Applied Biochemistry and Biotechnology

Part A: Enzyme Engineering and Biotechnology

Ashok Mulchandani • Editor-In-Chief
Department of Chemical and Environmental Engineering
Bourns Hall, Room A242
University of California
Riverside, CA 92521
E-mail: adani@engr.ucr.edu

Advisory Board

Howard H. Weetall • Founding Editor
US Environmental Protection Agency • Las Vegas, NV

David R. Walt • Former Editor-In-Chief
Department of Chemistry • Tufts University • Medford, MA

Isao Karube
Research Center for Advanced Science and Technology • University of Tokyo • Tokyo 153, Japan

Klaus Mosbach
Department of Pure and Applied Biochemistry • University of Lund • Lund, Sweden

Shuichi Suzuki
Saitama Institute of Technology • Saitama, Japan

Associate Editors

Wilfred Chen
Department of Chemical and Environmental Engineering • University of California • Riverside, CA

Elisabeth Csoregi
Department of Biotechology • University of Lund • Lund, Sweden

David W. Murhammer
Department of Chemical and Biochemical Engineering • University of Iowa • Iowa City, IA

Anup K. Singh
Biosystems Research Department • Sandia National Laboratories • Livermore, CA

Assistant Editor

Priti Mulchandani
Department of Chemical and Environmental Engineering • University of California • Riverside, CA

Editorial Board

M. Aizawa, *Tokyo Institute of Technology, Tokyo, Japan*
M. A. Arnold, *University of Iowa, Iowa City, IA*
L. Bachas, *University of Kentucky, Lexington, KY*
T. T. Bachmann, *University of Stuttgartt, Stuttgart, Germany*
S. Belkin, *The Hebrew University of Jerusalem, Jerusalem, Israel*
Harvey W. Blanch, *University of California, Berkeley, CA*
H. J. Cha, *Pohang University of Science and Technology, Pohang, Korea*
Q. Chuan-Ling, *Institute of Zoology, Chinese Academy of Sciences, Beijing, China*
Nancy A. Da Silva, *University of California, Irvine, CA*
M. DeLisa, *Cornell University, Ithaca, NY*
M. Deshusses, *University of California, Riverside, CA*
J. S. Dordick, *Rensselaer Polytechnic Institute, Troy, NY*
M. E. Eldefrawi, *University of Maryland, Baltimore, MD*
M. B. Gu, K-JIST, *Gwangju, Korea*
R. K. Jain, *Institute of Microbial Technology, Chandigarh, India*
N. G. Karanth, *Central Food and Technology Research Institute, Mysore, India*
R. Kelly, *North Carolina State University, Raleigh, NC*
A. M. Klibanov, *M.I.T., Cambridge, MA*
U. J. Krull, *Erindale College, University of Toronto, Mississauga, Ontario, Canada*
M. R. Ladish, *Purdue University, West Lafayette, IN*
K. Lee, *Cornell University, Ithaca, NY*
Y. Y. Lee, *Auburn University, Auburn AL*
F. S. Ligler, *Naval Research Laboratory, Washington, DC*
R. Linhardt, *University of Iowa, Iowa City, IA*
A. Pandey, *Regional Research Laboratory, Trivandrum, India*
M. Pishko, *The Pennsylvania State University, University Park, PA*
V. Renugopalakrishnan, *Harvard Medical School, National University of Singapore*
D. Ryu, *University of California, Davis, CA*
M. Seibert, *National Renewable Energy Laboratory, Golden, CO*
W. Tan, *University of Florida, Gainsville, FL*
Mitsuyoshi Ueda, *Kyoto University, Kyoto, Japan*
S. D. Varfolomeyev, *M. V. Lomonosov Moscow State University, Moscow, Russia*
J.-H. Xu, *East China University of Science and Technology, Shanghai, China*
P. Wang, *University of Akron, Akron, OH*
C. E. Wyman, *University of California, Riverside, Riverside, CA*
H. Zhao, *Univeristy of Illinois, Urbana Champagne, IL*

Patents and Literature Reviews Editor:

Mark R. Riley
Dept. of Agricultural & Biosystems Engineering • Shantz Bldg. University of Arizona • Tucson, AZ 85721-0338

Reviews in Biotechnology Editor:

John M. Walker
University of Hertfordshire • Hatfield • Herts • UK

Volume 145, Numbers 1–3, March 2008
Copyright © 2008 Humana Press Inc. All Rights Reserved.
This publication is printed on acid-free paper. ♾
ANSI Z39.48-1984 (American National Standards Institute) Permanence of Paper for Printed Library Materials.

ISSN 0273-2289 (Print)/1559-0291(Online)

No part of this publication may be reproduced or transmitted in any form or by any means, electronic or mechanical, including photocopy, recording, or any information storage and retrieval system, without permission in writing from the copyright owner. All authored papers, editorials, news, comments, opinions, conclusions, or recommendations are those of the author(s), and do not necessarily reflect the views of the publisher.

Applied Biochemistry and Biotechnology is made available for abstracting or indexing in *Chemical Abstracts, Biological Abstracts, Current Contents, Science Citation Index, EMBASE/Excerpta Medica, Index Medicus, Cambridge Scientific Abstracts, Reference Update,* and related compendia.

Biotechnology for Fuels and Chemicals

The Twenty-Ninth Symposium

Presented as Volumes 145-148
of *Applied Biochemistry and Biotechnology*

Proceedings of the Twenty-Ninth Symposium
on Biotechnology for Fuels and Chemicals
Held April 29–May 2, 2007, in Denver, Colorado

Sponsored by

US Department of Energy's Office of the Biomass Program
US Department of Agriculture, Agricultural Research Service
National Renewable Energy Laboratory
Oak Ridge National Laboratory
Idaho National Laboratory
AdvanceBio LLC
Biotechnology Industry Association (BIO)
Broin Companies
Cargill
Dow Chemical Company
Iogen Corporation
KATZEN International, Inc.
Mascoma Corporation
Novozymes
Tate and Lyle Ingredients Americans,m Inc
Wynkoop Brewing Company

Editors
William S. Adney and James D. McMillan
National Renewable Energy Laboratory

Jonathan Mielenz
Oak Ridge National Laboratory

K. Thomas Klasson
Southern Regional Research Center, USDA–ARS

Applied Biochemistry and Biotechnology
Volumes 145-148, Complete, Spring 2008
Copyright © 2008 Humana Press
All Rights Reserved.

No part of this publication may be reproduced or transmitted in any form or by any means, electronic or mechanical, including photocopy, recording, or any information storage and retrieval system, without permission in writing from the copyright owner.

Applied Biochemistry and Biotechnology is abstracted or indexed regularly in *Chemical Abstracts, Biological Abstracts, Current Contents, Science Citation Index, Excerpta Medica, Index Medicus,* and appropriate related compendia.

Introduction to the Proceedings of the Twenty-Ninth Symposium on Biotechnology for Fuels and Chemicals

William S. Adney

National Renewable Energy Laboratory

Golden, CO 80401-3393

The Twenty-Ninth Symposium on Biotechnology for Fuels and Chemicals was held April 29 - May 2, 2007 in Denver, Colorado. Continuing to foster a highly interdisciplinary focus on bioprocessing, this symposium remains the preeminent forum for bringing together active participants and organizations to exchange technical information and update current trends in the development and application of biotechnology for sustainable production of fuels and chemicals. This annual symposium emphasizes advances in biotechnology to produce high-volume, low-price products from renewable resources, as well as to improve the environment. Topical foci include advanced feedstock production and processing, enzymatic and microbial biocatalysis, bioprocess research and development, opportunities in biorefineries, commercialization of biobased products, as well as other special topics.

Advances in commercialization of bioproducts continued apace this year, and the level of interest and excitement in expanding the use of renewable feedstocks continued to grow. Nonetheless, significant techno-economic challenges must be overcome to achieve widespread commercialization of biotechnological fuels and chemicals production, particularly to move the feedstock base beyond primarily sugar crops and cereal grains (starch) to include holocellulose (cellulose and hemicellulose) from fibrous lignocellulosic plant materials.

Participants from academic, industrial, and government venues gathered to discuss the latest research breakthroughs and results in biotechnology to improve the economics of producing fuels and chemicals. The total of 702 attendees represented an all-time conference high; this is almost a 46% increase over the 2006 conference attendance in Nashville. Of this total, approximately 45% of attendees were from academia (about half of this, 14% of the total attendees, were students), 31% were from

industry, and 22% were from government. A total of 78 oral presentations (including Special Topic presentations) and 350 poster presentations were delivered. The high number of poster submissions required splitting the poster session into two evening sessions. (Conference details are posted at http://www.simhq.org/meetings/29symp/index.html).

Almost 40% of the attendees were international, showing the strong and building worldwide interest in this area. Nations represented included Armenia, Australia, Belgium, Brazil, Canada, People's Republic of China, Republic of China, Denmark, Finland, France, Germany, Ghana, Hungary, India, Italy, Japan, Korea, Mexico, New Zealand, Nigeria, Norway, Portugal, South Africa, Spain, Sweden, Thailand, The Netherlands, and United Kingdom, as well as the United States.

One of the focus areas for bioconversion of renewable resources into fuels is conversion of lignocellulose into sugars and the conversion of sugars into fuels and other products. This focus is continuing to expand toward the more encompassing concept of the integrated multiproduct biorefinery—where the production of multiple fuel, chemical, and energy products occurs at one site using a combination of biochemical and thermochemical conversion technologies. The biorefinery concept continues to grow as a unifying framework and vision, and the biorefinery theme featured prominently in many talks and presentations. However, another emerging theme was the importance of examining and optimizing the entire biorefining process rather than just its bioconversion-related elements.

The conference continued to include two Special Topics sessions devoted to discussing areas of particular interest. This year the two topics were international biofuels developments and the evolving attitudes about biomass as a sustainable feedstock for fuels, chemicals and energy production. The first Special Topic session was entitled "International Energy Agency (IEA) Task #39–Liquid Biofuels." This session focused on recent international progress on production of liquid biofuels and was chaired by Jack Saddler of the University of British Columbia. The second Special Topic session was entitled, "'Outside of a Small Circle of Friends': Changing Attitudes about Biomass as a Sustainable Energy Supply," and was chaired by John Sheehan of NREL. This session focused on the evolving perceptions within the agricultural producer and environmental and energy efficiency advocacy communities that biomass has the potential to be a large volume renewable resource for sustainable production of a variety of fuel, chemical, and energy products.

The Charles D. Scott award for Distinguished Contributions in the field of Biotechnology for Fuels and Chemicals was created to honor Symposium founder Dr. Charles D. Scott who chaired this Symposium for its first ten years. This year, the Charles D. Scott award was presented to

Session Chairpersons

Session 1A: Feedstock Genomics and Development

Chairs: Wilfrid Vermerris, *University of Florida Genetics Institute*
Steve Thomas, *Ceres, Inc.*

Session 1B: Microbial Catalysis and Engineering

Chairs: Lisbeth Olsson, *BioCentrum-DTU,*
Martin Keller, *Oak Ridge national Laboratory*

Session 2: Enzyme Catalysis and Engineering

Chairs: Sarah Teter, *Novozymes*
Steve Decker, *National Renewable Energy Laboratory*

Session 3: Bioprocess Separations and Process R&D

Chairs: Robert Wooley, *National Renewable Energy Laboratory*
Dhinakar Kompala, University of Colorado

Session 4: Biorefineries and Advanced System Concepts

Chairs: David Glassner, *Natureworks, LLC*
Mark Laser, *Dartmouth College*

Session 5A: Feedstock Preprocessing and Supply Logistics

Chairs: Robert Anex, Iowa State University
Corey Radtke, Idaho National Laboratory

Session 5B: Feedstock Fractionation and Hydrolysis

Chairs: Susan Hennessey, E.I DuPont de Nemours and Co.
Nathan Mosier, Purdue University

Session 6: Industrial Biofuels and Biobased Products

Chairs: Dale Monceaux, AdvanceBio, LLC
Charles Abbas, Archer Daniels Midland

Organizing Committee

Jim McMillan, Conference Chairman, *National Renewable Energy Laboratory, Golden, CO*
William S. Adney, *Conference Co-Chairman, National Renewable Energy Laboratory, Golden, CO*
Jonathan Mielenz, Conference Co-Chairman, *Oak Ridge National Laboratory, Oak Ridge, TN*
K. Thomas Klasson, *Conference Co-Chairman, USDA-Agrigultural Research Service, New Orleans, LA*
Doug Cameron, *Khosla Ventures, Menlo Park, CA*
Brian Davison, *Oak Ridge National Laboratory, Oak Ridge, TN*
Jim Duffield, *Conference Secretary/Proceedings Coordinator, National Renewable Energy Laboratory, Golden, CO*
Bonnie Hames, *Ceres, Inc., Thousan Oaks, CA*
Chad Haynes, *USDA-Agricultural Research Service, Beltsville, MD*
Susan Hennessey, *DuPont, Inc., Wilmington, DE*
Thomas Jeffries, *USDA Forest Service, Madison, WI*
Lee Lynd, *Dartmouth College, Hanover, NH*
Amy Miranda *USDOE Ofice of the Biomass Program, Washington, DC*
Dale Monceaux, *AdvanceBio LLC, Cincinnati, OH*
Lisbeth Olsson, *Technical University of Denmark, Lyngby, Denmark*
Jack Saddler, *University of British Columbia, Vancouver, British Columbia, Canada*
Jin-Ho Seo, *Seoul National University, Seoul, Korea*
Sharon Shoemaker, *University of California, Davis, CA*
David Thompson, *Idaho National Laboratory, Idaho Falls,*
Charles Wyman, *Dartmouth College, Hanover, NH*
Gisella Zanin, *State University of Maringa, Maringa, PR, Brazil*

Acknowledgments

The continued success of the Symposium is due to the many participants, organizers, and sponsors, but is also the result of significant contributions by numerous diligent, creative and talented staff. In particular, Jim Duffield of NREL, conference secretary, provided timely advice and heroic persistence while maintaining an unfailingly upbeat attitude.

The National Renewable Energy Laboratory is operated for the US Department of Energy by Midwest Research Institute and Battelle under contract DE-AC36-99GO10337.

Oak Ridge National Laboratory is operated for the US Department of Energy by UT-Battelle, LLC under contract DE-AC05-00OR22725.

The submitted Proceedings have been authored by a contractor of the US Government under contract DE-AC36-99GO10337. Accordingly, the US Government retains a nonexclusive, royalty-free license to publish or reproduce the published form of this contribution, or allow others to do so, for US Government purposes.

Other Proceedings in this Series

1. "Proceedings of the First Symposium on Biotechnology in Energy Production and Conservation" (1978), *Biotechnol. Bioeng. Symp.* **8**.
2. "Proceedings of the Second Symposium on Biotechnology in Energy Production and Conservation" (1980), *Biotechnol. Bioeng. Symp.* **10**.
3. "Proceedings of the Third Symposium on Biotechnology in Energy Production and Conservation" (1981), *Biotechnol. Bioeng. Symp.* **11**.
4. "Proceedings of the Fourth Symposium on Biotechnology in Energy Production and Conservation" (1982), *Biotechnol. Bioeng. Symp.* **12**.
5. "Proceedings of the Fifth Symposium on Biotechnology for Fuels and Chemicals" (1983), *Biotechnol. Bioeng. Symp.* **13**.
6. "Proceedings of the Sixth Symposium on Biotechnology for Fuels and Chemicals" (1984), *Biotechnol. Bioeng. Symp.* **14**.
7. "Proceedings of the Seventh Symposium on Biotechnology for Fuels and Chemicals" (1985), *Biotechnol. Bioeng. Symp.* **15**.
8. "Proceedings of the Eigth Symposium on Biotechnology for Fuels and Chemicals" (1986, *Biotechnol . Bioeng. Symp.* **17**.
9. "Proceedings of the Ninth Symposium on Biotechnology for Fuels and Chemicals" (1988), *Appl. Biochem. Biotechnol.* **17,18**.
10. "Proceedings of the Tenth Symposium on Biotechnology for Fuels and Chemicals" (1989), *Appl. Biochem. Biotechnol.* **20,21**.
11. "Proceedings of the Eleventh Symposium on Biotechnology for Fuels and Chemicals" (1990), *Appl. Biochem. Biotechnol.* **24,25**.
12. "Proceedings of the Twelfth Symposium on Biotechnology for Fuels and Chemicals" (1991), *Appl. Biochem. Biotechnol.* **28,29**.
13. "Proceedings of the Thirteenth Symposium on Biotechnology for Fuels and Chemicals" (1992), *Appl. Biochem. Biotechnol.* **34,35**.
14. "Proceedings of the Fourteenth Symposium on Biotechnology for Fuels and Chemicals" (1993), *Appl. Biochem. Biotechnol.* **39,40**.
15. "Proceedings of the Fifteenth Symposium on Biotechnology for Fuels and Chemicals" (1994), *Appl. Biochem. Biotechnol.* **45,46**.
16. "Proceedings of the Sixteenth Symposium on Biotechnology for Fuels and Chemicals" (1995), *Appl. Biochem. Biotechnol.* **51,52**.
17. "Proceedings of the Seventeenth Symposium on Biotechnology for Fuels and Chemicals" (1996), *Appl. Biochem. Biotechnol* . **57,58**.
18. "Proceedings of the Eighteenth Symposium on Biotechnology for Fuels and Chemicals" (1997), *Appl. Biochem. Biotechnol.* **63–65**.
19. "Proceedings of the Nineteenth Symposium on Biotechnology for Fuels and Chemicals" (1998), *Appl. Biochem. Biotechnol.* **70–72**.
20. "Proceedings of the Twentieth Symposium on Biotechnology for Fuels and Chemicals" (1999), *Appl. Biochem. Biotechnol* . **77–79**.
21. "Proceedings of the Twenty-First Symposium on Biotechnology for Fuels and Chemicals" (2000), *Appl. Biochem. Biotechnol.* **84–86**.
22. "Proceedings of the Twenty-Second Symposium on Biotechnology for Fuels and Chemicals" (2001), *Appl. Biochem. Biotechnol.* **91–93**.

23. "Proceedings of the Twenty-Third Symposium on Biotechnology for Fuels and Chemicals" (2002), *Appl. Biochem. Biotechnol.* **98–100**.
24. "Proceedings of the Twenty-Fourth Symposium on Biotechnology for Fuels and Chemicals" (2003), *Appl. Biochem. Biotechnol.* **105–108**.
25. "Proceedings of the Twenty-Fifth Symposium on Biotechnology for Fuels and Chemicals" (2004), *Appl. Biochem. Biotechnol.* **113–116**.
26. "Proceedings of the Twenty-Sixth Symposium on Biotechnology for Fuels and Chemicals" (2005), *Appl. Biochem. Biotechnol.* **121–124**.
27. "Proceedings of the Twenty-Seventh Symposium on Biotechnology for Fuels and Chemicals" (2005), *Appl. Biochem. Biotechnol.* **121–124**.
28. "Proceedings of the Twenty-Eighth Symposium on Biotechnology for Fuels and Chemicals" (2005), Appl. Biochem. Biotechnol. **121–124**.

This symposium has been held annually since 1978. We are pleased to have the proceedings of the Twenty-Ninth Symposium currently published in this special issue to continue the tradition of providing a record of the contributions made.

The Thirtieth Symposium will be May 4-7, 2008 in New Orleans, Louisiana. More information on the 28th and 29th Symposia is available at the following websites: http://www1.eere.energy.gov/biomass/biotech_symposium/ and http://www.simhq.org/meetings/29symp/index.html. We welcome comments or discussions relevant to the format or content of the meeting.

TABLE OF CONTENTS

Volume 145 Numbers 1–3

Session 1A

Introduction to Session 1A: Feedstock Genomics and Development
W. Vermerris 1

High-resolution Thermogravimetric Analysis For Rapid Characterization of Biomass Composition and Selection of Shrub Willow Varieties
M. J. Serapiglia • K. D. Cameron • A. J. Stipanovic • L. B. Smart 3

Assessment of Bermudagrass and Bunch Grasses as Feedstock for Conversion to Ethanol
W. F. Anderson • B. S. Dien • S. K. Brandon • J. D. Peterson 13

Session 1B

Rapid Isolation of the *Trichoderma* Strain with Higher Degrading Ability of a Filter Paper and Superior Proliferation Characteristics Using Avicel Plates and the Double-Layer Selection Medium
H. Toyama • M. Nakano • Y. Satake • N. Toyama 23

A Comparison of Simple Rheological Parameters and Simulation Data for *Zymomonas mobilis* Fermentation Broths with High Substrate Loading in a 3-L Bioreactor
B.-H. Um • T. R. Hanley 29

Effects of Oxygen Limitation on Xylose Fermentation, Intracellular Metabolites, and Key Enzymes of *Neurospora crassa* AS3.1602
Z. Zhang • Y. Qu • X. Zhang • J. Lin 39

Fermentation of Acid-pretreated Corn Stover to Ethanol Without Detoxification Using *Pichia stipitis*
F. K. Agbogbo • F. D. Haagensen • D. Milam • K. S. Wenger 53

Bioethanol Production from Uncooked Raw Starch by Immobilized Surface-engineered Yeast Cells
J.-P. Chen • K.-W. Wu • H. Fukuda 59

Effects of Gene Orientation and Use of Multiple Promoters on the Expression of *XYL1* and *XYL2* in *Saccharomyces cerevisiae*
J. Y. Bae • J. Laplaza • T. W. Jeffries 69

Bioreactors for H_2 Production by Purple Nonsulfur Bacteria
S. A. Markov • P. F. Weaver 79

Solid-state Fermentation of Xylanase from *Penicillium canescens 10-10c* in a Multi-layer-packed Bed Reactor
A. A. Assamoi • J. Destain • F. Delvigne • G. Lognay • P. Thonart 87

Ethanol Production from Wet-Exploded Wheat Straw Hydrolysate by Thermophilic Anaerobic Bacterium *Thermoanaerobacter* BG1L1 in a Continuous Immobilized Reactor
T. I. Georgieva • M. J. Mikkelsen • B. K. Ahring 99

Succinic Acid Production from Cheese Whey using *Actinobacillus succinogenes* 130 Z
C. Wan • Y. Li • A. Shahbazi • S. Xiu 111

Volume 146 Numbers 1–3

Session 2

Introduction to Session 2: Enzyme Catalysis and Engineering
S. R. Decker • S. Teter 1

Production of Cyclodextrins by CGTase from *Bacillus clausii* Using Different Starches as Substrates
H. F. Alves-Prado • A. A. J. Carneiro • F. C. Pavezzi • E. Gomes • M. Boscolo • C. M. L. Franco • R. da Silva 3

Effects of pH and Temperature on Recombinant Manganese Peroxidase Production and Stability
F. Jiang • P. Kongsaeree • K. Schilke • C. Lajoie • C. Kelly 15

Xylanase Production by *Bacillus circulans* D1 Using Maltose as Carbon Source
D. A. Bocchini • E. Gomes • R. Da Silva 29

Immobilization of Fungal β-Glucosidase on Silica Gel and Kaolin Carriers
H. K. Karagulyan • V. K. Gasparyan • S. R. Decker 39

Immobilization of *Yarrowia lipolytica* Lipase—a Comparison of Stability of Physical Adsorption and Covalent Attachment Techniques
A. G. Cunha • G. Fernández-Lorente • J. V. Bevilaqua • J. Destain • L. M. C. Paiva • D. M. G. Freire • R. Fernández-Lafuente • J. M. Guisán 49

Heterologous Expression of *Aspergillus niger* β-D-Xylosidase (XlnD): Characterization on Lignocellulosic Substrates
M. J. Selig • E. P. Knoshaug • S. R. Decker • J. O. Baker • M. E. Himmel • W. S. Adney 57

Cloning, Expression and Characterization of a Glycoside Hydrolase Family 39 Xylosidase from *Bacillus Halodurans* C-125
K. Wagschal • D. Franqui-Espiet • C. C. Lee • G. H. Robertson • D. W. S. Wong 69

Heterologous Expression of Two Ferulic Acid Esterases from *Penicillium funiculosum*
E. P. Knoshaug • M. J. Selig • J. O. Baker • S. R. Decker • M. E. Himmel • W. S. Adney 79

Evaluation of a *Hypocrea jecorina* Enzyme Preparation foro Hydrolysis of Tifton 85 Bermudagrass
E. A. Ximenes • S. K. Brandon • J. Doran-Peterson 89

A Novel Technique that Enables Efficient Conduct of Simultaneous Isomerization and Fermentation (SIF) of Xylose
K. Rao • S. Chelikani • P. Relue • S. Varanasi 101

The Effects of Wheat Bran Composition on the Production of Biomass-Hydrolyzing Enzymes by *Penicillium decumbens*
X. Sun • Z. Liu • Y. Qu • X. Li 119

Integrated Biosensor Systems for Ethanol Analysis
E. M. Alhadeff • A. M. Salgado • O. Cós • N. Pereira Jr. • F. Valero • B. Valdman 129

β-D-Xylosidase from *Selenomonas ruminantium*: Catalyzed Reactions with Natural and Artificial Substrates
D. B. Jordan 137

Hydrolysis of Ammonia-pretreated Sugar Cane Bagasse with Cellulase, β-Glucosidase, and Hemicellulase Preparations
B. A. Prior • D. F. Day 151

Monoglycerides and Diglycerides Synthesis in a Solvent-Free System by Lipase-Catalyzed Glycerolysis
P. B. L. Fregolente • L. V. Fregolente • G. M. F. Pinto • B. C. Batistella • M. R. Wolf-Maciel • R. M. Filho 165

Immobilization of *Candida Antarctica* Lipase B by Adsorption to Green Coconut Fiber
A. I. S. Brigida • Á. D. T. Pinheiro • A. L. O. Ferreira • L. R. B. Gonçalves 173

Methods and Supports for Immobilization and Stabilization of Cyclomaltodextrin Glucanotransferase from *Thermoanaerobacter*
A. E. Amud • G. R. P. da Silva • P. W. Tardioli • C. M. F. Soares • F. F. Moraes • G. M. Zanin **189**

Response Surface Methodology as an Approach to Determine Optimal Activities of Lipase Entrapped in Sol-Gel Matrix Using Different Vegetable Oils
R. C. Pinheiro • C. M. F. Soares • H. F. de Castro • F. F. Moraes • G. M. Zanin **203**

Improving Activity of Salt-Lyophilized Enzymes in Organic Media
A. P. Borole • B. H. Davison **215**

Protease Production by Different Thermophilic Fungi
M. M. Macchione • C. W. Merheb • E. Gomes • R. da Silva **223**

Non-ionic Surfactants and Non-Catalytic Protein Treatment on Enzymatic Hydrolysis of Pretreated Creeping Wild Ryegrass
Y. Zheng • Z. Pan • R. Zhang • D. Wang • B. Jenkins **231**

Volume 147 Numbers 1–3

Session 3

Separate and Concentrate Lactic Acid Using Combination of Nanofiltration and Reverse Osmosis Membranes
Y. Li • A. Shahbazi • K. Williams • C. Wan 1

Parameter Estimation for Simultaneous Saccharification and Fermentation of Food Waste Into Ethanol Using Matlab Simulink
R.A. Davis 11

Lignin Peroxidase from Streptomyces viridosporus T7A: Enzyme Concentration Using Ultrafiltration
L.M.F. Gottschalk • E.P.S. Bon • R. Nobrega 23

Oxygen-controlled Biosurfactant Production in a Bench Scale Bioreactor
F.A. Kronemberger • L.M.M. Santa Anna I A.C.L.B. Fernandes • R.R. Menezes • C.P. Borges • D.M.G. Freire 33

Continuous Production of Ethanol from Starch Using Glucoamylase and Yeast Co-Immobilized in Pectin Gel
R.L.C. Giordano • J. Trovati • W. Schmidell 47

Lipase Production in Solid-State Fermentation Monitoring Biomass Growth of Aspergillus niger Using Digital Image Processing
J.C.V. Dutra • S. da C. Terzi • J.V. Bevilaqua • M.C.T. Damaso • S. Couri • M.A.P. Langone • L.F. Senna 63

The Effects of Surfactants on the Estimation of Bacterial Density in Petroleum Samples
A.S. Luna • A.C.A. da Costa • M.M.M. Gonçalves • K.Y.M. de Almeida 77

An Alternative Application to the Portuguese Agro-Industrial Residue: Wheat Straw
D.S. Ruzene • D.P. Silva • A.A. Vicente • A.R. Gonçalves • J.A. Teixeira 85

The Use of Seaweed and Sugarcane Bagasse for the Biological Treatment of Metal-contaminated Waters Under Sulfate-reducing Conditions
M.M.M. Gonçalves • L.A. de Oliveira Mello • A.C.A. da Costa 97

Development of Activity-based Cost Functions for Cellulase, Invertase, and Other Enzymes
C.C. Stowers • E.M. Ferguson • R.D. Tanner 107

Session 4

Reaction Kinetics of the Hydrothermal Treatment of Lignin
B. Zhang • H.-J. Huang • S. Ramaswamy 119

Hydrodynamic Characterization of a Column-type Prototype Bioreactor
T. Espinosa-Solares I M. Morales-Contreras • F. Robles-Martínez • M. García-Nazariega • C. Lobato-Calleros 133

Thermal Effects on Hydrothermal Biomass Liquefaction
B. Zhang • M. von Keitz • K. Valentas 143

Volume 148 Numbers 1–3

Session 5A

Bundled Slash: A Potential New Biomass Resource for Fuels and Chemicals
P. H. Steele • B. K. Mitchell • J. E. Cooper • S. Arora **1**

Session 5B

Pretreatment Characteristics of Waste Oak Wood by Ammonia Percolation
J.-S. Kim • H. Kim • J.-S. Lee • J.-P. Lee • S.-C. Park **15**

Pretreatment of Whole-Crop Harvested, Ensiled Maize for Ethanol Production
M. H. Thomsen • J. B. Holm-Nielsen • P. Oleskowicz-Popiel • A. B. Thomsen **23**

Enzymatic Hydrolysis and Ethanol Fermentation of High Dry Matter Wet-Exploded Wheat Straw at Low Enzyme Loading
T. I. Georgieva • X. Hou • T. Hilstrøm • B. K. Ahring **35**

A Comparison between Lime and Alkaline Hydrogen Peroxide Pretreatments of Sugarcane Bagasse for Ethanol Production
S. C. Rabelo • R. M. Filho • A. C. Costa **45**

Substrate Dependency and Effect of Xylanase Supplementation on Enzymatic Hydrolysis of Ammonia-Treated Biomass
R. Gupta • T. H. Kim • Y. Y. Lee **59**

Alkali (NaOH) Pretreatment of Switchgrass by Radio Frequency-based Dielectric Heating
Z. Hu • Y. Wang • Z. Wen **71**

Session 6

Biological Hydrogen Production Using Chloroform-treated Methanogenic Granules
B. Hu • S. Chen **83**

Effect of Furfural, Vanillin and Syringaldehyde on *Candida guilliermondii* Growth and Xylitol Biosynthesis
C. Kelly • O. Jones • C. Barnhart • C. Lajoie **97**

Production and Characterization of Biodiesel from Tung Oil
J.-Y. Park • D.-K. Kim • Z.-M. Wang • P. Lu • S-C. Park • J.-S. Lee **109**

Yeast Biomass Production in Brewery's Spent Grains Hemicellulosic Hydrolyzate
L. C. Duarte • F. Carvalheiro • S. Lopes • I. Neves • F. M. Gírio **119**

Lipase-Catalyzed Transesterification of Rapeseed Oil for Biodiesel Production with *tert*-Butanol
G.-T. Jeong • D.-H. Park **131**

Bioethanol Production Optimization: A Thermodynamic Analysis
V. H. Álvarez • E. C. Rivera • A. C. Costa • R. M. Filho • M. R. Wolf Maciel • M. Aznar **141**

Oxidation in Acidic Medium of Lignins from Agricultural Residues
G. A. A. Labat • A. R. Gonçalves **151**

Kinetic Modeling and Parameter Estimation in a Tower Bioreactor for Bioethanol Production
E. C. Rivera • A. C. da Costa • B. H. Lunelli • M. R. Wolf Maciel • R. M. Filho **163**

Analysis of Kinetic and Operational Parameters in a Structured Model for Acrylic Acid Production through Experimental Design
B. H. Lunelli • E. C. Rivera • E. C. Vasco de Toledo • M. R. Wolf Maciel • R. Maciel Filho **175**

Optimization of Oligosaccharide Synthesis from Cellobiose by Dextransucrase
M. Kim • D. F. Day **189**

Fermentation Kinetics for Xylitol Production by a *Pichia stipitis* D-Xylulokinase Mutant Previously Grown in Spent Sulfite Liquor
R. C. L. B. Rodrigues • C. Lu • B. Lin • T. W. Jeffries **199**

Selective Enrichment of a Methanol-Utilizing Consortium Using Pulp and Paper Mill Waste Streams
G. R. Mockos • W. A. Smith • F. J. Loge • D. N. Thompson **211**

Evaluation of Cashew Apple Juice for the Production of Fuel Ethanol
Á. D. T. Pinheiro • M. V. P. Rocha • G. R. Macedo • L. R. B. Gonçalves **227**

Atmospheric Pressure Liquefaction of Dried Distillers Grains (DDG) and Making Polyurethane Foams from Liquefied DDG
F. Yu • Z. Le • P. Chen • Y. Liu • X. Lin • R. Ruan **235**

Bacterial Cellulose Production by *Acetobacter xylinum* Strains from Agricultural Waste Products
S. Kongruang **245**

Special Topic B

Overview of Special Session B—Compositional and Structural Analysis of Biomass
B. Hames **257**

What can be Learned from Silage Breeding Programs?
A. J. Lorenz • J. G. Coors **261**

Permethylation Linkage Analysis Techniques for Residual Carbohydrates
N. P. J. Price **271**

Appl Biochem Biotechnol (2008) 145:1–2
DOI 10.1007/s12010-008-8224-1

Introduction to Session 1A: Feedstock Genomics and Development

Wilfred Vermerris

Published online: 12 April 2008
© Humana Press 2008

Genomics research aimed at improving bioconversion properties of feedstocks received a major impetus as a result of the Feedstock Genomics program jointly operated by the U.S. Department of Energy (DOE) and the U.S. Department of Agriculture (USDA). In addition, oil company BP established the Energy Biosciences Institute in collaboration with the University of California-Berkeley, Lawrence Berkeley National Laboratory, and the University of Illinois in Urbana-Champaign. This was followed later on in the year by the establishment of three DOE-funded bioenergy centers. The need to switch from petroleum-based duels to biofuels was underscored by the report of Working Group II of the United Nations-sponsored International Panel on Climate Change (IPCC), in which the wide-spread effects of greenhouse gas emissions on the global climate were presented. IPCC and former U.S. vice-president Al Gore received the 2007 Nobel Peace Prize for their efforts to quantify and disseminate the effects of global warming.

The presentations in Session 1A reflected this new impetus, as evidenced by two oral presentations from recipients of USDA–DOE funding, Dr. William Rooney (Texas A&M University, College Station, TX, USA) and Dr. Rick Dixon (Noble Foundation, Ardmore, OK, USA). Dr. Rooney discussed his research on the development of sorghum for bioenergy production. Photoperiod-sensitive sorghums do not transition to the reproductive stage and can produce large amounts of biomass, as high as 27 Mg ha^{-1}. He also discussed genetic approaches to identify genes controlling sugar accumulation, cell wall composition, and biomass production in sorghum. Dr. Dixon presented his research on the transgenic down-regulation of monolignol biosynthetic genes in alfalfa. Conversion of alfalfa biomass appeared to be primarily dependent on lignin content as opposed to lignin subunit composition. The down-regulation of some of the genes resulted in a noticeable reduction in the total amount of biomass, an undesirable side effect. The impact of lignin content and composition was also discussed by Dr. William Anderson (USDA, Tifton, GA, USA), Dr. James Coors (University of Wisconsin-Madison, WI, USA), and Dr. Gautham Sarath (USDA, Lincoln, NE, USA) in their presentations on Bermudagrass, maize, and switchgrass, respectively. In maize, lignin content appeared to impact biomass conversion

W. Vermerris (✉)
University of Florida Genetics Institute, Gainesville, FL 32610, USA
e-mail: wev@ufl.edu

properties, just like in alfalfa, whereas in Bermudagrass and switchgrass lignin subunit composition appeared to be a more critical factor.

The need to establish reliable methods for the evaluation of biomass conversion properties was expressed in several of the presentations. Methods that were originally developed for the analysis of forage quality seem to provide a reasonable approximation of biomass conversion potential in some species (maize), but not in other species (Bermudagrass). Ms. Michelle Serapiglia (SUNY-ESF, Syracuse, NY, USA) discussed how thermogravimetric analyses may be applicable to determine lignin content and composition in shrub willow. The oral session was concluded with a presentation by Dr. Steven Thomas (Ceres, Inc., Thousand Oaks, CA, USA) on ways in which genetic diversity in switchgrass can be catalogued and exploited for the development of superior germplasm.

Several poster presentations in this session focused on the chemical basis of biomass conversion and the development of methods to determine which features contributed to a more rapid bioprocessing. Approaches included the use of atomic force microscopy, fluorescently labeled cellulases, near infrared reflectance spectroscopy and fluorescence spectroscopy. Other topics represented in the poster presentations included the production of cell wall-degrading enzymes *in planta*, and plant breeding approaches, including the incorporation of mutations and the introduction of transgenes to facilitate biomass processing of a variety of species, including sorghum, wheat, corn, shrub willow, and switchgrass.

Appl Biochem Biotechnol (2008) 145:3–11
DOI 10.1007/s12010-007-8061-7

High-resolution Thermogravimetric Analysis For Rapid Characterization of Biomass Composition and Selection of Shrub Willow Varieties

Michelle J. Serapiglia · Kimberly D. Cameron · Arthur J. Stipanovic · Lawrence B. Smart

Received: 21 May 2007 / Accepted: 19 September 2007 /
Published online: 19 October 2007
© Humana Press Inc. 2007

Abstract The cultivation of shrub willow (*Salix* spp.) bioenergy crops is being commercialized in North America, as it has been in Europe for many years. Considering the high genetic diversity and ease of hybridization, there is great potential for genetic improvement of shrub willow through traditional breeding. The State University of New York—College of Environmental Science and Forestry has an extensive breeding program for the genetic improvement of shrub willow for biomass production and for other environmental applications. Since 1998, breeding efforts have produced more than 200 families resulting in more than 5,000 progeny. The goal for this project was to utilize a rapid, low-cost method for the compositional analysis of willow biomass to aid in the selection of willow clones for improved conversion efficiency. A select group of willow clones was analyzed using high-resolution thermogravimetric analysis (HR-TGA), and significant differences in biomass composition were observed. Differences among and within families produced through controlled pollinations were observed, as well as differences by age at time of sampling. These results suggest that HR-TGA has a great promise as a tool for rapid biomass characterization.

Keywords Cellulose · Hemicellulose · Lignin · *Salix* · Wood composition

Introduction

Reliance on petroleum-based transportation fuels has raised national concern with respect to homeland security, energy independence, depletion of petroleum resources, and impact on

M. J. Serapiglia · K. D. Cameron · L. B. Smart (✉)
Department of Environmental and Forest Biology, State University of New York
College of Environmental Science and Forestry, 1 Forestry Drive, Syracuse, NY 13210, USA
e-mail: lbsmart@esf.edu

A. J. Stipanovic
Department of Chemistry, State University of New York College of Environmental Science and Forestry,
1 Forestry Drive, Syracuse, NY 13210, USA

the environment. The production of biofuels from dedicated energy crops and agricultural crop residues grown sustainably within the USA could help alleviate these problems. Currently, the vast majority of ethanol fuel produced in the USA is made from a single feedstock, corn grain, harvested from an annual crop. Achieving the goal of replacing 30% of the US petroleum consumption with biofuels and bioproducts by 2030 will require the use of perennial crops as well as the current annual crops [1]. As extraction techniques and conversion processes improve and become more cost effective, sustainable perennial woody crops, such as fast-growing willow shrubs, will become the preferred feedstocks. Shrub willow (*Salix* spp.), a high-yielding perennial crop with a short harvest cycle of only 3 to 4 years, is considered a suitable energy crop for much of North America [2, 3] and can be grown on underutilized agricultural land [3, 4]. There are multiple environmental benefits to growing shrub willow and excellent potential for genetic improvement through traditional breeding [5].

Researchers at the State University of New York College of Environmental Science and Forestry (SUNY-ESF) have developed a breeding program for the genetic improvement of shrub willow for increased biomass production [4]. There are more than 300 species of *Salix* worldwide with little domestication and high genetic diversity [6]. Since 1994, SUNY-ESF has collected and planted more than 750 accessions of shrub willow and established the largest willow-breeding program in North America [3, 4]. From these accessions, breeding efforts begun in 1998 have produced more than 5,000 progeny. Between 1998 and 2007, more than 200 families have been generated through controlled pollination. Crosses completed in 1998 and 1999 produced more than 2,000 individuals that have been screened in field trials for high biomass, form, and disease resistance [4, 7]. Selected groups of superior clones from crosses performed in 1998 and 1999 were planted in selection trials in 2001 and 2002, respectively. Growth improvements as high as 40% greater than a reference clone have been observed [4].

If shrub willow is to be used as a feedstock for the production of bioproducts or biofuels, the bioconversion process must become more efficient and cost effective. This can be partially achieved by selecting varieties with biomass composition that is better suited to the conversion process. Composition of the biomass is critical to the efficiency of processing and product yield, whether it is used to produce liquid fuels such as ethanol or polymers such as biodegradable plastics. Lignocellulosic biomass displays considerable recalcitrance to biochemical conversion because of the inaccessibility of its polymer components to enzymatic digestion and the release or production of fermentation inhibitors during pretreatment. If the ratio of hemicellulose, cellulose, and lignin in a woody biomass feedstock was optimized for the specific biochemical conversion method, then expensive and chemically harsh pretreatment methods could be reduced or avoided [8].

The development of a high-throughput process for the analysis of willow biomass will allow for selection of improved varieties with more favorable biomass composition in the willow breeding program. Traditional wet chemistry techniques for the analysis of biomass require strong acids and time-consuming processes resulting in a method whereby only 20 samples per week per person can be analyzed [9]. Current advancements in analytical methods include infrared spectroscopy (Fourier transform infrared [FT-IR] and near-infrared [NIR]) and pyrolysis molecular beam mass spectroscopy (pyMBMS) [10–13]. Multivariate analyses are often used in conjunction with these methods. To increase accuracy and improve throughput, development and further improvement of new analytical methods is required.

This project focuses on the development of high-resolution thermogravimetric analysis (HR-TGA) as a rapid, low-cost method for the analysis of biomass composition of shrub willow. The goal is to provide an alternative method for biomass analysis that is faster and

more cost effective than existing techniques with comparable or enhanced accuracy. This method can quantitatively resolve complex mixtures based on the characteristic thermal decomposition temperature of each component. It is well established that the pyrolytic decomposition of woody plant tissues in inert atmospheres occurs at the lowest temperature for hemicellulose (250–300 °C), followed by cellulose (300–350 °C) and lignin (300–500 °C) [14]. HR-TGA has already been applied to the analysis of lignocellulosic material and has shown to be useful in compositional analysis [15, 16]. Our work applies this method in analysis of willow varieties produced in the SUNY-ESF breeding program.

Materials and Methods

Source Material and Tissue Collection

Willow stem biomass samples were collected in January 2006 from two field trials growing at the Tully Genetics Field Station (Tully, NY; Table 1). Individuals sampled from the 2001 selection trial have clone IDs with the designation "98XX," where 98 indicates the year of the cross and XX the number of the family. Clones sampled from the 2002 selection trial were bred in 1999 and have IDs beginning with the designation "99." Samples from the reference clones SV1, SX61, SX64, and SX67 were collected from both selection trials. Samples were collected from three replicate plants for each of the 95 clones (Table 1) as follows: 15-cm sections including bark were cut from the base, middle, and top of one representative canopy stem. These stem sections were dried to a constant weight at 65 °C and then ground in a Wiley mill with a 20-mesh screen. The ground material from the three sections of each stem was pooled and homogenized. Each of the three replicates was analyzed in triplicate, for a total of nine analyses per clone. Samples from the 1999 families

Table 1 Families and reference clones in this study.

Family ID	Species	Number of progeny analyzed
9870	*S. sachalinensis*×*S. miyabeana*	4
9871	*S. sachalinensis*×*S. miyabeana*	4
98101	*S. dasyclados*×*S. miyabeana*	2
9882	*S. purpurea*×*S. purpurea*	4
9970	*S. sachalinensis*×*S. miyabeana*	13
9979	*S. purpurea*×*S. miyabeana*	1
9980	*S. purpurea*×*S. miyabeana*	1
99113	*S. purpurea*×*S. purpurea*	3
99201	*S. viminalis*×*S. miyabeana*	4
99202	*S. viminalis*×*S. miyabeana*	15
99207	*S. viminalis*×*S. miyabeana*	7
99208	*S. viminalis*×*S. miyabeana*	2
99217	*S. purpurea*×*S. miyabeana*	12
99227	*S. purpurea*×*S. purpurea*	2
99232	*S. purpurea*×*S. purpurea*	2
99239	*S. purpurea*×*S. purpurea*	15
SV1	*S. dasyclados*	–
SX61	*S. sachalinensis*	–
SX64	*S. miyabeana*	–
SX67	*S. miyabeana*	–

were collected after the third growing season after coppice, while samples from the 1998 individuals were collected one growing season after coppice. Samples of both ages were collected from the reference clones SV1, SX61, SX64, and SX67.

High-resolution Thermogravimetric Analysis

All willow samples were analyzed using a Thermogravimetric Analyzer 2950 (TA Instruments, New Castle, DE) with the TA Universal Analysis 2000 software. The method used for all samples was "high-resolution dynamic" with a heating rate of 20 °C min^{-1}, a final temperature of 600 °C, a resolution of 4.0, and a sensitivity value of 1.0. The electro-balance was purged with nitrogen at a flow rate of 44 L min^{-1}, and the furnace was purged with compressed air with a flow rate of 66 mL min^{-1}. For each analysis, 10 mg of dry tissue was used.

The percent dry weight for each stem biomass component (hemicellulose, cellulose, and lignin) was calculated by designating weight loss cutoff points on the generated thermogram (Fig. 1). The initial mass of the sample was corrected for water loss (change in weight from starting temperature to around 129 °C). Hemicellulose content was designated to be the weight loss between 245 and 290 °C, cellulose between 290 and 350 °C, and lignin between 350 and 525 °C. These cutoff points were identical for each sample, providing relative differences among the clones.

Statistical Analysis

All statistical analyses were performed using SAS® version 9.1.2 at a critical α=0.05. SAS PROC GLM and PROC NESTED were used to analyze all TGA data and to evaluate the

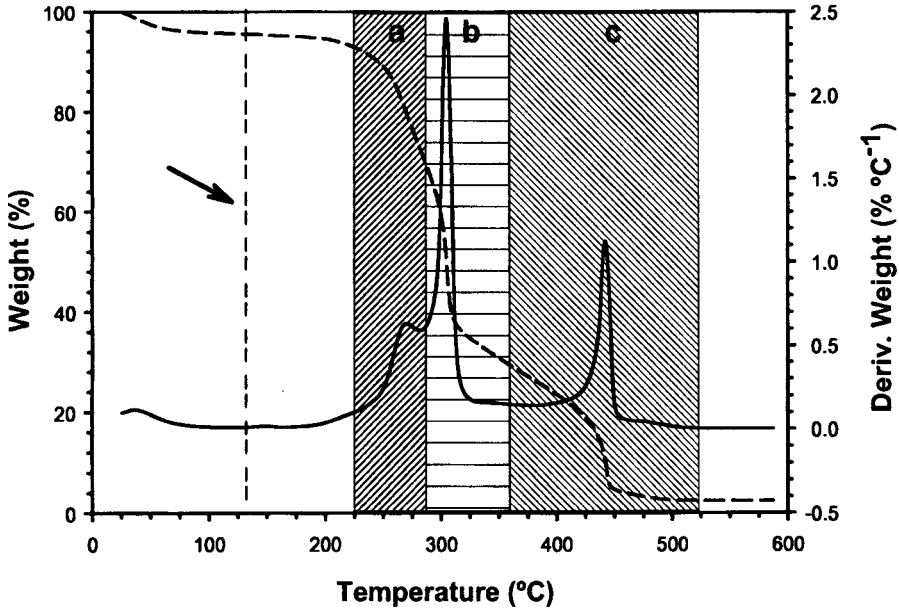


Fig. 1 TGA thermogram of biomass from reference willow clone *S. dasyclados* 'SV1.' *Arrow* indicates cutoff line for water loss correction (129 °C). *Block A*: weight loss representative of hemicellulose (245–290 °C). *Block B*: weight loss representative of cellulose (290–350 °C). *Block C*: weight loss representative of lignin (350–525 °C)

differences in biomass composition. When a significant interaction ($P<0.05$) was observed, Tukey's mean studentized range test was used to determine significant differences among clones. The variance components for the total data set, between and within clones, and within instrumental run were estimated with PROC NESTED. The multivariate analyses PROC CLUSTER and PROC CANDISC (discriminate analysis) were performed to identify groupings among specific clones.

Results and Discussion

As the breeding and domestication of crops to serve as feedstocks for biofuels and bioenergy is a very recent priority, there is urgent need to focus or refocus the aim of energy crop breeding programs to the optimization of biomass composition, while maintaining and improving high yield as the most critical trait. Characterizing and identifying differences in biomass composition among the varieties produced through conventional breeding demands techniques that are relatively fast, precise, and inexpensive. To refine the selection strategy of the willow breeding program with the aim of identifying varieties that have biomass composition that is well matched with the requirements of the intended downstream conversion technology, we have embarked on the development of HR-TGA as a rapid, low-cost method for analyzing and screening the biomass of hundreds or thousands of unique willow genotypes. Based on the initial results obtained in this study, HR-TGA may be an advantageous tool for the willow breeding program.

Utilizing this HR-TGA method, we were able to identify significant differences in the relative cellulose, hemicellulose, and lignin content among 95 willow clones. Statistical analysis provided variance components among clones, experimental replication, and instrumental replication. The total variation observed in the data set was relatively low, but more than 50% of the total variation was attributed to clonal variation. Instrument variation accounted for a maximum of 25% of total variation. The observed experimental and instrumental variation suggests that either more experimental replications or instrumental runs would help reduce variation, but the error is relatively small compared to the means; therefore, this is not a critical issue. This small error was generated using a remarkably small sample size of only 10 mg, which is indicative of the precision of the instrument. Small sample size, speed of analysis, and the ease of sample preparation for instrumental analysis are other advantages associated with this analytical method. Currently, one instrument can analyze 16 samples per day with a run time per sample of 90 min. As the instrument has an autosampler, it can process 16 samples before more samples need to be loaded. With further refinement of this analysis, the run time might be shortened. In addition, multiple instruments can be utilized to increase the daily throughput.

No discrete groupings or clusters were observed among the clones when plotted in a 3D graph (Fig. 2). Several multivariate analyses were performed, but all proved to be inconclusive and are not presented here. Most of the willow clones analyzed have similar biomass composition; however, there are several clones that have distinctively more or less cellulose, hemicellulose, or lignin (Fig. 2). This could be very important in future selection of willow varieties optimized for a particular application.

Among all clones analyzed, cellulose content ranged from 29 to 40%, hemicellulose content ranged from 23 to 30%, and lignin content ranged from 27 to 35% (data not shown). Individuals with the greatest relative amount of one component were significantly different from individuals with the least amount. The individual willow clones that were selected for analysis were purposefully chosen with an eye to their genetic diversity. In

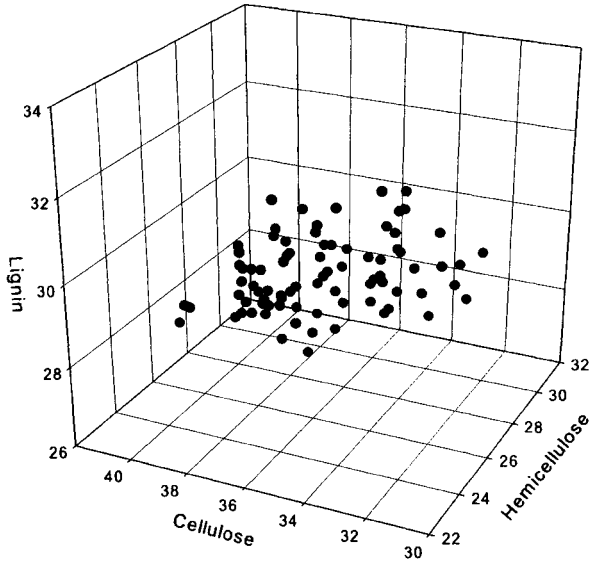


Fig. 2 3D plot of cellulose, hemicellulose, and lignin components for all the 1999 progeny and reference clones analyzed

building a breeding collection at SUNY-ESF, genetically diverse individuals were collected throughout the mid-western and northeastern USA, in addition to accessions from Japan, China, Ukraine, Sweden, and Canada. The range of cellulose, hemicellulose, and lignin content observed here may be an indication of the genetic diversity present in the various clones and will be very beneficial for future breeding efforts.

In the four largest families of the 1999 progeny, significant differences were observed in cellulose and hemicellulose content among siblings in each family (Table 1; Fig. 3; family 9970 data not shown). Significant differences in lignin composition were observed only in families 99217 and 99239 (Fig. 3). Families 9970, 99202, and 99217 are the result of interspecific hybridization, while family 99239 is the result of an intraspecific cross of *S. purpurea*. The siblings of the intraspecific cross displayed the greatest variability, compared with the siblings of the three interspecific hybrids. Kopp et al. [17] have shown that there can be great variability in seedling height growth among individuals produced from an intraspecfic cross of *S. eriocephala*. The variability among the progeny of intraspecific crosses is interesting in light of genetic studies of *Populus* spp. utilizing extensive amplified fragment length polymorphism analyses that have shown that interspecific variability is significantly greater than intraspecific variability [18, 19].

The willow biomass samples collected 1 year after coppice had significantly greater lignin content and lower cellulose content than the samples collected 3 years after coppice. The mean lignin content for the third-year samples was 29.5%, compared to a mean lignin content of 31.7% for the first-year samples, with the highest mean lignin content for a clone of more than 35% (data not shown). Samples were collected from the reference clones SV1, SX61, SX64, and SX67 after one season and three seasons postcoppice. The differences in composition based on stem age are shown in Fig. 4. Cellulose content was significantly lower in the 1-year-old growth compared to the 3-year-old growth. Inversely, lignin content was significantly higher in the younger growth. Hemicellulose appeared to be unaffected by the difference in years. Lignin content in bark is greater than that of wood [20, 21]; therefore, the greater lignin content in 1-year-old biomass may be due to greater bark content as a result of smaller stem diameters. Analyses with hybrid poplar clones have

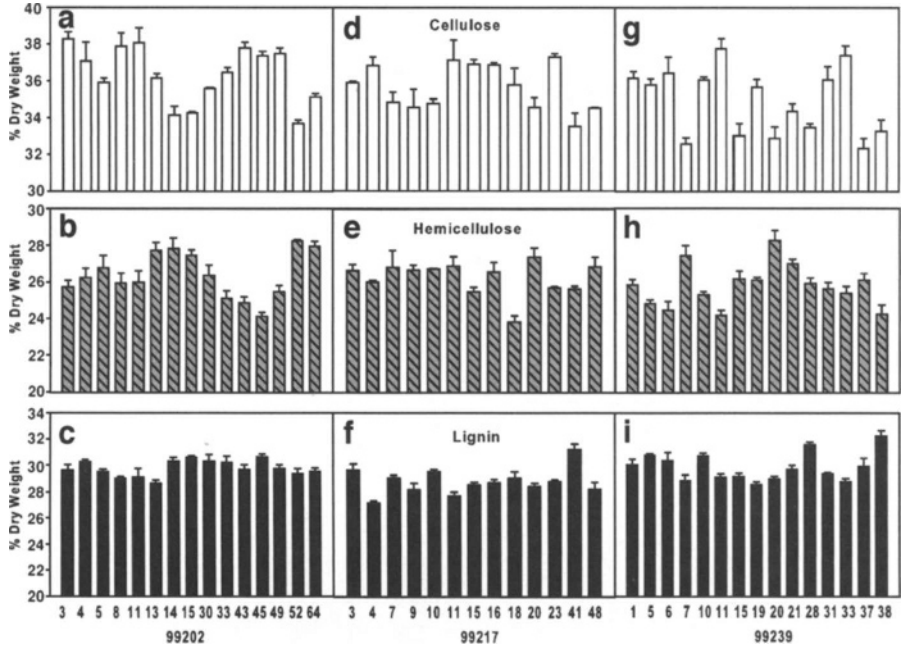


Fig. 3 Cellulose, hemicellulose, and lignin content of progeny in families 99202 (**a–c**), 99217 (**d–f**), and 99239 (**g–i**). *Bars* indicate mean±SE of three experimental replicates, each of which was analyzed using three instrumental replicates. *X*-Axis indicates the clone IDs for specific progeny individuals in each family

shown that lignin content of bark can be two times greater than that of the wood [20]. In 5-year-old stems from shrub willow stands in Sweden, bark represents approximately 19% of the total biomass. Small-diameter stems had a higher bark-to-wood ratio, and stems larger than 55 mm had a constant bark-to-wood ratio [22]. One-year-old twigs had bark content reaching 54% of the total biomass, compared to 18–27% for older stems [22]. Further analysis of bark content would be required to determine the impact of bark on the overall biomass composition of these clones.

The other analytical methods involving biomass composition that are currently in development (FT-IR, NIR, and pyMBMS) are able to resolve and quantify individual sugar composition. This is not possible with HR-TGA; however, in conjunction with ^{1}H nuclear magnetic resonance (NMR), sugar residues can be identified, and their abundance can be determined. Carbohydrate compositional profiles of lignocellulosic biomass can be accurately quantified based on the 600 MHz ^{1}H-NMR spectrum of unpurified acid hydrolyzates wherein the hemicellulose and cellulose fractions of biomass have been reduced to a mixture of sugars in acidic solution [23].

Conclusions

Preliminary HR-TGA analysis has shown that this technique can be used to identify compositional differences in shrub willow stem biomass among high-yielding clones selected in the breeding program at SUNY-ESF. To further refine this technique, a set of rigorously characterized reference biomass samples of shrub willow clones representing a

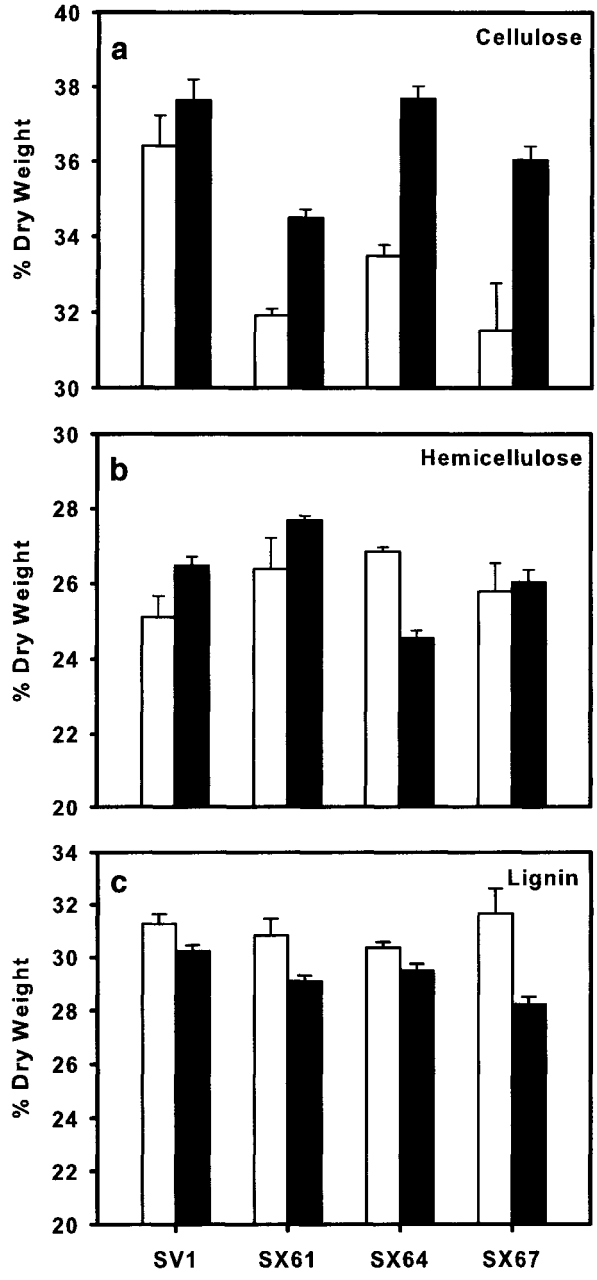


Fig. 4 Cellulose (**a**), hemicellulose (**b**), and lignin (**c**) content of different aged biomass samples from the reference clones. *White bars* represent 1 year growth after coppice; *black bars* represent 3-year growth after coppice. *Bars* indicate the mean±SE of three experimental replicates, each of which was analyzed using three instrumental replicates

range of varying compositions are being used to develop a neural network tool that will reliably and accurately interpret HR-TGA thermograms of unknown samples. HR-TGA in combination with ^{1}H-NMR can be a powerful, high-throughput tool used to identify unique compositional features in shrub willow and improve selection in the breeding program.

Acknowledgments This work was funded by the McIntire–Stennis Cooperative Forestry Research Program of the US Department of Agriculture. The authors would also like to acknowledge funding of the willow breeding program at SUNY-ESF from the New York State Energy Research and Development Authority (NYSERDA). Appreciation is also expressed to Dr. Larry Abrahamson, Dr. Tim Volk, Dr. Ed White, and Dr. Bill Winter for their support and advice as collaborators with this research and to Mark Appleby and Ken Burns for excellent technical support.

References

1. Perlack, R. D., Wright, L. L., Turhollow, A., Graham, R., Stokes, B., & Erbach, D. (2005). *Tech. Rep. ORNL/TM-2005/66*. Oak Ridge, TN: Oak Ridge National Laboratory.
2. Volk, T. A., Verwijst, T., Tharakan, P. J., Abrahamson, L. P., & White, E. H. (2004). *Frontiers in Ecology and the Environment, 2*, 411–418.
3. Volk, T. A., Abrahamson, L. P., Nowak, C. A., Smart, L. B., Tharakan, P. J., & White, E. H. (2006). *Biomass and Bioenergy, 30*, 715–727.
4. Smart, L. B., Volk, T. A., Lin, J., Kopp, R. F., Phillips, I. S., Cameron, K. D., et al. (2005). *Unasylva, 221*(56), 51–55.
5. Kopp, R. F., Smart, L. B., Maynard, C. A., Isebrands, J. G., Tuskan, G. A., & Abrahamson, L. P. (2001). *The Forestry Chronicle, 77*, 287–292.
6. Argus, G. W. (1997). *Infrageneric classification of Salix (Salicaceae) in the New World*. Ann Arbor, MI: The American Society of Plant Taxonomists.
7. Kopp, R. F. (2000). Ph.D. thesis, State University of New York College of Environmental Science and Forestry.
8. Himmel, M. E., Ding, S. Y., Johnson, D. - K., Adney, W. S., Nimlos, M. R., Brady, J. W., et al. (2007). *Science, 315*, 804–807.
9. US DOE (2006). *US Department of Energy Office of Science and Office of Energy efficiency and renewable energy*. Available at: doegenomestolife.org/biofuels/.
10. Labbe, N., Rials, T. G., Kelley, S. S., Cheng, Z. - M., Kim, J. - Y., & Li, Y. (2005). *Wood Science and Technology, 39*, 61 77.
11. Hames, B. R., Thomas, S. R., Sluiter, A. D., Roth, C. J., & Templeton, D. W. (2003). *Applied Biochemistry and Biotechnology, 105*, 5–16.
12. Kelley, S., Rials, T., Snell, R., Groom, L., & Sluiter, A. (2004). *Wood Science and Technology, 38*, 257–276.
13. Tuskan, G. A., West, D., Bradshaw, H. D., Neale, D., Sewell, M., Wheeler, N., et al. (1999). *Applied Biochemistry and Biotechnology, 77*, 55–65.
14. Shafizadeh, F., & Chin, P. P. S. (1977). In I. S. Goldstein (Ed.) *Wood technology: Chemical aspects* (vol. *43*, pp. 57–81). Washington, DC: American Chemical Society Symposium Series.
15. Cozzani, V., Lucchesti, A., Stoppato, G., & Maschio, G. (1997). *Canadian Journal of Chemical Engineering, 75*, 127–133.
16. Stipanovic, A. J., Goodrich, J., & Hennessy, P. (2004). In *American Chemical Society Symposium on "Novel Analytical Tools in the Characterization of Polysaccharides"*. Cellulose and Renewable Materials Division.
17. Kopp, R. F., Smart, L. B., Maynard, C., Tuskan, G., & Abrahamson, L. P. (2002). *Theoretical and Applied Genetics, 105*, 106–112.
18. Cervera, M. T., Remington, D., Frigerio, J. - M., Storme, V., Ivens, B., Boerjan, W., et al. (2000). *Canadian Journal of Forest Research, 30*, 1608–1616.
19. Cervera, M. T., Storme, V., Soto, A., Ivens, B., Van Montagu, M., Rajora, O. P., et al. (2005). *Theoretical and Applied Genetics, 111*, 1440–1456.
20. Blankenhorn, P. R., Bowersox, T. W., Kuklewski, K. M., Stimely, G. L., & Murphy, W. K. (1985). *Wood and Fiber Science, 17*, 148–158.
21. Kenney, W. A., Gambles, R. L., & Sennerby-Forsse, L. (1992). In C. Mitchell, J. Forb-Robertson, T. Hinckley, & L. Sennerby-Forsse (Eds.) *Ecophysiology of short rotation forest crops* pp. 267–284. Elsevier: Essex, England.
22. Adler, A., Verwijst, T., & Aronsson, P. (2005). *Biomass and Bioenergy, 29*, 102–113.
23. Kiemle, D. J., Stipanovic, A. J., & Mayo, K. E. (2004). In P. Gatenholm, & M. Tenkanen (Eds.), *ACS Symposium Series 864* pp. 122–139. Washington, DC: American Chemical Society.

Appl Biochem Biotechnol (2008) 145:13–21
DOI 10.1007/s12010-007-8041-y

Assessment of Bermudagrass and Bunch Grasses as Feedstock for Conversion to Ethanol

William F. Anderson · Bruce S. Dien · Sarah K. Brandon · Joy Doran Peterson

Received: 7 May 2007 / Accepted: 4 September 2007 /
Published online: 27 November 2007
© Humana Press Inc. 2007

Abstract Research is needed to allow more efficient processing of lignocellulose from abundant plant biomass resources for production to fuel ethanol at lower costs. Potential dedicated feedstock species vary in degrees of recalcitrance to ethanol processing. The standard dilute acid hydrolysis pretreatment followed by simultaneous sacharification and fermentation (SSF) was performed on leaf and stem material from three grasses: giant reed (*Arundo donax* L.), napiergrass (*Pennisetum purpureum* Schumach.), and bermudagrass (*Cynodon* spp). In a separate study, napiergrass, and bermudagrass whole samples were pretreated with esterase and cellulose before fermentation. Conversion via SSF was greatest with two bermudagrass cultivars (140 and 122 mg g^{-1} of biomass) followed by leaves of two napiergrass genotypes (107 and 97 mg g^{-1}) and two giant reed clones (109 and 85 mg g^{-1}). Variability existed among bermudagrass cultivars for conversion to ethanol after esterase and cellulase treatments, with Tifton 85 (289 mg g) and Coastcross II (284 mg g^{-1}) being superior to Coastal (247 mg g^{-1}) and Tifton 44 (245 mg g^{-1}). Results suggest that ethanol yields vary significantly for feedstocks by species and within species and that genetic breeding for improved feedstocks should be possible.

Keywords Biomass · Bioethanol · Bermudagrass · Energy crops

W. F. Anderson
Coastal Plain Experiment Station, ARS-USDA, Tifton, GA, USA

B. S. Dien
NCAUR, ARS-USDA, Peoria, IL, USA

S. K. Brandon · J. D. Peterson
Department of Microbiology, University of Georgia, Athens, GA, USA

W. F. Anderson (✉)
Crop Genetics and Breeding Research Unit, USDA/ARS, P.O. Box 748, Tifton, GA 31793, USA
e-mail: Bill.Anderson@ars.usda.gov

Introduction

Among the perennial grass species that have been cited as potential feedstocks for production in the Southeast are giant reed (*Arundo donax* L.), napiergrass (*Pennisetum purpureum* Schumach.) and bermudagrass (*Cynodon* spp), which have all shown superior dry matter yields compared to switchgrass. Each has potential production advantages and disadvantages for the Southeast.

In Southeastern United States, a significant portion of arable land is planted in pasture grasses with the most widely grown being bermudagrass. In addition to being popular as a forage crop, bermudagrass has the benefit of having preexisting cultivars specifically bred for increased rumen digestibility. Work on forage rumen digestibility has suggested that the binding of aromatic components to cell wall carbohydrates inhibits enzymatic release of sugars and are found within the more recalcitrant tissues of plants [1]. Lignocelluloses vary in the amount and type of aromatics responsible for recalcitrance; some materials are virtually nonconvertible, i.e., highly lignified, while others are only esterified with phenolic acids and can be modified to provide available carbohydrates [2]. Phenolic acids that occur within grass cell walls (*p*-coumaric and ferulic acids [2]) are associated with lignin, and because they are recalcitrant to biodegradation [3, 4], they serve as a barrier for releasing sugars for subsequent ethanol fermentation [5].

In some cultivars of bermudagrass bred for high digestibility (e.g., Coastcross-1), the level of ester-linked phenolics have been found to be reduced within specific cell wall tissues compared to the parents [6]. Prior studies indicate a negative relationship between both ester- and ether-linked ferulic acid concentrations and extent of digestibility among bermudagrass cultivars [7]. The ferulic acid linkages between lignin and cell wall polysaccharides impede microbial break down of cell walls [8]. Alternatively, in highly digestible bermudagrass Tifton 85, the ratio of ether- to ester-linked phenolic acids has been lowered, resulting in improved bioconversion [9, 10]. Ruminal bacteria and fungi produce enzymes that can break the ferulate ester, but none are able to break the tougher ether linkage. It would be of interest to discover if these same ligno-cellulosic linkages also have a direct effect on enzymatic conversion of biomass to sugars in a biorefinery setting.

Napiergrass has value as feedstock for biomass in Southern United States because of high dry matter yields. In a test at Tifton, Georgia, napiergrass (var. Merkeron) (27,764 kg ha^{-1}) out-yielded Tifton 85 bermudagrass (17,578 kg ha^{-1}) and Alamo switchgrass (16,220 kg ha^{-1}) [11]. Yields of napiergrass lines tested in southern and central Florida, grown on a range of soil and cultural practices including sewage effluent and phosphate mining sites, were between 30,000 and 60,000 kg ha^{-1} $year^{-1}$ [12]. Napiergrass yields in northern areas of the South have ranged from the 20,000 to 30,000 kg ha^{-1} $year^{-1}$ [13]. Other data also supports the observation that napiergrass produces more dry matter than other grasses or legumes [14]. It grows in bamboo-like clumps and may reach 7 m in height. The species is well adapted to soil conditions ranging from low fertility acid soils to slightly alkaline and has good drought tolerance due to its deep fibrous root system [15]. Photosynthetic efficiency and water use efficiency of napiergrass is higher than other crops, including giant reed. These traits could lead to much higher sustainable yields than already attained, reducing acreage needed for biomass feedstocks and reducing transport costs. Giant reed has also been identified as a prime biomass source for fuel and an alternative crop for paper/pulp or wood substitutes. The high yield potential and low input demands of giant reed make it an attractive biomass crop [16].

Little is known on the comparative conversion efficiency of these feedstocks to ethanol via saccharification and fermentation. The objectives of this study were to: (1) compare leaf

and stem material from the three grasses for ethanol production via simultaneous saccharification and fermentation (SSF), and (2) better elucidate the differences between bermudagrass genotypes and napiergrass when fermented with pretreatment enzymes.

Methods and Materials

Study 1: Three Species Comparison

Plant Material Preparation

Mature plant samples of three potential dedicated bioenergy feedstock crops were harvested for evaluation of cell wall characteristics. Three stem samples each of clonal collections from Cicily and Fitzgerald, GA of giant reed (*Arundo donax* L.) and genotypes Merkeron and N190 of napiergrass (*Pennisetum purpureum* Schumach.) were harvested from nursery plots grown at Tifton, GA. on November 1, 2004 after a full season of growth. Samples were cut with a knife at 20 cm from ground level. Three samples each of Coastal and Tifton 85 bermudagrass were harvested by hand scissors on November 1, 2004 from nursery plots that had been staged by cutting to 10 cm on August 9, 2004. Leaves were separated from stems for all samples, and weighed. Samples were then dried, weighed, and ground with a Wiley mill and filtered through a 1-mm screen before analyses.

Digestibility and Fiber Analyses

Ground leaf and stem samples of bermudagrass, napiergrass, and giant reed were subjected to *in vitro* dry matter digestibility (IVDMD) as described by Tilley and Terry [17]. Neutral detergent fiber (NDF), acid detergent fiber (ADF), and acid detergent lignin (ADL) were determined sequentially [18] using the Ankom filter bag (Ankom Technology Corp., Fairport, NY) method [19] and sulfuric acid.

Saccharification and Fermentation

Each leaf and stem sample was pretreated and converted to ethanol by SSF in triplicate. Dry weights were determined by drying at 105°C. Samples (1.5 g, dry basis) were mixed in 25 ml Corning bottles with 1.75% *w/v* sulfuric acid (8.5 ml) and treated at 121°C for 1 h. Bottles were then cooled to room temperature and neutralized by adding 1.2 ml sterile 10% *w/v* $Ca(OH)_2$ solution—$Ca(OH)_2$ was kept in suspension during additions by stirring- and 0.55 sodium citrate buffer (1 M, pH 4.5). Further nutrients were supplied by adding 1.1 ml 10× yeast–peptone (200 g/l peptone, 100 g/l yeast extract). Enzyme loadings consisted of 5 FPU GC 220 cellulase/g biomass, and 12 U Novozyme 188 cellobiase/g biomass. The bottles were finally inoculated with *Saccharomyces cerevisiae* D5A. The inoculum was prepared by transferring the yeast from a glycerol culture stored at −80°C to YPD plates (10 g/l yeast extract, 20 g/l peptone, 20 g/l glucose, and 20 g/l agar to solidify), then transferring it to 10 ml YPD at 3°C. It was transferred 18 h later to 25 ml YPD supplemented with 50 g/l glucose at 35°C and allowed to grow for an additional 18 h before being concentrated to an optical density (OD) A600nm=50 in 1× diluent (8.5 g NaCl, 0.3 g anhydrous KH_2PO_4, 0.6 g anhydrous Na_2HPO_4, 0.4 g peptone/l). The yeast was added in the fermentation culture to a final optical density (600 nm, OD) of 0.5,

approximately 0.11 ml/bottle. Bottles were incubated at 35°C with 150 rpm mixing. Bottles were fitted with septa-lined caps and vented with inserted needles for CO_2 exhaust. Fermentations were sampled after 72 h for ethanol and remaining sugars, which were measured by high performance liquid chromatography (HPLC). Samples were analyzed for sugars and acids using a SpectraSYSTEM liquid chromatography system (Thermo Finnigan, San Jose, CA) equipped with an organic acid column (Aminex HPX-87H Column, 300×7.8 mm, Bio-Rad Laboratories, Inc, Hercules, CA) and a refractive index detector (RI-150, Thermo Finnigan).

Study 2: Bermudagrass and Napiergrass Comparison

Plant Material Preparation

Bermudagrass (var. Tifton 85, Tifton 44, Coastal and Coastcross II) and napiergrass (var. Merkeron) plots were fertilized with 225 kg ha^{-1} 5:10:15 (N, P_2O_5, K_2O) on March 10, 2004, then staged on July 20, 2006 by mowing bermudagrass plots to 10 cm napiergrass plots to 20 cm. After 4 weeks, bermudagrass plots were mowed to 10 cm to obtain 4-week old samples. On September 14, 2004 the plots were cut at 10 cm for bermudagrass and 20 cm for napiergrass. Two random samples of cut grass from each variety/age plot were gathered and weighed immediately after cutting. The grass samples were weighed wet before drying in an oven set at 40°C. The dry samples were weighed and ground with a Wiley mill using a 1-mm screen (20 mesh). Ground samples were subjected to enzyme pretreatment.

Whole ground plant material (0.5 g dry weight per tube in triplicate) from 4-week-old bermudagrass and 8-week-old napiergrass samples were incubated with 1.0 g/tube (4,393 IU/g) of Depol 740 l in buffer essentially as previously described [5]. The esterase-treated material was centrifuged, and the supernatant removed and frozen for subsequent chemical analysis. The residue was dried, weighed, and then incubated with similarly buffered cellulase (Sigma C-8546) at 400 IU/tube for 72 h. Samples were stored at −80°C until use in fermentations.

Fermentation Protocol

The inoculum was prepared by transferring *Escherichia coli* LY01 [20, 21] from a glycerol culture stored at −80 °C to Luria Bertani (LB) plates (Fisher Scientific, Fair Lawn, New Jersey) with an additional 20 g/l glucose and 40 mg/l chloramphenicol. Plates were incubated at 35 °C for 18 h. A single colony was transferred to 50 ml LB supplemented with 50 g/l glucose and 40 mg/l chloramphenicol at 35 °C and incubated for 18 h. Bacteria were added in the fermentation culture to a final optical density (550 nm, OD) of 1.0 [22]. To increase sugar concentration for fermentation, the esterase-treated samples were combined with the cellulase-treated samples for fermentations in 125 ml Erlenmeyer flasks with caps. Flasks were autoclaved to reduce potential contamination during fermentation. Filter sterilized Spezyme® CP (4.8 FPU) was added to the fermentations, and flasks were incubated in a shaking water bath (100 rpm) at 35 °C for 24 h. Samples were taken at 0 and 24 h. These were filtered (Spin-X® Centrifuge Tube Filter 0.22 μm) and then analyzed by gas chromatography (Shimadzu GC-8A, Inj/Dec 250 °C, Column 65 °C, 30 m, ID 0.53 mm, Film 3 μm) with 2.0% isopropanol as an internal standard essentially as previously described [22]. Values presented were corrected for ethanol contributions from enzymes containing sugar stabilizers and from media components.

Monosaccharide and Phenolic Acid Determination

Monosaccharides were measured by adding 0.2 ml of the enzyme supernatant and 0.2 ml of a standard solution of inositol in a 2-ml vial. The solution was freeze dried and the simple sugars measured as their silyl ethers by GCL using DMF as the solvent and Sylon BTZ (Supelco, Bellefonte, PA) (*N,O*-Bis(trimethylsilyl)acetamide, Trimethylsilylimidazole, Trimethylchlorosilane, 3:2:3) as the derivatizing reagent. Phenolic acids were measured by GLC as their silyl ethers using *N,O*,bis(trimethylsilyl) trifloroacetamide (BSTFA) as previously described [23].

All data was analyzed statistically using PROC GLM [24] for comparisons among plant material and PROC CORR for correlations among traits.

Results

In vitro dry matter digestibility (IVDMD) of leaves was much higher than for stems except in the case of bermudagrass (Table 1). Neutral detergent fiber (NDF) generally correlated with digestibility as measured by IDVMD. The acid detergent fiber (ADF) of the napiergrass and giant reed leaves and both bermudagrass plant components was significantly different from the woody stem tissue of napiergrass and giant reed. This leaf/stem differentiation was also reflected in results of acid detergent lignin (ADL). In general, ethanol production correlated most closely with ADL (r=−0.78, p<0.0001), with IVDMD (r=0.64, p=0.0001), and with ADF (r=−0.62, p=0.0004).

The most efficient conversion of biomass to ethanol was with leaves and stems of bermudagrass (Table 1). Next, the leaves of the bunch grasses, napiergrass and giant reed, produced the greatest ethanol yields by SSF. Merkeron napiergrass stems also digested well. Tifton 85 plant parts produced significantly more ethanol than Coastal bermudagrass, which is consistent with digestibility data. Substantial sugar remained after 72 h of fermentation (102 g mg^{-1}) for stems of the Cicily giant reed (*Arundo donax*) clone compared to the other samples. The stem of the Fitzgerald clone of giant reed had similar

Table 1 *In vitro* dry matter digestibility (IVDMD), neutral detergent fiber (NDF), acid detergent fiber (ADF), acid detergent lignin (ADL), and ethanol production of leaf and stem tissues of 12-week-old bermudagrass (*Cynodon* sp.), mature napiergrass (*Pennisetum purpureum*) and giant reed (*Arundo donax*) grown at Tifton, GA. 2004.

Species	Genotype	Tissue	% IVDMD[a]	NDF[a]	ADF[a]	ADL[a]	Ethanol mg/g[a]
Cynodon sp.	Tifton 85	Leaf	47.1 c	77.6 g	35.0 abc	2.93 a	139.6 a
Cynodon sp.	Tifton 85	Stem	49.2 c	77.5 g	37.2 cd	4.04 b	141.1 a
Cynodon sp.	Coastal	Leaf	35.4 e	77.0 fg	33.7 ab	3.85 b	121.7 b
Arundo donax	Cicily	Leaf	54.1 b	67.6 ab	36.7 bcd	3.82 b	109.0 bc
Pennisetum purpureum	Merkeron	Leaf	58.5 a	69.4 bc	36.0 abcd	3.04 a	106.7 bc
Pennisetum purpureum	Merkeron	Stem	43.5 d	74.2 def	48.1 ef	6.95 c	105.3 c
Pennisetum purpureum	N 190	Leaf	46.8 c	73.0 de	38.3 d	3.53 ab	96.7 cd
Arundo donax	Fitzgerald	Leaf	52.4 b	65.5 a	33.7 a	4.14 b	84.8 d
Pennisetum purpureum	N 190	Stem	35.9 e	74.1 def	49.1 f	7.90 d	84.0 d
Arundo donax	Fitzgerald	Stem	22.6 g	75.4 efg	49.9 f	8.98 e	47.2 e
Arundo donax	Cicily	Stem	29.0 f	71.9 cd	45.9 e	8.67 e	44.2 e

[a] Means with the same letter are not significantly different (p=0.05).

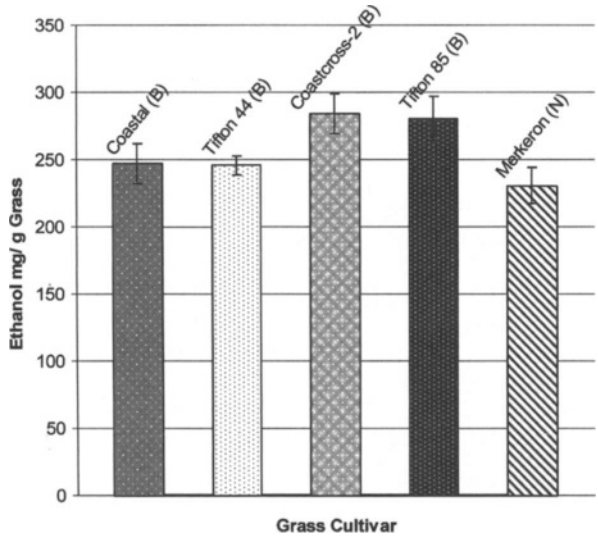


Fig. 1 Ethanol yields (mg/g grass) of 4-week-old bermudagrass cultivars and 8-week-old Merkeron napiergrass harvested at Tifton, GA 2004 and fermented by *Escherichia coli* strain LY01 after pretreatment with esterase and cellulase for 24 h

ethanol yields but much less residual sugar (21.7 mg g^{-1}). Released glucose from leaves of all species was almost completely converted to ethanol as observed by the low residual glucose (2 mg g^{-1}). Inhibitory compounds may be present in giant reed stems, and to a lesser extent, in napiergrass stems. Xylan-associated monosaccharides were equally released during pretreatment of all samples (average of 201 mg g^{-1}), which represents potential increases in ethanol production with xylose-fermenting *Saccharomyces*.

Tifton 85 and Coastcross II yielded the highest amounts of ethanol after enzyme treatment with esterase and cellulase (Fig. 1). These cultivars also had the highest concentrations of glucose after enzymatic pretreatments (Table 2). Pretreatment of Merkeron napiergrass resulted in the greatest dry weight loss. Much of that loss may have been due to hemicellulose as evidenced by the higher yields of xylose, which is the major component of hemicellulose in grasses. Although the Merkeron napiergrass sugar release

Table 2 Percent dry weight (DW) loss, ferulic acid, *para*-coumaric acid, and free sugars released in filtrate after pretreatments with commercial esterase and cellulase for bermudagrass (B) at 4 weeks and napiergrass (N) genotypes at 8 weeks of age[a].

Genotype	Age[b] (weeks)	Percent DW loss (%)	Ferulic acid (mg/g)	P-Coumaric acid (mg/g)	Xylose (mg/g)	Glucose (mg/g)
Coastal (B)	4	33.1 de	0.44±0.04	0.31±0.01	4.7±0.1	84.0±4.7
Tifton 85 (B)	4	41.8 b	0.64±0.02	0.46±0.01	9.2±0.4	112.2±2.0
Tifton 44 (B)	4	32.2 e	0.51±0.11	0.37±0.04	5.5±2.5	78.5±3.8
CC II (B)	4	38.5 c	0.44±0.03	0.30±0.01	6.1±0.1	112.9±4.1
Merkeron (N)	8	55.4 a	0.74±0.10	0.47±0.10	12.7±5.0	91.6±13.8

[a] Values are the sum of subsequent incubations with esterase for 24 h and then cellulase for 72 h

[b] Plant age in weeks of regrowth

was greater than that of Coastal and Tifton 44, the ethanol production was the lowest of the five cultivars tested.

Discussion

The results indicate that bermudagrass would be a superior feedstock for conversion to ethanol via saccharification and fermentation. Under normal harvest procedures, bermudagrass is cut, dried, and baled for hay at maturities of between 4 and 5 weeks. The quality is much better at that time with IVDMD of 60% or better for Tifton 85 [9]. Even at 12 weeks of age and at IVDVD levels of 47%, the observed ethanol yield was much better than observed for napiergrass or giant reed leaves. Superior dry matter yield is not the only aspect to consider when assessing species as potential bioenergy crops in the Southeast. Bermudagrass has the advantage of being an established crop. Growers of bermudagrass hay thus would have an alternative market for hay. If fields cannot be cut in a timely manner for animal forage, older hay would have sufficient quality to be used in an ethanol plant. The ethanol yields from napiergrass and giant reed leaves are comparable to switchgrass (Dien, personal communication); however, stem material is not conducive to fermentation at full maturity when applying a low severity pretreatment (Table 1) and stem made up the majority of the dry matter for giant reed (83%) and napiergrass (59%). The stems would require a harsher pretreatment or may be better suited for thermo-chemical conversion to biofuels. Eight-week-old whole napiergrass (leaves and stems) appears suitable as a feedstock for fermentation (Table 2) under a two or three harvest per year management system.

Bermudagrass yielded more ethanol compared to napiergrass with both the dilute acid pretreatment and enzymatic pretreatments. There appears to be significant enough variation among bermudagrass cultivars (Fig. 1) to warrant breeding and selection for improved cultivars for the biofuels industry. In a previous study, bermudagrasses and napiergrass were treated with esterase alone and the resulting sugars fermented to ethanol. Tifton 85 yielded the most ethanol, followed by Coastcross II, Tifton 44, and Coastal bermudagrass. Ethanol production from napiergrass was lowest of the five grass cultivars tested [5]. The solids were recovered, dried, then treated with cellulase and a second, separate, sugar stream fermented to ethanol. Because of the small volumes of material and the dilute sugar concentrations, the amount of ethanol produced in each individual stream was low. In this study, the grasses were treated with esterase followed by cellulase; however, the samples were combined, and washing steps were reduced in an effort to keep the sugar stream more concentrated. Adding esterases and cellulases together in one pretreatment was not as effective as sequential treatments (data not shown), presumably due to inhibition of the cellulases by the phenolics released by the esterases. The combined sugar streams in buffer were autoclaved to prevent microbial contaminant interference with sugar fermentation to ethanol. Regardless of the differences in protocols, the same hierarchy of performance was observed with Tifton 85 and Coastcross II producing more ethanol than Tifton 44 and Coastal for the bermudagrasses and Merkeron napiergrass producing the least amount of ethanol in both studies. Results from the current study illustrate greater differences in some of the cultivars than observed in the previous study [5]. Phenolic compounds, liberated during the enzyme pretreatment, are known to have an inhibitory effect on microorganisms; however, ferulic acid and para-coumaric acid concentrations alone do not explain the reduction in ethanol yield from Merkeron napiergrass. Future studies will examine this inhibition more closely and will compare fermentations with phenolics removed before inoculation.

Overall ethanol yields were much higher in the second study which used enzymatic pretreatments. Bermudagrass and napiergrass plant samples were much less mature in the second study, but more importantly, fermentation was enhanced by using *Escherichia coli* strain LY01, which converts xylan sugars and the glucans. *Saccharomyces cerevisiae* D5A that was used in the first study does not ferment xylans. Ethanol yields were brought closer to maximization by combining the esterase–cellulase pretreatment of younger plant material and the more efficient fermenting agent.

The significant correlation between IVDMD for forage and ethanol production in these results indicate that breeding for improved forage quality via IVDMD may be sufficient for selection of improved feedstock for ethanol. More work is required to determine whether selecting for lignin content or ADL would be an effective indirect method of measuring for conversion efficiency.

In conclusion, bermudagrass appears to be a viable feedstock for ethanol. Leaves of the bunchgrasses napiergrass and giant reed have potential as feedstock through fermentation; however, due to the high stem to leaf ratio of giant reed, it would be more suited to thermochemical conversion. Sufficient genetic variability among bermudagrass lines should allow for improvement in ethanol yields through breeding.

Acknowledgements Enzymatically pretreated materials were supplied by Dr. Danny E. Akin; sugarand phenolic acid data were provided by W. Herbert Morrison III.

References

1. Grabber, J. H. (2005). *Crop Science, 45*, 820–831.
2. Hartley, R. D., & Ford, C. W. (1989). In N. G. Lewis & M. G. Paice (Eds.), *Plant cell wall polymers: Biogenesis and biodegradation* (pp. 137–145). Washington, D.C., American Chemical Society.
3. Akin, D. E. (1989). *Agronomy Journal, 81*, 17–25.
4. Akin, D. E., & Chesson, A. (1989). *Proceedings of the International Grassland Congress, 16*, 1753–1760.
5. Anderson, W. F., Peterson, J., Akin, D. E., & Morrison, W. H. III. (2005). *Applied Biochemistry and Biotechnology, 121–124*, 303–310.
6. Akin, D. E., Ames-Gottfried, N., Hartley, R. D., Fulcher, R. D., & Rigsby L. L. (1990). *Crop Science, 30*, 396–401.
7. Hill, G. M., Gates, R. N., West, J. W., Watson, R. S. & Mullinix, B. G. (2001). *Journal of Animal Science, 79*(1), 235.
8. Jung, H. G., & Allen, M. S. (1995). *Journal of Animal Science, 73*, 2774–2790.
9. Burton, G. W., Gates, R. N., & Hill, G. M. (1993). *Crop Science, 33*, 644–645.
10. Mandedebvu, P., West, J. W., Hill, G. M., Gates, R. N., Hatfield, R. D., Mullinix, B. G., et al. (1999). *Journal of Animal Science, 77*, 1572–1586.
11. Bouton J. (2002). In *Bioenergy crop breeding and production research in the southeast*, ORNL/SUB-02-19XSV810C/01.
12. Prine, G. M., Stricker, J. A. & McConnell, W. V. (1997), *Proc. 3rd Biomass Conference of the America: Making a Business from Biomass in Energy, Environment, Chemicals, Fibers and Materials, 1*, 227–235.
13. Prine, G. M., Mislevy, P. ,Stanley, R. L., Jr., Dunavin, L. S. & Bransby,D. I.. (1991). In D. L. Klass (Ed.), *Proc. final program of conference on energy from biomass and wastes XV.* Paper No. 24, 8p.
14. Vincente-Chandler, J., Abruna, F., Caso-Costas, R., Figarella, J., Silva, S., & Pearson, R. (1974). *University of Puerto Rico Bulletin*, 233.
15. Hanna, W. W., Chaparro, C. J., Mathews, B. W., Burns, J. C., & Sollenberger, L. E. (2004). In L. E. Moser, B. L. Burson, & L. E. Sollenberger (Eds.), *American society of agronomy monograph series* (pp. 503–535). Madison, WI: American Society of Agronomy.
16. Lewandowski, I., Scurlock, J. M. O., Lindvall, E., & Christou, M. (2003). *Biomass and Bioenergy, 25*, 335–361.
17. Tilley, J. M. A & Terry, R. A. (1963). *Journal of the British Grassland Society, 18*, 104–111.

18. Van Soest, P. J., Robertson, J. B., & Lewis, B. A. (1991). *Journal of Dairy Science, 74*, 3583–3597.
19. Vogel, K. P., Pederson, J. F., Masterson, S. D., & Toy, J. J. (1999). *Crop Science, 39*, 276–279.
20. Yomano, L. P., York, S. W., & Ingram, L. O. (1998). *Journal of Industrial Microbiology and Biotechnology, 20*, 132–138.
21. Gonzalez, R., Tao, H., Purvis, J. E., York, S. W., Shanmugam, K. T., & Ingram, L. O. (2003). *Biotechnology Progress, 19*, 612–623.
22. Doran, J. B., Cripe, J., Sutton, M., & Foster, B. (2000). *Applied Biochemistry and Biotechnology, 84–86*, 141–152.
23. Morrison, W. H., III, Akin, D. E., Ramaswamy, G. & Baldwin, D. (1996), *Textile Research Journal, 66*, 651–656.
24. SAS Institute. (1999). *Version 7 SAS Inst.* Cary, NC.

The use of trade, firm or corporation names in this publication is for the information and convenience of the reader. Such use does not constitute an official endorsement or approval by the U.S.D.A. of any product or service to the exclusion of others that may be suitable.

Appl Biochem Biotechnol (2008) 145:23–28
DOI 10.1007/s12010-007-8036-8

Rapid Isolation of the *Trichoderma* Strain with Higher Degrading Ability of a Filter Paper and Superior Proliferation Characteristics Using Avicel Plates and the Double-Layer Selection Medium

Hideo Toyama · Megumi Nakano · Yuuki Satake · Nobuo Toyama

Received: 22 April 2007 / Accepted: 27 August 2007 /
Published online: 11 September 2007
© Humana Press Inc. 2007

Abstract The cost of cellulase is still a problem for bioethanol production. As the cellulase of *Trichoderma reesei* is applicable for producing ethanol from cellulosic materials, the cellulase productivity of this fungus should be increased. Therefore, we attempted to develop a system to isolate the strain with higher degrading ability of a filter paper and superior proliferation characteristics among the conidia treated with the mitotic arrester, colchicine. When green mature conidia of *T. reesei* RUT C-30 were swollen, autopolyploidized, and incubated in the double-layer selection medium containing Avicel, colonies appeared on the surface earlier than the original strain. When such colonies and the original colony were incubated on the Avicel plates, strain B5, one of the colonies derived from the colchicine-treated conidia, showed superior proliferation characteristics. Moreover, when strain B5 and the original strain were compared in the filter paper degrading ability and the cellulose hydrolyzing activity, strain B5 was also superior to the original strain. It was suspected that superior proliferation characteristics of strain B5 reflects higher filter paper degrading ability. Thus, we concluded that the *Trichoderma* strain with higher degrading ability of a filter paper and superior proliferation characteristics can be isolated using Avicel plates and the double-layer selection medium.

Keywords Cellulase · Cellulose · Conidia · Nuclei · *Trichoderma* · Filter paper

The cellulolytic fungus *Trichoderma reesei* is well known to produce stable cellulase useful for saccharification of cellulose and is widely used for production of commercial cellulase [1, 2]. Fuel ethanol must be produced from cellulosic resources to prevent global warming [3]. The cellulase of this fungus is applicable for producing ethanol from cellulosic materials, but the cost is still a problem [4]. Thus, the cellulase productivity of this fungus

H. Toyama (✉) · M. Nakano · Y. Satake · N. Toyama
Minamikyushu University, Kirishima 5-1-2, Miyazaki 880-0032, Japan
e-mail: wonder@iris.dti.ne.jp

must be increased. For this purpose, a system must be developed to rapidly isolate cellulase hyperproducers of this fungus. We earlier formed autopolyploids of this fungus using polyploidizer with swollen conidium [5]. Moreover, we could develop a double-layer selection medium that can rapidly isolate the strains with higher degrading ability of crystalline cellulose [6]. However, the proliferation characteristics of the selected strains varied.

In this study, we attempted to isolate the *Trichoderma* strain with higher degrading ability of a filter paper and superior proliferation characteristics using Avicel plates and the double-layer selection medium among the conidia treated with colchicine. *Trichoderma reesei* Rut C-30 (ATCC56765) was used as a model strain [7]. The strain was incubated on potato dextrose agar (PDA) medium (BBL, Cockeysville, MD, USA) at 28°C and preserved at 4°C. PDA medium was used as the medium for conidial formation. A mycelial block (2×2 mm^2) of the original strain was placed on the center of a PDA plate and incubated for 10 days at 28°C to generate green mature conidia. The conidia were suspended in distilled water and filtered with a glass filter (3G-2 type, Iwaki Glass, Funakoshi, Tokyo, Japan) to remove hyphae. These conidia were collected by centrifugation at 5,510×*g* for conidial swelling.

The conidia were then added to the medium for conidial swelling and incubated for 6 h using a rotary shaker (TAITEC NR-30, Koshigaya, Japan) at 28°C. The agitation speed was 160 rpm. The Mandels' medium used for the basic medium consisted of $(NH_4)_2SO_4$ (Wako, Osaka, Japan), 1.4 g; KH_2PO_4 (Wako), 2.0 g; urea (Wako), 0.3 g; $CaCl_2$ (Wako), 0.3 g; $MgSO_4$ $7H_2O$ (Wako), 0.3 g; $FeSO_4$ $7H_2O$ (Wako), 0.005 g; $MnSO_4$ H_2O (Wako), 0.0016 g; $ZnSO_4$ H_2O (Wako), 0.0014 g; $CoCl_2$ (Wako), 0.0020 g; and distilled water, 1,000 mL (pH 6.0) [8]. Mandels' medium containing 1.0% (w/v) glucose (Wako) and 0.5% (w/v) peptone (Difco, Detroit, MI, USA) was used as the medium for conidial swelling.

After incubation, the swollen conidia were collected by centrifugation at 5,510×*g* and added to the medium for autopolyploidization followed by incubation for 7 days at 28°C. Mandels' medium containing 0.1% (w/v) colchicine (Wako), 1.0% (w/v) glucose, and 0.5% (w/v) peptone was used as the medium for autopolyploidization. After incubation, the medium was filtrated with a glass filter 3G-2. The treated swollen conidia in the filtrate were collected by centrifugation and washed with distilled water followed by preservation in distilled saline at 4°C.

For the double-layer selection medium, the upper-layer medium containing 100 mL of Mandels' medium containing 3.0 g Avicel (Funakoshi), 0.5 g peptone, 0.3 mL polyoxyethylene (10) octylphenylther (Triton X-100) (Wako), and 3.0 g agar (pH 6.0) was overlayed on the bottom-layer medium, which contained 100 mL of Mandels' medium containing 3.0 g Avicel, 0.5 g peptone, 0.3 mL Triton X-100, 3.0 g agar (Difco), and conidia in a deep glass plate (150 mm in diameter and 60 mm in depth) (pH 6.0), followed by incubation. Colchicine-treated swollen conidia were added to the bottom layer and left for 30 min at 4°C to harden the agar. After the agar hardened, the upper-layer selection medium was overlaid and left for 30 min at 4°C to allow the agar to harden. The treated-swollen conidia were then incubated at 28°C. The colony appearance was observed during incubation. Colonies began to appear on the surface of the medium after 4 days of incubation. After 6 days of incubation, there were many colonies on the surface, but the colony diameters varied.

Five larger colonies were selected as B1, B2, B3, B4, and B5 from the colonies appearing on the surface of the selection medium, and their growth characteristics were compared with the original strain using the Avicel medium. Two Avicel plates were used for a strain. Mandels' medium containing 1.0% (w/v) Avicel, 0.5% (w/v) peptone, 3.0% (w/v) agar, and

0.1% (v/v) Triton X-100 was used as the Avicel medium. A mycelial block (2×2 mm^2) of the original strain or the selected strains was placed on the Avicel medium and incubated for 13 days at 28°C. The colony diameter was measured by a digital caliper (Mitsutoyo, Koshigaya, Japan) to calculate the average value. It was found that the colony diameter of strain B5 was 1.56 times larger than that of the original strain, as shown in Table 1. Figure 1 shows the superior proliferation characteristics of strain B5 compared with the original strain.

The five selected strains and the original strain were compared in filter paper degrading ability. A mycelial block (2×2 mm^2) of the selected strains or the original strain was added to 50 mL of the medium for enzyme production in a 100-mL Erlenmeyer flask, followed by incubation for 5 days using a rotary shaker (TAITEC NR-30) at 28°C. The agitation speed was 160 rpm. Two flasks were used for a strain. Mandels' medium containing 1.0% (w/v) Avicel and 0.5% (w/v) peptone was used as the medium for enzyme production. After incubation, the medium was filtered with a glass filter (3G-2 type) to remove hyphae. The filtrate was used as the enzyme solution. The pH of the enzyme solution was adjusted to 5.0 using 0.1 N HCl, and the filter paper degrading ability of the filtrate was evaluated. The addition of 0.1 N HCl did not collapse the filter paper. Five milliliters of the enzyme solution and a filter paper (10×10 mm^2) (Whatman, no. 2, Maidstone, UK) were added to an L-type glass tube (120×68 mm) and incubated for 30 min at 50°C using a Monod shaker (TAITEC Monod Shaker Personal-11) at an agitation speed of 75 strokes per minute. The time of collapse of the filter paper was then measured using a digital stopwatch (Citizen, Tokyo, Japan). The term "collapse" was defined as the condition when the reaction mixture contained only fibers without fragments of a filter paper. After collapse, the reaction mixture was filtered with another filter paper (no. 2 Whatman), and the amount of reducing sugar in the filtrate was measured using 3,5-dinitrosalicylic acid (Wako) [9]. As shown in Table 2, strain B5 collapsed the filter paper within 15 min, but the original strain took 25 min. Moreover, the amount of reducing sugar in the L-type glass tube of strain B5 was over four times larger than that of the original strain. These results indicate that the filter paper degrading ability of strain B5 is over four times greater than that of the original strain.

From the above results, the cellulose hydrolyzing activity of strain B5 was compared with that of the original strain. As the substrates of enzyme reaction, 1.0 g of Avicel, CMC-Na (D.S.0.7–0.8) (Wako), or Salicin (Wako) was added to 100 mL of 0.1 M acetate buffer (pH 5.0). Two milliliters of the enzyme solution was added to 4 mL of substrate in a glass tube (185×18.5 mm) and incubated by a reciprocal shaker (THOMASTAT T-22S, Tokyo,

Table 1 The colonial diameter of the original strain and the selected strains, B1–B5.

Strains	Colonial diameter (mm)
T. reesei Rut C-30	28.32±1.03
B1	41.25±1.23
B2	34.03±1.18
B3	36.23±1.38
B4	35.41±1.05
B5	44.24±1.15

A mycelial mat (2×2 mm^2) was incubated on the Avicel medium for 13 days at 28°C. The colonial diameter was measured by a digital caliper. Two plates were used per strain.

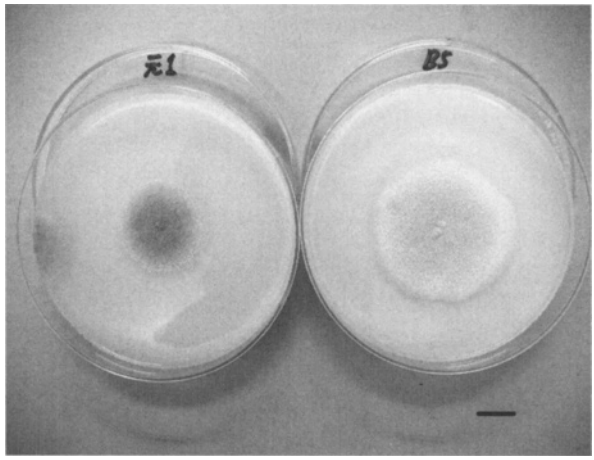


Fig. 1 Colonies of the original strain and strain B5. *Left*: *T. reesei* Rut C-30. *Right*: strain B5. Mycelial blocks (2×2 mm^2) of the original strain and strain B5 were incubated on Avicel plates for 13 days at 28°C. *Bar* indicates 1.0 cm

Japan) for 1 h at 50°C at an agitation speed of 125 strokes per minute. The glass tubes containing the Avicel substrate were tilted on the shaker and shaken by hand every 30 min to avoid the precipitation of Avicel. The reaction mixture was filtered with filter paper (Whatman, no. 2), and the amount of reducing sugar was measured using 3,5-dinitrosalicylic acid. Activity was defined as the amount of enzyme producing reducing sugar equivalent to 1 μmol of glucose per minute. Consequently, the Avicel and Salicin hydrolyzing activity of strain B5 increased by a factor of 1.4 times and 3.0 over the original strain, respectively, as shown in Table 3. The CMC-Na hydrolyzing activity of strain B5, however, was almost the same as that of the original strain. Moreover, the mycelial amount of strain B5 decreased less than that of the original strain.

We discuss here why strain B5 showed superior proliferation on an Avicel medium. Strain B5 is one of the colonies that appeared earlier on the double-layer selection medium. This suggested that strain B5 could rapidly saccharify the Avicel in the selection medium. Hence, we suspected that strain B5 possesses higher Avicel hydrolyzing ability, and the results of the measurement of enzyme activity confirmed this. Thus, we considered that strain B5 could quickly break through the selection medium containing Avicel and show superior proliferation on an Avicel medium because of its higher Avicel and Salicin

Table 2 Evaluation of degrading ability of a filter paper.

Strains	Collapse time of a filter paper (min)	Amount of reducing sugar (mg)
T. reesei Rut C-30	25	0.425
B1	22	0.975
B2	24	0.774
B3	24	0.652
B4	25	0.682
B5	15	1.730

A filter paper (10×10 mm^2) was added to 5 ml of enzyme solution in an L-type glass tube and incubated at 50°C using a Monod shaker. After 15 min of shaking, the amount of reducing sugar was measured using 3,5-dinitrosalycilic acid.

Table 3 Measurement of cellulose hydrolyzing activity.

Strains	Avicel hydrolyzing activity	CMC-Na hydrolyzing activity	Salicin hydrolyzing activity (IU/ml)	Mycelial weight (mg)
T. reesei Rut C-30	19	68	2	320
B5	26	67	6	283

A mycelial mat (2×2 mm^2) was incubated in the medium for enzyme production in a 100-ml Erlenemyer flask for 5 days at 28°C using a rotary shaker. The amount of reducing sugar was measured using 3, 5-dinitrosalicylic acid. Two flasks were used for a strain. These values are average.

hydrolyzing ability. The higher filter paper degrading ability of strain B5 also seems to be owed to its higher Avicel and Salicin hydrolyzing ability.

Next, we discuss why Avicel and Salicin hydrolyzing activity increased more than those of the original strain. In this study, unsynchronized green mature conidia were used. When such conidia were treated with colchicine, their nuclear diameter and number varied (data not shown). We consider that the cellulose hydrolyzing ability of such conidia also varies. We therefore think that strain B5 possessing higher Avicel and Salicin hydrolyzing ability was selected through the selection using the double-layer selection medium among such conidia.

The nuclear diameter and number of conidia of strain B5 were compared with those of the original strain. The diameter and number of conidia were observed using Giemsa staining after 5 N HCl treatment for 40 min at 60°C, after which, microphotographs were taken [10]. The conidia of strain B5 was mononucleate similar to the conidia of the original strain shown in Fig. 2 [11]. However, the nuclear diameter of strain B5 enlarged more than that of the original strain. From these results, strain B5 seemed to be polyploid or aneuploid. When strain B5 was incubated on an Avicel medium, no sector was segregated, which means that this strain is genetically stable and polyploid. Therefore, the increase of Avicel and Salicin hydrolyzing ability of strain B5 is suspected to be related with autopolyploidization. From these results, we conclude that the strain with higher filter paper degrading ability and superior proliferation characteristics can be rapidly selected using Avicel plates and the double-layer selection medium.

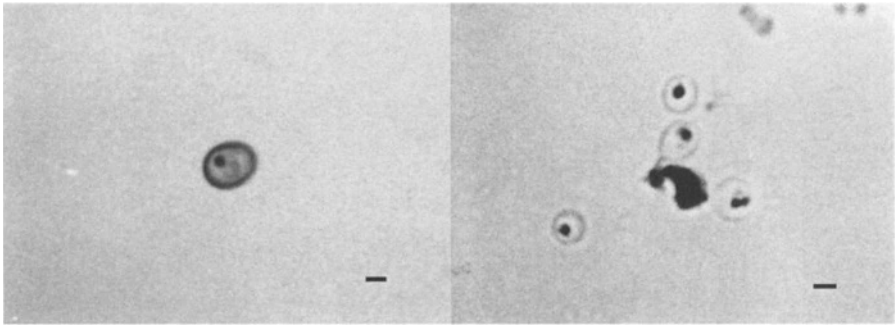


Fig. 2 Nuclear staining of the conidia derived from the original strain and strain B5. *Left*: *T. reesei* Rut C-30. *Right*: strain B5. Conidia were fixed on a slide glass by heating and treated with HCl at 60°C. After HCl treatment, conidia were washed with water followed by nuclear staining using Giemsa solution. *Bar* indicates 1.0 μm

Acknowledgments We wish to thank Tsukishima Kikai and Yakult Honsha for their cooperation.

References

1. Nevalainen, H., Suominen, P., & Taimisto, K. (1994). *Journal of Biotechnology, 37*(3), 193–200.
2. Reese, E. T., & Mandels, M. (1980). *Biotechnology and Bioengineering, 22*(2), 323–335.
3. Farrell, A. E., Plevin, R. J., Turner, B. T., Jones, A. D., O'Hare, M., & Kammen, D. M. (2006). *Science, 311*(5760), 506–508.
4. Tu, M., Chandra, R. P., & Saddler, J. N. (2007). *Biotechnology Progress, 23*(2), 398–406.
5. Toyama, H., & Toyama, N. (2000). *Applied Biochemisty and Biotechnology, 84–86*, 419–429.
6. Toyama, H., Yamagishi, N., & Toyama, N. (2002). *Applied Biochemistry and Biotechnology, 98–100*, 257–263.
7. Ghosh, A., Ghosh, B. K., Trimino-Vazquez, H., Eveleigh, D. E., & Monenecourt, B. S. (1984). *Archives of Microbiology, 140*, 126–133.
8. Mandels, M., & Sternberg, D. (1976). *Journal of Fermentation Technology, 54*, 267–286.
9. Miller, G. L. (1959). *Analytical Chemistry, 31*, 426–428.
10. Friend, K., Chen, S., & Ruddle, F. (1976). *Somatic Cell Genetics, 2*, 183–188.
11. Rosen, D., Edelman, M., Galun, E., & Danon, D. (1974). *Journal of General Mirobiology, 83*, 31–49.

Appl Biochem Biotechnol (2008) 145:29–38
DOI 10.1007/s12010-007-8105-z

A Comparison of Simple Rheological Parameters and Simulation Data for *Zymomonas mobilis* Fermentation Broths with High Substrate Loading in a 3-L Bioreactor

Byung-Hwan Um · Thomas R. Hanley

Received: 2 May 2007 / Accepted: 19 November 2007 /
Published online: 3 January 2008
© Humana Press Inc. 2007

Abstract Traditionally, as much as 80% or more of an ethanol fermentation broth is water that must be removed. This mixture is not only costly to separate but also produces a large aqueous stream that must then be disposed of or recycled. Integrative approaches to water reduction include increasing the biomass concentration during fermentation. In this paper, experimental results are presented for the rheological behavior of high-solids enzymatic cellulose hydrolysis and ethanol fermentation for biomass conversion using Solka Floc as the model feedstock. The experimental determination of the viscosity, shear stress, and shear rate relationships of the 10 to 20% slurry concentrations with constant enzyme concentrations are performed with a variable speed rotational viscometer (2.0 to 200 rpm) at 40 °C. The viscosities of enzymatic suspension observed were in range of 0.0418 to 0.0144, 0.233 to 0.0348, and 0.292 to 0.0447 Pa s for shear rates up to 100 reciprocal seconds at 10, 15, and 20% initial solids (w/v), respectively. Computational fluid dynamics analysis of bioreactor mixing demonstrates the change in bioreactor mixing with increasing biomass concentration. The portion-loading method is shown to be effective for processing high-solids slurries.

Keywords High-solids fermentation · Rheology · Bioreactors · Non-Newtonian fluids · Computational fluid dynamics (CFD)

Nonmenclature

τ shear stress, Pa
τ_y yield shear stress, Pa
n flow behavior index, dimensionless
K consistency index constant, Pa s^n
R^2 linear regression correlation coefficient, dimensionless

B.-H. Um · T. R. Hanley (✉)
Department of Chemical Engineering, Samuel Ginn College of Engineering, Auburn University, Auburn, AL 36849, USA
e-mail: hanley@auburn.edu

Introduction

Production of fuel ethanol from lignocellulosic biomass has the potential to reduce world dependence on petroleum while decreasing net emissions of carbon dioxide, the principal greenhouse gas [1]. There continue to be times, however, when ethanol cannot compete economically with gasoline or petroleum derivatives of fossil fuels. The opportunity therefore exists for process improvements in the conversion of biomass to fuel alcohol, resulting in more favorable production economics. High-solids loading fermentation is a process improvement aimed at increasing both the rate of fermentation and the final ethanol concentration, thereby reducing processing costs [2–4]. Positive economic advantages associated with a high-solids saccharification process over a conventional low-solids process include lower capital costs because of the reduced volume, lower operating costs because of less energy required for heating and cooling, lower downstream processing costs because of higher product concentrations, and reduced disposal and treatment costs because of lower water usage [5, 6].

Understanding the rheology of concentrated biomass slurries is important for designing equipment and predicting process performance. Specifically, the shear rate in a mixing tank is an important parameter controlling many important industrial processes. Fundamentally, shear rate affects processes involving mixing of Newtonian and non-Newtonian fluids, generating/dispersing liquid/liquid droplets, and producing fine gas bubbles for gas-to-liquid mass transfer.

Stirred tanks are typically used for the thermo-chemical fermentation. To simulate the flow of cellulosic slurries in stirred tanks, the rheological properties of these suspensions must be known. This high-solids slurry definition can be regarded as the solids region where the slurry viscosity is highly non-Newtonian at approximately 12 to 15% insoluble solids [7]. High-solids slurries such as corn stover typically range from 10 to 40% solids [8].

The primary objective of this study is to investigate the rheological behavior of high-solids cellulosic slurries, to fit an appropriate model to the experiment data and to determine the distribution of turbulent viscosity during ethanol fermentation. The results of this work will be used to investigate high-solids saccharification followed by fermentation (SFF) for biomass conversion using Solka Floc, a delignified pulp, as the model feedstock. Additionally, the results can be employed for a larger bioreactor design using computational fluid dynamics.

Materials and Methods

Materials

Solka Floc (Fiber Sale and Development, Urbana, OH), a delignified spruce pulp, was the biomass used as the raw material in this work. The composition of this material was analyzed according to National Renewable Energy Laboratory (NREL) standard procedures 001, 002, and 006. The glucan content was 88%.

Enzyme and Microorganism

Commercially produced Spezyme CP and Novozyme 188 were used for enzymatic hydrolysis. The cellulosic enzyme Spezyme CP, secreted by *Trichoderma longibrachiatum*,

formerly *Trichoderma reesei*, was procured from Genencor International (Palo Alto, CA). The enzyme had an activity of 82 GCU/g (provided by the manufacturer) and 55 IFPU/mL as determined by NREL standard procedure 006. Novozym 188 purchased from Sigma (Cat. no. G-0395) was used for cellulose hydrolysis with a volume ratio of 4 IFPU Celluclast/CBU Novozyme to alleviate end-product inhibition by cellobiose.

The recombinant *Zymomonas mobilis* strain ATCC 39679, carrying the plasmid pZB4L (designated as *Zm* 39679:pZB4L), was provided by M. Zhang (NREL, Golden, CO). Stock cultures were stored in glycerol at −70 °C.

Preculture and Inoculation Procedures

A 2.0-mL aliquot of a glycerol-preserved culture was removed from cold storage (freezer) and transferred to 200 mL of complex RM medium (yeast, KH_2PO_4, glucose, and water) containing about 2% (w/v) glucose and 2% (w/v) xylose supplemented with tetracycline (20 mg/L) in a 500-mL Erlenmeyer flask and grown overnight at 30 °C.

Batch fermentations were inoculated by transferring around 10% (v/v) of the overnight flask culture directly to the stirred-tank bioreactor (BioFlo® 3000, New Brunswick Scientific, Edison, NJ). For the fermentations, the initial cell density was monitored spectrophotometrically to give an optical density at 600 nm in the range 0.4 to 0.5 corresponding to growth in the midexponential phase.

Saccharification Followed By Fermentation

To maximize the glucose and ethanol concentrations, substrate concentrations were employed from 10 to 20% on a dry basis, corresponding to cellulose concentrations of 8 to 17%. In several experiments employing a traditional batch enzyme reaction and fermentation of high substrate concentrations (>10%), there is no visible liquid phase because of complete absorption of liquid by the biomass. In this state, no sugar and ethanol products were produced for tests between 10 and 20%. To overcome this problem, the Solka Floc was added to the reactions in three equal portions at 4-h intervals during both enzyme reaction and fermentation up to the 20% final substrate concentration. Then, the inoculum prepared as 10% by volume of the total working volume (2 L) was transferred into the reactor after enzymatic hydrolysis for 48 h. The enzyme loading was 30 FPU per gram of cellulose, supplemented by β-glucosidase to prevent product inhibition by cellobiose. The SFF experiments were operated for 96 h, initially at 50 °C for saccharification and finally at 30 °C for fermentation.

The substrate and nutrient media were autoclaved (120 °C for 20 min), but the enzyme solutions were not sterile. The Solka Floc slurry, diluted to different dry weights of solid material (10, 13, 15, and 20%), was used as a substrate.

Viscosity Measurement of High Solid Suspension

The viscosity of the suspension at different biomass concentration was measured by Modular Compact Rheometer Physica MCR 300 (Paar-Physica). Controlled shear-stress measurements were done using the concentric cylinder system with a FL 100/6W impeller at temperatures of 30, 40, and 50 °C. Samples were mixed before measurements were taken. Then, an appropriate volume was placed into the viscometer, allowing several minutes for the temperature to stabilize. The rheological measurements were performed three times for each value of biomass concentration using a fresh sample each time.

Models and Methods

Vessel Geometry

The cylindrical mixing tank simulated in this study has an ellipsoidal bottom with four equally spaced, wall-mounted baffles extending from the vessel bottom to the free surface, stirred by two centrally located six-blade Rushton turbine impellers. The tank diameter measured 0.138 m, and the baffle width was 0.008 m. The impeller diameter was 0.046 m ($D/T=3$) for both impellers. The distance between the impellers was 0.061 m. The bottom impeller center was positioned at a distance $C=T/3$ off the tank bottom. The liquid level was equal to the tank diameter, $Z/T=1.3$.

The suspension was a fermentation broth with various viscosities. The impellers were mounted on a 0.0025-m-diameter shaft rotating at 120 rpm corresponding to a range of Reynolds number of 50 to 300.

CFD Simulation Model and Tool Package

The CFD simulation employed the following setting: Type, 3D cylindrical; analysis model, multiple reference frame; turbulent model, Standard k–ε model; Mixsim V. 2.1.10; and FLUENT V. 6.2.20. The computational grid was defined by 570,000 unstructured, nonuniformly distributed, 182,000 nodes and tetrahedral cells. When refining the mesh, care was taken to place additional mesh points in the regions of high gradient around the blades and discharge region. Simulations were typically considered converged when the scaled residuals (continuity, X, Y, Z-velocity, k, and ε), normalized relative to the maximum circulating flow, fell below 6E-04 by iteration 5,000.

Results and Discussion

Rheological Behavior of Enzymatic Hydrolysis Suspension

Figure 1a–c shows the dependence of the apparent viscosity of the enzyme hydrolysis suspension on biomass concentration. It clearly demonstrates a dramatic decrease of viscosity at the reloading point (i.e., after the initial 4 h). The experimental determination of the viscosity–shear rate and shear stress–shear rate relationships of the various formulation suspensions with different concentrations was performed with a variable speed rotational viscometer (2 to 200 rpm).

The viscosities observed were in range of 0.0418 to 0.0144, 0.233 to 0.0348, and 0.292 to 0.0447 Pa s for shear rates up to 100 reciprocal seconds and substrate concentrations of 10, 15, and 20% initial solids (w/v) measured at 50 °C, respectively. The fermentation experimental shear stress–shear rate curves are depicted in Fig. 1d.

In the fermentation, experimental results are presented for the rheological behavior of high-solids ethanol fermentation for biomass conversion using Solka Floc as the model feedstock. A recombinant strain of *Z. mobilis* 39679:pZB4L was used in SFF processes as a function of varying initial concentration of Solka Floc and constant enzyme dosage. The initial viscosities ranged from 0.024 to 0.028, 0.423 to 0.067, and 0.840 to 0.087 Pa s for shear rates up to 100 reciprocal seconds at combined temperatures (50 and 30 °C) at 10, 15, and 20% initial solids (w/v), respectively. At 120 rpm, the viscosities were 0.019, 0.078, and 0.105 Pa s at 10, 15, and 20% initial solids (w/v), respectively. One can see that the

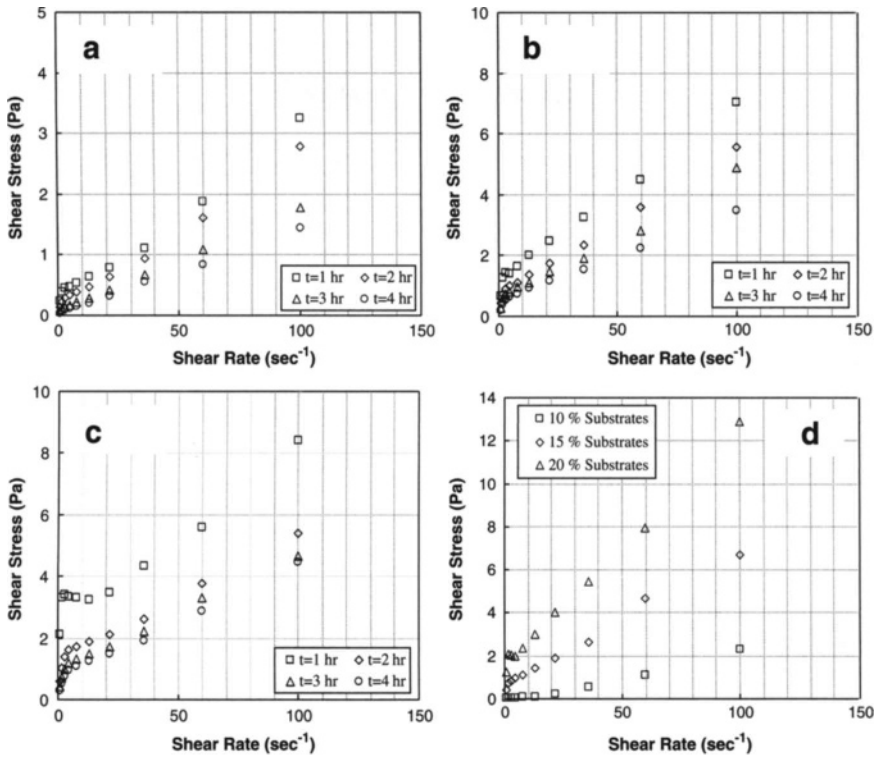


Fig. 1 Shear stress as a function of shear rate for different times during the initial 4-h enzymatic hydrolysis and fermentation. **a** 10, **b** 15, and **c** 20% solids concentration. **a**–**c** Enzyme condition: 30 FPU/g of glucan, pH 4.8 to 5.0, 50 °C, 120 rpm. **d** SFF condition: 30 FPU/g of glucan, pH 4.8 to 5.0, 30 °C 120 rpm, *Zymomonas mobilis*, strain 39679:pZB4L

rheological behavior of suspensions of the fermentation broth significantly changes with its concentration and reaction conditions. At all concentrations, both enzymatic suspension and fermentation broths exhibit an overall pseudoplastic behavior with two Newtonian regions. At relatively high solid concentrations loaded by the portion method, constant viscosity was observed, indicating Newtonian behavior for slurries at low and high shear rates during initial enzymatic hydrolysis and SFF process.

Rheological Parameter Estimation for the Pseudoplastic Suspension

Several researchers reported viscoelastic behavior of yeast suspensions. Labuza et al. [9] reported shear-thinning behavior of baker's yeast (*S. cerevisiae*) in the range of 1 to 100 reciprocal seconds at yeast concentrations above 10.5% (w/w). The power law model was successfully applied. More recently, Mancini and Moresi [10] also measured the rheological properties of baker's yeast using different rheometers in the concentration range of 25 to 200 g dm^{-3}. While the Haake rotational viscometer confirmed Labuza's results on the pseudoplastic character of yeast suspension, the dynamic stress rheometer revealed definitive Newtonian behavior. This discrepancy was attributed to the lower sensitivity of Haake viscometer in the range of viscosity tested (1.5 to 12 mPa s). Speers et al. [11] used a controlled shear-rate rheometer with a cone-and-plate system to measure viscosity of

Table 1 Determination of rheological parameter as function of time during initial 4-h enzymatic hydrolysis.

	Herschel–Bulkley model				Bingham model			Casson model			Power law		
	$\tau = \tau_y + K\dot{\gamma}^n$				$\tau = \tau_y + K\dot{\gamma}$			$\tau^{0.5} = (\tau_y)^{0.5} + n(\dot{\gamma})^{0.5}$			$\tau = K\dot{\gamma}^n$		
	τ_y (Pa)	K	n	R^2	τ_y (Pa)	n	R^2	τ_y (Pa)	n	R^2	K	n	R^2
Reaction time (10% solid concentration)													
t=1 h	0.391	0.012	1.175	0.996	0.360	0.022	0.994	0.226	0.100	0.982	0.269	0.404	0.948
t=2 h	0.213	0.019	1.024	0.995	0.209	0.021	0.995	0.335	0.107	0.990	0.155	0.507	0.972
t=3 h	0.099	0.009	1.176	0.994	0.081	0.171	0.992	0.031	0.108	0.987	0.063	0.669	0.973
t=4 h	0.065	0.005	1.294	0.995	0.044	0.014	0.988	0.013	0.105	0.983	0.037	0.766	0.972
Reaction time (15% solid concentration)													
t=1 h	1.191	0.060	0.987	0.998	0.763	0.071	0.931	0.759	0.1611	0.991	0.835	0.403	0.958
t=2 h	0.713	0.055	0.968	0.997	0.731	0.048	0.997	0.424	0.156	0.993	0.489	0.466	0.967
t=3 h	0.577	0.044	0.975	0.996	0.589	0.040	0.996	0.338	0.144	0.992	0.399	0.476	0.969
t=4 h	0.354	0.057	0.887	0.991	0.400	0.036	0.990	0.213	0.143	0.990	0.292	0.532	0.975
Reaction time (20% solid concentration)													
t=1 h	2.707	0.036	1.083	0.972	2.658	0.052	0.926	1.488	0.115	0.930	2.363	0.205	0.859
t=2 h	0.960	0.140	0.730	0.981	1.173	0.044	0.976	0.815	0.133	0.983	0.854	0.353	0.966
t=3 h	0.600	0.154	0.693	0.987	0.827	0.041	0.979	0.535	0.138	0.989	0.589	0.408	0.978
t=4 h	0.372	0.158	0.677	0.986	0.573	0.041	0.978	0.358	0.144	0.988	0.424	0.464	0.981

Condition: 30 FPU/g of glucan, pH 4.8 to 5.0, 50 °C, 120 rpm. Substrates were added to the reactions in portion loading during hydrolysis up to the 20% final substrate concentration.

suspensions of flocculating and nonflocculating strains of *S. cerevisiae* and *S. uvarum*. They used the Bingham model for description of viscoelastic flow behavior of cell suspension.

The normal procedure for the estimation of the model parameters for pseudoplastic fluids with a yield stress using rheological models employs nonlinear regression of the viscometric data from a concentric cylinder geometry with a numerical package, minimizing the sum of error squares. Nonlinear fits to various data with a statistics package (RHEOLPLUS) has sometimes given a best fit with negative yield values, which is meaningless. Therefore, the first point at low shear stress was not considered in the regression analysis.

Figure 1 shows shear stress curves as a function of shear rate at different time during initial enzymatic hydrolysis and fermentation processes. The yield stress values are shown

Table 2 Determination of rheological parameter as function of time during the initial SFF process.

Percent (w/v) substrates	Herschel–Bulkley model				Bingham model			Casson model			Power law		
	$\tau = \tau_y + K\dot{\gamma}^n$				$\tau = \tau_y + K\dot{\gamma}$			$\tau^{0.5} = (\tau_y)^{0.5} + n(\dot{\gamma})^{0.5}$			$\tau = K\dot{\gamma}^n$		
	τ_y (Pa)	K	n	R^2	τ_y (Pa)	n	R^2	τ_y (Pa)	n	R^2	K	n	R^2
10	0.029	0.002	1.554	0.998	0.014	0.011	0.980	0.001	0.105	0.970	0.016	0.973	0.968
15	0.306	0.177	0.756	0.985	0.467	0.068	0.978	0.256	0.201	0.988	0.425	0.549	0.979
20	0.735	0.259	0.740	0.996	1.016	0.089	0.981	0.625	0.216	0.996	0.866	0.461	0.970

Condition: 30 FPU/g of glucan, pH 4.8 to 5.0, 120 rpm, *Zymomonas mobilis*, strain 39679:pZB4L. Temperature=30 °C. Substrates were added to the reactions in four portions during fermentation up to 20% final substrate concentration. The substrate and nutrient media were autoclaved (120 °C and 20 min).

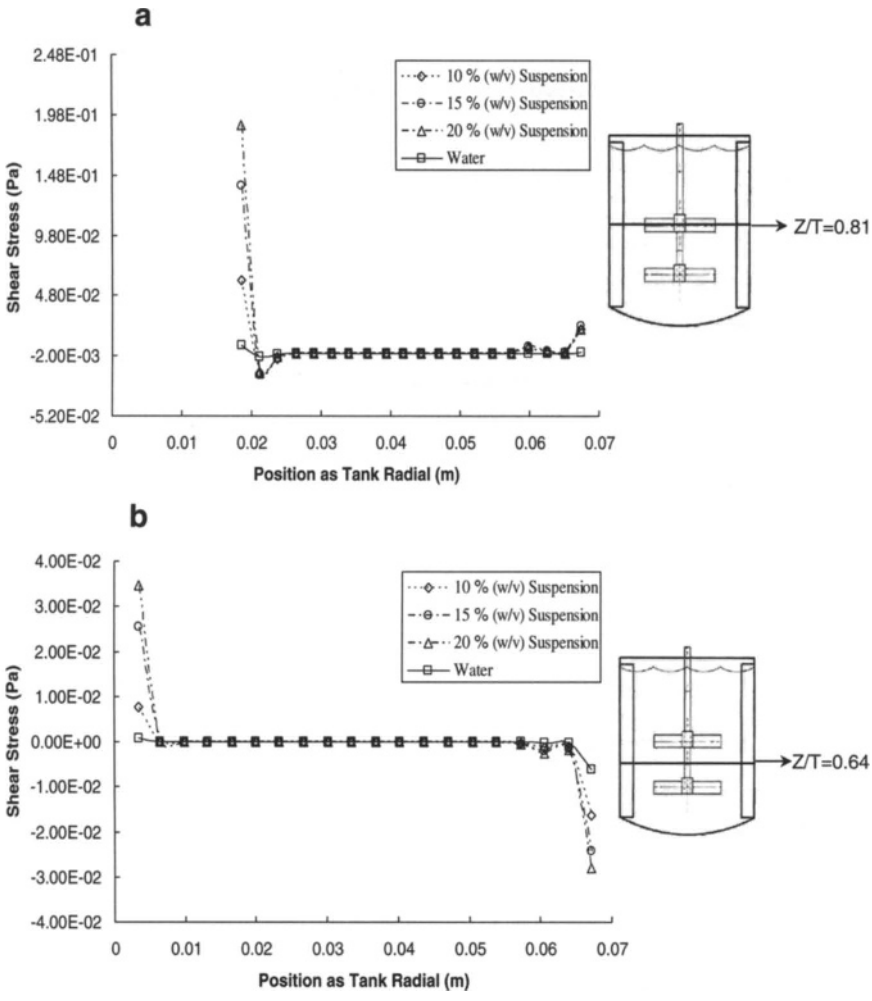


Fig. 2 Shear stress profiles as a function of tank radial position at different tank heights. **a–c** SFF condition: 30 FPU/g of glucan, pH 4.8 to 5.0, 120 rpm, *Zymomonas mobilis*, strain 39679:pZB4L

in Tables 1 and 2. Shear stress–shear rate data of the enzymatic hydrolysis suspension and fermentation broth were tested for various rheological models (Herschel–Bulkley, Bingham, Casson, and power law models).

Four models (Herschel–Bulkley, Casson, Bingham, and power law) were used to fit the experimental data and to determine the yield stress of the slurries. Table 1 list the results obtained for the different parameters used to fit the experimental data of fermentation suspensions at the various concentrations. The Herschel–Bulkley model fits the data satisfactorily over the whole experimental range at 10 to 20% solids concentration. On the other hand, the Bingham and Casson equations are in excellent agreement with results of the enzymatic suspension and fermentation broth testing at 10 and 20%, respectively (Table 1). The results of the power law model (n and K) were compared to those power law parameters obtained with the impeller method. The Herschel–Bulkley, Bingham, and the

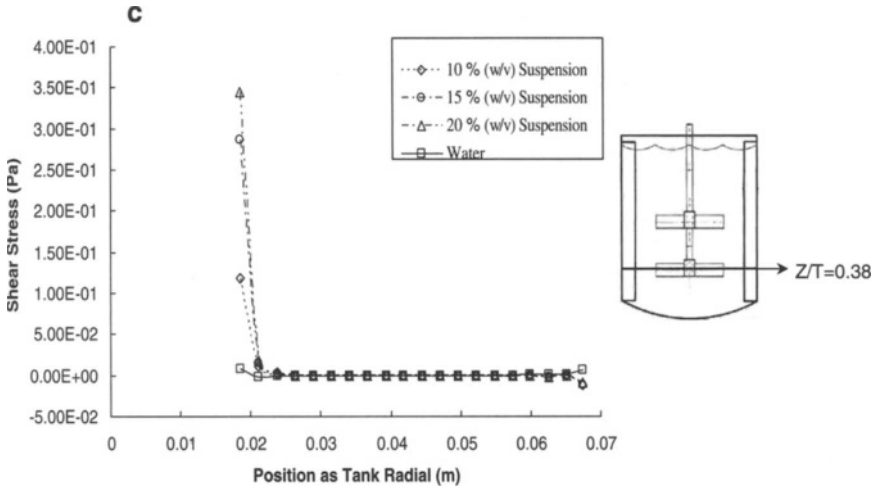


Fig. 2 (continued)

Casson models were used to compare their yield stress results to those calculated with the direct methods, the stress growth and impeller methods. Table 2 shows the parameters obtained when the experimental shear stress–shear rate data for the fermentation suspensions were fitted with all models at initial process. The correlation coefficients (R^2) between the shear rate and shear stress are from 0.994 to 0.995 for the Herschel–Bulkley model, 0.988 to 0.994 for the Bingham, 0.982 to 0.990 for the Casson model, and 0.948 to 0.972 for the power law model for enzymatic hydrolysis at 10% solids concentration (Table 1). The rheological parameters for Solka Floc suspensions were employed to determine if there was any relationship between the shear rate constant, k, and the power law index flow, n. The relationship between the shear rate constant and the index flow for fermentation broth at concentrations ranging from 10 to 20% is shown on Table 2. The yield stress obtained by the FL 100/6W impeller technique decreased significantly as the function of time and concentration during enzyme reaction and fermentation.

Simulation of Shear Stress and Turbulent Viscosity in the 3-L Mixing Tank

The viscous fermentation broth used in this project exhibited pseudoplastic rheology that is modeled quite well over a wide range of shear rates by the power law model. Consequently, the power law was used to model fluid rheology in this study for at 10, 15, 20% solids concentration. The upper and lower limits for n in this study were obtained from experiments with fermentation broth (*Z. mobilis* cultures) and ranged from 0.46 to 0.97 during the portion batch fermentation.

An understanding of the velocity flow fields is a prerequisite to understanding mixing and the key physical parameters such as shear stress, flow fluctuations, and vorticity fields. The circumferential-averaged shear stresses are plotted for the different solid concentrations as a function of tank radial position on three different panels by the z direction in Fig. 2. The fluid suspension near the impeller blade is accelerated by an imbalance of shear forces. The average maximum values determined by circumferential averaging model in the middle of tank were 0.008 τ_{avg} for 10%, 0.025 τ_{avg} for 15%, and 0.035 τ_{avg} for 20%.

Figure 3 shows the contour of the distribution of the turbulent viscosity, modeled by three different flow behavior indexes. The maximum viscosity was found in the midpoint (z=0.09m) of the tank: 0.084 Pa s for 10%, 0.050 Pa s for 15%, and 0.039 Pa s for 20%. With higher values of n, the fluid viscosity was less affected by shear, and the fluid encountered a resistance that significantly impeded flow in the wall region.

Results for average shear stress and contour distributions of viscosity over the range of tank radial position in the mixing tank illustrated that the fluid viscosity was significantly reduced in the high shear stress regions. Consequently, the fluid moved rapidly through this region.

Conclusions

The rheological analysis of high-solids substrates in the bioreactor during the enzymatic hydrolysis and ethanol fermentation showed a dramatic decrease in viscosity as a function of time. Initial reaction time and specifically biomass concentration were found to affect the bioreactor hydrodynamics. Adoption of high-solids substrates loading by portion method in the 3-L bioreactor showed significant reduction in viscosity with a dramatic acceleration of net liquid flow with increasing biomass quantity. Rheological analysis revealed a direct dependence of temperature and concentration of biomass in the bioreactor on the apparent viscosity of fermentation broths.

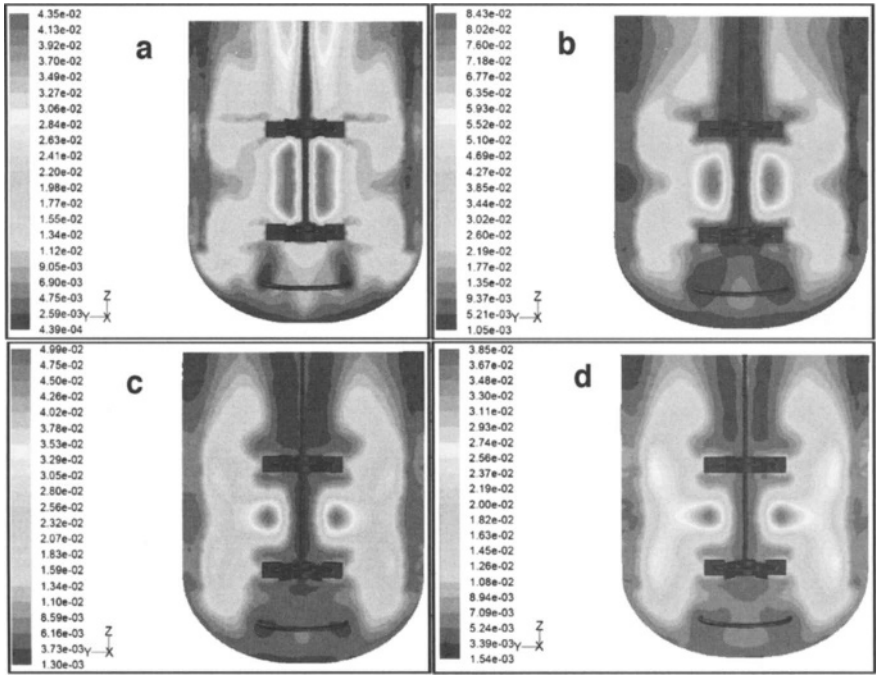


Fig. 3 Distribution of turbulent viscosity (kg/m s) in a bench scale reactor (2-L working volume). **a** Water, **b** 10, **c** 15, and **d** 20% solids concentration. **b–d** SFF condition: 30 FPU/g of glucan, pH 4.8 to 5.0, 120 rpm, *Zymomonas mobilis*, strain 39679:pZB4L

For the operation of a high-solids bioreactor for an ethanol production system, the bioreactor should operate below the critical biomass concentration to ensure efficient operation in a desirable mixing regime. The SFF process can be operated with relatively high solids loading up to a maximum solids loading of 20% w/v; however, increasing concentration affects fluid transport, mixing, and solids distribution negatively. The hydrodynamic results in the 3-L bioreactor can be used a priori or during the bioprocess to optimize operational parameters to avoid any occurrence of undesirable bioreactor stalling and to maximize the process productivity.

Acknowledgments The authors are grateful for the support of the Dahlem Supercomputer Laboratory at the University of Louisville. We also wish to thank Mr. Nathan P. Johnson and Dr. Eric Berson for their valuable discussion and the technical support of this project.

References

1. Renewable Fuels Association (REF) (2006). *Ethanol industry outlook: from niche to nation*. Washington, DC: USDA.
2. Ingledew, W. M. (1993). Yeast for production of fuel ethanol. In A. H., Rose, & J. S., Harrison (Eds.) *The yeast. Yeast technology*(vol. 5, 2nd ed.). New York, NY: Academic.
3. Varga, E., Klinke, H. B., Réczey, K, & Thomsen, A. B. (2004). *Biotechnology and Bioengineering, 88*, 567–574.
4. Philippidis, G. P., & Hatzis, C. (1997). *Biotechnology Progress, 13*(3), 222–231.
5. Lübbert, A., & Jørgensen, B. S. (2001). *Journal of Biotechnology, 85*(2), 187–212.
6. Mohagheghi, A., Tucker, M., Grohman, K., & Wyman, C. E. (1992). *Applied Biochemistry and Biotechnology, 33*, 67–81.
7. Pimenova, N. V., & Hanley, T. R. (2003). *Applied Biochemistry and Biotechnology, 105*(108), 353–364.
8. Ranatunga, T. D., Jervis, J., Helm, R. F., McMillan, J. D., & Wooley, R. J. (2000). *Enzyme and, Microbial Technology, 27*, 240–247.
9. Labuza, T. P., Barrera Santos, D., & Roop, R. N. (1970). *Biotechnology and Bioengineering, 12*, 123–134.
10. Mancini, M., & Moresi, M. (2000). *Journal of Food Engineering, 44*, 225–231.
11. Speers, R. A., Durance, T. D., Tung, M. A., & Tou, J. (1993). *Biotechnology Progress, 9*, 267–272.

Appl Biochem Biotechnol (2008) 145:39–51
DOI 10.1007/s12010-007-8038-6

Effects of Oxygen Limitation on Xylose Fermentation, Intracellular Metabolites, and Key Enzymes of *Neurospora crassa* AS3.1602

Zhihua Zhang · Yinbo Qu · Xiao Zhang · Jianqiang Lin

Received: 7 May 2007 / Accepted: 29 August 2007 /
Published online: 25 September 2007
© Humana Press Inc. 2007

Abstract The effects of oxygen limitation on xylose fermentation of *Neurospora crassa* AS3.1602 were studied using batch cultures. The maximum yield of ethanol was 0.34 g/g at oxygen transfer rate (OTR) of 8.4 mmol/L·h. The maximum yield of xylitol was 0.33 g/g at OTR of 5.1 mmol/L·h. Oxygen limitation greatly affected mycelia growth and xylitol and ethanol productions. The specific growth rate (μ) decreased 82% from 0.045 to 0.008 h^{-1} when OTR changed from 12.6 to 8.4 mmol/L·h. Intracellular metabolites of the pentose phosphate pathway, glycolysis, and tricarboxylic acid cycle were determined at various OTRs. Concentrations of most intracellular metabolites decreased with the increase in oxygen limitation. Intracellular enzyme activities of xylose reductase, xylitol dehydrogenase, and xylulokinase, the first three enzymes in xylose metabolic pathway, decreased with the increase in oxygen limitation, resulting in the decreased xylose uptake rate. Under all tested conditions, transaldolase and transketolase activities always maintained at low levels, indicating a great control on xylose metabolism. The enzyme of glucose-6-phosphate dehydrogenase played a major role in NADPH regeneration, and its activity decreased remarkably with the increase in oxygen limitation.

Keywords *Neurospora crassa* · Oxygen limitation · Xylose · Xylitol · Ethanol

Z. Zhang · Y. Qu (✉) · X. Zhang · J. Lin
State Key Lab of Microbial Technology, Shandong University, Jinan 250100, China
e-mail: quyinbo@sdu.edu.cn

Z. Zhang
e-mail: zhangzhihua@mail.sdu.edu.cn

X. Zhang
e-mail: x_zha14@yahoo.ca

J. Lin
e-mail: jianqianglin@sdu.edu.cn

Present address:
X. Zhang
Biology Department, Concordia University, 7141 Sherbrooke West, Montreal, Quebec, Canada H4B 1R6

Introduction

Lignocellulosics are the most abundant renewable resource in the world, and bioconversion of lignocellulosics into fuel ethanol could contribute to renewable energy supplies. Hemicelluloses, the second most abundant polysaccharides in nature, represents about 20–30% of agricultural residues [1]. The utilization of hemicellulose is essential for whole components utilization of lignocellulosic materials, as well as for the economy of the bioconversion process in industrial applications.

Xylose is the main product of enzymatic hydrolysis of angiosperm hemicellulose. In the past, it was regarded that xylose was unfermentable, until Wang et al. [2] found that some microbes were able to utilize xylose to produce ethanol in 1980. Now, more than 100 kinds of microbes that are capable of fermenting xylose have been found, including bacteria, fungi, and yeasts [3].

In fungi, xylose is reduced to xylitol by NADH- or NADPH-dependent xylose reductase (XR) and thereafter is oxidized to xylulose by NAD^+-dependent xylitol dehydrogenase (XDH). The xylulose is phosphorylated, channeled into the pentose phosphate pathway [3]. XR of most fungi, including most yeasts, prefers NADPH to NADH. Because of the cofactor preference of XR (NADPH) and XDH (NAD^+), redox imbalance occurs under anaerobic condition [4]. Therefore, the oxygen-limited rather than anaerobic condition is ideal for bioconversion of xylose to ethanol, so that the accumulated reduced cofactor can be oxidized to reach redox balance. A critical level of oxygen should exist for the highest ethanol yield and productivity.

Since the 1980s, there have been many studies on yeast xylose fermentation [5–8] but fewer studies on filamentous fungi. *Neurospora crassa* has both abilities of producing cellulase and hemicellulase and fermenting glucose and xylose; therefore, it maybe can be used in a consolidated processing [9–11]. In this study, the effects of oxygen limitation on xylose fermentation of *N. crassa* have been investigated. Comparisons of the metabolic rates, intracellular metabolite concentrations, and key enzyme activities under various oxygen-limited conditions were carried out.

Materials and Methods

Microorganism

N. crassa AS3.1602 (orn^-) was purchased from the China General Microbiological Culture Collection Center (Beijing, China) and was routinely maintained on potato dextrose agar slant (potato extract, 200 g/L; dextrose, 20 g/L; agar, 1.5–2.5%) at 4 °C.

Medium and Cultivation Conditions

The culture medium composed of the following (g/L): KH_2PO_4, 2.0; $MgSO_4$, 0.3; $CaCl_2$, 0.3; peptone, 5.0; yeast extract, 3.0; $FeSO_4 \cdot 7H_2O$, 0.005; $ZnSO_4$, 0.0014; $MnSO_4 \cdot 4H_2O$, 0.0016; $CoCl_2$, 0.002; pH 5.0. The carbon source was described in specific later.

The mycelia were inoculated directly from the potato slants into 300-mL flasks containing 100 mL of culture medium added with 1.0% xylose as carbon source. The inocula were precultured for 48 h at 30 °C and shaken at 200 rpm. After 48 h, the precultivated broth was transferred into flasks containing 2.0% xylose and cultivated under various oxygen-limited conditions as described later, at 37 °C and 150 rpm. Samples were

taken every 24 h for analysis of cell and metabolite concentrations in fermentation broth. Mycelia were collected at the exponential phase of fermentation for assays of intracellular intermediate metabolite concentrations and key enzyme activities.

Determination of Oxygen Transfer Rate

Oxygen transfer rate (OTR) was determined using the sodium sulfite oxidation method [12]. OTRs were measured for standard Erlenmeyer flasks of 500-mL flask, 200-mL flask, 100-mL flask, 100-mL serum flask, and 100-mL serum flask filled with nitrogen, containing 100 mL of medium, respectively, shaken at 150 rpm at 37 °C. The OTRs of different oxygen-limited conditions were 12.6, 8.4, 5.1, 3.3, and 0 mmol/L·h, respectively.

Substrate and Products Analysis

Xylose, xylitol, and ethanol were analyzed using LC-10AD high-performance liquid chromatography (Shimadzu, Japan), equipped with an HPX-87H Aminex column (Bio-Rad) and a RID-10A refractive index detector. The column was maintained at 55 °C and eluted with 5 mmol/L H_2SO_4 at a flow rate of 0.4 mL/min.

Intracellular Metabolite Analysis

The extraction of intracellular metabolites was performed according to the method of Ruijter and Visser [13]. The samples for phosphorylated carbohydrate and organic acid analysis were concentrated using solid phase extraction (SPE) and vacuum evaporation, respectively, and stored at −70 °C before assays. The SPE was performed according to the method of Smits et al. [14].

Intracellular metabolites were analyzed using Dionex DX 500 high-pressure anion exchange chromatography (Dionex, USA) equipped with a Dionex GP40 gradient pump and a Dionex ED40 electrochemical detector.

Malate, citrate and isocitrate, pyruvate, 3-phosphoglycerate, and phosphoenolpyruvate (PEP) were analyzed using an AS11-HC column (250×4 mm, Dionex) and a conductivity detector. Solvent A of H_2O and solvent B of 100 mmol/L of NaOH were used to make a time-dependent gradient elution solution: initial 95% of A and 5% of B (0–5 min), followed by a linear decrease in A to 60% and a linear increase in B to 40% (5–43 min), then, a linear increase in A to 95% and a linear decrease in B to 5% (43–45 min), and finally, 95% of A and 5% of B (45–50 min). The flow rate for each gradient was 0.9 mL/min.

Glucose-6-phosphate (G6P), fructose-6-phosphate (F6P), fructose-1,6-bisphosphate (FBP), ribose-5-phosphate (R5P), and erythrose-4-phosphate (E4P) were analyzed using a CarboPac PA20 column (150×3 mm, Dionex) and a pulsed amperometric detector. The detector was equipped with a working gold electrode and a reference electrode consisting of a Ag/AgCl combination. The following potential–time sequences were used: 0.1 V (0–0.4 s), −2.0 V (0.41–0.42 s), 0.6 V (0.43 s), −0.1 V (0.44–0.5 s). The gradient elution system was according to Panagiotou et al. [15].

The protein content was measured using the Bradford method [16].

Enzyme Assays

For the measurement of intracellular enzyme activities, mycelia were collected at the exponential growth phase of fermentation. Mycelia were washed three times with 0.9%

NaCl and lysed using a FastPrep FP120 cell disrupter (Qbiogene, USA). After centrifugation at 4 °C, the supernatants were stored at −70 °C for further assays.

XR (EC 1.1.1.21), XDH (EC 1.1.1.9), xylulokinase (XK, EC 2.7.1.17), and ethanol dehydrogenase (ADH, EC 1.1.1.1) activities were measured as described by Eliasson [17].

FBP aldolase (ALD, EC 4.1.2.13), pyruvate kinase (PK, EC 2.7.1.40), transaldolase (TAL, EC 2.2.1.2), $NADP^+$-dependent isocitrate dehydrogenase (IDH, EC 1.1.1.41), G6P dehydrogenase (G6PDH, EC 1.1.1.49), and malate dehydrogenase (MDH, EC 1.1.1.37) activities were measured as described by Bergmeryer [18].

The activities of pyruvate decarboxylase (PDC, EC 4.1.1.1), phosphofructokinase (PFK, EC 2.7.1.11), and transketolase (TKL, EC 2.2.1.1) were measured as described by Postma et al. [19], Tian et al. [20], and Selivanov et al. [21], respectively.

All assays were carried out at 37 °C, and the samples were measured using UV2550 spectrophotometer (Simadzu, Japan) at 340 nm wavelength.

Enzyme units (U) are defined as micromoles of oxidized or reduced coenzymes per minute under assay conditions. Specific activities are expressed as U/mg total cell protein.

Biomass Measurement

The biomass was measured using the perchloric acid method [22].

Results and Discussion

Xylose Fermentation of *N. crassa* at Various Oxygen-limited Conditions

Xylose fermentation was carried out at OTRs of 12.6, 8.4, 5.1, 3.3, and 0 mmol/L·h, respectively. Xylose uptake rates of exponential growth phase decreased with the increase in oxygen limitation. At OTR of 12.6 mmol/L·h, cell growth was fast, and there was little xylose remained after 24 h (Fig. 1). However, at anaerobic conditions (OTR of 0 mmol/L·h), cell growth was limited, almost no increase in cell concentration appeared, and 12.2 g/L of xylose remained after 10 days of fermentation.

Oxygen limitation had great effects on ethanol and xylitol productions. As shown in Table 1, the maximum conversion of xylose to ethanol was 66% at OTR of 8.4 mmol/L·h, with the ethanol concentration of 6.7 g/L and ethanol yield of 0.34 g/g. The maximum conversion of xylose to xylitol was 34% at OTR of 5.1 mmol/L·h, with the xylitol concentration of 6.7 g/L and xylitol yield of 0.33 g/g. It has been reported that the ratio of ethanol to xylitol is influenced by oxygen [23–25]. Schvester et al. [26] found that during xylose fermentation using *Pachysolen tannophilus*, ethanol began to accumulate only after oxygen was exhausted. In the present research on *N. crassa*, it was found that OTR of 8.4 mmol/L·h was optimal for ethanol production, while OTR of 5.1 mmol/L·h was optimal for xylitol production. More oxygen was needed for production of ethanol than xylitol to reach the maximum conversion and yield. *Candida boidinii* NRRL Y-17213 showed a similar pattern in flask cultivation [27]. Whereas, *C. boidinii* NRRL Y-17213 got the highest ethanol yield at OTR of 10 mmol/L·h and the highest xylitol yield at OTR of 14 mmol/L·h, when OTR varied from 10 to 30 mmol/L·h in fermentor [4].

At low xylose level, ethanol concentration reduced rapidly (Fig. 1). No byproducts of acetic acid and lactic acid were found (data not shown), which suggested that ethanol was

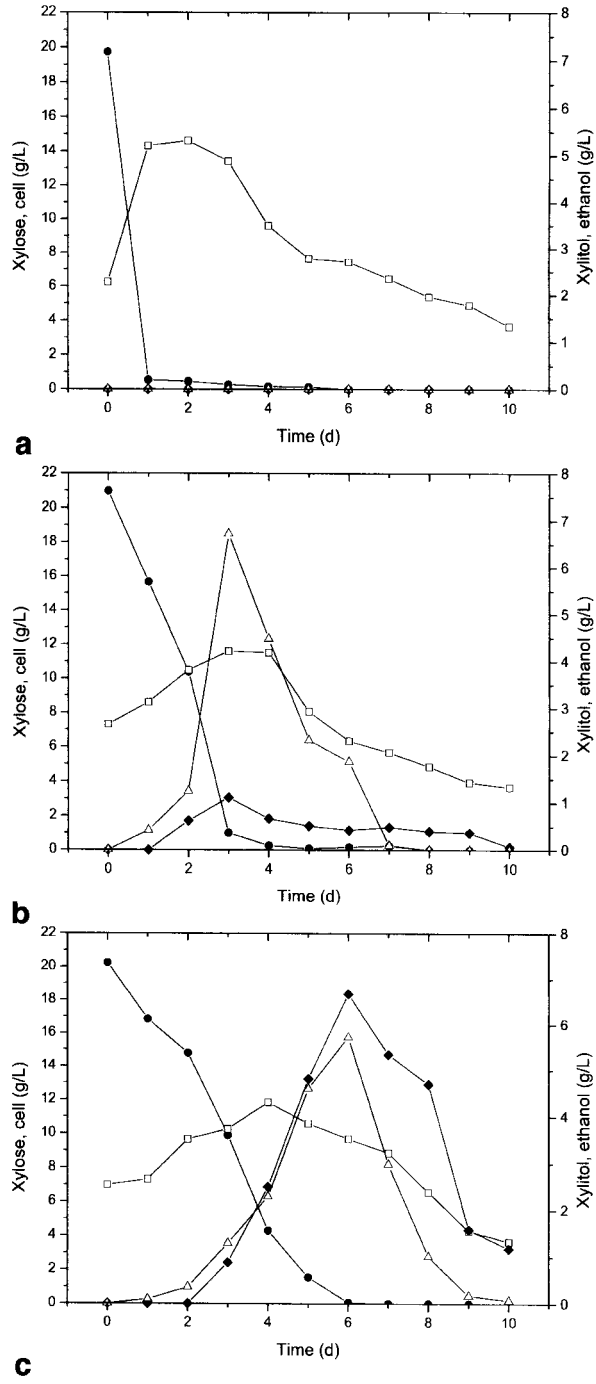
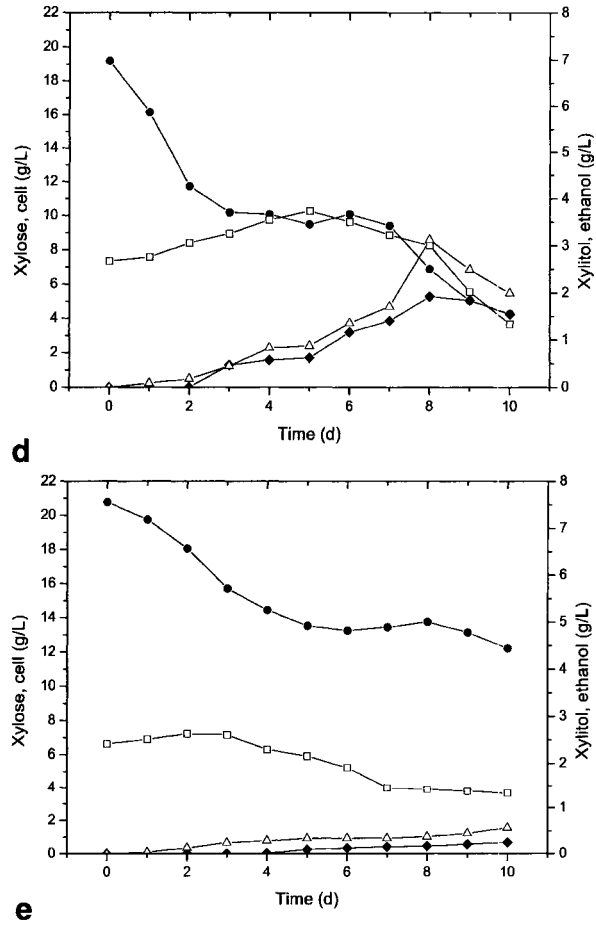


Fig. 1 The time course of substrate, products and cell concentrations (g/L) for *N. crassa* batch cultures using xylose as carbon source. The values are the averages of at least four measurements from two fermentations. OTR: 12.6 (**a**), 8.4 (**b**), 5.1 (**c**), 3.3 (**d**), and 0 mmol/L·h (**e**). Xylose (*filled circles*), cell (*open squares*), xylitol (*filled diamonds*), and ethanol (*open triangles*)

Fig. 1 (continued)



utilized by the cells. Xylitol uptake rate was low at high ethanol levels. When ethanol concentration decreased to a lower level, xylitol uptake rate increased obviously (Fig. 1), which indicated that xylitol uptake was inhibited by ethanol.

Intracellular Metabolite Profiles at Various Oxygen-limited Conditions

Xylose fermentation was carried out at OTRs of 12.6, 8.4, and 0 mmol/L·h, respectively. Mycelia were collected at the exponential growth phase, and the intracellular metabolites were assayed.

As shown in Fig. 2, intracellular metabolite concentrations decreased with the increase in oxygen limitation, except for G6P/E4P and pyruvate. PEP was never detected in all tested conditions, same with the results obtained using *Candida tropicalis* [28].

To compare the values at the same level of xylose uptake rate, the intracellular metabolite concentrations were divided by the corresponding xylose uptake rates [29]. These calculations (Fig. 3) showed accumulation of all intracellular metabolites with the increase in oxygen limitation, indicating a faster metabolism at higher OTRs. When OTRs

Table 1 The influence of oxygen limitation on xylose fermentation of *N. crassa*.

OTR (mmol/L·h)	Xylose consumption[a] (mmol/L·h)	Ethanol				Xylitol			
		Maximal concentration (g/L)	Volumetric productivity (g/L·h)	Yield (g/g)	Conversion[b] (%)	Maximal concentration (g/L)	Volumetric productivity (g/L·h)	Yield (g/g)	Conversion (%)
12.6	5.4±0.1[c]	0	0	0	0	0	0	0	0
8.4	1.5±0.04	6.7±0.4	0.093±0.006	0.34±0.02	66±4	1.1±0.1	0.015±0.001	0.06±0.01	5.6±0.5
5.1	0.94±0.05	5.7±0.4	0.040±0.002	0.28±0.02	56±4	6.7±0.2	0.046±0.001	0.33±0.02	34±2
3.3	0.84±0.03	3.1±0.2	0.016±0.001	0.25±0.02	50±3	1.9±0.03	0.010±0.0001	0.16±0.02	16±2
0	0.28±0.03	0.57±0.06	0.0024±0.0002	0.066±0.003	13±1	0.24±0.01	0.0010±0.0001	0.028±0.002	2.9±0.2

[a] Xylose consumption during exponential growth.

[b] The ethanol conversion rate was calculated with 1 mol xylose producing 1.67 mol ethanol.

[c] The values are the averages and standard deviations of at least four measurements from two fermentations.

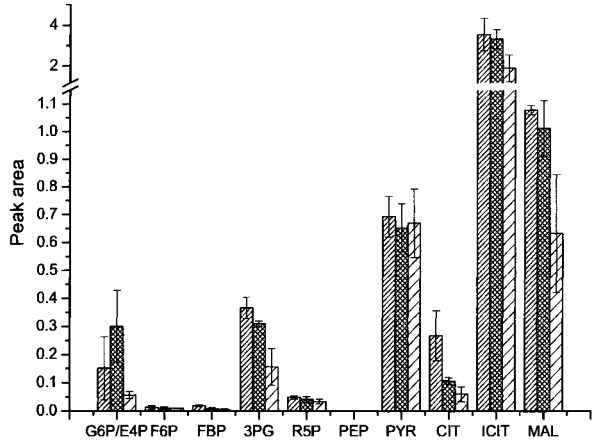


Fig. 2 Intracellular metabolite profiles of *N. crassa* batch cultures at various OTRs using xylose as carbon source. OTR: 12.6 (▨), 8.4 (▩), and 0 mmol/L·h (▨). Bars represent the peak areas divided by the protein concentration. The values are the averages and standard deviations of at least four measurements from two fermentations. *G6P* Glucose-6-phosphate, *E4P* erythrose-4-phosphate, *F6P* fructose-6-phosphate, *FBP* fructose-1,6-bisphosphate, *3PG* 3-phosphoglycerate, *R5P* ribose-5-phosphate, *PEP* phosphoenolpyruvate, *PYR* pyruvate, *CIT* citrate, *ICIT* isocitrate, *MAL* malate

varied from 12.6 to 0 mmol/L·h, the accumulations of all detected intracellular metabolites increased more than 2.8-fold. The most remarkable accumulation happened on pyruvate, F6P, R5P, and malate, whose accumulations increased more than tenfold. These four metabolites were of glycolysis, the pentose phosphate pathway, and the tricarboxylic acid cycle, respectively, which showed that oxygen limitation affected the whole cell metabolism.

Intracellular Enzyme Activities at Various Oxygen-limited Conditions

Xylose fermentation was carried out at five OTRs, and mycelia were collected at the exponential growth phases for intracellular enzyme assays. The results are shown in Fig. 4. The cells incubated at low OTRs might not have fully adapted to the aeration conditions,

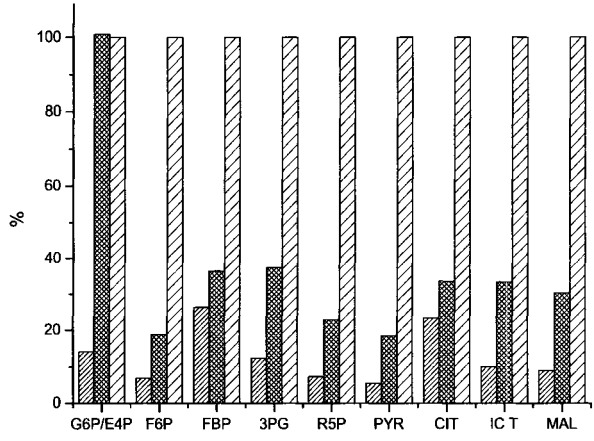


Fig. 3 Intracellular metabolite concentrations divided by corresponding xylose uptake rate at various OTRs, normalized by the values at OTR of 0 mmol/L·h as 100%. OTR: 12.6 (▨), 8.4 (▩), and 0 mmol/L·h (▨)

and the enzyme titers might not be representative.

The activities of XR, XDH, and XK decreased with the increase in oxygen limitation (Fig. 4a), which could be a reason for the decrease in xylose uptake rate under oxygen-limited conditions.

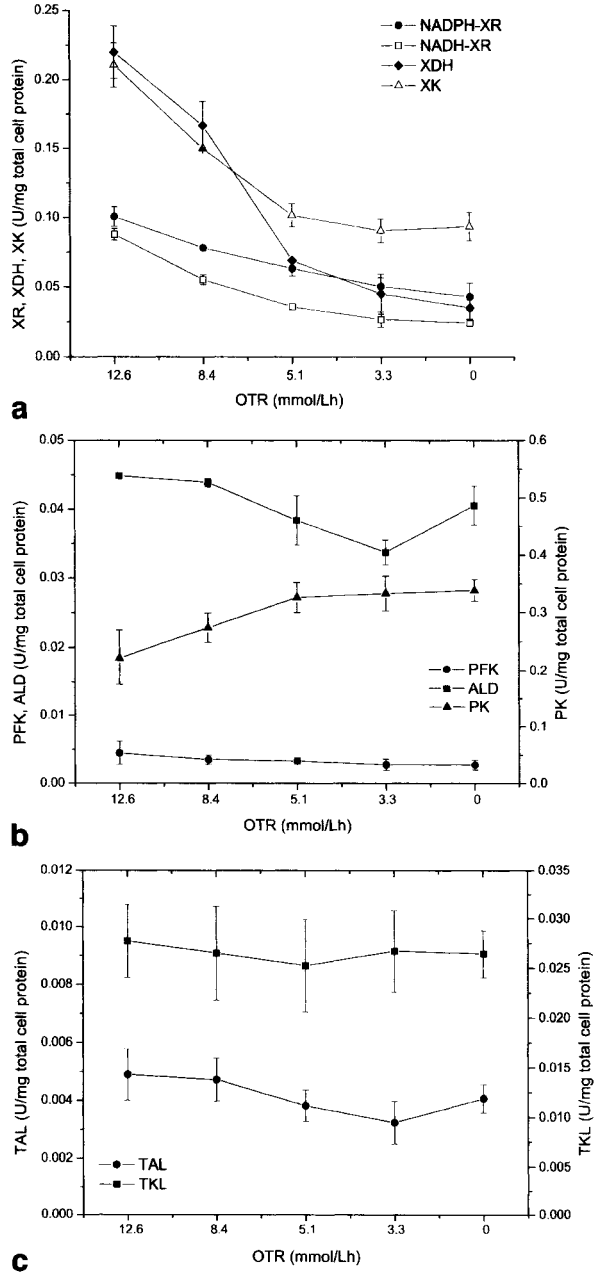
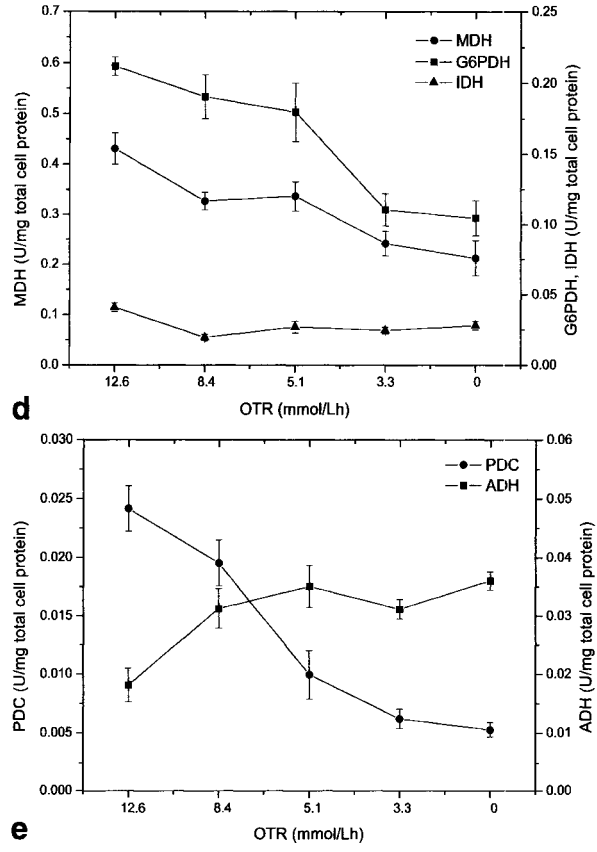


Fig. 4 a–e Specific intracellular enzyme activity profiles of *N. crassa* at various OTRs using xylose as carbon source. The values are the averages and standard deviations of at least four measurements from two fermentations. *XR* Xylose reductase, *XDH* xylitol dehydrogenase, *XK* xylulokinase, *PFK* phosphofructokinase, *ALD* fructose-1,6-bisphosphate aldolase, *PK* pyruvate kinase, *TAL* transaldolase, *TKL* transketolase, *MDH* malate dehydrogenase, *IDH* isocitrate dehydrogenase, *G6PDH* glucose-6-phosphate dehydrogenase, *PDC* pyruvate decarboxylase, *ADH* ethanol dehydrogenase

Fig. 4 (continued)



XR and XDH are the first two enzymes in the xylose metabolic pathway. Xylose is converted to xylitol by NADPH-XR or NADH-XR. Then, xylitol is converted to xylulose by NAD^+-XDH. The ratio of NADH-XR to NADPH-XR activity of *N. crassa* was lower than 1 (Fig. 5), which is the same as most of the fungi. At OTR of 12.6 mmol/L·h, the ratio was 0.87. The ratio decreased with the increase in oxygen limitation and remained at 0.55 when OTR was below 5.1 mmol/L·h. For most xylose-fermenting fungi, XR has a preference for NADPH to NADH, although there is an exception reported by Vandeska et al. to have the NADH-XR/NADPH-XR activity ratio larger than 1 for *C. boidinii* [4]. At OTR of 14 mmol/L·h, the NADH-XR/NADPH-XR activity ratio and xylitol yield were reported being the highest values of 5.88 and 0.48 g/g, respectively [4].

At OTRs of 12.6 and 8.4 mmol/L·h, the ratios of NADH-XR/XDH and NADPH-XR/XDH were low, about 0.45. However, the ratio increased rapidly, especially for NADPH-XR/XDH, with the increase in oxygen limitation. At anaerobic conditions (OTR of 0 mmol/L·h), the ratio of NADPH-XR/XDH reached 1.22, which was 165% larger than the value at OTR of 12.6 mmol/L·h (Fig. 5).

The activities of XR and XDH decreased with the increase in oxygen limitation (Fig. 4a), which indicated that an increase in XR and XDH activities could lead to the increase in xylose metabolic rate. Karhumaa et al. [30] increased XR and XDH activities in *Saccharomyces cerevisiae* by genetic manipulation, which significantly increased ethanol but decreased xylitol productions. Not only XR and XDH activities but also the XR/XDH

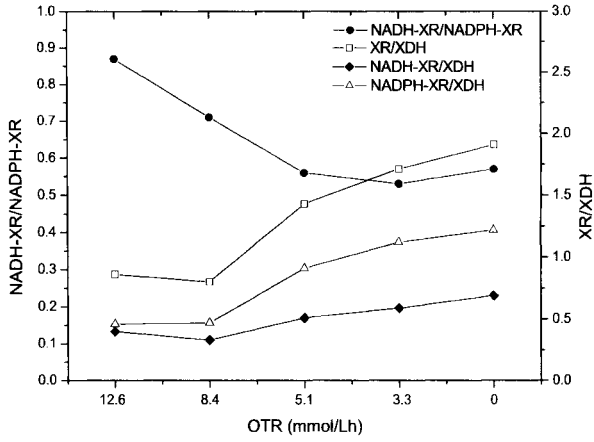


Fig. 5 Effects of oxygen limitation on the NADH-XR and NADPH-XR ratio and the XR/XDH ratio

ratio is important for xylose metabolism. It was reported that a XR/XDH ratio of 1:10 was optimal in minimizing xylitol formation in xylose-utilizing *S. cerevisiae* [31]. For *N. crassa*, the XR/XDH ratio is much higher than 1:10, which indicated that the activity of XDH was low for efficient ethanol fermentation, and the increase in XDH activity might decrease the xylitol accumulation.

XK activity decreased with the increase in oxygen limitation (Fig. 4a). XK is a key enzyme in xylose metabolism and fulfills the initial steps of xylose metabolism together with XR and XDH, to convert xylose to xylitol, and then to xylulose in series. After that, xylulose is phosphorylated and channeled into the pentose phosphate pathway. The decrease in XK activity could be another reason for the decrease in xylose uptake rate under oxygen-limited conditions. It was reported that overexpression of the *XKS1* gene encoding xylulose kinase significantly increased xylose utilization and ethanol production in recombinant *S. cerevisiae* [32].

Oxygen limitation had little influence on the intracellular enzyme activities of PFK and ALD that were in the upstream of glycolysis, while activated PK that was in the downstream of glycolysis converting PEP to pyruvate (Fig. 4b). PK is an important regulatable enzyme in glycolysis and is inhibited by adenosine triphosphate (ATP) [33]. The decreased ATP production rate under oxygen-limited conditions could alleviate the inhibiting effect of ATP on PK.

Oxygen limitation had little effect on the activities of TAL and TKL. When OTR varied from 0 to 12.6 mmol/L·h, TAL and TKL activities always maintained at low levels (Fig. 4c). TAL and TKL activities always maintained at low levels, to show big control effects on xylose metabolism. Walfridsson et al. [34] overexpressed TAL in XR- and XDH-expressing *S. cerevisiae*, which increased the cell growth but not ethanol production. Karhumaa et al. [30] found that increased XR and XDH activities redirected the production from xylitol to ethanol, whereas the rate of xylose consumption was governed by the overexpressed nonoxidative pentose phosphate pathway.

MDH activity reduced by 51%, decreased from 0.43 to 0.21 U/mg total cell protein when OTR varied from 12.6 to 0 mmol/L·h, with the decrease in intracellular malate concentration of 42% (Fig. 2).

Both G6PDH and IDH could generate NADPH. Activity of G6PDH decreased with the increase in oxygen limitation, while oxygen had no effect on IDH. G6PDH activity was much higher than IDH activity (Fig. 4d), which indicated that G6PDH was the main

enzyme in NADPH regeneration. IDH was not regulated by oxygen, similar with the results obtained using *Debaryomyces hansenii* [35].

Oxygen limitation showed reverse effects on PDC and ADH (Fig. 4e). The former decreased and the latter increased with the increase in oxygen limitation. At OTR of 8.4 mmol/L·h, the activities of both enzymes were high, and ethanol yield was the highest.

Conclusion

In this study, the effects of oxygen limitation on xylose fermentation of *N. crassa* AS3.1602 were investigated in batch cultures. With the increase in oxygen limitation, xylose uptake and cell growth rates decreased. Oxygen had great effects on ethanol production. With the increase in oxygen limitation, the metabolic fluxes of ethanol production changed gradually. At OTR of 8.4 mmol/L·h, the productivity and final concentration of ethanol reached the highest values.

Intracellular metabolites were determined at various OTRs. Concentrations of most of the intracellular metabolites decreased with oxygen limitation. The cells incubated at low aeration rates might not have fully adapted to the aeration conditions, and the enzyme titers might not be representative. Intracellular enzyme activities of XR, XDH, and XK, the first three enzymes in the xylose metabolic pathway, decreased with the increase in oxygen limitation, resulting in the decreased xylose uptake rate. When OTR varied from 12.6 to 0 mmol/L·h, TAL and TKL activities always maintained at low levels, indicating a great control on xylose metabolism. The enzyme of G6PDH played a major role in NADPH regeneration, and its activity decreased remarkably with the increase in oxygen limitation.

This work provides intracellular information of xylose metabolism of *N. crassa* AS3.1602 under oxygen-limited conditions, which is useful for the understanding of the metabolic controls for future genetic modification or condition optimization for improvement of ethanol production of this strain.

Acknowledgments This work was supported by grants from the National Natural Science Foundation (30270044) and the National Basic Research Program (2003CB716006) of the People's Republic of China.

References

1. Ladisch, M. R., Lin, K. W., Voloch, M., & Tsao, G. T. (1983). *Enzyme and Microbial Technology, 5*, 82–102.
2. Wang, P. Y., Shopsis, C., & Schneider, H. (1980). *Biochemical and Biophysical Research Communications, 94*, 248–254.
3. Skoog, K., & Hahn-Hägerdal, B. (1987). *Enzyme and Microbial Technology, 10*, 66–80.
4. Vandeska, E., Kuzmanova, S., & Jeffries, T. W. (1995). *Journal of Fermentation and Bioengineering, 80*, 513–516.
5. Alexander, M. A., Chapman, T. W., & Jeffries, T. W. (1988). *Applied Microbiology and Biotechnology, 28*, 478–486.
6. Hahn-Hägerdal, B., Hallborn, J., Jeppsson, H., Olsson, K., Skoog, K., & Walfridsson, M. (1993). In J. N. Saddler (Ed.) *Bioconversion of forest and agricultural residues* pp. 231–290. Wallingford, UK: CABI.
7. Walfridsson, M., Anderlund, M., Bao, X., & Hahn-Hägerdal, B. (1997). *Applied Microbiology and Biotechnology, 48*, 218–224.
8. Ryabova, O. B., Chmil, O. M., & Sibirny, A. A. (2003). *FEMS Yeast Research, 4*, 157–164.
9. Rao, M., Mishra, C., Keskar, S., & Srinivasan, M. C. (1985). *Enzyme and Microbial Technology, 7*, 625–628.
10. Rawat, U., Bodhe, A., Deshpande, V., & Rao, M. (1993). *Biotechnology Letters, 15*, 1173–1178.

11. Phadtare, S. U., Rawat, U. B., & Rao, M. B. (1997). *FEMS Microbiology Letters, 146*, 79–83.
12. Cooper, C. M., Fernstrom, G. A., & Miller, S. A. (1944). *Industrial and Engineering Chemistry, 36*, 504–509.
13. Ruijter, G. J. G., & Visser, J. (1996). *Journal of Microbiological Methods, 25*, 295–302.
14. Smits, H. P., Cohen, A., Buttler, T., Nielsen, J., & Olsson, L. (1998). *Analytical Biochemistry, 261*, 36–42.
15. Panagiotou, G., Christakopoulos, P., Villas-Boas, S. G., & Olsson, L. (2005). *Enzyme and Microbial Technology, 36*, 100–106.
16. Bradford, M. M. (1976). *Analytical Biochemistry, 72*, 248–254.
17. Eliasson, A. (2000). *Applied and Environmental Microbiology, 66*, 3381–3386.
18. Bergmeryer, H. U. (1983). *Methods of enzymatic analysis*. New York: Wiley.
19. Postma, E., Verduyn, C., Scheffers, W. A., & Van Dijken, J. P. (1989). *Applied and Environmental Microbiology, 55*, 468–477.
20. Tian, K. L., Lin, J. Q., Liu, X. M., Liu, Y., & Zhang, C. K. (2003). *Acta Microbiologica Sinica, 43*, 593–598.
21. Selivanov, V. A., Kovina, M. V., Kochevova, N. V., Meshalkina, L. E., & Kochetov, G. A. (2004). *FEBS Letters, 567*, 270–274.
22. Lin, J. Q., Lee, S. M., & Koo, Y. M. (2000). *Biotechnology and Bioprocess Engineering, 5*, 382–385.
23. Gong, C. H., Chen, L. F., & Tsao, G. T. (1981). *Biotechnology Letters, 3*, 130–135.
24. Suikko, M. L., & Drazic, M. (1983). *Biotechnology Letters, 5*, 107–112.
25. Jeffries, T. W. (1981). *Biotechnology and Bioengineering Symposium, 11*, 5–324.
26. Schvester, P., Robinson, C. W., & Moo-Yong, M. (1983). *Biotechnology and Bioengineering Symposium, 13*, 131–152.
27. Winkelhausen, E., Amartey, S. A., & Kuzmanova, S. (2004). *Engineering in Life Sciences, 4*, 150–154.
28. Skoog, K., & Hahn-Hägerdal, B. (1989). *Biotechnology Techniques, 3*, 1–6.
29. Skoog, K., & Hahn-Hägerdal, B. (1990). *Applied and Environmental Microbiology, 56*, 3389–3394.
30. Karhumaa, K., Fromanger, R., Hahn-Hägerdal, B., & Gorwa-Grauslund, M. F. (2007). *Applied Microbiology and Biotechnology, 73*, 1039–1046.
31. Eliasson, A., Hofmeyr, J. H. S., Pedler, S., & Hahn-Hägerdal, B. (2001). *Enzyme and Microbial Technology, 29*, 288–297.
32. Toivari, M. H., Aristidou, A., Ruohonen, L., & Penttilä, M. (2001). *Metabolic Engineering, 3*, 236–249.
33. Shen, T., & Wang, J. Y. (1991). *Biochemistry*. Beijing: Education.
34. Walfridsson, M., Hallborn, J., Penttila, M., Keränen, S., & Hahn-Hägerdal, B. (1995). *Applied and Environmental Microbiology, 61*, 4184–4190.
35. Nobre, A., Duarte, L. C., Roseiro, J. C., & Girio, F. M. (2002). *Applied Microbiology and Biotechnology, 59*, 509–516.

Appl Biochem Biotechnol (2008) 145:53–58
DOI 10.1007/s12010-007-8056-4

Fermentation of Acid-pretreated Corn Stover to Ethanol Without Detoxification Using *Pichia stipitis*

Frank K. Agbogbo · Frank D. Haagensen · David Milam · Kevin S. Wenger

Received: 9 May 2007 / Accepted: 14 September 2007 /
Published online: 20 October 2007
© Humana Press Inc. 2007

Abstract In this work, the effect of adaptation on *P. stipitis* fermentation using acid-pretreated corn stover hydrolyzates without detoxification was examined. Two different types of adaptation were employed, liquid hydrolyzate and solid state agar adaptation. Fermentation of 12.5% total solids undetoxified acid-pretreated corn stover was performed in shake flasks at different rotation speeds. At low rotation speed (100 rpm), both liquid hydrolyzate and solid agar adaptation highly improved the sugar consumption rate as well as ethanol production rate compared to the wild-type strains. The fermentation rate was higher for solid agar-adapted strains compared to liquid hydrolyzate-adapted strains. At a higher rotation speed (150 rpm), there was a faster sugar consumption and ethanol production for both the liquid-adapted and the wild-type strains. However, improvements in the fermentation rate between the liquid-adapted and wild strains were less pronounced at the high rotation speed.

Keywords Corn stover · Ethanol · Sulfuric acid · *Pichia stipitis* · Adaptation · Detoxification

Introduction

Economically feasible processes for biomass conversion to ethanol requires the fermentation of the sugars generated in the pretreatment and hydrolysis steps. In agricultural residues and hardwoods, xylose constitutes about 45% of the total sugars, and therefore xylose conversion to ethanol is important for high yields. Dilute acid hydrolysis of cellulosic biomass generates inhibitory compounds such as furfural, hydroxymethyl furfural, and acetic acid [1]. These inhibitors affect the ability of yeasts to ferment the hydrolyzates, and therefore a detoxification step is usually included in fermenting acid

F. K. Agbogbo (✉) · F. D. Haagensen (✉) · D. Milam · K. S. Wenger
Novozymes North America, 77 Perry Chapel Church Road, P.O. Box 576, Franklinton, NC 27525, USA
e-mail: fkagbo@yahoo.com
e-mail: fhaa@novozymes.com

hydrolyzates [1, 2]. Detoxification may include the use of chemicals [3] and may require additional process steps [4, 5], which add up to the total process costs.

Previous studies have identified *Pichia stipitis* as a good candidate for xylose fermentation of agricultural residues that have been subjected to an acid-catalyzed pretreatment process [6–8]. An issue with using this microorganism for fermentation is that the pretreated slurries reportedly have been found to be inhibitory to the growth of *P. stipitis* at high substrate concentrations, reducing the sugar consumption as well as ethanol production rates [9–11]. Ethanol production rates have also been linked to the availability of oxygen to *P. stipitis* during fermentation of synthetic media and pretreated lignocellulosic slurries because of the microaerophilic nature of the yeast during ethanol metabolism [12–15].

As an alternative to detoxification methods, improvement in *P. stipitis* ability to grow and ferment in acid-pretreated slurries (through conditioning or adaptation) have been pursued in some studies [16–18]. To our knowledge, there has been no study on how aeration (agitation) affects the improvements in fermentation observed from adaptation. This study looks at how aeration (agitation) affects fermentation speed in adapted and unadapted strains of *P. stipitis*.

Materials and Methods

Microorganism and Medium

Stock culture of *P. stipitis* CBS 6054 was grown on yeast extract, peptone, and xylose agar plates at 30 °C for 3 days. The agar plates contain 10 g/L yeast extract, 20 g/L peptone, 20 g/L xylose, and 20 g/L agar. Colonies from the plates were grown overnight in a filter-sterilized fermentation medium containing 1.7 g/L yeast nitrogen base (without amino acid or ammonium sulfate), 2.27 g/L urea, 6.56 g/L peptone, and 20 g/L xylose. Nutrient solution (50× the concentration used) was prepared by dissolving 1.7 g of yeast nitrogen base, 2.27 g of urea, and 6.56 g of peptone in 20 mL of water.

Hydrolysis of Dilute Acid-pretreated Corn Stover

The pretreatment conditions for the dilute H_2SO_4 acid-pretreated corn stover used in this study have been reported elsewhere [19]. Acid-pretreated corn stover (12.5% total solids) was neutralized with NH_4OH and hydrolyzed with Celluclast 1.5 L (15 filter paper units/g total solids [TS]) and Novozyme 188 (16.8 cellobiase units/g TS) at 50 °C and pH 5.0 for 48 h. The hydrolyzate was neutralized to pH 6.0 and filter sterilized.

Adaptation

Liquid adaptation was performed by growing cells overnight in the filter-sterilized corn stover hydrolyzate. Solid agar adaptation was performed by growing cells on agar plates containing 10 g/L yeast extract, 20 g/L peptone, 20 g/L agar, and corn stover hydrolyzate.

Fermentation

Fermentations were performed in sterile 125-mL Erlenmeyer flasks (with 0.2 μm vent cap) in an air-shaker incubator at 30 °C at the speed of 100 rpm [A] and 150 rpm [B]. Each Erlenmeyer flask contained 50 mL of corn stover hydrolyzate, 1 mL of nutrient solution,

and 2 mL of inoculum (initial cell concentration 2 g/L), and 1.5 ml of phosphate buffer. Samples were taken from the Erlenmeyer flasks at different time intervals, centrifuged, and put in high-performance liquid chromatography (HPLC) vials. Separation and quantification of sugars and ethanol were performed using HPLC analysis with a Biorad® HPX-87H column at 60 °C and RI detection at 40 °C. The mobile phase was 5 mM H_2SO_4 with a flow rate of 0.5 mL/min.

Results and Discussion

Comparison of Wild Strains and Liquid-adapted Strains of *Pichia stipitis*

The performance of the wild-type (unadapted) and liquid hydrolyzate-adapted strains of *P. stipitis* was compared on 12.5% corn stover hydrolyzate at 100 rpm (Fig. 1). The liquid-adapted strains used glucose at a faster rate compared to the unadapted strains. After 96 h of fermentation, the liquid-adapted strains were beginning to use xylose, while the wild strains did not consume any of the xylose. Because xylose consumption begins after glucose is consumed [12], a faster glucose consumption rate with the liquid-adapted strains allowed *P. stipitis* to start consuming xylose earlier than the wild strain. Therefore, a longer fermentation time will be required to use all the sugars in the wild strains compared to the liquid-adapted strains. A complete consumption of xylose will require fermentation past the 96 h used in this study. The ethanol production rate in the liquid-adapted strain was also higher than the unadapted strains. Our observation is similar to results obtained from previous studies on hydrolyzates [16–18].

Comparison of Wild Strains and Solid Agar-adapted Strains of *Pichia stipitis*

Fermentation results for the unadapted and solid agar-adapted strains of *P. stipitis* on 12.5% corn stover hydrolyzate at 100 rpm are shown in Fig. 2. The solid agar adaptation improved both the sugar consumption rate as well as the rate of ethanol production. The solid agar-

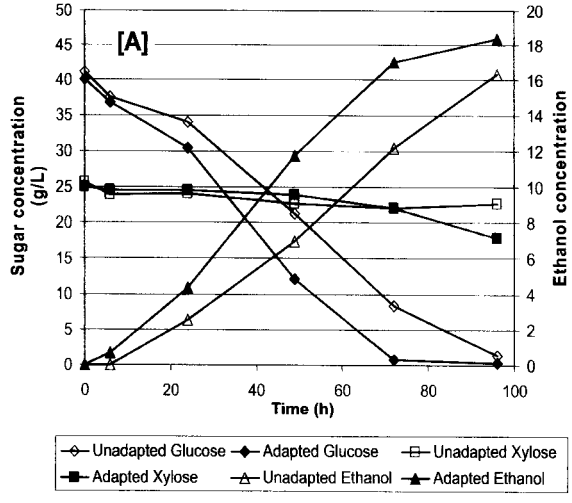


Fig. 1 Comparison of fermentation results from unadapted strains and liquid-adapted strains of *P. stipitis* at 100 rpm

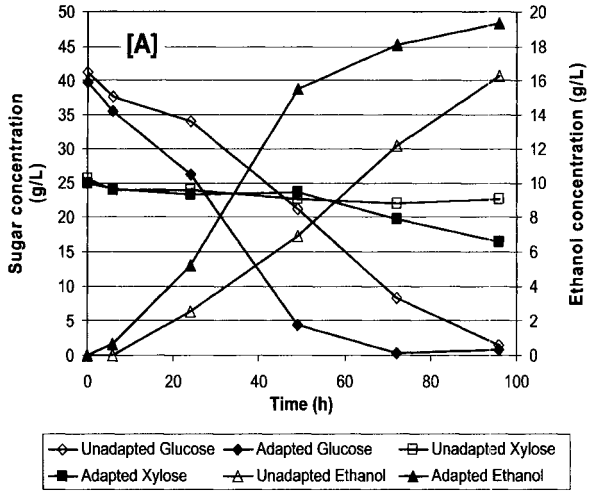


Fig. 2 Comparison of fermentation results from unadapted strains and solid agar-adapted strains of *P. stipitis* at 100 rpm

adapted strains started using xylose after 96 h of fermentation, while the wild strains did not consume xylose. In this study, fermentation was stopped at 96 h, which is not sufficient time for complete sugar utilization at 100 rpm. The conversion of all the sugars to ethanol will require less time with the solid agar-adapted strains compared to the wild strains. The observed increased rate of substrate utilization and ethanol production using solid agar adaptation was higher than the results for liquid-adapted strains.

Comparison of Wild Strains and Liquid-adapted Strains at Optimized Conditions

The fermentation results for the wild stains and liquid-adapted strains of *P. stipitis* on 12.5% hydrolyzate at 150 rpm rotation speed are shown in Fig. 3. The difference in fermentation speed between the wild and liquid-adapted strains were minimal at 150 rpm. The presence

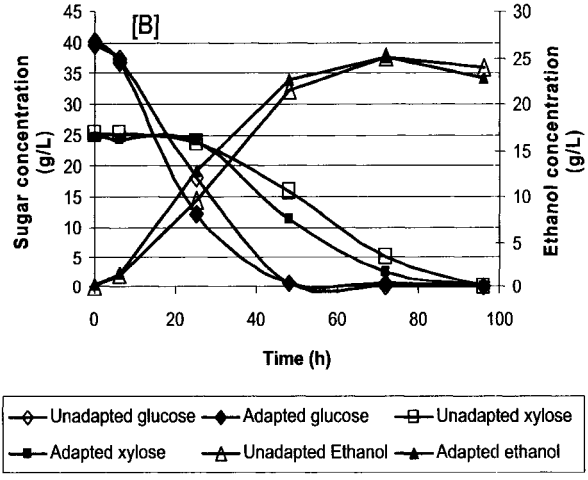


Fig. 3 Comparison of fermentation results from unadapted strains and liquid-adapted strains of *P. stipitis* at 150 rpm

of oxygen enhances the ability of *P. stipitis* to cope with inhibitory compounds in undetoxified corn stover. A summary of the fermentation results are shown in Table 1. From Table 1, liquid and solid agar adaptation increased the sugar consumed from 64 to 72% at 100 rpm after 96 h of fermentation. However, when rotation speed in the flask was increased to 150 rpm, 92% of the total sugar was consumed within 72 h of fermentation.

The sugar consumption rates and ethanol production for both the wild and liquid-adapted strains of *P. stipitis* were higher at 150 rpm rotation speed compared to 100 rpm. The high sugar consumption and ethanol production rate at 150 rpm is attributed to higher aeration and good mixing. Because xylose conversion starts after glucose is consumed, a faster glucose consumption reduces the time it takes for xylose consumption to begin and therefore reduces the total time it takes to complete fermentation. At rotation speeds of 100 rpm where aeration was low, it took a longer time to complete glucose consumption, and therefore xylose consumption could not start in wild strains.

In a recent study, it was found that a high initial cell concentration increased the rate of xylose utilization and ethanol formation in *P. stipitis* [20]. Results from our previous work [20] and this work suggest that there are two options available for using *P. stipitis* for biomass fermentation. The first option is to operate at suboptimal conditions of low aeration where adaptation or a high initial cell concentration improves the speed of the fermentation. The second option is to operate at optimal fermentation conditions where microaerophilic conditions need to be maintained. Choosing between these two options under industrial conditions will require cost benefit analysis to determine the most viable option.

Conclusion

Adaptation of *P. stipitis* to both liquid hydrolyzate and agar resulted in an increase in sugar consumption and ethanol production in undetoxified acid-pretreated corn stover. However, the improvements observed in the fermentation rate were less pronounced at rotation speeds of 150 rpm compared to 100 rpm in shake flask experiments. At less optimal conditions of aeration (100 rpm), adaptation significantly improved fermentation rate. However, at increased aeration rates (150 rpm), the improvements in fermentation because of liquid adaptation were less pronounced. In using *P. stipitis* for the fermentation of biomass hydrolyzates, adaptation could be used to improve fermentation rate at less aeration rates, but at optimal aeration rates, the benefits of adaptation seems to be less pronounced.

Table 1 Summary of fermentation results.

Substrates	Unadapated (100 rpm)	Liquid adapted (100 rpm)	Solid adapted (100 rpm)	Unadapted (150 rpm)	Liquid adapted (150 rpm)
Ethanol concentration (g/L)	16.3±0.51	18.4±0.20	19.4±0.12	25.0±0.28	25.1±0.21
Ethanol yield (g ethanol/g sugars consumed)	0.38±0.01	0.39±0.01	0.41±0.01	0.42±0.01	0.41±0.01
Fermentation time (h)	96	96	96	72	72
Sugar consumed (%)	64±2	72±2	73±0	92±1	95±0

All errors are±1 SD

Fermentations were performed using 50 mL media in 125-mL Erlenmeyer flasks at 30 °C in a shaker incubator at 100 and 150 rpm.

Acknowledgment This investigation was funded by the US DOE project managed by Abengoa Bioenergy R&D. The authors thank the sponsors for their support.

References

1. Palmqvist, E., & Hahn-Hägerdal, B. (2000). *Bioresource Technology, 74*, 17–24.
2. Persson, P., Andersson, J., Gorton, L., Larsson, S., Nilvebrant, N. O., & Jonsson, L. J. (2002). *Journal of Agricultural and Food Chemistry, 50*, 5318–5325.
3. Van Zyl, C., Prior, B. A., & du Preez, J. C. (1988). *Applied Biochemistry and Biotechnology, 17*, 357–369.
4. Clark, T. A., & Mackie, K. L. (1984). *Journal of Chemical Technology and Biotechnology, 34B*, 101–110.
5. Tran, A. V., & Chambers, R. P. (1986). *Enzyme and Microbial Technology, 8*, 439–444.
6. Chandrakant, P., & Bisaria, V. S. (1998). *Critical Reviews In Biotechnology, 18*, 295–331.
7. Hahn-Hagerdal, B., Karhumaa, K., Fonseca, C., Spencer-Martins, I., & Gorwa-Grauslund, M. F. (2007). *Applied Microbiology and Biotechnology, 74*, 937–953.
8. Lee, J. (1997). *Journal of Biotechnology, 56*, 1–24.
9. Amartey, S., & Jeffries, T. (1996). *World Journal of Microbiology & Biotechnology, 12*, 281–283.
10. Delgenes, J. P., Moletta, R., & Navarro, J. M. (1996). *Enzyme and Microbial Technology, 19*, 220–225.
11. Fenske, J. J., Hashimoto, A., & Penner, M. H. (1998). *Applied Biochemistry and Biotechnology, 73*, 145–157.
12. Agbogbo, F. K., Coward-Kelly, G., Torry-Smith, M., & Wenger, K. S. (2006). *Process Biochemistry, 41*, 2333–2336.
13. Laplace, J. M., Delgenes, J. P., Moletta, R., & Navarro, J. M. (1991). *Applied Microbiology and Biotechnology, 36*, 158–162.
14. Roberto, I. C., Demancilha, I. M., Felipe, M. G. A., Silva, S. S., & Sato, S. (1994). *Arquivos de Biologia e Tecnologia, 37*, 55–63.
15. Skoog, K., Jeppsson, H., & Hahnhagerdal, B. (1992). *Applied Biochemistry and Biotechnology, 34–5*, 369–375.
16. Amartey, S., & Jeffries, T. (1996). *World Journal of Microbiology & Biotechnology, 12*, 281–283.
17. Nigam, J. N. (2001a). *Journal of Applied Microbiology, 90*, 208–215.
18. Nigam, J. N. (2001b). *Journal of Biotechnology, 87*, 17–27.
19. Schell, D. J., Farmer, J., Newman, M., & McMillan, J. D. (2003). *Applied Biochemistry and Biotechnology, 105–108*, 69–85.
20. Agbogbo, F. K., Coward-Kelly, G., Torry-Smith, M., Wenger, K. S., & Jeffries, T. W. (2007). *Applied Biochemistry and Biotechnology, 136–140*, 653–662.

Appl Biochem Biotechnol (2008) 145:59–67
DOI 10.1007/s12010-007-8054-6

Bioethanol Production from Uncooked Raw Starch by Immobilized Surface-engineered Yeast Cells

Jyh-Ping Chen · Kuo-Wei Wu · Hideki Fukuda

Received: 9 May 2007 / Accepted: 14 September 2007 /
Published online: 4 October 2007
© Humana Press Inc. 2007

Abstract Surface-engineered yeast *Saccharomyces cerevisiae* codisplaying *Rhizopus oryzae* glucoamylase and *Streptococcus bovis* α-amylase on the cell surface was used for direct production of ethanol from uncooked raw starch. By using 50 g/L cells during batch fermentation, ethanol concentration could reach 53 g/L in 7 days. During repeated batch fermentation, the production of ethanol could be maintained for seven consecutive cycles. For cells immobilized in loofa sponge, the concentration of ethanol could reach 42 g/L in 3 days in a circulating packed-bed bioreactor. However, the production of ethanol stopped thereafter because of limited contact between cells and starch. The bioreactor could be operated for repeated batch production of ethanol, but ethanol concentration dropped to 55% of its initial value after five cycles because of a decrease in cell mass and cell viability in the bioreactor. Adding cells to the bioreactor could partially restore ethanol production to 75% of its initial value.

Keywords Bioethanol · Immobilized cells · Recombinant cells · Bioreactor

Introduction

Bioethanol produced from biomass resources by fermentation is the most promising biofuel and the starting material of various chemicals. Starch is a cheap, clean, nontoxic, renewable carbon source for bioethanol production [1]. In the process currently employed for industrial-scale ethanol production from starchy materials, starch is first hydrolyzed by adding a liquefying enzyme, α-amylase (EC 3.2.1.1), to avoid gelatinization and then

J.-P. Chen (✉) · K.-W. Wu
Department of Chemical and Materials Engineering, Chang Gung University, Kwei-San, Taoyuan 333 Taiwan, Republic of China
e-mail: jpchen@mail.cgu.edu.tw

H. Fukuda
Division of Molecular Science, Graduate School of Science and Technology, Kobe University, Nada-ku, Kobe 657-8501, Japan

cooked at high temperature (140–180 °C). The liquefied starch is then hydrolyzed to glucose with a saccharifying enzyme, glucoamylase (EC 3.2.1.3). Finally, the glucose is converted to ethanol by yeast cells [2]. Traditional processes for bioethanol production from starch are expensive. There are two main reasons for the high costs, one being that as the yeast *Saccharomyces cerevisiae* cannot utilize starchy materials, large amounts of amylolytic enzymes need to be added. On the other hand, the starchy materials need to be cooked at a high temperature to obtain a high ethanol yield.

To improve the conventional high-temperature-cooking fermentation system, efficient processes for one-step bioconversion of starch into ethanol have been developed. Starch-utilizing yeast displaying amylolytic enzymes on the cell surface have been constructed for producing ethanol from soluble starch at high yield using a flocculating *S. cerevisiae* strain displaying *Rhizopus oryzae* glucoamylase on the cell surface [3–5]. Further improved ethanol productivity was reported by developing yeast strains that display *R. oryzae* glucoamylase and codisplay or secrete *Bacillus stearothermophilus* α-amylase [6]. Direct ethanol production in a single step was also performed using low-temperature-cooked corn starch as the sole carbon source instead of soluble starch using a yeast strain displaying only glucoamylase on the cell surface or yeast strains displaying glucoamylase and either codisplaying or secreting α-amylase [7]. These strains cannot, however, ferment raw starch to ethanol. Recently, instead of the *B. stearothermophilus* α-amylase, α-amylase from the lactic acid bacterium *Streptococcus bovis* 148 was codisplayed with *R. oryzae* glucoamylase on the surface of a yeast strain by using the C-terminal half of α-agglutinin and the flocculation functional domain of Flo1p as anchor proteins [8]. Extracellular α-amylase secreted from *S. bovis* 148 is known to have a strong ability to hydrolyze and be adsorbed onto raw corn starch [9]. This recombinant yeast, YF207/pGA11/pUFLA, not only can hydrolyze raw starch and ferment ethanol in a short time but also keep the flocculation ability for convenient immobilization in a porous carrier.

Cell immobilization is an effective method of improving the efficiency of substrate utilization and productivities of various fermentation processes. The concept of cell immobilization provides a promising strategy for the use of recombinant yeast cells in a bioreactor for easy scale up and industrial production of bioethanol. However, to use this technology in fuel ethanol production, the immobilized carrier must be cheap, and cell immobilization should be achievable with minimal additional cost. In addition, the carrier should preferentially be also biodegradable and renewable considering the nature of intended purpose of its fermentation product. Loofa sponge is available in abundance at lower prices and is an environment friendly material with sustainable sourcing. This natural plant sponge consists of a fibrous network and can be obtained from the dried fruit of *Luffa cylindrica*. It was found to be a very economical and excellent support matrix for immobilization of both nonflocculating and flocculating cells because of its high porosity, high specific pore volume, stable physical properties, nontoxicity, and low cost [10, 11]. This could be promising for achieving large-scale and economical production of bioethanol by immobilized yeast cells.

Although genetically engineered yeast cells has been used for direct production of ethanol from raw starch, only free cell systems have been studied with no data on reusability, and few immobilized cell systems have been reported [12]. In the present study, we have developed a process for direct production of bioethanol from insoluble raw starch using surface-engineered *S. cerevisiae*. The flocculating recombinant yeast strain codisplaying α-amylase and glucoamylase on its surface could be conveniently immobilized within the loofa sponge at high cell density for direct production of bioethanol in a packed-bed bioreactor.

Materials and Methods

Microorganism, Media, and Free Cell Fermentation

A genetically engineered *S. cerevisiae* strain YF207/pGA11/pUFLA coexpressing the glucoamylase from *R. oryzae* and α-amylase from *S. bovis* on cell surface was used in the experiment [8]. Yeast cells were aerobically grown in 100 mL of SDC medium (6.7 g/L yeast nitrogen base without amino acids [Difco] with appropriate amino acids and nucleotides, 20 g/L glucose, and 20 g/L casamino acids) for cultivation under selective condition at 30°C and 150 rpm for 48 h. The cell pellet collected by centrifugation at 6,000×*g* for 10 min was used to inoculate 100 mL YPS medium (10 g/L yeast extract, 20 g/L polypeptone, and 200 g/L insoluble raw starch). Ethanol fermentation from uncooked insoluble starch was carried out at 30 °C under anaerobic condition with agitation at 150 rpm for 240 h. For repeated batch fermentation, the flocculated cells were separated from the culture broth by centrifugation at 6,000×*g* for 10 min and replaced with 100 mL fresh YPS medium. The initial cell density was adjusted to 10 to100 g cell dry weight (CDW) per liter. The dry weight of cells corresponds to 0.15 times the wet weight of cells.

Fermentation with Immobilized Cells in a Bioreactor

Loofa sponge was cut from the peripheral part of the dried fruit of *L. cylindrica* with 1×1×12 cm size and soaked in deionized (DI) water for 24 h followed by extensively washing under running DI water. Three pieces of loofa sponge were weighed (6 g) after drying at 70 °C for 24 h and spirally packed into a column (diameter=3 cm, length= 15 cm). For cell immobilization, 50 g CDW/L yeast cells in 200 mL YP medium (10 g/L yeast extract and 20 g/L polypeptone) was placed in a 250-mL flask, and the cell-containing medium was pumped through the column by a peristaltic pump. The void in the reactor was calculated to be 71.4±7.2%. The recirculation flow rate was adjusted from 10 to 35 mL/min. Cell concentration in the flask was monitored with time to determine the extent of immobilization and the immobilization efficiency (defined as the mass of cells immobilized divided by that of cells added). For fermentation, 200 mL YPS medium was pumped through the column containing the immobilized cells at 20 mL/min after loading the column at the optimum flow rate for immobilization. For repeated batch fermentation with the immobilized cells, the whole culture broth was removed and replaced with 200 mL fresh YPS medium every 7 days. The YPS medium bottle was stirred at 150 rpm to avoid settling of raw starch, and fermentation was carried out anaerobically at 30 °C.

Measurement of Starch and Ethanol Concentration

Cells were separated from the fermentation broth by centrifugation at 6,000 rpm for 10 min. The supernatant was removed and determined for ethanol concentration by gas chromatograph (model GC-8A; Shimadzu Seisakusho, Kyoto, Japan), fitted with a flame-ionization detector and a glass column (3.0 mm×3.1 m) packed with Unisole 3000 (GL Science, Tokyo, Japan). The conditions for analysis are: column temperature 210 °C, temperature of injector and detector 270 °C, and nitrogen carrier gas flow rate 25 mL/min.

For determination of starch concentration, starch was first hydrolyzed with glucoamylase to glucose. Glucoamylase from *Aspergillus niger* (6,100 U/mL, Sigma) was used for measurement of starch concentration after diluted 100 times with distilled water. Culture broth of 0.1 mL and 0.8 mL DI water were preincubated at 30 °C for 5 min before adding

0.1 mL enzyme solution, and the mixture was incubated at the same temperature for 30 min by shaking at 150 rpm. The reaction was stopped by boiling the mixture for 10 min and centrifuged at×10,000 rpm for 1 min, and the concentration of glucose was determined using a glucose test kit from Human (Glucose Liquicolor). Glucose concentration in the culture broth was similarly determined using the glucose test kit.

Results and Discussion

Fermentation with Free Yeast Cells

The direct fermentation using surface-engineered recombinant *S. cerevisiae* strain YF207/pGA11/pUFLA, which coexpresses the glucoamylase from *R. oryzae* and α-amylase from *S. bovis*, can directly produce ethanol from raw starch. To study the influence of cell concentration on the production of ethanol, fermentation runs were carried out with cell concentrations ranging from 10 to 100 g/L. As shown in Table 1, ethanol concentration increases with increasing cell concentration until reaching 50 g/L, after which no statistical difference ($p<0.05$, one-way analysis of variance) in ethanol concentrations was found between runs carried out with higher cell concentrations. The starch consumption rate and ethanol productivity also shows similar dependence on cell concentrations. However, the ethanol yield from sugar consumed ($Y_{P/S}$) was independent of cell concentration ranging from 0.39 to 0.49, which corresponds to 80 to 96% of the theoretical yield from sugar (0.51 g of ethanol produced per g of sugar consumed). Taken together, 50 g/L was chosen as the best cell density under the experiment conditions, and this value was used in the following studies.

To test the stability of the ethanol production capability of recombinant yeast cells, the cells were recovered by low-speed centrifugation after 7 days and reused for fermentation for up to seven cycles. As shown in Fig. 1, the concentration of ethanol in each consecutive cycle shows no statistical difference ($p<0.05$) between each repeated runs and ranging from 48 to 58 g/L (day 7) for each fermentation cycle.

Cell Immobilization

With the excellent reusability of free recombinant yeast cells, using immobilized cells in a bioreactor could facilitate the reuse of cells and scale up the process. The immobilization of

Table 1 Effects of cell density on ethanol fermentation with free recombinant yeast cells at day 10.

Cell density (g CDW/L)	Starch consumption rate (g starch/h)	Ethanol concentration (g/L)	$Y_{P/S}$[a]	R_P (g h^{-1} L^{-1})[b]
100	0.741	57.12±4.12*	0.40	0.238
75	0.765	55.43±3.45*	0.39	0.231
50	0.741	56.11±4.60*	0.41	0.234
25	0.680	49.68±1.21	0.39	0.207
10	0.383	34.97±4.68	0.49	0.146

[a] $Y_{P/S}$ Product yield (g ethanol produced/g sugar consumed)

[b] R_P Productivity (g ethanol produced h^{-1} L^{-1})

*No statistical difference, $p<0.05$

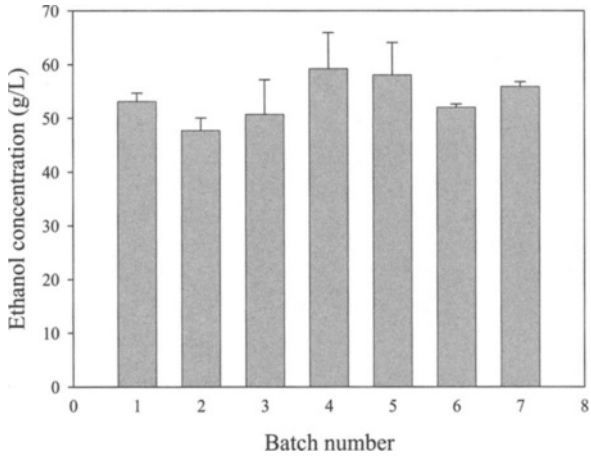


Fig. 1 Repeated batch fermentations with free recombinant yeast cells. Fermentation time for each batch=7 days. Initial cell density=50 g CDW/L

flocculation yeast in a porous carrier is a challenging task considering the size of the flocculated mass. Traditional method for cell immobilization by entrapment in polymeric gel beads is not suitable for construction of fixed-bed bioreactors with the constraints of physical properties for these gel matrices. Alternatively, for cell immobilization by adsorption, the carrier must be highly porous with large pore size to accommodate the flocculated cells. However, the carrier must also have good mechanical strength to withstand the high pressure drop associated with a packed-bed bioreactor. The loofa sponge with pore size around 800 μm was chosen in this study. During the immobilization step, cell suspension was continuously circulated through the column from the top for cell attachment to the loofa sponge. As can be seen from Fig. 2, the efficiency of cell immobilization could reach 100% within 120 min irrespective of flow rates. However, for flow rates above 30 mL/min, cell immobilization could be completed within 20 min. This flow rate was thus chosen as the optimum flow rate for cell immobilization and used in all future fermentation studies.

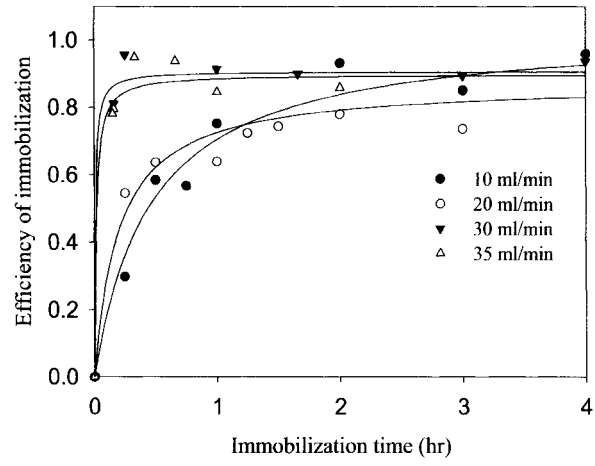


Fig. 2 The effects of recirculation flow rate on cell immobilization efficiency in a packed-bed bioreactor. Cell density=50 g/L

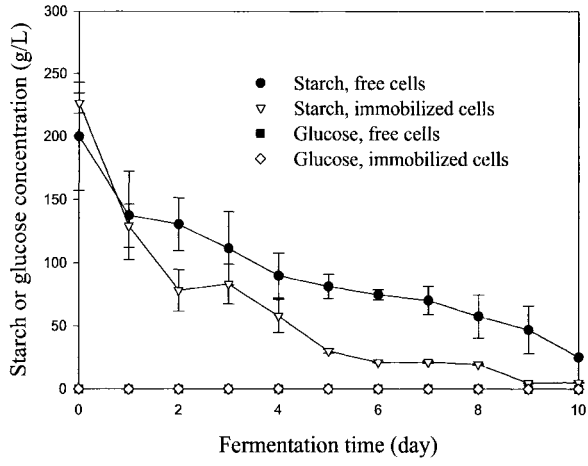


Fig. 3 Starch and glucose concentrations during batch fermentation with free and immobilized recombinant yeast cells. Cell density=50 g/L

Fermentation with Immobilized Yeast Cells

Fermentation by immobilized cells was studied in the fixed-bed bioreactor by circulating the starch-containing medium (YPS medium) through the column at 20 mL/min under anaerobic condition. As can be seen from Fig. 3, starch concentration decreases quickly to 0 after 9 days for the immobilized cell system, and the starch consumption rate for the immobilized cells system is 50% higher than that for the free cell system (1.116 vs 0.741) using the same cell density (50 g/L) for fermentation. Glucose concentration in the fermentation broth remained at close to 0 throughout the fermentation period for both systems (Fig. 3). Increase in ethanol concentrations also shows similar trends for both systems up to day 5 where ethanol concentration reaches 42 g/L, and there is no statistical difference in ethanol concentration for both systems up to day 7 ($p<0.05$). However, no further increase in ethanol concentration was found for the immobilized cell system after day 5. In contrast, the ethanol concentration continues to increase throughout the

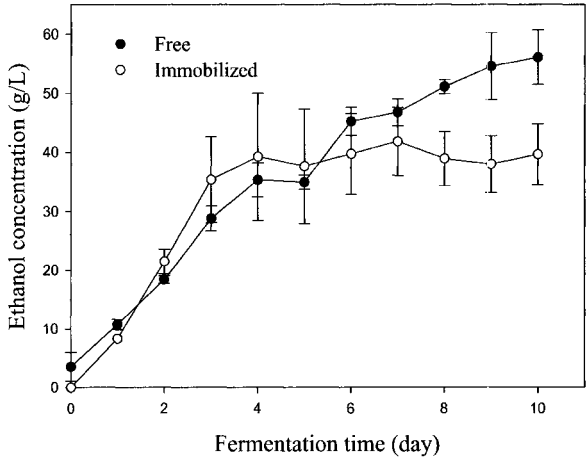


Fig. 4 Ethanol concentrations during batch fermentation with free and immobilized recombinant yeast cells. Cell density=50 g/L

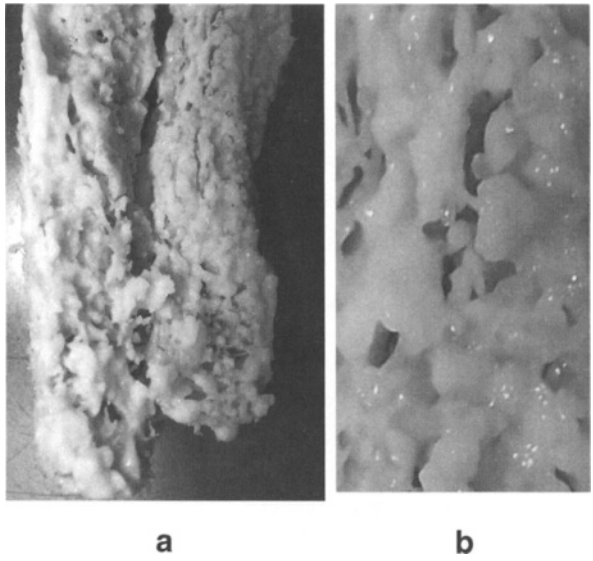


Fig. 5 Attachment of starch granules to the **a** center and **b** the surface of loofa sponge during fermentation with immobilized recombinant yeast cells

fermentation period for the free cell system, and the ethanol concentration reaches 53 g/L at day 7 (Fig. 4). The productivities of ethanol were 0.316 and 0.249 g h^{-1} L^{-1} for free and immobilized cells systems at day 7, respectively.

It is not reasonable to expect a higher starch consumption rate for the immobilized cell system without a concomitant increase in ethanol concentration. Because raw starch granules will be trapped within the pores of the loofa sponge with time when circulated through the carrier, it can be inferred that the amount of starch consumed and rate of starch consumption observed for the immobilized system will be overestimated. During initial fermentation up to day 5, the immobilized cell system is as effective as the free cell system for producing ethanol from raw starch (Fig. 4). Nonetheless, limited diffusion of starch to the immobilized cells at the later stage of fermentation, where the cell surface was covered with stationary starch granules, will limit the supply of starch and hydrolysis reaction to

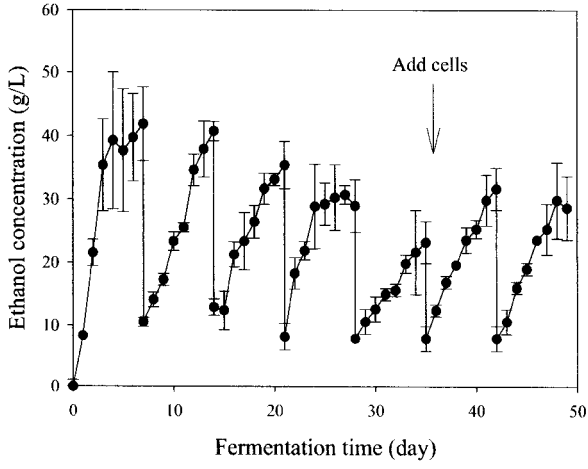


Fig. 6 Repeated batch fermentation with immobilized recombinant yeast cells. Fermentation time for each batch=7 days. Initial cell density=50 g/L. Cells were added at day 35

Table 2 Summary of repeated batch fermentation with immobilized recombinant yeast cells.

Batch number	Starch consumption rate (g starch/h)	Ethanol concentration (g/L)	$Y_{P/S}$[a]	R_P (g h^{-1} L^{-1})[b]
1	1.116	41.81±5.78	0.28	0.249
2	0.893	40.75±1.47	0.34	0.243
3	0.833	35.40±3.74	0.32	0.211
4	0.720	28.94±4.18	0.31	0.172
5	0.697	23.23±3.31	0.25	0.138
6	0.803	31.56±3.30	0.30	0.187
7	0.774	28.63±5.01	0.30	0.170

Fermentation time for each batch=7 days. Initial cell density=50 g/L. Cells were added after batch 5.

[a] $Y_{P/S}$ Product yield (g ethanol produced/g sugar consumed)

[b] R_P Productivity (g ethanol produced h^{-1} L^{-1})

produce glucose. This could be inferred from the appearance of the loofa sponge matrix during fermentation with immobilized cells where white starch granules could be seen to cover the immobilized cells layer in the loofa sponge (Fig. 5). A similar situation will not happen in the case of free cells where starch could be freely contacted with cells by shaking.

Repeated Batch Fermentation with Immobilized Cells

Figure 6 gives the results of repeated batch fermentation with immobilized cells in the bioreactor. Ethanol concentrations decrease with batch numbers, and the ethanol

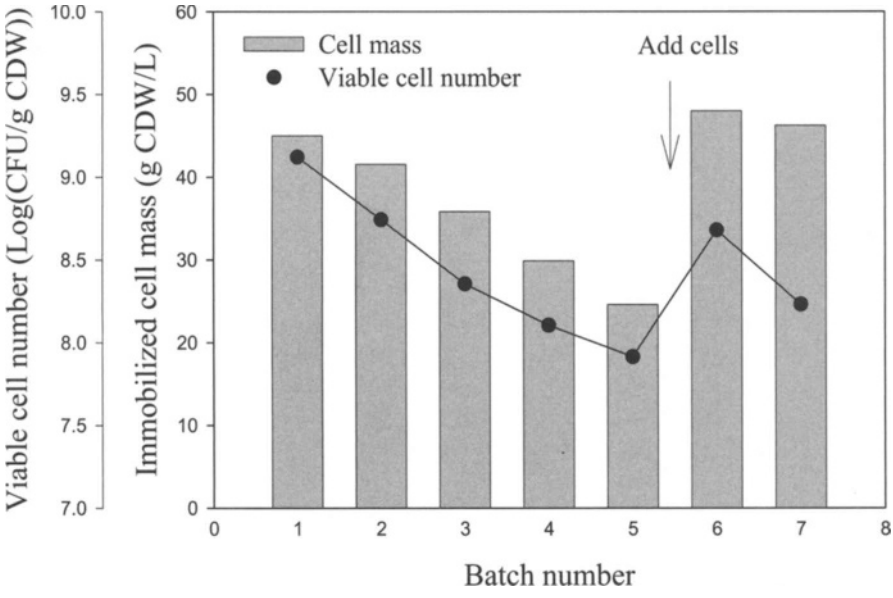


Fig. 7 Cell mass and viable cell number of immobilized recombinant yeast cells during repeated batch fermentation. Fermentation time for each batch=7 days. Initial cell density=50 g/L. Cells were added at day 35. *CDW* Cell dry weight, *CFU* colony-forming unit

concentration after batch 5 drops to 55% of its initial value. Starch consumption rate and ethanol productivity also show similar trends (Table 2). The reasons for diminished ethanol production may arise from loss in cell mass or cell viability. The cell density in the bioreactor after each batch was determined from the amount of cells lost from the carrier and recovered in the culture medium after each batch. The results in Fig. 7 indicates that about 10% cell mass was lost in each run with cell density decreased from 50 to 24.6 g/L at the end of cycle 5. In contrast, the cell viability decreased more than one order from $10^{9.1}$ to $10^{7.9}$ colony-forming unit per g CDW. To compensate for the lost cells, the cell mass was brought to initial value (50 g/L) by immobilizing new cells in the bioreactor at the end of cycle 5. However, the number of viable cells can only be raised to 42% of its initial value with the dead cells left in the bioreactor. Under such condition, ethanol production in cycle 6 could be restored to 75% of that in the first cycle (31.6 g/L; Fig. 6 and Table 2).

References

1. Spencer-Martins, I., & Van Uden, N. (1977). *European Journal of Applied Microbiology, 4*, 29–35.
2. Knox, A. M., du Preez, J. C., & Kilian, S. G. (2004). *Enzyme and Microbial Technology, 34*, 453–460.
3. Kondo, A., Shigechi, H., Abe, M., Uyama, K., Matsumoto, T., & Takahashi, S., et al. (2002). *Applied Microbiology and Biotechnology, 58*, 291–296.
4. Murai, T., Ueda, M., Yamamura, Z. M., Atomi, H., Shibasaki, Y., & Kamasawa, N., et al. (1997). *Applied and Environmental Microbiology, 63*, 1362–1366.
5. Murai, T., Ueda, M., Kawaguchi, T., Arai, M., & Tanaka, A. (1998). *Applied and Environmental Microbiology, 64*, 4857–4861.
6. Shigechi, H., Uyama, K., Fujita, Y., Matsumoto, T., Uedac, M., & Tanaka, A., et al. (2002). *Journal of Molecular Catalysis B: Enzymatic, 17*, 111–222.
7. Shigechi, H., Fujita, Y., Koh, J., Ueda, M., Fukuda, K., & Kondo, A. (2000). *Biochemical Engineering Journal, 18*, 149–153.
8. Shigechi, H., Koh, J., Fujita, Y., Matsumoto, T., Bito, Y., & Ueda, M., et al. (2004). *Applied and Environmental Microbiology, 70*, 5037–5040.
9. Satoh, E., Uchimura, T., Kudo, T., & Komagata, K. (1997). *Applied and Environmental Microbiology, 63*, 4941–4944.
10. Ogbonna, J. C., Liu, Y. C., Liu, Y. K., & Tanaka, H. (1994). *Journal of Fermentation and Bioengineering, 78*, 437–442.
11. Ogbonna, J. C., Mashima, H., & Tanaka, H. (2001). *Bioresource Technology, 76*, 1–8.
12. Kobayashi, F., & Nakamura, Y. (2004). *Biochemical Engineering Journal, 21*, 93–101.

Appl Biochem Biotechnol (2008) 145:69–78
DOI 10.1007/s12010-007-8076-0

Effects of Gene Orientation and Use of Multiple Promoters on the Expression of *XYL1* and *XYL2* in *Saccharomyces cerevisiae*

Ju Yun Bae · José Laplaza · Thomas W. Jeffries

Received: 10 May 2007 / Accepted: 2 October 2007 /
Published online: 24 October 2007
© Humana Press Inc. 2007

Abstract Orientation of adjacent genes has been reported to affect their expression in eukaryotic systems, and metabolic engineering also often makes repeated use of a few promoters to obtain high expression. To improve transcriptional control in heterologous expression, we examined how these factors affect gene expression and enzymatic activity in *Saccharomyces cerevisiae*. We assembled D-xylose reductase (*XYL1*) and D-xylitol dehydrogenase (*XYL2*) in four ways. Each pair of genes was placed in two different tandem (1→2→ or ←1←2), convergent (1→←2), and divergent (←1 2→) orientations in autonomous plasmids. The *TEF1* promoter was used to drive *XYL1* and the *TDH3* promoter to drive *XYL2* in each of the constructs. The effects of gene orientation on growth, transcription, and enzyme activity were analyzed. The transcription level as measured by quantitative PCR (q-PCR) correlated with enzyme activities, but our data did not show a significant effect of gene orientation. To test the possible dilution of promoter strength due to multiple use of the same promoter, we examined the level of expression of *XYL1* driven by either the *TEF1* or *TDH3* promoter when carried on a single copy plasmid. We then co-expressed *XYL2* from either a single or multicopy plasmid, which was also driven by the same promoter. *XYL2* transcript and enzyme expression increased with plasmid copy number, while the expression of *XYL1* was constant regardless of the number of other *TEF1* or *TDH3* promoters present in the cell. According to our data, there is no significant effect of gene orientation or multiple promoter use on gene transcription and translation when genes are expressed from plasmids; however, other factors could affect expression of adjacent genes in chromosomes.

Keywords Yeast · Metabolic engineering · Promoter saturation · Gene orientation · *S. cerevisiae* · Gene expression · Enzyme activities

J. Y. Bae · T. W. Jeffries
Molecular and Environmental Toxicology Center, University of Wisconsin, Madison, WI 53705, USA

J. Laplaza · T. W. Jeffries (✉)
USDA Forest Service, Forest Products Laboratory, 1 Gifford Pinchot Drive, Madison, WI 53726, USA
e-mail: twjeffri@wisc.edu

Present address:
J. Laplaza
Cargill, Minneapolis, MN, USA

Introduction

Yeasts have become important hosts for heterologous gene expression [1]. For optimal metabolic engineering, it is necessary to control gene expression quantitatively. Genome structure and function are known to correlate, and Williams et al. found co-expression of neighboring genes in *Arabidopsis* [2]. This pattern has been observed for many eukaryotic genomes [3–5]. Gene orientation has been suggested as one of the mechanisms for co-expression [2, 6]. For example, effects of divergent gene orientation or tandem orientation can be found in co-expressed genes in plants [7, 8]. Prescott et al. [9] identified transcriptional repression of convergently arranged genes in yeast, which was explained by transcriptional collision. These findings imply that intergenic regions between adjacent genes can have important roles in transcription. Deletion of regions between the two ORFs caused decreased transcription in yeast [10, 11]. In *Saccharomyces cerevisiae* the intergenic region has regulatory function [12, 13] and different base compositions according to the orientation of neighboring ORFs [14].

In the present study, we have manipulated the orientation of the D-xylose reductase (*XYL1*) and D-xylitol dehydrogenase (*XYL2*) genes to model the effect of two different tandem (1→2→ or ←1←2), convergent (1→←2), and divergent (←1 2→) orientations. Two strong promoters were used—translation elongation factor promoter (*TEF1*p) and glyceraldehyde 3-phosphate dehydrogenase promoter (*TDH3*p). *XYL1* and *XYL2* used their own terminator sequences. The effect of gene orientation on growth, transcription, and enzyme activities were analyzed in *S. cerevisiae*.

We also investigated the promoter effectiveness in the condition of multiple use of the same promoter. To test this, we examined the expression level of *XYL1* with co-expression of single or multiple copies of *XYL2*. Both *TEF1*p and *TDH3*p were tested separately. We found increased *XYL2* transcription and enzyme activities of multiple copies of *XYL2* with constant expression and activities of *XYL1*. Both *TEF1*p and *TDH3*p showed the same pattern.

Materials and Methods

Strains, Media, and Cultivation Conditions S. cerevisiae strain L2612 (MATα leu2–3 leu2–112 ura3–52 trp1–298 can1 cyn1 gal$^+$) was used for transformation of all the constructed gene plasmids. Enzymatic manipulation and cloning of DNA were performed as described in Sambrook and Russell [15]. Yeast transformants with *URA3* or *TRP1* selectable markers were cultivated in yeast synthetic complete (YSC) medium containing 6.7 g of yeast nitrogen base/l without amino acids plus 20 g of glucose/l, 20 g of agar/l, and an appropriate mixture of nucleotides and amino acids. Yeast cells were cultured in a 125-ml flask with 50 ml medium at 30°C and 200 rpm.

Plasmid Construction to Test Gene Orientation Polymerase chain reaction (PCR) was used to amplify and create in-frame fusions of D-xylose reductase (*XYL1*) and D-xylitol dehydrogenase (*XYL2*) with the *TEF1* and *TDH3* promoters, respectively. Gene 1 (*TEF1+XYL1*) and 2 (*TDH3+XYL2*) were assembled into two different tandem (1→2→ or 1←2←), convergent (1→←2), and divergent (←1 2→) orientations in pRS316 (*URA3* CEN/ARS) plasmid (Fig. 1). Each construct was sequenced to confirm the structure.

Plasmid Construction to Examine Promoter Dilution XYL1 was amplified and fused with the *TEF1* or *TDH3* promoter by PCR as above. This fragment was then inserted into pRS316

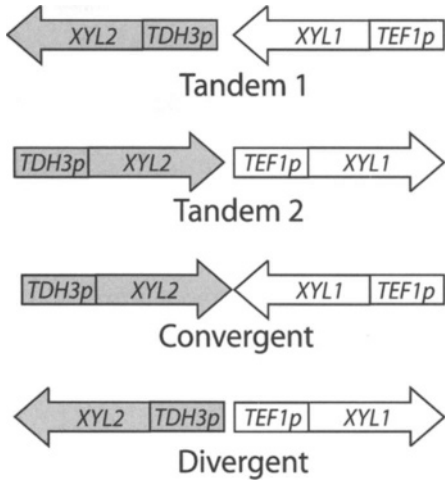


Fig. 1 Four constructs with gene 1 (*TEF1* promoter+*XYL1*) and gene 2 (*TDH3* promoter+*XYL2*). The genes for xylose reductase (*TEF1*+*XYL1*) and xylitol dehydrogenase (*TDH3*+*XYL2*) were assembled into two different tandem (1→2→ or 1←2←), convergent (1→←2), and divergent (←1 2→) orientations in pRS316 (*URA3* CEN/ARS) plasmid. *URA3* was the selectable marker for all constructs

plasmid. *XYL2* was amplified and fused with *TEF1* or *TDH3* promoter by PCR. This fragment was inserted into pRS314 (*TRP1* CEN/ARS) or pRS424 (*TRP1* 2 μm origin; Fig. 5).

Yeast Transformation All yeast transformations were performed as described in Gietz and Woods [16]. Transformants of gene orientation test were selected on yeast synthetic complete (YSC) dropout medium (Ura^-) containing 20 g of glucose/l. Transformants of promoter dilution examination were selected on Ura^-, Trp^- YSC dropout medium containing 20 g of glucose/l.

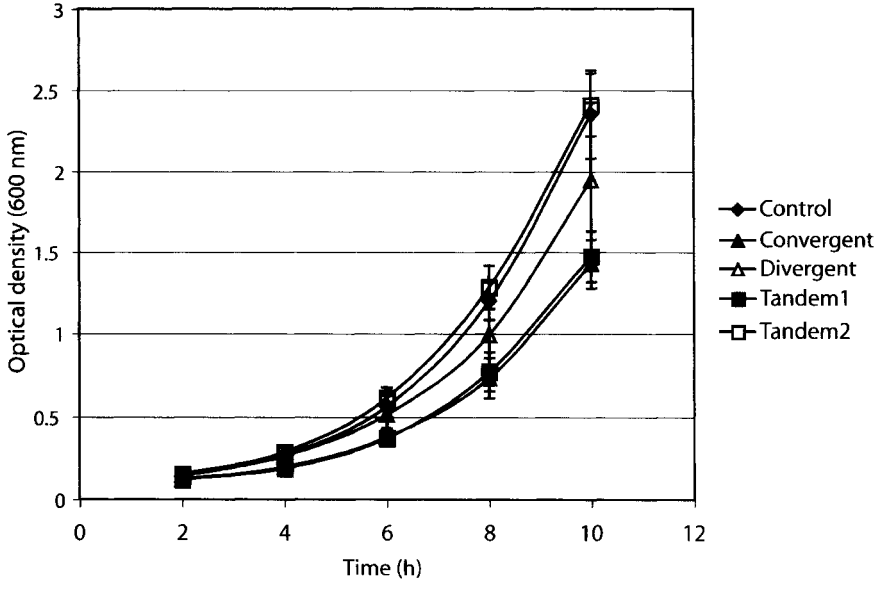


Fig. 2 Growth of strains with different gene orientations. Each stain was cultured in a 125-ml flask with 50 ml medium at 30°C and 200 rpm. OD_{600} value was the mean of three replicates, and *error bar* represents SD

Table 1 Growth rate of each strain of different gene orientations.

Strains	Doubling time[a] (h)
Control	2.7
Tandem1	2.68
Convergent	3.07
Divergent	2.88
Tandem2	2.61

[a] Doubling time (Td)=$(t_2-t_1)/\mu$; $\mu=\ln(cd_2/cd_1)$ (cd_1 Cell density at time t_1, cd_2 cell density at time t_2) cd_1 was OD_{600} value at 4 h (t_1) and cd_2 at 8 h (t_2).

Cell Growth Experiments For the growth rate measurement, overnight cultures were diluted to the initial OD_{600} of 0.1. Three replicates of each strain were performed. Initial cell growth (OD_{600}, <2) was used for calculation of the specific growth rate.

Preparation of RNA Total RNA was prepared from each transformant as described by Rose et al. [17].

Relative Quantitative Reverse Transcriptase-Polymerase Chain Reaction For each RT reaction, 5 μg of total RNA was reverse-transcribed with avian myeloblastosis virus-reverse transcriptase (Promega, Madison, WI). Relative quantitative reverse transcriptase-polymerase chain reaction (RT-PCR) primers were designed to XYL1 (5′-GATACCTTCGT CAATGGCCTTCT-3′ and 5′-TTCGAC GGTGCCGAAGA-3′), XYL2 (5′-CAA GACCGGTGGTTCTGAAGA-3′ and 5′- CCAGTA CATTCCAAAACGACGTT-3′), and *ACT1* (5′-TGGATTCCGGTGATGGTGTT-3′ and 5′- TCAAAATGGCGTGAGGTA GAGA-3′) using Primer Express software (Applied Biosystems). We used SYBR green PCR master mix (Applied Biosystems) and an ABI PRISM 7000 sequence detection system (Applied Biosystems) to perform RT-PCR. PCR conditions were as recommended by the

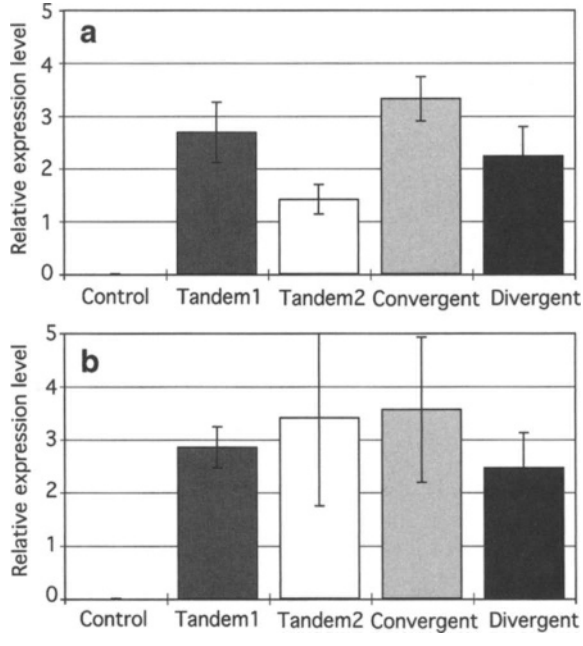


Fig. 3 *XYL1* (**a**) and *XYL2* (**b**) expression in each strain with different gene orientation. Graph represents the average±SD of three replicates

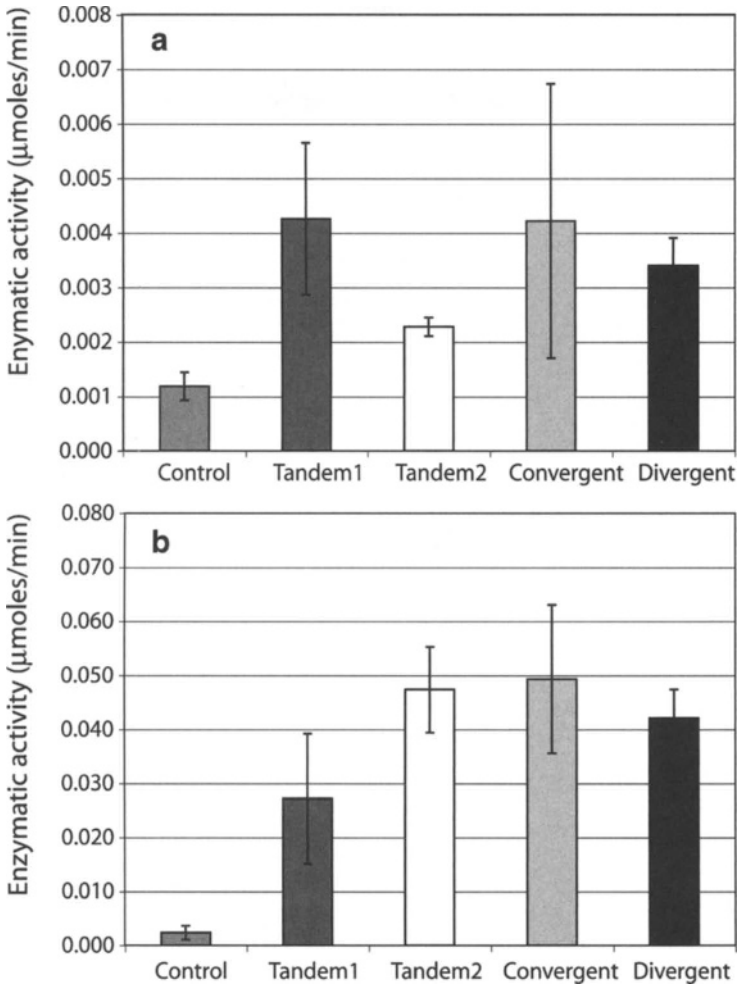


Fig. 4 *XYL1* (**a**) and *2* (**b**) enzyme activities in each strain of different gene orientation. Graph represents the average±SD of three replicates

manufacturer except that one-half of the reaction volume was used: 7.5 pmol of each primer was used in cycles of 50°C for 2 min and 95°C for 10 min, and 40 cycles of 95°C for 15 s and 60°C for 1 min. Relative quantification for copy number of *XYL1* and *XYL2* was performed using both the standard curve method and the comparative C_T method [18]. The C_T value of serial dilution of *Pichia stipitis* genomic DNA (30, 3, 0.3, 0.003, 0.0003, and 0.00003 ng) with *ACT1* primers was used to construct a standard curve. Then, the relative copy numbers of the *XYL1* and *XYL2* were calculated by comparison with *ACT1*. All reactions were performed in triplicate.

Enzymatic Assay Cells were harvested by centrifugation at 10,000×*g* for 10 min. The pellet was washed and suspended in buffer (100 mM phosphate buffer, 1 mM EDTA, 5 mM β-mercaptoethanol [pH 7.0]). The suspended cells were mixed with glass beads (Sigma), vortexed at maximum rate in bursts of 30 to 120 s, and then cooled on ice. The cell debris

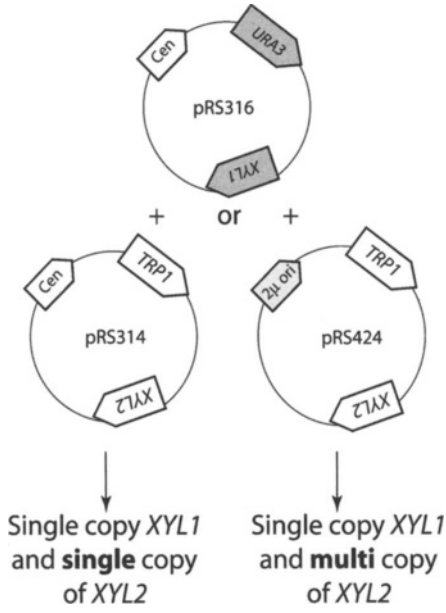


Fig. 5 Experimental strategy to identify the effect of multiple use of same promoter. Each stain has a single copy of *XYL1* with variation of *XYL2* expression. The construct with 2μ *ori* had multicopy gene expression. *TEF1* and *TDH3* promoter were examined separately

and glass beads were separated by centrifugation for 10 min at 15,000×*g*. In vitro activities of xylose reductase (with NADPH and NADH) and xylitol dehydrogenase (with NADH) in the supernatant were determined by using a previously described method [19]. All reactions were performed in triplicate. The unit was μmol min^{-1} mg^{-1}.

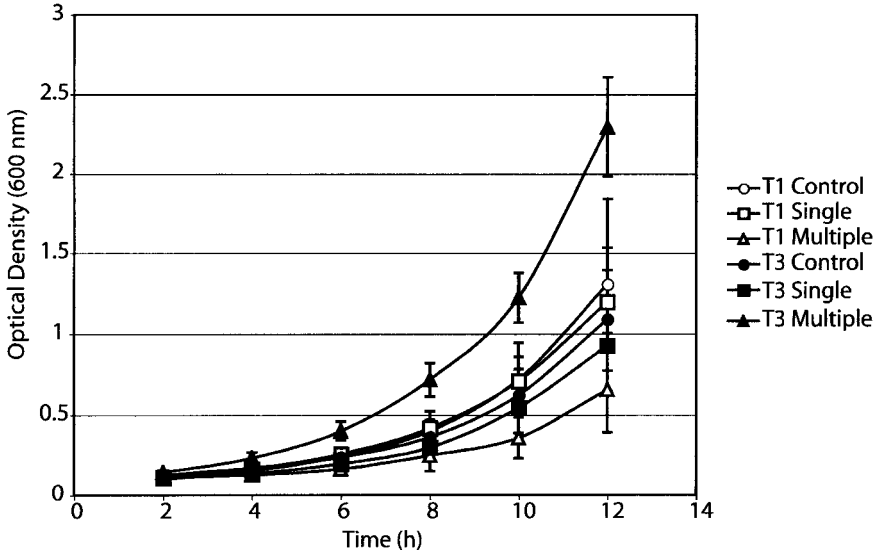


Fig. 6 Growth of each strain with variation of *XYL2* expression. Each stain was cultured in a 125-ml flask with 50 ml medium at 30°C and 200 rpm. OD_{600} value was the mean of three replicates, and the *error bar* represents SD. Every construct had a single copy of *XYL1* with either *TEF1* promoter (T1) or TDH3 promoter (T3). *T1 Control* No XYL2, *T1 single* single copy of XYL2, *T1 Multiple* multicopy of XYL2, *T3 Con* no XYL2, *T3 single* single copy of XYL2, *T3 Multiple* multicopy of XYL2

Table 2 Growth rate of each strain with variation of *XYL2* expression.

Strains	Doubling time[a] (h)
T1Control	4.28
T1Single	4.43
T1Multiple	6.04
T3Control	5.45
T3Single	5.17
T3Multiple	3.6

[a] Doubling time (Td)=$(t_2-t_1)/\mu$; $\mu=\ln(cd_2/cd_1)$ (cd_i Cell density at time t_1, cd_2 cell density at time t_2) cd_1 was OD_{600} value at 8 h (t_1) and cd_2 at 4 h (t_2)

Results and Discussion

Effect of Gene Orientation on Cell Growth, Transcription, and Translation We constructed single copy expression vectors with two genes inserted in four different orientations (Fig. 1). Each of these was transformed into the *S. cerevisiae* host. The control consisted of the host strain carrying the parental vector without any gene inserts. Yeast strains bearing

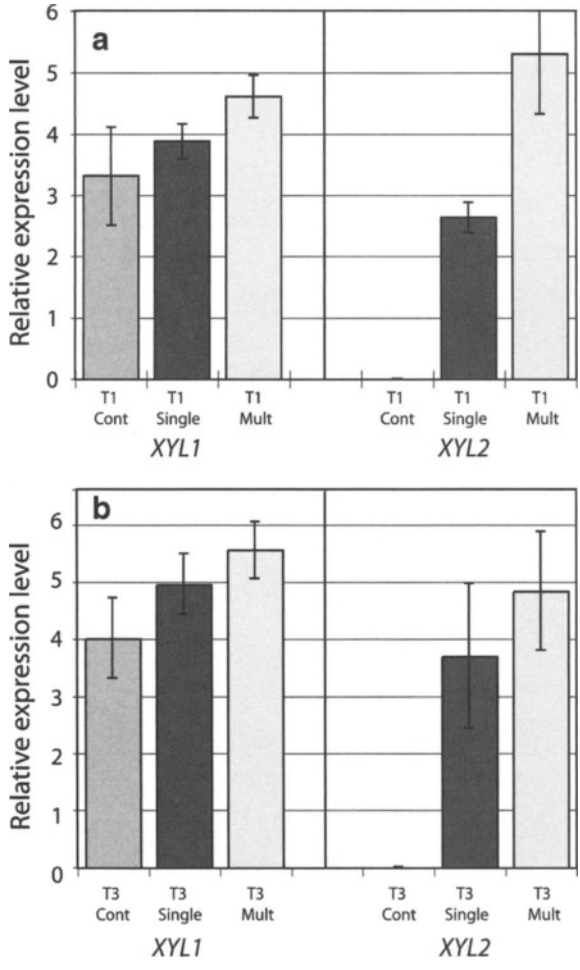


Fig. 7 *XYL1* (**a**) and *2* (**b**) expression in each strain with variation of *XYL2* expression. Graph represents the average±SD of three replicates. Every construct had a single copy of *XYL1* with either *TEF1* promoter (T1) or TDH3 promoter (T3). *T1 Cont* No XYL2, *T1 Single* single copy of XYL2, *T1 Mult* multicopy of XYL2, *T3 Cont* no XYL2, *T3 Single* single copy of XYL2, *T3 Mult* multicopy of XYL2

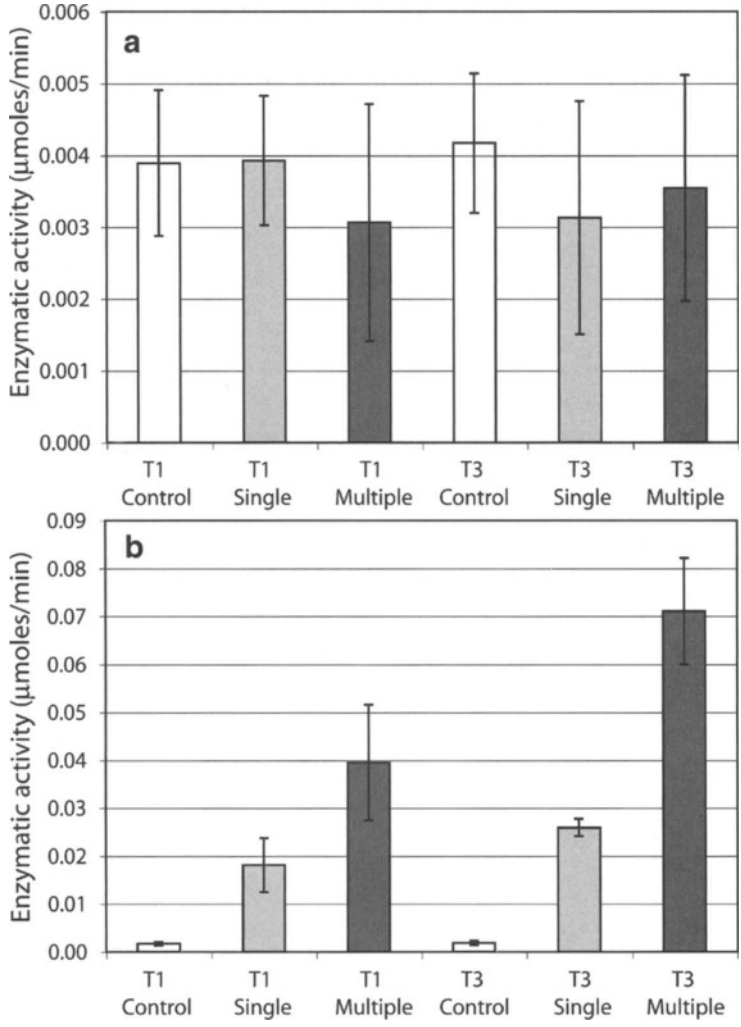


Fig. 8 *XYL1* (**a**) and *2* (**b**) enzyme activities in each strain with variation of *XYL2* expression. Graph represents the average ± SD of three replicates. Every construct had a single copy of *XYL1* with either *TEF1* promoter (T1) or TDH3 promoter (T3). *T1 Control* No XYL2, *T1 Single* single copy of XYL2, *T1 Multiple* multicopy of XYL2, *T3 Control* no XYL2, *T3 Single* single copy of XYL2, *T3 Multiple* multicopy of XYL2

vectors with the divergent (←1 2→) and tandem2 (1←2←) gene orientations showed similar growth rates with the control (Fig. 2). Yeast strains bearing vectors with the convergent (1→←2) and tandem1 orientations (1→2→) showed slightly retarded growth rates compared with the control. Strains with the tandem2 orientation showed the fastest growth rates (doubling time (Td)=2.61 h), and strains with the convergent orientation were the slowest (Td=3.07 h) (Table 1).

We could not detect significant differences in the gene expression profiles of *XYL1* and *XYL2* among these various strains (Fig. 3). *XYL2* enzyme activities were higher than *XYL1*

overall (Fig. 4), but no significant difference could be detected in enzymatic activities among the various orientations.

Effect of Multiple Use of Same Promoter We examined promoter dilution effect using *TEF1* and *TDH3* promoter, separately. Control was carrying single copy of *XYL1* expression vector and no *XYL2* expression vector (Fig. 5). Other stains contained single or multiple copies of the *XYL2* expression vector with single copy of *XYL1* expression vector. Therefore, we could identify if there was any change of *XYL1* expression due to *XYL2* overexpression. Figure 6 and Table 2 show the growth rates of each strain. The strain bearing the *TDH3* promoter with multiple copies of *XYL2* (T3 multiple) showed the highest growth rate (Td=3.6 h). The strain with the *TDH3* promoter with a single copy of *XYL2* (T3 single) had a slow growth rate compared to the T3 multiple strain (Td=5.17 h). The stain bearing the *TEF1* promoter with multicopy vector of *XYL2* (T1 multiple) showed the slowest growth rate (Td=6.04 h). In the case of *TEF1*, the single copy of *XYL2* (T1 single) had faster growth rate compared to T1 multiple (Td=4.43 h). According to these data, overexpression of *XYL2* had different growth effects with each promoter. To determine whether this difference is from the multiple use of the same promoter or other factors, however, will require more studies.

Transcription of *XYL1* and *2* showed an increase in *XYL2* with a multicopy vector bearing *XYL2*, and there was no effect on *XYL1* expression due to *XYL2* overexpression (Fig. 7).

Enzyme activities showed correlation with the transcript expression level for each construct, and *XYL1* had no influence due to co-expression of *XYL2* (Fig. 8).

According to our data, there was no significant effect of gene orientation or multiple promoter use on gene transcription and translation. However, our data were based on plasmid expression. The expression of adjacent genes in chromosomes can be affected by several other factors in addition to gene orientation. The base composition of intergenic regions and chromatin structure can have influence on gene expression [14]. It has been reported that distance between genes, gene length, and number of exons are also important parameters for expression level [20]. Moreover, genes with similar promoter regions show significantly higher correlations in expression profiles even though the actual expression level depends on the genes [21]. There is a complex relationship between regulatory elements and gene expression [22]. Therefore, we need to consider several critical factors that can influence expression in host genome.

References

1. Piontek, M., Hagedorn, J., Hollenberg, C. P., Gellissen, G., & Strasser, A. W. (1998). *Applied Microbiology and Biotechnology, 50*, 331 338.
2. Williams, E. J., & Bowles, D. J. (2004). *Genome Research, 14*, 1060–1067.
3. Cohen, B. A., Mitra, R. D., Hughes, J. D., & Church, G. M. (2000). *Nature Genetics, 26*, 183–186.
4. Lercher, M. J., Urrutia, A. O., & Hurst, L. D. (2002). *Nature Genetics, 31*, 180–183.
5. Lercher, M. J., Blumenthal, T., & Hurst, L. D. (2003). *Genome Research, 13*, 238–243.
6. Qi, X., Bakht, S., Leggett, M., Maxwell, C., Melton, R., & Osbourn, A. (2004). *Proceedings of the National Academy of Sciences of the United States of America, 101*, 8233–8238.
7. Hesberg, C., Hansch, R., Mendel, R. R., & Bittner, F. (2004). *Journal of Biological Chemistry, 279*, 13547–13554.
8. Tsuchiya, T., Takesawa, T., Kanzaki, H., & Nakamura, I. (2004). *Gene, 335*, 141–149.
9. Prescott, E. M., & Proudfoot, N. J. (2002). *Proceedings of the National Academy of Sciences of the United States of America, 99*, 8796–8801.
10. Valerius, O., Brendel, C., Duvel, K., & Braus, G. H. (2002). *Journal of Biological Chemistry, 277*, 21440–21445.

11. Springer, C., Valerius, O., Strittmatter, A., & Braus, G. H. (1997). *Journal of Biological Chemistry, 272*, 26318–26324.
12. Martens, J. A., Laprade, L., & Winston, F. (2004). *Nature, 429*, 571–574.
13. Schmitt, S., & Paro, R. (2004). *Nature, 429*, 510–511.
14. Marin, A., Wang, M., & Gutierrez, G. (2004). *Gene, 333*, 151–155.
15. Sambrook, J., & Russell, D. W. (2001). *Molecular cloning: a laboratory manual*, 3 vols., (3rd ed.). Cold Spring Harbor, N.Y.: Cold Spring Harbor Laboratory Press.
16. Gietz, R. D., & Woods, R. A. (2002). *Methods in Enzymology, 350*, 87–96.
17. Rose, M. D., Winston, F. M., & Hieter, P. (1990). *Methods in yeast genetics: a laboratory course manual.* Cold Spring Harbor, N.Y.: Cold Spring Harbor Laboratory.
18. De Preter, K., Speleman, F., Combaret, V., Lunec, J., Laureys, G., Eussen, B. H., et al. (2002). *Modern Pathology, 15*, 159–166.
19. vanKuyk, P. A., de Groot, M. J., Ruijter, G. J., de Vries, R. P., & Visser, J. (2001). *European Journal of Biochemistry, 268*, 5414–5423.
20. Chiaromonte, F., Miller, W., & Bouhassira, E. E. (2003). *Genome Research, 13*, 2602–2608.
21. Park, P. J., Butte, A. J., & Kohane, I. S. (2002). *Bioinformatics, 18*, 1576–1584.
22. Lee, T. I., Rinaldi, N. J., Robert, F., Odom, D. T., Bar-Joseph, Z., Gerber, G. K., et al. (2002). *Science, 298*, 799–804.

Appl Biochem Biotechnol (2008) 145:79–86
DOI 10.1007/s12010-007-8032-z

Bioreactors for H_2 Production by Purple Nonsulfur Bacteria

Sergei A. Markov · Paul F. Weaver

Received: 11 May 2007 / Accepted: 27 August 2007 /
Published online: 13 September 2007
© Humana Press Inc. 2007

Abstract Two types of laboratory-scale bioreactors were designed for H_2 production by purple nonsulfur bacteria. The bioreactors employed a unique type of hydrogenase activity found in some photosynthetic bacteria that functions in darkness to shift CO (and H_2O) into H_2 (and CO_2). The mass transport of gaseous CO into an aqueous bacterial suspension was the rate-limiting step and the main challenge for bioreactor design. Hollow-fiber and bubble-train bioreactors employing immobilized and free-living bacteria have proven effective for enhancing the mass transfer of CO. The hollow-fiber bioreactor was designed so that both a growth medium and CO (10% in N_2) passed from the inside of the fibers to the outside within the bioreactor. Bacteria were immobilized on the outer surface of the hollow fibers. Hydrogen production from CO at an average rate of 125 ml g cdw^{-1} h^{-1} (maximum rate of 700 ml g cdw^{-1} h^{-1}) was observed for more than 8 months. The bubble-train bioreactor was built using polyvinyl chloride (PVC) tubing, wound helically on a vertical cylindrical supporting structure. Small bubbles containing CO were injected continuously through a needle/septum connection from the gas reservoir (20% CO). Up to 140 ml g cdw^{-1} h^{-1} of H_2 production activity was observed using this bioreactor for more than 10 days.

Keywords Biohydrogen · Purple bacteria · Bioreactor · Water–gas shift reaction · Hollow fibers

Introduction

Hydrogen (H_2) is considered a fuel with low environmental impact as its combustion product (water) is non-polluting. Hydrogen is a renewable energy carrier; it can be produced from water again. The conventional industrial methods for H_2 production are costly and the problem has been to find a cheaper way to produce hydrogen. Biological H_2

Dr. Paul Weaver is deceased.

S. A. Markov (✉) · P. F. Weaver
Biology Department, SSC A225, Austin Peay State University, P.O. Box 4718,
Clarksville, TN 37041, USA
e-mail: markovs@apsu.edu

production by microbial species has a number of advantages and it could be a cost-effective alternative to the current industrial methods of H_2 production. Some microscopic bacteria produce H_2 using water as the source of electrons and sunlight as the energy source. Microbiological H_2 production based on sunlight and water is very attractive for practical applications. It holds the promise of generating a renewable fuel as a result of the availability of large amounts of solar light and water and the ability of H_2 to produce water again.

A unique type of H_2-producing activity was found in a strain of nonsulfur purple photosynthetic bacterium by Uffen [1]. Cultures of Uffen's strain in a complex organic medium carry out a water–gas shift reaction in darkness to produce H_2 according to the equation:

$$CO + H_2O \rightarrow CO_2 + H_2$$

Since the time of Uffen's discovery, numerous strains of photosynthetic bacteria, including *Rubrivivax gelatinosus* CBS, have been isolated at the National Renewable Energy Laboratory (NREL) in Colorado, USA. These bacteria utilize CO in light and in darkness and do not require complex organic substrates [2, 3]. In addition, these strains will quantitatively shift the CO component of synthesis gas (*e.g.*, from thermally gasified biomass) into H_2. During the shift reaction, the bacterial cells produce hydrogen from water as verified by experiments with ^3H_2O [4]. However, purple bacteria do not use light energy directly to produce H_2 from water during the shift reaction.

Data collected at NREL suggest that the water–gas shift reaction is far more rapid than the rate at which CO can be supplied to the bacterial culture [5]. Mass transport of gaseous CO into an aqueous bacterial suspension is thus the rate-limiting step in the process of shift reaction and was the main challenge during bioreactor design for the current study. In this study, two types of simple laboratory-scale hollow-fiber and bubble-train bioreactors employing immobilized and free-living *Rubrivivax gelatinosus* CBS were analyzed. The bioreactor with immobilized cells was built around bundles of hollow fibers composed of semipermeable polymeric membranes. Salts and gases can freely diffuse through these membranes. Bacterial cells, because of their larger size, cannot pass through the membrane. Bacterial cells that can grow on hollow fibers are called immobilized cells. Immobilization leads to an increase/stabilization of H_2 production for several months or more [6]. Little is known about the mechanisms that induce changes in H_2-producing activity when cells are immobilized. Many microorganisms exist naturally in an immobilized-like state, either on a surface of soil particles or in symbiosis with other organisms. The second type of a bioreactor (bubble-train bioreactor) was constructed out of transparent polyvinyl chloride (PVC) tubing.

Materials and Methods

Bacterial Culture

Before inoculation into bioreactors *Rubrivivax gelatinosus* CBS was grown in closed 250-mL volume flasks using basic basal medium without yeast extract [7] plus 10% CO, shaken and illuminated with incandescent lamps (35 W m^{-2}). Cell dry weight was determined by trapping the bacteria on Whatman # 114 filter paper and drying the cell suspensions at 90°C to a constant weight.

Bioreactors

Two types of bioreactors were designed and constructed. The first one (Fig. 1) consisted of:

1. A 250×33 mm AM-4OM-SD cartridge with hydrophilic cuprammonium rayon hollow fibers (Asahi Medical Co., Ltd, Japan). The total surface area of the 180-μm-diameter hollow fibers was 0.8 m^2, and the cartridge volume outside the fibers was 48 mL.
2. A H_2 measurement port, where H_2 and CO_2 were vented from the bioreactor cartridge.
3. A CO gas cylinder (10% in N_2). CO flow rates were in the range of 0.05–0.5 mL/min.
4. A peristaltic pump (Masterflex, Cole-Palmer Instrument, Niles, IL) for adding the basal medium caused by evaporation from the bioreactor cartridge (one time per week).
5. A medium reservoir
6. A pH controller for automatically adjusting the pH of the medium to 6.8 caused by CO_2 build-up.

The bioreactor was designed such that both the basal growth medium and the CO passed from the inside to the outside of the fibers within the column. A bacterial cell inoculum (0.65 g/L) readily adsorbed to the outer surface of the hollow fibers, and the column was maintained in the darkness.

The second bioreactor was a 0.5-L (liquid volume), 0.8-m-tall device as diagrammed in Fig. 2. This bioreactor was constructed from:

1. A 9.8-m transparent PVC tube (Tygon, Akron, OH), with a 6.3 mm inner diameter, wound helically on a vertical cylindrical supporting structure.
2. A pump (Masterflex, Cole-Palmer Instrument) for circulating (pumping speed 15 mL min^{-1}) the bacterial suspension (0.36 mg cdw mL^{-1}).
3. A needle injector for 20% CO in N_2 (2 mL min^{-1}).
4. A 300-mL gas reservoir.

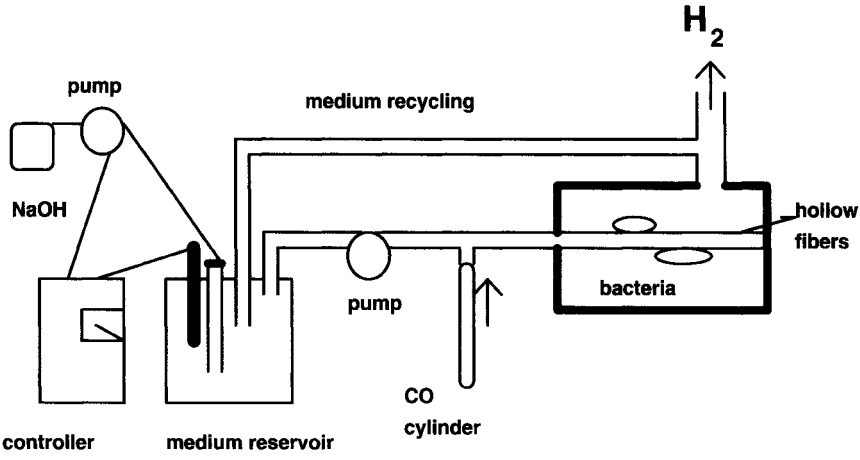


Fig. 1 Schematic diagram of a hollow-fiber bioreactor for continuous shifting of CO into H_2 by *Rubrivivax gelatinosus* CBS

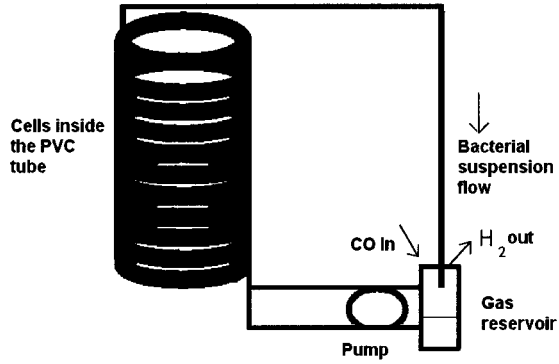


Fig. 2 Schematic diagram of a helical PVC tubular bioreactor to shift CO into H_2 by *Rubrivivax gelatinosus* CBS

The bioreactor was designed so that small bubbles containing CO were injected continuously through a needle/septum connection from the gas reservoir (initially 20% CO). The bubbles rose with the pumped medium (3.5-min transit time) from the bottom of the bioreactor to the top. The high surface area of the bubble train promoted enhanced mass transport of gaseous CO into the aqueous bacterial suspension. To keep the pH of the medium from dropping as a result of carbonic acid build-up, the gas phase of the bioreactor was degassed with N_2 once daily, after which CO (20% in a N_2 balance) was reinjected into the system. The bioreactor was covered with a black cloth to prevent photosynthetic H_2 consumption from exposure to ambient light according to the reaction: $2H_2 + CO \rightarrow (CH_2O)_n + H_2O$.

The bioreactor was inoculated with bacterial culture at cell density of 0.65 g/L.

The bioreactors did not require sterilization because CO is either toxic to, or will not support the growth of, most potential invading organisms. Both bioreactors were maintained at room temperature (25–26°C).

Measurement of Hydrogen Production

Hydrogen production rates were measured using a Varian Model 3700 gas chromatograph (Walnut Creek, CA) equipped with a molecular sieve 5A column and a thermal conductivity detector. Argon was used as the carrier gas.

Scanning Electron Microscopy

Immobilized bacterial cells were examined using the freeze-drying method. Cells were fixed in 2.5% glutaraldehyde in 0.1 M phosphate buffer, pH 7.2 (containing 6% sucrose wt/vol) for 24 h at 25°C and then washed in the same buffer containing 12% sucrose (wt/vol). The specimens were freeze-dried. Dried specimens were coated with gold and examined in a model JSM 25 S scanning microscope (Jeol Ltd., Japan) at accelerating voltage of 10 kV.

Results

H_2 Production by the Hollow-Fiber Bioreactor

Before construction of the hollow-fiber bioreactor, the adhesion of bacterial cells to hollow fibers was studied in batch cultures. Cells were immobilized on 2-cm-long pieces of

hydrophilic cuprammonium rayon hollow fibers. The degree of immobilization of cells was assessed by examining the attachment of the cells using scanning electron microscopy (Fig. 3). Bacterial cells almost entirely covered the hollow-fiber surfaces. Because of this high degree of immobilization, a cuprammonium rayon hollow-fiber cartridge was selected for construction of the bioreactor.

Hydrogen production in hollow-fiber bioreactor by *Rubrivivax gelatinosus* CBS from CO at an average rate of 125 ml g cdw^{-1} h^{-1} (maximum rate of 700 ml g cdw^{-1} h^{-1}) was observed for more than 8 months (Fig. 4). No detectable remaining levels of CO (<18 ppm) in the effluent gas were observed during this period.

H_2 Production by the Bubble-Train Bioreactor

Continuous H_2 production by *Rubrivivax gelatinosus* CBS at rates up to 140 ml g cdw^{-1} h^{-1} was observed in a bubble-train bioreactor for more than 10 days (Fig. 5). Rates of H_2 production were low at first, probably because of the exposure of the bacterial culture to O_2 during bacterial transfer to the bioreactor. Once more favorable anaerobic conditions were established for the bacteria in the bioreactor, rates of H_2 production started to increase. At the higher rates, 2 h was sufficient to shift all of the added CO in the reservoir gas phase into H_2. No detectable level of CO remained in the gas phase (less than 18 ppm). The bulk of the added CO was shifted during the first hour after feeding. Repetitive batch feeding of CO (the gas phase was changed once a day and reestablished with 20% CO in N_2) maintained the culture in a highly active state.

Hydrogen production as a function of the distance from the gas injection port within the bubble-train bioreactor was studied in a separate experiment as well. For this experiment, the PVC tube used within the bioreactor was much longer (50 m long versus the original 9.8 m). Rubber stoppers were inserted at regular intervals along the bioreactor tube. Samples of the gas phase were taken and H_2 production and CO utilization was determined. The results of this study are shown in Fig. 6. The highest H_2 production rate (as well as the CO consumption rate) was observed within 10 m from the CO injection port. Apparently, a long PVC is not necessary for the bioreactor construction, at least not from the point of H_2 production and CO consumption.

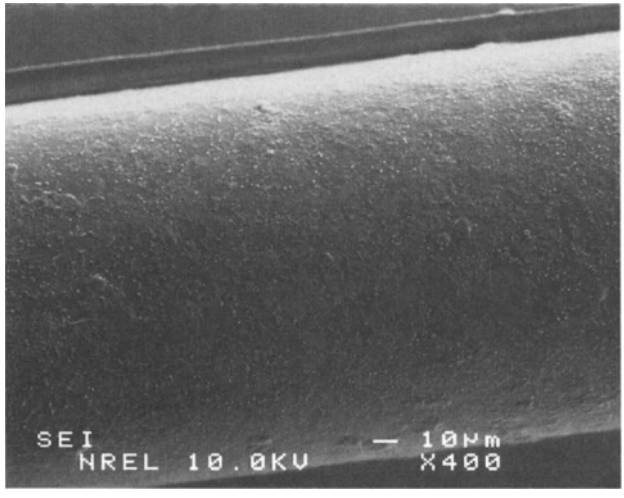


Fig. 3 Scanning electron microscopy of *Rubrivivax gelatinosus* CBS immobilized on cuprammonium rayon hollow fiber (AM-4OM-SD)

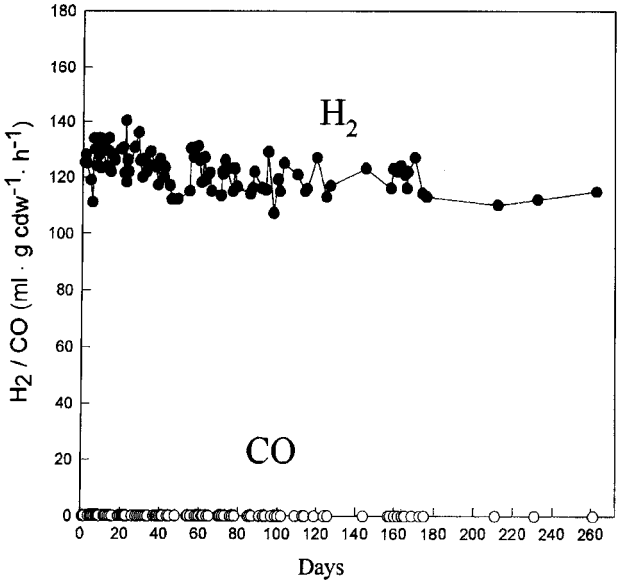


Fig. 4 Continuous shifting of CO into H_2 by *Rubrivivax gelatinosus* CBS in a hollow-fiber bioreactor

Discussion

In this study, two types of bioreactors were tested for H_2 production by purple nonsulfur bacterium using a shift reaction. The main idea was to improve mass transport of gaseous CO into an aqueous bacterial suspension. A simple method of using hollow fiber membrane technology to enhance mass transfer of CO has proven effective, but is likely too expensive for commercial applications at the present time. Different types of membrane-based

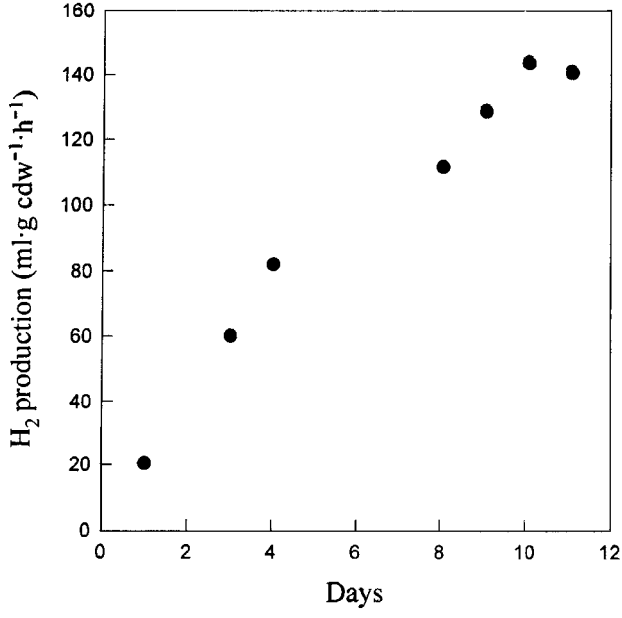


Fig. 5 Shifting of CO into H_2 by *Rubrivivax gelatinosus* CBS in the PVC tubular bioreactor

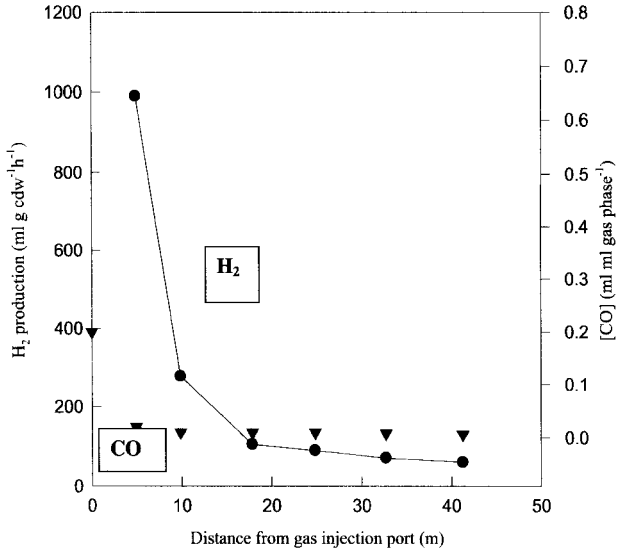


Fig. 6 Shifting of CO into H_2 by *Rubrivivax gelatinosus* CBS as a function of distance from CO injection port in the PVC tubular bioreactor

bioreactors such as a spiral sheet membrane bioreactor can be scaled up using a prototype already available for filtration applications with cartridges produced by Amicon, Inc (Beverly, MA). The price for that type of membrane bioreactors could be more affordable. The cost of the bubble-train bioreactor described here is significantly less than that of any type of membranous bioreactors or any type of bioreactor that uses immobilized cells. This bioreactor exhibited superior mass transfer rates as well.

The gaseous product from both bioreactors, enriched in H_2 (20% H_2) and devoid of any remaining CO, was sufficiently clean for direct injection into a H_2 fuel cell. In fact, the effluent gas from the hollow-fiber bioreactor has been directly injected into small millivolt fuel cells and shown capable of generating enough electricity to power small motors and lamps. No negative effect on the fuel cells was noted.

Carbon monoxide for the water–gas shift reaction may derive from a synthesis gas (predominantly CO) obtained by a thermochemical gasification of biomass (*e.g.*, wood waste). Growth and H_2 production using this synthesis gas was recently reported for another purple nonsulfur bacterium *Rhodospirillum rubrum* [8].

Carbon monoxide for the shift reaction may also come from other microorganisms. A number of bacteria are able to degrade different molecules such as chlorophyll with the release of CO [9].

Acknowledgements This work was supported by the U.S. Department of Energy Hydrogen Program. The authors thank Asahi Medical Co., Ltd. (Japan) for supplying the hollow fibers.

References

1. Uffen, R. L. (1976). *Proceedings of the National Academy of Sciences of the United States of America, 73*, 3298–3302.
2. Weaver, P., Maness, P.-C., Markov, S., & Martin, S. (1997). in Proceedings of the 1997 U.S. DOE Hydrogen Program Review, May 21–23, 1997, Herndon, Virginia, pp. 33–40.
3. Maness, P.-C., & Weaver, P. (2002). *International Journal of Hydrogen Energy, 27*, 1407–1411.

4. Kondratieva, E. N., & Gogotov, I. N. (1983). *Advances in Biochemical Engineering Biotechnology, 28*, 139–191.
5. Markov, S. A., Weaver, P. F., & Seibert, M. (1996) *Hydrogen energy progress XI. Proceedings of the 11th World hydrogen energy conference*, Stuttgart, Germany, 23–28 June 1996, pp. 2619–2624.
6. Hall, D. O., & Rao, K. K. (1989). *Chimica Oggi, 7*, 41–47.
7. Schultz, J., & Weaver, P. F. (1981). *Journal of Bacteriology, 149*, 181–190.
8. Do, Y. S., Smeenk, J., Broer, K. M., Kisting, C. J., Brown, R., Heindel, T. J., et al. (2007). *Biotechnology and Bioengineering*. (Published Online: 19 Oct 2006).
9. Uffen, R. L. (1981). *Enzyme and Microbial Technology, 3*, 197–206.

Appl Biochem Biotechnol (2008) 145:87 98
DOI 10.1007/s12010-007-8077-z

Solid-state Fermentation of Xylanase from *Penicillium canescens 10–10c* in a Multi-layer-packed Bed Reactor

Antoine A. Assamoi · Jacqueline Destain · Frank Delvigne · Georges Lognay · Philippe Thonart

Received: 15 May 2007 / Accepted: 2 October 2007 /
Published online: 26 October 2007
© Humana Press Inc. 2007

Abstract Xylanase is produced by *Penicillium canescens 10–10c* from soya oil cake in static conditions using solid-state fermentation. The impact of several parameters such as the nature and the size of inoculum, bed-loading, and aeration is evaluated during the fermentation process. Mycelial inoculum gives more production than conidial inoculum. Increasing the quantity of inoculum enhances slightly xylanase production. Forced aeration induces more sporulation of strain and reduces xylanase production. However, forced moistened air improves the production compared to production obtained with forced dry air. In addition, increasing bed-loading reduces the specific xylanase production likely due to the incapacity of the *Penicillium* strain to grow deeply in the fermented soya oil cake mass. Thus, the best cultivation conditions involve mycelial inoculum form, a bed loading of 1-cm height and passive aeration. The maximum xylanase activity is obtained after 7 days of fermentation and attains 10,200 U/g of soya oil cake. These levels are higher than those presented in the literature and, therefore, show all the potentialities of this stock and this technique for the production of xylanase.

Keywords Multi-layer-packed bed reactor · *Penicillium canescens* · Solid-state fermentation · Soya oil cake · Xylanase

Introduction

Microbial xylanases are enzymes with biotechnological potential in many industrial processes, such as pre-bleaching of kraft pulp, improvement of the digestibility of animal

A. A. Assamoi · J. Destain (✉) · F. Delvigne · P. Thonart
Unité de Bio-industries, Faculté Universitaire des Sciences Agronomiques de Gembloux,
2, Passage des Déportés, Gembloux 5030, Belgium
e-mail: destain.j@fsagx.ac.be

G. Lognay
Unité de Chimie Analytique, Faculté Universitaire des Sciences Agronomiques de Gembloux,
2, Passage des Déportés, Gembloux 5030, Belgium

feed, juice clarification, degumming of vegetal fibers such as jute, ramie, and hemp [1–8], and bioethanol production from lignocellulosic compounds [9, 10]. A variety of microorganisms, including bacteria, yeasts, and filamentous fungi are reported to produce xylanolytic enzymes [1–8] using solid-state cultivation systems and submerged liquid cultivation processes. Most of the researches are focused on submerged culture, which allows control of the pH and the temperature of the medium and several environmental factors (homogenization of the medium, aeration, and shearing) required to optimize microbial growth [3, 7]. Thus, the availability of informations about xylanase production in solid-state bioreactors is limited [11].

However, solid-state fermentation has gained renewed interest from researchers in recent years and is often employed for the production of xylanases because of a number of economical and practical advantages, such as its simplicity, low capital costs for equipment and operating, high volumetric productivity, lower space requirements, and easier downstream processing [1, 11–13]. The tray reactor is currently the most popular technology, particularly in oriental countries, for koji or food fermentation. However, this technology suffers from its limited capacity and poor aeration control [14]. Thus, other types of reactors are investigated, including the packed-bed reactor, which has the potential to overcome the disadvantages of the tray reactor [14]. The packed-bed reactor allows using several trays (beds) of the medium simultaneously, whereas the tray technology uses only one bed of the medium in the reactor. Some applications of the packed-bed reactor in solid state fermentation are recently summarized, and the important operating parameters are identified as the air flow rate, the particle size of the substrate, and the bed loading [14]. However, the main parameters to be measured and controlled generally in solid-state fermentation processes are the temperature, the aeration homogeneity, the pH, and the water bed content [12].

This paper investigates the potential of xylanase production in solid-state fermentation from soya oil cake by *Penicillium canescens 10–10c* using a multi-layer-packed bed reactor. Previous studies reported xylanase production by this strain in solid-state fermentation from wheat straw in flasks [1].

Materials and Methods

Strain

P. canescens 10–10c is supplied by G.I Kvesidatse, Institute of Plant Biochemistry, Academy of Sciences, Tbilisi Georgia.

Culture Conditions

The enzymatic production medium is composed by 20% of soya oil cake (5-mm particles size) and 80% of a nutritive solution composed by casein peptone at 0.75% (*w/v*) and $Na_2HPO_4.2H_2O$ at 1% (*w/v*) in distilled water. The 5-mm particle size soya oil cake was obtained after crushing the whole soya oil cake with a hammer mill (Gladiator, Ets J. Mondelaers S.P.R.L, Bruxelles, Belgium) equipped with a 5-mm diameter grid. Enzymatic production medium is autoclaved in the enamel metallic trays ($17 \times 11 \times 5$ cm^3) and then placed horizontally in four distinct layers in the multi-layer-packed bed reactor as shown in Fig. 1. Enzymatic production medium is inoculated by conidia (5.10^5 or 10^7 spores/gram of soya oil cake) or mycelia issued from conidia. Bed loading varied between 50 to 250 g of soya oil cake/layer (respectively, 0.5 to 2.5 cm). In the first case, enzymatic production medium contained in the reactor is directly

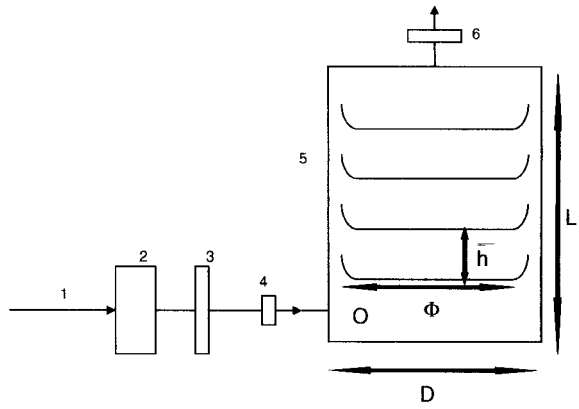


Fig. 1 Schematic diagram of the multi-layer-packed bed reactor system. *1* Circuit of air; *2* rotameter; *3* inlet filter; *4* humidifier system; *5* reactor (*L* length; *D* diameter); *6* outlet filter; *Φ* diameter of a circular layer; *h* distance between two layers; *O* air distributor

inoculated by the whole conidial suspension, whereas in the second case, a mycelial inoculum (one day old spores preculture) on 1/10 of enzymatic production medium is used as inoculum. The mycelial preculture is used to inoculate the 9/10 of the enzymatic production medium in the reactor. Production is led under static conditions at 30 °C. Passive aeration is compared to forced aeration (dry or moistened air). After production during, respectively, 3, 7, and 12 days, the fermented soya oil cake from each layer is extracted and assayed for xylanase activity, moisture content, and ergosterol content (after lyophylization). The experiments are conducted in triplicate, and the mean value is selected.

Multi-layer-packed Bed Reactor

The multi-layer-packed bed reactor (Fig. 1) contains four distinct circular layers (Φ=28.5 cm) separated each one by a distance h of 6 cm. The circular layers are composed of meshes (diameter<2 mm) facilitating the circulation of the air in the fermented medium. The dimensions of the reactor are 42 cm length L×33 cm diameter D. The distribution of air is carried out by an opening O on the reactor. In the case of forced not-moistened air, compressed air goes directly through a rotameter and then in the reactor. In the case of forced moistened air, compressed air issued from the rotameter goes through a bottle containing distilled water before going in the reactor. Filters ($\varnothing$=0. 20 μm, PTFE Midisart 2000, Sartorius Technologies, Vilvoorde, Belgium) are positioned at the inlet and at the outlet of the reactor to filter the air.

Enzyme Extraction

The fermented soya oil cake of each layer from the multi-layer-packed bed reactor is complemented with distilled water at 75% (*v*/*w*). The solution obtained is centrifuged at 10,000 RPM for 15 min at 4 °C (Avanti™ J-25 I, Beckman, Palo Alto, USA) to remove the fermented soya oil cake. This extract solution is filtrated through a folded filter ($\varnothing$= 150 mm, 595 1/2, ref. no. 10311645; Schleilcher and Schuell, Dassel, Germany). The clear supernatant filtrate is used as the enzyme source.

Enzyme Assay

Xylanase activity is measured according to Bailey et al. [15] using 1% birchwood xylan as substrate (X0502, EC 232-760-6, Sigma-Aldrich Chemie GmbH, Steinheim, Germany). Reducing sugars are assayed by dinitrosaycylic acid method with xylose as the standard

[16]. One unit of xylanase activity is defined as the amount of enzyme releasing 1 μmol of reducing sugar equivalent to xylose per minute. Xylanase activity is evaluated per layer. Each test is done in triplicate. To determine the total enzymatic activity obtained during each experiment, enzymatic activities of the four layers are added, and the average is evaluated. The average value is validated when the variation between tests values are less than 8.0%.

Moisture Content Analysis

Fifteen grams of fresh fermented soya oil cake from each layer is dried during 48 h at 105 °C until a stable weight is obtained. Moisture content is determined by the difference between the fresh matter and the dried mater. Then, the percentage of the ratio moisture content/fresh matter of the fermented soya oil cake during the process is determined by layer. Each test is done in triplicate. To determine the total moisture content of the fermented soya oil cake during each experiment, moisture contents of the fours layers are added, and the average value is evaluated. The variation between tests values are less than 8.0%.

Ergosterol Analysis

To extract ergosterol, the fermented soya oil cake of each layer is lyophilized (Lyophylizator Liogamma, Koeltechniek Louw, Rotselaar, Belgium). About 100 mg of the lyophilized sample in 2.5 ml of 4% (*w/v*) methanolic solution of NaOH is saponified for 30 min at 80 °C. After cooling to room temperature, 3 ml of hexane is added. The hexane phase (upper phase) is transferred to new test tubes. Three hexane extractions are performed. The three hexane fractions are combined and evaporated under vacuum at 30 °C. The dried residue is dissolved in 1.0 ml of methanol. Ergosterol is measured by high performance liquid chromatography (Hewlett-Packard 1100 Agilent Technologies, Diegem, Belgium) after filtration of the samples through on a 0.2-μm pore-size filter (Chromofil PET-20/15 MS-Macherey-Nagel, Duren, Germany). Ten microliters of the sample is injected on a C18 column (length, 150 mm; ID, 3.0 mm; Alltech, Lokeren, Belgium). Ergosterol is eluted with a mixture of methanol acetonitrile 90:10 (*v/v*) at a flow rate of 0.40 ml/min and at 30 °C. Peaks are detected at a wavelength of 282 nm. A standard solution of ergosterol (Acros Organics; Geel, Belgium) in methanol is used for quantifications purposes. Standards and blanks are treated in the same manner. Each test is done in triplicate. To determine the total ergosterol content obtained during each experiment, ergosterol content of the four layers are added, and the average is evaluated. The variation between tests values are less than 8.0%.

Results and Discussion

Xylanase Production in Passive Aeration Conditions

In preliminary studies at small scale in flask and in enamel metallic trays (submitted for publication), several cheap substrates (soya oil cake, soya meal, wheat bran, complete bran, and pulp sugar beet) have been tested. The best substrates were issued from soya. However, soya oil cake gave better production than soya meal. The average of best activities were obtained after 7 days, 14,485±1,090 U/g in flasks and 8,133±540 U/g in enamel metallic trays. To improve the scale up of the production, we have decided to test xylanase production in a multi-layer-packed bed reactor. The fermentations conditions are similar.

Firstly, impacts of bed loading, type of inoculum, and cultivation duration on the enzyme production in the multi-layer-packed bed reactor have been studied. Bed loading varied between 50 to 250 g of soya oil cake/layer.

Figure 2 shows that the mycelial inoculum gives higher xylanase activity than conidial inoculum. The highest specific production (7,900 U/g) and the highest total production (1,020,000 U) are observed after 7 days incubation with 100 g (2X, 1-cm bed thickness) and 150 g (3X, 1.5-cm bed thickness) of soya oil cake, respectively. Xylanase first increases and then decreases with increasing the bed loading of soya oil cake. The *Penicillium* strain sporulated and was unable to colonize the entire culture medium. The microorganism growths primarily at the surface of the culture medium and colonizes the entire medium when depth is comprised between 0.5 cm to 1 cm (visual observation). Similar observations were reported in the cases of penicillin production by *Penicillium chrysogenum* and in alkaline protease production by *Teredinobacter turnirae* using agricultural wastes under solid state fermentation [17, 18]. With mycelial inoculum, the lag phase during the strain growth is reduced. The strain grows quickly and, therefore, produces more xylanase. Production increases with the cultivation duration until the seventh day and then decreases. Many works describe this phenomenon as a sudden increase and subsequent decrease in enzymes activities during the cultivation period [5]. The sporulation of the strain reduces the enzymatic activity [19, 20]. Maybe, the xylanase produced during days 1–7 is consumed or denaturated after onset of sporulation during days 7–12. These assumptions had to be verified.

Ergosterol level is an indicator of the strain growth. Figure 3 indicates that it decreases slightly when the bed loading increases. About 100 g of fermented soya oil cake allows obtaining higher values of ergosterol. Ergosterol content is affected by the inoculum form and the time of cultivation. Mycelial inoculum gives more ergosterol content than conidial inoculum. Twelve days cultivation duration gives the highest ergosterol content.

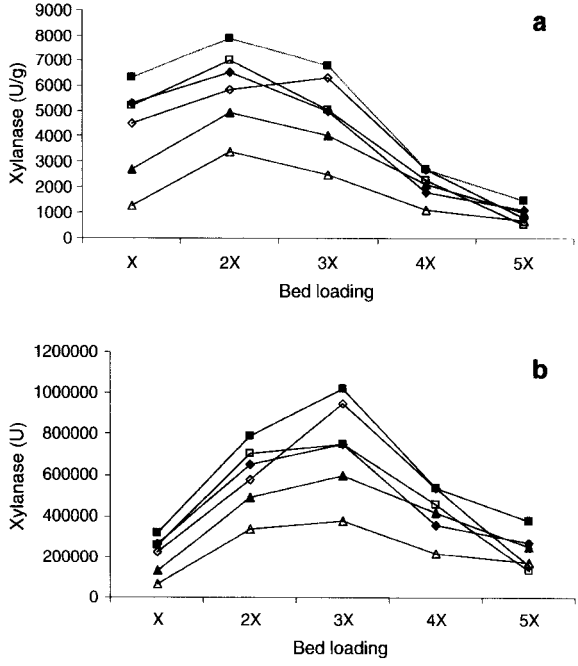


Fig. 2 Xylanase production in the multi-layer-packed bed reactor with passive aeration conditions; **a** specific activity, **b** total activity. *X* represents 50 g of soya oil cake supplemented with 200 ml of the nutritive solution [casein peptone at 0.75% (*w/v*) and $Na_2HPO_4.2H_2O$ at 1% (*w/v*) in distilled water]. Inoculum is 5.10^5 spores/gram of soya oil cake or the results of the development of these spores in 1 day (mycelia). The ratio values are averages based on addition of the enzymatic activity from the four layers, and the experiment was performed in triplicate. The deviation standard was below 8% in all cases. Conidial inoculum: 3 days (*open triangle*), 7 days (*open square*), 12 days (*open rhombus*). Mycelial inoculum: 3 days (*closed triangle*), 7 days (*closed square*), 12 days (*closed rhombus*)

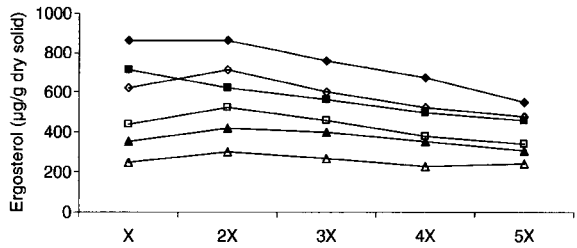


Fig. 3 Evolution of ergosterol content during xylanase production in the multi-layer-packed bed reactor in passive aeration conditions. The ratio values are averages based on addition of the ergosterol content from the four layers, and the experiment was performed in triplicate. The deviation standard was below 8% in all cases. *Symbols* are identical to those of the Fig. 2

Impact of Forced Air on Xylanase Production

To enhance oxygen transfer during the process in the multi-layer-packed bed reactor, xylanase production is realized with forced air (moistened or dry) at 0.1, 0.5, and 1 l/min. The other parameters of the culture remain identical to those used before.

Figures 4 and 5 show that aeration affects the parameters of the culture. For the three air flows tested, moistened air gives best activities than dry air. The higher xylanase productions appear at 0.1 l/min moistened air after 7 days (4,000 U/g) with the mycelial inoculum (Fig. 4) and after 12 days (2,300 U/g) with the conidial inoculum (Fig. 5). The xylanase production increases during days 3–7 in all the cases. However, during days 7–12, the xylanase production increases slowly or decreases. Maybe, this weak increase of xylanase activity after the seventh day is caused by the effects of forced aeration. Indeed, this situation did not appear in passive aeration. It has clearly established in submerged fermentation that *P. canescens* is very sensitive to hydrodynamic stress generated by aeration and mixing of the medium [21–23]. A lowering stress due to aeration would be beneficial as well for the synthesis of several enzymes by filamentous microorganisms in general as for the synthesis of xylanase by *P. canescens* in particular [21–23].

Figures 6 and 7 show ergosterol content during *P. canescens* growth. Ergosterol content is related to the *Penicillium* strain growth. As we can see, ergosterol content increases with

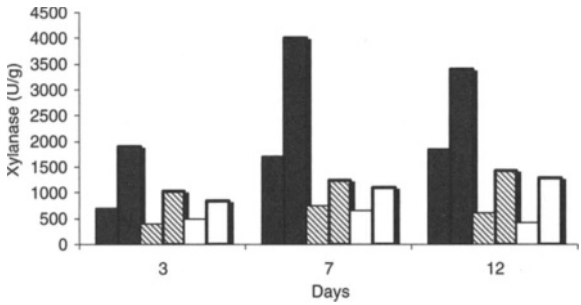


Fig. 4 Xylanase production in the multi-layer-packed bed reactor with active aeration conditions. Mycelial inoculum, bed loading of 50 g of soya oil cake. The ratio values are averages based on addition of the enzymatic activity from the four layers, and the experiment was performed in triplicate. The deviation standard was below 8% in all cases. Ambient air 0.1 l/min (*black*); Moistened air 0.1 l/min (*shaded black*); ambient air 0.5 l/min (*stripes*); moistened air 0.5 l/min (*shaded stripes*); ambient air 0.1 l/min (*white*); moistened air 0.1 l/min (*shaded white*)

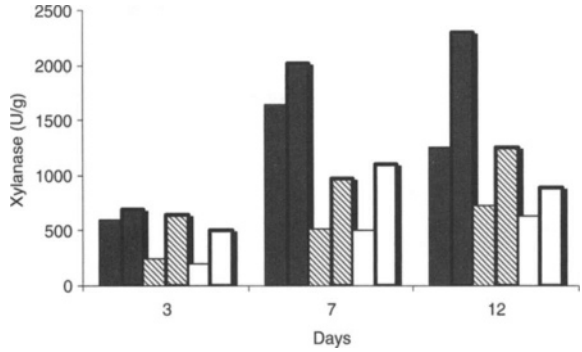


Fig. 5 Xylanase production in the multi-layer-packed bed reactor with active aeration conditions conidial inoculum, bed loading of 50 g soya oil cake. The ratio values are averages based on addition of the enzymatic activity from the four layers, and the experiment was performed in triplicate. The deviation standard was below 8% in all cases. *Symbols* are identical to those of the Fig. 4

time. Forced moistened air at 1 l/min gives the higher ergosterol content, and the lowest content is obtained at 0.1 l/min forced dry air. Visual observations of culture show also that aeration does appear to have a pronounced effect on spore formation. Indeed, with forced dry air, conidia formation takes place rapidly, and it is visible at the second day. With forced moistened air, spore formation is less important and appeared at the fifth day. With passive aeration, spore formation appears at the seventh day of fermentation. The temperature at the inner of the reactor is not controlled during the process. Maybe, formation of spores is favored by a fall of the temperature in the reactor and/or by a stress of the strain caused by forced air injection [21]. In addition, literature indicates many other examples where xylanase production decreases with forced aeration level [11, 24–26]. Moreover, forced aeration could cause a cellular mortality and enzymatic damage [27, 28]. Oxygen could be toxic for aerobic strains at critical values [19]. It could also inhibit or inactivate the enzymes [25]. Forced dry air decreases also the moisture content during the fermentation until the microorganisms cannot grow well (Fig. 8). With passive aeration, moisture content remains constant. Our results suggest that the optimum operating conditions includes 100 g bed loading (1-cm thickness), mycelial inoculum, and passive aeration. However, when using lower bed loading, the advantage of the process for scaling-up is lost. Increasing bed loading reduces production (Fig. 9). To improve xylanase production, we decide to increase

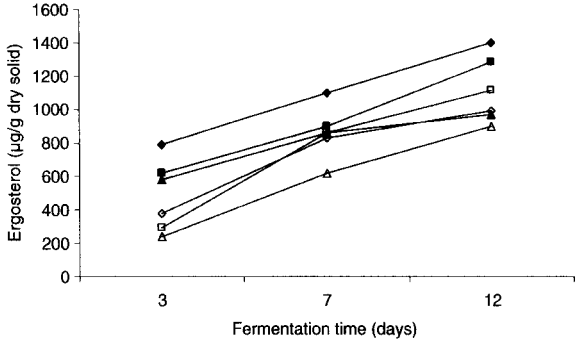


Fig. 6 Evolution of ergosterol content during xylanase production in the multi-layer-packed bed reactor with active aeration conditions, mycelial inoculum, bed loading of 50 g soya oil cake. The ratio values are averages based on addition of the ergosterol content from the four layers, and the experiment was performed in triplicate. The deviation standard was below 8% in all cases. Ambient air 0.1 l/min (*open triangle*); moistened air 0.1 l/min (*closed triangle*); ambient air 0.5 l/min (*open square*); moistened air 0.5 l/min (*closed square*); ambient air 1 l/min (*open rhombus*); moistened air 1 l/min (*closed rhombus*)

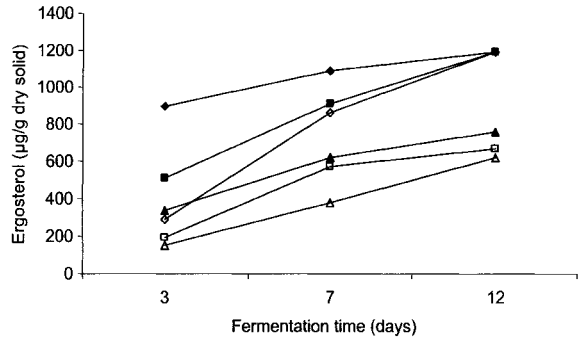


Fig. 7 Evolution of ergosterol content during xylanase production in the multi-layer-packed bed reactor with active aeration conditions, conidial inoculum, bed loading of 50 g of soya oil cake. The ratio values are averages based on addition of the ergosterol content from the four layers, and the experiment was performed in triplicate. The deviation standard was below 8% in all cases. *Symbols* are identical to those of the Fig. 6

quantity of initial inoculum to 10^7 spores/gram of soya oil cake. Better production (10,200 U/g of soya oil cake) is obtained with mycelial inoculum and about 100 g of soya oil cake in passive aeration condition (Table 1). Therefore, during solid-state fermentation xylanase production by *P. canescens*, it is desirable not to use active aeration if temperature is not controlled.

Comparison of Fermentations in Flasks, Enamel Metallic Trays and in the Multi-layer-packed Bed Reactor

Table 2 presents a comparison of the fermentation parameters used in the framework of this study by the multi-layer-packed bed reactor and data from experiments conducted in flasks and in enamel metallic trays using the same substrate and the same strain in passive aeration. It is evident that in flasks, xylanase production is higher than in the multi-layer-packed bed reactor and in the enamel metallic trays. A major difference in these three systems tested is the depth (bed height) of the fermented soya oil cake. Indeed, the production requires an appropriate thickness of medium for the microbial growth, the complete colonization of the medium, and not sporulation of the strain. A great quantity of inoculum enhances slightly the production. However, we think that it is not the best solution to improve the production. Indeed, with a low quantity of inoculum and an appropriate depth of medium, the entire

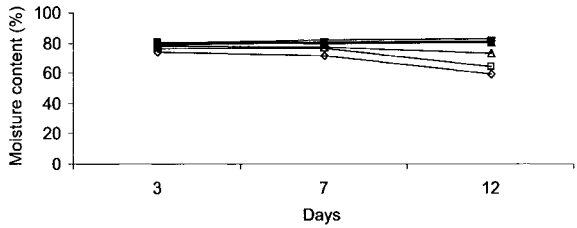


Fig. 8 Evolution of moisture content during xylanase production in the multi-layer-packed bed reactor in active aeration conditions, bed loading of 50 g of soya oil cake. The ratio values are averages based on addition of the moisture content from the four layers, and the experiment was performed in triplicate. The deviation standard was below 8% in all cases. Passive aeration (*feature*); ambient air 0.1 l/min (*open triangle*); moistened air 0.1 l/min (*closed triangle*); ambient air 0.5 l/min (*open square*); moistened air 0.5 l/min (*closed square*); ambient air 1 l/min (*open rhombus*); moistened air 1 (*closed rhombus*)

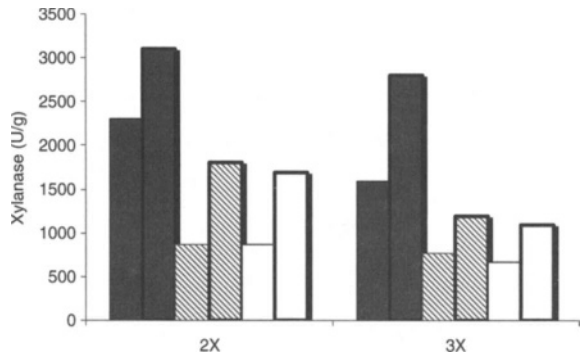


Fig. 9 Xylanase production in the multi-layer-packed bed reactor with active aeration conditions, mycelial inoculum (X=50 g of soya oil cake + 5.10^5 spores/gram). The ratio values are averages based on addition of the enzymatic activity from the four layers, and the experiment was performed in triplicate. The deviation standard was below 8% in all cases. *Symbols* are identical to those of the Fig. 4

medium will be colonized but tardily, and the level of the production would be equivalent to production obtained with a great quantity of inoculum in the same cultural conditions. However, a rigorous control of the sporulation of *P. canescens* is strongly recommended. One of the possible solutions would consist to increase the cultural surface by increasing the dimensions of the layers in the reactor.

Comparison of This Work and Others in the Literature

The number of publications on solid-state fermentation in a large scale in general and on xylanase production in particular is very small. The majority of the works are limited to studies in flasks. Indeed, many problems appear that limit production during the scaling-up. The aerobic microbes grow at the surface of the culture medium and cannot grow in-depth in the solid cultural mass. Thus, with *Thermoascus aurantiacus* in a double-jacketed glass column, better xylanase production was 1,597 U/g [11]. This activity is obtained after 10 days cultivation with only 8 g of bagasse at an airflow rate of 6 l/(h g). A static environment gave 71 U/g. The authors noted that the best conditions of the process required better oxygen transfer, which depends on the porosity of the substrate and interparticular spaces. This loading is very weak compared to bed loading used in our studies with the multi-layer-packed bed reactor. *T. aurantiacus* strain in a 2-l rotating drum bioreactor gave optimal xylanase activity (4,490 U/g) from 100 g of dry wheat straw after 7 days cultivation duration [29]. This activity is obtained at a humidified air flow rate of 10 l/min/kg dry wheat straw. Initial moisture content was 80%. This activity is two times inferior to the optimal activity (10,200 U/g of soya oil cake) obtained in the present study. This confirms the hyperproductor character of xylanase by the strain *P. canescens*. Khamgkhang and Wisutharom [30] used a packed bed fermenter, with a diameter and height ratio of 1 to produce xylanase. They obtained only 497 U/g dry solid, and overheating problems occurred that limit production. Prasertsri [31] obtained with a tray fermenter a maximum of 1,764 U/g dry solid of xylanase. Although the xylanase concentration in tray is high, the larger area requirement in tray fermenters is the limitation of large scale production. With *Aspergillus sulphurous*, the xylanase activity of the dry koji was more than 1,000 U/g when the medium temperature and water activity are balanced [32]. However, the xylanase activity of the dry koji was only 650 U/h if the solid state fermentation is carried out naturally. In our cultivation conditions, 10,200 U/g of xylanase is obtained in passive aerations after 7 days incubation. Bed loading of 100 g of soya oil cake (1-cm bed height) is required to obtain this activity. This production is better obtained compared to other works reported in literature. However, this comparison must be considered with care because of

Table 1 Xylanase production in the multi-layer-packed bed reactor with a great quantity of inoculum (10^7 spores/gram of soya oil cake).

Inoculum form	Air flow rate (l/min)	Bed loading (g)	Xylanase (U/g)	Final moisture content (%)	Ergosterol (mg/g dry solid)
Spore	Passive	50	8,100	82	6.7
Spore	Passive	100	7,100	82	8.6
Spore	Passive	150	5,700	82	7.6
Spore	Passive	200	3,800	82	6.7
Spore	Passive	250	1,380	82	5.7
Mycelia	Passive	50	9,200	82	10.9
Mycelia	Passive	100	10,200	82	11.9
Mycelia	Passive	150	8,500	82	10
Mycelia	Passive	200	5,100	82	9
Mycelia	Passive	250	3,800	82	7.1
Spore	0.1	50	2,980	77	6.2
Spore	0.1	100	3,100	77	9
Spore	0.1	150	1,800	77	7.6
Spore	0.1	200	1,600	77	6.7
Spore	0.1	250	1,100	77	5.7
Spore	0.1[a]	50	4,800	80	7.1
Spore	0.1[a]	100	5,100	80	8.6
Spore	0.1[a]	150	2,450	80	7.6
Spore	0.1[a]	200	1,800	80	6.7
Spore	0.1[a]	250	1,300	80	5.7
Mycelia	0.1	50	4,700	77	8.1
Mycelia	0.1	100	3,600	77	9.5
Mycelia	0.1	150	2,550	77	10.5
Mycelia	0.1	200	1,200	77	8.6
Mycelia	0.1	250	870	77	7.6
Mycelia	0.1[a]	50	7,380	80	9
Mycelia	0.1[a]	100	6,150	80	10
Mycelia	0.1[a]	150	4,000	80	9.5
Mycelia	0.1[a]	200	2,900	80	9
Mycelia	0.1[a]	250	3,000	80	8.1

All the values presented are mean value of triplicates. Standard deviations were essentially within 2–8%.

[a] Cultures were conducted with moistened air.

Table 2 Comparison of fermentations in flasks, enamel metallic trays, and in the multi-layer-packed bed reactor.

Parameters	Flask	Enamel metallic trays	Multi-layer packed bed reactor
Maximum xylanase production (U/g)	14,485	8,133	10,200
Productivity (U/g/day)	2,069	1,162	1,457
Initial inoculum (spores/gram of soya oil cake)	1×10^6	5×10^5	1×10^7
Form of inoculum	Spore	Spore	Mycelia
Bed loading (g of soya oil cake)	5	50	100/layer
Bed height of fermented soya oil cake (cm)	0.5	1	1

nonstandardization of the different reactors used during all the works. Indeed, in function of the desired scale production, the objectives to be reached vary according to the reactor. In the studies, problems occurred concerning bed loading, aeration conditions, and heat accumulation in the medium. In our case, one of the main problems is the sporulation of the strain when production is done with forced aeration, although no control of cultivation temperature is realized during our studies. Maybe, this production would be enhanced with association of a low moistened air flow rate and rigorous control of cultivation temperature at 30 °C. Therefore, it is probable that forced aeration in the form of steam vapor at 30 °C would be advantageous for the strain growth and so the xylanase production. This system has been used in other work [29, 32].

Conclusion

The present work has established the potential of a laboratory multi-layer-packed bed reactor for xylanase production in solid-state fermentation by *P. canescens*. Optimal production obtained is largely superior to those related in literature. Two problems are identified. Initially, the forced aeration causes sporulation of the *Penicillium* strain and so decreases xylanase production. In addition, increasing the cultural surface more than 100 g/layer of soya oil cake (1-cm bed height) decreases significantly xylanase production and constitutes a disadvantage for this process. To increase efficiency of the multi-layer-packed bed reactor, we can increase the dimensions of the layers. Why not associate mixing the culture medium, moistened air, and a rigorous control of the temperature at the inner the reactor? Another approach would be to develop a reactor in this direction to improve the production.

Acknowledgements We are very grateful to Quentin Denis (Unité de Chimie Analytique) for his helpful assistance in ergosterol analysis and Adeline Gillet (Unité de statistique, Informatique et Mathématique apliquées) for the councils on the ANOVA test of our data. We also thank the Government of the Côte d'Ivoire for financial assistance.

References

1. Bakri, Y., Jacques, Ph., & Thonart, Ph. (2003). *Applied Biochemistry and Biotechnology, 105–108*, 737–747.
2. Bocchini, D. A., Oliveira, O. M. M. F., Gomes, E., & Silva, Da. R. (2005). *Process Biochemistry, 40*, 3653–3659.
3. Oliveira, L. A., Porto, A. L. F., & Tambourgi, E. B. (2006). *Bioresource Technology, 97*, 862–867.
4. Senthilkumar, S. R., Ashokkumar, B., Raj, C. K., & Gunasekaran, P. (2005). *Bioresource Technology, 96*, 1380–1386.
5. Shah, A. R., & Madamwar, D. (2005). *Process Biochemistry, 40*, 1763–1771.
6. Virupaksi, S., Babu, G. K., Gaikwad, S. R., & Naik, G. R. (2005). *Process Biochemistry, 40*(1), 431–435.
7. Xiong, H., Von Weymarn, N., Turunen, O., Leisola, M., & Pastinen, O. (2005). *Bioresource Technology, 96*, 753–759.
8. Yang, S. Q., Yan, Q. J., Jiang, Z. Q., Li, L. T., Tian, H. M., & Wang, Y. Z. (2006). *Bioresource Technology, 97*, 1794–1800.
9. Tabka, M. G., Herpoël-Gimbert, I., Monod, F., Asther, M., & Sigoillot, J. C. (2006). *Enzyme and Microbial Technology, 39*, 897–902.
10. Öhgren, K., Vehmaanperä, J., Siika-Aho, M., Galbe, M., Viikari, M., & Zacchi, G. (2007). *Enzyme and Microbial Technology, 40*, 607–613.
11. Milagres, A. M. F., Santos, E., Piovan, T., & Roberto, I. C. (2004). *Process Biochemistry, 39*, 1387–1391.
12. Bellon-maurel, V., Orliac, O., & Christen, P. (2003). *Process Biochemistry, 38*, 881–896.
13. Lareo, C., Sposito, A. F., Bossio, A. L., & Volpe, D. C. (2006). *Enzyme and Microbial Technology, 38*, 391–399.

14. Lu, M. Y., Maddox, I. S., & Brooks, J. D. (1998). *Proccess Biochemistry, 33*(2), 117–123.
15. Bailey, M. J., Biely, P., & Poutanen, K. (1992). *Journal of Biotechnology, 23*, 257–270.
16. Miller, G. L. (1959). *Analytical Chemistry, 31*, 426–428.
17. Barrios-Gonzalez, J., Tomasini, A., & Viniegra, G. L. G. (1988). Solid state fermentation in bioconversion of agro-industrial raw materials. Proceedings of the seminar, Orstom-Montpellier (France), Montpellier, 25–27 July 1988.
18. Elibol, M., & Moreira, A. R. (2005). *Process Biochemistry, 40*, 1951–1956.
19. Gaspar, A. (1999). PhD thesis, Faculté Universitaire des Sciences Agronomiques de Gembloux, Belgium.
20. Bakri, Y. (2003). PhD thesis, Faculté Universitaire des Sciences Agronomiques de Gembloux, Belgium.
21. Gaspar, A., Cosson, T., Roques, C., & Thonart, Ph. (1997). *Applied Biochemistry and Biotechnology, 67*, 45–58.
22. Gaspar, A., Strodiot, L., & Thonart, Ph. (1998). *Applied Biochemistry and Biotechnology, 7072*, 535–545.
23. Bakri, Y., Jacques, Ph., Shi, K. L., & Thonart, Ph. (2002). *Applied Biochemistry and Biotechnology, 98–100*, 1037–1047.
24. Arzumanov, T., Jenjins, N., & Roussos, S. (2005). *Process Biochemistry, 40*, 1037–1042.
25. Palma, M. B., Milagres, A. M. F., Prata, A. M. R., & De Mancilha, M. I. (1996). *Proccess Biochemstry, 31*(2), 141–145.
26. Robinson, P. D. (1984). *Biotechnology Letters, 6*, 119–122.
27. Evrard, J. F. (1991). Engineer thesis, Faculté Universitaire des Sciences Agronomiques de Gembloux, Belgium.
28. Kunas, K. T., & Papoutsakis, E. T. (1990). *Biotechnology and Bioengineering, 36*, 476–483.
29. Kalogeris, E., Iniotaki, E., Topakas, E., Christakopoulos, P., Kekos, D., & Macris, B. J. (2003). *Bioresource Technology, 86*, 207–213.
30. Khamgkhang, S., & Wisutharom, A. B. (1997). Project in Department of Chemical Engineering, Kasetsart University, Bangkok.
31. Prasertsri, A. M. (1999). PhD thesis, Kasetsart University at Bangkok.
32. Wenqing, L., Defa, L., & Yubo, W. (2003). *Enzyme and Microbial Technology, 32*, 305–311.

Appl Biochem Biotechnol (2008) 145:99–110
DOI 10.1007/s12010-007-8014-1

Ethanol Production from Wet-Exploded Wheat Straw Hydrolysate by Thermophilic Anaerobic Bacterium *Thermoanaerobacter* BG1L1 in a Continuous Immobilized Reactor

Tania I. Georgieva · Marie J. Mikkelsen · Birgitte K. Ahring

Received: 15 May 2007 / Accepted: 23 July 2007 /
Published online: 1 September 2007
© Humana Press Inc. 2007

Abstract Thermophilic ethanol fermentation of wet-exploded wheat straw hydrolysate was investigated in a continuous immobilized reactor system. The experiments were carried out in a lab-scale fluidized bed reactor (FBR) at 70°C. Undetoxified wheat straw hydrolysate was used (3–12% dry matter), corresponding to sugar mixtures of glucose and xylose ranging from 12 to 41 g/l. The organism, thermophilic anaerobic bacterium *Thermoanaerobacter* BG1L1, exhibited significant resistance to high levels of acetic acid (up to 10 g/l) and other metabolic inhibitors present in the hydrolysate. Although the hydrolysate was not detoxified, ethanol yield in a range of 0.39–0.42 g/g was obtained. Overall, sugar efficiency to ethanol was 68–76%. The reactor was operated continuously for approximately 143 days, and no contamination was seen without the use of any agent for preventing bacterial infections. The tested microorganism has considerable potential to be a novel candidate for lignocellulose bioconversion into ethanol. The work reported here also demonstrates that the use of FBR configuration might be a viable approach for thermophilic anaerobic ethanol fermentation.

Keywords Ethanol · Wet-explosion · Thermophilic anaerobic bacteria · Wheat straw · Fluidized bed reactor · Lignocellulose

Introduction

The use of bioethanol in the transportation sector can reduce the current dependence of petroleum and reduce greenhouse gas emission, in particular, CO_2. These facts have

T. I. Georgieva · M. J. Mikkelsen · B. K. Ahring (✉)
BioScience and Technology Group, BioCentrum-DTU, Technical University of Denmark,
Building 227, 2800 Lyngby, Denmark
e-mail: bka@biocentrum.dtu.dk

M. J. Mikkelsen
BioGasol ApS, DTU, Building 205, Lyngby 2800, Denmark

increased the necessity of using alternative raw materials in addition to corn and sugar cane, which are nowadays the primary feedstock used for the production of fuel ethanol. Lignocellulosic biomass, like wood and agricultural residues (e.g., wheat straw, rice straw, corn stover, sugar cane bagasse), is an abundant renewable raw material for fuel ethanol production.

Wheat straw is one of the most important global feedstocks for ethanol production. Wheat straw is the major crop residue in Europe and the second largest agricultural residue in the world [1]. Potential global annual production of bioethanol from wheat straw (104 million cubic meters) could replace 75 million cubic meters of gasoline, or about 6.8% of the global gasoline consumption [1]. Wheat straw is the main agricultural waste product in Denmark and likely to be the lignocellulosic raw material used in a future Danish industrial bioethanol process. Since 2002, two pilot plants (IBUS and MaxiFuels) for production of ethanol from wheat straw have been inaugurated in Denmark.

Wheat straw, like other lignocellulosic materials, contains lignin, which tightly binds cellulose and hemicelluloses together, forming a complex, rather resistant structure. To make the cellulose and hemicellulose carbohydrates more susceptible to enzymatic hydrolysis and further microbial conversion, the lignocellulose must first be pretreated. However, the pretreatment conditions are severe, and various degradation products (e.g., acetic acid, furans, and phenols) are generated, which have an inhibitory effect on microbial growth and metabolism [2, 3]. To reduce the inhibitory effect of lignocellulosic hydrolysates, an additional detoxification step is needed [2, 3]. The inclusion of a detoxification process using a recombinant strain of *Escherichia coli* [4] has been found to increase the cost of ethanol production from acid-hydrolyzed willow by 22%. In this regard, the development of inhibitory-tolerant strains that are capable of tolerating toxicity of various hydrolysates is of large commercial interest.

Xylose is the major sugar present in the hemicellulose fraction of agricultural residues, such as wheat straw. Because the raw material cost is greater than one-third of the overall ethanol production cost [5], fermentation of xylose together with glucose is needed to improve the economics of any lignocellulosic-based bioethanol process.

Pentose-fermenting organisms are found among bacteria, yeast, and fungi, with the yeast *Pichia stipitis*, *Candida shehatae*, and *Pachysolen tannophilus* being the most promising naturally occurring xylose fermenting microorganisms [6]. However, the disadvantage with these organisms is their susceptibility to the inhibitors in the undetoxified hydrolysates and the difficulty in maintaining the oxygenation at optimal levels for optimum performance [7]. Metabolic engineering has been extensively used to develop recombinant strains of traditionally used ethanol producers like *Saccharomyces cerevisiae* and *Zymomonas mobilis*, and enteric bacteria such as *E. coli*, that will efficiently ferment mixed sugars glucose and xylose, and in some cases, arabinose [5, 6, 8]. However, cofermentation of a mixture of glucose with xylose and other sugars is commonly accomplished with either "glucose repression" or "xylose sparing" [2, 8] and instability of the plasmid carrying the xylose utilization genes in the presence of glucose over a longer time period [9]. In addition, recombinant organisms exhibit low tolerance to the inhibitors in undetoxified hydrolysates [5].

Thermophilic anaerobic bacteria are an alternative for pentose fermentation [10, 11]. The increased interest in these microorganisms arises from their ability to metabolize naturally both pentose and hexose sugars found in lignocellulosic hydrolysates. Moreover, there are a large number of potential advantages associated with the production of ethanol at higher temperatures, including high bioconversion rates, low risk of contamination, and energy

savings due to cost reduction via cooling, mixing, and distillation. However, these organisms are excluded from being seriously considered for bioethanol production primarily because of (1) low ethanol yields associated with the production of fermentation products other than ethanol, (2) limited data under conditions of practical interest including high substrate concentrations and real hydrolysate media, and (3) a lack of consensus in the literature on their tolerance to ethanol [10].

Because no one strain meets the requirement for efficient fermentation of lignocellulose, the development of industrial organisms capable of simultaneously fermenting the broad range of sugars present in lignocellulosic hydrolysates (particularly glucose and xylose) and tolerating the hydrolysate inhibitors is still a challenge [8]. In addition to the required industrial fermentation organism, continuous fermentation with high cell density (cell immobilization or cell recycle) could optimize the feasibility of the bioethanol production process by increasing ethanol productivity, ethanol concentrations and continuous ethanol removal [2, 11].

It was found that the wild-type strain *Thermoanaerobacter* BG1 could grow and produce ethanol from hemicellulose hydrolysate of wheat straw with the same ethanol yield as found for synthetic medium. To increase the ethanol yield of this organism, lactic acid production was eliminated by knocking out the lactate dehydrogenase gene, resulting in the strain *Thermoanaerobacter* BG1L1. It has been found that *Thermoanaerobacter* BG1L1 tolerates ethanol concentration of 8.3% (v/v), and thus, the ethanol tolerance of this strain is one of the highest found for thermophilic anaerobic bacteria [12]. Therefore, the objective of the present work was to investigate the cofermentation of glucose and xylose derived from undetoxified wet-exploded wheat straw by an immobilized cell culture of *Thermoanaerobacter* BG1L1.

Materials and Methods

Microorganism

The strain used in this study was *Thermoanaerobacter* BG1L1, which is a lactate dehydrogenase-deficient mutant of the thermophilic anaerobic bacterial strain BG1. The strains *Thermoanaerobacter* BG1 and BG1L1 have been deposited in the German Collection of Microorganisms and Cell Cultures as patented strains.

Media and Inoculum Preparation

Inoculum was prepared by growing cells in 100-ml vials containing 45 ml anaerobic synthetic medium (BA medium) [13], amended with 1 g/l yeast extract but without cystein. The medium was neutralized and flushed for 15 min with a mixture of N_2/CO_2 (4:1) to ensure anaerobic conditions before autoclaving at 140°C for 20 min. Prior to inoculation, the medium was reduced with a sterile anaerobic solution of sodium sulfide to a final concentration of 0.5 g/l. Xylose and vitamins were further added from filter-sterilized anaerobic solutions of D-xylose and vitamins DSMZ medium No141 (German Collection of Microorganisms and Cell Cultures) to initial concentrations of 5 g/l and 10 ml/l, respectively. The medium was inoculated with 10% (v/v) culture and incubated overnight at 70°C in the dark without shaking.

Wet-Explosion Pretreatment

Straw pellets were obtained from DONG Energy pellet plant in Køge, Denmark. Wheat straw pellets were pretreated by wet-explosion. Wheat straw pellets (200 g) were mixed with water (1 l) in a 3.5-l reactor and heated for 10 min. Hydrogen peroxide was added to reach a final wet-oxidation condition of 3% oxygen per dry matter content (DM, w/w) when the temperature was 170°C. The biomass was flashed as soon as all hydrogen peroxide had reacted with the biomass. The pretreated wheat straw out of the reactor was with a DM of 14% and consisted of hemicellulose, cellulose and lignin.

Hydrolysate Medium

Different pretreated wheat straw suspensions were prepared by the addition of a corresponding volume of water to give a concentration of 20–80% (wt/v), equivalent to wet-exploded wheat straw of 3–12% DM. The pH was raised to 5 with 10 M NaOH and the suspensions were autoclaved at 120°C for 20 min. After autoclavation the enzyme mixture of Celluclast and Novozyme 188 (3:1 v/v) (Novozymes A/S, Bagsvaerd, Denmark) was aseptically added to give 10 FPU /g-cellulose. Enzymatic hydrolysis was carried out in a shaker at 50°C for 2–4 days. After enzyme hydrolysis, the wet-exploded wheat straw hydrolysate was centrifuged at 4,000 rpm for 30 min at 4°C to remove the particulate matter. After hydrolysate centrifugation, the supernatant was collected and the pH was adjusted with 10 M NaOH to pH=7, followed by further supplements of yeast extract, minerals, trace metals, and vitamins as used in the anaerobic synthetic medium (BA). Finally, the hydrolysate medium (WEH) was flushed for 45 min with a gas mixture of N_2/CO_2 (4:1), and 250 mg/l Na_2S was added to ensure anaerobic conditions.

Reactor Set-up

A schematic diagram of the reactor set-up used in the present study is shown in Fig. 1. The reactor was a water-jacketed glass column with a working volume of 200 ml. The influent entered from the bottom of the reactor and the feeding was controlled by a peristaltic pump. Recirculation flow was achieved by using an identical peristaltic pump to ensure up-flow velocities in the reactor of 1 m/h. The pH was maintained at 7.0 by the addition of 1 or 2 M NaOH. Liquid samples were taken from a sampling port located on the top of the reactor, close to the reactor outlet. The experiments were performed at 70°C using external heating and the recirculation of hot water in the glass jacket.

Reactor Start-up and Operation

The reactor was loaded with 75 ml granular carrier material [14], and finally, the entire reactor system, including tubing and recirculation reservoir, was autoclaved at 120°C for 30 min. Before use, the reactor system was gassed for 15 min with N_2/CO_2 (4:1) to ensure anaerobic conditions and filled with BA medium with an initial xylose concentration of 10 g/l. The reactor was started up in batch mode by inoculation with 80 ml of cell suspension with an optical density (OD_{578}) of 0.9–1. The batch mode of operation was maintained for 24 h to allow cells to attach and to immobilize on the carrier matrix. After the batch run, the system was switched to continuous mode, applying a hydraulic retention time (HRT; the volume of the reactor divided by the influent flowrate) of 8 h and up-flow velocity of 1 m/h. To achieve operational stability, the reactor was run for 7 days under

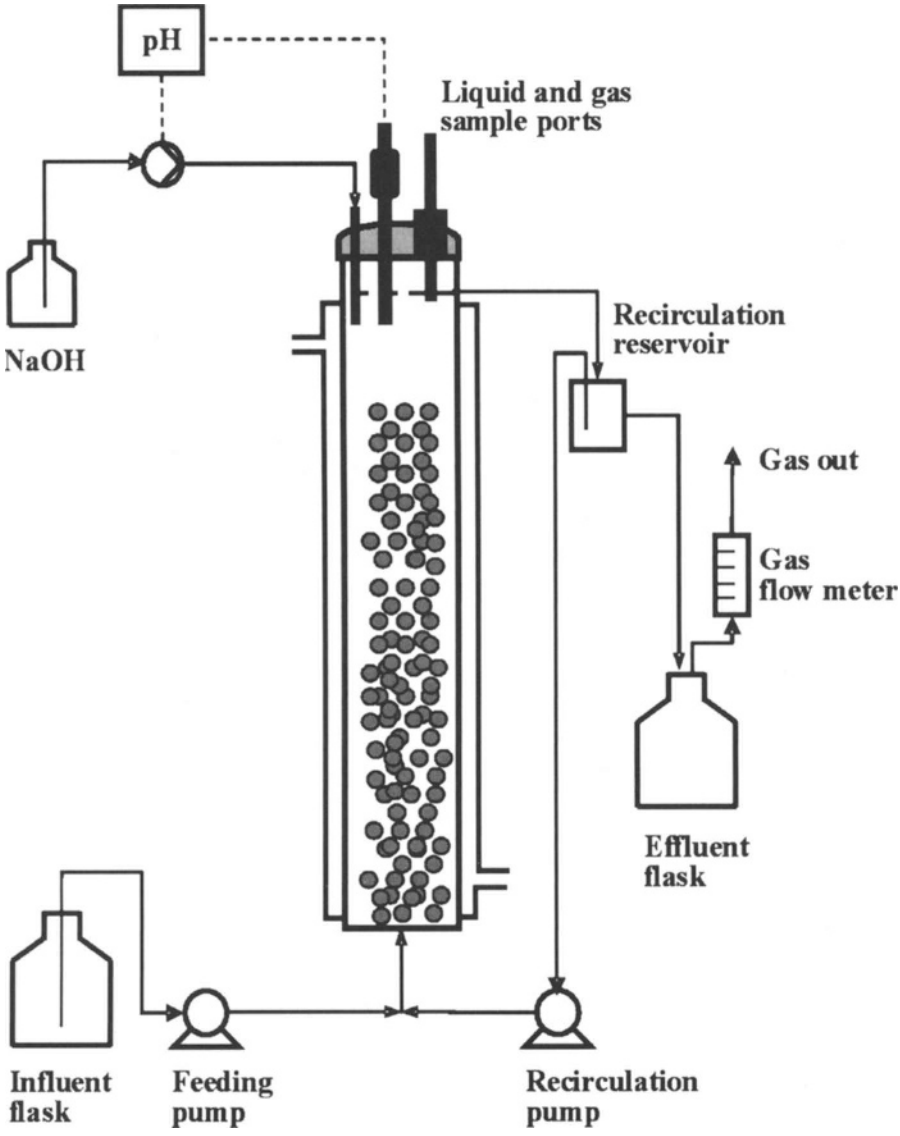


Fig. 1 A schematic diagram of the experimental set-up of the reactor

these operational conditions. After that, the fermentation started with 20% WEH as an influent at a HRT of 2 days. Unless otherwise stated, the HRT was 2 days. During the experiment, the concentration of WEH was gradually increased from 20 to 80% whenever steady state was achieved. The criteria for steady-state conditions were that all parameters must be held constant for at least five residence times. The reactor performance at different steady states was monitored by measuring the sugar and end-fermentation product concentrations. The values presented in the paper are the average of data taken at least over five residence times at steady state, and the standard deviation was less than 5%.

During the experiment, sterile syringes and needles were used to take the samples from the influent and effluent, and the samples were stored at −20°C until analysis.

Estimation of Ethanol Loss: Carbon and Redox Balances

The redox and carbon balances were used to determine the amount of carbon in the form of ethanol loss by stripping off to the gas phase. Lactic acid production at steady state conditions was less than 0.03 g/g; thus, it was excluded from carbon and redox balance calculations. For biomass production, biomass yield of 0.045 g/g was assumed [15, 16] with biomass composition $CH_{1.65}N_{0.23}O_{0.45}$ [17]. When growing the strain in batch culture, the carbon balance was almost closed (SD±2%), indicating that no other end products are formed than that included in redox and carbon balances.

Carbon recovery (Eq. 1) was determined as carbon in biomass and products formed divided by the total amount of sugar carbon consumed. For carbon recovery calculations, the amount of CO_2 produced was determined from the catabolic pathway of xylose and glucose, assuming that 1 mol CO_2 is produced for each mole of ethanol and acetic acid [15, 17–19]. Carbon balance can be written as:

$$CR[\%] = \frac{3(C_{EtOH}/M_{EtOH} + C_{Ace}/M_{Ace}) + C_{BM}/M_{BM}}{5C_{Xyl}/M_{Xyl} + 6C_{Glu}/M_{Glu}} \times 100 \quad (1)$$

where Ci is the concentration of compound i, i.e., substrate consumed or product produced (g/l) and Mi is the molecular weight of compound i (g/mol).

The redox balance was calculated based on fermentation products (ethanol and acetate) and biomass plus stoichiometrically associated production of H_2 accompanying the production of acetic acid [15, 17–19] as written:

$$RB[\%] = \frac{\gamma_{EtOH}\phi_{EtOH}C_{EtOH}/M_{EtOH} + \gamma_{Ace}\phi_{Ace}C_{Ace}/M_{Ace} + \gamma_{BM}\phi_{BM}C_{BM}/M_{BM} + 2N_{H2}}{\gamma_{Xyl}\phi_{Xyl}C_{Xyl}/M_{Xyl} + \gamma_{Glu}\phi_{Glu}C_{Glu}/M_{Glu}} \times 100 \quad (2)$$

As the degree of reduction of xylose and glucose are equal, Eq. 2 can be reduced to Eq. 3:

$$RB[\%] = \left(\frac{Y_{EtOH}\gamma_{EtOH} + Y_{Ace}\gamma_{Ace} + Y_{Lac}\gamma_{Lac} + Y_{BM}\gamma_{BM} + 2Y_{H2}}{\gamma_{Glu/Xyl}}\right) \times 100 \quad (3)$$

where: γ is degree of reduction representing the electron content per C-mole for organic compounds or per mole for inorganic compounds; ϕ is the number of carbon atoms per mole of compound; N_{H2} is the concentration of H_2 (mol/l); and Y is product yield: for organic compounds, it is C-mole product per C-mole substrate and for H_2, it is H_2-mole per C-mole substrate.

The redox balance verified that missing product was with a high degree of reduction (5.7–5.9), confirming that the primary product missing is ethanol because the ethanol degree of reduction is 6. To validate the values of ethanol loss, ethanol evaporation rate was also determined experimentally in an experimental set-up identical to the one used for the WEH fermentations with medium containing 10 g/l xylose and 10 g/l ethanol. Measured ethanol concentrations in the effluent were used to estimate ethanol evaporation

rate (0.02 g l^{-1} h^{-1}). The ethanol concentrations, as directly measured by high-performance liquid chromatography (HPLC), were then corrected for loss of ethanol by applying this ethanol evaporation rate. The corrected ethanol concentrations fitted well with the ethanol values calculated from carbon and redox balances. Therefore, redox balance was used throughout the paper to determine ethanol loss, assuming that the missing percentage in the degree of reduction was due to ethanol loss, and to correct ethanol concentrations presented in the paper for loss of ethanol.

Analytical Methods

Glucose, xylose, and end-fermentation products (ethanol, acetate, and lactate) were quantified using an HPLC-RI equipped with an Aminex HPX-87H column (Biorad, Hercules, CA, USA) at 60°C with 4 mM H_2SO_4 as eluent and with a flowrate of 0.6 ml/min. In addition, the ethanol and acetate measurements were validated using an HP 5890 Series II gas chromatograph with flame-ionization detection and a silica capillary column (cross-linked polyethylene glycol-TPA; 30 m×0.53 mm). Prior to HPLC and gas chromatograph analysis, 1-ml samples were acidified with 10 μl 20% H_2SO_4 and 30 μl 17% phosphoric acid, respectively, and centrifuged at 10,000 rpm for 10 min, followed by filtration through a 0.45-μm membrane filter.

Test for Contamination

A 1-ml sample was taken from the reactor and chromosomal DNA was purified using the DNA purification kit from A&A Biotech (Gdynia, Poland). PCR reactions were setup using the Pfu polymerase (MBI Fermentas, St. Leon-Rot, Germany) and the primers B-all 27F (GAG TTT GAT CCT GGC TCA G) and B-all 1492R (ACG GCT ACC TTG TTA CGA CTT), which anneal to bacterial rDNA. The fragments were purified using the Qiaex II kit from Qiagen (Valencia, CA, USA), treated with PNK (MBI Fermentas), cloned into pBluescript SK+ (Stratagene, Cedar Creek, TX, USA) treated with CIAP (MBI Fermentas), and transformed into *E. coli* Top10 (Invitrogen, Carlsbad, CA, USA). Fifty clones were picked and the inserts were amplified using B-all 27F and B-all 1492R primers. The resulting fragments were digested with *Alu*I and *Mbo*I restriction enzymes (MBI Fermentas) and were run on a 3% agarose gel. Only one digestion pattern was found. Two fragments were sent for sequencing (MWG Biotech, Ebersberg, Germany) and were identified as strain *Thermoanaerobacter* BG1L1. PCR reactions were also run annealing, respectively, to regions upstream and downstream of the lactate dehydrogenase. Otherwise, the same reaction conditions as for the B-all primers, were used. The obtained fragments were cloned (as above); 26 were analyzed by restriction length polymorphism. Again, this resulted in only one pattern. Two fragments were sequenced.

Results

Thermophilic anaerobic ethanol fermentation of wet-exploded wheat straw hydrolysate was investigated using an immobilized culture of a lactate dehydrogenase-deficient mutant strain *Thermoanaerobacter* BG1L1. The fermentations were carried out in a lab-scale fluidized bed reactor (FBR) at 70°C. Whenever steady state was achieved, the concentration of WEH was increased gradually from 20 to 80% (wt/v), corresponding to sugar mixtures of glucose and xylose ranging from 12 to 41 g/l. Fermentation performance of tested strain

under steady state conditions was evaluated by sugar utilization, product formation (ethanol, acetate, and lactate) and ethanol yield. The results, including influent sugars and acetate concentrations, are summarized in Table 1. The experiment started with a HRT of 2 days to prevent substrate limitation due to short sugar residence time in the reactor and to enable the organism to adapt to the new environment.

With increasing of WEH concentration from 20 to 80%, the ethanol concentration in the effluent increased gradually from 4.6 to 14.42 g/l, yielding relatively high and stable ethanol yields in the range 0.39–0.42 g per gram sugars consumed, corresponding to 76–83% of the theoretically possible yield (Table 1). When the fermentation started with 80% WEH, the process continued at a HRT of 3 days to avoid kinetic limitation i.e., low reaction rate compared to substrate loading rate caused by higher concentration of inhibitors present at higher WEH concentrations. Increasing the HRT from 2 to 3 days was apparently effective with respect to utilized sugars, and 3% higher overall sugar conversion was seen compared to 60% WEH (Table 1).

Glucose utilization was higher than 90% for all tested WEH suspensions, whereas xylose conversion remained lower, between 72 and 80%. The lowest sugar conversions of 90 and 72%, respectively, for glucose and xylose were seen at 40% WEH. This could be attributed to a technical problem with the pH control system because the pH value was maintained around 6.5–6.7 instead of pH 7, and the reactor operated under these conditions (pH 6.5–6.7) with 40% WEH until the end of the experiment. The overall sugar conversion efficiency to ethanol for all these experiments was in a range of 68–76% (Table 1).

Acetate was the main by-product with a yield of 0.08–0.11 g/g (Table 1). High initial acetate concentrations (2.86–6.02 g/l) in the feed streams resulted in a rather high concentration of nearly 10 g/l acetate in the effluent at the highest WEH concentration tested (Table 1). In all fermentations, only trace amounts of lactate were produced (<0.03 g/g, data not shown) as expected, because the strain is a lactate dehydrogenase-deficient mutant. These data also show that deletion of the lactate dehydrogenase was stable over a long period of time.

During the experiment, which lasted for 143 days, the reactor was checked regularly for contamination by purifying chromosomal DNA from reactor samples, and no species other than *Thermoanaerobacter* BG1L1 were found. The deletion of the lactate dehydrogenase was also found to be stable, as shown by sequencing of the lactate dehydrogenase region.

Discussion

In a preliminary study on continuous cofermentation of glucose–xylose mixtures in a laboratory medium, the strain *Thermoanaerobacter* BG1L1 showed promising ethanol yields up to 0.45 g/g and an ethanol productivity of 1 g l^{-1} h^{-1} required for an economically feasible lignocellulose-based bioethanol process [20]. However, microorganisms producing high ethanol yields in laboratory media do not necessarily ferment lignocellulosic substrates efficiently because of the presence of a broad range of inhibitory compounds. Therefore, evaluation of fermentative performance of microbial candidates in lignocellulosic hydrolysates of industrial interest is crucial because the fuel ethanol production will be based on these substrates rather than laboratory media [21]. Thus, the fermentative performance of *Thermoanaerobacter* BG1L1 in cofermenting glucose and xylose present in undetoxified wet-exploded wheat straw hydrolysate was studied to verify the potential of this strain as a candidate for bioethanol production from lignocellulosic biomass. In this study, wet-exploded wheat straw hydrolysate was used as a lignocellulosic substrate

Table 1 Summary of ethanol production from undetoxified WEH by immobilized cells of the thermophilic anaerobic bacterium *Thermoanaerobacter* BG1L1 in a FBR operated at 70°C and pH 7.

HRT (days)	WEH (wt/v) %	Influent			Effluent				Sugar conversion			Yield[a]		Y_{EtOH}[b] %	CE[c] %	CR[d] %
		Glu (g/l)	Xyl (g/l)	Ace (g/l)	Glu (g/l)	Xyl (g/l)	Ace (g/l)	EtOH[e] (g/l)	Glu (%)	Xyl (%)	Total[f] (%)	Ace (g/g)	EtOH (g/g)			
2	20	8.77	3.04	2.86	0.37	0.60	3.76	4.60	95.8	80.2	91.8	0.08	0.42	83	76	103.0
2	40	16.22	8.02	3.51	1.62	2.23	5.39	8.38	90.0	72.2	84.1	0.09	0.41	80	68	99.9
2	60	22.17	11.18	4.84	1.45	2.68	7.91	11.57	93.4	76.0	87.6	0.10	0.40	78	68	99.4
3	80	27.24	14.08	6.02	1.11	2.76	9.98	14.42	95.9	80.4	90.6	0.11	0.39	76	68	97.7

[a] Yield on sugars consumed

[b] Ethanol yield given as percentage of theoretical possible yield of 0.51 g/g

[c] Conversion efficiency is calculated by dividing the ethanol yield based on the glucose and xylose concentrations present in the influent by theoretical possible yield of 0.51 g/g

[d] CR carbon recovery

[e] Ethanol corrected for loss of ethanol based on redox balance

[f] Total sugar consumed (i.e., glucose plus xylose)

because it is likely to be the lignocellulosic feedstock for fuel ethanol production in the MaxiFuels pilot plant, Denmark.

To counteract possible bacterial contamination, the wet-exploded wheat straw was sterilized using autoclavation (120°C for 20 min). Autoclavation of wet-oxidized wheat straw (121°C; for 10–20 min) has recently been reported to increase the concentration of phenol acids, formic acid, glycolic acid, and malic acid by 30–40% and of acetic acid by 75% [22]. Despite the facts that wet-exploded wheat straw was temperature-sterilized and the hydrolysate was undetoxified, strain *Thermoanaerobacter* BG1L1 was capable of fermenting WEH with relatively high ethanol yields of 0.39–0.42 g per gram of sugars consumed (equivalent to 76–83% of theoretical ethanol yield) (Table 1). The ethanol yields are comparable with those previously obtained in a defined BA medium with similar glucose–xylose concentrations [20]. These results reveal that inhibitors present in the hydrolysate did not significantly affect the ethanol yield. Strain resistance to hydrolysate toxicity could be attributed to long-term continuous strain adaptation to inhibitors present in the hydrolysate coupled with the use of high cell mass concentrations (cell immobilization). Employing high cell densities for fermentation of lignocellulosic hydrolysates has previously been shown to overcome hydrolysate toxicity [2]. Recent studies with immobilized thermophilic yeast have demonstrated that immobilization increases tolerance to substrates, ethanol, and high osmolarity and stabilizes the fermentation capacity of the system in a wide range of pH and temperature conditions [23].

The lowest sugar conversions of 90 and 72%, respectively, for glucose and xylose were seen at 40% WEH. This could be attributed to a technical problem with the pH control system because the pH value dropped to 6.5–6.7 instead of pH 7. The reactor operated under these conditions (pH 6.5–6.7) with 40% (DM) WEH until the end of the experiment with this WEH concentration. The low sugar conversion at 40% WEH compared to all other substrate concentrations constitutes an example of the influence of small pH deviations on the fermentation. This is consistent with previous reports that pH is a crucial variable parameter during the fermentation of lignocellulosic hydrolysates, especially at high organic acid concentrations, because the inhibitory effects of organic acids increase with decreasing pH due to more acids being in the more toxic undissociated form [3]. Although process unbalance was caused by the loss of pH control, the long-term reactor performance (143 days) was demonstrated with respect to sugar conversions, ethanol yields, contamination, and stable lactate dehydrogenase strain mutation.

Continuous fermentation has previously been tested for cellulosic substrates (e.g., glucose conversion) by thermophilic anaerobic bacteria [24, 25]; however, the present study is, to our best knowledge, the first one dealing with continuous cofermentation of glucose and xylose derived from lignocellulosic biomass using these microorganisms.

Very limited data have been published regarding cofermentation of glucose and xylose present in wheat straw hydrolysate. Immobilized cells of yeast *Pachysolen tannophiluc* gave significantly lower ethanol yield (0.32 g per gram of sugars consumed from 35 g/l reducing sugars) and sugar efficiency (63.4%) during continuous fermentation of wheat straw hydrolysate than these reported here [26]. Recently, comparable ethanol production yields for recombinant *E. coli* FBR5 (0.33–0.41 g per gram of sugars available) have been reported for fermentation of similar glucose–xylose mixtures (41–46 g/l) present in undetoxified alkaline peroxide-treated wheat straw [27] and undetoxified dilute acid-pretreated wheat straw [28].

The ethanol yields obtained in this study are considerably higher than those reported for fermentation of the undetoxified hemicellulose fraction of wheat straw by various pentose-utilizing yeasts and are comparable with the highest yield of 0.41 g per gram of sugars

available achieved by batch culture of *P. stipitis* from detoxified hydrolysate [29]. The ethanol yields and sugar utilization presented in this paper are also somewhat higher than those (0.24–0.36 g per gram of sugars consumed) obtained from both undetoxified and detoxified wheat straw acid hydrolysates by the thermophilic bacterium *Bacillus stearothermophilus* T-13 during continuous fermentation with cell recycle [30]. The results obtained are also comparable to those from simultaneous saccharification and fermentation of the cellulose fraction from wheat straw by *S. cerevisiae* (0.35–0.42 g per gram of glucose potential in pretreated material) [31–33] and by thermotolerant yeast strain of *Kluyveromycess* species (0.32–0.41 g per gram of glucose potential in pretreated material) [34, 35].

The experimental data reported here seem rather encouraging in view of the feasibility of the tested strain (*Thermoanaerobacter* BG1L1) as a novel candidate for fuel bioethanol fermentation from lignocellulose. The high ethanol yield, the high sugar conversion, and the resistance to hydrolysate toxicity seen in this study provide additional evidence supporting the previous suggestions based on demonstrated high ethanol tolerance by *Clostridium thermosaccharolyticum* and *Thermoanaerobacter ethanolicus*: that the practicality of thermophilic anaerobic bacteria for industrial bioethanol production should be reevaluated [36, 37]. This study has also demonstrated that the use of FBR technology might be a viable approach for ethanol production by thermophilic anaerobic bacteria. Work is already under way to test the strain's performance in other undetoxified hydrolysates, and future experiments are under consideration to ferment higher-input sugar concentrations (e.g., higher biomass concentrations) and to optimize the process parameters to improve ethanol productivity.

Acknowledgements We thank Novozymes A/S for providing enzymes Celluclast and Novozyme 188. We further thank Thomas Andersen and Gitte Hinz-Berg from BioCentrum for excellent technical help.

Reference

1. Kim, S., & Dale, B. E. (2004). *Biomass and Bioenergy, 26*, 361–375.
2. Olsson, L., & Hahn-Hägerdal, B. (1996). *Enzyme and Microbial Technology, 18*, 312–331.
3. Palmqvist, E., & Hahn-Hägerdal, B. (2000). *Bioresource Technology, 74*, 25–33.
4. Von Sivers, M., Zacchi, G., Olsson, L., & Hahn-Hägerdal, B. (1994). *Biotechnology Progress, 10*, 555–560.
5. Dien, B. S., Cotta, M. A., & Jeffries, T. W. (2003). *Applied Microbiology and Biotechnology, 63*, 258–266.
6. Aristidou, A., & Penttila, M. (2000). *Current Opinion in Biotechnology, 11*, 187–198.
7. Saha, B. C. (2003). *Journal of Industrial Microbiology and Biotechnology, 30*, 279–291.
8. Zaldivar, J., Nielsen, J., & Olsson, L. (2001). *Applied Microbiology and Biotechnology, 56*, 17–34.
9. Moniruzzaman, M., Dien, B. S., Skory, C. D., Chen, Z. D., Hespell, R. B., Ho, N. W. Y., et al. (1997). *World Journal of Microbiology and Biotechnology, 13*, 341–346.
10. Klapatch, T. R., Hogsett, D. A. L., Baskaran, S., Pal, S., & Lynd, L. R. (1994). *Applied Biochemistry and Biotechnology, 45–46*, 209–223.
11. Lynd, L. R. (1989). In *Advances in biochemical engineering/biotechnology* (vol 38, pp. 1–52). New York: Springer.
12. Georgieva, T. I., Mikkelsen, M. J., & Ahring, B. K. (2007). *Central European Journal of Biology*, DOI 10.2478/s11535-007-0026-x.
13. Sommer, P., Georgieva, T., & Ahring, B. K. (2004). *Biochemical Society Transactions, 32*, 283–289.
14. Schmidt, J. E., & Ahring, B. K. (1999). *Applied and Environmental Microbiology, 65*, 1050–1054.
15. Desai, S. G., Guerinot, M. L., & Lynd, L. R. (2004). *Applied Microbiology and Biotechnology, 65*, 600–605.
16. Lynd, L. R., Baskaran, S., & Casten, S. (2001). *Biotechnology Progress, 17*, 118–125.
17. Hild, H. M., Stuckey, D. C., & Leak, D. J. (2003). *Applied Microbiology and Biotechnology, 60*, 679–686.

18. Hill, P. W., Klapatch, T. R., & Lynd, L. R. (1993). *Biotechnology and Bioengineering, 42*, 873–883.
19. Lynd, L. R., Weimer, P. J., van Zyl W. H, & Pretorius, I. S. (2002). *Microbiology and Molecular Biology Reviews, 66*, 506–577.
20. Georgieva, T., & Ahring, B. K. (2007). *29th Symposium on Biotechnology for Fuels and Chemicals*, 51.
21. Zaldivar, J., Roca, C., Le Foll, C., Hahn-Hägerdal, B., & Olsson, L. (2005). *Bioresource Technology, 96*, 1670–1676.
22. Klinke, H. B., Thomsen, A. B., & Ahring, B. K. (2004). *Applied Microbiology and Biotechnology, 66*, 10–26.
23. Banat, I. M., Nigam, P., Singh, D., Marchant, R., & Mchale, A. P. (1998). *World Journal of Microbiology and Biotechnology, 14*, 809–821.
24. Hörmeyer, H. F., Tailliez, P., Millet, J., Girard, H., Bonn, G., Bobleter, O., et al. (1988). *Applied Microbiology and Biotechnology, 29*, 528–535.
25. Lynd, L. R., Grethlein, H. E., & Wolkin, R. H. (1989). *Applied and Environmental Microbiology, 55*, 3131–3139.
26. Kaur, H. R. P. (1989). *Biological Wastes, 30*, 301–308.
27. Saha, B. C., & Cotta, M. A. (2006). *Biotechnology Progress, 22*, 449–453.
28. Saha, B. C., Iten, L. B., Cotta, M. A., & Wu, Y. V. (2005). *Process Biochemistry, 40*, 3693–3700.
29. Nigam, J. N. (2001). *Journal of Biotechnology, 87*, 17–27.
30. Amartey, S. A., Leung, P. C. J., Baghaei-Yazdi, N., Leak, D. J., & Hartley, B. S. (1999). *Process Biochemistry, 34*, 289–294.
31. Alfani, F., Gallifuoco, A., Saporosi, A., Spera, A., & Cantarella, M. (2000) *Journal of Industrial Microbiology and Biotechnology, 25*, 184–192.
32. Felby, C., Klinke, H. B., Olsen, H. S., & Thomsen, A. B. (2003). *Applications of Enzymes to Lignocellulosics, 855*, 157–174.
33. Mohagheghi, A., Tucker, M., Grohmann, K., & Wyman, C. (1992). *Applied Biochemistry and Biotechnology, 33*, 67–81.
34. Ballesteros, M., Oliva, J. M., Negro, M. J., Manzanares, P., & Ballesteros, I. (2004). *Process Biochemistry, 39*, 1843–1848.
35. Szczodrak, J. (1988). *Biotechnology and Bioengineering, 32*, 771–776.
36. Baskaran, S., Ahn, H. J., & Lynd, L. R. (1995). *Biotechnology Progress, 11*, 276–281.
37. Burdette, D. S., Jung, S. H., Shen, G. J., Hollingsworth, R. I., & Zeikus, J. G. (2002). *Applied and Environmental Microbiology, 68*, 1914–1918.

Appl Biochem Biotechnol (2008) 145:111–119
DOI 10.1007/s12010-007-8031-0

Succinic Acid Production from Cheese Whey using *Actinobacillus succinogenes* 130 Z

Caixia Wan · Yebo Li · Abolghasem Shahbazi · Shuangning Xiu

Received: 15 May 2007 / Accepted: 27 August 2007 /
Published online: 22 September 2007
© Humana Press Inc. 2007

Abstract *Actinobacillus succinogenes* 130 Z was used to produce succinic acid from cheese whey in this study. At the presence of external CO_2 supply, the effects of initial cheese whey concentration, pH, and inoculum size on the succinic acid production were studied. The by-product formation during the fermentation process was also analyzed. The highest succinic acid yield of 0.57 was obtained at initial cheese whey concentration of 50 g/L, while the highest succinic acid productivity of 0.58 g h^{-1} L^{-1} was obtained at initial cheese whey concentration of 100 g/L. Increase in pH and inoculum size caused higher succinic acid yield and productivity. At the preferred fermentation condition of pH 6.8, inoculum size of 5% and initial cheese whey concentration of 50 g/L, succinic acid yield of 0.57, and productivity of 0.44 g h^{-1} L^{-1} were obtained. Acetic acid and formic acid were the main by-products throughout the fermentation run of 48 h. It is feasible to produce succinic acid using lactose from cheese whey as carbon resource by *A. succinogenes* 130 Z.

Keywords Succinic acid · Cheese whey · Lactose · Fermentation · *Actinobacillus succinogenes*

Introduction

Succinic acid, known as amber acid or butanedioic acid, is a four-carbon dicarboxylic acid produced as an intermediate of the tricarboxylic acid cycle (TCA) [1, 2]. Succinic acid and its derivative have wide industrial applications such as the feedstock of food and pharmaceutical products, as the intermediate of chemical synthesis of surfactants, detergents, green solvents, and biodegradable plastics, and also as ingredients of animal feeds to stimulate animal and

C. Wan · Y. Li (✉)
Department of Food, Agricultural, and Biological Engineering,
The Ohio State University, 1680 Madison Ave.,
Wooster, OH 44691, USA
e-mail: li.851@osu.edu

A. Shahbazi · S. Xiu
Department of Natural Resources and Environmental Design,
North Carolina A&T State University, 1601 East Market Street,
Greensboro, NC 27411, USA

plant growth [2–5]. Currently, most of commercial succinic acid is produced through petrochemical process, which brings environmental pollution and the concerns of sustainable development [2, 3]. The production of succinic acid by microbial fermentation is a simple and environmentally friendly process [4, 6, 7]. However, to date, biobased succinic acid is not yet competitive with petrochemical-based acid, mainly owing to high production cost [8]. There is a need to develop cost-effective conversion technology to produce succinic acid from renewable resource such as food processing waste [9–11].

Many anaerobic and facultative anaerobic microbes produce succinic acid as the fermentation end product [5]. *Actinobacillus succinogenes* 130Z, originally isolated from bovine ruminal contents, is a facultatively anaerobic, capnophilic and Gram-negative bacteria, which has been considered as the most potential succinic acid producer to produce a significant amount of succinic acid from glucose under anoxic condition [12]. This strain 130Z also showed distinctive ability to convert a broad range of carbon sources such as arabinose, cellobiose, fructose, xylose, and reduced sugar to succinate as the major end product and acetate, formate, lactate, and ethanol as the minor end products [13]. This strain has an advantage over other previously reported succinic acid producers because it can tolerate the presence of high concentration of succinic acid or its salt [14].

It was reported that *A. succinogenes* 130Z and its variant strain FZ6 produced 66.4 and 105.8 g/L of succinic acid with the yield of 0.67 and 0.8 from glucose, respectively, which indicated *A. succinogenes* had huge potential to be developed as a commercial succinic acid producer [13, 14]. Continuous and repeat-batch biofilm fermentation of succinic acid by strain 130Z demonstrated a significant increase in succinic acid productivity (7 g h^{-1} L^{-1}) and yield (86.7%) [15]. Environmental and physiological studies showed that CO_2 level and pH were the most critical factors affecting both cell growth and succinic acid formation. Increase in CO_2 supply and electron donor resulted in increase of succinic acid production and less formation of by-products such as ethanol and formate. This is most likely due to the increased PEP carboxylation to oxaloacetate rather than PEP conversion to pyruvate, where the pathway was regulated by the level of CO_2 and electron donors [16].

Whey is produced as a by-product during cheese making and as a potentially environmental pollutant due to its high biological oxygen demand (BOD) [17]. Whey consists mainly of 6 to 7% solids, of which 70 to 80% is lactose and 10 to 15% soluble proteins, lactate, and other mineral salts [11]. It can be directly used as feed additive and also has a continuing interest to be alternatively utilized as the low-cost substrate to produce value-added biochemicals such as lactic acid [17, 18]. Previous studies showed that *Actinobacillus succiniciproducens* and *Mannheimia succiniproducens* can ferment whey directly into succinic acid [11, 19]. However, the studies concerning the fermentation of succinic acid from cheese whey using A. *succinogenes* have not been reported.

The objectives of this study were to develop fermentative protocol for succinic acid production from cheese whey by *A. succinogenes* and study the effect of environmental and nutritional factors such as external CO_2 supply, pH, inoculum size, and initial whey concentration on succinic acid production.

Materials and Methods

Organism and Growth Conditions

A. succinogenes 130Z (ATCC 55618) was obtained from the American Type Culture Collection (Rockville, MD). Cells were grown in 250 mL sealed anaerobic bottles

containing 150 mL of medium with CO_2 as the gas phase, unless stated otherwise. The growth medium contained per liter deionized water: 5 g yeast extract, 3 g K_2HPO_4, 1 g NaCl, and 1 g $NaHCO_3$. The medium was autoclaved for 15 min at 121 °C in an anaerobic bottle with N_2 as headspace. Cheese whey (Davisco Foods International, Inc., Eden Prairie, MN; final concentration of 20 g/L) was separately sterilized (10 min at 110 °C) and aseptically added to the medium. pH was adjusted to 6.8 using a few drops of concentrated sterile sulfuric acid. The reduced medium was inoculated with 1.5 mL of glycerol stock and incubated at 37 °C for 20 h.

The batch fermentation was conducted in a 2.5-L fermentor (New Brunswick Scientific Co. Edison, NJ) with 1.2 L fermentation medium containing per liter: 50–100 g cheese whey, 5 g yeast extract, 10 g peptone, 3 g K_2HPO_4, 1 g NaCl, 0.02 g $CaCl_2 \cdot H_2O$, and 0.02 g $MgCl_2 \cdot 6H_2O$. Cheese whey was separately autoclaved (10 min at 110 °C) and mixed with the nutrients in the fermentor. The pH was maintained at 6.8 using 10 N NaOH during the fermentation run, unless stated otherwise. The agitation rate and temperature were maintained at 200 rpm and 38 °C, respectively. Filter-sterile CO_2 was sparged into the medium at a constant flow rate of 0.5 vvm. The inoculum was added to the fermentor after pH, agitation, CO_2 sparging, and temperature were adjusted. Foam was controlled by adding antifoam 204 (Sigma Chemical Co., St. Louis, MO). Sample was withdrawn at an interval of 2 h during the first 8 h and an interval of 12 h during the rest of fermentation run. The fermentation experiment lasted for 48 h.

Analytical Method

The concentration of lactose and fermentation products such as succinic acid and acetic acid was determined by high-performance liquid chromatography (Waters, Milford, MA) with a KC-811 ion exclusion column and a waters 410 differential refractometer detector. The mobile phase was 0.1% H_3PO_4 solution at a flow-rate of 1 mL/min. The temperature of the detector and of the column ware maintained at 35 and 60 °C, respectively. The succinic acid yield was expressed as the amount of succinic acid produced from 1 g lactose consumed during the fermentation process.

Results and Discussions

Effect of Initial Cheese Whey Concentration

In the previous studies, it was reported that initial concentration of carbon source could influence the cell growth and succinic acid production throughout the fermentation [20]. The effect of initial cheese whey concentrations on succinic acid formation was shown in Fig. 1 Maximum succinic acid concentration of 27.9 g/L was obtained at 48 h when the initial concentration of cheese whey was 100 g/L. The succinic acid concentration increased rapidly from 6 to 24 h corresponding to the rapid consumption of lactose during this period.

Initial cheese whey concentration had a significant effect on the succinic acid yield ($P<0.03$) and productivity ($P<0.02$). After 48 h of fermentation, the highest succinic acid yield of 0.57 was obtained at initial cheese whey concentration of 50 g/L. The succinic acid productivity increased from 0.44 to 0.58 g h^{-1} L^{-1} when the initial whey concentration increased from 50 to 100 g/L (Fig. 2). The highest succinic acid productivity of 0.95 g h^{-1} L^{-1} was obtained at 24 h with the initial whey concentration of 75 g/L, while the productivity

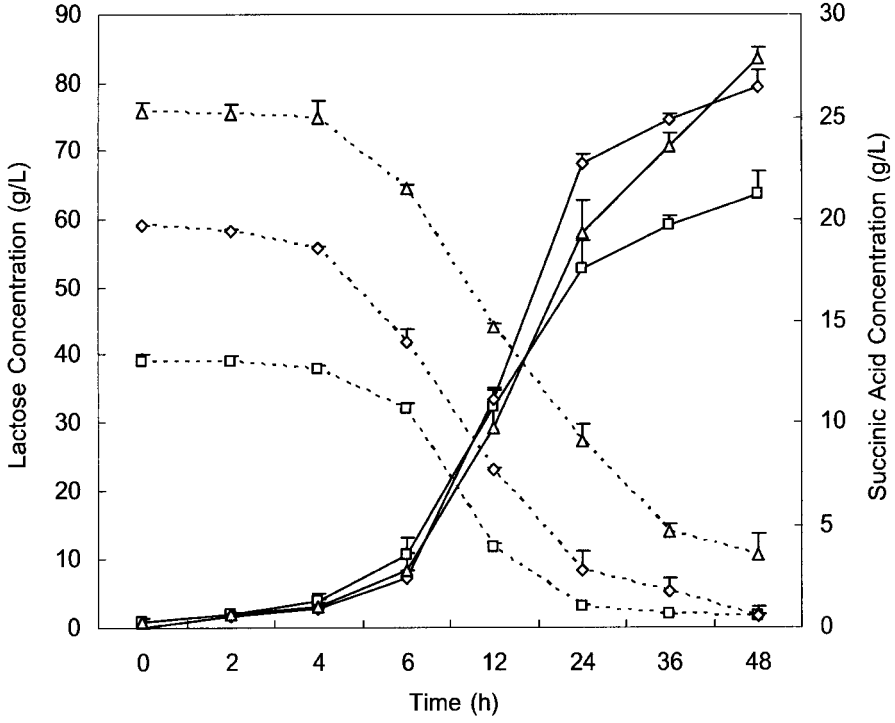


Fig. 1 Effect of initial cheese whey concentration on lactose and succinic acid concentration (pH 6.8, inoculum size of 5%). *Solid line and dash line* represent the succinic acid concentration and the lactose concentration, respectively. *Symbols* represent different cheese whey concentrations of 50 (*empty squares*), 75 (*empty diamonds*), and 100 g/L (*empty triangles*)

at 48 h was 0.44 g h^{-1} L^{-1} (Fig. 2). The rapid increase in succinic acid concentration from 12 to 24 h led to the higher productivity at 24 h. In our study, it was demonstrated that strain 130Z could directly ferment lactose from cheese whey with less single sugar such as galactose and glucose produced due to the degradation of lactose (data no shown).

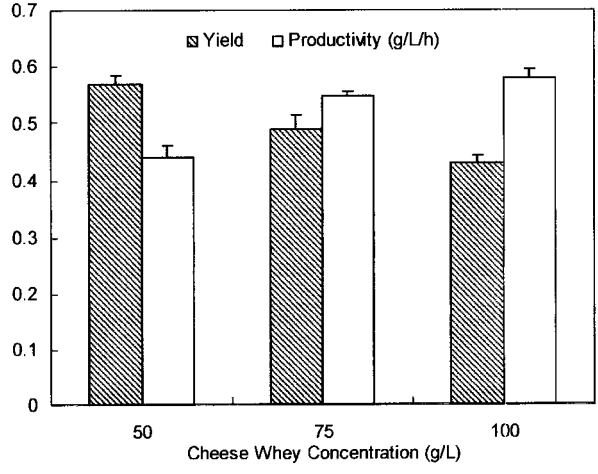


Fig. 2 Effect of initial cheese whey concentration on the succinic acid yield and productivity (pH 6.8, inoculum size of 5%, fermentation time of 48 h)

Effect of the pH

The pH is an important environmental factor that affects cell growth and CO_2/HCO_3^- ratio which played a crucial role in the fermentative succinic acid production. Samuelov et al. [11] reported that low pH resulted in increase of the activity of the key enzymes of the PEP carboxykinase pathways, which led to the flux of PEP towards more succinic acid formation. However, low pH also had adverse effect on the cell growth [16]. The optimal pH or range for succinic acid production by anaerobic or facultatively anaerobic microorganism such as *Bacteroides fragilis*, *A. succiniciproducens*, *M. succiniciproducens* MBEL 55E, *Enterococcus facalis*, and *A. succinogenes* was 7.0, 6.8, 6.0–7.5, 7–8, and 6.0–7.4, respectively [7, 11, 14, 16, 21, 22].

The effect of pH on succinic acid production using cheese whey as carbon source by *A. succinogenes* 130 Z was shown in Fig. 3. The concentration of succinic acid increased from 19.1 to 21.2 g/L with pH increase from 6.2 to 6.8, while the succinic acid concentration at pH 6.8 and 7.2 were very close. The succinic acid yield and productivity at pH 6.8 and 7.2 were also very close, while that at pH 6.2 were much lower (Fig. 4). However, the effects of pH ranging from 6.2 to 7.2 on the succinic acid yield ($P>0.13$) and productivity ($P>0.35$) were not significant. Although similar succinic acid productivity and yield were obtained at pH 6.8 and 7.2, more alkaline is needed to maintain a higher pH during fermentation run. In this study, the preferred pH for succinic acid production from cheese whey was 6.8.

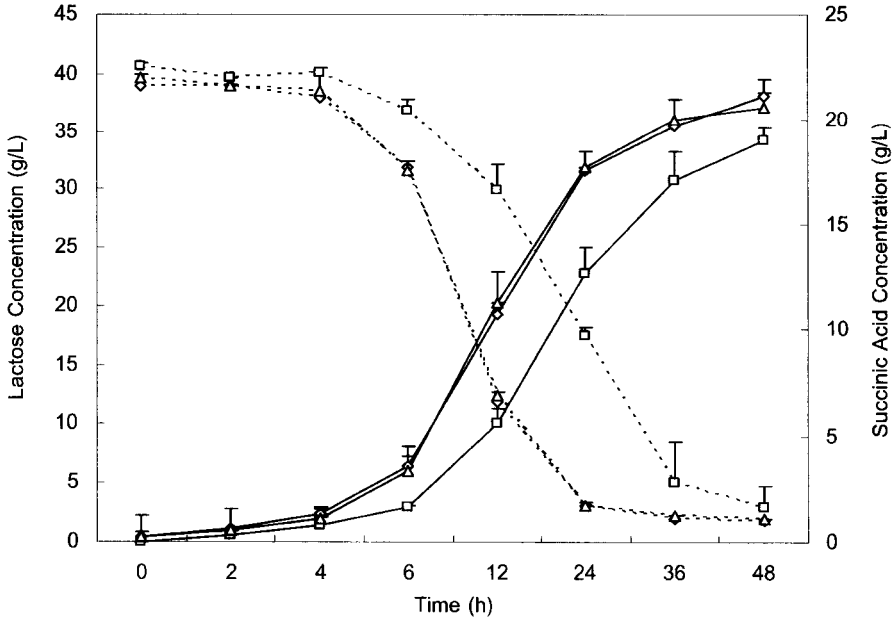


Fig. 3 Effect of pH value on lactose and succinic acid concentration (initial cheese whey concentration of 50 g/L, inoculum size of 5%). *Solid line* and *dash line* represent the succinic acid concentration and the lactose concentration, respectively. Symbols are the pH values of 6.2 (*empty squares*), 6.8 (empty diamonds), 7.2 (*empty triangles*)

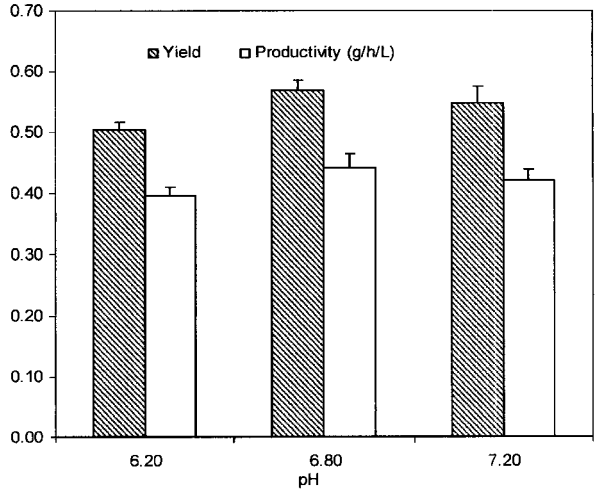


Fig. 4 Effect of pH on the succinic acid yield and productivity (initial cheese whey concentration of 50 g/L, inoculum size of 5%, total fermentation time of 48 h)

Effect of Inoculum Size

The effect of inoculum size on succinic acid production is shown in Fig. 5. Higher succinic acid concentration was observed at the inoculum size of 10% than that at 2 and 5%

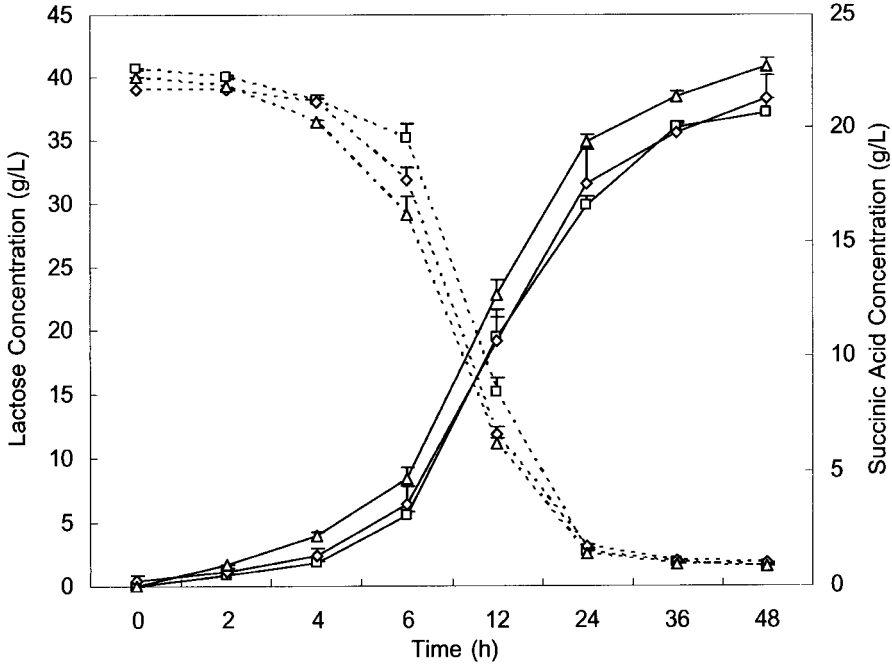


Fig. 5 Effect of inoculum size on lactose and succinic acid concentration (initial cheese whey concentration of 50 g/L, pH 6.8). *Solid line* and *dash line* represent the succinic acid concentration and the lactose concentration, respectively. *Symbols* are the inoculum sizes of 2 (*empty squares*), 5 (*empty diamonds*), 10% (*empty triangles*)

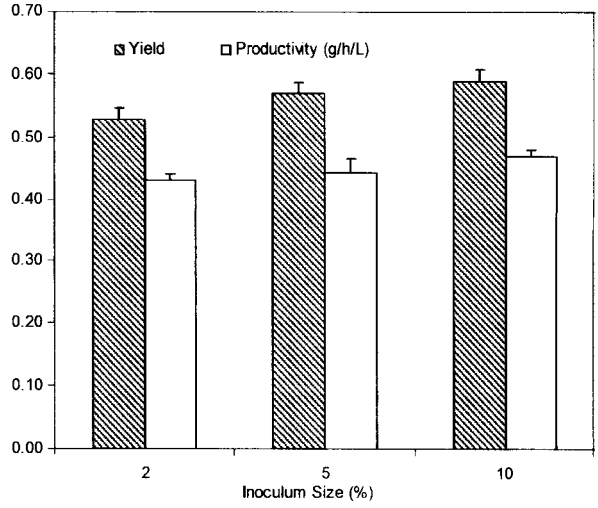


Fig. 6 Effect of inoculum size on the succinic acid yield and productivity (initial cheese whey concentration of 50 g/L, pH of 6.8, total fermentation time of 48 h)

throughout the fermentation run. The reason could be that the increase in the inoculum density shortened the lag period and increased the final cell concentration, which resulted in the less fermentation time required to reach the maximum succinic acid concentration [22]. It can be seen from Fig. 6 that maximum succinic acid yield (0.59) and productivity (0.47 g h^{-1}

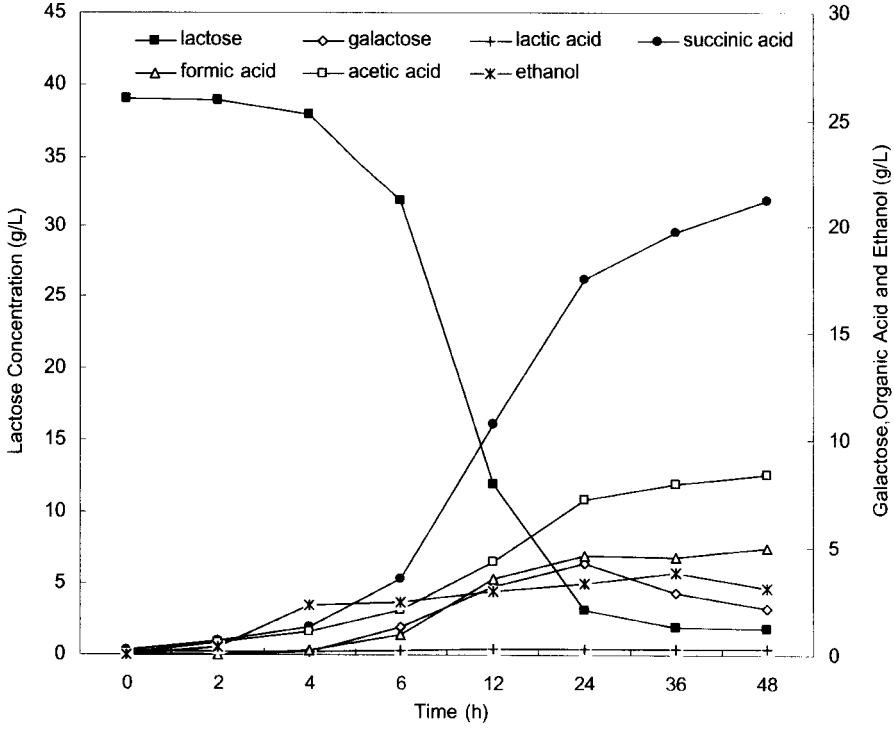


Fig. 7 Distribution of end products during the fermentative succinic acid production (initial cheese whey concentration of 50 g/L, pH of 6.8, and inoculum size of 5%)

L^{-1}) were obtained at inoculum size of 10%. However, the effects of inoculum sizes on succinic acid yield ($P>0.11$) and productivity ($P>0.36$) were not significant.

The Production of By-Products

Under anoxic condition of succinic acid production, phoshpoenolpyruvate (PEP), one of the central intermediates during mixed acid fermentation, is converted by two enzymes in *A. succinogenes* 130Z named PEP carboxykinase (PPCK) and pyruvate kinase [16, 23]. PPCK is a CO_2-fixing enzyme that converts PEP to oxaloacetate toward the flux to the formation of succinic acid [20, 23]. Pyruvate kinase converts PEP to pyruvate, which is consequently converted to end fermentation by-products such as acetic acid, formic acid, and ethanol [16].

The end fermentation products at initial cheese whey concentration of 50 g/L, pH 6.8 and inoculum size of 5% under non-limiting CO_2 supply (0.5 vvm CO_2 sparging) are shown in Fig. 7. Acetic acid and formic acid were the main by-products, and there was no observation of lactic acid production throughout the fermentation run. The concentration of acetic acid increased more rapidly than that of other by-products along with the dramatic increase of succinic acid concentration from 6 to 24 h. No further increase of formic acid was observed after 24 h, while there was a slight increase in the concentration of acetic acid. The galactose concentration resulting from lactose degradation slightly decreased after 24 h possibly due to the fermentation of galactose by *A. succinogenes* 130Z at the low total carbohydrate concentration.

Conclusion

This study shows that *A. succinogenes* 130Z can effectively convert cheese whey to succinic acid. Therefore, cheese whey, waste stream from dairy industry, can be used in the cost-effective fermentative production of succinic acid.

Higher succinic acid productivity and lower yield were obtained when the initial cheese whey concentration increased from 50 to 100 g/L. Increase in succinic acid productivity and yield was also obtained with increased pH range from 6.2 to 7.2. The highest succinic acid yield of 0.57 was obtained at pH 6.8. Higher succinic acid yield and productivity were obtained when the inoculum size increased from 2 to 10%, but the effect was not significant. Under non-limiting CO_2 supply, acetic acid and formic acid were the main by-products during the succinic acid production from cheese whey using *A. succinogenes* 130Z. Further studies need to be conducted to determine the optimized fermentation parameters for maximum succinic acid production from cheese whey using *A. succinogenes* 130Z.

Acknowledgements The authors thank Michele R. Mims for the assistance in sample analysis. Financial support from USDA CSREES Evans-Allen Program is also greatly appreciated.

References

1. Gottschalk, G. (1986). *Bacterial Metabolism*, 2nd ed. New York: Springer-Verlag, pp. 242–249.
2. Zeikus, J. G., Jain, M. K., & Elankovan, P. (1999). *Applied Microbiology and Biotechnology, 51*, 542–552.
3. Song, H., & Lee, S. Y. (2006). *Enzyme and Microbial Technology, 39*, 352–361.

4. Landucci, R., Goodman, B., & Wyman, C. (1994). *Applied Biochemistry and Biotechnology, 45-46*, 678–696.
5. Zeikus, J. G. (1980). *Annual Review of Microbiology, 34*, 423–464.
6. Lee, P. C., Lee, W. G., Lee, S., & Chang, H. N. (2001). *Biotechnology and Bioengineering, 72*, 41–48.
7. Lee, P. C., Lee, S. Y., Hong, S. H., & Chang, H. N. (2002). *Applied Microbiology and Biotechnology, 58*, 663–668.
8. Huh, Y. S., Jun, Y. S., Hong, K. H., Song, H., Lee, S. Y., & Hong, W. H. (2006). *Process Biochemistry, 41*, 1461–1465.
9. McKinlay, J. B., Zeikus, J. G., & Vieille, C. (2005). *Applied and Environmental Microbiology, 71*, 6651–6656.
10. Kim, D. Y., Yim, S. C., Lee, P. C., Lee, W. G., Lee, S. Y., & Chang, H. N. (2004) *Enzyme and Microbial Technology, 35*, 648–653.
11. Samuelov, N. S., Datta, R., Mahendra, K. J., & Zeikus, J. G. (1999). *Applied and Environmental Microbiology, 65*, 2260–2263.
12. Guettler, M. V., Rumler, D., & Jain, M. K. (1999). *International Journal of Systematic Bacteriology, 49*, 207–216.
13. Guettler, M. V., Jain, M. K., & Rumler D. (1996). *US Patent* 5,573,931.
14. Guettler, M. V., Jain, M. K., & Soni, B. K. (1996) *US Patent* 5,504,004.
15. Urbance, S. E., Pometto, A. L., DiSpirito, A. A., & Denli, Y. (2004). *Applied Microbiology and Biotechnology, 65*, 664–670.
16. Van der Werf, M. J., Guettler, M. V., Jain, M. K., & Zeikus, J. G. (1997). *Archives of Microbiology, 167*, 332–342.
17. Li, Y.B., Shahbazi, A., & Coulibaly, S. (2006). *Transaction of the ASABE, 49*, 1–5.
18. Gonzalez, S. M. I. (1996). *Bioresource Technology, 57*, 1–11.
19. Lee, P. C., Lee, S. Y., Hong, S. H., & Chang, H. N. (2003). *Bioprocess and Biosystems Engineering, 26*, 63–67.
20. Lee, P. C., Lee, W. G., Kwon, S., Lee, S. Y., & Chang, H. N. (1999). *Enzyme and Microbial Technology, 24*, 549–554.
21. Isar, J., Agarwal, L., Saurabh, S., & Saxena, R. K. (2006). *Anaerobe, 12*, 231–237.
22. Wee, Y. J., Yun, J. S., Kang, K. H., & Ryu, H. W. (2002). *Applied Microbiology and Biotechnology, 98–100,* 1093–1104.
23. Kim, P., Laivenieks, M., Vieille, C., & Zeikus, J.G. (2004). *Applied and Environmental Microbiology, 70*, 1238–1241.

Appl Biochem Biotechnol (2008) 146:1–2
DOI 10.1007/s12010-008-8223-2

Introduction to Session 2: Enzyme Catalysis and Engineering

Stephen R. Decker · Sarah Teter

Published online: 12 April 2008
© Humana Press 2008

The role of enzymes in biomass-to-fuels is rapidly expanding from a narrow focus on the hydrolysis of cellulose remaining after pretreatment to a more comprehensive approach, where increasing attention is focused on noncellulase activities, including hemicellulases, lignin-modifying, and accessory enzymes. This transition is being driven from several directions. Foremost is the realization that pretreatment may be best viewed as an activation or preconditioning step in the hydrolysis of biomass. Pretreatment conditions severe enough to produce highly accessible biomass for subsequent enzymatic conversion may be saddled with the significant problems of high cost, yield losses, and inhibitor formation. Mild severities may significantly reduce these problems; however, lower severity pretreatment results in higher recalcitrance, and often higher chemical complexity compared to more severely pretreated biomass.

The broadening diversity of biofuel feedstocks, the varied thermochemistry of the dozen or so pretreatment technologies, and a wide range of severities for each pretreatment all contribute to a complex picture when assessing the nature of the substrate to be converted by biomass-to-fuels enzymes. The likelihood that a single enzyme system will be able to efficiently deconstruct a wide variety of highly complex pretreated substrates is considered to be low. This complexity, however, can be addressed through several variations in the enzyme system employed, including more aggressive enzyme loadings, increased specific activities, altered substrate specificities, and tailoring enzyme cocktails to specific causes of recalcitrance. Although each approach has its limitations and benefits, it is readily apparent that matching the enzyme activities to a given substrate may be a route for cost-effective minimization of the drawbacks of more severe pretreatments, while maintaining the yields and efficiencies required for an economical biomass conversion process.

Session 2, Enzyme Catalysis and Engineering, addressed many of the issues detailed above. The main session focused on the functionality of natural enzyme systems in the

S. R. Decker (✉)
National Renewable Energy Laboratory, 1617 Cole Boulevard, Golden, CO 80401, USA
e-mail: steve_decker@nrel.gov

S. Teter
Novozymes, Inc., 1445 Drew Avenue, Davis, CA 95618, USA

hydrolysis of a diverse range of feedstocks under different process conditions. Hydrolysis of insoluble chitin and soluble chitosan by a three-enzyme system was shown to be directly affected by the binding residues near the catalytic site. More insights were gained into the mechanism of multi-enzyme cellulose hydrolysis by *Trichoderma reesei*. In more process-related research, the effect of ethanol on enzymatic hydrolysis of biomass was investigated, as was the conversion of two niche-feedstocks, barley straw and canary grass, to ethanol. Session 2A examined the role of hemicellulase activities such as ferulic acid esterase, β-xylosidase, β-xylanase, and α-L-arabinofuranosidase in the hydrolysis of biomass. Session 2B focused on the noncatalytic parameters involved in enzyme hydrolysis of biomass. The effect of water was a dominant theme in these talks and a new mechanism of binding by the Family 1 carbohydrate binding module based on molecular modeling was presented.

Overall, Session 2 provided a very good panoramic snapshot of the current research focusing on enzymes for biomass conversion. The diversity and quality of the work indicate that this area of biomass conversion research is very vigorous and is continuing to expand in scope. As feedstock diversity and pretreatment protocols continue to expand, the role of enzymes will become increasingly critical to maintaining high yields, low losses, and efficient conversion rates. The synergy between the biomass-to-fuel trinity of feedstock diversity, pretreatment thermochemistry, and enzyme activity will be the cornerstone of a successful biomass conversion industry.

Appl Biochem Biotechnol (2008) 146:3–13
DOI 10.1007/s12010-007-8093-z

Production of Cyclodextrins by CGTase from *Bacillus clausii* Using Different Starches as Substrates

H. F. Alves-Prado · A. A. J. Carneiro · F. C. Pavezzi · E. Gomes · M. Boscolo · C. M. L. Franco · R. da Silva

Received: 15 May 2007 / Accepted: 1 November 2007 /
Published online: 15 December 2007
© Humana Press Inc. 2007

Abstract Cyclodextrins (CDs) are cyclic oligasaccharides composed by D-glucose monomers joined by α-1,4-D glicosidic linkages. The main types of CDs are α-, β- and γ-CDs consisting of cycles of six, seven, and eight glucose monomers, respectively. Their ability to form inclusion complexes is the most important characteristic, allowing their wide industrial application. The physical property of the CD-complexed compound can be altered to improve stability, volatility, solubility, or bio-availability. The cyclomaltodextrin glucanotransferase (CGTase, EC 2.4.1.19) is an enzyme capable of converting starch into CD molecules. In this work, the CGTase produced by *Bacillus clausii* strain E16 was used to produce CD from maltodextrin and different starches (commercial soluble starch, corn, cassava, sweet potato, and waxy corn starches) as substrates. It was observed that the substrate sources influence the kind of CD obtained and that this CGTase displays a β-CGTase action, presenting a better conversion of soluble starch at 1.0%, of which 80% was converted in CDs. The ratio of total CD produced was 0:0.89:0.11 for α/β/γ. It was also observed that root and tuber starches were more accessible to CGTase action than seed starch under the studied conditions.

Keywords CGTase · Cyclodextrin · *Bacillus clausii* · Soluble starch · Corn starch · Cassava starch · Sweet potato starch · Waxy corn starch

Introduction

Cyclomaltodextrin glucanotranferase (CGTase, EC 2.4.1.19) is a member of the α-amylase family (family 13) of glycosylhydrolases, an important group of starch

H. F. Alves-Prado · A. A. J. Carneiro · F. C. Pavezzi · E. Gomes · M. Boscolo · R. da Silva (✉)
Laboratorio de Bioquímica e Microbiologia Aplicada, IBILCE, UNESP,
Rua Cristóvão Colombo nº 2265, 15054-000 São José do Rio Preto, São Paulo, Brazil
e-mail: dasilva@ibilce.unesp.br

C. M. L. Franco
Laboratorio de Amido do Depto de Engenharia e Tecnologia de Alimentos, IBILCE, UNESP,
São José do Rio Preto, SP, Brazil

processing enzymes (1). This group of enzymes exhibits a broad diversity in reaction specificities. However, while amylases generally hydrolyze glucosidic bonds in the starch molecules, CGTases catalyse mainly transglycosylation reactions, with hydrolysis being a minor activity (1–3). The major activity is intramolecular transglycosylation or cyclization reaction, leading to the formation of nonreducing cyclic oligosaccharides, named cyclodextrins (CDs). The main types of CDs are α-, β-, and γ-CDs consisting of six, seven, and eight glucose monomers in cycles, respectively. Their structure has a hydrophilic outer surface and a hydrophobic cavity. Because of their ability to form inclusion complexes with many organic molecules, CDs and their derivatives have become increasingly useful in pharmaceutical, food, cosmetics, analytical chemistry, agriculture, and biotechnology (4–6).

The majority of the CGTases usually produce a mixture of α-, β-, and γ-CD, and the product ratio can vary depending on condition and reaction time. These require CDs purification and separation, which becomes a rather elaborate, costly, and time-consuming part of an industrial production process. Hence, efforts are being made not only to increase the CDs yield but also to improve conditions of enzymatic reaction of the CGTases toward a particular CD. Protein engineering of the enzyme has promising results for changing the product specificity (7, 8). On the other hand, addition of selective complexant agents and organic solvents to the reaction mixture has also shown to significantly influence the ratios of α-, β-, and γ-CDs and their yields. Many works have shown that different substrates can determine the kind of product obtained from enzymatic reaction CDs (9–16).

In this work, the profile of CD production by the action of CGTase from *Bacillus clausii* strain E16 in soluble starch and maltodextrin was studied. Furthermore, the action of this CGTase in the presence of other starch botanical sources such as cassava starch, sweet potato starch, corn starch, and waxy corn starch were analyzed.

Materials and Methods

Materials

CDs (α-, β-, γ-CD), glucoamylase, and maltodextrin (dextrose equivalent 13.0–17.0) were purchased from Sigma (St. Louis, MO). Soluble starch was obtained from Mallinckrodt (Paris, France), corn and cassava starches were obtained from Cargil (São Paulo, Brazil), and sweet potato and waxy corn starches were donated by Starch Laboratory of the Food Science and Technology Department (IBILCE-UNESP, SP, Brazil). Yeast extract was obtained from Difco (Detroit, USA), and peptone was obtained from Biobrás (Minas Gerais, Brazil). Other chemicals of analytical grade were obtained from Merck (Darmstadt, Germany).

Bacterial Strain and CGTase Production

CGTase used in this study was obtained from *B. clausii* E16 that was isolated and identified by Alves-Prado et al. (17, 18). The microorganism was grown in shake flasks (250 mL) containing culture medium (50 mL) composed (g/L) of soluble starch 13.4, peptone 4.9, yeast extract 5.9, K_2HPO_4 1.0, $MgSO_4.7H_2O$ 0.2, and Na_2CO_3 12.5 (separately sterilized), pH 10.1 (18), on a rotatory shaker at 200 cycles per min. After 48 h, the bacterial cells were harvested by centrifuging at 10,000×*g* for 10 min at 5 °C, and the clear supernatants were used as crude enzyme.

Enzymatic Assay

Two methods were used; one is the iodine method that was used to determine dextrinization or the ratio of hydrolysis of the starch, and the other is the phenolphthalein method that was used to determine CD formation. Starch-dextrinizing activity was determined in accordance with Fuwa (19) and Pongasawasdi and Yagisawa (20) with slight modifications. The reaction mixture containing 100 μL of diluted enzyme aliquot and 300 μL of 0.5% soluble starch prepared in 0.1 M acetate buffer, pH 5.5, was incubated at 55 °C for 10 min. The enzyme reaction was stopped by the addition of 4.0 mL of 0.2 M HCl solution. Then, 0.5 mL of iodine solution (0.3 g/L I_2 and 3.0 g/L KI) was added to form an amylose–iodine complex with residual amylose. The final volume was adjusted to 10 mL with distilled water. The absorbance of the blue color of the amylose–iodine complex was measured by spectrophotometer at 700 nm, and a decrease in absorbance was verified, when compared to a control tube with heat-inactivated enzyme. One unit of enzyme activity was defined as the quantity of enzyme that reduces the blue color of the starch–iodine complex by 10% per minute.

CGTase activity was measured as β-CD-forming activity based on the phenolphthalein method (21) with slight modifications as described in Alves-Prado et al. (18). One hundred microliters of diluted enzyme aliquot was added to 800 μL of 1% soluble starch prepared in 100 mM acetate buffer, pH 5.5, and incubated at 55°C for 10 min. The enzyme reaction was stopped by the addition of 4.0 mL of 0.25 M Na_2CO_3 solution, and 0.1 mL of 1 mM phenolphthalein solution was added to the reaction mixture. The absorbance was measured at 550 nm, and a decrease in absorbance was compared to a control reaction mixture with inactive enzyme (100°C for 30 min). One unit of enzyme activity was defined as the amount of enzyme that produced 1 μmol of β-CD per minute using a standard curve with β-CD.

Protein Determination

Protein concentration was estimated according to the Hartree–Lowry method, using bovine serum albumin as the standard (22).

CGTase Purification

The CGTase was produced in 500-mL Erlenmeyer flasks, containing 80 mL culture medium with soluble starch as substrate, in a rotary shaker at 35 °C, for 48 h at 200 cycles per min. The cells were removed from the culture by centrifugation at 10,000×*g* for 10 min at 5 °C. The supernatant containing crude CGTase was concentrated by ultrafiltration using the Pellicon® system (Millipore, Beldford, MA). The concentrated CGTase was subjected to a gel filtration chromatography on a Sephadex superfine G-50 column (2.6 cm diameter× 100 cm length) pre-equilibrated with 20 mM Tris–HCl buffer (pH 7.5), containing 20 mM NaCl. The elution was carried out in the same buffer at a flow rate of 0.3 mL/min at room temperature, and 4 mL fractions were collected using a fraction collector (Pharmacia Biotech Frac-100, Sweden). The active CGTase fractions were concentrated by Centricon® (amicon bioseparations, Millipore). The partially purified CGTase was confirmed by sodium dodecyl sulfate–polyacrylamide gel electrophoresis (23).

Effect of Soluble Starch and Maltodextrin on CD Formation

Soluble starch and maltodextrin (1.0 and 2.5% w/v) prepared in acetate buffer, 100 mM, pH 5.5, were homogenized by heating in a boiling water bath. Four hundred microliters of

enzyme (adjusted to 10 U of dextrinizing activity per gram of substrate) was added to 100 mL of each substrate, and it was incubated in a shaker under agitation of 100 cycles per min at 55 °C for 24 h. Aliquots of 1 mL were transferred to 2-mL tubes, closed, and immediately heated in a boiling water bath. All samples were submitted to hydrolysis with amyloglucosidase (Sigma) and filtered through a 0.45-μm cellulose acetate membrane (Millipore). The CD formed in the reaction mixture was detected by high-performance liquid chromatography (HPLC). All experiments were done in triplicate.

Effect of Kind of Starches on CD Formation

The CGTase action was evaluated on cassava starch, sweet potato starch, corn starch, and waxy corn starch. Substrates' concentrations were at 2.5%. Enzyme, conditions, and quantity were conducted as described above, except that aliquot samples were withdrawn periodically until 24 h. In an independent experiment, starches were gelatinized by autoclave process. The percentage of starch converted into CDs was calculated by ratio of total grams of CDs formed divided per gram of starch and multiplied per 100.

CD Quantification

The CD formed in the reaction mixture was detected by HPLC. Conditions for HPLC were based on that described by Sato et al. (24). The HPLC system consisted of Jasco PU 990 pump (Jasco, Japan) connected to a Shodex RI 72 refractive index detector. In this system, it was connected a Zorbax-NH_2 column (250×4.6 mm, 5 μm, Aligent Technologies) installed in a column oven Dionex STH 585 (Dionex Softron GmbH, Germany) at 35 °C. It was used a mixture of acetonitrile/water (65:35 v/v) with the flow rate of 0.8 mL/min. All experiments were done in triplicate.

Results and Discussion

CGTase Purification

After 48 h of fermentation, the supernatant from the *B. clausii* strain E16 culture was used for partial purification of the CGTase. The supernatant containing crude enzyme was first concentrated by ultrafiltration and subsequently purified by gel filtration. The gel filtration profile and purity degree of enzyme is shown in Fig. 1.

Effect of Soluble Starch and Maltodextrin on CD Formation

CD production was evaluated on 1.0 and 2.5% of maltodextrin and soluble starch by CGTases action. After 24 h, the products formed were analyzed by HPLC. The ratio conversion in α-, β-, and γ-CD of the maltodextrin and soluble starch hydrolyzed by CGTase from *B. clausii* strain E16 is shown in Table 1.

It can be observed that there are differences in quantity and types of CD formed in accordance with the substrate used for CGTase action. In the presence of maltodextrin, the CD production was of three types, α-, β-, and γ-CD, while in soluble starch, there was production of only two types of CDs, β- and γ-CD, and no α-CD was observed. Many other CGTase studies have shown similar results, with the production of the β-CD

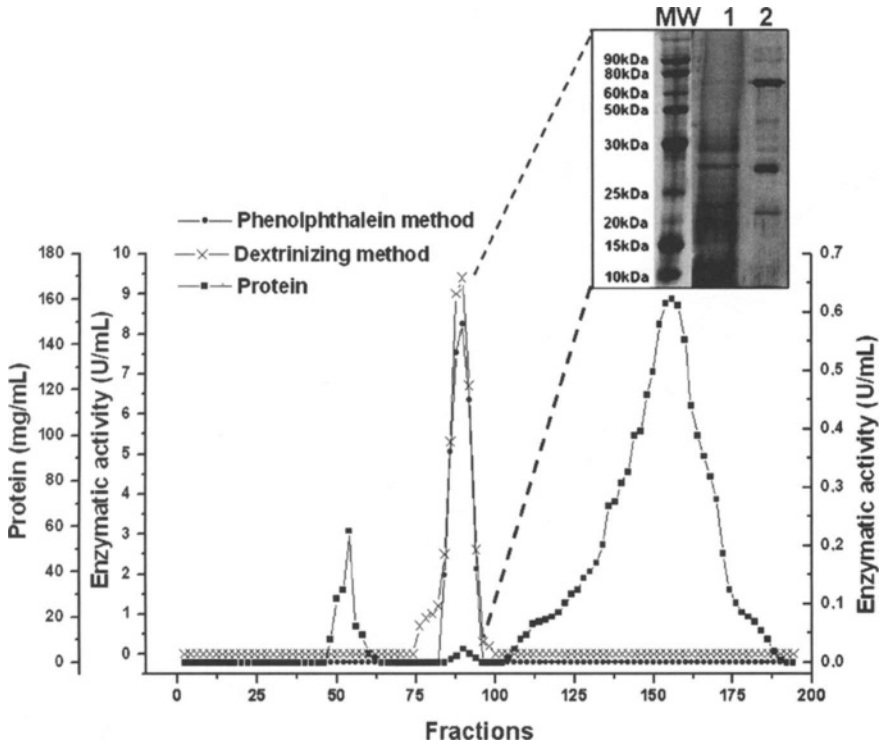


Fig. 1 Gel filtration process profiles on purification of the CGTase from *Bacillus clausii* strain E16, with illustration of electrophorese SDS-PAGE. MW: molecular weight; 1: crude CGTase; 2: partially purified CGTase

prevailing (9, 12, 13, 15, 16, 27, 28, 29). The better conversions were observed on 1.0% soluble starch, which showed a major conversion (80%) or in 2.5% maltodextrin (41%; Table 1). CGTase from *B. clausii* strain E16 produced preferentially, on soluble starch, β- (89%) and γ-CD (11%) in higher concentrations, similar to CGTase from *Bacillus* sp. AL-6 (25) that produces only β- and γ-CD in the presence of soluble starch. The authors have observed that it was possible to improve γ-CD yield when ethanol was added to the reaction mixture of hydrolysis. Charoenlap et al. (26) reported a CGTase from *B. circulans* (TISTR 907) as being highly specific for β-CD formation because its distributions of α-, β-, and γ-CDs were 7, 65, and 28%, respectively, from soluble starch. In this respect, we can also consider CGTase from *B. clausii* strain E16 as specific for β-CD formation. The

Table 1 Effect of maltodextrin and soluble starch on CDs production by CGTase from *Bacillus clausii* strain E16, after 24 h of hydrolysis.

Substrate	CD production (mg/mL)				CD
	α-CD	β-CD	γ-CD	Total	Conversion (%)
Maltodextrin 1.0%	0.41±0.03	1.20±0.13	0.51±0.07	2.12	21.0
Maltodextrin 2.5%	1.64±0.06	5.27±0.11	3.46±0.13	10.37	41.0
Soluble starch 1.0%	0	7.09±0.10	0.90±0.20	7.99	80.0
Soluble starch 2.5%	0	3.09±0.14	0.73±0.13	3.82	15.2

GTase from the *B. circulans* NRRL B380 using soluble starch as a substrate exhibited only 40% distribution of β-CD (27).

Effect of Kind of Starch on CD Formation

Soluble starch was a better substrate than maltodextrin for CD production, so other substrates were also used for CD production. The content and structural characteristics of amylose and amylopectin present in starches may vary depending of their botanical sources. So, it was interesting to investigate this parameter regarding to CD formation under CGTase action. Cassava starch, sweet potato starch, corn starch and waxy corn starch were used.

Generally, starches contain about 20 to 30% of amylose and 70 to 80% of amylopectin, and these concentrations change with the botanical source of starch. Cassava starch, sweet potato starch, corn starch, and waxy corn starch showed, respectively, 17.0, 20.7, 25, and less than 1% of amylose (28, 29, 30). The ratio amylose/amylopectin is an important factor to consider for CD production. The helicoidal structure of amylose with loops of six to seven glucose units can contribute with action of CGTase on α- and β-CD formation (2).

In Table 2, it can be observed that after 24 h of hydrolysis, 22 and 21% of cassava starch and sweet potato starch, respectively, were converted into β- and γ-CD. Corn starch (7.3%) was converted into β- and γ-CD, and only 1.5% of waxy corn starch was converted into β-CD.

In the results shown, cassava starch and sweet potato starch were more susceptible to CGTase action than corn starch, which has the highest percentage of amylose. However, another factor that should be considered is the lipid concentration of the starch. Root starches (cassava) and tuber starches (sweet potato) show low lipid quantities, less than 0.1%, while in cereal starches (corn), the lipid quantities are high, around 0.5 to 1.0% (30, 31, 32). Most of the lipid components of cereal grains are concentrated in the germ. The lipids of the endosperm have been classified as starch lipids, which are those associated with starch granule, and nonstarch lipids, which are those contained in the spherosome dispersed throughout the endosperm. Therefore, in cereal starches, amylose and lipid may form a complex, amylose–lipid, which is very stable and dissociates only at very high temperatures (30, 31, 33). The lower action of CGTase on corn starch can be due to the fact that part of amylose is engaged in lipid complexation. To analyze this hypothesis, an intense thermal treatment during homogenization of starches was done. Cassava, sweet potato, and corn starches were homogenized in a boiling water bath (Table 2 and Fig. 2) or were homogenized in a boiling water bath and then submitted to a gelatinization process in autoclave for 10 min at 121 °C and 1 atm (Table 3 and Fig. 3). Then, the starch solutions were submitted to CGTase action.

Table 2 Effects of starches from different botanical sources on CD production by CGTase from *Bacillus clausii* strain E16, homogenized by heating in a boiling water bath.

Botanical sources (2.5%)	CD production (mg/mL)				CD conversion (%)
	α-CD	β-CD	γ-CD	Total	
Cassava starch	0	4.75±0.28	0.73±0.11	5.48	22.0
Sweet potato starch	0	4.39±0.17	0.81±0.10	5.20	21.0
Corn starch	0	1.83±0.13	0	1.83	7.3
Waxy corn starch	0	0.30±0.06	0	0.30	1.5

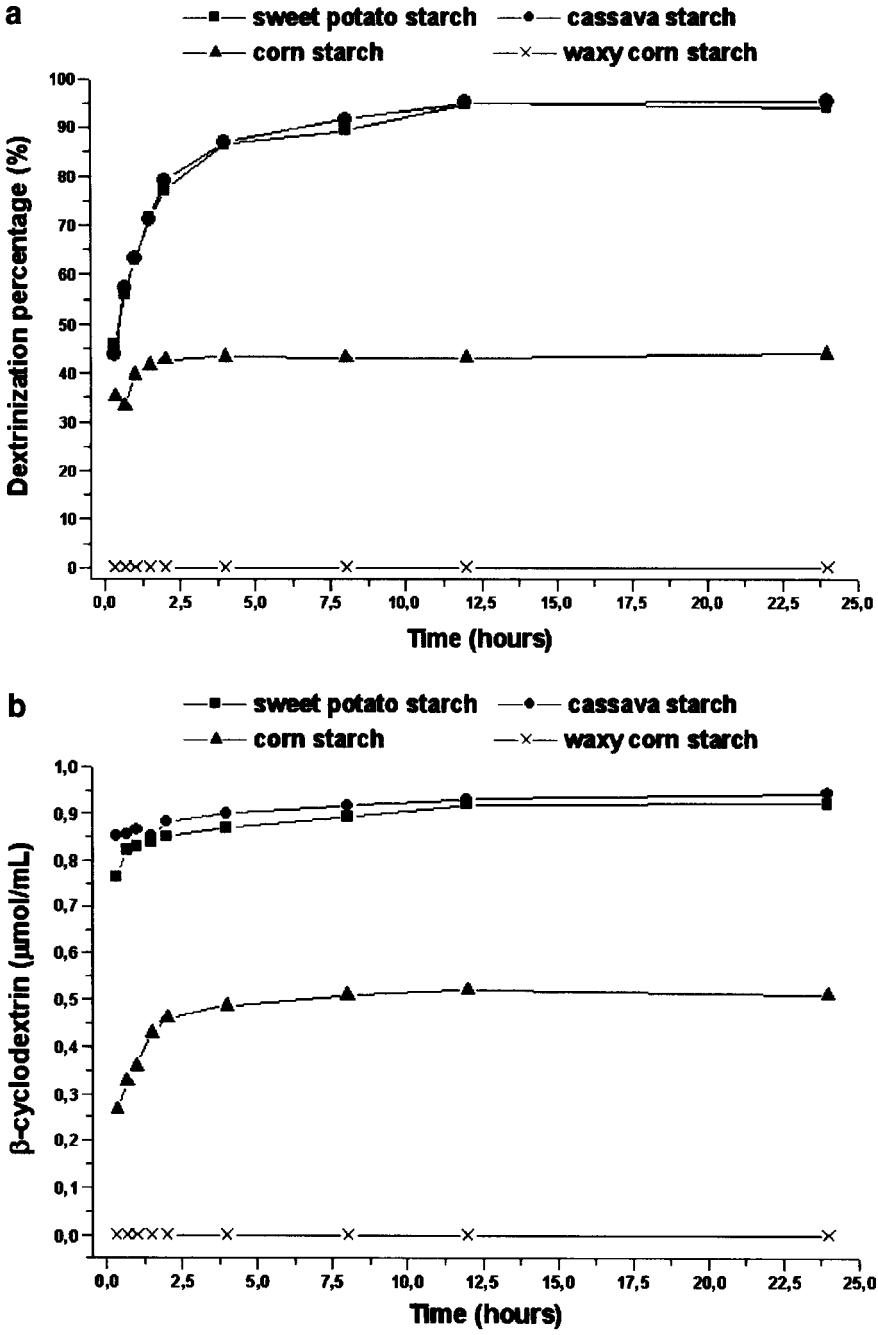


Fig. 2 CD production by action of CGTase from *Bacillus clausii* strain E16 on starches from different botanical sources. **a** Dextrinization percentage, **b** CD formation

Table 3 Effect of starches from different botanical sources on CD production by CGTase from *Bacillus clausii* strain E16, gelatinized by autoclave.

Botanical sources (2.5%)	CD production (mg/mL)				CD conversion (%)
	α-CD	β-CD	γ-CD	Total	
Cassava starch	0	4.92±0.21	1.03±0.11	5.95	24.0
Sweet potato starch	0	5.21±0.37	1.05±0.07	6.26	25.0
Corn starch	0	2.60±0.35	0.20±0.09	2.80	11.0
Waxy corn starch	0	1.58±0.12	0	1.58	6.3

Analyses of the time course of CD formation after gelatinization in boiling water bath through dextrizing (a) and phenolphthalein (b) methods are shown in Fig. 2. There was a better CD formation in cassava and sweet potato starches. At 4 h, it was shown that the homogenization in boiling water bath (conventional process) yield a maximum dextrinization of 95% for cassava and sweet potato starches, 42% for corn starch, and 0% for waxy corn starch. The time course of dextrinization with the gelatinization in boiling water bath followed by autoclaving (Fig. 3) showed an increased percentage of dextrinization (10%) for cassava and sweet potato starches. For corn starch, the dextrinization percentage increased 79% (42 to 79) in regard to conventional homogenization processes, and also, there was a conversion (25%) from waxy corn starch. The same characteristic was observed in regard to β-CD formation (Fig. 3b), in which an increase in conversion of 8% (0.88 to 0.95) for cassava and sweet potato starches and 66% (0.48 to 0.8) for corn starch were observed, and there was also a small conversion for waxy corn starch (0.15 μmol/mL). Therefore, these results suggest that the amylose–lipid complex present in corn starch granules reduces the CGTase action.

Table 3 shows the CD produced after 24 h quantified by HPLC. The data show a better CD production under the new homogenization condition when compared with heating in a boiling water bath. It was also observed that there was a significant increase in CD conversion when corn starch was used (2.6 against 1.8 mg/L, for β-CD). The increase in total CD yield was approximately 50%, and some γ-CD (0.2 g/L) could be quantified. The increase in total CD for cassava and sweet potato starch was lower, 8 and 20%, respectively. The ratio of CD production for α-, β-, and γ-types from cassava and sweet potato starches were similar, 0:0.83:0.16, and for corn starch, it was 0:0.93:0.07. Furthermore, there was increase in ratio of CD conversion with all starches gelatinized by autoclave. These results reinforce the idea that the amylose–lipid complex present in cereal starches can influence CGTase action and thus CD formation. Gawande and Patkar (34) have observed a low CD conversion using CGTase from *Klebsiella pneumoniae* AS-22 on a corn starch solution. Using CGTase from *Brevibacterium* sp no. 9605, Mori et al. (10, 11) have observed 1% lower conversion when using corn starch than when using sweet potato starch. Similar results were observed by Goel and Nene (12) who obtained a better CD conversion using CGTase from *Bacillus firmus* in cassava starch than in corn starch.

In accordance with these results, it can be said that CD formation by CGTase from *B. clausii* strain E16 depends not only on the amount of amylose but also on the ability of amylose and lip to form a amylose–lipid complex in the starch. Corn starch showed an increase of β- and γ-CD production when gelatinized in an autoclave. Production of γ-CD was not observed when this starch was homogenized by heating in a boiling water bath. This demonstrates that the gelatinization process of starch is an important factor with regard to CD production process. Waxy corn starch, which is rich in amylopectin, also produced a small amount of β-CD. A mix of α-, β-, and γ-CDs was produced when CGTases from *K.*

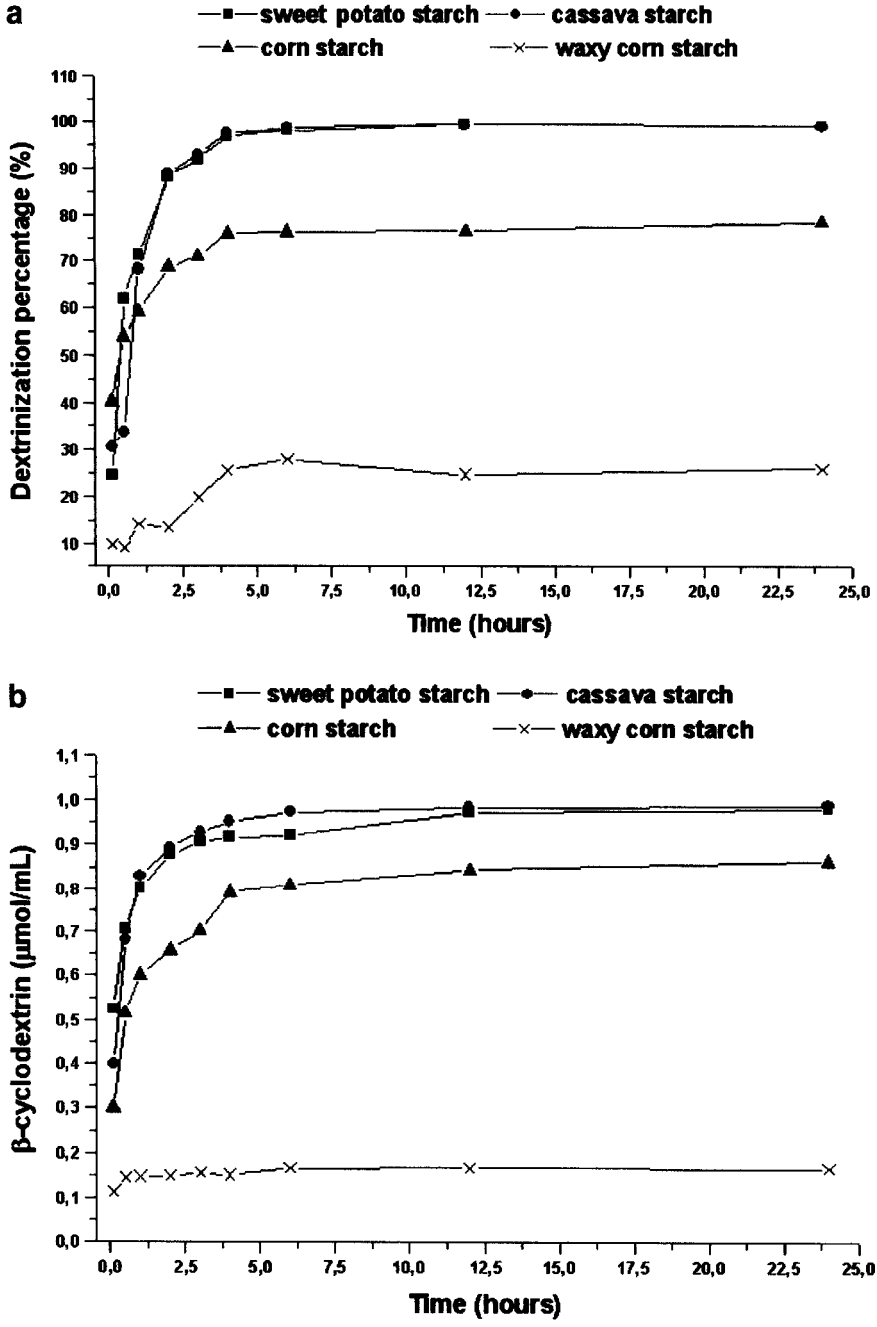


Fig. 3 CD production by action of CGTase from *Bacillus clausii* strain E16 on starches from different botanical sources, gelatinized on autoclave. **a** dextrinization percentage; **b** CD formation

pneumoniae AS-22 (34) and *Brevibacterium* sp. no. 9605 (10) were used. However, the CGTases from *B. firmus* (12, 29, 34) and *B. clausii* E16 produced only β- and γ-CD from different starches. The formation of only two types of CDs during hydrolysis processes is important in the separation process because it is easier to separate the CDs produced, which is interesting for industrial application.

Conclusions

CGTase from *B. clausii* strain E16 was specific for β-CD formation displaying a β-CGTase action. The distributions of α-, β-, and γ-CDs were 0, 89, and 11%, respectively, on soluble starch. The starches from different botanical sources influenced quantities and types of CD formed. It was also observed that root and tuber starches were more accessible to CGTase action. The process of starch homogenization can interfere whit the CGTase action and, consequently, on the CD formation. The gelatinization of starches by the autoclave process improves the CD production, mainly for cereal starches.

Acknowledgments Heloiza Ferreira Alves-Prado is grateful for the Pós-doctorate fellowship funded by FAPESP (Fundação de Amparo à Pesquisa do Estado de São Paulo, São Paulo, Brazil). The authors also acknowledge the financial support of FAPESP and CNPq (Conselho Nacional de Desenvolvimento Científico e Tecnológico, Brazil).

References

1. Van Der Veen, B. A., Uitdehaag, J. C. M., Dijkstra, B. W., & Dijkhuizen, L. (2000). *Biochimica et Biophysica Acta, 1543*, 336–360.
2. Bender, H. (1986). *Advances in Biotechnological Processes, 6*, 31–71.
3. Alves-Prado, H. F., Gomes, E., & DaSilva, R. (2002). *Boletim Sociedade Brasileira de Ciência e Tecnologia de Alimentos, 36*, 43–54.
4. Starnes, R. R. (1990). *Cereal Foods World, 35*, 1094–1099.
5. Martin del Valle, E. M. (2004). *Process Biochemistry, 39*, 1033–1046.
6. Hedges, A. R. (1998). *Chemical Reviews, 98*, 2035–2044.
7. Kim, Y. H., Bae, K. H., Kim, T. J., Park, K. H., Lee, H. S., & Byun, S. M. (1997). *Biochemistry and Molecular Biology International, 41*, 227–234.
8. Van Der Veen, B. A., Uitdehaag, J. C. M., Alebeek, G-J. W. M., Smith, L. M., Dijkstra, B. W., & Dijkhuizen, L. (2000). *Journal of Molecular Biology, 296*, 1027–1038.
9. Pongsawasdi, P., & Yagisawa, m. (1988). *Agricultural and Biological Chemistry, 52*, 1099–1103.
10. Mori, S., Hirose, S., Oya, T., & Kitahata, S. (1994). *Bioscience, Biotechnology, and Biochemistry, 58*, 1968–1972.
11. Mori, S., Goto, M., Mase, T., Matsuura, A., Oya, T., & Kitahata, S. (1995). *Bioscience, Biotechnology, and Biochemistry, 59*, 1012–1015.
12. Goel, A., & Nene, S. (1995). *Biotechnology Letters, 14*, 411–416.
13. Maréchal, L. R., Rosso, A. M., Maréchal, M. A., Krymkiewicz, N., & Ferrarotti, S. A. (1996). *Cellular and Molecular Biology, 42*, 659–664.
14. Rendleman, J. A., Jr. (1997). *Biotechnology and Applied Biochemistry, 26*, 51–61.
15. Yamamoto, K., Zhang, Z. Z., & Kobayashi, S. (2000). *Journal of Agricultural and Food Chemistry, 48*, 962–966.
16. Higuti, I. H., Silva, P. A., & Nascimento, A. J. (2004). *Brazilian Archives of Biology and Technology, 47*, 135–138.
17. Alves-Prado, H. F., Gomes, E., & DaSilva, R. (2002). *Brazilian Journal of Food Technology, 98*, 189–196.
18. Alves-Prado, H. F., Bocchini, D. A., Gomes, E., Baida, L. C., Contiero, J., Roberto, I. C., et al. (2007). *Applied Biochemistry and Biotechnology, 136–140*, 27–40.
19. Fuwa, H. (1954). *Journal of Biochemistry, 41*, 583–603.

20. Pongsawasdi, P., & Yagisawa, M. (1987). *Journal of Fermentation Technology, 65*, 463–467.
21. Mäkelä, M. J., Korpela, T. K., Puisto, J., & Laakso, S. V. (1988). *Journal of Agricultural and Food Chemistry, 36*, 83–88.
22. Hartree, E. F. (1972). *Analytical Biochemistry, 48*, 422–427.
23. Laemmli, U. K. (1970). *Nature, 27*, 680–685.
24. Sato, M., Yagi, Y., Nagano, H., & Ishikura, T. (1985). *Agricultural and Biological Chemistry, 49*, 1189–1191.
25. Fujita, Y., Tsubouchi, H., Inagi, Y., Tomita, K., Ozaki, A., & Nakanishi, K. (1990). *Journal of Fermentation and Bioengineering, 70*, 150–154.
26. Charoenlap, N., Dharmsthiti, S., Sirisansaneeyakul, S., & Lertsiri, S. (2004). *Bioresource Technology, 92*, 49–54.
27. Larsen, K. L., Christensen, H. J. S., Mathiesen, F., Pedersen, L. H., & Zimmermann, W. (1998). *Applied Microbiology and Biotechnology, 50*, 314–317.
28. Martins, R. F., & Hatti-Kaul, R. (2002). *Enzyme and Microbial Technology, 30*, 116–124.
29. Matioli, G., Zanin, G. M., Guimarães, M. F., & Moraes, F. F. (2000). *Applied Biochemistry and Biotechnology, 84–86*, 955–962.
30. Buléon, A., Colonna, P., Planchot, V., & Ball, S. (1998). *International Journal of Biological Macromolecules, 23*, 85–112.
31. Thomas, D. J., & Atwell, W. A. (1999). *Starchs: pratical guides for the food industry* pp. 1–11. St. Paul, MN: Eagan.
32. Swinkels, J. B. (1985). *Starch/Stärke, 15*, 17.
33. Morrison, W. R. (1988). *Journal of Cereal Science, 8*, 1–15.
34. Gawande, B. N., & Patkar, A. Y. (2001). *Enzyme and Microbial Technology, 28*, 735–743.

Appl Biochem Biotechnol (2008) 146:15–27
DOI 10.1007/s12010-007-8039-5

Effects of pH and Temperature on Recombinant Manganese Peroxidase Production and Stability

Fei Jiang · Puapong Kongsaeree · Karl Schilke · Curtis Lajoie · Christine Kelly

Received: 15 May 2007 / Accepted: 29 August 2007 /
Published online: 5 October 2007
© Humana Press Inc. 2007

Abstract The enzyme manganese peroxidase (MnP) is produced by numerous white-rot fungi to overcome biomass recalcitrance caused by lignin. MnP acts directly on lignin and increases access of the woody structure to synergistic wood-degrading enzymes such as cellulases and xylanases. Recombinant MnP (rMnP) can be produced in the yeast *Pichia pastoris* αMnP1-1 in fed-batch fermentations. The effects of pH and temperature on recombinant manganese peroxidase (rMnP) production by *P. pastoris* αMnP1-1 were investigated in shake flask and fed-batch fermentations. The optimum pH and temperature for a standardized fed-batch fermentation process for rMnP production in *P. pastoris* αMnP1-1 were determined to be pH 6 and 30 °C, respectively. *P. pastoris* αMnP1-1 constitutively expresses the manganese peroxidase (*mnp1*) complementary DNA from *Phanerochaete chrysosporium*, and the rMnP has similar kinetic characteristics and pH activity and stability ranges as the wild-type MnP (wtMnP). Cultivation of *P. chrysosporium* mycelia in stationary flasks for production of heme peroxidases is commonly conducted at low pH (pH 4.2). However, shake flask and fed-batch fermentation experiments with *P. pastoris* αMnP1-1 demonstrated that rMnP production is highest at pH 6, with rMnP concentrations in the medium declining rapidly at pH less than 5.5, although cell growth rates were similar from pH 4–7. Investigations of the cause of low rMnP production at low pH were consistent with the hypothesis that intracellular proteases are released from dead and lysed yeast cells during the fermentation that are active against rMnP at pH less than 5.5.

F. Jiang · P. Kongsaeree
Department of Biomedical and Chemical Engineering, Syracuse University,
121 Link Hall, Syracuse, NY 13244-1240, USA

K. Schilke · C. Lajoie · C. Kelly (✉)
School of Chemical, Biological, and Environmental Engineering, Oregon State University,
102 Gleeson Hall, Corvallis, OR 97331-2701, USA
e-mail: ckelly@engr.orst.edu

F. Jiang
Cell Genesys, Inc., 500 Forbes Boulevard, South San Francisco, CA 94080, USA

P. Kongsaeree
G C Hanford MFG Company, 304 Oneida St., Syracuse, NY 13201, USA

Keywords Manganese peroxidase · Yeast · *Pichia* · Biofuels · Proteases

Introduction

Microorganisms have evolved a variety of enzymes for degrading the different components of lignocellulosic material, including cellulose (cellulases), hemicellulose (xylanases), and lignin (heme peroxidases), and effectively recycle plant biomass in the environment to CO_2 and H_2O. Manganese peroxidase (MnP) is an extracellular heme peroxidase that catalyzes the H_2O_2-dependent oxidation of Mn(II) to Mn(III). Mn(III) chelates organic acids to create the diffusible oxidants that attack phenolic lignin structures [1]. Both wild-type MnP (wtMnP) from a white-rot fungus [2] and recombinant MnP (rMnP) from the yeast *Pichia pastoris* [3] have been shown to be effective for removing lignin from cellulose fibers in pulp bleaching experiments [4]. However, potential applications of rMnP in pulp and paper manufacture and biofuels production are limited by enzyme production costs.

Production of rMnP from *P. pastoris* for pulp bleaching experiments was previously conducted at pH 6 [4]. A medium pH of 4.5 resulted in very low rMnP concentrations, although the wtMnP is commonly produced in *P. chrysosporium* cultures at this pH. This observation was also surprising in that Gu et al. [3] found that rMnP purified from *P. pastoris* cultures shares similar characteristics with the wtMnP and is active at pH 4.5 and relatively stable from pH 3.0 to 6.0. Further experiments on the effect of pH on rMnP were thereby conducted in this study to determine why rMnP is not observed in low pH yeast cultures, although white-rot fungi typically produce wtMnP at low pH, and the purified *P. pastoris* rMnP appears to be as stable as the wtMnP at low pH.

The effects of pH, temperature, and buffer type on the stability of purified wtMnP from white-rot fungi have been previously investigated. Sutherland and Aust [5] found that wtMnP from the white-rot fungus *P. chrysosporium* was most stable at pH 5.5 and temperatures at or below 37 °C. They also found that the presence of Ca^{2+} is essential to maintain MnP activity. However, Mielgo et al. [6, 7] found that *P. chrysosporium* MnP stability and activity was optimal at pH 4.5 and 30 °C. Recently, the optimal pH for wtMnP from the white rot fungus *Irpex lacteus* was found to be from 5.5–6.5. [8, 9]. Banci et al. [10] observed that rMnP produced by *Escherichia coli* lost its activity immediately after treatment with buffers of pH<3.0 or pH>8.0.

P. pastoris fermentations are often conducted at pH 6, but *P. pastoris* also grows well at a pH range from 2.8 to 6.5 [11]. The optimal pH for expression of active recombinant proteins in *P. pastoris* fermentations has been found to vary widely, with even small changes having dramatic effects on expression. *P. pastoris* can also be grown over a broad temperature range, with 30 °C most commonly employed for fermentations. However, the production levels of some recombinant proteins at this temperature are unsatisfactory or even unobservable. Because of the instability of some recombinant proteins or susceptibility to proteolytic activity, decreasing the fermentation temperature below 30 °C often increases the yield of active antibodies and other proteins. For example, Jahic et al. [12] reported a doubling in the expression of a fusion protein when the temperature was lowered from 30 to 20 °C, although the observed cell growth rates were similar at both temperatures. The authors speculated that this was caused by a substantial reduction in serine protease activity at 20 °C.

Cassland and Jönsson [13] suggested that the higher recombinant protein yield often observed at lower temperatures is caused by a decrease in protein misfolding and aggregation, as well as a reduction in proteolytic degradation. The existence of proteases

has been widely observed during the expression of recombinant proteins in high-cell density *P. pastoris* fermentations [11, 12, 14–19], and addition of protease inhibitors has been shown to be effective in reducing proteolytic activity against certain recombinant proteins [11, 12, 17, 19]. The fermentation conditions reported for the optimized expression of various proteins in *P. pastoris* are summarized in Table 1 [20–32]. It can be concluded that the optimum pH and temperature for the production of recombinant proteins by *P. pastoris* strongly depends on the particular protein.

The current research describes the effect of pH and temperature on *P. pastoris* growth and rMnP production in both shake flask and bioreactor cultivation. Results of these experiments suggest that intracellular proteases are released from dead and lysed yeast cells during the fermentation that are active against rMnP at pH less than 5.5.

Materials and Methods

Analytical Methods

Cell Density by Spectrophotometry Yeast cell density was estimated by optical density at 600 nm (OD_{600}). Liquid broth samples were diluted in a normal saline solution (0.9% NaCl) or deionized water to achieve an optical density less than 0.4 in a final volume of 1 ml. The diluted cell solution was transferred to disposable semimicro cuvettes, and the absorbance at 600 nm was measured with a Spectronic Genesys 20 spectrophotometer (Thermo Electron, Waltham, MA). Normal saline solution or diluted heme solution were

Table 1 Optimal pH and temperature conditions reported for the expression of recombinant proteins by *Pichia pastoris*.

pH	Temperature (°C)	Protein expressed	Putative effect	Reference
3.0	25	A33 single-chain Fv antibody fragment	Protease inhibition	[20]
3.0	30	Mouse and rat collagen gelatins	Protease inhibition	[21]
4.0	20	Cellulose-binding *Cissus antartica* lipase B	Increased expression	[12]
4.5	30	Coffee bean α-galactosidase	Increased expression	[22]
5.0	–	120 kDa HIV-1 envelope protein	Protease inhibition	[23]
6.0	16	Bovine β-1,4-galactosyltransferase I	Increased expression	[24]
6.0	23	Herring anti-freeze protein (hAFP)	Increased expression	[25]
6.0	25	Galactose oxidase	Stabilized structure	[26]
6.0	28	Human cystatin C protein	Increased expression	[27]
6.0	30	*Trametes versicolor* laccase	Protease inhibition	[16]
–	19	*Trametes versicolor* laccase	Increased expression	[13]
6.0	–	Human serum albumin	Increased expression	[11]
6.0	–	Mouse epidermal growth factor (mEGF)	Increased expression	[14]
7.0	28	Hookworm anticoagulant peptide	Protease inhibition	[28]
7.5 – 8.0	15	Single-chain Fv antibody fragment	Increased expression	[17]
7.7 – 8.3	–	Prourokinase–annexin V chimeric protein	Protease inhibition	[29]
8.0	28	A/Victoria/3/75 (H_3N_2) hemagglutinin[1]	Increased expression	[30]
8.5	20	*Trametes versicolor* laccase[1]	Protease inhibition	[31]
10.0	20	Human μ-opioid receptor fusion protein[1]	Increased expression	[32]

Medium pH is outside of normal *P. pastoris* growth range (pH 2.8–6.5).

used to zero the spectrophotometer. A standard curve was prepared to correlate dry weight (g/l) to optical density. The resulting correlation was dry weight (g/l)=0.3×optical density.

MnP Activity Assay MnP activity was measured by monitoring the oxidation of 2,6-dimethoxyphenol (2,6-DMP) at 469 nm [33]. The reaction mixtures contained 0.4 mM $MnSO_4$, 50 mM sodium malonate (pH 4.5), 0.1 mM 2,6-DMP, and MnP enzyme. The extinction coefficient, ε_{469}, for the orange-brown dimeric product 2,2′,6,6′-tetramethoxydibenzo-1,1′-diquinone is 49,600 $m^{-1}\cdot cm^{-1}$ at 469 nm. MnP activity is expressed as the micromoles of product formed per minute (units)/liter (U/l). The culture samples (1 ml) were centrifuged at 10,000×*g* for 5 min to pellet yeast cells and heme particles, and the clear culture supernatant (10–100 μl) was added to the reaction mixture. Deionized water was added to a final volume of 1 ml. Addition of H_2O_2 to a concentration of 0.1 mM was used to initiate reactions at room temperature, and the absorbance at 469 nm was measured after 1 min.

Strains

P. pastoris SMD1168H (*his*$^+$ *pep4*$^-$) is a protease-deficient strain developed by Invitrogen, Carlsbad, CA. *P. pastoris* SMD1168H αMnP1-1 (*P. pastoris* αMnP1-1) was constructed by electroporating the plasmid pαAMNP [3] into *P. pastoris* SMD1168H. This plasmid contains *mnp1* complementary DNA (cDNA; *P. chrysosporium*) downstream of a constitutive glyceraldehyde-3-phosphate dehydrogenase promoter and a *Saccharomyces cerevisiae* á-factor secretion signal sequence. The plasmid integrates into the host chromosome and contains the *Sh ble* gene that confers resistance to the broad spectrum antibiotic Zeocin. The transformed *P. pastoris* αMnP1-1 was routinely cultured on YPD medium (1% yeast extract, 2% peptone, and 2% dextrose) in agar plates and shake flasks at 30 °C for inoculation of experimental cultures.

Shake Flask Cultivation

Shake flask experiments were performed in buffered glycerol-complex medium (BMGY), modified by substituting glucose for glycerol. The modified BMGY medium consisted of the following (weight percent): yeast extract (1%), peptone (2%), potassium phosphate buffer at pH 6.0 (200 mM) or sodium malonate buffer at pH 4.5 (200 mM), yeast nitrogen base (with ammonium sulfate, without amino acids) (1.34%), biotin (4×10^{-5}%), and glucose (2%).

Exogenous hemin (minimum 80%, Sigma-Aldrich, St Louis, MO) was added as dry powder to the modified BMGY medium after autoclaving. Zeocin (100 mg/l) was also added to inhibit bacterial contamination. Shake flask experiments were conducted with 20 ml medium in 125 ml baffled flasks on an Innoun 4230 refrigerated rotary shaker incubator (250 rpm; New Brunswick Scientific Co., Inc., Edison, NJ) at 25 or 30 °C. For pH experiments, 1 M sodium malonate buffer was used in pH 4.0, 4.5, and 5.0 media; 1 M potassium phosphate buffer was used for pH 5.5, 6.0, 6.5, and 7.0 media. HCl or NaOH (10 N) were added to adjust medium pH.

The *P. pastoris* αMnP1-1 inoculum was prepared with 100 ml YPD medium in a 500 ml shake flask at 250 rpm and 30 °C. After 24 h, the inoculum was separated through centrifugation and washed with sterile normal saline solution (0.9% NaCl). The washed inoculum was then added to each flask to achieve an initial cell density of approximately 0.15 g/l dry cell weight.

Bioreactor Fed-Batch Fermentation

Fed-batch fermentations with *P. pastoris* αMnP1-1 were performed using 3.0-l BioFlo 100 fermentors (New Brunswick Scientific Co. Inc.). The suspended cell, fed-batch cultivation was divided into two stages: batch and fed-batch cultivation with glucose. *P. pastoris* αMnP1-1 inoculum cultures (100 ml) were grown in YPD medium and used to inoculate 1 l of medium in the bioreactors.

Batch fermentations were conducted in basal salts medium (BSM) containing 4% glucose and were prepared as follows [31]:

Basal Salt Medium (BSM) For 1l final volume, the following ingredients were dissolved completely in distilled–deioinized water: phosphoric acid (85% H_3PO_4), 26.7 ml; calcium sulfate ($CaSO_4 \cdot 2H_2O$), 0.93 g; potassium sulfate (K_2SO_4), 18.2 g; magnesium sulfate ($MgSO_4 \cdot 7H_2O$), 14.9 g; potassium hydroxide (KOH), 4.13 g; glucose, 40.0 g. The medium was autoclaved, and 4 ml of PMT1 trace salt solution were aseptically added per liter of BSM.

PMT1 trace salts For 1l final volume, the following ingredients were dissolved completely in distilled–deionized water: cupric sulfate ($CuSO_4 \cdot 5H_2O$), 6.0 g; sodium iodide (NaI), 0.08 g; manganese sulfate·H_2O ($MnSO_4 \cdot H_2O$), 3.0 g; sodium molybdate ($Na_2MoO_4 \cdot H_2O$), 0.2 g; boric acid (H_3BO_4), 0.02 g; cobalt chloride ($CoCl_2 \cdot 6H_2O$), 0.5 g; zinc chloride ($ZnCl_2$), 20.0 g; ferrous sulfate ($FeSO_4 \cdot 7\ H_2O$), 65.0 g; biotin, 0.2 g; sulfuric acid (H_2SO_4), 5.0 ml. The solution was filter sterilized and stored at room temperature.

Fermentation conditions were set at 25 or 30 °C, with agitation (800 rpm) and 1.5 l of air per liter of culture volume/minute. The pH was maintained at 6.0 by the addition of 30% ammonium hydroxide. For pH experiments, 30% phosphoric acid was added slowly for one-time pH adjustments from 6.0 to 4.5 either at the beginning or during the course of the fermentation as indicated. The level of dissolved oxygen was monitored using an Ingold galvanic electrode. One milliliter of Antifoam 204 (Sigma-Aldrich) was added before inoculation. When the carbon source was depleted as indicated by a sharp rise in oxygen concentration, the fed-batch cultivation was initiated. During glucose fed-batch, 50% glucose solution mixed with 12 ml of PMT1 per liter was continuously added at a rate of 12 ml/h to keep the dissolved oxygen in the medium broth above 30% saturation. Heme (0.1 g/l) was added as dried powder at the beginning of the fed-batch phase.

Enzyme Purification and Stability Experiments

Recombinant manganese peroxidase (rMnP) was concentrated from *P. pastoris* αMnP1-1 cultures (pH 6.0) by high-speed (10,000×*g*) centrifugation to remove the yeast cells and heme particulates, acetone precipitation (equal volumes of acetone and culture supernatant), dialysis (0.1 M pH 6.0 KH_2PO_4/K_2HPO_4 buffer) to concentrate the rMnP and remove salts, and freeze-drying. The final rMnP activity was concentrated from approximately 2,000 U/l in the fermentation broth to 30,000 U/l in the final concentrated solution [4]. For enzyme stability experiments in defined buffers, fermentation broth (with yeast cells) or supernatant fractions, the initial rMnP activity was adjusted at the start of the experiment through the addition of concentrated rMnP to about 1,500 U/l. Enzyme stability

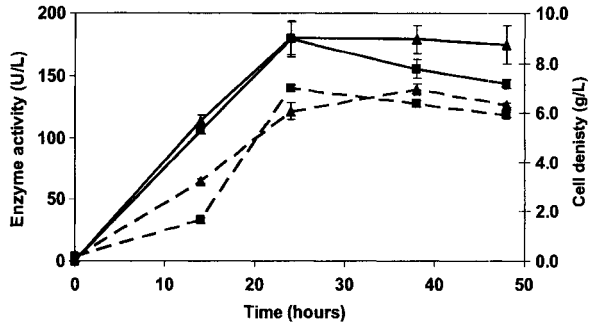


Fig. 1 Effects of temperature on cell growth and rMnP activity (U/l) in *P. pastoris* αMnP1-1 shake flask cultivation (pH 6). *Solid line* Enzyme activity (U/l), *dashed line* cell density (g/l). Symbols are as follows: *triangle* 25 °C, *square* 30 °C

experiments were conducted with 20 ml of solution in 125 ml baffled flasks on a rotary shaker incubator (250 rpm; New Brunswick Scientific Co., Inc.) at 30 °C.

Four different protease inhibitors [10 μM pepstatin, 20 μM E-64, 1 mM phenylmethylsulfonyl fluoride (PMSF), and 1 mM ethylenediaminetetraacetic acid (EDTA)] were examined for their effects on rMnP stability. These inhibitors were dissolved in either distilled water or ethanol and then added into 20 ml of pH 4.5 culture supernatant either separately or in combination. The 125 ml baffled flasks were incubated on a rotary shaker as described above. The rMnP activities were measured at appropriate time intervals.

Results and Discussion

Production of MnP at Different Temperatures

Lowering the temperature of *P. pastoris* αMnP1-1 shake flask or bioreactor fermentations from 30 to 25 °C did not result in appreciable changes in cell growth rate or production of recombinant enzyme as indicated by cell density and rMnP activity measurements (Figs. 1 and 2). A higher cell density was achieved at 25 °C (52.6 g/l) than at 30 °C (42.1 g/l) in the fed-batch fermentations, but this did not result in a corresponding increase in rMnP activity (Fig. 2).

This is in contrast to many reports in which expression of active recombinant protein by *P. pastoris* was increased by up to 30 times by lowering the temperature from 30 to 15–25 °C

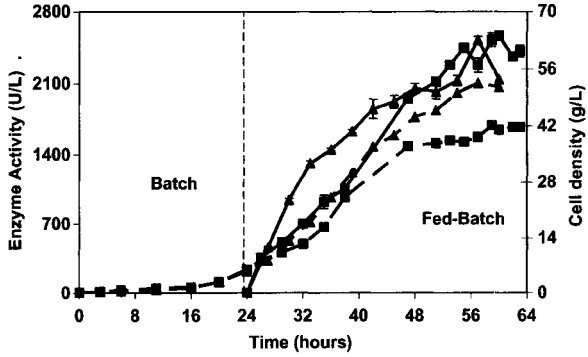


Fig. 2 Effects of temperature on cell growth and rMnP activity (U/l) in *P. pastoris* αMnP1-1 bioreactor fed-batch fermentations (pH 6). *Solid line* Enzyme activity (U/l), *dashed line* cell density (g/l). Symbols are as follows: *triangle* 25 °C, *square* 30 °C

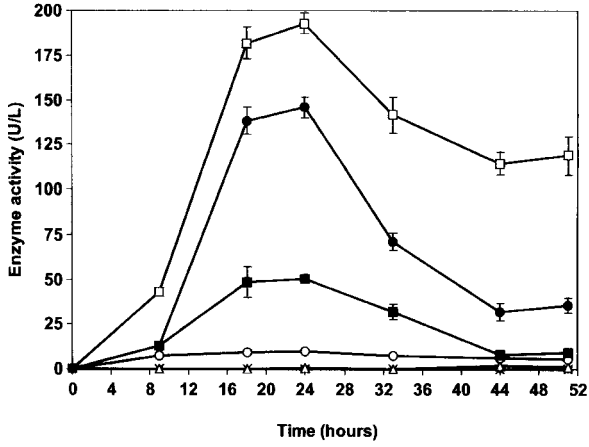


Fig. 3 Effects of pH on rMnP activity (U/l) in shake flask cultivation of *P. pastoris* αMnP1-1 (30 °C). Symbols are as follows: *cross* pH 4.0, *empty diamond* pH 4.5, *empty triangles* pH 5.0, *empty circles* pH 5.5, *empty squares* pH 6.0, *filled circles* pH 6.5, *filled squares* pH 7.0

[12, 13, 17, 20, 24, 25, 31]. The effect of lowering the temperature is typically attributed to decreased proteolysis and unfolding of the protein. The lack of a clear increase in the rMnP yield by *P. pastoris* αMnP1-1 upon lowering the fermentation temperature suggests that, at pH 6, spontaneous denaturation and protease activity do not limit the final active rMnP enzyme yield.

Production of MnP at Different pH

Varying the pH of shake flask cultures from pH 4.5 to 7 had little effect on *P. pastoris* cell growth. At pH 4, the cell density decreased to approximately half that of cultures at higher pH (data not presented). Little to no rMnP activity was observed during 48 h of cultivation at pH 4.0, 4.5, 5.0, or 5.5 (Fig. 3). After 24 h, the cultures at pH 6.0, 6.5, and 7.0 produced the highest enzyme activities (193, 147, and 51 U/l, respectively).

In fed-batch fermentations, growth rates at pH 4.5 and 6.0 (Fig. 4) were also similar, with short lag periods after large pH adjustments from pH 6 to 4.5 (Figs. 5 and 6). Growth of *P. pastoris* αMnP1-1 throughout this pH range is consistent with previously reported results [11, 17, 28].

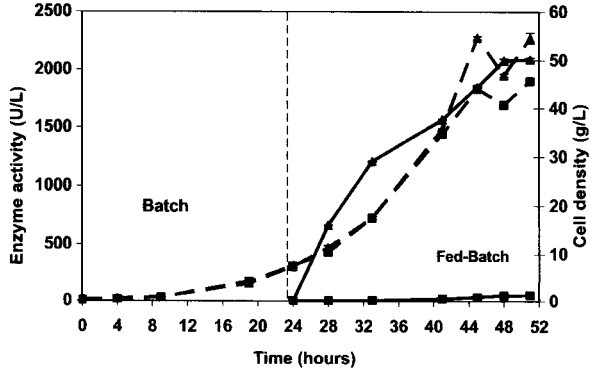


Fig. 4 Comparison of pH 4.5 and 6 *P. pastoris* αMnP1-1 fed-batch fermentations (30 °C). *Solid line* rMnP activity (U/l), *dashed line* cell density (dry weight, g/l). Symbols are as follows: *triangles* pH 6.0 during the whole cultivation, *squares* pH 4.5 during the whole cultivation

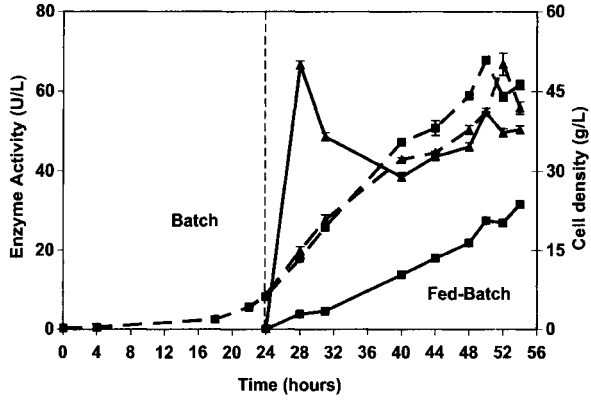


Fig. 5 Effects of reducing the pH from 6 to 4.5 at the beginning of the fed-batch phase. *Solid line* rMnP activity (U/l), *dashed line* cell density (dry weight g/l). Symbols are as follows: *triangle* pH 6.0 for batch/pH 4.5 for fed batch, *square* pH 4.5 during the whole cultivation

In bioreactors maintained at pH 4.5 throughout the batch and fed-batch phases, the rMnP enzyme activity was very low (54 U/l) compared with activities greater than 2,000 U/l in pH 6.0 fermentations at the end of the fed-batch phase (Fig. 4). Decreasing the culture pH from 6.0 to 4.5 at the start of the fed-batch phase also resulted in little rMnP accumulation in the medium (Fig. 5). Decreasing the culture pH from 6.0 to 4.5 after 20 h in the fed-batch phase resulted in a rapid loss of more than 1,000 U/l rMnP activity from the rMnP produced at pH 6 (Fig. 6). The failure of *P. pastoris* αMnP1-1 to produce appreciable amounts of rMnP at low pH and the decline in rMnP activity upon lowering the cultivation pH are somewhat unexpected. *P. pastoris* grows equally well at pH 6 and 4.5, and wtMnP and rMnP are both stable and active at pH 4.5 [3]. Furthermore, the wtMnP host (*P. chrysosporium*) is known to produce active wtMnP at pH 4.5 [34]. Because of the rapid inactivation of rMnP in cultures at pH 4.5, a pH of 6.0 was chosen for the routine cultivation of *P. pastoris* αMnP1-1, and further experiments were undertaken to investigate the cause of low rMnP production at low pH.

rMnP Stability

Recombinant MnP produced by *P. pastoris* αMnP1-1 in pH 6 fed-batch fermentations was not stable in pure pH 6.0 buffers (Fig. 7). In 0.01 M potassium phosphate buffer, rMnP activity decreased by 25% in 4 h, and a somewhat higher activity loss rate was observed in

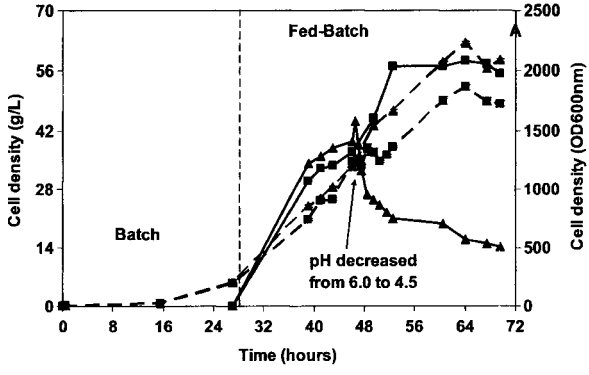


Fig. 6 Effects of reducing the pH from 6 to 4.5 during the middle of the fed-batch phase. *Solid line* rMnP activity (U/l), *dashed line* cell density (dry weight g/l). Symbols are as follows: *triangle* transition from pH 6.0 to 4.5 during the middle of fed-batch, *square* pH 6.0 during the whole cultivation

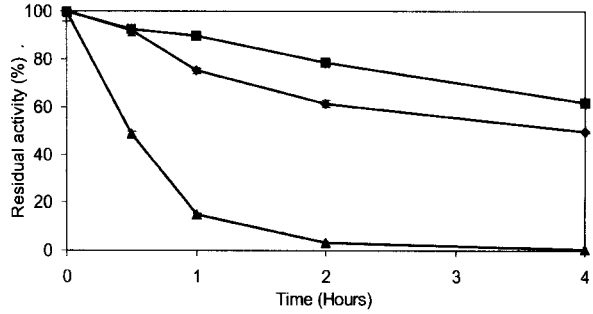


Fig. 7 Stability of rMnP in pH 6.0 buffers (30 °C). Symbols are as follows: *diamonds* 0.1 M phosphate buffer, *squares* 0.01 M phosphate buffer, *triangles* 0.01 M sodium citrate buffer

0.1 M potassium phosphate buffer. A much more rapid decrease in rMnP activity was observed in 0.01 M sodium citrate buffer (also pH 6); the enzyme half-life in this buffer was less than 30 min (Fig. 7).

These experimental data are well-described by first-order kinetics, with best-fit half-lives of 6.7, 3.4, and 0.4 h for 0.01 M phosphate, 0.1 M phosphate, and 0.01 M sodium citrate buffers, respectively. These purified buffers may lack essential co-factors that could stabilize the rMnP, such as calcium, manganese, and iron. As Ca^{2+} ion is essential for MnP activity, chelation of calcium ions by citrate (and to a lesser extent, phosphate) is probably the mechanism for the observed first-order kinetics of inactivation in these buffers. These attempts to determine the effect of pH on rMnP activity in defined buffers were ultimately deemed unsuccessful, as the rates of inactivation in potassium phosphate (0.1 and 0.01 M) and sodium citrate (0.01 M) buffers were observed to be considerably higher than in the bioreactor culture supernatant.

Recombinant MnP concentrated from pH 6 *P. pastoris* αMnP1-1 fed-batch fermentations was also added to pH 4.5 fed-batch fermentations and pH 4.5 and 6 cultures and culture supernatants. In culture supernatants obtained from pH 6.0 bioreactor fermentations, rMnP was stable for up to 6 h before a measurable loss of activity occurred, and only 25% of the initial activity was lost after 24 h incubation (Fig. 8). In supernatant from pH 4.5 fermentations, 25% of rMnP activity was lost during the first 6 h, and another 25% decrease occurred in the following 18 h. However, a much higher rate of loss of rMnP activity was observed in whole pH 4.5 culture, from which the yeast cells were not removed via centrifugation, than in either of the cell-free supernatants (Fig. 8). The rate of loss of rMnP activity in pH 4.5 bioreactor cultures and culture supernatant was higher in samples obtained after 72 h of fermentation than in samples taken after only 48 h. As before, the

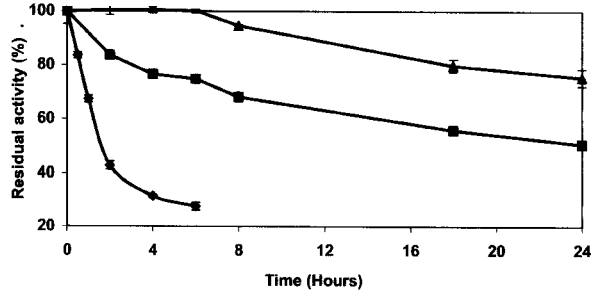


Fig. 8 rMnP stability in cultures and culture supernatants from pH 4.5 and 6.0 *P. pastoris* αMnP1-1 fed-batch fermentations (30 °C). Symbols are as follows: *triangles* pH 6.0 culture supernatant, *square* pH 4.5 culture supernatant, *diamond* pH 4.5 culture

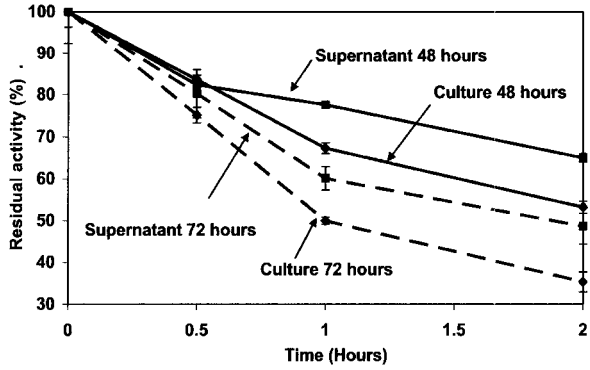


Fig. 9 rMnP stability in cultures and culture supernatants taken 48 and 72 h after the start of *P. pastoris* αMnP1-1 pH 4.5 fed-batch fermentations (30 °C). *Solid line* Samples at 48 h, *dashed line* samples at 72 h. Symbols are as follows: *diamonds* culture, *squares* culture supernatant

presence of yeast cells substantially increased the rate of loss of rMnP activity (Fig. 9). Also, the activity of concentrated rMnP added directly into the medium of an ongoing pH 4.5 bioreactor fermentation 20 h after the start of the fed-batch phase declined rapidly, with 50% of the activity lost within the first 2 h (Fig. 10).

Whereas it is known that the negatively charged yeast cell surface strongly adsorbs mono- and divalent ions, such as Ca^{2+} [35, 36], the cells in the whole culture were grown in calcium-rich media, and Ca^{2+} binding sites would likely be saturated. Thus, simple biosorption of calcium does not explain the very fast inactivation of rMnP in whole culture. A complex or cooperative mechanism is suggested by the failure of first-order kinetics to describe the inactivation of rMnP in any of these media (c.f. Fig. 7).

Proteases

The results of the rMnP stability experiments are consistent with the hypothesis that intracellular proteases released from dead cells during the fermentation are active against rMnP at pH 4.5. The rapid onset of rMnP inactivation during fermentation following a pH adjustment from 6.0 to 4.5 suggests that these proteases are produced at both pH 6 and 4.5, but are only active against rMnP at the lower pH. Lowering the temperature of the stability test in pH 4.5 culture supernatant from 30 to 20 °C slowed the rate of rMnP activity loss (Fig. 11), consistent with reduced activity of proteases against rMnP at lower temperatures. However, the lower temperatures would likely also favor the active enzyme conformation, so the observed rMnP inactivation cannot necessarily be attributed to the action of proteases.

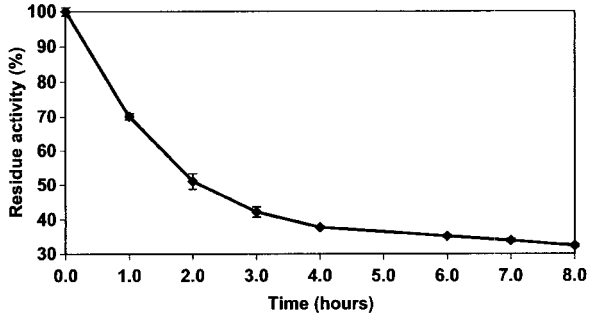


Fig. 10 Stability of rMnP added to pH 4.5 *P. pastoris* αMnP1-1 fed-batch fermentations (30 °C) 20 h after the start of the fed-batch phase

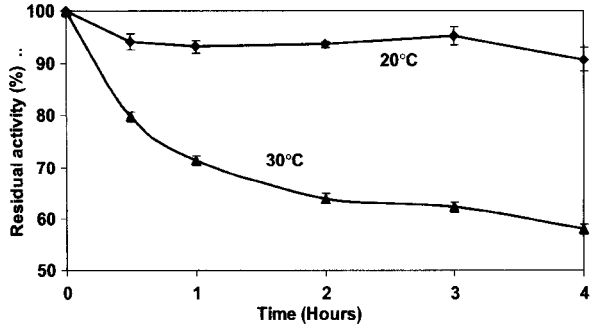


Fig. 11 rMnP stability in 20 and 30°C culture supernatant from *P. pastoris* αMnP1-1 pH 4.5 fed-batch fermentations (30 °C). Symbols are as follows: *diamond* 20 °C, *triangles* 30 °C

A comparison of the rate of inactivation of rMnP in whole culture and culture supernatants from *P. pastoris* αMnP1-1 fed-batch fermentations at pH 4.5 (Fig. 12) indicates that the rate of loss of activity in the presence of cells is approximately 100 U l^{-1} h^{-1} higher than in the culture supernatant. In both cases, the rate of rMnP degradation is initially high, presumably because of the action of proteases, and then decreases from approximately 650 to150 U l^{-1} h^{-1} during the first hour. The initial rapid inactivation is followed by a slower inactivation of rMnP over the next few hours, similar to the degradation rate observed in pH 6 culture supernatants (Fig. 8). This slower rate of loss of rMnP activity may be caused by denaturation of the enzyme.

Further attempts to obtain direct evidence for the action of intracellular acidic proteases against rMnP using protease inhibitors and defined buffers were inconclusive. Addition of the protease inhibitors pepstatin (10 μM), E-64 (20 μM), and PMSF (1 mM) to pH 4.5 culture supernatant did not decrease the rate of rMnP inactivation, suggesting that aspartic, cysteine, and serine proteases, respectively, in the culture supernatant were not active against rMnP. The presence of EDTA (1 mM) was found to inhibit rMnP activity, probably by chelation of essential Ca^{2+} ions or heme Fe^{3+}, and thus, could not be used to detect the activity of metalloproteases (data not shown). Analysis for peptide fragments by sodium dodecyl sulfate polyacrylamide gel electrophoresis (SDS-PAGE) was also inconclusive because of the highly variable molecular weight of the intact hyperglycosylated protein. Further progress in elucidating the role of proteases at low pH will probably require the preparation of substantially pure rMnP, as well as a suitable defined buffer or medium in which to conduct stability studies.

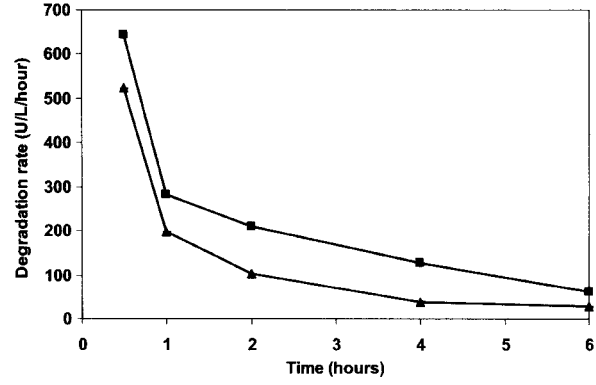


Fig. 12 Rate of degradation of rMnP added to cultures and culture supernatants from pH 4.5 *P. pastoris* αMnP1-1 fed-batch fermentations (30 °C). Symbols are as follows: *squares* pH 4.5 culture, *triangles* pH 4.5 supernatant

It does not appear that the production of active proteases limits the rMnP enzyme titer during pH 6 fermentations, but this possibility was not directly addressed and cannot be entirely eliminated. The production of rMnP in *P. pastoris* αMnP1-1 at pH 6 may be sufficiently practical for most industrial applications, such as pulp bleaching [2, 4]. Although rMnP is not produced effectively by *P. pastoris* αMnP1-1 at pH 4.5, the concentrated preparations of rMnP expressed at pH 6 exhibit activity at pH 4.5 similar to the wtMnP. Presumably these preparations could be used, perhaps with further purification to remove residual proteases, for low pH applications.

Acknowledgment This work was supported by the National Science Foundation grants BES-0536128 and BES-0328031.

References

1. Kirk, T. K., & Cullen, D. (1998). In R. A. Young & M. Akhtar (Eds.), *Environmentally friendly technologies for the pulp and paper industry* (pp. 273–307). New York, NY: Wiley.
2. Harazono, K., Kondo, R., & Sakai, K. (1996). *Applied and Environmental Microbiology, 62*(3), 913–917.
3. Gu, L., Lajoie, C. A., & Kelly, C. J. (2003). *Biotechnology Progress, 19*(5), 1403–1409.
4. Jiang, F., Kongsaeree, P., Charron, R., Lajoie, C., Xu, H., Scott, G., & Kelly, C. (2007). *Biotechnology and Bioengineering* (in press).
5. Sutherland, G. R. J., & Aust, S. D. (1996). *Archives of Biochemistry and Biophysics, 332*(1), 128–134.
6. Mielgo, I., Palma, C., Guisan, J. M., Fernandez-Lafuente, R., Moreira, M. T., Feijoo, G., et al. (2003). *Enzyme and Microbial Technology, 32*, 769–775.
7. Urek, R. O., & Pazarlioglu, N. K. (2004). *Process Biochemistry, 39*, 2061–2068.
8. Shin, K. S., Kim, Y. H., & Lim, J. S. (2005). *Journal of Microbiology, 43*(6), 503–509.
9. Baborova, P., Moder, M., Baldrian, P., Cajthamlova, K., & Cajthaml, T. (2006). *Research in Microbiology, 157*(3), 248–253.
10. Banci, L., Bartalesi, I., Ciofi-baffoni, S., Tien, M. (2003). *Biopolymers, 72*, 38–47.
11. Sreekrishna, K., Barr, K. A., Hoard, S. A., Prevatt, W. D., Torregrosa, R. E., Levingston, R. E., et al. (1990). Topic 09-37B. In S. G. Oliver & R. Wickner (Eds.), 15th International Congress on Yeast Genetics and Molecular Biology, 1990, Hague, The Netherlands. *Yeast, 6*(Special Issue), S447.
12. Jahic, M., Gustavsson, M., Jansen, A. K., Martinelle, M., & Enfors, S. O. (2003). *Journal of Biotechnology, 102*, 45–53.
13. Cassland, P., & Josson, L. J. (1999). *Applied Microbiology and Biotechnology, 52*, 393–400.
14. Clare, J. J., Romanos, M. A., Rayment, F. B., Rowedder, J. E., Smith, M. A., Payne, M. M., et al. (1991). *Gene, 105*, 205–212.
15. Cregg, J. M., Vedvick, T. S., & Raschke, W. C. (1993). *Bio/Technology, 11*, 905–910.
16. Jönsson, L. J., Saloheimo, M., & Penttila, M. (1997). *Current Genetics, 32*, 425–430.
17. Shi, X., Karkut, T., Chamankhah, M., Alting-Mees, M., Hemmingsen, S. M., & Hegedus, D. (2003). *Protein Expression and Purification, 28*(2), 321–330.
18. Sinha, J., Plantz, B. A., Zhang, W., Gouthro, M., Schlegel, V., Liu, C. P., et al. (2003). *Biotechnology Progress, 19*, 794–802.
19. Sinha, J., Plantz, B. A., Inan, M., & Meagher, M. M. (2004). *Biotechnology and Bioengineering, 89*(1),102–112.
20. Damasceno, L. M., Pla, I., Chang, H. J., Cohen, L., Ritter, G., Old, L. J., et al. (2004). *Protein Expression and Purification, 37*(1), 18–26.
21. Werten, M. W. T., Bosch, T. J. V. D., Wind, R. D., Mooibroek, H., & Wolf, F. A. D. (1999). *Yeast, 15*, 1087–1096.
22. Zhu, A., Monahan, C., Zhang, Z., Hurst, R., Leng, L., & Goldstein, J. (1995). *Archives of Biochemistry and Biophysics, 324*(1), 65–70.
23. Clare, J., Scorer, C., Buckholz, R., & Romanos, M. (1998). *Methods in Molecular Biology, 103*, 209–225.
24. Bencurova, M., Rendic, D., Fabini, G., Kopecky, E. M., Altmann, F., & Wilson, I. B. H. (2003). *Biochimie, 85*, 413–422.
25. Li, Z., Xiong, F., Lin, Q., d'Anjou, M., Daugulis, A. J., Yang, D. S. C., et al. (2001). *Protein Expression and Purification, 21*(3), 438–445.

26. Whittaker, M. M., & Whittaker, J. W. (2000). *Protein Expression and Purification, 20*(1), 105–111.
27. Pritchett, J., & Baldwin, S. A. (2004). *Journal of Industrial Microbiology and Biotechnology, 31*, 553–558.
28. Inan, M., Chiruvolu, V., Eskridge, K. M., Vlasuk, G. P., Dickerson, K., Brown, S., et al. (1999). *Enzyme and Microbial Technology, 24*, 438–445.
29. Ohya, T., Morita, M., Masami, M., Shinobu, K., & Kaoru, K. (2002). *Journal of Bioscience and Bioengineering, 94*(5), 467–473.
30. Saelens, X., Vanlandschoot, P., Martinet, W., Maras, M., Neirynck, S., Contreras, R., et al. (1999). *European Journal of Biochemistry, 260*, 166–175.
31. Hong, F., Meinander, N. Q., & Jönsson, L. J. (2002). *Biotechnology and Bioengineering, 79*, 438–449.
32. Sarramegna, V., Demange, P., Milon, A., & Talmont, F. (2002). *Protein Expression and Purification, 24*, 212–220.
33. Wariishi, H., Valli, K., & Gold, M. H. (1992). *Journal of Biological Chemistry, 267*, 23688–23695.
34. Tien, M., & Kirk, T. K. (1983). *Science, 221*(4611), 661–663.
35. Vasudevan, P., Padmavathy, V., & Dhingra, S. C. (2002). *Bioresource Technology, 82*(3), 285–289.
36. Wang, J., & Chen, C. (2006). *Biotechnology Advances, 24*(2), 427–451.

Appl Biochem Biotechnol (2008) 146:29–37
DOI 10.1007/s12010-007-8051-9

Xylanase Production by *Bacillus circulans* D1 Using Maltose as Carbon Source

D. A. Bocchini · E. Gomes · R. Da Silva

Received: 15 May 2007 / Accepted: 5 September 2007 /
Published online: 27 October 2007
© Humana Press Inc. 2007

Abstract *Bacillus circulans* D1 is a good producer of extracellular thermostable xylanase. Xylanase production in different carbon sources was evaluated and the enzyme synthesis was induced by various carbon sources. It was found that D-maltose is the best inducer of the enzyme synthesis (7.05 U/mg dry biomass at 48 h), while D-glucose and D-arabinose lead to the production of basal levels of xylanase. The crude enzyme solution is free of cellulases, even when the microorganism was cultivated in a medium with D-cellobiose. When oat spelt xylan was supplemented with D-glucose, the repressive effect of this sugar on xylanase production was observed at 24 h, only when used at 5.0 g/L, leading to a reduction of 60% on the enzyme production. On the other hand, when the xylan medium was supplemented with D-xylose (3.0 or 5.0 g/L), this effect was more evident (80 and 90% of reduction on the enzyme production, respectively). Unlike that observed in the xylan medium, glucose repressed xylanase production in the maltose medium, leading to a reduction of 55% on the enzyme production at 24 h of cultivation. Xylose, at 1.0 g/L, induced xylanase production on the maltose medium. On this medium, the repressive effect of xylose, at 3.0 or 5.0 g/L, was less expressive when compared to its effect on the xylan medium.

Keywords Xylanase · Maltose · Induction · Repression · *Bacillus circulans*

D. A. Bocchini · E. Gomes · R. Da Silva (✉)
Laboratório de Bioquímica e Microbiologia Aplicada, IBILCE—Instituto de Biociências Letras e Ciências Exatas, UNESP—Universidade Estadual Paulista, Rua Cristóvão Colombo, 2265, São José do Rio Preto, São Paulo CEP 15054-000, Brazil
e-mail: dasilva@ibilce.unesp.br

Introduction

Xylanases (1,4-β-D-xylan xylanohydrolases, EC 3.2.1.8) are hydrolytic enzymes that catalyze the endohydrolysis of the β-1,4 backbone in xylan, the main polysaccharide of the hemicellulose fraction in plant cell walls [1]. Endoxylanases are reported to be produced mainly by microorganisms, including several species of fungi and bacteria [2–4].

Xylanases are enzymes of great potential for industrial applications. They are mainly used in the pretreatment of Kraft pulp, improving bleachability of pulp while decreasing consumption of chlorine chemicals [5, 6]. These enzymes are also used as additives to pig and poultry cereal-based diets, to improve nutrient utilization [7], in flour improvement for bakery products [8], in saccharification of agricultural, industrial and municipal wastes [9], and in juice and wine clarification [1].

Xylanase production by microorganisms, which were grown on a variety of carbon sources, has been studied, and the role of these substrates as inducers or repressors has been evaluated [10–13]. In general, xylanases are enzymes liable to induction, synthesized in media containing xylan or xylan residues [14]. However, in some cases, xylan may be a poor inducer of xylanase synthesis [15]. In many microorganisms, this enzyme synthesis is liable to catabolite repression in the presence of more readily assimilable carbon sources, such as glucose or xylose [16]. However, syntheses of constitutive xylanases were also reported [17–19]. In the present work, the effect of various carbohydrates on xylanase production by *Bacillus circulans* D1 were investigated.

Materials and Methods

Microorganism

The thermophilic and alkalophilic bacterial strain *Bacillus circulans* D1 used in this study was isolated in a previous work [20]. Stock cultures were maintained in a complex medium containing xylan as carbon source [21], with the addition of agar (15.0 g/L).

Media and Culture Conditions

The mineral media used for xylanase production was composed of KH_2PO_4 (0.5 g/L), K_2HPO_4 (0.5 g/L), KCl (0.5 g/L), NH_4NO_3 (0.5 g/L), $(NH_4)_2SO_4$ (0.5 g/L), $MgSO_4$ $7H_2O$ (0.2 g/L), $FeCl_3$ $6H_2O$ (0.01 g/L), and Na_2CO_3 (5.0 g/L; separately sterilized) supplemented with different carbon sources (birchwood xylan, oat spelt xylan, D-glucose, D-cellobiose, D-galactose, D-arabinose or D-maltose). *B. circulans* D1 was grown in 40 mL of medium, at 45 °C, for 48 h, under 200 rpm. To provide inoculum, cells were grown in 20 mL of mineral medium containing D-glucose as carbon source (5.0 g/L). In the log phase, cells were collected and separated aseptically from the supernatant solution by centrifugation (10 °C, 10,000×*g*, 15 min) and washed three times with NaCl 8.0 g/L. Cells were resuspended in the same volume of sterile mineral medium and used as inoculum (8×10^7 cells/mL).

Induction Experiments

The microorganism was grown in mineral medium supplemented with 1.0 to 10.0 g/L of the carbon source and also in a mineral medium with oat spelt xylan or D-maltose, with the addition of glucose or xylose. Samples were collected from the culture and centrifuged at

10,000×*g* for 15 min. The cell-free supernatant was used as crude enzyme. The experiments were performed in duplicate.

Growth Measurement

Growth was determined by cell dry weight. During cultivation, samples of 1.0 mL were taken and centrifuged at 10,000×*g* for 15 min. Centrifuged cells were dried at 65 °C to a constant weight. The results were expressed in mg of dry cell/mL.

Enzyme Assay

Xylanase activity was assayed by measuring reducing sugars released as xylose, using a dinitrosalycylic acid method [22]. The reaction mixture containing 0.9 mL of the substrate solution of birchwood xylan (5.0 g/L) in acetate buffer (pH 5.0, 0.1 M) and 0.1 mL of the crude enzyme solution was incubated at 60 °C for 10 min. One unit of enzyme activity was defined as the amount of enzyme releasing 1 μmol of xylose per minute, under the cited assay conditions.

Results

Effect of Different Carbon Sources on Xylanase Production

To determine the effects of different carbon sources on the production of extracellular xylanase by *B. circulans* D1, the microorganism was grown in a medium with birchwood xylan, oat spelt xylan, D-xylose, D-maltose, D-galactose, D-cellobiose, D-glucose, or D-arabinose (2.5 g/L). Cellular growth and xylanase production were observed on all sugars tested, except on xylose. The medium containing arabinose afforded the smallest cellular growth and enzyme production (Table 1). At 2.5 g/L, maltose was the best substrate for xylanase production, followed by galactose and oat spelt xylan. The data shown in Table 1 indicate that oat spelt xylan is better than birchwood xylan for xylanase induction in *B. circulans* D1. Xylanase production on the medium with cellobiose was very close to that obtained on the medium with oat spelt xylan. Cellobiose may induce the synthesis of cellulases in some microorganisms, but the crude enzymatic extract obtained with the cultivation of *B. circulans* D1 in this substrate is free of cellulases activities (data not

Table 1 Xylanase production by *B. circulans* D1 at 48 h of cultivation media containing different carbon sources at 2.5 g/L.

Substrate	Xylanase (U/mL)	Specific activity (U/mg dry biomass)
Maltose	9.18	7.05
Galactose	5.71	5.56
Oat spelt xylan	8.25	5.26
Cellobiose	4.61	4.53
Birchwood xylan	4.17	2.44
Glucose	5.03	3.86
Arabinose	0.50	0.82
Xylose	Nd	-

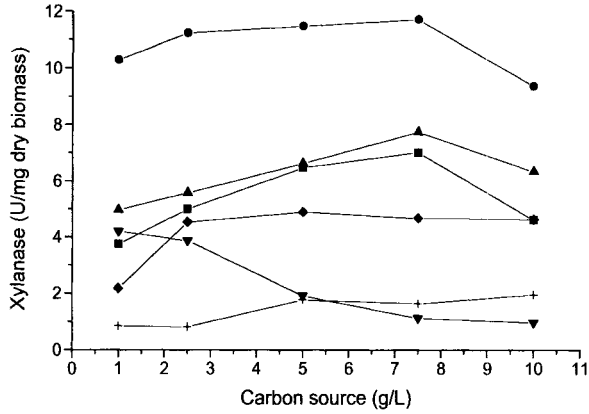


Fig. 1 Effect of carbon sources concentration on xylanase production by *B. circulans* D1, after 48 h of cultivation. Oat spelt xylan (*squares*); D-maltose (*circles*); D-galactose (*triangles*); D-glicose (*inverted triangles*); D-cellobiose (*diamonds*); D-arabinose (*plus signs*)

shown). This fact was reported in previous works [6, 20], and it is an important characteristic for this enzyme application on biobleaching of kraft pulps.

Effect of Sugar Concentration on Xylanase Production

To better evaluate the effects of carbon sources on xylanase production, experiments were carried out using different concentrations of each substrate. The results are presented in Fig. 1. Highest levels of xylanase production were obtained using maltose as the carbon source. Xylanase production on media with xylan was very close to that obtained in medium with galactose. For these substrates, 7.5 g/L seems to be the best concentration for the enzyme production. On cellobiose, the highest xylanase production was observed at 2.5 g/L of this substrate. Apparently, concentrations of cellobiose above 2.5 g/L did not influence xylanase production. The repressive effect of glucose is clearly observed (Fig. 2), as xylanase production decreased as glucose concentration increased. Xylanase production tended to increase as arabinose concentration increases, but only basal levels of the enzyme were obtained.

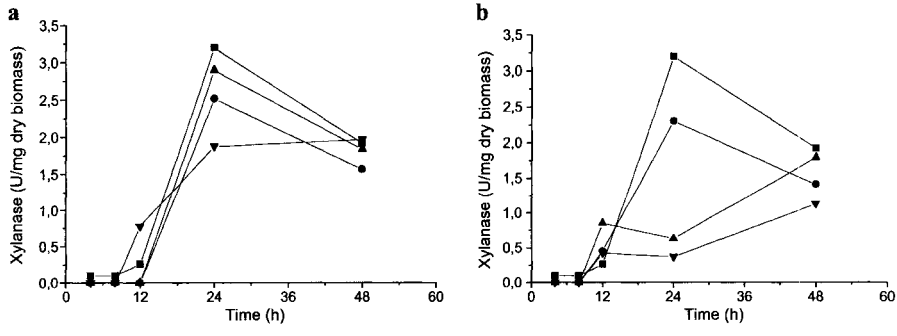


Fig. 2 Xylanase production by *B. circulans* D1 in mineral medium with oat spelt xylan (10.0 g/L; *squares*) and oat spelt xylan (10.0 g/L) plus glucose (**a**) or xylose (**b**) at 1.0 (*circles*), 3.0 (*triangles*) or 5.0 g/L (*inverted triangles*)

Effect of D-glucose or D-xylose on Xylanase Production in the Xylan Medium

The microorganism was grown in a mineral medium with oat spelt xylan (10.0 g/L) supplemented with D-xylose or D-glucose (1.0, 3.0 or 5.0 g/L). The presence of glucose did not strongly influence xylanase production when used at concentrations up to 3.0 g/L (Fig. 2a). The repressive effect of glucose was observed at 5.0 g/L, when a reduction of 40% (1.88 U/mg dry biomass) on the enzyme production was observed at 24 h (Fig. 2a). The addition of xylose repressed the enzyme production (Fig. 2b). This effect was evident at 24 h, when xylose was used at 3.0 or 5.0 g/L, leading to a decrease of 80 and 90% on the productivity (0.63 and 0.37 U/mg dry biomass, respectively).

Effect of D-glucose or D-xylose on Xylanase Production in the Maltose Medium

Because maltose was a good inducer for xylanase production by *B. circulans* D1, the addition of xylose or glucose to the maltose medium was evaluated. As shown in Fig. 3, the presence of glucose or xylose in the maltose medium afforded xylanase production from the first hours of cultivation. However, when the microorganism was cultivated on maltose as the sole carbon source, there was no enzyme induction until 12 h of cultivation, which suggests that maltose was used to support the microbial growth. On the other hand, when glucose or xylose was used with maltose, these sugars were probably used to support growth, while maltose accumulated in the cell and exerted its inducer effect.

Xylanase synthesis on maltose medium was more sensitive to glucose repression when compared to the enzyme synthesis on the xylan medium (Fig. 3a). At 24 h, xylanase production was at the same level in the medium with maltose and maltose plus glucose at 1.0 g/L. However, glucose at 3.0 or 5.0 g/L repressed enzyme production after 24 h of cultivation, leading to a reduction of 55% on specific activity (about 2.30 U/mg dry biomass; Fig. 3a).

The repressive effect of xylose on xylanase synthesis was milder on the maltose medium than on the xylan medium. Xylanase production was induced, at 24 h, when the maltose medium was supplemented with xylose at 1.0 g/L, and xylanase repression was observed, at 24 h, only when 3.0 or 5.0 g/L of xylose was added, leading to a reduction of 22 and 57%, respectively, on the productivity (Fig. 3b).

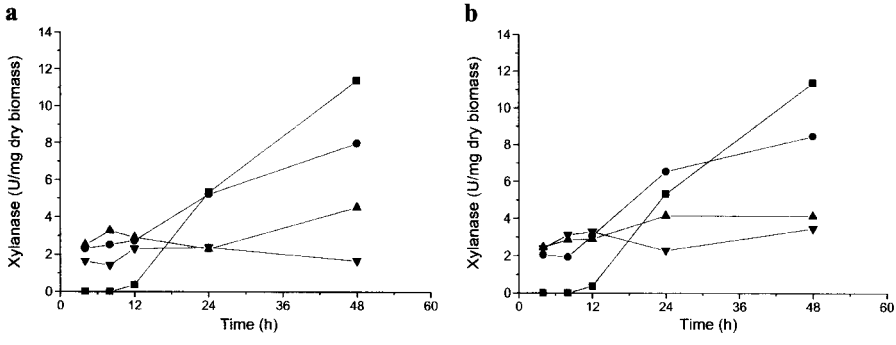


Fig. 3 Xylanase production by *B. circulans* D1 in a mineral medium with (*squares*) maltose (10.0 g/L) and maltose (10.0 g/L) supplemented with glucose (**a**) or xylose (**b**)1.0 (*circles*) , 3.0 (*triangles*), or 5.0 g/L (*inverted triangles*)

Discussion

The data presented in this work regarding xylanase production by *B. circulans* D1 point out the presence of a constitutive xylanase, produced in media with different carbon sources, besides xylan. In many of the reports regarding xylanase production, there is the occurrence of constitutive enzymes [23–26].

Xylanase production by *B. circulans* was induced by a variety of carbon sources, and among the tested substrates, maltose was the best inducer. These data suggest two modes of enzyme expression: one gene that codes for a constitutive xylanase and another gene that codes for a xylanase subject to induction or a single gene that constitutively expresses basal levels of the enzyme and that also is susceptible to induction by specific sugars.

Kyu et al. [10] also reported xylanase production by the strain *B. circulans* B_6 on a variety of carbon sources. However, they reported xylanase levels smaller than those cited in this work. Their results showed xylanase productions of 0.15 and 0.20 U/mg dry biomass after 5 days of cultivation in media containing maltose or galactose (at 2.5 g/L), respectively, whereas *B. circulans* D1 produced on average of 7.05 and 5.56 U/mg dry biomass after 48 h of cultivation on the same carbon sources. The authors reported that D-arabinose did not afford xylanase production, which is in agreement with our results, as only basal levels of the enzyme were obtained on this substrate.

Xylanase production on maltose has been cited for some microorganisms [27, 28], but the authors did not provide details about the enzyme production on this substrate. The data reported in the present work indicated that xylanase synthesis on the maltose medium was more sensitive to glucose repression and less sensitive to xylose repression, when compared to the enzyme synthesis on the xylan medium. From these data, we can infer that xylanase synthesis by *B. circulans* D1 is regulated by different ways when the microorganism is cultivated on xylan or maltose.

From the data obtained with the cultivation of *B. circulans* D1 on the maltose medium, we can infer that when used with maltose, glucose and xylose are preferentially consumed to support microbial growth, while maltose acts as xylanase inducer. Thus, maltose and xylose/glucose are probably transported by different systems. In *B. subtilis*, maltose is transported by a symport sugar-proton [29], but the gene *malP* for the enzyme II was identified, indicating that maltose can also be transported by the phosphotransferase transport system (PTS) [30]. Regarding glucose and xylose, these sugars can be transported by PTS or others transport systems in *Bacillus* species [31–36].

Cellobiose induces xylanase synthesis in some microorganisms [24], but sometimes, this enzyme is associated with cellulases. The crude enzymatic extract produced by *B. circulans* D1 on cellobiose is free of cellulases. This is important data that confirm the enzyme potential for application in biobleaching processes [6].

In the present work, we reported that the cultivation of *B. circulans* D1 in the medium with arabinose lead to basal level of xylanase production, as observed for other *Bacillus* species [37]. However, this carbon source can act as xylanase inducer in some microorganisms [38–40].

Lower xylanase production was also observed when *B. circulans* D1 was cultivated in the medium with glucose. Repression by glucose is common for catabolite extracellular enzymes [14, 41, 42]. However, glucose does not repress xylanase synthesis by some microorganisms [19, 24].

It was not possible to detect variation on cellular growth when *B. circulans* D1 was cultivated in xylose as sole carbon source, at 2.5 g/L. No growth in the medium containing xylose was reported by Lindner et al. [19], when cultivating *B. subtilis* in a medium

containing 1.0 g/L of this substrate as the carbon source. This may be due to the fact that there is no effective uptake system for xylose in some *Bacillus* species. In these cases, small amounts of xylose that are necessary for enzymes induction, such as xylanases, are possibly taken up in an unspecific way [19].

Conclusion

The results showed in this research indicate that *B. circulans* D1 is a promising microorganism regarding to xylanase production, as the amounts of enzyme obtained were similar to or higher than those cited in the scientific literature in works dealing with *Bacillus* species. The enzyme synthesis is not necessarily related to the presence of xylan in the cultivation medium. Maltose was the best inducer of xylanase production, and the microorganism showed versatility in the utilization of other carbon sources.

Acknowledgments Daniela Alonso Bocchini is grateful for the Ph.D. fellowship funded by FAPESP (Fundação de Amparo à Pesquisa do Estado de São Paulo, São Paulo, Brazil). The authors also acknowledge the financial support of FAPESP and CNPq (Conselho Nacional de Desenvolvimento Científico e Tecnológico, Brazil).

References

1. Biely, P. (1985). Microbial xylanolytic systems. *Trends in Biotechnology, 3*, 286–289.
2. Bi, R., Sun, X., & Ren, S. (2000). The study on xylanase fermentation by *Aspergillus niger* sp. *Industrial Microbiology, 30*, 53.
3. Balakrishnan, H., Srinivasan, M. C., Rele, M. V., Chaundhari, K., & Chandwadkar, A. J. (2000). Effect of synthetic zeolites on xylanase production from an alkalophilic *Bacillus* sp. *Current Science, 79*, 95.
4. Maheswari, M. U., & Chandra, T. S. (2000). Production and potential applications of xylanase from a new strain of *Streptomyces cuspidosporus*. W. *Journal of Microbiology and Biotechnology, 16*, 257.
5. Damiano, V. B., Bocchini, D. A., Gomes, E., & Da Silva, R. (2003). Application of crude xylanase from *Bacillus licheniformis* 77–2 to the bleaching of eucalyptus Kraft pulp. W. *Journal of Microbiology and Biotechnology, 19*, 139–144.
6. Bocchini, D. A., Damiano, V. B., Gomes, E., & Da Silva, R. (2003). Effect of *Bacillus circulans* D1 thermostable xylanase on biobleaching of eucalyptus Kraft pulp. *Applied Biochemistry. Biotechnology, 106*(1–3), 393–402.
7. Bedford, M. R., & Classen, H. L. (1992). The influence of dietary xylanase on intestinal viscosity and molecular weight distribution of carbohydrates in rye-fed broiler chick. In J. Visser, G. Beldman, M. A. Kusters-Van Someren, & A. G. J. Voragen (Eds.) *Xylans and xylanases* (pp. 361–370). Amsterdam: Elsevier.
8. Wong, K. K. Y., & Saddler, J. N. (1992). Applications of hemicellulases in the food, feed and pulp industries. In M. P. Coughlan, & G. P. Hazlewood (Eds.) *Hemicelluloses and hemicellulases* (pp. 127–143). London: Portland Press.
9. Gilbert, H. J., & Hazlewood, G. P. (1993). Bacterial cellulases and xylanases. *Journal of General Microbiology, 139*, 187–194.
10. Kyu, K. L., Ratanakhanokchai, K., Uttapap, D., & Tanticharoen, M. (1994). Induction of xylanase in *Bacillus circulans* B_6. *Bioresource Technology, 48*, 163–167.
11. Flores, M. E., Perea, M., Rodríguez, O., Malváez, A., & Huitrón, C. (1996). Physiological studies on induction and catabolite repression of β-xylosidase and endoxylanase in Streptomyces sp. CH-M-1035. *Journal of Biotechnology, 49*, 179–187.
12. Liu, W., Lu, Y., & Ma, G. (1999). Induction and glucose repression of endo-β-xylanase in the yeast *Trichosporon cutaneum* SL409. *Process Biochemistry, 34*, 67–72.
13. Dhillon, A., Gupta, J. K., Jauhari, B. M., & Khanna, S. (2000). A cellulase-poor, thermostable, alkalitolerant xylanase produced by *Bacillus circulans* AB 16 grown on rice straw and its application in biobleaching of eucalyptus pulp. *Bioresource Technology, 73*, 273–277.

14. Balakrishnan, H., Srinivasan, M. C., & Rele, M. V. (1997). Extracellular protease activities in relation to xylanase secretion in an alkalophilic *Bacillus* sp. *Biotechnology Letters, 18*, 599–601.
15. Avalos, O. P., Noyola, T. P., Plaza, I. M., & Torre, M. (1996). Induction of xylanase and β-xylosidase in Cellulomonas flavigena growing on different carbon sources. *Applied Microbiology and Biotechnology, 46*, 405–409.
16. Beg, Q. K., Bhushan, B., Kapoor, M., & Hoondal, G. S. (2000). Production and characterization of thermostable xylanase and pectinase from a *Streptomyces* sp. QG-11-3. *Journal of Industrial Microbiology & Biotechnology, 24*, 396–402.
17. Khanna, S., & Gauri, P. (1993). Regulation, purification and properties of xylanase from *Cellulomonas fimi. Enzyme and Microbial Technology, 15*, 990–995.
18. Khasin, A., Alchanati, I., & Shoham, Y. (1993). Purification and characterization of a thermostable xylanase from *Bacillus stearothermophilus* T-6. *Applied and Environmental Microbiology, 59*, 1725–1730.
19. Lindner, C., Stülke, J., & Hecker, M. (1994). Regulation of xylanolytic enzymes in *Bacillus subtilis. Microbiology, 140*, 753–757.
20. Bocchini, D. A., Alves-Prado, H., Baida, L. C., Roberto, I. C., Gomes, E., & Da Silva, R. (2002). Optimization of xylanase production by *Bacillus circulans* D1 in submerged fermentation using response surface methodology. *Process Biochemistry, 38*, 727–731.
21. Horikoshi, K. (1971). Production of alkaline enzymes by alkalophilic microorganisms. *Agricultural Biology and Chemistry, 35*(11), 1783–1791.
22. Miller, G. L. (1959). Use of dinitrosalicylic acid reagent for determination of reducing sugars. *Analytical Chemistry, 31*, 426–428.
23. Wang, P., Ali, S., Mason, J. C., Sims, P. F. G., & Broda, P. (1992). Xylanases from *Streptomyces cyaneus*. In J. Visser, M. A. Kusters-van Someran, & A. G. J. Voragen (Eds.) *Xylans and xylanases* (p. 225). Amsterdam: Elsevier.
24. Srivastava, R., & Srivastava, A. K. (1993). Characterization of a bacterial xylanase resistant to repression by glucose and xylose. *Biotechnology Letter, 15*(8), 847–852.
25. Zhao, Y., Chany, C. J., II, Sims, P. F. G., & Sinnott, M. L. (1997). Definition of the substrate specificity of the sensing xylanase of *Streptomyces cyaneus* using xylooligosaccharide and celloolidosaccharide glycosides of 3,4-dinitrophenol. *Journal of Biotechnology, 57*, 181.
26. Sá-Pereira, P., Mesquita, A., Duarte, J. C., Barros, M. R. A., & Costa-Ferreira, M. (2002). Rapid production of thermostable cellulase-free xylanase by a strain of *Bacillus subtilis* and its properties. *Enzyme and Microbial Technology, 30*, 924–933.
27. Pham, P. L., Taillandier, P., Delmas, M., & Strehaiano, P. (1998). Production of xylanases by *Bacillus polymyxa* using lignocellulosic wastes. *Industrial Crops and Products, 7*, 195–203.
28. Sigoillot, C., Lomascolo, A., Record, E., Robert, J. L., Asther, M., & Sigoillot, J. C. (2002). Lignocellulolytic and hemicellulolytic system of *Pycnoporus cinnabarinus*: isolation and characterization of a cellobiose dehydrogenase and a new xylanase. *Enzyme and Microbial Technology, 31*, 876–883.
29. Tangney, M., Buchanan, C. J., Priest, F. G., & Mitchell, W. J. (1992). Maltose uptake and its regulation in *Bacillus subtilis. FEMS Microbiology Letters, 97*, 191–196.
30. Reizer, J., Bacehm, S., Reizer, A., Arnauld, M., Saier, M. H., Jr, & Stülke, J. (1999). Novel phosphotransferase system genes revealed by genomic analysis: the complet complement of PTS proteins encoded within the genome of *Bacillus subtilis. Microbiology, 145*, 3419–3429.
31. Gonzy-Tréboul, G., de Waard, J. H., Zagorec, M., & Postma, P. W. (1991). The glucose permease of the phosphotransferase system of *Bacillus subtilis*: evidence for II^{Glc} and III^{Glc} domains. *Molecular Microbiology, 5*, 1241–1249.
32. Fiegler, H., Bassias, J., Jankovic, I., & Brückner, R. (1999). Identification of a gene in Staphylococcus xylosus encoding a novel glucose uptake protein. *Journal of Bacteriology, 181*, 4929–4936.
33. Scarlatos, P., & Dahl, M. K. (1998). The glucose kinase of *Bacillus subtilis. Journal of Bacteriology, 180*, 3222–3226.
34. Tangney, M., Priest, F. G., & Mitchell, W. J. (1993). Two glucose transport systems in bacillus licheniformis. *Journal of Bacteriology, 175*, 2137–2142.
35. Schmiedel, D., Kintrup, M., Küster, E., & Hillen, W. (1997). Regulation of expression, genetic organization and substrate specificity of xylose uptake in *Bacillus megaterium. Molecular Microbiology, 23*, 1053–1062.
36. Krispin, O., & Allmansberger, R. (1998). The *Bacillus subtilis* AraE protein displays a broad substrate specificity for several substrates. *Journal of Bacteriology, 180*, 3250–3252.
37. Piñaga, F., Peña, J. L., & Vallés, S. (1993). Xylanase production by *Bacillus polymyxa. Journal of Chemical Technology and Biotechnology, 57*, 327–333.

38. Bataillon, M., Nunes Cardinali, A. P., & Duchiron, F. (1998). Production of xylanases from a newly isolated alkalophilic thermophilic *Bacillus* sp. *Biotechnology Letters*, *20*(11), 1067–1071.
39. Leathers, T. D., Detroy, R. W., & Bothast, R. J. (1986). Induction and glucose repression of xylanase from a color variant strain of *Aureobasidium pullulans*. *Biotechnology Letters*, *8*, 867–872.
40. Dobberstein, J., & Emeis, C. C. (1989). β-Xylanase produced by *Aureobasidium pullulans* CBS 584475. *Applied Microbiology and Biotechnology*, *32*, 262–268.
41. Toda, K. (1981). Induction and repression of enzymes in microbial culture. *Journal of Chemical Technology and Biotechnology*, *31*, 775–790.
42. Biely, P. (1982). Catabolite repression of β-xylanase synthesis in the yeast *Cryptococcus albidus*. *Biologia*, *37*, 799–807.

Appl Biochem Biotechnol (2008) 146:39–47
DOI 10.1007/s12010-007-8065-3

Immobilization of Fungal β-Glucosidase on Silica Gel and Kaolin Carriers

Hakob K. Karagulyan · Vardan K. Gasparyan · Stephen R. Decker

Received: 20 May 2007 / Accepted: 26 September 2007 /
Published online: 31 October 2007
© Humana Press Inc. 2007

Abstract β-Glucosidase is a key enzyme in the hydrolysis of cellulose for producing feedstock glucose for various industrial processes. Reuse of enzyme through immobilization can significantly improve the economic characteristics of the process. Immobilization of the fungal β-glucosidase by covalent binding and physical adsorption on silica gel and kaolin was conducted for consequent application of these procedures in large-scale industrial processes. Different immobilization parameters (incubation time, ionic strength, pH, enzyme/support ratio, glutaric aldehyde concentration, etc.) were evaluated for their effect on the thermal stability of the immobilized enzyme. It was shown that the immobilized enzyme activity is stable at 50 °C over 8 days. It has also been shown that in the case of immobilization on kaolin, approximately 95% of the initial enzyme was immobilized onto support, and loss of activity was not observed. However, covalent binding of the enzyme to silica gel brings significant loss of enzyme activity, and only 35% of activity was preserved. In the case of physical adsorption on kaolin, gradual desorption of enzyme takes place. To prevent this process, we have carried out chemical modification of the protein. As a result, after repeated washings, enzyme desorption from kaolin has been reduced from 75 to 20–25% loss.

Keywords β-glucosidase · Immobilization · Silica gel · Kaolin · Thermostability · Corn stover · Enzymatic hydrolysis

Introduction

β-Glucosidase is a key enzyme in the process of enzymatic hydrolysis of cellulose to glucose, functioning primarily to hydrolyze cellobiose to two glucoses [1]. β-Glucosidase

H. K. Karagulyan (✉) · V. K. Gasparyan
Institute of Biotechnology, 14 Gyurjyan str., Yerevan, Armenia
e-mail: hackarag@yahoo.com

S. R. Decker
Chemical and Biosciences Center, National Renewable Energy Laboratory, 1617 Cole Blvd, Golden, CO 80401, USA

can also demonstrate activity on cello-oligomers, and although the activity varies, it generally decreases with increasing chain length. The cellulase complex from the main fungal producers normally contains small amounts of β-glucosidase, which may limit the overall cellulose hydrolysis rate, as cellobiose inhibits activity of other enzymes of cellulose complex [2]. β-Glucosidase is also subject to end-product inhibition, with removal of glucose significantly enhancing the enzyme activity rate.

The cost of enzyme preparations has been decreasing in recent years; however, it continues to affect considerably the price of ethanol obtained from cellulosic raw materials. Increased enzymatic hydrolysis efficiency is one way to reduce the enzyme cost in bioethanol production. Another method is enzyme recycle and reuse. Immobilization of biocatalysts allows for their economic reuse and development of continuous bioprocess. Although immobilization poses problems of substrate accessibility and binding for most endo- and exocellulases, β-glucosidase exhibits characteristics amenable to immobilization, such as activity on soluble substrates and the lack of a carbohydrate-binding module. Among the possible approaches, immobilization of β-glucosidase is one prospective solution to the problem.

The variety of protein immobilization methods can be reduced to two main approaches: physical adsorption and covalent binding with the carrier. Both approaches have their advantages and shortcomings [3–6]. The advantage of adsorption is simplicity, as usually no cross-linking reagents or activation steps are required. As a result, adsorption is cheap, easily carried out, and tends to be less destructive to the enzyme than chemical means of the attachments. The shortcoming of physical binding is non-stability of the bonds between enzyme and carrier. In covalent binding, the bonds between carrier and protein are very firm, resulting in a highly stable conjugate, but very often the enzyme activity drops significantly.

We have examined several carrier matrices for their ability to immobilize β-glucosidase, including activated charcoal, nylon, chitosan, bentonite, kaolin, silica gel, and titanium dioxide. The results indicated that immobilization by covalent binding on silica gel and by physical adsorption on kaolin were the most prospective methods for improvement of the economic parameters of enzymatic hydrolysis of cellulose. Here, we report on these two supports.

Materials and Methods

Enzyme Assays and Stability Determination

Determination of glucose was carried out by glucose oxidase/peroxidase method [7]. The activity of β-glucosidase was determined as follows: the enzyme preparation was diluted 10- to 50-fold depending on the initial activity. Substrate used was a 1% (*v*/*w*) solution of cellobiose (Sigma) in 0.05 M sodium acetate buffer pH 5.0. Fifty microliters of enzyme solution were added to 5 ml of substrate incubated at 45 °C. After 30 min, test tubes were placed into a boiling water bath for 10 min. Concentration of glucose formed in the process of reaction was determined by the method mentioned above. Activity units of β-glucosidase were expressed as μMol of glucose/min ml^{-1} of enzyme preparation.

The thermal stability of free and immobilized enzyme preparations was determined by incubation at 70 °C, pH 5.0 (0.05 M sodium acetate buffer). Every 10 min, aliquots were taken, and β-glucosidase activity was determined.

Enzyme Immobilization

To remove low molecular weight compounds that interfere with enzyme activity, 20 ml of Novozym 188 was dialyzed against 1.5 l of 0.15 M solution of sodium acetate buffer (pH 5.5) for 2 days. After 24 h, the solution was replaced by fresh buffer. To examine the effect of hydrophobicity of the β-glucosidase on non-covalent immobilization, a subset of β-glucosidase was acetylated. Protein acetylation was carried out by acetic anhydride by a modified method according to Ansari [8]. Four milliliters of acetic anhydride was added to 65 ml of the final solution of the enzyme for acetylation of free amino groups of lysine and arginine. The mixture was incubated at 25 °C for 2 h. After acetylation, the obtained preparation was dialyzed against 1 l of 3 M solution of sodium acetate for deacetylation of other amino acids. Dialysis medium was replaced twice during 2 days.

Silanization of silica gel was carried out according to Walters [9]. Silica gel 40/100 was silanized by (γ-aminopropiltriethoxysilane). Procedure involved 5 h boiling of 10% silica gel suspension with 10% silane solution. The silica gel was then washed exhaustively by decantation to remove excess of silane. The silanized silica gel was activated by glutaric aldehyde at 37 °C for 24 h with periodic mixing. As increased concentrations of glutaric aldehyde bring to decreased activity of immobilized enzyme, we have used glutaric aldehyde in final concentration 1.5%. Exhaustive decantation of supernatant was conducted to remove excess of glutaric aldehyde. Finally, silica gel was suspended in 0.01 M phosphate buffer pH 6.8, containing 0.05 M NaCl. Conjugation of the β-glucosidase to activated silica gel was conducted. Conjugation was conducted at 37 °C during 24 h with periodic mixing in 0.01 M phosphate buffer pH 6.8 NaCl 0.05 M. The amount of enzyme was varied from 3.46 to 17.3 mg/ml of silica gel suspension.

Kaolin granules were prepared from dry powdered kaolin after hydration to 45–48% moisture. The obtained paste was rubbed through a metal sieve with a mesh diameter 0.6 mm to make granules with the maximal length of 1 mm and baked at 550 °C for 2 h. The kaolin granules were washed in aliquots of 1 g in 50 ml distilled H_2O by centrifugation. After washing several times, dialyzed Novozym 188 was added to 1 ml of the kaolin suspension in a final buffer concentration of 50 mM sodium acetate. The amount of enzyme was varied from 3.46 to 17.3 mg/ml of kaolin suspension. After incubation during 2 h at 40 °C with mixing, the suspension was centrifuged for removal of non-bound protein,and activity of the absorbed protein was determined by standard glucose oxidase/peroxidase method.

Determination of Immobilization Parameters

Retained Enzyme After binding of enzyme to carrier, the mix was washed by centrifugation to remove unbound protein. The amount of enzyme bound to each carrier was determined by difference after determination of residual protein content from the supernatants after washing the carrier/enzyme conjugate.

K_m Measurement Approximate K_m values were determined using a range of cellobiose concentrations in 50 mM acetate buffer, pH 5.0. Enzyme was added to the pre-equilibrated substrate, and buffer and glucose were determined after reaction by the method above. As reproducible aliquots were difficult to obtain for immobilized enzyme samples, the samples were dried to determine dry weight, and the amount of enzyme present in the reaction was calculated based on the retained enzyme value for each carrier and normalized to 10 mg of enzyme.

Thermal Stability The thermal stability of the β-glucosidase was determined by measuring activity over time after incubation at 70 °C. Samples were taken at 10 min intervals, cooled on ice, and activity determined on cellobiose as above. The thermal stability of β-glucosidase from Novozym188 was determined for free native enzyme, bound native enzyme, free acetylated enzyme, and bound acetylated enzyme.

Desorption The procedure of evaluation of enzyme desorption from the carrier was as follows: after incubating the enzyme with the carrier in corresponding conditions, the suspension was centrifuged. The precipitate was then washed by buffer solution and centrifuged once more. This procedure was repeated three times by tenfold quantity of the buffer. Then, we joined all the portions of supernatants; after which, we measured the activity of the immobilized enzyme and the activity of the supernatant. We have also measured preliminarily the activity of the enzyme solution that was used for immobilization. Based on the correlation between activities, we calculated the level of desorption of the enzyme from the carrier.

Fluidized Bed Reactor To determine the amenability of immobilized enzyme to process conditions, a fluidized bed reactor was used to measure continuous glucose production from cellobiose. We used granulated kaolin with immobilized acetylated β-glucosidase in the fluidized bed reactor. A thermostatically controlled column with a diameter of 1.6 cm and a height of 18 cm was used as the reactor. After filling, the part of the column filled with kaolin granules made 30 ml. The column was preliminary washed by the buffer during 24 h to wash out the non-absorbed enzyme and fine part of the carrier, after which, we measured the activity of β-glucosidase in the effluent solution. We assessed the level of conversion of the substrate into glucose by running 100 g/l cellobiose solution through the column in 50 mM sodium acetate buffer solution. The correlation between the level of conversion of the substrate and the velocity of running of the solution through the column was defined by varying the flow rate through the column.

Digestion of Pretreated Corn Stover

Pretreated corn stover was graciously provided by the National Renewable Energy Laboratory (Golden, Colorado). The stover was pretreated at 190 °C at 30% solids with 0.048 g H_2SO_4/g dry biomass. The reactor residence time was approximately 1 min. After pretreatment, the composition of the corn stover was 59.9% glucan, 4.74% xylan, 0.69% arabinan, 0.2% mannan, 0.47% galactan, 25.53% lignin, 2.44% protein, and 3.4% ash. Digestions were carried out using a commercial cellulase (Spezyme CP, Genencor, Intl.) augmented with β-glucosidase (Novozym 188, Novozymes Inc., Davis, CA., 250 CBU/g) immobilized on kaolin as above. Protein was determined by Biuret method according to Gornall et al. [10] or dye binding method according to Bradford [11].

Enzymatic hydrolysis of pretreated corn stover was conducted at 10% solid concentration in 50 mM sodium acetate buffer (pH 5.0) in Erlenmeyer flasks. Into each flask was added 50 ml of 10% PCS suspension, and 0.5 ml of the enzyme solution was diluted to the level that provides necessary enzyme activity.

Spezyme CP was loaded at 5 FPU/g cellulose for cellulase-only digestions and 2.5 FPU/g cellulose when assayed with β-glucosidase present. β-glucosidase was added at 15 CBU/g cellulose. Flasks were preincubated at 45 °C on the rotary shaker at 150 rpm for 10 min, and

the enzymes were added to start the hydrolysis. Aliquots of 2 ml were taken at different time points, immediately chilled on ice, and centrifuged at 5,000×*g* for 10 min. Glucose analyses were performed on the resultant supernatants.

To obtain statistically valid data, all the experiments have been carried out four times for each series, and within each series, the experiments were replicated five times for each investigated parameter. The results of replications were averaged. The deviations between the results of replications did not generally exceed 6%.

Results and Discussion

Choice of Immobilization Method

We have studied various carriers that are applicable for immobilization of β-glucosidase (activated charcoal, chitosan, nylon, bentonite, kaolin, silica gel, etc.) and determined several parameters essential for practical application of the immobilized enzyme. Initial work using almond β-glucosidase evaluated the binding parameters for the various carriers tested. Taking into account the main parameters, we have found that covalent binding with silica gel and physical adsorption on kaolin granules are the most efficient methods of immobilization. Table 1 presents the data of immobilization of β-glucosidase on the indicated carriers.

As Table 1 demonstrates, silica gel is superior to kaolin in some parameters (K_m, thermostability, desorption); however, the relative costs of the two carriers and superiority of kaolin in enzyme binding capacity and retention suggest that kaolin is much more economically favored for large-scale processes compared to silica gel. The primary drawback to kaolin is its propensity to lose enzyme by desorption over long exposure times. Taking into account the fact that desorption of the enzyme from the carrier in the process of fermentation may become a determinative factor, we made an attempt to improve this parameter by changing the hydrophobicity of the enzyme preparation. We carried out acetylation of the enzyme preparation and compared the native and acetylated preparations with respect to several parameters. Table 2 demonstrates data on the level of binding of the enzyme with the carrier. Acetylation of β-glucosidase, which is aimed at increasing the hydrophobicity of protein molecule surface, increases the level of binding of the enzyme with the carrier.

The results indicate that acetylation of the enzyme considerably improves immobilization stability of the process. Acetylation of the enzyme reduces enzyme desorption resulting

Table 1 Comparison of immobilization methods.

Enzyme immobilization parameter	Kaolin	Silica gel
K_m, (mM cellobiose)	1.8	10
Enzyme/support ratio, mg/g	140	55
Retained, %	95	35
Thermostability, min[a]	11	21
Desorption, %[b]	22	0

[a] Enzyme half-life at t=70 °C

[b] Desorbed activity was determined after washing of column by 200× volume of buffer solution.

Table 2 Adsorption of native and acetylated preparation of β-glucosidase on kaolin.

Conjugates	Activity (initial)	Activity (100× wash)	Activity (300× wash)	Activity (500× wash)
Kaolin/native enzyme	0.63	0.56	0.46	0.44
Kaolin/acetylated enzyme	0.69	0.64	0.62	0.61

from washing by greater than fourfold compared to native protein. As the activity of the acetylated enzyme is equivalent to native (or slightly better), this represents an important step in enabling the reuse and recycle of β-glucosidase in biomass processing. The kaolin immobilized acetylated β-glucosidase was also evaluated in a fluidized bed reactor for continuous production of glucose from cellobiose. The powdered kaolin was unusable for this purpose, as it either diluted out of the column (upflow) or packed tightly to very high back pressure (downflow); the granulated kaolin was used. The two kaolin forms showed equivalent capacities and activities of bound enzyme, although the granulated form exhibited a slightly higher binding capacity. After washing the column for 24 h, β-glucosidase activity was determined for the effluent. We did not observe any appreciable enzyme desorption from the column. During velocity experiments with cellobiose solutions, the column performed at a stable rate until the velocity 40 ml/h, at which point, the residence time of the cellobiose apparently exceeded the reaction rate and glucose production decreased (Fig. 1).

Comparative Analysis of Thermostability of Native and Acetylated Enzyme

Another essential factor is the change of thermostability of the enzyme as a consequence of chemical modification and immobilization. We have determined the thermostability of free and immobilized forms of native and acetylated β-glucosidase. The results of these measurements are presented in Figs. 2 and 3.

As the results presented in Figs. 2 and 3 indicate, thermostability of free, native β-glucosidase is quite high, and after the immobilization on kaolin, it decreases slightly. Acetylation of the enzyme causes substantial decrease of thermostability. Thus, if the native enzyme preserves approximately 45% of its initial activity at 70 °C during 10 min, the acetylated enzyme at the same conditions preserves only 18% of its initial activity. Although acetylation of β-glucosidase decreased the thermostability of the enzyme

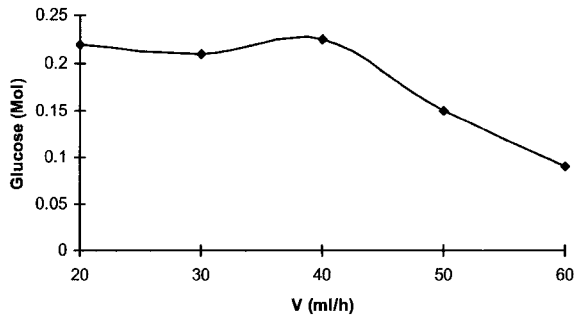


Fig. 1 Glucose production in a fluidized bed reactor by immobilized β-glucosidase

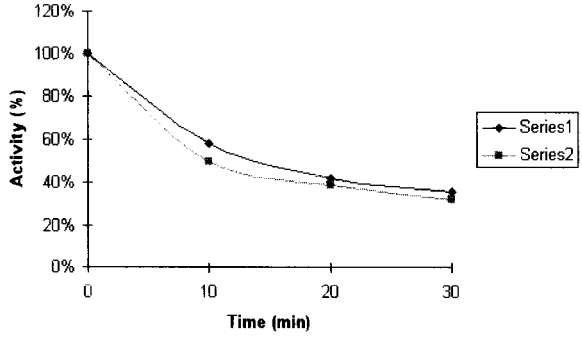


Fig. 2 Thermostability of β-glucosidase from Novozym 188 preparation in free and immobilized forms. *1* Free enzyme, *2* immobilized enzyme, *t* 70 °C, pH 5.0

compared to the native enzyme, immobilization restored much of the thermostability to near-native levels.

Chemical modification of the enzyme and its immobilization may cause either increase or decrease of thermostability [12–14] depending on the enzyme, nature of the carrier, and the method of immobilization. As the data from Nagamoto et al. [15] indicates, thermostability of β-glucosidase immobilized on chitosan increases, and the enzyme works successfully at 70 °C during 12 h. Such considerable increase of thermostability that we observed is due to the covalent binding of the enzyme and the carrier.

Taking into account the fact that acetylated enzyme adsorbs on the carrier more firmly, acetylation can be regarded as a possible way to improve the immobilization characteristics of β-glucosidase.

Enzymatic Hydrolysis of Pretreated Corn Stover

To evaluate the practical application of immobilized β-glucosidase for hydrolysis of pretreated corn stover, we have carried out enzymatic hydrolysis in flasks with the use of cellulase and immobilized β-glucosidase. Taking into account the fact that Spezyme CP contains a certain quantity of β-glucosidase, we used reduced quantities of Spezyme CP in our experiments—5 U/g of glucan instead of normally used 15–40 U/1 g of glucan. This allowed us to better evaluate the effect of immobilized β-glucosidase in the process of hydrolysis of corn stover. The obtained results are presented in Fig. 4.

As Fig. 4 shows, the addition of immobilized β-glucosidase to the preparation Spezyme accelerates substantially the production of glucose and increases the level of hydrolysis. Taking into account the contents of glucan in PCS and basing on the obtained results, we

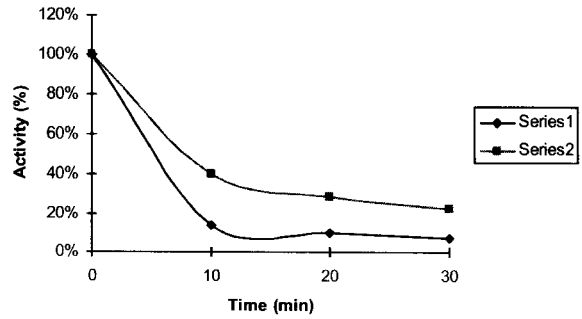


Fig. 3 Thermostability of acetylated β-glucosidase from Novozym 188 preparation in free and immobilized forms. *1* Free enzyme, 2 immobilized enzyme, *t* 70 °C, pH 5.0

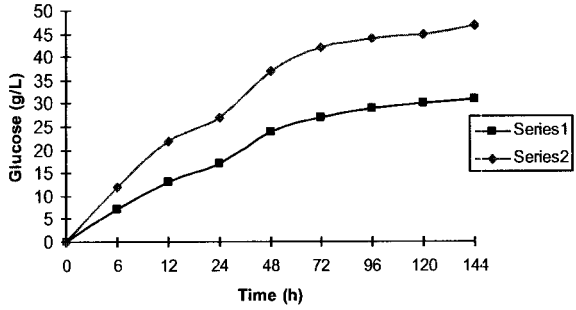


Fig. 4 Glucose formation from washed pretreated corn stover (PCS) by kaolin-immobilized beta-glucosidase (Novozym188) and cellulase. Pretreated corn stover 10% (*w*/*v*) solids, *t* 5 °C, pH 5.0. Series (1) 5 FPU cellulose/g glucan. Series (2) 5 FPU cellulase per g glucan+15 CBU β

can see that when using Spezyme, the level of conversion of glucan into glucose reaches about 50% after 144 h, while the addition of immobilized β-glucosidase enhances the conversion to 79%. For comparison, we can present the data [16, 17] where the authors studied possibility of application of immobilized β-glucosidase for the winemaking industry. The stability of β-glucosidase immobilized on chitosan pellets and Duolite A-568 resin was studied. In the case of chitosan, authors point out considerable stability of the enzyme (half-life 1.2 years). According to our data at 50°C, the activity of β-glucosidase immobilized on kaolin does not change notably for 300 h (observed time). Consequently, in the process of simultaneous saccharification and fermentation, i.e., at the temperature 35 °C, the immobilized enzyme is reusable at least five to six times during 1/5–2 months. Although our indices for time span of the enzyme usability are lower than those from the literature, it should be taken into notice that in the mentioned work, the immobilization carried out by covalent binding. If we take into account all the factors that determine the costs of enzymatic hydrolysis, we will see that our approach has certain advantages.

During enzyme hydrolysis of biomass, Spezyme CP supplemented with immobilized β-glucosidase gave satisfactory results of saccharification of pretreated corn stover, increasing the digestion rate and extent while enabling the reduction of cellulase loading. Thus, immobilization of β-glucosidase on kaolin can be regarded as a prospective method for multiple use of the enzyme at ethanol production from cellulose-containing raw materials.

Conclusion

Studies of immobilization on different carriers indicate that immobilization on silica gel or kaolin is the most prospective for application in the future, although the potential economic benefits appear much more favorable for kaolin. Comparison of immobilization characteristics of β-glucosidase immobilized on silica gel and on kaolin has shown that the kaolin method has more advantages, as it is considerably cheaper and more efficient. The feasibility of preliminary acetylation of the enzyme preparation requires further investigation. We have to take into consideration additional expenses necessary for acetylation and the issue of the decrease of the enzyme activity after acetylation.

These preliminary studies indicate a good potential for the use of immobilized β-glucosidase in the enzymatic conversion of biomass to sugars. Significant work, however, needs to be continued to evaluate efficacies under more process-relevant conditions.

References

1. Reese, E. T. (1975). Cellulose as a Chemical and Energy Resource, Symposium No.5 of Biotechnology and Bioengineering, 77–80.
2. Gallifuoco, A., & Ercole, L. D. (1998). *Process Biochemistry, 33*, 163–168.
3. Gomez, J. M., Romero, M. D., & Fernandes, T. M. (2005). *Catalysis Letters, 101*, 275–278.
4. Ortega, N., & Busto, M. D. (1998). *Bioresource Technology, 64*, 105–111.
5. Calsavara, L. P., De Moraes, F. F., & Zanin, G. M. (2001). *Applied Biochemistry and Biotechnology, 91–93*, 615–626.
6. Roy, K. S., Raha, S. K., Dey, S. K., & Chakrabarty, S. L. (1989). *Enzyme and Microbial Technology, 11/7*, 431–435.
7. Morin, L. G., & Prox, J. (1973). *Clinical Chemistry, 19*, 959–962.
8. Ansari, A. A. (1975). *Journal of Biological Sciences, 250*, 1625–1632.
9. Walters, R. R. (1988). In P. D. G. Dean, W. S. Jonson, & F. A. Middle (Eds.), *Affinity Chromatography* (pp. 42–44). Oxford-Washington D. C.: IRL Press.
10. Gornall, A. C., Bardawill, C. J., & David, M. M. (1949). *Journal of Biological Chemistry, 177*(3), 751–766.
11. Bradford, M. M. (1976). *Analytical Biochemistry, 72*, 248–254.
12. Tyagi, R., Roy, I., Agarwal, R., & Gupta, M. N. (1998). *Biotechnology and Applied Biochemistry, 28*, 201–206.
13. Siddiqui, K. S., Sagib, A. A., Rashid, M. N., & Rajoka, M. I. (2000). *Enzyme and Microbial Technology, 27*(7), 467–474.
14. Ichicawa, S., Takano, K., Kuroiva, T., Hiruta, O., Sato, S., & Mukataka, S. (2002). *Journal of Bioscience and Bioengineering, 92*(2), 201–206.
15. Nagamoto, H., Matsushita, Y., Sugamoto, K., & Matsui, T. (2005). *Bioscience, Biotechnology and Biochemistry, 69*(1), 128–136.
16. Gallifuoco, A., Alfani, F., Cantarella, M., Spagna, G., & Pifferi, P. G. (1999). *Process Biochemistry, 35* (1–2), 179–185.
17. Gueguen, Y., Chemardin, P., Pien, S., Arnaud, A., & Galzy, P. (1997). *Journal of Biotechnology, 55*(3–4), 151–156.

Appl Biochem Biotechnol (2008) 146:49–56
DOI 10.1007/s12010-007-8073-3

Immobilization of *Yarrowia lipolytica* Lipase—a Comparison of Stability of Physical Adsorption and Covalent Attachment Techniques

Aline G. Cunha · Gloria Fernández-Lorente · Juliana V. Bevilaqua · Jacqueline Destain · Lúcia M. C. Paiva · Denise M. G. Freire · Roberto Fernández-Lafuente · Jose M. Guisán

Received: 21 May 2007 / Accepted: 27 September 2007 /
Published online: 9 November 2007
© Humana Press Inc. 2007

Abstract Lipase immobilization offers unique advantages in terms of better process control, enhanced stability, predictable decay rates and improved economics. This work evaluated the immobilization of a highly active *Yarrowia lipolytica* lipase (YLL) by physical adsorption and covalent attachment. The enzyme was adsorbed on octyl–agarose and octadecyl–sepabeads supports by hydrophobic adsorption at low ionic strength and on MANAE–agarose support by ionic adsorption. CNBr–agarose was used as support for the covalent attachment immobilization. Immobilization yields of 71, 90 and 97% were obtained when *Y. lipolytica* lipase was immobilized into octyl–agarose, octadecyl–sepabeads and MANAE–agarose, respectively. However, the activity retention was lower (34% for octyl–agarose, 50% for octadecyl–sepabeads and 61% for MANAE–agarose), indicating that the immobilized lipase lost activity during immobilization procedures. Furthermore, immobilization by covalent attachment led to complete enzyme inactivation. Thermal deactivation was studied at a temperature range from 25 to 45°C and pH varying from 5.0 to 9.0 and revealed that the hydrophobic adsorption on octadecyl–sepabeads produced an appreciable stabilization of the biocatalyst. The octadecyl–sepabeads biocatalyst was almost tenfold more stable than free lipase, and its thermal deactivation profile was also modified. On the other hand, the

A. G. Cunha · L. M. C. Paiva · D. M. G. Freire (✉)
Instituto de Química, Universidade Federal do Rio de Janeiro, Centro de Tecnologia (CT), Lab. 549–2 and 536-B, Cidade Universitária, Ilha do Fundão, CEP 21945-970 Rio de Janeiro, Brazil
e-mail: freire@iq.ufrj.br

G. Fernández-Lorente · R. Fernández-Lafuente · J. M. Guisán
Department of Biocatalysis, Institute of Catalysis, CSIC, Campus UAM, Cantoblanco, 28049 Madrid, Spain

J. V. Bevilaqua
Centro de Pesquisa e Desenvolvimento Leopoldo Américo Miguez de Mello (CENPES), Petrobras, Brazil

J. Destain
Centre Wallon de Biologie Industrielle, Faculté universitaire des Sciences agronomiques, Gembloux, Belgium

Y. lipolytica lipase immobilized on octyl–agarose and MANAE–agarose supports presented low stability, even less than the free enzyme.

Keywords Immobilized lipase · *Y. lipolytica* · Biocatalysis · Glutaraldehyde · Hydrophobic supports

Introduction

Microbial lipases (acylglycerol acylhydrolase, EC 3.1.1.3) have been employed in a broad range of applications such as treatment of wastewater with high oil and grease content [1], synthesis of low chain fatty esters as component for cosmetics and surfactants and in production of pharmaceuticals intermediates [2, 3]. Over the past few years, attractive processes have appeared using enzymes as biocatalysts for the synthesis of fine chemicals [4]. Furthermore, biocatalysis has been considered as the most efficient way of producing chiral drugs. However, one of the most important drawbacks of the use of lipases for asymmetric synthesis is the poor water solubility of the majority of organic compounds, while most enzymes present very low stability and activity in organic media. One of the best enzymatic approaches to carry out the production of enantioenriched or enantiopure compounds is based on the application of lipases in organic medium [2, 3, 5]. In this way, microbial lipases are effective biocatalysts due to high-substrate specific activity, good stability in organic solvents, stereoselectivity and also produce low impact on the environment. In fact, the use of lipases in organic solvents has already proved to be an excellent methodology for the preparation of chiral drugs [2, 6].

Reports on immobilization of enzymes first appeared in the 1960s [7]. Since then, immobilized enzymes have been widely used in the processing of a variety of products and in the synthesis of chiral products [6, 8]. The advantages of immobilized over soluble enzymes arise from their enhanced stability and ease of separation from the reaction media, leading to significant savings in enzyme consumption [3]. Lipase immobilization offers important and unique advantages in terms of better process control when the reactions are processed in nonaqueous media. Furthermore, immobilized preparations are frequently more stable than free enzyme and can be easily recycled, which is of crucial importance in industrial processes. Enzyme immobilization can also avoid deleterious effects caused by organic solvents such as enzyme denaturation and agglomeration [1, 9]. The improvement on enzyme stability by immobilization cannot be easily predicted as it is dependent on several factors and even the explanation for the observed stabilization may be diverse [10–14].

Immobilization methods range from binding to prefabricated carrier materials to packaging in enzyme crystals or powders. Adsorption is the most usual methodology for lipase immobilization because it presents minor deleterious effects on the enzyme activity, and it is a low-cost method [3]. Polymeric resins and materials containing hydrophobic groups are often described as good supports for lipase immobilization. Hydrophobic adsorption on porous supports in which the inner shell is covered with thick layer of hydrophobic compounds causes the interfacial activation phenomenon. It has been stressed in the literature that most lipases present a 'lid' controlling the access to the active site [15, 16]. Thus, in the hydrophobic adsorption, the enzyme recognizes those supports as a lipid/water interface. As a consequence, it leads to conformation changes exposing the catalytic residues toward the solvent making the binding site accessible to the substrate. The hyperactivation phenomenon is usually observed as a consequence of this method of immobilization which provides stabilization of the active open form of the enzyme [17, 18].

In this context, the present work evaluates the behavior of a highly active *Yarrowia lipolytica* lipase immobilized by two different techniques such as adsorption on hydrophobic (octyl–agarose, octadecyl–sepabeads) and hydrophilic supports (MANAE–agarose) with covalent attachment using cyanogens–bromide–agarose (CNBr–agarose) and cross-linking of YLL immobilized on MANAE–agarose with glutaraldehyde.

Materials and Methods

Materials

Lipase from *Y. lipolytica* was obtained from Centre Wallon de Biologie Industrielle, Faculté Universitaire des Sciences Agronomiques, Gembloux, Belgium. Octyl–agarose, CNBr–agarose and agarose 4BCL were obtained from Hispanagar S.A. (Burgos, Spain). Octadecyl–sepabeads was donated by Resindion S.R.L. Mitsubishi Chemical Co. (Milan, Italy). *p*-Nitrophenyl-butyrate (*p*NPB), Triton X-100 and Cetyl-trimetyl-ammonium bromide (CTAB) were obtained from Sigma Chemical Co. (St. Louis, USA). All other chemicals were of analytical or chromatographic grade.

Methods

Protein Determination

The amount of protein in all samples was determined as described by Lowry et al. [19] using bovine serum albumin as standard.

Yarrowia lipolytica Lipase

Lipase from *Yarrowia lipolytica* was produced in a 2,000-l fermentor containing (*w/v*) 1% of glucose, 3% of whey powder, 0.8% of ammonium sulphate, 1% of corn steep syrup and 0.5% of olive oil. After 30 h of fermentation, the culture broth was centrifuged, and the supernatant was dried by lyophilization [20]. The lyophilized powder was than diluted in sodium phosphate buffer 5 mM, pH 7.0 in a final protein concentration of 0.11 mg/ml.

Enzyme Activity

Yarrowia lipolytica lipase (YLL) activity was performed by continuously measuring the increase in the absorbance in 348 nm produced by the release of *p*-nitro-phenol in the hydrolysis 0.4 mM *p*-nitrophenyl-butyrate (*p*NPB) in 25 mM sodium phosphate buffer pH 7 and 28°C. The reaction was initialized by addition of 0.2 ml of lipase suspension to 2.5 ml of substrate solution. One international unit (IU) of *p*NPB was defined as the amount of immobilized YLL necessary to hydrolyze 1 μmol of *p*NPB per minute in assay conditions [21].

Immobilization of Yarrowia lipolytica Lipase

Immobilization on Hydrophobic Supports Standard preparations of octyl–agarose or octadecyl–sepabeads (hydrophobic supports) consisted first in exhaustively washing the supports with distilled water. After that, 1 g of the support was suspended in 10 ml of YLL solution in sodium phosphate buffer 5 mM pH 7, and the mixture was shaken at 25°C and

250 rpm for 2 h, washed with distilled water and stored at 4°C. Periodically, samples of the suspensions and the supernatants were withdrawn, and hydrolytic activity was measured using *p*NPB as substrate as described earlier.

Immobilization on Hydrophilic Supports

By ionic adsorption Amino-glyoxyl–agarose (MANAE–agarose), used as hydrophilic support, was prepared as described by Fernandez-Lafuente et al. [22]. Standard immobilization procedure consisted of the addition of 1 g of the support to 10 ml of enzymatic solution containing Triton X-100 0.1% in phosphate buffer 5 mM pH 7. The mixture was shaken at 25°C and 250 rpm for 2 h, washed with distilled water and stored at 4°C. Periodically, samples of the suspensions and the supernatants were withdrawn and enzymatic activity was measured using *p*NPB as substrate as described above.

By Covalent Attachment

With CNBr–Agarose One gram of CNBr–agarose support was added to 10 ml of YLL solution containing 0.1% (*v*/*v*) Triton X-100. The suspension was stirred (250 rpm) at 4°C for 20 min. After that, it was firstly washed with bicarbonate buffer 0.1 M pH 8.3 and then the suspension was gently stirred for 2 h with 0.1 M Tris–HCl pH 8, filtered and stored at 4°C. Immobilization process was followed by measuring the hydrolytic activity using *p*NPB as substrate.

MANAE–Agarose Cross-linked with glutaraldehyde One gram of the YLL immobilized onto MANAE–agarose was incubated with 1% (*v*/*v*) glutaraldehyde solution in sodium phosphate buffer 5 mM pH 7 and 25°C for 1 h, under mild stirring. After that, the suspension was washed with 5 mM phosphate buffer and then filtered and stored at 4°C. The samples of the suspensions were withdrawn, and YLL activity was measured using *p*NPB as substrate as described above.

Parameters of Immobilization

The yield of the immobilization (η) and the activity retention (R) were calculated according Eqs. 1 and 2.

$$\eta(\%) = \frac{U_A - U_E}{U_A} \times 100 \tag{1}$$

$$R(\%) = \frac{U_H}{U_A - U_E} \times 100 \tag{2}$$

where:

U_A added units or units of activity offered for immobilization
U_E output units or units of activity in the solution after immobilized procedure
U_H immobilized units or units of immobilized enzyme.

Kinetic Parameters of Thermal Inactivation

The thermal inactivation assays of soluble YLL and immobilized preparations on octyl–agarose, octadecyl–sepabeads and MANAE–agarose were carried out incubating the same amount of lipase in three different buffers at 45°C: 25 mM sodium acetate pH 5, 25 mM sodium phosphate pH 7 and 25 mM sodium carbonate pH 9. Periodically, residual enzyme activity was estimated by hydrolysis of *p*NPB. Soluble enzyme was submitted to the same conditions.

The half-life ($t_{1/2}$) time was calculated according to Eqs. 3 and 4:

$$E = E_0 \exp(-kt) \tag{3}$$

$$t_{1/2} = \frac{\ln 2}{k} \tag{4}$$

Where

E enzyme specific activity for a reaction in a time=t(U/g);
E_0 enzyme specific activity for t=0 (U/g);
k observed deactivation rate constant;

Results and Discussion

Immobilization of YLL through adsorption process even on hydrophobic or ionic supports was quite fast. In both cases, the immobilization procedures were completed after 50 min of contact time between the support and enzyme, resulting in immobilization yield up to 97% when *Y. lipolytica* lipase was immobilized in MANAE–agarose. Immobilization yield was slightly lower for enzyme immobilization on octadecyl–sepabeads (90%) and achieved 71% when octyl–agarose was used. The activity retention values were lower for every preparation (34% for octyl–agarose, 50% for octadecyl–sepabeads and 61% for MANAE–agarose), indicating that the immobilized lipase lost activity during immobilization procedures.

Among the two hydrophobic supports, octadecyl–sepabeads presented the best result concerning YLL immobilized activity (15.5 U/g), as its activity was over twice higher than YLL immobilized onto octyl–agarose (7.0 U/g). The other immobilization parameters calculated (immobilization yield and activity retention) were also better for octadecyl–sepabeads (Table 1). These results were probably related with the chemical nature of hydrophobic supports. When a very hydrophobic support like octadecyl–sepabeads is used, there might be an increment of the affinity between the support and the substrate that

Table 1 Immobilization yield (η) and activity retention (R) of *Y. lipolytica* lipase on different supports and hydrolytic activity of the immobilized enzyme.

YLL preparation	Hydrolytic activity ($U_H/g_{support}$)	η (%)	R (%)
Octyl–agarose	7.0	71	34
Octadecyl–sepabeads	15.5	90	59
MANAE–agarose	17.0	97	61
MANAE–agarose–glutaraldehyde	0	97	0
BrCN–agarose	0.6	99	2

promote an increase in substrate concentration in the microenvironment of the enzyme leading to higher enzyme activity. Petkar et al. [23], studying immobilization of lipases on different hydrophobic supports, demonstrated that hydrolytic activity was higher when immobilized in very hydrophobic supports as octadecyl–sepabeads.

On the other hand, the ionic adsorption of *Y. lipolytica* lipase on MANAE–agarose showed activity retention, immobilization yield and immobilized activity of 61%, 97% and 17 U/g, respectively (Table 1). The use of ionic adsorption has been very successfully used for lipase immobilization [24]. Although, the above results are better than the YLL lipase immobilized by adsorption in polypropylene support [25], they showed that these immobilization procedures did not lead to lipase hyperactivation phenomenon, as it was described for lipases of different sources [17, 18]. Hyperactivation of the lipase when immobilized on very hydrophobic octadecyl–sepabeads derivative probably occurs because it occurred with the "open structure" of the lipase that is also much more active than the corresponding "closed" structure even when undergoing multipoint covalent immobilization. In our study, this phenomenon was not observed probably due to the absence of the lid in this *Y. lipolytica* lipase [26].

Although immobilization of YLL onto BrCN–agarose and MANAE–agarose–glutaraldehyde led to higher immobilization yield, the resulted immobilized biocatalysts had almost null activity (Table 1). The immobilization of YLL onto MANAE–agarose support by CNBr-mediated covalent interaction or glutaraldehyde cross-linking with resin amino groups has probably led to inactivation of the enzyme. Covalent interaction is followed by the formation of a Schiff base between aldehyde groups and Lys residues placed on the enzyme surface. This sort of interaction is likely to result in undesired mobility restriction of the enzyme or even displacement of the active site which may inactivate the YLL lipase [3].

Thermal stability study was performed for soluble YLL and immobilized onto octyl–agarose, octadecyl–sepabeads and MANAE–agarose (Figs. 1 and 2). Previous results (not shown) with immobilized and soluble YLL showed that those preparations maintained 100% activity when incubated at pH 5 during 24 h at 25°C and 3 h at 37°C. However, at 50°C, they were very unstable losing 80% enzyme activity in less than 2 h. Based on these results, stability curves were carried out at 45°C at three different values of pH: 5, 7 and 9 as described in the Materials and Methods section. Figures 1 and 2 showed that octadecyl–sepabeads preparations for both pH 5 and 7 presented an expressively higher stability than the soluble enzyme.

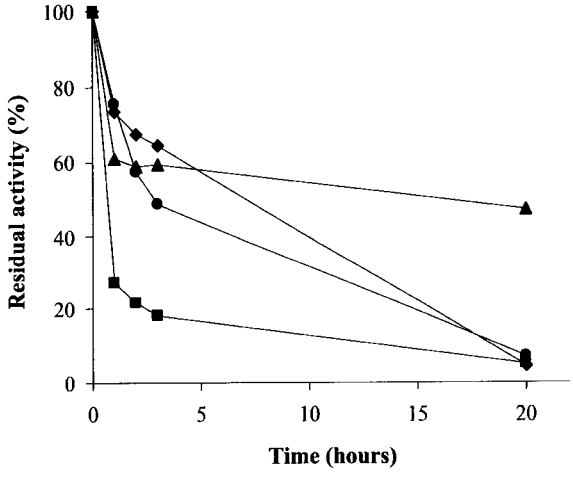


Fig. 1 Thermal stability of the different immobilized preparations and soluble YLL. Experiments were carried out in sodium acetate buffer 25 mM pH 5 and 45°C. Soluble YLL (*filled diamonds*) and immobilized on (*filled squares*) octyl–agarose, (*filled triangles*) octadecyl–sepabeads, (*filled circles*) MANAE–agarose

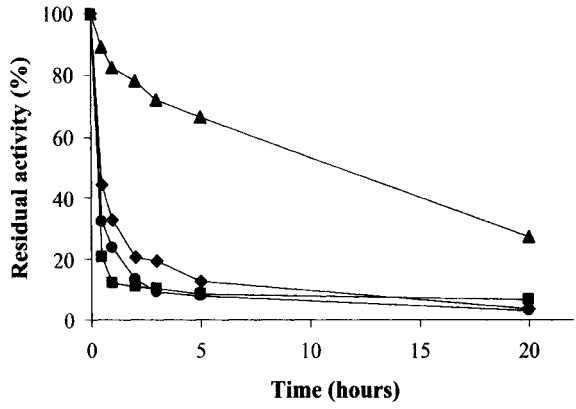


Fig. 2 Thermal stability of the different immobilized preparations and soluble YLL. The inactivation courses were carried out in 25 mM sodium phosphate buffer pH 7 and 45°C. YLL immobilized on (*filled squares*) octyl–agarose, (*filled triangles*) octadecyl–sepabeads, (*filled circles*) MANAE–agarose and (*filled diamonds*) soluble

However, for those experiments carried out at pH 9, all immobilized preparations and the soluble enzyme showed a very slight stability losing activity in less than 1 h.

Table 2 shows half-life time and inactivation coefficient for YLL soluble and immobilized on different supports. The enzyme immobilized on MANAE–agarose support presented lower stability than the soluble enzyme, perhaps because the immobilized derivative has been prepared in the presence of detergent to ensure the enzyme desegregation could be monomers, while soluble enzyme as dimers [27, 28]. Random immobilization may not really improve enzyme rigidity; even in some cases, the enzyme stability may decrease after immobilization [10–14], e.g., if the support is able to establish undesired interactions with the enzyme.

The YLL lipase immobilized onto octadecyl–sepabeads was the most stable one in all conditions, presenting half-life ten times higher than the soluble preparation at pH 7.0. Palomo et al. [8] demonstrated that the interfacial adsorption on a hydrophobic resin (octadecyl–sepabeads) was the best immobilization technique for *B. thermocatenulatus* lipase. This immobilized preparation, retaining 100% of the initial activity at high temperature, is even better than the covalent immobilization by multipoint interaction on glyoxyl support, where the lipase retained only 80% activity.

Wilson et al. [27] working with lipase QL from *Alcaligens* sp immobilized in different supports also found that for octadecyl–agarose preparation, the stability enhanced about 20 times when compared with animated supports or multipoint covalent immobilization.

Table 2 Kinetic (k and $t_{1/2}$) parameters of thermal inactivation of the soluble *Y. lipolytica* and immobilized onto different supports.

YLL preparation	$t_{1/2}$ (h)	k (h^{-1})	Experimental conditions
Soluble	4.7	0.15	
Octyl–agarose	1.4	0.48	pH 5
Octadecyl–sepabeads	26.6	0.03	45°C
MANAE–agarose	2.9	0.24	
Soluble	0.9	0.72	
Octyl–agarose	0.7	1.06	pH 7
Octadecyl–sepabeads	10.5	0.06	45°C
MANAE–agarose	0.7	0.93	

Conclusion

This work shows that lipase from *Y. lipolytica* does not undergo hyperactivation phenomenon that is largely observed for lipases from other sources when immobilized in hydrophobic supports [12, 13]. However, immobilization by physical adsorption showed to be the key for the immobilization process and especially in very high hydrophobic supports that are by far, the best way to get an optimal compromise between activity and stability. Our results also showed that YLL lost activity when immobilized by multipoint covalent attachment.

Acknowledgements Financial support was gratefully received from PETROBRÁS, FUJB, FAPERJ and CAPES. The authors are also grateful to Prof Rodrigo Volcan Almeida for his contribution.

References

1. Cammarota, M. C., & Freire, D. M. G. (2006). *Bioresource Technology, 97*, 2195–2210.
2. Gotor-Fenandez, V., Brieva, R., & Gotor, V. (2006). *Journal Molecular Catalysis B: Enzymatic, 40*, 111–120.
3. Mateo, C., Palomo, J. M., Fernandez-Lorente, G., Guisán, J. M., & Fernandez-Lafuente, R. (2007). *Enzyme and Microbial Technology, 40*, 1451–1463.
4. Koeller, K. M., & Wong, C.-H. (2001). *Nature, 409*, 232–240.
5. Bevilaqua, J. B., Lima, L. M., Cunha, A. G., Barreiro, E. J., Alves, T. L. M., & Paiva, L. M. C., et al. (2005). *Applied Biochemistry and Biotechnology, 121*, 117–128.
6. Shibatane, T., Omori, K., Akatsuka, H., Kawai, E., & Matsumae, H. (2000). *Journal of Molecular Catalysis B: Enzymatic, 10*, 141–149.
7. Mosbach, K. (1971). *Science American, 224*, 26–32.
8. Palomo, J. M., Segura, R. L., Fernandez-Lorente, G., Guisán, J. M., & Fernandez-Lafuente, R. (2007). *Enzyme and Microbial Technology, 40*, 704–707.
9. Villeneuve, P., Muderhwa, J. M., Graille, J., & Haas, M. J. (2000). *Journal of Molecular Catalysis B: enzymatic, 9*, 113–148.
10. Gupta, M. N. (1991). *Biotechnology Applied Biochemistry, 14*, 1–11.
11. Klibanov, A. M. (1982). *Advanced Applied Microbiology, 29*, 1–28.
12. Klibanov, A. M. (1983). *Biochemical Society Transactions, 11*, 19–20.
13. Mozhaev, V. V., Melik-Nubarov, N. S., Sergeeva, M. V., Sikrnis, V., & Martinek, K. (1990). *Biocatalysis, 3*, 179–87.
14. Nanalov, R. J., Kamboure, M. S., & Emanuiloda, E. I. (1993). *Biotechnology Applied Biochemistry, 18*, 409–416.
15. Jaeger, K. E., Dijkstra, B. W., & Reetz, M. T. (1999). *Annual Review of Microbiology, 53*, 315–351.
16. Aloulou, A., Rodriguez, J. A., Fernandez, S., Osterhout, D., Puccinelli, D., & Carriere, F. (2006). *Biochimica et Biophisica Acta, 1761*, 995–1013.
17. Fernandez-Lafuente, R., Armisén, P., Sabuquillo, P., Fernández-Lorente, G., & Guisán, J. M. (1998). *Chemistry and Physics of Lipids, 93*, 185–197.
18. Palomo, J. M., Muñoz, G., Fernández-Lorente, G., Mateo, C., Fernández-Lafuente, R., & Guisán, J. M. (2002). *Journal of Molecular Catalysis B: Enzymatic, 19*, 279–286.
19. Lowry, O., Rosenbrough, M., Farr, A., & Randall, R. (1951). *Journal of Biological Chemistry, 193*, 265–275.
20. Destain, J., Roblain, D., & Thonart, P. (1997). *Biotechnology Letters, 19*, 105–107.
21. Cabrera, Z., Palomo, J. M., Fernandez-Lorente, G., Fernandez-Lafuente, R., & Guisan, J. M. (2007). *Enzyme and Microbial Technology, 40*, 1280–1285.
22. Fernandez-Lafuente, R., Rosell, C. M., Rodriguez, V., Santana, C., Soler, G., & Batisda, A., et al. (1993). *Enzyme and Microbial Technology, 15*, 546–550.
23. Petkar, M., Lali, A., Caimi, P., & Daminati, M. (2006). *Journal of Molecular Catalysis B: enzymatic, 9*, 83–90.
24. Palomo, J. M., Segura, R. L., Fernandez-Lorente, G., Pernas, M., Rua, M. L., & Guisán, J. M., et al. (2004). *Biotechnology Progress, 20*, 630–635.
25. Oliveira, D., Feihrmann, A. C., Dariva, C., Cunha, A. G., Bevilaqua, J. V., & Destain, J., et al. (2006). *Journal of Molecular Catalysis B: Enzymatic, 39*, 117–123.
26. Lipase Engineering Database is available as http://www.led.uni-stuttgardt.de/.
27. Wilson, L., Palomo, J. M., Fernández-Lorente, G., Illanes, A., Guisan, J. M., & Fernandez-Lafuente, R. (2006). *Enzyme and Microbial Technology, 38*, 975–980.
28. Palomo, J. M., Fuentes, M., Fernández-Lorente, G., Mateo, C., Guisán, J. M., & Fernández-Lafuente, R. (2003). *Biomacromolecules, 4*, 1–6.

Appl Biochem Biotechnol (2008) 146:57–68
DOI 10.1007/s12010-007-8069-z

Heterologous Expression of *Aspergillus niger* β-D-Xylosidase (XlnD): Characterization on Lignocellulosic Substrates

Michael J. Selig · Eric P. Knoshaug · Stephen R. Decker · John O. Baker · Michael E. Himmel · William S. Adney

Received: 25 May 2007 / Accepted: 26 September 2007 /
Published online: 8 November 2007
© Humana Press Inc. 2007

Abstract The gene encoding a glycosyl hydrolase family 3 xylan 1,4-beta-xylosidase, *xlnD,* was successfully cloned from *Aspergillus niger* strain ATCC 10864. The recombinant product was expressed in *Aspergillus awamori*, purified by column chromatography, and verified by matrix-assisted laser desorption ionization, tandem time of flight (MALDI-TOF/TOF) mass spectroscopy of tryptic digests. The T_{max} was determined using differential scanning microcalorimetry (DSC) to be 78.2 °C; the K_m and k_{cat} were found to be 255 μM and 13.7 s^{-1}, respectively, using *p*NP-β-D-xylopyranoside as substrate. End-product inhibition by D-xylose was also verified and shown to be competitive; the K_i for this inhibition was estimated to be 3.3 mM. XlnD was shown to efficiently hydrolyze small xylo-oligomers to monomeric xylose, making it a critical hydrolytic activity in cases where xylose is to be recovered from biomass conversion processes. In addition, the presence of the XlnD was shown to synergistically enhance the ability of an endoxylanase, XynA from *Thermomyces lanuginosus*, to convert xylan present in selected pretreated lignocellulosic substrates. Furthermore, the addition of the XynA/XlnD complex was effective in enhancing the ability of a simplified cellulase complex to convert glucan present in the substrates.

Keywords Xylosidase · Xylanase · Xylo-oligomer · Pretreatment · Lignocellulose · Cellobiohydrolase

Introduction

Xylan is a major structural heterogeneous polysaccharide found in plant biomass and represents the second most abundant polysaccharide in the biosphere, after cellulose. The abundance of xylan and its integral association within the plant cell wall makes it a key

M. J. Selig (✉) · E. P. Knoshaug · S. R. Decker · J. O. Baker · M. E. Himmel · W. S. Adney
National Renewable Energy Laboratory, Chemical and Biosciences Center, 1617 Cole Blvd., Golden, CO 80401, USA
e-mail: michael_selig@nrel.gov

target for hydrolysis and conversion to fermentable sugars. However, because of its complex structure and heterogeneity, the natural bioconversion of xylan requires a diverse suite of synergistic enzymes [1, 2]. After pretreatment, it is often necessary to enzymatically hydrolyze the remaining xylan and xylo-oligomers present in hydrolyzates. In the context of a large-scale biorefinery, xylan breakdown and conversion represents a significant cost barrier to the development of the lignocellulose-to-ethanol industry [3].

To convert xylan to chemical fuels, it must first be reduced to monomeric components, primarily D-xylose; however, other side-chain sugars such as arabinose are also candidates for conversion. Enzyme activities associated with the complete hydrolysis of the xylan backbone include xylan 1,4-β xylosidase (β-xylosidase, EC 3.2.1.37) which removes successive D-xylose residues from the nonreducing ends of xylo-oligosaccharides and endo-1,4-β-xylanase (EC 3.2.1.8), which randomly cleaves 1,4-β-D-xylosidic backbone linkages releasing xylo-oligomers of variable lengths [1, 4]. Exo-xylanases are also involved in this process; however, few examples are known [5]. The random action of endoxylanases typically results in only a portion of xylan hydrolyzed being broken down to monomeric xylose, which makes the presence of β-xylosidase activity key for recovering monomeric xylose from xylan [4]. The production of such xylanolytic activities has been observed in a number of organisms, although the historical production of xylanases for industry, primarily for biobleaching of pulp and paper, has typically been done in fungi [6, 7]. Furthermore, the discovery and improvement of these enzymes is the focus of considerable research for the development of biorefineries and in the pulp and paper industry.

In this study, we report the successful heterologous expression of a functional and well-studied *Aspergillus niger* β-xylosidase (*xlnD*) in *Aspergillus awamori*. The intent was to build a sizable stock of this enzyme activity for use throughout a number of enzymatic studies. Previous experience in our laboratory with the *A. awamori* expression system [8], particularly regarding expression levels and the ease of product purification, led to its' selection as the host organism. After purification, the kinetic and thermal properties of the enzyme were assessed to confirm whether or not the expression produced a functioning form of the protein. To show the utility of the enzyme, we have probed the ability of XlnD to hydrolyze small xylo-oligomers and investigated the ability of this enzyme to work in concert with an endoxylanase, XynA from *Thermomyces lanuginosus,* to hydrolyze xylan in pretreated lignocellulosic substrates. We have also investigated the ability of the XynA/XlnD complex to work in synergy with a simplified cellulase mix to more effectively convert glucan present in pretreated substrates.

Materials and Methods

Cloning of xlnD Sequence

Genomic DNA from *A. niger* (ATCC 10864) grown in CM-glucose media [8] was isolated using the DNeasy Plant Maxi Kit as per the manufacturer's directions (Qiagen, cat. no. 68161). The coding sequence for the gene XlnD (Z84377) was amplified with the polymerase chain reaction (PCR) using PfuTurbo polymerase (Stratagene, cat. no. 600250) and the MasterAmp PCR Optimization Kit with ammonium sulfate (Epicentre, cat. no. MOS02N). Primers used for the PCR are listed in Table 1. The following touchdown PCR cycle parameters were used: denaturing parameters, 95 °C for 1 min, annealing parameters, 60 °C for 30 s, extension parameters, 72 °C for 3 min (repeat previous cycles lowering the annealing temperature by 2 °C with every cycle until an annealing temperature of 52 °C is

Table 1 PCR Primers used for cloning and mutagenesis; start and stop codons are underlined, restriction sites used for cloning are in bold (*BbvCI* and *XbaI*) and the base pair change to knockout the BbvCI restriction site is underlined in bold.

Primer name	Sequence
XlnDfor	**CCTCAGC**AATGGCGCACTCAATGTCTCGT
XlnDrev	**TCTAGA**CTACTCCTTCCCCGGCCACTTCAGCA
XlnDmutflor	GCTGCCGCTGCCGC**C**GAGGCCATCCTCGCC
XlnDmutrev	GGCGAGGATGGCCTC**G**GCGGCAGCGGCAGC

reached, then 28 cycles of 95 °C for 30 s, 52 °C for 30 s, 72 °C for 3 min, followed by a final extension at 72 °C for 10 min). The PCR product was cloned into pCR2.1-TOPO (Invitrogen, cat. no. K4510–20) for recovery and mutagenesis to remove the internal *BbvCI* site. Site-directed mutagenesis was preformed on the pCR2.1-TOPO-XlnD construct using the QuickChange Site-Directed Mutagenesis Kit as described (Stratagene, cat. no. 200518). The primers used for site-directed mutagenesis are listed in Table 1. The mutated construct was recovered and confirmed to have lost the additional *BbvCI* site by restriction analysis. The mutated gene was then subcloned into pFE2 for fungal expression. Plasmid DNA of the expression vector-gene construction from a large scale isolation (Qiafilter Plasmid Maxi Kit, Qiagen, cat. no. 12262) was sequenced using the Applied Biosystems Automated 3730 DNA Analyzer and Big Dye Terminator chemistry with AmpliTaq-FS DNA Polymerase at the Cornell Biotechnology Resource Center. *A. awamori* (ATCC 22342) was transformed as described [8]. Spores from potential transformants were frozen to −80 °C for later use.

Production of XlnD Protein

Protein production was carried out in 2.8 l Fernbach flasks using CM medium as described previously [8]. Seed cultures of the transformed spores were prepared in CM media containing 300 μg/ml Zeocin and were incubated for 4 to 5 days before transferring to the 2.8-l flasks containing 1 l of CM media with 100 μg/ml Zeocin. XlnD production was monitored during the fermentations by sodium dodecyl sulfate-polyacrylamide gel electrophoresis (SDS-PAGE) and activity analysis on *p*NP-β-D-xylopyranoside. Upon harvesting, the fermentation broths were clarified by filtration through Miracloth (Novagen, Madison, WI) and 70 μm polypropylene filter cloth; the broth was then frozen and stored at −20 °C. Before protein purification, the broth was thawed and refiltered through a 141-grade Ahlstrom glass microfiber filter.

Protein Purification

The filtered XlnD fermentation broth was initially concentrated into 20 mM Bis–Tris buffer at pH 6.8 in a 300 ml stirred ultrafiltration cell from Amicon (Beverly, MA) with a 30,000 Da molecular weight cut-off membrane. The protein was then bound to a Source Q anion exchange column (96 ml) and eluted over a 0 to 1 M NaCl gradient into 20 mM Bis–Tris at pH 6.8. The eluted XlnD peak was then reconcentrated and rerun on the Source Q column. From this run, the XlnD fractions were then pooled and buffer-exchanged into 20 mM acetate buffer at pH 5.0 with 100 mM NaCl on a Superdex 200 size exclusion column. The purity of the purified fractions was assessed by SDS-PAGE, and the protein content was assessed by measuring the absorbance at 280 nm and by bicinchoninic acid (BCA) assay with bovine serum albumin (BSA) run as a standard.

Additional proteins used in this study, the endoxylanase XynA, the cellobiohydrolase Cel7A, and a cellobiase were all purified from commercial sources. Cel7A and XynA were purified as described previously [9]. In brief, the XynA was isolated from a Sigma *T. lanuginosus* endoxylanase prep by sequential anion exchange and size exclusion chromatography steps. The Cel7A was isolated from a *Trichoderma reesei* cellulase preparation (Spezyme CP, Genencor, Copenhagen, Denmark), by multiple anion exchange steps followed by cellulose affinity chromatography and clean-up by size exclusion chromatography (SEC). The cellobiase was purified as previously described [10] from an *A. niger* cellobiase preparation (Novo 188, Novozymes, Bagsvaerd, Denmark).

Thermal Analysis of Purified XlnD

Thermal analysis of the purified XlnD protein was performed by differential scanning microcalorimetry (DSC) in a Microcal (Northampton, MA) VP-ITC system. All portions of this analysis were conducted in 20 mM sodium acetate buffer at pH 5.0 with 100 mM NaCl (SEC buffer). The XlnD was analyzed at a nominal protein concentration of 50 nM and scanned from 30 to 95 °C at a rate of 60 °C/h.

Determination of Initial Rate Kinetics on *p*-nitrophenol β-D xylopyranoside

Initial rate kinetic assays were conducted at 37 °C in 50 mM citrate buffer at pH 4.8 in 96-well microtiter plates using *p*-nitrophenol β-D-xylopyranoside. For all assays, the XlnD was loaded at 1.5 μg/ml of reaction, and initial substrate concentrations were varied from 0.1 to 3.2 mM. The release of *p*NP was monitored every 15 s for the initial 10 min of each reaction by measuring the absorbance at 405 nm on a SpectraMax 190 UV/VIS microplate scanner from the Molecular Devices (Sunnyvale, CA). End product inhibition by D-xylose was confirmed by running identical assays to those described above with initial D-xylose concentrations ranging from 3.33 to 40 mM. Triplicate analyses of all assays were run at all conditions. All parameters estimated in this study were calculated using standard Michaelis–Menten kinetics as described previously [11].

Assessment of Efficacy in Converting Simple Xylo-Oligomers

The ability of the XlnD to convert simple xylo-oligomers was initially assessed on low DP (up to DP6) preparations purchased from Megazyme (Wicklow, Ireland). Solutions of xylobiose, xylotriose, xylotetrose, xylopentose and xylohexaose, 1.5 mg/ml, were incubated in 50 mM citrate buffer at 50 °C for 1 and 24 h in the presence of a 5-mg/g xylan loading of XlnD. A mixed solution of xylobiose (~1.5 mg/ml), xylotriose, xylotetraose, and xylohexose (1.0 mg/ml each) was also incubated in the presence of a 0.5-mg/g xylan loading of XlnD and analyzed for oligomeric and monomeric xylose by high-performance liquid chromatography (HPLC) at 10, 30, 60, and 120 min.

Digestions with Oat Spelt Xylan

The ability of XlnD to convert xylo-oligomers resulting from endoxylanase action was determined using oat spelt xylan (Sigma Chemical) and the purified XynA. Digests containing only XynA were run at loadings between 0.25 and 50 mg/g xylan; digestions with XlnD were run at loadings ranging from 0.25 to 10.0 mg/g xylan at a near-optimal

XynA loading (2.5 mg/g xylan). All digestions were run in duplicate at 50 °C in 50 mM, pH 4.8, citrate buffer, and sampled at 24 h for analysis by HPLC.

Digestions on Pretreated Corn Stover

Corn stover used for this study was harvested in 2003 at the Kramer Farm in Wray, Colorado. The stover was pretreated either in-house at the National Renewable Energy Laboratory or received via subcontract from the CAFI [12] pretreatment group members. The samples selected for this study were pretreated by alkaline peroxide (NREL), sulfite steam explosion (UBC), ammonia fiber explosion (MSU), and dilute sulfuric acid (NREL) methods. The composition of the pretreated stover was determined by a two-stage sulfuric acid hydrolysis treatment according to the NREL Laboratory Analytical Procedure titled "Determination of Structural Carbohydrates and Lignin in Biomass" [13]. The pretreatment conditions and compositional information for each substrate are listed in Table 2.

Digestions were run on the pretreated substrates with XlnD and XynA loaded at 1.0 and 2.5 mg/g xylan, respectively. Digestions with these loadings were run with each individual enzyme and the combination of the two. In addition, the same loadings were run in combination with the purified Cel7A and cellobiase at nominal loadings of 50 and 5 mg/g glucan, respectively. All digestions were run for 24 h at 50 °C in 50 mM citrate buffer at pH 4.8; after which, the hydrolysates were sampled for analysis by HPLC.

HPLC Analysis

HPLC analysis of digestion hydrolysates was conducted on an 8 mm × 300 mm Shodex (Kawasaki, Japan) SP0810 Sugar Column at 80 °C with water running at 0.6 ml/min as the eluent.

Results and Discussion

Cloning and Expression

The gene encoding XlnD was amplified and isolated from genomic DNA of *A. niger* using the PCR and cloned into the pCR2.1-TOPO vector. The coding sequence was then subcloned into our fungal expression vector pFE2 [8] at the *BbvCI* and *XbaI* sites to allow for expression driven by the glucoamylase promoter and secretion based on the gene's native signal sequence. The DNA sequence showed that introns were not present, and there were no

Table 2 Pretreated corn stover substrates; pretreatment information and glucan, xylan and lignin content as a fraction of the pretreated material.

Pretreatment	Source	Pretreatment Information	Glucan	Xylan	Lignin
Alkalnine peroxide	NREL	1.0% hydrogen peroxide; pH 11.5; 3 h at 50 °C	0.58	0.27	0.06
Dilute acid	NREL	Low severity sulfuric acid pretreatment in Sunds at NREL	0.54	0.14	0.27
Sulfite steam explosion	CAFI2-UBC	190C; 5 min; 3% SO_2; 20% solids	0.60	0.11	0.01
AFEX	CAFI2-MSU	90 °C; 60% moisture; ammonia loading of 1.0 kg/KG	0.37	0.20	0.05

Table 3 Matching peptide fragments from MALDI TOF/TOF analysis of Trypsin Digested XlnD; analyzed at the Cornell Proteomics and mass spectrometry core facility at Cornell University in Ithaca, NY.

Start AA	End AA	Sequence	Observed MW
65	78	SHLICDETATPYDR	1,677.7577
79	104	AASLISFTLDELIANTGNTGLGVSR	2,633.3792
105	122	LGLPAYQVWSEALHGLDR	2,025.05
150	164	TLIHQIASIISTQGR	1,637.9381
165	171	AFNNAGR	749.4118
172	185	YGLDVYAPNINTFR	1,642.8271
172	191	YGLDVYAPNINTFRHPVWCR	2,375.1667
186	191	HPVWGR	751.4315
192	224	GQETPGEDSLAAVYAYEYITGIQGPDPESNLK	3,511.6707
231	245	HYAGYDIENWHNHSR	1,898.8374
368	376	DDIEQGVIR	1,044.5609
394	399	ANNPYR	734.4005
428	438	NSNNVLPLTEK	1,228.6628
532	546	ESIAWPGNQLDLIQK	1,711.8864
596	607	DIITGKKNPAGR	1,269.7437
608	640	LVTTQYPASYAEEFPATDMNLRPEGDNPGQTYK	3,719.7461
730	737	KWLVGWDR	1,059.6017
731	737	WLVGWDR	931.5106
738	747	LGEVKVGETR	1,087.6412
738	750	LGEVKVGETRELR	1,485.7902
748	760	ELRVPVEVGSFAR	1,458.8146
751	760	VPVEVGSFAR	1,060.6046
761	782	VNEDGDWVVFPGTFELALNLER	2,520.2102

amino acid differences between our cloned sequence and the sequence reported in GenBank for XlnD (*A. niger* CBS 120.49). Peptide sequences derived from trypsin digests followed by MALDI TOF/TOF MS analysis was used for positive identification of the purified enzyme. This analysis was performed at the Cornell Proteomics and Mass Spectrometry core facility at Cornell University in Ithaca, NY. From the analysis, 23 peptides were matched representing ~38% mass coverage of the entire amino acid sequence (Table 3).

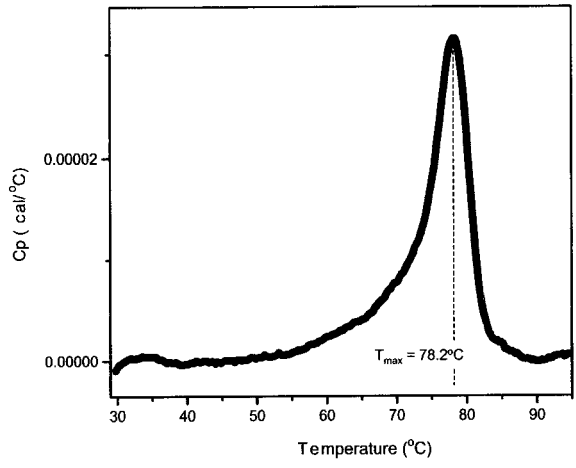


Fig. 1 DSC scan of the purified XlnD protein; the protein was scanned from 30 to 95 °C in 20 mM acetate buffer, pH 5.0 with 100 mM NaCl, at a scanning rate of 60 °C/h. T_{max} was estimated to be 78.2 °C

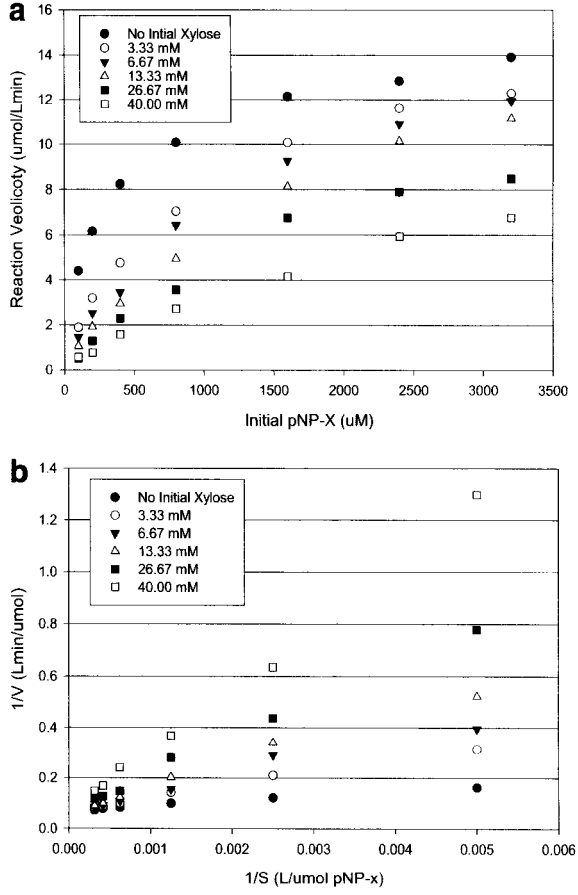


Fig. 2 Assays with the purified XlnD on *p*NP-x, run at 37 °C in 50 mM citrate buffer at pH 4.8; **a** reaction rate vs substrate concentration and **b** Michaelis–Menten plots of data from assays with varying initial D-xylose concentrations

Thermal Analysis of XlnD

Analysis by DSC (Fig. 1) revealed the purified XlnD to have a high thermal denaturation point. By this method, the T_{max} of the protein was estimated to be 78.2 °C; repeat scans on the protein verified this value. In addition, a rescan (data not shown) of the deconvoluted protein showed the XlnD was unable to refold after thermal collapse. This data is in agreement with previously published temperature vs activity data indicating the thermostable nature of the *A. niger* XlnD [14, 15] and is a strong indication that our expression was successful in retaining thermostability of the protein.

Activity Analysis on pNP-beta-D-xylopyranoside

Initial activity analysis on *p*NP-X showed the kinetic behavior of our purified XlnD to be in agreement with previously published work regarding the β-xylosidase enzyme from *A. niger* [16, 17]. From triplicate assays at each substrate loading, the K_m and k_{cat} of the protein were estimated to be 254.8±6.8 μM and 13.7±0.7 s^{-1}, respectively (note that all deviations presented are the standard deviations between values obtained for each parameter as determined from each replicate assay set). Assays with increasing amounts

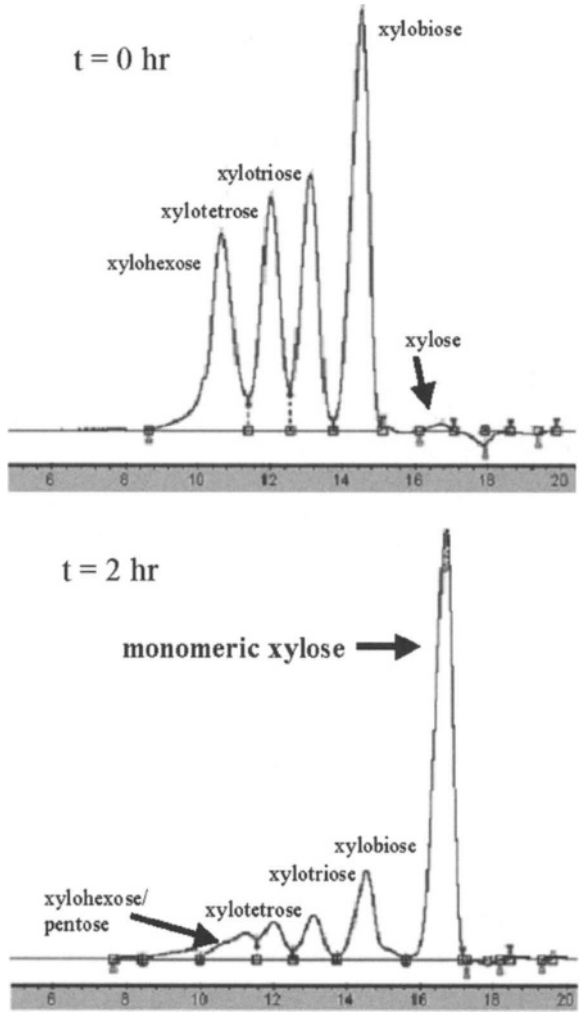


Fig. 3 HPLC chromatograms from 0 to 2 h digestions of a mixed solution of xylobiose, xylotriose, xylotetraose, and xylohexose; 0 and 2 h sampling times are shown

of initial D-xylose (Fig. 2a) confirmed the end-product inhibition of the enzyme by D-xylose as described by Tavobilov and coworkers [16, 17]. Michaelis–Menten plots (Fig. 2b) of initial reaction rate and substrate data for each initial D-xylose loading show the slopes of each plot to have very similar *y*-intercepts (0.0073±0.0004 min/μM), indicating that the inhibition by D-xylose is most likely competitive. Based on the assumption that the inhibition is competitive, the K_i was estimated from the data to be 3.35±0.78 mM. Overall, the strong agreement between our analysis and published kinetic data for the *A. niger* β-xylosidase proves we have successfully expressed an active and useful form of this enzyme using the A. awamori system.

Efficacy in Converting Xylo-Oligomers

Digestions of prepared xylo-oligomers with the XlnD demonstrated the enzymes ability to quickly hydrolyze small oligomers. The 5 mg/g oligomer loading of the XlnD was observed to

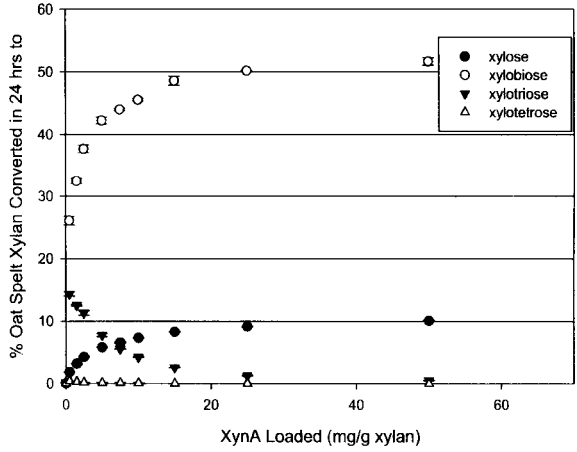


Fig. 4 Twenty-four-hour digestions of oat spelt xylan with varying loadings of XynA presented as the percent of xylan converted to xylotetrose, xylotriose, xylobiose, and xylose. All error bars represent the SD replicate assays

completely hydrolyze 1.5 mg/ml solutions of individual xylo-oligomers up to xylohexose within 2 to 3 h (data not shown). This enzyme showed no cross-reactivity with cellobiose, even for extended periods (24 h). Figure 3 depicts the rapid hydrolysis of a mixed solution of xylo-oligomers over a 2-h period. The negligible effect of this enzyme on cellobiose will make this enzyme a useful tool for reducing xylan degradation to monomeric xylose release, without directly hydrolyzing sugars released by cellulose hydrolysis. This enzyme will be of particular use when studying the effects of specific hemicellulases on the ability of cellobiohydrolases to release cellobiose from lignocellulosic materials. In addition, the ability of the enzyme to rapidly hydrolyze low molecular weight oligomers may prove useful in the treatment of high molecular weight xylo-oligomer containing hydrolysates from pretreatments of lignocellulose.

Digestions of oat spelt xylan with purified XynA and the XlnD further show the utility of the β-xylosidase activity in a real lignocellulosic system. For example, in Fig. 4, we show how the endoxylanase primarily degrades the xylan to xylobiose and xylotriose; and to a lesser extent, xylose. Shown in Fig. 5, xylan converted by XynA in the presence of small quantities of XlnD is entirely converted to monomeric xylose during the 24-h incubation

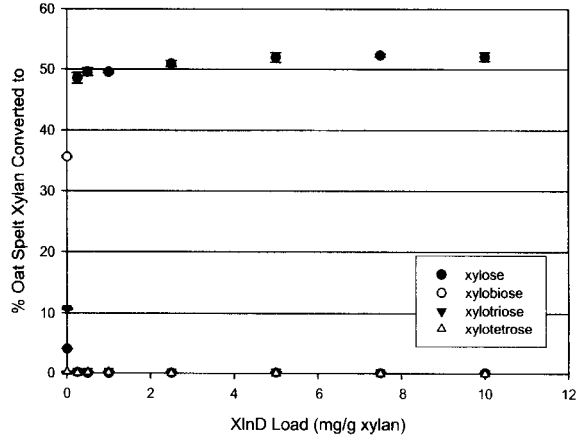


Fig. 5 Twenty-four-hour digestions of oat spelt xylan with a nominal XynA loading of 2.5 mg/g xylan and varying loadings of the purified XlnD enzyme. The data is presented as the percent of xylan converted to xylotetrose, xylotriose, xylobiose, and xylose. All *error bars* represent the SD between replicate assays

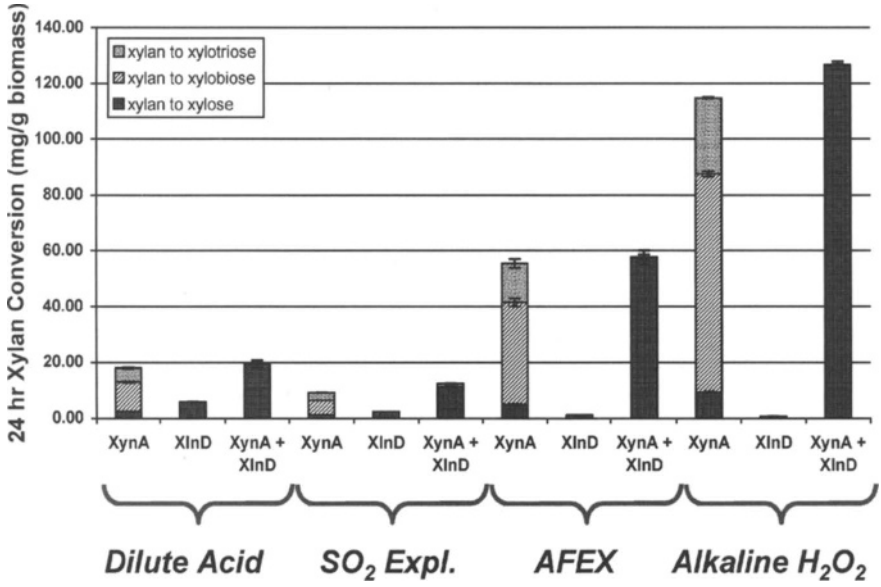


Fig. 6 Twenty-four-hour digestions of pretreated corn stover with individual and combined loadings of XynA and XlnD. XynA and XlnD were loaded at 2.5 and 1.0 mg/g xylan, respectively. All *error bars* represent the SD between replicate assays

time. Results from a 1-h incubation (data not shown) with both XynA and XlnD are nearly identical to the 24-h digest (lower overall yields), with only trace amounts of xylobiose present in solution at the lowest XlnD loadings. This result is a good indication that the XlnD is fairly capable of keeping pace with the release of xylo-oligomers by the endoxylanase.

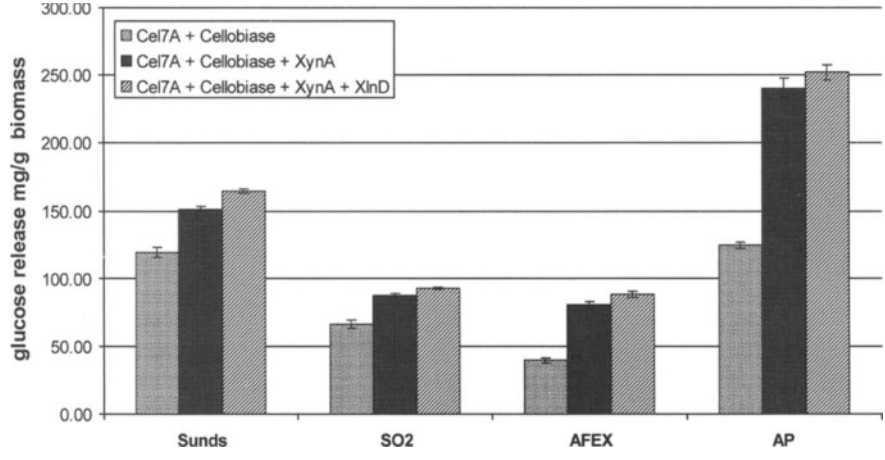


Fig. 7 Twenty-four-hour digestions of pretreated corn stover with a nominal mix of purified Cel7A and cellobiase (50 and 5 mg/g cellulose, respectively) with individual and combined loadings of XynA and XlnD. XynA and XlnD were loaded at 2.5 and 1.0 mg/g xylan, respectively. All *error bars* represent the SD between replicate assays

Effects on the Saccharification of Pretreated Corn Stover

In Fig. 6, we show that the addition of XlnD contributes to the degradation of xylan present in pretreated corn stover substrates. In this work, the XlnD has a significant impact on the quantity of monomeric xylose that can be recovered from the pretreated substrates, while also allowing for mild improvements in the total amount of xylan converted (i.e., compared to digestions with only XynA). In Fig. 7, we show how enzymatic xylan removal can have a significant and synergistic impact on the conversion of cellulose by the simplified cellulase system: Cel7A and a cellobiase. In this work, the mild enhancement in xylan conversion with the addition of XlnD correlates to slightly higher recoveries of glucose from the pretreated biomass. The overall synergy we have observed between these simplified xylanolytic and cellulolytic systems is in agreement with previously published work showing synergism between unpurified cellulase and xylanase systems on lignocellulosic materials [18, 19]. From these data (Fig. 7), we show that the enhancement of cellulose conversion by simultaneous enzymatic xylan conversion is most significant for substrates that have higher post-pretreatment xylan content (i.e., AFEX and alkaline peroxide stover).

Conclusions

We have successfully expressed an *A. niger* β-xylosidase, XlnD, in *A. awamori*. The expressed XlnD was purified and successfully identified by MALDI-TOF/TOF analysis to be the correct protein. Activity analysis on *p*NP-X showed the XlnD to behave in accordance with previously published work on the *A. niger* β-xylosidase indicating that this enzyme was successfully expressed in this heterologous system. In addition, we have shown that the purified XlnD has high thermal stability and is effective in converting low molecular weight xylo-oligomers to monomeric xylose. When working in concert with a purified endoxylanase, the presence of the XlnD permits complete recovery of the hydrolyzed xylan to monomers, and thus, provides some enhancement in total xylan conversion. This enhancement in xylan conversion translates to additional improvements in the performance of a simplified cellobiohydrolase/cellobiase system over the significant gains observed with the addition of the endoxylanase XynA. Overall, our data suggests that activities, such as XlnD, are crucial to the biomass conversion process and that discovery of new, and perhaps, even more active versions of these enzymes is thus warranted.

Acknowledgements This work was funded by the DOE Office of the Biomass Program. We would also like to acknowledge the CAFI pretreatment group for providing some of the corn stover samples used in this study and Cornell Proteomics and Mass Spectrometry core facility for providing MS data regarding the identification of our purified enzyme.

References

1. Collins, T., Gerday, C., & Feller, G. (2005). *Fems Microbiology Reviews*, *29*(1), 3–23.
2. Christov, L. P., & Prior, B. A. (1993). *Enzyme and Microbial Technololgy*, *15*(6), 460–475.
3. Jeffries, T. W., & Jin, Y. S. (2000). *Advances in Applied Microbiology*, *47*, 221–268.
4. Schlacher, A., et al. (1996). *Journal of Biotechnology*, *49*(1–3), 211–218.
5. Ghosh, M., & Nanda, G. (1994). *Applied and Environmental Microbiology*, *60*(12), 4620–4623.
6. Beg, Q. K., et al. (2001). *Applied Microbiology and Biotechnology*, *56*(3–4), 326–338.

7. Christov, L. P., Akhtar, M., & Prior, B. A. (1996). *Holzforschung, 50*(6), 579–582.
8. Adney, W. S., et al. (2003). *In applications of enzymes to lignocellulosics* pp. 403–437. Washington: American Chemical Society.
9. Decker, S. R., & Selig, M. J. (2006). D Milestone: enzyme enhanced conversion of low severity pretreated biomass, DOE, Editor. NREL. p. 1–31.
10. Himmel, M. E., et al. (1993). *Applied Biochemistry and Biotechnology, 39*, 213–225.
11. Nelson, D. L., & Cox, M. M. (2000). *Lehninger principles of biochemistry* (3rd ed.). New York, NY: Worth Publishers.
12. Wyman, C. E., et al. (2005). *Bioresource Technology, 96*(18), 2026–2032.
13. Sluiter, A., Hames, B., Ruiz, R., Scarlata, C., Sluiter, J., & Templeton, D.(2004). Determination of structural carbohydrates and lignin in biomass, DOE, Editor. National Renewable Energy Laboratory.
14. Pedersen, M., et al. (2007). *Biotechnology Letters, 29*(5), 743–748.
15. Uchida, H., et al. (1992). *Journal of Fermentation and Bioengineering, 74*(3), 153–158.
16. Tavobilov, I., Rodionova, N., & Bezborodov, A. (1983). PrikladnaaÃ biohimiaÃ i mikrobiologia, *19*(2), 232–239.
17. Rodionova, N. A., Tavobilov, I. M., & Bezborodov, A. M. (1983). *Journal of Applied Biochemistry, 5*, 300–312.
18. Yu, P. Q., et al. (2003). *Journal of Agricultural and Food Chemistry, 51*(1), 218–223.
19. Murashima, K., Kosugi, A., & Doi, R. H. (2003). *Journal of Bacteriology, 185*(5), 1518–1524.

Appl Biochem Biotechnol (2008) 146:69–78
DOI 10.1007/s12010-007-8055-5

Cloning, Expression and Characterization of a Glycoside Hydrolase Family 39 Xylosidase from *Bacillus Halodurans* C-125

Kurt Wagschal · Diana Franqui-Espiet · Charles C. Lee · George H. Robertson · Dominic W. S. Wong

Received: 18 April 2007 / Accepted: 14 September 2007 /
Published online: 10 October 2007
© Humana Press Inc. 2007

Abstract The gene encoding a glycoside hydrolase family 39 xylosidase (*BH1068*) from the alkaliphile *Bacillus halodurans* strain C-125 was cloned with a C-terminal His-tag, and the recombinant gene product termed BH1068(His)$_6$ was expressed in *Escherichia coli*. Of the artificial substrates tested, BH1068(His)$_6$ hydrolyzed nitrophenyl derivatives of β-D-xylopyranose, α-L-arabinofuranose, and α-L-arabinopyranose. Deviation from Michaelis–Menten kinetics at higher substrate concentrations indicative of transglycosylation was observed, and k_{cat} and K_m values were measured at both low and high substrate concentrations to illuminate the relative propensities to proceed along this alternate reaction pathway. The pH maximum was 6.5, and under the conditions tested, maximal activity was at 47°C, and thermal instability occurred above 45°C. BH1068(His)$_6$ was inactive on arabinan, hydrolyzed xylooligosaccharides, and released only xylose from oat, wheat, rye, beech, and birch arabinoxylan, and thus, can be classified as a xylosidase with respect to natural substrate specificity. The enzyme was not inhibited by up to 200 mM xylose. The oligomerization state was tetrameric under the size-exclusion chromatography conditions employed.

Keywords Alkaliphile · Xylosidase · Glycoside hydrolase family 39 · Hemicellulose degradation

Introduction

Enzymes that can be harnessed for the breakdown of hemicellulose in cereal crops, and crop fiber biomass are becoming increasingly important because of their pivotal role in the utilization of these renewable energy sources. Hemicelluloses (xylans, arabinoxylans) are widely found as structural components in plant cell walls, where they cross-link with lignin and are extensively hydrogen-bonded to cellulose [1]. Structurally, xylans are heteropolysaccharides consisting of a linear β-D-(1→4)-linked xylopyranoside backbone that,

K. Wagschal (✉) · D. Franqui-Espiet · C. C. Lee · G. H. Robertson · D. W. S. Wong
USDA Agricultural Research Service, Western Regional Research Center,
800 Buchanan Street, Albany, CA 94710, USA
e-mail: kwagschal@pw.usda.gov

depending on the tissue source, is variously substituted with arabinose and other substituents. The xylose backbone of cereal xylans can be substituted with (1→2)- and/or (1→3)-linked α-L-arabinofuranosyl, α-D-glucuronic acid, and *O*-2 and/or *O*-3-linked acetate groups. Enzymes that hydrolyze non-reducing terminal β-D-xylopyranoside linkages and release xylose in an *exo*-manner from substrates such as xylooligosaccharides and arabinoxylan, and from synthetic substrates such as *p*-nitrophenyl-β-D-xylopyranoside are classified as xylan 1,4-β-xylosidases (xylosidases; EC 3.2.1.37). Xylosidases are key enzymes in the breakdown of biomass. Their action produces xylose from xylooligosaccharide mixtures that are produced by endo-xylanases. Moreover, because some xylanases can be inhibited by their xylooligosaccharide product, xylosidases can have a synergistic effect with endo-xylanase hydrolysis [2, 3]. Xylosidases and their potential biotechnological application have been the subject of several reviews [4–6]. In addition to the breakdown of hemicellulosic biomass for fuel and chemical feedstock use, xylosidases may also find use in cellulose pulp biobleaching processes [7].

Numerous enzymes with the ability to hydrolyze the various hemicellulose linkages have been isolated, most of them from microbial sources [6]. We describe in this paper the cloning with a C-terminal His-tag of the gene annotated *BH1068* from *Bacillus halodurans* C-125 genomic DNA, an alkalophilic bacterium with a known genomic sequence, and the subsequent expression, purification, and biochemical characterization of the encoded xylosidase gene product termed BH1068(His)$_6$.

Materials and Methods

Cloning BH1068 from Genomic DNA into pET 22 b(+)

Bacillus halodurans C-125 genomic DNA was obtained from the American Type Culture Collection (Manassas, VA, USA). The gene *BH1068* (1,509 bp, GenBank accession number BA000004) was amplified in a polymerase chain reaction using the following primers:

BH1068bl-5′: ATGAAAACAGTAGTTGTAAATGATCGTTC
BH1068–3′: GGATACTCGAGATACGAAGGAATCAGCCGA

The cloning strategy consisted of a 5′ blunt end and a 3′ *Xho*I cohesive terminal, and a pET-22b(+) vector was used for expressing the *BH1068* with a C-terminal His-tag. The amplified fragment was gel-purified using Promega SV gel and polymerase chain reaction (PCR) clean-up system (Promega, Madison, WI, USA). The product was digested with *Xho*I and subsequently purified using the Promega system. The expression vector used was pET22b(+) digested with *Nde*I *and Xho*I. The digested vector was gel purified using the Promega System. Given that *BH1068* contains an internal *Nde*I site, the enzyme T4 DNA polymerase (Promega) was used to fill the 5′ end of the digested pET22 b(+) vector and convert it into a blunt end. Fragment and vector were ligated using T4 DNA ligase (Promega). BL21-Gold (DE3) chemically competent cells (Stratagene) were transformed with the construct.

BH1068(His)$_6$ Expression and Purification

The expression host *Escherichia coli* BL21(DE3) was transformed with the expression plasmid pET22b(+) containing the BH1068(His)$_6$ insert, streaked onto Luria–Bertani agar plates amended with 50 μg/ml carbenicillin (Sigma; LB_{carb}), and incubated overnight at 37°C.

Positive transformants were selected based on enzymatic hydrolysis of *p*-NP-β-D-xylopyranoside (described below) and restriction digestion of the plasmids. A single positive transformant was used to inoculate a 15-ml seed culture of *E. coli*, which was then grown in LB_{carb} broth at 37°C at 250 rpm for 16 h with 0.5% glucose added to repress protein expression. A 5-ml aliquot was used to inoculate 200 ml LB_{carb}, which was grown at 37°C to $OD_{600\,nm}$=2–3. Then 1 mM isopropylthiogalactoside was added to induce protein expression, and incubation was allowed to proceed at 16°C at 250 rpm for 16 h. Fifty milliliter aliquots were pelletted and the pellets stored frozen at −80°C. Cell lysis and release of soluble proteins were achieved by adding to each pellet 3.5 ml Bug-Buster solution (EMD Biosciences) containing 40 U/ml r-lysozyme (EMD Biosciences), 0.5 mM phenylmethylsulfonylfluoride, 25 U/ml benzonase, and 5 mM β-mercaptoethanol (BME; all from Sigma). Cells were incubated in the lysis solution for 20 min at room temperature, cooled to 0–4°C, and centrifuged to remove cell debris. The protein was purified using Ni-NTA resin (Qiagen) according to the manufacturer's instructions by first adjusting the supernatant solution to 300 mM NaCl, 10 mM imidazole, and 50 mM phosphate buffer (pH 8.0). The composition of the wash buffer used was 50 mM phosphate buffer (pH 8.0) containing 1 mM BME, 1 μl/ml Calbiochem protease inhibitor cocktail set III (EMD Biosciences), 300 mM NaCl, and 10 mM imidazole. The protein was eluted using the same buffer, except that the imidazole concentration was increased to 250 mM. Fractions containing the enzyme were buffer exchanged using NAP-5 desalting columns (Amersham Biosciences, Piscataway, NJ, USA) into 50 mM phosphate (pH 6.0), 10% glycerol, and 1 ul/ml protease inhibitor cocktail set III, and stored at −80°C. Protein concentrations were determined using Coomassie Plus reagent (Pierce Biotechnology, Rockford, IL, USA) following the manufacturer's protocol. Enzyme fractions were analyzed using polyacrylamide gel electrophoresis (PAGE, 4–12%, reducing) following the manufacturer's protocol (Invitrogen). Final protein purity was estimated to be 55% by gel densitometry performed using an AlphaImager imaging system (Alpha Innotech Corp., San Leandro, CA, USA).

Molecular Weight Determination

The molecular weight of the His-tagged protein was estimated by gel filtration chromatography using an Amersham/Pharmacia HiPrep 16/60 Superdex 200 10/300 GL column (Amersham Biosciences). The running buffer was 50 mM phosphate (pH 7.4), 150 mM NaCl, and 1 mM dithiothreitol (DTT). A standard curve was generated with low-molecular weight (13.7 to 67 kDa) and high-molecular weight (158 to 669 kDa) standards (Amersham Biosciences).

Enzyme Assays

For assays using nitrophenyl (NP) glycosides as substrates (Sigma, St. Louis, MO, USA or Research Products International Corporation, Mt. Prospect, IL, USA), the enzyme activity was determined by measuring the change in absorbance at 400 nm caused by NP release using a SpectraMax M2 spectrophotometer equipped with a temperature controller (Molecular Devices, Sunnyvale, CA, USA). Time-course studies using saturating substrate concentrations were initially performed with *p*-NP-XylP to establish the linearity of hydrolysis rate with respect to time at 45°C. In a typical kinetic assay, 190 μl of 50 mM phosphate (pH 6.5) containing 0.1% bovine serum albumin (BSA; Sigma) and varying substrate concentrations was pre-incubated at 45°C for 5 min, then 10-μl enzyme solution was added and mixed to initiate the reaction. Generally, 16 different substrate

concentrations were used to assess the kinetic parameters; the assays were performed in quadruplicate, and the amount of enzyme was chosen so that the proportion of substrate hydrolyzed at the end of the data acquisition period was 10% or less (Table 1). The kinetic parameters V_{max} and K_m for the aryl-glycoside substrates were calculated by non-linear regression fitting of the data to the Michaelis–Menten equation using the program GraFit 5 (Erithacus Software, Surrey, UK). The inhibition constant K_i for xylose was determined using a kinetic spectrophotometric assay wherein velocity was measured in the absence of added xylose, and then in the presence of 30, 60, 90, 120, and finally, 200 mM xylose using *p*-NP-XylP concentrations ranging from 30 to 2,000 μM, 50 mM phosphate (pH 6.5) and 20 nM BH1068(His)$_6$. Xylose at the various concentrations and BH1068(His)$_6$ were preincubated in the assay buffer for 10 min at 45°C, and the reaction initiated by adding *p*-NP-XylP.

The hydrolysis of the natural substrate xylobiose (Wako Chemicals USA, Inc., Richmond, VA, USA) was assessed using 380 nM BH1068(His)$_6$ and substrate concentrations of 1,040 μM to 16 mM, 100 mM phosphate buffer (pH 6.5), and a 35-min incubation at 45°C (Table 1). Xylotriose (Wako Chemicals USA, Inc., Richmond, VA, USA) and xylotetraose (Megazyme Ltd., Wicklow, Ireland) were also tested as substrates at concentrations ranging from 112 to 4480 μM for the former, and 104 μM to 16 mM for the latter. Enzyme activity resulting in xylose release was then assessed using an enzyme-coupled assay for xylose as described [8].

Activity Versus pH Profile

The effect of pH on the apparent V_{max} (Fig. 1) was measured using endpoint assays utilizing an equal volume of 1 M Na_2CO_3 to quench the reactions and raise all the pH values to ~pH 11. Reactions were carried out at 45°C using 4 mM *p*-NP-XylP, 68 nM BH1068(His)$_6$, 0.1% BSA, and incubation for 40 min at 35°C, followed by quenching with an equal volume of 1 M Na_2CO_3 and absorbance measurement at 400 nm. The buffers used to generate the pH curve were 100 mM citrate for pH 3 to 6.5, 100 mM phosphate for

Table 1 Michaelis–Menten kinetic parameters for hydrolysis of *p*-NP-AraF, *p*-NP-AraP, *p*- and *o*-NP-XylP, and xylobiose.

Substrate[a]	Concentration range (μM)	*K*m (μM)	k_{cat} (s^{-1})	k_{cat}/*K*m (mM^{-1} s^{-1})
p-NP-AraF	16–160	140±59.4	0.0043±0.0011	0.031±0.015
	16–4267	6030±419	0.080±0.0039	0.013±0.001
p-NP-AraP	16–160	713±148	0.15±0.03	0.21±0.06
	16–4267	4540±440	0.82±0.05	0.18±0.02
p-NP-XylP	10–150	30.1±2.97	0.184±0.006	6.10±0.64
	10–4515	3270±907	1.73±0.286	0.53±0.17
o-NP-XylP	10–375	11.5±5.76	0.235±0.021	20.4±10.3
	10–4,000	262±98.0	0.518±0.059	1.98±0.77
Xylobiose	1,040–16,000	30,900±8,100	0.35±0.07	0.011±0.004

[a] BH1068 enzyme concentrations were 163 nM for both *p*-NP-AraF and *p*-NP-AraP, 19 nM for both *p*- and *o*-NP-XylP, and 380 nM for xylobiose. Reaction conditions were 100 mM PO_4, pH 6.5, 45°C with 0.1% BSA. Ten percent or less conversion for *p*-NP-XylP, 8% or less conversion for *o*-NP-XylP, 5% or less conversion for *p*-NP-AraF, 7% or less conversion for *p*-NP-AraP, 2% or less conversion for xylobiose.

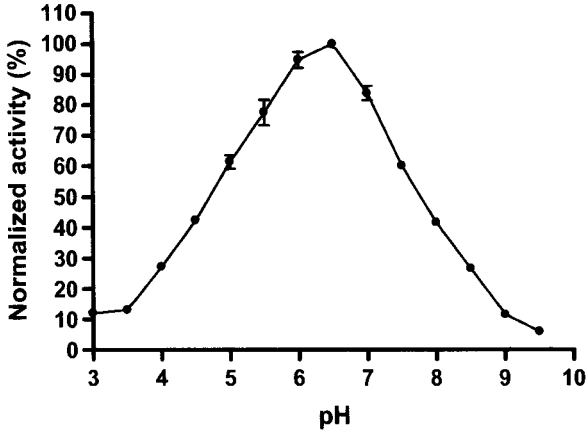


Fig. 1 Relative enzyme activity at the indicated pH values. Enzyme activity was determined with 4 mM *p*-NP-XylP (*circle*). Reaction conditions were as described in "Materials and Methods"

pH 6.5 to 8.0, and 100 mM AMPSO for pH 8.0 to 9.5. Reported values are the average of six determinations.

Thermostability Profiles and Temperature Versus V_{max}

The effect of temperature on enzyme stability (Fig. 2) was determined by first measuring the rate of *p*-NP-XylP hydrolysis before thermal challenge. The assays were performed in triplicate, and the reaction conditions were 45°C, 50 mM phosphate, pH 6.5, 0.1% BSA, 4 mM *p*-NP-XylP, and 19 nM BH1068(His)$_6$. Then 50-µl aliquots of the enzyme solution were transferred to a 96-well PCR plate and subjected to incubation at a series of temperatures ranging from 30 to 88.5°C for 10 min using a temperature gradient PCR machine (MJ Research, Watertown, MA, USA). After thermal treatment, the enzyme activity was again measured to allow calculation of the residual activity. The residual activity was then normalized to the highest recorded initial activity. The data shown in Fig. 2 are the average of either two or three measurements.

The effect of temperature on the apparent V_{max} was determined by performing endpoint assays using 64 nM BH1068(His)$_6$, 50 mM HPO_4 pH 6.5, 0.1% BSA, and 4 mM *p*-NP-

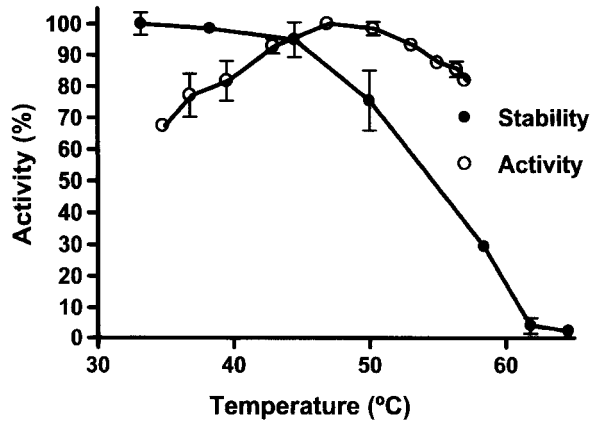


Fig. 2 Enzyme stability at the indicated temperatures (*filled circle*) and enzyme activity (relative V_{max}) at the indicated temperatures (*open circle*). Reaction conditions were as described in "Materials and Methods"

XylP. BH1068(His)$_6$ was incubated for 30 min at the various temperatures, quenched with an equal volume of Na_2CO_3, and *p*-NP release quantitated at 400 nm using a standard curve generated on the same microtiter plate. The data shown in Fig. 2 are the average of either three or four measurements.

Substrate Specificity

Capillary electrophoresis (CE) was used to monitor the degradation of the following natural polymeric substrates: sugar beet arabinan, rye flour arabinoxylan, wheat medium viscosity arabinoxylan (all from Megazyme), birchwood xylan, beechwood xylan, and oat spelt xylan (all from Sigma). The composition of these natural substrates were specified by the supplier as follows. The sugar beet arabinan substrate consisted of a 1,5-α-linked arabinose backbone to which 1,3-α-linked and possibly some 1,2-α-linked L-arabinofuranosyl groups were attached. Approximately 60% of the main-chain arabinofuranosyl residues were substituted by single 1,3-linked arabinofuranosyl groups. The cereal grain natural arabinoxylan substrates had homopolymeric backbones of (1–4)-β-D-xylopyranosyl residues substituted with (1–2)- and/or (1–3)-α-linked L-arabinofuranosyl branch units. The wheat arabinan medium viscosity arabinoxylan had an arabinose/xylose/other sugars ratio of 37:61:2. The rye flour arabinoxylan had a sugar composition of arabinose/xylose/other sugars of 49:48:3. The oat spelt xylan used contained minimally 70% xylose and maximally 10% arabinose and 15% glucose. The xylans from the two hardwoods, birchwood and beechwood, that were also tested were each specified as containing >90% xylose residues. Reaction conditions were overnight incubation at 37°C in 115-μl volume of reaction buffer containing 100 mM phosphate, pH 6.5, 1 μl/ml Calbiochem protease inhibitor cocktail III, 5 mM DTT, 0.1% BSA, and natural substrate concentrations between 0.9 and 2.2 mg/ml and 2.9 μM BH1068(His)$_6$. The samples were centrifuged, and a 100-μL aliquot from each reaction was lyophilized before derivatization. The reaction products formed using xylobiose as the substrate were also analyzed by CE, where the reaction conditions were 380 nM enzyme and 20 mM xylobiose, and reaction conditions were the same as those used for the other natural substrates. For the xylobiose reactions, 4 μl aliquots were removed at time 0 and, subsequently, at 30-min intervals, and the reaction quenched by heating to 100°C. 1-Aminopyrene-3,6,8-trisulphonate (APTS) derivatization was performed by adding 6 μl 100 mM APTS in 15% acetic acid and 12 μl 1 M $NaBH_3CN$ in tetrahydrofuran (THF) and allowing the derivatization reaction to occur overnight at 37°C. The samples were then stored at −20°C, and aliquots were diluted 200 to 400-fold before capillary electrophoresis. Analyses were performed on a P/ACE MDQ capillary electrophoresis system (CE, Beckman Coulter, Inc., Fullerton, CA, USA). Separations were performed using a 20-cm uncoated fused-silica capillary column of 50 μm internal diameter (MicroSolv Technology Corp., Long Branch, NJ, USA). Analyses were carried out at 25°C with an applied voltage of 30 kV using 50 mM phosphate, pH 7.4, as the running electrolyte. A typical run schedule was 0.5 min at 50 psi 0.1 N HCl, 0.5 min at 50 psi H_2O, 0.5 min at 50 psi 0.1 N NaOH, 0.5 min at 50 psi 1 M phosphate at pH 7.4, 4 min at 80 psi 50 mM phosphate at pH 7.4, conditioning at 30 kV for 5 min, injection 5 s at 0.5 psi, and separation at 30 kV. The detection system was a Beckman laser-induced fluorescence detector using an excitation wavelength of 488 nm and detection at 520 nm.

Action on the following artificial aryl-glycoside substrates was tested: *p*-NP-β-D-xylopyranoside (*p*-NP-XylP), *o*-NP-β-D-xylopyranoside (*o*-NP-XylP), *p*-NP-α-L-arabinofuranoside (*p*-NP-AraF), *p*-NP-α-L-arabinopyranoside (*p*-NP-AraP), *p*-NP-β-D-glucopyranoside, *p*-NP-β-D-fucopyranoside, *p*-NP-β-D-galactopyranoside, and *p*-NP-β-D-mannopyranoside (all from Sigma or Research Products International Corporation). Reaction conditions were

37 nM BH1068(His)$_6$, 4 mM aryl-glycoside substrate, 100 mM phosphate buffer at pH 6.5, 0.1% BSA, and 45°C. NP group release was monitored by measuring the change in absorbance at 400 nm.

Results and Discussion

Sequence Analysis

The xylosidases from several bacterial species have been characterized and, based on amino acid sequence similarity, have been classified into glycoside hydrolase (GH) families 3, 39, 43, 52, and 54 in the CAZy classification (P. M. Coutinho and B. Henrissat, http://www.afmb.cnrs-mrs.fr/CAZY) [9]. Phylogenetic analysis of the evolutionary relationship of the amino acid sequence of *BH1068* revealed greatest similarity to GH 39 proteins from *Geobacillus stearothermophilus* T-6 (UniProt Q9ZFM2; 65% identity, 76% consensus), *Thermoanaerobacterium saccharolyticum* (UniProt P36906; 62% identity, 72% consensus), and *Clostridium cellulolyticum* H10 (NCBI protein id ZP_01574178; 61% identity, 73% consensus). These enzymes are all members of the GH family 39 and are predicted to have xylosidase activity. Thus, based on amino acid sequence, BH1068(His)$_6$ belongs to GH family 39; this family has both β-D-xylosidase (EC 3.2.1.37) and α-L-iduronidase (EC 3.2.1.76) as known activities.

Alignment of the amino acid sequences of BH1068(His)$_6$ with xylosidases whose active site residues are known [10, 11] shows high homology around the active-site residues, with Glu160 predicted to be the acid/base catalyst and Glu279 predicted to be the nucleophile (*vide infra*).

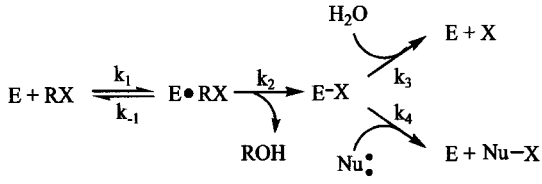
Oligomerization State

The protein BH1068(His)$_6$ eluted as a single peak during gel filtration chromatography with an apparent MW value of ~235 kDa. Thus, the protein eluted as a tetramer under the conditions employed since the calculated subunit MW is 59.3 kDa based on the amino acid sequence predicted for the His-tagged protein. This is in contrast to the results of another study of BH1068(His)$_6$ wherein the data did not allow differentiation between dimeric and trimeric states for the C-terminal His-tagged enzyme [12]. However, the closely related β-xylosidases from *T. saccharolyticum* (62% identity, 72% consensus) and from *Geobacillus stearothermophilus* T-6 (65% identity, 76% consensus) have both been crystallized, and their quaternary structures shown to be tetrameric [10, 11].

Enzyme Kinetic Parameters

The catalytic mechanism of hydrolysis is conserved for all members within a given sequence-based GH family [13, 14] and has been reported to result in retention of the anomeric center in GH family 39 glycohydrolases. In the case of retaining hydrolytic enzymes, a double-displacement reaction ensues [15], and for GH, a pair of carboxyl groups are a central feature of the catalytic site. For retaining GH, one active-site carboxylate acts as a nucleophile where it attacks the sugar anomeric center to form an enzyme-bound covalent intermediate (xylosylation, k_2), whereas the other carboxylate groups acts as a general acid/base catalyst where it protonates the glycosidic oxygen concomitantly with bond cleavage in the first step (general acid catalysis) and deprotonates water in the second step (general base catalysis), resulting in formation of a β-sugar hemiacetal product (dexylosylation, k_3; Eq. 1)

[16–18]. Alternatively, another substrate molecule or other nucleophile can react with the covalent intermediate E–X in a transglycosylation reaction (k_4). This can lead to non-Michaelis–Menten kinetics when the apparent V_{max} continues to increase with increasing substrate concentration caused by an increase in k_4.



(1)

Time-course studies initially performed established that the rate of *p*-NP-XylP substrate hydrolysis under saturating conditions was linear with respect to time (R^2>0.99) for at least 35 min at 45°C. The Michaelis–Menten parameters for hydrolysis of *p*-NP-AraF, *p*-NP-AraP, *o*- and *p*-NP-XylP and xylobiose are shown in Table 1. For all of the substrates tested, deviation from Michaelis–Menten kinetics with increasing substrate concentration was observed, suggesting the participation of transglycosylation in the kinetic scheme. Transglycosylation has previously been observed for a related GH 39 xylosidase from *T. saccharolyticum* with the substrate xylobiose [8, 19] and also with aryl glycosides [8, 17]. *p*-NP-AraF was a very poor substrate, and the kinetic parameters obtained were not precise at low substrate concentrations because of an extremely low k_{cat}. Nevertheless, it can be concluded that while the K_m values for *p*-NP-AraF and *p*-NP-AraP were in the same range at both the low and high substrate concentrations tested, the k_{cat} values for the arabinopyranose aryl glycoside were roughly an order of magnitude greater than the corresponding values for the arabinofuranose congener, with the net result being the specificity factor k_{cat}/K_m was about tenfold larger for *p*-NP-AraP. The K_m for *o*-NP-XylP was in the low micromolar range, and a precise value was not obtained because the lowest substrate concentration tested was on the order of the K_m value for the substrate. However, the xylopyranoside substrates are clearly preferred over the arabinopyranoside substrates, with a 30-fold higher k_{cat}/K_m value at low substrate concentration ranges for *p*-NP-XylP than for the corresponding C4 epimer *p*-NP-AraP. It was interesting to note that the enzyme showed a lesser propensity for transglycosylation with *o*-NP-XylP compared to the *p*-NP analog, where k_{cat} at higher substrate concentrations only doubled for the *o*-NP isomer, compared to a tenfold difference for the *p*-NP isomer. Contributing significantly to the observed differences in hydrolysis rates and propensities for transglycosylation of *o*- and *p*-NP-XylP are differences in the noncovalent enzyme/substrate interactions (e.g., hydrogen bonding) of these stereoelectronically different leaving groups in the active site and the attendant differences in stabilization of their respective oxocarbenium ion-like transition states [16]. Thus, results similar to BH1068(His)$_6$ have previously been reported for a GH family 52 β-xylosidase, where k_{cat} *o*-NP-XylP/k_{cat} *p*-NP-XylP was ~4, whereas K_m values were similar [20]. On the other hand, similar k_{cat} values for *o*- and *p*-NP-XylP hydrolysis have been reported for a phylogenetically closely related GH family 39 β-xylosidase [21].

When xylobiose was tested as a substrate, deviation from Michaelis–Menten kinetics consistent with transglycosylation activity was observed at higher substrate concentrations (up to 16 mM xylobiose was tested). Capillary electrophoresis analysis of the reaction products from xylobiose hydrolysis showed production of significant xylose and xylotriose, corroborating the transglycosylation activity inferred by the kinetic data. Thus, under the

reaction conditions described, after 30 min, roughly 1/2 of the xylobiose had been consumed, yielding xylose and xylotriose in a ~4:1 ratio. Two peaks in the region corresponding to xylotriose were observed on the electropherogram, and it is not clear at this time if that is caused by different isomers of xylotriose being formed. While it appears that the enzyme was able to release xylose from both xylotriose and xylotetraose, the enzyme was inhibited by substrate concentrations greater than ~2 mM for either substrate. Substrate inhibition by xylotriose (K_i=1.7 mM) and no inhibition by xylobiose have previously been observed for a closely related *Thermoanaerobacterium* sp. GH family 39 β-D-xylosidase [8] and for an arabinofuranosidase isolated from a compost starter mixture[22]. The enzyme was not inhibited by up to 200 mM xylose, which is a potentially useful bioprocess characteristic. There is considerable variability in the susceptibility of xylosidases to product inhibition. For example, xylosidase from the fungus *Scytalidium thermophilum* was likewise not inhibited by up to 200 mM xylose [23], whereas a xylosidase from the thermophile *Caldocellum saccharolyticum* had a K_i for xylose of 40 mM [24].

Substrate Specificity

To assign the substrate specificity of BH1068(His)$_6$, a series of artificial and natural substrates were tested. Whereas it has previously been reported that BH1068(His)$_6$ is unable to cleave *p*-NP-AraF and weakly hydrolyzes *p*-NP-β-D-glucopyranoside [12], in this study BH1068(His)$_6$ was able to cleave the arabinofuranosyl, arabinopyranosyl, and xylopyranosyl synthetic aryl substrates, whereas no activity was detected with the other aryl-glycoside synthetic substrates tested. D-xylopyranose, L-arabinofuranose, and L-arabinopyranose are all spatially similar, thereby, rationalizing the multifunctional α-L-arabinofuranosidase/α-L-arabinopyranosidase/β-D-xylosidase activity of BH1068(His)$_6$ with respect to hydrolysis of synthetic substrates containing the relatively good leaving groups *o*-NP (p*K*a=7.22) or *p*-NP (p*K*a=7.18). In the natural substrate, however, the leaving groups are either xylose or arabinose moieties, which are very poor leaving groups with p*K*a>12. When hydrolysis of natural substrate glycosidic bonds by BH1068(His)$_6$ was tested, only release of xylose was observed by CE from rye, wheat, oat-spelt, beech, and birch arabinoxylan. Also, it was found that BH1068(His)$_6$ does not hydrolyze sugar beet arabinan containing (1–3)-α-linked L-arabinofuranosyl branch units. With respect to natural substrate specificity, it can, therefore, be concluded that BH1068(His)$_6$ is specific for hydrolyzing xylopyranosyl units.

pH Curve

Whereas alkaliphiles such as *B. halodurans* C-125 grow optimally at pH values above 9, the intracellular pH range is thought to be in the range between 7 and 8.5, and the pH optima of intracellular enzymes would be expected to be in this range [25]. A sharp pH optima was observed at pH 6.5 for BH1068(His)$_6$, in the same range as that found for several other xylanolytic activities isolated from this organism. Thus, two types of xylanase from *Bacillus halodurans* C-125 have been expressed in *E. coli*; xylanase N had a pH optima between 6 and 7, whereas xylanase A had a broad activity range from pH 6 to 10 [26]. A GH family 8 reducing-end xylose-releasing exooligoxylanase gene has also been expressed from this organism (*BH2105*) and was found to have a pH optimum of 6.2 to 7.3 [27]. Similar pH optima were also found for four xylanases isolated from thermophilic *Bacillus* strains; the optima for strains W1 and W3 was pH 6.0, and for strains W2 and W4, the optima were between pH 6 and 7 [28].

Thermal Stability and T_{max}

The enzyme was stable for 10 min up to 45°C, whereas the activity decreased rapidly to ~30% after 10 min at 55°C (Fig. 2). The temperature maximum (T_{max}) was found to be 47°C under the conditions tested (30 min endpoint assays), whereupon activity rapidly diminished, possibly because of enzyme thermal instability.

Acknowledgment The mention of firm names or trade products does not imply that they are endorsed or recommended by the US Department of Agriculture over other firms or similar products not mentioned. All programs and services of the US Department of Agriculture are offered on a non-discriminatory basis without regard to race, color, national origin, religion, sex, age, marital status, or handicap.

References

1. Bajpai, P. (1997). *Advances in Applied Microbiology, 43*, 141–195.
2. Rahman, A. K. M. S., Sugitani, N., Hatsu, M., & Takamizawa, K. (2003). *Canadian Journal of Microbiology, 49*, 58–64.
3. Sørensen, H. R., Pedersen, S., Viksø-Nielsen, A., & Meyer, A. S. (2005). *Enzyme and Microbial Technology, 36*, 773–784.
4. Saha, B. C. (2003). *Journal of Industrial Microbiology & Biotechnology, 30*, 279–291.
5. Biely, P. (2003). In J. R. Whitaker, A. G. J. Voragen, & D. W. S. Wong (Eds.) *Handbook of food enzymology* pp. 879–915. New York: Marcel Dekker.
6. Shallom, D., & Shoham, Y. (2003). *Current Opinion in Microbiology, 6*, 219–228.
7. Beg, Q. K., Kapoor, M., Mahajan, L., & Hoondal, G. S. (2001). *Applied Microbiology and Biotechnology, 56*, 326–338.
8. Wagschal, K., Franqui-Espiet, D., Lee, C. C., Robertson, G. H., & Wong, D. W. S. (2005). *Applied and Environmental Microbiology, 71*, 5318–5323.
9. Coutinho, P. M., & Henrissat, B. (1999). In H. J. Gilbert, D. Davies, B. Henrissat, & B. Svensson (Eds.) *Recent advances in carbohydrate bioengineering* pp. 3–12. Cambridge: The Royal Society of Chemistry.
10. Czjzek, M., David, A. B., Bravman, T., Shoham, G., Henrissat, B., & Shoham, Y. (2005). *Journal of Molecular Biology, 353*, 838–846.
11. Yang, J. K., Yoon, H. J., Ahn, H. J., Lee, B. I., Pedelacq, J. D., & Liong, E. C., et al. (2004). *Journal of Molecular Biology, 335*, 155–65.
12. Smaali, I., Rémond, C., & O'Donohue, M. J. (2006). *Applied Microbiology and Biotechnology, 73*, 582–590.
13. Davies, G., & Henrissat, B. (1995). *Structure, 3*, 853–859.
14. Gebler, J., Gilkes, N., Claeyssens, M., Wilson, D., Beguin, P., & Wakarchuk, W., et al. (1992). *Journal of Biological Chemistry, 267*, 12559–12561.
15. Koshland, D. E. (1953). *Biological Reviews, 28*, 416–436.
16. Zechel, D. L., & Withers, S. G. (2000). *Accounts of Chemical Research, 33*, 11–18.
17. Vocadlo, D. J., Wicki, J., Rupitz, K., & Withers, S. G. (2002). *Biochemistry, 41*, 9727–9735.
18. Ly, H. D., & Withers, S. G. (1999). *Annual Reviews of Biochemistry, 68*, 487–522.
19. Lee, Y.-E., & Zeikus, G. (1993). *Journal of General Microbiology, 139*, 1235–1243.
20. Bravman, T., Belakhov, V., Solomon, D., Shoham, G., Henrissat, B., Baasov, T., & Shoham, Y. (2003). *Journal of Biological Chemistry, 278*, 26742–26749.
21. Vocadlo, D. J., Wicki, J., Rupitz, K., & Withers, S. G. (2002). *Biochemistry, 41*, 9736–9746.
22. Wagschal, K., Franqui-Espiet, D., Lee, C. C., Kibblewhite-Accinelli, R. E., Robertson, G. H., & Wong, D. W. S. (2007). *Enzyme and Microbial Technology, 40*, 747–753.
23. Zanoelo, F. F., de Lourdes Teixeira de Moraes Polizeli, M., Terenzi, H. F., & Jorge, J. A. (2004). *Journal of Industrial Microbiology & Biotechnology, 31*, 170–176.
24. Hudson, R. C., Schofield, L. R., Coolbear, T., Daniel, R. M., & Morgan, H. W. (1990). *Biochemical Journal, 273*, 645–650.
25. Horikoshi, K. (2004). *Proceedings of the Japan Academy, Series B, 80*, 166–178.
26. Honda, H., Kudo, T., Ikura, Y., & Horikoshi, K. (1985). *Canadian Journal of Microbiology, 31*, 538–542.
27. Honda, Y., & Kitaoka, M. (2004). *Journal of Biological Chemistry, 279*, 55079–55103.
28. Okazaki, W., Akiba, T., Horikoshi, K., & Akahoshi, R. (1985). *Agricultural and Biological Chemistry, 49*, 2033–2039.

Appl Biochem Biotechnol (2008) 146:79–87
DOI 10.1007/s12010-007-8074-2

Heterologous Expression of Two Ferulic Acid Esterases from *Penicillium funiculosum*

Eric P. Knoshaug · Michael J. Selig · John O. Baker · Stephen R. Decker · Michael E. Himmel · William S. Adney

Received: 25 May 2007 / Accepted: 27 September 2007 /
Published online: 7 December 2007
© Humana Press Inc. 2007

Abstract Two recombinant ferulic acid esterases from *Penicillium funiculosum* produced in *Aspergillus awamori* were evaluated for their ability to improve the digestibility of pretreated corn stover. The genes, *faeA* and *faeB*, were cloned from *P. funiculosum* and expressed in *A. awamori* using their native signal sequences. Both enzymes contain a catalytic domain connected to a family 1 carbohydrate-binding module by a threonine-rich linker peptide. Interestingly, the carbohydrate binding-module is N-terminal in FaeA and C-terminal in FaeB. The enzymes were purified to homogeneity using column chromatography, and their thermal stability was characterized by differential scanning microcalorimetry. We evaluated both enzymes for their potential to enhance the cellulolytic activity of purified *Trichoderma reesei* Cel7A on pretreated corn stover.

Keywords Ferulic acid esterase · Hemicellulose · Cellulose · Biomass digestion · Heterologous expression

Introduction

The use of lignocellulosic materials from agricultural crops for the production of fuels and chemicals has received a considerable amount of interest recently and is a major part of the Advanced Energy Initiative outlined by the President of the United States in both the 2006 and 2007 State of the Union addresses [1]. Currently, ethanol derived from biomass is produced by the conversion of either sugar or starch containing crops. The production of

E. P. Knoshaug (✉)
National Bioenergy Center, National Renewable Energy Laboratory, Golden, CO 80401, USA
e-mail: eric_knoshaug@nrel.gov

M. J. Selig · J. O. Baker · S. R. Decker · M. E. Himmel · W. S. Adney
Chemical and Biosciences Center, National Renewable Energy Laboratory, Golden 80401 CO, USA

ethanol from lignocellulosic agricultural residues has become increasingly important due to the volumetric limitations of using corn kernels and will directly address the United States goal of reducing gasoline usage by 20% in the next 10 years [1]. Examples of underutilized lignocellulosic materials that are produced in large quantities worldwide include maize stem, wheat, barley, rice, and rye straw.

Lignocellulosic materials, having a structure and composition that is recalcitrant to degradation, require pretreatment followed by enzymatic hydrolysis to obtain soluble sugars for fermentation. It is thus critical that pretreatment and enzymatic saccharification maximize the release of these soluble sugars. One barrier to efficient sugar release is the degree of accessibility of the crystalline cellulose to the saccharification enzymes. Plant cell walls are structurally complex with networks of cross-linked hemicellulose and lignin intercalated between the cellulose fibrils. The natural breakdown of plant cell wall material requires the synergistic action of several enzymes including those that break ester cross-links between lignin and xylan. Ferulic acid is a hydroxycinnamic acid that cross-links hemicelluloses and lignin in plant cell walls through ester linkages [2]. This lignin/carbohydrate complex may contribute to the natural recalcitrance of biomass to microbial degradation. Microbial feruloyl esterases (EC 3.1.1.73) are generally secreted, catalyze the hydrolysis of ester and ether bridges between hydroxycinnamic acids and polysaccharides and/or lignins in plant cell walls, and have been classified into four groups based on substrate utilization: A, B, C, D [3].

An important characteristic of enzymes having plant cell wall deconstruction activities is the presence of a carbohydrate binding module (CBM). These modules have been found on enzymes with a wide range of activities and are crucial to targeting the enzyme at the substrate level leading to increased activity on insoluble substrates [4]. Interestingly, the majority of known fungal ferulic acid esterases do not contain CBMs. Those without CBMs include FaeA and FaeB from *Aspergillus niger* [5, 6], FaeB and FaeD from *Neurospora crassa* [7, 8], and FaeC from *Talaromyces stipitatus* [9]. However, while the gene encoding FaeB from *T. stipitatus* has not been fully sequenced, it does show significant sequence homology to FaeB from *Penicillium funiculosum*, which does have a CBM [10]. This lack of a CBM in the majority of the ferulic acid esterases is somewhat surprising, as CBMs have been shown to be required for maximal utility for a variety of cellulolytic enzymes [4].

Here, we report the heterologous expression of two ferulic acid esterases from *P. funiculosum* and their ability to enhance the release of cellobiose by *Trichoderma reesei* Cel7A from pretreated corn stover.

Materials and Methods

Media, Strains, Plasmid Construction, and Genetic Techniques

Genomic DNA from *P. funiculosum* ATCC 62998 grown in CM-glucose media [11] was isolated using the DNeasy Plant Maxi Kit (Qiagen, cat. no. 68161) as per the manufacturer's directions. The genes *faeA* (AJ312296) and *faeB* (AJ291496) were amplified by the PCR and the appropriate primers (Table 1) for sub-cloning into the fungal expression vector, pFE2 [11]. The following cycle parameters and the PfuTurbo polymerase (Stratagene, cat. no. 600250) were used; 99 °C 10 min, 30 cycles of 95 °C for 30 s, 58 °C for 1 min, 72 °C for 2:30 min, followed by a final extension at 72 °C for 5 min. The PCR product was cloned into the pCR2.1-TOPO vector (Invitrogen, cat. no. K4510–20) for recovery then sub-cloned into the

Table 1 PCR primers.

Primer name	Sequence
FaeAfor	**CCTCAGC**AATGGTGAAATCGTACATTATCGGGGCAT
FaeArev	**TCTAGA**TTAGTGGAATAGAGAGAAGAAACTCCAGAT
FaeBfor	**CCTCAGC**ATGGCGATTCCCTTGGTCCT
FaeBrev	GA**TCTAGA**TCACAGGCACTGGGAATAATAATCGT

Start and stop codons are underlined. Restriction sites used for sub-cloning into pFE2 are in bold (*Bbv*CI and *Xba*I).

pFE2 vector for fungal expression. Plasmid DNA of the expression vector–gene construction from a large-scale isolation (Qiafilter Plasmid Maxi Kit, Qiagen, cat. no. 12262) was sequenced using the Applied Biosystems Automated 3730 DNA Analyzer and Big Dye Terminator chemistry with AmpliTaq-FS DNA Polymerase at the Cornell Biotechnology Resource Center. *Aspergillus awamori* ATCC 22342 was transformed as described [11]. Spores from potential transformants were frozen for later use.

Protein Expression and Purification

Frozen *A. awamori* spores were thawed and inoculated into 50 ml CM-maltose medium and grown at 32 °C, 225 rpm in 250 ml baffled flasks. After 2–3 days, the cultures were transferred to 1.0 l CM-maltose fermentation medium in 2,800 ml Fernbach flasks and grown in the above conditions. The flasks were harvested by filtration through Miracloth (Calbiochem, cat. no. 475855) after 4–6 days of growth and frozen at −20 °C. The broth was thawed and clarified through a glass fiber filter (Pall Life Sciences, cat. no. 66084). Protein was allowed to precipitate out in 90% ammonium sulfate for 2 days at 4 °C, then centrifuged at 9,000×*g* for 20 min at 4 °C for removal from the supernatant. Precipitated protein was dissolved in 20 mM Bis–Tris at pH 6.8 and desalted on a Pharmacia Hi-Prep Desalting (GE Healthcare Bio-Sciences, Uppsala, Sweden) column into 20 mM Bis–Tris pH 6.8. The desalted proteins were separated by anion exchange chromatography using a FineLine Pilot 35 column (GE Healthcare Bio-Sciences, Uppsala, Sweden) packed with 96 ml of Resource SourceQ (GE Healthcare Bio-Sciences, Uppsala, Sweden) in 20 mM Bis–Tris pH 6.8 as the running buffer over a 0- to 1-M NaCl gradient. Both proteins eluted in a sharp peak within the initial 5% of the salt gradient. Purified FaeA was then buffer-exchanged into 20 mM sodium acetate, 100 mM NaCl at pH 5.0 (SEC buffer) using a 26/60 SuperDex200 size exclusion chromatography (SEC) column (GE Healthcare Bio-Sciences, Uppsala, Sweden) aliquoted, and stored at −80 °C. Pooled FaeB fractions were further purified on a Resource ISO (1 ml) HIC column (GE Healthcare Bio-Sciences, Uppsala, Sweden) running 20 mM sodium acetate buffer at pH 5.0 over a 1.5- to 0-M ammonium sulfate gradient. Purified FaeB was then buffer-exchanged, aliquoted, and stored as above. Purity of the proteins was verified by sodium dodecyl sulfate-polyacrylamide gel electrophoresis (SDS-PAGE), and each was quantified by absorbance at 280 nm. Purified proteins were sequenced at the Cornell Proteomics and Mass Spectrometry core facility as described [12]. *T. reesei* Cel7A was purified chromatographically from Spezyme CP (Genencor International Inc., Palo Alto, CA) via two anion exchange steps followed by an affinity step. Spezyme CP was diafiltered into 20 mM Bis–Tris pH 6.2 using an Amicon CH-2 hollow fiber concentrator (Amicon, Beverly, MA.) equipped with PM10 cartridges and

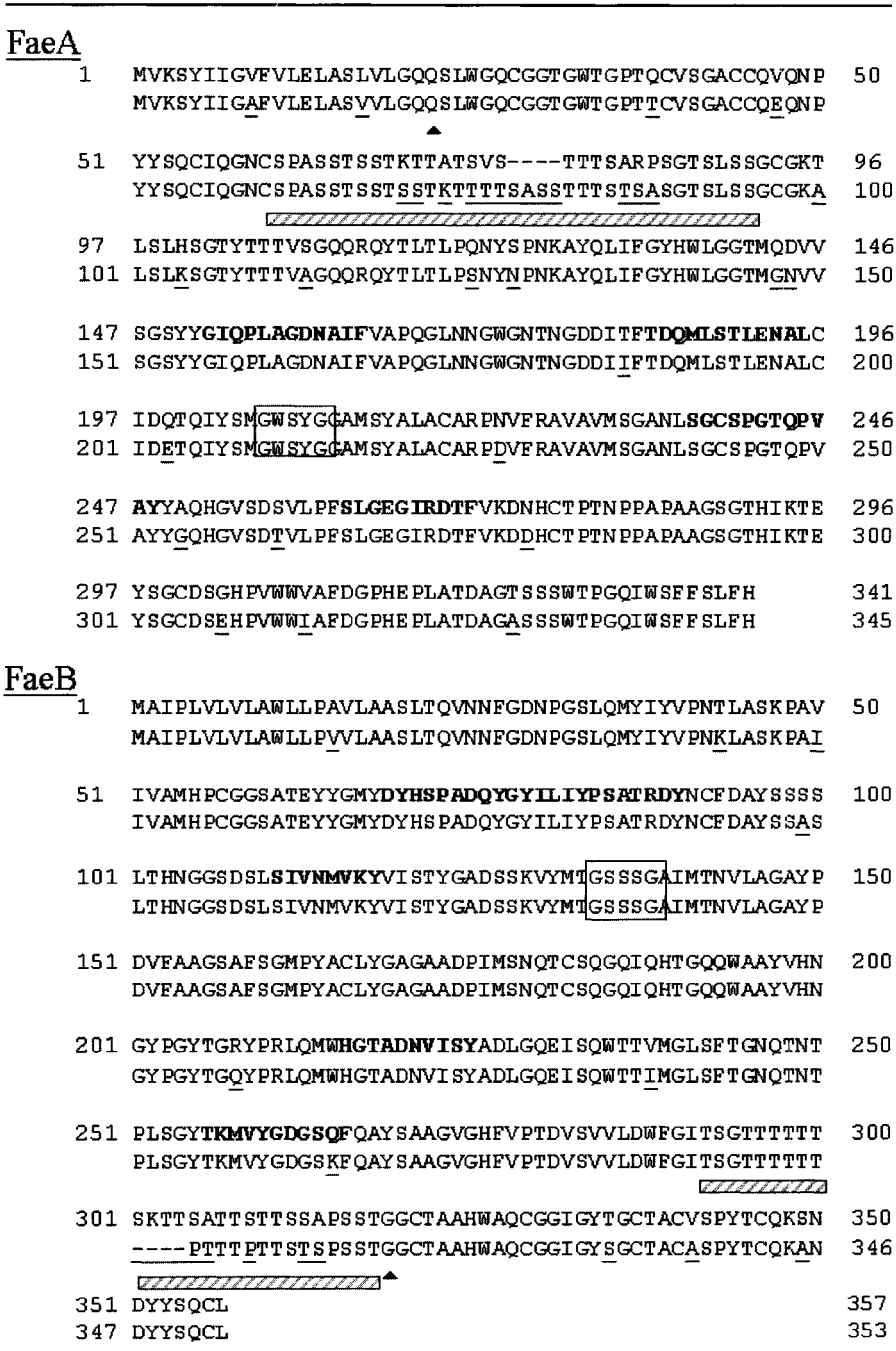


Fig. 1 Alignments of our sequence (*top*) and the sequences deposited in GenBank (*bottom*). Amino acids are *numbered on either end* and differences in AA sequences are *underlined*. Peptides isolated by sequencing are in *bold*. *Symbols* are located under the corresponding sequences: *closed triangles*; Putative start of the family 1 CBM. *Hatch filled boxes* delineate linker regions. The GXSXG sequence of the conserved serine protease motif is *enclosed in a box*

loaded onto a 53-ml DEAE anion exchange column (GE Healthcare Bio-Sciences, Uppsala, Sweden). Bound proteins were eluted with a linear 0 to 1.0 M NaCl gradient in the same buffer. Fractions containing Cel7A were pooled, desalted, and loaded onto a 200-ml SourceQ anion exchange column (GE Healthcare Bio-Sciences, Uppsala, Sweden). Cel7A was eluted with a 0.0- to 1.0-M NaCl gradient, and active fractions were pooled and bound to SigmaCell 101 (SigmaAldrich, St. Louis, MO) with cellulose loadings of 0.1 g/ml. After binding overnight at 4 °C, the cellulose was washed twice with SEC buffer via centrifugation (4,000×*g*) to remove unbound protein. Bound Cel7A was eluted with 100% ethylene glycol and concentrated with a 10-kDa PES MWCO membrane in a stirred pressure cell (Amicon, Beverly, MA.) before buffer exchange on a 26/60 SuperDex200 SEC column into SEC buffer.

Protein Stability Measurements

The thermal stability of the proteins was measured by differential scanning microcalorimetry (DSC) using a Microcal model VP-DSC calorimeter (Microcal, Inc., Northampton, MA), with data analysis by Origin for DSC software (Microcal). Thermograms were collected for samples containing 50 μg/ml protein at pH 5.0 in SEC buffer. Calorimeter scan rate was 60 °C/h.

Ferulic Acid Esterase Activity Analysis

Activity of the purified enzymes was assessed on methyl ferulate (methyl 4-hydroxy 3-methoxy cinnamate, MF). Assays were run for 30 min at 50 °C in 50 mM citrate buffer at pH 4.8 with initial MF concentrations of 50 to 750 μM and an enzyme concentration of 50 nM. The reactions were terminated after 30 min by boiling for 10 min and analyzed for MF and ferulic acid content via C18 high performance liquid chromatography (HPLC) over a 0 to 100% acetonitrile gradient with 0.1% formic acid in all solutions. Preliminary isothermal titration calorimetry (ITC) on both ferulic acid esterase proteins was conducted in SEC buffer on a Microcal VP-ITC system. All reactions were carried out at 37 °C using MF as a substrate.

Corn Stover Digestions

The corn stover used for this study was harvested in 2003 at the Kramer Farm in Wray, Colorado. The stover was pretreated in a flow-through hot water pretreatment reactor at Dartmouth College under subcontract with the National Renewable Energy Laboratory (NREL). The pretreatment was conducted at 200 °C for 16 min with a 2.5% (*w*/*v*) solid loading. Carbohydrate and lignin composition of the pretreated material was determined by a two-stage sulfuric acid hydrolysis treatment using NREL Laboratory Analytical Procedure "Determination of Structural Carbohydrates and Lignin in Biomass" [13]. Briefly, 300 mg of biomass is hydrolyzed by 3.0 ml 72% (*w*/*v*) H_2SO_4 for 1 h at 30 °C with stirring every 5–10 min. After dilution to 4% H_2SO_4 (*w*/*v*), the sample was autoclaved at 121 °C for 1 h. Aliquots were analyzed by UV absorbance for acid soluble lignin, gravimetrically for acid-insoluble lignin, and by HPLC for structural sugars. The glucan, xylan, and lignin content of the pretreated material was 0.59, 0.14, and 0.19 g/g, respectively. Digestions were run with 2.5 mg FaeA or FaeB /g cellulose in addition to 10 mg Cel7A/g cellulose for 24 h at 50 °C in 50 mM citrate buffer, pH 4.8, with the biomass loaded to achieve a 1.0% (*w*/*v*) glucan concentration in solution. FaeA and FaeB were assessed separately and in combination with each other.

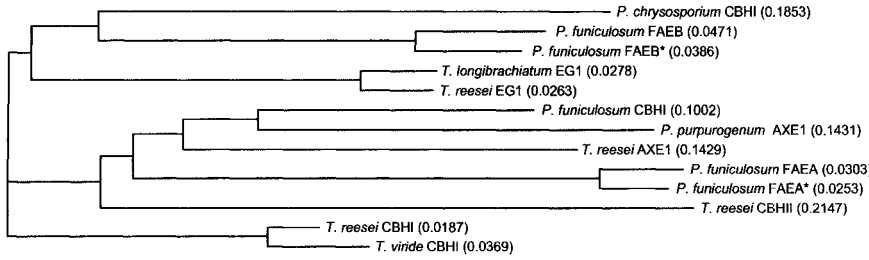


Fig. 2 Relatedness of FaeA and FaeB Family One CBMs. *asterisks*: denotes our sequence for FaeA or FaeB

Results and Discussion

Cloning and Heterologous Expression

The genes *faeA* and *faeB* were amplified from genomic DNA of *P. funiculosum* using the PCR and cloned into the pCR2.1-TOPO vector. The genes were then sub-cloned into the fungal expression vector pFE2 [11] at the *Bbv*CI and *Xba*I sites to allow for fungal expression driven by the glucoamylase promoter with secretion based on the gene's native signal sequence. The sequence of the cloned DNA revealed that one intron was present in each gene. These introns were left intact and were properly processed by *A. awamori* as shown by the expression of a functional protein.

Several amino acid differences between our cloned sequences and the sequences reported in GenBank for *faeA* (AJ312296; no specific strain designation was given) and *faeB* (AJ291496; *P. funiculosum* IMI-134756), respectively, were present (Fig. 1). It is not surprising and quite common that minor AA sequence differences are present in the same proteins from different strains. Peptide sequences derived from chymotrypsin digests followed by nano-liquid chromatography/mass-spectrometry/mass spectrometry (LC-MS/MS) analysis were used for positive identification of the purified enzymes. Four peptides were recovered for each protein representing 13 and 14% coverage of FaeA and FaeB, respectively (Fig. 1).

Both enzymes have a family 1 CBM; however, they differ in that the carbohydrate binding module is N-terminal in FaeA and C-terminal in FaeB (Fig 1). This situation mirrors that of Cel6A (N-terminal CBM) and Cel7A (C-terminal CBM) of *T. reesei*. The

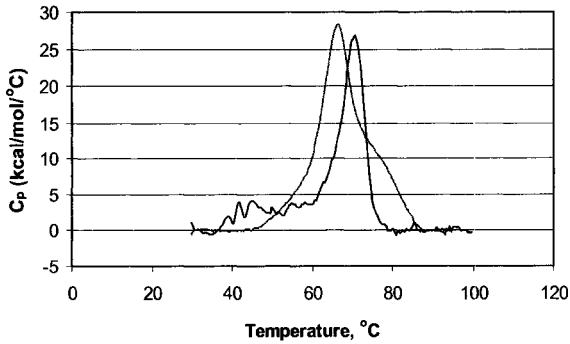


Fig. 3 Thermal stability of FaeA and FaeB. DSC thermograms were acquired as described in the Materials and Methods section

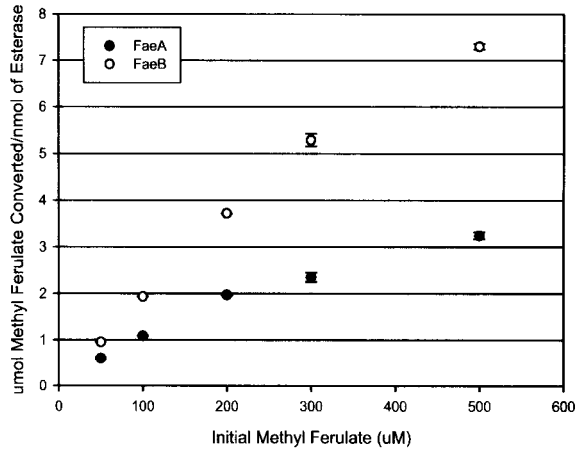


Fig. 4 Activity of the two esterases on methyl ferulate. *filled circles*: FaeA; *empty circles*: FaeB

CBM's of our sequences have two and three AA differences for FaeA and FaeB, respectively, compared to the sequences listed in GenBank. As a result of these AA differences, the sequences we cloned are slightly closer to their respective branch points than for the sequences currently deposited in GenBank as estimated by the neighbor-joining method [14] (Fig. 2). We did not characterize the CBM–cellulose interaction of FaeA and FaeB. Both enzymes bound effectively to Sigmacell 101 as a step in our initial purification, but due to concerns about the effects of eluting with ethylene glycol, we did not use this step in our final purification scheme (data not shown). It is curious that enzymes that do not act on crystalline cellulose have a CBM that effectively binds crystalline cellulose. One hypothesis is that the CBM allows the enzyme to maintain a higher effective concentration near its preferred substrate; thus, by binding to cellulose, the ferulic acid esterases can more effectively target their activity. In this regard, the enzymes from *P. funiculosum* are unique in possessing CBMs, and as more ferulic acid esterases are sequenced and characterized, it will be interesting to see whether the majority of these enzymes contain or lack CBMs.

Thermal Stability Determination

The enzyme FaeB has previously been described [10], but thermal stability was not measured. In addition, the sequence for *FaeA* has been deposited in GenBank; however,

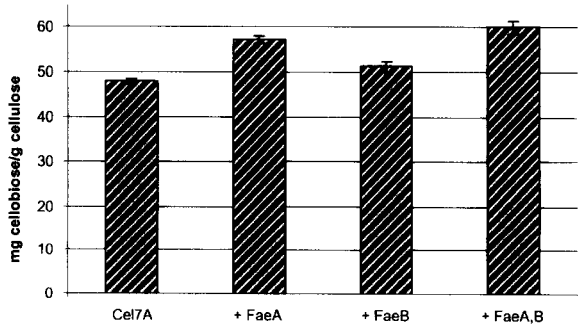


Fig. 5 Digestion of hot water pretreated corn stover with various enzyme combinations. Digestions were carried out for 24 h as described in the Materials and Methods section

there are no reports concerning that enzyme. Thermograms acquired by DSC showed that FaeB is slightly more thermally stable (T_{max} = 70.4 °C) than FaeA (T_{max} = 66.3 °C) when heterologously expressed (Fig. 3). Due to possible differences in the extent of glycosylation, their thermal stabilities when expressed in a recombinant host may differ from those when the proteins are expressed in their native host [15].

Activity Assays and Corn Stover Digestions

Activity assays on MF show that both esterases have activity when heterologously expressed in *A. awamori* (Fig. 4). FaeB was more active than FaeA, hydrolyzing the bulk of the available substrate during the 30-min incubation period. The identical loading of FaeA, in most cases, only consumed about half of the initial MF in each assay. Both enzymes are known to be active on MF with group A enzymes preferring methoxy substitutions on the phenolic ring, while group B enzymes prefer the hydroxyl substitutions [3]. In addition, preliminary ITC experiments with MF were run on both ferulic acid esterase proteins. The reactions of both proteins appears to be mildly endothermic, with apparent heats of reaction estimated as ~1,400 and ~2,000 cal/mol of MF reacted for FaeA and FaeB, respectively. The relatively small heats of reaction have made detailed kinetic analysis of the proteins on this substrate difficult to accurately discern in the presence of baseline drift in the calorimetry runs.

Previously, we have reported the presence of FaeA to be beneficial during the hydrolysis of hot water pretreated corn stover by the cellobiohydrolase Cel7A [16]. In this study, FaeA had a significant impact on Cel7A performance, releasing an additional 19% cellobiose, whereas the benefits of FaeB addition were smaller, releasing only an additional 7% cellobiose. The combination of the two esterase enzymes, however, had an additive gain releasing an additional 25% cellobiose (Fig. 5). Clearly, adding additional accessory enzyme activities can be beneficial in maximizing the enzymatic saccharification of recalcitrant lignocellulosic agricultural residues such as corn stover.

Conclusions

The ferulic acid esterase genes, *faeA* and *faeB*, from *P. funiculosum* were expressed in *A. awamori*, and after purification, the proteins were identified as FaeA and FaeB, respectively, by nano-LC/MS/MS peptide sequencing analysis. The heterologously expressed enzymes were determined to be active as judged by their ability to hydrolyze MF to ferulic acid and by their ability to increase the cellobiose release in digestions of pretreated corn stover with Cel7A. Additional studies involving the digestion of biomass with various enzymatic components will be critical to gain a more comprehensive understanding of the synergistic effects of individual enzymes on biomass deconstruction and will help in deconvoluting the myriad enzymatic pathways fungi have evolved to degrade complex recalcitrant materials present in their native habitats. With a better understanding of these synergisms, the development of an enzymatic suite capable of this same degradation in a timely fashion in the modern biorefinery will be greatly facilitated.

Acknowledgements We acknowledge Dartmouth College for the pretreatment of the corn stover and the MS-based protein identification service work provided by the Cornell Proteomics and Mass Spectrometry core facility. This work was funded by the Department of Energy Office of the Biomass Program.

References

1. *Advanced Energy Initiative*, House, T. W., Editor, (2006), National Economic Council.
2. Sun, R. C., Sun, X. F., & Zhang, S. H. (2001). *Journal of Agricultural and Food Chemistry, 49*, 5122–5219.
3. Crepin, V. F., Faulds, C. B., & Connerton, I. F. (2004). *Applied Microbiology and Biotechnology, 63*(6), 647–652.
4. Linder, M., & Teeri, T. T. (1997). *Journal of Biotechnology, 57*(1–3), 15–28.
5. De Vries, R. P., Michelsen, B., Poulsen, C. H., Kroon, P. A., Van Den Heuvel, R. H. H., et al. (1997). *Applied and environmental microbiology, 63*(12), 4638–4644.
6. De Vries, R. P., Vankuyk, P. A., Kester, H. C. M., & Visser, J. (2002). *Biochemical Journal, 363*, 377–386.
7. Crepin, V. F., Faulds, C. B., & Connerton, I. F. (2004). *Applied Microbiology and Biotechnology, 63*(6), 567–570.
8. Crepin, V. F., Faulds, C. B., & Connerton, I. F. (2003). *Biochemical Journal, 370*, 417–427.
9. Garcia-Conesa, M. T., Crepin, V. F., Goldson, A. J., Williamson, G., Cummings, N. J., Connerton, I. F., et al. (2004). *Journal of Biotechnology, 108*, 227–241.
10. Kroon, P. A., Williamson, G., Fish, N. M., Archer, D. B., & Belshaw, N. J. (2000). *European Journal of Biochemistry, 267*, 6740–6752.
11. Adney, W. S., Chou, Y. C., Decker, S. R., Ding, S. Y., Baker, J. O., Kunkel, G., et al. (2003). *Heterologous expression of Trichoderma reesei 1,4-beta-D-glucan cellobiohydrolase (Cel 7A). in Applications of Enzymes to Lignocellulosics*. Washington, Amer: Chemical Soc.
12. Morris, R. M., Fung, J. M., Rahm, B. G., Zhang, S., Freedman, D. L., Zinder, S. H., & Richardson, R. E. (2007). *Applied and Environmental Microbiology, 73*(1), 320–326.
13. Sluiter, A., Hames, B., Ruiz, R., Scarlata, C., Sluiter, J., & Templeton, D. (2004). *Determination of Structural Carbohydrates and Lignin in Biomass*, DOE, Editor, National Renewable Energy Laboratory.
14. Saitou, N., & Nei, M. (1987). *Molecular Biology and Evolution, 4*, 406–425.
15. Chu, F. K., Trimble, R. B., & Maley, F. (1978). *Journal of Biological Chemistry, 253*, 8691–8693.
16. Selig, M. J., Knoshaug, E. P., Adney, W. S., Himmel, M. E., & Decker, S. R. (2007). Synergistic enhancement of cellobiohydrolase performance on pretreated corn stover by addition of xylanase and esterase activities. *Bioresource Technology* (2007). DOI 10.1016/j.biortech.2007.09.064.

Appl Biochem Biotechnol (2008) 146:89–100
DOI 10.1007/s12010-007-8129-4

Evaluation of a *Hypocrea jecorina* Enzyme Preparation for Hydrolysis of Tifton 85 Bermudagrass

E. A. Ximenes · S. K. Brandon · J. Doran-Peterson

Received: 30 May 2007 / Accepted: 13 December 2007 /
Published online: 29 January 2008
© Humana Press Inc. 2008

Abstract Tifton 85 bermudagrass, developed at the ARS-USDA in Tifton, GA, is grown on over ten million acres in the USA for hay and forage. Of the bermudagrass cultivars, Tifton 85 exhibits improved digestibility because the ratio of ether- to ester-linked phenolic acids has been lowered using traditional plant breeding techniques. A previously developed pressurized batch hot water (PBHW) method was used to treat Tifton 85 bermudagrass for enzymatic hydrolysis. Native grass (untreated) and PBHW-pretreated material were compared as substrates for fungal cultivation to produce enzymes. Cellulase activity, measured via the filter paper assay, was higher for fungi cultivated on PBHW-pretreated grass, whereas the other nine enzyme assays produced higher activities for the untreated grass. Ferulic acid and vanillin levels increased significantly for the enzyme preparations produced using PBHW-pretreated grass and the release of these phenolic compounds may have contributed to the observed reduction in enzyme activities. Culture supernatant from Tifton 85 bermudagrass-grown fungi were combined with two commercial enzyme preparations and the enzyme activity profiles are reported. The amount of reducing sugar liberated by the enzyme mixture from *Hypocrea jecorina* (after 192 h incubation with untreated bermudagrass) individually or in combination with feruloyl esterase was 72.1 and 84.8%, respectively, of the commercial cellulase preparation analyzed under the same conditions.

Keywords Bermudagrass · *Trichoderma* · *Hypocrea* · Cellulases · Hemicellulases

Introduction

Global demand for food is expected to double within the next 50 years, and global demand for transportation fuels is expected to increase even more rapidly [1]. Diversion of ethanol production from food and feed can be reduced if other agricultural and forestry products are considered for this purpose [2]. There is also a great need for renewable energy supplies

E. A. Ximenes · S. K. Brandon · J. Doran-Peterson (✉)
204 Biological Sciences, Microbiology Department, University of Georgia,
Athens, GA 30602-2605, USA
e-mail: jpeterso@uga.edu

that do not cause significant environmental harm. Biofuels such as cellulosic ethanol have potential to provide fuel supplies with greater environmental benefits than either petroleum or current food-based biofuels [3].

Crops such as bermudagrass (*Cynodon dactylon* L.) have the capacity to produce large quantities of lignocellulose as substrates for biofuels production. Bermudagrass is already grown on 10–15 million acres throughout the southern United States for hay and forage. Genetic improvements in digestibility obtained by traditional plant breeding [4, 5] are directly related to the ability to digest the biomass with enzymes [6]. Tifton 85 is a variety of bermudagrass with improved animal digestibility developed at the ARS-USDA (Tifton, GA). Phenolic acids occurring within grass cell walls are associated with lignin and are recalcitrant to biodegradation [7, 8], thus inhibiting sugar release from the biomass [6]. Prior studies indicate a negative relationship between ether-linked ferulic acid concentrations and extent of digestibility among bermudagrass cultivars [9]. Tifton 85 bermudagrass exhibits improved digestibility because the ratio of ether- to ester-linked phenolic acids has been lowered using traditional plant breeding techniques [4, 5].

Three steps are involved in bioconversion of grasses to ethanol: (1) a pretreatment process to reduce substrate recalcitrance, (2) enzymatic hydrolysis of cellulose and hemicellulose components to simple sugars, and (3) fermentation of the sugars to ethanol. The first two steps are considered to be economic hurdles for full-scale process commercialization [10, 11]. Pretreatments help to increase the rate and extent of hydrolysis by chemicals, enzymes, or microorganisms, and improve the action of enzymes to increase sugar yields. An ideal pretreatment is cost-effective and avoids the loss of potential sugars and formation of inhibitory by-products [2]. Pressurized batch hot water pretreatment (PBHW) [12] of plant materials provides an effective way to pretreat cellulosic material by disrupting hemicellulose before enzymatic hydrolysis without using chemicals such as sulfuric acid, lime, or ammonia. Liquid water at 220°C has a pH of approximately 5.5 as a result of an ion product of 10^{-11} [13], and exposure of biomass causes liberation of acetyl groups from hemicellulose and increases depolymerization. These reactions decrease the pH of the solution further, mimicking very dilute acid hydrolysis, a common technique which uses low concentrations of acid in hot water to break down hemicellulose [14]. PBHW-pretreated grass was investigated as a substrate for enzyme production using *Hypocrea jecorina*.

The ascomycete *Hypocrea jecorina* (anamorph: *Trichoderma reesei*) is currently used for commercial manufacturing of cellulase and hemicellulase products and has been proposed as the most promising organism for production of enzymes for lignocellulose conversion to fermentable sugars [15]. In addition to a long history of safe commercial use, this fungus secretes significant quantities of enzymes and has well-developed genetic systems [16, 17]. *H. jecorina* strains have been cultivated on different lignocellulosic substrates to generate an enzyme cocktail suited for a particular substrate. Certain natural substrates may induce secreted enzymes suited to degrade particular combinations of polysaccharides and chemical bonds found in the carbon source [18].

The goal of this study was to determine the enzyme profile of *H. jecorina* when grown either on untreated or PBHW-pretreated Tifton 85 bermudagrass and to compare enzyme cocktails produced in this fashion to commercially available preparations. Commercial enzyme preparations are very effective at hydrolyzing biomass; however, they are expensive, although this cost may decrease in the near future. If an enzyme cocktail produced by growing *H. jecorina* on Tifton 85 bermudagrass showed enhanced activity, it could translate into cost savings for the overall grass-to-ethanol process. Enzyme preparations thus obtained were also evaluated for release of sugars and phenolic

compounds from PBHW-pretreated Tifton 85 bermudagrass, either alone or in combination with commercially available feruloyl esterase. These results were compared to those obtained from commercial enzyme preparations. In addition, the important inhibitory effects of phenolic compounds, such as ferulic acid, on cellulase activity of preparations were explored. Economically viable enzyme production and amelioration of enzyme inhibition are of crucial importance when designing grass-to-ethanol processes.

Materials and Methods

Materials, Microbial Strains, and Medium

H. jecorina (anamorph *T. reesei*) NRRL 11460 (Rut C-30) was provided by Dr. Xin-Liang Li [from the ARS Culture Collection (NCAUR, Peoria, IL)]. The fungus was routinely propagated in potato dextrose agar (PD) containing 0.4% (*w/v*) potato and 2.0% (*w/v*) dextrose supplemented with 2% (*w/v*) agar for solid medium. Tifton 85 bermudagrass was provided by Dr. William F. Anderson (ARS-USDA, Tifton, GA). All chemicals and media ingredients were of research quality. The experiments were performed in triplicate. Values obtained were very similar; therefore, to facilitate reading, standard deviations are not presented in the tables. In the graphs, standard deviations are presented as error bars.

PBHW Pretreatment of Tifton 85 Bermudagrass

Pressurized batch hot water (PBHW) pretreatment was conducted in a 2-l pressure vessel (Model 4600 Parr Instrument Co., Moline, IL), surrounded by retractable ceramic heaters [12]. Tifton 85 bermudagrass (15 g) was placed in a 500-μm (35 mesh) stainless steel basket, which was immersed in 1,450 ml of deionized water in the vessel. The sample was treated at 230°C for 2 min essentially as previously described [12]. Hydrolyzed solids were dried at 40°C for 90 min using a fluidized bed drier (Endecott, FBD2000, London, UK), and stored at 4°C until further use.

H. Jecorina Flask Cultures

Conidia spores (approximately 1×10^7) were transferred to a shake flask (250 ml) containing 50 ml PD medium. The flask was shaken at 250 rpm at 28°C for 48 h. A 5% (*v/v*) inoculum was transferred to 50 ml of production medium in a 250-ml Erlenmeyer flask. Production media for *H. jecorina* contained per liter 15.0 g KH_2PO_4, 20.0 g corn steep liquor (Sigma-Aldrich, St. Louis, MO), 5 g NH_4SO_4, 0.5 g $Mg(SO_4)_2 \cdot 7H_2O$, 1.0 ml Tween 80, and 30 ml solution of untreated or PBHW-pretreated Tifton 85 bermudagrass containing a 2.0 g of grass. Basal medium was adjusted to pH 4.8 with 1 M NaOH. The fungus was grown at 28°C with agitation (250 rpm) for 8 days. Flasks were sampled daily (2 ml). For evaluation of the inhibitory effect of ferulic acid on cellulase activities, *H. jecorina* was grown as described above on untreated bermudagrass with different concentrations of ferulic acid (0, 0.02, 0.06, and 0.10% *w/v*).

Bermudagrass Digestion Assay

Tifton 85 bermudagrass solids recovered after PBHW treatment at 230°C at a solids loading of 5% (*w/v*) were hydrolyzed by commercial (Spezyme CP, Danisco, Genencor Division,

Rochester, NY; and DEPOL 740LL, Biocatalysts Ltd., Cardiff, Wales, UK) and *H. jecorina* preparations (supernatant of samples collected after 8 days of growth on 4% *w/v* solids untreated or PBHW-pretreated Tifton 85 bermudagrass). The performance of the enzyme preparations were compared by standardizing either xylanase (400 IU/ g grass) or FPAase (8 FPU/ g grass) units. Assays were conducted at 50°C, pH 4.8, with an agitation of 100 rpm for 24 h, under sterile conditions. Samples were boiled, centrifuged (10,000 rpm/ 4°C), and supernatant was collected and kept at −20°C until further analysis. Reducing sugars, sugar composition and phenolic compounds were analyzed after the enzymatic hydrolysis.

Enzyme Assays

Enzyme activities in the presence of 1% *w/v* substrates (Sigma-Aldrich) including oat-spelt xylan, polygalacturonic acid, carboxymethylcellulose (CMC, low viscosity), 15 mmol/ l cellobiose, and 2.5 mmol/l *p*-nitrophenyl (*p*-NP) conjugated substrates were determined at 50°C in the presence of 50 mmol/l sodium acetate buffer, pH 4.8 using published methods [19, 20]. Filter paper activity (FPAase) was assayed as described by Mandels et al. [21]. Release of reducing sugars was determined according to Miller [22]. Glucose determination for the cellobiase assay used a D-glucose (GOPOD Format) assay kit from Megazyme (Megazyme International Ireland Ltd., Co. Wicklow, Ireland). One unit of cellulase (for CMC as substrate), cellobiase, xylanase and polygalacturonase activities was defined as the release of one μmol of glucose, xylose or galacturonic acid, respectively, per min. For *p*-NP conjugated substrates, one unit of activity was defined as one μmol of *p*-NP released per min.

Protein Content

The protein content of the commercial enzyme preparations and the fungal supernatant samples were determined using the Bradford assay [23].

Analysis of Soluble Carbohydrates

A 25-μl filtered liquid sample was blown to dryness by nitrogen after adding 50 μl of MeOH containing 91 μg of phenyl glucose as the internal standard. Two drops of acetonitrile were also added to dried samples and then blown to dryness again. Silylation was performed by adding 50 μl of both trimethylsilane (TMS) and N, O-Bis (trimethylsilyl) trifluoroacetamide (BSTFA) to dried samples by incubation at 75°C for 30 min. Arabinose, xylose, and glucose, both α and β conformations, and sucrose concentrations were determined for 1 μl aliquots of silylated sugar derivatives by gas chromatography (model 5890, Hewlett Packard Inc., Atlanta, GA) using J&W (Agilent, Wilmington, DE) DB-5 capillary column (30 M×0.25 mm I.D.). The temperature program started at 100°C, and increased to 320°C at a rate of 6°C/min. Injector temperature was 250°C and detector temperature was 350°C.

Ferulic Acid Determination

The procedure for ferulic acid determination was adapted from a chlorogenic acid quantification protocol [24]. A 100-μl sample was diluted with 100 μl dH_2O. 50 μl of MeOH containing 0.0041 mg of chrysin was added as an internal standard. Ferulic and p-coumaric acid concentrations were determined for 20 μl aliquots of the solution by reverse-phase HPLC (model 1050, Hewlett Packard) using an H_2O/MeOH linear gradient from 10% (*v/v*) to 100%

MeOH in 35 min and a flow rate of 1 ml/min. The column was a 250×4.6 mm i.d., 5 μm Ultrasphere C18 (Beckmann Instruments, Norcross, GA). The detector was a diode array system, and 340 nm was used for further analysis. Each solvent contained 0.1% (*v*/*v*) H_3PO_4. Response factors were determined with pure authentic compounds (Sigma-Aldrich). Quantification of ferulic acid was based on the internal standard (chrysin) and peak identification was based on co-chromatography (spiking) and spectral analysis.

Results and Discussion

Hydrolytic Enzyme Production by *H. Jecorina* Grown on Untreated or PBHW-pretreated Tifton 85 Bermudagrass

Tifton 85 bermudagrass has been used for fermentations using both yeast and engineered bacteria with commercially available cellulase mixtures generating the sugars that are subsequently fermented to ethanol [9, 12, 19]. This is the first report of Tifton 85 bermudagrass as a substrate for production of different enzyme activities. The goal of this study was to determine the enzyme profile of *H. jecorina* when grown either on untreated or PBHW-pretreated Tifton 85 bermudagrass. All activities were similar or higher for the fungus grown on untreated bermudagrass (Table 1). These results agree with those of Acebal et al. [25] where ammonia treated wheat was used as the substrate. Using *T. reesei* (*H. jecorina*) QM9414, growth was maximal with alkali-pretreated straw, however cellulase yields expressed as activity units were higher when the alkali pretreatment was omitted [31]. These results are in contrast to those obtained during cultivation of the *H. jecorina* on liquid hot water (LHW) treated DDGS, where the enzyme activities were equal to or better than those using untreated DDGS [19]. The results obtained for xylanase production using untreated bermudagrass as substrate are similar to those obtained for *T. reesei* (*H. jecorina*) Rut C-30 cultured in LHW-treated DDGS and corn fiber, and *T. reesei* (*H. jecorina*) QM9414 cultured in corn fiber (Table 2). On the other hand, considerably higher enzyme production results were reported for these two *Hypocrea* strains when grown in corn fiber arabinoxylan (Table 2) [26]. Efficient inducers of xylanase production in *H. jecorina* include xylan, xylan hydrolysis intermediates (xylobiose, D-xylose), lactose, L-sorbose, L-arabinose and sophorose [27, 28]. In addition, cellulose is known to induce xylanases [28, 29]. However, the mechanisms by which the hydrolytic enzymes are induced are still not well understood [18, 30].

When grown on cellulose (50 g/l), the production of α-arabinosidase activity by *H. jecorina* Rut C-30 reached its highest value of 0.009 IU/ml after 106 h [18]. Higher α-arabinosidase activity (0.56 IU/ml and 0.28 IU/ml, respectively) was produced by *H. jecorina* when grown on untreated and PBHW-pretreated bermudagrass after a longer incubation (192 h; Table 1). When cultivated in LHW-treated DDGS, even greater amounts of α-arabinosidase activity was produced (1.86 IU/ml) [19].

Maximum polygalacturonase (PG) activity produced by *H. jecorina* Rut C-30 when grown on cellulose (50 g/l) was 0.10 U/ml measured after 128 h of incubation. Total PG activity on sugar beet as substrate was 0.82 U/ml, while 0.12 U/ml was produced by another strain (QM9414) when grown on the same substrate [31]. Our results show that when cultivated in untreated bermudagrass, *H. jecorina* produces similar levels of PG activity (0.60 IU/ml; Table 1) after 8 days of incubation. Under conditions tested, no PG activity was detected when the fungus was cultivated in PBHW-pretreated bermudagrass (Table 1).

Similar results were obtained for FPAase activity whether the fungus was grown on PBHW-pretreated bermudagrass (Tables 1 and 2) or LHW-treated DDGS, although the two

Table 1 Comparison of *H. jecorina* enzyme profile after 8 days growth on untreated or 230°C PBHW-pretreated Tifton 85 bermudagrass as substrate with that of commercial preparations.

	FPAase (FPU)	CMCase (IU/ml)	β-glucosidase (ρ-NPG) (IU/ml)	Cellobiase (CBU)	Xylanase (IU/ml)	β-xylosidase (IU/ml)	α-arabinofuranosidase (IU/ml)	α-galactosidase (IU/ml)	Polygalacturonase (IU/ml)	Amylase (IU/ml)	Protein (mg/ml)
H. jecorina (untreated bermudagrass)	0.53	14.8	0.21	0.25	85.0	0.53	0.56	0.60	0.60	0.31	0.058
H. jecorina (230°C PBHW-pretreated bermudagrass)	1.16	11.5	0.12	0.17	32.2	0.70	0.28	0.15	0.19	0.00	0.051
Spezyme CP[a]	48.1	3,086.0	65.1	79.2	2,411.1	4.30	Not determined	1.03	5.90	31.8	37.5
Depol 740L[b]	0.50	876.5	32.6	26.8	2,100.0	2.86	Not determined	0.20	1.12	1.63	8.60

[a] Commercial enzyme preparation (Danisco, Genencor Division, Rochester, NY)

[b] Commercial enzyme preparation (Biocatalysts Ltd., Cardiff, Wales, UK)

Table 2 The effect of various carbon sources on production of xylan-degrading enzymes by different *H. jecorina* (*T. reesei*) strains.

Organism	Substrate	Cultivation conditions	Substrate for determination of enzyme activity	Xylanase (IU/ml)	Reference
H. jecorina Rut C-30	Untreated Tifton 85 bermudagrass	Shake flask 28°C, 192 h	1% oat spelt xylan	85.0	This work
H. jecorina Rut C-30	PBHW-pretreated Tifton 85 bermudagrass	Shake flask 28°C, 192 h	1% oat spelt xylan	32.0	This work
H. jecorina Rut C-30	LHW- DDGS	Shake flask 28°C, 132 h	1% oat spelt xylan	93.4	18
H. jecorina QM 9414	corn fiber	Shake flask 28°C, 192 h	1% oat spelt xylan	98.5	24
H. jecorina Rut C-30	corn fiber	Shake flask 28°C, 192 h	1% oat spelt xylan	86.1	24
H. jecorina QM 9414	Corn fiber Xylan	Shake flask 28°C, 192 h	1% oat spelt xylan	221	24
H. jecorina Rut C-30	Corn fiber Xylan	Shake flask 28°C, 192 h	1% oat spelt xylan	621	24

substrates are very different. The tendency to produce higher FPAase activity when grown in PBHW- or LHW-treated substrate was observed in both cases (Fig. 1a; Table 1). On the other hand, LHW-treated DDGS was a better substrate for the production of β-glucosidase and β-xylosidase [19]. Xylanase activity was higher in the fungal culture grown on untreated bermudagrass than when the fungus was cultivated on PBHW-pretreated bermudagrass (Fig. 1b; Table 1). Starch is not present in grass [32], which could explain the very low levels of amylase activity found (Table 1). The same pattern of reducing sugars release was observed for the fungus grown in both conditions tested (Fig. 2). There was not a significant difference in terms of protein production after 8 days growth on either of the substrates evaluated (Table 1).

PBHW-pretreated Tifton 85 Bermudagrass Digestion Assay: Production of Soluble Carbohydrates and Inhibition by Phenolic Compounds

After we determined the enzyme profile of *H. jecorina* grown on either untreated or PBHW-pretreated Tifton 85 bermudagrass, we compared our enzyme preparations to the commercial cellulase preparation, Spezyme CP (Genencor International, Rochester, NY). *H. jecorina* is the source for this commercial preparation; however, Spezyme CP was not made specifically for the degradation of grass. Kabel et al. [33] have pointed out that the choice of an efficient enzyme preparation is dependent rather on substrate characteristics than on standard enzyme activities measured. Therefore, we compared the commercial preparation results with the enzyme mixture produced by growing the fungus in untreated or PBHW-pretreated bermudagrass. These enzyme preparations were evaluated individually or in combination with a commercial feruloyl esterase (Depol 740L). Studies were conducted by standardizing xylanase activity for Spezyme CP and the *H. jecorina* preparations for 400 IU/g grass. Cellulase activity was standardized for 8 FPU/g grass.

The amount of reducing sugars released by the enzyme mixture from *H. jecorina* (after 8 days incubation with untreated bermudagrass) individually or in combination with feruloyl esterase was 72.1 and 84.8%, respectively, of the Spezyme CP preparation

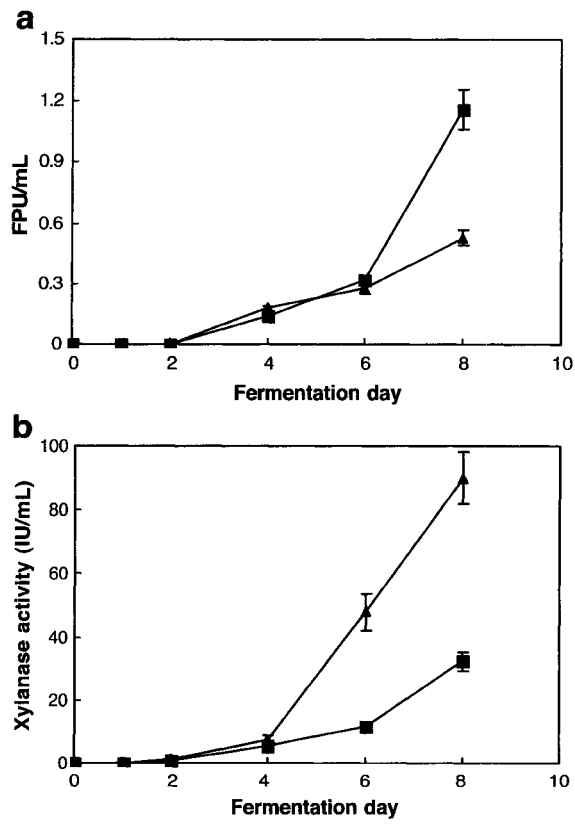


Fig. 1 Cellulase (Filter Paper Unit=FPU) (**a**) and Xylanase (**b**) and activities produced by *H. jecorina* after growth on 230°C PBHW-pretreated (*filled square*) and untreated (*filled triangle*) Tifton 85 bermudagras. Standard deviations are presented by error bars

analyzed under the same conditions (Table 3). It is important to note that although Depol 740L is mainly a feruloyl esterase commercial preparation there are other enzyme activities present, most notably xylanase activity. The addition of Depol 740L to Spezyme CP and to the *H. jecorina* enzyme preparation increased reducing sugars by 11.4 and 24.2%, respectively (Table 3). It is unclear if the increase in reducing sugars liberated was due to synergism between enzymes from our *H. jecorina* preparation with the feruloyl esterase or the action of xylanases and/or other enzymes present in this commercial preparation. The

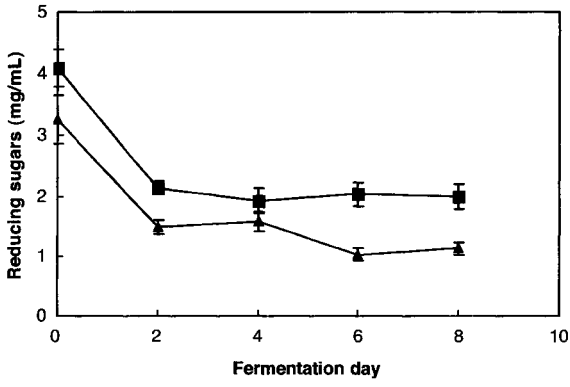


Fig. 2 Reducing sugars released from grass by *H. jecorina* after grown on 230°C PBHW-pretreated (*filled square*) or untreated (*filled triangle*)Tifton 85 bermudagrass. Standard deviations are presented by error bars

Table 3 Reducing sugar and monomeric sugar composition for *H. jecorina* enzyme preparations and commercial enzymes for the hydrolysis of 230°C PBHW-pretreated bermudagrass[a].

	Reducing sugars (mg/ml)	Reducing sugars (mg/g grass)	Glucose	Xylose	Arabinose	Ferulic acid (mg/g grass)
Spezyme CP	19.5	391.2	221.4	72.0	0.78	0.25
H. jecorina preparation[b]	14.1	282	132.8	64.0	0.77	0.26
Depol 740L (Feruloyl esterase)	10.9	218	94.8	63.3	7.48	0.88
Spezyme+ Depol 740L	22.0	440	123.3	85.9	3.73	0.36
H. Jecorina +Depol 740L	18.6	373	92.6	78.4	3.7	0.54

[a] Xylanase activity standardized for 400 IU/g grass for Spezyme CP and *H. jecorina* enzyme preparations; Feruloyl activity used: 7.8 IU/g grass; Cellobiase activity used: 78.2 CBU/ g grass

[b] Using a preparation taken from the fungus grown on untreated bermudagrass after 8 days of cultivation

dinitrosalycilic acid (DNS) colorimetric assay has been commonly used for cellulose/ cellulase studies for the quantification of the number of reducing sugars associated with the soluble face, such as glucose, cellobiose, as well as low-DP cellooligosaccharides, although the DNS assay tends to overestimate absolute numbers of reducing ends per unit mass cellulose [34].

When cellulase activity was standardized for 8 FPU/g d wt grass for both cellulase preparations, there was no significant difference in reducing sugars released (Table 4). For the 230°C PBHW-pretreated bermudagrass with 7.8 IU Depol 740L/g d wt grass added, doubling the cellulase did not increase reducing sugar (data not shown). There was not a significant increase in reducing sugar when commercial feruloyl esterase was added to the *H. jecorina* preparation as observed in Table 3 (with higher xylanase units of activity). Overall, the fungus grown on the untreated grass gave a better balanced enzyme mixture for the degradation of the PBHW-pretreated substrate. Vanillin and ferulic acid levels were higher in the PBHW-pretreated grass samples and increased during incubation with *H. jecorina* enzymes (data not shown). The phenolic compounds appear to be more easily

Table 4 Comparison of *H. jecorina* enzyme preparations to commercial enzymes for the hydrolysis of 230°C PBHW-pretreated bermudagrass[a].

	Reducing sugars (mg/ml)	Reducing sugars (mg/g grass)	Glucose	Xylose	Arabinose	Ferulic acid (mg/g grass)
Spezyme CP	16.05	321	218.1	60.5	0.45	0.17
H. jecorina preparation[b]	15.8	316	180.9	51.2	1.27	0.21
Spezyme CP+Depol 740L	19.5	390	122.8	71.2	8.04	0.36
H. jecorina+Depol 740L[b]	16.9	338	115.9	89.2	1.85	0.39
H. jecorina preparation+Cellobiase[b]	17.6	352	230.1	47.9	0.13	0.27
Spezyme CP+Cellobiase	18.2	364	306.8	53.0	0.15	0.12
Spezyme CP+Depol 740L+ Cellobiase	23.0	460	230.9	54.5	1.04	0.42

[a] Cellulase (FPAase) activity standardized for 8 FPU/g grass for Spezyme CP and *H. jecorina* enzyme preparations; Feruloyl activity used: 7.8 IU/g grass; Cellobiase activity used: 78.2 CBU/ g grass

[b] Using a preparation taken from the fungus grown on untreated bermudagrass after 8 days of cultivation

liberated from the PBHW-pretreated grass and may be inhibiting certain enzyme components, although further studies are needed to confirm this hypothesis.

Phenolic compounds, freed from lignin, are known to inhibit extracellular cellulases and hemicellulases produced by fungi, although cellulase preparations can differ significantly in their sensitivity to lignin [35–37]. The mechanism of enzyme inhibition may involve both the adsorption of enzyme to the major particulate lignin component and the interactions with the minor low-molecular lignin component [5]. Vohra et al. [35] reported that Avicelase, CMCase and β-glucosidase activities were reduced when *H. jecorina* was grown in Avicel in the presence of different concentrations of lignin, vanillin and ferulic acid. In the case of ferulic acid, the β-glucosidase activity was the most affected, although the ferulic acid had little effect on the growth of the fungus itself. DNS reducing sugar estimation was not affected by the phenolic concentration used in their investigations. We also observed this effect in the *H. jecorina* cellulase activity, when the fungus was grown on untreated bermudagrass for 8 days in the presence of different ferulic acid concentrations. All the activities tested (FPAase, CMCase and β-glucosidase) were drastically reduced in the presence of 0.02% (*w/v*) ferulic acid (Fig. 3). In addition, when our *H. jecorina* cellulase preparations and the commercial feruloyl esterase were combined, the sugar compositional analysis showed that glucose production from PBHW-pretreated bermudagrass decreased in comparison to the amount liberated by each enzyme mixture alone (Tables 3 and 4). Even when a third enzyme, a commercial β-glucosidase to supplement the insufficient cellobiase activity from *H. jecorina* preparations, was added to the Spezyme CE and feruloyl esterase treatment, the inhibitory effect was also observed (Table 4). For both cellulolytic enzyme preparations acting only in the presence of the feruloyl esterase compared to their action individually, the amount of xylose and arabinose released was increased. It is unclear if this increase is related to some synergism between the two enzyme preparations or due to the hemicellulolytic activity present in the Depol 740L preparation.

Considering that the microorganism source for the Spezyme CP enzyme preparation is also *H. jecorina*, our results using a different approach confirm previous work showing that low molecular weight phenolic compounds are inhibitory to the action of cellulases from *H. jecorina*. Vohra et al. [35] demonstrate that at least some of *H. jecorina* cellulases are inhibited in the presence of different concentrations of ferulic acid. *H. jecorina* itself does not produce feruloyl esterase activity [12], so it may not be surprising that the cellulases do not seem to act in synergism with feruloyl esterases and are inhibited by the esterase

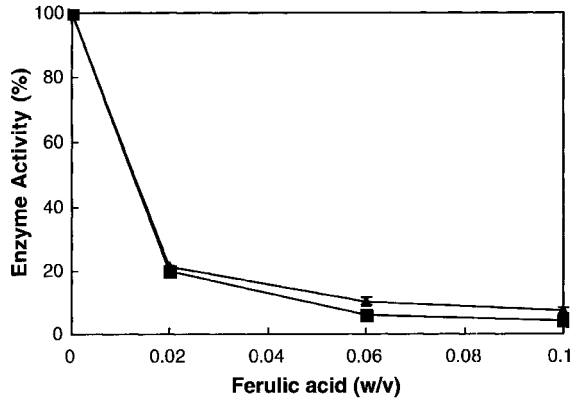


Fig. 3 Effect of ferulic acid on the cellulase activities of *H. jecorina* after grown on untreated bermudagrass. The activities tested were: FPAase (*filled triangle*) and β-glucosidase (*filled square*). The CMCase activity was reduced to almost 0% in the presence of 0.02% (*w/v*) ferulic acid. Standard deviations are presented by error bars

products. Berlin et al. [20, 38] have discussed the engineering or selection of enzymes with reduced affinity for lignin as a potential strategy to improve enzymes for hydrolysis of lignocellulosic substrates. Perhaps this approach would be helpful when cellulase activity is needed in the presence of substantial amounts of phenolic compounds. *H. jecorina* has been successfully engineered for the over-expression of homologous and heterologous genes coding for different hydrolytic enzymes [17, 39], and future work will explore the engineering of *H. jecorina* enzymes for resistance to phenolic compounds.

Ferulic acid, ρ-coumaric acid, and vanillin are low-molecular-weight phenolic compounds frequently isolated from forages [37]. Ferulic acid is a precursor to natural vanillin, and may be used as a UV absorber and antioxidant in skin care formulations. Phenolic compounds, especially ρ-coumaric acid, act as an inhibitor of microbial growth and enzyme activities and may have potential value as natural compounds for pest control [9]. Ferulic acid, in particular, seems to have an inhibitory effect on the cellulase action from the *H. jecorina* and Spezyme CP preparations. Interestingly, when feruloyl esterase was used in combination with Spezyme CP and the *H. jecorina* preparations, less ferulic acid was released from the PBHW-pretreated bermudagrass, compared to the amount of ferulic acid liberated by Depol 740L alone (Table 3). In developing a methodology for using bermudagrass for ethanol and co-products production, incubating with the feruloyl esterase, removing the phenolics, then treating with cellulases has worked well [6], although this maybe costly. Alternatively, *H. jecorina* may be engineered for the expression of cellulases less susceptible to inhibition by phenolic compounds, or other sources of non-phenolic acid inhibited cellulolytic enzymes may be used.

Acknowledgements We would like to acknowledge Drs. E. Timothy Davies and Zeynep Cvetkovich for support with the small fermentation reactor, and Ms. Amruta Jangid for her technical assistance.

References

1. Fedoroff, N. V., & Cohen, J. E. (1999). *Proceedings of the National Academy of Sciences of the United States of America, 96*, 5903–5907.
2. Sun, Y., & Cheng, J. J. (2005). *Bioresource Technology, 96*, 1599–1606.
3. Hill, J., Nelson, E., Tilman, D., Polasky, S., & Tiffany, D. (2006). *Proceedings National Academy of Sciences, 103*, 11206–11210.
4. Burton, G. W., Gates, R. N., & Hill, G. M. (1993). *Crop Science, 33*, 644–645.
5. Mandedebvu, P., West, J. W., & Hill, G. M. (1999). *Journal of Animal Science, 77*, 1572–1586.
6. Anderson, W. F., Peterson, J., Akin, D. E., & Morrisson III, W. H. (2005). *Applied Biochemistry and Biotechnology, 121–124*, 303–310.
7. Akin, D. E. (1989). *Agronomy Journal, 81*, 17–25.
8. Akin, D. E., & Chesson, A. (1989). *Proceedings of the International Grassland Congress, 16*, 1753–1760.
9. Hill, G. M., Gates, R. N., West, J. W., Watson, R. S., & Mullinix, B. G. (2001). *Journal of Animal Science, 79*, 235.
10. Wingren, A., Galbe, M., & Zacchi, G. (2003). *Biotechnology Progress, 19*, 1109–1117.
11. Berlin, A., Balakshin, M., Gilkes, N., Kadla, J., Maximenko, V., Kubo, S., et al. (2006). *Journal of Biotechnology, 125*, 198–209.
12. Brandon, S. K., Eiteman, M. A., Patel, K., Richbourg, M., Miller, D., & Peterson, J. D. (2008). *Journal of Chemical Technology and Biotechnology, 83*(6) (in press).
13. Allen, S. G., Kam, L. C., Zemann, A. J., & Antal, M. J. (1996). *Industrial Engineering Chemical Research, 35*, 2709–2715.
14. Hamelinck, C. N., Hooijdonk, G. V., & Faaij, A. P. C. (2005). *Biomass Bioenergy, 28*, 384–410.
15. Potera, C. (2006). *Microbe, 1*, 317–322.
16. Hazell, B. W., Te, , O, V. S. J., Bradner, J. R., Berquist, P. L., & Nevalainen, K. M. H. (2000). *Letters in Applied Microbiology, 30*, 282–286.

17. Li, X.-L., Skory, C. D., Ximenes, E. A., Jordan, D. B., Dien, B. E., Hughes, S. R., et al. (2007). *Applied Microbiology Biotechnology, 74*, 1264–1275.
18. Olsson, L., Christensen, T. M. I. E., Hansen, K. P., & Palmqvist, E. A. (2003). *Enzyme Microbial Technology, 33*, 612–619.
19. Ximenes, E. A., Dien, B. S., Ladisch, M. R., Mosier, N., Cotta, M. A., & Li, X.-L. (2007). *Applied Biochemistry Biotechnology, 137–140*, 171–183.
20. Berlin, A., Gilkes, N., Kurabi, A., Bura, R., Tu, M., Kilburn, D., et al. (2005b). *Applied Biochemistry Biotechnology, 121–124*, 163–170.
21. Mandels, M., Andreotti, R., & Roche, C. (1976). *Biotechnology Bioengineering, 6*, 17–34.
22. Miller, G. L. (1959). *Analytical Chemistry, 31*, 426–428.
23. Bradford, M. (1976). *Analytical Biochemistry, 72*, 248–254.
24. Peterson, J. K., Harrison, H. F., Snook, M. E., & Jackson, D. M. (2005). *Allelopathy Journal, 16*, 239–249.
25. Accbal, C., Castillon, M. P., Estrada, P., Mata, I., Costa, E., Aguado, J., et al. (1986). *Applied Microbiology and Biotechnology, 24*, 218–223.
26. Li, X.-L., Dien, B. S., Cotta, M. A., Wu, Y. V., & Saha, B. D. (2005). *Applied Biochemistry Biotechnology, 121–124*, 321–334.
27. Zeilinger, S., Mach, R. L., Schindler, M., Herzog, P., & Kubicek, C. P. (1996). *Journal of Biological Chemistry, 271*, 25624–25629.
28. Xu, J., Nogawa, M., Okada, H., & Morikawa, Y. (1998). *Bioscience Biotechnology Biochemistry, 62*, 1555–1559.
29. Xiong, H., Turunen, O., Pastinen, O., Leisola, , & von Weymarn, M. N. (2004). *Applied Microbiology Biotechnology, 64*, 353 358.
30. Aro, N., Pakula, T., & Penttilä, M. (2205). *FEMS Microbiology Review, 29*, 719 739.
31. Markovic, O., Slezárik, A., & Labudová, I. (1985). *FEMS Microbiology Letters, 27*, 267–271.
32. Anger, M., Malcharek, A., & Kunbauch, W. (2002). *Journal of Applied Botany, 76*, 47–51.
33. Kabel, M. A., van der Maarel, M. J. E. C., Klip, G., Voragen, A. G. J., & Schols, H. A. (2006). *Biotechnology Bioengineering, 93*, 56–63.
34. Kongruang, S., Han, M. J., Breton, C. I. G., & Penner, M. H. (2004). *Applied Biochemistry Biotechnology, 113–116*, 213–231.
35. Vohra, R. M., Shirkot, C. K., Dhawan, S., & Gupta, K. G. (1980). *Biotechnology Bioengineering, 22*, 1497–1500.
36. Sharma, A., Milstein, O., Vered, Y., Gressel, J., & Flowers, H. M. (1985). *Biotechnology Bioengineering, 27*, 1095–1101.
37. Martin, S. A., & Akin, D. E. (1988). *Applied Environmental Microbiology, 54*, 3019–3022.
38. Berlin, A., Gilkes, N., Kilburn, D., Bura, R., Markov, A., Skomarovsky, A., et al. (2005a). *Enzyme Microbial Technology, 37*, 175–184.
39. Salles, B., Valentino, T., Moreland, G., Bergquist, P., Filho, E. X. F., Ximenes, E. A., & Nevalainen, H. (2007). *Biotechnology Letters, 29*, 1195–1201.

Appl Biochem Biotechnol (2008) 146:101–117
DOI 10.1007/s12010-007-8122-y

A Novel Technique that Enables Efficient Conduct of Simultaneous Isomerization and Fermentation (SIF) of Xylose

Kripa Rao · Silpa Chelikani · Patricia Relue · Sasidhar Varanasi

Received: 18 June 2007 / Accepted: 11 December 2007 /
Published online: 28 February 2008
© Humana Press Inc. 2007

Abstract Of the sugars recovered from lignocellulose, D-glucose can be readily converted into ethanol by baker's or brewer's yeast (*Saccharomyces cerevisiae*). However, xylose that is obtained by the hydrolysis of the hemicellulosic portion is not fermentable by the same species of yeasts. Xylose fermentation by native yeasts can be achieved via isomerization of xylose to its ketose isomer, xylulose. Isomerization with exogenous xylose isomerase (XI) occurs optimally at a pH of 7–8, whereas subsequent fermentation of xylulose to ethanol occurs at a pH of 4–5. We present a novel scheme for efficient isomerization of xylose to xylulose at conditions suitable for the fermentation by using an immobilized enzyme system capable of sustaining two different pH microenvironments in a single vessel. The proof-of-concept of the two-enzyme pellet is presented, showing conversion of xylose to xylulose even when the immobilized enzyme pellets are suspended in a bulk solution whose pH is sub-optimal for XI activity. The co-immobilized enzyme pellets may prove extremely valuable in effectively conducting "simultaneous isomerization and fermentation" (SIF) of xylose. To help further shift the equilibrium in favor of xylulose formation, sodium tetraborate (borax) was added to the isomerization solution. Binding of tetrahydroxyborate ions to xylulose effectively reduces the concentration of xylulose and leads to increased xylose isomerization. The formation of tetrahydroxyborate ions and the enhancement in xylulose production resulting from the complexation was studied at two different bulk pH values. The addition of 0.05 M borax to the isomerization solution containing our co-immobilized enzyme pellets resulted in xylose to xylulose conversion as high as 86% under pH conditions that are suboptimal for XI activity. These initial findings, which can be optimized for industrial conditions, have significant potential for increasing the yield of ethanol from xylose in an SIF approach.

Keywords Xylose · Xylulose · Urea · Urease · Borate · Simultaneous isomerization and fermentation · Ethanol

K. Rao · S. Varanasi (✉)
Department of Chemical and Environmental Engineering, The University of Toledo, Toledo, OH 43606, USA
e-mail: Sasidhar.varanasi@utoledo.edu

S. Chelikani · P. Relue
Department of Bioengineering, The University of Toledo, Toledo, OH 43606, USA

Introduction

Ethanol is being hailed as the fuel of the future. Interest in the production of fuel ethanol from renewable sources has increased significantly. For fuel ethanol production to become a practical reality, cheaper substrates and more efficient production processes are needed [1, 2]. Biomass, which includes all plant and plant-derived material, forms a potential renewable source of sugars that can be fermented to produce fuel ethanol and a variety of other fuels and chemicals. In addition to the many benefits common to renewable energy, biomass is particularly attractive because it is currently the only renewable sustainable energy source for liquid transportation fuel.

Lignocellulosic biomass consists of three major components: cellulose (~40–50%), hemicellulose (~25–35%), and lignin (~15–20%) [3]. Of these, cellulose and hemicellulose constitute the polysaccharides that can be hydrolyzed to sugars that could be fermented to ethanol. In biomass, the majority of cellulose is a crystalline polymer of glucose that is relatively difficult to hydrolyze into its monomeric sugar residues. Hemicellulose is a short-branched polymer of pentose and some hexose sugars that surround the cellulose fibrils and is much less organized [4]. The pentose sugars consist primarily of xylose and to a smaller extent arabinose, whereas the hexose sugars are usually galactose and mannose. Because of its relatively open structure, the hemicellulose fraction is easier to convert to its sugar monomers by various pretreatment techniques than the cellulose fraction.

For the conversion of lignocellulosic biomass to bioethanol to be economically feasible, it is imperative that the hemicellulose-derived monomeric sugars be fermentable along with the glucose derived from cellulose. Unfortunately, no known native microorganisms are able to efficiently ferment both glucose and xylose to ethanol. Wild-type *Saccharomyces cerevisiae* strains can readily ferment glucose and other sugar components of biomass like mannose, fructose, and galactose [5]. Xylose, which forms a major portion of hemicellulose, cannot be fermented by the same native strains of yeast. Several non-*Saccharomyces* strains of yeast, such as *Pichia stipitis* and *Candida shehatae*, are known to ferment pentose sugars more efficiently than other yeasts [6]. In such yeasts, the xylose metabolism pathway goes from xylose to xylitol to xylulose [7, 8]. In other yeast strains and bacteria and fungi, xylose can also be converted to xylulose via a single enzyme, xylose isomerase (XI). Several yeasts, including *S. cerevisiae*, that cannot ferment xylose are able to ferment xylulose, the ketose isomer of xylose [9–12]. Considerable effort has been focused on the genetic modification of microorganisms so that both xylose and glucose can be efficiently metabolized using the same organism [13–25].

Although genetically modified organisms have potential for fermentation of pentose and hexose sugars, their genetic stability, overall ethanol yield, and ability to survive under the conditions of industrial fermentation are unproven [26, 27]. Hence, an alternative approach to fermentation of xylose to ethanol involves using native yeast strains with the addition of exogenous enzymes for the isomerization of xylose. In this approach, the production of xylulose is accomplished using immobilized glucose/xylose isomerase [11, 28–30]. The appeal for this approach is that XI, along with amylase and protease, is among the most widely and cheaply available commercial enzyme [31]. Hydrolysate from lignocellulosic biomass will contain both xylose and glucose. The affinity of XI for xylose is typically 1 to 2 orders of magnitude greater than its affinity for glucose; hence, isomerization of xylose to xylulose will dominate over isomerization of glucose to fructose [31]. However, any fructose formed is readily fermentable by *Saccharomyces* to produce ethanol, so fructose formation is not a cause for concern.

Although XI is capable of converting xylose to xylulose, under conditions where XI has significant activity, the equilibrium ratio of xylose/xylulose is typically high (on the order

of 5:1) [32–34]. Hence, xylose isomerization does not have a favorable forward equilibrium. One way to increase xylose conversion is to drive the isomerization forward by removal of the product xylulose. Simultaneous isomerization and fermentation (SIF), where the isomerization of xylose and the fermentation of xylulose to ethanol occur simultaneously in the same vessel, is one method for increasing xylose utilization. However, SIF does have inherent limitations because of the pH range over which XI is active. All commercially available XI's have optimal activity at pH 7 to 8, and the XI activity drops sharply as the pH decreases. In contrast, the optimal pH for the fermentation is in the range of 4 to 5. The large pH difference associated with these two steps poses a problem for conducting SIF efficiently. The SIF can be carried out at a compromised pH between 4 and 7, but the results are less than optimal for both reactions [11]. Efforts to isolate a XI with optimal activity at significantly lower pH for SIF were also noted in the literature [30]. However, it does not appear that this enzyme has the same level of activity as displayed by the commercially available enzymes.

To overcome the disparity in the optimal pH's for the isomerization and fermentation, our group [29, 35, 36] proposed a novel scheme of isomerization that incorporates urease co-immobilized with xylose isomerase. This technique uses XI immobilized in a porous pellet for isomerization and the immobilized urease enzyme for pH control (Fig. 1). These co-immobilized enzyme pellets are dispersed in a fermentation broth, which contains urea in addition to the other necessary ingredients for fermentation. Theoretically, it is possible to sustain a significant pH gradient between the bulk liquid and the core region of the pellet

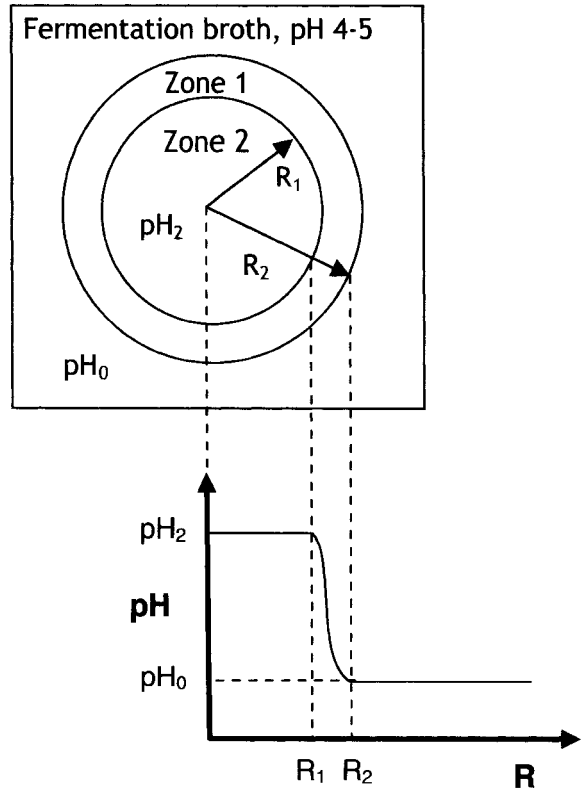


Fig. 1 Cross-section of a Sweetzyme™ pellet showing the steady-state pH profile developed when urease is co-immobilized in the pellet and urea is added to the fermentation broth. The pH in the fermentation broth is pH_0, which is typically in the range of 4 to 5. Zone 1 (outer layer) of the pellet contains immobilized urease and represents the region of the pellet where the pH changes with radial position as ammonia is produced by the consumption of urea. Zone 2 (core) represents the region of the pellet which is at pH_2, the elevated pH. The boundary between zones 1 and 2 represents either the point where all urea is consumed or the penetration depth of urease into the pellet

[29] because as hydrogen ions diffuse into the pellet, they are neutralized by the ammonia produced in the hydrolysis of urea by urease. The XI, which is maintained at a higher pH in the inner core of the pellet, then catalyzes the isomerization of the xylose to xylulose; xylulose diffuses from the pellet and is then available for fermentation in the bulk solution.

Although our co-immobilized enzyme approach is able to sustain the necessary pH difference between isomerization and fermentation steps in SIF [35], the overall production rate of ethanol in SIF will still be limited by the total concentration of xylulose available to the yeast [9]. Under normal equilibrium conditions, the xylulose concentration is usually at best one fifth of the xylose concentration. Hence, other avenues of shifting the equilibrium towards higher xylulose formation will further increase the rate of ethanol production.

One effective means of shifting the equilibrium toward increased xylulose formation is the addition of sodium tetraborate to the isomerization media [37–39]. Borate ion has been reported to shift the equilibrium between xylose and xylulose in XI catalyzed isomerization from 80:20 to 30:70. The borate ion binds more tightly to xylulose than xylose, effectively reducing the product concentration, and thus shifts the equilibrium toward increased xylulose formation. Interestingly, this ability of borate to bind to xylulose is pH dependent, with higher pH (6 to 7.5) favoring binding [40]. Thus, as the pH increases, the concentration of free xylulose decreases. Therefore, the rate of fermentation of xylulose in the presence of borate is also pH dependent, with lower pH leading to higher free xylulose concentrations and thus higher yields and rates of ethanol production [40]. In this regard, our co-immobilized enzyme strategy, which provides different microenvironments for isomerization and fermentation, is naturally benefited by the addition of borate to the fermentation broth. Inside the pellet, the pH is elevated, XI is active, and the isomerization equilibrium is favored by strong borate binding to xylulose. In contrast, in the low pH fermentation broth, borate has a reduced binding to xylulose and thus produces a higher free xylulose concentration for fermentation to ethanol.

In previous papers and patents, we have introduced our novel system and provided proof of concept for the co-immobilized enzyme pellet system [29, 35, 36, 49, 50]. In this paper, we present results of experiments that illustrate the effectiveness of our co-immobilized enzyme system for isomerization under conditions optimal for fermentation by common *S. cerevisiae*. We have changed the media composition in an effort to both shift the equilibrium in favor of xylulose production and improve XI activity [51]. In addition to borate, we also investigated the effect of metal ion addition to the kinetics and equilibrium of the isomerization reactions as certain divalent metal ions have been shown to increase the long-term activity of XI [41, 42]. This paper provides results of these experiments in our co-immobilized enzyme system and their potential impact on SIF enhancement.

Materials and Methods

Chemicals Novo Sweetzyme™ (Sigma Aldrich G4166 ≥350 U/g with activity based on isomerization of glucose to fructose), which is immobilized glucose isomerase produced from *Streptomyces murinus*, was used for the isomerization of xylose. The glucose isomerase has optimal activity for glucose/fructose isomerization at pH 7.5 and 60°C (as per the manufacturer). The Sweetzyme™ pellets were dry, brown, cylinder-shaped granules with a diameter of approximately 1–3 mm. Jack bean urease (Sigma U4002, 70,400 U/g) was used for generating the co-immobilized enzyme pellets used in the isomerization studies. Urease has optimal activity at pH 7.0 and 25°C (as per manufacturer). Both enzymes were stored at 4 °C.

Additional chemicals, including xylose, urea, borax, magnesium chloride, cobalt chloride, sodium citrate, and Tris were all purchased from Sigma Aldrich (St. Louis, MO).

Immobilization of Urease on Sweetzyme™ Pellets For co-immobilization of urease on the Sweetzyme™ pellets, 500 ml of 1 g/l urease solution and 2 g of Sweetzyme pellets was added to a 1-l beaker [35]. The beaker was left on the benchtop at room temperature for 24 h. The pellets were separated from the solution by decanting and gravity filtration and dried on a paper towel at room temperature for 24 h or until dry. Co-immobilized pellets were stored at 4 °C until use. Activity of immobilized urease was measured at pH 7.5 and 25°C using a standard assay procedure that measures the rate of ammonia liberation [43]. The urease activities obtained with our immobilization procedure were in the range of 550–577 U/g pellets, where a unit liberates 1 μmol of ammonia per minute under the assay conditions.

Measurement of Xylose Isomerization Kinetics and Equilibrium All experiments were carried out at 34 °C in a volume of 25 ml in 50-ml shake flasks agitated at 130 rpm in an incubated shaker. Each experiment was conducted in duplicate. All experiments used 60 g/l xylose, and unless otherwise noted, 5.2 g/l of enzyme pellets (0.13 g) was used for each experiment. Buffered solutions used in making the isomerization media were 0.01 M Tris buffer (pHed to 7.5 using 0.01 M NaOH) and 0.05 M sodium citrate buffer (pHed to 4.5 using citric acid). The pH was measured at the beginning of the experiments but was not monitored throughout. We have observed a small drift in pH of less than 1 unit over the course of 48 hrs. Even with this drift, the pH of the bulk solution stayed within the range suitable for fermentation and well-below the pH optimum of XI (pH 7.5). In experiments with co-immobilized pellets, urea concentration was 0, 0.01, or 0.1 M.

Analytical Techniques and Data Analysis To analyze experiments for xylose and xylulose concentration, a 200-μl sample was collected at each time point. The sample was diluted 1:3 with deionized water and then filtered through a 0.2 μm filter. Xylose and xylulose calibration standards with concentrations ranging from 0.25 to 80 g/l in pH 4.5 citrate buffer were prepared in a similar manner. All standards and samples were analyzed by high performance liquid chromatography (HPLC) using a 30-μl injection volume with a 100-μl injection loop. The HPLC unit used was a Shimadzu Series 10A HPLC unit equipped with a SIL-10Ai autosampler and a refractive index detector (RID 10A). A Bio-Rad Aminex HPX-87 P (300×7.8 mm) ion exchange column was used for sugar analysis using a mobile phase of deionized water with a flow rate 0.6 ml/min and a temperature of 80 °C. This column was successful in separating xylose and xylulose. To determine if the xylulose–borate complex dissociated and eluted separately, solutions of borate and borate with xylulose were injected, and the area of the borate peak was measured. As the height of the borate peak was independent of xylulose concentration, we concluded that the xylulose–borate complex dissociated into xylulose and borate, and the xylulose peak represented total xylulose in the mixture. Finally, data for xylose and xylulose concentration at each time point were summed and normalized to 60 g/l total concentration to eliminate variability and to close the mass balance. All xylulose concentrations reported in the presence of borate represent the total xylulose (free xylulose + xylulose-borate complex) concentration. All experiments were performed in duplicate, and data were very reproducible; data shown is representative of one run. Figures were generated in Origin 7.0 (Northampton, MA, USA).

Results and Discussion

The experimental results are organized as follows. The first set of experiments was designed to demonstrate the ability of the co-immobilized pellet system to achieve two

different pH microenvironments within a single vessel—one optimal for XI activity and the other suitable for conducting fermentation. After these experiments, the ability of sodium tetraborate decahydrate (borax) to alter the kinetics and shift the xylose/xylulose equilibrium was investigated in the unaltered and co-immobilized pellet systems. Next, the mass of co-immobilized enzyme pellets was changed, and the effect on the kinetics and approach to equilibrium for the xylose isomerization are presented. Finally, the effect of added metal ions on the isomerization are presented and discussed.

Demonstration of the Sustainability of Two-pH Environments in a Single Vessel

Unaltered Pellets As an initial control experiment, the isomerization of xylose to xylulose was studied using Sweetzyme™ pellets, as received, before co-immobilization with urease. The time course of xylose consumption and xylulose formation was monitored for an initial xylose concentration of 60 g/l with 0.13 g pellets at 34 °C. The isomerization mixture was buffered at pH 7.5, which is the optimal pH for XI activity. As seen in Fig. 2, curve A, the concentration of xylulose steadily increased and reached an equilibrium value of about 9 g/l, suggesting an equilibrium xylose/xylulose ratio of nearly 6:1 under these conditions. When the same experiment was repeated at a reduced pH of 4.5, no xylulose was detected in the reaction mixture, even after 40 h (data not shown). At a pH of 4.5, XI is 3 pH units below its optimum and displays essentially no activity.

XI/Urease Co-immobilized Pellets We next modified the SweetzymeTM pellets by adsorbing urease onto the pellets. The co-immobilized enzyme pellets (0.13 g) were added to reaction media containing 60 g/l xylose buffered to pH 4.5. As with the unaltered pellets, no xylulose formation was observed under these conditions even after 48 h (see Fig. 2, curve C). Next, 0.01 M urea was added to the bulk solution buffered to a pH of 4.5. Formation of xylulose was observed in the presence of urea, and the concentration of xylulose in the reaction medium gradually increased to reach a value of about 5 g/l by 48 h (see Fig. 2, curve B).

The production of ammonia by urea hydrolysis catalyzed by immobilized urease in the pellets raises the internal pH within the core of the pellets as shown in Fig. 1. The interior

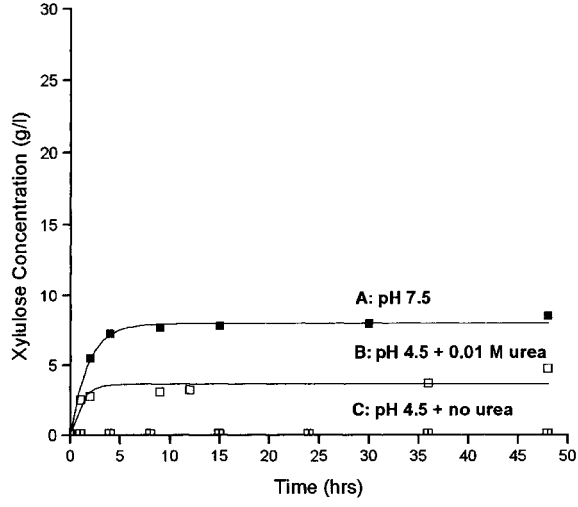


Fig. 2 Proof-of principle that two pH microenvironments are developed in the co-immobilized enzyme system via urea hydrolysis. *Solid symbols* are used for unaltered Sweetzyme™; *open symbols* are used for the XI/urease co-immobilized pellets. The three experiments shown are *A* pH 7.5; *B* pH 4.5 with 0.01 M urea, and *C* pH 4.5 with no urea; each used 0.13 g pellets. Unaltered Sweetzyme™ yielded no xylulose production at pH 4.5 (data not shown). Xylulose production shown for *B* indicates that XI has activity when urea is added

pH must be well above the bulk pH of 4.5 for the XI within the pellets to be catalytically active. Therefore, when the xylose in the bulk solution diffuses into the pellets and reaches a higher pH region where XI is active, xylose isomerizes to form xylulose. At the same time, the continuous production of ammonia in the outer layer (Zone 1, Fig. 1) of the co-immobilized pellets also tends to neutralize any hydrogen ions that diffuse into the core of the pellets from the bulk solution, thereby sustaining the pH difference between the interior of the pellets and the external solution.

Because the rate of isomerization in curve B is lower than that obtained at pH 7.5 in unaltered pellets, it suggests that the interior pH is not maintained at 7.5 but at a suboptimal pH, either above or below 7.5. If the interior pH is suboptimal, then the XI activity will be lower than that in the unaltered pellets at pH 7.5, and we expect that the time required to reach equilibrium will be longer. If XI activity is reduced in the co-immobilized pellets, the time required for isomerization may ultimately exhaust the urea from the bulk solution, at which point XI activity will be lost, and the isomerization reaction will cease.

The interior pellet pH is a function of the urease loading and the urea concentration profile in the pellet. The K_m for urease hydrolysis of urea is 2.9 mM, [29] so with 0.01 M (10 mM) urea, we are initially consuming urea at approximately 78% of V_{max} at the surface of the pellet. Increasing the bulk concentration of urea will result in increased ammonia production and an increase in the interior pellet pH. Depending upon whether the interior pH is above or below the pH for optimum XI activity, an increase in interior pH will decrease or increase the rate of xylose isomerization. To achieve optimal isomerization in the co-immobilized pellet system, the urea concentration in the bulk solution can be optimized for a specific urease loading and should be maintained at a constant concentration throughout the isomerization to allow maximal, constant XI activity.

Although our system has not been optimized to achieve the most favorable internal pH for XI activity, we are able to demonstrate significant XI activity in our co-immobilized enzyme pellets at a bulk pH of 4.5 with 0.01 M urea. As the overall production rate of ethanol is limited by the total concentration of xylulose available to the yeast [9], it is important to determine if we can modify our experimental conditions to favorably enhance the isomerization and the xylose/xylulose proportions. Hence, the next experiments focus on addition of borate to the reaction medium in an effort to enhance the isomerization kinetics and favorably shift the equilibrium. Results for both unaltered and co-immobilized enzyme pellets are presented.

Effect of Sodium Tetraborate Addition on Xylose Isomerization

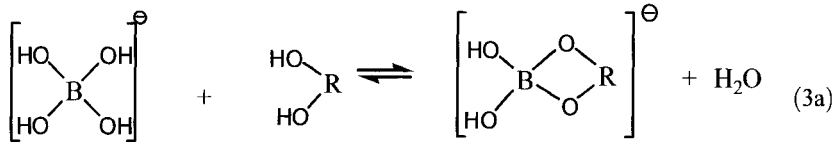
Mechanism of Sugar–Borate Complexation It has been suggested that borate leads to a shift in the equilibrium isomerization because of the binding of tetrahydroxyborate ions to aldose and ketose sugars. At near neutral pH, tetrahydroxyborate ions can be formed by hydrolysis of borax ($Na_2B_4O_5(OH)_4{\cdot}8H_20$) [44]:

$$B_4O_5(OH)_4^{2-}+5H_2O \leftrightarrow 3B(OH)_3+B(OH)_4^-+OH^- \quad (1)$$

The boric acid produced in the above reaction is a weak-acid (p*K*a~9) that ionizes to a slight extent by reaction with water at neutral pH to form additional tetrahydroxyborate ions:

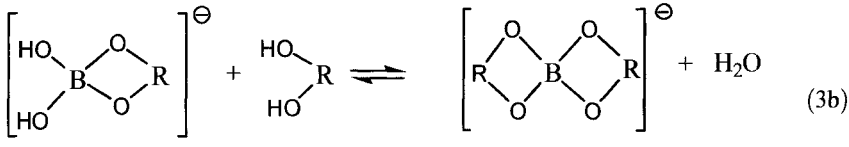
$$B(OH)_3+H_2O \leftrightarrow B(OH)_4^-+H^+ \quad (2)$$

The tetrahydroxyborate ions produced in the above reactions are able to complex with adjacent hydroxyls on sugar molecules. As shown in Eqs. 3a and 3b, each tetrahydroxyborate ion can bind up to two molecules of sugar in a two-step process.



(3a)

Tetrahydroxyborate ion **Sugar** **Mono-complex**



(3b)

Monocomplex **Sugar** **Di-complex**

Borate is able to complex, via the above mechanism, more readily with the open-chain structure of xylulose as compared to the cyclic hemiacetal form of xylose [44]. This binding preference leads to a shift in the xylose/xylulose isomerization equilibrium in favor of xylulose formation.

Unaltered Pellets First, the effect of sodium tetraborate on the kinetics and equilibrium of isomerization for unaltered XI pellets in a buffer of pH 7.5 was studied. These data are shown in Fig. 3, curve A. When compared with the corresponding data obtained in the absence of borate (Fig. 2, curve A), it is clear that even at this low concentration (0.05 M), borate is able to shift the equilibrium significantly in favor of higher xylulose production. The equilibrium concentration of xylulose reaches~30 g/l, which is more that three times

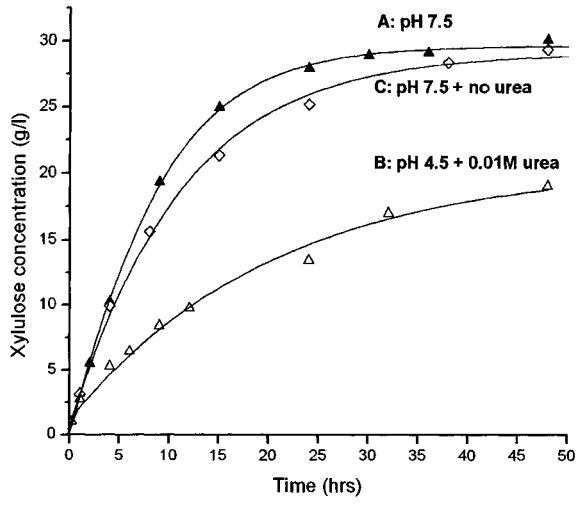


Fig. 3 Borate is able to favorably shift the xylose/xylulose equilibrium for both unaltered and co-immobilized enzyme pellets. *Solid symbols* are used for unaltered Sweetzyme™; *open symbols* are used for the XI/urease co-immobilized pellets. The three experiments shown are *A* pH 7.5; B pH 4.5 with 0.01 M urea, and *C* pH 7.5 with no urea. All three experiments show a significant shift in the equilibrium toward xylulose production. However, only the conditions represented by curve *B* are conducive for simultaneous isomerization and fermentation

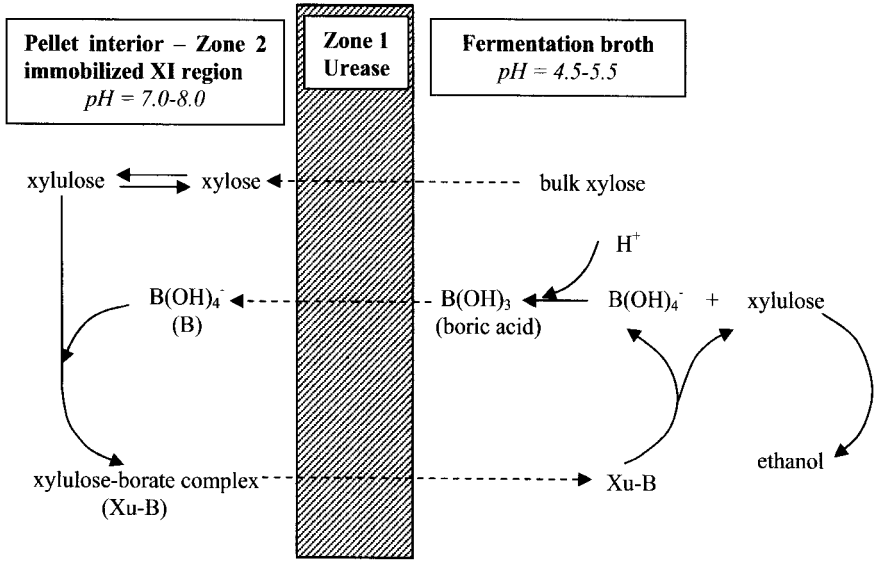


Fig. 4 Role of xylulose–borate complexation in the co-immobilized enzyme system. When sodium tetraborate (borax) is added to solution, it dissociates into tetrahydroxyborate (borate, *B*) ion and boric acid. In the pellet interior, higher pH favors tighter xylulose–borate binding, which effectively reduces the xylulose concentration in the interior and forces the isomerization forward. In the bulk, the lower pH has an uncoupling effect on the Xu–B complex, making the dissociated xylulose readily available to the yeast. Removal of xylulose via fermentation further forces dissociation of the xylulose–borate complex. *Dashed lines* represent transport of species; *solid lines* represent reactions

that seen without borate (~9 g/l). Borate addition leads to an increased conversion of xylose and a shift in the equilibrium xylose/xylulose ratio from about 6:1 to about 1:1.

Urease Co-immobilized Pellets The effect of urease immobilization on the pellets has a negligible impact on the overall kinetics and equilibrium achieved at pH 7.5 as shown in Fig. 3, curves A and C (both run without urea). The immobilized urease may add a small mass transfer resistance, which could account for the slowing of the kinetics seen as the xylose concentration decreases. Next, upon adding urea (0.01 M) to the citrate buffer solution, we again see significant formation of xylulose with our co-immobilized pellet system, with xylulose reaching a concentration of~17 g/l by 48 h. This value is much higher than the corresponding level reached without borate addition, which was about 5 g/l (see Fig. 2, curve B, and Fig. 3, curve B).

As suggested by reactions given in Eqs. 1 and 2, the formation of tetrahydroxyborate ions is affected by the pH of the medium, and consequently, the ability of borax to shift the xylose/xylulose isomerization equilibrium is also a function of pH. At low pH (4 to 5), very few tetrahydroxyborate ions are formed (as the second reaction does not occur) and accordingly borax is less likely to have any influence on the isomerization equilibrium. On the other hand, in the higher pH range (6 to 8), the tetrahydroxyborate ion concentration reaches appreciable levels, and these ions bind strongly to xylulose (Eq. 3), shifting the isomerization equilibrium.

As shown in Fig. 4, in our two-pH environment system, we expect that the core region of the pellets (where the pH is high and XI is active) provides conditions conducive to

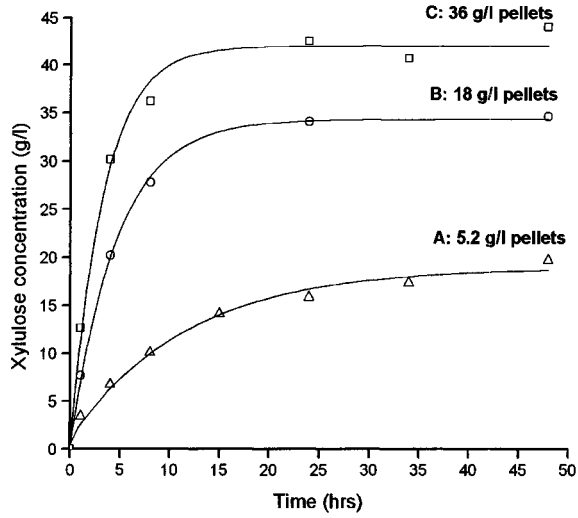


Fig. 5 Effect of XI/urease activity on the isomerization kinetics and xylose/xylulose production for the co-immobilized enzyme pellets. All pellets were from the same co-immobilization batch and have the same urease and XI activities per gram of pellet at pH 7.5. The initial urea concentration used in all experiments was 0.01 M. The improvement in the xylulose yields with increased enzyme loading can be attributed to the dual role of tetrahydroxyborate ions in our co-immobilized pellet system

strong binding of xylulose to tetrahydroxyborate ions and formation of the xylulose–borate complex (Xu–B). However, in the bulk solution where the pH is low, very little borate–sugar complex formation takes place. The likely net result of this two-pH environment in the context of SIF is that boric acid diffuses into the pellets, is converted to tetrahydroxyborate ions (Eq. 2), binds to xylulose, and ferries xylulose from inside the pellet to the bulk solution outside. In the low pH bulk solution, the Xu–B releases xylulose and the borate ions recombine with hydrogen ions to form boric acid. Thus, tetrahydroxyborate, in addition to shifting the isomerization equilibrium, facilitates the removal of xylulose from the core of the pellets into the bulk where xylulose can be readily metabolized by yeast to ethanol. Xylose feed solutions isomerized in the presence of 0.05 M borate have been used in fermentation studies with yeast, and no inhibition of yeast by borate have been observed [45].

Effect of Co-immobilized Pellet Mass on Isomerization

The activity of the Sweetzyme™ pellets co-immobilized with urease depends on many factors [29]. These factors include the concentration of urea and the pH in the bulk solution and the activity of urease immobilized in the outer layer (Zone 1) of the pellet. These factors influence the production of ammonia and the neutralization of the diffusing hydrogen ions and hence the size of the active XI zone (Zone 2).

In Fig. 5, transient xylulose production is shown as a function of total co-immobilized pellet mass. All pellets used were from the same co-immobilization batch and have the same urease and XI loadings. Experiments were conducted at 34 °C and pH 4.5 with 0.01 M urea, 0.05 M sodium tetraborate, and an initial xylose concentration of 60 g/l. Experiments shown in curves B and C have 3.3 (18 g/l) and 6.6 (36 g/l) times more of each enzyme compared to curve A (5.2 g/l). At time zero in all experiments, the interior pH increases rapidly to values closer to the optimum for XI activity as ammonia is produced. In experiments B and C, the increased mass of urease and XI will cause a more rapid decrease in the bulk urea and xylose concentrations than in A. As the bulk urea concentration decreases, the ammonia production per pellet decreases and the interior pH also starts to decrease. This drop in pH occurs earlier in cases where the total urease mass (activity) is higher, leading to an accompanying loss in specific XI activity. From the data shown in Fig. 5, the average specific XI activity was

Table 1 Effect of co-immobilized pellet mass on isomerization kinetics and xylulose production.

Experiment	Mass of pellets (g)	Ave. XI activity in first hour (U)	Specific XI activity in first hr (ave; U/g pellet)	Final [Xylulose] (g/l)
A	0.13	7.8	58.5	20.0
B	0.45	20.4	45.3	34.4
C	0.9	34.9	38.8	44.0

Total XI is proportional to the pellet mass, but the XI activity measured over the first hour depends on the internal pH profile within the pellet. As pellet mass increases, the bulk urea concentration decreases more rapidly and the changing internal pH profile results in an apparent decrease in specific XI activity. Although urea consumption and loss of XI activity occurs most rapidly for the highest pellet mass, the total xylulose produced while the XI is active is the greatest.
1 U=1 μmol of xylulose produced per minute at 34 °C and bulk pH of 4.5.

calculated for the first hour of isomerization; these results are summarized in Table 1. The average specific XI activity (based on xylulose production per g of pellets at pH 4.5) decreases with increasing pellet mass. However, the corresponding total XI activity is higher, resulting in a much more rapid production of xylulose and much higher xylulose yield by 48 h.

It is noteworthy that the xylulose concentration (~44 g/l) at 48 h for the highest pellet mass is substantially higher than the value achieved (~30 g/l) with unaltered pellets at pH 7.5 with the same borate concentration (Fig. 3 curve A). For an unaltered Sweetzyme™ pellet, the kinetics of the isomerization depend on the XI activity, but the equilibrium is governed solely by the thermodynamics and is unaffected by the XI activity and pellet mass. In our co-immobilized pellet system, we are seeing xylulose conversions that are higher than those possible with the unaltered pellets at pH 7.5. As mentioned in the context of Fig. 3 and illustrated in Fig. 4, in our co-immobilized pellet system, tetrahydroxyborate acts to shift the equilibrium by binding to xylulose and also shuttles complexed xylulose from the pellet interior to the bulk solution. We believe that this dual role of tetrahydroxyborate is responsible for the significant improvement in xylose conversion seen in our co-immobilized pellet system when a pH gradient is established.

Effect of Urea

The urea concentration in the bulk media will affect the rate and quantity of ammonia produced and hence the maintenance of the pH gradient within the co-immobilized enzyme pellet. The urea concentration will also determine the volume of the active XI core, and this will in turn influence the kinetics of the isomerization and the extent of isomerization. In Fig. 6, transient xylulose production is shown as a function of urea concentration. All pellets used were from the same co-immobilization batch and have the same urease and XI loadings. Experiments were conducted at 34 °C and pH 4.5 with either 0.01 M (curve A) or 0.1 M urea (curve B), 0.05 M sodium tetraborate, and an initial xylose concentration of 60 g/l.

As seen in these the two experiments, the rate of xylose isomerization is very similar for the first 4 h. For both cases, the concentration of urea is significantly higher than the K_m for urease so the internal pH profiles within the pellet are likely to be similar. As the pellets also have the same XI loading, xylulose production is equivalent in both. However, by 8 h, urea consumption in A results in a decrease in reaction velocity for urea hydrolysis. With reduced ammonia production, the internal volume of the pellet with active XI decreases, and a drop in xylulose production relative to B is observed. Based on the results shown for A, urea hydrolysis is no longer effective at maintaining the two pH microenvironments by 24 h.

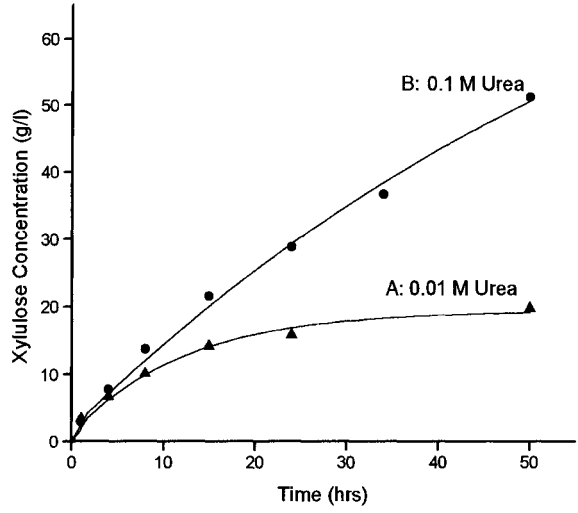


Fig. 6 Effect of initial urea concentration on the isomerization kinetics and xylulose production for the co-immobilized enzyme pellets. Both experiments use 0.13 g pellets from the same co-immobilization batch and have the same urease and XI activities per gram of pellet at pH 7.5. The decrease in the rate of isomerization and xylulose production seen in *A* is because of consumption of urea. Urea concentration is initially higher than the K_m for urease, but as the urea concentration drops, the reaction velocity and ammonia production decrease, resulting in a loss of the pH gradient within the pellet. In *B*, the urea concentration is high enough that the rate of xylulose isomerization does not appear to be affected by urea consumption over the entire 48-h period

For B, with a much higher initial urea concentration, the active zone for xylose isomerization is maintained for a much longer period of time (>48 h). The final xylulose concentration measured at 48 h was~52 g/l, corresponding to a xylose/xylulose ratio of ~1:6.5.

Effect of Co-immobilized Pellet Mass on Isomerization in Presence of Excess Urea

The effects of pellet mass and urea concentration on the final composition of the isomerization solution are summarized in Fig. 7. Pellet mass ranged from 0.13 to 0.9 g per experiment, whereas the initial urea concentrations were either 0.01 or 0.1 M. For 0.01 M urea (B and C), the increase in pellet mass results an increase in rate of xylulose production (see also Fig. 5) as well as an increase in the total xylulose produced. However, none of the experiments with 0.01 M urea reach a xylulose yield as high as that achieved when 0.1 M urea is added. For 0.1 M urea (D and E), the increase in pellet mass also results in an increase in the rate of xylulose production and a reduction in the time required to reach the final solution composition, but the final xylulose yields remain unchanged. Although increasing the pellet mass (more XI) increases the isomerization kinetics, urea plays an essential role in maintaining XI activity and achieving high xylulose yields. The co-immobilized enzyme system, by virtue of the unique two-pH microenvironments and the borate shuttling of xylulose to the bulk, results in conversion of xylose to xylulose (~86%) that is significantly higher than that achievable with the native XI at its optimal pH.

Effect of Metal Ion Addition on Xylose Isomerization

In addition to evaluating the effectiveness of borate in favorably shifting the xylose to xylulose equilibrium, we were also concerned with maintaining sustained optimal activity of

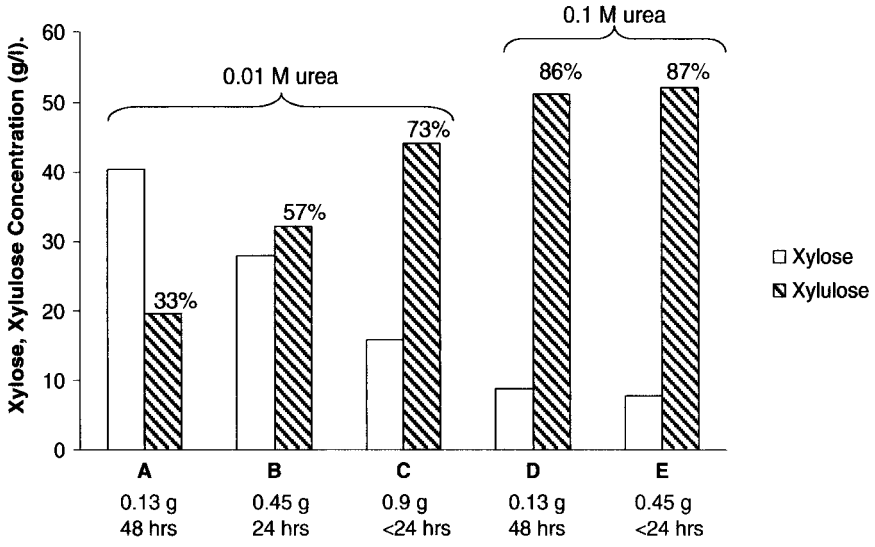


Fig. 7 Effect of initial urea concentration and mass of pellets on xylulose production for the co-immobilized enzyme pellets. All pellets were from the same co-immobilization batch and have the same urease and XI activities per g pellet at pH 7.5. The percentage conversion to xylulose is given *above the bars* for each experiment. The time indicated on the *x*-axis represents the time of apparent equilibrium for all experiments. With 0.01 M urea (*A*, *B*, and *C*), increasing the pellet mass results in a significant increase in xylulose formation. With 0.1 M urea (*D* and *E*), the final xylulose production is only minimally increased by increasing the mass of pellets

XI for long time periods. The XI enzyme requires metal ions for activity, and these ions can be depleted during the isomerization [46]. It has been suggested that improvement in long-term activity of XI can be realized by the addition of Mg^{2+}, and Co^{2+} ions to the medium [47, 48].

In these experiments, unaltered Sweetzyme™ at pH 7.5 was used. In the absence of borate, addition of metal ions results in a small shift in the isomerization toward xylulose (Fig. 8, curves A and B). In the presence of borate, a similar shift in the isomerization is

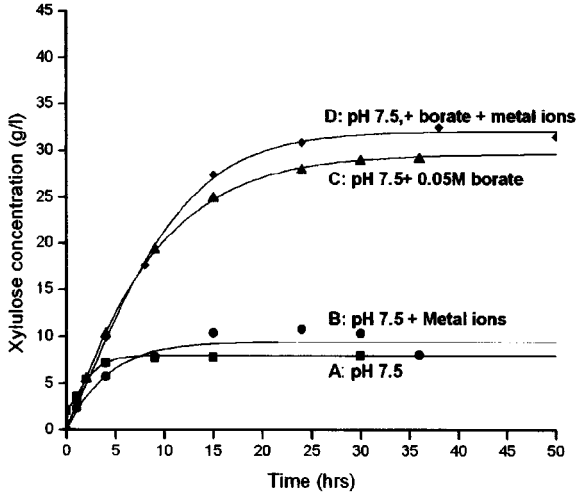


Fig. 8 Addition of metal ions results in a small shift in the isomerization toward xylulose, but the effect is not as significant as the shift associated with addition of sodium tetraborate. If added, sodium tetraborate was 0.05 M, and metal ions were 20 mM $MgCl_2$ and 1 mM $CoCl_2$. All data shown are for unaltered Sweetzyme™ at pH 7.5. The four experiments shown differ by additives and are *A* no additives, *B* metal ions, *C* borate, and *D* borate and metal ions

observed (Fig. 8, curves C and D). Thus, metal ions either alone or in conjunction with borate provide an incremental improvement in the xylulose production, but the effect is not as significant as the shift associated with addition of sodium tetraborate.

Summary and Conclusions

One of the crucial issues in ethanol production from lignocellulosic biomass is the ability to convert both the hexose (C6) and pentose (C5) sugars resulting from the saccharification of its cellulose and hemicellulose portions. In this paper, a method for producing high yields of xylulose from xylose isomerization (the principal C5 sugar from hemicellulose) is presented, as xylulose can be converted to ethanol by native *S. cerevisiae* along with glucose (C6 sugar).

In our experiments at pH 7.5 and 34 °C with SweetzymeTM pellets, we found that starting with 60 g/l of xylose; we could shift the equilibrium concentration of xylulose from~9 to~30 g/l by the addition of 0.05 M borax. The positive shift in equilibrium results from the selective complexation of xylulose to the tetrahydroxyborate ions formed from borax at this pH. Although the xylulose production is significantly enhanced with borate, if the isomerization and the fermentation steps are sequential, only half of the available xylose may be converted to ethanol.

Simultaneous isomerization and fermentation (SIF) is expected to drive the isomerization forward and lead to higher xylose utilization. Unfortunately, the pH optima for the isomerization (~7.5) and the fermentation (~4.5) steps are vastly different. The approach we have taken is to develop a novel technique for SIF that is capable of sustaining two different pH-microenvironments in a single vessel—one optimal for xylose isomerization and the other optimal for fermentation of xylulose. The technique involves co-immobilization of urease with xylose isomerase. We have shown that it is possible to sustain a significant pH gradient between the bulk liquid and the core region of the pellet by adding urea to the fermentation broth.

Using our co-immobilized enzyme system in media supplemented with borate, we have obtained xylose conversions that are higher than those possible with the native XI pellets operating under optimal pH at the same borate concentration. The advantage of the co-immobilized enzyme system results from the pH-dependent nature of borate/xylulose binding, and Fig. 4 summarizes our hypothesis as to why isomerization is enhanced in our system. The results presented demonstrate the effectiveness of our co-immobilized enzyme system for isomerization under conditions optimal for fermentation by common *S. cerevisiae*. As the overall production rate of ethanol in SIF is limited by the total concentration of xylulose available to the yeast [9], our technique significantly improves upon currently available options for SIF.

Acknowledgement This research was sponsored by SuGanit Systems, Inc. (Reston, VA). A US provisional patent has been filed on this technology and is licensed to SuGanit Systems, Inc.

References

1. Zaldivar, J., Nielsen, J., & Olsson, L. (2001). Fuel ethanol production from lignocellulose: a challenge for metabolic engineering and process integration. *Applied Microbiology and Biotechnology*, *56*(1–2), 17–34.

2. Office of Science, US DOE. (2005). Breaking the biological barriers to cellulosic ethanol: A research roadmap resulting from the biomass to biofuels workshop, December 2005. Rockville, MD: US Department of Energy.
3. Holtzapple, M. T. (1993). Chapters, cellulose, hemicelluloses, and lignin. In M. J. Sadler (Ed.), *Encyclopedia of food science, food technology and nutrition* (pp. 758–767, 2324–2334, 2731–2738). London: Academic.
4. Somerville, C., Bauer, J. G. B., Facette, M., Hamann, T., Milne, J., Osborne, E., Paredez, A., Persson, S., Raab, T., Vorwerk, S., & Youngs, H. (2004). Toward a systems approach to understanding plant cell walls. *Science*, *306*(5705), 2206–2211.
5. Van Maris, A. J. A., Abbott, D. A., Bellissimi, E., Van Den Brink, J., Kuyper, M., Luttik, M. A. H., Wisselink, H., Scheffers, A. W., Van Dijken, J. P., & Pronk, J. T. (2006). Alcoholic fermentation of carbon sources in biomass hydrolysates by Saccharomyces cerevisiae: current status. *Antonie van Leeuwenhoek*, *90*(4), 391–418.
6. Prior, B. A., Kilian, S. G., & Dupreez, J. C. (1989). Fermentation of d-xylose by the yeasts *Candida shehatae* and *Pichia stipitis*. *Process Biochemistry*, *24*, 21–32.
7. Tantirungkij, M., Nakashima, N., Seki, T., & Yoshida, T. (1993). Construction of xylose-assimilating Saccharomyces cerevisiae. *Journal of Fermentation and Bioengineering*, *75*(2), 83–88.
8. Wang, P. Y., Shopsis, C., & Schneider, H. (1980). Fermentation of a pentose by a yeasts. *Biochemical and Biophysical Research Communications*, *94*, 248–254.
9. Chiang, L. C., Gong, C. S., Chen, L. F., & Tsao, G. T. (1981). D-Xylulose fermentation to ethanol by Saccharomyces cerevisiae. *Applied and Environmental Microbiology*, *42*(2), 284–289.
10. Hsaio, H. Y., Chiang, L. C., Ueng, P. P., & Tsao, G. T. (1982). Sequential utilization of mixed monosaccharides by yeasts. *Applied and Environmental Microbiology*, *43*(4), 840–845.
11. Gong, C. S., Chen, L. F., Flickinger, M. C., Chiang, L. C., & Tsao, G. T. (1981). Production of ethanol from D-xylose by using D-xylose isomerase and yeasts. *Applied and Environmental Microbiology*, *41*(2), 430–436.
12. Yu, S., Jeppsson, H., & Hahn-Gaegerdal, B. (1995). Xylulose fermentation by Saccharomyces cerevisiae and xylose fermenting yeast strains. *Applied Microbiology and Biotechnology*, *44*, 314–320.
13. Sarthy, A. V., Mcconaughy, B. L., Lobo, Z., Sundstrom, J. A., Furlong, C. E., & Hall, B. D. (1987). Expression of the Escherichia coli xylose isomerase gene in Saccharomyces cerevisiae. *Applied and environmental microbiology*, *53*(9), 1996–2000.
14. Kotter, P., Amore, R., Hollenberg, C. P., & Ciriacy, M. (1990). Isolation and characterization of the Pichia stipitis xylitol dehydrogenase gene, XYL2, and construction of a xylose-utilizing Saccharomyces cerevisiae transformant. *Current genetics*, *18*(6), 493–500.
15. Amore, R., Kotter, P., Kuster, C., Ciriacy, M., & Hollenberg, C. P. (1991). Cloning and Expression in Saccharomyces cerevisiae of the NAD(P)H- dependent xylose reductase- encoding gene (XYL1) from the xylose assimilating yeast Pichia stipitis. *Gene*, *109*, 89–97.
16. Moes, C. J., Pretorius, I. S., & Van Zyl, W. H. (1996). Cloning and expression of the Clostridium thermosulfurogenes D-xylose isomerase gene (xylA) in Saccharomyces cerevisiae. *Biotechnology Letters*, *18*(3), 269–274.
17. Walfridsson, M., Bao, X., Anderlund, M., Lilius, G., Buelow, L., & Hahn-Gaegerdal, B. (1996). Ethanolic fermentation of xylose with Saccharomyces cerevisiae harboring the Thermus thermophilus xylA gene, which expresses an active xylose (glucose) isomerase. *Applied and Environmental Microbiology*, *62*(12), 4648–4651.
18. Hahn-Hagerdal, B., Wahlbom, C. F., Gardonyi, M., Van Zyl, W. H., Otero, R. R. C., & Jonsson, L. J. (2001). Metabolic engineering of Saccharomyces cerevisiae for xylose utilization. *Advances in Biochemical Engineering/Biotechnology*, *73*, 53–84.
19. Jeppsson, M., Johansson, B., Hahn-Gaegerdal, B., & Gorwa-Grauslund, M. F. (2002). Reduced Oxidative Pathway flux in recombinant xylose-utilizing strains improves the ethanol yield from xylose. *Applied and Environmental Microbiology*, *69*, 5892–5897.
20. Johansson, B., & Hahn-Gaegerdal, B. (2002). The non-oxidative pentose phosphate pathway controls the fermentation rate of xylulose, but not of xylose in Saccharomyces cerevisiae. *FEMS Yeast Research*, *2*, 277–282.
21. Verho, R., Londesborough, J., Penttilae, M., & Richard, P. (2003). Engineering redox cofactor regeneration for improved pentose fermentation in Saccharomyces cerevisiae. *Applied and Environmental Microbiology*, *69*(10), 5892–5897.
22. Gardonyi, M., & Hahn-Hagerdal, B. (2003). The Streptomyces rubiginosus xylose isomerase is misfolded when expressed in Saccharomyces cerevisiae. *Enzyme and Microbial Technology*, *32*(2), 252–259.
23. Kuyper, M., Harhangi, H. R., Stave, A. K., Winkler, A. A., Jetten, M. S. M., De Laat, W. T. A. M., Den Ridder, J. J. J., Op Den Camp, H. J. M., Van Dijken, J. P., & Pronk, J. T. (2003). High-level functional

expression of a fungal xylose isomerase: the key to efficient ethanolic fermentation of xylose by Saccharomyces cerevisiae? *FEMS Yeast Research*, *4*(1), 69–78.
24. Kuyper, M., Winkler, A. A., Van Dijken, J. P., & Pronk, J. T. (2004). Minimal metabolic engineering of Saccharomyces cerevisiae for efficient anaerobic xylose fermentation: a proof of principle. *FEMS Yeast Research*, *4*, 655–664.
25. Kuyper, M., Toirkens, M. J., Diderich, J. A., Winkler, A. A., Van Dijken, J. P., & Pronk, J. T. (2005). Evolutionary Engineering of mixed-sugar utilization by a xylose-fermenting Saccharomyces cerevisiae strain. *FEMS Yeast Research*, *5*, 925–934.
26. Dien, B. S., Cotta, M. A., & Jeffries, T. W. (2003). Bacteria engineered for fuel ethanol production: current status. *Applied Microbiology and Biotechnology*, *63*, 258–266.
27. Jeffries, T. W. (2006). Engineering yeasts for xylose metabolism. *Current Opinion in Biotechnology*, *17*, 320–326.
28. Linden, T., & Hahn-Gaegerdal, B. (1989). Fermentation of lignocellulose hydrolysates with yeasts and xylose isomerase. *Enzyme and Microbial Technology*, *11*, 583–589.
29. Byers, J. P., Fournier, R. L., & Varanasi, S. (1992). A Feasibility Analysis of a Novel Approach For the Conversion of Xylose to Ethanol. *Chemical Engineering Communications*, *112*, 165–187.
30. Chandrakant, P., & Bisaria, V. S. (2000). Simultaneous bioconversion of glucose and xylose to ethanol by Saccharomyces cerevisiae in the presence of xylose isomerase. *Applied Microbiology and Biotechnology*, *53*, 301–309.
31. Bhosale, S. H., Rao, M. B., & Deshpande, V. V. (1996). Molecular and industrial aspects of glucose isomerase. *Microbiological Reviews*, *60*(2), 280–300.
32. Mitsuhashi, S., & Lampen, J. O. (1953). Conversion of D-xylulose to D-xylose in extracts of Lactobacillus pentosus. *Journal of Biological Chemistry*, *204*, 1011–1018.
33. Hochester, R. M., & Watson, R. W. (1954). Enzymatic isomerization of D-xylose to D-xylulose. *Archives of Biochemistry and Biophysics*, *48*, 120–129.
34. Tewari, Y. B., Steckler, D. K., & Goldberg, R. N. (1985). Thermodynamics of the conversion of aqueous xylose to xylulose. *Biophysical Chemistry*, *22*, 181–185.
35. Byers, J. P., Shah, M. B., Fournier, R. L., & Varanasi, S. (1993). Generation of pH gradient in an immobilized enzyme system. *Biotechnology and Bioengineering*, *42*, 410–429.
36. Fournier, R. L., Byers, J. P., Varanasi, S., & Chen, G. (1996). Demonstration of pH control in a commercial immobilized glucose isomerase. *Biotechnology and Bioengineering*, *52*, 718–722.
37. Boeseken, J. (1949). The use of boric acid for the determination of the configuration of carbohydrates. *Advances in Carbohydrate Chemistry*, *4*, 189.
38. Foster, A. B. (1957). Zone electrophoresis of carbohydrates. *Advances in Carbohydrate Chemistry*, *12*, 81.
39. Mendicino, J. F. (1960). Effect of borate on the alkali-catalyzed isomerization of sugars. *Journal of the American Chemical Society*, *82*(18), 4975–4979.
40. Hsaio, H. Y., Chiang, L. C., Chen, L. F., & Tsao, G. T. (1982). Effects of borate on isomerization and yeast fermentation of high xylulose solution and acid hydrolysate of hemicellulose. *Enzyme and Microbial Technology*, *4*, 25–31.
41. Allen, K. N., Lavie, A., Glassfeld, A., Tanada, T. N., Jerrity, D. P., Carlson, S. C., Farber, G. K., Petsko, G. A., & Ringe, D. (1994). Role of the divalent metal ion in sugar binding, ring opening and isomerization by D-xylose isomerase; replacement of a catalytic metal by an amino acid. *Biochemistry*, *33*, 1488–1494.
42. Liu, H. H., & Shi, Y. (1997). The reaction pathway of the isomerization of D-xylose catalysed by the enzyme D-xylose isomerase: A theoretical study. *Proteins: Structure, Function and Genetics*, *27*, 545–55.
43. Worthington, C. E. (1972), Enzymatic assay of urease from Jack Beans (E.C.3.5.1.5). In Worthington Enzyme Manual (pp. 146–148). Freehold, NJ: Worthington Biochemical Corporation.
44. Rizzi, G. P. (2007). On the effect of tetraborate ions in the generation of colored products in thermally processed glycine-carbohydrate solutions. *Journal of Agricultural and Food Chemistry*, *55*, 2016–2019.
45. Hsiao, H. Y., Chiang, L. C., Chen, L. F., & Tsao, G. T. (1982). Effects of borate on isomerization and yeast fermentation of high xylulose solution and acid hydrolysate of hemicellulose. *Enzyme and Microbial Technology*, *4*, 25–31.
46. Pastinen, O., Visuri, K., Schoemaker, H. E., & Leisola, M. (1999). Novel reactions of xylose isomerase from Streptomyces rubiginosus. *Enzyme and Microbial Technology*, *25*, 695–700.
47. Callens, M., Kersters-Hilderson, H., Van Opstal, O., & De Bruyne, C. K. (1988). Catalytic properties of D-xylose isomerase from Streptomyces violaceoruber. *Enzyme and Microbial Technology*, *8*(11), 696–700.
48. Callens, M. H., Tomme, P., Kesters-Hilderson, W., Cornelis, R., Vangrysperre, W., & Debruyne, C. K. (1988). Metal ion binding to D-xylose isomerase from Streptomyces violaceoniger. *Biochemistry Journal*, *250*, 285–290.

49. Fournier, R. L., Varanasi, S., Byers, J. P. "Bilayer pellet containing immobilized xylose isomerase and urease for the simultaneous isomerization and fermentation of xylose to ethanol," US Patent # 5,254, 468.
50. Fournier, R. L., Varanasi, S., Byers, J. P. "Method of producing products with a bilayer pellet containing a coimmobilized enzyme system that maintains a pH difference," US Patent # 5,397,700.
51. Varanasi, S., Rao, K., & Relue, P. "A Novel technique that enables efficient fermentation of xylose and hexose sugars from biomass hydrolasates using native non-GMO yeasts," US provisional patent application filed 01/4/08.

Appl Biochem Biotechnol (2008) 146:119–128
DOI 10.1007/s12010-007-8049-3

The Effects of Wheat Bran Composition on the Production of Biomass-Hydrolyzing Enzymes by *Penicillium decumbens*

Xianyun Sun · Ziyong Liu · Yinbo Qu · Xuezhi Li

Received: 22 April 2007 / Accepted: 5 September 2007 /
Published online: 22 September 2007
© Humana Press Inc. 2007

Abstract The effects of the starch, protein, and soluble oligosaccharides contents in wheat bran on the extracellular biomass-hydrolyzing enzymes activities released by *Penicillium decumbens* mycelia grown in batch fermentations have been examined. The results showed increased starch content correlated directly with an increase in released amylase activity but inversely with the levels of secreted cellulase and xylanase. High amounts of protein in wheat bran also reduced the activities of cellulase, xylanase and protease in the culture medium. The effects of the soluble and insoluble components of wheat bran and cello-oligosaccharides supplements on production of extracellular cellulase and xylanase were compared. The soluble cello-oligosaccharides compositions in wheat bran were proved to be one of the most significant factors for cellulase production. According to the results of this research, determining and regulating the composition of wheat bran used as a fermentation supplement may allow for improved induction of cellulase and xylanase production.

Keywords *Penicillium decumbens* · Wheat bran · Biomass · Cellulase · Xylanase

Introduction

Penicillium species with the ability to produce high cellulase and hemicellulase titres have been described [1, 2]. Also, they have the advantage of containing higher glucosidase activity than *Trichoderma* [2]. So, *Penicillium* species have great potential for hydrolysis of lignocellulosic materials. *Penicillium decumbens* 114-2 was fast-growing cellulolytic fungus that isolated from soil [3] and its catabolic repression-resistant mutants have been used industrially for biomass hydrolysis [4, 5]. In previous study, wheat bran supplements have been shown to promote the growth of *P. decumbens*, and increase the cellulase and β-glucosidase activities released by *P. decumbens* mycelia [6], but the basis of this stimulation is still unknown.

X. Sun · Z. Liu · Y. Qu (✉) · X. Li
State Key Laboratory of Microbial Technology, Shandong University, Jinan 250100, China
e-mail: quyinbo@sdu.edu.cn

Wheat bran is the outer ~15% of the wheat seed and is composed predominantly of non-starch carbohydrates (~58%), starch (~19%) and crude protein (~18%), with the non-starch polysaccharides being primarily ~70% arabinoxylans, ~24% cellulose and ~6% β-(1,3) (1,4)-glucan [7–10]. Reports have showed wheat bran or acid-hydrolyzed wheat bran can increase cellulase production by filamentous fungi [6, 9, 11, 12]. Also, wheat-bran culture gave the richest gene expression profile of hydrolytic enzymes from *Aspergillus oryzae* among the three tested media [13]. However, which factor in wheat bran being important for cellulase synthesis is unknown yet.

It is generally believed that oligosaccharides play an important role in regulating the synthesis of wood-degrading enzymes [14, 15], and oligosaccharides has been proved to be converted to inducer (such as sophorose and gentiobiose) by transglucosylation [16–19]. So, we supposed that oligosaccharides may exist in autoclaved wheat bran, which may play an important role in increasing the production of the extracellular biomass-hydrolyzing enzymes by *P. decumbens*. The experiments reported here were undertaken to identify the components in wheat bran responsible for the stimulation of growth and the increased production of the industrially important biomass-degrading enzymes by *P. decumbens*. The knowledge obtained may provide a scientific platform for further improvement of the processes that employ this fungus for biomass conversion.

Materials and Methods

Microorganism and Culture Conditions

P. decumbens 114-2 stock cultures were grown on wheat bran extract agar slants for 6 days at 30 °C to allow sporulation. Spores were then washed from the agar surface using sterile water, and aliquots of the resulting spore suspensions were inoculated to liquid media of 50 ml in 300 ml flasks sterilized by autoclaving at 115 °C for 30 min. The media used contained one or more carbon sources, as noted in the text and figure legends, dissolved in Mandel's solution [3], namely (per liter): 3 g KH_2PO_4, 2.6 g $NaNO_3$, 0.5 g $MgSO_4{\cdot}7H_2O$, 0.5 g $CaCl_2$, 0.5 g urea, 7.5 mg $FeSO_4{\cdot}7H_2O$, 2.5 mg $MnSO_4{\cdot}H_2O$, 3.6 mg $ZnSO_4{\cdot}7H_2O$, 3.7 mg $CoCl_2{\cdot}6H_2O$ and 1 g peptone (pH 5.5). The inoculated media were incubated for 4.5 days (the time point of maximum enzyme activities and steady growth phases of *P. decumbens*) at 30 °C, 180 rpm on rotary shakers.

Enzyme Assays

Accumulated *P. decumbens* biomass was removed by centrifugation, and aliquots of the resulting supernatants were diluted and assayed for enzyme activities. One unit of all enzyme activities is defined as the amounts of the enzyme that liberates 1 μmol of product per minute under the assay conditions used.

(1) Cellulase activity was measured by reducing sugar released from filter paper (Whatman No.1) and from carboxymethylcellulose with glucose as the standard [20–22].
(2) β-glucosidase activity was assayed using salicin as the substrate [23]. Dilutions of supernatant (0.5 ml) were incubated with 1 ml of 1% (*w/v*) solution of salicin in 0.2 M acetate buffer (pH 4.8) at 50 °C for 30 min and the DNS method was used to quantify the reducing sugar released.

(3) Xylanase activity was assayed by measuring the reducing sugars liberated from 1% (*w/v*) xylan (from oat spelts, Sigma) suspended in acetate buffer (0.2 M, pH 4.8) when incubated with aliquots of diluted supernatant at 50 °C for 30 min [24]. The amounts of reducing sugars released were determined using the DNS assay with xylose as the standard sugar.
(4) Amylase activity was measured using 1% (*w/v*) soluble starch dissolved in acetate buffer (0.2 M, pH 4.8) as the substrate. Reaction mixtures were incubated for 10 min at 40 °C and the reducing sugars released were measured using the DNS assay with maltose as the standard sugar.
(5) Protease activity was measured using 1% (*w/v*) casein as substrate dissolved in 0.1 M phosphate buffer (pH 3.0). Aliquots (2 ml) of diluted supernatant were mixed with 2 ml of 1% (*w/v*) casein and the reaction mixtures incubated at 40 °C for 10 min. An equal volume of trichloroacetic acid (0.4 l) was added to the reaction mixture, after filtration, the tyrosine released was quantified by the absorbance of the filtrate at 275 nm (A_{275}).

Biomass Determination

The biomass was measured using the perchloric acid method [25]. Mycelium suspension was mixed with an equal volume of 1-M perchloric acid, and the mixture was incubated at 100 °C for 20 min. After centrifugation at 10,000 g for 10 min, the absorbance at 260 nm (A_{260}) of dilutions of the resulting supernatant was measured. For control experiments, the minimal amounts of biomass in cell-free supernatants were measured. Standard curve was plotted by known amounts of biomass.

Determination of Starch, Soluble Sugars and Protein Contents of Wheat Brans

The starch content in wheat bran was determined enzymatically as described by Holm et al. [26]. To determine the contents of soluble sugars and protein in 10% (*w/v*) wheat bran, microcrystalline cellulose (MCC, from cotton, Shanghai Hengxin Co.) and CF11 cellulose powder (from cotton, Whatman), these polymers were suspended in water and autoclaved at 115 °C for 30 min. The resulting solutions were filtered through 0.45-μm filters and the mono- and oligosaccharide contents of the filtrates were identified and quantified by high performance liquid chromatography (HPLC) at 75 °C using a Bio-Rad HPX-42C column with water as the eluent. The amounts of protein present in the filtrates were determined by using Bradford assay [27] with bovine serum albumin used as the standard.

Data Analysis

All results are given as the mean ± standard deviation, with the numbers of independently repeated experiments listed. Statistical analyses were fulfilled by the *t* test.

Results

The Effects of Starch and Wheat Bran on Synthesis of Cellulase and Xylanase

The amounts of biomass and cellulase and xylanase activities released into the supernatant of *P. decumbens* grown in media that contained a total of 3% (*w/v*) polymeric carbon

substrate were shown in Fig. 1. All growth media contained 1% microcrystalline cellulose (MCC) plus 2% wheat bran, or 2% wheat starch or a mixture of wheat bran and wheat starch (in the ratios 2:1, 1:1 or 1:2) that in total constituted 2% carbon source substrate. With the increase of wheat bran content, mycelial biomass, cellulase, β-glucosidase and xylanase activities in the supernatant increased but amylase activity reduced. The cultures grown on 1% MCC and 2% wheat starch with no wheat bran produced the lowest levels of cellulase, β-glucosidase, xylanase and amylase activity. As expected, the presence of starch, including the starch in wheat bran, apparently promoted amylase synthesis but starch alone did not support robust growth or substantial release of xylanase and cellulase by *P. decumbens*. There were no detectable differences in the amounts of cellulase or xylanase activity present in the supernatants of the different cultures, when these activities were calculated in terms of the biomass. The lower levels of cellulase and xylanase activities in the supernatants of cultures grown with starch therefore resulted from the reduced mycelia growth and as opposed to a regulatory reduction in enzyme synthesis or secretion.

Effects of Wheat Bran Granule Size on Synthesis of Cellulase and Xylanase

There were no detectable differences in the cellulase and xylanase activities in the supernatants of *P. decumbens* cultures grown in media supplemented with wheat bran where particles were size-separated by passage through a 1.5-mm filter compared to samples where media were not size-separated (*A* and *B* of Fig. 2). However, at smaller granule sizes, the net starch content increased and this resulted in increased amylase production but reduced total mycelial growth and lowered levels of cellulase and xylanase released (Fig. 2).

Effects of Wheat Protein Plus Wheat Bran on Cellulase and Xylanase Synthesis

Cultures were grown in media containing 1% MCC plus 2% wheat bran, or 2% wheat protein, or a mixture of wheat bran and wheat protein (ratios of 2:1, 1:1 and 1:2) that together constituted 2% carbon polymer solutions. Cultures grown with only MCC and wheat protein grew less well than cultures supplemented with wheat bran. Increasing the wheat protein to wheat bran ratio did not reduce the amounts of mycelial growth (Fig. 3)

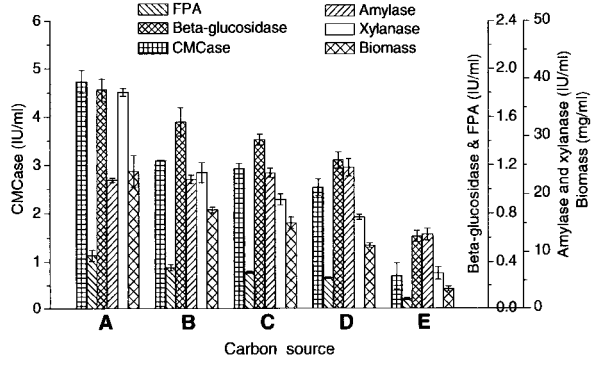


Fig. 1 Effects of starch and wheat bran on growth and production of extracellular cellulase, xylanase and amylase by *P. decumbens*. Cultures were grown and the levels of biomass and extracellular enzymes were measured as described in the "Materials and Methods" section. All cultures contained 1% MCC plus as additional carbon sources: *A* 2% wheat bran; *B* 0.7% wheat starch plus 1.4% wheat bran; *C* 1% wheat starch plus 1% wheat bran; *D* 1.4% wheat starch plus 0.7% wheat bran; and *E* 2% wheat starch

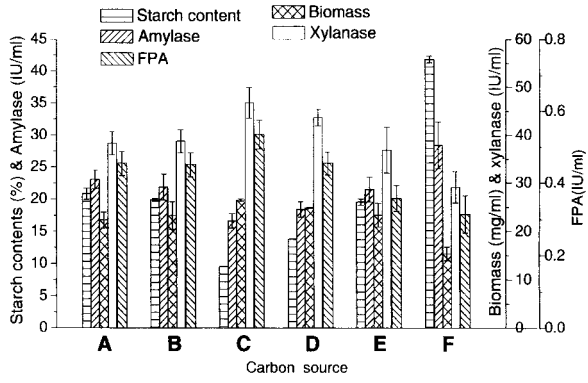


Fig. 2 Effects of granule size of wheat bran on growth and production of extracellular cellulase, xylanase and amylase by *P. decumbens*. All cultures contained 1% MCC plus 2% wheat bran: *A* all sizes of wheat bran granules; *B* wheat bran granules that passed through a 1.5-mm filter; *C* to *F* wheat bran granules with diameters of 0.45 to 0.8 mm, 0.3 to 0.45 mm, 0.2 mm to 0.3 mm, and <0.2 mm, respectively

but the amounts of cellulase, xylanase and protease released were reduced. Together, the fact that 0.1% peptone has presented in Mandel's solution, the obtained data indicated high amounts of protein in wheat bran repressed the synthesis or secretion of cellulase, xylanase and protease by *P. decumbens*, which was consistent with the observation that acid-hydrolyzed protein inhibited cellulase production by *Trichoderma reesei* [9].

Comparison of the Effects of the Soluble and Insoluble Components of Wheat Bran on Cellulase and Xylanase Synthesis

A 10% wheat bran suspension in water was autoclaved for 30 min at 115 °C and the resulting soluble (liquor) and insoluble components (residue) were separated by filtration. The liquor and residue fractions were then used alone or mixed with 1% MCC as carbon sources for *P. decumbens* growth. The biomass in cultures grown on wheat-bran liquor plus MCC was less than that on wheat-bran residues plus MCC, but the cellulase activity released was higher (Fig. 4). The liquor apparently contained a factor that stimulated cellulase synthesis and/or secretion. In contrast, the xylanase activity in the supernatants of cultures supplemented with wheat-bran liquor was lower than that in cultures supplemented with the wheat-bran residues, which were in consistent with the residues having higher hemicellulose content.

In the absence of MCC, total biomass accumulation, and also the cellulase and xylanase activities present in the supernatant were ~50% lower in cultures grown on only wheat bran

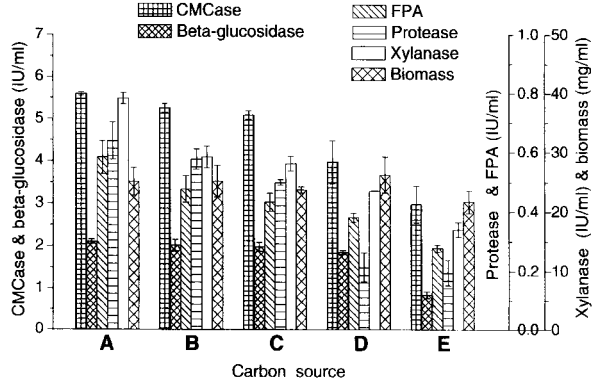


Fig. 3 Effects of protein and wheat bran on growth and production of extracellular cellulase, xylanase and protease by *P. decumbens*. All cultures contained 1% MCC plus as additional carbon sources: *A* 2% wheat bran; *B* 1.4% wheat bran plus 0.7% wheat protein; *C* 1% wheat bran plus 1% wheat protein; *D* 0.7% wheat bran plus 1.4% wheat protein; and *E* 2% wheat protein

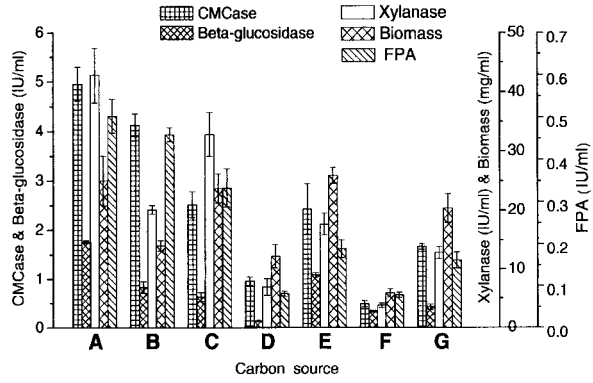


Fig. 4 Effects of the water soluble and insoluble components of wheat bran on growth and production of extracellular cellulase and xylanase by *P. decumbens*. The carbon sources were: *A* 1% MCC plus 2% wheat bran; *B* 1% MCC plus 2% wheat bran liquor; *C* 1% MCC plus 2% wheat bran residues; *D* 3% MCC; *E* 3% wheat bran; *F* 3% wheat bran liquor; *G* 3% wheat bran residues

liquor than on only wheat bran residues. Apparently in the liquor overall concentration of substrate, carbon was lower and levels of cellulose and hemicellulose were too low to stimulate cellulase and xylanase synthesis. Consistent with this interpretation, when *P. decumbens* cultures were grown on wheat bran with or without MCC, similar amounts of biomass accumulated but the cellulase and xylanase activities in the supernatant were much lower in the absence of MCC. Wheat bran alone did not therefore provide sufficient cellulose for maximum cellulase and xylanase production and release by *P. decumbens* mycelia.

Soluble Protein, Mono- and Oligosaccharide Composition of Wheat Bran and Cellulose Powder

HPLC and Bradford method analysis of the water soluble components from a 10% suspension of wheat bran revealed the presence of proteins (0.83 mg/ml), monosaccharides (glucose, xylose and arabinose), small oligosaccharides (xylobiose and xylotriose) and some larger oligosaccharides, apparently tetra-, penta-, and hexa-saccharides. In contrast, boiling suspensions of MCC and cellulose powder CF11 resulted in solutions that contained very little soluble protein, mono- or oligosaccharides (Fig. 5). Based on these results and the discovery that *P. decumbens* cultures grew better and released more cellulase and xylanase when grown with MCC plus wheat bran than on MCC plus soluble protein, it seems that the soluble oligosaccharides in wheat bran are the primary stimulators of cellulase and xylanase synthesis in *P. decumbens* cultures.

Stimulation of Growth and Production of Cellulase and Xylanase by the Soluble Components of Wheat Bran

Cultures of *P. decumbens* were grown with 2% MCC plus 0.5, 1, 2, 5 or 10% (*v*/*v*) of wheat-bran liquor. The total amounts of biomass accumulated, and the levels of cellulase and xylanase released to the supernatant did increase with increasing amounts of added wheat-bran liquor, but the increases were not directly proportional (Fig. 6).

Studies of 12 different *Penicillium* species have demonstrated that there was a coinduction between cellulolytic and xylanolytic activities whether the substrate was cellulose or xylan, whereas activities of cellulolytic enzymes were generally higher during growth on cellulose than on xylan [28]. The conclusion was further confirmed by our studies of *P. decumbens* (data not shown). Together with the above results of starch and protein experiments, it must be the high levels of water soluble cello-oligosaccharides

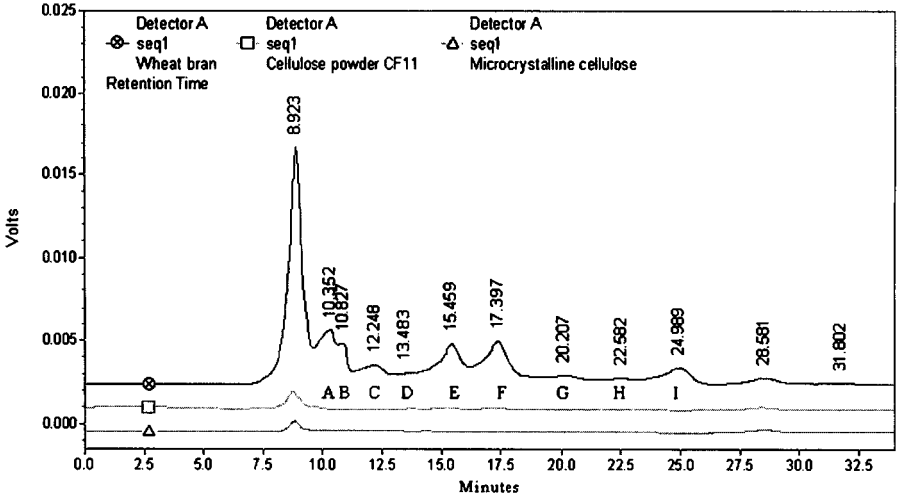


Fig. 5 HPLC separation of the water-soluble sugars extracted from wheat bran, MCC and cellulose powder CF11. Based on known standards, the elution peaks labeled A through I contained hextose, pentose, tetraose, xylotriose, xylobiose, glucose, xylose and arabinose, respectively

present in wheat bran that have positive effects on inducing higher levels of cellulase production.

Effects of Cello-oligosaccharides on Production of Extracellular Cellulase and Xylanase

To further confirm the conclusion, the effects of cello-oligosaccharides supplements on the production of cellulase and xylanase were examined. As shown in Table 1, the cultures containing 2% MCC plus 0.05% cellobiose or 0.05% cello-oligosaccharides (the mixture of cellotetraose, cellopentose and cellohextose) and the control with only 2% MCC were compared. There was no detectable difference in biomass accumulated among these three cultures, but the amounts of extracellular cellulase, β-glucosidase and xylanase increased with the supplement of cello-oligosaccharides or cellobiose in the medium. This further demonstrated that soluble cello-oligosaccharides composition of wheat bran was one of the most significant factors in enhancing cellulase production.

Discussion and Conclusions

The experiments reported were undertaken to understand the empirical observation wheat bran additions to industrial-scale batch fermentation improve biomass hydrolysis by *P. decumbens*. The results obtained have established that the starch content of wheat bran is an important, potentially negative factor, as high starch contents stimulate amylase production, but do not support high levels of mycelial growth, cellulase or xylanase production. Similarly, although the addition of high amount wheat protein did not inhibit growth, it did result in a reduction in the levels of cellulase, xylanase and protease released to the medium. In contrast, the high levels of water-soluble cello-oligosaccharides present in wheat bran, concentrations that are much higher than in cellulose-only preparations, have

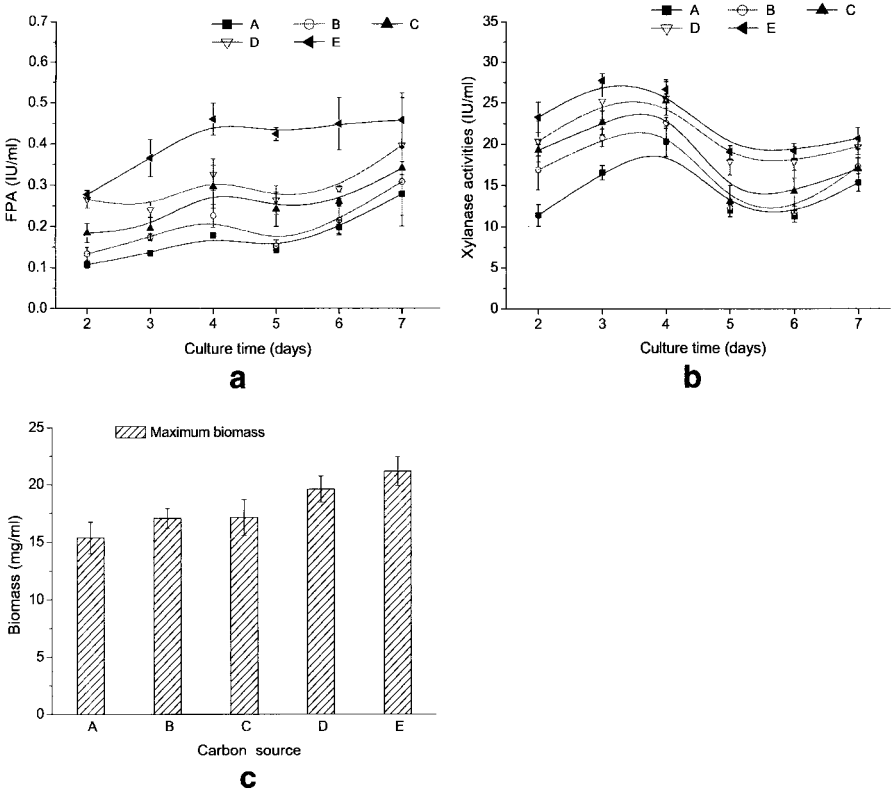


Fig. 6 Effects of the water soluble components of wheat bran supplements on growth and production of extracellular cellulase and xylanase by *P. decumbens*. Cultures were grown as described in the "Materials and Methods" and samples of the supernatant were collected assayed for (**a**) cellulase (FPA) and (**b**) xylanase over a 1 week period. (**c**) The maximum biomass accumulated was determined after 2 days. All cultures contained 2% MCC plus A through E additions of 0.5%, 1%, 2%, 5% or 10% soluble components of wheat bran, respectively

positive effects in terms of inducing higher levels of cellulase production during shorter fermentation time.

It had shown that the regulation of cellulase formation was significantly different between *Penicillium* and *Trichoderma* [16]. In *T. reesei* and *P. purpurogenum*, the inducers are sophorose and gentiobiose, respectively. In *P. purpurogenum*, constitutive cellulase

Table 1 Effects of cellobiose and cello-oligosaccharides supplements on growth and production of extracellular cellulase and xylanase (enzyme activities per gram mycelia mass).

	2% MCC	2% MCC+0.05% CB	2% MCC+0.05% COS
CMCase ($IU \cdot g^{-1}$)	115±27	147±27	133±25
FPA ($IU \cdot g^{-1}$)	8.06±0.99	9.25±1.61	9.04±0.74
β-glucosidase ($IU \cdot g^{-1}$)	8.82±2.59	11.13±1.68	12.89±2.35
Xylanase ($IU \cdot g^{-1}$)	800±66	1041±117	1121±148
Biomass ($g \cdot l^{-1}$)	9.52±0.94	9.67±1.53	9.10±0.19

MCC microcrystalline cellulose, *CB* cellobiose, *COS* cello-oligosaccharides (the mixture of cellotetraose, cellopentose and cellohextose)

degrades cellulose to cello-oligosaccharides and glucose as these saccharides enter the cell. The intracellular β-glucosidase converts cello-oligosaccharides to glucose, gentiobiose and other disaccharides. Gentiobiose induces mass synthesis of cellulase and then the synthesized cellulase is secreted to the outside of the cell [16, 17]. Experimental evidence was reported that the activity of extracellular basal cellulase is the rate-limiting event in induction of synthesis of the cellulase transcripts by cellulose [29]. This paper showed that wheat bran contained plenty of cello-oligosaccharides, and the amounts of extracellular cellulase, β-glucosidase and xylanase increased with the supplement of cello-oligosaccharides or cellobiose in culture medium. Therefore, higher content of soluble cello-oligosaccharides in culture medium of wheat bran can induce higher levels of cellulase production during shorter fermentation time. This is consistent with previous reports that acid-hydrolyzed wheat bran increased cellulase production by *T. reesei* and *P. decumbens*, and that the levels of released enzymes correlated with the mono- and oligosaccharide contents of the wheat bran [9, 11, 12]. It seems likely that inducers of cellulase synthesis, such as sophorose, are generated directly by acid-hydrolysis of wheat bran. Hrmova et al. [14] also reported that mixed disaccharides, could play an important role in regulating the synthesis of wood-degrading enzymes. Therefore, it can be seen from above discussions that cello-oligosaccharides can accelerate synthesis of filamentous fungi cellulase.

Taken together, the results of this research demonstrate the importance of knowing and regulating the starch and soluble protein contents of wheat bran supplements from different sources when adding wheat bran to stimulate cellulase and xylanase production by *P. decumbens*. Our results also predict that adding cello-oligosaccharides directly to *P. decumbens* fermentation could significantly improve industrial-scale biomass hydrolysis by *P. decumbens*.

Acknowledgments This work was supported by National Natural Science Foundation of China (grant no. 30570049) and State Key Development Program for Basic Research of China (grant no. 2003CB716006). The authors are grateful to Prof. John N. Reeve (Department of Microbiology, Ohio State University, USA) for valuable insights and discussions on the manuscript.

References

1. Brown, J. A., Collin, S. A., & Wood, T. M. (1987). *Enzyme and Microbial Technology, 9*, 176–180.
2. Jørgensen, H., Mørkeberg, A., Krogh, K. B. R., & Olsson L. (2005). *Enzyme and Microbial Technology, 36*, 42–48.
3. Qu, Y. B., Gao, P. J., & Wang, Z. N. (1984). *Acta Mycologica Sinica (Chinese), 3*, 238–243.
4. Qu, Y. B., Zhao, X., Gao, P. J., & Wang, Z. N. (1991). *Applied Biochemistry and Biotechnology, 28/29*, 363–368.
5. Mo, H., Zhang, X., & Li, Z. (2004). *Process Biochemistry, 39*, 1293–1297.
6. Qu, Y. B., Gao, P. J., & Wang, Z. N. (1987). *Journal of Shandong University (Chinese), 22*, 97–103.
7. Carre, B., & Brillouet, J. M. (1986). *Journal of the Science of Food and Agriculture, 37*, 341–351.
8. Ralet, M. C., Thibault, J. F., & Della-Valle, G. (1990). *Journal of Cereal Science, 11*, 793–812.
9. Wayman, M., & Chen, S. (1992). *Enzyme Microbiology Technology, 14*, 825–831.
10. Maes, C., & Delcour, J. A. (2002). *Journal of Cereal Science, 35*, 315–326.
11. Xu, H., Qian, W., Zhu, M. T., Cai, C. P., & Gao, P. J. (1997). *Food and Fermentation Industries (Chinese), 23*, 15–17.
12. Palmarola-Adrados, B., Chotěborská, P., Galbe, M., & Zacchi, G. (2005). *Bioresource Technology, 96*, 843–850.
13. Maeda, H., Sano, M., Maruyama, Y., Tanno, T., Akao, T., Totsuka, Y., et al. (2004). *Applied Microbiology and Biotechnology, 65*, 74–83.
14. Hrmova, M., Petrakova, E., & Biely, P. (1991). *Journal of General Microbiology, 137*, 541–547.
15. Schmoll, M., & Kubicek, C. P. (2003). *Acta Microbiologica et Immunologica Hungarica, 50*, 125–145.

16. Suto, M., & Tomita, F. (2001). *Journal of Bioscience and Bioengineering, 92*, 305–311.
17. Kurasawa, T., Yachi, M., Suto, M., Kamagata, Y., Takao, S., & Tomita, F. (1992). *Applied and Environmental Microbiology, 58*, 106–110.
18. Kubicek, C. P. (1987). *Journal of General Microbiology, 133*, 1481–1487.
19. Claeyssens, M., van Tilbeurgh, H., Kramerling, J. P., Berg, J., Vrsanska, M., & Biely, P. (1990). *Biochemical Journal, 270*, 251–256.
20. Miller, G. L. (1959). *Analytical Chemistry, 31*, 426–428.
21. Ghose, T. K. (1987). *Pure and Applied Chemistry, 59*, 257–268.
22. Wood, T. M., & Bhat, K. M. (1988). *Methods in Enzymology, 160*, 87–112.
23. Chahal, D. S. (1985). *Applied and Environmental Microbiology, 49*, 205–210.
24. Bailey, M. J., Biely, P., & Poutanen, K. (1992). *Journal of Biotechnology, 23*, 257–270.
25. Lin, J. Q., Lee, S. M., & Koo, Y. M. (2000). *Biotechnology and Bioprocess Engineering, 5*, 382–385.
26. Holm, J., Bjorck, I., Drews, A., & Asp, N. G. (1986). *Starch/Starke, 38*, 224–226.
27. Bradford, M. M. (1976). *Analytical Biochemistry, 72*, 248–254.
28. Krogh, K. B., Morkeberg, A., Jorgensen, H., Frisvad, J. C., & Olsson, L. (2004). *Applied Biochemistry and Biotechnology, 113*, 389–401.
29. Carle-Urioste, J. C., Escobar-Vera, J., El-Gogary, S., Henrique-Silva, F., Torigoi, E., Crivellaro, O., et al. (1997). *Journal of Biological Chemistry, 272*, 10169–10174.

Appl Biochem Biotechnol (2008) 146:129–136
DOI 10.1007/s12010-007-8130-y

Integrated Biosensor Systems for Ethanol Analysis

Eliana M. Alhadeff · Andrea M. Salgado · Oriol Cós · Nei Pereira Jr · Francisco Valero · Belkis Valdman

Received: 29 April 2007 / Accepted: 14 December 2007 /
Published online: 23 January 2008
© Humana Press Inc. 2008

Abstract Different integrated systems with a bi-enzymatic biosensor, working with two different methods for ethanol detection—flow injection analysis (FIA) or sequential injection analysis (SIA)—were developed and applied for ethanol extracted from gasohol mixtures, as well as for samples of alcoholic beverages and fermentation medium. A detection range of 0.05–1.5 g ethanol/l, with a correlation coefficient of 0.9909, has been reached when using FIA system, working with only one microreactor packed with immobilized alcohol oxidase and injecting free horseradish peroxidase. When using both enzymes, immobilized separately in two microreactors, the detection ranges obtained varied from 0.001 to 0.066 g ethanol/l, without on-line dilution to 0.010–0.047 g ethanol/l when a 1:7,000 dilution ratio was employed, reaching correlation coefficients of 0.9897 and 0.9992, respectively. For the integrated biosensor SIA system with the stop–flow technique, the linear range was 0.005–0.04 g/l, with a correlation coefficient of 0.9922.

Keywords Flow injection analysis · Sequential injection analysis · Ethanol · Alcohol oxidase · Horseradish peroxidase · Biosensor

Introduction

Ethanol is a biofuel extensively used nowadays as one of the most interesting substitutes for petroleum. In Brazil, since 1975, an important government program has introduced ethanol as automotive biofuel, mostly obtained from sugar-cane fermentation. Ethanol may be used in cars working with the hydrated form (95wt% ethanol), or mixed with gasoline as anhydrous ethanol in a proportion varying from 22% to 25% (*v/v*), or in the new flex-fuel

E. M. Alhadeff (✉) · A. M. Salgado · N. Pereira Jr · B. Valdman
Escola de Química, Centro de Tecnologia, Universidade Federal do Rio de Janeiro, Ilha do Fundão, Cidade Universitaria, CEP.: 21.949-900, Rio de Janeiro, Brazil
e-mail: ema@eq.ufrj.br

O. Cós · F. Valero
Depto. de Enginyeria Química, Escola Técnica Superior d'Enginyeria, Universitat Autònoma de Barcelona, 08193 Bellaterra, Barcelona, Spain

models, thus evidencing the need to find ways of measuring correctly ethanol's level in biofuel quality control. Ethanol analysis is also required for monitoring and control of an alcoholic fermentation bioprocess, in food industries and in clinic and forensic areas. High-sensitivity analytical systems, using enzymatic reactions and aiming to achieve a high confidence and fast response signal, have been applied to quantify low ethanol concentrations [1]. Among those, flow injection analysis (FIA) is a very promising technique for being reliable, reproducible, reagent-saving and readily automated. FIA systems have also been applied for ethanol detection either in alcoholic beverages as for gasohol mixtures, using sequential enzymatic microreactors, packed with enzymes such as alcohol oxidase and horseradish peroxidase, immobilized on chitosan or glass beads [2–4]. A real alternative to FIA systems is the sequential injection analysis (SIA) technique due to its more versatile sample-handling capability [5]. SIA systems were successfully employed in bioprocess automation and control, working either with free or immobilized enzymes [6–9]. For ethanol analysis, biosensor systems have also been reported, although working with an expensive NAD^+ co-factor-dependent enzyme [7, 9–10]. In this work, different integrated biosensor analysis systems have been developed to obtain a colorimetric method to analyze ethanol in diluted samples. The advantages of using optical determinations, which avoid interferences on the response signal caused by the electrochemical mechanism on the electron transference, through bio and/or mediator molecules to the electrode surface, have been aggregated to achieve an efficient analytical device [11]. The colorimetric biochemical reaction results in a coloured stable product, which could be detected in accordance with Lambert–Beer law. Other advantages of working with FIA and SIA methods should be mentioned, such as the economic aspects inherent to the reduction of reagent and sample volumes required for each analysis [12].

Materials and Methods

Chemicals

All reagents were analytical grade and have been acquired from Sigma Chemical, St. Louis, MO, USA, unless otherwise informed. Alcohol oxidase (AOD, Sigma) and horseradish peroxidase (HRP, Toyobo of Brazil) were immobilized separately on aminopropyl glass beads treated with 2.5% (*v*/*v*) glutaraldehyde, as previously described [3]. The composition of the indicator solution was: 4-aminophenazone 0.395 g/l and phenol 0.875 g/l, prepared in a 0.1 M sodium phosphate buffer solution (pH 7), which was also used as carrier [3, 13]. Reactions were carried out at room temperature (20°C). The ethanol samples were diluted with 0.1 M sodium phosphate buffer solution (pH 7).

Enzymatic Reactions

$$\text{Ethanol} + O_2 \xrightarrow{\text{AOD}} \text{Acetaldehyde} + H_2O_2$$

$$2H_2O_2 + 4\text{-aminophenazone} + \text{phenol} \xrightarrow{\text{HRP}} \text{monoimino-p-benzoquinone-4-phenazone} + H_2O$$

The resulting coloured product, monoimino-p-benzoquinone-4-phenazone, has been detected with a spectrophotometer at 470 nm.

The Integrated Biosensor Flow Injection Analysis Systems

The Flow Injection Analysis system consisted of Técniques Mesura Instrumentació (TMI) modules, a five-channel peristaltic pump, an eight-channel injection valve, an eight-channel distribution valve and a colorimeter, connected to an interface and to an IBM-personal computer (PC) microcomputer. Two sequential microreactors, made of acrylic, each one with 0.91 ml of void volume, with 3:1 length-to-diameter ratio, were used. Both enzymes were immobilized separately on glass beads (80–120 mesh) and packed in both microreactors, working in sequence. The beads were supported in the microreactor by a 110-mesh nylon screen and two rubber O-rings, having an external diameter of 11.4 mm. The FIA system was used for quantifying ethanol extracted from gasohol blends, working with different conditions: (1) one microreactor, packed with immobilized AOD and injection of free HRP and reagent solution; and (2) two microreactors with immobilized AOD and HRP and having different strategies for diluting the concentrated ethanol samples (off-line and on-line).

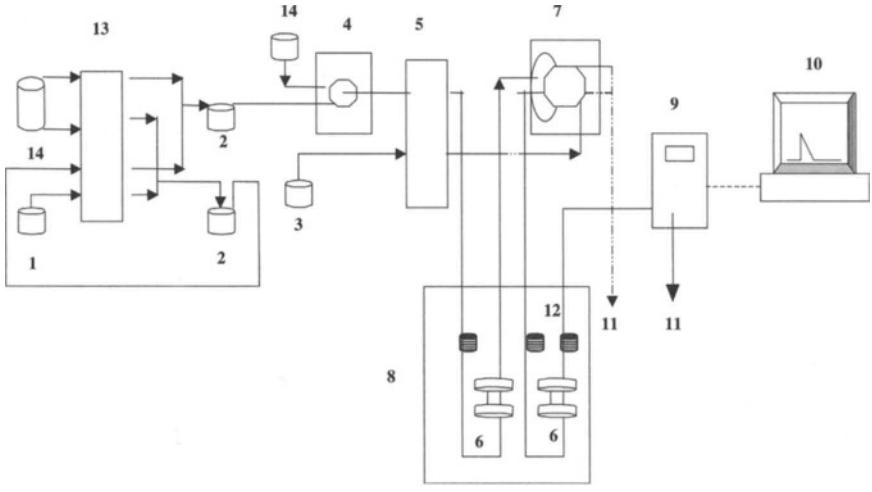
The Sequential Injections Analysis System of the Integrated Biosensors

The analyser has comprised interfaces of four modules (Easy Technologies, Cerdanyola del Vallés, Spain) connected by a RS-485 protocol and powered by a single 12V/2.5 A source. The system included a five-way eight-roller peristaltic pump (Model 1201/06-5-0), a 470 nm colorimeter (Model 1203/470/Z10), a module with two rotary valves of the three-port type (Model 1202/3) and a six-port rotary valve (Cheminert 4162510, Valco Instruments, Houston, TX, USA). The SIA system was made of polytetrafluoroethylene (PTFE) tubing (0.8 mm i.d.), connected to polyvinylchloride (PVC) fittings. One-meter length of PTFE tubing was used as a holding coil. Samples and reagent solutions were aspirated and fed to the system via the six-port rotary valve by two automatic micro-burettes (Crison MicroBU 2031, Alella, Spain) with two syringes, 1 ml and 0.5μl (Hamilton 1002 Teflon Luer Lock, Hamilton Bonaduz AG, Bonaduz, Switzerland). A PC via an RS-485/RS-232 interface controlled all the elements. Operations of the SIA analyser and data acquisition were PC-controlled using specific software developed in C^{++} language. The SIA system with two acrylic microreactors, having a 0.91-ml void volume each, was packed separately with the AOD- and HRP-immobilized enzymes. The SIA integrated system worked with the stop–flow technique, at the first AOD-immobilized microreactor. The time between sample frequency and linear range was settled in 120 s. The SIA system was used to measure ethanol content in alcoholic beverages and in fermented medium, working with the two microreactors described above and off-line sample dilutions.

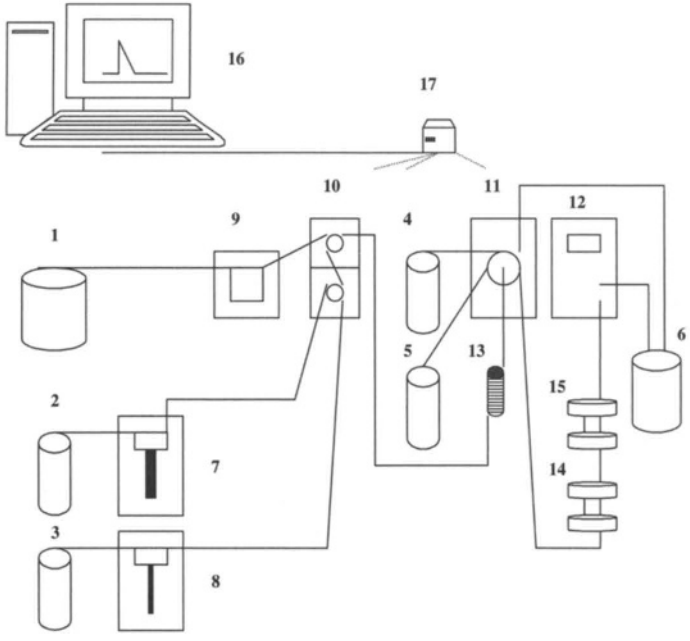
Figure 1a and b shows the schematic structure of the FIA and SIA systems proposed in this work, respectively. Each system had been tested, after calibration, on both response signal repeatability and stability of the immobilized enzymes, when reused in successive analysis. The results were compared to gas chromatography and high-performance liquid chromatography, having shown good agreement [3, 4, 12].

Results and Discussion

Five integrated FIA systems have been proposed to measure ethanol extracted from gasohol, and changes were conducted to introduce an on-line dilution process of the



a



b

samples. The proposed SIA system was applied to quantify ethanol samples, which had been previously diluted.

Table 1 shows the description of the different proposed integrated systems, namely, as FIA I, II, III, IV-I, IV-II and, finally, SIA-I. The adjustment of the FIA systems was reached,

Fig. 1 **a** The FIA IV-I and II integrated biosensor systems; *1* concentrated sample solution, *2* diluted sample solution, *3* reagent solution, *4* eight-channel distribution valve, *5* peristaltic pump, *6* microreactors, *7* eight-way injection valve, *8* temperature chamber control, *9* colorimeter, *10* micro computer, *11* waste, *12* coil, *13* peristaltic pump for sample dilution, *14* phosphate buffer. **b** The SIA integrated biosensor system; *1*, *2* and *3* phosphate buffer solution; *4* ethanol diluted sample; *5* reagent solution; *6* waste; *7* 1,000-μl micro-burette; *8* 500-μl micro-burette; *9* peristaltic pump; *10* two three-way valves; *11* six-channel distribution valve; *12* colorimeter; *13* serpentine; *14* AOD-immobilized microreactor; *15* HRP-immobilized microreactor, *16* computer; *17* Interface RS-232/RS-485

as proposed in this work, to amplify the response signal and to fit the data in a linear range. For the proposed FIA integrated biosensor systems, the flow rate that showed the best profile for the response signal was 3.6 ml/min. Seventy analyses of ethanol samples were measured with the immobilized AOD and free HRP integrated biosensor system FIA-I in 7 days [3]. The integrated biosensor FIA-II system worked with an immobilized HRP packed in a second microreactor that was adapted to the integrated system. A second peristaltic pump was included into the original FIA-II integrated system to dilute the sample by on-line automated control proceeding. A chamber was also adapted to the FIA-III integrated system to study the effect of the temperature on the bi-enzymatic reaction, as shown in Fig. 1a. The experiments were performed with FIA-IV-I and FIA-IV-II at controlled temperature of 25°C. For the integrated biosensor SIA-I system, the best profile of the response signal was obtained with 7.4 ml/min [12] with two microreactors working in series. The detection limit values have been calculated as three times the standard deviation of the background noise [12].

The detection range of 0.05 to 1.5 g ethanol/l, obtained with the system FIA-I, working with only one microreactor, was changed to 0.001 to 0.066 g ethanol/l when a second microreactor was introduced in the FIA-I line, packed with the immobilized HRP (integrated system II), to reuse both enzymes in successive analysis. That instrument permitted the analysis of low ethanol contents, in highly diluted solutions. The analysis cost will decrease once the immobilized enzymes could be reused, in successive measurements, always using the same immobilized lot. On the other hand, the enzymes lose the activity when they are reused in successive analyses [4].

Figure 2 shows the calibration curves obtained working with the proposed integrated biosensor FIA systems II, III and IV, including the SIA integrated system I. The calibration curves were adjusted to a hyperbolic correlation for the different configuration systems investigated. The original system FIA-I was modified to detect correctly the linear range and improve the accuracy and sensitivity of the analysis results. For the FIA and SIA

Table 1 Description of FIA and SIA integrated systems.

Integrated system		Immobilized enzymes	Dilution	Detection range (g ethanol/l)	Linear range (g ethanol/l)	Detection limit (g ethanol/l)
FIA	I	AOD[a]	Off-line	0.05–1.5	nd	4.1×10^{-2}
	II	AOD and HRP	Off-line	0.001–0.066	0.001–0.023	9.4×10^{-3}
	III	AOD and HRP	1:2,150	0.001–0.087	0.001–0.033	9.5×10^{-3}
	IV-I	AOD and HRP	1:1,580	0.033–0.127	nd	8.3×10^{-3}
	IV-II	AOD and HRP	1:7,000	0.010–0.047	0.010–0.047	8.4×10^{-3}
SIA	I	AOD and HRP	Off-line	0.005–0.1	0.005–0.04	2.1×10^{-3}

nd Not determined

[a] Injection of free HRP solution

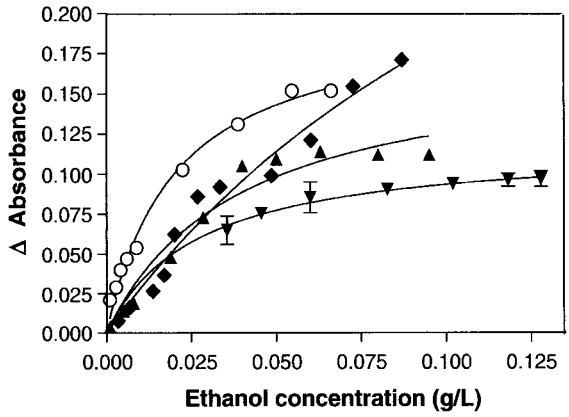


Fig. 2 Calibration curves for integrated biosensor systems FIA; II (*open circle*), III (*closed diamond*), IV-1 (*closed inverted triangle*) and SIA-I (*closed upright triangle*)

systems proposed in this study, the linear range fitted circa 0.01 to 0.047 g ethanol/l, which enables to analyze properly low ethanol concentrations in samples from different origins.

The proposed integrated FIA and SIA biosensor systems permitted to obtain good response signal reproducibility, with a maximum relative error of 12% for system VI-1, working with on-line dilution (1:1,580) and 2% for the SIA integrated system I. A small change in analysis per hour was observed: 19 (h^{-1}; FIA-I) and 15 (h^{-1}; FIA-II, III, IV-I and IV-II), when a second peristaltic pump was used to dilute the real samples, working with an automated dilution system [3, 4]. For the SIA system, the sample frequency was around seven analyses per hour, working with an off-line dilution method and a time schedule, which included a cleaning colorimeter and stop–flow steps at the AOD-immobilized microreactor to increase the response signal value [12].

Figure 3 shows the stability of the immobilized enzymes for the SIA systems when testing the samples of standard ethanol solution, in which continuous and stop–flow strategies were compared. After 3 days, 60% of the bi-enzymatic activity has been retained for the stop–flow strategy, although 20% had been lost after the first day in the same maintaining conditions. When ethanol samples were analyzed using the SIA integrated system, 60 measurements were performed, and the immobilized AOD and HRP lots were reused during two consecutive days after a new calibration.

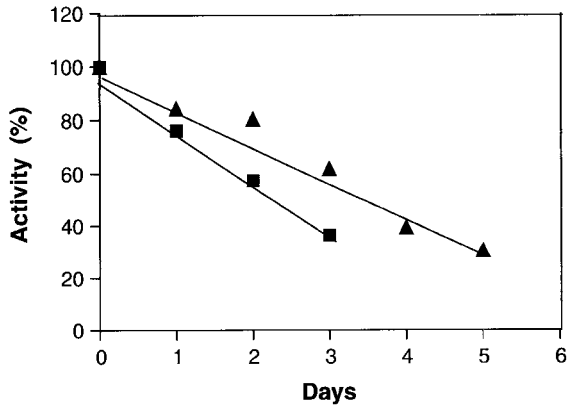


Fig. 3 SIA bi-enzymatic activity working with 7.4 ml/min flow; (*closed diamond*) continuous feed; (*closed square*) 120 s stop–flow into the immobilized AOD microreactor

Figure 4 shows the influence of the temperature on the response signal working with the FIA system for 0.1 g/l ethanol samples. The results have shown that the absorbance value had decreased from 0.1105 ± 0.0007 at 25°C to 0.0313 ± 0.0015 at 45°C. The decrease of the absorbance values may be explained by enzyme inactivation, when the temperature was increased from 25°C to 45°C and by the reuse of the immobilized enzymes in successive analysis [4] during the course of the experiment.

The accuracy of the proposed methods was evaluated for real sample analysis. The results obtained for real samples made with FIA integrated system IV-I (extracted ethanol from gasohol mixtures) with on-line dilution and with SIA integrated system I (alcoholic beverages and fermented medium) with off-line dilution have agreed fairly with those obtained by using high-performance liquid chromatography (HPLC) standard method [12]. The samples of extracted ethanol were obtained from red gasohol and yellow gasohol mixtures received from different distributors. Slightly different values were obtained when compared to the nominal 25% *v/v* ethanol, claimed by vendors of commercial gasohol mixture samples, although a relative deviation of 12.7% was observed for a red gasohol (1:1,589) diluted sample [4]. In addition, low relative deviations were also obtained for alcoholic beverages when compared with the HPLC measurements, with a maximum value of 7.3% for white wine diluted samples and 4.7% for fermented medium, as presented in previous work [12] for measurements made with the SIA system. The low relative deviations found in this work were similar to those observed with amperometric and colorimetric ethanol biosensors reported in the literature [7, 9–10].

Conclusions

A highly advantageous and robust method for ethanol analysis was developed working with a continuous injection flowing integrated system (FIA) and with a stop–flow sequential injection integrated system (SIA). A change on FIA-I system sensitivity, which worked with one microreactor for the immobilized AOD and free HRP, was obtained when a second microreactor, for the immobilized HRP (FIA-II) was introduced into the integrated system. Ethanol was analyzed using an on-line dilution system, showing good reproducibility and reliability (FIA-III, FIA-IV-I and FIA-IV-II). An economy on the analytical method was observed when the immobilized enzymes were reused in several analyses. In addition, savings on reagent and sample volumes were achieved for the

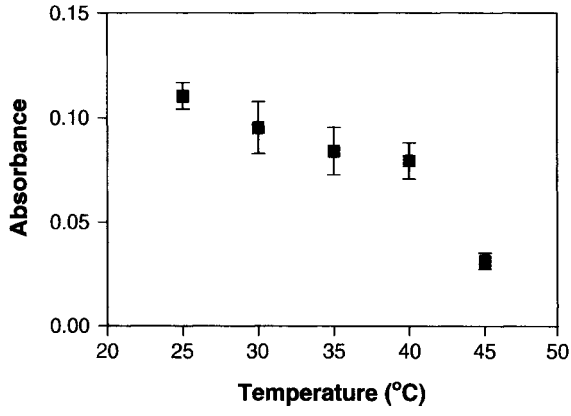


Fig. 4 The influence of temperature on response signal

sequential injection analysis proposed system (SIA-I), working with a stop–flow strategy into the AOD-immobilized microreactor. No pretreatment of the samples was needed; a simple dilution for the adequate linear range was enough to analyze 60 ethanol samples from different origins.

Acknowledgments We acknowledge the support received from the BI-EURAM Project of the Alpha Program-EU. We also would like to thank Toyobo of Brazil for gently donating the horseradish peroxidase. We also acknowledge LABCOM-EQ/UFRJ and Refinaria de Petróleos Manguinhos, for donating, respectively, the different samples of gasohol mixture and gasoline A.

References

1. Patel, P. D. (2002). *Trends in Analytical Chemistry, 21*, 96–115.
2. Taniai, T., Sukurragawa, A., & Okitani, T. (2001). *Journal of Association of Official Analytical Chemists International, 84*(5), 1475–1483.
3. Alhadeff, E. M., Salgado, M. A., Pereira, N., Jr., & Valdman, B. (2004). *Applied Biochemistry and Biotechnology, 113*, 125–136.
4. Alhadeff, E. M., Salgado, M. A., Pereira, N., Jr., & Valdman, B. (2005). *Applied Biochemistry and Biotechnology, 121*, 361–372.
5. van Staden, J. F., & Stefan, R. I. (2004). *Talanta, 64*, 1109–1113.
6. Surribas, A., Cos, O., Montesinos, J. L., & Valero, F. (2003). *Biotechnology Letters, 25*, 1795–1800.
7. Lapa, R. A. S., Lima, J. L. F. C., & Pinto, I. V. O. S. (2003). *Food Chemistry, 81*, 141–146.
8. Masini, J. C., Rigobello-Masini, M., Salatino, A., & Aidar, E. (2001). *Latin American Applied Research, 31*, 463–468.
9. Niculescu, M., Erichsen, T., Sukharev, V., Kereny, Z., Csregi, E., & Schuhmann, W. (2002). *Analytica Chimica Acta, 463*, 39–51.
10. Segundo, M. A., & Rangel, A. O. S. S. (2002). *Analytica Chimica Acta, 458*, 131–138.
11. Coi, M. M. F. (2004). *Microchemical Acta, 148*, 107–132.
12. Alhadeff, E. M., Salgado, M. A., Cos, O., Pereira, N., Jr., Valero, F., & Valdman, B. (2007). *Applied Biochemistry and Biotechnology, 136–140*, 17–26.
13. Salgado, A. M., Folly, R. O. M., Valdman, B., Cós, O., & Valero, F. (2000). *Biotechnology Letters, 22*, 327–330.

Appl Biochem Biotechnol (2008) 146:137–149
DOI 10.1007/s12010-007-8064-4

B-D-Xylosidase from *Selenomonas ruminantium*: Catalyzed Reactions with Natural and Artificial Substrates

Douglas B. Jordan

Received: 5 May 2007 / Accepted: 26 September 2007 /
Published online: 17 October 2007
© Humana Press Inc. 2007

Abstract Catalytically efficient β-D-xylosidase from *Selenomonas ruminantium* (SXA) exhibits pK_as 5 and 7 (assigned to catalytic base, D14, and catalytic acid, E186) for k_{cat}/K_m with substrates 1,4-β-D-xylobiose (X2) and 1,4-β-D-xylotriose (X3). Catalytically inactive, dianionic SXA ($D14^-E186^-$) has threefold lower affinity than catalytically active, monoanionic SXA ($D14^-E186^H$) for X2 and X3, whereas $D14^-E186^-$ has twofold higher affinity than $D14^-E186^H$ for 4-nitrophenyl-β-D-xylopyranoside (4NPX), and $D14^-E186^-$ has no affinity for 4-nitrophenyl-α-L-arabinofuranoside. Anomeric isomers, α-D-xylose and β-D-xylose, have similar affinity for SXA. 4-Nitrophenol competitively inhibits SXA-catalyzed hydrolysis of 4NPX. SXA steady-state kinetic parameters account for complete progress curves of SXA-catalyzed hydrolysis reactions.

Keywords Fuel ethanol · Glycoside hydrolase · GH43 · Hemicellulose · pH dependence · Stereochemistry · Inhibitor · Assay method

Introduction

B-D-Xylosidase/α-L-arabinofuranosidase from the ruminal anaerobic bacterium *Selenomonas ruminantium* (SXA) is a bifunctional glycoside hydrolase possessing β-D-xylosidase activity (EC 3.2.1.37) and α-L-arabinofuranosidase activity (EC 3.2.1.55) [1–3]. Its amino acid sequence places SXA within glycoside hydrolase family 43 (GH43) and structural clan F in the CAZy database (carbohydrate active enzymes database, http://www.cazy.org/) [4, 5]. Because of its exceptionally efficient catalysis of xylooligosaccharide hydrolysis [3], its arabinofuranosidase function for cleaving arabinose side chains from arabinoxylooligosac-

The mention of firm names or trade products does not imply that they are endorsed or recommended by the U.S. Department of Agriculture over other firms or similar products not mentioned.

D. B. Jordan (✉)
Fermentation Biotechnology Research Unit, National Center for Agricultural Utilization Research, U.S. Department of Agriculture, Agricultural Research Service, 1815 N. University Street, Peoria, IL 61604, USA
e-mail: douglas.jordan@ars.usda.gov

charides [1], and its good stability properties [2], SXA has potential utility in industrial processes where it could serve double duty in depolymerizing complex carbohydrates (i.e., arabinoxylans) of herbaceous biomass to simple sugars for subsequent fermentation to fuel ethanol and other bioproducts [6–9]. In this regard, it is particularly important, from an efficiency viewpoint, to engage a catalytically powerful β-D-xylosidase in saccharification of xylans: for example, even in an all-enzymatic saccharification process, the β-D-xylosidase would be required to catalyze hydrolysis of more glycosidic bonds than other enzymes in the process (e.g., β-xylanases that cleave larger polymers of D-xylose, xylans, to xylooligosaccharides), and benefits of the process cannot fully be realized until this ultimate step of saccharification is complete.

X-ray structures have been determined for GH43 β-xylosidases isolated from *Bacillus subtilis*, *Bacillus halodurans*, *Clostridium acetobutylicum*, and *Geobacillus stearothermophilus*, which have 53–70% protein sequence identity with SXA [3, 10]. The structures describe homotetrameric proteins with monomers comprising two domains: an N-terminal, five-bladed β-propeller domain that contains the two-subsite, funnel-shaped active site, which has a single route for access by ligands; and a C-terminal β-sandwich domain that serves to restrict the size of the active site. Structures of catalytically impaired mutant enzymes from *G. stearothermophilus* in complex with 1,4-β-D-xylobiose [10] are highly useful for modeling ligands in the active site of SXA, particularly as the eight amino acid residues in the vicinity of the xylose moiety of the nonreducing end of xylobiose, which occupy subsite −1, are fully conserved in SXA.

Structure–function studies have secured that SXA catalyzes hydrolysis of substrates with inversion of anomeric stereochemistry, implicating a single transition state with the catalytic base (D14) serving to activate a water molecule for addition to substrate and the catalytic acid (E186) serving to protonate the leaving group [3]; SXA catalyzes the hydrolysis of a single residue from the nonreducing end of the substrate without processivity so that all products of the hydrolysis reaction are removed from the active site before initiating another catalytic cycle [3]; and the β-xylosidase and α-arabinofuranosidase activities share the single active site of the SXA protomer [3].

Besides the determination that 4NPX is tenfold faster than 4NPA as substrate for SXA [3], there are additional differences between the competing substrates (Fig. 1). Similar to 4NPX, SXA-catalyzed hydrolysis of 4NPA proceeds with inversion of anomeric stereochemistry. However, unlike the α-D-xylose product of the SXA-catalyzed hydrolysis of 4NPX, which has a half-life of ~ 1 h for mutarotation (Fig. 1a), the β-L-arabinofuranose product of SXA-catalyzed hydrolysis of 4NPA more rapidly undergoes mutarotation and ring reorganization to arabinopyranose, which dominates at equilibrium [3]. Secondly, whereas catalytically inactive, dianionic SXA ($D14^{-}E186^{-}$) forms a dead end, binary complex with 4NPX that has a twofold tighter binding constant than the productive complex comprising catalytically active, monoanionic SXA ($D14^{-}E186^{H}$) and 4NPX (Fig. 1b), SXA in the dianionic form does not bind 4NPA [3]. Thirdly, whereas 4NPX forms a ternary, inhibited complex (SXA-D-xylose-4NPX), 4NPA does not [11]. In this work, pH profiles of steady-state kinetic parameters for SXA-catalyzed hydrolysis of 1,4-β-D-xylobiose (X2) and 1,4-β-D-xylotriose (X3) are determined for comparison with those of 4NPX and 4NPA and analyzing the affinity of catalytically inactive $D14^{-}E186^{-}$ SXA for the natural substrates. SXA affinities for D-xylose preparations enriched in α-D-xylose or β-D-xylose content are determined to assess whether SXA recognizes its reaction product (α) better than its anomeric isomer. The affinity of 4-nitrophenol for SXA is determined to assess whether its inhibition constant needs to be included in describing SXA-catalyzed hydrolysis of 4NPX. Lastly, an improved procedure is established for quenching SXA-

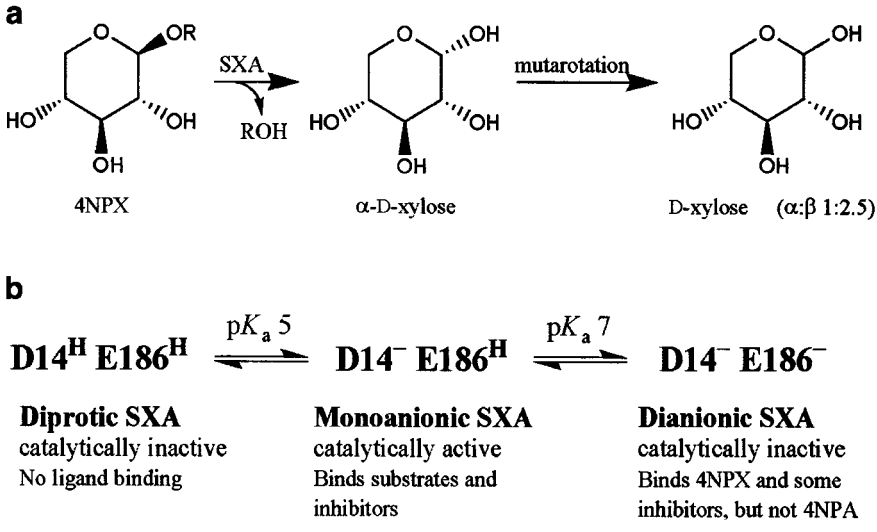


Fig. 1 Properties of SXA-catalyzed hydrolysis of 4-nitrophenyl-β-D-xylopyranoside (4NPX). **a** Stereochemistry. SXA catalyzes hydrolysis of 4NPX with inversion of anomeric configuration. Mutarotation, off the enzyme, converts α-D-xylose to its equilibrium mixture (α:β ratio of 1:2.5) with a half-life of ~1 h [3]. R = 4-nitrophenyl. **b** Diprotic model. pK_as 5 and 7, assigned to catalytic base (D14) and catalytic acid (E186), respectively, govern catalysis and binding of ligands [3]

catalyzed reactions for high performance liquid chromatography (HPLC) analysis of products.

Materials and Methods

Materials and General Methods

Buffers, 4-nitrophenol (4NP), 4-nitrophenyl-β-D-xylopyranoside (4NPX), 4-nitrophenyl-α-L-arabinofuranoside (4NPA), and D-xylose (X1) were obtained from Sigma-Aldrich (St. Louis, MO). 1,4-β-D-Xylobiose (X2), 1,4-β-D-xylotriose (X3), 1,4-β-D-xylotetraose (X4), 1,4-β-D-xylopentaose (X5), and 1,4-β-D-xylohexaose (X6) were from Megazyme (Wicklow, Ireland). Water was purified through a Milli-Q unit (Millipore; Billerica, MA). All other reagents were reagent grade and high purity. The gene encoding β-xylosidase from *S. ruminantium* GA192 was cloned and expressed in *Escherichia coli* as described [1]. SXA, produced in *E. coli*, was purified to homogeneity, as judged from sodium dodecyl sulfate-polyacrylamide gel electrophoresis (SDS-PAGE) analysis, by using reverse phase and anionic exchange chromatography steps as described [3] with the addition of a final desalting, gel filtration step employing a 2.6×30 cm column of Bio-Gel P-6 DG desalting gel (Bio-Rad; Hercules, CA), equilibrated and developed with 20 mM sodium phosphate, pH 7.0. Concentrations of homogeneous SXA protomers (active sites) were determined by using an extinction coefficient at 280 nm of 129,600 $M^{-1}cm^{-1}$, calculated from amino acid composition [3, 12]. A Cary 50 Bio UV-Visible spectrophotometer (Varian; Palo Alto, CA), equipped with a thermostatted holder for cuvettes, was used for spectral and kinetic determinations. A model SX.18MV-R stopped-flow (Applied Photophysics; Leatherhead, UK) with a thermostatted compartment for syringes and reaction chamber and a 2-mm path length for absorbance measurements was used for rapid kinetic studies. Kinetic simulations

were through the computer program KINSIM: Chemical Kinetics Simulation System, 32-bit DOS-Extended Version 4.0, March 1997 [13]. Delta extinction coefficients (product–substrate) at 360, 380, and 400 nm were determined for each buffer condition by subtracting the molar absorbance of 4NPX from that of 4-nitrophenol (4NP) [3]. The concentration of 4NP was determined by using the published extinction coefficient of 18.3 $mM^{-1}cm^{-1}$ at 400 nm for 4NP in NaOH [14]. Concentrations of 4NPX and 4NPA were determined by incubating substrate with excess enzyme until an end point was reached, adding an aliquot (10–100 μl) to 0.99–0.90 ml 0.1 M NaOH, recording the absorbance at 400 m and using the extinction coefficient of 18.3 mM^{-} cm for 4NP in NaOH.

HPLC Analysis of Reactions

Products from SXA-catalyzed hydrolysis of substrates X2–X6 and 4NPX were separated and quantified by using a DX500 HPLC system with an ED40 electrochemical detector (pulsed amperometry), AS3500 autosampler, PA-100 (4×250 mm) anion exchange column, and Chromeleon software (Dionex, Sunnyvale, CA). Samples (25 μl) were injected onto the column equilibrated with 0.1 M NaOH and developed with a 5-min linear gradient (0.1 M NaOH to 33 mM sodium acetate) at ~25°C and a flow rate of 1 ml min^{-1}. Several concentrations of the products of interest (e.g., D-xylose and X2) were used to establish standard curves on the same day experimental samples were run. Substrate concentrations were determined by HPLC analysis of samples incubated with excess SXA for complete conversion to D-xylose.

Kinetics with Substrates X2–X6

For determination of steady-state kinetic parameters of X2–X6 substrates, 0.5-ml reaction mixtures contained varied substrate concentrations (0.9–13 mM) in 100 mM succinate–NaOH, pH 5.3 at 25°C. For pH studies of SXA-catalyzed hydrolysis of X2 and X3, buffers of constant ionic strength (I=0.3 M), adjusted with NaCl, were used as indicated (replacing 100 mM succinate–NaOH, pH 5.3): 100 mM succinate–NaOH (pH 4.3–6), 100 mM sodium phosphate (pH 6–8), and 30 mM sodium pyrophosphate (pH 8–9.2). Before (time= 0 min) and after (time=0.5–2 min) initiating reactions with enzyme (7 μl SXA in 20 mM sodium phosphate, pH 7.0), 100-μl aliquots of reaction mixtures were removed and quenched with an equal volume of 0.2 M sodium phosphate pH 11.3 at 0°C (so that quenched mixtures were pH 10.5–11) and diluted by adding 1 mM sodium phosphate, pH 10.5–11 at 0°C as necessary (typically 200–800 μl added to 200 μl quenched samples) to adjust concentrations of reactants and products to fall within the linear range of standard curves. Samples were kept on wet ice or the HPLC autosampler at 5°C until analyzed by HPLC. Initial rates, calculated from linear regressions of the [D-xylose] produced vs time, were fitted to Eq. 1 to determine steady-state kinetic parameters. Parameter, k_{cat}, is expressed in moles of substrate hydrolyzed per second per mole enzyme active sites (protomers); thus, for substrate X2, the [D-xylose] produced was divided by two to provide the [X2] hydrolyzed, whereas for X3–X6, the [D-xylose] produced was taken as the concentration of substrate hydrolyzed.

Reaction Progress Curves

For X2, 2-ml reactions contained 100 mM succinate–NaOH, pH 5.3 at 25°C. Concentrations of SXA (protomer) and X2 are indicated in the figure legends. Before

(time=0) and after initiating reactions with enzyme (7 μl SXA in 20 mM sodium phosphate, pH 7.0), 100-μl aliquots of reaction mixtures were removed, quenched with an equal volume of 0.2 M sodium phosphate pH 11.3 at 0°C, and diluted with 1 mM sodium phosphate, pH 10.5–11 (as above) before HPLC analysis.

For 4NPX, 1.5-ml reactions contained 100 mM succinate–NaOH, pH 5.3 at 25°C and concentrations of 4NPX and SXA (protomer) as indicated in the figure legends. Before (time=0) and after initiating reactions with enzyme (7 μl SXA in 20 mM sodium phosphate, pH 7.0), 10–100 μl aliquots of reaction mixtures were removed and added to cuvettes containing 900–990 μl 0.1 M NaOH (final volume=1,000 μl); absorbencies at 400 nm were recorded and converted to molarities by using the extinction coefficient of 18.3 mM^{-1} cm^{-1} for 4NP in NaOH [14].

Determination of Inhibition Constants

For D-xylose inhibition of SXA-catalyzed hydrolysis of 4NPX, 1-ml reactions contained varied concentrations (0.2–7 mM) of 4NPX and varied concentrations (0, 20, 60, and 150 mM) of D-xylose in 100 mM succinate–NaOH, pH 5.3 at 25°C. Reactions were initiated by adding enzyme (7 μl SXA in 20 mM sodium phosphate, pH 7.0), and reaction progress was monitored continuously for 0.3 min at 380 nm to determine initial rates (fitted to lines). For determination of steady-state kinetic parameters, initial rates were fitted to Eq. 2 (competitive inhibition) and Eq. 3 (noncompetitive inhibition).

For inhibition of SXA-catalyzed hydrolysis of 4NPA by two D-xylose preparations having different ratios of α and β anomeric isomers, the stopped-flow instrument was used to allow rapid execution of three to five replicates for each reaction condition. The experiment relies on the experimentally determined production of α-D-xylose from SXA-catalyzed hydrolysis of 4NPX and 1,4-β-D-xylose (X2), the experimentally determined half-life (~ 1 h) of α-D-xylose mutarotation to its equilibrium position (α:β ratio of 1:2.5), and the experimentally determined α:β ratio of 6:1 for D-xylose as the immediate product from the SXA-catalyzed hydrolysis of X2 [3]; from the latter, it can be inferred that the reducing D-xylose moiety of X2 has an anomeric isomer ratio of 2.5:1 (α:β). Left syringe of the stopped-flow contained 0.951, 1.90, or 9.51 mM 4NPA in 100 mM succinate-NaOH, pH 5.3 at 25°C. When the α:β ratio of D-xylose was 6:1, the right syringe contained 5.07 μM SXA and 0, 8.6, or 17.2 mM X2 in 100 mM succinate–NaOH, pH 5.3 at 25°C. After 6 min preincubation to ensure complete conversion of X2 to D-xylose, reactions were initiated by injecting 50 μl from each syringe through the mixing cuvette, and absorbance was recorded for 20 s at 360 nm to determine initial rates (fit to line). When the α:β ratio of D-xylose was 1:2.5, the right syringe contained 5.07 μM SXA and 0, 20, or 40 mM D-xylose in 100 mM succinate–NaOH, pH 5.3 at 25°C. After 6 min preincubation (to mimic those containing X2), reactions were initiated by injecting 50 μl from each syringe through the mixing cuvette, and absorbance was recorded for 20 s at 360 nm to determine initial rates (fit to line). For determination of steady-state kinetic parameters, initial rates were fitted to Eq. 2 (competitive inhibition).

For inhibition of SXA-catalyzed hydrolysis of 4NPX by 4NP, 1-ml reactions contained varied concentrations of 4NPX, 0 or 9.4 mM 4NP and 7.09–33.8 nm SXA (protomer) in 100 mM succinate–NaOH, pH 5.3 at 25°C. Before (time=0) and after (up to 6 min) initiating reactions by adding enzyme (7 μl SXA in 20 mM sodium phosphate, pH 7.0), 100-μl aliquots of reaction mixtures were removed and quenched with an equal volume of 0.2 M sodium phosphate pH 11.3 at 0°C, and diluted with 1 mM sodium phosphate, pH 10.5–11 (as above) before HPLC analysis. Concentrations of D-xylose produced vs time

were fitted to lines for determination of initial rates. For determination of steady-state kinetic parameters, initial rates were fitted to Eq. 2 (competitive inhibition).

Equations

Data were fitted to equations by using the computer program Grafit (Erithacus Software; Horley, UK) [15]. Symbol definitions for equations 1, 2, 3: v is the observed initial (steady-state) rate of catalysis, k_{cat} is the maximum rate of catalysis, S is the substrate concentration, K_m is the Michaelis constant, I is the inhibitor concentration, K_i is the dissociation constant for I from the EI complex, and K_{is} is the substrate dissociation constant from the EIS complex. For Eqs. 4, 5, 6, 7, p is the determined parameter at a single pH, P is the pH-independent value of the parameter, K_a is the acid dissociation constant of the group affecting P, H^+ is the proton concentration, K_{a1} is the acid dissociation constant of the first group affecting P, K_{a2} is the acid dissociation constant of the second group affecting P, P_1 is the limit of p associated with K_{a1}, and P_2 is the limit of p associated with K_{a2}.

$$v = \frac{k_{cat} * S}{K_m + S} \tag{1}$$

$$v = \frac{k_{cat} * S}{K_m\left(1 + \frac{I}{K_i}\right) + S} \tag{2}$$

$$v = \frac{k_{cat} * S}{K_m\left(1 + \frac{I}{K_i}\right) + S\left(1 + \frac{K_m * I}{K_{is} * K_i}\right)} \tag{3}$$

$$p = \frac{P}{1 + \frac{H^+}{K_a}} \tag{4}$$

$$p = \frac{P}{1 + \frac{K_a}{H^+}} \tag{5}$$

$$p = \frac{P}{1 + \frac{H^+}{K_{a1}} + \frac{K_{a2}}{H^+}} \tag{6}$$

$$p = \frac{P_1}{1 + \frac{H^+}{K_{a1}} +} + \frac{P_2 - P_1}{1 + \frac{H^+}{K_{a2}}} \tag{7}$$

Results and Discussion

An improved method for quenching SXA reactions was established for determination of steady-state kinetic parameters with xylooligosaccharide substrates X2–X6 (Table 1). The improved quenching method raises the pH of reaction mixtures to ~ pH 11, where SXA is inactive (pK_a=7 for k_{cat}/K_m) and lowers the temperature; it produces much lower background concentrations, stemming from hydrolysis of oligosaccharide substrates off the enzyme to D-xylose and smaller xylooligosaccharides, than the acid-quenching method employed previously [3], thus, allowing better estimations of rates, particularly at higher concentrations of substrate. In direct comparison to previous determinations at pH 5.3 and 25°C [3], the respective k_{cat}/K_{m1} values for X2, X3, X4, X5, and X6 are lower by 9, 1, 12, 34, and 25% and the respective k_{cat} values are lower by 55, 45, 39, 49, and 15%. The lower k_{cat} values do not affect previous KINSIM simulations of reaction progressions for SXA-catalyzed hydrolysis of X4 and X6 (*3*) because initial X4 and X6 substrate concentrations of the reactions were low (30% of K_m) where parameter k_{cat}/K_m governs rates, and as indicated, there are relatively small differences between the new and previously determined k_{cat}/K_m values. Also, SXA remains the most active β-xylosidase known for promoting hydrolysis of xylooligosaccharides with k_{cat} and k_{cat}/K_m values at pH 5.3 and 25°C that are higher than those of the second most active β-xylosidase known from the literature, the enzyme from *Bacillus pumilus* [16], determined at its pH optimum (pH 7.15) and 25°C, by factors of 10 (X2), 32 (X3), 31 (X4), 20 (X5), and 27 (X6) for k_{cat} and factors of 14 (X2), 16 (X3), 15 (X4), 10 (X5), and 13 (X6) for k_{cat}/K_m. For comparison, k_{cat} and k_{cat}/K_m values of SXA with substrate 4NPX at pH 5.3 and 25°C [3] are higher than those determined for the *B. pumilus* enzyme at pH 7.15 and 25°C [16] by factors of 4 and 5, respectively.

pH dependencies of SXA-catalyzed hydrolysis of X2 and X3 were determined using buffers of constant ionic strength (I=0.3 M) from pH 4.3 to 9.2 (Figs. 2 and 3); denaturation of SXA at lower pH values precludes their analysis [2]. pH dependencies of k_{cat}, k_{cat}/K_m, and $1/K_m$ are similar in shape for X2 and X3, and similar pK_a values were determined (legends to Figs. 2 and 3). A small difference between the two substrates is that pK_a can be determined for the acidic limb of k_{cat} with X3 (pK_{a1} 3.21), but no acidic limb is seen for k_{cat} with X2; the inability to determine the pK_a for X2 stems from the inability to analyze SXA kinetics below pH 4.3. Extension by 2 pH units of the pK_a for k_{cat} over that of k_{cat}/K_m (pK_{a1} 4.8) would not be unusual [17]. Lower pK_a values for k_{cat} (pK_{a1}~3.6) than k_{cat}/K_m (pK_{a1} ~ 5.0) for the acidic limbs are also seen with substrates 4NPX and 4NPA [3]. pH dependencies of $1/K_m$ indicate that catalytically inactive, dianionic SXA ($D14^-E186^-$) has 2.9-fold and 3.1-fold lower affinity than catalytically active, monoanionic SXA ($D14^-E186^H$) for X2 and X3, respectively. In contrast, $D14^-E186^-$ has 1.9-fold higher

Table 1 Steady-state kinetic parameters of SXA acting on xylooligosaccharides[a].

Substrate	k_{cat} (s^{-1})	k_{cat}/K_m ($mM^{-1}\ s^{-1}$)	K_m (mM)
1,4-β-d-xylobiose (X2)	185±3	90.2±2.5	2.06±0.08
1,4-β-d-xylotriose (X3)	95.1±1.5	44.8±1.5	2.12±0.10
1,4-β-d-xylotetraose (X4)	91.6±2.3	33.3±2.0	2.75±0.23
1,4-β-d-xylopentaose (X5)	77.2±3.6	27.0±2.4	2.86±0.38
1,4-β-d-xylohexaose (X6)	81.5±2.0	26.1±1.2	3.12±0.21

[a] Reactions contained varied concentrations of substrate in 100 mM succinate–NaOH, pH 5.3 at 25 °C. Initial-rate data were fitted to Eq. 1; SEs (±) are indicated.

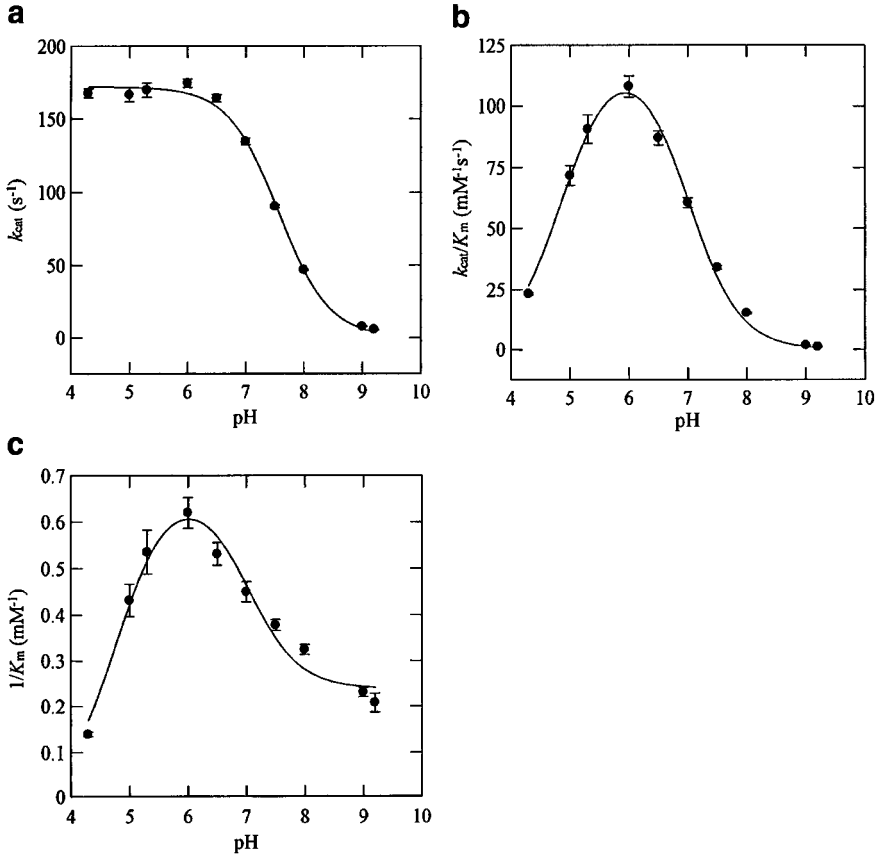


Fig. 2 pH dependence of steady-state kinetic parameters for 1,4-β-D-xylobiose hydrolysis catalyzed by SXA at 25°C. Initial rates were determined from reactions in buffers of constant ionic strength (I=0.3 M) and kinetic parameters were determined by fitting initial-rate data to Eq. 1; SEs (±) are indicated. **a** k_{cat} vs pH. The curve was generated by fitting k_{cat} values vs pH to Eq. 5: pK_a=7.57±0.03, pH-independent k_{cat}=172±2. **b** k_{cat}/K_m vs pH. The curve was generated by fitting k_{cat}/K_m values vs pH to Eq. 6: pK_{a1}=4.86±0.06, pK_{a2}= 7.01±0.05, pH-independent k_{cat}/K_m=123±5. **c** $1/K_m$ vs pH. The curve was generated by fitting $1/K_m$ values vs pH to Eq. 7: pK_{a1}=4.78±0.11, pK_{a2}=7.03±0.17, middle limit $1/K_m$=0.682±0.048, upper limit $1/K_m$=0.238±0.022

affinity than catalytically active, monoanionic SXA ($D14^{-}E186^{H}$) for 4NPX, and $D14^{-}E186^{-}$ has no affinity for 4NPA [3].

Inhibition of SXA-catalyzed hydrolysis of 4NPX by D-xylose was determined at pH 5.3 and 25°C by using a continuous spectrophotometric method: $K_i^{D\text{-xylose}}$ of 9.63±0.30 mM and $K_{is}^{D\text{-xylose•4NPX}}$ of 15.9±2.1 mM were determined by fitting the data to Eq. 3, describing noncompetitive (or "mixed") inhibition. For comparison with actual reaction progression data acquired by following production of 4NP spectroscopically, values of k_{cat}^{4NPX} (32.1±0.5), K_m^{4NPX} (0.716±0.032), $K_i^{D\text{-xylose}}$ (9.63±0.30 mM), and $K_{is}^{D\text{-xylose•4NPX}}$ (15.9±2.1 mM) were used as inputs to KINSIM for simulations of four reaction progressions of SXA-catalyzed hydrolysis of 1 mM 4NPX and 5 mM 4NPX at pH 5.3 and 25°C (Fig. 4). Whereas the simulations adequately describe the two progressions at 1 mM 4NPX, the simulations fail to account for the production of 4NP towards the end of 4NPX consumption of the two progressions containing 5 mM 4NPX. Two possibilities, which could rationalize the

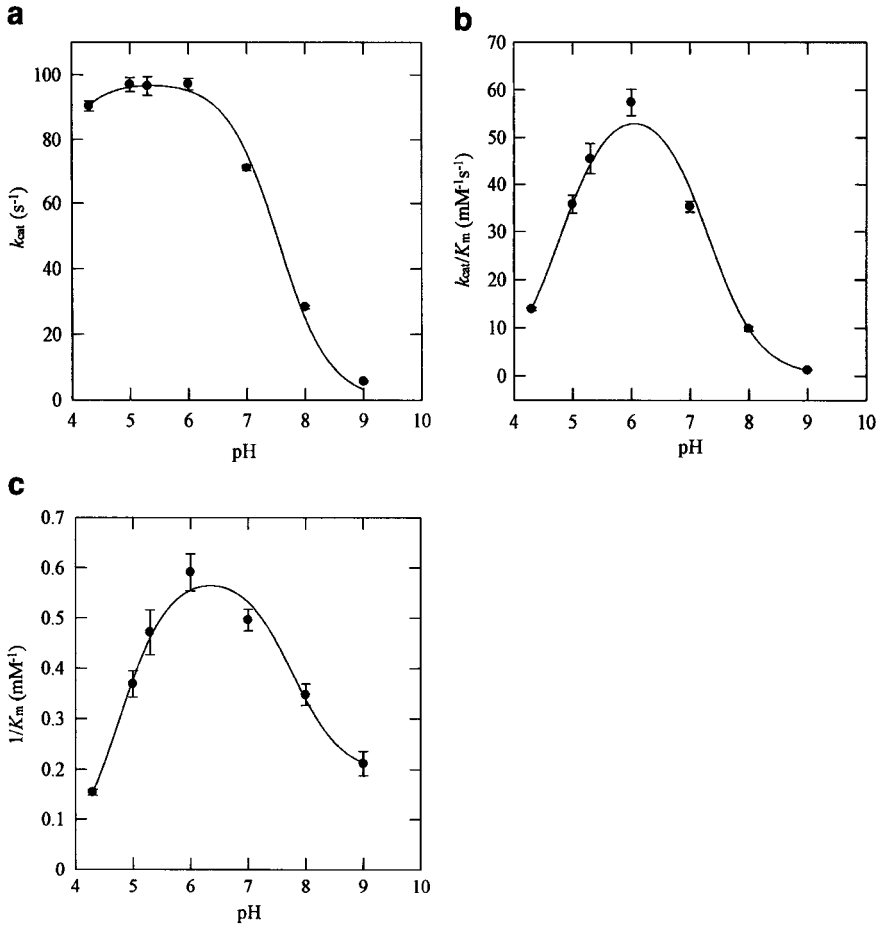


Fig. 3 pH dependence of steady-state kinetic parameters for 1,4-β-D-xylotriose hydrolysis catalyzed by SXA at 25°C. Initial rates were determined from reactions in buffers of constant ionic strength (I=0.3 M), and kinetic parameters were determined by fitting initial-rate data to Eq. 1; SEs (±) are indicated. **a** k_{cat} vs pH. The curve was generated by fitting k_{cat} values vs pH to Eq. 6: pK_{a1}=3.21±0.27, pK_{a2}=7.53±0.06, pH-independent k_{cat}=98.0±2.3. **b** k_{cat}/K_m vs pH. The curve was generated by fitting k_{cat}/K_m values vs pH to Eq. 6: pK_{a1}=4.80±0.06, pK_{a2}=7.30±0.04, pH-independent k_{cat}/K_m=58.9±3.3 mM^{-1} s^{-1}. **c** $1/K_m$ vs pH. The curve was generated by fitting $1/K_m$ values vs pH to Eq. 7: pK_{a1}=4.76±0.05, pK_{a2}=7.76±0.14, middle limit $1/K_m$=0.594±0.027, upper limit $1/K_m$=0.191±0.017

discrepancies, were addressed experimentally. The first of these is that the $K_i^{D\text{-xylose}}$ (9.63 mM) input of the simulation was determined from inhibition studies with D-xylose, predominantly in the β conformation (α:β ratio of 1:2.5 at equilibrium), whereas the product of SXA-catalyzed hydrolysis of 4NPX is temporally in the α conformation (half life~1 h) before mutarotation establishes equilibrium favoring the β conformation [3]; potentially, α-D-xylose has greater affinity than β-D-xylose for SXA. To address this, X2 was preincubated with SXA for 6 min to fully convert to D-xylose with α:β ratio of 6:1 [3] before initiating reactions with varied concentrations of 4NPA for determination of $K_i^{D\text{-xylose}}$ to compare with $K_i^{D\text{-xylose}}$, determined from reactions with SXA preincubated with D-xylose (α:β ratio of 1:2.5) before initiating reactions with varied concentrations of 4NPA. In contrast to 4NPX, SXA-catalyzed hydrolysis of 4NPA is competitively inhibited by D-xylose. From the data collected with D-xylose (α:β

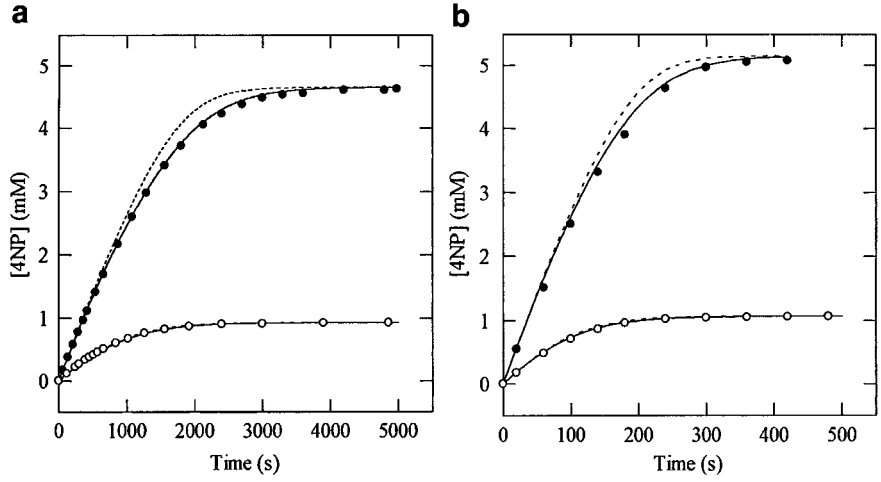


Fig. 4 Progress curves of 4NPX hydrolysis catalyzed by SXA. Reactions contained 100 mM succinate–NaOH, pH 5.3 at 25°C. [4NP] was determined spectrophotometrically. Curves were generated from the KINSIM calculations, assuming rapid equilibrium binding, with the indicated [enzyme] and [4NPX] and the following as inputs: $E+S <=> E•S$ (K_m^{4NPX}=0.716±0.032 mM); $E•S=>E+P+Q$ (k_{cat}^{4NPX}=32.1±0.5 s^{-1}); E•P <=> E+P ($K_i^{D\text{-xylose}}$=9.63±0.30 mM); E•Q <=> $E+Q$ (K_i^{4NP}=6.28±0.55 mM); EP•4NPX <=> EP+4NPX ($K_{is}^{D\text{-xylose•4NPX}}$=15.9±2.1 mM). *Solid curves* included all parameters as inputs in the KINSIM simulations; *dotted curves* excluded the K_i^{4NP} term in the simulations. **a** Reactions were initiated by addition of enzyme to give initial reaction conditions of 52 nM SXA and 0.93 mM 4NPX (*empty circles*) or 104 nM SXA and 4.65 mM 4NPX (*filled circles*). **b** Reactions were initiated by addition of enzyme to give initial reaction conditions of 520 nM SXA and 1.07 mM 4NPX (*empty circles*) or 1040 nM SXA and 5.15 mM 4NPX (*filled circles*)

ratio of 6:1), $K_i^{D\text{-xylose}}$ of 11.9±0.3 was determined (Fig. 5a). From the data collected with D-xylose (α:β ratio of 1:2.5), $K_i^{D\text{-xylose}}$ of 11.8±0.3 was determined (Fig. 5b). If, for example, all inhibitory activity resided in the α anomeric isomer and β-D-xylose had no affinity for SXA, then $K_i^{D\text{-xylose}}$ for D-xylose with α:β ratio of 1:2.5 would be threefold that for D-xylose with α:β ratio of 6:1. Therefore, the two anomeric isomers of D-xylose possess similar affinities for SXA, and corrections, on the basis of α and β content, cannot account for the overestimation of reaction progress by the simulations in comparison to the actual progressions of Fig. 4. Similarly, from stopped-flow reactions at pH 7.0 (100 mM sodium phosphate, adjusted with NaCl to ionic strength of 0.3 M) and 25°C, $K_i^{D\text{-xylose}}$ values for inhibition of SXA-catalyzed hydrolysis of 4NPA were similar when the D-xylose solutions contained α:β anomeric isomer ratios of 1:2.5 ($K_i^{D\text{-xylose}}$=5.15±0.08 mM) or 6:1 ($K_i^{D\text{-xylose}}$=4.97±0.05 mM).

The second possible cause for discrepancies between the simulated and actual progressions is the unaccounted for potential of product 4NP to inhibit the SXA-catalyzed hydrolysis of 4NPX. To address this, K_i^{4NP} for inhibition of SXA-catalyzed hydrolysis of 4NPX was determined at pH 5.3 and 25°C by using HPLC analysis of D-xylose produced from 4NPX to determine catalyzed rates in the absence and presence of 4NP and fitting the rate data to Eq. 2, describing competitive inhibition (Fig. 6). By including the determined value of K_i^{4NP} (6.28±0.55 mM) in the simulations of SXA-catalyzed hydrolysis of 4NPX, better agreement with actual reaction progressions is generated (Fig. 4).

For comparison with actual reaction progress data acquired by HPLC quantification of D-xylose and 1,4-β-D-xylobiose (X2) concentrations, steady-state values for k_{cat}^{X2} (185±3 s^{-1}), K_m^{X2} (2.06±0.08 mM) and $K_i^{D\text{-xylose}}$ (9.63±0.30 mM) were used for KINSIM inputs for simulations of SXA-catalyzed reactions containing 0.922 mM X2 and 7.31 mM X2 (Fig. 7).

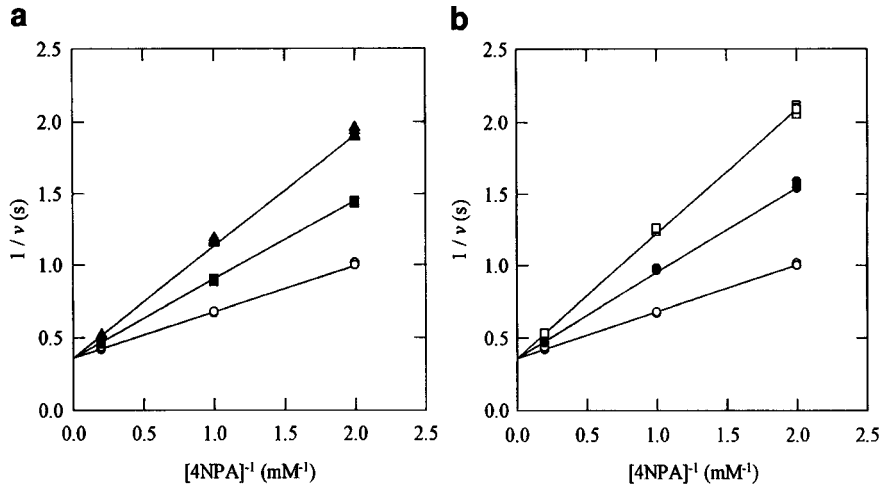


Fig. 5 Influence of D-xylose anomeric stereochemistry on inhibition of SXA-catalyzed hydrolysis of 4NPA at pH 5.3 and 25°C. Left syringe of stopped-flow instrument contained varied 4NPA concentrations in 100 mM succinate–NaOH, pH 5.3 at 25°C. Right syringe contained the indicated concentrations of SXA and D-xylose (or 1,4-β-D-xylobiose) in 100 mM succinate–NaOH, pH 5.3 and 25°C. Contents of the syringes were preincubated 6 min at 25°C, to achieve full conversion of 1,4-β-D-xylobiose to D-xylose, before initiating 20-s reactions (by mixing 50 μl from each syringe) and recording linear absorbance changes at 360 nm for determination of initial rates (v in moles 4NP produced per second per mole SXA protomer). **a** D-Xylose α:β ratio of 6:1. Right syringe of stopped flow contained 5.07 μM SXA, and the following concentrations of 1,4-β-D-xylobiose: 0 (*empty circles*), 8.6 mM (*filled squares*), and 17.2 mM (*filled triangles*). Lines were generated by fitting initial rate data to Eq. 2 (competitive inhibition): $K_i^{D\text{-xylose}}$=11.9±0.3 mM, k_{cat}^{4NPA}= 2.78±0.01 s^{-1}, k_{cat}/K_m^{4NPA}=3.16±0.04 mM^{-1} s^{-1}, and K_m^{4NPA}=0.880±0.13 mM. **b** D-Xylose α:β ratio of 1:2.5. Right syringe of stopped flow contained 5.07 μM SXA, and the following concentrations of D-xylose: 0 (*empty circles*), 20 mM (*filled circles*), 40 mM (*empty squares*). Lines were generated by fitting initial rate data to Eq. 2 (competitive inhibition): $K_i^{D\text{-xylose}}$=11.8±0.3 mM, k_{cat}^{4NPA}=2.79±0.01 s^{-1}, k_{cat}/K_m^{4NPA}=3.10± 0.04 mM^{-1} s^{-1}, and K_m^{4NPA}=0.900±0.013 mM

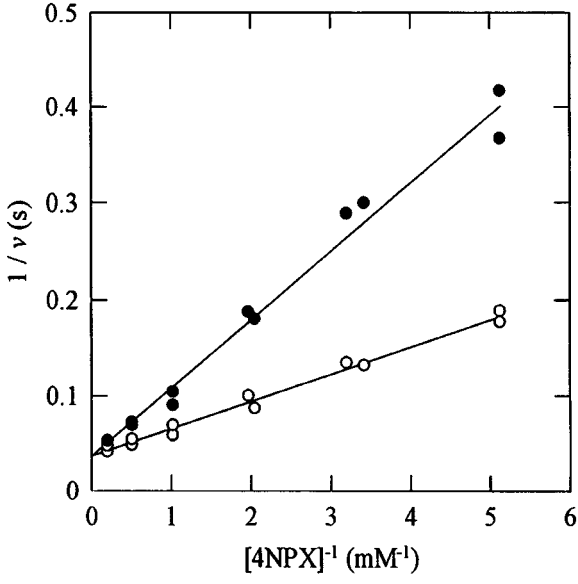


Fig. 6 Inhibition of SXA-catalyzed hydrolysis of 4NPX by 4-nitrophenol (4NP) at pH 5.3 and 25°C. Reactions contained 0 (*empty circles*) or 9.4 mM 4NP (*filled circles*), 7.09–33.8 nm SXA, and varied concentrations of 4NPX in 100 mM succinate–NaOH, pH 5.3 at 25°C. Concentrations of D-xylose produced were quantified by HPLC for determination of initial rates (v). Lines were generated by fitting initial rates to Eq. 2 (competitive inhibition): K_i^{4NP}=6.28±0.55 mM, k_{cat}^{4NPX}=26.7±1.1 s^{-1}, and K_m^{4NPX}=0.758±0.059 mM

The simulations adequately describe reaction progress at both high and low X2 concentrations, conditions where the $K_i^{D\text{-xylose}}$ term is more and less important, respectively, to the calculations. Thus, the xylobiose reactions substantiate that α and β anomeric conformations of D-xylose have similar affinities for SXA.

Conclusions

The small discrepancies between the actual and simulated (when not including K_i^{4NP} in the calculations) progress curves for SXA-catalyzed hydrolysis of 4NPX (Fig. 4) prompted experiments to determine K_i values for 4NP and the two preparations of D-xylose with different anomeric isomer ratios. Determinations that the two anomeric isomers of D-xylose have similar K_i values and that 4NP binds to SXA and inhibits catalysis allow more accurate predictions of SXA-catalyzed reactions (Figs. 4 and 7). Of course the absence of complicating factors, such as subunit cooperativity (SXA is a homotetramer) and transglycosylation back reactions, simplify the parameters needed for kinetic simulations. The ability to simulate reaction progress could have utility in engineering saccharification processes. Undoubtedly, the lack of complicating factors (cooperativity, transglycosylation), which lower rates of hydrolysis, favors the effectiveness of SXA in saccharification processes.

Based on the twofold tighter binding of 4NPX by the catalytically inactive, dianionic SXA ($D14^-E186^-$) than by the catalytically active, monoanionic SXA ($D14^-E186^H$), it might have been projected that X2 and X3 would share this property of forming relatively high-affinity, dead-end complexes, which would be detrimental to the usefulness of SXA at

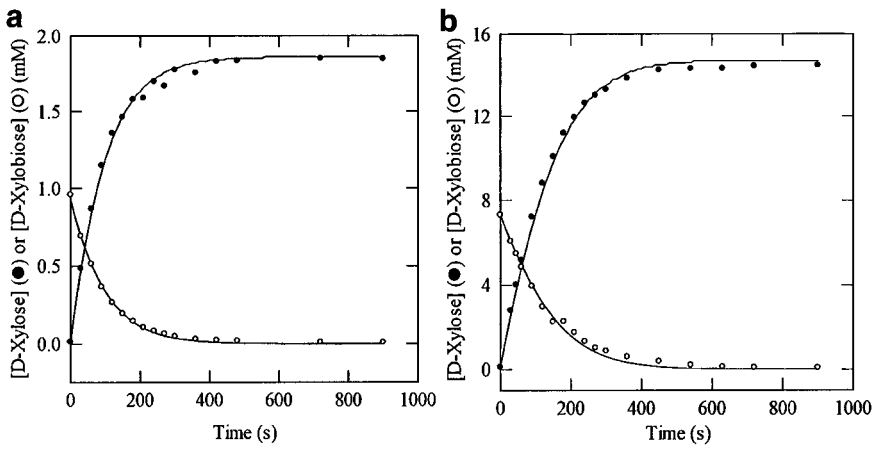


Fig. 7 Progress curves of 1,4-β-D-xylobiose (X2) hydrolysis catalyzed by SXA. Reactions contained 100 mM succinate–NaOH, pH 5.3 at 25 °C. Curves were generated from the KINSIM calculations, assuming rapid equilibrium binding, with the indicated [enzyme] and [X2] and the following as inputs: $E + X2 <=> E{\bullet}X2$ (K_m= 2.06±0.08 mM); $EX2 => E+X1+X1$ (k_{cat}^{X2}=185±3 s^{-1}); $E{\bullet}X1 <=> E+X1$ ($K_i^{D\text{-xylose}}$=9.63±0.32 mM). Determined K_m^{X2} and k_{cat}^{X2} values at pH 5.3 at 25 °C are from Table 1, and determination of $K_i^{D\text{-xylose}}$ at pH 5.3 at 25 °C is described in the text. **a** Reaction contained 152 nM SXA, 0.922 mM X2, and 0.0146 mM X1 (contaminant of X2); concentrations of X1 (*filled circles*) and X2 (*empty circles*) were monitored by HPLC. **b** Reaction contained 303 nM SXA, 7.31 mM X2, and 0.111 mM X1 (contaminant of X2); concentrations of X1 (*filled circles*) and X2 (*empty circles*) were monitored by HPLC

higher pH. Determination of threefold weaker binding of X2 and X3 by $D14^{-}E186^{-}$ than by $D14^{-}E186^{H}$ favors the effectiveness of SXA as a catalyst.

Acknowledgments I thank Jay D Braker for excellent technical assistance in contributing to this work.

References

1. Whitehead, T. R., & Cotta, M. A. (2001). *Current Microbiology, 43*, 293–298.
2. Jordan, D. B., Li, X-L., Dunlap, C. A., Whitehead, T. R., & Cotta, M. A. (2007). *Applied Biochemistry and Biotechnology, 137-140*, 93–104.
3. Jordan, D. B., Li, X-L., Dunlap, C. A., Whitehead, T. R., & Cotta, M. A. (2007). *Applied Biochemistry and Biotechnology, 141*, 51–76.
4. Henrissat, B. (1991). *Biochemistry Journal, 280*, 309–316.
5. Henrissat, B., & Davies, G. J. (1997). *Current Opinion in Structural Biology, 7*, 637–644.
6. Saha, B. C. (2003). *Journal of Industrial Microbiology & Biotechnology, 30*, 279–291.
7. Saha, B. C. (2000). *Biotechnology Advances, 18*, 403–423.
8. Gray, K. A., Zhao, L., & Emptage, M. (2006). *Current Opinion in Chemical Biology, 10*, 141–146.
9. Shallom, D., & Shoham, Y. (2003). *Current Opinion in Microbiology, 6*, 219–228.
10. Brüx, C., Ben-David, A., Shallom-Shezifi, D., Leon, M., Niefind, K., Shoham, G., et al. (2006). *Journal of Molecular Biology, 359*, 97–109.
11. Jordan, D. B., & Braker, J. D. (2007). *Archives of Biochemistry and Biophysics, 465*, 231–246.
12. Gill, S. C., & von Hippel, P. H. (1989). *Analytical Biochemistry, 182*, 319–326.
13. Barshop, B. A., Wrenn, R. F., & Frieden, C. (1983). *Analytical Biochemistry, 130*, 134–145.
14. Kezdy, F. J., & Bender, M. L. (1962). *Biochemistry, 1*, 1097–1106.
15. Leatherbarrow, R. J. (2001). Grafit Version 5, Erithacus Software Ltd., Horley, U.K.
16. Van Doorslaer, E., Kersters-Hilderson, H., & De Bruyne, C. K. (1985). *Carbohydrate Research, 140*, 342–346.
17. Cleland, W. W. (1982). *Methods in Enzymology, 87*, 390–405.

Appl Biochem Biotechnol (2008) 146:151–164
DOI 10.1007/s12010-007-8084-0

Hydrolysis of Ammonia-pretreated Sugar Cane Bagasse with Cellulase, β-Glucosidase, and Hemicellulase Preparations

Bernard A. Prior · Donal F. Day

Received: 8 May 2007 / Accepted: 16 October 2007 /
Published online: 20 November 2007
© Humana Press Inc. 2007

Abstract Sugar cane bagasse consists of hemicellulose (24%) and cellulose (38%), and bioconversion of both fractions to ethanol should be considered for a viable process. We have evaluated the hydrolysis of pretreated bagasse with combinations of cellulase, β-glucosidase, and hemicellulase. Ground bagasse was pretreated either by the AFEX process ($2NH_3$: 1 biomass, 100 °C, 30 min) or with NH_4OH (0.5 g NH_4OH of a 28% [*v*/*v*] per gram dry biomass; 160 °C, 60 min), and composition analysis showed that the glucan and xylan fractions remained largely intact. The enzyme activities of four commercial xylanase preparations and supernatants of four laboratory-grown fungi were determined and evaluated for their ability to boost xylan hydrolysis when added to cellulase and β-glucosidase (10 filter paper units [FPU]: 20 cellobiase units [CBU]/g glucan). At 1% glucan loading, the commercial enzyme preparations (added at 10% or 50% levels of total protein in the enzyme preparations) boosted xylan and glucan hydrolysis in both pretreated bagasse samples. Xylanase addition at 10% protein level also improved hydrolysis of xylan and glucan fractions up to 10% glucan loading (28% solids loading). Significant xylanase activity in enzyme cocktails appears to be required for improving hydrolysis of both glucan and xylan fractions of ammonia pretreated sugar cane bagasse.

Keywords Ammonia pretreatment · Sugar cane bagasse · Hydrolysis · Cellulase · Hemicellulase

Introduction

With the rapid increase in oil prices over the past decade together with the uncertainty about reliable future supplies, alternative sources of liquid fuels have recently received extensive

B. A. Prior · D. F. Day
LSU Agricultural Center, Audubon Sugar Institute, St. Gabriel, LA 70776, USA

Present address:
B. A. Prior (✉)
Department of Microbiology, University of Stellenbosch, Private Bag X1, Matieland 7602, South Africa
e-mail: bap@sun.ac.za

attention. Increased ethanol demand as an attractive liquid biofuel has resulted in extensive fermentation facilities being constructed worldwide. Whereas ethanol production from food crops will expand over the next decade, a stage will be reached where insufficient crop substrates will be available to satisfy liquid fuel demands. Lignocellulose biomass, a low cost substrate, is available in much larger amounts than food crops and can be hydrolyzed to sugars. Therefore, biomass can serve as a useful substrate to produce a wide range of commodity chemicals in addition to ethanol [1]. However, the heterogeneous nature of lignocellulose results in a biomass that is recalcitrant to enzymatic hydrolysis and where the component fermentable sugars released are more expensive than those obtained from food crops. This situation has started to change as more efficient and cost-effective enzymes have become available [2, 3].

Sugar cane bagasse is a lignocellulose biomass produced in large amounts as a byproduct from sugar extraction in volumes that will continue with increased worldwide sugar production. Considerable amounts of bagasse are currently used as a combustible energy source, for paper pulp production, or animal feed. However, a relatively high carbohydrate (hemicellulose and cellulose) and medium lignin content make bagasse an attractive substrate for ethanol production, but bioconversion of both carbohydrate fractions to ethanol must be considered for a viable process. Pretreatment of bagasse is necessary to reduce its recalcitrance to enzymatic hydrolysis. Previous studies have reported the pretreatment of sugar cane bagasse with either physical or chemical methods such as acid [4], steam [5], or alkali [6, 7]. Dilute sulfuric acid has been widely used to pretreat sugar cane bagasse [4, 8] and results in the hemicellulose fraction being released as pentoses such as xylose and arabinose. Without detoxification, the subsequent fermentation of the hydrolysate can be seriously inhibited. Alkali pretreatment leaves the hemicellulose fraction relatively intact. The ammonia freeze explosion (AFEX) process is a particularly attractive pretreatment for sugar cane bagasse [7] as ammonia can be potentially recycled whereas only some hemicellulose is removed and the formation of sugar degradation products are minimized [9, 10]. Furthermore, this process enables both the cellulose and hemicellulose fractions to be hydrolyzed enzymatically.

We have evaluated the degree of hydrolysis of sugar cane bagasse pretreated by the AFEX process or with NH_4OH with combinations of cellulase, β-glucosidase, and hemicellulase enzymes. Significant xylanase activity in enzyme cocktails appears to be required for greater hydrolysis of both glucan and xylan fractions of ammonia pretreated sugar cane bagasse.

Materials and Methods

Pretreatment of Sugar Cane Bagasse

Bagasse from sugar cane (*Saccharum officinarum*) was obtained from the Raceland Raw Sugar Corp. sugar mill, Raceland, LA, USA and ground to a particle size less than 12 mm. Ground sugar cane bagasse was submitted to MBI International, Lansing, MI, USA for pretreatment using the AFEX process [7]. Briefly, approximately 1 kg of the bagasse was treated in a 1-gal reactor at 100 °C for 30 min with a 2:1 ammonia loading to biomass and 40% moisture level. After pretreatment, bagasse was removed from the reactor, dried to remove ammonia, and stored in sealed plastic bags at 4 °C. Ground sugar cane bagasse (2.5 kg) was also pretreated by adding a 28% stock solution of NH_4OH to achieve a final concentration

of 0.02 g NH_3/g water in a final water mass of 20 kg. The slurry was placed in a pressure reactor and heated at 160 °C for 60 min. The solid mass was removed from the slurry by filtration through muslin cloth and washed with 40 kg of water. Less than 1% of the carbohydrate in the bagasse, detected as monosaccharides, was found in the pretreatment effluents.

Analysis of the Composition of Sugar Cane Bagasse and Pretreated Bagasse

The carbohydrate composition and lignin were determined using the NREL laboratory analytical procedures (http://www1.energy.gov/biomass/analytical_procedures.html). The moisture content of the bagasse samples was determined using a moisture analyzer (Computrac MAX 1000, Arizona Instrument Corporation, Tempe, AZ, USA).

Enzyme Preparations

Commercial Preparations

A commercial preparation produced by *Trichoderma reesei* (Spezyme CP) and supplied by Genencor (Rochester, NY, USA) was used as the cellulase enzyme in this study. This preparation was supplemented with a β-glucosidase preparation (Novozym 188) produced by *Aspergillus niger* and supplied by Sigma (C6105). Various commercial xylanase preparations were kindly provided by various North American suppliers, and their cellulolytic and hemicellulolytic activities were evaluated (Table 1). BioCat xylanase was in powder form and was suspended in 100 mM sodium acetate buffer (pH 5) at a concentration of 10 mg/ml before use.

Laboratory-produced Enzyme Preparations

Thermomyces lanuginosus strains SSBP and ATCC 34626 and *Aspergillus carneus* ABO 372 were obtained from the culture collection of the Department of Microbiology at the University of Stellenbosch, South Africa. The fungi were maintained on malt extract agar plates. With a sterilized needle, samples were inoculated into 1 ml YPD (10 g/l yeast extract, 20 g/l peptone, 20 g/l glucose) and cultivated for 2 days respectively at the optimum temperature for the fungus (*T. lanuginosus*, 50 °C; *A. carneus*, 30 °C) with shaking. The contents of each inoculant were decanted into 200 ml growth medium (0.67% yeast nitrogen base with amino acids, 0.2% L-asparagine monohydrate, 0.5% KH_2PO_4), containing 4 g of AFEX pretreated sugar cane bagasse or 4 g beechwood xylan (Sigma) as carbon source and cultivated for 5 days at the optimum temperature. Fungal growth was clearly visible in the flasks after 4 days. The culture fluid was filtered through four layers of muslin cloth and then centrifuged at 5,000×*g* for 10 min to remove fungal debris. After centrifugation, 0.1% sodium azide was added to the supernatant to prevent microbial growth and concentrated by filtration through an Amicon concentration apparatus using a 10-kDa membrane filter.

Enzyme and Protein Assays

The filter paper activity of the enzyme samples was determined at 50 °C according to standardized NREL filter paper assay [11]. Carboxymethylcellulase (CMCase; endoglucanase) and Avicelase (exoglucanase) activity was determined by measuring the release of reducing

Table 1 Specific activities (mean of triplicate determinations±standard deviation) of cellulolytic and hemicellulolytic enzymes of selected preparations.

Enzyme and source	Protein concentration mg/ml	Filter paper activity U/mg	Endoglucanase (CMCase) U/mg	Exoglucanase (Avicelase) U/mg	β-glucosidase U/mg	β-xylanase U/mg	β-xylosidase U/mg	α-arabinofuranosidase U/mg
Cellulase (Spezyme CP) *T. reesei*	51.81±5.66	1.40	21.8±2.1	0.09±0.02	1.82±0.08	15±2	0.56±0.02	0.38±0.04
β-glucosidase (Novozym 188) *A. niger*	38.01±1.2	0	1.0±0.2	0.35±0.05	14.75±0.45	10±1	0.22±0	0.09±0.1
Xylanase (Multifect) *T. reesei*	7.63±0.39	0.04	6.3±0.6	0.46±0.07	3.30±0.10	209±10	4.90±0.58	3.21±0.40
Xylanase (PowerPulp TX200A) *Trichoderma*	3.34±0.07	0.42	5.6±2.0	0.31±0.09	1.07±0.13	369±10	1.27±0.01	0.98±0.04
Xylanase (FibreZyme LBL) unknown	28.81±1.00	1.27	97.1±7.6	0.38±0.05	3.09±0.21	69±1	0.94±0.03	0.68±0.03
Xylanase (BioCat; 10 mg/ml) *Trichoderma longibrachiatum*	0.51±0.01	1.43	78.6±10.5	9.50±0.79	4.65±0.26	1235±57	5.87±0.31	5.07±0.45
A. carneus ABO372[a]	0.23	ND	43.3±11.0	0.20±0.03	2.64±0.21	156±5	0.50±0.02	0.19±0.01
T. lanuginosus SSBP[b]	0.47	ND	4.8±1.7	0.05±0.02	0.46±0.02	2498±34	0.09±0.01	0.11±0.01
T.lanuginosus ATCC 34626[b]	0.32	ND	5.6±1.6	0.03±0.01	0.91±0.06	2764±137	0.12±0.01	0.08±0.01
T. lanuginosus ATCC 34626[c]	0.14	ND	19.3±5.5	0.16±0.03	0.66±0.03	8238±64	0.19±0.03	0

ND: not determined

[a] Fungus grown in medium containing AFEX-pretreated bagasse at 30 °C.

[b] Fungus grown in medium containing AFEX-pretreated bagasse at 50 °C.

[c] Fungus grown in medium containing beechwood xylan at 50 °C.

sugars from 3% carboxymethylcellulose (Sigma) and 3% Avicel (FMC Biopolymer pH-102), respectively, at 50 °C and pH 5.0 (100 mM acetate buffer) for 10 min [12]. β-Xylanase activity was determined by following the release of reducing sugars from a 1% birchwood xylan (Sigma) solution at 50 °C for 5 min [13]. One unit of activity was defined as the amount of enzyme that released either 1 μmol of glucose or xylose as reducing sugar equivalents per min.

β-Glucosidase, β-xylosidase, and α-arabinofuranosidase activities were determined by following the release of 4-nitrophenol from 4-nitrophenyl-β-D-glucopyranoside, 4-nitrophenyl-β-D-xylopyranoside, and 4-nitrophenyl-α-L-arabinopyranoside (Sigma), respectively, for 15 min at 50 °C and pH 4.0 (50 mM Na acetate buffer). The reaction was stopped by the addition of 1 M Na_2CO_3, and the absorbance was read at 410 nm from a 4-nitrophenol standard curve. One unit of activity was defined as the amount of enzyme that released 1 μmol of 4-nitrophenol per min.

The protein concentration was determined using the Coomassie Brilliant Blue dye-binding method (BioRad; [14]).

Batch Hydrolysis of Pretreated Sugar Cane Bagasse and Avicel

Enzymatic saccharification experiments of pretreated samples were performed in triplicate in 20 ml glass scintillation vials at 50 °C and 100 rpm for 72 h as described in the NREL (LAP-009) procedure. Briefly, the reaction mixture contained 0.1 g glucan (cellulose dry weight; except with the substrate loading experiment), 0.5 ml 1 M sodium citrate buffer (pH 4.8), 40 μl tetracycline (10 mg/ml), 30 μl cycloheximide (10 mg/ml), Spezyme CP and Novozym 188 in a ratio of 1:2/g glucan, and distilled water to give a final volume of 10 ml. Adjustments were also made for the addition of various activities of commercial and laboratory-produced xylanases. The moisture content in the AFEX-pretreated bagasse (24.53%) and NH_4OH-pretreated bagasse (78.42%) was included in the calculation of the total volume. Avicel (FMC Biopolymer pH-102; 4.54% moisture) was also included as a control. Substrate blanks excluded the enzyme activities whereas enzyme blanks excluded the substrates, and the degree of hydrolysis was used to correct data. Samples were withdrawn initially and after 72 h, and centrifuged at 10,000 rpm in Eppendorf tubes to remove the biomass. Subsequently, the liquid portion was filtered through a 0.45 μm (pore size) Whatman GD/X filter and the liquid was subjected to HPLC analysis. HPLC analysis was conducted using an isocratic system using a refractive index detector (Spectra System, RI 150, Thermo Electron, Milan, Italy). Sugars were separated on an Aminex-HPX-87P column (BioRad) at a flow rate of the mobile phase (deionized water) of 0.6 ml/min and at 85 °C for 30 min.

Calculations

The percent hydrolysis of the glucan fraction of sugar cane bagasse was calculated by adding the glucose concentration to double the cellobiose concentration. This value was multiplied by 0.9 to correct for hydration (each glucose molecule had one molecule of water added during hydrolysis) and divided by the grams of glucan.

Statistical Analysis

A two-way analysis of variance (ANOVA) was performed to determine if any significant differences ($p<0.05$) occurred between factors. Bonferroni and bootstrap multiple comparisons were preformed with STATISTICA version 7.0 (Stat-Soft, Tulsa, OK, USA).

Results and Discussion

Analysis of sugar cane bagasse revealed a composition (dry biomass) of 25.0% lignin, 38.4% glucan, 24.1% xylan, and 1.9% arabinan. After pretreatment with the AFEX process or NH_4OH, the composition consisted of 22.6 and 21.1% lignin, 41.7 and 56.6% glucan, 20.4 and 24.0% xylan, respectively, and 1.2% arabinan for both AFEX and dilute ammonia treatment. Both pretreatment processes resulted in an increase in the glucan concentration and left the hemicellulose fraction of bagasse largely intact. Alkali pretreatments are reported to only partially hydrolyze the hemicellulose fraction to oligomers [9, 15]. In this study, it is apparent that solubilization might also depend on the substrate type as the xylan concentration of the pretreated bagasse was only slightly less than that of the raw sugar cane bagasse.

The cellulolytic and hemicellulolytic activities of six commercial enzyme preparations are shown in Table 1. Filter paper activity could be detected only in some samples and the highest activities were obtained in the BioCat xylanase, Spezyme CP, and FibreZyme LBL. The samples showed a considerable range in CMCase (an indicator of endo-β-1,4-glucanase activity) and Avicelase (an indicator of exoglucanase activity). BioCat xylanase preparation showed the highest specific activity of the various cellulolytic enzymes. Novozym 188 had the highest β-glucosidase activity. The β-xylanase specific activities of the six commercial samples ranged between 10 and 1,235 U/mg. Especially notable was the low β-xylanase activities of Novozym 188 and Spezyme CP, two enzyme preparations commonly used in the hydrolysis of lignocellulose. The hemicellulolytic enzyme profiles of a number of preparations were evaluated to establish which might be appropriate for addition to a cellulase/β-glucosidase enzyme mixture. The BioCat, PowerPulp TX200A, and Multifect preparations were found to have the highest xylanase activity. Furthermore, BioCat xylanase, Multifect xylanase, and PowerPulp TX200A revealed specific β-xylosidase activity >1 and BioCat xylanase and Multifect xylanase were found to have the highest α-arabinofuranosidase activity. Four other commercial xylanase preparations were analyzed but their hemicellulolytic enzyme profiles were deemed not to be appropriate for further evaluation (data not shown). The results suggest that these xylanase preparations might be suitable to boost hydrolysis of sugar cane bagasse to a mixture of hexoses and pentoses when added to a cellulase/β-glucosidase enzyme mixture.

The cellulolytic and hemicellulolytic enzyme profiles of a number of selected fungi were also evaluated (Table 1). The selection of the fungi was based on their properties determined in previous research. *A. carneus* ABO374 was isolated from soil in the Southern Cape region of South Africa and found to efficiently release reducing sugars from wheat straw. The *T. lanuginosus* strains SSBP and ATCC 34626 were shown to be very efficient producers of xylanases, and the β-xylanase activity could be maintained up to 60 °C [16, 17]. The *A. carneus* strain cultivated on AFEX-pretreated sugar cane bagasse produced the highest specific activities of cellulolytic enzymes and β-glucosidase of the fungal strains tested. *T. lanuginosus* strain SSBP produced lower cellulolytic specific activities when compared with ATCC 34626 when cultivated under similar conditions. Most activities of cellulolytic enzymes were higher with strain ATCC 34626 when it was grown on beechwood xylan than on AFEX-pretreated bagasse, suggesting that pure xylan is a better substrate for enzyme production. The highest specific β-xylanase activity was produced by strain ATCC 34626 when cultivated on beechwood xylan, whereas lower activity was found when the *T. lanuginosus* strains were grown on AFEX-pretreated bagasse, and much lower β-xylanase activity was produced by *A. carneus* (Table 1). These results revealed values that were higher than those found in the commercial samples. *A. carneus* produced

the highest activity of β-xylosidase and α-arabinofuranosidase whereas the *T. lanuginosus* strains produced much lower activities of these auxiliary enzymes, as has been reported previously [16].

Spezyme CP is a commercial cellulolytic enzyme preparation produced by *Trichoderma reesei* (Table 1) and has been widely used in the hydrolysis of cellulose-rich biomass. However, this preparation lacks adequate β-glucosidase activity [9] to achieve complete hydrolysis to glucose, resulting in cellobiose accumulation. Therefore, Spezyme CP is usually supplemented with β-glucosidase to promote hydrolysis. In the literature, the ratios of cellulase to β-glucosidase have ranged widely and have depended upon the nature of the lignocellulose material to be hydrolyzed. For example, ratios of 1 filter paper unit (FPU):2 cellobiase units (CBU) [18] and 1 FPU:3.2 CBU [3] have been used to hydrolyze various softwood substrates and barley straw, respectively, whereas Martin et al. [4] used a ratio of 1 FPU:5.4 CBU and the NREL procedure (LAP-009) recommended a ratio of approximately 1 FPU:1 pNPGU to hydrolyze steam pretreated sugar cane bagasse. A ratio of 1 FPU:2 CBU was selected for the hydrolysis experiments in this study, and the ratio was based on the reported commercial enzyme activities of 60 FPU/ml for Spezyme CP and 282 CBU/ml for Novozym 188. Based on the data in Table 1, our calculated ratio was 1 FPU of Spezyme CP:3.3 β-glucosidase units of Novozym 188.

Figure 1 shows the effect of three concentrations of Spezyme CP/Novozym 188 (in an activity ratio of 1:2) on the hydrolysis of NH_4OH-pretreated and AFEX-pretreated bagasse and Avicel (1% glucan loading). As the enzyme level increased, greater amounts of glucose and xylose were released from the bagasse samples. No cellobiose was detected in any of the samples suggesting that the β-glucosidase activity was not limiting in any of the enzyme mixtures. Arabinose was only released in low concentrations from the AFEX-pretreated bagasse. At a 10 FPU:20 CBU/g glucan ratio, the greatest amount of glucose was released from Avicel followed by the AFEX-pretreated bagasse. A significant increase ($p<0.05$) in the release of glucose and xylose from NH_4OH-pretreated and AFEX-pretreated bagasse was observed when the enzyme amount was raised from 10:20 to 30:60. Greater amounts of enzyme activity (60:120) failed to significantly ($p>0.05$) increase the release of glucose and xylose. Only a marginal increase in the amount of glucose ($p>0.05$) released from Avicel was observed with greater enzyme activity, which indicated that the 10:20 enzyme mixture was close to the saturation level for hydrolysis. At the lowest enzyme level, only 28% and 33% of the glucan in respective NH_4OH-pretreated and AFEX-pretreated bagasse samples were hydrolyzed to glucose, whereas 66% of the Avicel glucan was hydrolyzed, suggesting that some glucan was inaccessible in the bagasse samples to enzyme hydrolysis. At the highest enzyme level (60 FPU/g glucan:120 CBU/g glucan), 68% and 78% of the glucan was hydrolyzed in the respective bagasse samples and Avicel samples. Increasing the level of enzyme appeared to have a much lower impact on the hydrolysis of Avicel than on bagasse. This might be because of a synergistic effect of the other enzymes present in the Spezyme CP/Novozym 188 acting on the cellulose and hemicellulose components in bagasse.

Four xylanase preparations with suitable activity profiles were evaluated for their ability to boost the hydrolysis by Spezyme CP and Novozym 188 (10 FPU:20 CBU/g glucan) of NH_4OH-pretreated and AFEX-pretreated bagasse and Avicel (Fig. 2). As these enzyme preparations contain multiple cellulolytic and hemicellulolytic activities (Table 1), the protein concentration was used as the basis to supplement the Spezyme CP/Novozym mixture instead of using the activity of a single enzyme such as xylanase. All enzyme preparations added at 10% and 50% protein levels resulted in increases in the release of glucose (Fig. 2a, c, e, g) and xylose (Fig. 2b, d, f, h). However, in most instances, significant

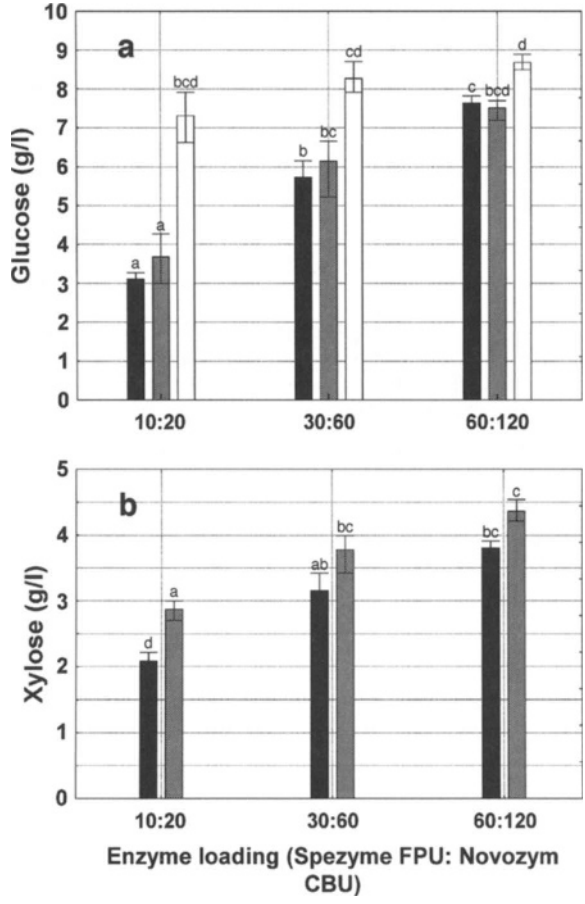


Fig. 1 Release of glucose (**a**) and xylose (**b**) from ammonium hydroxide-pretreated (*black bars*) and AFEX-pretreated (*gray bars*) sugar cane bagasse and Avicel (*white bars*) (1% glucan loading) by Spezyme CP and Novozym 188 (1:2 activity ratio/g glucan). The total protein concentration of Spezyme CP/Novozym 188 mixture was 1.146 (10:20 ratio), 3.438 (30:60 ratio), and 6.876 (60:120 ratio) mg/g glucan. *Vertical lines* indicate 95% bootstrap confidence intervals and means of *bars with identical letters* are not significantly different ($p>0.05$)

differences ($p>0.05$) were not revealed, and only a significant increase in xylose release was observed when Multifect xylanase was added at the 10% protein level to AFEX-pretreated bagasse. Little, none, or trace amounts of cellobiose were detected in these hydrolysates, indicating that β-glucosidase was not limiting under the conditions used. Low concentrations of arabinose were detected in some hydrolysates but no relationship could be found between the levels of the various enzyme preparations applied (data not shown). In all instances, higher levels of glucose and xylose were released from the AFEX-pretreated bagasse than the NH_4OH-pretreated bagasse, and in many cases, these differences were significant ($p<0.05$). The degree of hydrolysis of the glucan of the NH_4OH-pretreated bagasse increased from 26% to 43%, 44%, and 55% when Multifect, FibreZyme LBL, and BioCat xylanases were added, respectively, at the 50% protein level. However, the degree of hydrolysis of the AFEX-pretreated bagasse was greater and increased from approximately 42% to 61%, 54%, 55%, and 73% when Multifect, PowerPulp, FibreZyme LBL, and BioCat xylanases were added at the 50% protein levels. It is interesting to note that the addition of Multifect and PowerPulp xylanase but not FibreZyme LBL or BioCat xylanase to the enzyme mixture increased the release of glucose from Avicel, but bore no relationship to the levels of cellulolytic enzyme activities (Table 1). PowerPulp and Multifect xylanase added at the 50% protein level increased the hydrolysis of Avicel from 65% to 80% and 76%, respectively. Table 1 shows

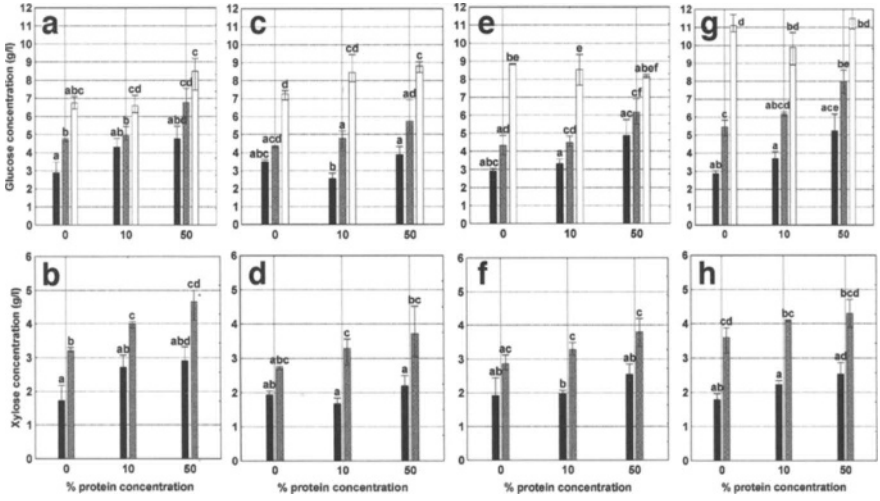


Fig. 2 Release of glucose (**a**, **c**, **e**, g) and xylose (**b**, **d**, **f**, **h**) from ammonium hydroxide-pretreated (*black bars*) and AFEX-pretreated (*checked bars*) sugar cane bagasse and Avicel (*open bars*) (1% glucan loading) by Spezyme CP (10 FPU/g glucan) and Novozym 188 (20 CBU/g glucan). Xylanase from Multifect (**a**, **b**), PowerPulp (**c**, **d**), FibreZyme LBL (**e**, **f**) and BioCat (**g**, **h**) added at 10% and 50% protein to the total protein concentration of Spezyme CP/Novozym 188 mixture (1.146 mg protein/g glucan). *Vertical lines* indicate 95% bootstrap confidence intervals and means of *bars with identical letters* are not significantly different ($p>0.05$)

that both xylanase preparations had relatively low cellulolytic enzyme activities and, therefore, these results point to the possibility that the xylanase might act synergistically in the hydrolysis of cellulose by cellulase.

The impact of laboratory-produced enzymes, added at a 10% protein level on hydrolysis by Spezyme CP and Novozym 188 (10 FPU:20 CBU) is shown in Fig. 3. Enzymes produced by *A. carneus* failed to boost the hydrolysis of NH_4OH-pretreated and AFEX-pretreated bagasse. The enzyme preparations produced by *T. lanuginosus* strains all produced an increase of xylose release from NH_4OH-pretreated and AFEX-pretreated bagasse, but little or no increase in glucose release was observed. *T. lanuginosus* ATCC 34626, grown on beechwood xylan, was the most effective of the various laboratory-produced enzyme preparations in increasing the amount of xylose released, and this could be related to the high specific xylanase activity (Table 1). No clear relation between enzyme preparation of the laboratory-grown fungi and the release of glucose from Avicel was observed. The failure of *A. carneus* to boost xylose release from NH_4OH-pretreated and AFEX-pretreated bagasse might be because of the low xylanase activity (Table 1). The percent hydrolysis of the glucan fraction of NH_4OH-pretreated and AFEX-pretreated bagasse increased from 29% to 40% and from 49% to 54%, respectively, by the addition of an enzyme preparation from *T. lanuginosus* ATCC 34626, grown on beechwood xylan. As shown in the studies with the commercial xylanase preparations, greater amounts of sugar were released from the AFEX-pretreated bagasse than from the NH_4OH-pretreated bagasse when the laboratory-produced enzymes were added to Spezyme CP and Novozym 188, suggesting that the AFEX-pretreated bagasse is more easily hydrolyzed.

As the Multifect xylanase was shown to be one of the most effective xylanase preparations in boosting the hydrolysis of bagasse, the effect on glucan substrate loading on the hydrolysis of NH_4OH-pretreated and AFEX-pretreated bagasse by Spezyme CP and Novozym 188 with and without Multifect xylanase was evaluated (Fig. 4). As a result of

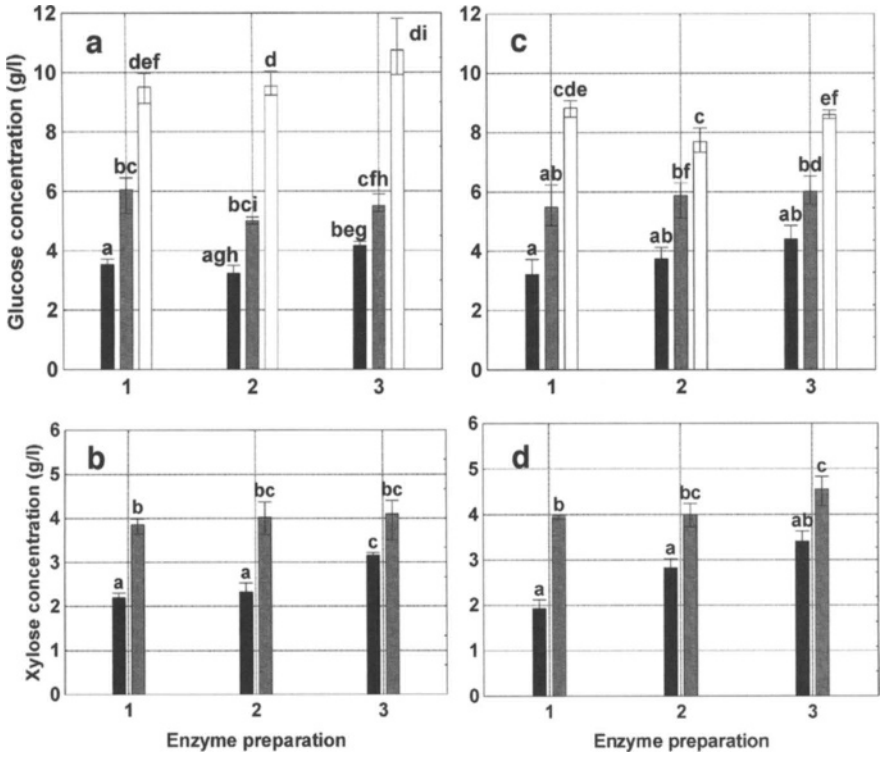
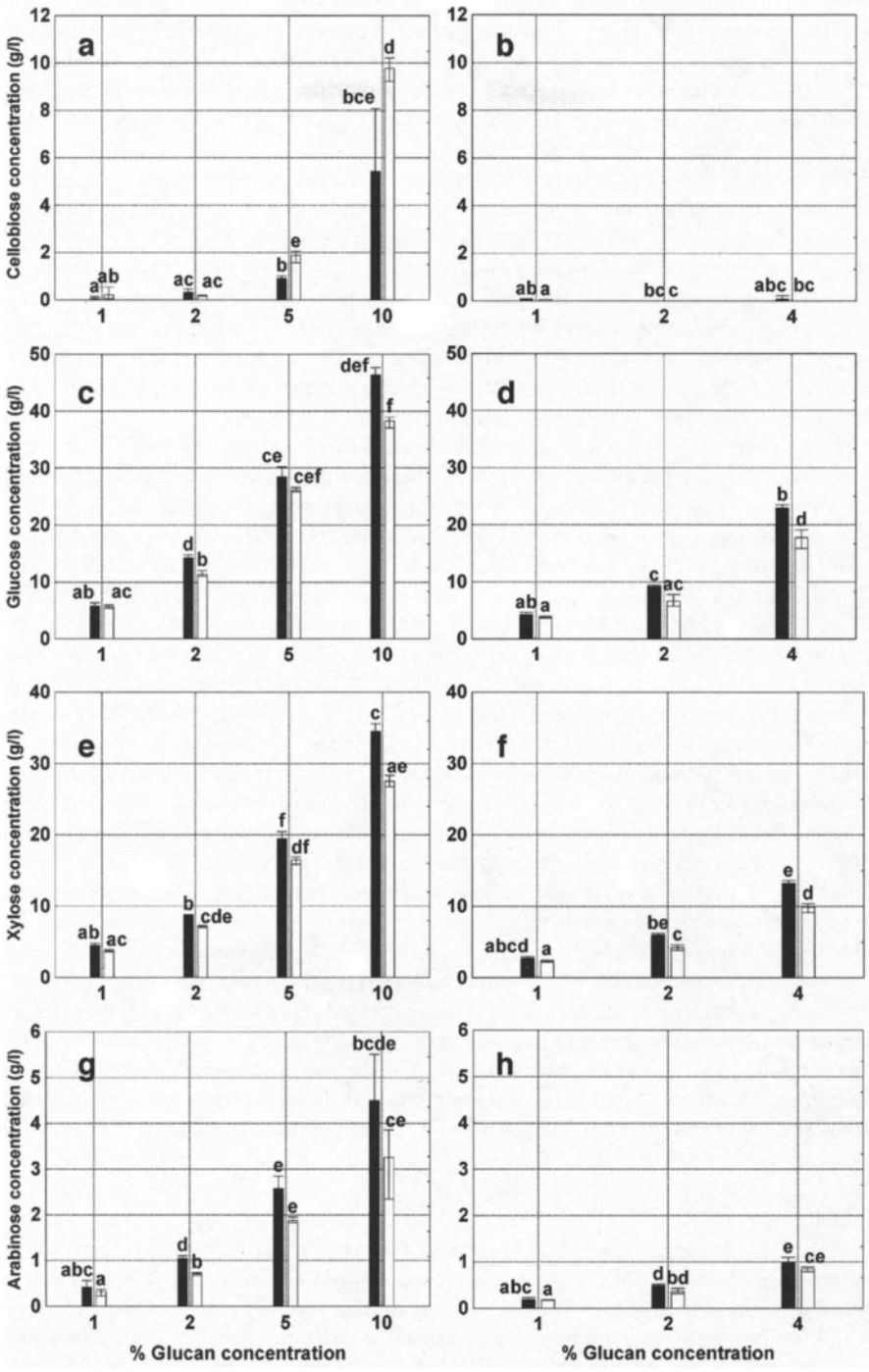


Fig. 3 Release of glucose (**a**, **c**) and xylose (**b**, **d**) from ammonium hydroxide-pretreated (*solid bars*) and AFEX-pretreated (*gray bars*) sugar cane bagasse and Avicel (*open bars*) (1% glucan) when hydrolyzed with Spezyme CP (10 FPU/g glucan) and Novozym 188 (20 CBU/glucan) without (*a1*, *c1*) or with the addition of crude enzyme preparations (10 % protein added) of *A. carneus* ABO372 (*a2*, *b2*), *T. lanuginosus* SSBP (*a3*, *b3*), *T. lanuginosus* ATCC 34626 (AFEX-pretreated bagasse as growth substrate; *c2*, *d2*), or *T. lanuginosus* ATCC 34626 (beechwood xylan as growth substrate; *c3*, *d3*). The total protein concentration of Spezyme CP/Novozym 188 mixture was 1.146 mg/g glucan. *Vertical lines* indicate 95% bootstrap confidence intervals and means of *bars with identical letters* are not significantly different ($p>0.05$)

the high moisture content of the NH_4OH-pretreated bagasse, a maximum glucan substrate loading of only 4% could be tested, whereas the AFEX-pretreated bagasse could be tested up to 10% glucan substrate loading. At all substrate loadings, there were greater amounts of xylose, arabinose, and glucose released when Multifect xylanase was present, although the differences in sugars accumulated in hydrolysates with and without Multifect xylanase were only significant ($p<0.05$) in some instances (Fig. 4). Notable is the significantly ($p<0.05$) higher amount of xylose released from AFEX-pretreated and NH_4OH-pretreated bagasse at 10% and 4% glucan loading, respectively (Fig. 4e, f). However, it was apparent that greater amounts of both glucose and xylose were released from the AFEX-pretreated bagasse than the NH_4OH-pretreated bagasse at an equivalent glucan loading. Whereas cellobiose

Fig. 4 Release of cellobiose (**a**, **b**), glucose (**c**, **d**), xylose (**e**, **f**), and arabinose (**g**, **h**) from various concentrations (% glucan) of AFEX-pretreated (**a**, **c**, **e**, **g**) and ammonium hydroxide-pretreated (**b**, **d**, **f**, **h**) sugar cane bagasse by Spezyme CP (10 FPU/g glucan) and Novozym (20 CBU/g glucan) with (*solid bars*) and without (*open bars*) the addition of Multifect xylanase (10% protein;). The total protein concentration of Spezyme CP/Novozym 188 mixture was 1.146 mg/g glucan. *Vertical lines* indicate 95% bootstrap confidence intervals and means of *bars with identical letters* are not significantly different ($p>0.05$)


a
b
c
d
e
f
g
h
Cellobiose concentration (g/l)
Glucose concentration (g/l)
Xylose concentration (g/l)
Arabinose concentration (g/l)
% Glucan concentration
% Glucan concentration

accumulation was negligible at the various substrate loading of NH_4OH-pretreated bagasse (Fig. 2b), a significant amount of cellobiose was accumulated as the substrate loading of AFEX-pretreated bagasse was increased and the accumulation was significantly exacerbated ($p<0.05$) by absence of the Multifect xylanase (Fig. 2a). This suggests that additional β-glucosidase activity might be necessary at higher loadings of AFEX-pretreated bagasse. β-Glucosidase improves cellulose hydrolysis by reducing end-product inhibition of cellulolytic enzymes because of the accumulation of cellobiose. Evidently, at high substrate loading, the inhibition of β-glucosidase by glucose accumulation may have occurred [19], and glucan hydrolysis could be improved by further optimization of the ratio and levels of cellulase: β-glucosidase or by using a β-glucosidase preparation more resistant to glucose inhibition. A simultaneous saccharification and fermentation to ethanol system may also reduce end-product inhibition and not require additional β-glucosidase [9]. It is surprising to note that the percent hydrolysis of the glucan fraction of bagasse appeared to be unaffected by the load increase (data not shown).

A regression analysis of the relationship between xylanase activity added and sugar release found that increasing units of enzyme activity had significant impact on the release of glucose and of xylose (Fig. 5). The relationship between xylanase activity was significant ($p<0.01$) with commercial xylanases added to AFEX-pretreated ($p=0.0087$; Fig. 5g) and NH_4OH-pretreated ($p=0.0048$; Fig. 5h) bagasse, as well with laboratory-produced xylanases added to AFEX-pretreated ($p=0.0057$; Fig. 5i) and NH_4OH-pretreated ($p<0.0001$; Fig. 5j) bagasse. These results suggest that addition of xylanase boosts xylose release, and this was especially significant with the laboratory-produced xylanase on the NH_4OH-pretreated bagasse. When the release of glucose was analyzed, the addition of commercial xylanase had a highly significant effect on AFEX-pretreated ($p<0.0001$; Fig. 5a) and NH_4OH-pretreated ($p<0.0001$; Fig. 5b) bagasse. The effect of the laboratory-produced xylanase on glucose release was only significant on the NH_4OH-pretreated ($p<0.0021$; Fig. 5d) but not the AFEX-pretreated ($p=0.2137$; Fig. 5c) bagasse. These results point to the xylanase in the commercial preparations, in conjunction with possibly other cellulolytic enzymes acting in synergy to hydrolyze the bagasse. The laboratory-produced xylanase preparations mostly lacked cellulolytic activity (Table 1). The release of glucose from Avicel was only significant ($p=0.0004$) with the commercial xylanase preparations (Fig. 5e), whereas no relationship was observed between xylanase activity and glucose release when laboratory-produced xylanase preparations were added (Fig. 5f). This observation again points to the cellulolytic activities in the commercial xylanase preparations playing an important role in cellulose hydrolysis but the xylanase itself does not appear to have any specific activity on the cellulose and on glucose release. A similar observation was made by Berlin et al. [18] from their studies on the hydrolysis of softwood substrates. However, more in depth investigations with purified cellulolytic and hemicellulolytic enzymes could help to confirm these observations.

Conclusions

In conclusion, enzyme preparations have been assayed for their activities and certain preparations have been identified as being most suitable for use in hydrolysis experiments. A lack of detailed knowledge about the nature of the substrate after pretreatment (porosity, size, insolubility, and crystallinity of the macroscopic particles) required us to follow an empirical approach in this study. Furthermore, the role of each enzyme in the crude enzyme preparations is difficult to assess but fundamental studies have pointed to each enzyme as having a complementary role in the sequential hydrolysis of lignocellulose [9]. The boost in

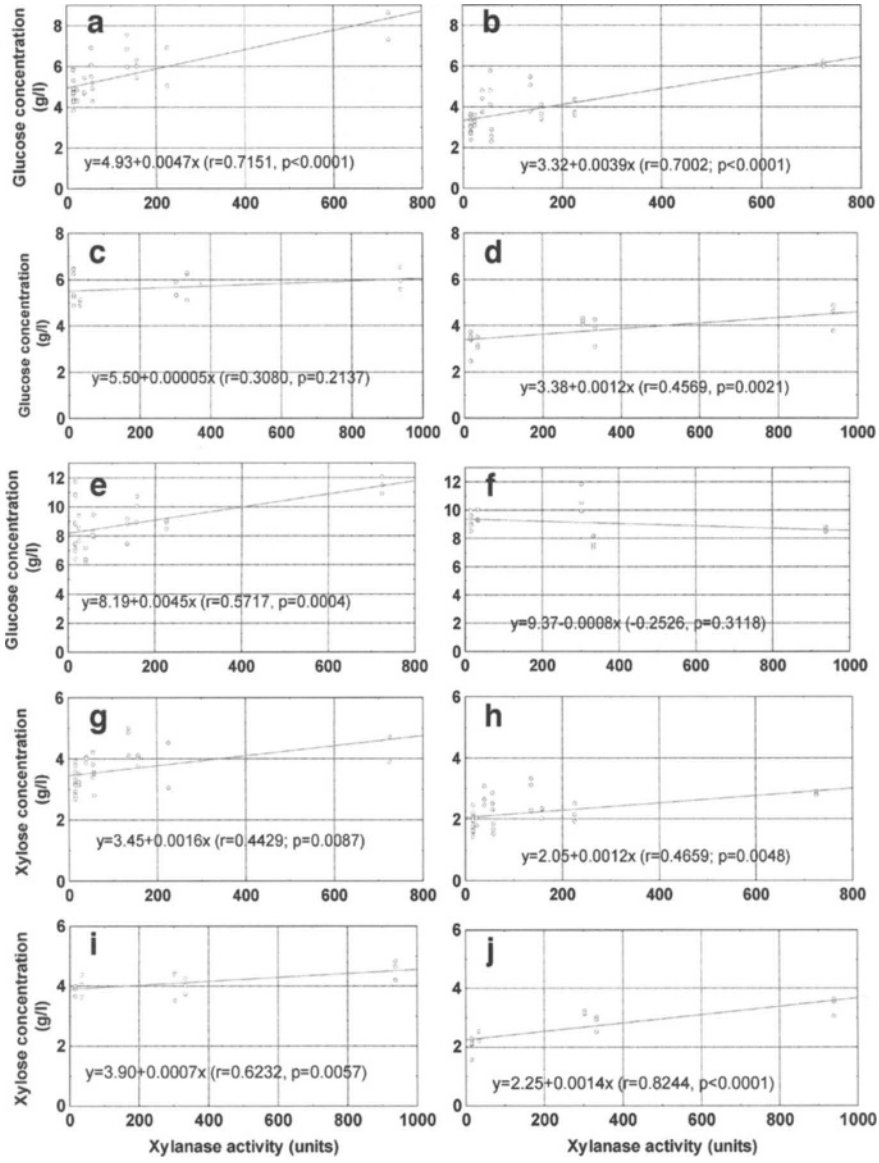


Fig. 5 Regression analysis of glucose (**a**–**f**) and xylose (**g**–**j**) release from AFEX-pretreated bagasse (**a**, **c**, **g**, **i**), NH_4OH-pretreated bagasse (**b**, **d**, **h**, **j**), and Avicel (**e**, **f**) hydrolyzed with Spezyme CP (10 FPU/g glucan) and Novozym 188 (20 CBU/g glucan) and supplemented with xylanase (10% protein addition) from either commercial (**a**, **b**, **e**, **g**, **h**) or laboratory-grown sources (**c**, **d**, **f**, **i**, **j**). The total protein concentration of Spezyme CP/Novozym 188 mixture was 1.146 mg/g glucan

hydrolysis of the xylan fraction but also the glucan fraction of pretreated bagasse by the addition of 10% protein level of a xylanase preparation to the Spezyme CP/Novozym 188 mixture could be interpreted in a number of ways. Previous studies have pointed to the removal of hemicellulose by xylanases increasing the accessibility of cellulose to cellulases [18]. The separation of the lignin fraction from the hemicellulose could also be important in

the overall hydrolysis as lignin acts as a competitive absorbent for cellulase and β-glucosidase [9] and the auxiliary enzymes present in the preparations used in this study might play a significant role. Future work should tailor the levels of xylanases to be added to cellulase/β-glucosidase enzyme mixtures to achieve substantial hydrolysis of AFEX-pretreated and NH_4OH-treated sugar cane bagasse. The development of an optimal cellulase/β-glucosidase/xylanase enzyme mixture is necessary to achieve efficient and economic bagasse hydrolysis.

Acknowledgements We thank Benito Stradi, Giovanna DeQueiroz, and Chang-Ho Chung for the helpful discussions and preparation of the ammonium hydroxide-pretreated bagasse, Farzaneh Teymouri for the preparation of the AFEX-pretreated bagasse, Chardcie Verret and Brian White for the assistance with the analysis of the sugars, and Daan Nel at the University of Stellenbosch for the assistance with the statistical analysis.

References

1. Lynd, L. R., Wyman, C. E., & Gerngross, T. U. (1999). *Biotechnology Progress, 15*, 777–793.
2. Knauf, M., & Moniruzzaman, M. (2004). *International Sugar Journal, 106*, 147–150.
3. Rosgaard, L., Pedersen, S., Cherry, J. R., Harris, P., & Meyer, A. S. (2006). *Biotechnology Progress, 22*, 493–498.
4. Martin, C., Galbe, M., Wahlbom, C. F., Hahn-Hägerdal, B., & Jönsson, L. J. (2002). *Enzyme and Microbial Technology, 31*, 274–282.
5. Kaar, W. E., Gutierrez, C. V., & Kinoshita, C. M. (1998). *Biomass and Bioenergy, 14*, 277–287.
6. Fox, D. J., Gray, P. P., Dunn, N. W., & Marsden, W. L. (1987). *Journal of Chemical Technology and Biotechnology, 40*, 117–132.
7. Holtzapple, M. T., Jun, J.-H., Ashok, G., Patibandla, S. L., & Dale, B. E. (1991). *Applied Biochemistry and Biotechnology, 28/29*, 59–74.
8. Van Zyl, C., Prior, B. A., & du Preez, J. C. (1988). *Applied Biochemistry and Biotechnology, 17*, 357–369.
9. Lynd, L. R., Weimer, P. J., van Zyl, W. H., & Pretorius, I. S. (2002). *Microbiology and Molecular Biology Reviews, 66*, 506–577.
10. Mosier, N., Wyman, C., Dale, B., Elander, R., Lee, Y. Y. Holtzapple, M., et al. (2005). *Bioresource Technology, 96*, 673–686.
11. Adney, B., & Baker, J. (1996). NREL laboratory analytical procedure. In *Laboratory Analytical Procedure No. 006*. Golden, CO: National Renewable Energy Laboratory.
12. Wood, T. M., & Bhat, K. M. (1988). *Methods in Enzymology, 160*, 87–112.
13. Bailey, M. J., Biely, P., & Poutanen, K. (1992). *Journal of Biotechnology, 23*, 257–270.
14. Bradford, M. M. (1976). *Analytical Biochemistry, 72*, 248–254.
15. Dale, B. E., & Moriera, M. J. (1982). *Biotechnology and Bioengineering Symposium, 12*, 31–43.
16. Singh, S., Pillay, B., Dilsook, V., & Prior, B. A. (2000). *Journal of Applied Microbiology, 88*, 975–982.
17. Singh, S., Pillay, B., & Prior, B. A. (2000). *Enzyme and Microbial Technology, 26*, 502–508.
18. Berlin, A., Gilkes, N., Kilburn, D., Bura, R., Matkov, A., Skomatovsky, A., et al. (2005). *Enzyme and Microbial Technology, 37*, 175–184.
19. Dekker, R. F. H. (1986). *Biotechnology and Bioengineering, 28*, 1438–1442.

Appl Biochem Biotechnol (2008) 146:165–172
DOI 10.1007/s12010-008-8133-3

Monoglycerides and Diglycerides Synthesis in a Solvent-Free System by Lipase-Catalyzed Glycerolysis

Patricia Bogalhos Lucente Fregolente · Leonardo Vasconcelos Fregolente · Gláucia Maria F. Pinto · Benedito César Batistella · Maria Regina Wolf-Maciel · Rubens Maciel Filho

Received: 30 November 2007 / Accepted: 20 December 2007 /
Published online: 22 February 2008
© Humana Press Inc. 2008

Abstract Five lipases were screened (*Thermomyces lanuginosus* free and immobilized forms, *Candida antarctica* B, *Candida rugosa*, *Aspergillus niger*, and *Rhizomucor miehei*) to study their ability to produce monoglycerides (MG) and diglycerides (DG) through enzymatic glycerolysis of soybean oil. Lipase from *C. antarctica* was further studied to verify the enzyme load (wt% of oil mass), the molar ratio glycerol/oil, and the water content (wt% of glycerol) on the glycerolysis reaction. The best DG and MG productions were in the range 45–48% and 28–30% (*w/w*, based on the total oil), respectively. Using immobilized lipases, the amount of free fatty acids (FFA) produced was about 5%. However, the amount of FFA produced when using free lipases, with 3.5% extra water in the system, is equivalent to the MG yield, about 23%. The extra water content provides a competition between hydrolysis and glycerolysis reactions, increasing the FFA production.

Keywords Monoglycerides · Diglycerides · Lipase-catalyzed glycerolysis · Soybean oil

Introduction

Monoglycerides (MG) and diglycerides (DG) are widely used as emulsifiers in foods, cosmetics, and pharmaceutical products [1–3]. Often, mixtures of MG and DG are used in these applications because they are cheap and give proper performance [4]. Besides these applications, a great number of studies on DG in human dietary have been carried out. The use of DG replacing triglyceride (TG) in food has been studied to prevent lipid accumulation in abdominal tissue and, therefore, prevent some diseases related to obesity. Researchers recently showed that long-term ingestion of dietary oil containing mainly DG

P. B. L. Fregolente (✉) · L. V. Fregolente · G. M. F. Pinto · B. C. Batistella · M. R. Wolf-Maciel · R. M. Filho
Separation Process Development Laboratory, Chemical Engineering School, State University of Campinas, 13081 970 Campinas, São Paolo, Brazil
e-mail: lucente@feq.unicamp.br

M. R. Wolf-Maciel
e-mail: wolf@feq.unicamp.br

reduces body fat accumulation in humans as compared to TG oil with a similar fatty acid composition [5–7]. Industrially, the production of MG and DG consists on the interesterification of TG with glycerol (GL), in the presence of inorganic catalysts at high temperatures (220–260 °C). This reaction is known as glycerolysis and produces approximately 50% MG content mixture. Due to the high temperatures used, undesirable sub-products are formed [8, 9]. Currently, food industries present interest on the production of more healthful products due to the market requirements, like products free of sub-products of polymerization reactions and of fats in the *trans* configuration. The product produced by this strategy has several drawbacks, e.g., low yield, dark color, and burnt taste [10]. Thus, the substitution of the chemical synthesis of MG and DG for the enzymatic route is presented as an attractive alternative because, in this process, low temperatures and near neutral pH are used to prevent the formation of undesirable products [11]. An efficient alternative to produce high yield of MG is the use of solvent or a mixture of solvents to improve the miscibility of substrates. However, the optimization of the solvent media is complex considering the interaction between solvents and enzymes and the safety requirements for food applications [12].

Lipase-catalyzed glycerolysis of oils and fats using solvent-free system at atmospheric pressure and lower temperature have attracted interest in both academic and industrial fields. Because of the possibility of further separation of the reaction products by vacuum distillation, lower energy requirements, selectivity of the enzymes [13], and possibility of recoverability and recyclability of immobilized enzymes [14], it is believed to be a practical alternative method for MG and DG production.

In this work, MG and DG are produced through lipase-catalyzed glycerolysis of soybean oil in a batch reactor using *Candida antarctica* B, *Thermomyces lanuginosus*, *Rhizomucor miehei*, *Candida rugosa*, and *Aspergillus niger* lipases, in a solvent-free system.

Materials and Methods

Materials

Commercial refined soybean oil was used. Glycerol (99%, 0.5% of water content) was supplied by Synth (Diadema, Brazil). *C. antarctica* B (CA-IM, immobilized lipase), *T. lanuginosus* (TL-IM and TL-L, immobilized and free lipases, respectively), *A. niger* (AN-L, free lipase), and *R. miehei* (RM-IM, immobilized lipase) were generously supplied by Novozymes A/S (Bagsvaerd, Denmark). *C. rugosa* (CR-IM, immobilized lipase) was supplied by Sigma Chemicals Co. Lipase from *R. miehei* is immobilized by adsorption on a macroporous anion exchange resin phenolic type. This is a thermostable 1,3-specific lipase preparation that can be used at temperatures between 30 and 70 °C. Novozyme 435 B is the lipase from *C. antarctica* immobilized on a macroporous acrylic resin. It is also a thermostable lipase preparation with a maximum activity in the range 70–80 °C. The immobilization matrix of TL IM lipase is silicon dioxide.

Glycerolysis Reaction

The enzymatic glycerolysis reaction was carried out in batch system. The reaction mixture consisted of glycerol and soybean oil in different molar ratios (glycerol/oil), immobilized or free lipase (the amount of lipase was based on the weight of oil), and an extra 3.5% of water (based on the glycerol amount). A water thermostatic bath was used to control the

temperature, which ranged from 40 to 70 °C. The reaction was stirred using a magnetic stirrer at 300 rpm. The reaction was stopped after 24 h by heating the reaction until 90 °C for 15 min, as described by Tuter et al. [15]. Samples of the reaction mixture were filtrated to remove the lipases before analysis.

Determination of Lipase Hydrolytic Activity

The method is based on the speed at which the enzyme hydrolyzes tributyrin at pH 7.0. The butyric acid that is formed is titrated with sodium hydroxide and the consumption of the latter recorded as a function of time. One unit (lipase activity unit) is the amount of enzyme that releases 1 μmol titratable butyric acid per minute of reaction at 37 °C.

Analysis of Glycerides by HPSEC

The determination of the composition of the acylglycerols, FFA and GL, were performed using a gel-permeation chromatography (GPC), also called high-performance size-exclusion chromatography (HPSEC) [16]. The chromatographic system consists of an isocratic pump, model 515 HPLC Pump (Waters, Milford, MA, USA), a differential refractometer detector model 2410 (Waters), and an oven for columns maintained at 40 °C by a temperature control module (Waters). Two HPSEC columns Styragel HR 0.5 and HR 1 (Waters) were connected in series. These columns are packed with styrenedivinylbenzene co-polymer. The mobile phase used was high-performance liquid chromatography-grade tetrahydrofuran from Tedia Inc. (Fairfield, OH, USA), and the flow rate was 1 ml/min. The typical pressure at this flow rate was 450 PSI (3,102 kPa). All the standards were obtained from Supelco, Inc. (Bellefonte, PA, USA). The products of reaction, DG, MG, and FFA, as well as TG and GL are separated because of the differences of molar weight.

Results

Screening of Lipases for the Enzymatic Glycerolysis of Soybean Oil

To select the most suitable lipase for the production of DG and MG through enzymatic glycerolysis reactions, different lipases were examined under the same experimental conditions. The reaction products are presented as mass fraction (%) of TG, DG, MG, and FFA. The mass percentage of TG, DG, MG, and FFA after 24 h of reaction for each lipase is presented in Fig. 1. In all cases, lipases led to the high production of DG. As can be seen, RM-IM lipase does not present a satisfactory performance to produce DG and MG, as it presented lower lipase activity (Table 1). Furthermore, according to Bornscheuer and Kazlauskas [17] and Mukherjee [18], this lipase present more selectivity for short chain fatty acids (10–6 carbons), which are not significantly present in soybean oil. The fatty acids compositions of the starting material was 22.8% of C18:1, 43.4% of C18:2, and 16.8% of C18:3. Under the reaction conditions, CR-IM lipase also did not obtain satisfactory results on the production of DG and MG. Figure 1 shows that glycerolysis catalyzed by CA-IM lipase presented the highest yield of DG and MG. According to Ferreira-Dias et al. [11], the aquaphilicity (Aq) of the supports might be used as an indicator of their affinity for water and, this way, evaluate possible differences in hydrophilicity between the supports used in the immobilized lipases. The support used to immobilize CA-IM lipase presents lower hydrophilicity than the support used as immobilization matrix for

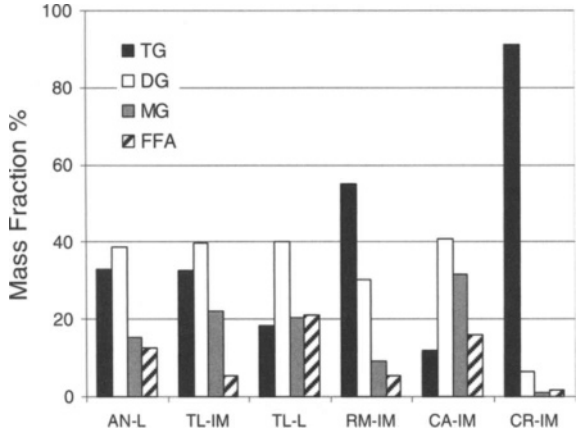


Fig. 1 Glycerolysis of soybean using various lipases. Conditions: T=40°C, substrate molar ratio glycerol/oil=4, 10% enzyme load (wt% of oil mass), 3.5% water content (wt% of glycerol mass), 24 h of reaction

RM-IM lipase [11]. The observed results may be explained by a different affinity of glycerol (hydrophilic compound) for each immobilization matrices. According to Ferreira-Dias et al. [11], the support of the RM-IM presents Aq about six times higher than that of CA-IM, leading to higher glycerol concentrations in the microenvironment; the formation of a glycerol layer around the lipase particles restraining the contact between the lipase and the hydrophobic substrates (TG and DG) may occur [11]. Besides the strong activity, the high performance in the production of MG and DG obtained by CA-IM also can be explained because its support presents low Aq, decreasing the unavailable caused by GL in the interface lipase-oil.

TL-L and AN-L resulted in the production of high amount of FFA (considered byproducts), even with lesser MG production, compared to other lipases as CA-IM and TL-IM. In this case, an extra 3.5% of water content was added to the system, which already contained a concentration similar to water from free lipase (lipase in aqueous solution). Therefore, with the mixture containing an excess of water, a competition between glycerolysis and hydrolysis occurs. In this case, the hydrolysis can predominate in relation to glycerolysis reaction, producing high amount of FFA (principal characteristic of hydrolysis reaction).

Effect of Water Content

Enzymes require a minimum amount of water to maintain their structure and flexibility. Water content is necessary because these enzymes act at the oil–water interface, allowing

Table 1 Initial lipases hydrolytic activity in the tributyrin substrate.

Lipases	Commercial name	Lipase activity (U/mg)
RM-IM	Lipozyme IM	39.1
TL-IM	Lipozyme TL IM	145
TL-L	Lipozyme TL 100L	246
AN-L	Palatase 20000L	230
CA-IM	Novozyme 435	1,056
CR-IM	Sigma—typeVII	800

the formation of an acyl–enzyme complex. As can be seen in Fig. 2(a), the conversion of TG for the reaction that contains 3.5% of water is 48.15% higher than the reaction without extra water in the same conditions [Fig. 2(b)]. The reaction illustrated in Fig. 2(b) occurred because of the minimum of 0.5% water present on glycerol. The production of DG and MG are, respectively, 23% and 58% lower when the enzymatic glycerolysis is carried out in the absence of extra water content.

According to Table 2, free lipases in the absence of extra water content produce around 50–57% lesser FFA because of the decrease in the competition between glycerolysis and hydrolysis reaction. Similarly, the mass fractions of DG and MG for both free lipases increase, 15% and 13% of DG and MG for TL-L and 11% and 8% of DG and MG for AN-L, respectively, prevailing glycerolysis reaction. Reaction employing TL-L in the absence of extra water can be compared with glycerolysis reaction using TL-IM lipase in relation to the compositions of DG and MG. However, the use of free lipases presents disadvantages, such as impossibility of recycle to the system.

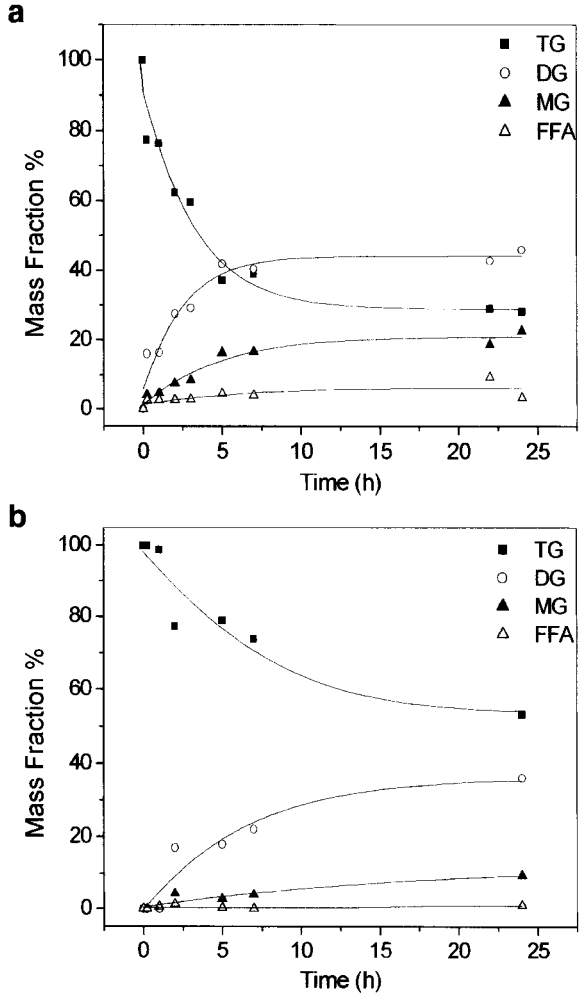


Fig. 2 Time course of the enzymatic glycerolysis reaction using 10% of TL-IM lipase (oil mass) at 40 °C, substrate molar ratio glycerol/oil=8, **a** 3.5% water content (wt% of glycerol mass), **b** absence of extra water content

Table 2 Effect of water content in the glycerol on DG, MG, and FFA productions for TL-L and AN-L lipases.

Absence extra water (a); extra 3.5% water (b) (wt% of glycerol mass). T=50 °C, molar ratio glycerol/oil=8, 10% enzyme load (wt% of oil mass), 24 h of reaction. Standard error=±0.72.

Mass fraction (%)					
Lipases		TG	DG	MG	FFA
TL-L	(a)	19.47	47.00	22.87	10.65
	(b)	18.46	40.20	20.37	20.96
AN-L	(a)	31.14	44.88	16.66	7.31
	(b)	33.13	38.89	15.30	12.66
TL-IM	(b)	29.43	44.59	21.41	4.56

Effect of Enzyme Load

The effect of the amount of lipase was investigated using immobilized lipase from *C. antarctica* B, as it presented higher performance to produce DG and MG. Figure 3(a) and (b) shows the kinetics of the enzymatic glycerolysis of soybean oil in a solvent-free system,

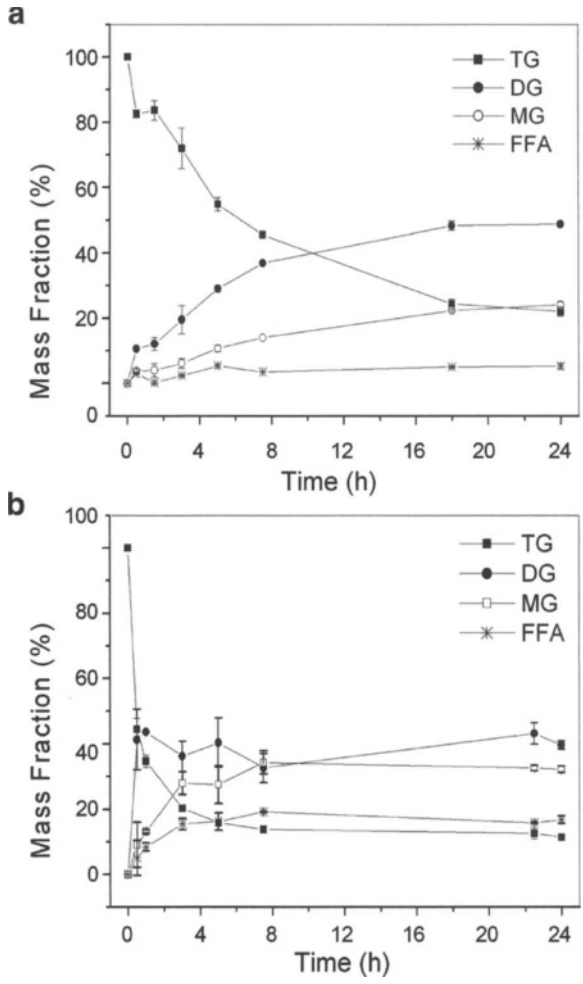


Fig. 3 Time course of the enzymatic glycerolysis reaction using CA-IM (wt% of oil mass) at 50 °C, substrate molar ratio glycerol/oil=8, **a** 2% CA-IM, **b** 10% CA-IM

using 2% [Fig. 3(a)] and 10% [Fig. 3(b)] of CA-IM at 70 °C. As can be seen, in adding 2% of CA-IM, the reaction reaches the equilibrium slower. The compositions of DG and MG are 48.76% and 24.02%, respectively, and the production of byproducts is minimized, around 5.2% of FFA after 24 h. The same behavior of the reaction is verified when 5% of CA-IM is used in the same conditions. The production of DG and MG are similar, 48.28% and 24.64%, respectively, and the mass fraction of FFA is 5.83% after 24 h. In contrast, the reaction equilibrium is reached quickly when 10% of CA-IM is used; however, the production of FFA is higher, around 12.5%, after 24 h. The yield of MG is 27% higher than reactions with 2% and 5% of lipase; however, the excess of lipase and the increase in the production of FFA are strong disadvantages.

Conclusions

The lipase CA-IM was the most efficient in producing DG and MG in a solvent-free system through the catalyzed lipase glycerolysis of soybean oil. The maximum production reached, after 24 h of reaction, for DG and MG was 48% and 32%, respectively. CA-IM presented higher hydrolysis activity and, also, its immobilization matrix presents low hydrophilicity, which provided a good interaction lipase–oil. Water content influences directly on the production of MG, as the lipase acts at the oil–water interface. However, excess of water content leads to the competition between glycerolysis and hydrolysis reaction. The addition of extra water in glycerolysis reactions using free lipases produces high amount of FFA, once the system with excess water is favorable, for the lipases conduct hydrolysis rather than the glycerolysis reaction. The glycerolysis reaction reaches the equilibrium quickly when high amount of lipases (10%) is used; however, lower quantities of CA-IM (2%) catalyzes the reaction slower and producing lower quantity of by-products (FFA). It implies the reduction of lipase load to catalyze the production of DG and MG, decreasing the cost of enzymes in an enzymatic process.

Acknowledgments The authors are grateful for the financial support of CNPq and FAPESP.

References

1. Kristensen, J. B., Xu, X., & Mu, H. (2005). *Journal of the American Oil Chemists' Society, 82*, 329–334.
2. Kaewthong, M., Sirisansaneeyakul, S., Prasertsan, P., & H-Kittikun, A. (2005). *Process Biochemistry, 40*, 1525–1530.
3. Chang, C., & Bodmeier, R. (1998). *International Journal of Pharmaceutics, 173*, 51–60.
4. Fureby, A. M., Tian, L., Adlercreutz, P., & Mattiasson, B. (1997). *Enzyme and Microbial Technology, 20*, 198–206.
5. Taguchi, H., Nagao, T., Watanabe, H., Onizawa, K., Matsuo, N., & Tokimitsu, I. (2001). *Lipids, 36*, 379–382.
6. Maki, C. K., Davidson, M., Tsushima, R., Matsuo, N., Tokimitsu, I., Umporowicz, D. N., et al. (2002). *American Journal of Clinical Nutrition, 76*, 1230 1236.
7. Meng, X., Zou, D., Shi, Z., Duan, Z., & Mao, Z. (2006). *Lipids, 39*, 37–41.
8. Sonntag, N. O. V. (1982). *Journal of the American Oil Chemists' Society, 59*, A795–A802.
9. Fregolente, L. V., Batistella, C. B., Maciel, R., & Wolf-Maciel, M. R. (2005). *Journal of the American Oil Chemists' Society, 82*(9), 673–678.
10. Bornscheuer, U. T. (1995). *Enzyme and Microbial Technology, 17*, 578–586.
11. Ferreira-Dias, S., Correia, A. C., Baptista, F. O., & Fonseca, M. M. R. (2001). *Journal of Molecular Catalysis. B, Enzymatic, 11*, 699–711.
12. Yang, Y., Vali, S. R., & Ju, Y. (2003). *Journal of the Chinese Institute of Chemical Engineers, 34*, 617–623.

13. Noureddini, H., & Harmeier, S. E. (1998). *Journal of the American Oil Chemists' Society, 75*, 1359–1365.
14. Guo, Z., & Xu, X. (2006). *Green Chemistry, 8*, 54–62.
15. Tuter, M., Aksoy, H. A., Ustun, G., Riva, S., Secundo, F., & Ipekler, S. (2003). *Journal of the American Oil Chemists' Society, 80*, 237–241.
16. Schoenfelder, W. (2003). *European Journal of Lipid Science and Technology, 105*, 45–48.
17. Bornscheuer, U. T., Kazlauskas R. J. (1999). *Hydrolases in organic synthesis: Regio- and stereoselective biotransformations*. Weinheim: Wiley-VCH, pp. 164–167.
18. Mukherjee, K. D. (1998). Lipid biotechnology. In C. C. Akoh, & D. B. Min (Eds.)*Food lipids* (pp. 589–639). New York: Marcel Dekker.

Appl Biochem Biotechnol (2008) 146:173–187
DOI 10.1007/s12010-007-8072-4

Immobilization of *Candida antarctica* Lipase B by Adsorption to Green Coconut Fiber

Ana I. S. Brígida · Álvaro D. T. Pinheiro · Andrea L. O. Ferreira · Luciana R. B. Gonçalves

Received: 9 May 2007 / Accepted: 27 September 2007 /
Published online: 27 October 2007
© Humana Press Inc. 2007

Abstract An agroindustrial residue, green coconut fiber, was evaluated as support for immobilization of *Candida antarctica* type B (CALB) lipase by physical adsorption. The influence of several parameters, such as contact time, amount of enzyme offered to immobilization, and pH of lipase solution was analyzed to select a suitable immobilization protocol. Kinetic constants of soluble and immobilized lipases were assayed. Thermal and operational stability of the immobilized enzyme, obtained after 2 h of contact between coconut fiber and enzyme solution, containing 40 U/ml in 25 mM sodium phosphate buffer pH 7, were determined. CALB immobilization by adsorption on coconut fiber promoted an increase in thermal stability at 50 and 60 °C, as half-lives ($t_{1/2}$) of the immobilized enzyme were, respectively, 2- and 92-fold higher than the ones for soluble enzyme. Furthermore, operational stabilities of methyl butyrate hydrolysis and butyl butyrate synthesis were evaluated. After the third cycle of methyl butyrate hydrolysis, it retained less than 50% of the initial activity, while Novozyme 435 retained more than 70% after the tenth cycle. However, in the synthesis of butyl butyrate, CALB immobilized on coconut fiber showed a good operational stability when compared to Novozyme 435, retaining 80% of its initial activity after the sixth cycle of reaction.

Keywords *Candida antarctica* lipase B · Enzyme immobilization · Coconut fiber · Physical adsorption · Methyl butyrate hydrolysis · Butyl butyrate synthesis

A. I. S. Brígida
Escola de Química, Centro de Tecnologia,
Universidade Federal do Rio de Janeiro, Bloco E,
60455-760 Rio de Janeiro, Rio de Janeiro, Brazil

Á. D. T. Pinheiro · A. L. O. Ferreira · L. R. B. Gonçalves (✉)
Departamento de Engenharia Química,
Universidade Federal do Ceará, Campus do Pici, Bloco 709,
60455-760 Fortaleza, Ceará, Brazil
e-mail: lrg@ufc.br

Introduction

Most proteins, amongst them enzymes, are large amphiphatic molecules, and this characteristic makes them intrinsically surface-active molecules, which might lead them to adsorb in some interfaces [1]. Thus, enzyme immobilization by adsorption occurs through a binding between an enzyme and a solid support. Depending on the nature of the surface, enzyme binding may be the result of ionic interactions, physical adsorption, hydrophobic bonding, Van der Waals attractive forces, or a combination of these interactions. This technique, although simple and of low cost, possesses disadvantages, such as low linking energy between enzyme and support, which may cause enzyme desorption in presence of the substrate or when it is subjected to variations on temperature, pH, and ionic force. However, although immobilized enzymes are susceptible to desorption, immobilization by adsorption is one of the most used techniques in the attainment of insoluble biocatalysts [2].

In literature, a great number of publications [3–11] using immobilized lipases by physical adsorption is observed. Initially, porous glass beads, diatomaceous earth, silica, and alumina were the commonest support used for lipase immobilization. However, recently, ionic exchange resins, celite, and biopolymers are preferred [3]. Some factors that influenced in lipase immobilization were discussed, e.g., use of hydrophilic or hydrophobic supports [4, 5], enzyme loading and coupling time [6, 7], and electrostatic interactions [8]. An increase in its stability on organic solvents [7], as well as on thermal and operational stabilities [5, 9, 10], was obtained after immobilization of lipases by adsorption. Furthermore, in some cases, an improvement on specific activity of lipase is achieved by fixing it to the support in its open-form conformation [11].

Candida antarctica lipase B (CALB) is a triacylglycerol hydrolase (E.C. no. 3.1.1.3) and also an effective carboxylesterase that has a molecular weight of 33 kDa and an isoeletric point (p*I*) of 6.0 [12]. Because of its stereospecificity and regioselectivity, CALB has been used as biocatalyst in several applications such as cosmetics, food, and pharmaceutical industries [13–15]. Several supports have been proposed to CALB immobilization, e.g., silica functionalized with octyltriethoxysilane [9], duolite A568 [5], EP 100 [16], silica gel [17], CoFoam [18], activated carbon [19], octyl-agarose, octadecyl-Sepabeads, and hydrophobin-agarose [20]. When CALB was adsorbed on functionalized silica, for instance, interesting results were obtained on the *N*-acylation of ethanolamine with lauric acid. The catalyst remained fully active after 15 cycles of reaction, similar to the result obtained using Novozyme 435 [9], a commercial biocatalyst prepared by lipase immobilization on a macroporous polyacrylic resin.

The high cost of some available commercial support is promoting a search for cheaper substitutes. Low-cost supports can be organic (chitin, chitosan) or inorganic ($CaCO_3$) [21]. From organic group, it has been detached from lignocellulosic agroindustrial waste supports, such as saw dust, straw, wood chips/shavings, rice husk [22], spent grains [23], rice straw [21, 24], cellulignin [25], and coconut fiber [26, 27]. These studies showed that agroindustrial wastes are a suitable raw material source for immobilization matrixes. Previous studies [27] had shown that green coconut fiber is a suitable support for lipase immobilization by covalent attachment, as an increase in thermal and operational stabilities were obtained when compared with the soluble enzyme.

Thus, in order to produce a low-cost immobilized lipase, the objective of this work is to evaluate the immobilization of CALB by adsorption on green coconut fiber. For this purpose, the influence of contact time, lipase concentration, and pH of lipase solution during the adsorption step on the biocatalyst activity and stability was investigated.

Materials and Methods

Materials

Commercial soluble and immobilized lipase B from *C. antarctica* (Lipozyme® CALB L and Novozyme 435, respectively) were kindly donated by Novozymes Latin America (Araucária, Brazil), with 1,780 U/ml and 1,039 U/g of hydrolytic activity for Lipozyme® CALB L and Novozyme 435, respectively. Methyl butyrate was from Sigma-Aldrich Chemical (St. Louis, MO, USA). Butyric acid and butanol were purchased from Merck (Rio de Janeiro, Brazil). Molecular sieve 4A ($Na_2O[Al_2O_3(5.0SiO_2)]12H_2O$) was from W. R. Grace (Massachusetts, MA, USA). The support used for enzyme immobilization was green coconut fiber that was kindly donated by Embrapa Agroindústria Tropical, Ceará State, Brazil. Other chemicals were of analytical grade.

Support

Green coconut fiber was obtained from green coconut husk through a process developed by Embrapa Agroindustria Tropical [28]. It was cut and sieved to obtain particles between 32 and 35 mesh. It was then washed with distilled water and dried at 60 °C before being used as immobilization matrix.

Protein Determination

Protein content was determined according to the Bradford method [29] using bovine serum albumin as a standard. Adsorbed protein was calculated by Eq. 1, where: P_{ads} is the adsorbed protein for gram of fiber (μg/g), P_o (μg/ml) and P_{sob} (μg/ml) are, respectively, protein concentration on the supernatant before and after adsorption, V is volume of lipase solution used during immobilization, and m_{fiber} is the mass of fiber used during immobilization.

$$P_{ads} = \frac{(P_o - P_{sob}) \times V}{m_{fiber}} \tag{1}$$

Preparation of Immobilized Enzyme

Immobilized enzyme was obtained by adsorption, at room temperature, by contacting enzyme solution and support in 5 ml syringes, stirred using the apparatus presented in a previous work [27]. For each gram of dry support, 10 ml of lipase solution in 25 mM sodium phosphate buffer was used. After immobilization, the biocatalyst was separated by filtration, rinsed with phosphate buffer (10 ml), and dried at vacuum for 10 min. In this study, recovered activity was defined as the ratio of enzymatic activity of the immobilized enzyme and the total units of soluble lipase that disappeared from the supernatant during immobilization [19]. Immobilization yield was defined as the difference between enzyme activity in the supernatant before and after immobilization divided by the enzyme activity in the supernatant before immobilization [29].

Assay of Hydrolytic Activity: Methyl Butyrate Hydrolysis

Hydrolytic activity of immobilized or soluble enzyme was determined by methyl butyrate hydrolysis [30]. Experiments were performed using an automatic titrator (pHstat) and

50 mM NaOH as titrating agent. The pH was set at 7.0. The reaction was initiated with the addition of 0.1 ml of soluble enzyme solution, 0.4 g of CALB immobilized on fiber, or 0.03 g of Novozyme 435 to a 30-ml methyl butyrate solution dissolved in 25 mM phosphate buffer pH 7.0. In this work, 1 U of enzymatic activity was defined as the amount of enzyme that hydrolyzes 1 μmol of methyl butyrate per minute at pH 7.0 and 28 °C.

Esterification Yield: Butyl Butyrate Synthesis

Stock solutions of butyric acid (150 mM) and butanol (150 mM) were prepared in *n*-heptane. Experiments were set up in 250-ml flasks containing 20 ml of stock solution, 1 g of molecular sieve 4A, and 0.3 g of the immobilized CALB or 0.012 g of Novozyme 435. The flasks were kept at 30 °C under agitation at 150 rpm for 24 h [31]. The consumption of butyric acid was measured by titration with 0.02 M NaOH and using phenolphthalein as indicator. The total acid content before reaction was determined by titration of a blank sample, without enzyme. The esterification yield was calculated from the decrease in butyric acid concentration after 24 h of reaction.

Operational Stability: Methyl Butyrate Hydrolysis

Immobilized enzyme stability was assayed by using 0.4 g of the immobilized CALB on fiber or 0.01 g of Novozyme 435 in successive batches of methyl butyrate hydrolysis. The operational conditions were the same as described for the assay of hydrolytic activity. At the end of each batch, the immobilized lipase was removed from the reaction medium, washed with phosphate buffer to remove any remaining substrate or product, dried under vacuum (10 min), and assayed again. The residual activity of the biocatalyst was calculated in terms of percentage of activity (U) of the immobilized enzyme measured after each cycle compared with the activity of the immobilized enzyme before the first cycle.

Operational Stability: Synthesis of Butyl Butyrate

Immobilized enzyme stability was assayed by using 0.3 g of the immobilized CALB on fiber or 0.012 g of Novozyme 435 in successive batches of butyl butyrate synthesis. Assay conditions were the same as described for the determination of esterification yield. At the end of each batch, the immobilized lipase was removed from the reaction medium and rinsed with hexane (20 ml) to extract any substrate or product eventually retained in the matrix. After 1 h at room temperature, the immobilized derivative was introduced into a fresh medium. The residual conversion is given as percentage of initial conversion of butyric acid (first cycle of synthesis) under standard conditions (described in "Esterification Yield: Butyl Butyrate Synthesis").

Thermal Stability

Thermal stability of soluble or immobilized enzyme was determined by incubating the biocatalyst in 100 mM sodium phosphate buffer pH 7.0 at 50 or 60 °C. Periodically, samples were withdrawn, and their residual activities were assayed by the hydrolysis of methyl butyrate. Residual activity is given as percentage of initial activity (hydrolytic activity before incubation). Thermal deactivation curves have been described following the

deactivation model proposed by Henley and Sadana (1985) referenced by Arroyo et al. [10]; see Eq. 2.

$$A = \left(100 + \frac{\alpha_1 k_1}{k_2 - k_1} - \frac{\alpha_2 k_2}{k_2 - k_1}\right) e^{-k_1 t} + \left(\frac{\alpha_2 k_1}{k_2 - k_1} - \frac{\alpha_1 k_1}{k_2 - k_1}\right) e^{-k_2 t} + \alpha_2 \quad (2)$$

where A is the residual activity in time t, k_1 and k_2 are first-order deactivation rate coefficients, and α_1 and α_2 ratios of specific activities (E_1/E and E_2/E, respectively) to the different states, see Eq. 3.

$$E \xrightarrow{k_1} E_1 \xrightarrow{k_2} E_2 \quad (3)$$

First-order deactivation rate coefficients (k_1 and k_2) and ratios of specific activities to the different states (α_1 and α_2) were estimated from experimental data. Biocatalyst half-life ($t_{1/2}$) was estimated by Eq. 2, using the estimated parameters (k_1, k_2, α_1, and α_2) and making A equal to 50%. In this work, stabilization factor (F) was considered as the ratio of immobilized enzymes' half-lives to soluble enzyme half-life [27].

Results and Discussion

Immobilization of *C. antarctica* Lipase B on Coconut Fiber by Adsorption

Influence of Contact Time and Enzyme Concentration on the Immobilized Enzyme Properties

Adsorption kinetic was investigated, and the influence of contact time between coconut fiber and lipase, at different enzyme concentrations from 0 U/ml (control without enzyme) to 90 U/ml, were evaluated. No hydrolytic activity was detected when the fiber without immobilized enzyme (control) was used as catalyst. Figure 1 pictures the influence of different initial concentrations of lipase in the supernatant (E_0 equal to 30, 60, or 90 U/ml) on the hydrolytic activity of immobilized CALB. The experimental data were subjected to statistical analysis (analysis of variance). At the probability level of $p<0.05$ (data not shown), it was observed that immobilized amount increases as time increased until 2 h (in

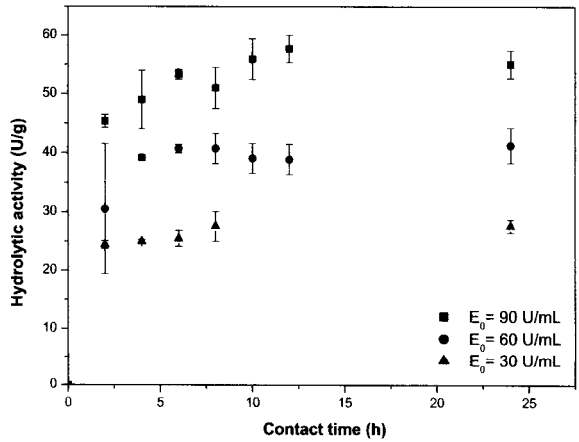


Fig. 1 Effect of contact time on the hydrolytic activity of lipase immobilized on coconut fiber by adsorption using initial enzyme concentrations of 30 U/ml (*closed triangle*), 60 U/ml (*closed circle*), or 90 U/ml (*closed square*)

case of E_0=30 U/ml and E_0=60 U/ml) or 6 h (E_0=90 U/ml), which is probably the point of dynamic balance between adsorption and desorption [32]. Furthermore, after 2 h of contact between enzyme and support, no expressive changes in hydrolytic activity of immobilized CALB was observed, as, after this time, loading amounts were almost 70–80% of the maximum loading achieved for the three initial concentrations studied. These results indicate that immobilization was achieved in a short time.

In subsequent experiments, to evaluate the influence of enzyme loading on the properties of the immobilized enzyme, contact time was set in 2 h, and enzyme concentration in the supernatant, during incubation, was changed from 30 to 500 U/ml (Fig. 2). It can be seen that hydrolytic activity of the immobilized enzyme enhances with increasing lipase concentration in the supernatant. However, the higher value of hydrolytic activity achieved by adsorption of CALB on coconut fiber (135.14 U/g) was still lower than the hydrolytic activity of Novozyme 435 (1,039 U/g, determined according to the methodology described in "Assay of Hydrolytic Activity: Methyl Butyrate Hydrolysis"), a commercial derivative.

Recovered activity and immobilization yield were calculated, and results are listed in Table 1. It can be observed that recovered activity increased when the initial enzyme concentration in the supernatant (E_0) was increased to 60 and 90 U/ml, but it remained almost constant for the other concentrations studied. Immobilization yield, on the other hand, decreased when high concentrations of enzyme were used (60 to 150 U/ml, compared to 30–40 U/ml). When E_0=90 U/ml, the highest value of recovered activity was obtained, which suggests that protein molecules are probably immobilized at close proximity to each other, which may prevent deactivation caused by enzyme unfolding by covering the support surface. In other words, when enzyme load was increased, more enzyme molecules were immobilized and less area of the support is available for lipase to spread itself, which may prevent loss in activity [31].

Nevertheless, when higher concentrations of lipase in the supernatant were used, E_0= 150 U/ml, recovered activity decreased, and immobilization yield was enhanced (Table 1). According to the literature [4, 6, 9, 10], protein adsorption is not restricted to a monolayer on the support, and adsorption of secondary layers has been reported. Therefore, when E_0= 150 U/ml, probably a second layer of lipase was adsorbed on the first layer, leading to an improvement on immobilization yield, as more enzyme molecules were adsorbed. However, although more molecules were immobilized on coconut fiber, not all of them

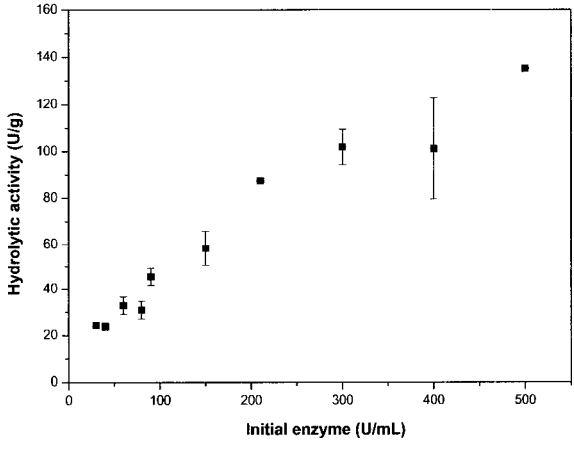


Fig. 2 Hydrolytic activity of immobilized enzyme as a function of initial enzyme activity in the supernatant. Lipase was immobilized on coconut fiber by adsorption after 2 h of contact time at room temperature

Table 1 Influence of enzyme concentration on recovered activity and immobilization yield.

Concentration of enzyme (U/ml)	Recovered activity (%)	Immobilization yield (%)
30	32.9	33.4
40	32.9	33.4
60	42.1	9.0
80	33.3	14.0
90	86.9	5.2
150	39.6	9.5
210	0	0
300	0	0
400	0	0
500	0	0

CALB immobilized by adsorption on coconut fiber at pH 7 and room temperature

were available to the substrate, causing a decrease in recovered activity. Coconut fiber surface does not have a porous structure, and it has a low surface area [27]. This poor surface area limits the number of enzyme molecules to be immobilized, facilitating the multilayer adsorption of proteins.

In order to evaluate the formation of enzyme multilayers [10], thermal stability studies of lipase immobilized in coconut fiber, obtained by using E_0=40 U/ml or E_0=280 U/ml, were performed at 60 °C. The thermal deactivation model (Eq. 2) was fitted to experimental data (Fig. 5), and the model parameters are listed in Table 2.

At 60 °C, the deactivation of soluble CALB and the immobilized CALB, obtained at pH 7.0 and E_0=280 U/ml, followed a first-order pattern. The other biocatalyst tested followed a double exponential decay. In all cases, $k_1 > k_2$, $\alpha_1 < 100\%$, and $\alpha_2 = 0$ (Table 2 and Eq. 2). According to the literature [10], the small values of parameter k_2 mean that there is a good stabilization of the enzymatic state E_1.

By comparing the remaining activity of the intermediate state E_1, expressed by α_1, for the two biocatalysts obtained at pH 7.0 and different initial enzyme activities in the supernatant, it is possible to evaluate the formation of lipase multilayers during adsorption. The intermediate of CALB-7A, CALB immobilized at pH 7 using E_0= 40 U/ml, has higher activity (α_1=59.2%) than the intermediate of CALB-7B (α_1=14.3%), CALB immobilized at pH 7 using E_0=280 U/ml, probably because of the formation of multilayers on CALB-7B. Due to this enzyme aggregation, lipase is weakly linked, and it is quickly deactivated [10]. As it can be seen, CALB-7A is 4.6-fold more stable than CALB-7B.

Effect of pH on the Adsorption of C. antarctica Lipase B on Coconut Fiber

According to the literature, hydrophobic interactions should not be affected by changes in the pH of adsorption. On the other hand, if electrostatic forces are important, changes over the isoelectric point of lipase will have a large impact on the binding constants [6]. Therefore, in this work, the effect of pH in the adsorption of *C. antarctica* lipase B on coconut fiber was investigated. The results of lipase adsorption, after 2 h of contact between coconut fiber and enzyme solution (E_0=40 U/ml), are presented in Fig. 3. Similar profiles for hydrolytic activity of immobilized lipase and adsorbed protein on fiber can be observed, with two plateau regions. This behavior is typical of ionic supports [6], and adsorption is governed by electrostatic forces. The same enzyme (CALB), when immobilized on a

Table 2 Kinetics parameters of thermal deactivation, at 50 and 60 °C, of soluble CALB, CALB immobilized by adsorption on coconut fiber and Novozyme 435.

Enzyme	k_1 (h^{-1})	k_2 (h^{-1})	α_1	α_2	$t_{1/2}$ (h)	F
Soluble CALB (T=50 °C)	0.0791	–	4.53	–	7.813	1
CALB-7A (T=50 °C)	0.0309	–	4.412	–	16.180	2
Soluble CALB (T=60 °C)	7.153	0.0000	99.908	0	0.0968	1
CALB-7A (T=60 °C)	1.642	0.0204	59.236	0	8.92	92
CALB-7B (T=60 °C)	0.451	0.0000	14.25	0	1.94	20
CALB-4A (T=60 °C)	0.503	0.0215	36.436	0	2.92	30
CALB-5A (T=60 °C)	0.521	0.0096	29.885	0	2.37	24
Novozyme 435 (T=60 °C)	0.955	0.0043	81.280	0	114.04	1178

CALB-7A CALB immobilized by adsorption on coconut fiber at pH 7, using E_0=40 U/ml; *CALB-7B* CALB immobilized by adsorption on coconut fiber at pH 7, by using E_0=280 U/ml; *CALB-4A* CALB immobilized by adsorption on coconut fiber at pH 4, by using E_0=40 U/ml; *CALB-5A* CALB immobilized by adsorption on coconut fiber at pH 5, by using E_0=40 U/ml.

hydrophobic support (activated carbon), did not show important differences on the amount of bound protein for the different values of pH studied [19].

Considering that green coconut fiber is a lignocellulosic material, interactions between charged groups and/or dipoles of lipase and cellulose were expected. Furthermore, when electrostatic interactions are the driven force of adsorption, the amount of adsorbed protein is pH-dependent, i.e., dependent on the charge of the protein and, possibly, the sorbent [8]. For better understanding immobilization of CALB on coconut fiber, it is important to imagine the distribution of charges of CALB, based on its isoelectric point of 6 [12], and coconut fiber, supposing an isoelectric point of 2 [33]. Based on these suppositions, a maximum plateau value would be expected for pH values smaller than 6, as enzyme is positively charged and fiber, negatively charged. This behavior was experimentally confirmed; higher values of hydrolytic activities were obtained when enzyme was immobilized between pH 3 and 6. Moreover, as hydrolytic activity and adsorbed protein profiles are similar, only lipase molecules must be adsorbed. It is known [19] that the crude extract used has contaminant proteins, but the obtained results show that they are not adsorbed on coconut fiber and that lipase is preferentially adsorbed from the crude extract.

The two plateaus on Fig. 3, constant specific activity values, indicate that there is a stability of the enzyme structure on the range of pH studied. For some enzymes, there may be partial destruction of cystine residues (in alkaline solutions) or hydrolysis of the labile peptide bonds (in acid solutions), as observed by Akova and Ustun [34] during adsorption of *Nigella sativa* lipase on Celite. Other authors [8] have also found similar values of specific activity for the different pH values studied for the adsorption of lipase from *Candida rugosa*.

Immobilization parameters (recovered activity and immobilization yield) were calculated for the biocatalyst with higher hydrolytic activities (adsorptions performed between pH 3 and 6), and results are presented in Fig. 4. It can be observed that best results for recovered activity and immobilization yield were obtained at pH 4 and at 5 or 6, respectively.

Although the amount of *C. antarctica* lipase type B adsorbed to coconut fiber was nearly independent on the pH of adsorption (between pH 3 and 6), immobilization yield and recovered activity were dependent on the pH of adsorption because interactions between the molecule and its environment influence the structure of a protein molecule, and these interactions are pH-dependent [8].

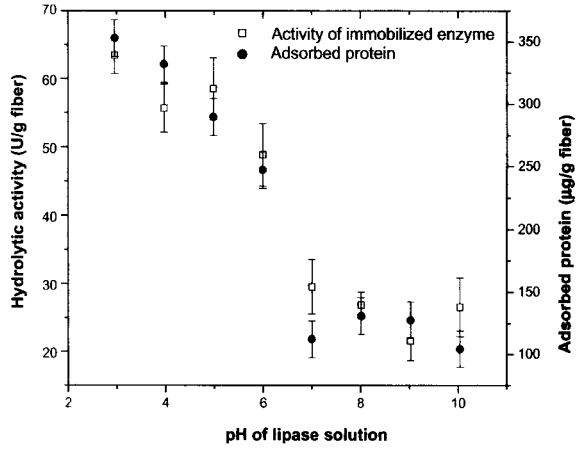


Fig. 3 Effect of the pH of immobilization on the amount of adsorbed protein (*closed circle*) and on the hydrolytic activity (*open square*). Lipase was immobilized on coconut fiber by adsorption after 2 h of contact time at room temperature

Based on the obtained results, immobilized enzyme prepared at pH 4 (CALB-4) and 5 (CALB-5) were selected for thermal stability studies at 60 °C. Table 2 shows the kinetic parameters of thermal deactivation at 60 °C estimated by fitting deactivation model, Eq. 2, to experimental data. It can be observed that the deactivation profiles of CALB-4 and CALB-5 were similar, as k_1 and k_2 are almost the same. However, by comparing the half-lives of CALB-4 and CALB-5 to CALB-7A, it can be observed that the biocatalyst prepared at pH 7 is 3- and 3.8-fold more stable than the ones prepared at pH 4 and 5, respectively. Considering that CALB has an optimum pH between 7 and 8 [35], when the enzyme is adsorbed on coconut fiber at pH 7, a favorable molecule conformation is preserved, being, therefore, more thermal stable than CALB-4 and CALB-5. Therefore, lipase immobilized at pH 7 was selected for further kinetic, operational, and thermal stability studies.

Properties of CALB Immobilized on Coconut Fiber by Adsorption

Based on the results obtained so far, CALB-7A, CALB immobilized on coconut fiber after 2 h of contact between the support and an enzyme solution containing E_0=40 U/ml, in

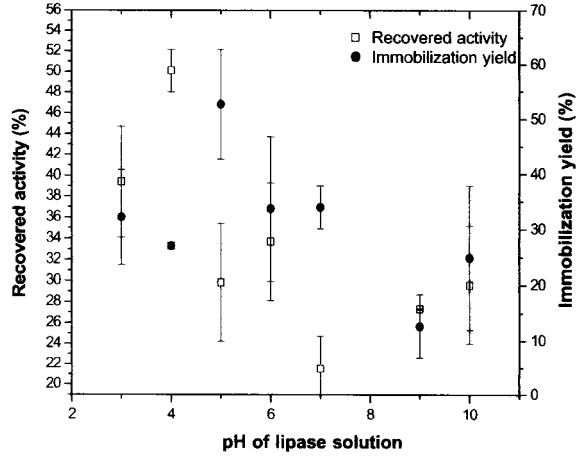


Fig. 4 Effect of pH enzyme solution on the recovered activity (*open square*) and immobilization yield (*closed circle*) of lipase immobilization on coconut fiber by adsorption after 2 h of contact time at room temperature

25 mM sodium phosphate buffer pH 7, was selected for comparative studies with a commercial immobilized CALB, Novozyme 435, and soluble CALB. A low enzymatic loading was selected to ensure lipases were immobilized in monolayers.

Thermal Stability

Thermal stabilities of CALB immobilized on coconut fiber were investigated at 50 and 60 °C, and results were compared to the stability of soluble CALB and Novozyme 435 (Fig. 5 and Table 2). It can be observed, by analyzing stabilization factors (F) on Table 2, that immobilization of CALB on coconut fiber promoted an improvement on thermal stabilities, as CALB-7A is 2- and 92-fold more stable than soluble CALB at 50 and 60 °C, respectively. Other authors [19] obtained similar results when immobilizing the same enzyme on activated carbon by adsorption; immobilized CALB was 2-fold more stable than soluble enzyme with $t_{1/2}$=8 h to thermal stability studies at 50 °C.

The thermal stability at 60 °C of CALB-7A was significantly higher than that of the soluble enzyme, with a stabilization factor of 92.15 (Table 2). In a previous study [27], when CALB was immobilized on coconut fiber by covalent attachment at pH 7 and 10, the immobilized enzyme was, respectively, 67- or 364-fold more stable than the soluble enzyme. Making a comparison between the thermal stabilization achieved by adsorption and covalent immobilization, it can be observed that the forces involved in immobilization of CALB on coconut fiber by adsorption are stronger than the bind between enzyme and support, formed during immobilization by covalent attachment at pH 7. Nevertheless, it is not stronger than the interaction that occurred at pH 10. Other authors [9], when immobilizing CALB by adsorption in octyl silica, obtained a biocatalyst with half-life of around 2 h, which is less stable than CALB-7A prepared in this work ($t_{1/2}$= 8.92 h).

The thermal stability at 60 °C of Novozyme 435, however, is higher than that of CALB-7A (Fig. 5). After 10 h of incubation at 60 °C, Novozyme 435 retained more than 70% of its initial activity, whereas CALB-7A retained only 50%. The higher stability of Novozyme 435 may be due to the hydrophobic nature of the support used for immobilization. When hydrophobic supports are used, the hydrophobic areas surrounding the enzyme active center are involved in adsorption, which stabilizes the active form of lipase [11].

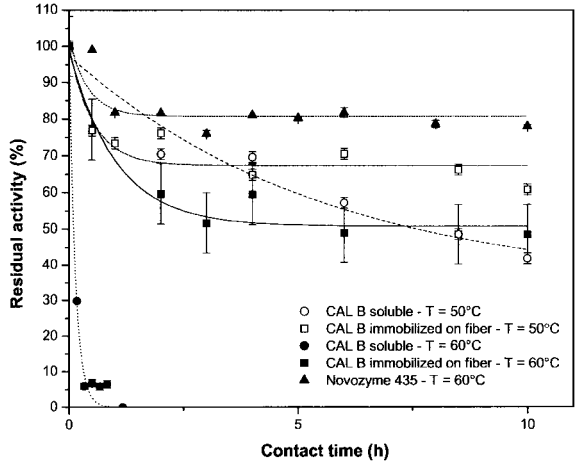


Fig. 5 Thermal stability of derivatives of lipase B from *Candida antarctica* obtained by adsorption, incubated in 0.1 M sodium phosphate buffer, pH 7, at 50 or 60 °C

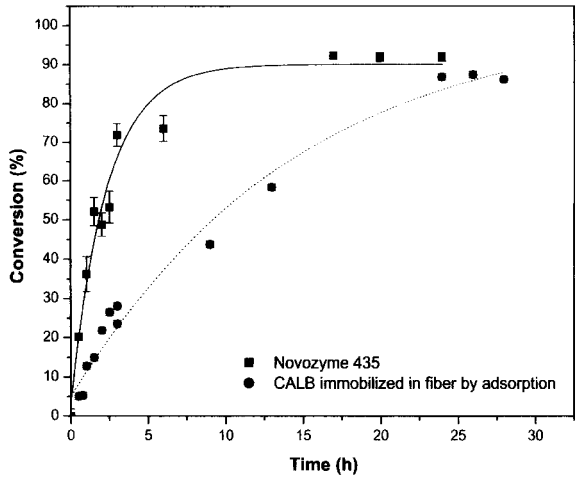


Fig. 6 Conversion of butyric acid in butyl butyrate synthesis catalyzed by immobilized lipase B of *Candida antarctica* on coconut green fiber (*closed circle*) and Novozyme 435 (*closed square*)

Time Course of Butyl Butyrate Synthesis Catalyzed by Immobilized CALB

Figure 6 shows the time course of butyl butyrate synthesis catalyzed by CALB-7A and Novozyme 435. It can be observed that at the beginning, the reaction catalyzed by Novozyme 435 achieved higher conversions quickly. It is known that the enzyme load in Novozyme 435 is higher than in CALB-7A, which explains the fast reaction rate of this well-characterized commercial biocatalyst. However, when equilibrium was reached, conversion values were very similar for both, 87.7% when using CALB-7A and 92.1% when using Novozyme 435. Rodrigues et al. [19] achieved equilibrium conversion values of 92.1 and 84.8% for Novozyme 435 and CALB immobilized on activated carbon, respectively, for the same reaction. Brigida et al. [27] achieved equilibrium conversion of 91.7% using CALB immobilized on coconut fiber by covalent attachment.

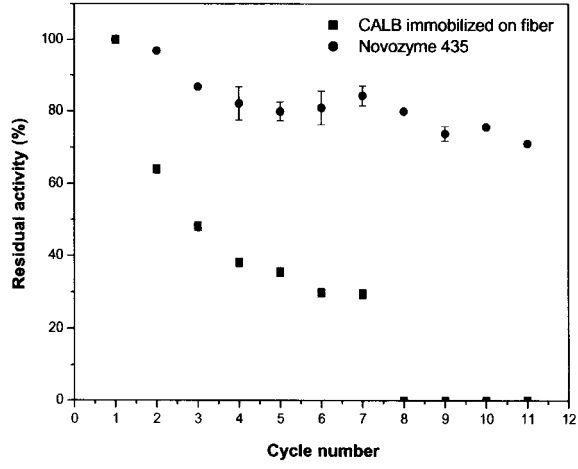


Fig. 7 Operational stability of (*closed square*) lipase type B of *Candida antarctica* adsorbed on green coconut fiber and (*closed circle*) Novozyme 435 in subsequent batches of methyl butyrate hydrolysis

Operational Stability

Reusability of immobilized CALB was tested in subsequent cycles of methyl butyrate hydrolysis. It can be observed in Fig. 7 that CALB-7A retained less than 50% of its initial hydrolytic activity after the third cycle of reaction whereas Novozyme 435 retained almost 70% after the tenth cycle (Fig. 7). Other authors [36] observed that CALB immobilized on activated carbon retained more than 55% of its initial activity after the sixth cycle of methyl butyrate hydrolysis. The worse operational stability of CALB immobilized on coconut fiber, when compared to CALB immobilized on activated carbon and to Novozyme 435, may be due to enzyme desorption during reaction, induced by the hydrophobic substrate, and by the low enzyme load adsorbed. As discussed before, the driven forces of CALB adsorption on coconut fiber are electrostatic interactions that are weaker than hydrophobic interactions, which predominate on Novozyme 435 and CALB adsorbed on activated carbon. Furthermore, both activated carbon and the resin used in the preparation of Novozyme 435 are porous support with high superficial area available for enzyme immobilization, allowing obtaining of high enzyme load. Coconut fiber, on the other hand, does not have a porous structure, and it has a low surface area [27], making it difficult to achieve high enzyme loads.

The effect of repeated use on immobilized lipase activity was also investigated in the synthesis of butyl butyrate, and results are pictured in Fig. 8. CALB-7A showed a good operational stability, retaining 80% of its initial activity after the sixth cycle of reaction, when compared to Novozyme 435, which remained fully active. Other authors [19, 37], when they studied the immobilization of *C. antarctica* type B and *C. rugosa* lipase by adsorption, obtained poor results of operational stability of synthesis. When *C. antarctica* type B lipase was immobilized on activated carbon, the immobilized enzyme retained, after six cycles, only 10% of its initial stability [19]. Both niobium oxide (crystalline and amorphous) supports, used for the immobilization of *C. rugosa*, showed poor operational stability resulting in high activity lost (over 75%) after five recycles [37]. Brigida et al. [27] found that CALB immobilized on coconut fiber by covalent attachment at pH 7 and 10 retained, respectively, only 65 and 30% of residual conversion after six cycles of reaction. Therefore, CALB-7A is a suitable biocatalyst to be used in organic synthesis rather than in hydrolysis reactions.

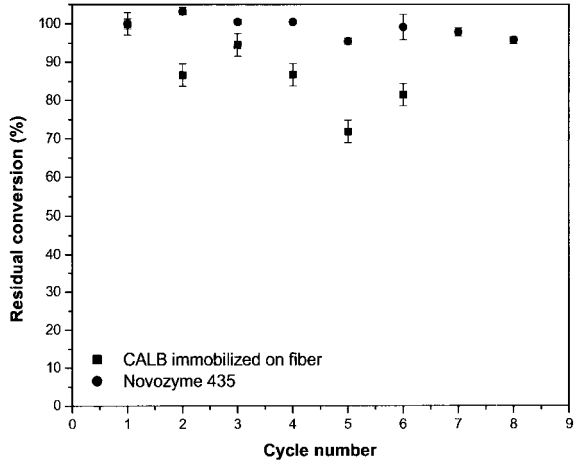


Fig. 8 Operational stability of (*closed square*) lipase type B of *Candida antarctica* adsorbed on green coconut fiber and (*closed circle*) Novozyme 435 in subsequent batches of butyl butyrate synthesis

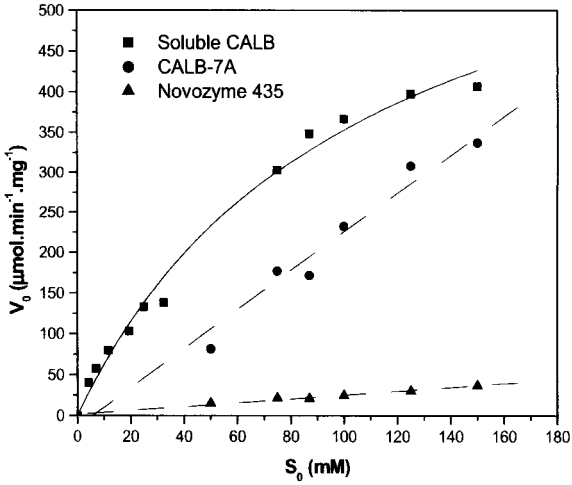


Fig. 9 Initial rate of hydrolysis of methyl butyrate by soluble lipase (*closed square*), lipase immobilized on green coconut fiber (*closed circle*) and Novozyme 435 (*closed triangle*) in fully aqueous medium. The *solid line* represents the fit of Michaelis–Menten model to experimental data. The *dashed lines* represent a linear regression of the experimental data. The amount of adsorbed protein (50 mg/g of catalyser) in Novozyme 435 was determined by Secundo et al. [42]

Hydrolysis of Methyl Butyrate: Kinetic Parameters

Initial reaction rates were determined at different initial methyl butyrate concentrations ranging from 4 to 150 mM. Higher concentrations could not be used because the substrate is not fully soluble in the aqueous medium upon this limit [38].

Figure 9 shows the initial hydrolysis rate of increasing concentrations of methyl butyrate, and Table 3 shows the estimated parameters. It can be seen that hydrolysis rate increases with substrate concentration for the three biocatalysts investigated. However, soluble enzyme follows a Michaelis–Menten-type kinetics with a value of K_M and V_{max} of around 80.65±39.7 mM and 625.01±168.5 μmol min^{-1} mg^{-1}, respectively, while immobilized enzymes, both CALB-7A and Novozyme 435, follow first-order kinetics. There are some reasons to explain the different behavior of the immobilized enzyme compared to the soluble enzyme. The immobilized enzyme residues are in an environment that is different from that of the soluble enzyme in the bulk solution, which may lead to apparent enzyme kinetics. Furthermore, immobilized enzyme might be influenced by mass transfer effects, i.e., substrate and products diffusion through a stagnant film that may surround the support (external diffusion) and through the pores of the support (internal diffusion) [39].

Enzyme activity can be reduced by mass-transfer effects as immobilization means the deliberate restriction of enzyme mobility, which can also affect the mobility of solutes [40].

Table 3 Kinetic parameters of free, immobilized lipase B from *Candida antarctica* obtained by adsorption and Novozyme 435.

Enzyme	Hydrolytic activity	K_m (mM)	V_{max} (μmol.min^{-1}.mg^{-1})
CALB soluble	40 U/mL	33.57	444.44
Immobilized CALB by adsorption at pH 7	27 U/g	49.37	341.30
Novozyme 435*	1,047 U/g	178.11	70.68

* The amount of adsorbed protein (50 mg/g of catalyser) in Novozyme 435 was determined by Secundo et al. [42].

These phenomena can lead to reduced reaction rate and to decrease efficiency compared to soluble enzyme, which can be observed in Fig. 9.

Although Novozyme 435 possesses high activity per gram of support, it has a low specific activity (20.94 U/mg protein) when compared to CALB-7A (245.45 U/mg protein). Higher values of specific activity at low degree of adsorption in cellulose have been reported [8] when compared to hydrophobic materials. Moreover, diffusional limitations are less significant in coconut fiber, as immobilization occurs on the surface due to the absence of porous. The support used to prepare the biocatalyst Novozyme 435, a macroporous resin, may be affect by both internal and external diffusional resistances. The influence of different particle sizes and different specific surface areas on the rate of enzymatic reaction has been investigated [41], and higher values of specific activity were also obtained for low specific surface area.

Conclusions

In the present work, green coconut fiber was successfully used to immobilize lipase B from *C. antarctica* by adsorption. During adsorption studies, it was observed that adsorption equilibrium was achieved after a contact time of 2 h (in case of E_0=30 U/ml and E_0=60 U/ml) or 6 h (E_0=90 U/ml). Moreover, an improvement of hydrolytic activity of immobilized CALB is also observed with increasing concentrations of lipase offered to immobilization. This increase in activity is due to formation of multilayers, confirmed by thermal stability essays. Two plateaus of enzyme activity were observed when the pH of lipase solution during adsorption was varied in the range studied. This behavior is typical of an ionic support. At 50 and 60 °C, the adsorbed enzyme was, respectively, 2- and 92-fold more stable than the soluble enzyme. At 60 °C, however, Novozyme 435's stability was higher than that of CALB-7A. After 10 h of incubation at 60 °C, Novozyme 435 retained more than 70% of its initial activity, whereas CALB-7A retained only 50%. Last but not least, operational stabilities studies of butyl butyrate synthesis, compared to a commercial derivative, showed that CALB-7A is a suitable biocatalyst to be used in the synthesis of flavors.

Acknowledgments The authors would like to thank the Brazilian research-funding agencies FUNCAP (State of Ceará), FINEP, and CNPq (Federal).

References

1. Hlady, V., & Buijs, J. (1996). *Current Opinion in Structural Biology, 7*, 72–77.
2. Kennedy, J. F., White, C. A., & Melo, E. H. M. (1988). *Chimica Oggi, 5*, 21–29.
3. Villeneuve, P., Muderhwa, J. M., Graille, J., & Haas, M. J. (2000). *Journal of Molecular Catalysis B, Enzymatic, 9*, 113–148.
4. Al-Duri, B., & Yong, Y. P. (2000). *Biochemical Engineering Journal, 4*, 207–215.
5. Koops, B. C., Papadimou, E., Verheij, H. M., Slotboom, A. J., & Egmond, M. R. (1999). *Applied Microbiology and Biotechnology, 52*, 791–796.
6. Gitlesen, T., Bauer, M., & Adlercreutz, P. (1997). *Biochimica Et Biophysica Acta, 1345*, 188–196.
7. Panzavolta, F., Soro, S., D'Amato, R., Palocci, C., Cernia, E., & Russo, M. V. (2005). *Journal of Molecular Catalysis B, Enzymatic, 32*, 67–76.
8. Geluk, M. A., Norde, W., Van Kalsbeek, H. K. A., & Van't Riet, K. (1992). *Enzyme and Microbial Technology, 14*, 748–754.
9. Blanco, R. M., Terreros, P., Pérez, M. F., Otero, C., & González, G. (2004). *Journal of Molecular Catalysis B, Enzymatic, 30*, 83–93.

10. Arroyo, M., Sánchez-Montero, J. M., & Sinisterra, J. V. (1999). *Enzyme Microbial Technology, 24*, 3–12.
11. Mateo, C., Palomo, J. M., Fernandez-Lorente, G., Guisan, J. M., & Fernandez-Lafuente, R. (2007). *Enzyme Microbial Technology, 40*, 1451–1463.
12. Uppenberg, J., Hansen, M. T., Patkar, S., & Jones, A. (1994). *Structure, 2*, 293–308.
13. Pirozzi, D., & Grego Jr., G. (2004). *Enzyme Microbial Technology, 34*, 94–100.
14. Yadav, G. D., & Lathi, P. S. (2003). *Biochemical Engineering Journal, 16*, 245–252.
15. Foresti, M. L., & Ferreira, M. L. (2005). *Catalysis Today, 107–108*, 23–30.
16. Cao, L., Bornscheuer, U. T., & Schmid, R. D. (1999). *Journal of Molecular Catalysis B, Enzymatic, 6*, 279–285.
17. Lozano, P., Diego, T., Sauer, T., Vaultier, M., Gmouh, S., & Iborra, J. L. (2007). *Journal of Supercritical Fluids, 40*, 93–100.
18. Vasudevan, P. T., López-Cortés, N., Caswell, H., Reyes-Duarte, D., Plou, F. J., & Ballesteros, A., et al. (2004). *Biotechnology Letters, 26*, 473–477.
19. Rodrigues, D. S., Cavalcante, G. P., Ferreira, A. L. O., & Gonçalves, L. R. B. (2007). *Chemical and Biochemical Engineering Quarterly* (in press).
20. Palomo, J. M., Muñoz, G., Fernández-Lorente, G., Mateo, C., Fernández-Lafuente, R., & Guisán, J. M. (2002). *Journal of Molecular Catalysis B, Enzymatic, 19-20*, 279–286.
21. Pereira, E. B., Zanin, G. M., & Castro, H. F. (2003). *Brazilian Journal of Chemical Engineering, 20*, 343–355.
22. D'Souza, S. F., & Godbole, S. S. (2002). *Journal of Biochemical and Biophysical Methods, 52*, 59–62.
23. Rocha, C., Ducso, L., Gonçalves, M. P., & Teixeira, J. A. (2005). Spent-grains and zeolites as potencial carriers for trypsin immobilization, 4 Mercosur Congress on Process Systems Engineering Proceedings (CD-ROM), Costa Verde, Brasil.
24. Freitas, L., Mendes, A. A., & Castro, H. F. (2003). *Anais da Associacao Brásileira de Química, 52*, 124–128.
25. Castro, H. F., Lima, R., & Roberto, I. C. (2001). *Biotechnology Progress, 17*, 1061–1064.
26. Dey, G., Nagpal, V., & Banerjee, R. (2002). *Applied Biochemistry and Biotechnology, 102-103*, 303–313.
27. Brigida, A. I. S., Pinheiro, A. D. T., Ferreira, A. L. O., Pinto, G. A. S., & Gonçalves, L. R. B. (2007). *Applied Biochemistry and Biotechnology, 136-140*, 67–80.
28. Rosa, M. F., Bezerra, F. C., Brígida, A. I. S., & Brígido, A. K. L. (2002), Aproveitamento de resíduos da indústria da água de coco verde como substrato agrícola: I—Processo de obtenção, VI Seminário Nacional de Resíduos Sólidos Proceedings (CD-ROM), Gramado, Brasil.
29. Adriano, W. S., Costa-Filho, E. H., Silva, J. A., Giordano, R. L. C., & Goncalves, L. R. B. (2005). *Brazilian Journal of Chemical Engineering, 22*, 529–538.
30. Bastida, A., Sabuquillo, P., Armisen, P., Fernandez-Lafuente, R., Huguet, J., & Guisán, J. M. (1998). *Biotechnology and Bioengineering, 58*, 486 493.
31. Oliveira, P. C., Alves, G. M., & Castro, H. F. (2000). *Biochemical Engineering Journal, 5*, 63–71.
32. Wang, Z. -G., Wang, J. -Q., & Xu, Z. -K. (2006). *Journal of Molecular Catalysis B, Enzymatic, 42*, 45–51.
33. Pino, G. H., Mesquita, L. M. S., Torem, M. L., & Pinto, G. A. S. (2006). *Minerals Engineering, 19*, 380–387.
34. Akova, A., & Ustun, G. (2000). *Biotechnology Letters, 22*, 355–359.
35. Petersen, M. T. N., Fojan, P., & Petersen, S. B. (2001). *Journal of Biotechnology, 85*, 115–147.
36. Rodrigues, D. S., Bezerra, T. G., Bruno, L. M., & Gonçalves, L. R. B. (2004), Imobilização de lipase B de *Candida antarctica* em suporte hidrofóbico, XV Congresso Brasileiro de Engenharia Química Proceedings (CD-ROM), Curitiba, Brasil.
37. Castro, H. F., Silva, M. L. C. P., & Silva, G. L. J. P. (2000). *Brazilian Journal Of Chemical Engineering, 17*, 849–857.
38. Bastida, A., Sabuquillo, P., Armisen, P., Fernández-Lafuente, R., Huguet, J., & Guisán, J. M. (1998). *Biotechnology and Bioengineering, 58*, 486–493.
39. Silva, E. A. B., Souza, A. A. U., Rodrigues, A. E., & Souza, S. M. A. G. U. (2006). *Brazilian Archives of Biology and Technology, 49*, 491–502.
40. Tischer, W., & Kasche, V. (1999). *Trends in Biotechnology, 17*, 326–335.
41. Park, E. Y., Sato, M., & Kojima, S. (2006). *Enzyme and Microbial Technology, 39*, 889–896.
42. Secundo, F., Carrea, G., Soregaroli, C., Varinelli, D., & Morrone, R. (2001). *Biotechnology and Bioengineering, 73*, 157 163.

Appl Biochem Biotechnol (2008) 146:189–201
DOI 10.1007/s12010-007-8092-0

Methods and Supports for Immobilization and Stabilization of Cyclomaltodextrin Glucanotransferase from *Thermoanaerobacter*

Ana Elisa Amud · Gercio Rodrigo Presa da Silva · Paulo Waldir Tardioli · Cleide Mara Faria Soares · Flavio Faria Moraes · Gisella Maria Zanin

Received: 9 May 2007 / Accepted: 1 November 2007 /
Published online: 16 January 2008
© Humana Press Inc. 2007

Abstract *Thermoanaerobacter* cyclomaltodextrin glucanotransferase (CGTase) was immobilized using different supports and immobilization methods to study the effect on activity recovery. The enzyme covalently attached into glyoxyl-silica showed low activity recovery of 1.5%. The hydrophobic adsorption of the enzyme on Octadecyl-Sepabeads yielded also low activity recovery, 3.83%, and the enzyme could easily leak from the support at low ionic strength, although the immobilization yield was satisfactory, approximately 76%. The CGTase encapsulated in a sol–gel matrix gave an activity recovery of 6.94% and maximum cyclization activity at 60 °C, at pH 6.0. The half-time life at 60 °C, pH 6.0, in the presence of substrate was 100 min, which was lower than that of the free enzyme. The best activity recovery in this work (6.94%) is approximately five times smaller than that obtained previously using glyoxyl-agarose as support and covalent immobilization. Thus, the best support and method we tested so far for immobilization of CGTase is covalent attachment on glyoxyl-agarose.

Keywords CGTase · Toruzyme® · Glyoxyl-silica · Octadecyl-sepabeads · Sol–gel encapsulation · Multipoint attachment · Hydrophobic adsorption

Introduction

Cyclomaltodextrins (CDs) are cyclic oligosaccharides that are produced by the action of the CGTase enzyme (CD glucanotransferase, EC 2.4.1.19) on liquefied starch [1–3]. They have

A. E. Amud · G. R. P. da Silva · F. F. Moraes · G. M. Zanin (✉)
Chemical Engineering Department, State University of Maringa, Av. Colombo 5790, Bloco D-90, 87020-900 Maringa, PR, Brazil
e-mail: gisella@deq.uem.br

P. W. Tardioli
Mathematics Department, State University of Maringa, Maringa, PR, Brazil

C. M. F. Soares
Tiradentes University, Aracaju, SE, Brazil

countless applications in various industries [4–8] because they have a nonpolar cavity, which favors the encapsulation of a great variety of organic molecules [3, 6] conferring improved physicochemical properties, such as greater chemical resistance to environmental factors, higher solubility, and reduced volatility.

Immobilization of the CGTase enzyme has been pursued as a means of insolubilizing and stabilizing the enzyme molecule to allow using its catalytic activity continuously and repeatedly. However, the activity recovery of the immobilized CGTase is usually very low [9]. Therefore, we have set a research line with the main focus of immobilizing the *Thermoanaerobacter* extremely heat-stable CGTase [10], by different methods and supports, seeking high activity recovery. In this article, we report the immobilization of CGTase by three different methods: covalent multipoint attachment on glyoxyl-silica, physical adsorption on octadecyl-Sepabeads, and sol–gel encapsulation.

Enzyme immobilization by multipoint attachment into macroporous solid supports (for example, silica) activated with glyoxyl groups (monolayer of aliphatic aldehydes moderately away from the support surface) is a technique that has been extensively used since 1987 for the immobilization of different enzymes. For example, Pereira et al. [11] immobilized Penicillin G acylase on glyoxyl-silica (140 μmol of aldehyde groups per gram of silica) and obtained 100% activity recovery. Silica is an adequate support because it is inexpensive and easily regenerated. The formation of glyoxyl (aldehyde) groups on the silica is achieved by silanization with 3-glyxidoxypropyl-trimetoxysilane (GPTMS), followed by acidic hydrolysis to open the oxirane ring and to obtain vicinal hydroxy groups. Finally, the aldehyde groups are formed by oxidation with sodium periodate. The degree of activation of the support (i.e., the number of aldehyde groups on the silica surface) is related to the intensity of the multi-interaction between enzyme and support [11].

Physical adsorption of enzymes into solid supports is an immobilization technique commonly used, mainly when the enzyme has a low cost or is thermostable. The advantages of this technique are that reaction conditions are gentle and, when inactivated, the enzyme can easily be eluted from the support, which can be regenerated by a new charge of active enzyme. Its chief disadvantage is the fact that under the reaction conditions, the enzyme may be eluted from the support, and this is highly undesirable.

Octadecyl-Sepabeads is an epoxy-acrylic resin, which has octadecyl hydrophobic groups covering its surface. In comparison with conventional hydrophobic supports, it has the advantage of having pores with large surfaces that facilitates intense interaction with proteins. In addition, it becomes a very rigid support after extensive intercrosslinking with porousgenic agents, hence appropriate for application in packed-bed or stirred-tank reactors.

Octadecyl-Sepabeads particles do not swell when transferred from a buffered aqueous solution to an anhydrous medium, and they can be used in all reaction media [12]. The adsorption of enzymes in Octadecyl-Sepabeads was first proposed by Palomo et al. [12] for the immobilization of lipases. The idea behind this method was to take advantage of the enzyme affinity for hydrophobic interfaces as a strategy of immobilization.

In our work, CGTase immobilization into Octadecyl-Sepabeads by adsorption was tried hoping to obtain a biocatalyst with higher activity recovery, given the gentle conditions for obtaining this derivative (low ionic strength, pH 7.0, and room temperature).

The encapsulation of enzymes in a sol–gel matrix is an immobilization method in which the enzymes are incorporated into hybrid organic–inorganic hydrophobic materials (alkylsilanes) [13]. The sol–gel process can easily be recognized because it is the synthesis route in which at a certain time, there is the transition from the sol to the gel system. In contrast to the conventional methods, which require high temperatures for the fusion of vitreous silica, the sol–gel technique uses low temperatures for the hydrolysis and

condensation reactions, which are ideal for a great variety of organic molecules sensible to high temperatures, as the class of proteins that can denature and loose their biological activity [14]. Enzyme immobilization by the sol–gel process has been extensively used because the physicochemical characteristics of the biocatalysts obtained by this method qualify the sol–gel matrices as ideal supports for the encapsulation of biological materials and enzymes [14, 15], giving very satisfactory results.

Materials and Methods

Materials

Toruzyme® 3.0 L (a liquid preparation of CGTase from *Thermoanaerobacter* sp.) was a kind gift from Novozymes A/S (Bagsvaerd, Denmark). It contained 5.0 mg of protein/mL and had a specific activity of 32.26 U/mg of protein, previously determined by Tardioli et al. [9]. One unit was defined as the amount of enzyme that produces 1 μmol of β-CD per min at 60 °C, using 0.5% w/v dextrin solution prepared in 10 mM sodium citrate buffer, pH 6.0. Dextrin 10 from cornstarch was supplied by Fluka Chemie AG (Buchs, Switzerland), and soluble starch was supplied by Acros Organics (New Jersey, USA). Octadecyl-Sepabeads (epoxy-acrylic resin covered with octadecyl groups) was a gift from CSIC-ICP (Madrid, Spain). Controlled pore silica (CPS) was a gift from Sucrerie Vanciennes (France). The CPS particles had an average diameter of 0.42 mm, with a particle-size distribution range of 0.351–0.589 mm, previously determined by Tardioli et al. [16]. GPTMS was purchased from Aldrich. Sodium borohydride was supplied by Sigma Chemical (St. Louis, MO), and sodium periodate was purchased from Nuclear (Diadema, Brazil). Tetraethylortosilicate (TEOS), the encapsulation reagent, was purchased from Across Organic (New Jersey, USA). β-CD and γ-CD were acquired from Sigma Chemical and Wacker Consortium (Munich, Germany), respectively. All other reagents were of analytical grade.

β-CD Colorimetric Assay

The concentration of β-CD was measured by the dye-extinction colorimetric method using phenolphthalein, as described by Tardioli et al. [9].

Enzymatic Activity Assays

Enzymatic activity of soluble and immobilized CGTase was measured at 60 °C and pH 6.0 by assaying the initial reaction rate of β-CD production using 0.5% (w/v) maltodextrin solution as substrate. The full protocol can be accessed from Tardioli et al. [9].

Preparation of CGTase Glyoxyl-Silica Derivative

Support Activation The glyoxyl-silica support with high concentration of aldehyde groups was prepared as described by Pereira et al. [11] with slightly modifications.

The silica was washed with nitric acid solution (10%, v/v) for 30 min at room temperature. Then, the silica was washed with the same acidic solution and with acetone/water solutions at increasing concentrations (25, 50, 75, and 100% v/v of acetone). The treated silica was

dried in an oven for 1 h at 40 °C. The silanization reaction with GPTMS was accomplished at 25 °C, pH 8.5, for 1 h under gentle agitation, using 30 mL of 5% (w/v) GPTMS solution per gram of dried silica. The solution pH was constantly adjusted with diluted KOH solution. Then, the silanized support was washed with distilled water and acetone/water solutions at increasing concentrations (25, 50, 75, and 100% v/v of acetone) and dried at 40 °C for 1 h.

The epoxy groups formed during the silanization step were hydrolyzed by sulfuric acid (0.1 M) for 2 h at 85 °C, using 30 mL of acid solution per gram of dried silica. The glyceryl-silica support was washed with distilled water and acetone/water solutions, as described above, over a sintered glass filter under vacuum. After the last washing, the support was dried at 40 °C for 1 h. The glyoxyl-silica support was finally obtained by oxidation of the glyceryl groups to glyoxyl groups, using sodium periodate (1 h of reaction at room temperature, 200 μmol of periodate per gram of glyceryl-silica support). Under these conditions, the support had 113.4 μmol of aldehyde groups per gram of silica.

CGTase Immobilization Five grams of glyoxyl-silica support were added to 49 mL of enzyme solution in 0.1 M sodium bicarbonate, pH 10.05, at 25 °C and kept under gentle stirring. Enzymatic activities from the initial enzyme solution and from the final supernatant, after 5 h of reaction, were assayed. The initial enzyme solution had an activity of approximately 3.93 U/mL. The immobilized enzyme derivative was reduced with sodium borohydride (1 mg/ml, 25 °C, 30 min), as described by Blanco and Guisán [17]. After 30 min of reduction, the CGTase-glyoxyl derivative was washed with an excess of distilled water.

A blank, under the same immobilization conditions, using untreated silica instead of activated silica, was used to verify if CGTase was adsorbed on silica. It was observed that the nonactivated silica-CGTase suspension, after 5 h at 25 °C, pH 10.05, still showed 96% of the initial activity present in the suspension. After reduction with sodium borohydride, washing, and suck drying under vacuum, the resulting solid had no enzymatic activity.

Preparation of CGTase Octadecyl-Sepabeads Derivative

Hydration of the Support Eight grams (dried mass) of octadecyl-Sepabeads support were suspended in 100 mL of acetone/water solution (80% v/v). The air was removed from the suspension using ultrasound. Then, the support was washed with 100 mL of acetone/water solution (50% v/v), acetone/water solution (20% v/v), distilled water in excess, and phosphate buffer (10 mM, pH 7.0). The hydrated support was filtered under vacuum and suck dried. The mass of the hydrated support was 18.104 g.

CGTase Adsorption Hydrated support (6.79 g) was added in 73 mL of an enzymatic solution (7.88 U/mL of solution) prepared in phosphate buffer (10 mM, pH 7.0). The suspension was gently agitated for 2 h at room temperature. Then, the immobilized enzyme was washed with distilled water, filtered under vacuum and suck dried.

Enzymatic activities from the initial enzyme solution and from the supernatant after 30, 60, and 120 min of reaction were assayed.

Desorption Assay One gram of CGTase–Sepabeads (CGTase immobilized on octadecyl-Sepabeads) was suspended in 20 mL of citrate buffer (10 mM, pH 6.0) and kept under

agitation for 5 h. The supernatant activity was assessed in a span of 1 h to verify the amount of enzyme that leaked from the support.

Preparation of CGTase Encapsulated into a Sol–Gel Matrix

The protocol used was described by Soares et al. [13]. Sixty-two milliliters of TEOS (manipulated under argon atmosphere because it is highly hydroscopic) were diluted in 72 mL of absolute ethanol (99%) inside a 250-mL three-neck round-bottom flask that was then connected to a fractional distillation apparatus. The flask was half-immersed in glycerin at 45 °C, and the ethanolic solution was stirred for 5 min. Then, 0.22 mL of hydrochloric acid (37%) diluted in 10 mL of ultrapure water (prehydrolyzing solution) was added slowly through a funnel, drop by drop, for about 1 min. The quantities of TEOS and hydrochloric acid were taken as to give the molar ratio of 2.1:0.01. After completing the addition of the prehydrolyzing solution, the mixture was kept under agitation for 90 min at 45 °C. Then, 6 mL of the CGTase stock solution diluted in 14 mL of ultrapure water (30 mg of protein, 960 U) were added. Finally, 2 mL of ammonium hydroxide diluted in 12 mL of absolute ethanol (hydrolyzing solution, 1:6) were added slowly through a funnel, drop by drop, for approximately 1 min, and a transparent homogeneous solution was obtained. After this latter addition, the solution was left at rest (without agitation), at 45 °C for 60 min under an inert atmosphere. After the resting period, the material was sealed off inside the flask and kept for 18 h (aging time), at 4 °C. The biocatalyst was then transferred to a Buchner funnel and washed with 3 vol of 60 mL heptane. The material was sucked dry for 10 min for removing residual water, then washed with 90 mL acetone, and after being further sucked dry for 10 min, it was left in a desiccator for 24 h.

The biocatalyst mass obtained was 90.01 g, with 23% humidity, determined by the Karl Fischer automated titration model D18, Mettler.

Morphologic Characterization of Sol–Gel-encapsulated CGTase

The biocatalyst morphology was characterized in relation to the superficial area, pore diameter, and volume of pores.

Physical Characterization with the BET Equipment

Samples of pure silica matrix and the sol–gel-encapsulated CGTase were analyzed with the NOVA 1200 Quantachrome equipment to obtain the particles' superficial area, pore mean diameter, and volume.

Thermoporometry

The mean pore diameter of the pure silica matrix and the sol–gel-encapsulated CGTase was determined by thermoporometry, according to the method described by Iza et al. [18]. The water freezing and boiling temperatures were analyzed with a Shimadzu calorimeter, model DSC-50, equipped with an accessory section containing liquid nitrogen used for the cooling of water located inside the pores of the sample material. The samples with 10 to 20 mg were conditioned in aluminum capsules and an excess of solvent (water) was maintained. The material was cooled up to the freezing point of nitrogen (−30 °C) and latter kept at −20 °C for 10 min. The temperature was then reduced to −30 °C and subsequently raised by

1°C/min, up to the temperature of the thermodynamic equilibrium for the solidification of water inside the pores (from 0 to −5 °C). From the thermogram obtained, the sample mean pore diameter was determined according to Eq. 1:

$$\mathrm{Dp}\ (\text{Å}) = 0.02 \times \left[\left(\frac{64.67}{\Delta T}\right) + 0.57\right] \quad (1)$$

where Dp is the mean pore diameter and $\Delta T = T - T_0$ is the porous material temperature triple point of saturation with water.

Physicochemical Characterization of the Sol–Gel-encapsulated CGTase

The hydrophobic matrix (pure silica) and the sol–gel-encapsulated CGTase, produced from the precursor TEOS were characterized by thermogravimetric analysis (TGA) and Fourier transform infrared spectroscopy (FTIR).

Thermogravimetric Analysis

Samples of the pure silica sol–gel matrix and encapsulated CGTase were taken for TGA with a TGA-50 Shimadzu Thermogravimetric Analyzer, and the mass loss as a function of temperature was registered at a heating rate of 20 °C/min from room temperature to 1,000 °C. Initial mass samples varied from 2 to 6 mg.

Fourier Transform Infrared Spectroscopy

FTIR was used for characterization of the pure silica sol–gel matrix and encapsulated CGTase with a FTIR BOMEM MB-100 spectrophotometer in the wavelength range 400–4,000 cm^{-1}.

Catalytic Properties of the Soluble and Encapsulated CGTase

Soluble and sol–gel-encapsulated CGTase were characterized with respect to thermal stability and enzymatic activity as a function of temperature and reaction pH.

Activity as a Function of Temperature and Reaction pH

CGTase activity was measured at the following temperatures (40, 50, 70, 80, and 90 °C) and pH 6.0 (pH of maximum catalytic activity), keeping fixed the biocatalyst mass (307.5 mg). Samples of the reaction medium were taken in duplicates at the times of 0 and 25 min and added to a test tube containing 20 μL of 5 M HCl. These tubes were immersed in boiling water for 5 min to inactivate the enzyme. After cooling, a sample was taken to determine β-CD concentration using the phenolphthalein colorimetric method. The same assay was conducted from pH 4.0 to 10.0 and 60 °C, the temperature for maximum enzyme activity.

Biocatalyst Thermal Stability

Suspensions of the immobilized CGTase were prepared in sodium citrate buffer 10 mM, pH 6.0, containing maltodextrin 0.5% (w/v) and incubated at 60 °C for 3 h. At regular time intervals, the residual activity of the immobilized enzyme was measured.

Results and Discussion

Immobilization of CGTase on Different Supports and Methods

The results for the immobilization of CGTase from *Thermoanaerobacter* sp. in glyoxyl-silica, hydrophobic adsorption in octadecyl-sepabeads, and encapsulation into the sol–gel matrix are shown at Table 1.

Usually, activity loss occurs as a consequence of enzyme immobilization because of many causes, for example, steric hindrances (the immobilized enzyme molecule may be inappropriately oriented in relation to the porous surface, and the active site may not be accessible to the substrate), intraparticle diffusional resistance (an effect more severe in the case of sol-gel encapsulation), or tridimensional conformal changes in the enzyme molecule (induced by enzyme-support multipoint covalent link attachments).

In a previous work, Tardioli et al. [9] have immobilized CGTase from *Thermoanaerobacter* sp. by covalent attachment into glyoxyl-agarose particles and obtained an activity recovery of about 32%, that is, five times the highest values obtained in this work (6.94% with sol–gel encapsulation). It is thought that with the latter method, in addition to the causes listed above for immobilized enzyme activity loss, the immobilization conditions and reagents used by the sol–gel method contribute to enzyme deactivation.

Although the activity recovery of the immobilized CGTase in glyoxyl-silica was low, a result of the same magnitude, 2.5%, was obtained by Tardioli et al. [16] using CGTase from *Bacillus* sp. and silica silanized with γ-amino-propyl-trietoxi-silane (γ-APTS) and activated by glutaraldehyde.

The activity recovery of the CGTase adsorbed in octadecyl-sepabeads was higher than that obtained with covalent attachment in glyoxyl-silica, but the latter support can be considered more appropriate for immobilization of this enzyme because it was weakly adsorbed into the octadecyl-sepabeads, being easily desorbed even at low ionic strength (25% desorbed with at 10 mM buffer).

In general, results of the same magnitude as in this work were obtained for the activity recovery of immobilized CGTase by many different authors [9]. There are three exceptional cases reported of activity recovery equal to or higher than 74%: two of them use adsorption

Table 1 Activity results for the immobilization of CGTase from *Thermoanaerobacter sp.* using different supports and methods.

Method (Support)	Conditions	U_I (U/g)	U_{IT} (U/g)	RI (%)	U_{EI} (U/g)	RA (%)
Covalent attachment (silica-glyoxyl)[a]	25 °C, pH 10.05, 5 h	38.4	38.4	100	0.59	1.54
Adsorption (Octadecyl-Sepabeads)	25 °C, pH 7.0, 2 h	84.7	64.3	75.9	2.46	3.83
Encapsulation (sol–gel)	Note 1	10.7[b]	10.7	100	0.74	6.94

U_I The enzymatic charge offered for immobilization in U/g of support, U_{IT} the enzymatic charge theoretically immobilized in U/g of support, *RI* the immobilization yield, defined as $(U_{IT}/U_I)\times 100$, U_{EI} the measured immobilized enzyme activity, in U/g of biocatalyst, *RA* the activity recovered in the immobilized enzyme, defined as $(U_{EI}/U_{IT})\times 100$, *Note 1* gelation/encapsulation=45 °C, ethanolic/acid medium, 155 min, aging=18 h at 4 °C, drying=suck dried by vacuum, followed by a 24-h resting period in a desiccator

[a] All the results of this immobilization are the averages of duplicates.

[b] The enzymatic charge per gram of support, U_I, was calculated from the biocatalyst mass obtained after the process of gelation/encapsulation (90.01 g) and the offered enzymatic charge (960 U).

in resins as the immobilization method, and a third uses a high-silica fabric treated with γ-APTS and glutaraldehyde. The highest activity recovery reported is 95%, and in this case, CGTase was fused with ten lysine residues and electrostactically immobilized in a cation exchanger resin [19]. For the case of CGTase from *Thermoanaerobacter* sp., the highest activity recovery reported is 10.2%. The hydrophobic support Eupergit C was used, and the enzyme was immobilized by covalent attachment [20]. From these observations and the results of our work, it may be concluded that CGTase is very sensitive to its microenvironment of immobilization, and it seems worthy protecting the enzyme, such as in the case that attached ten lysine residues to the enzyme.

Temperature Dependence of the CGTase Activity

Figure 1 shows the relative activity of the soluble and sol–gel-encapsulated CGTase, measured at pH 6.0 and temperatures from 40 to 90 °C. The soluble enzyme showed a maximum activity in the temperature range of 80–90 °C, which is in accord with Norman and Jorgensen [10] and Tardioli et al. [9]. However, the sol–gel-encapsulated CGTase has shown a shift in the maximum temperature range to around 60 °C, which demonstrates that the conformal changes that occurred at the tridimensional enzyme shape made it more susceptible to thermal inactivation.

The thermal stability of an immobilized enzyme is another important factor for the selection of an immobilization method. A method that shifts the maximum catalytic activity for a region of higher temperatures is undoubtedly preferred. Tardioli et al. [9] obtained greater thermal stability for a *Thermoanaerobacter* sp. CGTase covalently bound to glyoxyl-agarose; the temperature range shift for the maximum activity was from 80 to 85 (for the free enzyme) to just above 90 °C (for the immobilized enzyme).

pH Dependence of the CGTase Activity

Figure 2 shows that the CGTase from the *Thermoanaerobacter* sp. in the soluble form has the maximum activity in the pH range from 5.0 to 6.0 at 60 °C, corroborating data from Norman and Jorgensen [10], but the sol–gel-encapsulated enzyme showed maximum

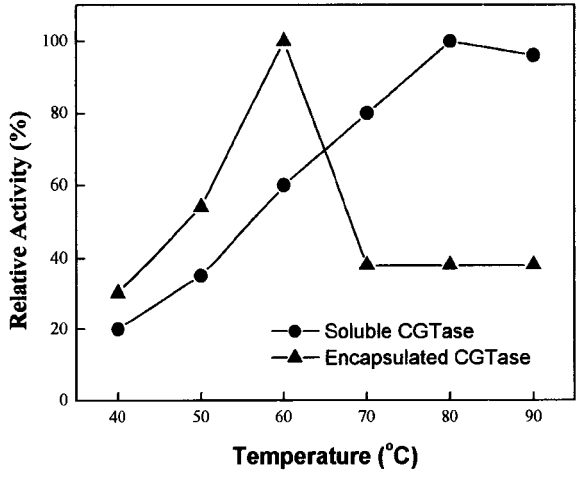


Fig. 1 Effect of temperature on the cyclization activity (Effect of temperature on the cyclization activity (β-CD formation rate) of the free and sol–gel encapsulated CGTase at pH 6.0. The maximum catalytic activity in each case was normalized to 100%

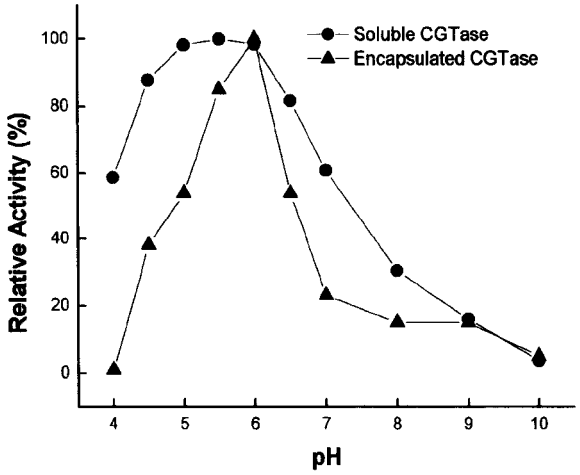


Fig. 2 Relative cyclization activity (β-CD formation rate) for free and sol–gel-encapsulated CGTase at 60 °C and pH 4.0 to 10.0 with 10 mM buffers: sodium citrate (pH 4.0–6.5), Tris–HCl (pH 7.0–9.0), and bicarbonate (pH 10.0). The substrate was maltodextrin 5 g L^{-1}, and the maximum catalytic activity in each case was normalized to 100%

activity at pH 6.0, and below or above this pH value, the immobilized enzyme activity has an abrupt drop that is not observed around the maximum region of the free enzyme. This sharp drop in activity adds strength to the conclusion that CGTase encapsulation by the sol–gel technique has caused detrimental conformal changes to the enzyme.

Thermal Stability of the Sol–Gel-encapsulated CGTase

Figure 3 presents the thermal deactivation as a function of time for the sol–gel-encapsulated CGTase incubated at 60 °C and pH 6.0 (citrate buffer). These results demonstrate a low thermal stability of the encapsulated enzyme that at 60 °C has a half-life of approximately 100 min and is practically inactivated after 3 h. In addition, they are consistent with the shift of the maximum catalytic activity to a lower temperature range, as the enzyme was encapsulated, and reinforce the conclusion that deleterious conformal changes occurred

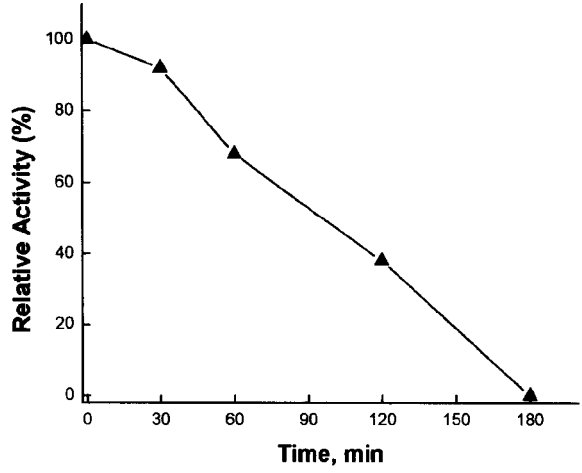


Fig. 3 Thermal deactivation as a function of time for the sol–gel-encapsulated CGTase incubated at 60 °C and pH 6.0 (citrate buffer 10 mM and maltodextrin 5 g L^{-1})

when the enzyme was encapsulated. Norman and Jorgensen [10] informed that the CGTase from *Thermoanaerobacter* sp. in soluble form retains more than 95% of its activity when incubated at 75 °C in acetate buffer, pH 5.5, for 60 min in the absence of substrate.

Morphologic Characterization of Sol–Gel-encapsulated CGTase

The morphologic characterization of the immobilized enzyme is important to correlate the biocatalyst performance with porous structure parameters. BET analysis, which is usually based on N_2 isothermal adsorption at 77 K, allows determining the solid-specific surface area, total pore volume, pore size distribution, and mean pore diameter. It is not recommended for solids with a low specific surface area (<5 m^2 g^{-1}). Table 2 shows the specific surface area, mean pore diameter, and total pore volume determined by BET for the pure sol–gel silica matrix having TEOS as the precursor and the same matrix with the encapsulated CGTase.

For the encapsulated CGTase, a significant reduction in surface area was observed, while pore diameter and volume remained practically constant.

With the objective of studying the biocatalyst textural properties, N_2 adsorption isotherms were obtained (Fig. 4), and according to the International Union Pure and Applied Chemistry nomenclature, they are of type IV, which indicates that the solid contains a large proportion of mesopores (1.8–6 nm), and this facilitates the substrate access to the catalytic site of the immobilized enzyme.

TGA and FTIR Analyses of the Sol–Gel-encapsulated CGTase

The encapsulated CGTase mass loss as a function of temperature, calculated by TGA [21], is shown in Fig. 5. The temperature range used was divided in three regions for interpretation: Region I (0 to 130 °C) shows a relatively large mass loss, probably caused by loss of water and organic residues, region II (130 to 620 °C) has also a large mass loss, probably caused by decomposition of organic compounds including the enzyme, and region III (620 to 1,000 °C) shows sample mass stabilization corresponding to the final carbonization of the residual organic mater.

FTIR analysis was also used to study the efficiency of the sol–gel enzyme encapsulation method that uses TEOS as precursor. The silica matrix gelation procedure produces a tridimensional reticulate formed by interacting polymeric inorganic chains that form a holding net around the enzyme, and FTIR can be used to follow this encapsulating process. The FTIR spectrograms obtained for the pure silica matrix and the encapsulated CGTase are shown at Fig. 6.

The CGTase characteristic peaks are the bands at 1,650 and 1,600 cm^{-1} related to primary and secondary amino groups. They can be seen at the biocatalyst spectrogram (Fig. 6) and are in accord with the bands described in the literature [22].

Table 2 Morphologic characteristics of the support prepared with TEOS as precursor (pure silica matrix) and the biocatalyst (sol–gel-encapsulated CGTase).

Material	Superficial area (m^2 g^{-1})	Mean pore diameter (nm)	Total pore volume (cm^3 g^{-1})
Pure silica	607	1.80	0.37
Sol–gel-encapsulated CGTase	484	1.79	0.36

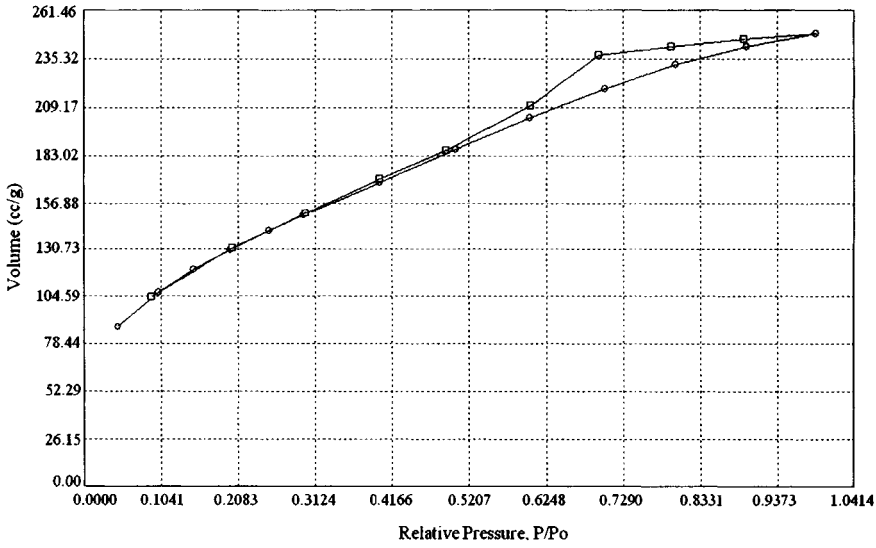


Fig. 4 Nitrogen adsorption (*squares*) and desorption (*circles*) isotherms measured at 77 K for the sol–gel-encapsulated CGTase

Figure 6 shows in addition the characteristic bands of pure silica, that is, 950 (Si-O-Si, axial deformation), 810 (Si-O-Si, axial deformation), and 600 cm^{-1} (Si-O-Si, angular deformation) [23, 24]. The characteristic peaks for the hydroxyl group bonds can also be observed in the range of 3,400 cm^{-1} [23].

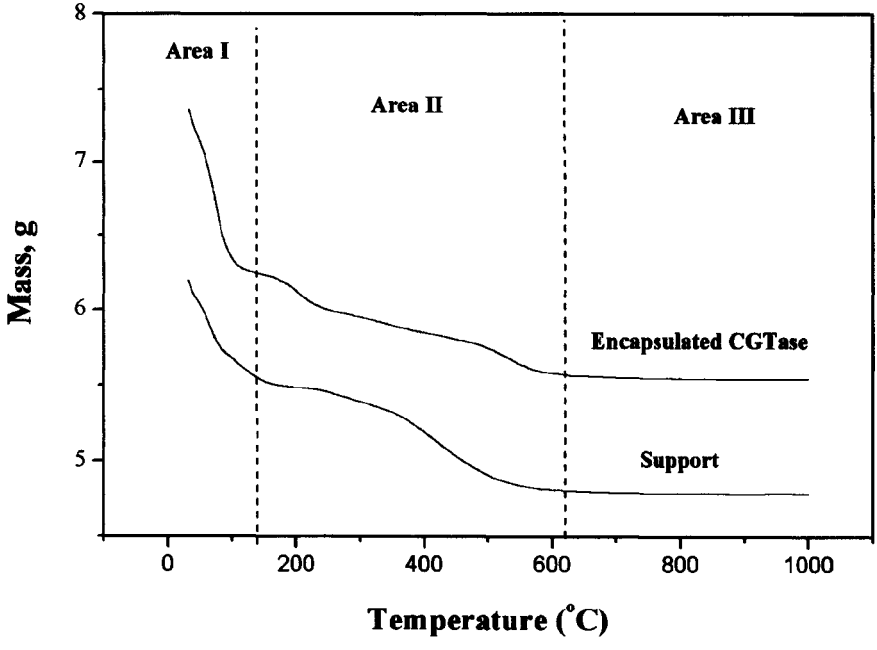


Fig. 5 TGA of the pure silica matrix (*support*) and the sol–gel encapsulated CGTase, prepared using TEOS as precursor

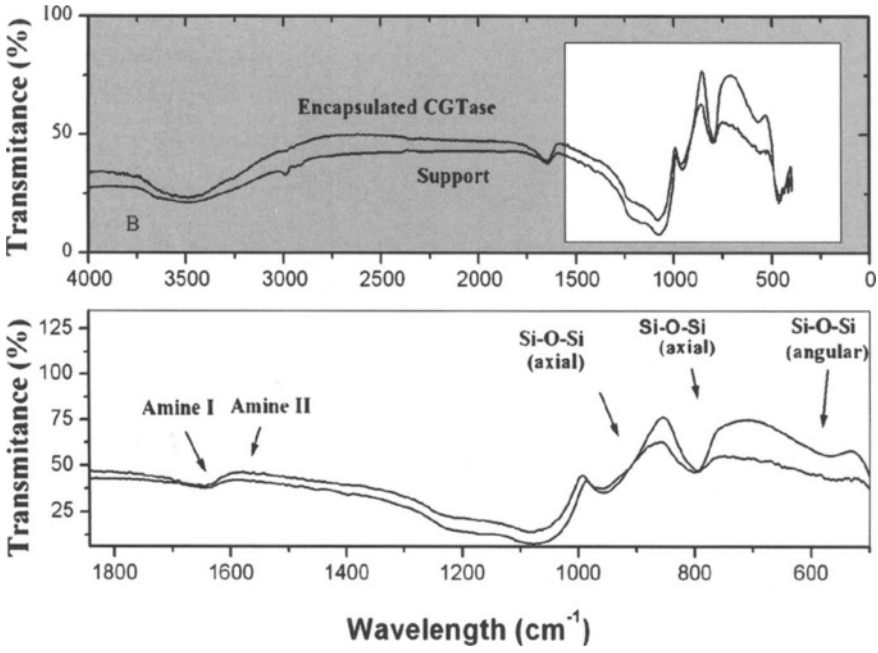


Fig. 6 FTIR spectrograms for the pure silica matrix and the sol-gel encapsulated CGTase, prepared with TEOS as precursor

Conclusions

The covalent immobilization of CGTase into silica particles activated with linear aldehyde groups (glyoxyl-silica) at 25 °C, pH 10.05, by 5 h resulted in a yield of immobilization of approximately 100% and activity recovery of 1.54%. Hydrophobic adsorption on Octadecyl-Sepabeads at 25 °C, pH 7.0, by 2 h gave approximately 76% of immobilization yield and 3.83% of activity recovery. In addition, the enzyme-support binding was shown to be very weak, in this case, losing approximately 25% of the enzyme from the support under low ionic force. Encapsulation of CGTase using the sol–gel technique produced the best results: 100% yield of immobilization and 6.94% of activity recovery.

The temperature of maximum cyclization activity downshifted from 80–90 (for the soluble enzyme) to 60 °C (for the sol–gel-encapsulated CGTase) at pH 6.0. However, both, soluble and encapsulated CGTases exhibited almost the same pH for maximum cyclization activity.

The thermal stability of the sol–gel-encapsulated CGTase was not satisfactory. The approximate half-life time was only 100 min at 60 °C, pH 6.0, in the presence of substrate (maltodextrin 0.5%, w/v). After 3 h of incubation, the enzyme was nearly completely inactivated.

Encapsulation of CGTase by the sol–gel technique strongly influenced the superficial area of the formed gel, but the influence on pore average diameter and total pore volume was negligible.

Among all the methods and supports already tested by our group for the immobilization of CGTase, the covalent link of the enzyme to agarose activated with glyoxyl groups (glyoxyl-agarose) was the most efficient, giving an immobilization yield of practically

100% and an activity recovery of 32% [9]. Consequently, this method warrants further studies that will be carried out by adding enzyme active site protectors, such as polyethylene glycol, β-CD, or acarbose, which could lead to higher activity recoveries that we seek.

Acknowledgments The authors thank the support of the Brazilian research grant agencies CNPq, CAPES, and Fundação Araucária. The authors also thank Novozymes A/S and Roberto Fernández-Lafuente from CSIC-ICP (Madrid, Spain) for the gift of the Toruzyme® 3.0 L and Octadecyl-Sepabeads support, respectively.

References

1. Szejtli, J (1990). *Carbohydrate Polymers, 12*, 375–392.
2. Fromming, K. H., & Szejtli, J. (1994). *Cyclodextrins in pharmacy.* Dordrecht: Kluwer.
3. Szejtli, J (1988). *Cyclodextrin technology.* Dordrecht: Klumer.
4. Vaution, C., Hutin, M., Gomot, F., & Duchêne, D. (1987). In D. Duchêne (Ed.), *Cyclodextrins and their industrial uses* (Chapter 8). Paris: Editions de Santé.
5. Pszczola, D. E (1988). *Food Technologist, 42*, 96–100.
6. Bekers, O., Uijtendaal, E. V., Beijnen, J. H., Bult, A., & Underberg, W. J. M. (1991). *Drug Development and Industrial Pharmacy, 17*(11), 1503–1549.
7. Uekama, K. (2002). *Journal of Inclusion Phenomena and Macrocyclic Chemistry, 44*, 3–7.
8. Hashimoto, H (2002). *Journal of Inclusion Phenomena and Macrocyclic Chemistry, 44*, 57–62.
9. Tardioli, P. W., Zanin, G. M., & Moraes, F. F. (2006). *Enzyme and Microbial Technology, 39*, 1270–1278.
10. Norman, B. E., & Jorgensen, S. T. (1992). *Denpun Kagaku, 39*(2), 101–108.
11. Pereira, G. H. A., Guisán, J. M., & Giordano, R. L. C. (1997). *Brazilian Journal of Chemical Engineering, 14*(4), 327–331.
12. Palomo, J. M., Munoz, G., Fernandez-Lorente, G., Mateo, C., Fernandez-Lafuente, R., & Guisán, J. M. (2002). *Journal of Molecular Catalysis, B, Enzymatic, 19–20*, 279–286.
13. Soares, C. M. F., Santos, O. A. A., Castro, H. F., Moraes, F. F., & Zanin, G. M. (2004). *Journal of Molecular Catalysis, B, Enzymatic, 29*, 69–79.
14. Mansur, H. S., Oréfice, R. L., Vasconcelos, W. L., Silva, R. F., & Lobato, Z. P. (1999). *Revista de Biotecnologia*, 16–18.
15. Kauffmann, C., & Mandelbaum, R. T. (1998). *Journal of Biotechnology, 62*, 169–176.
16. Tardioli, P. W., Zanin, G. M., & Moraes, F. F. (2000). *Applied Biochemistry and Biotechnology, 84–86*, 1003–1019.
17. Blanco, R. M., & Guisán, J. M. (1989). *Enzyme and Microbial Technology, 11*, 360–366.
18. Iza, M., Worley, S., Danumah, C., Kaliagine, S., & Bousmira, M. (2000). *Polymer, 41*, 5885–5893.
19. Kweon, D. H., Kim, S. G., Han, N. S., Lee, J. H., Chung, K. M., & Seo, J. H. (2005). *Enzyme and Microbial Technology, 36*, 571–578.
20. Martin, M. T., Plou, F. J., Alcalde, M., & Ballesteros, A. (2003). *Journal of Molecular Catalysis. B: Enzymatic, 21*, 299–308.
21. Brinker, C. J., & Scherer, G. M. (1990). *Sol–gel science the physics and chemistry of sol–gel processing* (2nd ed.). New York: McGraw-Hill.
22. Murray, M., Rooney, D., Van Neikerk, M., Montenegro, A., & Weatherley, L. R. (1997). *Process Biochemistry, 32*, 479–486.
23. Ramos, M. A., Gil, M. H., Schact, E., Matthys, G., Mondelaers, W., & Figueiredo, M. M. (1998). *Powder Technology, 99*, 79–85.
24. Assis, O. B. G. (2003). *Brazilian Journal of Chemical Engineering, 20*(3), 339–342.

Appl Biochem Biotechnol (2008) 146:203–214
DOI 10.1007/s12010-007-8088-9

Response Surface Methodology as an Approach to Determine Optimal Activities of Lipase Entrapped in Sol–Gel Matrix Using Different Vegetable Oils

Rubiane C. Pinheiro · Cleide M. F. Soares · Heizir F. de Castro · Flavio F. Moraes · Gisella M. Zanin

Received: 13 May 2007 / Accepted: 18 October 2007 /
Published online: 26 March 2008
© Humana Press Inc. 2007

Abstract The conditions for maximization of the enzymatic activity of lipase entrapped in sol–gel matrix were determined for different vegetable oils using an experimental design. The effects of pH, temperature, and biocatalyst loading on lipase activity were verified using a central composite experimental design leading to a set of 13 assays and the surface response analysis. For canola oil and entrapped lipase, statistical analyses showed significant effects for pH and temperature and also the interactions between pH and temperature and temperature and biocatalyst loading. For the olive oil and entrapped lipase, it was verified that the pH was the only variable statistically significant. This study demonstrated that response surface analysis is a methodology appropriate for the maximization of the percentage of hydrolysis, as a function of pH, temperature, and lipase loading.

Keywords Lipase · Canola oil · Soybean oil · Olive oil · Sol–gel encapsulation

Introduction

Recently, Reetz and others have published a number of studies showing that adding organically modified silanes (precursors), such as methyltrimethoxysilane or poly (dimethylsiloxane), to tetraethoxysilane (TEOS) during hydrolysis can produce a protein-doped organicinorganic hybrid material that is hydrophobic [1–7]. Systems already tested

R. C. Pinheiro · F. F. Moraes · G. M. Zanin (✉)
Chemical Engineering Department, State University of Maringa, Av. Colombo 5790, E-46, 87020-900 Maringá, PR, Brazil
e-mail: gisellazanin@maringa.com.br

C. M. F. Soares
Instituto de Tecnologia e Pesquisa (ITP), Universidade Tiradentes, Aracaju, SE, Brazil

H. F. de Castro
Escola de Engenharia de Lorena, Universidade de São Paulo, Caixa Postal 116, 12600-970 Lorena, SP, Brazil

for lipases from either microbial or animal sources include the utilization of different precursors, alternative stabilizing additives (polyvinyl alcohol, albumin, gelatin, and others), and several solvents (methanol, ethanol, and others) [1, 3, 7]. The behavior of the sol–gel-encapsulated lipase systems depends on the physical and structural properties of the support and the physical and chemical properties of the lipase used [7–9]. We recently developed a bioactive organically modified silicate through sol–gel processing, starting with silica matrices produced by acid- and base-catalyzed hydrolysis of TEOS, in the presence of the additive polyethylene glycol (PEG) [6]. This is a modified methodology previously established for a chemical catalyst [6, 8], and to our knowledge, it has not been used by other groups for encapsulating the enzyme lipase. The encapsulation of *Candida rugosa* lipase (CRL) in sol–gel prepared by the hydrolysis of alkyl-substituted silanes like TEOS, in the presence of PEG, showed considerably high hydrolytic and esterification activities. This result was attributed to the interactions mediated by the hydrophobic–hydrophilic nature of CRL [6]. The hydrolysis of triglyceride esters to yield free fatty acids and glycerol represents an important group of chemical reactions relevant to the industrial processing of natural oils and fats. Hydrolysis is the primary reaction for production of free fatty acids that may then be interesterified, transesterified, or converted into high-value fatty alcohols. The mainstream current technologies for hydrolysis are based on high-temperature, high-pressure contacting processes with steam or superheated liquid water, involving high temperatures and high-pressure equipment requirements. The best known process is the Colgate Emery process [10], which typically requires operating temperatures of 250 °C and a reaction pressure of 50 bar. Enzymic fat splitting (hydrolysis) has been studied extensively using enzymes immobilized on hydrophobic polymeric supports [11, 12] and also using enzymes freely attached at a liquid–liquid interface [13]. In this latter technique, one of the primary physical requirements is the provision of a free interface at which the lipase can catalyze the reaction, and the overall rate of reaction can be enhanced using dispersions of aqueous phase in oil substrate and vice versa. Another requirement is the enhancement of mass transfer processes necessary for the supply of reaction substrate from the corresponding bulk phases. In this study, we examined the hydrolysis of vegetable oil and focused upon phenomena that affect the process feasibility of using lipolytic hydrolysis as a viable alternative to conventional techniques. The objective was also to establish operational conditions that allow a desirable working region where a high hydrolysis percentage of olive, canola, and soybean oils can be attained. The high hydrolysis percentage is important for the biotechnological process of biodiesel and fatty acids. The response surface methodology (RSM) was used as an approach for the maximization of the percentage of hydrolysis for different oils.

Experimental Procedures

Enzyme and Chemicals

Commercial CRL (Type VII—product no. L1754) was purchased from Sigma Chemical (St Louis, MO). This lipase is substantially free of α-amylase and protease and contains lactose as an extender. Nominal-specific lipase activity was 104.94 U mg^{-1} protein. PEG (MW 1,450, Merck) was used as a stabilizing agent. The silane precursor TEOS was supplied by Across Organic (New Jersey, USA) and used without further purification. Ethanol (minimum 99%), ammonia (minimum 28%), hydrochloric acid (minimum 36%), and gum Arabic were from Synth (São Paulo, Brazil). Olive oil (low acidity), soybean oil, and

canola oil were purchased at a local market. Water was purified by reverse osmosis and deionized through a Milli-Q four-cartridge organic-free water purification system. Other chemicals were of analytical grade and used as received.

The percentage of different fatty acids varies according to oil origin, and the mean molar mass of the fatty acids in the oil is required for calculating the percentage of oil hydrolysis. The fatty acid composition of each tested oil in this work is given at Table 1. It can be observed that canola and olive oils are richest in oleic acid (57.71 and 69.00%, respectively) and soybean oil has the greatest amount of linoleic and linolenic fatty acids (54.50 and 8.30, respectively). Some components present in small quantities are not analyzed and consequently the sum of percentage composition values does not add up to 100%. Then for calculating the mean molar mass of the fatty acids in the oil it is necessary to first normalize the composition according to Eq. 1:

$$x_{N_i} = \frac{x_i}{\sum_i^n x_i} \tag{1}$$

where x_i is the percentage mass fraction of component i, x_{N_i} is the normalized mass fraction of component i, and n is the number of fatty acids present in the oil.

Then, the mean molar mass of the fatty acids in the oil ($\overline{M}$) is calculated as:

$$\overline{M} = \sum_i^n M_i x_{Ni} \tag{2}$$

where M_i is the molar mass of the fatty acid i.

The oil lipids mean molar mass ($\overline{\mathrm{MO}}$) is given by Equation (3):

$$\overline{\mathrm{MO}} = G + 3\overline{M} - 3W \cong 38.05 + 3\overline{M} \tag{3}$$

where G is the molar mass of glycerol (92.0935 g/mol) and W is the molar mass of water (18.0152 g/mol).

Encapsulation of Lipase from *Candida rugosa* in Sol–Gel Matrices

The methodology previously established by Soares et al. [6] was used as briefly described: 30 mL of TEOS was dissolved in 36 mL of absolute ethanol under nitrogen-inert atmosphere.

Table 1 Fatty acids composition for different vegetable oils.

Name	Short	Molar mass (g mol^{-1})	Soybean oil (% w/w)	Canola oil (% w/w)	Olive oil (% w/w)
Palmitic	C16:0	256.42	10.50	5.11	13.85
Oleic	C18:1	282.26	22.30	57.71	69.00
Linoleic	C18:2	278.43	54.50	22.45	12.25
Linolenic	C18:3	276.43	8.30	6.28	<0.1
Palmitileic	C16:3	254.42	<0.1	<0.2	1.90
$\overline{M}$=oil fatty acids mean molar mass (g mol^{-1})[a]	–	–	276.71	279.42	277.54
$\overline{\mathrm{MO}}$=oil lipids mean molar mass (g mol^{-1})[a]	–	–	868.18	876.31	870.67

Composition Source: [14]

[a] These table values were calculated in this work using Eq. 2 for $\overline{M}$ and Eq. 3 for $\overline{\mathrm{MO}}$, after normalizing the fatty acids composition to 100% (Eq. 1).

To this, 0.22 mL of hydrochloric acid dissolved in 5 mL of ultrapure water was slowly added, and the mixture was agitated (200 rpm) for 90 min at 35 °C. Then, 10 mL of lipase solution (18.29 mg mL^{-1}), PEG solution (5 mg mL^{-1}, 8 mL added), and 1 mL of ammonium hydroxide dissolved in 6 mL of ethanol were added (hydrolysis solution), and the mixture was kept under static conditions for 4 h to obtain the chemical condensation. The bulk gel was washed with heptane and acetone and dried under vacuum at room temperature for 24 h [6].

Hydrolysis Tests

For the free lipase hydrolysis tests, the substrate was prepared by mixing 30–70 mL of the selected oil with 70–30 mL of gum Arabic solution (7% w/v) containing free CRL (Table 2) and fixing the free lipase loading values (1 mL, 5 mg mL^{-1}).

For the encapsulated lipase runs, the substrate was prepared with 50% oil to water ratio and the percentage of hydrolysis was investigated by running enzymatic hydrolysis according to an experimental design with three different temperatures (30, 37, and 44 °C), pH values (4.0, 7.0, and 10.0) and encapsulated lipase-loading values (6, 7.5, and 9 mg mL^{-1}; Table 3).

Determination of the Percentage of Oil Hydrolysis

The percentage of oil hydrolysis (POH) was determined by titration of the released fatty acids and defined as the percentage weight of free fatty acids in the sample, in comparison with the maximum theoretical amount of free fatty acids that could be produced if all the oil in the sample was hydrolyzed:

$$\mathrm{POH}\ (\%) = \frac{N_a \times 0.02 \times 10^{-3} \times MM}{W_t \times f_0 \times f_1} \times 100 \tag{4}$$

where:

f_0 fraction of oil in the sample at the start of reaction (g_{lipids}/g_{sample})

f_1 ratio of the mass of fatty acids produced at total hydrolysis to the mass of oil ($g_{fatty\ acids}/g_{lipids}$)

Table 2 Free enzyme: Effect of pH, temperature, and oil/water ratio on the hydrolysis of olive, canola, and soybean oils.

Runs	pH	Temperature (°C)	Oil/water ratio (%)	Olive oil POH (%)	Canola oil POH (%)	Soybean oil POH (%)
1	4	30	40	11.13	3.91	4.80
2	10	30	40	4.64	5.54	4.29
3	4	44	40	11.69	3.85	4.98
4	10	44	40	4.47	4.16	4.30
5	4	30	60	5.13	3.10	2.83
6	10	30	60	0.74	0.62	1.76
7	4	44	60	5.99	3.12	2.03
8	10	44	60	0.91	1.16	1.23
9	7	37	50	6.55	6.47	5.97
10	7	37	50	6.89	6.13	5.77
11	7	37	50	6.83	7.22	7.43
12	7	37	50	7.30	6.43	7.07
13	7	37	50	7.65	6.65	6.65

[a] Values reached after a reaction time of 4 h

Table 3 Encapsulated CRL: effect of factors on the hydrolysis of olive, canola, and soybean oils.

Runs	pH	Temperature (°C)	Loading Biocatalyst (mg mL^{-1})	Olive oil[a] POH (%)	Canola oil[a] POH (%)	Soybean oil[a] POH (%)
1	4	30	6.0	6.89	6.08	6.86
2	10	30	6.0	1.84	2.09	1.32
3	4	44	6.0	7.48	6.77	6.38
4	10	44	6.0	1.75	1.24	1.43
5	4	30	9.0	7.86	5.76	6.88
6	10	30	9.0	2.20	2.13	1.35
7	4	44	9.0	7.17	6.92	7.40
8	10	44	9.0	1.95	1.70	1.53
9	7	37	7.5	2.68	2.43	2.54
10	7	37	7.5	2.63	2.45	3.14
11	7	37	7.5	3.34	2.39	2.82
12	7	37	7.5	2.86	2.31	2.91
13	7	37	7.5	3.09	2.32	2.76

[a] Values reached after a reaction time of 4 h

$\overline{M}$ mean molar mass of fatty acids in the oil which was calculated from the composition data presented in Table 1, according to Eq. 2 (g mol^{-1})
N_a volume of sodium hydroxide solution required during titration of the fatty acids (mL)
W_t weight of the sample (g)

Note that Eq. 4 is similar to that found in Rooney and Weatherle [15], but it has the factor f_1 that was missing in the earlier work. Given the composition of an oil molecule and its hydrolysis reaction that requires three molecules of water, the factor f_1 can be calculated as:

$$f_1 = \frac{\text{mass of free fatty acids at total hydrolysis}}{\text{mass of oil}} = \frac{3\,\overline{M}}{\overline{\text{MO}}} \cong \frac{1}{1 + \frac{12.68}{\overline{M}}} \tag{5}$$

where $\overline{\text{MO}}$ is given by Eq. 3 and $\overline{M}$ is calculated with Eq. 2.

Experimental Design with Response Surface Methodology

The results of the experimental design were analyzed using the software STATISTICA®, USA as a function of pH, temperature, and lipase loading. The coefficients were generated by regression analysis. The quality of the fit by the models was evaluated by examining the coefficients (R^2) and p (analysis of variance).

Results and Discussion

Free Lipase

A central composite experimental design leading to a set of 13 experiments with different variable value combinations for finding the maximal region of the percentage of hydrolysis, as a function of pH, temperature, and concentration of reactants (oil-to-water ratio), is shown at Table 2 for free lipase. The percentage of hydrolysis (POH%) ranged from 0.62 to

11.69%, according to the experimental condition. When lower pH (4) and lower substrate concentration (30%) for olive oil were used, the POH was higher, whereas in the case of canola and soybean oils, better results were observed using 50% oil–water ratio at 37 °C, pH 7 (Table 2).

Tables 4 and 5 show the variables' effects and interactions for free lipase as obtained from the factorial design analysis for canola and soybean oil, respectively. It can be seen that the oil/water ratio is the most important variable, with a negative effect, which means that an increase in the oil/water ratio leads to a decrease in the percentage of hydrolysis (POH%).

On the contrary, Table 6 shows the effects of the variables and their interactions on the percentage of hydrolysis for olive oil, and it can be seen that for olive oil, the pH and concentration of reactants (oil–water ratio) were statistically significant at 95% of confidence. The interactions between the variables were not statistically significant in the range studied for all the three types of oils studied. For free lipase, at 70% oil–water ratio (not shown at Table 2), all oil suspensions have shown a percentage of hydrolysis (POH%) lower than that observed at 50% oil–water ratio, suggesting substrate mass transfer limitations at the highest oil concentrations.

Analysis of variance (Tables 4, 5, and 6) shows that the statistical significance for the responses of the percentage of hydrolysis is appropriate because a high determination coefficient (R^2) of 0.98542, 0.90664, and 0.95227 was obtained for olive, canola, and soybean, respectively. In this part of the study, RSM was used as an approach for determining the region where the percentage of hydrolysis is maximized for the oils tested

Table 4 Effect and ANOVA for the free and encapsulated CRL on the hydrolysis of canola oil obtained by the experimental design employing three levels.

	Effect	Standard error	*p*	SS	*Df*	MS
Free CRL						
Mean/Interc.	3.18	±0.16	0.000007			
Curvature	*6.80*	*±0.53*	*0.000051*	*35.53*	*1*	*35.53*
(1) pH	−0.62	±0.33	0.115881	0.79	1	0.79
(2) Temperature	−0.22	±0.33	0.532231	0.10	1	0.10
(3) Concentration	*−2.37*	*±0.33*	*0.000805*	*11.20*	*1*	*11.20*
1 by 2	−0.20	±0.33	0.570550	0.08	1	0.08
1 by 3	*−1.59*	*±0.33*	*0.004725*	*5.06*	*1*	*5.06*
2 by 3	0.50	±0.33	0.185929	0.51	1	0.51
Error				1.08	5	0.18
Total SS				54.34	12	
Encapsulated CRL						
Mean/Interc.	*4.29**	*±0.02*	*0.000000**			
Curvature	*−3.57**	*±0.07*	*0.000000**	*9.87**	*1*	*9.87**
(1) pH	*−4.82**	*±0.03*	*0.000000**	*46.47**	*1*	*46.47**
(2) Temperature	*0.15**	*±0.03*	*0.016772**	*0.044**	*1*	*0.044**
(3) Loading	0.087	±0.03	0.096542	0.015	1	0.015
1 by 2	*−0.81**	*±0.03*	*0.000007**	*1.349**	*1*	*1.349**
1 by 3	*0.18**	*±0.03*	*0.008934**	*0.062**	*1*	*0.062**
2 by 3	*0.23**	*±0.03*	*0.002696**	*0.109**	*1*	*0.109**
Error				0.018	5	0.003
Total SS				57.939	12	

For free CRL, R^2 =0.95227; for encapsulated CRL, R^2 =0.99926

Table 5 Effect and ANOVA for the free and encapsulated CRL on the hydrolysis of soybean oil obtained by the experimental design employing three levels.

	Effect	Standard error	*p*	SS	*df*	MS
Free CRL						
Mean/Interc.	3.28	±0.22	0.000027			
Curvature	*6.63**	*±0.72*	*0.000254**	*33.78**	*1*	*33.78**
(1) pH	−0.77	±0.45	0.146278	1.18	1	1.18
(2) Temperature	−0.29	±0.45	0.550681	0.16	1	0.16
(3) Concentration	*−2.63**	*±0.45*	*0.002014**	*13.81**	*1*	*13.81**
1 by 2	0.02	±0.45	0.959938	0.001	1	0.001
1 by 3	−0.17	±0.45	0.718635	0.06	1	0.06
2 by 3	−0.38	±0.45	0.433811	0.29	1	0.29
Error				1.99	5	0.39
Total SS				51.27	12	
Encapsulated CRL						
Mean/Interc.	*4.34**	*±0.09*	*0.000000**	*5.80**	*1*	*5.80**
Curvature	*−2.75**	*±0.29*	*0.000232**	*65.78**	*1*	*65.78**
(1) pH	*−5.72**	*±0.18*	*0.000001**	*0.02**	*1*	*0.02**
(2) Temperature	0.09	±0.18	0.653743	0.19	1	0.19
(3) Loading	0.31	±0.18	0.151864	0.01	1	0.01
1 by 2	0.06	±0.18	0.732805	0.11	1	0.11
1 by 3	−0.24	±0.18	0.245813	0.16	1	0.16
2 by 3	0.28	±0.18	0.182921	5.80	1	5.80
Error				0.33	5	0.33
Total SS				72.37	12	

For free CRL, R^2 =0.90664; for encapsulated CRL, R^2 =0.98905

(Fig. 1), confirming that in the ranges studied, temperature (30–44 °C) is at its optimum and pH (4 to 10) is optimum in the lower range of the 4 to 7 interval.

According to Fu et al. [16], a complete hydrolysis can be achieved by either lengthening the reaction time at low free enzyme concentration or increasing the enzyme concentration for a shorter reaction time, to achieve 90–98% hydrolysis with coconut oil and other oils, and lipase from *Aspergillus* sp. The former is preferable for industrial production when using an expensive enzyme.

Encapsulated Lipase

Table 3 shows that for the encapsulated lipase, the region where the percentage of hydrolysis is maximized as a function of pH, temperature, and lipase loading. POH data for canola oil showed significant effects in the statistical analyses for pH and temperature and also for the interactions between pH and temperature and temperature and biocatalyst loading (Table 4). For the olive and soybean oils, it was verified that with encapsulated lipase, the pH was the only variable statistically significant (Tables 5 and 6).

The analysis of variance (Tables 4, 5, and 6) showed that the statistical significance of the responses for the percentage of hydrolysis is appropriate because a high determination coefficient R^2=0.98229, 0.99926, and 0.98905 was obtained for olive, canola, and soybean oil, respectively. Statistical analyses showed significant effects for pH and demonstrate high statistical significance ($p<0.05$) at 95% confidence level. Tables 3, 4, 5, and 6 and Fig. 2 indicate a region of higher POH where the temperature is around 37 °C, and there is maximum loading of the entrapped lipase for the tested oils. These results were

Table 6 Effect and ANOVA for the free and encapsulated CRL on the hydrolysis of olive oil obtained by the experimental design employing three levels.

	Effect	Standard error	*P*	SS	*df*	MS
Free CRL						
Mean/Interc.	*5.59**	*±0.14*	*0.000000**			
Curvature	*2.91**	*±0.44*	*0.001195**	*6.53**	*1*	*6.53**
(1) pH	*−5.79**	*±0.26*	*0.000004**	*67.18**	*1*	*67.18**
(2) Temperature	0.36	±0.26	0.249549	0.25	1	0.25
(3) Concentration	*−4.78**	*±0.26*	*0.000011**	*45.80**	*1*	*45.80**
1 by 2	−0.36	±0.26	0.249549	0.25	1	0.25
1 by 3	*1.06**	*±0.26*	*0.011774**	*2.24**	*1*	*2.24**
2 by 3	0.15	±0.26	0.578532	0.05	1	0.05
Error				0.74	5	0.15
Total SS				123.04	12	
Encapsulated CRL						
Mean/Interc.	*4.86**	*±0.12*	*0.000000**			
Curvature	*−3.61**	*±0.38*	*0.000220**	*10.00966*	*1*	*10.00966*
(1) pH	*−5.67**	*±0.24*	*0.000002**	*64.30002*	*1*	*64.30002*
(2) Temperature	−0.12	±0.24	0.645975	0.02653	1	0.02653
(3) Loading	0.32	±0.24	0.233711	0.20399	1	0.20399
1 by 2	−0.05	±0.24	0.800594	0.00789	1	0.00789
1 by 3	−0.03	±0.24	0.915946	0.00137	1	0.00137
2 by 3	−0.38	±0.24	0.170894	0.28420	1	0.28420
Error				0.55633	5	0.11127
Total SS				75.39000	12	

For free CRL, R^2 =0.98542; for encapsulated CRL, R^2 =0.98229

experimentally confirmed, and the POH was determined for different vegetable oils using an experimental design. Similar values have been found for fatty acids as previously obtained by our group in other studies [6, 17]. This study demonstrated that the statistical analysis is an efficient tool to unfold the influences of pH, temperature, and lipase loading on the POH.

The results of the experimental design for the encapsulated lipase were also analyzed by the RSM using the software STATISTICA® to find the region where a high POH for canola, soybean, and olive oils can be obtained as a function of pH, temperature, and lipase loading. A high percentage of hydrolysis is important for the biotechnological production processes of biodiesel and fatty acids.

Analyzing the curvatures in Tables 4, 5, and 6, one concludes that the POH profile approximates to the optima region for the tested oils utilizing entrapped enzyme. RSM for entrapped lipase (Fig. 2) shows that the typical POH profiles is different from that of free lipase (Fig. 1), while the pH effect is very significant for the entrapped lipase (Fig. 2) with all tested oils; for the free enzyme, the POH is more affected by pH only for olive oil. Maximum hydrolysis was observed at lower pH for the entrapped lipase, whereas for the free enzyme, the maximum hydrolysis occurred at pH 7, for canola and soybean oils. POH was generally smaller for lower loadings of entrapped enzyme, as shown in Tables 3, 4, 5, and 6. This could be due to the limitation of substrate diffusion toward the biocatalyst surface and into the pores of the support because of its microporous structure.

Recently, the RSM has been used to determine the kinetic constants of enzymatic reactions as well as for the optimization of reactions. Boyaci [18] used RSM and the

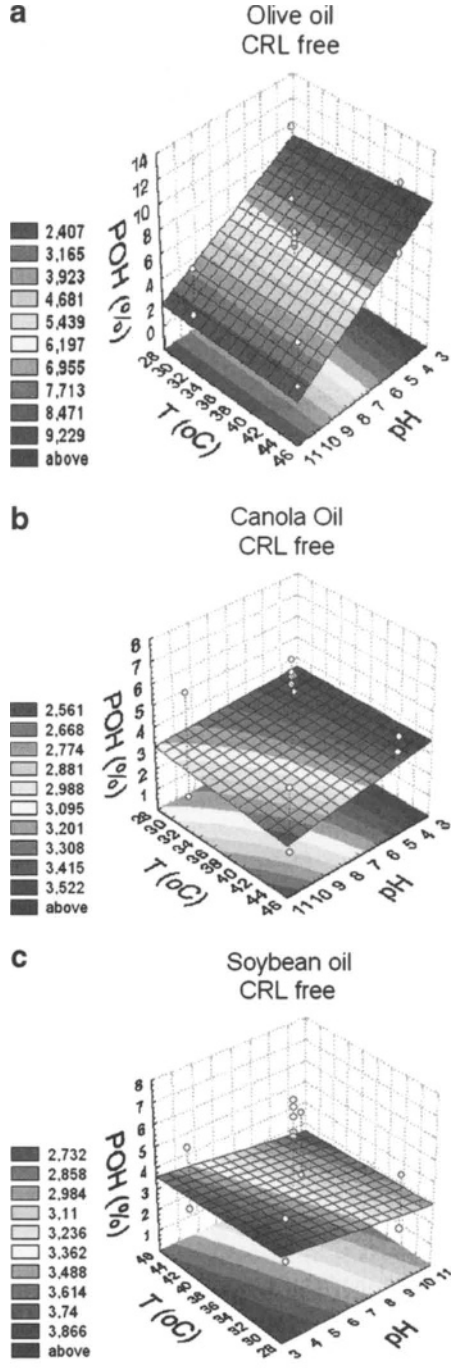


Fig. 1 Surface response plot of free CRL hydrolysis of olivc (**a**), canola (**b**), and soybean oil (**c**) showing the POH dependence on pH, temperature, and substrate concentration

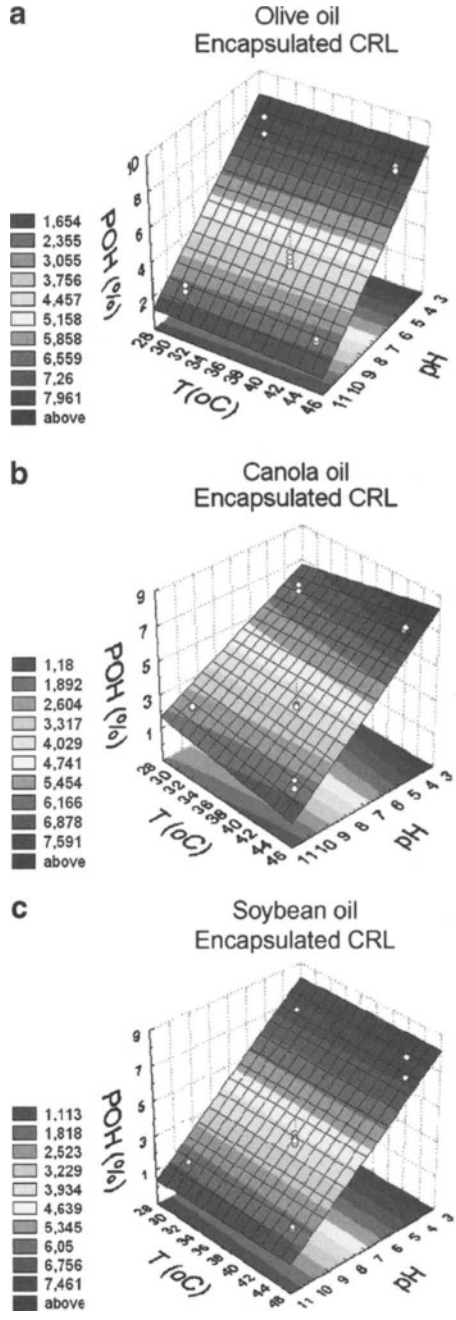


Fig. 2 Surface response plot of encapsulated CRL hydrolysis of olive (**a**), canola (**b**), and soybean oil (**b**) showing the POH dependence on pH, temperature, and lipase loading

conventional method to determine the kinetic constants of glucose oxidase as a function of reaction temperature and pH. The accuracy of the RSM for determining K_m and V_{max} was tested by comparing the results of these two methods. According to the author, reasonable results in the range of tested parameters were reached. A quite good correlation between the

kinetic constants of horse liver alcohol dehydrogenase obtained from conventional methods and those obtained from RSM was also reported by Andersson and Adlercreutz [19].

Conclusions

For free lipase, the POH varied from 0.62 to 11.69%, for temperatures from 30 to 44 °C, pH from 4 to 10, and oil/water ratio from 40 to 70%. The results show that the initial concentration of reactants (oil-to-water ratio) is the most important variable, with a negative effect, which means that an increase in the oil/water ratio leads to a decrease in the POH. In the case of canola and soybean oils, better results were observed using 50% oil–water ratio at 37 °C, pH 7, whereas for olive oil, the pH and concentration of reactants (oil–water ratio) were statistically significant at 95% of confidence, giving higher POH when lower pH (4) and lower substrate concentration (30%) were used for olive oil. The interactions between the variables were not statistically significant in the range studied for all the three types of oils studied. For free lipase, at 70% oil–water ratio, all oil suspensions have shown a POH lower than that observed at 50% oil–water ratio, suggesting substrate mass transfer limitations at the highest oil concentrations. Analysis of variance showed that the statistical significance for the POH responses were appropriate because a high determination coefficient (R^2) was obtained for the three oils. The RSM was used for determining the region where the percentage of hydrolysis is maximized for the oils tested and showed that in the range of the variables studied, temperature is approximately at its optimum (30–44 °C) and the lower pHs between 4 and 7 are optimum for the oils tested.

For the encapsulated lipase, the analysis of variance of the POH data showed that the statistical significance obtained is appropriate too because a high determination coefficient (R^2) resulted for the three oils. Statistical analyses showed significant effects for pH only and demonstrate high statistical significance at 95% confidence level. The results of the experimental design for the encapsulated lipase were also analyzed by the RSM to find the region where a high POH for the tested oils can be obtained as a function of pH, temperature, and lipase loading, giving temperatures approximately 37 °C and maximum entrapped lipase loading (9 mg mL^{-1}). The POH profiles obtained by the RSM show the optima region for the tested oils hydrolyzed by the entrapped lipase and the typical profiles for encapsulated lipase differs from that of free lipase, while the pH effect is very significant for the entrapped lipase with all tested oils; for the free enzyme, the POH is more affected by pH only for olive oil. Maximum hydrolysis was observed at lower pH for the entrapped lipase, whereas for the free enzyme, the maximum hydrolysis occurred at pH 7, for canola and soybean oils. Decreasing immobilized enzyme loading resulted in a reduction in the POH, and this effect was attributed to microporous diffusion limitations. A high percentage of hydrolysis is important for the processes of production of biodiesel and fatty acids.

This study demonstrated that the RSM is appropriate for the maximization of the hydrolysis of olive, canola, and soybean oils by free and sol–gel-entrapped lipase as a function of pH, temperature, and enzyme loading. Examining the curvature of the RSM graphics allowed concluding that the profiles studied approximate to the optima for the experiments carried out using different vegetable oils. This methodology also makes it possible to locate a desirable working region where a better performance for the hydrolysis reaction can be achieved.

Acknowledgments We acknowledge financial assistance from Coordenação de Aperfeiçoamento de Pessoal de Ensino Superior (CAPES), Conselho Nacional de Desenvolvimento Científico e Tecnológico (CNPq), and Fundação Araucária.

References

1. Reetz, M. T., Zonta, A., & Simpelkamp, J. (1996). *Biotechnology and Bioengineering, 49*, 527–534.
2. Reetz, M. T. (1997). *Advanced Materials, 9*, 943–954.
3. Reetz, M. T., Zonta, A., Vijayakrishnan, V., & Schimossek, K. (1998). *Journal of Molecular Catalysis. A, Chemical, 134*, 251–258.
4. Ghosh, S., & Bhattacharyya, D. K. (1995). *Journal of the American Oil Chemical Society, 72*, 1541–1544.
5. Buisson, P., Hernandez, C., Pierre, M., & Pierre, A. C. (2001). *Journal of Non-Crystalline Solids, 285*, 295–302.
6. Soares, C. M. F., Santos, O. A. S., Olivo, J. E., Castro, H. F., de Moraes, F. F., & Zanin, G. M. (2004). *Journal of Molecular Catalysis. B, Enzymatic, 29*, 69–79.
7. Kunkova, G., Szilva, J., Hetflejs, J., & Sabata, S. (2003). *Journal of Sol–Gel Science and Technology, 26*, 1183–1187.
8. Dutoit, D. C. M., Schneider, M., Fabrizioli, P., & Baiker, A. (1996). *Chemistry of Materials, 8*, 734–743.
9. Unger, K. K. (1979). *Porous silica its properties and use as support in column liquid chromatography* (p. 376). New York: Elsevier.
10. Orthoefer, F. (1996). Bailey's handbook of industrial oils and fats (5th ed., p. 1). New York: Wiley (chapter 2).
11. Bailie, P. M., McNerlan, S. E., Robinson, E., & Murphy, W. R. (1995). The immobilisation of lipases for the hydrolysis of fats and oils. Transactions of the Institution of Chemical Engineers, 73(Part C), 71–76.
12. Murray, M., Rooney, D., Van Niekerk, M., Montenegro, A., & Weatherley, L. R. (1997). *Process Biochemistry, 32*(6), 479–486.
13. Niekerk, M. V., & Weatherley, L. R. (1996). Electrostatically enhanced enzymatic hydrolysis of vegetable oil. *Transactions of the Institution of Chemical Engineers, 74*(C1), 22–26.
14. Socinol Indústria E Comércio (2000). Fábrica Sítio Bela Vista—Bairro Capotuna, C.P: 66, CEP: 13828.
15. Rooney, D., & Weatherle, L. R. (2001). *Process Biochemistry, 36*, 947–953.
16. Fu, X., Zhu, X., Gao, K., & Duan, J. (1995). *Journal of the American Oil Chemical Society, 72*, 527–531.
17. Soares, C. M. F., Santos, O. A. A., de Castro, H. F., Itako, J. E., de Moraes, F. F., & Zanin, G. M. (2006). *Journal of Non-Crystalline Solids, 352*, 3469–3477.
18. Boyaci, I. H. (2005). *Biochemical Engineering Journal, 25*, 55–62.
19. Andersson, M., & Adlercreutz, P. (1999). *Biotechnology Techniques, 13*, 903–907.

Appl Biochem Biotechnol (2008) 146:215–222
DOI 10.1007/s12010-007-8033-y

Improving Activity of Salt-Lyophilized Enzymes in Organic Media

Abhijeet P. Borole · Brian H. Davison

Received: 14 May 2007 / Accepted: 27 August 2007 /
Published online: 15 September 2007
© Humana Press Inc. 2007

Abstract Lyophilization with salts has been identified as an important method of activating enzymes in organic media. Using salt-activated enzymes to transform molecules tethered to solid surfaces in organic phase requires solubilization of enzymes in the solvents. Methods of improving performance of salt-lyophilized enzymes, further, via chemical modification, and use of surfactants and surfactants to create fine emulsions prior to lyophilization are investigated. The reaction system used is transesterification of *N*-acetyl phenylalanine ethyl ester with methanol or propanol. Initial rate of formation of amino acid esters by subtilisin Carlsberg (SC) was studied and found to increase two to sevenfold by either chemical modification or addition of surfactants in certain solvents, relative to the salt (only)-lyophilized enzyme. The method to prepare highly dispersed enzymes in a salt-surfactant milieu also improved activity by two to threefold. To test the effect of chemical modification on derivatization of drug molecules, acylation of bergenin was investigated using chemically modified SC.

Keywords Subtilisin Carlsberg · Salt lyophilization · Nonaqueous media · Drug derivatization · Bergenin · Acylation · Surfactant · PEG

Introduction

Derivatization of drug candidates to prepare diversified libraries has traditionally been done via combinatorial chemistry. There have been several reports on using enzymes for drug derivatization, and this combined with high-throughput screens has led to the development of the field of combinatorial biocatalysis [1–3]. Derivatization of molecules with certain ligands such as acyl and aromatic moieties introduces the need to conduct reactions in

The submitted manuscript has been authored by a contractor of the US Government under contract No. DE-AC05-00OR22725. Accordingly, the US Government retains a nonexclusive, royalty-free license to publish or reproduce the published form of this contribution, or allow others to do so, for US Government purposes.

A. P. Borole (✉) · B. H. Davison
Biosciences Division, Oak Ridge National Laboratory, Oak Ridge, TN 37831-6226, USA
e-mail: borolea@ornl.gov

organic media, which improves the solubility of the reacting substrates. However, enzymes typically have lower activities in organic media [4]. The increasing application of biocatalytic processes in pharmaceutical, food, and fine chemical industries has resulted in methods to improve the activity and stability of enzyme biocatalysts in organic media [5–7]. These methods include immobilization techniques [8]; stabilization via lyophilization with lyoprotectants [9], salts [10], or addition of surfactants [11, 12]; chemical modification with amphiphilic or hydrophobic polymers [13, 14]; and activation by addition of salts during lyophilization [10, 13].

The salt-based lyophilization method has shown activation of up to four orders of magnitude for enzymatic reactions in organic media [10, 13, 15]. Whereas this method improves activity, it does not improve solubility of the enzymes. Additionally, if the substrates are attached to surfaces, such as in microwell plates [16] to perform sequential derivatization, solubilization of enzymes would certainly help in increasing the rate of conversion of the attached substrates. The goal of this work was to investigate the effect of chemical modification and surfactant addition on transesterification rate of salt-lyophilized subtilisin Carlsberg (SC) in organic solvents. SC is a protease from *Bacillus licheniformis* capable of transesterifying alkyl esters. The chemical modification and surfactant addition can potentially assist in protein solubilization and thus improve the rate of the reaction. The enzyme was modified with polyethylene glycol (PEG) and an alkyl group, 14 carbons long, followed by salt-lyophilization to study the effect of chemical modification. Two surfactants, Aerosol OT (AOT) and Tween 20 (T 20), were studied to determine the effect on activity in various organic solvents. Bergenin was used as a model drug substrate to demonstrate enzymatic transformation in organic media.

Materials and Methods

Chemical Modification of Enzyme

The enzyme SC was modified with methoxy PEG (molecular weight 5,000) activated with p-nitrophenyl carbonate (Sigma, M-3903). The enzyme (240 mg) was dissolved in 100 mM potassium phosphate buffer pH 7.8 and stirred with 480 mg (~10 × molar equivalent) PEG for a period of 2 h. The reaction was monitored by release of the p-nitrophenyl group (absorbance at 405 nm). The modified enzyme was purified from the solution by washing with phosphate buffer in an ultrafiltration cell (Amicon, Model 8050) using a 30,000-Da molecular weight cut-off membrane, over several hours. The modified enzyme was then lyophilized as described below.

A double modification of SC with two groups, a C14 alkyl group and PEG, was conducted to obtain a PEG-C14-SC. The enzyme SC has 10 lysine groups accessible for chemical ligation. The PEG-C14-SC was prepared by first modifying the SC with methoxy PEG using a molar ratio of 1:2, enzyme/methoxy PEG, followed by modification with tetradecaldehyde. The first modification (with methoxy PEG) was conducted over a 2-h period, followed by washing in an ultrafiltration cell as described above. The procedure for the C14 modification consisted of dissolving 240 mg of SC modified with PEG in a 50:50 mixture of potassium phosphate buffer and ethanol, followed by addition of 400 mg of sodium cyanoborohydride, followed by the addition of 40.8 mg of tetraldehyde suspended in 2 mL ethanol. The mixture was stirred over a period of 2 h, followed by a washing step in an ultrafiltration cell to remove excess reagent.

Salt-Lyophilization of Enzyme

Native and modified SC were lyophilized with 0, 50, 75, and/or 99% salt concentration (in the lyophilized preparation). The salt mixture used contained 75% sodium bicarbonate and 25% sodium acetate by weight [13], with the total salt concentration at 1 M in the salt–SC solution used for lyophilization. The solution also contained 1 mg/mL potassium phosphate, pH 7.8, to buffer the lyophilized enzyme. The salt–SC solutions were lyophilized for a period of 36 h at −50°C and 8 μm Hg.

Enzyme Assays

The reaction system used for studying the activity of SC was transesterification of *N*-acetyl phenylalanine ethyl ester (APEE) with n-propanol or methanol. A solution of APEE was prepared in propanol and added into reaction vials giving a final propanol concentration of 0.85 mM and APEE concentration of 20 mM. The solvents studied were hexane, toluene, and methanol. In case of methanol, the reaction of interest was methanolysis of the ester. The total solvent volume used was 3 or 5 mL. Hexane and toluene were used after overnight saturation with distilled water, whereas methanol solvent used was prepared by adding 1 vol% deionized water to neat methanol. The reactions were carried out for a period of 4 h, to obtain a linear rate representing V_{max}. Aliquots of 300 μL were collected at five different time points between 20 min after the start of the reaction and the end of the run, and they were analyzed by gas chromatography (GC) or high-pressure liquid chromatography (HPLC). The concentration vs. time data between 20 and 240 min were plotted to obtain an initial rate of reaction. This plot was linear with R^2 between 0.90 and 0.99.

The effect of the surfactants AOT (Fischer Scientific) and T 20 (Sigma, P-7949) was assessed by adding these surfactants into the reaction vials at the beginning of the experiment as a solution or suspension in the solvent being studied. The amount of surfactant was equal to the amount of the enzyme–salt mixture (about 5–10 mg per reaction). The reactions were carried out in Teflon-lined screw-cap vials with shaking at 200 rpm and at 37°C with pyrene as an internal standard at 0.5 mM. A control with no enzyme was also run with each experiment. No conversion was obtained in the control reactions. The error in the rate calculations was estimated by obtaining a cumulative error in measurements that went into the rate equation. This included the experimentally determined slope of concentration vs. time plot (R^2 between 0.90 and 0.99), error in weighing the enzyme catalyst and assessment of enzyme concentration in the salt-enzyme preparation. The errors in these analyses were 1–10%, 0–4%, and 1–9%, respectively. This results in a total error in the range 2–23%.

Derivatization of Bergenin

Bergenin is a model compound for flavonoids [17] exhibiting several pharmacologically relevant effects including antioxidant, free radical scavenging, metal ion chelation, and nuclear type II estrogen-binding antagonism. Bergenin (Sigma, B-6776) was derivatized with ethyl acetate to obtain bergenin 4,11-diacetate and bergenin 4-acetate [2, 18]. The experiment was conducted by adding 200 mM bergenin dissolved in methanol into 20-mL scintillation vials. The solvent (methanol) was volatilized, followed by addition of 2 mL toluene containing 5% dimethyl sulfoxide (giving 2 mM bergenin in the reaction vessel).

The ethyl acetate concentration in the reaction vessel was 100 mM. The reaction was carried out by shaking at 200 rpm at 40°C for a period of 66 h.

Surfactant-Assisted Salt Enzyme Nanodispersions

A preparation of the SC was made by adding the surfactant to the enzyme prior to lyophilization. This was done as follows: The enzyme SC was dissolved in the buffered salt solution, which was then dispersed into a solvent by addition of surfactants. The solvent used in this experiment was hexanol and the surfactants studied were AOT and T 20. The amount of surfactant was equal to the total amount of salt + SC (by weight), with the salt concentration being 1 M. The volume ratio of solvent/aqueous phase was 9:1. The two-phase mixture was emulsified by placing it in an untrasound water bath (Bransonic Ultrasonics, Model 3210R-DTH) for 2–3 min, after which the emulsion was frozen in place by keeping the sample in liquid nitrogen for 10 min. The frozen sample was then lyophilized for a period of 36 h at 8 μm of Hg and −50°C.

Analytical

Samples in methanol were analyzed by HPLC, and samples in toluene or hexane were analyzed by GC. The HPLC method used a C18 column (Shimadzu Premier C18, 5 μ) with acetonitrile–water mixture as mobile phase with gradient from 70 to 100% acetonitrile and UV detection at 280 nm. The GC method consisted of a 0.53 mm × 15 m DB5 column, with helium as the carrier gas, injector and detector temperatures of 250°C, and an oven temperature of 210°C.

Results and Discussion

Effect of Chemical Modification and Surfactants

Activity of Salt–Enzyme Preparations in Toluene and Hexane

Enzyme assays were conducted with native SC and PEG–SC to determine the effect of the PEG modification and addition of surfactant. The initial rate of transesterification was obtained by using the initial linear portion of the product formation curve. As indicated earlier, the data points (between 20 and 240 min) produced a linear plot, with an R^2 between 0.95 and 0.99. The results (Table 1) indicate that surfactants decreased rate of APEE transesterification in hexane for the native enzyme lyophilized with 99% salt; however, an enhancement of rate was observed in toluene. AOT has been shown to improve the rate of enzymatic reactions in certain organic solvents with pure enzymes and not in the presence of salts [19–21]. AOT can form either a micelle around the enzyme (in the presence of water) or can directly complex the enzyme in neat organic solvents. This is the first study, to our knowledge, investigating the effect of chemical modification and surfactants on salt-lyophilized enzymes. The idea behind using surfactants was to enable complexation of the salt–enzyme particle by the surfactant in the form of a reverse micelle to improve interaction with the substrate present in the solvent phase. Alternately, the substrate APEE itself may complex with the surfactant and improve its partitioning into the salt–enzyme phase, similar to a desolvation effect. Whereas the data suggest a beneficial effect of surfactant and chemical modification, the mechanism of rate enhancement is not completely clear.

Table 1 Initial rate of transesterification (V_{max}, mM/g SC-min) of APEE in hexane and toluene in presence of different surfactants.

	Hexane		Toluene	
	Native SC	PEG–SC	Native SC	PEG–SC
None	310	480	37	45
AOT	190	470	68	100
T 20	330	420	35	93

The estimated total error in calculation of the rates is 23% (maximum). This error is cumulative error in measurement of product concentration by GC and determination of enzyme concentration during weighing and lyophilization procedure.

The presence of AOT resulted in an about twofold increase in initial rate of conversion in toluene, whereas T 20 did not improve activity. A similar effect was also observed with PEG-modified SC (PEG–SC). The PEG attachment by itself did not increase the rate of reaction significantly, although a larger enhancement was observed with the surfactants. In the case of T 20, PEG modification resulted in a twofold increase in activity, not observed with the native enzyme. With hexane as solvent, the PEG modification resulted in a slight increase in activity compared to the activity of the native enzyme. However, given the 23% estimated error (Table 1) in determination of the rate, this difference is not significant. Whereas the surfactant AOT appeared to negatively affect the activity in hexane for the native enzyme, the PEG modification appeared to reduce this deleterious effect.

Activity of Salt–Enzyme Preparations in Methanol

The activity of the native and modified SC was also studied for the reaction: methanolysis of APEE, using the substrate, methanol, itself as a solvent. This was done for three different salt–enzyme preparations, consisting of 99% salt, 50% salt, and no added salt (except that present in buffer). It was found that the PEG modification resulted in a six- to sevenfold increase in the initial rates of conversion for the cases with no surfactant and with T 20 (Table 2). AOT was found to reduce the activity of the enzyme preparations in all experiments conducted in the solvent methanol. Previous reports on enzymatic conversion in organic solvents have shown the effect of the solvent dielectric constant on enzyme activity for salt-free enzymes [22]. Relationship between activity of AOT and PEG-modified SC to the hydrophobicity coefficient of various solvents has also been studied [20], however, only for the enzymes without salt-lyophilization. The decrease in activity of enzymes in organic solvents is attributed to the decreased water availability in organic media. Additionally, as the dielectric constant increases, the potential for removal of the

Table 2 Initial rates of conversion (V_{max}, mM/g SC-min) of APEE to APME in methanol.

	99% salt			50% salt			No salt (except buffer salts)		
	None	AOT	T 20	None	AOT	T 20	None	AOT	T 20
Native SC	370	330	220	26	15	34	45	20	37
PEG–SC	2420	750	2880	52	21	54	25	NA	25
PEG-C14-SC	420	250	410	7	NA	7	5.5	0.2	4.8

The estimated total error in calculation of the rates is 23% (maximum), as described in Table 1.

Table 3 APEE transesterification in millimolars per gram SC-min using SSENDs catalyst in hexane and comparison with reactions with native SC in presence of surfactants added postlyophilization.

	AOT	T 20
SC–AOT	1,050±330	
SC–T 20		730±80
Native SC	380	450

Note that the AOT and T 20 were not readded in the reactions with SSENDs catalyst (but they were present in the preparation due to addition before lyophilization). The surfactants indicated below were added (postlyophilization) only in the experiment with the native SC. The standard deviation for the SSEND samples is for duplicate experiments.

layer of hydration from enzyme microenvironment increases. The inclusion of salts with the enzymes, in essence, reduces the effect of solvents on the enzyme microenvironment and on the hydration layer, thereby increasing activity of the enzymes in organic media. A relationship between solvent parameters and salt-lyophilized enzymes has, however, not been reported. From our results, the addition of surfactants or chemical modification of enzymes appears to introduce additional complexity into the interaction between the enzyme and the solvent, further complicating any relationship that can be derived. A comparison of the enhancement in rate observed with 98 and 50% salt is not linear and resembles what has been reported with preparations without use of surfactants [23]. Further work is necessary to understand the enhancement observed in the rate of transesterification reactions. This is being pursued by systematically deriving catalytic efficiencies for various solvents in the presence and absence of surfactants and chemical modifications.

Surfactant-Assisted Salt Enzyme Nanodispersions

To increase dispersion or surface area of salt–enzyme preparations in organic media, a method of preparing surfactant-assisted salt enzyme nanodispersions (SSENDs) was explored. The goal was to create a fine dispersion of the salt enzyme lyophilized particles with the use of a surfactant prior to lyophilization by creation of a fine emulsion, followed by removal of solvent and water by lyophilization. Microscopic observation of the emulsion indicated a submicron dispersion of the aqueous phase in the solvent. The results of the enzyme assay using SSENDs catalyst is shown in Table 3. This experiment was conducted in hexane to determine if such a preparation can enhance activity of the enzyme because postlyophilization addition of the surfactant did not improve the rate of the reaction. The results show that a two- to threefold higher rate can be obtained by preparation of the salt–SC using the SSENDs preparation method.

Table 4 Acylation of bergenin by native and chemically modified SC in hexane and toluene.

	Bergenin 4,11-diacetate	Bergenin 11-acetate
Native SC	20	5
PEG–SC	20	6
PEG-C14-SC	18	5

Rate is given in millimolars per gram SC-min. The response factor for bergenin was used for quantitation of the products.

Derivatization of Bergenin

One of the goals of this study was to identify experimental conditions for biotransformations in organic media and apply them to derivatization of drug candidates. Along these lines, derivatization of bergenin was studied using chemically modified SC to determine change in the rate of reaction. Bergenin consists of two hydroxyl groups capable of acylation by lipase biocatalysis, at positions 4 and 11 [18]. Thus, alteration of specificity due to introduction chemical modification was also investigated. The results (Table 4) indicate that the chemical modification did not introduce any significant change in specificity or rate of the reaction.

Conclusions

Effect of surfactants and chemical modification was studied on salt-lyophilized SC in organic solvents. Modification with PEG was found to enhance the initial rate of transesterification marginally in toluene but about five- to sixfold in methanol. Addition of AOT to the reaction mixture was found to enhance the rate by about threefold in toluene, but reduced it in hexane and methanol. The combined effect of the presence of salt, surfactant, and solvent appears to result in a complex interaction with the enzyme resulting in an, as yet, unpredictable change in the reaction rate as a result of a change in its microenvironment. Further work to determine catalytic efficiencies for a variety of solvents and surfactants is necessary to better understand the interactions. Creation of fine emulsions of enzyme–salt solutions prior to lyophilization using surfactants appears to enhance the activity of lyophilized biocatalysts prepared using the SSENDs method. Finally, conversion of bergenin in toluene was not affected significantly by chemical modification of the enzyme. Further work investigating the effect of surfactants on bergenin conversion is under way.

Overall, chemical modification and surfactants appear to offer moderate enhancements in some cases compared to salt-lyophilized enzymes. However, these enhancements are small compared to the original advantages of salt lyophilization.

Acknowledgements The authors wish to acknowledge support from the National Institute of Health under the Bioengineering Research Partnerships. Initial project direction and assistance from Dr. Jonathan Dordick is greatly appreciated.

References

1. Altreuter, D. H., & Clark, D. S. (1999). *Current Opinion in Biotechnology, 10*, 130–136.
2. Michels, P. C., Khmelnitsky, Y. L., Dordick, J. S., & Clark, D. S. (1998). *Trends in Biotechnology, 16*, 210–215.
3. Rich, J. O., Michels, P. C., & Khmelnitsky, Y. L. (2002). *Current Opinion in Chemical Biology, 6*, 161–167.
4. Dordick, J. S. (1992). *Biotechnology Progress, 8*, 259–267.
5. Adamczak, M., & Krishna, S. H. (2004). *Food Technology and Biotechnology, 42*, 251–264.
6. Gupta, M. N., & Roy, I. (2004). *European Journal of Biochemistry, 271*, 2575–2583.
7. Lee, M. Y., & Dordick, J. S. (2002). *Current Opinion in Biotechnology, 13*, 376–384.
8. D'Souza, S. F. (1999). *Current Science, 77*, 69–79.
9. Dai, L. Z., & Klibanov, A. M. (1999). *Proceedings of the National Academy of Sciences of the United States of America, 96*, 9475–9478.

10. Morgan, J. A., & Clark, D. S. (2004). *Biotechnology and Bioengineering, 85*, 456–459.
11. Sawae, H., Sakoguchi, A., Nakashio, F., & Goto, M. (2002). *Journal of Chemical Engineering of Japan, 35*, 677–680.
12. Song, B. D., Ding, H., Wu, J. C., Hayashi, Y., Talukder, M., & Wang, S. C. (2003). *Chinese Journal of Chemical Engineering, 11*, 601–603.
13. Mine, Y., Fukunaga, K., Yoshimoto, M., Nakao, K., & Sugimura, Y. (2001). *Journal of Bioscience and Bioengineering, 92*, 539–543.
14. Wang, L. F., Zhu, G. Y., Wang, P., & Newby, B. M. Z. (2005). *Biotechnology Progress, 21*, 1321–1328.
15. Hudson, E. P., Eppler, R. K., & Clark, D. S. (2005). *Current Opinion in Biotechnology, 16*, 637–643.
16. Altreuter, D. H., Dordick, J. S., & Clark, D. S. (2003). *Biotechnology and Bioengineering, 81*, 809–817.
17. Prior, R. L., & Cao, G. (1999). *Proceedings of the Society for Experimental Biology and Medicine, 220*, 255–261.
18. Mozhaev, V. V., Buddc, C. L., Rich, J. O., Usyatinsky, A. Y., Michels, P. C., Khmelnitsky, Y. L., et al. (1998). *Tetrahedron, 54*, 3971–3982.
19. Bindhu, L. V., & Abraham, T. E. (2003). *Biochemical Engineering Journal, 15*, 47–57.
20. Kwon, O. H., Imanishi, Y., & Ito, Y. (1999). *Biotechnology and Bioengineering, 66*, 265–270.
21. Paradkar, V. M., & Dordick, J. S. (1994). *Biotechnology and Bioengineering, 43*, 529–540.
22. Clark, D. S. (2004). *Philosophical Transactions of the Royal Society of London Series B, Biological Sciences, 359*, 1299–1307.
23. Ru, M. T., Wu, K. C., Lindsay, J. P., Dordick, J. S., Reimer, J. A., & Clark, D. S. (2001). *Biotechnology and Bioengineering, 75*, 187–196.

Appl Biochem Biotechnol (2008) 146:223–230
DOI 10.1007/s12010-007-8034-x

Protease Production by Different Thermophilic Fungi

Mariana M. Macchione · Carolina W. Merheb · Eleni Gomes · Roberto da Silva

Received: 15 May 2007 / Accepted: 27 August 2007 /
Published online: 12 October 2007
© Humana Press Inc. 2007

Abstract A comparative study was carried out to evaluate protease production in solid-state fermentation (SSF) and submerged fermentation (SmF) by nine different thermophilic fungi – *Thermoascus aurantiacus* Miehe, *Thermomyces lanuginosus*, *T. lanuginosus* TO.03, *Aspergillus flavus* 1.2, *Aspergillus* sp. 13.33, *Aspergillus* sp. 13.34, *Aspergillus* sp. 13.35, *Rhizomucor pusillus* 13.36 and *Rhizomucor* sp. 13.37 – using substrates containing proteins to induce enzyme secretion. Soybean extract (soybean milk), soybean flour, milk powder, rice, and wheat bran were tested. The most satisfactory results were obtained when using wheat bran in SSF. The fungi that stood out in SSF were *T. lanuginosus*, *T. lanuginosus* TO.03, *Aspergillus* sp. 13.34, *Aspergillus* sp. 13.35, and *Rhizomucor* sp. 13.37, and those in SmF were *T. aurantiacus*, *T. lanuginosus* TO.03, and 13.37. In both fermentation systems, *A. flavus* 1.2 and *R. pusillus* 13.36 presented the lowest levels of proteolytic activity.

Keywords Protease · Thermophilic fungi · Solid state fermentation · Submerged fermentation · Wheat bran

Introduction

Proteases are enzymes that break down protein molecules through peptide bond hydrolysis [1]. They are commercially employed in many industrial processes. In foods, proteases have two main applications: in the processing of traditional food products and in the processing of new protein-based ingredients called functional foods [2]. Proteases are also used in other industrial segments such as leather industry, pharmaceutical, waste management, and the detergent industry. Currently, microbial proteases make up approximately 40% of total enzyme sales [3, 4].

M. M. Macchione · C. W. Merheb · E. Gomes · R. da Silva (✉)
Laboratório de Bioquímica e Microbiologia Aplicada,
IBILCE - Instituto de Biociências Letras e Ciências Exatas, UNESP - Universidade Estadual Paulista,
Rua Cristóvão Colombo, 2265 São José do Rio Preto, São Paulo CEP 15054-000, Brazil
e-mail: dasilva@ibilce.unesp.br

Proteinaceous material such as horn, feather, nail, hair, and cheese whey occur in nature as waste and can be converted, by proteases, into liquid concentrates or dry solids with high protein content and of nutritional value for food and feed. Thus, proteases provide potential application for the management of residues from various food processing industries such as poultry and cattle slaughterhouses and fishing and dairy industries [5, 6].

Microorganisms are capable of producing extracellular proteases that degrade proteins into amino acids to make their assimilation possible [7]. Many of them exhibit a very wide production due to their fast growing rate and thus have become potential sources of industrial enzymes [1].

Thermophilic fungi are known to produce thermostable enzymes. The use of these enzymes may present many advantages, especially in the food industry, due to the high processing temperatures that could be applied, which are related to an increase in reaction rates, improved solubility of reagents, and a decrease in mesophilic contamination. Besides thermal stability, these enzymes also exhibit higher stability towards other protein denaturating conditions such as extreme pH values and compounds such as ionic detergents and organic solvents, when compared to similar mesophilic enzymes [8].

In this study, nine thermophilic fungi were screened for the production of protease in solid and submerged cultivation mediums. Tested fungi were: *Thermoascus aurantiacus* Miehe, *Thermomyces lanuginosus*, *T. lanuginosus* TO.03, *Aspergillus flavus* 1.2, *Aspergillus* sp. 13.33, *Aspergillus* sp. 13.34, *Aspergillus* sp. 13.35, *Rhizomucor pusillus* 13.36 and *Rhizomucor* sp. 13.37. Five different substrates were used: soybean extract (soybean milk), soybean flour, milk powder, rice, and wheat bran.

Materials and Methods

Microorganisms and Inoculum

The fungi *T. aurantiacus*, *T. lanuginosus*, *T. lanuginosus* TO.03, *A. flavus* 1.2, *Aspergillus* sp. 13.33, *Aspergillus* sp. 13.34, *Aspergillus* sp. 13.35, *R. pusillus* 13.36, and *Rhizomucor* sp. 13.37, belong to the culture bank of the Laboratory of Applied Biochemistry and Microbiology, *Instituto de Biociências Letras e Ciências Exatas*, *Universidade Estadual Paulista*. They were inoculated in test tubes with Sabouraud and were incubated at 45°C for 4 days until complete growth. Afterwards, they were kept at room temperature until further use.

The mycelium was suspended in 7 mL of sterilized nutrient solution made up of 0.1% (w/v) $(NH_4)_2SO_4$, $MgSO_4.7H_2O$ and NH_4NO_3, and 1 mL of this mycelial suspension was used to inoculate the culture medium.

Fermentation Medium and Culture Conditions

Protease Production Profile by Solid-State Fermentation Mediums containing 10 g of wheat bran hydrated with 15 mL of nutrient solution, to approximately 60% moisture, were sterilized (120°C/40 min) in 250-mL Erlenmeyer flasks. The mediums were inoculated with mycelial suspension from each fungus and cultivated at 45°C for 8 days. Samples were taken every 24 h. The crude enzyme solution was obtained by adding 25 mL of water to the fermented material. Solids were removed by filtering through Whatman no. 1 filter paper and centrifuging at 10,000 rpm/20 min, and finally, the clear solution was assayed.

Protease Production Profile in Different Substrates by Solid-State Fermentation Mediums containing 10 g of soybean extract (soybean milk), soybean flour, milk powder, rice, and

wheat bran hydrated with 15 mL of nutrient solution, to approximately 60% moisture, were sterilized (120°C/40 min) in 250-mL Erlenmeyer flasks. The mediums were inoculated with mycelial suspension from each fungus and cultivated at 45°C during maximum production period as determined earlier. Experiments were carried out in duplicate; the results shown are average values. The crude enzyme solution was obtained by adding 25 mL of water to the fermented material. Solids were removed by filtering through Whatman no. 1 filter paper. For soybean extract, soybean flour, milk powder, and rice, centrifugation (10,000 rpm/20 min) was carried out prior to filtering.

Protease Production Profile by Submerged Fermentation Mediums containing 2.5 g of wheat bran hydrated with 22.5 mL of nutrient solution, to approximately 90% moisture, were sterilized (120°C/40 min) in 125-mL Erlenmeyer flasks.

The mediums were inoculated with mycelial suspension from each fungus and cultivated on rotary shaker (150 rpm) at 45°C for 8 days. Samples were taken every 24 h. The crude enzyme solution was obtained by centrifuging (12,000 rpm/10 min) and filtering through Whatman no. 1 filter paper.

Protease Production Profile in Different Substrates by Submerged Fermentation Mediums containing 2.5 g of soybean extract (soybean milk), soybean flour, milk powder, rice, and wheat bran hydrated with 22.5 mL of nutrient solution, to approximately 90% moisture, were sterilized (120°C/40 min) in 125-mL Erlenmeyer flasks. The mediums were inoculated with mycelial suspension from each fungus and cultivated on rotary shaker (150 rpm) at 45°C during maximum production period, as determined earlier. Experiments were carried out in two sets; the results shown are average values. The crude enzyme solution was obtained by centrifuging (12,000 rpm/10 min) and filtering through Whatman no. 1 filter paper.

Proteolytic Activity

Proteolytic activity was assayed as described by Kembhavi et al. [9], with modification. The reaction mixture was made up of 0.4 mL of casein (Sigma) 0.5% (w/v) in distilled water and 0.4 mL 0.2 M acetate buffer, pH 5.0, to which 0.2 mL of the crude enzyme solution was added. The reaction was carried out at 60°C and stopped after 30 min with 1 mL of 10% trichloroacetic acid (TCA). Test tubes were centrifuged at 5,000 rpm/5 min, and the absorbance of the supernatant was measured at 280 nm. An appropriate control was prepared in which the TCA was added before the enzymatic solution. One unit of enzyme activity (U) was arbitrarily defined as the amount of enzyme required to cause an increase of 0.01 in absorbance at 280 nm under the assay conditions.

Results and Discussion

Protease Production Profile by Solid-State Fermentation

Figure 1 shows the protease production profile in solid medium through 8 days, and it can be seen that six fungi, *T. lanuginosus*, *T. lanuginosus* TO.O3, *Aspergillus* sp. 13.33, *Aspergillus* sp. 13.34, *Aspergillus* sp. 13.35, and *Rhizomucor* sp. 13.37, exhibited maximum production on the third day. *Thermoascus aurantiacus* revealed maximum production from the third day up to the fourth. *Rhizomucor pusillus* 13.36 showed a plateau of production from the third day up to the fifth. *Aspergillus flavus* 1.2 showed a peak at the fifth day. The highest

production peak in Fig. 1 was reached by *T. lanuginosus*, with 945.2 U/mL followed by *Aspergillus* sp. 13.33, *Rhizomucor* sp. 13.37, *T. lanuginosus* TO.03, *Aspergillus* sp. 13.35, *Aspergillus* sp. 13.34, and *T. aurantiacus* with 844.6, 770.9, 730.0, 640.5, 469.6, and 258.3 U/mL, respectively, all on the third day. The lowest peak was obtained by *A. flavus* 1.2 with 117.6 U/mL on the fifth day. From these results, an incubation period of 3 or 4 days was chosen for the experiment of protease production in different substrates (Fig. 2). The variability of the results obtained from the sets was below 5% for each experiment.

Figure 1 shows that maximum enzyme production occurred on the third day for most fungi. The subsequent decrease in enzyme activity as fermentation time increased was probably due to degradation of the extracellular enzymes. When dealing with proteases, autolysis may occur, and in this case, it was probably higher than the production of new enzymes by the fungi, reaching an equilibrium as seen by the low and fairly constant activity remaining after the fifth up to the eighth day. Also, depletion of nutrients available to the microorganisms [10] or even cessation of production, because enzymes are primary metabolites [11], might have contributed to the decrease in enzyme activity.

Protease Production Profile in Different Substrates by Solid-State Fermentation

Substrates rich in proteins may act as protease inducers [12, 13]. Thus, a group of these substrates was chosen to verify their potential as protease producers.

Fermentation medium that yielded highest protease production by all fungi tested was wheat bran, as shown in Fig. 2. In addition to being a good inducer for proteolytic enzyme production, wheat bran is an agro-industrial residue from wheat flour production, which is of low cost and always available. Other factors that make wheat bran an excellent substrate for protease production in solid-state fermentation (SSF) are, besides its composition, its texture, which gives it an adequate surface area with good porosity, acting as physical support and allowing the fungi to access the nutrients [14].

The worst substrate tested was milk powder. This probably occurred due to its thin granularity, which ends up allowing a gathering of the particles when moist, causing stickiness. Moreover, the heat treatment during sterilization may have promoted Maillard reactions, which maybe affected the availability of amino acids in the medium, and also caramelization reactions, both leading to a darkening and modification of the medium's texture.

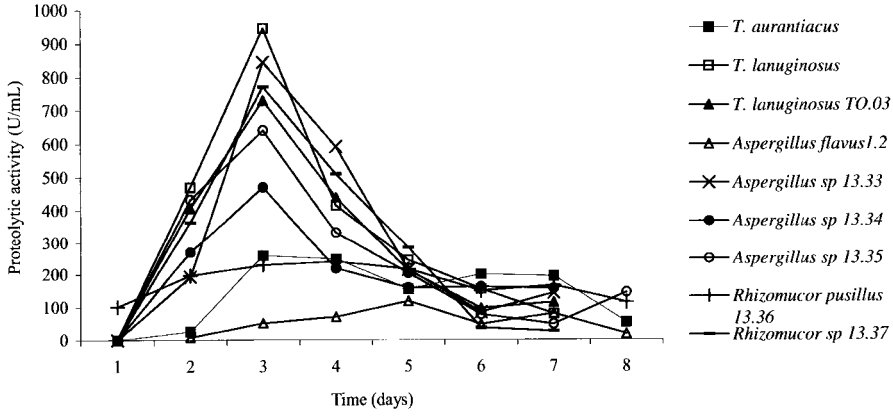


Fig. 1 Protease production profile by different thermophilic fungi in SSF using wheat bran as substrate

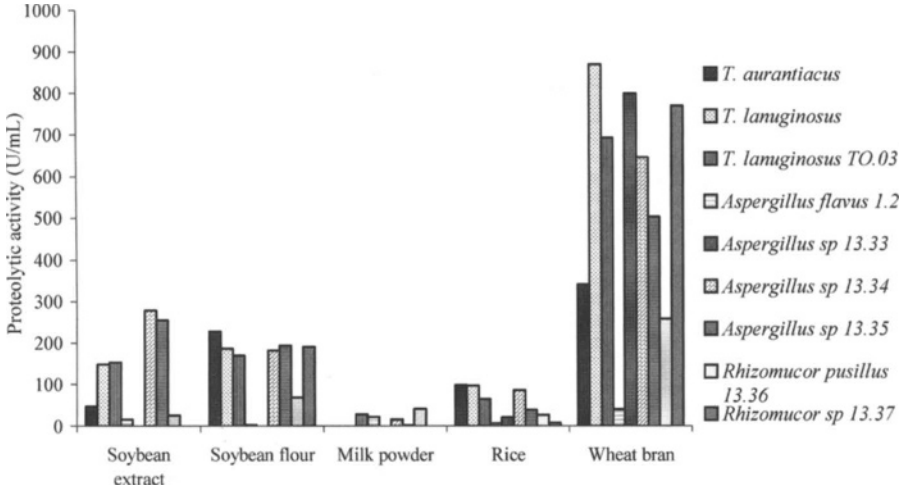


Fig. 2 Protease production by different thermophilic fungi in SSF using different substrates. *Thermoascus aurantiacus*, *T. lanuginosus*, *T. lanuginosus* TO.03, *Aspergillus* sp. 13.33, *Aspergillus* sp. 13.34, *Aspergillus* sp. 13.35, and *Rhizomucor* sp. 13.37: 3-day fermentation period. *Aspergillus flavus* 1.2 and *R. pusillus* 13.36: 4-day fermentation period

Soybean flour and soybean extract also exhibited, as main problems, thin granularity. The problem with rice was the difficulty in spreading the inoculum equally throughout the medium.

Protease Production Profile by Submerged Fermentation

Figure 3 shows protease production profile in liquid medium by submerged fermentation (SmF) through 8 days. It can be seen that most fungi exhibited maximum protease secretion

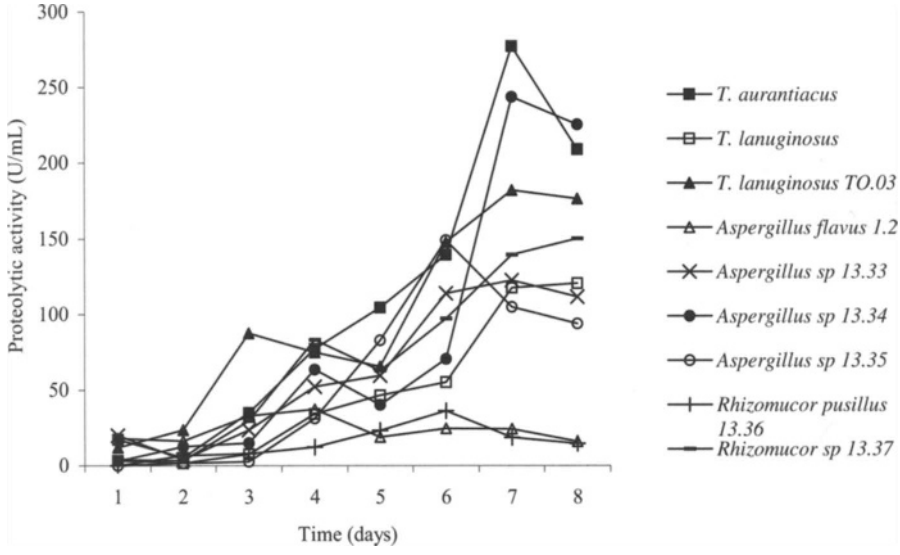


Fig. 3 Protease production profile by different thermophilic fungi in SmF using wheat bran as substrate

between the sixth and eighth days. The fungi *Aspergillus* sp. 13.35 and *R. pusillus* 13.36 showed maximum activity on the sixth day; fungus *T. aurantiacus* with the highest production (277.35 U/mL) and *T. lanuginosus*, *T. lanuginosus* TO.03, *Aspergillus* sp. 13.33, and *Aspergillus* sp. 13.34, also with high production (243.60 U/mL), showed maximum activity on the seventh day; and fungus *Rhizomucor* sp. 13.37 showed maximum activity on the eighth day. Hence, a 7-day incubation period for all fungi was adopted to continue with the SmF experiments using different substrates. It can also be seen in Fig. 3 that the lowest enzyme production was exhibited by *A. flavus* 1.2, with 37.22 U/mL on the fourth day.

Protease Production Profile in Different Substrates by SmF

Soybean extract and soybean flour were good inducers for protease production in SmF, as shown in Fig. 4. When compared to SSF, these results were similar. However, in SmF, there was a significant decrease in production when the substrate was wheat bran. Other researches have revealed that the SSF technique gives greater enzyme yield than SmF [10, 15]; however, there is not any established scale or method to compare product yield in SSF and SmF, and the exact reason for higher production in SSF is not well known yet [14]. It is known that the amount of enzyme produced varies with the cultivation medium used [16], meaning that the microorganism will behave differently according to the different types of substrates and conditions used for fermentation; thus, no defined medium has been established for the optimum production of protease from different microbial sources [17]. In SSF, the conditions may favor the growth of filamentous fungi, which generally grow in nature on solid material such as wood, leaves, and roots and other organic matter [18], explaining the higher enzyme yields. The major activity peaks occurred for *T. aurantiacus* on soybean extract (262.95 U/mL) and wheat bran (244.00 U/mL) and for *T. lanuginosus* TO.03 on soybean extract (185.02 U/mL) and soybean flour (193.55 U/mL).

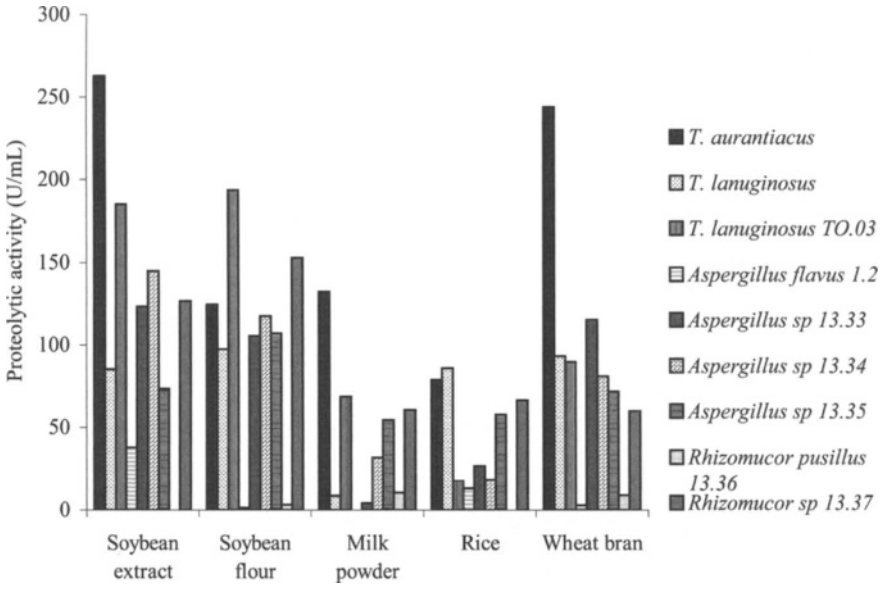


Fig. 4 Protease production by different thermophilic fungi in 7-day SmF using different substrates

The solubility of soybean extract, soybean flour, and milk powder had a positive influence on the results from SmF. For milk powder, the higher amount of water decreased the damaging effects of sterilization, especially regarding the texture, increasing enzyme production.

There was decrease in production in SmF when using rice, due to gelatinization, because it absorbed a lot of water during sterilization and incubation, decreasing the free water available for fermentation. The process was then similar to a SSF but with less substrate accessible for microbial growth. Similar results occurred when using wheat bran, where the biggest problem was probably the difficulty faced by the hyphae when penetrating the medium, besides the lower aeration due to the presence of water.

Cost and efficiency are major characteristics of enzymes for industrial application. Hence, it is desirable for the material used in the fermentation medium to be of low cost, available in large amounts, and continually renewable, which is exactly the case of agro-industrial residues, in addition to making microbial growth possible [19]. Thus, it should present in its composition carbon, nitrogen, and mineral sources, and, in the case of enzyme production, the presence of inducers is essential [18]. For the production of protease, substrates that contained proteins in its composition were chosen, and a nutrient solution was incorporated with the aim of making it suitable for the microorganism to grow in the desired fermentation [20].

Mediums used in submerged and solid fermentations present different characteristics. In SmF, the microorganism has more water available for its growth; there is the advantage of process control (pH, temperature, etc.) and it is easier to collect representative samples; and the heat and gases resulting from active growth can be easily dispersed, not causing a temperature increase. Some advantages of SSF are the possibility of using agro-industrial by-products offering the opportunity to process these residues, high product concentration, lower costs for enzyme recovery, less amount of liquid residues produced, and lower energy requirements [10, 14, 21].

Conclusions

The best condition for high protease production was using wheat bran in SSF. Soybean extract and soybean flour exhibited moderate production results for both types of fermentation; rice and milk powder did not present good results in either. Another type of sterilization can be suggested, such as filtration, when using medium made up of milk powder or even the addition of sterile water after the sterilization of dry material to improve the results. In spite of the fact that wheat bran was the best substrate for protease production, it should be noted that the inclusion of inducers such as the ones used in this work (powder milk, soybean flour, and soybean extract) might be beneficial as additives to the suitable solid substrate and should be further studied. SmF presented lower protease yields and longer fermentation time for maximum enzyme production.

Among the fungi tested, both strains of *T. lanuginosus* were revealed to be good protease producers in SSF. Fungi *Aspergillus* sp. 13.34, *Aspergillus* sp. 13.35, *Rhizomucor* sp. 13.37, *Aspergillus* sp. 13.33, and finally *T. aurantiacus* also stood out as good producers in this type of fermentation. Fungi *A. flavus* 1.2 and *R. pusillus* 13.36 exhibited the worst results due to the inconsistent curves and the low production peaks in all substrates tested. Thus, the most potent protease producer was *T. lanuginosus* in SSF with wheat bran.

Acknowledgement The authors would like to acknowledge the financial assistance provided by *Fundação de Amparo à Pesquisa do Estado de São Paulo.*

References

1. Eskin, N. A. M., Henderson, H. M., & Townsend, R. J. (1971). *Biochemistry of foods*. New York: Academic Press.
2. Nagodawithana, T., & Reed, G. (1993). *Enzymes in food processing* (3rd ed.). San Diego: Academic Press.
3. Gupta, R., Beg, Q. K., & Lorenz, P. (2002). *Applied Microbiology and Biotechnology, 59*, 15–32.
4. Rao, M. B., et al. (1998). *Microbiology and Molecular Biology Reviews, 62*, 597–635.
5. Kumar, C. G., & Takagi, H. (1999). *Biotechnology Advances, 17*, 561–594.
6. Anwar, A., & Saleemuddin, M. (1998). *Bioresource Technology, 64*, 175–183.
7. Zouari, N., & Jaoua, S. (1999). *Enzyme and Microbial Technology, 25*, 364–371.
8. Gusek, T. W., & Kinsella, J. E. (1988). *Food Technology, 42*, 102–106.
9. Kembhavi, A. A., Kulkarni, A., & Panti, A. (1993). *Applied Biochemistry and Biotechnology, 38*, 83–92.
10. Sandhya, C., et al. (2005). *Process Biochemistry, 40*, 2689–2694.
11. Sumantha, A., et al. (2005). *Food Technology and Biotechnology, 43*, 313–319.
12. Li, D. C., Yang, Y. J., & Shen, C. Y. (1997). *Mycological Research, 101*, 18–22.
13. Ong, P. S., & Gaucher, G. M. (1973). *Canadian Journal of Microbiology, 19*, 129–133.
14. Pandey, A. (2003). *Biochemical Engineering Journal, 13*, 81–84.
15. Wang, H. L., Vespa, J. B., & Hesseltine, C. W. (1974). *Applied Microbiology, 27*, 906–911.
16. Andrade, V. S., et al. (2002). *Brazilian Journal of Microbiology, 33*, 106–110.
17. Rao, Y. K., Lu, S., Liu, B., & Tzeng, Y. (2006). *Biochemical Engineering Journal, 28*, 57–66.
18. Germano, S., et al. (2003). *Enzyme and Microbial Technology, 32*, 246–251.
19. Fernandez, E. R. P. (2002). *Doctorate thesis*, Universidade Estadual Paulista, Rio Claro, Brasil.
20. Schmidell, W., et al. (2001). *Biotecnologia Industrial* (vol. 3). Edgard Blücher Ltda: São Paulo.
21. Souza, M. C. O. (1997). *Masters thesis*. Faculdade de Engenharia Química de Lorena, Lorena, Brasil.

Appl Biochem Biotechnol (2008) 146:231–248
DOI 10.1007/s12010-007-8035-9

Non-ionic Surfactants and Non-Catalytic Protein Treatment on Enzymatic Hydrolysis of Pretreated Creeping Wild Ryegrass

Yi Zheng · Zhongli Pan · Ruihong Zhang · Donghai Wang · Bryan Jenkins

Received: 21 May 2007 / Accepted: 27 August 2007 /
Published online: 27 September 2007
© Humana Press Inc. 2007

Abstract Our previous research has shown that saline Creeping Wild Ryegrass (CWR), *Leymus triticoides*, has a great potential to be used for bioethanol production because of its high fermentable sugar yield, up to 85% cellulose conversion of pretreated CWR. However, the high cost of enzyme is still one of the obstacles making large-scale lignocellulosic bioethanol production economically difficult. It is desirable to use reduced enzyme loading to produce fermentable sugars with high yield and low cost. To reduce the enzyme loading, the effect of addition of non-ionic surfactants and non-catalytic protein on the enzymatic hydrolysis of pretreated CWR was investigated in this study. Tween 20, Tween 80, and bovine serum albumin (BSA) were used as additives to improve the enzymatic hydrolysis of dilute sulfuric-acid-pretreated CWR. Under the loading of 0.1 g additives/g dry solid, Tween 20 was the most effective additive, followed by Tween 80 and BSA. With the addition of Tween 20 mixed with cellulase loading of 15 FPU/g cellulose, the cellulose conversion increased 14% (from 75 to 89%), which was similar to that with cellulase loading of 30 FPU/g cellulose and without additive addition. The results of cellulase and BSA adsorption on the Avicel PH101, pretreated CWR, and lignaceous residue of pretreated CWR support the theory that the primary mechanism behind the additives is prevention of non-productive adsorption of enzymes on lignaceous material of pretreated CWR. The addition of additives could be a promising technology to improve the enzymatic hydrolysis by reducing the enzyme activity loss caused by non-productive adsorption.

Y. Zheng (✉) · Z. Pan · R. Zhang · B. Jenkins
Biological and Agricultural Engineering Department, University of California, Davis,
One Shields Avenue, Davis, CA 95616, USA
e-mail: yizheng@ucdavis.edu

Z. Pan
Processed Foods Research Unit, USDA–ARS–WRRC, 800 Buchanan, St. Albany, CA 94710, USA

D. Wang
Biological and Agricultural Engineering Department, Kansas State University,
Manhattan, KS 66506, USA

Keywords Saline Creeping Wild Ryegrass · Cellulase · β-Glucosidase · Tween 20 · Tween 80 · Bovine serum albumin · Enzymatic hydrolysis · Avicel PH101 · Lignaceous residue

Abbreviations

CWR	Creeping Wild Ryegrass, *Leymus triticoides*
BSA	bovine serum albumin
FPU	cellulase activity
CBU	β-glucosidase activity
Tween 80	poly(oxyethylene)$_{20}$-sorbitan-monooleate
Tween 20	poly(oxyethylene)$_{20}$-sorbitan-monolaurate
SSF	simultaneous saccharification and fermentation
DI water	deionized water
HPLC	high-performance liquid chromatography

Introduction

For more than a decade, lignocellulosic biomass has been recognized as a high potential substrate for ethanol production [1]. At present, the major research interest is to develop effective processes for conversion of cellulose into ethanol through enzymatic hydrolysis with high yield and low cost. The main obstacle to the large-scale commercialization of lignocellulose-based ethanol is the significant enzyme cost contribution to the overall cost [2, 3]. To obtain high fermentable sugar yield and hydrolysis rate, high enzyme loading is normally needed along with prolonged process time [4–8]. Furthermore, enzyme recycling is difficult because of the enzyme adsorption on residual lignocellulosic material. Thus, it is necessary to develop technologies to improve the efficiency of enzymatic hydrolysis to make lignocellulose-based ethanol economically feasible.

Enzyme activity loss because of non-productive adsorption on lignin surface was identified as one of the important factors to decrease enzyme effectiveness, and the effect of surfactants and non-catalytic protein on the enzymatic hydrolysis has been extensively studied to increase the enzymatic hydrolysis of cellulose into fermentable sugars [7, 9–19]. The reported study showed that the non-ionic surfactant poly(oxyethylene)$_{20}$-sorbitan-monooleate (Tween 80) enhanced the enzymatic hydrolysis rate and extent of newspaper cellulose by 33 and 14%, respectively [20]. It was also found that 30% more FPU cellulase activity remained in solution, and about three times more recoverable FPU activity could be recycled with the presence of Tween 80. Tween 80 enhanced enzymatic hydrolysis yields for steam-exploded poplar wood by 20% in the simultaneous saccharification and fermentation (SSF) process [21]. Helle et al. [22] reported that hydrolysis yield increased by as much as a factor of 7, whereas enzyme adsorption on cellulose decreased because of the addition of Tween 80. With the presence of poly(oxyethylene)$_{20}$-sorbitan-monolaurate (Tween 20) and Tween 80, the conversions of cellulose and xylan in lime-pretreated corn stover were increased by 42 and 40%, respectively [23]. Wu and Ju [24] showed that the addition of Tween 20 or Tween 80 to waste newsprint could increase cellulose conversion by about 50% with the saving of cellulase loading of 80%. With the addition of non-ionic, anionic, and cationic surfactants to the hydrolysis of cellulose (Avicel, tissue paper, and reclaimed paper), Ooshima et al. [25] subsequently found that Tween 20 was the most effective for the enhancement of cellulose conversion, and anionic surfactants did not have any effect on cellulose hydrolysis. With the addition of Tween 20 in the SSF process for

ethanol production from softwood, Alkasrawi et al. [2] reported that the ethanol yield was increased by 8% in an even shorter time, and the amount of enzyme loading could be reduced by 50% while maintaining a constant yield. Kristensen et al. [3] reported that surfactants had a more pronounced effect on acid and steam-treated straw than ammonia and hydrogen-peroxide-treated straw. The addition of non-catalytic protein such as bovine serum albumin (BSA) was also used to enhance the enzymatic hydrolysis of cellulose in lignocellulosic biomass [26–28]. Addition of 17 g/l BSA produced about the same cellulose conversion as adding Tween 20 at 2.5 g/l for saccharose phosphate synthetase, but adding Tween 20 together with BSA did not increase cellulose conversion [7]. With addition of BSA for enzymatic hydrolysis of dilute acid pretreated corn stover, cellulose conversion was increased by 10% within 72 h, whereas 30% more cellulase activity (FPU) and 65% more β-glucosidase activity (CBU) remained free in solution [17]. In the same study, it was found that BSA did not affect Avicel hydrolysis and nor did it adsorb on Avicel, but it adsorbed on pretreated corn stover with high capacity. The possible reason for the difference between Avicel and corn stover was explained that BSA could adsorb onto a lignin surface and prevent the non-productive adsorption of enzymes onto lignin of corn stover, whereas Avicel has no lignin content to adsorb the enzymes. BSA was able to increase cellulose conversion up to 70% when it was added with cellulase for hydrolyzing wheat straw, but the effect depended on the substrate features derived by pretreatment methods [3].

Both Tween 20 and 80 are non-toxic and suitable for food and/or biotechnical use, such as stimulants for enzyme production by microorganisms [29–31] and additives in the SSF process for ethanol production [2]. BSA was used to improve the enzymatic conversion of lignocellulosic biomass because of its high affinity to lignin but little affinity to cellulose [17].

Although lots of work has been done on additives for enhancement of enzymatic hydrolysis of various substrates such as wood, corn stover, and wheat straw, saline Creeping Wild Ryegrass (CWR) has not previously been studied with addition of additives. Furthermore, the mechanisms for the enhancement of enzymatic hydrolysis by additives are not clear. Thus, more in-depth studies are needed to investigate such mechanisms. Two non-ionic surfactants (Tween 20 and 80) and a non-catalytic protein (BSA) were employed to do this study.

The specific objectives of this research were to investigate (1) the effect of additives on the cellulose conversion of pretreated CWR, (2) the possible mechanism behind the effect of additives on the enzymatic hydrolysis, (3) the effect of additives on the enzyme adsorption onto several substrates, including Avicel PH101, pretreated CWR, and lignaceous residue of pretreated CWR.

Materials and Methods

Non-ionic surfactants (Tween 20 and 80) and non-catalytic protein (BSA) were used to investigate if the enzymatic hydrolysis of pretreated CWR can be improved with various surface-active additives. The enzyme protein concentration and activities in solution were measured during enzymatic hydrolysis. Based on these data, the effect of additives on enzyme protein and activity was determined. All the experiments and experimental conditions are summarized in Table 1.

Pretreated CWR and Enzyme Preparations

The CWR was pretreated by dilute sulfuric acid under selected conditions [acid concentration=1.4% (*w*/*w*), temperature=165°C, and time=8 min; 32]. The pretreated CWR

Table 1 Experimental design.

Experiments	Additives (g/g dry solid)	Substrate loading (dry %, *w/w*)	Enzyme loading	Measurement
Effect of additives on enzymatic hydrolysis	Tween 20, Tween 80, BSA (0.1)	Pretreated CWR (8)	(15 FPU + 15 CBU)/g cellulose	Glucose and cellobiose concentration
Effect of additives on enzyme protein concentration and activity	Tween 20, BSA (0.1)			Enzyme protein concentration and activity
Effect of additive loading on enzymatic hydrolysis	Tween 20, BSA (0, 0.05, 0.1, 0.15, 0.2)			Glucose and cellobiose concentration and enzyme protein concentration and activity
Effect of additive on enzymatic hydrolysis	Tween 20 (0.1)	Avicel (8)		
Additive added after 8 h of hydrolysis	Tween 20 (0.1)	Pretreated CWR (8)		
Effect of additives on enzyme protein concentration and activity	Tween 20 (0.1)	Lignaceous residue (3)	(15 FPU + 15 CBU)/g dry solid	Enzyme protein concentration and activity
BSA adsorption	BSA (0.1)	Avicel (8) pretreated CWR (8) lignaceous residue (3)	–	BSA protein

The temperature and pH of the mixtures were 50°C and 4.8, respectively.

was washed to remove the soluble contents and acid. The washing was stopped until the pH of the filtrate reached 4.5. The washed pretreated CWR was then treated with cellulase (Novozymes, Celluclast 1.5 l, available from Sigma, Cat. no. C2730) supplemented with β-glucosidase (Novozyme188, Sigma, Cat. no. C6105). The enzymatic hydrolysis was performed in an incubator shaker at 150 rpm, pH=4.8, and temperature=50°C with cellulase and β-glucosidase loadings of 15 FPU and 15 CBU/g cellulose, respectively. The enzymatic hydrolysis conditions described in this paper was defined as a standard condition used throughout the entire paper, unless specified otherwise.

Additives and Avicel PH101

The additives tested in this study included non-ionic surfactants (Tween 20 and 80) and non-catalytic protein (BSA). They were purchased from Sigma-Aldrich (St. Louis, MO, USA). The Avicel PH101 was also purchased from Sigma-Aldrich.

Enhancement of Enzymatic Hydrolysis of Pretreated CWR by Additives

A batch enzymatic hydrolysis was conducted at 8% (*w/w*) of dry solid loading in a 50-mM citrate buffer (pH=4.8) containing 0.03% (*w/v*) sodium azide. The total working volume was 10 in 20 ml screw-capped vials. Before the addition of cellulase and β-glucosidase, the mixture of substrate and buffer was preheated in an incubator shaker under the temperature

of 50°C for 30 min to allow the substrate to disperse uniformly in the buffer. Tween 20, Tween 80, or BSA was then added into the vials at a loading of 0.1 g/g dry solid. The mixtures in vials were continuously heated in the incubator shaker for another 1 h for complete interaction between substrate and additives. Then, cellulase and β-glucosidase were added into vials immediately to initiate enzymatic hydrolysis. The time point of enzyme addition was recorded as time zero.

During the enzymatic hydrolysis, 1-ml aliquots were withdrawn from each vial by using micro-pippet (tips were cut) at start and at times of 8, 24, 48, and 72 h of hydrolysis to a series of 1.5-ml Eppendorf tubes. Before sampling, the vials were thoroughly shaken to make the mixture in vials as homogeneous as possible. The aliquots were immediately placed over a boiling water bath for 20 min to deactivate the enzymes as described by Helle et al. [22] and Desai and Converse [33]. After enzyme inactivation, each sample was centrifuged for 5 min at 12,000 rpm, and 500-ul supernatants were then removed to another series of 1.5-ml Eppendorf tubes. The supernatant samples were stored at 4°C for subsequent sugar analysis.

Effect of Tween 20 and BSA on Enzyme Protein Concentration and Activity

To study the effect of Tween 20 and BSA on enzyme protein concentration and activity, the enzyme protein concentration and activity were measured throughout the enzymatic hydrolysis of pretreated CWR. These experiments were conducted using the same procedure as described in "Enhancement of Enzymatic Hydrolysis of Pretreated CWR by Additives" except for the sampling procedure. In this experiment, 1-ml aliquots were withdrawn from each vial at start and times of 8, 24, 48, and 72 h using 1-ml syringes. These aliquots were then immediately filtered through syringe filters (Millex-GV4; polyvinylidene difluoride low protein-binding membrane; pore size, 0.2 μm; diameter, 4 mm, Millipore, Bedford, MA, USA) into another series of 1.5-ml Eppendorf tubes and diluted before analysis if necessary [15, 34]. The samples were stored at 4°C less than 1 h for subsequent protein concentration and enzyme activity measurements.

Effect of Tween 20 Loading on Enzymatic Hydrolysis of Pretreated CWR

The effect of Tween 20 loading on enzymatic hydrolysis of pretreated CWR was studied at five different loading levels, including 0, 0.05, 0.1, 0.15, and 0.2 g Tween 20/g-dry solid. At the end of 72 h hydrolysis, a 1-ml aliquot was withdrawn for sugars measurement. At the same time, another 1-ml aliquot was withdrawn for protein and enzyme activity measurement. For enzyme protein concentration and activity measurements, the sample pretreatment procedures before measurement were the same as described in "Effect of Tween 20 and BSA on Enzyme Protein Concentration and Activity."

Effect of Tween 20 on Enzymatic Hydrolysis of Avicel

The enzymatic hydrolysis and sampling procedures for Avicel was the same as described in "Enhancement of Enzymatic Hydrolysis of Pretreated CWR by Additives." Based on the experimental result from "Effect of Tween 20 Loading on Enzymatic Hydrolysis of Pretreated CWR," the ratio of Tween 20 to Avicel was decided to be 0.1 g Tween 20 to 1 g Avicel. A homogeneous aliquot of 1 ml was withdrawn at start and after 1, 2, 4, 8, 24, 48, and 72 h of hydrolysis. The aliquots were treated as "Effect of Tween 20 and BSA on Enzyme Protein Concentration and Activity" to obtain 500-ul supernatant samples. The

250-ul supernatant samples were then moved to other series of 1.5-ml Eppendorf tubes, which were heated in boiling water to deactivate the enzymes for sugar measurement as described in "Enhancement of Enzymatic Hydrolysis of Pretreated CWR by Additives." The rest of the 250-ul supernatant samples were used to measure enzyme protein concentration and activity.

Lignaceous Residue Preparation

Lignaceous residue of pretreated CWR was prepared by a limit enzymatic hydrolysis [13, 15, 16]. The total reaction volume was 400 ml in a 1-l Erlenmeyer flask. The pretreated CWR was hydrolyzed for 168 h with enzyme loading of 60 FPU and 75 CBU/g cellulose. These reaction conditions were enough to obtain almost complete hydrolysis of cellulose (98.5%) by monitoring the cellulose hydrolysis based on the released glucose and cellobiose concentrations in solution. The lignaceous residue after hydrolysis was sequentially washed with distilled DI water, 1.0 M NaCl, and distilled DI water. The prepared lignaceous residues were stored in the refrigerator under 4°C without drying for less than 24 h for further study.

BSA Adsorption to Avicel, Pretreated CWR, and Lignaceous Residue and Effect of Tween 20 on Enzyme Adsorption on Lignaceous Residue

To investigate the mechanism of the BSA on the improvement of enzymatic hydrolysis of pretreated CWR, the adsorptions of BSA on various substrates were studied [17]. Three sets of 20-ml vials were used to test the adsorption of BSA to Avicel, pretreated CWR, and lignaceous residue, respectively. The mixtures of citrate buffer (pH=4.8) with 8% (*w*/*w*) Avicel, 8% (*w*/*w*) pretreated CWR, or 3% (*w*/*w*) lignaceous residue were preheated to 50°C for 30 min. BSA was then added to the vials with the ratio of BSA to dry solid equal to 0.1 g BSA/g dry solid. The final working volume was 10 ml. One-milliliter aliquots were periodically withdrawn at start and after 1, 2, 4, 8, 24, 48, and 72 h. The aliquots were pretreated according to the procedures described in "Effect of Tween 20 and BSA on Enzyme Protein Concentration and Activity" for BSA protein concentration measurement.

For studying the effect of Tween 20 on the adsorption of enzymes on lignaceous residue, the mixtures of citrate buffer (pH=4.8), 3% (*w*/*w*) lignaceous residue, and Tween 20 were added to a 20-ml vial sequentially. The loading ratio between Tween 20 and lignaceous residue was 0.1 g Tween 20/g dry solid. The mixtures were then preheated to 50°C for 1 h for interaction between Tween 20 and lignaceous residue solids. Finally, the enzymes were loaded into vials with the loading of (15 FPU + 15 CBU)/g dry solid. The enzyme addition time point was set as time zero. Both enzyme protein concentration and activities were measured periodically (at start and after 1, 2, 4, 8, 24, 48, and 72 h of enzyme addition) according to the procedure described in "Effect of Tween 20 and BSA on Enzyme Protein Concentration and Activity."

Enzymatic Hydrolysis of Pretreated CWR With and Without the Presence of Tween 20 Added After 8 h of Hydrolysis

To investigate how the interaction between Tween 20 and pretreated CWR affect the enzymatic hydrolysis efficiency, the enzymatic hydrolysis of pretreated CWR with 0.1 g Tween 20/g dry solid added after 8 h of hydrolysis was studied. The results of this section were compared to those obtained in "Enhancement of Enzymatic Hydrolysis of Pretreated

CWR by Additives," in which Tween 20 was added before the addition of enzymes. During hydrolysis, 1-ml aliquots were taken at start and after 1, 2, 4, 8, 24, 48, and 72 h of hydrolysis. The sugars, enzyme protein concentration, and activity were measured.

Analytical Methods

The sugar contents such as glucose and cellobiose in the supernatant of liquid samples were analyzed on a high-performance liquid chromatography (HPLC; Shimadzu, Kyoto, Japan) equipped with a refractive index detector (RID-10A, Shimadzu, Kyoto, Japan). The time constant and range were set to be 1 s and ×64 (or ×8), respectively. All samples were filtered through small syringe filters (Millex-GV4; polyvinylidene difluoride low protein-binding membrane; pore size, 0.2 μm; diameter, 4 mm, Millipore) and diluted before analysis if necessary [15, 17, 34]. The HPLC analytical column was equilibrated with HPLC grade (18 MΩ) water at a flow rate of 0.6 ml/min overnight. An Aminex HPX-87P (Bio-Rad, Hercules, CA) column was used for sugar separations at 85°C, with the HPLC grade water as the mobile phase at a flow rate of 0.6 ml/min. The HPLC system was equipped with a Carbo-P refill cartridge (Bio-Rad) as a guard column to protect the analytical column from blocking.

The protein concentration in solution was measured by the Bradford protein assay using BSA as a standard (Bio-Rad). The Bradford colorimetric method cannot distinguish the BSA protein from enzyme protein. Therefore, no differentiation was possible between BSA and enzymes in solution other than by measuring the enzyme activity. The enzyme activities in solution including FPU and CBU were measured according to the methods described by Ghose [35].

All the experimental results were the average of two replicates, unless specified otherwise.

Results

Enhancement of Enzymatic Hydrolysis of Pretreated CWR by Additives

As shown in Fig. 1, the presence of Tween 80, Tween 20, BSA or (BSA + Tween 20) improved the enzymatic hydrolysis of pretreated CWR by 8 to 14% after 72 h of hydrolysis. The initial hydrolysis rate was also increased to some extent. The cellulose conversion was increased from approximately 75% (no additives) to 89, 88, and 83% with the presence of Tween 20, Tween 80, and BSA, respectively. Of all three additives, Tween 20 was the most effective additive on the improvement of cellulose conversion, followed by Tween 80 and BSA. The treatment of Tween 20, Tween 80, or BSA gave similar results at an enzyme loading of 15 FPU/g cellulose to those at enzyme loading of 30 FPU/g cellulose but without additive addition (Fig. 1). Therefore, the addition of surfactants and/or non-catalytic protein could help save enzyme loading without decreasing the hydrolysis yield. In addition, it was found that Tween 20 and BSA gave no further increase in cellulose conversion. Thus, the effect of Tween 20 on the hydrolysis of pretreated CWR might be similar to that of BSA [7].

To determine how additions of Tween 20 and BSA before adding enzymes affected adsorption of enzymes, the enzyme protein concentration and activities (FPU and CBU) in solution were measured for pretreated CWR, as reported in Figs. 2 and 3 for an enzyme loading of (15 FPU + 15 CBU)/g cellulose. Based on a free protein of 100% for the total

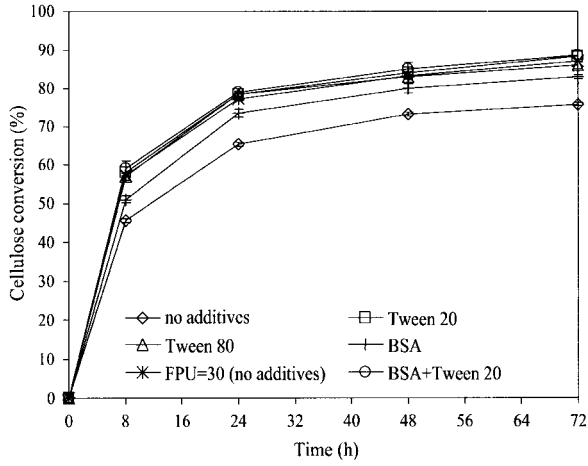


Fig. 1 Effect of additives on the cellulose conversion of pretreated CWR (the additive loading was 0.1 g additive/g dry solid and the enzyme loading was 15 FPU + 15 CBU/g cellulose)

protein concentration in solution at time zero, approximately 58% of initial enzyme protein remained in solution with the presence of Tween 20 after 72 h of interaction between enzyme and pretreated CWR (Fig. 2). However, only 15% of the initial enzyme protein remained free in solution without the addition of Tween 20. Because no differentiation was possible between BSA and enzymes in solution, enzyme protein concentration was not measured when BSA was used as an additive.

Based on a relative activity of 100% for the protein in solution at time zero, the cellulase activity (FPU) in solution dropped quickly to about 19% of its initial value within 72 h when no additives were present (Fig. 3). When Tween 20 or BSA was added to pretreated CWR before the addition of enzymes, the cellulase activity in solution only dropped to about 50% of its initial value after 72 h. With a similar trend, β-glucosidase activity (CBU) in solution dropped to approximately 5% of its initial value without additive addition but dropped far less to about 68% of the initial activity when Tween 20 or BSA was present. Based on the results from Figs. 2 and 3, a conclusion could be drawn that the Tween 20 and BSA can prevent the enzyme being adsorbed by substrate (cellulose or lignin content in the

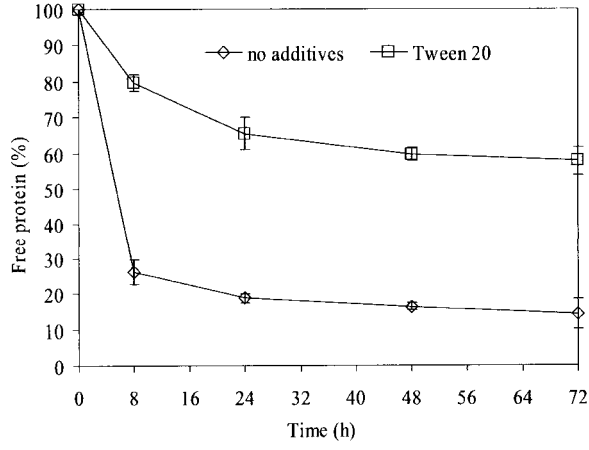


Fig. 2 Free enzyme protein in solution with and without Tween 20 during enzymatic hydrolysis

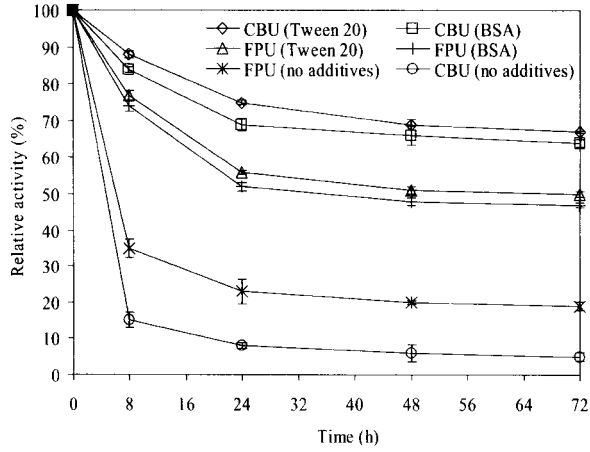


Fig. 3 Changes in relative enzyme activities with and without the addition of BSA or Tween 20 during enzymatic hydrolysis

pretreated CWR) and could increase the enzyme availability in solution for the hydrolysis of pretreated CWR.

Effect of Tween 20 Loading on Enzymatic Hydrolysis of Pretreated CWR

As shown in Fig. 4, cellulose conversion of pretreated CWR increased from 75 to 88% linearly with the increase of Tween 20 loading from 0 to 0.1 g Tween 20/g dry solid. When Tween 20 loading was higher than 0.1 g Tween 20/g dry solid, there was little increase in cellulose conversion. The changes of enzyme protein concentration and activities in solution followed similar trends to cellulose conversion (Fig. 5). With the presence of 0.1 g Tween/g dry solid, over 40% enzyme protein, 30% FPU and 60% CBU remained in solution after 72 h of hydrolysis. However, only about 6% protein, 17% FPU, and 20% CBU remained free without Tween 20 addition. The possible reason for these results of Figs. 4 and 5 was that non-productive adsorption sites in pretreated CWR were saturated by Tween 20 with the loading equal to or higher than 0.1 g Tween 20/g dry solid. Therefore, the loading of 0.1 g Tween 20/g dry solid could be a saturation value for Tween 20 to improve the cellulose conversion of pretreated CWR.

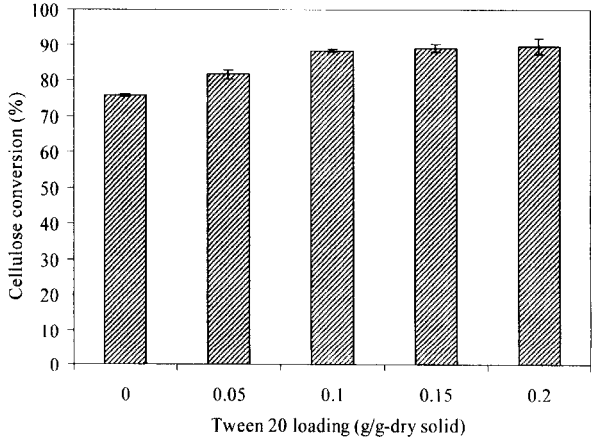


Fig. 4 Cellulose conversion of pretreated CWR after 72 h as a function of Tween 20 loading

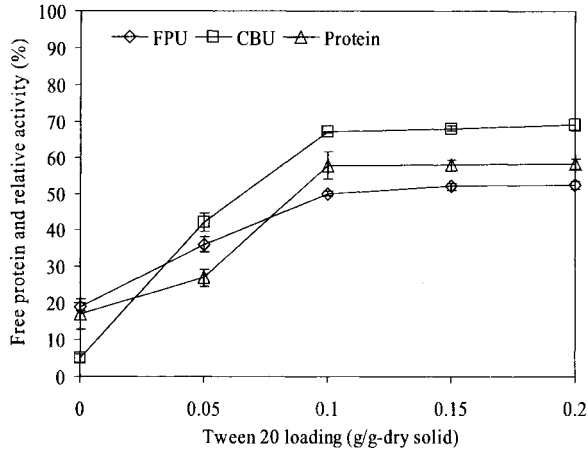


Fig. 5 Changes in free enzyme activities and protein concentration in the solution during enzymatic hydrolysis of pretreated CWR after 72 h as a function of Tween 20 loading

Considering the result from Fig. 1 that (0.1 g Tween 20 + 0.1 g BSA)/g dry solid gave no further increase of cellulose conversion compared with the addition of Tween 20 alone, a conclusion could be drawn that the mechanisms of Tween 20 and BSA on the improvement of enzymatic hydrolysis of pretreated CWR might be similar. If Tween 20 and BSA had significantly different mechanisms on the improvement of enzymatic hydrolysis, higher cellulose conversion should be expected after BSA was added to the solution with Tween 20 at saturation loading of 0.1 g/g dry solid.

Effect of Tween 20 on Enzymatic Hydrolysis of Avicel

When the substrate was Avicel, the cellulose conversion was slightly increased with Tween 20 addition, in contrast to the significant increase of cellulose conversion of pretreated CWR (Fig. 6). After 72 h, the cellulose conversion of Avicel was increased 3% with the presence of 0.1 g Tween 20/g Avicel.

The changes in enzyme protein concentration and activities in the solution during hydrolysis of Avicel were measured as functions of the addition of Tween 20 (Fig. 7).

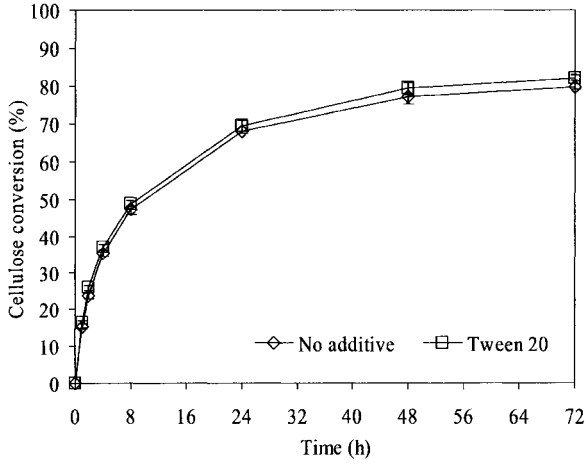


Fig. 6 Effect of Tween 20 on enzymatic hydrolysis of Avicel with 8% dry solid loading at 15 FPU + 15 CBU/g cellulose enzyme loading

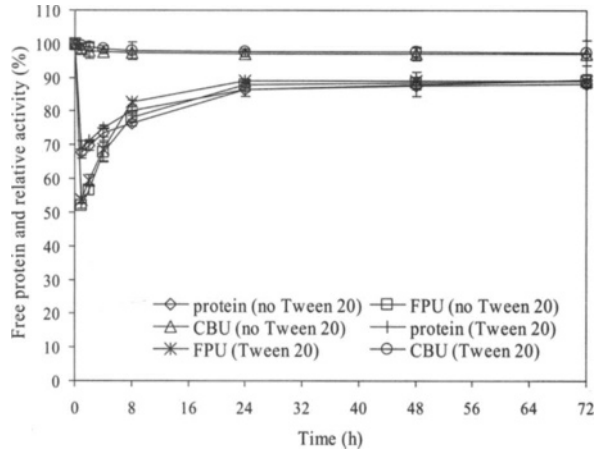


Fig. 7 Changes in free protein concentration and relative enzyme activities in solution during enzymatic hydrolysis of Avicel at 8% dry solid loading with and without Tween 20 addition

There were no significant changes about the enzyme protein, cellulase, and β-glucosidase activities with and without the addition of Tween 20, which corresponded to the performance of enzymatic hydrolysis present in Fig. 6. The free protein concentration and cellulase activity (FPU) in solution dropped rapidly to about 70 and 50% of their initial values, respectively, within the first 1 h. Both of them increased to about 80% after 8 h of hydrolysis. Then, they increased slightly until leveled off after 24 h. In addition, it was found that the β-glucosidase activity (CBU) just had few changes during the enzymatic hydrolysis of Avicel. After 72 h of hydrolysis, only about 3% β-glucosidase activity in solution was lost, which might indicate that small amount of β-glucosidase was adsorbed to Avicel, and/or that β-glucosidase activity was lost by thermal, mechanical, and/or other factors as reported by Moloney and Coughlan [36]. Ooshima et al. [37] found β-glucosidase could not adsorb on crystalline cellulose at the temperature of 50°C. If this is the case, we might conclude that the most β-glucosidase was deactivated during enzymatic hydrolysis by thermal, mechanical, and/or other factors. For cellulase, its activity loss from solution might be caused by the inactivation or adsorption on cellulose irreversibly. To our knowledge, little research has been done to distinguish between inactivation of cellulase and cellulase binding to cellulose during cellulosic hydrolysis. Mizutani et al. [38] compared the effects of Tween 20 on the hydrolysis of several cellulosic fibers with different crystallinity and found that the effectiveness of Tween 20 became higher with increased crystallinity of cellulosic substrates. Their results indicated that the surfactants could prevent some of the cellulase from adsorbing to non-productive sites on crystalline cellulose.

Comparing Figs. 2 and 3 with Fig. 7, it was found that the free enzyme protein concentration and activities in solution kept decreasing within the entire hydrolysis process of pretreated CWR, but they were slowly released back into solution after approximately 1 h hydrolysis of Avicel. Several studies have concluded that the reason for this difference was the presence of lignin content in the lignocellulosic biomass [7, 17, 22] in that the lignin adsorbed the enzymes irreversibly during the hydrolysis. The affinity of β-glucosidase to lignocellulosic biomass was much higher than that to Avicel. For cellulase, its affinity to lignocellulosic biomass was moderately higher than to Avicel. Although it is believed that lignin is a primary cause of the loss of enzyme protein and activities, the negative effect of crystallinity of cellulose might also exist. More research is needed to study the effect of cellulose crystallinity on the adsorption of hydrolytic enzymes.

BSA Adsorption to Avicel, Pretreated CWR, and Lignaceous Residue of Pretreated CWR

The adsorbed BSA on Avicel was only 2% of initial value after 72 h of interaction between BSA and Avicel (Fig. 8). When the adsorbent was changed to pretreated CWR or lignaceous residue of pretreated CWR, the free BSA concentration in the solution dropped to around 20% of the initial value within the first 1 h. For pretreated CWR and lignaceous residue, the relative adsorbed BSA were almost the same as each other. However, the adsorption capacities of lignaceous residue and pretreated CWR for BSA were calculated to be about 0.1 g BSA/g dry lignaceous residue and 0.08 g BSA/g dry pretreated CWR, respectively. In this study, the adjusted concentration of lignin content in pretreated CWR was almost the same as that of lignaceous residue in reaction vials. Based on the results of BSA adsorption on pretreated CWR and lignaceous residue, two hypotheses could be proposed. The first is that the cellulose content in pretreated CWR adsorbed little BSA, and only the lignin content in pretreated CWR could adsorb BSA. The other is that the cellulose content in pretreated CWR could adsorb some BSA, but the adsorption capacity of cellulose content was lower than that of lignin content of pretreated CWR. More research is needed to prove these hypotheses.

Effect of Tween 20 on Adsorption of Cellulase and β-glucosidase on Lignaceous Residue of Pretreated CWR

As shown in Fig. 9, the enzyme protein in the solution dropped rapidly either with or without the addition of Tween 20 within the first 1 h. From the first 1 h to the end of 72 h of adsorption, the free protein concentration in solution decreased much less rapidly, about 10% free protein concentration decrease either with or without Tween 20 addition. Over 50% more protein remained in the solution after 72 h when 0.1 g Tween 20/g dry lignaceous residue was present. The cellulase and β-glucosidase activities followed a similar change trend to free protein concentration in solution. Comparing with the adsorption without the addition of Tween 20, 60% more β-glucosidase activity and 30% more cellulase activity remained in solution after 72 h adsorption with Tween 20 addition. The results from Fig. 9 indicated that Tween 20 could prevent the non-productive adsorption of enzymes to lignin content in the pretreated CWR.

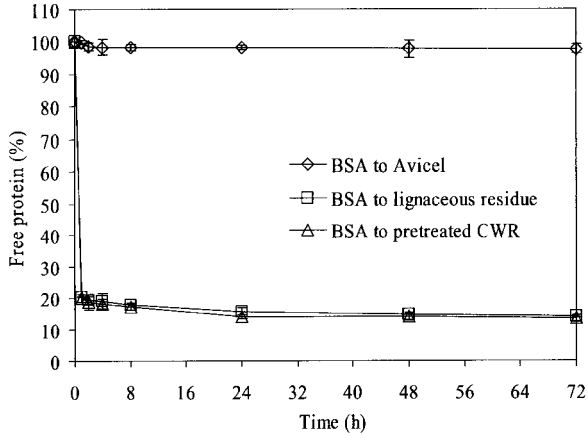


Fig. 8 BSA (0.1 g/g dry solid) adsorption to Avicel (8%, *w/w*), pretreated CWR (8%, *w/w*, containing lignin content equal to 3%, *w/w* of total reaction weight), and lignaceous residue of pretreated CWR (3%, *w/w*)

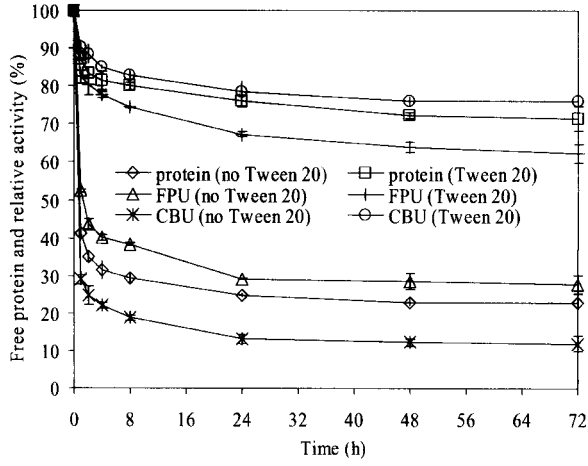


Fig. 9 Changes in free protein concentration and relative enzyme activities in solution during enzyme adsorption to lignaceous residue (3%, *w/w*) with and without Tween 20 addition (0.1 g Tween 20/g dry lignaceous residue)

Enzymatic Hydrolysis of Pretreated CWR With and Without Tween 20 Added after 8 h of Pretreated CWR Hydrolysis

Adding Tween 20 after 8 h of pretreated CWR hydrolysis had little effect on cellulose conversion (Fig. 10). The final cellulose conversion was improved by about 2%, which was much lower than the 14% more cellulose conversion achieved when Tween 20 was added before enzyme addition (Fig. 1).

In the same experiment presented in Fig. 10, the enzyme protein and activities were also measured, as shown in Fig. 11. The enzyme protein concentration in solution dropped quickly to about 40% of its initial value within the first 1 h of hydrolysis and to about 15% of initial value after 72 h of hydrolysis when no Tween 20 was added. At the end of 72 h, the free protein concentration in solution was increased to 17% of its initial value with Tween 20 added after 8 h of hydrolysis. When followed in a similar fashion, the cellulase and β-glucosidase activities dropped to about 20 and 5% of initial values, respectively, without the presence of Tween 20. While Tween 20 was added after 8 h of hydrolysis, only

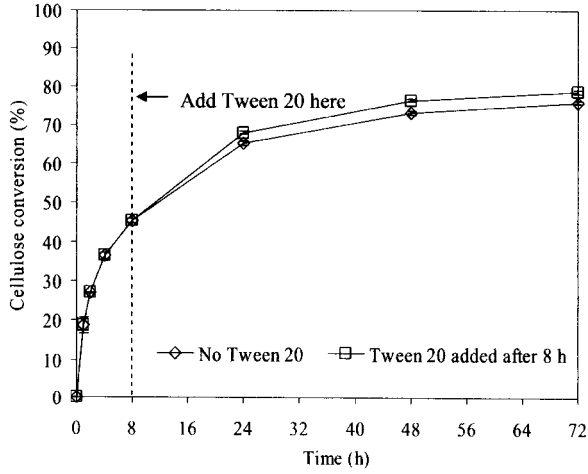


Fig. 10 Enzymatic hydrolysis of pretreated CWR (8%, *w/w*) with and without Tween 20 (0.1 g Tween 20/g dry pretreated CWR) added after 8 h of hydrolysis

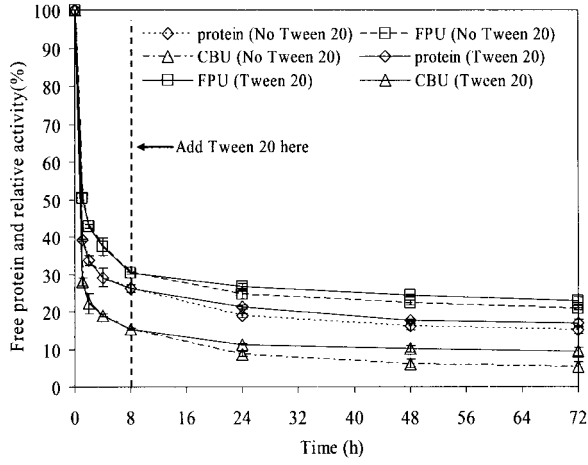


Fig. 11 Changes in free protein concentration and relative enzyme activities in solution during enzymatic hydrolysis of pretreated CWR with and without Tween 20 added after 8 h of hydrolysis presented in Fig. 10

2% more cellulase and 4% more β-glucosidase activities in solution were achieved than those without Tween 20 addition.

Considering Figs. 10 and 11, it might suggest that the primary effect of Tween 20 on cellulose conversion of pretreated CWR could be blocking non-productive adsorption of enzymes on substrate and not deactivation by some other mechanism. Comparing Figs. 2 and 3 with Fig. 11, it was found that adding Tween 20 before enzyme addition resulted in much higher enzyme protein and activities available in solution than when Tween 20 was added after enzyme addition. If Tween 20 can protect enzymes from deactivating and/or modifying the surface structure of the substrate, significantly more increased cellulose conversion should be expected. However, these results were not found in this study. Therefore, a conclusion could be drawn that the Tween 20 addition can prevent enzyme from adsorbing non-productively onto substrate, but cannot free most absorbed protein.

Discussions

Enhancement of cellulose conversion by adding various additives, including surfactants and non-catalytic proteins, to the hydrolysis mixture has been reported by many researchers. The mechanisms underlying the enhancement of enzymatic cellulose hydrolysis by the addition of surfactants and/or BSA have been the objective of intense research. Various mechanisms have been proposed that can be divided into three main categories: (1) stabilizing the enzyme by reducing thermal and/or mechanical shear forces [23, 39]; (2) changing the ultra structure of the substrate, making the cellulose more accessible to enzymes [22]; and (3) affecting enzyme-substrate interaction, e.g., enzymes are prevented from inactivation because of non-productive adsorption to lignin content in lignocellulosic biomass by steric repulsion [3, 7, 8, 17, 20, 22, 23, 40].

Kim et al. [41] reported that a significant deactivation was observed when cellulase was subjected to shear and/or exposed to air-liquid interface, which was thought to be far more severe and extensive than shear effect alone. By using sufficient additives (surfactants and non-catalytic proteins, e.g., BSA), cellulase deactivation can be, to some extent, prevented, and cellulase can be stabilized. This might be because the addition of non-ionic surfactants could reduce the contact of enzymes with the air–liquid interface because of the surface

activity of the surfactant [41]. Kaar and Holtzapple [23] proposed that the addition of Tween protected the enzymes from thermal deactivation because they found that the optimum temperature in Tween samples was 10°C higher than that of the Tween-free samples. However, Herskovits and Jaillet [42], Badley et al. [43], and Reese and Robbins [44] concluded that surfactants did not prevent heat or chemical inactivation of enzymes, and the interaction between surfactants and enzymes might lead to an increase in thermal deactivation. Employing fluorescence studies and measuring enzyme activity, Eriksson et al. [7] indicated that the difference of the denaturation temperature of enzymes was very small between with and without the addition of Tween 20, and enzymes were slightly stabilized by the addition of Tween 20 in thermal deactivation experiments. Therefore, Eriksson et al. [7] concluded that the positive effect on hydrolysis of Tween 20 could not be explained by a stabilizing effect of Tween 20 on the enzymes. In our research, results were consistent with the finding of Eriksson et al. [7, 11]. The increase of cellulose conversion became apparent immediately after additives were added (Figs. 1 and 6). Also, in contrast with models of cellulase inactivation without Tween 20, almost all cellulase (90%) and β-glucosidase (98%) were still active in solution after 72 h of hydrolysis with and/or without Tween 20 addition during the hydrolysis of Avicel (Fig. 7). Based on our results, additives had a negligible effect on the stabilization of enzymes.

Ballesteros et al. [21], Helle et al. [22], Kaar and Holtzapple [23], and Kurakake et al. [45] proposed that the surfactants could disrupt the lignocellulosic matrix and make more substrate available to the enzymes. If their theory could explain the effect of surfactants on enzymatic hydrolysis, an increase in enzyme adsorption at the beginning of enzyme addition should be expected because of more available active sites on substrate exposed to enzymes. However, this phenomenon was not detected in this research. Therefore, our findings on the changes of enzyme protein concentration and activities during hydrolysis of pretreated CWR with the presence of Tween 20 and/or BSA do not support their explanation. In contrast, increased enzyme protein concentration and activities in solution were observed with the increase of cellulose conversion in all pretreated CWR hydrolysis experiments (Figs. 1, 2, 3, 4, 5, 10, and 11). Moreover, the observed effect of BSA on the enzymatic hydrolysis of pretreated CWR was similar to surfactants, so that it is not easy to accommodate this result in a model requiring surfactant and, therefore BSA, to act by substrate disruption based on our and other's reported studies [7, 17].

Cellulose conversion of Avicel was only slightly increased by Tween 20 in contrast to that of pretreated CWR. Therefore, it may be likely that lignin content in the pretreated CWR plays a critical role in explaining the positive effect of Tween 20 on enzymatic hydrolysis because pretreated CWR has lignin content, but Avicel does not. Several findings in our study support this conclusion by studying enzyme protein and activities loss by the adsorption of enzyme on Avicel, lignaceous residue, and pretreated CWR: (1) The behavior of enzyme protein and activities loss by enzyme adsorption on pretreated CWR was similar to that on lignaceous residue with or without the addition of Tween 20; (2) BSA had the same effect as Tween 20 on the increased cellulose conversion of pretreated CWR. No additional effect was observed when BSA was added after the substrate was saturated by Tween 20. This result supports the conclusion that the effect of both Tween 20 and BSA on the enzymatic hydrolysis of pretreated CWR may be explained by the same mechanism; (3) pretreated CWR and lignaceous residue adsorbed a substantial amount of BSA, whereas Avicel adsorbed a small amount of BSA. Yang and Wyman [17] also found that BSA had little effect on the cellulose conversion of Avicel hydrolysis because Avicel adsorbed a substantial amount of cellulase but little BSA. It was proposed that the hydrophobic part of non-ionic surfactants binds to lignin on the pretreated CWR fibers through hydrophobic

interactions and/or hydrogen bonding, and the hydrophilic head group of the surfactant prevents the non-productive binding of the enzymes to lignin [8]. The modules of *Trichoderma reesei* cellulase have hydrophobic amino acids exposed on the surface [46], and these residues have been reported to be positioned for both optimal specific interaction with the cellulose [47] and non-specific interaction with lignin surfaces [16]. In addition, Berlin et al. [16] found *T. reesei* cellulase cores binding to lignin outside of the specific sites for cellulose binding. Therefore, the presence of hydrophobic residues on enzyme surfaces may result in non-specific adsorption to lignin surface. With the addition of surfactants, the hydrophobic interaction between lignin and enzymes could be disrupted by charges from surfactants [7]. Eriksson et al. [7] stated that this non-specific adsorption could have a stronger role with pretreated biomass compared to raw biomass because of the increased exposure of lignin surfaces in the pretreatment process. BSA was found to have hydrophobic sites, which could lead to the binding of fatty acids and adsorption on hydrophobic surfaces, such as lignin [28]. Therefore, the BSA effect on the hydrolysis could be explained by the similar mechanism of non-ionic surfactants, which is non-specific binding of BSA to lignin and the resulted decrease of non-productive adsorption of enzymes to lignin surfaces [17, 48].

As shown above, the improvement upon addition of surfactant of hydrolysis of Avicel was much lower than that of pretreated CWR. This result agreed well with findings by Eriksson et al. [7] who reported that surfactants and BSA were both viewed as preventing non-productive adsorption of cellulase on lignin. However, the contrary findings reported that the non-ionic surfactants could enhance the hydrolysis of cellulose such as Sigmacell 100 and Avicel and act differently from proteins [22, 25, 38]. Therefore, more research needs to be done to solve this discrepancy and better understand the mechanisms of additive effect.

Conclusions

The Tween-type non-ionic surfactants (Tween 20 and 80) and non-catalytic protein (BSA) were effective additives for enhancing the cellulose conversion of pretreated CWR. Tween 20 was the most effective among the three additives. When 0.1 g Tween 20/g dry solid was used, 14% more cellulose conversion was obtained comparing with without Tween 20 addition. With the addition of Tween 20, the cellulose conversion of pretreated CWR with the enzyme loading of 15 FPU/g cellulose was similar to that with the enzyme loading of 30 FPU/g cellulose. It is most likely possible to lower the enzyme loading by adding surfactants, e.g., Tween 20, while retaining the same degree of cellulose conversion. However, it has not been possible to perform economic evaluations on the feasibility of additive addition because of the lack of industrial scale prices of additives and enzymes. BSA and Tween 20 may have the same mechanism for improving the enzymatic hydrolysis of pretreated CWR. Enzyme protein concentration and activities were measured and could be correlated to cellulose conversion of Avicel and pretreated CWR with and without the presence of additives. When lignaceous residue of pretreated CWR was the absorbent, adsorbed protein decreased by 50% with the presence of Tween 20. At the same time, cellulase and β-glucosidase activities in solution were increased by 40 and 60%, respectively. The effect of Tween 20 on the adsorption of enzymes to lignaceous residue was similar to that on pretreated CWR. The results may be because of the prevention of non-productive adsorption of enzymes on lignin by Tween 20. However, more research is needed to fully understand the mechanisms of the effect of additive on cellulose conversion of lignocellulosic biomass.

Acknowledgment Authors would like to thank Novozymes Inc. for providing the enzymes and Red Rock Ranch for providing the biomass materials for this research. The funding support for this research was partially provided by a research grant from California Department of Water Resources (grant no. 4600002991).

References

1. Sheehan, J., & Himmel, M. (1999). *Biotechnology Progress, 15*, 817–827.
2. Alkasrawi, M., Erriksson, T., Borjesson, J., Wingren, A., Galbe, M., & Zacchi, G. (2003). *Enzyme and Microbial Technology, 33*, 71–78.
3. Kristensen, J. B., Borjesson, J. Bruun, M., Tjerneld, F., & Jorgensen, H. (2007). *Enzyme and Microbial Technology, 40*, 888–895.
4. Gregg, D. J., & Saddler, J. N. (1996). *Biotechnology and Bioengineering, 51*, 375–383.
5. Himmel, M. E., Ruth, M. F., & Wyman, C. E. (1999). *Current Opinion in Biotechnology, 10*, 358–364.
6. Wooley, R., Ruth, M., Glassner, D., & Sheehan, J. (1999). *Biotechnology Progress, 15*, 794–803.
7. Eriksson, T., Borjesson, J., & Tjerneld, F. (2002). *Enzyme and Microbial Technology, 31*, 353–364.
8. Borjesson, J., Peterson, R., & Tjernel, F. (2007). *Enzyme and Microbial Technology, 40*, 754–762.
9. Mooney, C., Mansfield, S., Touhy, M., & Saddler, J. (1998). *Bioresource Technology, 64*, 113–119.
10. Valjamae, P., Sild, V., Nutt, A., Pettersson, G., & Johansson, G. (1999). *European Journal of Biochemistry, 266*, 327–334.
11. Eriksson, T., Karlsson, J., & Tjerneld, F. (2002). *Applied Biochemistry and Biotechnology, 101*, 41–60.
12. Sutcliffe, R., & Saddler, J. N. (1986). *Biotechnology and Bioengineering Symposium, 17*, 749–762.
13. Ooshima, H., Burns, D. S., & Converse, A. O. (1990). *Biotechnology and Bioengineering, 36*, 446–452.
14. Lu, Y. P., Yang, B., Gregg, D., Saddler, J. N., & Mansfield, S. D. (2002). *Applied Biochemistry and Biotechnology, 98*, 641–654.
15. Palonen, H., Tjerneld, F., Zacchi, G., & Tenkanen, M. (2004). *Journal of Biotechnology, 107*, 65–72.
16. Berlin, A., Gilkes, N., Kurabi, A., Bura, R., Tu, M. B., Kilburn, D., et al. (2005). *Applied Biochemistry and Biotechnology, 121 124*, 163–170.
17. Yang, B., & Wyman, C. E. (2006). *Biotechnology and Bioengineering, 94*, 611–617.
18. Sewalt, V. J. H., Glasser, W. G., & Beauchemin, K. A. (1997). *Journal of Agricultural and Food Chemistry, 45*, 1823–1828.
19. Kim, S., & Holtzapple, M. T. (2006). *Bioresource Technology, 97*, 583–591.
20. Castanon, M., & Wilke, C. R. (1981). *Biotechnology and Bioengineering, 23*, 1365–1372.
21. Ballesteros, I., Oliva, J. M., Carrasco, J., Cabanas, A., Navarro, A. A., & Ballesteros, M. (1998). *Applied Biochemistry and Biotechnology, 70–72*, 369–381.
22. Helle, S. S., Duff, S. J. B., & Cooper, D. G. (1993). *Biotechnology and Bioengineering, 42*, 611–617.
23. Kaar, W. E., & Holtzapple, M. T. (1998). *Biotechnology and Bioengineering, 59*, 419–427.
24. Wu, J., & Ju, L.-K. (1998). *Biotechnology Progress, 14*, 649–652.
25. Ooshima, H., Sakata, M., & Harano, Y. (1986). *Biotechnology and Bioengineering, 28*, 1727–1734.
26. Tanaka, M., Takenawa, S., Matsuno, R., & Kamikubo, T. (1978). *Journal of Fermentation Technology, 56*, 108–113.
27. Kawamoto, H., Nakatsubo, F., & Murakami, K. (1992). *Mokuzai Gakkaishi, 38*, 81–84.
28. Haynes, H. A., & Nordc, W. (1994). *Colloids and Surfaces B, 2*, 517–566.
29. Reese, E. T., & Maguire, A. (1969). *Applied Microbiology, 17*, 242–245.
30. Reese, E. T., & Maguire, A. (1971). *Developments in Industrial Microbiology, 12*, 212–224.
31. Pardo, A. G. (1996). *Current Microbiology, 33*, 275–278.
32. Zheng, Y., Pan, Z., Zhang, R., Labvitch, J., Wang, D., Teter, S., et al. (2007). *Applied Biochemistry and Biotechnology, 136–140*, 423–435.
33. Desai, S. G., & Converse, A. O. (1997). *Biotechnology and Bioengineering, 56*, 650–655.
34. Medve, J., Karlsson, J., Lee, D., & Tjerneld, F. (1998). *Biotechnology and Bioengineering, 59*, 621–634.
35. Ghose, T. K. (1987). *Pure and Applied Chemistry, 59*, 257–268.
36. Moloney, A., & Coughlan, M. P. (1983). *Biotechnology and Bioengineering, 25*, 271–280.
37. Ooshima, H., Sakata, M., & Harano, Y. (1983). *Biotechnology and Bioengineering, 25*, 3103–3114.
38. Mizutani, C., Sethumadhavan, K., Howley, P., & Bertoniere, N. (2002). *Cellulose, 9*, 83–89.
39. Park, J. W., Takahata, Y., Kajiuchi, T., & Akehata, T. (1992). *Biotechnology and Bioengineering, 39*, 117–120.
40. Borjesson, J., Engqvist, M., Sipos, B., & Tjerneld, F. (2007). *Enzyme and Microbial Technology, 41*, 186–195.
41. Kim, M. H., Lee, S. B., & Ryu, D. D. Y. (1982). *Enzyme and Microbial Technology, 4*, 99–103.

42. Herskovitz, T. T., & Jaillet, H. (1969). *Science, 163*, 282–285.
43. Badley, R. A., Carruthers, L., & Phillips, M. C. (1977). *Biochimica et Biophysica Acta, 495*, 110–118.
44. Reese, E. T., & Robbins, F. M. (1981). *Journal of Colloid and Interface Science, 83*, 393–400.
45. Kurakake, M., Ooshima, H., Kato, J., & Harano, Y. (1994). *Bioresource Technology, 49*, 247–251.
46. Kraulis, P. J., Clore, G. M., Nilges, M., Jones, T. A., Pettersson, G., Knowles, J. K. C., et al. (1989). *Biochemistry, 28*, 7241–7257.
47. Reinikainen, T., Ruohonen, L., Nevanen, T., Laaksonen, L., Kraulis, P., Jones, T. A., et al. (1992). *Proteins: Struct. Funct. Genet. 14*, 475–482.
48. Yang, B., & Wyman, C. E. (2004). *US Patent* 0,185,542.

Appl Biochem Biotechnol (2008) 147:1–9
DOI 10.1007/s12010-007-8047-5

Separate and Concentrate Lactic Acid Using Combination of Nanofiltration and Reverse Osmosis Membranes

Yebo Li · Abolghasem Shahbazi · Karen Williams · Caixia Wan

Received: 15 May 2007 / Accepted: 4 September 2007 /
Published online: 25 September 2007
© Humana Press Inc. 2007

Abstract The processes of lactic acid production include two key stages, which are (a) fermentation and (b) product recovery. In this study, free cell of *Bifidobacterium longum* was used to produce lactic acid from cheese whey. The produced lactic acid was then separated and purified from the fermentation broth using combination of nanofiltration and reverse osmosis membranes. Nanofiltration membrane with a molecular weight cutoff of 100–400 Da was used to separate lactic acid from lactose and cells in the cheese whey fermentation broth in the first step. The obtained permeate from the above nanofiltration is mainly composed of lactic acid and water, which was then concentrated with a reverse osmosis membrane in the second step. Among the tested nanofiltration membranes, HL membrane from GE Osmonics has the highest lactose retention (97±1%). In the reverse osmosis process, the ADF membrane could retain 100% of lactic acid to obtain permeate with water only. The effect of membrane and pressure on permeate flux and retention of lactose/lactic acid was also reported in this paper.

Keywords Cheese whey · Lactic acid · Membrane · Nanofiltration · Reverse osmosis

Introduction

Cheese whey is an important by-product from the cheese manufacturing industry. Typically, 100 g of milk yields 10 g of cheese and 90 g of liquid whey. Cheese whey contains about 4.5–5% lactose, 0.6–0.8% soluble proteins, 0.4–0.5% (w/v) lipids, and varying concentrations of mineral salts [1]. Cheese whey disposal has long been a problem for the dairy industry. Most medium and small cheese producers still dispose of their whey or whey

Y. Li (✉) · C. Wan
Department of Food, Agricultural, and Biological Engineering, The Ohio State University,
1680 Madison Ave, Wooster, OH 44691-4096, USA
e-mail: li.851@osu.edu

A. Shahbazi · K. Williams
Department of Natural Resources and Environmental Design, North Carolina A&T State University,
1601 East Market Street, Greensboro, NC 27411, USA

permeate directly on farmland, which can pose an environmental risk. In response, regulations for land spreading of cheese whey are tightening and looking to ban land spreading of cheese whey. Ultrafiltration/diafiltration has been used to separate whey protein from lactose sugar and other components in the whey. Whey protein has found a good market as a food additive or protein supplement. The permeate stream after ultrafiltration/diafiltration is mainly composed of lactose, salts, and a lot of water, which can be dried to produce whey permeate powder (deproteinized whey). Drying of whey permeate need to remove large amount of water, which is an energy-intensive process. The lactose sugar fraction in cheese whey can be used to produce value-added products such as lactic acid, ethyl alcohol, and methane gas or to grow cells for an antibacterial compound, but this is not currently in full-scale production.

Lactic acid is a natural organic acid and has many applications in the pharmaceutical, food, and chemical industries. It is used as acidulant and preservative, and recently, its potential as substrate for the production of biodegradable plastic has been actively pursued. Approximately half of the world's supply of lactate is produced by fermentation process. Lactic acid has been produced by fermentation of sugar-containing substrates including cheese whey using *Lactobacillus helveticus* [2, 3] and *Lactobacillus casei* [4, 5] in most of the previous studies. *Bifidobacterium longum* was used to produce lactic acid in our previous research [6]. *B. longum* is a bacterium that can convert lactose into lactic acid and also produce an antibacterial compound, which can boost the immune system in its host [7].

The processes of lactic acid production include two key stages, which are (a) fermentation and (b) product recovery. The biggest challenge in lactic acid production lies in the recovery and not in the fermentation step [8]. A successful lactic acid recovery approach is that of continuous fermentation in a recycled reactor where the cells, protein, and lactose are separated by a filtration unit and returned to the fermentor, while the lactic acid is removed in the permeate.

Several different approaches and combinations have been applied for lactic acid recovery from fermentation broth. Neutralization with a base followed by filtration, concentration, and acidification is a traditional process for recovery of lactic acid; this process yields calcium salt as a by-product, causing high chemical cost and waste generation [9]. Other alternative lactic acid recovery processes such as solvent extraction, adsorption, direct distillation, nanofiltration, and electrodialysis have also been studied. The solvent extraction process is limited by unfavorable distribution coefficients and environmental problem because of the use of hazardous solvents. Adsorption process requires regeneration of ion exchange resin and also has the disadvantages such as short lifetime of adsorbents, low capacity, and additional filtration [10]. Direct distillation is an energy-intensive process, and it will causes product transformation, such as the polymerization of lactic acid [11]. Membrane technologies have been proving their advances in the fields of separation and purification. There has been a shift toward membrane separation processes because they are often more capital and energy efficient when compared with chemical separation processes [12]. Membrane processes have several advantages over many of the traditional separation techniques such as distillation, extraction, ion exchange, and adsorption. No energy-intensive phase changes or potentially expensive solvents or adsorbents are needed for membrane separations, and simultaneous separation and concentration of both inorganic and organic compounds is possible. Nanofiltration membrane with a molecular weight cutoff (MWCO) around 400 Da was demonstrated to retain about 97% of lactose and 12–35% of lactate at pH 3.3 in a nanofiltration membrane reactor [13]. In our previous research, ultrafiltration was used to separate cells and proteins from cheese whey fermentation broth. The obtained permeate was then passed through the nanofiltration unit to separate lactic acid from lactose [14].

Electrodialysis might also be an option, but it needs to remove large amounts of salt, which will increase the process cost [15].

The objectives of this study were: (1) to evaluate the performance of nanofiltration filtration membrane for separation of lactose from lactic acid in the fermentation broth and (2) to evaluate the performance of reverse osmosis for lactic acid concentration in the permeate of the nanofiltration. The diagram for the proposed process for lactic acid production and separation was shown in Fig. 1.

Materials and Methods

Fermentation

The whey powder used for the fermentation was obtained from Davisco Foods International (Eden Prairie, MN). The composition of the whey powder in percent w/w is as follows: 6.8% proteins, 78.6% lactose, 0.8% fat, and 4.4% moisture. The whey solution was made by mixing specific amount of whey powder to deionized (DI) water to obtain the designated

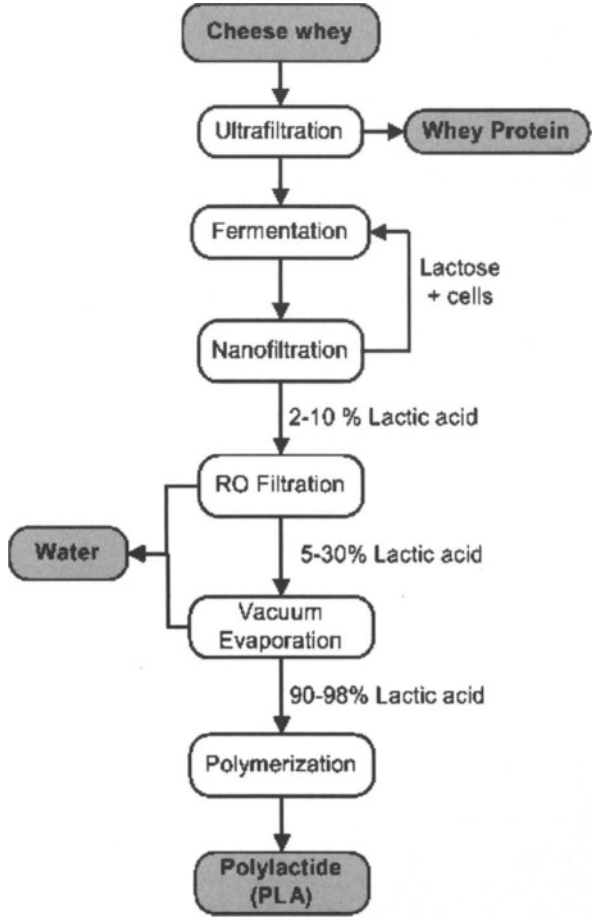


Fig. 1 Flow diagram for lactic acid production and separation from cheese whey

whey concentration. To sterilize the whey solution, it was autoclaved at 110°C for 10 min. The autoclaved cheese whey media was then fermented in a stirred 2.0-L bench-top fermentor with *B. longum*, which was obtained from the National Collection of Food Bacteria (NCFB 2259). The fermentation parameters were as follows: pH 5.5, temperature 37 °C, and agitation 150 rpm. The fermentation broth obtained at different tests was stored in freezer for the membrane separation tests.

Nanofiltration

A cross-flow nanofiltration module (SEPA CF II, GE Osmonics, Minneapolis, MN) was used for this process with a maximum operating pressure of 7.0 MPa. The surface area of the membrane is 140 cm^2. The holdup volume of the membrane unit is 70 mL. The fermentation broth was placed in a 5-L fermentation vessel to control the temperature, agitation, and pH. A bench-top pump (M03-S, Hydra cell, Minneapolis, MN) was used to pump the fermentation broth through the cross-flow membrane separation unit and recycle back to the fermentor (Fig. 2). The permeate was collected on a digital balance attached to a laptop computer with a RS-COM version 2.40 system (A&D, Milpitas, CA) that recorded the amount of permeate collected every 0.5 min. The fermentation broth was kept at constant temperature (37 °C), pH (5.5), and agitation (200 rpm). Transmembrane pressures of 1.4, 2.1, and 2.8 MPa were used in the nanofiltration tests. Each condition was tested twice, and each test lasted for 2 h. Samples of the original broth (before separation), permeate, and retentate were collected for analysis.

In this research, five nanofiltration membranes (CK, DK, DL, GE, and HL) obtained from GE Osmonics were tested. Table 1 shows the product specifications of the membranes.

Reverse Osmosis

The permeate collected from nanofiltration was placed in a 2-L fermentation vessel. Using the same system setup as that for nanofiltration, the lactic acid in the nanofiltration permeate was concentrated with reverse osmosis membrane. However, the pH was not regulated during reverse osmosis separation; only the temperature (37 °C) and agitation

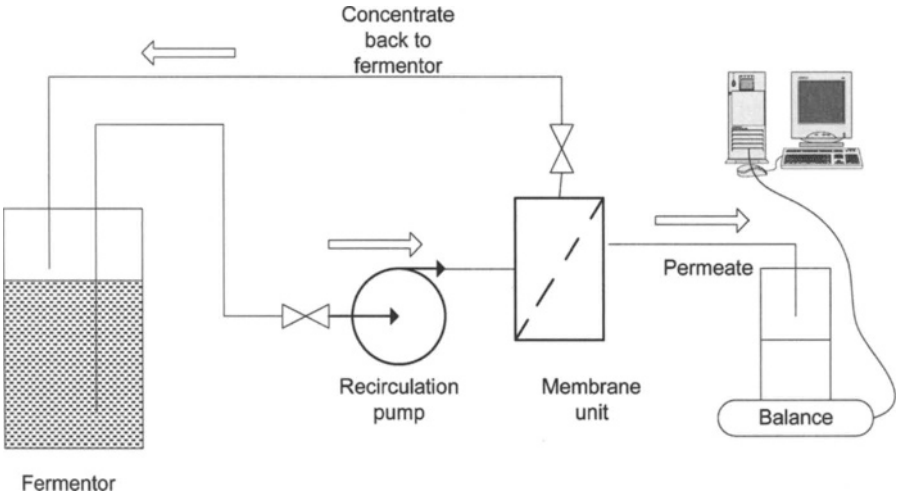


Fig. 2 Schematic diagram of the nanofiltration membrane separation system

Table 1 Product specifications for the five nanofiltration membranes tested.

Class	Polymer	Designation	Rejection size	MWCO (Da)
NF	Cellulose Acetate	CK	92% Na_2SO_4	175–15,000
NF	Thin film composites	DK	98% $MgSO_4$	0–400
NF	Thin film composites	DL	96% $MgSO_4$	0–400
NF	Thin film composites	HL	98% $MgSO_4$	0–400
NF	Composite polyamide	GE	1,000 Da	1,000–200,000

(200 rpm) were controlled. During reverse osmosis separation, two membranes were tested: DS 11 AG and ADF (GE Osmonics) at pressures of 4.1 and 5.5 MPa, respectively. Each test lasted for 75 min. There were two replications for each test. Samples of the original solution, permeate, and retentate were collected for analysis.

Membrane Cleaning

An alkali acid treatment method was applied to the membrane system (both nanofiltration and reverse osmosis separation) in the following steps: (a) fully open the recirculation and permeate valves, (b) flush with tap water for 5 min, (c) circulate 2 L of 4% phosphoric acid for 10 min, (d) rinse with tap water for 5 min, (e) circulate 2 L of 0.1 N NaOH solution for 10 min, and (f) rinse with 10 L of DI water for 5 min.

Analyses

Lactose, lactic acid, and acetic acid were determined by high-performance liquid chromatography (Waters, Milford, MA) with a KC-811 ion exclusion column and a Waters 410 differential refractometer detector. The mobile phase was 0.1% H_3PO_4 solution at a flow rate of 1 mL/min. The temperatures of the detector and of the column were maintained at 35 and 60 °C, respectively.

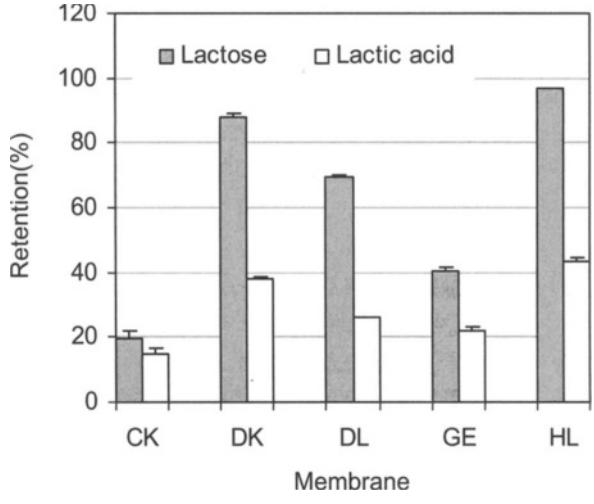


Fig. 3 Effect of membrane on lactose and lactic acid retention (2.1 MPa)

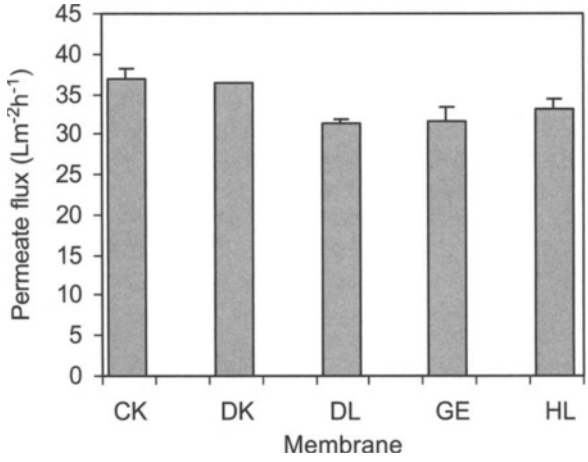


Fig. 4 Effect of membrane on permeate flux (2.1 MPa)

The performance of the membrane was evaluated by using two criteria: (a) permeate flux and (b) component retention. The permeate flux was calculated by measuring the quantity of permeate collected during a certain time and dividing it by the effective membrane area for filtration.

$$\text{Permeate flux} = \frac{\text{premeat volume}}{\text{membrane area} \times \text{time}} \quad \left(\text{L m}^{-2}\,\text{h}^{-1}\right) \tag{1}$$

The component retention (%) was defined as:

$$\text{Retention} = \left(1 - \frac{\text{concentration of component in the permeate}}{\text{concentration of component in the feed stream}}\right) \times 100 \tag{2}$$

Analysis of variance was performed using a statistical package from the SAS System (SAS Institute, Cary, NC).

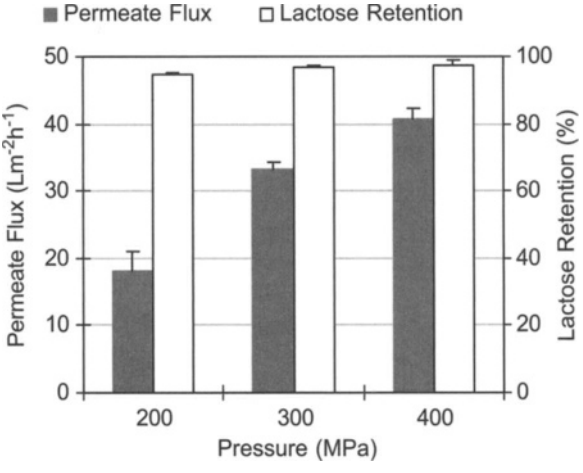


Fig. 5 Effect of pressure on permeate flux and lactose retention of HL membrane

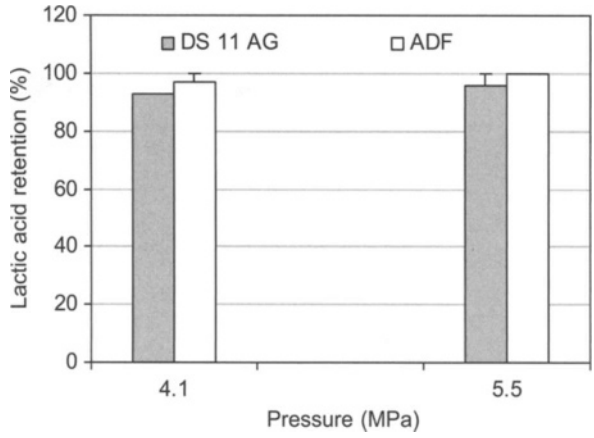


Fig. 6 Effects of pressure and membrane type on lactic acid retention of reverse osmosis separation

Results and Discussion

Nanofiltration

The concentration of lactose and lactic acid in the fermentation both varied with the fermentation conditions such as initial cheese whey concentration, pH, cell density, and fermentation time. The lactose concentration in most of the runs is less than 1%, and the lactic acid concentration is about 3%. The fermentation broth obtained from the fermentation tests was mixed, and the lactic acid and lactose concentration was adjusted to 5 and 2% for nanofiltration tests.

Five nanofiltration membranes, CK, DK, DL, GE, and HL, were tested at the same temperature (37 °C), pH (5.5), and pressure (2.1 MPa). The HL, DK, and DL membranes have the lowest MWCO, therefore allowing little or no solute to pass through the membrane, thereby increasing the lactose retention. The lactose retention of the HL, DK, and DL membrane was 96.8, 88.2, and 69.8%, respectively (Fig. 3). The lactic acid

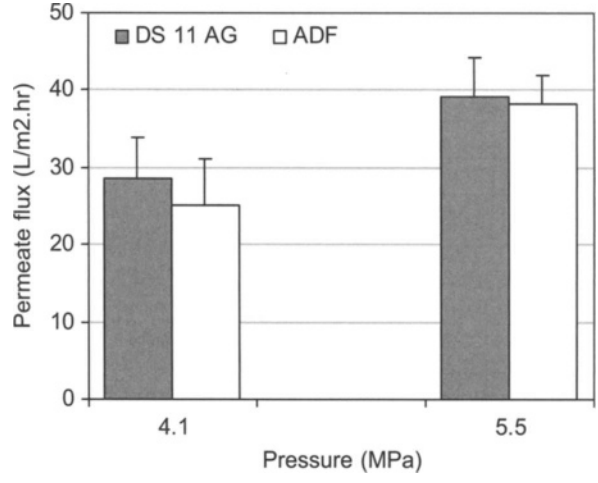


Fig. 7 Effects of pressure and membrane type on permeate flux of reverse osmosis separation

retention of the HL, DK, and DL membrane was 43.7, 38.0, and 26.1%, respectively. The permeate flux was also affected by the membrane type (Fig. 4). The CK membrane has the highest permeate flux of 36.8 L m^{-2} h^{-1}. The lowest permeate flux of 31.3 L m^{-2} h^{-1} was obtained with the DL membrane. The results of these tests show that the HL membrane was most efficient with almost 97% lactose retention and a permeate flux of 33.0 L m^{-2} h^{-1}.

The effects of pressure on lactose retention and permeate flux of the HL membrane were shown in Fig. 5. Permeate fluxes of 18.0, 33.2, and 40.6 L m^{-2} h^{-1} were obtained at pressure of 1.4, 2.1, and 2.8 MPa, respectively. The effect of pressure on lactose retention was not significant ($p>0.3$). The lactose retention kept almost constant at 97±1%. These observations are in agreement with literature data [10].

Reverse Osmosis

Reverse osmosis was applied to concentrate the lactic acid in the permeate of nanofiltration process. The permeate collected from nanofiltration with the HL membrane was used. Two reverse osmosis membranes (DS 11 AG and ADF) were tested at 4.1 and 5.5 MPa.

Slightly higher lactic acid retention was obtained with the ADF membrane compared to that of the DS 11 AG membrane (Fig. 6). The lactic acid retention for the ADF membrane was 96.7 and 100.0% at pressures of 4.1 and 5.5 MPa, respectively, while the lactic acid retention for the DS 11AG membrane was 92.6 and 96% at pressures of 4.1 and 5.5 MPa, respectively. The effect of membrane and pressure on lactic acid retention was not significant ($p>0.1$).

Figure 7 shows the results of permeate flux obtained with DS 11 AG and ADF membranes at pressures of 4.1 and 5.5 MPa. Higher permeate flux was obtained with DS 11AG membrane than that of the ADF membrane, but the effect of membrane on the permeate flux is not significant ($p>0.1$). The results show that permeate flux was significantly affected by the pressure ($p<0.005$). Higher permeate flux was obtained at a higher pressure.

Conclusion

Combined nanofiltration and reverse osmosis membranes could successfully separate and concentrate lactic acid from cheese whey fermentation broth. Nanofiltration membrane could retain about 97% of lactose to obtain permeate mainly containing lactic acid and water. The highest lactose retention of 97% was obtained with the HL membrane. The tested reverse osmosis membranes successfully separated lactic acid from water. Nearly 100% of lactic acid retention was obtained with the ADF membrane.

Further study needs to be conducted on the nanofiltration membrane to obtain 100% lactose retention and lower lactic acid retention. The economic analysis for the lactic acid recovery with membrane separation also needs to be analyzed and compared with that of other downstream processes.

References

1. Siso, M. I. G. (1996). *Bioresource Technology, 57*, 1–11.
2. Shahbazi, A., Mims, M. R., Li, Y., Shirley, V., Ibrahim, S. A., & Morris, A. (2005). *Applied Biochemistry and Biotechnology, 121–124*, 529–540.

3. Tango, M. S. A., & Ghaly, A. E. (2002). *Applied Microbiology and Biotechnology, 58*, 712–720.
4. Bruno-Barcena, J. M., Ragout, A. L., Cordoba, P. R., & Sineriz, F. (1999). *Applied Microbiology and Biotechnology, 51*, 316–324.
5. Senthuran, A., Senthuran, V., & Hatti-Kaul, R. (1999). *Journal of Biotechnology, 73*, 61–70.
6. Li, Y., Shahbazi, A., & Coulibaly, S. (2006). *Transactions of the ASABE, 49*(4), 1263–1267.
7. Song, S. H., Kim, T. B., Oh, H. I., & Oh, D. K. (2003). *World Journal of Microbiology & Biotechnology, 19*, 721–731.
8. Atkinson, B., & Mavituna, F. (1991). *Biochemical engineering and biotechnology handbook* (2nd ed., pp. 1181–1182). New York, NY: Stockton.
9. Wasewar, K. L. (2005). *Chemical and Biochemical Engineering Quarterly, 19*(2), 159–172.
10. Huang, C., Xu, T., Zhang, Y., Xue, Y., & Chen, G. (2007). *Journal of Membrane Science, 288*, 1–12.
11. Cockrem, M. C. M., & Johnson, P. D. (1993). *US Patent*, USP 5210296.
12. Ho, W., & Sirkar, K. (1992). *Membrane handbook*. New York: Chapman and Hall.
13. Jeantet, R., Maubois, J. L., & Boyaval, P. (1996). *Enzyme and Microbial Technology, 19*, 614–619.
14. Li, Y., & Shahbazi, A. (2006). *Applied Biochemistry and Biotechnology, 129–132*, 985–996.
15. Freger, V., Arnot, C., & Howell, J. A. (2000). *Journal of Membrane Science, 178*, 185–193.

Appl Biochem Biotechnol (2008) 147:11–21
DOI 10.1007/s12010-007-8045-7

Parameter Estimation for Simultaneous Saccharification and Fermentation of Food Waste Into Ethanol Using Matlab Simulink

Rebecca Anne Davis

Received: 15 May 2007 / Accepted: 4 September 2007 /
Published online: 6 October 2007
© Humana Press Inc. 2007

Abstract The increase in waste disposal and energy costs has provided an incentive to convert carbohydrate-rich food waste streams into fuel. For example, dining halls and restaurants discard foods that require tipping fees for removal. An effective use of food waste may be the enzymatic hydrolysis of the waste to simple sugars and fermentation of the sugars to ethanol. As these wastes have complex compositions which may change day-to-day, experiments were carried out to test fermentability of two different types of food waste at 27° C using *Saccharomyces cerevisiae* yeast (ATCC4124) and Genencor's STARGEN™ enzyme in batch simultaneous saccharification and fermentation (SSF) experiments. A mathematical model of SSF based on experimentally matched rate equations for enzyme hydrolysis and yeast fermentation was developed in Matlab Simulink®. Using Simulink® parameter estimation 1.1.3, parameters for hydrolysis and fermentation were estimated through modified Michaelis–Menten and Monod-type equations with the aim of predicting changes in the levels of ethanol and glycerol from different initial concentrations of glucose, fructose, maltose, and starch. The model predictions and experimental observations agree reasonably well for the two food waste streams and a third validation dataset. The approach of using Simulink® as a dynamic visual model for SSF represents a simple method which can be applied to a variety of biological pathways and may be very useful for systems approaches in metabolic engineering in the future.

Keywords Food waste · Hydrolysis · Ethanol · Simultaneous saccharification and fermentation · Matlab · Simulink® · Parameter estimation · Metabolic engineering

R. A. Davis (✉)
Department of Agricultural & Biological Engineering, Purdue University, 225 South University Street, West Lafayette, IN 47907-2093, USA
e-mail: davis160@purdue.edu

Nomenclature

C_{etoh}	ethanol concentration (g/l)
C_{fru}	fructose concentration (g/l)
C_{glc}	glucose concentration (g/l)
C_{gly}	glycerol concentration (g/l)
C_{mal}	maltose concentration (g/l)
C^{in}	inhibitory product concentration (g/l)
C_{starch}	starch concentration (g/l)
C_{suc}	sucrose concentration (g/l)
$C_{x,0}$	initial concentration (x=component g/l)
K_i	competitive inhibition constant (g/l)
Km	Michaelis–Menten constant (g/l)
K_s	uncompetitive inhibition constant of starch (g/l)
N	toxic power constant for glucose product inhibition
PME	processed ready-to-eat food
RICE	rice mixture
SSF	simultaneous saccharification and fermentation
V_m	maximal initial reaction rate (g l^{-1} h^{-1})
Y_{el}	fraction of glucose to ethanol ($1-Y_{el}$=fraction to glycerol)
$Y_{glc/mal}$	yield of glucose to maltose
$Y_{glc/starch}$	yield of glucose to starch
$Y_{hex/suc}$	yield of hexose to sucrose
$Y_{etoh/hex}$	yield of ethanol to hexose
$Y_{gly/hex}$	yield of glycerol to hexose

Introduction

In the USA alone, more than 91 billion pounds of edible food (27% of what is produced for consumption) are lost each year by the retail, consumer, and food service industries, almost all of which is unrecoverable [1]. Composting is one recovery path; however, it is time-consuming, location-dependent, and subject to contamination. At Purdue University, food waste from cafeteria trays is discarded separately from other trash and accounts for approximately 150 tons of food waste from residence halls and the Union. This does not include the waste from food prep. It is estimated that 340 tons per year of food waste is thrown in dumpsters or trash bins on Purdue campus (J. Zarate, West Lafayette, IN, 2006, personal communication).

A mobile or stand-alone unit which would controllably convert food waste into ethanol at a busy cafeteria or restaurant would be attractive if the economics were favorable. Using a black-box model, several components are considered important for monitoring the conversion into ethanol (Fig. 1).

Preliminary experiments determined that a loading of 0.8 g STARGEN™ enzyme (mixture of alpha-amylase and glucoamylase) and 90 g pre-grown *Saccharomyces cerevisiae* (ATCC4124) per liter of food waste slurry was sufficient. Under these conditions, hydrolysis and fermentation rates were not dependent on mass transfer limitations up to the maximum food waste slurry concentration of 400 g/l solids (104 g/l starch, 136 g/l mono- and disaccharides). To determine the final concentrations of ethanol and glycerol from initial concentrations of sugars and starch, datasets for hydrolysis and simultaneous saccharification and fermentation (SSF) of two types of food waste were used as fitting criteria for nonlinear

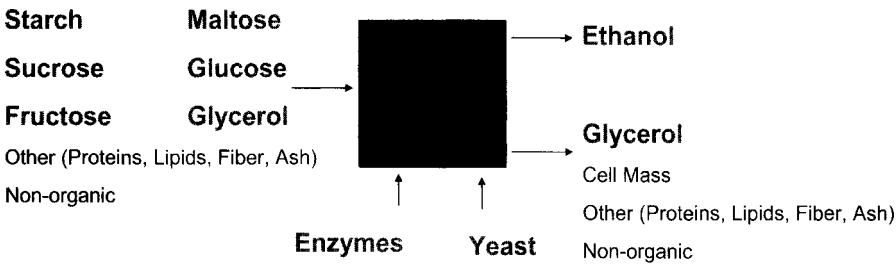


Fig. 1 The black-box model showing relevant inputs and outputs for SSF conversion of food waste

parameter estimation of kinetic model parameters. The kinetic models were based on established Michaelis–Menten and Monod-type equations.

The objective of this study was to generate a simple, editable, SSF black-box model template which could predict ethanol and glycerol production based on initial food waste conditions. With increased datasets and more advanced mathematical functions, these models and their predictive ability will continue to improve. The heterogeneous nature of food waste requires a robust model which can handle changing feed composition. These models, once improved, could serve as predictive tools to determine the expected ethanol productivity per year to control flow rates on a mobile unit or to determine the economic drivers of such a system.

Materials and Methods

Food Material

Two samples of homogenized food waste were used to match hydrolysis and SSF fermentation profiles to the kinetic models. The first sample was a mixture of processed ready-to-eat packaged food (PRE). LC analysis matched the composition of simple sugars and glycerol found on the PRE packages. Additional nutritional data on packages was used to determine starch (by difference), protein, ash, and lipids content. Theoretical ethanol yield for the PRE sample at a concentration of 100 g/l was 32.0 g/l.

The second food sample was a rice mixture which contained seaweed, egg, rice, imitation crab, and spinach. LC analysis was used to determine sugars and glycerol. Relative moisture, protein, lipid, ash, and carbohydrates were calculated based on USDA National Nutrient Database [2]. Theoretical ethanol yield for a 100 g/l sample was 34.6 g/l. Pictures of the dried, homogenized PRE mixture and the rice mixture are shown in Fig. 2a and b, respectively. Compositions of the two food mixtures are seen in Fig. 3. The PRE mixture (Fig. 3a) has less

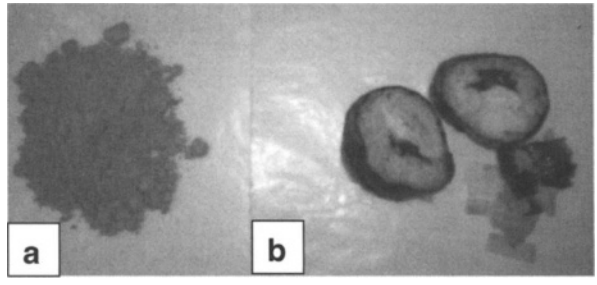


Fig. 2 Food waste (**a**) dried, homogenized PRE mixture (**b**) rice mixture

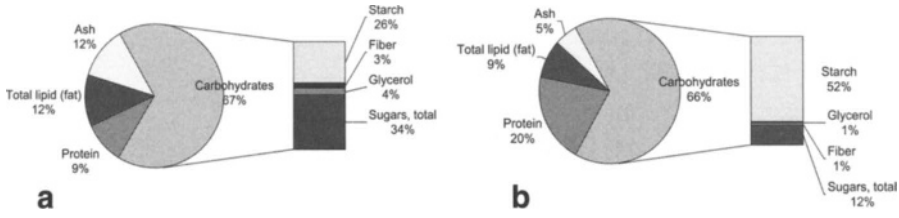


Fig. 3 Food waste composition on dry basis (**a**) PRE mixture (**b**) rice mixture

starch and more sugars (mono- and disaccharides), but the same overall composition of carbohydrates compared to the rice mixture (Fig. 3b).

A third set of data was prepared to represent a typical kitchen waste stream (food, plastic, paper, cardboard, etc.). Initial composition of the validation dataset was C_{starch}= 25 g/l, C_{glc}=5.7 g/l, C_{mal}=2.9 g/l, C_{suc}=1 g/l, C_{fru}=7.8 g/l, C_{gly}=1.2 g/l. This mixture was run under both hydrolysis only, and SSF conditions and the models created from the PRE and Rice mixture samples were compared as predictive models to the validation dataset. The PRE, Rice, and validation mixtures all had pH values of around pH=7 at 100 g/l concentration. The pH was not controlled throughout hydrolysis and SSF to mimic the simplest design scenario and lessen the model complexity.

Hydrolysis Procedure

Hydrolysis experiments were carried out in a G-24 Environmental Incubator (New Brunswick Scientific, Edison, NJ, USA) set on 250 rpm. Hydrolysis vessels were a 300-ml Erlenmeyer flask with sidearm sealed as in SSF experiments to allow identical conditions to SSF. The hydrolysis experiments were run at 27 °C (the optimal yeast growth temperature) to match the SSF experiments. The recommended conditions for STARGEN™ enzyme is between 20 and 40 °C.

The food slurry was allowed to shake for 1–5 min before STARGEN™ enzyme was added. Samples were taken in 1-ml volumes and pipetted into Optimum Tubes (Life Science, Colorado, USA). If the mixture was especially viscous or large pieces of matter were present, the pipette tips were cut to prevent clogging. The hydrolysis was ended by immediately spinning down samples in an Eppendorf centrifuge at RT for 5 min and 12,000 rpm then filtering the supernatant using a 3-ml syringe with Luer–Lok (Beckton Dickinson, NJ, USA) and 25-mm, 0.2-μm syringe filter (Fisher Scientific). The filtrate was stored in the freezer for future analysis.

SSF Procedure

SSF experiments were performed in a 300-ml Erlenmeyer flask with sidearm at 27 °C and 250 rpm. Yeast was pre-grown in 100 ml YEPD overnight until reaching 500–550 KU (~90 g/l), spun down, and then added to the food waste mixture. STARGEN™ enzyme was added, and the flasks were sealed with Saran wrap to allow fermentation to be carried out under largely anaerobic conditions. Figure 4 shows the two mixtures undergoing SSF.

Analytical Methods

LC columns were used to measure the simple sugars, glycerol, and ethanol. For monosaccharides, a YMC-Pack PolyamineII column (4.6×250 mm; Japan) with column

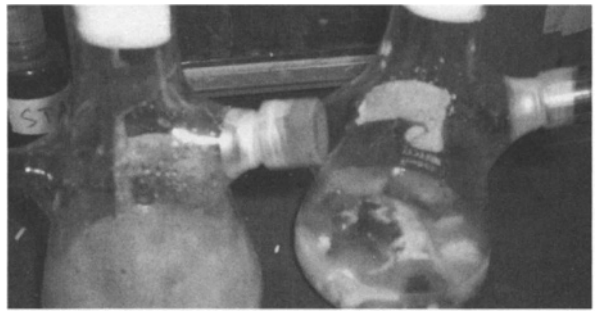


Fig. 4 Batch SSF experiments of food waste

heater (25 °C) was used, with an autoinjector (Hitachi AS-4000), pump (Hitachi L-6200), RI detector (Hitachi L-3350), and a computing integrator (Hitachi D-2500) at 40-μl injection volumes. The mobile phase was 75/25 Acetonitrile/DIW, degassed and filtered through a 0.2-μm nylon filter (Millipore).

For maltose, ethanol, and glycerol, an Aminex HPX-87H ion exchange column (Biorad, Hercules, CA, USA) with column heater (50 °C) was used with a Varian 9010 Solvent Delivery System, Waters 717plus Autosampler, Waters 2414 refractive index detector, and a Hewlett Packard HP3396G integrator at 50-μl injection volumes. The mobile phase was degassed 5 mM H_2SO_4 and filtered through a 0.2-μm nylon filter (Millipore).

Mathematical Models

Model Structure

The experimental and mathematical models were divided into two hierarchical steps, as seen in Fig. 5. First, hydrolysis experiments were conducted, and the hydrolysis time profile was matched to hydrolysis rate equations. A separate hydrolysis-only model was used to match the hydrolysis data to Michaelis–Menten based kinetics and to solve for unknown parameters. Second, SSF experiments were conducted using identical enzyme loading, and these datasets were matched to a complete SSF model. The SSF model incorporated the hydrolysis parameters from the first step and was used to solve for the unknown fermentation parameters using Monod-based kinetics.

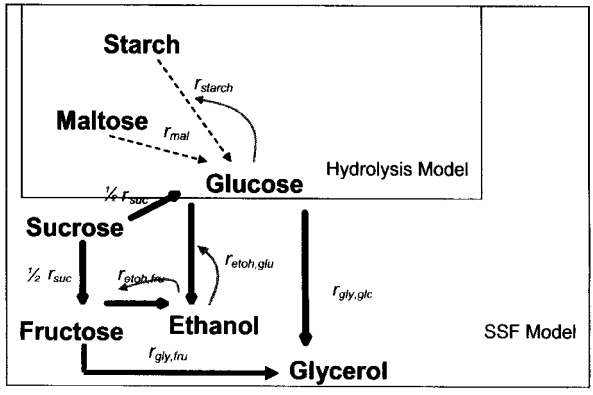


Fig. 5 Decomposition of hydrolysis and SSF models

Table 1 Balance equations for the hydrolysis model.

Hydrolysis model
$\frac{dC_{\text{starch}}}{dt} = -r_{\text{starch}}$
$\frac{dC_{\text{mal}}}{dt} = -r_{\text{mal}}$
$\frac{dC_{\text{glc}}}{dt} = Y_{\text{glc/mal}} r_{\text{mal}} + Y_{\text{glc/starch}} r_{\text{starch}}$

Tables 1 and 2 list the complete set of mass balance equations for the hydrolysis model and the SSF model. Dilution due to cell growth was not included in the model, nor was a cell mass balance. As cells were grown to maximal exponential phase before the batch runs and the fermentation was 90% complete in 5 h or less, any maintenance or growth requirements were neglected, and yield coefficients were used to determine the conversion yield for each reaction rate.

Simulink Model

The Matlab Simulink® Model was designed to represent the model structure and mass balance equations for SSF and is shown in Fig. 6. Shaded boxes represent the reaction rates, which have been lumped into subsystems. To solve the system of ordinary differential equations (ODEs) and to estimate unknown parameters in the reaction rate equations, the interface parameter estimation was used. This program allows the user to decide which parameters to estimate and which type of ODE solver and optimization technique to use. The user imports observed data as it relates to the input, output, or state data of the Simulink® model. With the imported data as reference, the user can select options for the ODE solver (fixed step/variable step, stiff/non-stiff, tolerance, step size) as well options for the optimization technique (nonlinear least squares/simplex, maximum number of iterations, and tolerance). With the selected solver and optimization method, the unknown independent, dependent, and/or initial state parameters in the model are determined within set ranges. For this study, nonlinear least squares regression was used with Matlab ode45, which is a Runge–Kutta [3, 4] formula for non-stiff systems. The steps of nonlinear least squares regression are as follows:

1. Guess initial values for parameters: K_{mm}, V_{mm}, K_{ms}, $Y_{\text{Glc/S}}$, etc. Set n(iteration)=0.
2. Solve for dy(t)/dt using Simulink simulation and iterative solver (ode45).
3. Use optimization algorithm to update parameters (nonlinear least square).
4. Check if minimization is reached $|J^{n+1}-J^{n}|<$ tolerance. If not, set $n=n+1$ and go back to step 2 for next iteration.

Table 2 Balance equations for the SSF model.

SFF model
$\frac{dC_{\text{starch}}}{dt} = -r_{\text{starch}}$
$\frac{dC_{\text{mal}}}{dt} = -r_{\text{mal}}$
$\frac{dC_{\text{glc}}}{dt} = Y_{\text{glc/mal}} r_{\text{mal}} + Y_{\text{glc/starch}} r_{\text{starch}} + \frac{1}{2} Y_{\text{hex/suc}} r_{\text{suc}} - r_{\text{etoh,glc}} - r_{\text{gly,glc}}$
$\frac{dC_{\text{suc}}}{dt} = -r_{\text{suc}}$
$\frac{dC_{\text{fru}}}{dt} = \frac{1}{2} Y_{\text{hex/suc}} r_{\text{suc}} - r_{\text{etoh,fru}} - r_{\text{gly,fru}}$
$\frac{dC_{\text{etoh}}}{dt} = Y_{el}\left[Y_{\text{etoh/hex}}\left(r_{\text{etoh,glc}} + r_{\text{etoh,fru}}\right)\right]$
$\frac{dC_{\text{gly}}}{dt} = (1 - Y_{\text{el}})\left[Y_{\text{gly/hex}}\left(r_{\text{gly,glc}} + r_{\text{gly,fru}}\right)\right]$

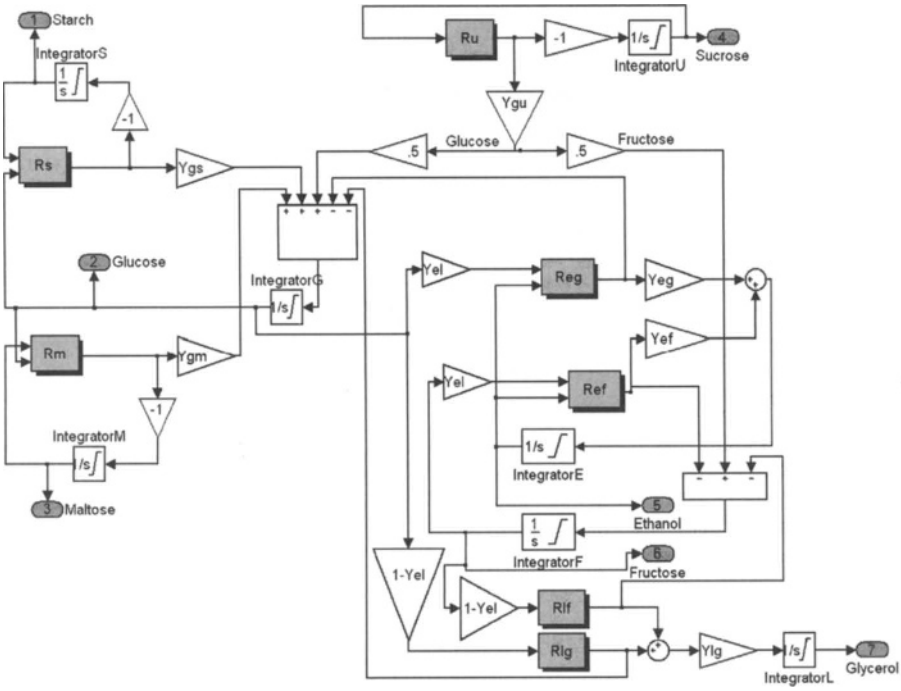


Fig. 6 Matlab Simulink model for SSF parameter estimation

The cost function, J, is a calculation of the squared errors for the two models to the datasets. If the minimization between the model-simulated results for each of the cases results in exactly the same system parameters, the cost function will be driven to zero.

Kinetic Rate Equations

Table 3 lists the kinetic rate expressions for each of the hydrolysis and fermentation reaction rates shown in Fig. 5 and in the mass balance equations of Tables 1 and 2. Each of the reaction rates were found to fit the data through trial and error, starting with the simplest model. For the hydrolysis reaction rates (r_{starch} and $r_{maltose}$), the simplest form was the Michaelis–Menten model without inhibition. For all other reaction rates which described fermentation kinetics, the simplest form was the Monod model without inhibition. More descriptive models were found in the literature and tested one by one until the set of kinetic rate equations with the best fit to the experimental data were determined. This was completed with the hydrolysis datasets first, then the complete SSF datasets.

The reaction rate for the hydrolysis of starch (Eq. 2.1 in Table 3) is a Michaelis–Menten type model, which considers competitive product inhibition of glucose and substrate inhibition of starch. The hydrolysis of maltose (Eq. 2.2 in Table 3) is represented by a Michaelis–Menten type model with competitive product inhibition. These equations were tested by Lopez et al. [3] for hydrolysis of chestnut puree by an alpha and glucoamylase mixture. As the enzyme STARGEN™ also contains amounts of alpha and glucoamylase, it was not surprising that they (Eqs. 2.1–2.2 in Table 3) fit the hydrolysis data better than non-inhibitory Michaelis–Menten kinetics.

Table 3 Kinetic rate equations.

Equations	Number	Reference
$r_{\text{starch}} = \frac{C_{\text{starch}} V_{m,\text{starch}}}{C_{\text{starch}} + K_{m,\text{starch}} \left(\frac{C_{\text{glc}}}{K_{i,\text{starch}}} + 1 \right) + K_{s,\text{starch}} C_{\text{starch}}^2}$	(2.1)	[4]
$r_{\text{mal}} = \frac{C_{\text{mal}} V_{m,\text{mal}}}{C_{\text{mal}} + K_{m,\text{mal}} \left(\frac{C_{\text{glc}}}{K_{i,\text{mal}}} + 1 \right)}$	(2.2)	[4]
$r_{\text{suc}} = \frac{C_{\text{suc}} V_{m,\text{suc}}}{C_{\text{suc}} + K_{m,\text{suc}}}$	(2.3)	
$r_{\text{etoh,glc}} = \frac{-C_{\text{glc}} V_{m,\text{glc}}}{C_{\text{glc}} + K_{m,\text{glc}}} \left(1 + \frac{C_{\text{etoh}}}{C_{\text{etoh}}^M} \right)^n$	(2.4)	[7]
$r_{\text{etoh,fru}} = \frac{-C_{\text{fru}} V_{m,\text{fru}}}{C_{\text{fru}} + K_{m,\text{fru}}} \left(1 + \frac{C_{\text{etoh}}}{C_{\text{etoh}}^M} \right)^n$	(2.5)	[7]
$r_{\text{gly,glc}} = \frac{C_{\text{glc}} V_{m,\text{gly}}}{C_{\text{glc}} + K_{m,\text{gly}}}$	(2.6)	
$r_{\text{gly,fru}} = \frac{C_{\text{fru}} V_{m,\text{gly}}}{C_{\text{fru}} + K_{m,\text{gly}}}$	(2.7)	

For the fermentation reaction kinetics, both the sucrose (Eq. 2.3 in Table 3) and glycerol reactions (Eqs. 2.6–2.7 in Table 3) used were simple Monod models without inhibition. Sucrose is hydrolyzed by invertase, an enzyme in the yeast cell envelope. When glucose levels are high, the invertase repressor genes are expressed, and when low, the expression is derepressed [4]. For sucrose, therefore, the hydrolysis into fructose and glucose is dependent on the concentration of glucose and is purely enzymatic; the sucrose molecule is not transported into the yeast cell. It is unclear at what concentration of glucose the invertase expression is repressed and whether the conversion is inhibited by either glucose of fructose. For simplicity, a simple Monod equation was used and found to fit the data well, with cost functions lower than modified Monod equations.

Glycerol formation is another pathway besides ethanol formation to replenish NAD+ and maintain redox balance in the cell. In addition, glycerol is important for osmoregulation where,

Table 4 Hydrolysis initial and kinetic parameters.

	100 g/l PRE	400 g/l PRE	Units
Initial conditions			
$C_{\text{starch},0}$	26.1	104	g/l
$C_{\text{mal},0}$	3.33	13.3	g/l
$C_{\text{glc},0}$	5.42	21.7	g/l
$C_{\text{suc},0}$	20.0	80.0	g/l
$C_{\text{fru},0}$	5.04	20.2	g/l
Evaluated parameters			
$V_{m,\text{starch}}$	417		$\text{g l}^{-1}\ \text{h}^{-1}$
$K_{m,\text{starch}}$	27		g/l
$K_{i,\text{starch}}$	0.5		g/l
$K_{s,\text{starch}}$	0.076		g/l
$V_{m,\text{mal}}$	343		$\text{g l}^{-1}\ \text{h}^{-1}$
$K_{m,\text{mal}}$	4.97		g/l
$K_{i,\text{mal}}$	0.77		g/l
$Y_{\text{glc/starch}}$	0.66		
$Y_{\text{glc/mal}}$	1.05		

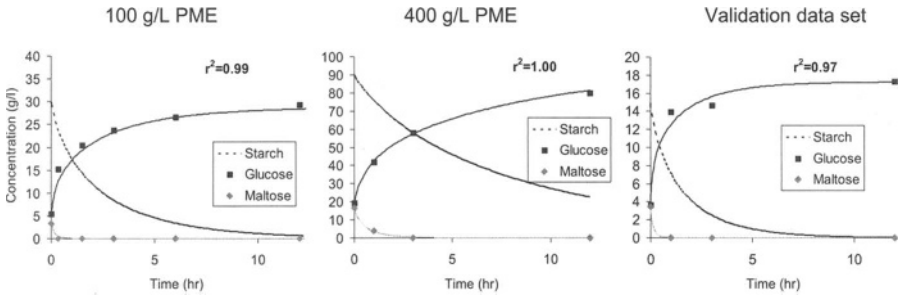


Fig. 7 Comparison of measured to simulated data for the hydrolysis experiments using the PRE mixture at 100, 400 g/l, and the validation data set

under conditions of decreased extracellular water activity, glycerol formation is increased [5]. Glycerol is produced at the expense of ethanol production and, after trial-and-error with product inhibition models, the simple Monod model gave best fits to the data based on the lowest resulting cost function.

Table 5 SSF initial and kinetic parameters.

	100 g/l PRE	100 g/l rice mixture	Units
Initial conditions			
$C_{starch,0}$	26.1	52.5	g/l
$C_{mal,0}$	3.33	0.66	g/l
$C_{glc,0}$	5.42	4.04	g/l
$C_{suc,0}$	20.0	3.090	g/l
$C_{fru,0}$	5.04	4.05	g/l
Fixed parameters			
$V_{m,starch}$	417		$g\ l^{-1}\ h^{-1}$
$K_{m,starch}$	27		g/l
$K_{i,starch}$	0.5		g/l
$K_{s,starch}$	0.076		g/l
$V_{m,mal}$	343		$g\ l^{-1}\ h^{-1}$
$K_{m,mal}$	4.97		g/l
$K_{i,mal}$	0.77		g/l
$Y_{glc/starch}$	0.66		
$Y_{glc/mal}$	1.05		
N	0.36		
$Y_{hex/suc}$	1.05		
C_{etoh}	100		g/l
$K_{m,glc}=K_{m,fru}$	0.315		g/l
Evaluated parameters			
$V_{m,suc}$	14.5		$g\ l^{-1}\ h^{-1}$
$K_{m,suc}$	2.7		g/l
$V_{m,glc}$	15		$g\ l^{-1}\ h^{-1}$
$V_{m,fru}$	4.2		$g\ l^{-1}\ h^{-1}$
$V_{m,glc}$	45.1		$g\ l^{-1}\ h^{-1}$
$K_{m,gly}$	101		g/l
$Y_{gly/hex}$	1.02		
Y_{el}	0.81		
$Y_{etoh/hex}$	0.511		

The utilization of glucose and fructose into ethanol uses the Levenspiel toxic inhibition equation for ethanol production [6]. This was used after more complex rate expressions including both substrate and product inhibition failed to improve model performance evidenced by failing to decrease the cost function.

Results and Discussion

Hydrolysis Results

Parameter estimate results from best fit kinetic expressions are listed in Table 4 for each of the hydrolysis reaction rates and yield coefficients. Using these parameters, Fig. 7 compares measured to simulated data for the hydrolysis experiments using the MRE mixture at 100, 400 g/l, and the validation dataset. The r^2 values, coefficient of determination, for glucose are 0.99, 1.00, 0.97, respectively, indicating a good fit to all three datasets.

SSF Results

The SSF parameters are listed in Table 5 and the measured and calculated data can be seen in Fig. 8. In modeling the fermentation reaction kinetics, it was found that for the parameter estimation simulations to match Matlab Simulink® simulations of the same model, the data had to be weighted. Giving higher weights to a data point means that the selected data point has more influence over the parameter estimates. If certain data points are more precisely

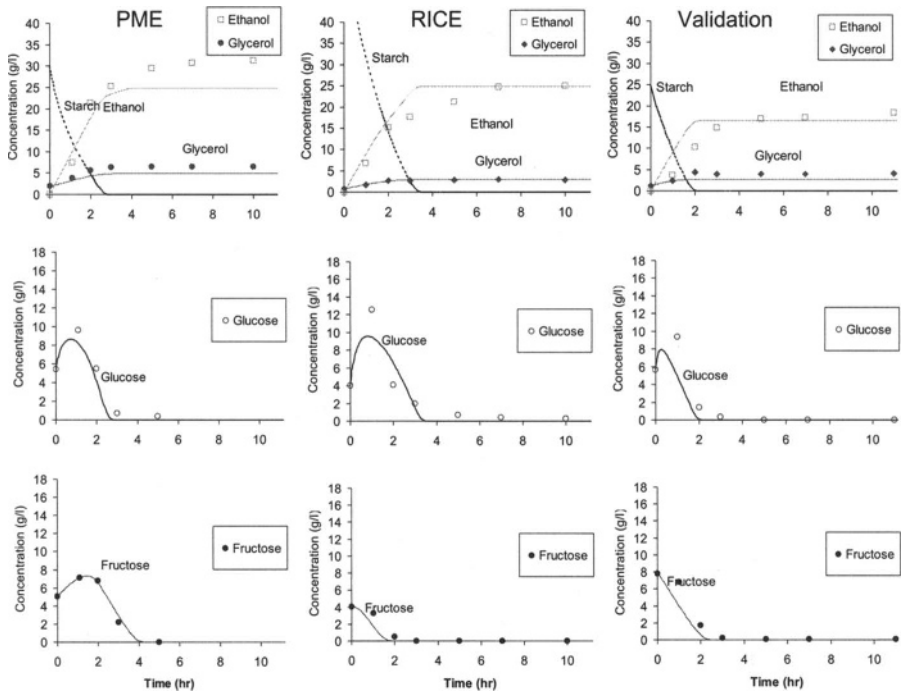


Fig. 8 Measured and simulated data for the SSF experiments using the PME mixture, the RICE mixture, and the validation data set

measured, for instance, then they should be given higher weighting then the points which are not precisely measured [7]. In the case of SSF, all but two trends (glucose and fructose) followed either an increasing or decreasing pattern. Given equal weighting, this meant that the optimization technique estimated the same, regardless of these two trends behaving differently (stiffer) than the other trends. The result of weighting the same led to what appeared to be converging solutions on the parameter estimation screen; however, there was misalignment of the glucose and fructose profiles. Giving higher weight to the measurements which change faster (and thus represent higher precision due to faster changing values than the other trends) gave the results in Table 5 using the following weighting factors: glucose and fructose (2), glycerol and ethanol (0.2), and maltose and sucrose (0.1).

Design

To determine a rough productivity evaluation, the validation dataset used in the models was made to represent a typical kitchen waste stream (food, plastic, paper, cardboard, etc.) Despite being mixed with other waste materials, the validation dataset fit the hydrolysis and SSF models well. If all Purdue food waste was at the concentrations in the SSF validation set and a stand-alone system converted food waste at the same yield, then 340 tons of food waste could be converted into 73 tons=146,000 lbs=22,500 gallons ethanol. The capital equipment would be quite high, making it difficult to achieve a short payback period. Energy required for ethanol separation and grinding is another factor, although electricity and heat may be provided cheaply if non-fermentable solids are thermochemically treated. More work needs to be done to analyze the economic feasibility of converting food waste to ethanol.

Conclusion

Hydrolysis and fermentation models were developed using two hydrolysis datasets and two SSF datasets and by using modified Michaelis–Menten and Monod-type kinetics. Validation experiments made to represent typical kitchen waste correlated well with both models. The models were generated in Matlab Simulink® and represent a simple method for implementing ODE system solvers and parameter estimation tools. These types of visual dynamic models may be useful for applying kinetic or linear-based metabolic engineering of bioconversion processes in the future.

Acknowledgements We would like to thank Defense Life Sciences (Mclean, VA) and Purdue Agricultural Research Programs for funding for this project and Genencor International for providing enzymes. Also thanks to Dr. Michael Ladisch, Dr. Nathan Mosier, and Dr. Miroslav Sedlak for their advice and help in many aspects of this project.

References

1. Kantor, L. S., & Lipton, K. (1997). *Food Review, 20*(1), 2–12.
2. USDA National Nutrient Database for Standard Reference. Retrieved September 2005 from http://www.nal.usda.gov/fnic/foodcomp/search/.
3. Lopez, C., Tarrado A., et al. (2006). *Enzyme and Microbial Technology, 39*(2), 252–258.
4. Walker, G. M. (1998). *Yeast physiology and biotechnology.* New York: Wiley.
5. Wang, Z. X., Zhuge, J., et al. (2001). *Biotechnology Advances, 19,* 201–223.
6. Levenspiel, O. (1980). *Biotechnology and Bioengineering, 22,* 1671–1687.
7. Handbook of Statistical Methods. Retrieved Jun 2006 from http://www.itl.nist.gov/div898/handbook/.

Appl Biochem Biotechnol (2008) 147:23–32
DOI 10.1007/s12010-007-8081-3

Lignin Peroxidase from *Streptomyces viridosporus* T7A: Enzyme Concentration Using Ultrafiltration

Leda M. F. Gottschalk · Elba P. S. Bon · Ronaldo Nobrega

Received: 18 May 2007 / Accepted: 10 October 2007 /
Published online: 20 March 2008
© Humana Press Inc. 2007

Abstract It is well known that lignin degradation is a key step in the natural process of biomass decay whereby oxidative enzymes such as laccases and high redox potential ligninolytic peroxidases and oxidases play a central role. More recently, the importance of these enzymes has increased because of their prospective industrial use for the degradation of the biomass lignin to increase the accessibility of the cellulose and hemicellulose moieties to be used as renewable material for the production of fuels and chemicals. These biocatalysts also present potential application on environmental biocatalysis for the degradation of xenobiotics and recalcitrant pollutants. However, the cost for these enzymes production, separation, and concentration must be low to permit its industrial use. This work studied the concentration of lignin peroxidase (LiP), produced by *Streptomyces viridosporus* T7A, by ultrafiltration, in a laboratory-stirred cell, loaded with polysulfone (PS) or cellulose acetate (CA) membranes with molecular weight cutoffs (MWCO) of 10, 20, and 50 KDa. Experiments were carried out at 25 °C and pH 7.0 in accordance to the enzyme stability profile. The best process conditions and enzyme yield were obtained using a PS membrane with 10 KDa MWCO, whereby it was observed a tenfold LiP activity increase, reaching 1,000 U/L and 90% enzyme activity upholding.

Keywords *Streptomyces viridosporus* · Lignin peroxidase · Ultrafiltration · Enzyme concentration · Enzyme stability

L. M. F. Gottschalk (✉) · E. P. S. Bon
Departamento de Bioquímica, IQ, CT, Universidade Federal do Rio de Janeiro, Rio de Janeiro, RJ 21949-900, Brazil
e-mail: ledagott@gmail.com

R. Nobrega
Programa de Engenharia Química, COPPE, CT, Universidade Federal do Rio de Janeiro, Rio de Janeiro, RJ, Brazil

Introduction

There has been a growing interest on the use of lignin peroxidase (LiP), manganese peroxidase, and laccase because of their ability to degrade both lignin and highly toxic phenolic compounds [1]. Regarding the use of biomass as a renewable material for the production of fuels and chemicals, the research on LiPs is of paramount importance because of their potential use for the degradation of the biomass lignin. It is well known that lignocellulose is a complex composite designed to resist degradation and that the enzymatic attack is effective for lignin removal. In biomass-free lignin, cellulose and hemicellulose moieties would be more prone to the attack by cellulases and hemicellulase enzymes. The production of ethanol from plant structural polysaccharides has become essential to improve energy availability, decrease air pollution, and diminish atmospheric CO_2 accumulation [2]. Regarding environmental pollution, the human activity has introduced a great variety of xenobiotic and recalcitrant chemicals into the environment, on a large scale, so that it is necessary to develop innovative bio-based technologies for its degradation [3]. Although the catalytic profile of peroxidase is potentially useful for the pretreatment of lignocellulosic materials [4] and in environmental pollution control [5], its application in industrial scale requires the production of a stable and low-cost biocatalyst.

Since its first characterization [6], several aspects of *Streptomyces viridosporus* T7A LiP production and characterization have been studied [7–10]. There is not a consensus regarding LiP molecular mass as different data have been reported according to the enzyme purification procedure. Although a molecular weight of 17,800 was estimated for the enzyme by sodium dodecyl sulfate polyacrylamide gel electrophoresis (SDS-PAGE) [6], different values were observed for LiP isoenzymes when they were purified by preparative PAGE and electroelution using unboiled (75,800) and boiled (67,100 and 37,100) samples. In addition, the Fergusson plot for the native polyacrylamide electrophoresis indicated a molecular weight of 134,000 [11]. The effect of the temperature and pH on the enzyme stability has been investigated. The enzyme showed to be stable in the pH range 3.0 to 8.2 in temperatures below 40 °C [10, 12]. Sensitivity toward temperature was observed upon the enzyme incubation at 50 °C for 30min at pH 5.5 or 7.0, which resulted on 25 and 38% activity loss, respectively [10, 12].

S. viridosporus LiP has been concentrated by ultrafiltration (UF) for further studies on the enzyme purification and the determination of its chemical and biochemical properties [10, 11, 13, 14]. However, there is no report on the UF operational conditions and on the enzyme activity recovery.

In enzymes, downstream processing activity loss is often observed. As the degree of product loss is critical to the economics of the separation process, the choice of the technique is guided by the preservation of the enzyme structure that is associated to their biological function [15]. One such technique, membrane technology, has been largely used because of its benefits such as: separation can be carried out under mild conditions and in a continuous mode, energy consumption is generally low, up-scaling is easy, membrane proprieties are variable and can be adjusted, no additives are required, and it can be easily combined with other separation processes [16]. Within this context, UF is a cost-effective method that allows both concentration and primary purification of enzymes under low temperature and pressure conditions. UF is also easy to scale-up in comparison to chromatography and electrophoresis. However, UF may present concentration polarization and fouling, which reduce the permeate flux below the theoretical capacity and modify membrane selectivity. This flux decline has a negative influence on the economics of a

given membrane operation and should be prevented [16]. The disadvantages of UF strongly depend on operation conditions and membrane characteristics, such as feed properties, membrane molecular weight cutoff (MWCO), transmembrane pressure (TMP) and cross-flow rate [17].

Our research group has studied *Streptomyces viridosporus* T7A LiP aiming the enzyme chemical characterization and the reduction in the enzyme production cost [7–9, 14]. In this study, LiP concentration by UF was investigated focusing on the effect of UF membrane MWCO and operation conditions. The recovery of fouled membranes using cleaning agents was also accessed.

Materials and Methods

Microorganism and Enzyme Production

S. viridosporus T7A (ATCC 39115) stock spores was maintained at −20 °C in a 20% (w/v) glycerol aqueous solution [18] after cell growth at 37 °C for 6–8 days on a medium composed of malt extract (3 g/L), yeast extract (3 g/L), peptone (5 g/L), glucose (10 g/L), and agar-agar (20 g/L). LiP was produced in batch submerged fermentations at 37 °C (bioreactor model Applikon, 3 L working volume) using an optimized growth medium (6.5 g/L yeast extract, 1 g/L corn oil, 5 g/L calcium carbonate, 0.20 g/L $MgSO_4.7H_2O$; 0.20 g/L NaCl; 0.05 g/L $CaCl_2$, and trace metal stock solution). The use of adequate aeration/agitation conditions (1.0 vvm and 400 rpm) allowed optimization of enzyme production and productivity [19]. Peak enzyme production was observed within 32 h of fermentation. At this time, the culture was filtered in Whatman no. 1 paper. This supernatant was used for UF experiments.

Lignin Peroxidase Activity

The LiP activity was determined by the enzymatic oxidation of 2,4-dichlorophenol (2,4-DCP) in the presence of H_2O_2 and 4-aminoantypirene (4-AAP) [20]. The 1.0-mL reaction mixture contained 164 μM 4-AAP (Sigma), 3 mM 2,4-DCP (Sigma), 4 mM hydrogen peroxide, and 200 μL of the culture supernatant in 50mM of potassium phosphate, pH 7.0. The reaction was initiated by the addition of hydrogen peroxide and the increase in absorbance at 510 nm was monitored for 1 min at room temperature. One unit of LiP activity corresponded to the increase in 1U of absorbance per minute under initial reaction rates. Extracellular LiP concentration was expressed as units of enzyme per liter of culture. LiP activity was measured in the feed before starting the UF process, in the concentrate and in the permeate to calculate the percentages of enzyme in each fraction and the losses of the process. Experiments were performed in duplicate, and standard error was lower than 10% of the mean.

Effect of pH and Temperature on LiP Stability

LiP stability was investigated by incubating the enzyme at 20, 25, 30, 40, and 50 °C for different time intervals at pH 7.0 and 8.0 (fermentation pH at the end of the enzyme production) to allow the design of adequate conditions for UF. After the incubation, the enzyme was placed in an ice bath, and the residual activity was measured under standard conditions. Experiments were performed in duplicate, and standard error was lower than 10% of the mean.

Ultrafiltration Unit and Operating Conditions

Membrane cutoff is not a clear-cut decision as it may not be a direct relationship between molecular mass and its response to the MWCO used in the UF process; the macromolecules may suffer structural deformation depending on the operational conditions and display a peculiar separation profile [21]. Thus, in this work, polysulfone (PS) membranes were used with MWCO of 10, 20, and 50 kDa (PS10, PS20, and PS50, respectively) and a cellulose acetate (CA) membrane with MWCO of 20 kDa (CA20), purchased from Dow Denmark. For the choices of membrane cutoff, the inconsistency on the reported LiP molecular mass was also taken into account. Ultrafiltration runs were performed in a laboratory-stirred cell (initial process volume of 50 mL and minimum working volume of 4 mL) showing an effective membrane area of 15.8 cm^2. Membranes were prewashed to eliminate residual solvent or impurities resulting from the manufacturing process. UF experiments were carried out in room temperature using microfiltered water under pressure of 1 to 3.0 bar. The measurement of the permeate flux indicated the initial hydraulic permeability before each run, taking into account the linear relationship between pressure and permeate flux [16]. Pressure was supplied by a nitrogen gas line. To reduce losses because of LiP adsorption on membrane surfaces and pore walls, all membranes were brought into contact with an enzyme solution during 1h before the experiments. For the UF experiments, 50 mL of LiP solution were transferred to the laboratory-stirred cell (200 rpm) and concentrated as already described. Permeate flux (J_{perm}) was obtained by measuring their volumes during each run. Feed and concentrate samples were taken in the beginning, during the UF process, and at the end of the runs. After the UF experiments, membranes were cleaned with microfiltered water for 30 min, using a pressure of 2 bar and 200 rpm. As water cleaning did not restore the initial permeate flux, a protocol to clean the membranes was further developed. All experiments were performed in duplicate, and standard error was lower than 10% of the mean.

UF Process Parameters

The slope of the corresponding flux–pressure curve corresponds to the hydraulic permeability coefficient (Lp), as shown by the Eq. 1:

$$\text{Hydraulic permeability coefficient(Lp)} = \frac{J_{perm}}{\Delta P} \tag{1}$$

The percentage of LiP in concentrate and in permeate was calculated as:

$$\text{LiP activity in concentrate (\%)} = \frac{\text{Total concentrate activity}}{(\text{Total concentrate activity} + \text{Total permeate activity})} \times 100 \tag{2}$$

$$\text{LiP activity in permeate (\%)} = \frac{\text{Total permeate activity}}{(\text{Total concentrate activity} + \text{Total permeate activity})} \times 100 \tag{3}$$

The LiP activity loss during the UF process was calculated as:

$$\text{LiP activity loss(\%)} = 100 - \frac{(\text{Total permeate activity} + \text{Total concentrate activity})}{\text{Total activity of feed solution}} \times 100 \tag{4}$$

The retention of LiP by the membrane was calculated as follows:

$$\text{Enzyme rejection } (\%) = 1 - \frac{\text{Permeate LiP activity}}{\text{Concentrate LiP activity}} \times 100 \quad (5)$$

The enzyme activity yield during membrane concentration of the feed was determined as the ratio of the final activity of the concentrate to the number of units at the beginning of the operation:

$$\text{Yield } (\%) = \frac{\text{Total concentrate activity}}{\text{Total activity of feed solution}} \times 100 \quad (6)$$

Results and Discussion

Enzyme Preparation and Stability Toward pH and Temperature

The supernatants of fermentations with peak enzyme concentrations in the range of 100 to 180 U/L [19] were used to study the enzyme stability toward incubation time, pH, and temperature. Data presented in Fig. 1a and b indicated for LiP a higher overall stability at pH 8.0 in comparison to pH 7.0, although a gradual enzyme inactivation, in both pH values, was observed in response to the temperature increase and incubation time. Upon incubation at pH 7.0 in the temperature range of 20 to 30 °C, for 4 h, a maximum activity loss of 25% was observed. Under comparative conditions, a more pronounced activity decrease was observed in pH 8.0. The results shows that the activity loss at pH 7.0 was less severe, within 76% of residual activity observed after incubation for 1 h at 50 °C in accordance to previous reports [10]. As at pH 7.0, the enzyme showed to be quite stable at 25 °C (maximum activity loss of 10% upon four hours of incubation), this pH and temperature were chosen for the subsequent UF experiments.

Membrane Selection for LiP Ultrafiltration

The first set of experiments, carried out to compare the performance of membranes with MWCO of 10, 20, and 50 kDa, were carried out using a pressure of 2 bar and 200 rpm agitation, to expose the systems to the same concentration polarization and fouling effects. Before and after the UF experiments, the membrane hydraulic permeability coefficient (Lp) was measured to evaluate the permeability loss.

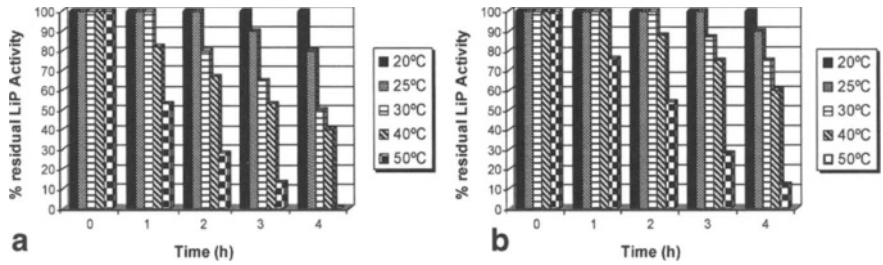


Fig. 1 Comparison of the effect of temperature on residual LiP activity on pH 8.0 and 7.0 (**a** and **b**, respectively)

The PS50 membrane showed to be the most permeable, as expected, with a permeability of 39.8 L/m^2 h bar, followed by the PS20 membrane that presented a permeability of 16.0 L/m^2 h bar. Surprisingly, the PS10 membrane permeability, of 20.7 L/m^2 h bar, was higher than that showed by the membrane PS20. This characteristic might be related to its global porosity and porous size distribution and density. LiP activity was measured in the feed before starting the UF and in the concentrate and in the permeate, at the end of the experiments. Results are summarized in Table 1. In UF experiments carried out with PS50, 83% of total enzyme activity was measured in permeate, in disagreement to previous reports that indicated for the enzyme a molecular mass around 50,000 [11]. The use of PS20 resulted on a better enzyme yield in the concentrate; nevertheless, 27% of total enzyme activity was still measured in permeate. The best results for LiP concentration were obtained using the PS10 membrane, which showed 90% retention of total enzyme activity in the concentrate, a rejection of 99% and a yield of 74%. This result was in agreement to the literature that reported a Lip molecular mass of 17,800 [6] and of 13,500 [14] using SDS-PAGE. In all UF experiments, LiP was concentrated around tenfold.

In the second set of experiments, UF were performed using a CA membrane with MWCO of 20 kDa. The pressure of 1 bar was used because this membrane showed a high initial permeability (37.7 L/m^2 h bar). Table 2 compares LiP UF results for PS10 and CA20 under the same process conditions (1 bar and 200 rpm). The use of PS10 resulted on 96% LiP activity retention on the concentrate (processing time of 340 min). As for results using the CA20 membrane, only 45% of LiP activity was measured in the concentrate (processing time of 65 min). As the CA10 membrane was not available at the time of the experiments, it was not possible to confirm the hypothesis that this membrane would conciliate the selectivity of the PS10 membrane with faster filtration characteristics of the hydrophilic CA membranes. The total PS10 permeability loss of 72% was considerably higher than that observed for CA20, of 12%. Our results are in agreement to previous reports where hydrophobic membrane like PS interacts more strongly with enzymes, being more prone to fouling, in comparison to hydrophilic polymers like CA membranes [22]. Besides, no LiP activity loss was observed for CA20 (0%), whereas 14% loss was measured for PS10,

Table 1 Comparison of $Lp_{initial}$, Lp loss, LiP activity in permeate and concentrate, rejection, yield, LiP activity loss, and UF processing time using membranes PS10, PS20, and PS50 for LiP concentration in a laboratory-stirred cell, with volume of 50 mL, pressure of 2 bar, and agitation of 200 rpm (permeate volume = 46 mL and concentrate volume = 4 mL).

Membrane	PS50	PS20	PS10
$Lp_{initial}$ (L/m^2 h bar)	39.8	16.0	20.7
Lp loss (%)	24	38	65
LiP activity in feed (UI/mL)	100	100	100
LiP activity in concentrate (UI/mL)	187	653	921
LiP activity in permeate (UI/mL)	79	20	9
Total feed LiP activity (UI)	5	5	5
Total concentrate LiP activity (UI)	0.75	2.61	3.68
Total permeate LiP activity (UI)	3.63	0.92	0.41
LiP activity in concentrate (%)	17	73	*90*
LiP activity in permeate (%)	83	27	10
Rejection (%)	58	97	*99*
Yield (%)	15	52	*74*
LiP activity loss (%)	12	29	18
UF process time (min)	30	75	105

Table 2 Comparison of $Lp_{initial}$, Lp loss, LiP activity in permeate and concentrate, rejection, yield, LiP activity loss, and UF processing time using membranes PS10 and CA20 for LiP concentration in a laboratory-stirred cell, with volume of 50 mL, pressure of 1 bar, and agitation of 200 rpm (permeate volume = 42 mL and concentrate volume = 8 mL).

Membrane	PS10	CA20
$Lp_{initial}$ (L/m^2 h bar)	24.1	37.7
Lp loss (%)	72	12
LiP activity in feed (UI/mL)	153	126
LiP activity in concentrate (UI/mL)	786	525
LiP activity in permeate (UI/mL)	6	120
Total feed LiP activity (UI)	7.65	6.3
Total concentrate LiP activity (UI)	6.29	4.2
Total permeate LiP activity (UI)	0.25	5.04
LiP activity in concentrate (%)	*96*	45
LiP activity in permeate (%)	4	55
Rejection (%)	*99*	77
Yield (%)	*82*	67
LiP activity loss (%)	14	*0*
UF Process Time (min)	340	65

indicating absence of LiP adsorption on the CA membrane. The rejection of LiP using PS10 was 99%, and the yield was 82%, being both values higher than that observed for CA20 that showed 77% rejection and 67% of yield.

Operational Conditions for LiP Ultrafiltration

According to the literature, TMP has a negative effect on the protein concentration because of membrane-fouling enhancement associated to TMP increase [17]. To evaluate the occurrence of pressure-related fouling, UF experiments were carried out using a PS10

Table 3 Comparison of $Lp_{initial}$, J_{perm} loss, LiP activity in permeate and concentrate, rejection, yield, LiP activity loss, and UF processing time using membrane PS10 for LiP concentration in a laboratory-stirred cell, with volume of 50 mL, pressure of 1, 2, and 3 bar, and agitation of 200 rpm.

Pressure	1 bar	2 bar	3 bar
$Lp_{initial}$ (L/m^2 h bar)	24.1	15.9	12.7
J_{perm} loss (%)	42	50	63
LiP activity in feed (UI/mL)	153	130	172
LiP activity in concentrate (UI/mL)	786	1,200	1,020
LiP activity in permeate (UI/mL)	6	10	14
Concentrate volume (mL)	8	4	6
Total feed LiP activity (UI)	7.65	6.5	8.6
Total concentrate LiP activity (UI)	6.29	4.8	6.12
Total permeate LiP activity (UI)	0.25	0.46	0.62
LiP activity in concentrate (%)	96	91	91
LiP activity in permeate (%)	4	9	9
Rejection (%)	99	99	98
Yield (%)	*82*	74	71
LiP activity loss (%)	*14*	21	35
UF Process Time (min)	340	250	*180*

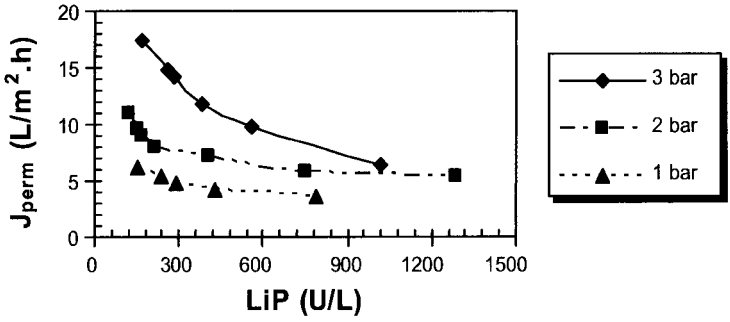


Fig. 2 Comparison of permeate flux values of PS10 membrane during LiP ultrafiltration using TMP of 1, 2, and 3 bar in relation to LiP activity

membrane under TMP of 1, 2, and 3 bar. New membranes with similar initial hydraulic permeability (around 15 L/m^2 h bar) were used in each run. A discrete permeate flux decrease was observed in all cases because of concentration polarization and fouling effects. Table 3 shows that higher initial permeate fluxes were observed in response to TMP increase, although the flux decreased sharply, resulting in a superior permeate flux loss (42, 50, and 63% for the TMP of 1, 2, and 3 bar, respectively). As the enzyme might be susceptible to shear stress and pressure, long processing times could lead to significant loss of enzyme activity [15]. In accordance to the literature, the use of 1bar resulted in the lowest LiP activity loss (14%) and the best yield (82%) even with the highest processing time (340 min). The increased in TMP to 2 and 3 bar resulted on an increase in activity loss to 21 and 35%, respectively. In addition, according to data presented in Fig. 2, a more pronounced decrease in the permeate flux was observed in response to the TMP increase. It is also shown that the increase in LiP initial concentration caused a decrease in permeate fluxes likely related to membrane polarization and fouling.

Membrane Cleaning and Reutilization

Maintenance of UF membrane performance requires the cleaning of fouled membranes [23]. Standard procedures involve the circulation of acid, caustic, and surfactant solutions through the system in a cyclic fashion [24]. In this study, fouled membranes were at first treated with H_2SO_4 6.0 N. This procedure was not adequate as it caused a further decrease in the membrane permeability, likely related to protein precipitation on the membrane surface. A subsequent treatment with NaOH 0.5 N restored to some extent the initial permeability. In a new set of experiments, NaOH 0.5 N was solely used resulting on the

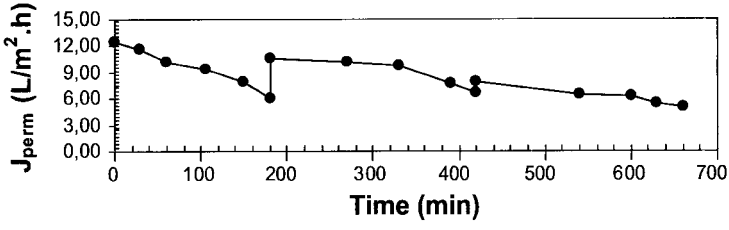


Fig. 3 Flux variation with time for PS10 membrane and flux restoration after cleaning procedure at 180 and 420 h

recovery of 93% of the initial membrane permeability. Afterward, the fouled PS10 membrane was cleaned upon circulation of 10 mL of NaOH 0.5 N (pH bellow 13 in agreement with manufacturer advice) for 20 min at 1 bar and 400 rpm. The cleaning efficiency of this procedure was evaluated, using a PS10 virgin membrane, in three LiP concentration experiments intercalated by a cleaning cycle. Although it was observed a flux decline after the first cleaning cycle, the flux of the subsequent experiments involving UF and cleaning runs showed to be quite stable (Fig. 3). Cleaning with the anionic surfactant SDS increased initial permeability of virgin membranes likely because of the modification of the membrane surface [24].

Final Remarks

In accordance to the enzyme stability data towards pH and temperature the UF experiments for LiP concentration were performed at pH 7.0 and controlled temperature of 25 °C. The best results were obtained using a PS10 membrane that showed 96% of enzyme activity retention in the concentrate. The CA20 membrane showed a lower decrease in total permeability (Lp) in comparison to the PS10 membrane suggesting a relative higher LiP adsorption and pore blocking.

Although the increase in the PS10 TMP from 1 to 3 bar was beneficial to the initial permeate flux, it was deleterious to the enzyme stability, decreasing the process yield. Considering the recovery of fouled membranes, the sole use of NaOH showed to be quite efficient for the PS10 membrane allowing its successful reuse in subsequent experiments. The LiP UF experiments carried out under optimized conditions allowed a tenfold LiP activity increase, reaching 1,000 U/L along with 90% enzyme activity upholding. This concentrate has a potential biotechnological application for the removal of lignin from lignocellulose materials widening its use prospects.

Acknowledgments This work was supported by the Brazilian Research Council/CNPq.

References

1. Minussi, R. C., Pastore, G. M., & Durán, N. (2007). *Bioresource Technology, 98*, 158–164.
2. Prasad, S., Singh, A., & Joshi, H. C. (2007). *Resources Conservation & Recycling, 50*, 1–39.
3. Ferreira-Leitao, V. S., Carvalho, M. E. A., & Bon, E. P. S. (2007). *Dyes and Pigments, 74*, 230–236.
4. Hernandezperez, G., Goma, G., & Rols, J. L. (1997). *Biotechnology Letters, 19*, 285–289.
5. Gilbert, M., Morosoli, R., Shareck, F., & Kluepfel, D. (1995). *CRC Critical Reviews in Biotechnology, 15*(1), 13–39.
6. Ramachandra, M., Crawford, D. L., & Hertel, G. (1988). *Applied and Environmental Microbiology, 54*, 3057–3063.
7. Macedo, J. M. B., Gottschalk, L. M. F., & Bon, E. P. S. (1999). *Applied Biochemistry and Biotechnology, 77-79*, 735–744.
8. Gottschalk, L. M. F., Macedo, J. M. B., & Bon, E. P. S. (1999). *Applied Biochemistry and Biotechnology, 77-79*, 771–778.
9. Macedo, J. M. B., Gottschalk, L. M. F., & Bon, E. P. S. (1999). *Brazilian Journal of Chemical Engineering, 16*, 163–169.
10. Lodha, S. J., Korus, R. A., & Crawford, D. L. (1991). *Applied Biochemistry and Biotechnology, 28*(29), 411–420.
11. Magnuson, T. S., Roberts, M. A., Crawford, D. L., & Hertel, G. (1991). *Applied Biochemistry and Biotechnology, 28*(29), 433–442.
12. Zerbini, J. E. (1994). M.S. thesis, Rio de Janeiro Federal University, Rio de Janeiro, Brasil.
13. Spiker, J. K., Crawford, D. L., & Thiel, E. C. (1992). *Applied Environment and Microbiology, 37*, 518–523.

14. Bon, E. P. S., Nascimento, H. J., Macedo, J. M. B., & Silva Jr, J. G. (1999). *Biotechnology Techniques*, *13*(5), 289–283.
15. Krstic, D. M., Antov, M. G., Pericin, D. M., Höflinger, W., & Tekic, M. N. (2007). *Biochemical Engineering Journal*, *33*, 10–15.
16. Mulder, M. (1991). Basic principles of membrane technology. The Netherlands: Kluwer.
17. Li, Z., Youravong, W., & H-Kittikun, A. (2006). *Bioresource Technology*, *97*, 2364–2370.
18. Hopwood, D. A., Bibb, M. B., Chater, K. F., Kieser, T., Bruton, C. J., Kieser, H. M. et al. (1985). Genetic manipulation of *Streptomyces*: A laboratory manual pp. 3–5. Norwich: The John Innes Foundation.
19. Gottschalk, L. M. F., Nobrega, R., & Bon, E. P. S. (2003). *Applied Biochemistry and Biotechnology*, *105*, 799–807.
20. Pasti, M. B., Hagen, S. R., Korus, R. A., & Crawford, D. L. (1991). *Applied Microbiology and Biotechnology*, *34*, 661–667.
21. Nobrega, R., & Balmann, H. (1989). *Journal of Membrane Science*, *45*, 17–36.
22. Salgin, S., Takaç, S., & Özdamar, T. H. (2006). *Journal of Colloid and Interface Science*, *299*, 806–814.
23. Kim, K. J., Sun, P., Chen, V., Wiley, D. E., & Fane, A. G. (1993). *Journal of Membrane Science*, *80*, 241–249.
24. Lee, H., Amy, G., Cho, J., Yoon, Y., Moon, S. H., & Kim, I. S. (2001). *Water Research*, *35*(14), 3301–3308.

Appl Biochem Biotechnol (2008) 147:33–45
DOI 10.1007/s12010-007-8057-3

Oxygen-controlled Biosurfactant Production in a Bench Scale Bioreactor

Frederico de Araujo Kronemberger · Lidia Maria Melo Santa Anna · Ana Carolina Loureiro Brito Fernandes · Reginaldo Ramos de Menezes · Cristiano Piacsek Borges · Denise Maria Guimarães Freire

Received: 8 May 2007 / Accepted: 14 September 2007 /
Published online: 12 October 2007
© Humana Press Inc. 2007

Abstract Rhamnolipids have been pointed out as promising biosurfactants. The most studied microorganisms for the aerobic production of these molecules are the bacteria of the genus *Pseudomonas*. The aim of this work was to produce a rhamnolipid-type biosurfactant in a bench-scale bioreactor by one strain of *Pseudomonas aeruginosa* isolated from oil environments. To study the microorganism growth and production dependency on oxygen, a nondispersive oxygenation device was developed, and a programmable logic controller (PLC) was used to set the dissolved oxygen (DO) concentration. Using the data stored in a computer and the predetermined characteristics of the oxygenation device, it was possible to evaluate the oxygen uptake rate (OUR) and the specific OUR (SOUR) of this microorganism. These rates, obtained for some different DO concentrations, were then compared to the bacterial growth, to the carbon source consumption, and to the rhamnolipid and other virulence factors production. The SOUR presented an initial value of about 60.0 mgO_2/g_{DW} h. Then, when the exponential growth phase begins, there is a rise in this rate. After that, the SOUR reduces to about 20.0 mgO_2/g_{DW} h. The carbon source consumption is linear during the whole process.

Keywords *Pseudomonas aeruginosa* · Biosurfactant · Oxygenation · Rhamnolipid · Bioreactor

F. A. Kronemberger (✉) · C. P. Borges
Instituto Alberto Luiz Coimbra de Pós Graduação e Pesquisa de Engenharia, Programa de Engenharia Química, Universidade Federal do Rio de Janeiro, Centro de Tecnologia, bloco G, sala 115—Cidade Universitária, P.O. Box 68502, 21945-970 Rio de Janeiro, RJ, Brazil
e-mail: frederico@peq.coppe.ufrj.br

L. M. M. Santa Anna
Gerência de Biotecnologia e Tratamentos Ambientais, Centro de Pesquisa e Desenvolvimento Leopoldo Américo Miguêz de Mello, Cidade Universitária, Rio de Janeiro, RJ, Brazil

A. C. L. B. Fernandes · R. R. Menezes · D. M. G. Freire
Departamento de Bioquímica, Instituto de Química, Universidade Federal do Rio de Janeiro, Rio de Janeiro, RJ, Brazil

Introduction and Objectives

The progresses in science and technology since the industrial revolution have been constantly raising the possibility of the exploration of natural resources. That exploration has been generating disturbances in the global elementary cycles. The introduction of exogenous chemical products to certain area can always surpass its capacity of self-remediation, resulting in the harmful accumulation of these products. Hydrocarbon contaminations in oil spills have been causing serious environmental problems, and extra consideration is being shown to the development and implementation of new technologies for the proper cleaning. Several methods of soil remediation are being developed as alternatives environmentally correct.

The main factor that limits the biodegradation of these pollutants is their limited availability to the native microorganisms. Hydrocarbons usually aggregate to soil components, which make the removal or degradation very difficult. Surface-active compounds reduce the superficial and interfacial tensions through the accumulation in the interface of immiscible fluids or of a fluid and a solid, increasing the availability and subsequent biodegradation. These compounds can be produced in a chemical or biochemical way and are denominated surfactants.

These substances are used industrially with several objectives, but for many years, they have been synthesized chemically. The biological surface-active compounds, biosurfactants, which began to be used in the last decades, are produced by some bacterial strains that degrade or transform petroleum components [1, 2]. These biosurfactants are getting notoriety because they can be used in several industrial applications, as a result of their biodegradability advantages, production from renewable sources, and functionality under extreme conditions [3].

Microorganisms are capable to produce a great variety of products with excellent surface-active properties. However, its use in certain applications depends on the production and purification costs for specific activities, if compared to the corresponding synthetic surfactants. Thus, the last works are concentrated in the identification of potentials surfactants, in the evaluation of their properties, and in the optimization of the fermentative processes for their production [4].

In the present moment, the biosurfactants are still not capable to compete economically with the chemically synthesized surfactants at the market because of the high production costs. That is result of the inefficient methodology of the bioprocessing, the low productivity of the microbial strains, and the need of using expensive substrates. Consequently, for the biosurfactants to reach a significant portion of the market, it is necessary a greater knowledge and ability for the manipulation of the producing strains metabolism, for the possibility of the use of cheaper substrates and the technological improvement of the production process.

Many biosurfactants and their productive processes were patented, but only some of them were commercialized. Nowadays, some products based in biosurfactants can be found at the international market, like PD5, produced by Pendragon Holdings, sold as an addictive for fuels based on a mixture of rhamnolipid biosurfactants and enzymes, EC-601, produced by EcoChem Organics, sold as a dispersive agent of water-insoluble hydrocarbons (rhamnolipids) and the products JBR, of Jeneil Biosurfactant, rhamnolipids in aqueous solutions with different purity degrees or in a semisolid form.

The cost of biosurfactants production is approximately from three to ten times larger than the one of chemical surfactants. Usually, the biosurfactants are produced during the growth of the microorganisms in hydrocarbons, which are usually expensive, increasing the

total cost of the process. However, other cheaper and water-soluble substrates, as glucose, glycerol, and ethanol, have been used. In this search for more economical raw materials for the biosurfactant production, the industrial effluents and the agriculture residues are shown as an excellent option [5].

In agreement with Gruber et al. [6], the prerequisites for the competitive production of biosurfactants are the attainment of products with great activity, produced from cheap substrates through economical viable processes and with high yields. A favorable economical aspect for the biosurfactants production in Brazil, from low-cost substrates, was the recent sanction of the Law 11.097 of January 13, 2005, which authorizes the introduction of the biodiesel in the Brazilian energetic matrix. The law establishes that in the next 3 years, the addition of 2% of biodiesel to the petroleum diesel will be authorized. In 2008, the mixture will be obligatory in this percentage, and it will be raised to 5% in 2013. Thus, some private projects are already in process for the new fuel production, with total installed capacity above 100 million liters per year. Because glycerol is the main byproduct of the biodiesel production, it can be used at a very low cost for the biosurfactant production [7]. The greater challenge then relapses in the technological development of an efficient productive process, with high yields, and in the reduction in the subsequent stages of recovery and purification of the product.

Most of the known biosurfactant-producing microorganisms need aerobic conditions for the production in an efficient way. However, the use of the conventional submerged aeration can lead to the formation of very stable foams, causing serious operational problems, and that is particularly valid for the rhamnolipid-type biosurfactant production. The high foam formation is still increased by the presence of extracellular proteins, resulting in great expenses for the process control, making the productive process impracticable. Mechanic foam breakers are not very efficient, and chemical antifoamy agents can alter the quality of the product and the pollutant potential of the final effluent of the bioreactor [6]. To overcome that difficulty, a different oxygenation process was used. It was similar to the one described by Gruber et al. [6] and to the other, used in alcoholic fermentations, patented by L'Air Liquide [8].

This oxygenation process is promising for the use in bioreactors, reaching good productivities. However, the oxygenation manual control was shown difficult and even inefficient because of the fact that the fermentations last approximately 7 days, demanding night operation of the unit.

Thus, an automated control system of that oxygenation was developed, using a Programmable Logical Controller (PLC) coupled to control equipment with electrical impulses. That system made possible the control and the attendance of the level of dissolved oxygen (DO) in the bioreactor and of the amount of oxygen transferred to the same.

It was also possible to evaluate the oxygen uptake rate (OUR) and the Specific OUR (SOUR) in all the phases of the *Pseudomonas aeruginosa* species bacterial growth, which are still not reported in the scientific literature, even when these bacteria, a pathogenic species involved in many diseases, are an important objective of study in the medical area. The expression of many virulence factors of *P. aeruginosa* is dependent of particular environmental conditions as the concentration of iron, readiness of nitrogen, temperature, and oxygen. Enzymes (proteases and elastases), just like the rhamnolipids and some toxins, are virulence factors of *P. aeruginosa*.

In this context, the main objective of this work was the evaluation of the DO concentration influence along fermentation in the production of biosurfactants (rhamnolipid type) using glycerol (byproduct of the biodiesel production) as the carbon source. The

microbial growth, the productivity, the consumption of the carbon source, and the production of proteins and of some extracellular enzymes related as virulence factors, as the proteases and, specifically, the elastase, were also evaluated.

The effectiveness of a cell-free rhamnolipid biosurfactant, produced by the same *P. aeruginosa* strain, in the removal of two different kinds of oil from impacted sandy soils was investigated by Santa Anna et al. [9]. The study indicates that the use of this biosurfactant was effective in reducing oil concentrations in impacted soil.

Biosurfactants: Definition and Classification

Surfactants are amphipathic molecules with both hydrophilic and hydrophobic (generally hydrocarbon) moieties that partition preferentially at the interface between fluid phases with different degrees of polarity and hydrogen bonding such as oil/water or air/water interfaces. These properties render surfactants capable of reducing surface and interfacial tension and forming microemulsions where hydrocarbons can solubilize in water or where water can solubilize in hydrocarbons. Such characteristics confer excellent detergency, emulsifying, foaming, and dispersing properties, which make surfactants some of the most versatile process chemicals.

A biosurfactant is defined as a surface-active molecule produced by living organisms, most of them being microorganisms. The main physiological function of biosurfactants is to allow the microorganisms growth in substrates immiscible in water, through the reduction in the interfacial tension between the phases, making the substrate available for the assimilation and metabolization [3].

Biosurfactant activities can be determined by measuring the changes in surface and interfacial tensions, stabilization or destabilization of emulsions, and hydrophilic–lipophilic balance. Surface tension at the air/water and oil/water interfaces can easily be measured with a tensiometer. The surface tension of distilled water is 72 mN/m, and the addition of surfactants lowers this value to about 30 mN/m [5].

Although there are a number of reports on the synthesis of biosurfactants by hydrocarbon-degrading microorganisms, some biosurfactants have been reported to be produced on water-soluble compounds such as glucose, sucrose, glycerol, or ethanol. The biosurfactant-producing microbes are distributed among a wide variety of genera.

Most of the known biosurfactants are glycolipids. They are carbohydrates in combination with long-chain aliphatic acids or hydroxyaliphatic acids. Among the glycolipids, the most recognized are the rhamnolipids, the trehalolipids, and the sophorolipids [5].

Rhamnolipids

Rhamnolipids, in which one or two molecules of rhamnose are linked to one or two molecules of β-hydroxydecanoic acid, are the best-studied glycolipids. Production of rhamnose-containing glycolipids was first described by Jarvis and Johnson [10]. The main glycolipids produced by *P. aeruginosa* are rhamnolipids of the types 1 and 2, L-rhamnosyl-β-hydroxydecanoyl-β-hydroxydecanoate and L-rhamnosyl-L-rhamnosyl-β-hydroxydecanoyl-β-hydroxydecanoate. Their structures can be seen in Fig. 1. The formation of rhamnolipid types 3 and 4 containing one β-hydroxydecanoic acid with one and two rhamnose units, methyl ester derivatives of rhamnolipids 1 and 2, and rhamnolipids with alternative fatty acid chains have also been reported [5].

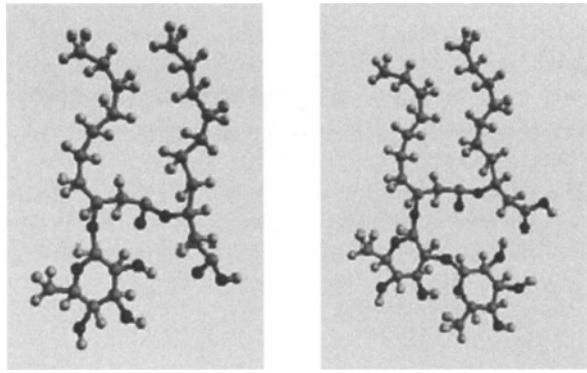


Fig. 1 The hard sphere model of rhamnolipids types 1 and 2 in their minimum energy positions: oxygen (*dark gray*), hydrogen (*light gray*), and carbon [11]

Materials and Methods

Maintenance of Microorganism and Preinoculum Preparation

The *P. aeruginosa* PA1 strain, previously selected from a petroleum environment as a good biosurfactant producer [12, 13], was preserved in glycerol 10% in an ultrafreezer at −80 °C. The preinoculum was cultivated in a plate with YPDA (yeast extract 0.3%, peptone 1.5%, dextrose 0.1%, and agar 1.2%) at 30 °C for 48 h and transferred to 1,000-ml flasks with 300 ml of a culture medium. After 24 h of cultivation, the fermentation medium containing the cells was stocked in cryotubes with 25% of glycerol and preserved at −18 °C to serve as a preinoculum pattern for all the fermentations.

Inoculum Preparation

The content of a cryotube was inoculated in 300 ml of a fermentation medium. The flasks were incubated in a rotatory shaker at 30 °C and 170 rpm for 40 h. At the end of that period, the cells of each flask were recovered by centrifugation (6,000 rpm for 15 min) and used as inoculum in the bioreactors.

Sterilization

The bioreactor, with the culture medium, was sterilized in an autoclave at 121 °C for 15 min before each production. The oxygenation system was sterilized with the circulation of a solution of sodium hypochlorite at 1% for 1 h. After this procedure, distilled sterilized water was circulated in the system for the elimination of chlorine residues. Only after this procedure, the inoculation of the microorganisms was accomplished.

Rhamnolipid production from *Pseudomonas aeruginosa*

The fermentations were accomplished in a BioFlo IIc bioreactor (Batch/Continuous Fermentor; New Brunswick Scientific; USA) with nominal capacity of 5.0 l of volume. The useful volume used in the fermentations was 3.0 l, and the temperature was maintained at 30 °C and the agitation in 100 rpm, with a Rushton 6-blade impeller. The oxygenation was nondispersive with the use of pure oxygen [14]. The culture medium was composed by

glycerol (3.0%) as the sole carbon source, $NaNO_3$ (0.1%), K_2HPO_4 and KH_2PO_4 (1.0%), and traces of iron (II) and magnesium sulfates [12].

Determination of the Biomass Concentration

The cellular concentration of the *P. aeruginosa* suspensions was determined through the light absorbance at 600 nm (MultiSpec-1501; Shimadzu, Japan). The absorbance value was converted in cell dry weight concentration (g/l) through a calibration curve.

Glycerol Quantification

The glycerol, the source of carbon used in the fermentations, concentration in the cell-free samples—the cells were removed by centrifugation at 6,000 rpm for 15 min—was evaluated by the enzymatic/colorimetric method for triglycerides determination (Enzymatic Triglyceride-Bioclin; Quibasa Basic Chemistry, MG-Brazil).

Rhamnolipid Quantification

The quantification of the rhamnolipids was carried through an indirect way, using the rhamnose as reference—the rhamnose is a byproduct of the acid hydrolysis of the rhamnolipids. A modified method described by Pham et al. [15] was used, where the rhamnolipids extraction phase was suppressed.

Nitrate Concentration

The nitrate concentration was determined through the colorimetric reaction of that ion with brucine sulfate. The absorbance values were measured (410 nm) and converted to milligram per liter values with a calibration curve [16].

Total Proteins Determination

The method used for the quantification of the extracellular proteins was described by Lowry et al. [17].

Protease Activity Determination

The protease activity was determined by the method described by Charney and Tomarelli [18] that is based on the formation of colored protein-derived compounds by the digestion of an azocasein solution with the proteolitic enzymes present in the enzymatic extract.

Elastase Activity Determination

A test based on the degradation of an elastin linked to Congo red was used for the elastase activity determination. The degradation of this substrate liberates that pigment, allowing the evaluation of the activity. The procedure was described by Braga et al. [19].

Results and Discussion

The first and clearest observation in the rhamnolipid production with the use of the nondispersive oxygenation is the foam absence in the vase containing the culture medium during the fermentative process. In this nondispersive oxygenation device, the interface between the liquid and the gaseous phase is well defined and fixed. The oxygen is transferred to the medium through this interface instead of being transferred through the bubble interface. As there is no bubbling in this system, the foam is not formed. The comparison between the production carried out in this work and a production with the conventional aeration can be observed in Fig. 2.

The foam absence is clearly noticed in Fig. 2a, corresponding to the fermentation with nondispersive oxygenation. To discard the possibility that the foam absence could be related to the absence of the biosurfactant in the medium, air was injected directly by a disperser, with low flow, simulating the conventional oxygenation. In a few seconds, the condition seen in the Fig. 2b was achieved. This fact once again proves the inefficiency of this fermentative process for the rhamnolipid production from *P. aeruginosa* with the conventional oxygenation by the means of bubbling.

The oxygen supply is a very important parameter in the rhamnolipid production. The largest modification in the productive process was the medium oxygenation, and special consideration was given to the DO concentration. The values were registered continuously with the use of a computer coupled initially to the DO sensor connected to the bioreactor and, later, to the PLC that controlled the necessary equipment for the oxygenation of the medium in the bioreactor.

The DO concentration control along the fermentations was initially accomplished manually. However, the difficulty of that control resulted in great variations in the DO concentration value during the fermentations. That variation was not desired, as the objective was to evaluate the influence of the amount of oxygen transferred and also of its concentration in the medium during the biosurfactant production. This fact justified the implementation of a control system with more efficient equipment connected to a PLC. The difference in the DO profile during fermentation with the manual-controlled system and with the use of the new system can be observed in the Fig. 3. It was noticed that the

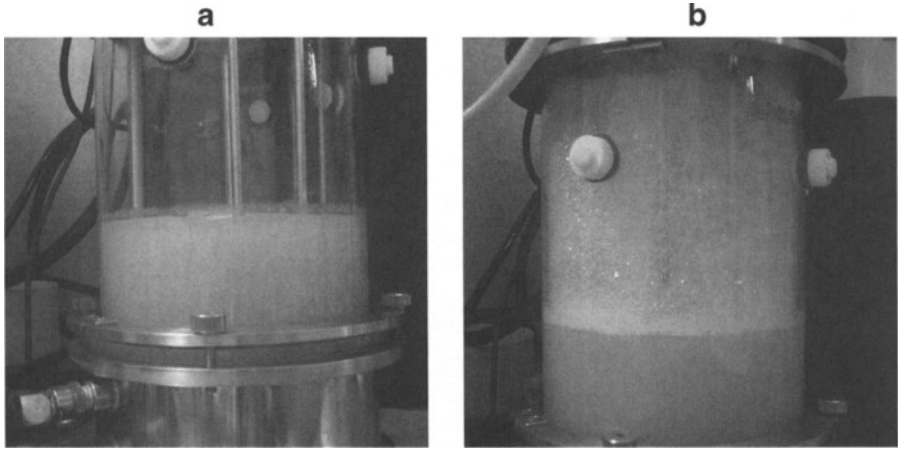


Fig. 2 Comparison between the rhamnolipid production with the conventional oxygenation and the one used in this work. **a** Nondispersive oxygenation. **b** Conventional oxygenation

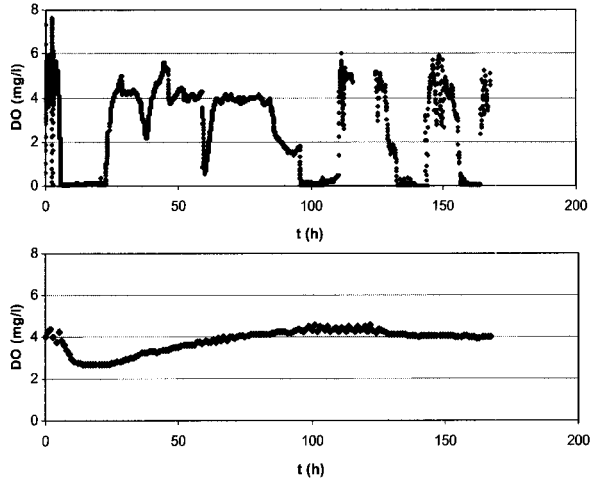


Fig. 3 Dissolved oxygen profile (mg/l) with time (h)—*t*—in fermentations with different controls for the nondispersive oxygenation system. *Above*, there is the manual control DO profile. In both fermentations, the DO set point was 4.0 mg/l

extreme DO variation during the fermentation process was over and that the desired investigation could continue.

Thus, the influence of the medium DO concentration in the fermentation was investigated. Fermentations were carried out with DO concentration set points at 1.0, 4.0, and 6.0 mg/l. Those values correspond, respectively, to 14, 57, and 86% of the saturation concentration of oxygen that was equal to 7.0 mg/l in the defined fermentation conditions. This value was calculated using an expression stated by Blanch and Clark [20] for the temperature and medium composition used in the experiments. The control system (with the PLC) actuated in the oxygenation device to raise the oxygenation rate (for example, raising the oxygen gas pressure) any time that the DO concentration in the medium got below the set point.

As all the oxygen was supplied to the medium through the nondispersive system and as there was no bubbling and the loss of that nutrient to the atmosphere was negligible, it was possible to affirm that the amount of the gas supplied, known by the previous characterization of the system, was exactly equal to the amount consumed by the bacteria. That made possible the analysis of the OUR, expressed in milligram of oxygen by liter per hour, and the SOUR, expressed in milligram of oxygen per gram of biomass in dry weight per hour. The SOUR was obtained by dividing the OUR by the biomass concentration during the fermentation.

An interesting fact was that the oxygen consumption profile was not affected by the variation of the DO concentration. The values found for these rates were also not affected by the change in the DO concentration, adjusted to 1.0, 4.0, or 6.0 mg/l. The profiles of the oxygen consumption during fermentation are presented in Fig. 4.

The variation in the oxygen consumption along the different phases of the cellular metabolism is clearly observed. After the adaptation phase, which lasts 4 h at the most, there is a significant increase in the OUR, which varies from 40.0 mg/l h to values above 100.0 mg/l h. Then, that value diminishes slowly until the stabilization in a value close to the initial. That behavior is also observed for the specific rate, SOUR, which confirms that the variation is not only related to the raise in the cellular concentration. The SOUR presents an increase from an initial value of 60.0 up to 85.0 mg/g h, diminishing later to a value around 20.0 mg/g h.

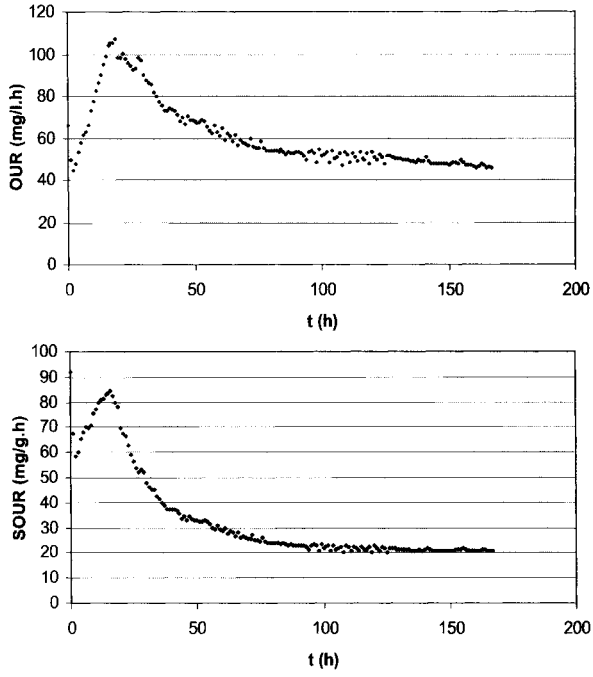


Fig. 4 Oxygen consumption in a fermentation (DO set point equal to 4.0 mg/l). *OUR* Oxygen uptake rate, in milligrams of oxygen per liter per hour, *SOUR* specific oxygen uptake rate, in milligrams of oxygen per cell dry weight in gram per hour

This raise in the oxygen consumption begins at 4 h of fermentation and lasts about 12 h, when the fermentation reaches 16 h. It is interesting to notice that this increase coincides with the exponential phase of the microbial growth, and it can be observed in Fig. 5. Thus, it can be concluded that the oxygen is an essential nutrient for the microbial growth, as it is consumed with a very high rate in that phase. It is still important to point out that the SOUR stays above 20.0 mg/g h along all the fermentations, being the oxygen also important to the cellular maintenance.

In Fig. 6, the biomass, glycerol, and rhamnolipid concentration are presented along fermentation. It is observed that the cellular behavior is simple, with the initial adaptation phase and the exponential growth phase, followed by the stationary one. Besides, the

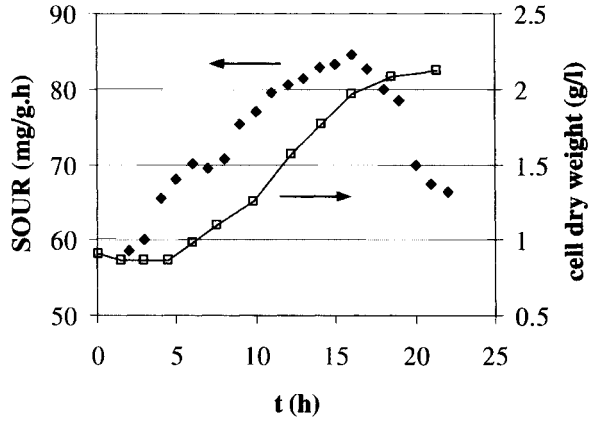


Fig. 5 Correlation between cell growth and SOUR in a rhamnolipid production by *Pseudomonas aeruginosa*. Biomass concentration in dry weight (g/l)×time (h) and SOUR in milligrams of oxygen per cell dry weight in gram per hour

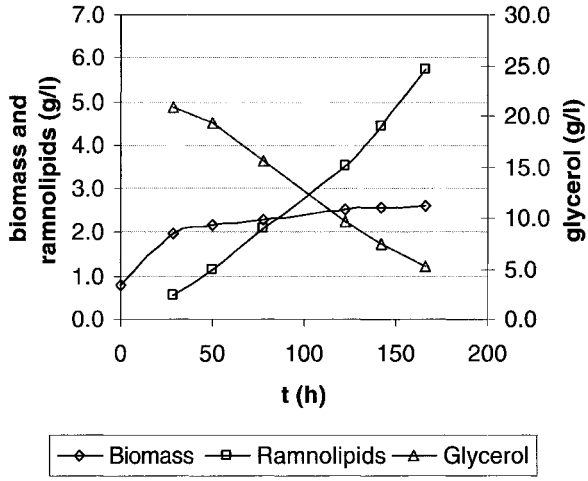


Fig. 6 Time variation of growth, rhamnolipid production, and glycerol consumption (in g/l) during *Pseudomonas aeruginosa* cultivation (DO set point equal to 4.0 mg/l)

consumption of the carbon source remains constant along the fermentation. That general behavior is not influenced by the DO concentration in the medium.

For the best understanding of the influence of the DO concentration in the fermentation, all results were compared with the values obtained in a conventional fermentation, carried out in an agitated flask. The biomass concentration was not influenced by the variation of the DO concentration. Besides, the values were similar to the one of the conventional fermentation, indicating that the cells have adapted to the oxygenation system. The values of the rhamnolipids and glycerol concentration along the fermentations are presented in Fig. 7.

The experiments with a DO set point of 4.0 mg/l are duplicate experiments. The experimental error is high in almost all biochemical reaction, and the rhamnolipid determination assay is not infallible. That is why there are two experiments in this middle point. In addition, all the discussion is made based in the global productivity instead of only in one single point.

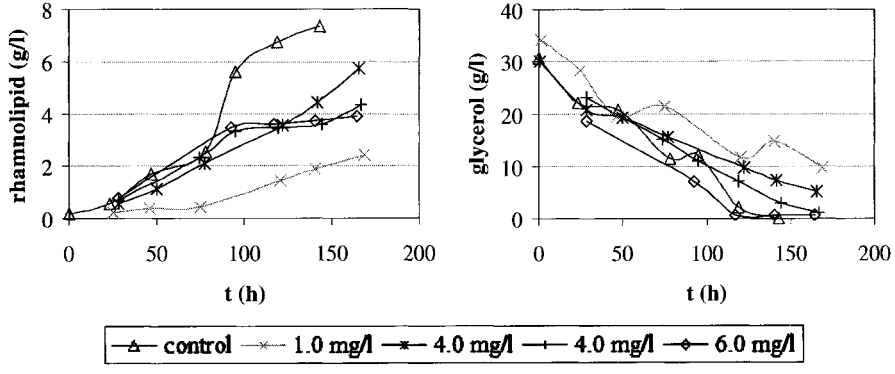


Fig. 7 Rhamnolipid and glycerol concentration (g/l) in fermentations with different DO set points—1.0, 4.0, and 6.0 mg/l—and the control conventional shake flask fermentation

It is noticed that both the rhamnolipid production and the glycerol consumption are reduced in the fermentation carried out with the lowest DO concentration, 1.0 mg/l. That amount of oxygen should be insufficient for the cells access to that nutrient that is shown to be necessary to the rhamnolipid production. The biosurfactant productivity under that condition is 15.0 mg/l h, and the rhamnolipid concentration reaches a value of about 2.0 g/l after 7 days of fermentation. It is also observed that until the third day of fermentation, the biosurfactant production is the same under all the other investigated conditions. The productivity values stay around 30.0 mg/l h of rhamnolipids for the bioreactor fermentations carried out with 4.0 and 6.0 mg/l of DO, while the productivity in agitated flasks equals to 60.0 mg/l h. For the fermentations carried out in the bioreactor, the reduction in the glycerol consumption with the decrease in the biosurfactant production can be observed, indicating a substrate in the product yield approximately constant with the variation of the DO concentration. Thus, it is noticed that the oxygenation system used in this work is efficient and makes possible the scale-up of the process. The great difficulty in scaling up biochemical processes is the oxygenation condition. In a conventional oxygenation system, the bubble dispersion in a big fermentation vessel is the greatest problem to maintain the oxygenation rate. With the proposed system, the oxygenation rate could be doubled simply by doubling the interface area. Therefore, when increasing the fermentation medium volume by a factor of two, the interfacial area of the oxygenation device should be doubled to keep the oxygenation conditions unchanged.

However, this process can still be improved, as the cells can reach greater productivities in other growth conditions. Furthermore, these productivity and yield values obtained for the bioreactor fermentation are comparable to the majority of the ones recently reported in the scientific literature for the rhamnolipid production by *P. aeruginosa* from low-cost materials, as seen in Table 1.

To complete the evaluation of the cellular metabolism behavior with the variation in the DO concentration, the nitrate and total protein concentrations and the protease and elastase activities were determined along the fermentations. The nitrogen source was consumed before 24 h of fermentation in all experiments. The results, normalized by the cellular concentration, are exhibited in Fig. 8. It can be observed that along most of the bioreactor fermentation, the protease and elastase activities are lower to the ones in the agitated flasks fermentation. This result is coherent with the fact that the proteases, including the elastase, and the rhamnolipids are virulence factors, and both are produced under a certain condition. The total proteins concentration values are similar along the 7 days of fermentation. This indicates that besides the virulence factors that are produced in a lower amount in the new system, other proteins could be secreted. These proteins could be somehow inhibiting the

Table 1 Rhamnolipid production by *Pseudomonas aeruginosa* from low-cost materials.

Reference	Carbon source	Rhamnolipid productivity (mg/l h)	Yield—$Y_{P/S}$ (%)
Present work	Glycerol	30	20
Jeong et al. [21]	Fish oil	31	37
Benincasa et al. [22]	Soapstock	210[a]	33
Santa Anna et al. [13]	Glycerol	19	13
Haba et al. [23]	Waste frying oil	27	–

[a] Considering only the stationary phase of cell growth

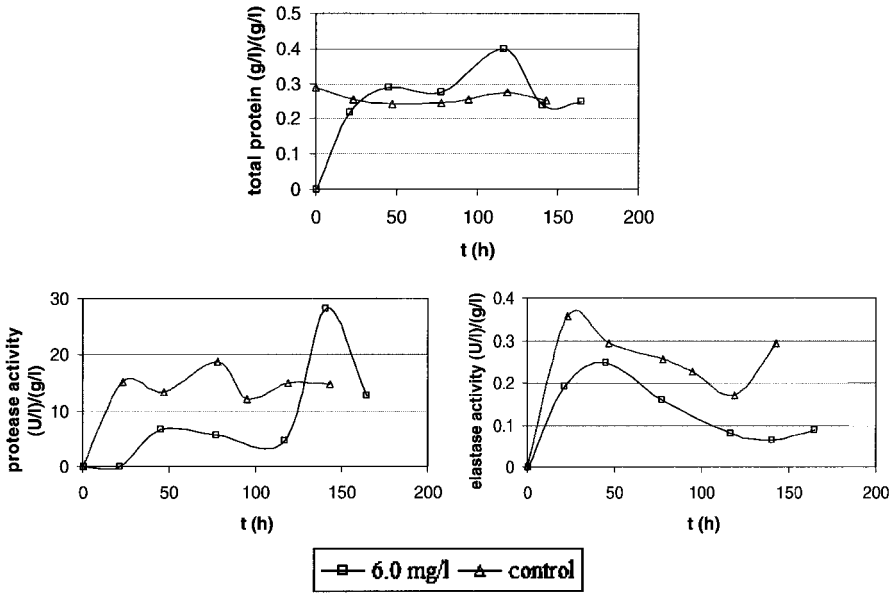


Fig. 8 Time variation of total proteins (g/l) and protease and elastase activities (U/l) during a rhamnolipid production in the bioreactor with the DO set point equal to 6.0 mg/l and in the conventional shake flask fermentation. All presented values are normalized by the biomass content

rhamnolipid production, or at least, they can be identified and used hereafter as indicators of the biosurfactant production inhibition.

Conclusions

The control system for the DO concentration developed was shown to be very efficient for the maintenance of a constant value for that parameter. An interesting observed fact was that the profile of oxygen consumption remained unaffected by the variation of the oxygen concentration. It is clearly observed the variation in the oxygen consumption oxygen along the different phases of the cellular metabolism. After the adaptation phase, which lasts 4 h at the most, there is a significant increase in the OUR. That behavior is also observed for the specific rate, SOUR, which confirms that the variation is not only related to the change in the values of cellular concentration. It is interesting to notice that the increase in the SOUR coincides with the microbial exponential growth phase. Thus, it can be concluded that the oxygen is an essential nutrient for the microbial growth, as it is consumed at a very high rate in that phase. It is still important to point out that the SOUR values remain above 20.0 mg/g h along all of the fermentations, being also important for the cellular maintenance.

The results presented in this work indicate that the proposed process is viable and promising, being a very good alternative for the rhamnolipids production, favoring the control and the scale-up of the production process.

References

1. Rahman, K. S. M., Banat, I. M., Thahira, J., Thayumanavan, T., & Lakshmanaperumalsamy, P. (2002). Bioremediation of gasoline contaminated soil by a bacterium consortium amended with poultry litter, coir pith and rhamnolipid biosurfactant. *Bioresource Technology, 81*, 25–32.
2. Rahman, K. S. M., Rahman, T. J., Kourkoutas, Y., Petsas, I., Marchant, R., & Banat, I. M. (2003). Enhanced bioremediation of n-alkane in petroleum sludge using bacterial consortium amended with rhamnolipid and micronutrients. *Bioresource Technology*, 90, 159–168.
3. Banat, I. M. (1995). Biosurfactants production and possible uses in microbial enhanced oil recovery and oil pollution remediation: a review. *Bioresource Technology, 51*, 1–12.
4. Parkinson, M. (1985). Bio-surfactants. *Biotechnology Advances*, 3, 65–83.
5. Desai, J. D., & Banat, I. M. (1997). Microbial production of surfactants and their commercial potential. *Microbiology and Molecular Biology Reviews, 61*(1), 47–64.
6. Gruber, T., Chmiel, H., Kappeli, O., Sticher, P., & Fiechter, A. (1993). Integrated process for continuous rhamnolipid biosynthesis. In N. Kosaric (Eds.) *Biosurfactants (surfactants science series)* (vol. 48, (pp. 157–173)). New York: Marcel Dekker.
7. Ma, F., & Hanna, M. A. (1999). Biodiesel production: a review. *Bioresource Technology, 70*, 1–15.
8. Cutayar, J., Poillon, D., & Cutayar, S. (1990). *Process for the controlled oxygenation of an alcoholic fermentation must or wort.* US Patent 4,978,545.
9. Santa Anna, L. M. M., Soriano, A. U., Gomes, A. C., Menezes, E. P., Gutarra, M. L. E., Freire, D. M. G., et al. (2007). Use of biosurfactant in the removal of oil from contaminated sandy soil. *Journal of Chemical Technology & Biotechnology, 82*(7), 687–691.
10. Jarvis, F. G., & Johnson, M. J. (1949). A glyco-lipid produced by *Pseudomonas aeruginosa*. *Journal of the American Chemical Society, 71*, 4121–4126.
11. Helvaci, S. S., Peker, S., & zdemir, G. (2004). Effect of electrolytes on the surface behavior of rhamnolipids R1 and R2. *Colloids and Surfaces B: Biointerfaces, 35*, 225–233.
12. Santa Anna, L. M. (2000). *Produção de biossurfactante do tipo ramnolipídeo por Pseudomonas sp.* M.S. thesis, Faculdade de Farmácia/Universidade Federal do Rio de Janeiro, Rio de Janeiro, RJ, Brazil.
13. Santa Anna, L. M., Sebastian, G. V., Menezes, E. P., Alves, T. L. M., Santos, A. S., & Pereira Jr., N., et al. (2002). Production of biosurfactants from *Pseudomonas aeruginosa* PA1 isolated in oil environments. *Brazilian Journal of Chemical Engineering, 19*(2), 159–166.
14. Santa Anna, L. M., Sebastian, G. V., Soriano, A. U., Gomes, A. C., Volpon, A., Freire, D. M. G., et al. (2004). *Biossurfactante e uso do mesmo em remediação de solos impactados por óleo.* Patent PI0405952-2, Petróleo Brasileiro S.A., Brazil.
15. Pham, T. H., Webb, J. S., & Rehm, B. H. A. (2004). The role of polyhydroxyalkanoate biosynthesis by Pseudomonas aeruginosa in rhamnolipid and alginate production as well as stress tolerance and biofilm formation. *Microbiology, 150*, 3405–3413.
16. ACS Committee on Analytical Reagents (2006). *Colorimetry and turbidimetry. Reagent chemicals: Specifications and procedures*10 edn, (pp. 32–41). Oxford: American Chemical Society–Oxford University Press.
17. Lowry, O. H., Rosebrough, N. J., Farr, A. L., & Randall, R. J. (1951). Protein measurement with the Folin phenol reagent. *Journal of Biological Chemistry, 193*, 265–275.
18. Charney, J., & Tomarelli, R. M. (1947). A colorimetric method for the determination of the proteolytic activity of duodenal juice. *Journal of Biological Chemistry, 171*, 501–505.
19. Braga, G. U. L., Messias, C. L., & Vencovsky, R. (1994). Estimates of genetic parameters related to protease production by *Metarhizium anisopliae*. *Journal of Invertebrate Pathology, 54*, 5–12.
20. Blanch, H. W., & Clark, D. S. (1997). *Biochemical engineering*. New York: Marcel Dekker.
21. Jeong, H., Lim, D., Hwang, S., Ha, S., & Kong, J. (2004). Rhamnolipid production by *Pseudomonas aeruginosa* immobilized in polyvinyl alcohol beads. *Biotechnology Letters, 26*, 35–39.
22. Benincasa, M., Contiero, J., Manresa, M. A., & Moraes, I. O. (2002). Rhamnolipid production by *Pseudomonas aeruginosa* LBI growing on soapstock as the sole carbon source. *Journal of Food Engineering, 54*, 283–288.
23. Haba, E., Espuny, M. J., Busquets, M., & Manresa, A. (2000). Screening and production of rhamnolipids by *Pseudomonas aeruginosa* 47T2 NCIB 40044 from waste frying oils. *Journal of Applied Microbiology, 88*, 379–387.

Appl Biochem Biotechnol (2008) 147:47–61
DOI 10.1007/s12010-007-8067-1

Continuous Production of Ethanol from Starch Using Glucoamylase and Yeast Co-Immobilized in Pectin Gel

Raquel L. C. Giordano · Joubert Trovati · Willibaldo Schmidell

Received: 9 May 2007 / Accepted: 26 September 2007 /
Published online: 8 November 2007
© Humana Press Inc. 2007

Abstract This work presents a continuous simultaneous saccharification and fermentation (SSF) process to produce ethanol from starch using glucoamylase and *Saccharomyces cerevisiae* co-immobilized in pectin gel. The enzyme was immobilized on macroporous silica, after silanization and activation of the support with glutaraldehyde. The silica–enzyme derivative was co-immobilized with yeast in pectin gel. This biocatalyst was used to produce ethanol from liquefied manioc root flour syrup, in three fixed bed reactors. The initial reactor yeast load was 0.05 g wet yeast/ml of reactor (0.1 g wet yeast/g gel), used in all SSF experiments. The enzyme concentration in the reactor was defined by running SSF batch assays, using different amount of silica–enzyme derivative, co-immobilized with yeast in pectin gel. The chosen reactor enzyme concentration, 3.77 U/ml, allowed fermentation to be the rate-limiting step in the batch experiment. In this condition, using initial substrate concentration of 166.0 g/l of total reducing sugars (TRS), 1 ml gel/1 ml of medium, ethanol productivity of 8.3 g/l/h was achieved, for total conversion of starch to ethanol and 91% of the theoretical yield. In the continuous runs, feeding 163.0 g/l of TRS and using the same enzyme and yeast concentrations used in the batch run, ethanol productivity was 5.9 g ethanol/l/h, with 97% of substrate conversion and 81% of the ethanol theoretical yield. Diffusion effects in the extra-biocatalyst film seemed to be reduced when operating at superficial velocities above 3.7×10^{-4} cm/s.

Keywords Ethanol · Cassava starch · *Saccharomices cerevisiae* · Glucoamylase · Packed-bed reactor · Simultaneous saccharification and fermentation

R. L. C. Giordano (✉) · J. Trovati
Chemical Engineering Department, Universidade Federal de São Carlos - UFSCar,
Washington Luiz, Km235, Monjolinho, São Carlos, SP, Brazil
e-mail: raquel@ufscar.br

W. Schmidell
Chemical Engineering and Food Enginering Department,
Universidade Federal de Santa Catarina-UFSC,
Florianópolis, SC, Brazil

Nomenclature

TRS	total reducing sugar, expressed as glucose concentration (g/l)
Et	ethanol concentration (g/l)
G	glucose concentration (g/l)
X_g	cell concentration in the gel (viable cells/g gel)
N_{viable}	average viable cell number in a square of the Neubauer chamber
M_{gs}	mass of the gel particles sample
Q_{feed}	feed volumetric flow rate (ml/h)
Q_r	recycle volumetric flow rate (ml/h)
RR1	recycle ratio in the first reactor
V_s	superficial velocity flux (cm/s)
U	unit of free enzyme
x_s	liquified starch (TRS) conversion
θ	residence time (h)=reactor volume/Q_{feed}
Pr_{et}	ethanol productivity (%)
η_{et}	ethanol yield (%)
theoretical yield	theoretical conversion of glucose to ethanol=0.51

Introduction

Brazil has been the major ethanol producer since the 1970s, with the implementation of the PROALCOHOL Program, using sugar cane as raw material [1]. In the last years, using the corn dry-grind process, USA has steadily increased its ethanol production, reaching in 2005, a figure similar to the one obtained in Brazil, around 4.2 billion gallons of ethanol per year [2].

The most important sources of biomass to produce bioethanol are clearly defined in the two more important producers. However, the increasing world demand for biofuels makes all the possible biomass eligible as raw materials. In Brazil, sugar cane distilleries only operate from March to November, the sugar cane crop period, and therefore, the option of a different feedstock that could extend the use of the industrial plant would be very attractive. Besides, culture rotating would improve the use of the soil that would be managed in a more sustainable manner.

Cassava, casava, or manioc (*Manihot esculenta*) is a plant native to South America that is extensively cultivated as an annual crop in tropical and subtropical regions for its edible starchy tuberous root, a major source of carbohydrate. It is a shrub with an average height of 1 m, and has a palmate leaf formation. Cassava roots contain a high concentration of carbohydrates (about 80%), mainly starch, significant amounts of calcium (50 mg/100 g), phosphorus (40 mg/100 g), and vitamin C (25 mg/100 g). Cassava gives the highest yield of food energy per cultivated area per day among crop plants, except possibly for sugarcane. Although the manioc roots are poor in protein and other nutrients, the leaves are a good source of protein if supplemented with the amino acid methionine. Whereas other crops such as yam, maize, banana, and plantain, cowpea, or sorghum and millet are eco-regionally specific, cassava is probably the only crop whose production cuts across all ecological zones.

The world cassava production in 2005 was 208 million tons, 55% in Africa, 32% in Asia (12% in Thailand), and 13% in Brazil. The global trade in cassava products in 2005 was 6.2 million tons. Dried cassava roots are used as raw material for compound animal feed, while

cassava starch is used for manufacture of paper, textiles, adhesives, and alcohol [3]. In Thailand, the construction of 12 cassava ethanol plants, with the total output of 3.4 million l/day by the next 2 years has just been approved. An assessment of the net energy and supply potentials to evaluate the utilization of cassava for fuel ethanol (CFE) in Thailand was performed [4]. This study showed that the CFE system is energy efficient, with positive net energy value and net renewable energy value of 8.80 and 9.15 MJ/l, respectively.

Centrifugation is a necessary step for the separation and recycle of the yeast cream in the Melle-Boinot process, the leading technology to produce ethanol from sugar cane that has been used in Brazil since the 1960s [1]. Centrifugation costs have a significant role in the production of ethanol via fermentation, and the use of immobilized microorganisms in the process avoids this step, thus reducing total costs. On using starch as raw material, the time and energy required for hydrolysis and the price of enzymes represent additional costs when compared to directly fermentable raw materials. Simultaneous saccharification and fermentation (SSF) involves the hydrolysis of the polysaccharides into glucose and its conversion to ethanol in the same vessel. Some advantages of this method, compared to separate hydrolysis and fermentation, are: the cost saving resulting from the reduction of the number of reactor vessels that are required (lower capital costs), the increased rate of hydrolysis due the lower inhibition by product, and the reduction of fermentation time [5]. The SSF process is already used in the conventional dry-grind corn process [6]. Immobilization of the enzyme and of the microorganism allows their reutilization, what may turn economically viable the use of high concentrations of the biocatalysts in the reactor, reducing reaction times. This technique has been extensively studied to reduce process costs [7–9]. Using immobilized glucoamylase and *Zymomonas mobilis*, the SSF process was compared to a separated hydrolysis and fermentation (SHF) process for the production of ethanol from starch in a fluidized bed reactor (FBR) [10]. This work showed that the SHF led to higher productivities than the SSF process, due to the low activity of the enzyme at 35°C, operation temperature for the SSF process. Economic analysis of the ethanol production in FBR reactors showed that there is operation and cost savings when this reactor configuration is used to produce ethanol from starch [11].

The fabrication of ethanol from liquefied manioc root flour syrup is studied here, using microorganism and enzyme co-immobilized in pectin gel. This process would be complementary to the fermentation of sugar cane molasses in sugar mills. In this process, glucoamylase (or amyloglucosidase) is first covalently immobilized in controlled porosity silica (CPS). After that, the derivative CPS-enzyme is co-immobilized with *Saccharomyces cerevisiae* in pectin gel. This technique makes operation at 30°C (optimum fermentation temperature) economically feasible because the immobilization of high loads of enzyme allows reaching high rates of hydrolysis in the reactor, even at such a low temperature. This strategy counterbalances the fact that the optimal operation temperature for glucoamylase is 60°C.

Pectin pellets are formed by the action of bivalent cations, such as calcium, that allow the formation of crossed bonds between the polymeric pectin precursors. The presence of calcium in the medium is essential to maintain gel integrity, thus avoiding the leaching of this cation [9].

Batch and continuous experiments were run. The continuous set-up consisted of three fixed-bed reactors in series, to allow the escape of the produced CO_2 in each reactor. Various process features were studied: determination, in batch experiments, of the most adequate rate between concentrations of enzyme and yeast in the reactor, investigation of the performance of continuous SSF in a packed-bed reactor, to analyze the influence of the superficial velocity on the performance of the continuous SSF process.

Materials and Methods

Materials Manioc root flour, from peeled, dried, and milled root, was purchased from "Ricieri Pechatt & Filhos", Araras, SP, Brazil; α-amylase P-500 (EC 3.2.1.1), was supplied by Pfizer S. A.; glucoamylase 200 L (EC 3.2.1.3), with 190 U/ml of activity (where 1 U is the quantity of enzyme that produces 1 g of glucose per hour, from 4% soluble starch at 60°C and pH 4.2) and 128 mg protein/ml, was donated by NOVO Industri do Brasil; commercial *S. cerevisiae* (60% of moisture), from Fleischmann SA; controlled pore silica (CPS) was supplied by Corning Glass Works (Corning, NY), with average pore size of 37.5 nm and internal porosity of 56.6% (diameter below 100 μm); citric pectin type 8002 supplied by Braspectina S.A. All the other reagents used were laboratory grade from different commercial sources.

Enzyme Immobilization Silica was silanized with a 5% *v/v* aminopropyltrietoxysilane solution, pH 3.3, 75°C, for 3 h at a liquid/solid ratio of 3 ml/g. The silica was then washed with water, dried at 105°C for 15 h, and activated with glutaraldehyde (2.5% hydrogenphosphate buffer, 0.1 M, pH 7.0) for 1 h at 20–25°C at a liquid/solid ratio of 5 ml/g, under stirring at the three stages.

Co-immobilization Pectin, 6 g, was dissolved in 78 ml distilled water, with subsequent addition of 6 ml sodium acetate buffer (1 M, pH 4.2) and 10 g wet yeast. Silica containing immobilized enzyme (206.5 U/g dried silica or 272.2 U/g dried silica) was then mixed with the suspension at the ratio of 1.5 g of wet silica–enzyme/20 g yeast–pectin suspension. One gram of dried silica corresponded to 1.5 of wet silica. Finally, the suspension was dropped in a 0.2 M $CaCl_2$ solution, and 18.5 g of 4 mm spherical particles were formed after curing in a refrigerator, for 18 to 20 h.

Manioc Root Flour Syrup A suspension of flour (approximately 300 g/l) in a 0.01-M NaOH/0.01 M $CaCl_2$ solution was prepared, adjusting the pH set between 6.0 and 6.5. Thereafter, the suspension was heated under stirring, and at 65°C, 0.3 g alpha-amylase per liter of suspension was added. This was kept at 90°C for 10 min, then boiled for 5 min, and vacuum filtered in syrup paper. For the fermentation, $NaH_2PO_4{\cdot}H_2O$ (1.0 g/l), $MgSO_4{\cdot}7H_2O$ (0.25 g/l), yeast extract (0.5 g/l), $CaCl_2$ (2.0 g/l), and urea (1.5 g/l) were dissolved and added to the liquefied starch solution.

Experimental Assays All experiments were performed at 30°C, initial pH of 4.0. Batch tests were carried out in glass flasks with 3 cm of internal diameter, in a reciprocal shaker, at 150 rpm. Each flask contained a known volume of substrate (liquefied cassava starch syrup) and an equal volume of biocatalyst beads. In continuous tests, a setup of three glass reactors was used with volumes of 35, 30, and 25 ml or 110, 104, and 100 ml, internal diameter of 5 cm, with or without recycle, and with exhaustion of the CO_2 formed in the first two stages in a water column. This allowed control of the reactors' internal pressure as shown in Fig. 1.

Analysis

TRS and Glucose Liquefied starch concentration was determined by dosing total reducing sugars (TRS), expressed in terms of glucose concentration, after enzymatic hydrolysis of the liquefied starch present in the sample, using glucoamylase, diluted 1:200 in acetate or

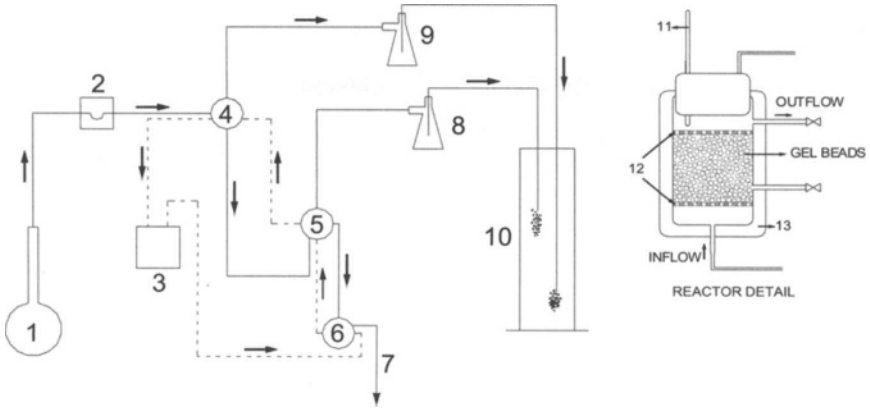


Fig. 1 Reactor system for continuous runs: *1* Feed flask, *2* pump, *3* bath; *4*, *5*, *6* reactors 1, 2, and 3, *7* effluent, *8*, *9* security flasks, *10* water/$CuSO_4$ column. A reactor detail: *11* thermometer, *12* stainless steel screen, *13* jacket. Water recirculation (*dashed line*); substrate (*line*)

citrate buffer 0.1 M, pH 4.2, at 45°C, for 30 min, followed by enzyme inactivation in boiling water, for 5 min [12].

TRS (grams of glucose/liter)=$(0.977\times(G_m-G_i)/0.9)+G_i$($G_m$=glucose concentration in the sample after enzymatic hydrolysis; G_i = glucose concentration in the sample before enzymatic hydrolysis; 0.977=empiric factor to convert in starch the glucose obtained by enzymatic hydrolysis of the liquefied starch=0.9/enzymatic hydrolysis yield, determined by Schmidell and Fernandes, 1977, using soluble starch, analytical grade [11]; 0.9= stoichiometric glucose/starch conversion factor). Glucose and TRS were dosed using a glucose-oxidase Kit (CELM S.A.)

Ethanol This is determined by oxidation with $K_2Cr_2O_7$, followed by titration with Fe $(NH_4)_2(SO_4)_2{\cdot}6H_2O$–Mohr salt [13] and using a Waters high performance liquid chromatography (HPLC), an ion exchange Shodex® column, at 80°C, refraction index detection, at 34°C, elution with Milli-Q water, flow rate of 1.0 ml/min. All samples were analyzed using the titration method. HPLC was used to confirm the results obtained with the titration method. The two methods led to very similar results.

Cellular Viability and Concentration Determined by counting cells in nine squares of a Neubauer chamber after dying them with methylene blue solution. Viable cells were not colored, and dead cells were blue; free yeast concentration was also obtained by filtering a known volume of cell suspension and drying the wet mass until the constant weight was achieved; viability and concentration of immobilized yeast were determined as already described, after dissolution of the pectin gel [1.0 g of cured pellets was dissolved in 20 ml of 5% ethylenediaminetetraacetic acid (EDTA) solution at constant agitation]. The cell concentration was calculated as:

$$X_g = \left(N_{viable}/4\times10^{-6}\right)\times\left(\left(20+\left(M_{gs}/\rho_g\right)\right)/M_{gs}\right)\times 10,$$

where:

X_g —cell concentration in the gel (viable cells/gram gel)
N_{viable} —average viable cell number in one square of the Neubauer chamber
20 —volume of EDTA solution (ml)
M_{gs} —mass of the gel particles sample
ρ_g —gel particles density
4×10^{-6} —volume of the one square of the chamber (ml)
10 —sample dilution factor in methylene blue solution

Bead density and diameter Bead density was determined before the beginning of the run and immediately after finishing it, using a pycnometer. After finishing the run, the liquid and the particles were collected and separated. The liquid volume was measured. The particles were first dried by contacting them with an absorbent paper, following the same procedure used before the beginning of the run. The pectin bead diameter was determined measuring the volume of 500 particles, using a pycnometer.

Soluble and Immobilized Enzyme Activity Soluble and immobilized enzyme activity was determined in standard conditions [14]: a unity (U) is the amount of enzyme that liberates 1 g of glucose in 1 h at 60°C, pH 4.2, from a 4% soluble starch solution. Amount of immobilized enzyme was calculated by the difference between the offered load and the remaining enzyme in the supernatant, after the immobilization procedure.

Starch Conversion (X_s) and Ethanol Yield (η_{et}) X_s was calculated as (TRS(*i* or feed)−TRS (*f* or outlet))/TRS(*i* or feed); η_{et} was calculated as (Et(*f* or outlet)/(TRS(*i* or feed)−TRS(*f* or outlet))×0.51).

Results and Discussion

Batch Experiments: Selecting Enzyme Concentration for the Continuous Experiments

The initial yeast concentration in the reactor, for all the SSF assays was 50 g wet yeast/l of reactor (0.1 g wet yeast/g gel). In previous continuous tests using the same equipment 50 g wet yeast/1 of reactor allowed obtaining increasing ethanol profile from the first to the third reactor, in the conversion of sucrose from molasses in ethanol (results not shown). In the present system, the liquefied starch has to be hydrolyzed inside the particle before the fermentation step, and therefore, the substrate availability to the microorganism is different. Nevertheless, as it was intended to operate the SSF process with the fermentation being the rate-limiting step, it was believed that the ethanol profile obtained with sucrose might be reproduced with hydrolyzed starch, using the same yeast concentration in the reactor. This yeast concentration in the reactor was then chosen and fixed to study the SSF process. The next step was to choose an enzyme concentration in the reactor that allowed keeping glucose available in the reaction medium, with the total hydrolysis time lower than the total fermentation time. In this way, fermentation would be the rate-limiting step. The experiments for choosing the enzyme concentration were performed in batch mode. Therefore, batch SSF tests were run, keeping the same yeast concentration—50 g wet yeast/ l of reactor (0.1 g wet yeast/g gel) and varying the amount of enzyme. Figure 2a,b shows

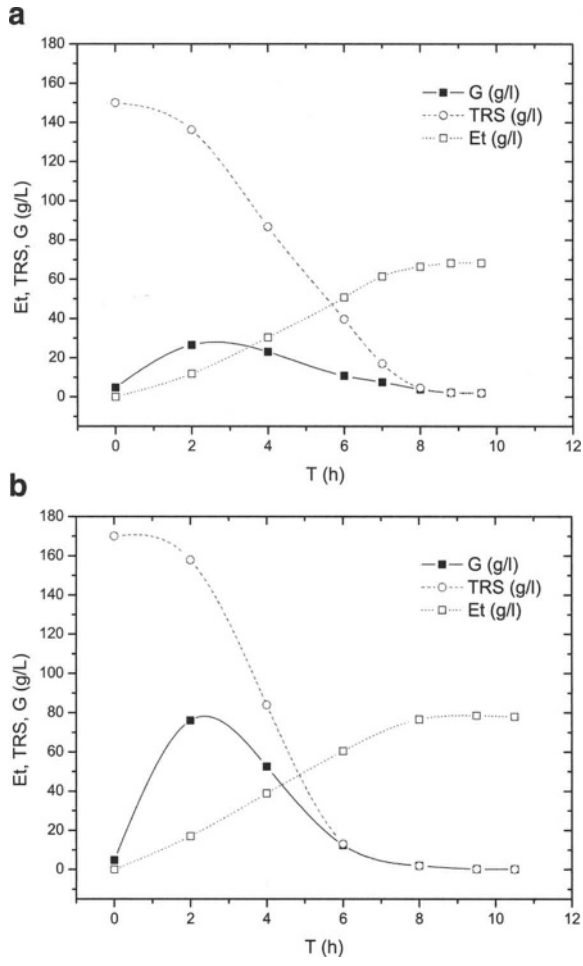


Fig. 2 Total reducing sugar (TRS), ethanol (Et), and glucose (G) concentrations with time (T), for operation of SSF process in discontinuous runs, under two different enzyme concentration in the reactor: **a** 2,860 U glucoamylase/l reactor; TRS_i=150.0 g/l; G_i=5.3 g/l; **b** 3,770 U glucoamylase/l reactor; TRS_i=166.0 g/l; G_i=4.8 g/l. Yeast concentration: 50 g wet yeast/l reactor; gel volume/medium volume=1.0. Batch runs

the obtained results for the two assayed conditions, 2,860 and 3,770 U/l, respectively. Observing the results showed in Fig. 2a, it can be seen that the hydrolysis is the rate-limiting step for the lower enzyme concentration tested. Figure 2b shows the results for the higher enzyme concentration, 3,770 U/l of reactor. Using this condition, the time for total hydrolysis of the liquefied starch was 6 h (TRS and glucose concentrations were equal), and the total fermentation time was 9.5 h. The maximum glucose concentration was 76.0 g/l, and maximum ethanol concentration was 78.5 g/l, which were reached, respectively, around 2 and 9.5 h.

It can be observed from the results presented in Fig. 2b that the system is well-balanced, using 3770 U/l and 50 g of wet yeast/l of reactor. There is always glucose available for the microorganism, the time for total hydrolysis is lower than for total fermentation, and therefore, starch hydrolysis is not the rate-limiting step. Productivity was 8.3 g/l/h, with 99.8% of conversion and yield of 0.47 (91% of the theoretical). This condition was then chosen to run the continuous SSF experiments.

Performance of the Continuous Reactor System

The three SSF continuous experiments were operated using 3,770 U/l of enzyme and 50 g of wet yeast/l of reactor, as determined in the batch runs. The first continuous run was performed with a total reactor volume of 90 ml (the volume was delimited by two stainless sieve), during 226 h, feeding 163.0 g/l of TRS. Flow rates changed from 8.1 to 44.0 ml/h. Sampling was made three residence times after changing the flow rate. Table 1 shows results of ethanol production and yeast concentration in the outlet of each reactor. Table 2 shows the concentrations of total reducing sugars and glucose.

Table 1 shows that the maximum ethanol concentration in this test was 67.7 g/l, in the outlet of the third reactor, for a flow rate of 8.1 ml/h. In this condition, the TRS and glucose concentrations were 3.3 and 0.8 g/l, respectively. The system is stable for all flow rates. The lowest flow rate, 8.1 ml/h, was more difficult to control, which was what led to some more pronounced oscillation of the variable values in this condition. It was expected in the continuous run that similar results than the ones obtained in the batch run will be achieved. As in batch operation, the cycle time is considerably longer than the reaction time, if the continuous process had reached a similar performance than the one obtained with the batch run; in the continuous operation, we could save cycle time (times to clean, to fill ant to empty the reactor). Therefore, from the industrial point of view, the continuous process would lead to higher productivities.

It is clear, however, that the operation of the SSF process in continuous reactors led to a worse performance than the one obtained in the batch experiments, with the same enzyme and yeast concentrations in the reactor and similar total reducing sugar concentration (initial, in the batch run and in the feed, for the continuous run). The concentration of free glucose in the effluent was lower than 1 g/l for all the tested flow rates, except for the two

Table 1 SSF continuous run 1.

T (h)	Q_{feed} (ml/h)	Et_1 (g/l)	Et_2 (g/l)	Et_3 (g/l)	Xef_1 cel/ml×10^7	Xef_2 cel/ml×10^7	Xef_3 cel/ml×10^7
23.0	8.1	52.3	63.1	63.1			
42.5	8.1	48.8	63.3	67.7			
54.0	8.1	47.9	58.7	66.0			
68.0	8.1	41.3	57.0	64.8	6.4	6.2	5.8
95.0	11.0	31.6	48.5	57.1			
114.0	11.0	32.8	49.3	57.0			
122.0	11.0	32.5	49.2	56.8			2.1
144.0	14.5	23.5	42.1	49.5			
152.0	14.5	23.5	42.0	50.1			
176.0	14.5	22.5	43.0	49.8		5.3	4.1
199.0	22.0	13.7	27.8	36.4			
203.5	22.0	13.7	25.0	38.2	3.8		
207.5	22.0	11.5	26.2	37.6			
222.0	44.0	11.7	20.8	28.0			
224.0	44.0	12.1	19.8	28.8			
226.0	44.0	11.3	19.4	28.0			

Ethanol concentration (Et) and effluent cell concentration (X_{ef}) in the outlet of reactors 1, 2, and 3, for different feed flow rates (Q_{feed}). TRS_{feed}=163 g/l; G_{feed}=3.9 g/l; enzyme concentration=3.77 U/ml reactor; initial yeast concentration=50.0 g wet yeast/ml of reactor; pH in the outlet of reactor 3=3.6

T Assay time.

Table 2 SSF continuous run 1.

T (h)	Q_{feed} (ml/h)	TRS_1 (g/l)	TRS_2 (g/l)	TRS_3 (g/l)	G_1 (g/l)	G_2 (g/l)	G_3 (g/l)
23	8.1	43.4	6.3	1	1.8	2.6	0.5
42.5	8.1	50.5	13.8	3.3	0.9	1	0.8
54	8.1	49.6	16.9	3.9	0.8	1.3	0.9
68.5	8.1	60	23	10	0.8	0.9	0.9
95.5	11	81	42.8	19.5	0.1	0.2	0.4
114.5	11	80.5	43.1	22.3	0.3	0.2	0.2
122.5	11	78.5	43	24.1	0.1	0.2	0.3
144	14.5	96.5	53.1	41.4	0.7	0.1	0.2
152	14.5	101	53.3	38.7	0.3	0.1	0.2
176	14.5	105.5	55.7	42.8	0.5	0.3	0.2
199	22	130.7	102	71.9	1	1	0.3
203.5	22	124.2	92.7	72.5	1	1	0.7
207.5	22	129.6	96.2	73.1	1	1	0.5
222	44	132	113.3	93.3	2.7	2.3	7.6
224	44	129	113.1	94.8	2.1	1	2.8
226	44	129.1	112.7	93.9	0	0	0

Total reducing sugar concentration (TRS) and glucose concentration (G), in the outlet of reactors 1, 2, and 3, for different feed flow rates (Q_{feed}).

T Assay time

first samples at 44 ml/h. Therefore, in this first continuous test, starch hydrolysis was the rate-limiting step.

Table 3 shows initial and final values for mass and volume of beads and initial and final cell concentration and cell viability of the yeast in the beads. Table 3 shows an increase in the mass and volume of beads after running the experiments for 226 h. All the detected bead alterations are more pronounced in the first reactor, where the reaction rates are the highest. The final bead density in the first reactor, 0.96 g/ml, decreased when compared to the initial bead density, 1.07 g/ml. A great amount of gas could be seen in the first reactor. The reactor system tested in this work (three reactors in series, with escape of CO_2 between two consecutives stages) had been designed to avoid the gas hold-up in the reactors. However, to keep the reactors under pressure (there were no pumps between the reactors), the CO_2 escaped in a water column (containing $CuSO_4$ for avoiding bed contamination), and some gas hold-up was still observed, mainly in the first reactor. Therefore, the designed

Table 3 SSF continuous run 1.

Reactor	Vr (ml)	M_{gi} (g)	M_{gf} (g)	V_{gf} (ml)	ρ_{gf} (g/ml)	ε_f	X_{gf} (cel/g gel)	Vb (%)
1	35	17.5	26.0	27.0	0.96	0.23	1.37×10^9	89
2	30	15	21.8	20.5	1.06	0.34	1.0×10^9	56
3	25	12.5	13.8	13.0	1.07	0.48	8.40×10^8	50

Bed characterization in the reactors 1, 2, and 3. Xg, Mg, Vg and ρg stand for cell concentration, mass, volume, and density of the beads, respectively.

ε Reactor porosity, Vr reactor volume, Vb viability. Subscripts: i initial, f final

ρg_i=1.07 g/ml; $Xg_i=1.8\times10^9$ viable cell/g gel; Vb_i=98%; ε_i=0.5

system only diminished the problem. The final cell concentration in the beads in each reactor decreased when compared to the initial one, the decrease being more pronounced in the third reactor. However, as the mass of beads increased, the total number of viable cells present in each reactor after 226 h ($X_{gf} \times M_{gf}$) was kept almost constant in the first reactor—from the initial 3.1×10^{10} to the final 3.2×10^{10} and decreased in the second and third ones—from the initial 2.6×10^{10} and 2.2×10^{10} to 1.2×10^{10} and 5.7×10^{9} in reactors 2 and 3, respectively. This was already expected, as the cells in the first reactor are living in better nutrition conditions than the ones in the second and third reactors. In the first reactor, the concentration of sugar is higher, and ethanol concentration is lower than in reactors 2 and 3. Some gel disruption was also observed, being always more significant in the first reactor and still more when the system was operated with recycle in the first reactor (runs 2 and 3). The leaching of calcium and the high production of CO_2 in the first reactor may be responsible for this problem. Gel disruption may be minimized by using particle size around 1 mm and adding 2–6 g/l of calcium chloride to the medium [9].

Figure 3 shows the results of ethanol, TRS, and glucose as function of the residence time, which was calculated considering the first reactor volume, the sum of reactors 1 and 2 volumes and the sum of the volumes of the three reactors. As it can be seen in Fig. 3, the concentration values obtained for residence times calculated considering only the first reactor operating with the lower flow rates shows a good agreement with the values obtained for the same residence time, calculated considering the sum of the volumes of the three reactors, operating with the higher flow rates.

Table 4 shows the calculated values of conversion, productivity, and yield for each residence time tested: the productivity for the maximum conversion reached in the continuous SSF (97%) was 5.9 g/l/h, with yield of 81%, for a residence time of 11.1 h, calculated using the average values of the four determined TRS and ethanol concentrations for this residence time. In the discontinuous SSF reactor, for the same enzyme and yeast concentrations, the results were: total conversion of TRS in glucose in 6 h and 99.8% of glucose/ethanol conversion in 9 h, with high concentrations of free glucose in the medium.

Possible causes for the worse performance of the continuous process may be the presence of severe external and/or internal diffusion effects, hold-up gas and channeling prob-

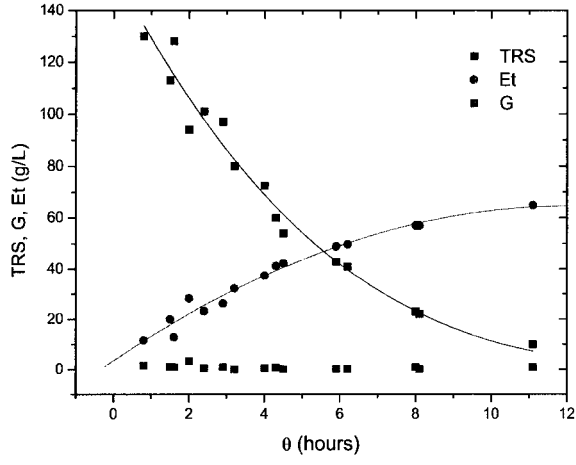


Fig. 3 SSF continuous run 1. Ethanol (Et), total reducing sugar (TRS), and glucose (*G*) concentrations with residence time (θ). θ values are related to: reactor 1 volume (35 ml); (reactor 1 + reactor 2) volume=65 ml; (reactor 1 + reactor 2 + reactor 3) volume=90 ml. TRS_{feed}= 163.0 g/l

Table 4 Ethanol concentration (Et), substrate conversion (x_s), ethanol productivity (Pr_{et}), and ethanol yield (η_{et}) for several residence time in the reactor (θ).

θ (h)	Et (g/l)	x_s	Pr_e (gEt/l h)	η_{et} (%)
0.8	11.7	0.2	14.6	69.0
1.5	20.0	0.31	13.3	77.0
1.6	13.0	0.21	8.1	74.0
2.0	28.3	0.42	14.1	81.0
2.4	23.2	0.38	9.7	73.0
2.9	26.3	0.40	9.1	79.0
3.2	32.3	0.51	10.1	76.0
4.0	37.4	0.56	9.4	80.0
4.3	41.3	0.63	9.6	79.0
4.5	42.4	0.67	9.4	76.0
5.9	49.0	0.74	8.3	79.0
6.2	49.5	0.75	8.0	79.0
8.0	57.0	0.86	7.1	80.0
8.1	57.0	0.86	7.0	80.0
11.1	65.4	0.97	5.9	81.0

TRS_{feed}=163 g/l. SSF continuous run 1.

lems in the bed. The decrease of the bead density in the first reactor, determined after finishing the run, indicates retention of the produced CO_2. It could be seen that some particles were floating in the first reactor in the beginning of the run, when there was space for that (the bed porosity decreased from 0.5, initial, to 0.23, final, in the first reactor). So, the exhaustion system proposed did not allow the complete escape of the large amount of gas produced in the first reactor, which was what implied a decrease in the real volume of the first reactor. The comparison between the performance of the batch and the continuous run is made considering around 9 h for the batch run and 226 h for the continuous one. It is a reasonable hypothesis that there might have been a preferential yeast growth near the silica, as glucose concentration is higher there. The considerable quantitative growth and the fact that yeast grows in clusters [15], near the substrate [16, 17], caused an increase in the tortuosity of the substrate course inside the gel. The access of the substrate to the enzyme in the interior of the silica might also be restrained, consequently lowering the hydrolysis rate in the continuous system. Therefore, as the continuous assay went by, a different distribution of the microorganism was established, which implied higher restrictions for the starch diffusion inside the biocatalyst. Gonçalves et al. [18] have modeled the hydrolysis of maltotriose catalyzed by glucoamylase immobilized in silica and co-immobilized in pectin gel, using a bi-disperse model. This study allowed the authors to estimate the maltotriose diffusivity in silica. Nevertheless, the presence of yeast may lead to different results. Finally, in the discontinuous run, the beads and medium were mixed at 150 rpm (in fact, oscillations/m, it was a reciprocal shaker), in glass flasks with a diameter of 3 cm, in what may lead to fluid velocities higher than the superficial flow rates of the fluid in the continuous test (run 1). In consequence, the external mass transport coefficient for the starch diffusion from the bulk to the particle surface may be lower in the continuous run, and the rate-limiting step in the process would be the diffusion of the liquefied starch from the bulk to the particle surface. If this last phenomenon was significant, increasing the superficial velocity would lead to an improvement in reactor productivity of the continuous run.

Influence of Superficial Velocity on the Performance of the Continuous SSF Reactor

To verify the possibility of limitation of the hydrolysis rate in the system by the external mass transport resistance, the bed height of the gel containing enzyme and co-immobilized yeast was increased. This was done to increase the total volume of the system (from 90 to 314 ml), without changing the flow area, and consequently, enabling higher superficial rates in the system for the same residence time. The use of recycle in the first reactor enabled obtaining even higher rates in this stage, where most of the conversion took place. TRS concentration in the feed decreases when operating the process with recycles. That implies a decrease in the driving force of starch diffusion through the external film and in the biocatalyst pores. Inherent reaction rates would also decrease. However, if the external diffusions effects were very high, the increase in the substrate mass transport coefficient may compensate the decrease of concentrations, thus, leading to an improvement in the reactor performance.

These effects were studied running two new continuous assays. In continuous run 2, the system was operated with a total volume of 314 ml (110, 104, and 100 ml, for reactors 1, 2, and 3, respectively), keeping constant the feed flow rate, 55 ml/h, with and without recycle in the first reactor. Only one recycle flow rate was tested, 67.2 ml/h. In continuous run 3, only the first reactor was operated, changing the feed and recycle flow rates. Table 5 shows operational conditions and respective average values of ethanol, TRS, and glucose concentrations obtained for related steady states, in the two new tests. Figure 4 shows ethanol production vs residence time for operational conditions operated without recycle, with superficial velocities up to 3.1×10^{-4} cm/s and above 3.7×10^{-4} cm/s.

Results in Table 5 show a worse performance of the system with recycle (always in the first reactor). All values of ethanol concentration obtained with recycle decreased when compared to the ones obtained without recycle. Therefore, the increase in the external mass transport coefficient was not sufficient to compensate for the decrease in the TRS concentration in the first reactor due to dilution. The concentration of free glucose in the effluent is still very low for both cases, with and without recycling. Only

Table 5 Ethanol (Et), total reduction sugar (TRS), and glucose (*G*) concentrations, for different operation conditions.

Run	Q_{feed} (ml/h)	RR1	Θ (h)	Et (g/l)	TRS (g/l)	*G* (g/l)
2	55	1.22	2	24.2	84.4	0
2	55	0	2	33.8	69.1	1.7
2	55	1.22	3.9	44.8	41.9	0,7
2	55	0	3.9	46.4	41.2	0
2	55	1.22	5.7	55.9	20.5	0.9
2	55	0	5.7	55.4	21.8	0.3
3	13.2	0	8.3	56.3	18.8	0.5
3	18.5	0	5.9	51.4	28.7	0
3	26.1	0	4.2	47.4	37.9	0
3	54.2	0	2	33.2	66	0
3	54.2	0.26	2	29.5	79.4	0
3	54.2	1.05	2	24.4	92.3	0

Q_f Feed flow, *RR1* recycle ratio=recycle flow=Q_r/Q_{feed}, θ residence time=reactor volume/Q_{feed}, TRS_{feed2}, TRS_{feed3}=feed TRS in the runs 2 and 3=144.0 and 151.0 g/l, respectively

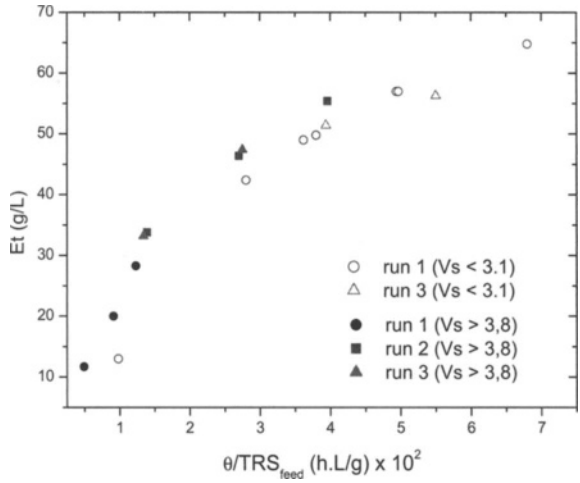


Fig. 4 Ethanol (Et) concentration with residence time/feed total reducing sugar (θ/TRS$_{feed}$), for two superficial velocities ranges: Vs≤3.1×10^{-4} cm/s and Vs≥3.8×10^{-4} cm/s, for the three SSF continuous runs

for the residence time of 2 h, without recycle, glucose concentration is higher than 1.0 g/l. However, the superficial velocities in runs 2 and 3 are higher than in run 1, and the comparison of the ethanol concentrations obtained for similar residence times in runs 1, 2, and 3 shows that the highest ethanol productivities are achieved for the highest volumetric flow rates.

Aiming at analyzing the influence of the superficial flow rates in the ethanol concentration, all the obtained results in the three continuous run, without recycle, are compared with respect to the respective superficial rates, as shown in Fig. 4. As the TRS feed used in the three assays were not exactly the same, the residence times are divided by the corresponding TRS feed concentration.

Analyzing the results in Fig. 4, it can be seen that the assays performed with velocities higher than 3.8×10^{-4} cm/s have better performance than the ones with velocities lower than 3.1×10^{-4} cm/s. Ethanol concentration values were higher for velocities equal to or bigger than 3.7×10^{-4} cm/s, indicating that limitation by external transport really exists. Despite this improvement, the results of the continuous system are still far from the batch process. The hydrolysis rate in the continuous process is lower when compared to the discontinuous tests, with no free glucose present in all operational conditions, including the ones with superficial velocities higher than 3.7×10^{-4} cm/s. The results of the assays with recycle in the first reactor (and consequently with increasing flow rates in this stage) support this conclusion.

Table 5 indicates a negative influence of the recycle on the performance of the reactor in this operational range (superficial velocities above 3.7×10^{-4} cm/s). Therefore, other phenomena may be contributing for the inferior performance of the continuous system: gas hold-up, channeling, and the intra-gel mass transport resistance due to yeast growth inside the particle during the long operation of the continuous runs.

Sun et al. [8] and Krishnan et al. [10] also found that starch hydrolysis was the rate-limiting step, when operating a SSF-fluidized bed reactor to produce ethanol from soluble starch and liquefied corn starch, respectively. The authors used immobilized glucoamylase co-immobilized with *Z. mobilis* in κ-carrageenan beads, a biocatalyst very similar to the one used in this work. Krishnan et al. [10], by testing the activity of the immobilized enzyme after deactivation of the microorganism using ethanol 75%, concluded that microorganism

growth was not responsible for the decrease of the starch hydrolysis rate in the continuous process. Mattos et al. [19] also found similar values when the glucose diffusivity in pectin gel was measured with and without immobilized yeast, supporting that conclusion. In that work, the authors deactivated the microorganism with formaldehyde 18.5%. However, living cells may lead to different results. The operation of the discontinuous process using repeated batch assays would allow the cell growth in the co-immobilized biocatalyst and could help to elucidate this point. Using a solution of 15% dry-milled corn starch previously liquefied by α-amylase, Krishnan et al. [10] achieved productivity of 9.1 g/l/h, with 89.3% of conversion, ethanol concentration of 36.44 g/l, without pH control, and operating at 35°C. In this work, a lower productivity, 5.9 g/l/h, but a higher ethanol concentration and conversion were reached, using similar starch concentrations in the feed, at 30°C and without pH control. They also compare the SSF process to the SHF process and found much better results for operating the hydrolysis and the fermentation steps separately. However, it is easier to operate packed beds than fluidized beds, and the SSF process demands less energy than the SHF one. Besides, the results obtained in this work with the SSF, operated in a packed bed system can still be improved. A small increase in the temperature, in the range between 30 and 35°C, may modify not only the relation between the hydrolysis/fermentation velocities but also the reaction/diffusion rates, thus improving the performance of the SSF packed bed reactor. The use of smaller bead diameters may be an option to change bed porosity, decrease diffusion effects, and consequently, improve the performance of the packed-bed reactor tested in this work. Therefore, further studies are still needed to allow a better comparison of the presented system with other possible ones.

Conclusions

A packed-bed reactor using glucoamylase immobilized in silica and co-immobilized with *S. cerevisiae* in pectin gel was stably operated during 226 h to produce ethanol from liquefied dry-milled manioc root starch.

Ethanol productivity of this SSF process reached 5.9 g/l/h, for a feeding of 163 g/l TRS concentration, with 97% of conversion and 65.4 g/l of ethanol. Our results showed that the presence of recycle in the first reactor led to a worse performance of the system. A better performance can be achieved operating the reactor with higher superficial velocities, indicating that operation of the packed bed using bead diameter smaller than 4.0 mm may lead to a better performance of the studied process.

Acknowledgments The authors acknowledge the financial support of CAPES and CNPq to this work.

References

1. Zanin, G. M., Santana, C. C., Bon, E. P. S., & Giordano, R. C. L., et al. (2000). *Applied Biochemistry and Biotechnology, 84-86*, 1147–1161.
2. Renewable Fuels Association. (2006). *http://www.ethanolrfa.org/industry/statistics/*.
3. Food Outlook. (2006). *Global Market Analysis*-n°1, June.
4. Nguyen, T. L. T., Gheewala, S. H., & Garivait, S. (2007). *Environmental Science & Technology, 41*, 4135–4142.
5. Hinman, N. D., Schell, D. J., Ryley, C. J., Bergeron, P. W., & Walter, P. J. (1992). *Applied Biochemistry and Biotechonology, 34*(5), 639–649.

6. Wang, P., Singh, V., Xue, H., Johnston, D. B., Rausch, K. D., & Tumbleson, M. E. (2007). *Cereal Chemistry, 84*(1), 10–14.
7. Yamade, K., & Fukushima, S. (1989). *Journal of Fermentation and Bioengineering, 67*, 97–101.
8. Sun, M. Y., Nghiem, N. P., Davison, B. H., Webb, O. F., & Bienkowski, P. R. (1998). *Applied Biochemistry and Biotechnology, 70/72*, 429–439.
9. Giordano, R. L. C., Gonçalves, L. R. B., Hirano, P. N., & Schmidell Netto, W. (2000). *Applied Biochemistry and Biotechnology, 84/86*, 643–654.
10. Krishnan, M. S., Nghiem, N. P., & Davison, B. H. (1999). *Applied Biochemistry and Biotechnology, 77/79*, 429–439.
11. Krishnan, M. S., Taylor, F., Davison, B. H., & Nghiem, N. P. (2000). *Bioresour. Technol., 75*, 99–105.
12. Schmidell, W., & Fernandes, M. V. (1977). *Revista de Microbiologia, 8*, 98–101.
13. Joslyn, M. A. (1970). *Methods in Food Analysis* (p. 4572nd ed.). NY: Academic Press.
14. Schmidell, W., & Menezes, J. R. G. (1986). *Revista de Microbiologia, 17*, 194–200.
15. Hannoun, B. J. M., & Stephanopoulos, G. (1986). *Biotechnology and Bioengineering, 28*, 829–835.
16. Wada, M., Kato, J., & Chibata, I. (1980). *Journal of Applied Microbioliogy and Biotechnology., 10*, 275–287.
17. Ogbonna, J. C., Amano, Y., & Nakamura, K. (1989). *Journal of Fermentation and Bioengineering, 67*(2), 92–96.
18. Gonçalves, L. R. B., Susuki, G., Giordano, R. C., & Giordano, R. L. C. (2001). *Applied Biochemistry and Biotechnology, 91-3*, 691–702.
19. Mattos, M. V. C., Giordano, R. C., & Giordano, R. L. C. (1996). *Brazilian Journal of Chemical Engineering, 13*(2), 63–70.

Appl Biochem Biotechnol (2008) 147:63–75
DOI 10.1007/s12010-007-8068-0

Lipase Production in Solid-State Fermentation Monitoring Biomass Growth of *Aspergillus niger* Using Digital Image Processing

Júlio C. V. Dutra · Selma da C. Terzi · Juliana Vaz Bevilaqua · Mônica C. T. Damaso · Sônia Couri · Marta A. P. Langone · Lilian F. Senna

Received: 9 May 2007 / Accepted: 26 September 2007 /
Published online: 27 November 2007
© Humana Press Inc. 2007

Abstract The aim of this study was to monitor the biomass growth of *Aspergillus niger* in solid-state fermentation (SSF) for lipase production using digital image processing technique. The strain *A. niger* 11T53A14 was cultivated in SSF using wheat bran as support, which was enriched with 0.91% (*m/v*) of ammonium sulfate. The addition of several vegetable oils (castor, soybean, olive, corn, and palm oils) was investigated to enhance lipase production. The maximum lipase activity was obtained using 2% (*m/m*) castor oil. In these conditions, the growth was evaluated each 24 h for 5 days by the glycosamine content analysis and digital image processing. Lipase activity was also determined. The results indicated that the digital image process technique can be used to monitor biomass growth in a SSF process and to correlate biomass growth and enzyme activity. In addition, the immobilized esterification lipase activity was determined for the butyl oleate synthesis, with and without 50% *v/v* hexane, resulting in 650 and 120 U/g, respectively. The enzyme was also used for transesterification of soybean oil and ethanol with maximum yield of 2.4%, after 30 min of reaction.

Keywords Lipase · Digital image processing · *Aspergillus niger* · Solid-state fermentation · Glycosamine · Vegetable oils · Biodiesel

J. C. V. Dutra · M. A. P. Langone · L. F. Senna
Departamento de Química Analítica, Universidade do Estado do Rio de Janeiro, Rua São Francisco Xavier 524, PHLC, IQ, sl 427, Maracanã, Rio de Janeiro, Brazil

S. da C. Terzi · S. Couri (✉)
Embrapa Agroindústria de Alimentos, Avenida das Américas 29501, Rio de Janeiro, Brazil
e-mail: scoury@ctaa.embrapa.br

J. V. Bevilaqua
CENPES, PETROBRAS, Av. Jequitiba 950 radial 5 sala 552, Rio de Janeiro, Brazil

M. C. T. Damaso
IT/DTA, Universidade Federal Rural do Rio de Janeiro, BR 465, Km 7, Seropédica, Brazil

Introduction

Lipases (triacylglycerol hydrolases, EC 3.1.1.3) are enzymes that catalyze reactions such as hydrolysis, interesterification, esterification, alcoholysis, acidolysis, and aminolysis [1]. There is an increasing interest in the development of lipase applications to oleochemical transformations to obtain esters of long-chain fatty acids, as monoalkyl esters of fatty acids [2]. Utilization of lipase as a catalyst for the production of biodiesel, defined as a mixture of monoalkyl esters, is a clean technology due to its nontoxic and environmental friendly nature, requiring mild operating conditions compared with chemical method [3].

Lipases are produced by animals, plants, and microorganisms. Microbial lipases have a great potential for commercial applications due to their stability, selectivity, and broad substrate specificity. Among the high number of lipases described in the literature, only the enzymes belonging to a few species have been demonstrated to have adequate stability and biosynthetic capabilities to allow routine use in organic reactions. The most productive species belong to the genera *Geotrichum*, *Penicillium*, *Aspergillus*, and *Rhizomucor* [4]. Nevertheless, the commercial lipases currently available are very costly and unsuitable for biodiesel production.

Fungal species are easily cultured in solid-state fermentation (SSF). This culture mode offers many advantages over commonly submerged fermentation (SF) processes, such as, the recovery of more concentrated products, smaller residues generation, reduced water consumption, and the possibility of using by-products as substrate [5]. There are several methods proposed to monitor the SSF process, such as the biomass estimation techniques, which permit to establish a relationship among growth kinetics, biomass morphology, and the fermentation product, providing important parameters to improve the operational fermentation process. However, the monitoring of filamentous fungi biomass growth in SSF is laborious and slightly accurate, mainly because of the difficulties in biomass/fermentation medium separation [6].

Some methodologies have been proposed as indirect measurements of biomass quantification, for example the production of primary metabolites [7], the variation in the electrical conductivity between biomass and the solid substrate [8] and the changes in the fermentation medium color determined by reflected light [9]. In most cases, the proposed methodology was compared to the glycosamine method, which is considered the classic method for biomass quantification. Within this method, the quitine, a monomer present on the cellular wall of fungi and yeast, is measured [10]. Nevertheless, this method can present errors due to the variation in the glycosamine content at different growth stages and to the low specificity of glycosamine quantification.

The use of software for digital image processing can be an alternative to the traditional chemical method, as it enables the correlation among the morphological biomass features and other variables of the fermentation process, mainly in submerged fermentation [11, 12]. However, a few works are found reporting the use of this methodology for biomass monitoring in solid-state fermentation [6, 13–16]. Recently, Couri et al. [6] showed that there is a correlation between the fungi growth area determined by image processing technique and the polygalacturonase activity produced by SSF.

The objective of the present work was to improve lipase production of *Aspergillus niger* under SSF conditions by supplementary carbon source addition and to verify whether the digital image processing can be used to monitor the biomass growth of *A. niger* 11T53A14. The methodology proposed in this work is similar to that presented by Couri et al. [6] and was based on the measurement of the hyphae area, which demanded that a contrast difference in the acquired image be obtained to separate the gray level image pixels in 0

(black) and 1 (white) [17]. In addition, the produced lipase was investigated as a biocatalyst in the alcoholysis of soybean oil with ethanol.

Experimental Methodology

Microorganism, Maintenance, and Propagation

A. niger 11T53A14, a mutant from the Embrapa Food Technology collection, was maintained on dry sand at −18°C, activated in basic agar slant, and propagated for a corn cob medium [18, 19].

Chemicals

The reagents employed were commercial soybean oil (Sadia, Brazil), analytical grade ethanol, butanol, oleic acid (extra pure), and hexane (Merck, Darmstadt, Germany). Methyl heptadecanoate (a chromatographic standard) was acquired from Sigma (St. Louis, USA). Sodium hydroxide and acetone were purchased from Vetec (Brazil).

Fermentation Mediums and Processes

Oil Selection

Initially, tests were performed to verify the best supplementary carbon source for lipase production, using the conditions described by Penha et al. [19]. The experiments were carried out in Erlenmeyer flasks (250 ml), and the fermentation medium consisted of 100 g of powdered wheat bran (60% moisture adjusted adding a 0.91% (*m/v*) ammonium sulfate solution, pH=7.0) and 2% *m/m* of vegetable oil (castor, soybean, olive, corn, and palm oils). The medium was mixed and sterilized at 1.0 atm for 15 min, and afterwards, inoculated with 10^7 spores/g substrate. All flasks were closed and incubated in a biochemical oxygen demand (BOD) environment, keeping the moisture and ventilation conditions constant, at 32°C for 96 h. Then, the samples were analyzed to determine the glycosamine content and the lipase activity.

Effect of Castor Oil Concentration in Lipase Production

Experiments were carried out using a SSF column reactor to enhance lipase production using castor oil as the carbon source. The experiments were carried out in glass columns (210 mm height and 22 mm diameter), filled with approximately 16.0 g of wheat bran and variable castor oil concentration (0, 2, and 4% *m/m*). The medium moisture was adjusted to 60% using the same procedures described earlier. The columns were inoculated with a suspension of 10^7 spores/g of substrate, incubated in a thermostatic bath at 32°C, and aerated with saturated air at a rate of 4 l/h. The experiment lasted 96 h and was monitored every 24 h, for determining the glycosamine content and the lipase activity.

Biomass Growth Monitoring

For the monitoring of fungi growth using image processing techniques, biomass was grown in Petri plates containing 16.0 g of wheat bran (60% moisture) enriched with 2%

m/m of castor oil. Twenty of these plates were then inoculated with 10^7 spores/g, and five plates were reserved to be used as the blank test of the fermentation process. The plates were covered, and the experiments took place at 32°C in a BOD environment, for 96 h, with moisture and ventilation conditions kept constant. All the samples had their images acquired every 24 h for image processing procedures, and simultaneously, a group of five plates was removed for determination of the glycosamine content and the lipase activity.

Glycosamine Determination

The content of glycosamine was determined by the method revised by Penman et al. [20], in which a solution composed of 5 ml of the dried fermented medium previously digested in 70% *v/v* sulfuric acid for 24 h and sterilized for 1 h at 120°C and 1 atm, was neutralized and mixed with acetyl acetone, ethanol and *p*-dimethylaminobenzaldehide. After 45 min, the reaction was completed, and the absorbance data could be measured by using a Perkin-Elmer Lambda 10 spectrophotometer, at 530 nm.

Lipase Activity Assay

Samples were drawn periodically during the fermentation, and the extracellular lipase activity was analyzed using an olive emulsion method [21]. The fatty acids released were determined by titration with 0.05 M NaOH. One lipase activity unit (U_h) was defined as the enzyme required to release 1 μmol of fatty acid per minute at 35°C, pH=7.0.

Image Acquisition and Processing

At each fermentation time, one image was acquired from all the Petri plates. The first group of images obtained at 0 h fermentation was achieved by applying simple random sampling. After this fermentation time, all image samples were acquired from the same place to permit the further subtraction of 0 h data. All the images were attained using a stereomicroscope Carl Zeiss STEMI 2000-CS, coupled to a digital camera Sony Cyber Shot DSC-S75, at the same conditions described by Couri et al. [6] that are focused and with high illumination. Afterwards, all images were processed using the software KS400®, release 2.0 (Kontron Electronic GMB). Morphological data were obtained by applying math operations, binary mask, and filters (both linear and nonlinear ones) [17]. Figure 1 presents an example of the image sequence produced by using the procedures of the image processing for a sample at 96 h of fermentation. In the developed subroutine, Fig. 1a was the original acquired image, showing the hyphae and the wheat bran substrate mixed. The hyphae boundaries were then enhanced by using a high-pass filter (Fig. 1b). Then, a fixed threshold was applied to this image to separate the gray levels in black (the substrate) and white (the hyphae area). Finally, a pruning tool was applied to remove the debris and reach the final image to be measured. All the acquired images were submitted to the same subroutine.

Statistical Analysis

The biomass growth and the lipase activity results were statistically evaluated using the software Statistica (Windows release 6.0). As the data did not present normal distribution, nonparametric statistic was used. Therefore, the Kruskal–Wallis test was performed to

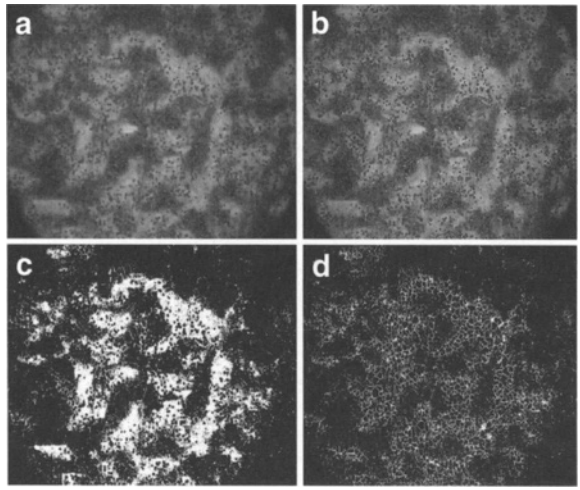


Fig. 1 Example of processing stages used to evaluate the images of biomass growth from solid-state fermentation (experimental condition: 24 h of fermentation): **a** acquired image; **b** a high-pass filter is applied; **c** a limited threshold is applied, and **d** debris are removed to reach the final image

evaluate all groups, while Mann–Whitney test was used to detect any differences between the groups. Parameters were considered statistically significant whenever the statistical analysis resulted in a p value less than 0.05. The experimental curves were fit using the software Microcal Origin® (Windows release 6.0).

Lipase Immobilization

The enzymatic extract produced was centrifuged, and the supernatant was dried by lyophilization. This dry product was solubilized in phosphate buffer (0.05 M, pH 7.0) and submitted to preferential immobilization by physical adsorption on hydrophobic support (Accurel® MP1000) according to Oliveira et al. [22].

Lipase Esterification Activity

The esterification activity of immobilized lipase was measured by the consumption of oleic acid at 45°C in the esterification reaction with butanol (equimolar ratio) with 3% *m/m* enzyme. One lipase activity unit (U_e) was defined as the amount of enzyme necessary to consume 1 μmol of oleic acid per minute under assay conditions. The enzyme activity was also evaluated in a reaction medium containing 50% *v/v* of hexane.

Lipase Catalyzed Transesterification (Biodiesel Synthesis)

The transesterification reactions between soybean oil and ethanol using 7% *m/m* of immobilized lipase at 40°C were conducted in closed 15 ml batch reactors, with constant mechanical stirring, coupled to condensers to avoid alcohol loss by volatilization. The water circulating in the condenser was cooled by a thermostatic bath. The reaction temperature was kept constant by circulating ethylene glycol from a thermostatic bath (Haake DC10) into the reactor's jacket. Reaction progress was monitored by taking duplicate samples (50 μl), which were diluted in hexane and mixed with methyl heptadecanoate as an internal standard before analysis by gas chromatography.

Chromatography Analysis

The samples were injected into a Varian gas chromatograph (CP-3380 model), equipped with a flame ionization detector (FID) and a CP WAX 52 CB capillary column 30 m×0.25 mm×0.25 μm, and a split injection system with a 1:20 ratio. Injector and detector temperatures were kept at 250°C. The oven was initially maintained at 200°C for 4.5 min, then heated up to 210°C, and kept constant at this temperature for 0.5 min. After that, it was heated to 220°C for 0.5 min. The oven was heated again to 250°C and maintained at this temperature for 1.5 min. Hydrogen was used as the carrier gas at a 1.8 ml/min flow rate; column pressure was set at 12 psi. A computer loaded with the Star Workstation 6.2 software was connected to the GC by a Star 800 Module Interface to automatically integrate the peaks obtained. Methyl heptadecanoate was the internal standard used.

Results and Discussion

Carbon Source Evaluation

Lipidic carbon sources (as vegetable oils) seem to be essential for obtaining high lipase yield in fermentation process due to their potential inducing ability [23–25]. Dalmau et al. [24] related that the mechanisms regulating biosynthesis vary widely in different microorganisms. Results obtained by these authors with *Aspergillus* showed that lipase production seems to be constitutive and independent of the addition of lipidic substrates to the culture medium, although their presence enhanced the level of lipase activity produced.

To study the ability of different supplementary carbon sources to enhance the lipase production, several kinds of vegetable oils (castor, soybean, olive, corn, and palm oils) were fed at 2% *m/m* to the fermentation process (Fig. 2). In the experimental conditions used, castor oil presented the best results, reaching lipase activity of 23.7 U/ml.

Rodriguez et al. [5] studied the effect of different triglycerides (olive, sunflower, corn, peanut walnut, and grape seed oils) on the production of lipases by culturing *Rhizopus homothallicus* in SSF. They observed that this fungal strain was able to produce similar high lipase activities with all studied oils. This is quite important as it proved that the

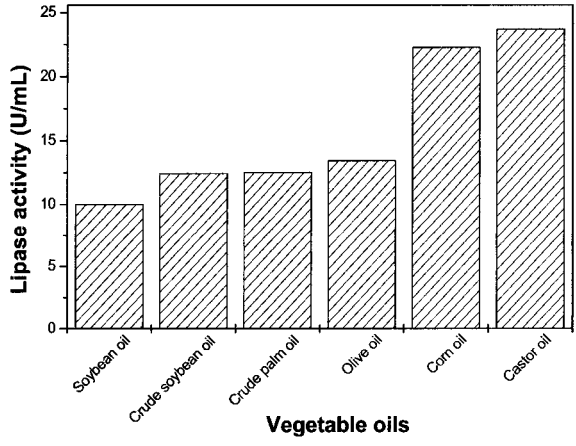


Fig. 2 Effect of feeding different vegetable oils as supplementary carbon sources (2% *m/m*) on lipase production by culturing *Aspergillus niger* 11T53A14 in SSF

cheapest and/or available oil could be used as a convenient carbon source for industrial scale lipase production.

Castor oil is largely produced in Brazil. Moreover, according to Fig. 2, the highest lipase activity was obtained with this vegetable oil. Therefore, different levels of this supplementary carbon source (0, 2, and 4% *m/m*) were added to respective batches of fermentation medium. As shown in Fig. 3, maximum lipase activity was obtained with 2% *m/m* of castor oil. This result is in agreement with that of Gombert et al. [26], who also studied the effects of different supplementary carbon sources concentration on lipase activity. They have shown that the best condition was obtained when 2% *m/m* of olive oil was added.

On the other hand, at the highest castor oil concentration studied (4% *m/m*), a significant drop in lipase activity was observed. Probably, the lipase production was repressed by the continuous release of fatty acid due to the castor oil hydrolysis in the fermentation broth. Li et al. [23] observed the inducing effect of oleic acid in lipase production and showed that when oleic acid concentration was higher than 0.4% *m/m*, it repressed lipase production.

Monitoring Biomass Growth in SSF

Design and operation of a fermentation process could be improved by using methodologies for biomass estimation, which permit to investigate the relationship among growth kinetic, biomass morphology, and the fermentation product. Biomass growth in SSF can be usually measured by indirect methods, as the variation in glycosamine content [19] or the production of a metabolite [7], in our case, the production of lipase.

The methodology proposed in this work was based on the area of the hyphae determined by image processing technique. For the sampling and image process procedures, it has been considered that the fungi grew as an isotropic interconnected system of tubules or fibers, surrounded by the fermentation medium. As the practical sections were very thick compared to the tubular diameter, the magnitude of the bias due to incorrect handling of any edge effect can be probably considered unimportant [27]. The results are shown in Fig. 4a. The proposed methodology was able to detect a significant growth trend during the SSF experiment ($p<0.003$) and a significant growth ($p<0.05$) between the samples at 24 and 48 h of fermentation. However, no significant difference could be noted among the other analyzed groups. Similar methodology used by Couri et al. [6], also detected a

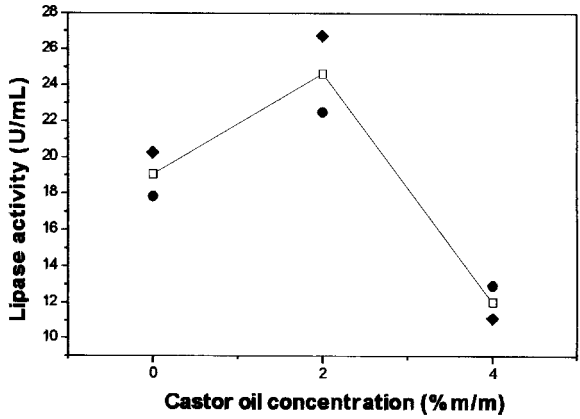


Fig. 3 Effect of castor oil concentration (% *m/m*) on lipase production by culturing *Aspergillus niger* 11T53A14 in SSF. *Filled circles*—experiment 1; *filled diamonds*—experiment 2; *empty squares*—average result

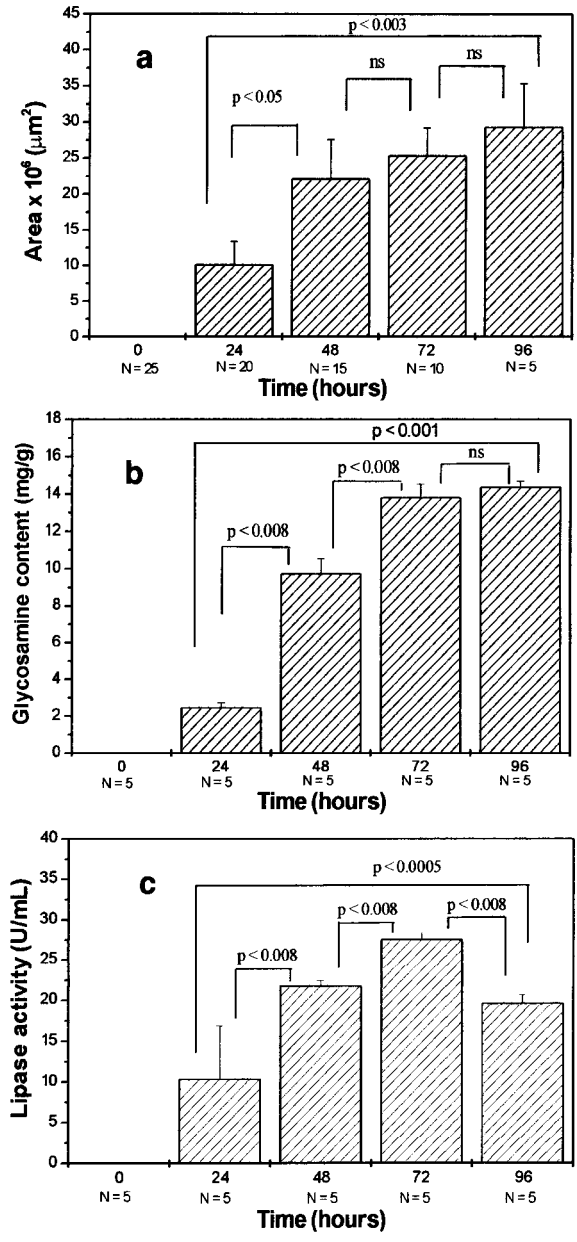


Fig. 4 Statistical results of the biomass growth and the enzyme production in solid-state fermentation: **a** Biomass growth measured by the digital image processing; **b** Biomass growth measured by the glycosamine method; **c** Lipase activity

significant growth trend ($p<0.000007$) and a significant difference ($p<0.003$) between zero and 24 h of fermentation, during the SSF production of polygalacturonase. Conversely, in the present work, there was no area measured in the initial point of fermentation. As reported by Couri et al. [6], a contrast difference is demanded in the digital processing technique, to separate the image pixels in 0 (black) and 1 (white), during the binary operation. As the wheat bran is a nonhomogeneous surface, a contrast difference between the grains in the bottom and at the surface of the Petri plate exists, causing the measurement

of some "data", even though no real hyphae is present. Therefore, an amount of area is always measured by the subroutine at 0 h fermentation, even though no growth occurred. This problem was avoided in the present work by acquiring the images from the same region of the Petri plate, so the blank value (0 h) could be discounted. Alternatively, the mathematical algorithm used for image processing was improved for 0 h fermentation, during the stage where a limited threshold is applied.

The variation of the glycosamine content within the fermentation time is shown in Fig. 4b. As it is widely known that the colorimetric methodology used to quantify the glycosamine in the fungi cell wall can also determinate other glycolized substances in the vegetal tissue, such as those present in the wheat bran [6, 19], in this analysis, the data obtained from the non-fermented medium (blank) have been previously discounted to avoid any interference in the results presented in this figure. The observed profile shows an intense growth up to 72 h, followed by a stationary stage after this fermentation time. There is a significant growing trend ($p<0.001$) in the glycosamine content during the SSF process and between the results obtained for 24 and 48 h ($p<0.008$) and 48 and 72 h ($p<0.008$) of fermentation. It suggests that at 72 h, the nutrient source was probably exhausted. Furthermore, knowing that the solid-state medium is a stress fermentation condition after the high enzyme production range, the microorganism can either keep its mass constant or overcome lyses processes.

The lipase activity varied significantly from 24 to 96 h of fermentation ($p<0.0005$), as shown in Fig. 4c. Moreover, there were also significant differences between 24 and 48 h ($p<0.008$), 48 and 72 h ($p<0.008$), and 72 and 96 h ($p<0.008$) of fermentation. It can be observed that the maximum lipase activity occurred at 72 h, followed by a decrease at 96 h of fermentation. Couri et al. [28] have shown similar effect for SSF production of polygalacturonase using *A. niger* 3T5B8. The authors related this effect to the possibility of protease production after the maximum point of enzyme activity, which could probably cause hydrolysis of the enzyme and decrease its activity.

It is interesting to note that this maximum was not observed for the results of glycosamine analysis or digital image processing (Fig. 4a and b). In the present work, images observed from 48 h on also presented spores on the surface, which were detected and also measured by the applied subroutine. The amount of these spores increased quickly from 72 to 96 h, probably by the substrate exhaustion, resulting in the area increase noted in the end of the experiment. Therefore, an enhancement of the method is needed to avoid the spore counting during the image processing.

Comparison Among the Biomass Quantification Methods

The determination of glycosamine content is the methodology usually used for comparison when a new biomass quantifying method is proposed. To verify if the digital image processing methodology could be applied for quantifying the microbial growth, its response to this parameter was then compared with the one produced by the glycosamine method. The results from both image and glycosamine experiments were plotted against each other to verify if any correlation between the methods would exist (Fig. 5). The correlation coefficient was higher than 0.97. Using a methodology similar to the one proposed in this study, Couri et al. [6] obtained a lower correlation coefficient ($R\approx0.86$) for comparison between the image processing and glycosamine results. The authors suggested that a high number of experiments was necessary to increase this correlation. In this work, the image process subroutine proposed also counted the spores' areas as hyphae, which could result in a higher difference between the analyses. However, it seems that this effect did not

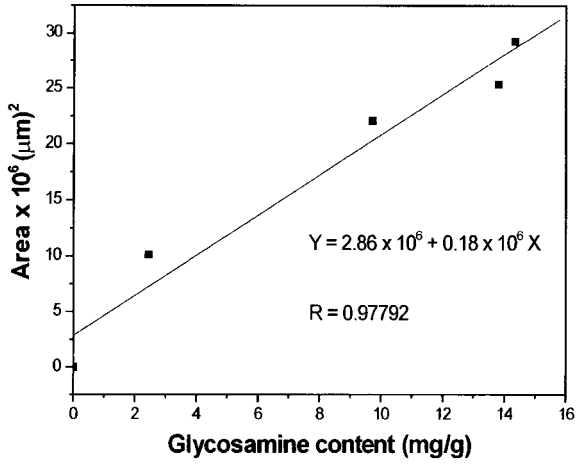


Fig. 5 Correlation between the digital processing analysis and the glycosamine methodologies

influence the correlation between the methods, as a high correlation coefficient value was obtained. The results suggest that the subtraction of the zero fermentation data may have enhanced the quality of the data.

The production of a primary metabolite, such as the lipase enzyme (whose production occurred during the same fermentation time of the biomass growth) can be related to the microbial growth [7]. Therefore, in the SSF experiments used in this work, the activity of lipase was also used as a reference to verify how efficient the applied methodologies to quantify the biomass growth during the process were. Therefore, a correlation between the enzyme activity and the results obtained for both image processing and glycosamine analysis is presented in Fig. 6. It can be observed that both curves present a correlation coefficient above 0.9, showing a direct and linear relationship between the two methodologies used to indirectly determine the biomass content and the enzyme activity.

Lipase Esterification Activity

One of the restrictions associated to the enzymatic route to biodiesel production is the cost of enzyme. So it is important to produce a lipase with lower cost and that it works out well

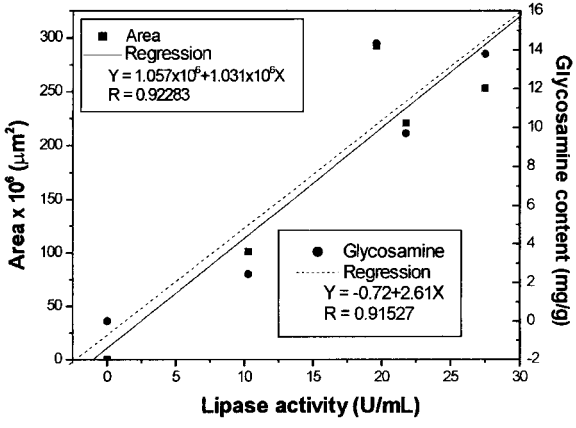


Fig. 6 Correlation between the lipase activity and the biomass contents indirectly measured by the glycosamine content and the digital image processing

for catalyzing the transesterification of vegetable oils with alcohols. The immobilized enzymes are generally known to give better catalytic performance in nonaqueous media. Therefore, in this work, the immobilization of the enzymatic extract obtained in SSF was performed. The carrier with enzyme was assayed for lipase esterification activity as described previously. The enzyme activity was determined by the initial reaction velocity in butyl oleate synthesis in a solvent-free system and in a reaction medium containing 50% *v/v* hexane, the values obtained were 120 and 650 U/g, respectively. As demonstrated by these results, the immobilized lipase produced by *A. niger* 11T53A14 presents considerable esterification activity. The commercial immobilized lipase Lipozyme RM-IM (Novozyme A/S) has an esterification activity of 2,250 U/g approximately, under the same conditions.

The time course curves of oleic acid consumption with immobilized lipase are shown in Fig. 7, and it can be seen that the fatty acid conversion was higher in the presence of hexane 50% *v/v*. At 45 min of reaction, oleic acid conversion in a solvent-free system was negligible; otherwise in a medium containing hexane 50% (*v/v*), the maximum conversion (approximately 30%) was observed.

The use of organic solvents in synthesis catalyzed by lipase has been reported. The nature of the solvent influences the activity and stability of the enzyme to a large extent. The polarity of the solvent plays a key role [29]. Log *P* has often been used to characterize solvents. Log *P* is defined as the logarithm of the partition coefficient of a substrate in the standard 1-octanol–water two-phase system. Normally, solvents with high log *P* values (log $P>4$, hydrophobic solvents) cause less inactivation of biocatalysts than more hydrophilic solvents [29]. The lipases have higher stability in a hydrophobic organic medium, such as hexane (log $P=3.5$).

According to the results shown in Fig. 7, in a solvent-free system, the enzyme drastically loses its activity after 30 min of reaction, indicating that the presence of hexane enhanced lipase stability.

Lipase Catalyzed Transesterification

As both methyl and ethyl alkyl esters are considered biodiesel, the enzymatic transesterification of soybean oil with ethanol was studied in this work. In Brazil, the production of ethyl esters is a sustainable technology, as ethanol can be easily produced from fermentable sugar (biomass).

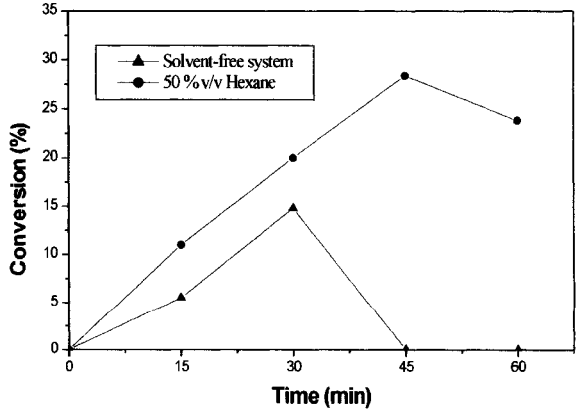


Fig. 7 Effect of hexane addition on oleic acid enzymatic conversion. Reaction conditions: oleic acid/butanol molar ratio of 1, with 3% (*m/m*) immobilized lipase from *A. niger* 11T53A14, at 45°C

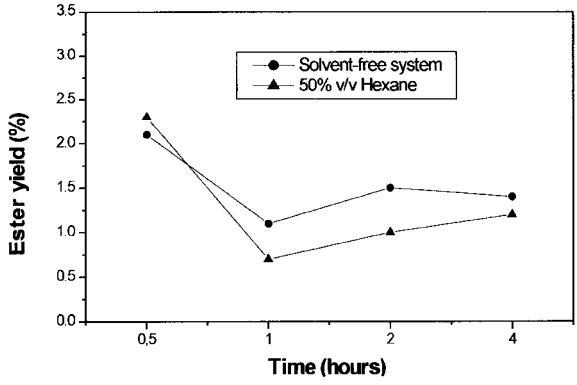


Fig. 8 Effect of hexane addition on the transesterification of soybean oil using an ethanol/soybean oil molar ration of 3 (stepwise ethanol addition: 1/3 at 0 h, 1/3 after 0.5 h, and 1/3 after 1 h), 7% *m/m* immobilized lipase from *A. niger* 11T53A14, at 40°C

The use of organic solvents is not indicated for biodiesel production due to the high risk of explosion and to the need of an additional step for solvent removal [30]. On the other hand, immobilized lipases show high conversion rates in nonpolar organic solvents. Therefore, there are several studies of triglyceride enzymatic alcoholysis in organic solvents [31]. Then, the effect of the addition of 50% *v/v* hexane was evaluated on the transesterification reaction of soybean oil with ethanol, at 40°C, with 7% *m/m* immobilized lipase and with the reactants' stoichiometric ratio (ethanol/soybean oil molar ratio of 3). The stepwise addition of ethanol (three consecutive steps) was used to avoid the lipase deactivation by a high initial alcohol concentration. However, the results (Fig. 8) show that even in these conditions, the yield of biodiesel obtained was only 2.4% after 30 min of reaction. This result is not in agreement with Bernardes et al. [32], who obtained yields of biodiesel higher than 50% using 7% *m/m* of commercial immobilized lipase (Lipozyme RM IM, Novozymes A/S) under similar reaction conditions (temperature of 50°C, with the stepwise addition of ethanol in three steps and using ethanol/soybean oil molar ratio of 3). These authors also evaluated the effect of the addition of 50% *v/v* hexane on the transesterification reaction of soybean oil with ethanol and verified that the use of hexane enhanced the biodiesel production. Therefore, the Fig. 8 results indicated that immobilized lipase produced by *A. niger* 11T53A14 is not suitable for transesterification reactions.

Conclusions

Lipase was produced by *A. niger* 11T53A14 using SSF process, using wheat bran as support. Several vegetable oils were tested as supplementary carbon sources, and the maximum lipase activity was achieved using castor oil. The best condition for producing the enzyme was evaluated in a column reactor, and it was obtained using 2% *m/m* of castor oil.

The results show that digital image process may be a promising tool to indirectly estimate of the biomass produced in SSF, by measuring the hyphae area in the acquired image. The correlation between the proposed methodology and the glycosamine determination was high and can be considered satisfactory, concerning the measurement of biological data. Moreover, the correlation between the proposed image processing methodology and the lipase activity was higher than 0.9, which agrees that the measured parameter (hyphae areas) might be applied to monitor the fungi growth at solid-state medium.

Acknowledgments The authors thank Petrobras for the financial support and D.Sc. Denise Maria Guimarães Freire for the lipase immobilization procedures. Lilian Ferreira de Senna and Marta Antunes Pereira Langone thank Prociência Program/UERJ.

References

1. Paiva, A. L., Balcão, V. M., & Malcata, F. X. (2000). *Enzyme and Microbial Technology, 27*, 187–204.
2. Guamgui, H., Karra-Chaâbouni, M., & Gargouri, Y. (2004). *Enzyme and Microbial Technology, 35*, 355–363.
3. Wang, H. X., Wu, H., Ho, C. T., & Weng, X. C. (2006). *Food Chemistry, 97*, 661-665.
4. Candenas, F., Castro, M. S., Sanchez-Montero, J. M., Sinisterra, J. V., Valmaseda, M., Elson, S. W., et al. (2001). *Enzyme and Microbial Technology, 28*, 145–154.
5. Rodriguez, J. A., Mateos, J. C., Nungaray, J., González, V., Bhagnagar, T., Roussos, S., et al. (2006). *Process Biochemistry, 41*, 2264–2269.
6. Couri, S., Merces, E. P., Neves, B. C. V., & Senna, L. F. (2006). *Journal de Microscopie, 224*, 290–297.
7. Okazaki, N., Sugama, S., & Tanaka, T. (1980). *Journal of Fermentation Technology, 58*, 471–476.
8. Peñaloza, W., Davey, C. L., Kell, D. B., & Hedger, J. N. (1991). *W orld Journal of Microbiology & Biotechnology, 7*, 248–259.
9. Murthy, M. V. R., Thakur, M. S., & Karanth, N. G. (1993). *Bioscience Bioelectrochemistry, 8*, 59–63.
10. Majeti, N., & Kumar, R. (2005). *Reactive & Functional Polymers, 46*, 1–27.
11. Cox, P. W., & Thomas, C. R. (1992). *Biotechnic Bioengeneering, 39*, 945–952.
12. Couri, S., Pinto, G. A. S., Senna, L. F., & Martelli, H. L. (2003). *Brazilian Journal of Microbiology, 33*, 1–6.
13. Nopharatana, M., Howes, T., & Mitchel, D. (1998). *Biotechnology Technique, 12*, 313–318.
14. Loera, O., & Viniegra-González, G. (1998). *Biotechnology Techology, 12*, 801–804.
15. Daniel, O., Schonholzer, F., & Zeyer, J. (1995). *Environmental Microbiology, 61*, 3910–3918.
16. Miri, T., Cox, P. W., & Fryer, P. J. (2003). *Biotechnology Letters, 25*, 295–300.
17. Gonzalez, R. C., & Woods, R. E. (1993). *Digital image processing*. New York: Addison-Wesley Publishing.
18. Couri, S., & Farias, A. X. (1995). *Brazilian Journal of Microbiology, 26*, 314–317.
19. Penha, E. M., Couri, S., Senna, L. F., Terzi, S. C., Neves, B. C. de V., & Alonso, S. P. (2006). *Brazilian Archives of Biology and Technology, 49*, 101–105.
20. Penman, D., Britton, G., Hardwick, K., Collin, H. A., & Isaac, S. (2000). *Mycological Research, 104*, 671–675.
21. Pereira, E. B., Castro, H. F., Moraes, F. F., & Zanin, G. M. (2001). *Applied Biochemistry and Biotechnology, 91–93*, 739–752.
22. Oliveira, D., Feihrmann, A. C., Dariva, C., Cunha, A. G., Bevilaqua, J. V., Destain, J., et al. (2006). *Journal of Molecular Catalysis. B, Enzymatic, 39*, 117–123.
23. Li, D., Wang, B., & Tan, T. (2006). *Journal of Molecular Catalysis. B, Enzymatic, 43*, 40–43.
24. Dalmau, E., Montesinos, J. L., Lotti, M., & Casas, C. (2000). *Enzyme and Microbial Technology, 26*, 657–663.
25. Couto, S. R., & Sanromán, M. A. (2006). *Journal of Food Engineering, 76*, 291–302.
26. Gombert, A. K., Pinto, A. L., Castilho, L. R., & Freire, D. M. G. (1999). *Process Biochemistry, 35*, 85–90.
27. Gundersen, H. J. G. (2002). *Journal de Microscopie, 207*, 155–160.
28. Couri, S., Terzi, S. C., Pinto, G. A. S., Freitas, S. P., & Costa, A. C. A. (2000). *Process Biochemistry, 36*, 255–261.
29. Carta, G., Gainer, J. L., & Gibson, M. (1992). *Enzyme and Microbial Technology, 14*, 904–910.
30. Shimada, Y., Watanabe, Y., Sugihara, A., & Toninaga, Y. (2002). *Journal of Molecular Catalysis B Enzymatic, 17*, 133–142.
31. Soumanou, M. M., & Bornscheuer, U. T. (2003). *Enzyme and Microbial Technology, 33*, 97–103.
32. Bernardes, O. L., Bevilaqua, J. V., Leal, M. C. M. R., Freire, D. M. G., & Langone, M. A. P. (2007). *Applied Biochemistry and Biotechnology, 136–140*, 105–114.

Appl Biochem Biotechnol (2008) 147:77–84
DOI 10.1007/s12010-007-8094-y

The Effects of Surfactants on the Estimation of Bacterial Density in Petroleum Samples

Aderval Severino Luna · Antonio Carlos Augusto da Costa · Márcia Monteiro Machado Gonçalves · Kelly Yaeko Miyashiro de Almeida

Received: 9 May 2007 / Accepted: 7 November 2007 /
Published online: 4 December 2007
© Humana Press Inc. 2007

Abstract The effect of the surfactants polyoxyethylene monostearate (Tween 60), polyoxyethylene monooleate (Tween 80), cetyl trimethyl ammonium bromide (CTAB), and sodium dodecyl sulfate (SDS) on the estimation of bacterial density (sulfate-reducing bacteria [SRB] and general anaerobic bacteria [GAnB]) was examined in petroleum samples. Three different compositions of oil and water were selected to be representative of the real samples. The first one contained a high content of oil, the second one contained a medium content of oil, and the last one contained a low content of oil. The most probable number (MPN) was used to estimate the bacterial density. The results showed that the addition of surfactants did not improve the SRB quantification for the high or medium oil content in the petroleum samples. On other hand, Tween 60 and Tween 80 promoted a significant increase on the GAnB quantification at 0.01% or 0.03% *m/v* concentrations, respectively. CTAB increased SRB and GAnB estimation for the sample with a low oil content at 0.00005% and 0.0001% *m/v*, respectively.

Keywords Sulphate-reducing bacteria (SRB) · General anaerobic bacteria (GAnB) · Petroleum · Surfactants · Most probable number (MPN)

Introduction

Sulfate-reducing bacteria (SRB) are some of the most common and problematic microorganisms of environmental and economic importance in petroleum industry. The effects caused by SRB activity are mainly the souring of oil and gas deposits and in problems related with microbially influenced corrosion (MIC). The toxic hydrogen sulfide produced may also present a health hazard to workers and may decrease oil quality by the souring of oil and gas [1].

A. S. Luna (✉) · A. C. A. da Costa · M. M. M. Gonçalves · K. Y. M. de Almeida
Programa de Pós-graduação em Engenharia Química, Instituto de Química,
Universidade do Estado do Rio de Janeiro, Rua São Francisco Xavier, 524-PHLC-sala 427,
Rio de Janeiro 20559-900, Brazil
e-mail: asluna@uerj.br

It is extremely difficult to estimate the costs related with corrosive processes attributed to the activity of microorganisms (SRB and other bacteria) in the oil industry. In recent years, the costs involving the control of the activity of SRB were significant with annual values estimated at approximately $150,000 per platform when only biocides are used to control microbial activity [2].

Considerable efforts have been made through the development of methods to SRB enumeration. In general, the most common methods to enumerate SRB fall into two categories: direct detection methods and culture methods. Although the direct detection methods are promising, they are still in the development phase and may have limitations when used in situ [3]. Recently, molecular techniques and the use of radiotracers are being investigated for the detection and enumeration of SRB and other anaerobic cells. However, although highly specific and reliable, they are not feasible for a routine control of microbial numbers at field conditions. Furthermore, these new techniques have high costs. Culture methods based on the most probable number (MPN) technique have been extensively used for several decades and remain the standard method for enumerating SRB.

In samples with hydrophobic compounds, enumeration of SRB and general anaerobic bacteria (GAnB) may be compromised because of the low solubilization of these compounds in the culture medium. The study of the influence of surfactants in the SRB and GAnB estimation in oil samples may become an alternative to improve the MPN method under these conditions. Surfactants are organic compounds that present both a hydrophobic part and a hydrophilic part in the same molecule. This hydrophilic part allows surfactants to be soluble in water, whereas the hydrophobic part causes them to concentrate at interfaces [4].

Based on the previous considerations, the aim of this work was to verify the effect of the addition of different types of surfactants: nonionic (Tween 60 and Tween 80), cationic (CTAB), and anionic (SDS), on SRB and GAnB enumeration in oil samples using the MPN technique.

Materials and Methods

The populations of SRB and GAnB considered in the tests were the indigenous population present in three different oil samples used:

Sample A—oil contaminated with water (kinematic viscosity=41.57 mm^2/s and 14.3% water);
Sample B—oil and water (kinematic viscosity=6.56 mm^2/s and 50.4% water);
Sample C—water contaminated with oil (kinematic viscosity=2.3 mm^2/s and 95.5% water).

These samples were obtained from oil storage tanks from Terminal São Sebastião, São Paulo, Brazil.

Microbial Enumeration

A 10-fold dilution series was used, from 10^0 to 10^8, for each group of microorganisms (SRB and GAnB). Firstly, 1 ml of the sample was injected into a vial containing 9 ml of anaerobic liquid medium and a vial containing 9 ml of a reducing solution. The vials were

then shaken, and a sterile syringe was used to draw out 1 ml of the reducing solution and inject this solution into a new medium vial and also into a new reducing solution vial. This procedure was repeated until the 10^8 dilution was reached. Inoculated flasks (n=3) were incubated at 30±1 °C for 28 days. The growth of SRB was indicated by the formation of a black FeS precipitate. The positive growth for GAnB was confirmed through the observation of turbidity in the culture medium. In the present work, the estimation of MPN cells was performed according to the method of Harrigan and McCance [5], which does not consider a normal distribution of results, but a binomial distribution.

Culture Media

The semisolid Postgate's E medium was used for SRB estimation. This medium had the following composition (per liter): sodium lactate, 7.0 ml; yeast extract, 1.0 g; NH_4Cl, 1.0 g; KH_2PO_4, 0.5 g; $MgCl_2{\cdot}6H_2O$, 1.83 g; $CaCl_2{\cdot}6H_2O$, 1.0 g; $FeSO_4{\cdot}7H_20$, 0.5 g; ascorbic acid, 0.1 g; agar–agar, 9 g; resazurin, 4 ml (0.025% *m/v*); NaCl, 35 g. The medium was prepared anaerobically and the pH was adjusted to 7.6 with NaOH 1 M. After that, 9 ml of this medium was dispensed in each flask and was autoclaved at 121 °C for 20 min. According to Postgate [1], the SRB require an environmental redox potential (Eh) of approximately −100 mV. To achieve this redox potential, sodium thioglycolate (12.4 g/l) was used as a reducing agent. This solution was added to the medium in aliquots of 0.1 ml before inoculation and after sterilization.

For GAnB enumeration, a medium was prepared under anaerobic conditions with the following composition (per liter): glucose, 5.0 g; peptone, 4.0 g; yeast extract, 1.0 g; resazurin 4 ml (0.025% *m/v*), at pH 7.6. After preparation, the medium was distributed into 9 ml flasks and sterilized in an autoclave at 121 °C for 20 min. Then, sodium thioglycolate (12.4 g/l) was added, as previously described.

The reducing solution contained (per liter): sodium thioglycolate, 0.124 g; ascorbic acid 0.1 g; and resazurin, 4 ml (0.025% *m/v*), at pH 7.6. After that, 9 ml of solution was dispensed in each flask and autoclaved at 121 °C for 20 min.

Surfactants and Tests

The main characteristics of Tween 60, Tween 80, CTAB, and SDS are presented in Table 1.

Ionic surfactants are more toxic for bacteria than nonionics [4]. Because of this fact, CTAB concentrations selected for the tests were lower than its critical micelle concentration (CMC) of 0.036% *m/v*. Corresponding solutions of each concentration were prepared and sterilized by vacuum filtration using a Millipore membrane of 0.45 μm pore diameter.

Table 1 Surfactants and their main characteristics.

Surfactant	Type	Molar mass (g/mol)	CMC (%)	HLB
Tween 60	Nonionic	1,311	0.003	14.9
Tween 80	Nonionic	1,309	0.001	15
CTAB	Cationic	364.5	0.036	–
SDS	Anionic	288.4	0.036	40

CMC: critical micellar concentration, *HLB*: hydrophilic–lipophilic balance

Results and Discussion

Effect of the Surfactants on the Estimation Bacterial Density of SRB

Figure 1 shows the quantification of SRB for samples A, B, and C in the presence of different concentrations of the surfactants: Tween 60 (a), Tween 80 (b), CTAB (c), and SDS (d).

The evaluation of the effect of the surfactant Tween 60 in sample A (Fig. 1a) showed that its addition did not contribute to the increase in SRB quantification in the sample with a larger oil content. The results were lower than the control test. Effects of the surfactants on microbial physiology vary from inhibitory, according to its toxicity, to growth stimulatory when the surfactant is used as substratum [4]. The complexity of these effects is well reported in literature with great variations in the results obtained [6–8].

In sample B, for all concentrations of the surfactant Tween 60, the results obtained were higher than the control test. However, when numbers were compared with those of the same magnitude, it would not be possible to consider a significant difference. In this case, the largest value for SRB (2.5×10^2 cells/ml) was obtained when the concentration of Tween 60 was 0.01% *m/v* (above of the CMC).

When the concentration of the surfactant is higher than its CMC, the surfactant can solubilize hydrophobic compounds because of the presence of micelles in the solution. According to some authors [4, 6, 8] the process of micellization leads to an increase in solubilization and, consequently, a higher degradation of these substances by microorganisms. However, when values much higher than the CMC are employed, a reduction is

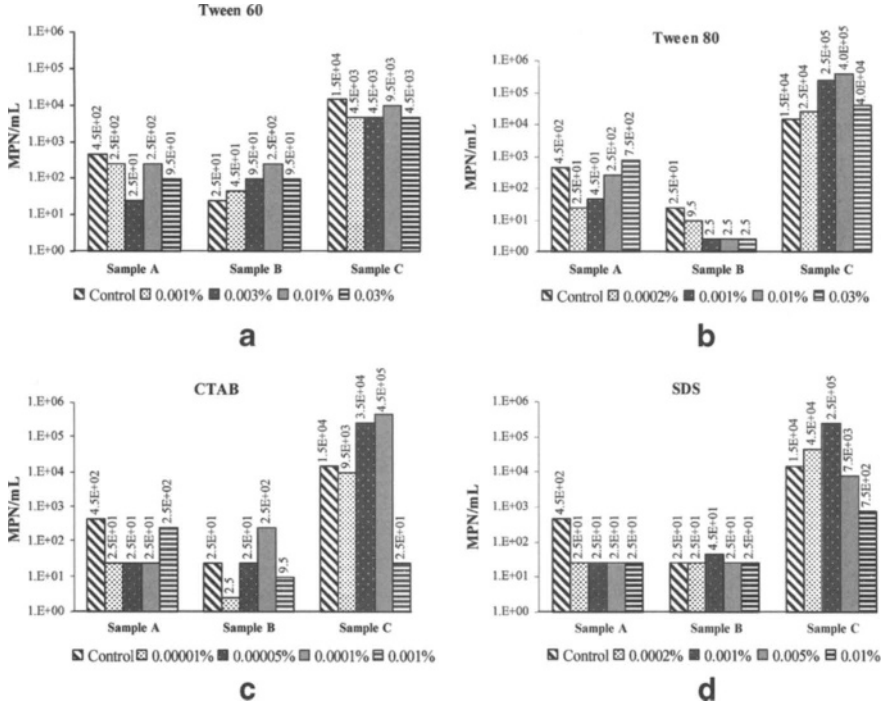


Fig. 1 Estimation of bacterial density of SRB, expressed by MPN (cells per milliliter), in the presence of different concentrations of the surfactants Tween 60 (**a**), Tween 80 (**b**), CTAB (**c**), and SDS (**d**)

observed in the degradation rate because of the inhibitory effect of the surfactant [9]. For sample C (Fig. 1a), all of the tested concentrations of Tween 60 showed results lower than the control test.

Figure 1b showed that the addition of surfactant Tween 80 was not favorable in the quantification of SRB in sample A. The analysis involved the comparison of estimated bacterial density, making it impossible to conclude about significant differences in the results as they presented that they are from the same magnitude. However, in the concentration of 0.03% *m/v*, the resulting quantification of 7.5×10^2 cells/ml was superior to the control test which showed a value of 4.5×10^2 cells/ml.

For sample B, it is also possible to observe that the addition of Tween 80 was not favorable to an increase in SRB quantification. The addition of surfactants in liquid systems will have two contradictory effects: solubilization of the hydrophobic compounds and stimulation of the biodegradation by microorganisms or inhibition of the cells bacterial adhesion in the interface, consequently reducing the biodegradation rate [4]. This last effect could have occurred in sample B composed of water and oil.

The results obtained for sample C (Fig. 1b) showed that the effect of surfactant Tween 80 was favorable for SRB quantification when used in concentrations of 0.001% and 0.01% *m/v*, reaching values of 2.5×10^5 and 4.0×10^5 cells/ml, respectively. According to the literature, biodegradation of polyaromatics hydrocarbons (PAHs) increased with the use of the synthetic surfactants, such as Triton-X, Brij 30, and Tween 80 [10]. The authors observed that when the concentration of the surfactants was below or near CMC, they did not see an improvement in solubilization. However, when concentrations above the CMC were tested, solubility increased.

Figure 1c shows that the addition of surfactant CTAB did not favor SRB quantification in sample A (oil contaminated with water). For sample B, when CTAB was used in a concentration of 0.0001% *m/v* (250 cells/ml), a 10-fold increase in comparison with the control test (25 cell/ml) was observed. In sample C, the addition of CTAB favored the quantification of SRB when used at 0.0001% *m/v*, resulting in a value of 4.5×10^5 cells/ml.

The inhibitory effects of CTAB are reported in the literature with a high diversity of results depending on the concentration. CTAB presented inhibitory effects in concentrations above 0.01% *m/v* in a study with *Pseudomonas putida* and *P. fluorescens* [11, 12]. On the other hand, Fengjiao et al. [13] showed that the inhibitory effect on the growth of *P. putida* was pronounced in concentrations above 0.001% *m/v*. In this work, the concentration of 0.001% demonstrated an inhibitory effect in samples B and C.

According to Fig. 1d, for sample A, all the tested concentrations presented values lower than the control test (450 cells/ml), showing that the addition of SDS did not promote an increase in SRB quantification, although solubilization of the oil in the sample was observed visually.

In sample B, the addition of SDS did not favor SRB quantification in any of the concentrations tested. On the other hand, the SDS concentration of 0.001% *m/v* used in sample C represented the largest increase in the SRB quantification, 2.5×10^5 cells/ml in comparison to the control test (1.5×10^4 cells/ml).

According to Lee et al. [14], anionic surfactants, like SDS, present characteristic detergents and low antimicrobial activity, except when used at high concentrations, which can induce the lysis of Gram-negative bacteria. This was also observed by Simões [12] in the study carried out with *P. fluorescens*. There is also the possibility that the stimulus of the bacterial growth could be associated with surfactant consumption. Suchanek et al. [15] observed that biodegradation of *n*-decane by a *Pseudomonas* strain was stimulated in the presence of SDS. The generation of an intermediate compound during surfactant

consumption seems to have enabled bacterial adhesion to the hydrocarbon, thus facilitating its biodegradation.

Effect of the Surfactants on the Estimated Bacterial Density of GAnB

Figure 2 shows the quantification results of GAnB for samples A, B, and C in the presence of surfactants Tween 60 (a), Tween 80 (b), CTAB (c), and SDS (d) with different concentrations.

Figure 2a showed that it is possible to observe that for all the samples evaluated (samples A, B, and C), Tween 60 presented the most favorable effect on the growth of GAnB at concentrations of 0.01% and 0.03%, above its CMC. Sample C presented the highest results in comparison to the control with values of 2.5×10^6 cells/ml. For sample B, the use of Tween 60 in its CMC also presented results higher than those observed in the absence of surfactant (9.5×10^2 cells/ml). For sample C, a marked increase in GAnB enumeration was achieved, at a concentration of 0.01 and 0.03% *m/v*, using Tween 60.

Figure 2b shows that the addition of surfactant Tween 80 in sample A promoted an increase in the enumeration when used at 0.01% and 0.03% *m/v*, both above the CMC (0.001% *m/v*) of the surfactant. The addition of Tween 80 in sample B did not cause favorable effects on the growth of GAnB in any of the tested concentrations; results were lower than the control test (9.5×10^2 cells/ml).

For sample C, it was observed that the addition of Tween 80 at the CMC (0.001% *m/v*) and in concentrations above CMC (0.01% and 0.03% *m/v*) showed superior results in comparison to those obtained in the absence of surfactants. GAnB quantifications were 3×

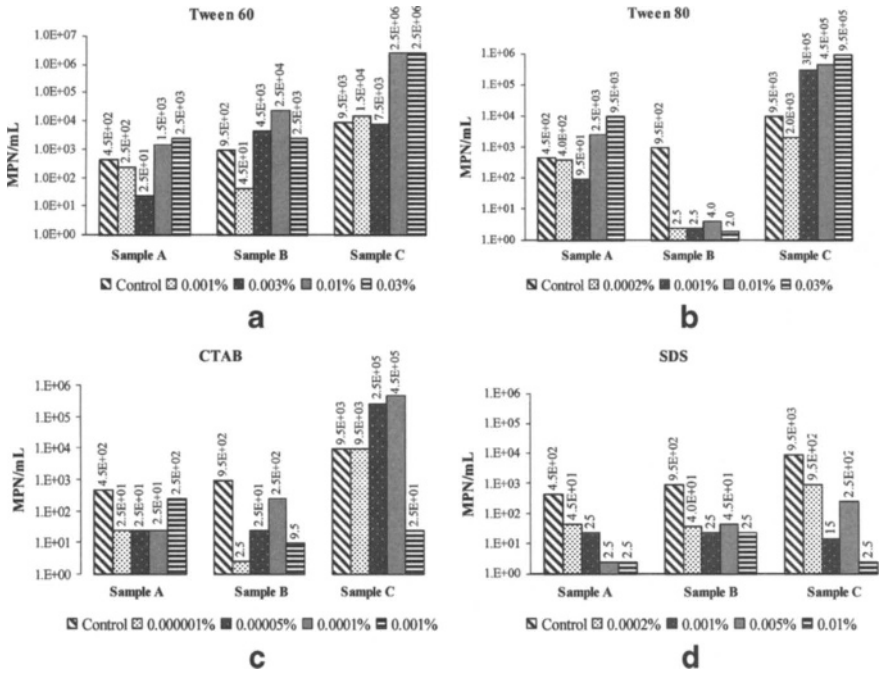


Fig. 2 Estimation of bacterial density of GAnB, expressed by MPN (cells per milliliter), in the presence of different concentrations of the surfactants Tween 60 (**a**), Tween 80 (**b**), CTAB (**c**), and SDS (**d**)

10^5, 4.5×10^5, and 9.5×10^5 cells/ml, respectively, indicating a favorable effect on GAnB quantification for samples with a low content of oil.

Figure 2c shows that in all tested concentrations, the addition of CTAB did not favor GAnB quantification in samples A and B. For sample C (water plus oil), a concentration of 0.0001% *m/v* of CTAB showed a higher value (4.5×10^5 cells/ml) in comparison to the control (9.5×10^3 cells/ml).

Figure 2d shows that the addition of the surfactant SDS did not cause a significant increase in GAnB quantification in any of the samples, at concentrations smaller than 0.01%. Although Margesin and Schinner [16] concluded that in concentrations smaller than 0.01% a significant increase in diesel oil biodegradation occurred, it is important to emphasize that, in the present work, crude oil was used.

Conclusions

- None of surfactants tested contributed to the quantification of SRB in the sample with the higher oil content (sample A). However, for the GAnB group, surfactants Tween 60 and Tween 80 caused favorable effects in the quantification.
- It was observed for sample B that the addition of Tween 60 and CTAB caused an increase in SRB quantification (10 times higher than the control—25 cells/ml) when used in concentrations of 0.01% and 0.0001% *m/v*, respectively. For GAnB, only Tween 60 contributed to a higher quantification when used at 0.01% *m/v* (2.5×10^4 cells/ml) compared to the control (9.5×10^2 cells/ml).
- Only Tween 60 did not show a positive effect for SRB quantification in sample C (water contaminated with oil). On the other hand, GAnB quantification was increased with the addition of all surfactants tested, except with the addition of SDS, leading to the highest concentration of cells (2.5×10^6 cells/ml).
- The importance of these findings to the petroleum industry relies on the underestimation about the use of biocides in continental platforms, oil storage tanks, and pipelines. Those environments are constantly subjected to anaerobic microbial activity, which are usually controlled through the addition of biocides in the absence of surfactants.

Acknowledgements The authors would like to thank the Brazilian Petrobras (BTA Division) for providing the samples and procedures to develop this work. This work is part of the M.Sc. Thesis of K.Y.M.A.

References

1. Postgate, J. R. (1984). *The sulfate reducing bacteria* (2nd ed.). Cambridge: Cambridge University Press.
2. Maxwell, S., Mutch, K., Hellings, G., Badalek, P., Charlon, P. (2002). *Corrosion 2002* Paper 02031.
3. Flemming, V., & Ingvorsen, K. (1998). *Applied and Environmental Microbiology, 64*, 1700–1707.
4. Volkering, F., Breure, A. M., & Rulkens, W. H. (1998). *Biodegradation, 8*, 401–417.
5. Harrigan, W. F., & McCance, M. E. (1976). *Laboratory methods in food and dairy microbiology.* London: Academic.
6. Tiehm, A. (1994). *Applied and Environmental Microbiology, 60*, 258–263.
7. Volkering, F., Breure, A. M., Andel, J. G., & Rulkens, W. H. (1995). *Applied and Environmental Microbiology, 61*(5), 1699–1705.
8. Guha, S., & Jaffe, P. R. (1996). *Environmental Science & Technology, 30*, 605–611.
9. Willumsen, P. A., Karlson, U., & Pritchard, P. H. (1998). *Applied Microbiology and Biotechnology, 50*, 475–483.
10. Kim, E. S., Lee, D. H., & Chang, H. W. (1998). *Geoscience Journal, 9*, 261–267.

11. Rodrigues, A. C., Brito, A. G., & Melo, L. F. (2001). *CEB-Paper, 190*, 4.
12. Simões, M. J. V. (2005). Ph.D. Thesis, Chemical and Biological Engineering, Minho University, Portugal.
13. Fengjiao, H., Xiaoqing, Z., & Zhenhua, L. (2006). *Sensors and Actuators B, 113*, 428.13–434.13.
14. Lee, C., Russel, N. J., & White, G. F. (1995). *Water Research, 29*(11), 2491–2497.
15. Suchanek, M., Kostal, J., Demnerova, K., & Kralova, B. (2000). *International Biodeterioration & Biodegradation, 45*, 27–33.
16. Margesin, R., & Schinner, F. (1998). *Chemosphere, 38*, 3463–3472.

Appl Biochem Biotechnol (2008) 147:85–96
DOI 10.1007/s12010-007-8066-2

An Alternative Application to the Portuguese Agro-Industrial Residue: Wheat Straw

Denise S. Ruzene · Daniel P. Silva · António A. Vicente · Adilson R. Gonçalves · José A. Teixeira

Received: 9 May 2007 / Accepted: 26 September 2007 /
Published online: 17 October 2007
© Humana Press Inc. 2007

Abstract The effects of alkaline treatments of the wheat straw with sodium hydroxide were investigated. The optimal condition for extraction of hemicelluloses was found to be with 0.50 mol/l sodium hydroxide at 55 °C for 2 h. This resulted in the release of 17.3% of hemicellulose (% dry starting material), corresponding to the dissolution of 49.3% of the original hemicellulose. The yields were determined by gravimetric analysis and expressed as a proportion of the starting material. Chemical composition and physico-chemical properties of the samples of hemicelluloses were elucidated by a combination of sugar analyses, Fourier transform infrared (FTIR), and thermal analysis. The results showed that the treatments were very effective on the extraction of hemicelluloses from wheat straw and that the extraction intensity (expressed in terms of alkali concentration) had a great influence on the yield and chemical features of the hemicelluloses. The FTIR analysis revealed typical signal pattern for the hemicellulosic fraction in the 1,200–1,000 cm^{-1} region. Bands between 1,166 and 1,000 cm^{-1} are typical of xylans.

Keywords Agro-industrial residue · Lignocellulosic materials · Wheat straw · Extraction · Hemicellulose · Papermaking

Introduction

Agro-industrial residues are renewable, costless, and widespread sources of chemicals. In recent years, there has been an increasing trend towards more efficient utilization of agro-industrial residues such as sugarcane bagasse, cereal straws, corn cob, brewer's spent grain, etc. Advances in industrial biotechnology offer actually potential opportunities for economic utilization of

D. S. Ruzene (✉) · D. P. Silva · A. A. Vicente · J. A. Teixeira
Institute for Biotechnology and Bioengineering, Centre of Biological Engineering, University of Minho, Campus de Gualtar, 4710-057 Braga, Portugal
e-mail: druzene@deb.uminho.pt

A. R. Gonçalves
Biotechnology Department, Engineering School of Lorena, University of São Paulo, P.O. Box 116, 12602-810 Lorena, São Paulo, Brazil

agro-industrial residues. Even if in most cases some of these materials are already used, e.g. burned (an application with low added value causing some environmental impact), the lignocellulosic nature and abundant availability make them an ideal substrate for chemical and/or microbial processes to obtain end products with high added value [1].

The agro-industrial residues are lignocellulosic materials constituted basically of cellulose, hemicelluloses, and lignin. Since society and the industries as a whole have a great interest in the integral use of agro-industrial residues, separation and extraction processes of the structural fractions of lignocellulosic materials are indispensable biotechnological processes for future and successful industrial applications. Currently overproduced and underutilized, the use of these materials is required to accomplish two main objectives: (a) reducing the existence of environmentally hazardous situations and (b) increasing the supply of energy or chemicals produced from renewable resources. Moreover, it is already well known that the cost of this raw material per unit of product can be reduced when all the components of the biomass are converted to added-value products [2, 3].

In many countries, the wheat straw is an abundant by-product from wheat production. Thus, wheat straw has potential to serve as a low-cost raw material for production of higher-value industrial products. Wheat straw is an agricultural by-product that is not used as industrial raw material at a significant scale in developed regions like Europe and North America. As a rough estimation, more than 170 million tons of wheat straw are produced yearly in Europe [4]. These amounts are enough to consider wheat straw as a source of renewable materials, particularly for the production of chemical derivatives from cellulose, hemicelluloses, and lignin.

Chemically, about 35–55% of the dry material is the glucose polymer cellulose, much of which is in a crystalline structure; while another 25–35% is hemicellulose, an amorphous polymer. The remainder is mostly lignin plus less amounts of minerals, waxes, and other compounds [3]. Cellulose is formed by beta-[1, 4] glucosyl linkages in a linear backbone, whereas hemicelluloses are branched polymers composed of several monosaccharides [5]. Fig. 1 shows the schematic illustration of the cellulose chain, while Fig. 2 shows the schematic illustration of xylans from Gramineae [5, 6].

Research has been done on the separation and structural characterization of the components. Alkali treatment of lignocellulosic substances such as wheat straw disrupts the cell wall by dissolving hemicellulose, lignin, and silica, by hydrolyzing uranic and acetic acid esters, and by swelling cellulose, decreasing its crystallinity. This increases the biodegradability of the cell walls due to cleavage of the bonds between lignin and hemicellulose or lignin and cellulose, allowing their preseparation [7, 8]. On the other hand, in the paper industry, it has been demonstrated that the addition of hemicelluloses as additive in the cellulosic pulp can improve some mechanical properties of the paper, among other features of papermaking [9, 10].

This work details our research on the integral use of agro-industrial residues, aiming at an economic and environmental-friendly process, together with recommendations for

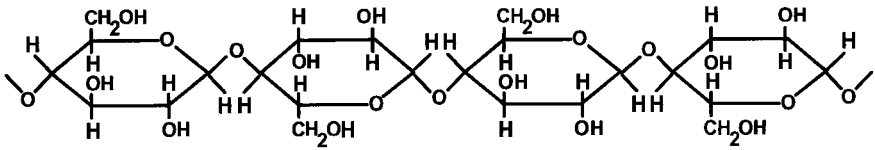


Fig. 1 Schematic illustration of the cellulose chain [5]

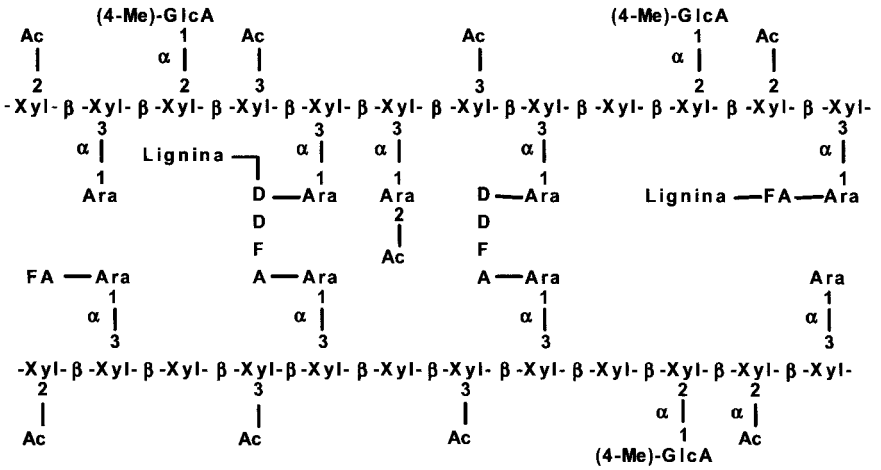


Fig. 2 Schematic illustration of xylans from Gramineae; *Xyl* 1,4-D-xylopiranose; *Ara* L-arabinofuranose; *Ac* acetyl; *(4-Me)-GlcA* (4-*O*-methyl)-D-glucopyranuronic acid; *FA* ferulic acid; *DDFA* dehydroferulic [6]

hemicellulose extraction processes from wheat straw, in order to make possible the use of this hemicellulose as additive in the papermaking industry, always keeping in mind the use of the other lignocellulosic fractions (cellulose and lignin) in other applications. Properties of wheat straw hemicelluloses worth exploiting are their ability to serve as

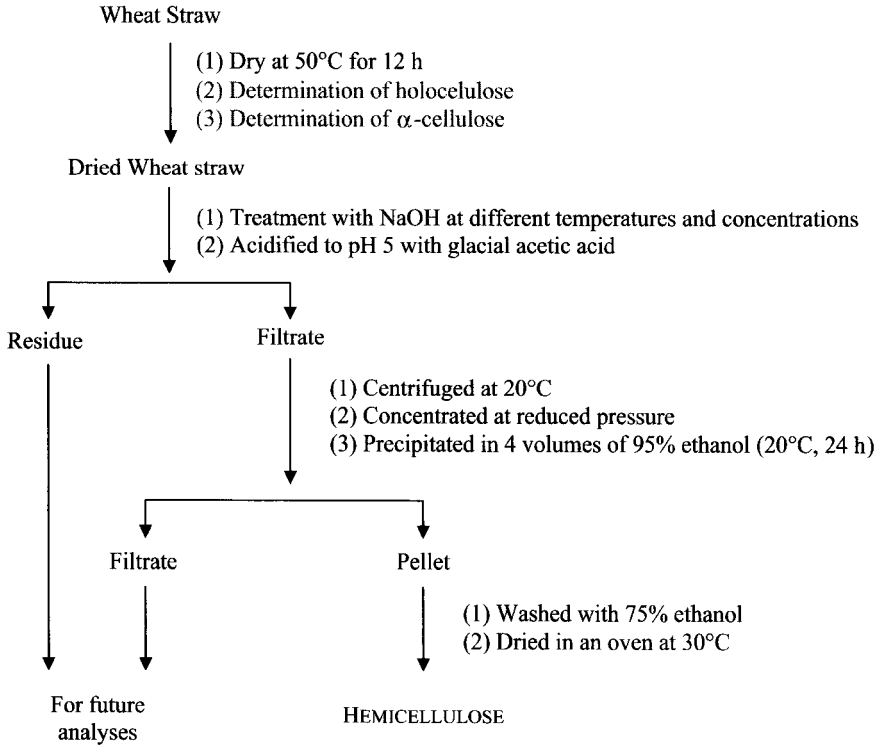


Fig. 3 Scheme for extraction of hemicelluloses from ground wheat straw

adhesives, thickeners, and stabilisers, and as film formers and emulsifiers [11]. Thus, future applications of agro-industrial residues in bioprocesses provide alternative substrates, economic and environmental-friendly process, and help in solving environmental problems which their disposal could cause.

Materials and Methods

Materials

Wheat straw was kindly supplied by a local farmer (Portugal) of the variety Rendego-breadweack, which was harvest July 2006 and storage in dry pocked 6–7% moisture; this material was not ensiled. After being dried at 50 °C in an oven for 12 h, the straw was cut into small pieces (1–3 cm), milled in a knives mill to pass through a 0.9-mm screen, and stored at room temperature. All chemicals used were of analytical or reagent grade. Experiments were performed in triplicate, and yields are given on a dry-weight (untreated straw) basis.

Chemical Composition of Wheat Straw

Approximately 2 g of ground wheat straw was treated with 10 ml of 72% H_2SO_4 with stirring at 45 °C for 7 min. The reaction was interrupted by adding 50 ml of distilled water, and the mixture was then transferred to a 500-ml Erlenmeyer flask and the volume brought to 275 ml. The flask was autoclaved for 30 min at 121 °C/1.05 bar for the complete hydrolysis of oligomers. The mixture was filtered and the hydrolysate brought to 500 ml. After filtration through a Sep-Pak C_{18} cartridge to remove aromatic compounds, the hydrolysate was analyzed in a MetaCarb 67H column at 45 °C by using a Jasco chromatograph with refraction-index detector. The mobile phase was 0.005 mol/l H_2SO_4 at 0.6 ml/min flow rate. Sugar concentrations, reported as xylan and glucan, were determined from calibration curves of pure compounds. Lignin in the solid residue was determined by gravimetric analysis [12].

Determination of Holocellulose

Approximately 5-g samples of dry ground straw (with known moisture content) were transferred to 250-ml Erlenmeyer flasks containing 160 ml of distilled water, 0.5 ml of acetic acid, and 1.5 g of sodium chlorite. The samples were heated for 60 min in a water bath at 70–80 °C with agitation every 10 min. Then, 0.5 ml of acetic acid and 1.5 g of sodium chlorite were added. This addition was repeated at 60-min intervals for 4 h reaction time. After 4 h, the Erlenmeyer flask was put in an ice bath and cooled to 10 °C. The samples were subsequently filtered in crucibles of porosity 2. The residue was washed with 1.6 l of hot distilled water under vacuum. The samples were finally washed with acetone and dried at room temperature [13, 14].

Determination of α-Cellulose

Approximately 1-g samples of holocellulose (with known water content) were transferred to 150-ml beakers and put in water bath at 20 °C. Then, 11.8 ml of 17.5% NaOH solution was added under stirring, 5 ml being added in the first 1 min, 3.4 ml in the next 45 s, and 3.4 ml

in the next 15 s. The samples were left at rest by 3 min, and then 13.6 ml of 17.5% NaOH was added during 10 min (3.4 ml initially with stirring, 3.4 ml at minute 2.5, 3.4 ml at minute 5, and 3.4 ml at minute 7.5). Samples were covered and left at 20 °C for 30 min. Afterwards, 33.4 ml of distilled water were added, and the mixture was left for another 30 min at 20 °C. The samples were filtered in a crucible of porosity 2, washed with 8 ml of 8.3% NaOH, and washed with 400 ml of distilled water. The volume was completed with acetic acid (50 ml) 2 mol/l and left at rest for 3 min. The samples were filtered to remove acetic acid, washed with 3 l of distilled water at room temperature, and dried overnight [13, 14].

Extraction of Hemicellulose

A sample of 5 g dry ground straw was treated with 200 ml NaOH solution (concentrations of 0.25 and 0.50 mol/l) for 2 h at different temperatures (30 and 55 °C). After the indicated period of treatment, the sample was acidified to pH 5 with glacial acetic acid, concentrated to about 30 ml under reduced pressure, and then filtered. The alkali-soluble hemicelluloses were then precipitated by pouring the concentrated supernatant fluid with four volumes of 95% ethanol (20 °C, 24 h). The precipitates were recovered by filtration, washed with 70% ethanol, and air dried. The scheme for fractionation of hemicelluloses from wheat straw is illustrated in Fig. 3.

Chemical Composition of Extracted Hemicellulose of Wheat Straw

Samples of 0.3 g of dry hemicellulose were treated with 3 ml of 72% H_2SO_4 under stirring at 30 °C for 1 h. The reaction was interrupted by adding 79 ml of distilled water, and the mixture was then transferred to a 250-ml Erlenmeyer flask. The flask was autoclaved for 1 h at 1.25 bar for the complete hydrolysis of oligomers. The mixture was filtered and the hydrolysate brought to 250 ml. After filtration through a Sep-Pak C18 cartridge to remove aromatic compounds, the hydrolysate was analyzed in a MetaCarb 67H at 45 °C by using a Jasco chromatograph with refraction-index detector. The mobile phase was 0.005 mol/l H_2SO_4 at 0.6 ml/min flow rate. Sugar concentrations, reported as xylan and glucan, were determined from calibration curves of pure compounds. Lignin was determined by gravimetric analysis [15].

Fourier Transform Infrared of Samples

Fourier transform infrared of samples (FTIR) spectra were obtained on a Fourier Transform Infrared Spectrophotometer (Bomem MB Series) operating at 4 cm^{-1} resolutions and using a KBr disc containing 1% finely ground samples.

Thermogravimetric Analyzer

Thermal stability of hemicelluloses was performed using thermogravimetric analysis (TGA) on a thermal analyzer (TA Instruments High-Resolution Model Q-500). The apparatus was continually flushed with nitrogen. The samples weighed between 10 and 13 mg and were run from room temperature to 600 °C at a rate of 10 °C/min.

Scanning Electron Microscopy

The samples were mounted on stubs, freeze dried, coated with gold, examined, and photographed in a Scanning Electron Microscope LEICA S 360.

Results and Discussion

In wheat straw, cellulose and hemicelluloses are the predominant components and comprise about 70% of the dry weight. The third major cell-wall component in straw is lignin. However, to determine the overall efficiency of any process of extraction or process designed to convert lignocellulosic polysaccharides to value-added products, it is first necessary to determine the composition of these lignocellulosic components. In this work, the sulfuric-acid-based method was used for this purpose, as it is one of the standard methods referenced in the literature. The composition of the wheat straw used is given in Table 1. These data were in good agreement with those presented in other works [16].

The fraction consisting of cellulose and hemicellulose or, in other words, the set of all carbohydrates in a lignocellulosic material, is also called holocellulose. Thus, holocellulose is the product obtained after selective removal of lignin, with very low residual-lignin content, minimal loss of polysaccharide, and minimal oxidative and hydrolytic degradation of cellulose. The α-cellulose is the part of material that is insoluble in strong NaOH (17.5%) and may also be designated by crystalline cellulose [5]. In this work, the values of holocellulose and α-cellulose are also shown in Table 1.

Extraction of hemicelluloses under alkaline conditions involves alkaline hydrolysis of ester linkages to liberate them from the lignocellulosic matrix followed by extraction in an aqueous medium. However, the liberation of the hemicellulosic component from the plant cell walls is restricted by the presence of lignin network as well as ester and ether lignin–hemicellulose linkages [17]. As can be seen from Table 2, the treatment of wheat straw solely with water and 0.25 and 0.50 mol/l NaOH at 30 and 55 °C for 2 h released 1.9, 8.2, 13.3, 2.3, 15.7, and 17.3% hemicelluloses (% dry starting material), corresponding to the dissolution of 5.4, 23.3, 37.9, 6.6, 44.7, and 49.3% of the original hemicelluloses, respectively. This calculation, which was used to convert the percent extracted hemicelluloses, was yield (%)/hemicellulose total (%). Thus, these results revealed that the extraction of the wheat straw was effective and that the highest extraction yield was obtained with 0.50 mol/l NaOH (49.3% of the total available hemicelluloses). Apparently, a part of the hemicelluloses is attached within the cell walls (the more acidic and branched fraction), while the major part of the hemicelluloses (the more linear and less acidic fraction) is embedded firmly in the cell wall [5]. It can be speculated that this difference in extractability of the hemicelluloses is a result of a different function/location of these polysaccharides in the cell wall.

Table 1 Chemical composition of the wheat straw.

Chemical components	Composition (%)
Glucan	36.7±0.6
Hemicelluloses	35.1±1.1
Xylan	32.6±1.1
Acetyl group	2.4±0.1
Total lignin	26.7±0.1
Soluble lignin	7.1±0.1
Klason lignin	19.6±0.1
Ash	1.3±0.3
Total chemical composition	99.8±0.5
Holocellulose	72.2±0.1
α-cellulose	51.5±1.1

Table 2 The yield and monosaccharide constituent of hemicelluloses (% dry matter).

Yield and constituents (%)	Birch wood	Wheat straw					
		Temperature (30 °C)			Temperature (55 °C)		
		Concentration NaOH (mol/l)			Concentration NaOH (mol/l)		
		0.0	0.25	0.50	0.0	0.25	0.50
Yield	–	1.9±0.3	8.2±0.5	13.3±0.6	2.3±0.2	15.7±0.3	17.3±0.4
Xylan	48.1	0	13.2±0.2	17.8±0.5	0	11.6±0.3	17.6±0.4
Arabinan	0	0	26.5±0.3	24.9±0.5	0	20.2±0.3	36.5± 0.4
Acetyl group	6.9	0	2.4±0.1	2.4±0.1	0	2.4±0.1	2.4±0.1

Alkaline solubilization of hemicelluloses is usually mentioned as responsible for the disruption and breakage of hydrogen bonds. In addition, all these ester-linked substituents of the hemicellulose and other cell-wall components can be cleaved by alkali [18]. This tends to increase hydrophilicity and hence solubility of the material.

However, to characterize the solubilized hemicelluloses of the wheat-straw samples, the four extracted fractions obtained and the commercial hemicellulose of birch wood (Sigma®) were hydrolyzed to determine their sugar constituents, and the results are given in Table 2. The major monosaccharide obtained was xylose of birch wood (48.1%), indicating the presence of a xylan. In the hemicelluloses of wheat straw, the major monosaccharide was arabinose (36.5%), indicating the presence of an arabinoxylan. However, these sugar concentrations were very low; which can likely be due to the methodology used to determined the chemical composition of the hemicellulose extracted from wheat straw.

Infrared spectroscopy is an effective way to identify the presence of certain functional groups in a molecule. Also, one can use the unique collection of absorption bands to confirm the identity of a pure compound or to detect the presence of specific impurities [19, 20]. The FTIR spectra of wheat straw and pretreated wheat straws (Fig. 4) initially appeared rather similar. However, in a closer examination, spectra of pretreated wheat straw with water (lines 2 and 3) were similar to those of untreated wheat straw (line 1), and spectra of NaOH pretreated wheat straw (lines 4–7) can be clearly distinguished from those of untreated wheat straw (line 1) by the disappearance of ester linkage absorption (1,733 cm^{-1} band).

The 1,653 cm^{-1} band is also a carbonyl stretching band due to para-substituted ketones or aryl aldehydes, which has the same absorbance among the seven FTIR spectra. The absorption ratios of the 1,250 cm^{-1} band (guaiacyl units) and the 1,321 cm^{-1} band (syringyl units) to 1,500 cm^{-1} band are similar for the four pretreated wheat straw samples (lines 4–7, Fig. 4) indicating high syringyl content (weak absorption at 1,250 cm^{-1}).

In the untreated straw sample (line 1, Fig. 2), the intensity of the 1,250 cm^{-1} band was much higher than that in NaOH pretreated straw (lines 4–7, Fig. 4), suggesting a relatively higher guaiacyl content in the original wheat straw. The broad band between 3,600 and 3,000 cm^{-1}, corresponding to vibrations of the hydroxyl groups, appeared to be similar in all spectra. Methyl, methylene, and methine group vibrations appeared at the 2,918 cm^{-1} band and were present in all straw spectra. The strong bands in the 1,157–892 cm^{-1} region can be attributed to the polysaccharides present in the wheat straw or pretreated wheat straw. It was also noted that the band at 1,053 cm^{-1}, which might be assigned to primary hydroxyl vibration, appeared in all the straw spectra.

The FTIR spectra of hemicelluloses extracted from birch wood (commercial xylan, line 1) and wheat straw hemicellulose extracted with 0.25 mol/l NaOH/30 °C (line 2),

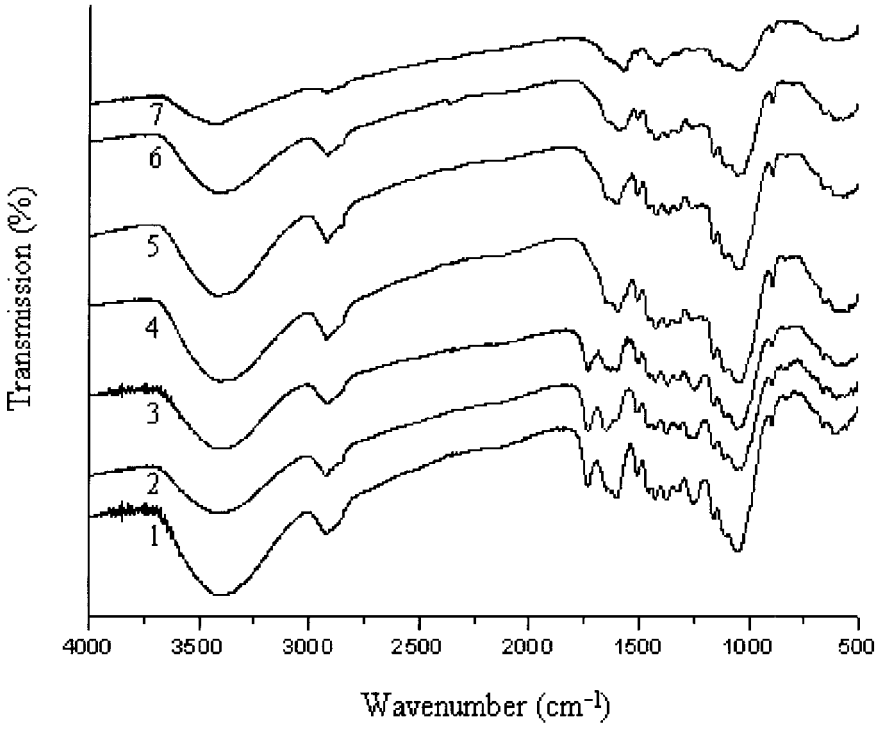


Fig. 4 FTIR spectra of untreated wheat straw (*line 1*), pretreated wheat straw with only water at 30 °C (*line 2*) and 55 °C (*line 3*), and pretreated wheat straw with 0.25 mol/l NaOH/30 °C (*line 4*), 0.50 mol/l NaOH/ 30 °C (*line 5*), 0.25 mol/l NaOH/55 °C (*line 6*), and 0.50 mol/l NaOH/55 °C (*line 7*); all the treatments for 2 h

0.50 mol/l NaOH/30 °C (line 3), 0.25 mol/l NaOH/55 °C (line 4), and 0.50 mol/l NaOH/ 55 °C (line 5) are illustrated in Fig. 5. As can be seen, the five spectral profiles and relative intensities of the bands were rather similar, indicating similar structures between the hemicelluloses. Similar features appeared in the spectra of lines 2–5 (Fig. 5), indicating analogous structures between the alkali-soluble hemicellulosic preparations.

The analysis of FTIR data showed that all hemicellulosic fractions clearly displayed the typical signal pattern for the hemicellulosic fraction and had a specific band maximum in the 1,200–1,000 cm^{-1} region. The absorption at 1,600 cm^{-1}, shown in all spectra is mainly associated with absorbed water [21]. Bands between 1,166 and 1,000 cm^{-1} are typical of xylans. The presence of the arabinosyl side chains is documented by the two low-intensity shoulders at 1,166 and 986 cm^{-1}.

As expected, the absence of a signal around 1,720 cm^{-1} for carbonyl stretching in all the four spectra indicated that the treatment with alkali under the conditions given did not significantly attack the glycosidic linkages and hydroxyl groups of hemicelluloses. The prominent band around 3,443 cm^{-1} represents the hydroxyl stretching vibrations of the hemicelluloses and water involved in hydrogen bonding. The absorbances at 3,422, 2,927, 1,468, 1,421, 1,388, 1,251, 1,166, 1,085, 1,049, 986, and 897 cm^{-1} in the spectra are associated with hemicelluloses. The lignin-related absorbance at 1,509 cm^{-1} is rather weak and poorly resolved, reflecting the low level of associated lignin in the hemicelluloses.

The prominent band at 1,046 cm^{-1} is attributed to the C–O, C–C stretching or C–OH bending in hemicelluloses [22]. The band at 897 cm^{-1}, which corresponds to the C1 group

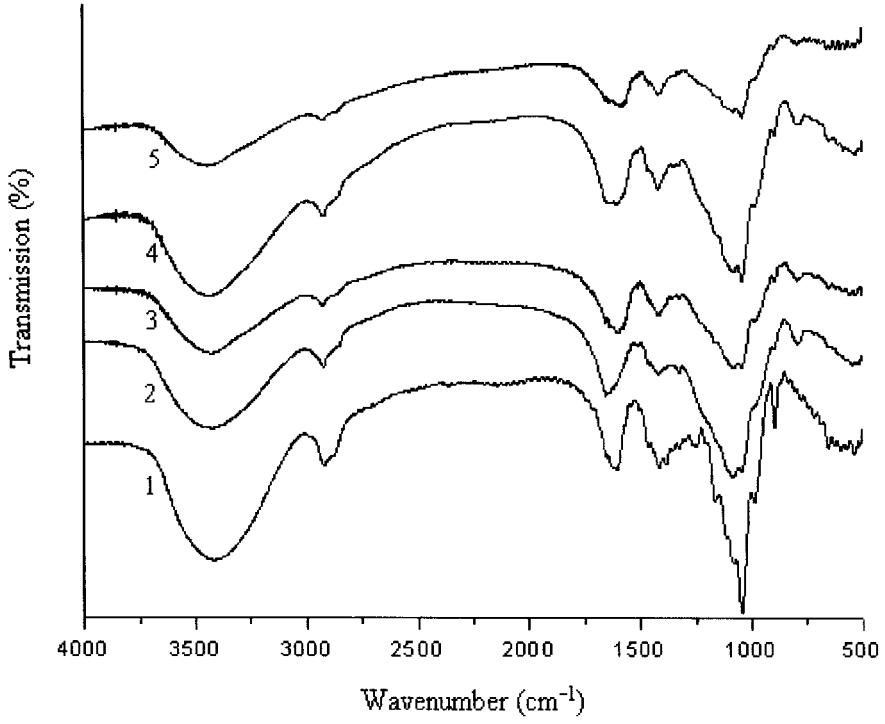


Fig. 5 FTIR spectra of commercial xylan from birch wood (*line 1*) and FTIR spectra of wheat straw hemicellulose extracted with 0.25 mol/l NaOH/30 °C (*line 2*), 0.50 mol/l NaOH/30 °C (*line 3*), 0.25 mol/l NaOH/55 °C (*line 4*), and 0.50 mol/l NaOH/55 °C (*line 5*); all the treatments for 2 h

frequency or ring frequency, is characteristic of beta-glycosidic linkages between the sugar units [23]. The presence of the arabinosyl side chains is identified by the low-intensity shoulder at 1,164 cm^{-1}, corresponding to the C–O–C vibration in hemicelluloses. The typical values of xylan in the spectra indicated that alkaline extraction treatment under the conditions used did not result in any significant change in the macromolecular structure of hemicelluloses.

TGA measures changes in weight of a sample with increasing temperature. Moisture content and presence of volatile species can be determined with this technique. In this work, the thermal properties (Fig. 6) of a commercial xylan from birch wood (line 1), wheat straw (line 2), hemicellulosic preparations after treatment with 0.50 mol/l NaOH/55 °C (line 3), 0.50 mol/l NaOH/30 °C (line 4), 0.25 mol/l NaOH/55 °C (line 5), and 0.25 mol/l NaOH/30 °C (line 6) for 2 h were studied by TGA. All these samples were found to be initially degraded at about 200 °C, and their maximum rates of weight loss were observed between 220 and 320 °C, except for the wheat straw sample (sample 2 in Fig. 6), with its maximum rate of weight loss observed between about 220 and 350 °C. As observed, the commercial xylan sample from birch wood and the wheat straw sample were stable up to 190 °C (lines 1 and 2, respectively), and the hemicellulosic preparations after treatment were stable up to 220 °C (lines 3, 4, 5, and 6, respectively). Beyond these temperatures, thermal degradation takes place. As can be seen (Fig. 6), at 30% weight loss, the decomposition temperatures of the degraded samples occurred at 270 °C (lines 1 and 3), 280 °C (lines 4 and 5), and 294 °C (lines 3 and 6). When scanning electron microscopy was used (Fig. 7), the fiber surface of

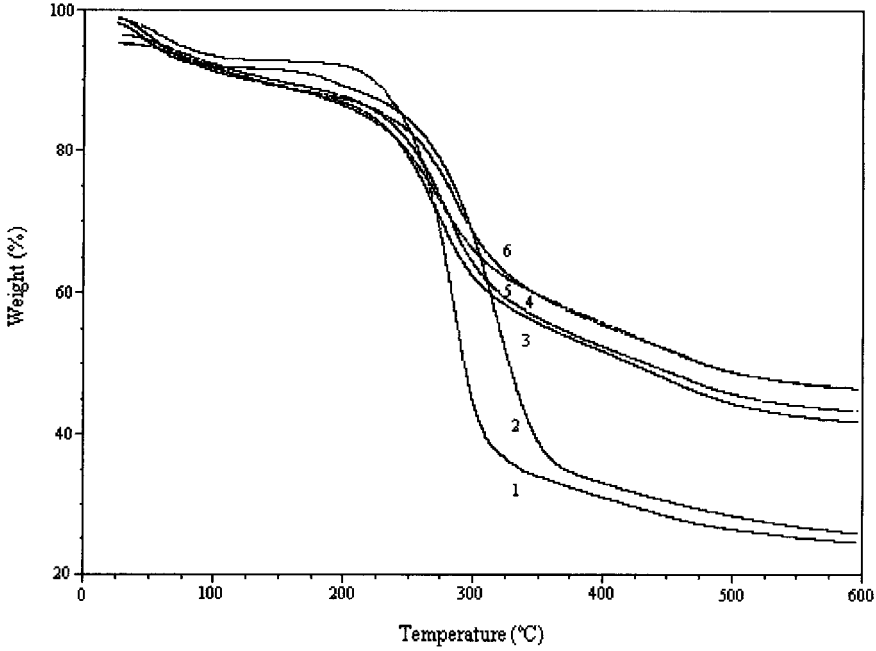


Fig. 6 TGA curves of commercial xylan from birch wood (*line 1*), wheat straw (*line 2*), and hemicellulosic preparations after treatment with 0.50 mol/l NaOH/55 °C (*line 3*), 0.50 mol/l NaOH/30 °C (*line 4*), 0.25 mol/l NaOH/55 °C (*line 5*), and 0.25 mol/l NaOH/30 °C (*line 6*) for 2 h

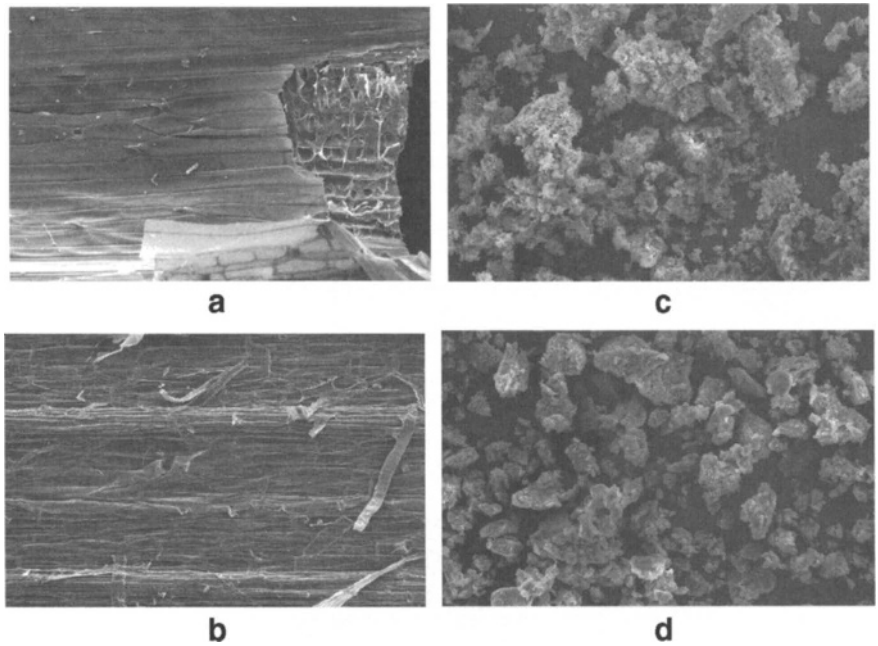


Fig. 7 Scanning electron microscopy of **a** wheat straw (magnification, ×150); **b** wheat straw treated with 0.25 mol/l NaOH (magnification, ×150); **c** extracted hemicellulose of birch wood (magnification, ×500); **d** extracted hemicellulose of wheat straw (magnification, ×500)

wheat straw clearly shows the modifications resulting from the NAOH action on the fiber structure (A and B). Wheat-straw hemicellulose (C) showed the similar appearance of the birch-wood hemicellulose (D) but with increased rugosity.

Conclusions

Hemicellulose could be extracted from wheat straw in a single stage using alkaline extraction process (0.50 mol/l NaOH) at 55 °C for 2 h, obtaining 17.3% of yield on dry base, corresponding to the dissolution of 49.3% of the original hemicellulose. Although being a preliminary study, these results suggest the potential of this process to hemicellulose extraction, making possible its biotechnological applications. The obtained material was identified as arabinoxylan by chemical analysis and characterized by FTIR spectroscopy and TGA. The analysis of FTIR (FTIR scans) showed typical signal pattern for the hemicellulosic factions. Microscopic evaluation shows some differences in the behavior of the hemicellulose when compared with birch-wood xylan.

This procedure shows potential to be employed as a part of a process leading to the integral use of lignocellulosic materials in different biotechnological processes. Thus, these future applications of agro-industrial residues in bioprocesses on the one hand provide alternative substrates and on the other hand help in solving environmental problems which their disposal could cause. Furthermore, many publications refer to the fact that the utilization of both cellulose and hemicellulosic sugars present in typical lignocellulosic biomass hydrolyzates is essential for the economical production, e.g., of bio-ethanol. However, the integral use not only of a hemicellulose fraction but also of the lignin can help in this concept of economical production of different products.

Acknowledgements The authors acknowledge the financial support from FCT (Fundação para a Ciência e Tecnologia/Portugal, SFRH/BPD/26156/2005 and SFRH/BPD/26108/2005), as well as from FAPESP (Fundação de Amparo a Pesquisa do Estado de São Paulo/Brazil) and CNPq (Conselho Nacional de Desenvolvimento Científico e Tecnológico).

References

1. Gonçalves, A. R., Benar, P., Costa, S. M., Ruzene, D. S., Moriya, R. Y., & Luz, S. M., et al. (2005). *Applied Biochemistry and Biotechnology, 121*, 821–826.
2. Küçük, M. M., & Demirbas, A. (1997). *Energy Conversion Management, 38*(2), 151–165.
3. Sun, Y., & Cheng, J. (2002). *Bioresource Technology, 83*, 1–11.
4. Montane, D., Farriol, X., Salvado, J., Jollez, P., & Chornet, E. (1998). *Journal of Wood Chemistry and Technology, 18*, 171.
5. Fengel, D., & Wegener, G. (1989). *Wood chemistry, ultrastructure, reactions* p. (p. 613). Berlin: Walter de Gruyter.
6. McDougall, G. J., Morrison, I. M., Stewart, D., Weyers, J. D. B., & Hillman, J. R. J. (1993). *Science of Food and Agriculture, 621*–20.
7. Jackson, M. G. (1977). *Animal Feed Science and Technology, 2*, 105–130.
8. Spencer, R. R., & Akin, D. E. (1980). *Journal of Animal Science, 51*(5), 1189–1196.
9. Lima, D. U., Oliveira, R. C., & Buckeridge, M. S. (2003). *Carbohydrate Polymers, 52*, 367–373.
10. Saake, B., Busse, T., & Puls, J. (2005). *Appita, 2*, 141–146.
11. Doner, L. W., & Hicks, K. (1997). *Cereal Chemistry, 74*, 176.
12. Rocha, G. J. M. (2000). PhD thesis, São Carlos/Universidade de São Paulo, Brazil,
13. Browing, B. L. (1963). *The chemistry of wood* p. (p. 574). New York: Interscience.
14. Ruzene, D. S., Gonçalves, A. R., Teixeira, J. A., & Pessoa De Amorim, M. T. (2007). *Animal Feed Science and Technology*, 136–140.

15. Ferraz, A., Rodriguez, J., Freer, J., & Baeza, J. (2000). *Bioresource Technology, 74*, 201–212.
16. Wilkie, K. C. B. (1979). *Advances in Carbohydrate Chemistry and Biochemistry, 36*, 215–264.
17. Ebringerová, A., & Heinze, T. (2000). *Macromolecular rapid communications, 21*, 542–556.
18. Ternrud, I. (1987). *Degradation of untreated and alkalitreated straw polysaccharides in ruminants.* Uppsala: The Swedish University of Agricultural Sciences.
19. Faix, O. (1991). *Holzforschung, 45*, 21–27.
20. Gonçalves, A. R., & Ruzene, D. S. (2001). *Applied Biochemistry and Biotechnology, 91–93*, 63–70.
21. Kacurakova, M., Belton, P. S., Wilson, R. H., Hirsch, J., & Ebringerova, A. (1998). *Journal of the Science of Food and Agriculture, 77*, 38–44.
22. Kacurakora, M., Ebringerova, A., Hirsch, J., & Hromadkova, Z. (1994). *Journal of the Science of Food and Agriculture, 66*, 423.
23. Gupta, S., Madan, R. N., & Bansal, M. C. (1987). *Tappi Journal, 70*, 113–114.

Appl Biochem Biotechnol (2008) 147:97–105
DOI 10.1007/s12010-007-8091-1

The Use of Seaweed and Sugarcane Bagasse for the Biological Treatment of Metal-contaminated Waters Under Sulfate-reducing Conditions

Márcia Monteiro Machado Gonçalves · Luiz Antonio de Oliveira Mello · Antonio Carlos Augusto da Costa

Received: 9 May 2007 / Accepted: 30 October 2007 /
Published online: 27 November 2007
© Humana Press Inc. 2007

Abstract When wetlands reach maximum treatment capacity to remove heavy metals, removal can still take place through precipitation as sulfide because of the biological reduction of sulfate. To achieve this goal, anaerobic conditions must be attained, a sulfate source must exist, and an adequate substrate for sulfate-reducing bacteria (SRB) is also required. In the present work, two ligneous-cellulosic materials, a brown seaweed and sugarcane bagasse, have been selected as substrates for SRB growth. Experiments were simultaneously conducted in continuous operation in two columns (0.57 L each), one containing the ligneous-cellulosic material plus inoculum and another containing only the ligneous-cellulosic material. In this work, the removal of cadmium and zinc was studied because of their presence in effluents from mining/metallurgy operations. Results obtained indicated that the inoculated reactor was able to treat the effluent more efficiently than the noninoculated reactor considering the time course of the tests.

Keywords Metal removal · Sulfate reduction · Sulfate-reducing bacteria (SRB) · Ligneous-cellulosic materials · Wetlands

Introduction

During the treatment of heavy-metal containing solutions, the use of constructed wetlands is thought of as an easy technological alternative when compared with conventional treatment methods. The term wetland is used to characterize natural ecosystems partially or totally flooded during the year. Observations about the ability of natural wetlands to change the quality of water led to the development of artificial ecosystems able to treat several classes of wastewater. Those ecosystems are called constructed wetlands, and the main

M. M. M. Gonçalves · L. A. de Oliveira Mello · A. C. A. da Costa (✉)
Instituto de Química, Programa de Pós-graduação em Engenharia Química,
Universidade do Estado do Rio de Janeiro, Rua São Francisco Xavier, 524—PHLC—sala 427,
Rio de Janeiro 20559-900, Brazil
e-mail: acosta@uerj.br

processes involved in the treatment of metals include adsorption by soil or sediment fractions, complexation by organic matter, plant uptake, and precipitation as carbonate or sulfide [1].

Several published reports on both natural and constructed wetlands affirm that metal removal from wastewater will continue indefinitely through the production of biogenic sulfides by sulfate-reducing bacteria (SRB) followed by precipitation. These microorganisms are responsible for sulfide production as long as sulfate is present in the influent and an organic substrate is provided [1–3]. Various organic wastes have been used as substrate for SRB such as wood dust [4], hay and straw [5], oak chips and sludge from a wastepaper recycling plant [6], and spent mushroom compost [7]. In these cases, these solid waste materials were able to sustain SRB growth for long periods without the addition of other substrates. According to Chang et al. [6], first the polysaccharide from waste material seems to be degraded by hydrolytic fermentative anaerobes to fatty acids and alcohols that support the growth of sulfidogens.

The objective of the present work was to evaluate the use of two ligneous-cellulosic materials, a brown seaweed and sugarcane bagasse, as substrates for SRB growth and to investigate their ability to remove heavy metals simulating constructed wetlands.

Materials and Methods

The experimental setup used in the study is comprised of one reservoir (10 L), from where the solution is fed, through peristaltic pumps, into two column reactors (0.57 L). Experiments were simultaneously conducted in both columns. The first one (column A) contained 40 g of ligneous-cellulosic material plus inoculum, and the second column (column B) contained just 40 g of ligneous-cellulosic material. The anaerobic sludge used as inoculum was obtained from the bottom of an upward-flow anaerobic sludge blanket (UASB) reactor from the effluent of a poultry-processing plant.

The influent composition was defined so as to simulate drainage wastewater from a metallurgical industry dam. Thus, the composition of this synthetic wastewater presented around 80 mg/L zinc, 2 mg/L cadmium, and 800 mg/L sulfate. Table 1 summarizes the main operational characteristics of the experimental runs investigated at 25±2 °C.

Influent and effluent sampling was undertaken twice a week from both columns, filtered through 0.45-μm filters, to measure chemical oxygen demand (COD), sulfate, and metals concentrations. At the end of each experiment, samples of the biomass were collected, and total solids (TS), volatile solids (VS), and SRB population were determined.

Sulfate, COD, TS, and VS determinations were performed according to standard methods [8]. Soluble cadmium and zinc concentrations were determined by atomic

Table 1 Operational conditions.

Run	Ligneous-cellulosic materials	Influent	pH		HRT (h)	
			Column A Effluent	Column B Effluent	Column A	Column B
I	100% seaweed (*Sargassum* sp.)	6.9±0.4	7.3–5.3[a]	6.6±0.3	16.6±1.3	16.8±1.3
II	50% seaweed + 50% bagasse	6.9±0.3	7.4–4.5[a]	6.8±0.4	17.4±2.7	16.8±2.3

[a] Maximum and minimum values

absorption spectrophotometry (Perkin-Elmer AAnalyst 300). The SRB were enumerated by the most probable number (MPN) technique (n=3), utilizing Postgate B semisolid medium [9]. Inoculated tubes were incubated at 35 °C for 28 days. The growth of SRB was indicated by the formation of a black FeS precipitate.

Results and Discussion

Consumption of Organic Matter

To evaluate the process of metal removal in relation to the consumption of organic matter, COD was measured in the effluent of columns A and B (Fig. 1). The COD of the influent solution, for all the runs conducted, was always below the detection limit of the method (15.0 mg/L). This was expected to occur once there is not a significant amount of oxidizable matter or organic compound in the influent solution.

The results of COD determination for run I showed that although the first sampling occurred after 7 days of operation, COD values obtained in the noninoculated column (column B) presented small availability of organic matter for the inoculated sludge in column A. The average COD from the seventh day of run until the end of the run was equal

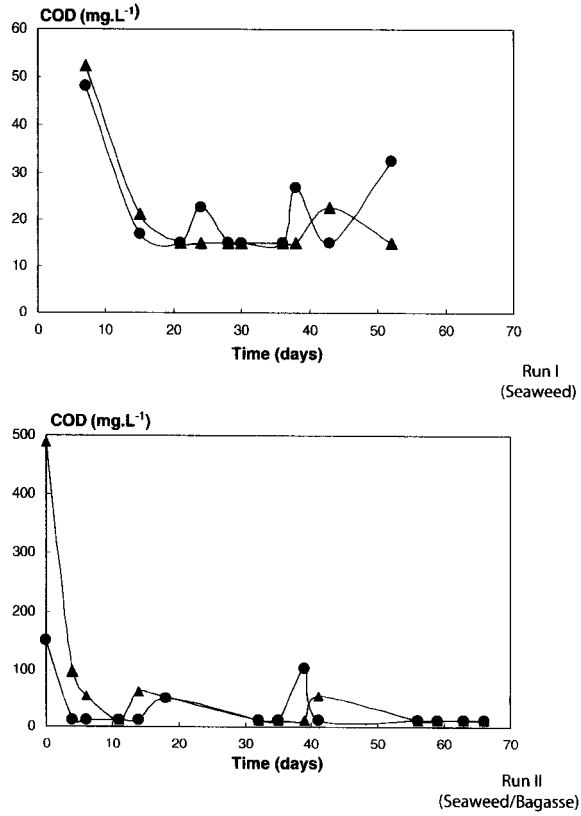


Fig. 1 COD concentration in the effluent of column A (with inoculum, *circles*) and column B (without inoculum; *triangles*) against time

to 22.2 mg/L in column A (inoculated) and 20.1 in column B, indicating that the availability or organic compounds to the bacteria was quite limited.

In Fig. 1, it can be observed that for some samples of run I (24th, 38th, and 52nd day), there was an increase in the COD value from the effluent from the inoculated column, probably because of the washout of particles from the inoculated sludge [10]. From the results presented in Fig. 1 for column B (noninoculated) during run II, it could be observed that because the organic material is more amenable to degradation, the available organic matter (as COD) was superior than previously observed (run I) for around 30 days. During this period, the difference between the COD measured in the effluent of the noninoculated column (column B) and the COD measured in the inoculated column (column A), corresponding to the organic matter used by the microbes, was around 92.0 mg/L, with a maximum value of 338.0 mg/L, in the first days of the experiment.

Bacterial Reduction of Sulfate Ions

The concentrations of sulfate ions in the influent to the reactors and effluent solutions from the columns are presented in Fig. 2. It could be observed that in all the runs performed, the concentration of sulfate in the effluent from column B (noninoculated) presented slightly higher values than the ones observed in the influent solution. This increase was probably due to the release of sulfate ions present in the structure of the seaweed. Thus, the amount

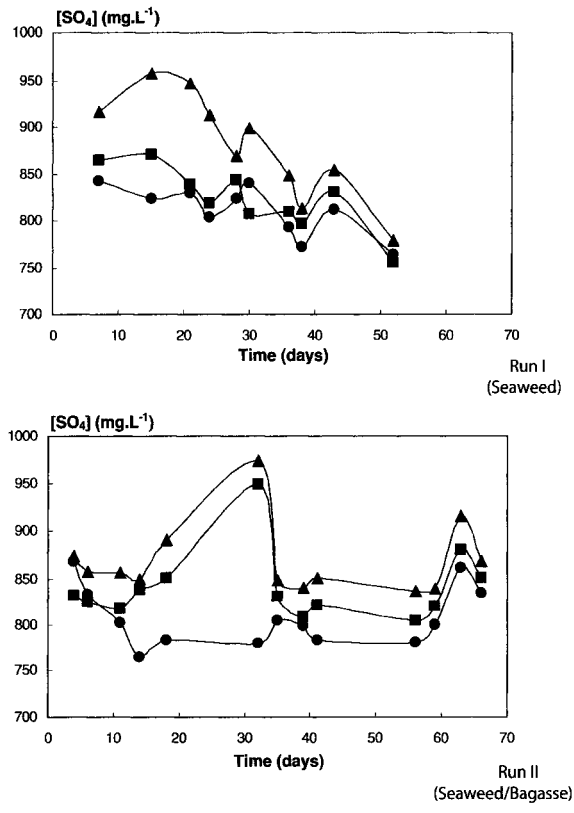


Fig. 2 Sulfate ion concentrations in the influent (*squares*), and effluent from columns A (with inoculum; *circles*) and B (without inoculum; *triangles*) against time

of sulfate available for SRB cells corresponds to the amount of sulfate present in the influent of the columns plus the amount of sulfate released by the seaweed. Based on these considerations, it could be concluded that the reduction of sulfate actually happened in all the experimental runs conducted.

To better understand these results obtained for column A (inoculated), Fig. 3 presents the amount of sulfate reduced by the bacteria against time. This amount of sulfate ions was calculated as the difference between the sulfate-loading rates in column B (available to SRB) and column A (mg SO_4^{2-}/L day).

It could be observed from these results that the biological reduction of sulfate obtained during run I did not show an adaptation period because of the fact that sulfate reduction was quantified from the seventh day of the run. The reduction of sulfate was followed up to the 21st day because of the availability of organic matter for metabolic processes.

A stoichiometric approach of the present sulfate reduction indicated that it would be necessary to have 140 mg SO_4^{2} /day, considering a hydraulic retention time equal to 16 h, to produce enough sulfide to remove all cadmium and zinc present in the effluent solution.

According to Chang et al. [6], when some ligneous cellulosic materials are used as the carbon source (such as hay or straw), the reduction of sulfate with further production of sulfide can be improved with the supplementation of electron donors easily accessible by the microbes, such as sucrose, peptone, and lactate. This can explain the marked increase in the efficiency of metal removal observed in run II, where seaweed was mixed with a certain quantity of sugarcane bagasse.

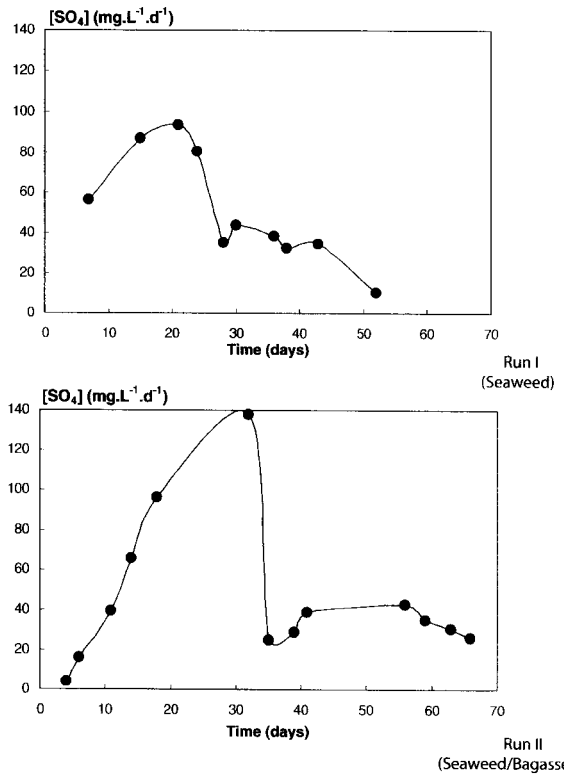


Fig. 3 Variation of amount of sulfate ions reduced by the SRB, expressed as sulfate loading rate against time for the inoculated column A

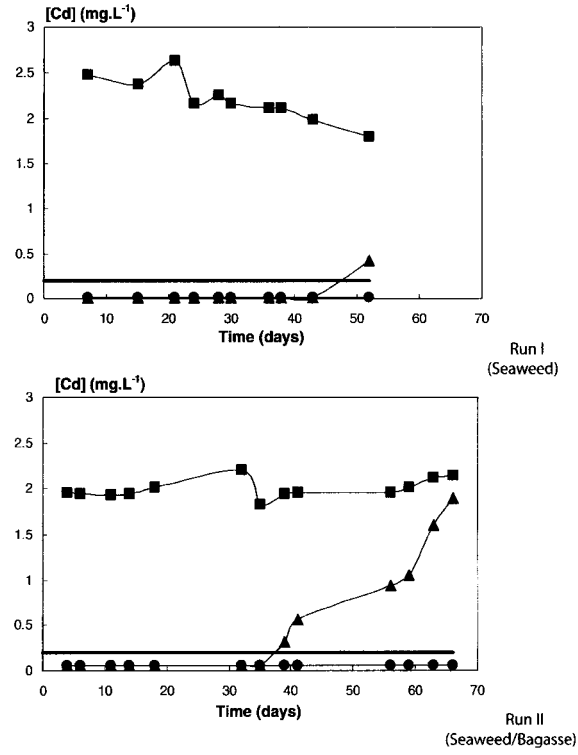


Fig. 4 Concentration of cadmium in the influent (*squares*), effluent from columns A (with inoculum; *circles*) and B (without inoculum; *triangles*), and local discharge limits (*straight solid line*)

Removal of Cadmium

Figure 4 shows the inlet and outlet cadmium concentrations obtained in both columns for runs I and II, as well as the local discharge limits. In run I, cadmium concentration was higher than the discharge limit (0.2 mg/L) from the 47th day of experiment in the column containing just the seaweed as the carbon source (0.43 mg/L). In column A, cadmium concentration was kept below the 0.2-mg/L limit during the entire course of the experiment because of the inoculation of the system. The average cadmium removal observed was equal to 99.5% in the inoculated column, while in the noninoculated column, it was equal to 97.2%.

During run II, where column A also contained anaerobic sludge, the increase in the availability of organic matter to the microbial population because of the addition of sugarcane bagasse confirmed the importance of the inoculation of SRB in the system. The concentration of cadmium was higher than 0.2 mg/L from the 39th day on, in the column containing only the mixed carbon sources, seaweed and sugarcane bagasse, reaching the value of 0.32 mg/L. On the other hand, the concentration of cadmium in the inoculated column was below 0.2 mg/L over the entire experiment. The average removal of cadmium in the columns was around 97.0% in the inoculated column and around 74.0% in the noninoculated column.

Removal of Zinc

In Fig. 5, the analytical results for zinc in the influent and effluent solutions is presented, as well as the local discharge limit for this metal (5.0 mg/L). During run I, zinc concentration

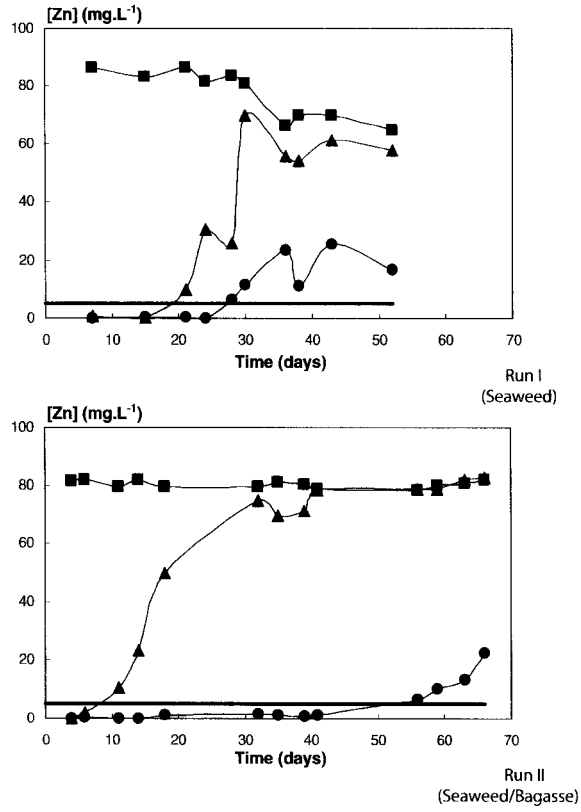


Fig. 5 Concentration of zinc in the influent (*squares*), effluent from columns A (with inoculum; *circles*) and B (without inoculum; *triangles*), and local discharge limits (*straight solid line*)

was higher than the discharge limit, from the 21st day (9.8 mg/L) in the noninoculated column (B) and from the 28th day (6.5 mg/L) in the column inoculated (A) with anaerobic sludge. The average removal of zinc observed was equal to 86.4% in the inoculated column and 49.6% in the column containing the seaweed only.

The increase in the availability of organic matter proved to be efficient in the removal of zinc during run II. In this run, zinc concentration was higher than the discharge limit (5.0 mg/L) from the 11th day (10.6 mg/L) in the column B and from the 56th day in the column A (6.9 mg/L). The average metal removal in the columns was equal to 94.4% in the inoculated and 32.6% in the column containing the seaweed and sugarcane bagasse only.

Beyond the biological process of sulfate reduction with subsequent metal precipitation as sulfides, other mechanisms of metal removal can be present during the runs, particularly in the inoculated column (A): precipitation as metals carbonates using the bicarbonate and/or carbonates formed during the reduction of sulfate by the SRB cells or by fermentation from other microorganisms, precipitation as metal hydroxides, complexing with substances excreted by the cells, and accumulation on the surface of cells, through reactions between metal ions and cell wall components [10].

Among those mechanisms, the most probable involved other than precipitation as sulfides are precipitation as metal carbonates and accumulation on the surface of the cell. This last one is due to the interaction of negative charges from biopolymers present on the outer structure of the cells and metal ions present in the solution [11].

Quantification of SRB Cells Present in the Sludge

The number of SRB cells was determined before and after each run performed. The results are presented in Fig. 6.

At the end of the experiment of run I, two distinct types of sludge could be individually identified based on color. Much of the total sludge was black, and a small part of the sludge was present as a gray precipitate, probably because of a higher concentration of zinc sulfide, a white precipitate. Because of this, the population of SRB cells in both types of sludge was quantified and also quantified in the inoculum. It could be noted that there was an 18-fold increase in the number of SRB cells present in the final black precipitate (19.0×10^6 cells/g VS) when compared to the inoculum (0.76×10^6 cells/g VS). However, in the final gray precipitate, the concentration of SRB slightly decreased because of an intense precipitation of ZnS. It is probable that the formation of this precipitate has contributed to decrease the activity of SRB cells, as observed in the study for the removal of metals in an UASB reactor using molasses and stillage as carbon sources for SRB [10].

During run II, an intense proliferation of photosynthetic microbes was observed in the reactors because of marked sunlight irradiation on the reactors. The number of SRB present in the final sludge (8.6×10^5 cells/g VS) was twice the number of cells in the inoculum (4.5×10^5 cells/g VS), although this increase was not remarkable. This fact can be related to the problems found in separating the final sludge from the remaining substrates (sugarcane bagasse and seaweed) still present in the reactors. Thus, those materials were considered in

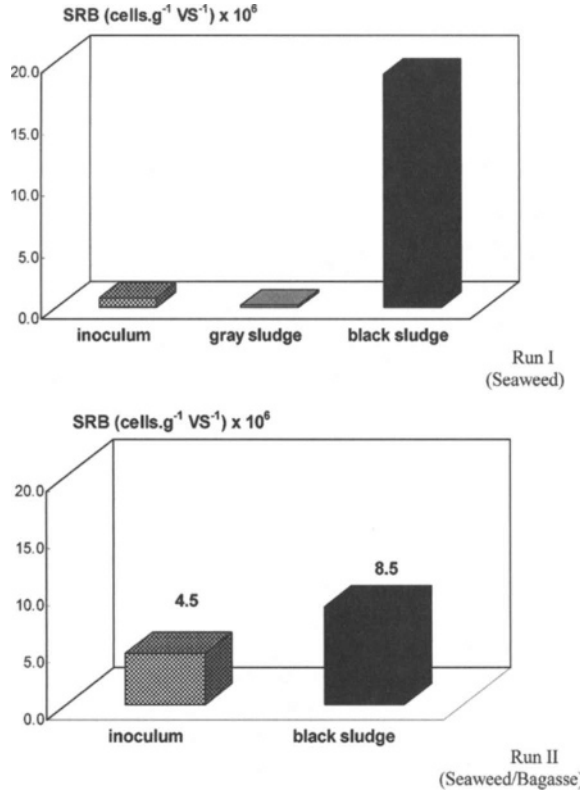


Fig. 6 Concentration of SRB cells (MPN of cells/g VS), in the inoculum and at the end of the experiments

the determination of VS, consequently reducing the enumeration of cells/g VS. It is probable that the number of SRB cells present in the final sludge is actually higher than the value reported.

Conclusions

The following are the conclusions for the study:

- The biological activity of SRB cells contributed to the process of precipitation of Cd and Zn, as compared to the noninoculated reactor, where physico-chemical mechanisms predominated.
- For run I (seaweed only), in the noninoculated column (B), Cd removal was high, but Zn removal was not so good. In this case, the predominating mechanism was biosorption of metals. On the other hand, in the inoculated column (A), both Cd and Zn removals were very high, confirming the importance of the production of sulfides by SRB cells.
- For run II (seaweed plus bagasse), in the noninoculated column (B), Cd and Zn removals were smaller than those obtained in run I. This was due to the presence of bagasse, which is not a suitable biosorbent material as the seaweed. On the other hand, in the inoculated column (A), both metals were efficiently precipitated as metal sulfides.
- The reduction of sulfate in run II was improved with the mixture of seaweed and bagasse as carbon sources, reflected in higher precipitation of Cd and Zn, as compared to run I.
- Although the production of sulfide was not enough to precipitate all zinc and cadmium present in the influent, other mechanisms also acted to improve the treatment process.
- In both runs, there was an increase in the MPN of SRB/g VS in the final sludge, in comparison to the inoculated sludge.

Acknowledgments The authors would like to thank Conselho Nacional de Desenvolvimento Científico e Tecnológico (CNPq) and Fundação Carlos Chagas Filho de Amparo à Pesquisa do Estado do Rio de Janeiro (FAPERJ) for financial support to conduct this research.

References

1. Lorion, R. (2001). *Constructed wetlands: Passive systems for wastewater treatment.* Available at: http://clu-in.org.
2. Sobolewski, A. (1996). Ecological Engineering, *6*, 259–271.
3. Hammack, R. W., Edenborn, H. M., & Dvorak, D. H. (1994). *Water Research*, *28*, 2321–2329.
4. Tutle, J. H., Dugan, P. R., & Randles, C. I. (1969). *Applied Microbiology*, *17*, 297–302.
5. Béchard, G., Yamazaki, H., Gould, W. D., & Bédard, P. (1994). *Journal of Environmental Quality*, *23*, 111–116.
6. Chang, I. S., Shin, P. K., & Kim, B. H. (2000). *Water Research*, *34*, 1269–1277.
7. Dvorak, D. H., Hedin, R. S., Edenborn, H. M., & Mcintire, P. E. (1992). *Biotechnology and Bioengineering*, *40*, 609–616.
8. American Public Health Association (1998). *Standard methods for the examination of water and wastewater* (20nd ed.). Washington: APHA.
9. Postgate, J. R. (1984). *The Sulphate-reducing Bacteria* (2nd ed.). Cambridge: Cambridge University Press.
10. Gonçalves, M. M. M. (2001). D.Sc. thesis, Federal University of Rio de Janeiro, Rio de Janeiro, Brazil.
11. Gomes, N. C. M., Hagler, L. C. S. M., & Savvaidis, I. (1998). *Revista de Microbiologia*, *29*, 85–92.

Appl Biochem Biotechnol (2008) 147:107–117
DOI 10.1007/s12010-007-8087-x

Development of Activity-based Cost Functions for Cellulase, Invertase, and Other Enzymes

Chris C. Stowers · Elizabeth M. Ferguson · Robert D. Tanner

Received: 11 May 2007 / Accepted: 18 October 2007 /
Published online: 13 December 2007
© Humana Press Inc. 2007

Abstract As enzyme chemistry plays an increasingly important role in the chemical industry, cost analysis of these enzymes becomes a necessity. In this paper, we examine the aspects that affect the cost of enzymes based upon enzyme activity. The basis for this study stems from a previously developed objective function that quantifies the tradeoffs in enzyme purification via the foam fractionation process (Cherry et al., Braz J Chem Eng 17:233–238, 2000). A generalized cost function is developed from our results that could be used to aid in both industrial and lab scale chemical processing. The generalized cost function shows several nonobvious results that could lead to significant savings. Additionally, the parameters involved in the operation and scaling up of enzyme processing could be optimized to minimize costs. We show that there are typically three regimes in the enzyme cost analysis function: the low activity prelinear region, the moderate activity linear region, and high activity power-law region. The overall form of the cost analysis function appears to robustly fit the power law form.

Keywords Cost function · Cellulase · Invertase · Foam fractionation · Separations cost

Introduction

Since the rapid development of the chemical industry in the 1940s, the chemical industry has morphed from a commodity chemical market into a specialty chemical market where bio-related products and processes have become increasingly important. Enzymes are now commonly used as catalysts to produce products such as proteins, sugars, and lipids as well as processing tools to enhance more traditional products, such as paper pulp. In fact,

C. C. Stowers · R. D. Tanner (✉)
Department of Chemical Engineering, Vanderbilt University, Nashville, TN 37235, USA
e-mail: Robert.D.Tanner@Vanderbilt.edu

E. M. Ferguson
Pediatrics Department/Judith B Ratner MD Office, George Washington University,
2150 Pennsylvania Ave NW, Washington, DC 20016, USA

enzyme industry sales are expected to increase to 2.2 billion dollars by 2010 [4]. It has been predicted that the kinetics of cost reduction for industrial enzymes will control the extent of how the enzyme market will grow [5]. Thus, cost analysis of enzymes is becoming an important factor for engineers and scientists dealing with mainstream bio-products.

The price of enzymes is often controlled by the method of production and more importantly the purification method [6]. Many enzymes can be isolated from common plants and microorganisms while others must be harvested from animals, particularly mammals such as pigs, rabbits, and even humans. Generally, enzymes isolated from common plants are less costly than those isolated from animals. Likewise, enzymes that require little purification are less costly. Some enzymes require additional processing beyond traditional standard processing, which includes foam fractionation, salting out, and liquid–liquid extraction [7]. These additional processing steps can become extremely costly and can lead to increased market cost of the enzyme. These processing steps often include standard gel chromatography and/or high performance/pressure liquid chromatography (HPLC).

In this study, we will explore whether an objective function, relating enzyme activity to cost, can be developed to establish the cost function of cellulase and other enzymes. We will determine the cost increase in crude cellulase (in terms of activity per mass) after processing used to enhance the purity and concentration of this protein. We shall start with a more generalized objective function comprised of measurable purification process responses to create our cost model and reduce that model to the specific cost function for this study. A previously developed objective function quantifies the tradeoff between maximizing the enzyme concentration in a separation process such as a foam fractionation process and minimizing the loss of enzyme mass and enzyme activity in that process [1] is shown below.

$$\Phi = (\mathrm{AR})^{a}(\mathrm{MR})^{b}(\mathrm{ER})^{c} \tag{1}$$

where AR=activity recovery=Afoam/Ai
MR=mass recovery=Mfoam/Mi
ER=enrichment recovery=Cfoam/Ci

Typically, a, b and c are positive in the case where Φ is a generalized, desired performance factor. On the other hand, as we shall see in the results section, when MR is replaced by purchase mass and Φ is replaced by \$/mg, b becomes negative. Here, we explore whether a generalized relationship between cost, activity, and recovered mass alone can characterize a cost function, and if so, determine the appropriate coefficients.

This approach to the development of cost-based processing can result in the lowering of product cost at each processing step by selecting the control variables which can maximize the respective Φ or minimize the cost-based functions at each step. In a foam-fractionation process, in particular, these control parameters are typically the pH and the foaming-gas superficial velocity [1]. In this approach, it is convenient to define Φ as a generalized value (or price) function. In this study, we define price as the price published in leading biochemical catalogs used in this study. Additional processing to generate higher purity enzyme will result in incremental increases in the value of Φ, which can be represented as the first derivative of the objective function with respect to activity. In particular, in this study, we shall compare the catalog values to a parameter fitted model for industrial enzymes to determine whether there are general trends and quantitative similarities between classes of enzymes. Our goal is to develop an objective function based on market values, making the model most useful from the purchasing (consumer) point of view. However, the

model could also be used from a manufacturing point of view to determine whether the production of certain products would be profitable by determining the economic value of a potentially new product before investment in production. In the initial part of this study, we will assume the second and third terms of the objective function model (Eq. 1), Φ, are constant and can be lumped into a new parameter γ. This permits the model to be simplified to the following equation, where the activity term is defined as activity per unit mass, as is often expressed in enzyme sales catalogs.

$$\Phi = \gamma(\mathrm{A})^{\mathrm{a}} \tag{2}$$

With this framework, our underlying assumption for the remainder of the work is that for a given enzyme, the processing cost is captured by the power law framework and by difference production (fermentation) costs are included within the constant γ. This is a good assumption since the majority of industrial enzymes are produced in a microbial environment or directly harvested from plants. These enzymes, such as cellulases, are often processed directly for activity [2, 3], which requires increasingly larger costs to reach higher activity. Enzymes generally used for medical applications, which are produced in a mammalian cell line or from animals, may tend to deviate from this assumption. Additionally, the cost of specialty enzymes, which are produced in only small quantities for R&D purposes, may be dictated by investment cost. We shall focus on industrial enzymes here.

The cost of storage for enzymes can also influence the cost of these chemicals at the customer level. It can be readily established that significant savings (greater than 25%) can be achieved by simply buying in bulk from an enzyme supplier. However, bulk storage costs of these enzymes are not negligible considering that most enzymes must be kept at −20°C. The additional cost of storage resulting from bulk purchases needs to be considered by engineers and scientists in industry. Thus, we present a slightly modified cost function, Φ, that accounts for the cost effects of buying in bulk quantity and the resulting enzyme storage.

$$\Phi = \gamma(A)^{a}\delta(M)^{b}(1 + \alpha * t) \tag{3}$$

where Φ=enzyme cost in \$/mg
M=mass purchase amount
t=storage time in weeks
a and b are dimensionless constants
γ, δ, and α have appropriate dimensions.

Two key observations can be made regarding this improved cost function. First, the cost per unit mass is directly proportional to activity and inversely proportional to the amount of mass purchased. This observation is fairly trivial knowing that if a customer wants a higher activity per unit mass product, it will cost more and the more purchased will warrant a decrease in price per unit. Secondly, the parameter b must be negative knowing that the price per unit should decrease as more product is purchased. The larger the absolute value of b, the more discount a consumer will receive for buying in bulk. Thus, the parameter b and the storage cost function (third term) must be balanced to attain the most cost-effective purchase amount for a given purchase. α has the units of 1/week (inverse time) and the parameters γ and δ have units dependent on the values of the coefficients a and b and the units of activity and mass are expressed, respectively. Of course, activity and the mass purchase amounts could be expressed in dimensionless form to generalize Eq. 3. It is also important to notice that the parameters γ and δ can be lumped into one single parameter. However, for our purposes, it is easier to now look at the two parameters separately so that

we can investigate the proposed model terms individually. The first term can be investigated as an independent activity dependent cost function, while the second term can be investigated to determine the effects of mass purchase amount on the cost function. This framework will allow us to empirically determine whether the simple models shown in Eqs. 2 and 3 can accurately relate enzyme activity and purchase amount to cost for industrial enzymes.

Materials and Methods

The enzyme market was investigated for the following enzymes: cellulase, invertase, collagenase, papain, alpha-amylase, and elastase. The market was surveyed by determining the cost per mg of enzyme from Fisher Scientific, Sigma-Aldrich, Carolina Biochemical, Worthington Biochemical, and Elastin Products Company [8–12]. If these suppliers sold a particular enzyme in different allotment sizes, the cost per mg was averaged over all allotments to determine an average price per mg from that particular supplier. This averaging was introduced here to reduce the market scattering of the data to enable us to more clearly observe the trend of enzyme activity on cost. Data were also collected for invertase from an available industrial market report [13]. Only enzymes that were sold in allotments in terms of mass were considered (those sold in terms of enzyme units were ignored). The activity per mg of each product was recorded along with the respective cost per mg. When the supplier gave an activity range, the lower limit of the range was selected to be the finite activity used in this study. Only enzymes that had reported activities with similar units were compared. A complete list of the data collected is shown in Table 1. The activity units between different enzymes varied because the enzyme activity was generally expressed as the amount of substrate utilized per unit time; however, the amount of substrate and time often varied between enzymes. A complete list of activities for enzymes used in this study is also shown in Table 1.

The data for price per mg for each enzyme were then plotted versus the corresponding activity per mg, and subsequent least-squares regression analysis was then performed. When more data were available for the lower activity purity range, the high purity data were weighted such that the number of high and low purity data points had equivalent power in the regressions, meaning each data set consisted of the same number of data points in the upper and lower purity range. If this normalization is not performed, the low purity data points will not allow the regression function to capture the dynamics associated with the high purity enzyme. Since data cannot be homogenously sampled over the entire activity domain, some form of normalization is necessary to fit the data over the entire activity domain. Performing a regression on the raw data, simply provides an excellent fit to the more numerous low range activity data points, but completely misses the scarce high-activity-range data. For the alpha amylase data, the regression technique was modified to compensate for an excessive number of data points available in the low purity regime. These data points were so low in the activity domain that they were not allowing the regression function to capture the dynamics associated with the high purity enzyme. In other words, the numerous data points for amylase in the low activity range were controlling the dynamics of the regression in the high activity range such that the regression did not fit the moderate to high activity data points. Thus, the three lowest data points were not included in the regression to provide the best qualitative fit to the data over the entire activity domain. All regression analysis was performed with Microsoft Excel Version XP using the built-in least squares algorithm. Several regressions were attempted including

Table 1 Data collected for several enzymes from different suppliers.

Enzyme	Activity (U/mg)	Price ($/mg)	Supplier	Activity unit definition
Invertase	20	0.00005	13	1 U hydrolyzes 1 μmol of saccharose per min
	100	0.01018	10	at pH=4.65 and T=25 °C
	200	0.05700	10	
	300	0.50600	10	
Papain	1.5	0.00072	10	1 U hydrolyzes 1 μmol of *N*-benzoyl-L-arganine-
	3	0.00097	10	ethyl ester per min at pH=6.2 and T=25 °C
	12	0.64983	10	
Elastase	3	1.04333	11	1 U cleaves 1 μmol of *N*-succinyl-L-alanyl-L-
	8	4.00000	11	alanyl-L-alanine-*p*-nitroanilide per min at
	18	1910.0	12	pH=8.0 and T=25 °C
	18	1928.7	9	
Alpha Amylase	1.5	0.00023	10	1 U liberates 1 mg of maltose from starch in
	20	0.09240	10	3 min at pH=6.9 and T=20°C
	30	0.00250	10	
	150	0.41700	10	
	380	0.16800	10	
	500	8.28000	10	
	1,000	97.200	10	
Cellulase	1	0.00223	10	1 U releases 0.01 mg of glucose per hour from
	6	0.00500	9	microcrystalline cellulose at pH=5.0
	25	0.02650	11	and T=37 °C
	45	0.10800	11	
	50	0.91000	8	

power law, exponential, polynomial, and linear fits. Power law regressions seemed to fit the best across all enzymes. This regression expression also passes through point (0,0). A similar algorithm was used to determine the enzyme cost as a function of purchase amount. The data for pricing and mass were normalized to cost per mg and inverse mass to suit the regression type limitations of Microsoft Excel.

Results

We found that there appears to be a generalized model for enzyme cost per mg in terms of enzyme activity. From the analyzed data, this simple two-parameter model follows a power law trend as depicted in the previously described Eq. 2. Here, it is found that a is approximately 3.7±0.6 and tends to vary only slightly from enzyme to enzyme. The parameter a describes the separation (purification) cost of these enzymes, since an increase in activity results in a power law growth in the cost function (the rate at which is controlled by the value of the parameter a). γ is dependent on the method of enzyme production and can vary greatly between enzymes, as shown in Table 2. Indeed, higher production cost, such as mammalian cell culture, will result in a larger value for γ, whereas lower production cost, such as observed in enzymes isolated from plants, generally results in a lower value for γ. This can be seen in Table 2 above, which shows elastase, which was isolated from a pig pancreas has a γ value of 0.005, whereas cellulase isolated from a fungus has a γ value of 3.00E-08. The generalized behavior of the enzymes quantified by γ and a is depicted in Figs. 1, 2, 3, 4 and 5.

Table 2 A list of fitted a and γ values and regression R^2 values for the simplified two parameter objective function model given in Eq. 2.

Parameter values			
	a	γ	R^2
Papain	3.48	8.00E-05	0.92
Elastase	4.32	0.005	0.95
Invertase	3.29	3.00E-09	0.99
Cellulase	4.18	3.00E-08	0.77
Alpha Amylase	3.45	3.00E-09	0.81

The data used to compute these parameters and generate the subsequent plots were collected from [6–10].

The equation relating the bulk price per mg is:

$$\Phi = \delta(M)^b \tag{4}$$

where b=−0.2 and δ=\$2.049 per $mg^{0.8}$ for papain (Figure not shown).

The negative parameter value for b, in Eq. 4, depicts the savings achieved by purchasing in bulk. Significant savings can be achieved when buying bulk enzymes, but this gain may be offset by storage costs. We have not quantified the tradeoffs associated with buying bulk and storage requirements (in Eq. 3). We expect that the parameters for capital costs of storage will vary greatly from facility to facility.

Figure 6 further elaborates on the enzyme cost relationship by segregating the enzyme activity domain into three regimes characterized by the method of separation.

In Fig. 6, the generalized function used was $y=4\times10^{-6}\times x^{3.7}$, where x is the activity per mg, and y is the cost per mg of the generalized enzyme. The parameter values used, γ=4×

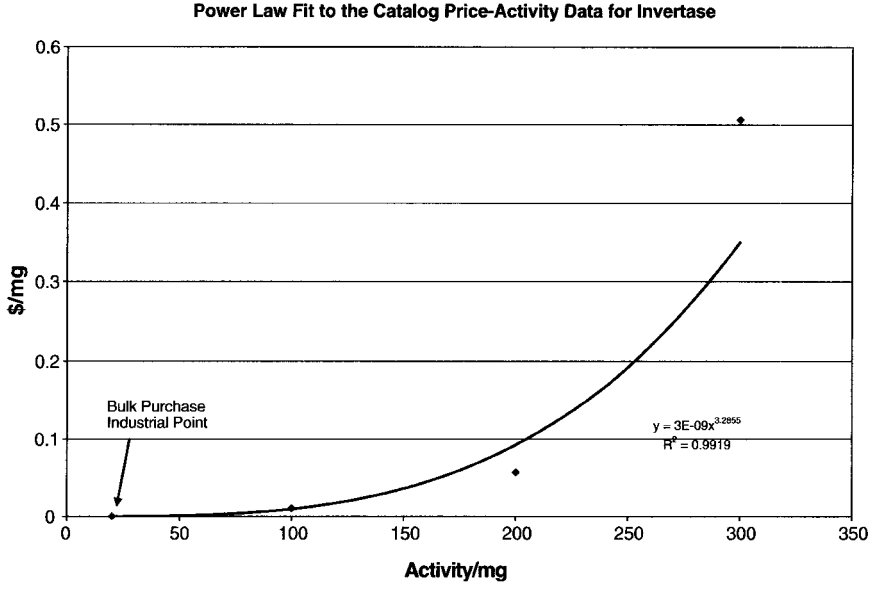


Fig. 1 Power law fit to the catalog price-activity data for invertase

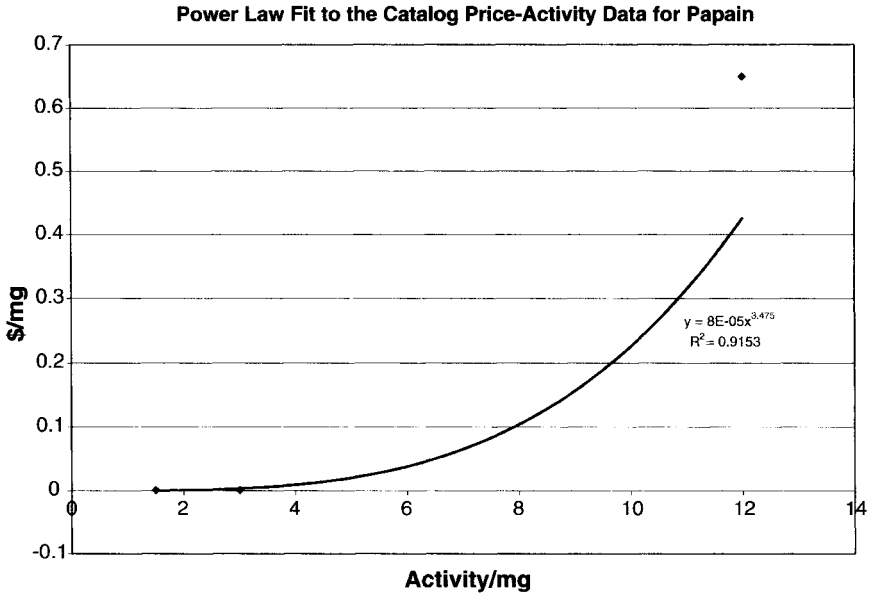


Fig. 2 Power law fit to the catalog price-activity data for papain

10^{-4} and $a=3.7$ were chosen arbitrarily, but lie within the realm of the parameters fitted to the collected data (see Table 2).

We now try to further interpret the possible meaning, in terms of separation cost, of Eq. 3. To do this analysis, we break up the enzyme activity domain into three parts: the low activity-prelinear region, the moderate activity linear region, and the high activity exponential region. We do this based on a general consensus seen within all the collected

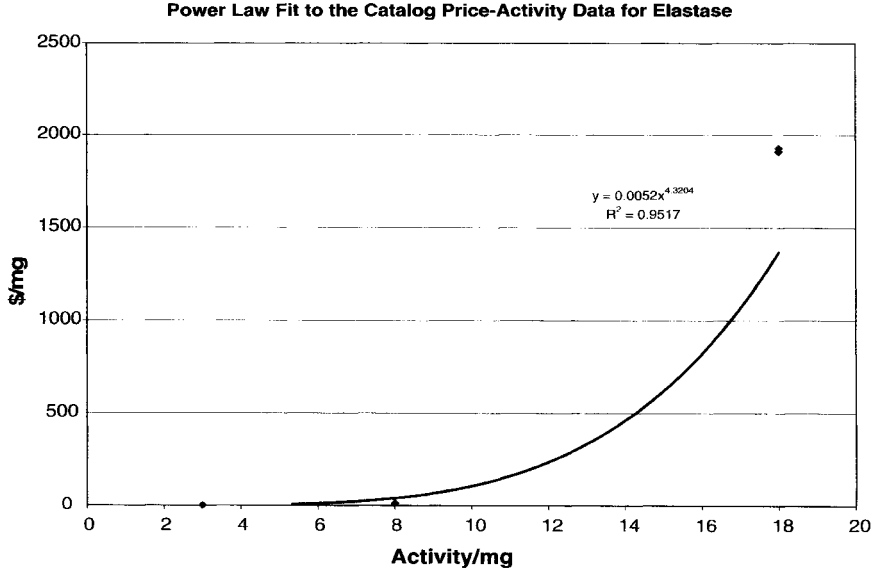


Fig. 3 Power law fit to the catalog price-activity data for elastase

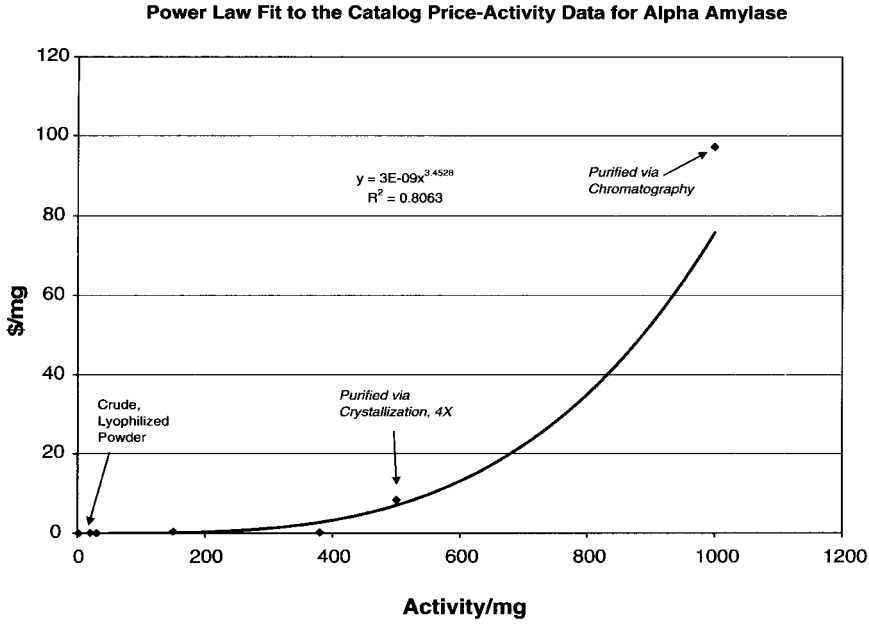


Fig. 4 Power law fit to the catalog pice-activity data for alpha amylase

data that the activity (and price) of each enzyme correlates with the separation techniques used. This correlation can be most easily seen for actual amylase data in Fig. 4.

The initial low activity prelinear region, is characterized by little change in cost per mg as activity per mg is increased. This region appears to be characterized by low purity

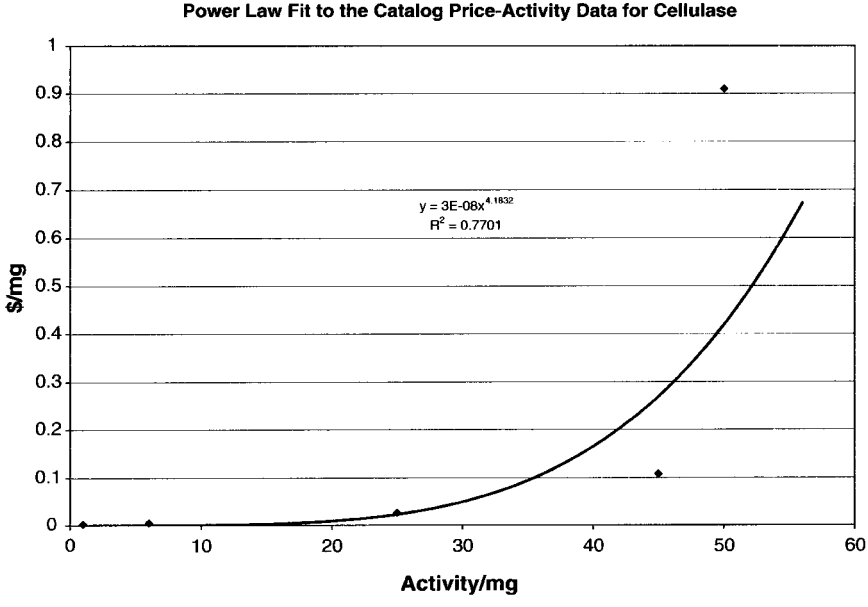


Fig. 5 Power law fit to the catalog price-activity data for cellulase

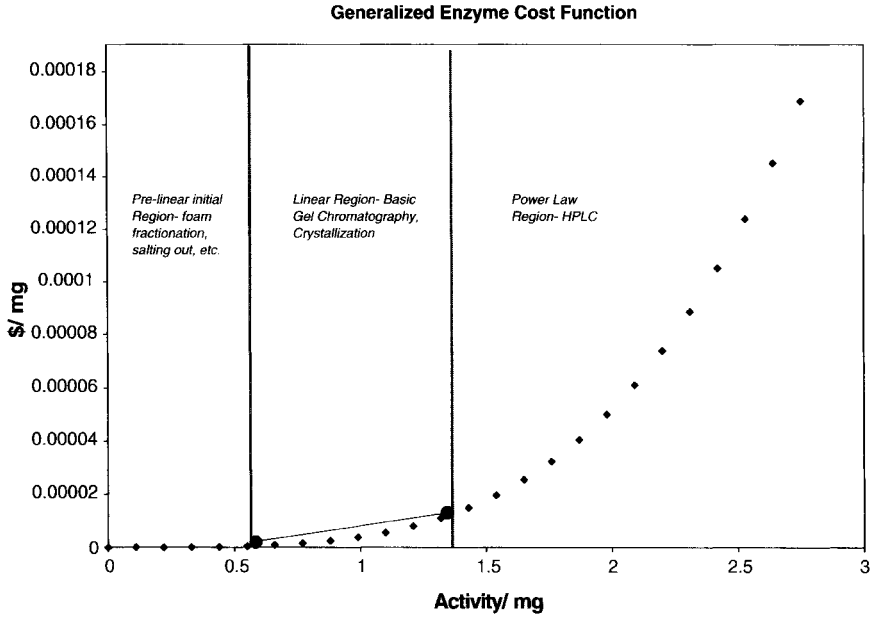


Fig. 6 Generalized enzyme cost function

enzymes harvested from plants (or other readily available sources such as fermentation broths) and purified via traditional low cost processes such as foam fractionation or salting out. These purification processes can be extended at little cost to generate increased enzyme activity. Since the additional processing within this region requires little additional capital cost and only modest operating costs, the change in enzyme cost per mg may be marginal.

The second region, the moderate activity region (linear), is characterized by nearly a linear change, over the narrow band of the $4\times10^{-6}\times x^{3.7}$ function, in cost per mg as activity is increased. This region is generally characterized by moderately pure enzymes that have been purified by more costly processing than the prelinear region. It appears that the majority of enzymes considered in this domain are purified via gel chromatography. The capital and operating costs of this processing are typically higher than the costs associated with foam fractionation and salting out processes [7]. Additional processing, for additional enzyme activity in this middle region where there is moderate activity, requires larger chromatography columns or larger affinity gels whose costs tend to increase linearly in price.

The third domain is characterized by the observable (empirical) power law growth in enzyme cost per mg with respect to activity. This domain extends to the highest purity of the desired enzyme and is generally comprised of enzymes that require expensive processing. The overall processing is thus generally a combination of salting out, foam fractionation, and multistage gel chromatography, but often includes a final purification step, which is generally HPLC. The capital and operating costs for HPLC are significantly higher than that of the other mentioned purification processes. Additional purification through HPLC generally requires running a sample multiple times on additional columns. During each step of HPLC, a large fraction of the enzyme is lost due to the inefficiencies of the process, making the increased cost per mg behave like a power law function when several steps are used in series.

The derivative of the generalized cost function shows the incremental change in cost as activity is increased. This derivative function, represented as $y=1.5\times10^{-5}\times x^{2.7}$ leads to some key observations. For example, the power law exponent is still larger than one. This observation holds for every enzyme analyzed in this study, which increases our confidence in the analysis of these enzymes. Even with a power greater than one, the cost will only change minimally with activities smaller than unity. Above unity, there will be a small region where price will increase only marginally as a function of activity. However, regardless of the value of the preexponential parameter, at some threshold where the activity per mass is greater than unity, the enzyme cost will begin increasing significantly and exponentially as a function of enzyme activity.

Conclusions

The significant conclusion and most interesting observation of this study is that there appears to be one simple function that estimates the cost of an enzyme in $ per mg as a function of activity, $\Phi=\gamma\,(A)^a$, where a appears to be a generalizable exponent of the order 3.7. The generalizable function appears to fit best over the low to moderate activity range, but often under-predicts enzyme cost in the high activity range. This implies that there may not be a simple two-parameter model that accurately captures the dynamics of enzyme activity related to cost over the entire activity domain. Additional data in the moderate to high activity range are needed to further characterize the limitations of Eq. 2. However, the function developed in this analysis is still useful as an estimation tool where little or no real data may be known.

The generalizable function can furthermore be analyzed in terms of three characteristic domains describing the enzyme cost with respect to activity. These domains can be useful when purchasing enzymes for industrial or laboratory purposes. For example, if a low purity enzyme is being purchased, it is logical to purchase the enzyme at that purity equivalent to the end of the prelinear phase of the generalized enzyme curve, denoted by the critical point located near an activity per mass ratio of 0.5 on the generalized enzyme cost function plot (Fig. 6), giving the buyer the most amount of active enzyme at a very low cost. A complimentary strategy for high purity enzymes would be to choose the activity of the upper end of the moderate activity linear range (the lower end of the high activity exponential domain). If processing cost is dependent on enzyme impurities, the cost of processing can be compared to the cost of increasing enzyme activity, by using Eq. 2 in a manner to minimize overall costs. Since the parameter a generally ranges between 3 and 4 between enzymes, a twofold increase in activity is generally associated with an eightfold increase in cost.

Since the parameters determined within this study were empirically computed from current market prices, these parameters are likely to change over long time-scales given the dynamic nature of any economic market. The enzymes used for this analysis are generally widely used proteins that, therefore, have fairly stable, well-developed markets. Enzymes used in small quantities for less industrial purposes may not follow similar trends since market fluctuations can be significant. This allows industrial enzymes to be best suited for this type of study since their market will be less dynamic than other enzymes that are still within market development. However, economies of scale will still play a factor, especially in enzymes that are expected to see a wide increase in use and production scale-up, such as cellulase. These changes will likely result in a scaling factor that will linearly decrease the value of γ. This observation is drawn from analyzing scale-up cost for typical bioprocessing

operations involved in enzyme purification that show linear cost reductions as scale increases [14]. Similarly, this observation can be made by looking at typical equipment scale-up cost. One of the most common protein purification methods is liquid chromatography [15]. Chromatography columns tend to scale up linearly since the capital cost for the column is minimal compared to the high resin cost, which is required in directly proportional amounts to column throughput. Scale-up of enzyme production is generally sublinear, but the data presented in this analysis demonstrates that purification costs tend to dominate overall product cost [15]. Regardless of changes in scaling due to market growth and scale-up, the functional forms determined for the relationship of enzyme activity and purchase amount to price should hold. The independent variables within Eq. 2 were shown to be directly related to the process variables for enzyme production. Although the model under-predicts enzyme cost for the high activity range, Eq. 2 still provides a useful tool for engineers to estimate enzyme cost based on activity.

References

1. Cherry, J., Ko, S., Grainger, R., Prokop, A., & Tanner, R. (2000). Developing an objective function to characterize the tradeoffs in salting out and the foam and droplet fractionation processes. *Brazilian Journal of Chemical Engineering, 17*, 233–238.
2. Zhang, Q., Lo, C.-M. & Ju, L.-K. (2007). Factors affecting foaming behavior in Cellulase fermentation by *Trichoderma reesei* Rut C-30. *Bioresource Technology, 98*(4), 753–760.
3. Lo, C.-M., Zhang, Q., Lee, P., & Ju, L-K. (2005). Cellulase production by *Trichoderma reesei* using Sawdust Hydrolysate. *Applied Biochemistry and Biotechnology, 121–124*, 561–573.
4. Graff, G., "Pharma Market Spur Increased Enzyme Demand" 3/1/2007 http://www.purchasing.com/article/CA6419082.html.
5. Poulsen, P. (1987). Trends in industrial applications of enzymes. Annals of the New York Academy of Sciences. *Enzyme Engineering, 501*, 413–419.
6. Nilesh; A., Kamat, M., & Arvind, L. (2004). Expanded bed affinity purification of bacterial α-amylase and Cellulase on composite substrate analogue-Cellulose matrices. *Process Biochemistry, 39*, 565–570.
7. Zhang, Q., Lo, C.-M., & Ju, L.-K. (2006). Affinity foam fractionation of Trichoderma Cellulase. *Applied Biochemistry and Biotechnology, 129–132*, 1051–1065.
8. Carolina Biochemical Corporation. http://www.carolina.com. (catalog information on enzymes). 4/1/07.
9. Fisher Scientific. http://new.fishersci.com. (catalog information on enzymes). 4/1/07.
10. Sigma-Aldrich Corporation. http://wwwsigmaaldrich.com. (catalog information on enzymes). 4/1/07.
11. Worthington Biochemical Corporation. http://www.worthington-biochem.com. (catalog information on enzymes). 4/1/07.
12. Elastin Products Company, Inc. http://www.elastin.com (catalogue information on enzymes) 4/1/07.
13. "Enzymatic Production of Invert Sugar", Ensymm Consulting for Biotechnology (2007). http://www.ensymm.com/pdf/ensymmProjectstudyreportInversugarproduction.pdf.
14. Cacciuttolo, M., & Arunakumari, A., " Scale-Up Considerations for Biotechnology-Derived Products" http://biomedical.rutgers.edu/doc/Scale%20Up%20of%20Biotechnology%20Products.pdf.
15. Blanch, H., & Clark, D. (1997). *Biochemical Engineering*. New York, NY: Marcel Dekker, pp. 678–682.

Appl Biochem Biotechnol (2008) 147:119–131
DOI 10.1007/s12010-007-8070-6

Reaction Kinetics of the Hydrothermal Treatment of Lignin

Bo Zhang · Hua-Jiang Huang · Shri Ramaswamy

Received: 7 May 2007 / Accepted: 27 September 2007 /
Published online: 23 October 2007
© Humana Press Inc. 2007

Abstract Lignins derived from abundant and renewable resources are nontoxic and extremely versatile in performance, qualities that have made them increasingly important in many industrial applications. We have shown recently that liquefaction of lignin extracted from aspen wood resulted in a 90% yield of liquid. In this paper, the hydrothermal treatment of five types of lignin and biomass residues was studied: Kraft pine lignin provided by MeadWestvaco, Kraft pine lignin from Sigma-Aldrich, organosolv lignin extracted from oat hull, the residues of mixed southern hardwoods, and switchgrass after hydrolysis. The yields were found dependent on the composition or structure of the raw materials, which may result from different pretreatment processes. We propose a kinetic model to describe the hydrothermal treatment of Kraft pine lignin and compare it with another model from the literature. The kinetic parameters of the presented model were estimated, including the reaction constants, the pre-exponential factor, and the activation energy of the Arrhenius equations. Results show that the presented model is well in agreement with the experiments.

Keywords Hydrothermal treatment · Degradation · Kinetic model · Kraft lignin · Biomass residue

Introduction

In the past decade, biomass feedstock, as an abundant, inexpensive and renewable resource, has emerged as an attractive alternative resource for producing easy-to-handle forms of

B. Zhang (✉)
BioTechnology Institute, University of Minnesota, 140 Gortner Labs, 1479 Gortner Avenue, St. Paul, MN 55108, USA
e-mail: zhan0260@umn.edu

H.-J. Huang · S. Ramaswamy
Department of Bioproducts and Biosystems Engineering, University of Minnesota, Kaufert Lab, 2004 Folwell Avenue, St. Paul, MN 55108, USA

energy such as gases, liquids, and charcoal. Cellulose and lignin represent two of the most prominent renewable carbon sources. Lignin, a second to cellulose as the most plentiful renewable carbon source on Earth, is an amorphous three-dimensional energy-rich phenolic biopolymer, which is deposited in all vascular plants and provides rigidity and strength to their cell walls. Currently, a limited supply of lignin is available as a by-product of the pulp and paper industry. However, in the near future, large quantities of lignin residue material will be available from biomass-to-ethanol processes and other biorefineries and associated processes [1].

So far, because it is an inexpensive feedstock, lignin is commonly used by combustion to provide heat and/or power. In general, however, using lignin for recovery of heat and power is not so economical because it can be used as a source of aromatic compounds. Therefore, it is very important to explore emerging technologies such as pyrolysis and gasification to produce multiproducts and obtain higher values. For example, liquefaction of lignin extracted from aspen wood resulted in a 90% yield of liquid, representing a significant added value, according to our recent research [2]. Converting lignin to higher-value fuel additives can significantly enhance the competitiveness of biorefinery technology. For this paper, the hydrothermal treatment of five types of lignins or biomass residues was studied. The liquid compounds produced by the reactions were identified by gas chromatography-mass spectroscopy (GC-MS). A kinetic model for the hydrothermal degradation of lignin was also presented and compared with another model from the literature. All the kinetic parameters of the presented model were estimated.

Materials and Methods

Materials

Indulin AT®, called Kraft pine lignin A in this study, was provided by MeadWestvaco. Kraft pine lignin B (catalog number 471003) was ordered from Sigma-Aldrich (St. Louis, MO, USA). Organosolv lignin was extracted from oat hull. The residues of mixed southern hardwoods and switchgrass, which were treated using a two-stage dilute acid hydrolysis process, were provided by the Tennessee Valley Authority.

Biomass Analytical Procedures

Moisture and ash content of the biomass were determined by the methods of LAP-001 and LAP-005, respectively, which are laboratory analytical procedures developed by the National Renewable Energy Laboratory. Structural analyses of the samples were carried out according to the American Society for Testing and Materials E1758–01 standard test methods. The composition of raw materials is listed in Table 1. The solubility of Kraft pine lignin A at room temperature is listed in Table 2.

Apparatus and Process

A 75-ml Parr high-pressure reactor (Parr Instrument, Moline, IL, USA) was used for hydrothermal treatment of the feedstock. The reactor consists of a reaction cylinder and a pressure gauge/valve assembly. An induction heating system, which allows the reduction of heat-up times by about two orders of magnitude, was customized by L.C. Miller, Monterey Park, CA, USA. For a typical run, 5 g of feedstock and 45 ml of distilled water were placed

Table 1 The composition of various lignocellulosic biomasses (air dried, % by weight).

	Kraft pine lignin A[a]	Kraft pine lignin B[b]	Organosolv lignin of oat hull	Hardwood residue	Switchgrass residue
Glucan	–	–	11.1	47.5	22.5
Xylan	–	–	30.9	7.6	2.3
Galactan	–	–	3.6	1.8	2.1
Arabinan	–	–	5.5	0.8	1.8
Mannan	–	–	–	0.8	2.9
Klason lignin	92.3	91	39.3	32.2	41.1
Sulfur	2.1	3.3	–	–	–
Moisture	5.6	5.7	6.1	5.2	3.1
Ash	–	–	1.4	0.94	23.2

– Not detectable

[a] Structural analyses were provided by MeadWestvaco.

[b] Structural analyses were provided by Sigma-Aldrich.

inside the cylinder. The cylinder was then sealed and purged with nitrogen gas at a flow rate of 80 ml/min to remove air and prevent secondary reactions such as thermal cracking and repolymerization. The reactor was heated to 300–374 °C at a heating rate of about 140 °C/min, and the desired temperature was held for 10 min. At the end of the reaction, the cylinder was cooled by soaking it in an ice bath for 5 min. Gases were sampled into a gas bag for later GC analysis. The gas fraction was determined by measuring the weight difference of the reactor before and after gas sampling. The liquid, including both water and heavy oil fractions, was collected for later GC-MS analysis. The procedure for separating of aqueous, water-insoluble, and solid phases in the liquid is shown in Fig. 1. First, the aqueous phase (approximately 50 ml) was poured into a centrifuge bottle. The water-insoluble fraction and the wall of the pressure reactor were washed with 50 ml acetone, then poured into the centrifuge bottle containing the aqueous phase, and centrifuged. The total amount of the supernatant liquid was referred to as the liquid fraction. The liquid fraction was air-dried at room temperature for 48–72 h to constant weight. The remaining solid after centrifugation was air-dried for 48–72 h to constant weight to yield the solid residue. Constant weight is defined as less than ±0.01 g change in the weight upon 12 h of re-drying the liquid or the residue.

The yield of each fraction from the hydrothermal treatment reaction is defined as:

$$\text{Gas yield}\,(\%) = (\text{weight of gas/weight of starting biomass}) \times 100$$

$$\text{Residue yield}\,(\%) = (\text{weight of residue/weight of starting biomass}) \times 100$$

$$\text{Liquid yield}\,(\%) = \begin{pmatrix} 1 - \text{weight of gas/weight of starting biomass} \\ - \text{weight of residue/weight of starting biomass} \end{pmatrix} \times 100$$

$$\text{The air-dried liquid yield}\,(\%) = (\text{weight of air - dried liquid/weight of starting biomass}) \times 100$$

The formula of liquid yield is universally true for the hydrothermal treatment process of biomass or biomass residues. However, because of Kraft pine lignin's unique solubility (Table 2), the formula of liquid yield can only be applied to Kraft pine lignin after the

Table 2 Solubility of Kraft pine lignin A at room temperature.

Solvent	Solubility (% *w/w*)
Water	2.8
Acetone	1.3
Methanol	3.4
Water/acetone (1:1)	>15

reaction reached the steady state. The difference between the liquid yield and the air-dried liquid yield is considered to be the moisture in the raw materials and volatile components of the liquid products. All experiments and analysis were performed in triplicate.

Chemical Analysis

The gaseous samples were analyzed using GC with MS5A, Pora PLOT Q (PPQ), and WAX columns and a thermal conductivity detector for the analysis of hydrogen, carbon monoxide, carbon dioxide, methane, and other gases [3]. The volume concentration of each gas of interest was calculated based on an external standard method.

Chemical compositions of the liquid products were identified using a Varian Saturn 3 GC/mass spectrometer with a HP-1 capillary column. The GC was programmed at 40 °C for 0.5 min and then increased at 10 °C/min to 300 °C, and finally held with an isothermal for 10 min. The injector temperature was 300 °C, and the injection size was 1 μl. The flow rate of the carrier gas (helium) was 0.6 ml/min. The ion source temperature was 230 °C for the mass-selective detector. The compounds were identified by comparison with the National Institute of Standards and Technology (NIST) Mass Spectral Database.

Results and Discussion

Mass Balance

The hydrothermal treatment process produces a gaseous phase, a solid phase, and a liquid phase. The gaseous and solid products were weighted directly. The liquid fraction was dried to yield the air-dried liquid. As shown in Table 3, the total amount of gaseous products,

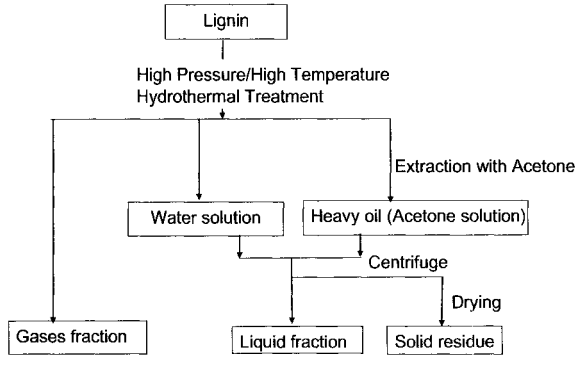


Fig. 1 Process for product separation after hydrothermal treatment

Table 3 Hydrothermal treatment of lignins and biomass residues at 374 °C.

	Hydrothermal treatment yield (% of total mass)				Gas yield (% of the total gaseous products)			
	Residue	Liquid	Gas	Air-dried liquid	H_2	CO	CH_4	CO_2
Kraft pine lignin A	37.6±1.3	57.8±2.1	4.6±1.6	33.9±2.2	3.0±1.1	7.4±3.3	12.7±2.2	76.9±4.1
Kraft pine lignin B	22.3±3.3	71.5±3.4	6.2±3.2	58.8±2.1	5.6±0.9	6.2±2.5	10.6±2.8	77.6±4.4
Organosolv lignin of oat Hull	12.1±2.7	79.1±2.8	8.8±3.7	42.8±6.1	2.1±0.9	19.7±3.2	0.3±0.2	77.9±4.9
Hardwood residue	24.2±3.1	56.3±5.1	19.4±2.0	17.6±1.7	3.8±1.2	22.9±3.4	8.0±0.7	65.3±3.7
Switchgrass residue	48.8±2.2	32.6±5.6	18.6±5.4	15.2±1.5	2.7±0.7	25.3±3.6	7.9±2.4	64.1±4.5
Aspen lignin[a] [2]	3.8±1.6	90.2±2.2	5.9±2.6	78.0±2.1	7.6±2.3	7.7±0.7	13.3±2.0	71.4±3.6

[a] Aspen lignin was treated at 350 °C for 10 min.

solid phase and air-dried liquids corresponds to 70–90% of the starting biomass. The other 10–30% is considered to be the result of moisture in the raw material that is 5–6% generally (Table 1) and volatile components in the liquid products, such as acetic acid, furfural, and guaiacol.

Thermochemical Conversion of Lignins and Biomass Residues

Lignins and biomass residues were treated at 374 °C and 22 MPa for 10 min. The yields of various lignins and biomass residues are listed in Table 3. The liquid yields of Kraft pine lignin A, Kraft pine lignin B, organosolv lignin of oat hull, hardwood residue, and switchgrass residue were 57.8, 71.5, 79.1, 56.3, and 32.6%, respectively.

The residue yields of Kraft pine lignins A and B, hardwood, and switchgrass were relatively high; a possible reason is that these raw materials were pretreated using either a pulping or hydrolysis process, which may result in unique structure of the raw materials. Another reason for the high residue yield from switchgrass is that it contains significant amount of ash, which is 23.2% of the total biomass. The ash in the switchgrass may be due to soil contamination. The yield of gaseous products from the lignins was 6–7% of the total biomass; applying a gasification process may require extremely high temperature or energy input.

Hardwood and switchgrass residues after a two-stage hydrolysis still contain significant amounts of cellulose (22–47%) and hemicellulose (9–11%). Hydrothermal treating fractions containing cellulose and/or hemicellulose resulted in a high yield of residue and gases. Our experiments reveal that a better pretreatment process needs to be developed.

Organosolv lignin of oat hull contains high amount of hemicellulose (~40%). When using organosolv lignin of oat hull as the raw material, the liquid products contain more volatile components than found using other materials; liquid products accounting for approximately 36% of the total mass were evaporated during the drying process.

The gaseous phase from hydrothermal treatment of lignins and biomass residues primarily consisted of hydrogen (H_2), carbon monoxide (CO), methane (CH_4), and carbon dioxide (CO_2), which were 2.1–7.6, 6.2–25.3, 0.3–13.3, and 64.1–77.9%, respectively (Table 3).

GC-MS Analysis of the Liquid Products

The components of the liquid products from various lignins and biomass residues were determined by GC-MS analysis. The mass-to-charge ratios of the components were checked

Table 4 The composition (% area) of the liquid products[a].

Retention time (min)	Possible structural formula	Chemical name	Kraft pine lignin A[b]	Organosolv lignin of oat hull	Hardwood residue	Switchgrass residue
3.3	$C_2H_4O_2$	Acetic acid	–	24.6	22.3	10.7
3.8	$C_3H_6O_2$	1-Hydroxy-2-propanone	–	6.8	2.6	0.9
7.5	$C_5H_4O_2$	Furfural	–	14.6	17.0	–
7.9	$C_6H_{12}O_2$	4-Hydroxy-4-Methyl-2-pentanone	1.7	–	–	–
10.0	$C_6H_{10}O_2$	2,5-Hexanedione	–	–	6.8	–
11.1	C_6H_6O	Phenol	–	–	–	1.5
12.9	$C_7H_8O_2$	Guaiacol	60.0	9.9	11.5	36.4
14.3	$C_8H_{10}O$	4-Ethyl-phenol	–	10.5	–	4.8
14.6	$C_8H_{10}O_2$	2-Methoxy-4-Methyl-phenol	0.7	3.6	3.7	14.7
15.9	$C_9H_{12}O_2$	4-Ethylguaiacol	10.6	17.9	3.7	16.9
16.6	$C_9H_{10}O_2$	2-Methoxy-4-vinylphenol	0.6	5.6	–	–
17.1	$C_8H_{10}O_3$	2,6-Dimethoxy-phenol	–	1.8	19.0	10.0
17.3	$C_{10}H_{14}O_2$	2-Methoxy-4-propyl-phenol	3.3	–	–	–
17.9	$C_8H_8O_3$	Vanillin	1.0	–	–	–
18.2	$C_9H_{12}O_3$	4-Methoxy-3-(methoxymethyl)-phenol	–	1.4	7.6	1.5
18.5	$C_{10}H_{12}O_2$	2-Methoxy-4-(1-propenyl)-(*e*)-phenol	1.4	–	–	–
18.9	$C_9H_{10}O_3$	1-(4-Hydroxy-3-methoxyphenyl)-ethanone	1.0	–	–	–
19.2	$C_{10}H_{14}O_3$	1,2,3-Trimethoxy-5-methyl-benzene	–	2.0	2.8	2.6
19.4	$C_{10}H_{12}O_3$	1-(4-Hydroxy-3-methoxyphenyl)-2-propanone	2.9	–	–	–
20.2	$C_{15}H_{16}$	1-Ethyl-3-(phenylmethyl)-benzene	–	1.3	1.1	–
20.9	$C_9H_{10}O_4$	4-Hydroxy-3-methoxy-benzeneacetic acid	3.4	–	–	–
22.2	$C_{11}H_{14}O_4$	Desaspidinol	–	–	1.9	–
25.6	$C_{16}H_{14}O_6$	1-Hydroxy-3,5,6-trimethoxy-9*h*-xanthen-9-one	2.8	–	–	–
27.5	$C_{21}H_{30}O_2$	Methyl dehydroabietate	10.6	–	–	–

– Not detectable

[a] The ratio was normalized in the detectable components.

[b] The composition of the liquid products from Kraft pine lignin B is similar to Kraft pine lignin A.

against the mass spectral library published by NIST. The GC peak areas are given in Table 4. The percentage values indicate the proportions of individual compounds in the liquid and do not represent the actual concentration of these compounds.

Within the GC detectable range, we identified the different composition of the liquid products from the various origins by using a GC-MS analysis. The liquid products from Kraft pine lignin contain mainly guaiacol and methyl dehydroabietate. The liquid products from oat hull, hardwood, and switchgrass contain acetic acid, 1-hydroxy-2-propanone, and/or furfural, which are the products of hemicellulose and cellulose. This further confirms that these three materials contain hemicellulose and cellulose. The liquid products have only two to three component differences from one biomass species to another. But the composition distributions are quite different among species (Table 4). So the composition of liquid products depends on the type of raw materials.

The liquid products from lignins may include high-molecular weight compounds that are not volatile and not detected by GC. To determine the degradation degree of Kraft lignin, polymer techniques, such as low-angle light scattering, need to be applied.

Effect of Time on the Hydrothermal Treatment of Kraft Pine Lignin A

The hydrothermal treatment was carried out using the designed batch pressure reactor equipped with an induction heating system. The heating time required to reach the final temperatures of 300 °C (10 MPa) and 374 °C (22 MPa) was 2.5 and 3 min, respectively. At the end of the chosen time of hydrothermal treatment, the reaction was stopped by putting the reactor in an ice bath. The aqueous phase (approximately 50 ml) was poured into a centrifuge bottle. The water-insoluble fraction and the wall of the pressure reactor were washed with 50 ml acetone and poured into the centrifuge bottle containing the aqueous phase, which resulted in a solution containing 50% water and 50% acetone, and then centrifuged. The solubility of Kraft pine lignin A in this mixture is greater than 15%, so the remaining residues were considered to be the charcoal or polymeric products produced by the hydrothermal treatment process.

Figure 2a shows the residue yields for treating Kraft pine lignin A at 300 and 374 °C, respectively. At 300 °C, the reaction reached the steady state within 12 min after the final temperature was reached (total approximately 15 min). The reaction was faster at 374 °C and reached the steady state within 3 min after the final temperature was reached (total approximately 6 min). The yields of gaseous products showed similar results (Fig. 2b). But the length of treatment time does not show obvious effects on the profile of gaseous products (Fig. 2c).

Mechanism of the Hydrothermal Treatment of Kraft Pine Lignin

The mechanism of degradation of poplar lignin was proposed by Bobleter and Concin [4]. They proposed a degradation mechanism consisting of two-phase reactions for the hydrothermal degradation of poplar lignin: first, a very fast reaction phase where lignin is degraded into the soluble fragments and then a slower reaction phase where the soluble fragments react with one another by recondensation. By observing the yields and GC-MS analysis of liquid products, hydrothermal treatment of Kraft pine lignin was found to follow similar mechanisms. The solubility of Kraft pine lignin in water is 2.7% at room temperature. With increasing temperature, the Kraft lignin becomes more water soluble within a very short time. Then there is a slow reaction phase, in which the Kraft lignin is degraded into small molecule compounds as shown by the GC peaks in Fig. 3a and b, and

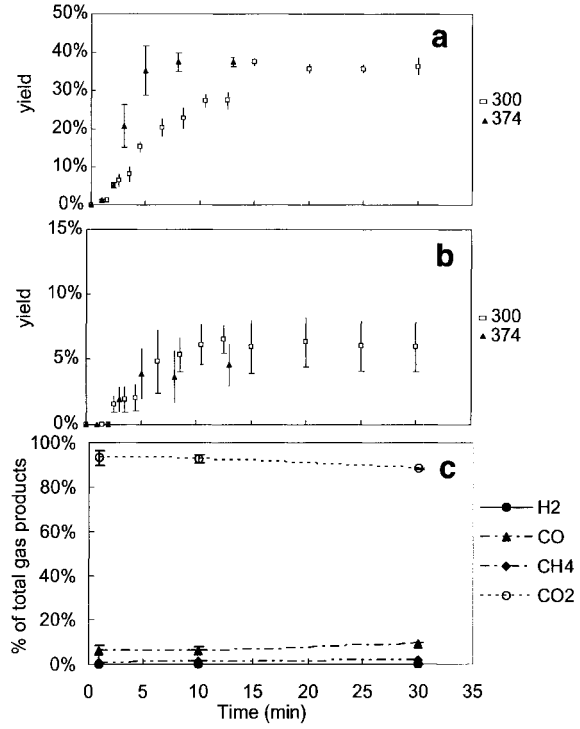


Fig. 2 Effect of time on the hydrothermal treatment of Kraft pine lignin A. **a** The yields of residue at 300 °C and 374 °C. **b** The yields of gases at 300 °C and 374 °C. **c** The yield of gaseous products. *Error bars* represent standard deviations calculated from the data obtained from at least three repeated experiments

these compounds interact and repolymerize or recondense into solid residue. As shown in Fig. 3c and d, most small-molecule compounds are gone after the elongated time except guaiacol and methyl dehydroabietate.

Kraft lignin refers to the lignin degradation products in spent liquors after pulping. During pulping, lignin undergoes more or less drastic degradation reactions depending on

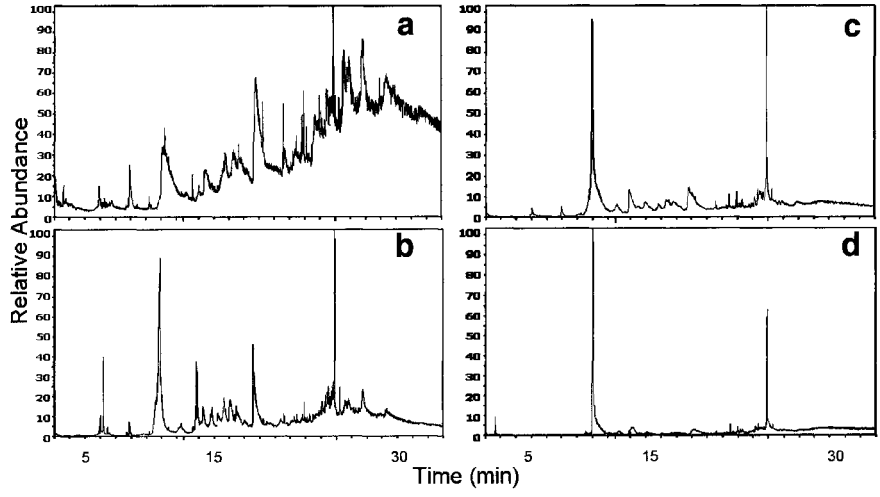


Fig. 3 GC snapshots of the liquid products from Kraft pine lignin A. Kraft pine lignin A was treated at 300 °C and 10 Mpa for 2 min **a**, 4 min **b**, 10 min **c** and 30 min **d**

the pulping conditions. The composition of Kraft lignin differs markedly from the composition of the native lignin [5]. The mechanism proposed here may not be applied directly to other biomasses or native lignin, but it gives a clue how the hydrothermal treatment process works.

Kinetic Model of the Hydrothermal Treatment of Kraft Pine Lignin

Detailed kinetic modeling of lignin hydrothermal treatment is very difficult because lignin can be degraded into tens of components as shown in Table 4, resulting in a large number of chemical reactions between different components in the reaction mixture. Therefore, few papers have been published on this, and lignin hydrothermal treatment or degradation is usually simulated kinetically with simplified models.

One of the simplified models is based on the mechanism of two-phase reactions, i.e., the fast and the slow reaction phases, at temperature in the range of 300–380 °C. In the first phase, lignin is degraded into soluble fragments, mainly consisting of low molecular components (e.g., monomers) and higher molecular components (oligomers). Almost all of the lignin was degraded in about 1 min, according to Bobleter and Concin [4]. Then, the reaction occurs in a slower phase where insoluble polymers and char were produced by condensation between soluble components and/or insoluble polymers.

For the fast degradation phase,

$$L \xrightarrow{k_1} L_L + L_H = L_S \tag{1}$$

where L represents lignin; L_L=low molecular fragments (mostly water-soluble monomers); L_H=higher molecular fragments (oligomers); and L_S=the sum of low and higher fragments (L_L+L_H) that are acetone–water soluble. In our case, L_S represents the liquid fractions, and k_1=reaction rate constant.

According to Eq. 1, the reaction rate for lignin is

$$\frac{d[L]}{dt} = -k_1[L] \tag{2}$$

Where $[L]$ is the lignin concentration in the lignin percent by weight at time t of the initial amount of lignin. The other concentration variables are in this same unit.

For the slow degradation phase, we assume that a part (c) of the soluble fragments reacts with all soluble components in the reaction mixture to form the insoluble polymers and char (P_L), i.e.,

$$c \cdot L_S + L_S \xrightarrow{k_2} P_L \tag{3}$$

in which k_2=reaction rate constant.

$$\frac{d[P_L]}{dt} = ck_2[L_S]^2 \tag{4}$$

Let $k_3=ck_2$, then

$$\frac{d[P_L]}{dt} = k_3[L_S]^2 \tag{5}$$

Based on the total balance, we have

$$[L] + [L_S] + [P_L] = [L_0] \tag{6}$$

Differentiation of both sides of Eq. 6 over time leads to

$$\frac{\partial[L]}{\partial t}+\frac{\partial[L_S]}{\partial t}+\frac{\partial[P_L]}{\partial t}=0 \tag{7}$$

Substitution of Eqs. 2 and 5 into 7 yields

$$\frac{\partial[L_S]}{\partial t}=k_1[L]-k_3[L_S]^2 \tag{8}$$

Therefore, Eqs. 2, 5, and 8 together form the whole kinetic model, which is called model 1 in this study.

Bobleter and Concin [4] used another model to simulate the degradation kinetics of poplar lignin. They assumed the insoluble polymer (P_L) exists during the first phase of quick reaction as a homogeneous suspension (P_L^*), which also reacts with the reactive soluble part ($c{\cdot}L_S$). Thus, $c{\cdot}L_S$ is able to react with both the soluble (L_S) and the suspended products (P_L^*), the sum of which corresponds to the total initial amount of lignin (L_0):

$$c\cdot L_S+L_0\xrightarrow{k_2'}P_L \tag{9}$$

From Eq. 9, the reaction rate for P_L is obtained:

$$\frac{d[P_L]}{dt}=ck_2'[L_0][L_S] \tag{10}$$

Let $k_3'=c[L_0]k_2'$, then

$$\frac{d[P_L]}{dt}=k_3'[L_S] \tag{11}$$

Derivation with steps similar to those for Eq. 8 yields

$$\frac{\partial[L_S]}{\partial t}=k_1[L]-k_3'[L_S] \tag{12}$$

Therefore, the whole kinetic model presented by Bobleter and Concin [4], called model 2 in this study, consists of Eqs. 2, 11, and 12.

Those two models are two sets of ordinary differential equations. As there is no dynamic data available for the first short-term (less than 1.5 min) phase, and according to the theory

Table 5 Estimated kinetic parameters (95% confidence intervals).

	300 °C		374 °C	
	Parameters (min^{-1})	SS	Parameters (min^{-1})	SS
Model 1	k_3=0.030±0.006	0.030	k_3=0.072±0.047	0.032
Model 2	k_3'=0.023±0.005	0.049	k_3'=0.053±0.027	0.043

SS Sum of the squares of the differences/residues between the model and the experimental values

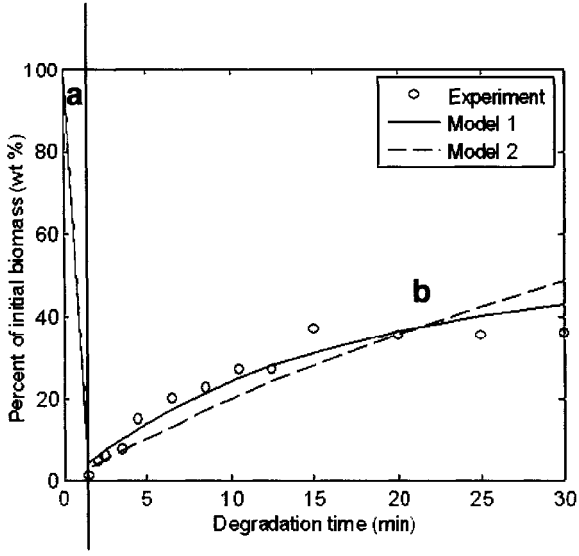


Fig. 4 Comparison of residues from the experiments, model 1, and model 2 at 300 °C. **a** Lignin degradation; **b** residue formation

of Bobleter and Concin [4], 90% of lignin was degraded within the first 1 min, k_1 in both models was first estimated by using Eq. 2 and assuming that 95% of Kraft lignin is degraded to the water-soluble form within the first 1.5 min, i.e., (t=0, L=1) and (t=1.5 min, L=5/100). The obtained k_1 is k_1=2.95 min^{-1}. Then, this value of k_1 was fixed when estimating the other parameters (k_3 or k_3') afterwards.

The unknown kinetic parameters (k_3 or k_3') of models 1 and 2 were estimated by the method of nonlinear least squares, in combination with solving the ordinary differential

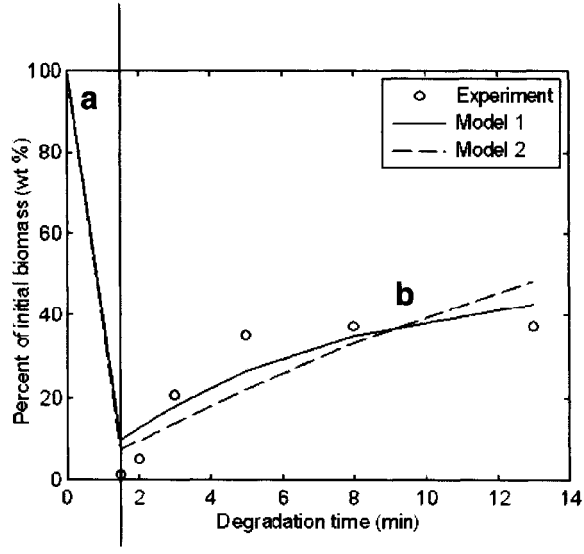


Fig. 5 Comparison of residues from experiments, model 1, and model 2 at 374 °C. **a** Lignin degradation; **b** residue formation

equations. The objective function for estimation of kinetic parameters by optimization (nonlinear least squares) is

$$\min_{k_3 \text{ or } k_3'} \sum_{i}^{N} \left(R_{\text{Cal},i} - R_{\text{Exp},i}\right)^2 \tag{13}$$

where N is the total number of experiments, the subscripts "Cal" and "Exp" represent the calculation values by the model and the experimental data, respectively, and R is the residues, i.e., the sum of undegraded lignin and the insoluble products:

$$R_i = L_i + P_{\text{L},i} \tag{14}$$

The parameters obtained are listed in Table 5.

Figure 4 shows the comparisons of residues for the experiments, model 1, and model 2 at 300 °C. The residue yield profiles at 374 °C (Fig. 5) has the same trend as seen in Fig. 4.

Table 5 shows that model 1 is better than model 2 because it has a smaller value of the sum of the squares of the residues/differences between the model and the experimental values. Figures 4 and 5 also show that the experimental data are better fitted to model 1 than to model 2.

It was proved that the lignin degradation can follow the Arrhenius equation [6]. Therefore, for model 1 to be used to predict lignin hydrothermal degradation, it is necessary to further estimate the pre-exponential factor (k_0) and the activation energy (E_a) in the Arrhenius equation

$$k = k_0 \exp\left(-\frac{E_a}{RT}\right) \tag{15}$$

By using Eq. 15 and the data of Table 5, k_0 and E_a were estimated for k_3 in model 1: k_0= 70.2 l/min, E_a=37 kJ/mol.

The activation energies of lignin degradation vary with the methods of isolating lignin from its biomass [6]. For instance, the activation energy for the lignin processed in sulfuric acid was 46 kJ/mol [7]. Therefore, the estimated activation energy (37 kJ/mol) here is at a reasonable level.

In summary, model 1 is in good agreement with the experiments and superior to model 2. The unknown kinetic parameters were estimated. However, it should be noted that this model could not be directly used in hydrothermal treatment of the other biomass. Modification of the model is required to ensure the accuracy of model prediction when applied to the other biomass.

Conclusions

The hydrothermal treatment of Kraft pine lignin, organosolv lignin of oat hull, mixed southern hardwood residue, and switchgrass residue after hydrolysis was studied. At 374 °C, the liquid yields of Kraft lignin, organosolv lignin, hardwood residue, and switchgrass residue were 57–71, 79.1, 56.3, and 29.7, respectively. The yields were found dependent on the composition or structure of the raw materials, which may result from different pretreatment processes. To select a suitable thermochemical conversion technol-

ogy for a raw material like lignin or biomass residue, each raw material needs to be evaluated individually.

A possible mechanism of the hydrothermal treatment of Kraft pine lignin was proposed. In addition, a kinetic model was established and compared with another model published elsewhere. All the kinetic parameters of the presented model were estimated. Good agreement was found between the model and the experiments.

Acknowledgements The University of Minnesota Initiative for Renewable Energy and the Environment (IREE) is gratefully acknowledged for its financial support. The authors would like to thank MeadWestvaco and Dr. Kwok-Choi Patrick Lee (Tennessee Valley Authority) for providing lignin, and our collaborators, Dr. Marc von Keitz, Dr. Kenneth Valentas, Dr. Ulrike W Tschirner, Dr. Vernon R Eidman, Dr. Steve Polasky, and Dr. Waleed Wafa Al-Dajani.

References

1. Zmierczak, W. W., & Miller, J. D. (2006). *WO2006119357.*
2. Zhang, B., von Keitz, M., & Valentas, K. (2007). *Abstracts of Papers of the American Chemical Society, 233*, AGRO 220.
3. Yu, F., Ruan, R., Chen, P., Deng, S., Liu, Y., & Lin, X. (2007). *Transactions of the ASABE, 50*, 175–180.
4. Bobleter, O., & Concin, R. (1979). *Cellulose Chemical Technology, 13*, 583–593.
5. Brunow, G., Lundquist, K., & , Gellerstedt, G. (1999). In E. Sjostrom, & R. Alen (Eds.) *Analytical methods in wood chemistry, pulping and papermaking* pp. 77–124. New York: Springer.
6. LeVan, S. L. (1989). In A. P. Schniewind (Ed.) *Concise encyclopedia of wood & wood-based material* pp. 271–273. Elmsford, NY: Pergamon Press.
7. Beall, F. C. (1969). *Wood Fiber, 1*, 215–226.

Appl Biochem Biotechnol (2008) 147:133–142
DOI 10.1007/s12010-007-8104-0

Hydrodynamic Characterization of a Column-type Prototype Bioreactor

Teodoro Espinosa-Solares · Marcos Morales-Contreras · Fabián Robles-Martínez · Melvin García-Nazariega · Consuelo Lobato-Calleros

Received: 8 May 2007 / Accepted: 30 November 2007 /
Published online: 3 January 2008
© Humana Press Inc. 2007

Abstract Agro-food industrial processes produce a large amount of residues, most of which are organic. One of the possible solutions for the treatment of these residues is anaerobic digestion in bioreactors. A novel 18-L bioreactor for treating waste water was designed based on pneumatic agitation and semispherical baffles. Flow patterns were visualized using the particle tracer technique. Circulation times were measured with the particle tracer and the thermal technique, while mixing times were measured using the thermal technique. Newtonian fluid and two non-Newtonian fluids were used to simulate the operational conditions. The results showed that the change from Newtonian to non-Newtonian properties reduces mixed zones and increases circulation and mixing times. Circulation time was similar when evaluated with the thermal and the tracer particle methods. It was possible to predict dimensionless mixing time (θ_m) using an equivalent Froude number (Fr_{eq}).

Keywords Flow pattern · Circulation time · Dimensionless mixing time · Froude number · Non-Newtonian behavior · Pneumatic agitation

Nomenclature

d_{eq} equivalent diameter (m)
Fr_{eq} equivalent dimensionless Froude number (–)
g gravitational acceleration (m s^{-2})
k consistency index (Pa s^n)

T. Espinosa-Solares · M. García-Nazariega
Departamento de Ingeniería Agroindustrial, Universidad Autónoma Chapingo, Apartado Postal no. 161, Chapingo 56230 Estado de México, México

M. Morales-Contreras · F. Robles-Martínez
Unidad Profesional Interdisciplinaria de Biotecnología del Instituto Politécnico Nacional, México City, DF, México

T. Espinosa-Solares (✉) · C. Lobato-Calleros
Posgrado en Ciencia y Tecnología Agroalimentaria, Universidad Autónoma Chapingo, Chapingo, Estado de México, México
e-mail: espinosa@correo.chapingo.mx

n flow behavior index (–)
R^2 coefficient of determination (–)
t_c circulation time (s)
t_m mixing time (s)
U_f superficial velocity of the fluid (m s^{-1})
$\dot{\gamma}$ shear rate (s^{-1})
θ_m dimensionless mixing time (–)
τ shear stress (Pa)

Introduction

Biodigester design and operation for anaerobic digestion must usually balance hydrodynamic efficiency and microbial performance. While transport phenomena are improved by increasing the hydrodynamic conditions, excessive mixing could compromise the metabolic activity of the anaerobic consortia. Gómez et al. [1], working with anaerobic codigestion of primary sludge and the fruit and vegetable fraction of municipal solid wastes, reported that the absence of agitation resulted in a reduction in the specific gas production. In contrast, excess of shear force resulting from the digestate being passed through a pump or a mixer for long periods of time can disrupt the microbial communities dependent upon each other for fermentation. It has been reported by Shigematsu et al. [2] that mesophyllic acetate-degrading methanogenic consortia modify their structure when the dilution rate is changed. Sheng et al. [3], studying the role of extracellular polymeric substances (EPS) on the stability of sludge flocs under shear conditions, demonstrated that external layers are easily dispersible by shear forces. This fact confirms the findings of Ong et al. [4] regarding the decrease in the production of EPS when excessive mixing was used during the cattle manure biomethanization. Espinosa-Solares et al. [5], working with chicken litter in a pilot plant anaerobic digester, reported that the poor consortia performance could be attributed to excessive mechanical work on the slurry; the fermentation mass was recycled six times in 24 h.

Several authors have reported a non-Newtonian behavior for anaerobic digestion media. Hashimoto and Chen [6], working with poultry waste slurries with 5.2% of total solids (TS), found a behavior flow index (n) of 0.28 and a consistency index (k) of 0.700 Pa s^n. Similar results were found by Chen [7] for beef-cattle manure; when the TS concentration was 6.2%, n and k were 0.73 and 0.070 Pa s^n, respectively. In the case of dairy cattle manure with 5.4% TS, Achkari-Begdouri and Goodrich [8] reported flow properties within the ranges of $0.69 \leq n \leq 0.77$ and $0.032 \leq k$ (Pa s^n) ≤ 0.065. For higher concentrations of dairy cattle manure (10% TS), the flow properties found by El-Mashad et al. [9] indicated a higher shear-thinning behavior ($0.31 \leq n \leq 0.34$; $10.5 \leq k$ (Pa s^n) ≤ 13.0) than the one found by Achkari-Begdouri and Goodrich [8]. To improve the performance of anaerobic digesters, flow properties have to be considered, particularly when a change in rheology is involved. Hydrodynamic characterization is a useful tool to define adequate performance of a bioreactor. Long-term operation geared toward a target efficiency of the bioreactor depends ultimately on the nature of the flow pattern obtained [10]. Espinosa-Solares et al. [11] studied flow patterns in stirred vessels using Newtonian and non-Newtonian fluids. These authors proposed a correlation between the dimensionless Froude number and the vortex length. This research group extended the previous study to assess dimensionless mixing time under different hydrodynamic conditions [12]. It was shown that rheological properties, gassing rate, and hydrodynamics played major roles in mixing time (t_m) when

the Froude number ranged from 0.40 to 0.71 and the dimensionless flow number varied from 0.00 to 0.06. Hence, mixing time is another key parameter for designing mixing systems. It has been defined by several authors as the time required to reach a specified degree of homogeneity [13, 14]. In fact, mixing time is a global index of mixing [15] and, consequently, the result of imposed hydrodynamics. As an initial approach for understanding the effect of mixing on anaerobic digestion, the hydrodynamics of a novel bioreactor was characterized. Thus, the aim of the present research was to study the mixing performance of this bioreactor, both qualitatively, via flow patterns, and quantitatively, using mixing and circulation times. The device was designed for wastewater treatment with both Newtonian and non-Newtonian model fluids, which mimic fermentation conditions. The column bioreactor includes semispherical baffles to improve aggregate retention in the bioreactor when the medium is mixed by pumping. The purpose of the top baffle is to promote mixing, while the bottom baffle is intended to favor sedimentation of large aggregates.

Materials and Methods

The novel bioreactor used was developed at the Instituto Politécnico Nacional. The column length is 1.152 m with an internal diameter of 0.144 m; it includes a draft tube (0.655 m high, 0.063 m inner diameter), two semispherical baffles, and a recirculation system. Figure 1 shows detailed measurements of the equipment. Fluid recirculation was achieved using a centrifugal pump (Little Giant, Oklahoma City, OK). The general flow starts when the fluid leaves the pump (marked as current 1 in Fig. 1) and enters the column, flowing through the draft tube. Once the fluid reaches the top baffle, part of the liquid goes downward, and the other could go upward. The fluid returns to the pump either through currents 2 and 3 (Fig. 1). Currents 4 and 5 are used, respectively, only during filling and flushing of the column reactor.

Experiments were conducted at room temperature. Water was used as the Newtonian fluid. Non-Newtonian liquids included aqueous solutions of Xanthan gum (Keltrol T, Kelco-Merck) as shear-thinning fluids. Solutions were prepared at constant ionic strength by adding 0.1% (w/v) NaCl. These fluids were selected because they had similar rheological properties to several anaerobic media [6–9] and they are clear fluids that allowed flow pattern visualizations.

The steady shear viscosity function was evaluated using a dynamic shear rheometer RHEOPLUS/32 V2.62 rheometer (Anton Paar, Messtechnik, Stuttgart, Germany) provided with cone-plate geometry, in which the rotating cone was 50 mm in diameter and cone angle was 1°. The viscosity for the shear-thinning fluids in the linear region was well fitted by the Ostwald–de Waele model (Eq. 1). The flow behavior index (n) of the non-Newtonian fluids varied from 0.34 to 0.53, the consistency index (k) between 0.086 and 0.637 Pa s^n, and their density was 1,020 kg m^{-3}. Deionized water was used throughout.

Flow patterns were visualized by adding tracer particles to the fluid, following the method reported by Espinosa-Solares et al. [11]. κ-Carrageenan particle tracers were introduced into the system through the recirculation tube at the top. A digital video camera was used to follow the particle trajectory through the bioreactor. The particle trajectory was drawn using bioreactor-scale sketches.

$$\tau = k\left(\dot{\gamma}\right)^n \tag{1}$$

Mixing time was determined using the thermal method reported by Espinosa-Solares et al. [12]. A small amount of the same working fluid at 40 °C above the working temperature was injected through the system pump. Mixing time was evaluated by means of the

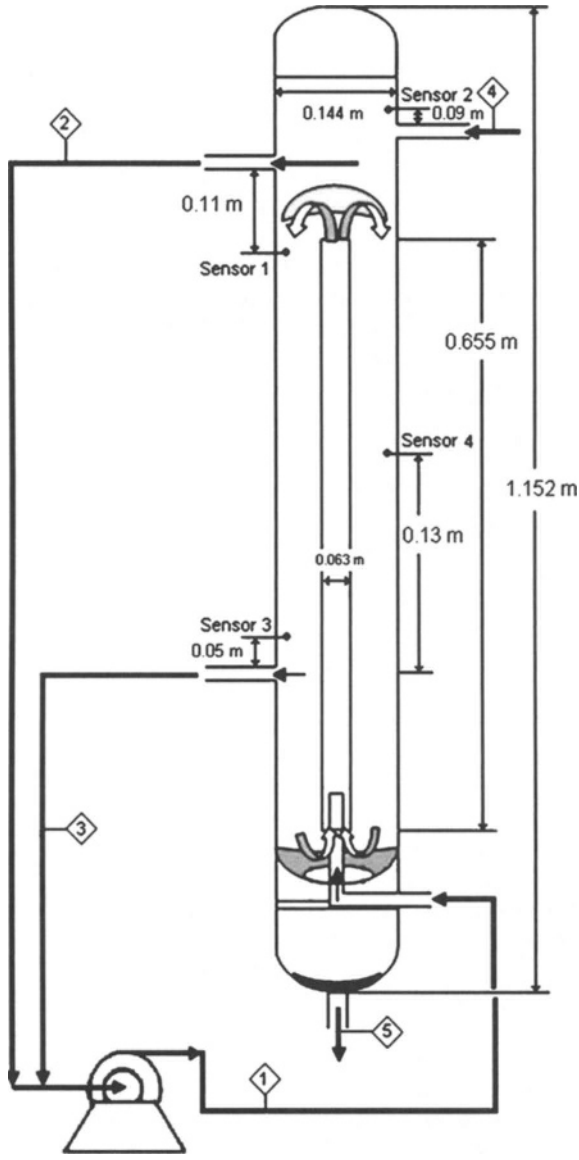


Fig. 1 Experimental setup

evolution of fluid temperature distribution in the vessel after adding the thermal tracer. For that purpose, temperature changes in the vessel were measured by four thermocouples (k-type). The signals of the probes were acquired by an interface (model FDR98/061) from Pico Technology Limited (London, UK). Figure 1 shows the location of the thermocouples. Mixing is complete when uniform temperature distribution inside the tank is achieved [16]. Full details of the method were reported by Espinosa-Solares et al. [12]. Figure 2 shows the typical results of the thermal technique.

Circulation time (t_c) was evaluated using the particle tracers and the signals obtained by the thermal tests. For the tracers, circulation time was defined as the time required for the

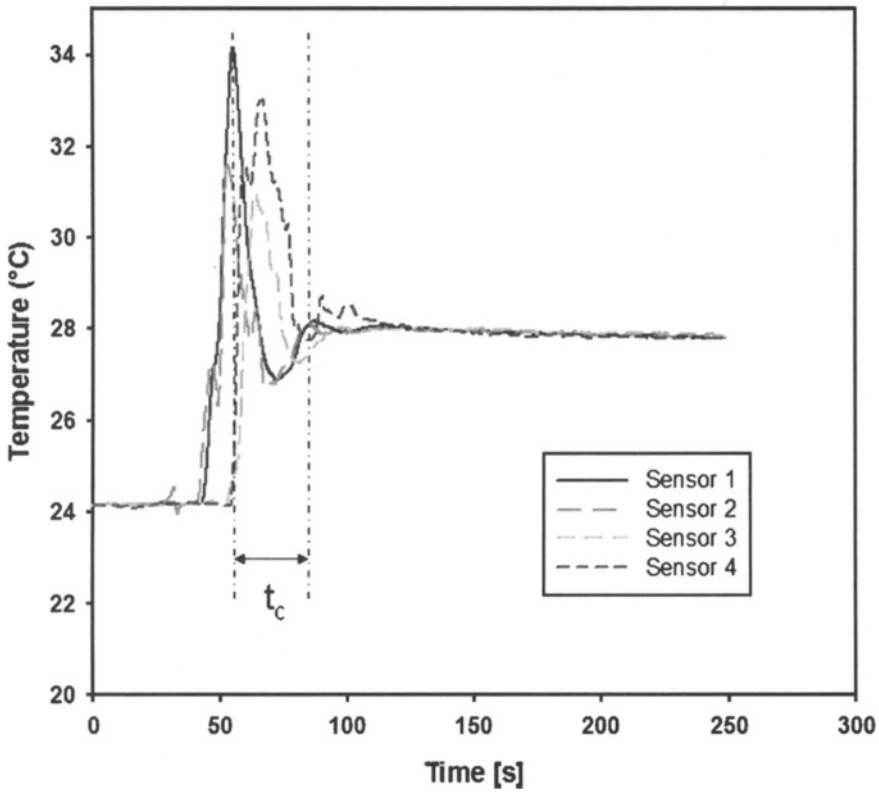


Fig. 2 Mixing time evaluation

particle to complete a circuit through the bioreactor. In the case of the thermal technique, circulation time was considered to be the time between first two consecutive peaks in the diagram obtained with the thermal method described previously. In all the cases, it was used only the signal of the sensor 1. Dimensionless mixing time was evaluated using mixing and circulation times obtained by the thermal method in the same manner as defined for airlift reactors [15]. Definition of the parameter is presented in Eq. 2, where θ_m represents the number of complete circuits needed in the bioreactor to achieve mixing. Dimensionless equivalent Froude number, Fr_{eq}, was evaluated with Eq. 3, where U_f, g, and d_{eq} represent fluid velocity, gravitational acceleration, and equivalent diameter of the annular section, respectively. The letter defined as the diameter of a circular section with the same area of the annular space; thus, the equivalent diameter enables the same flow rate as in the annular section.

$$\theta_m = \frac{t_m}{t_c} \tag{2}$$

$$Fr_{eq} = \frac{U_f^2}{g\, d_{eq}} \tag{3}$$

Results and Discussion

Flow Patterns

Figure 3 shows the flow patterns observed in the bioreactor using Newtonian (Fig. 3a, n= 1.00, k=0.001 Pa s^n) and two non-Newtonian fluids (Fig. 3b, n=0.53, k=0.086 Pa s^n; Fig. 3c, n=0.34, k=0.637 Pa s^n). It was found that the flow is generally similar, having pattern differences mainly in the draft tube and at the top section of the system. These differences depend on the rheological properties of the fluid. The fluid flows through the system beginning at the pump and continues to the bioreactor by the draft tube. When the fluid flows through the baffle at the top, it begins to flow down. Once the fluid reaches the exits marked 2 and 3 in Fig. 1, part of the fluid is suctioned into the pump input, while another part of the fluid continues flowing down to the semispherical baffle at the bottom of the bioreactor where it is incorporated into the flow imposed by the fluid coming from the pump.

The flow patterns that develop in different zones of the bioreactor are described as follows. Two patterns were observed in the draft tube; with the Newtonian fluid, as soon as the particle enters the draft tube until approximately 20 cm above the flow entrance, a rapid motion was observed. Passing this zone, the particle flows up in a straight line or in zigzag. In contrast, using non-Newtonian fluids, the particle movement is not so fast in the bottom 20 cm. This difference could be attributed to the smaller expected viscosity when the Newtonian fluid was used. After this point, the particles flow upward in a pattern similar to that obtained with the Newtonian fluid.

Agitation in the bioreactor is promoted mainly by the top baffle. In the Newtonian fluid, a well-defined zone of 16 cm, having small loops, was observed. In non-Newtonian fluids, these loops were occasionally observed. In this case, the top baffle improves the flow in the bioreactor in a manner similar to the helical flow promoter proposed by Wu and Merchuk [17].

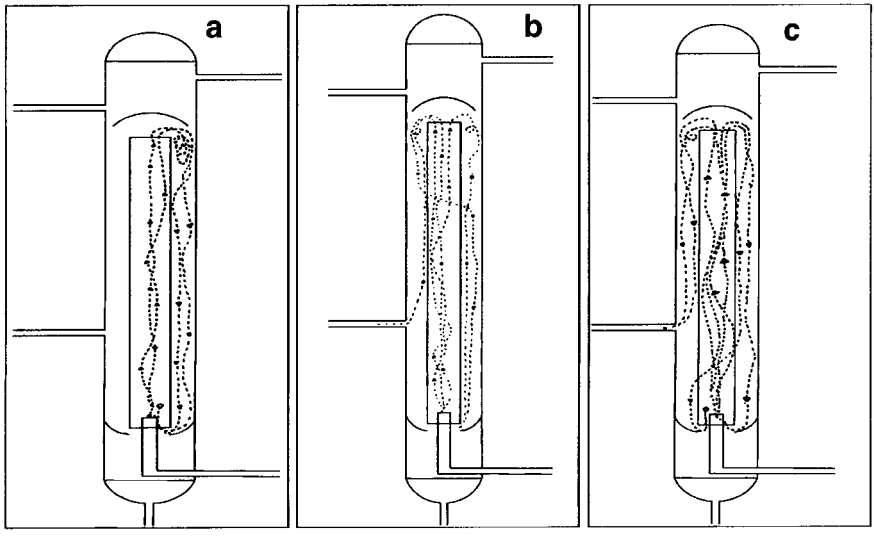


Fig. 3 Flow patterns using **a** Newtonian fluid (viscosity 1 mPa s) and two non-Newtonian fluids **b** n=0.53, k=0.086 Pa s^n and **c** n=0.34 and k=0.637 Pa s^n

The flow in the annular section of the bioreactor is toward the baffle located at the bottom. The main flow is through the zone on the side opposite to the recirculation tubes. This flow pattern is more dominant in the Newtonian fluid (Fig. 3a), which could be attributed to the creation of a main flow where the particle is trapped. In all cases, the top baffle is important in keeping the particles within the body of the bioreactor. For the shear-thinning fluid with n=0.53 and k=0.086 Pa s^n, it was detected that particles are slightly suctioned by the recirculation tube at the bottom of the bioreactor (Fig. 3b). This flow is more dominant with a higher shear-thinning fluid (n=0.34 and k=0.637 Pa s^n, Fig. 3c).

Summarizing, the main recycling flow of the fluid, for a low-viscosity Newtonian fluid (0.001 Pa s), is from the draft tube to the vicinity of the top recirculation tube (indicated as 2 in Fig. 1). For non-Newtonian fluids with moderate shear-thinning behavior ($0.34 \leq n \leq 0.53$, and $0.034 \leq k$ (Pa s^n) ≤ 0.637), the recycling flow is also from the draft tube to the vicinity of the recirculation top tube; however, the flow through the bottom recirculation tube (indicated as 3 in Fig. 1) becomes more important as shear thinning increases (Fig. 3b and c). The shear-thinning behavior of the fluids indicates that viscosity changes as shear rate does. Thus, according the Ostwald–de Waele model presented in Eq. 1, for the non-Newtonian fluid with n=0.53 and k=0.086 Pa s^n, viscosity changes from 0.010 to 0.040 Pa s when shear rate passes from 100 to 5 s^{-1}. In the case of another non-Newtonian fluid (n= 0.34 and k=0.637 Pa s^n), viscosity increases from 0.030 to 0.220 Pa s with the same shear rate variation. Thus, the increments in viscosity are, respectively, close to 410 and 720%. Any fluid dissipates energy while it flows because of viscosity forces. Thus, because no additional power is supplied along the flow pattern, it is expected a velocity reduction and consequently a decrement on shear rate as much as the fluid follows the path. The opposition to the flow at the bottom of the bioreactor in non-Newtonian fluids is attributed to the increment in the viscosity occasioned by a reduction in shear rate in that section of the bioreactor.

The baffle at the bottom has an apparently neutral effect on agitation; it does, however, allow particle separation. It was observed that particles with a mean weight of 0.01 g are incorporated into the flow described previously. At the same time, particles with a mean weight of 0.06 g settled. This section of the bioreactor should be adjusted to allow the separation of a specific particle size to satisfy specific needs, such as large sludge particles that could lose efficiency.

Circulation and Mixing Time

It was observed that hydrodynamics plays an important role in circulation time (Table 1). The increase in flow velocity reduces t_c. It is important to note in Table 1 that both techniques resulted in similar values for t_c for Newtonian and non-Newtonian fluids. Taking the t_c obtained by the tracer method as reference, the difference with t_c by thermal method ranges from 11 to 25%. Table 1 shows that t_c depends on flow properties; as flow index reduces, increasing at the same time the consistence index, t_c increases.

Figure 4 shows mixing time as a function of the fluid velocity. The effect of the increase in fluid velocity in reducing mixing time is expected. For example, for the fluid with highest shear-thinning behavior assessed here (n=0.34, k=0.637 Pa s^n), when the velocity increases from 1.84×10^{-3} to 3.61×10^{-3} m s^{-1}, mixing time decreases from 582 to 310 s. The reduction of mixing time by increasing velocity has been reported for draft tube airlift vessels by Gouveia et al. [18] and Sánchez Mirón et al. [15] using water as a working fluid. These research groups observed the trend with superficial aeration velocity below 0.045 and at 0.010 m s^{-1}, respectively. Mixing time in the bioreactor follows the exponential

Table 1 Circulation times for several hydrodynamic conditions.

U_f (m s^{-1})	n (–)	k (Pa s^n)	t_c tracer method (s)	t_c thermal method (s)
6.71×10^{-3}	1.00	0.001	24	27
1.14×10^{-2}	1.00	0.001	24	30
1.30×10^{-2}	1.00	0.001	37	33
2.86×10^{-3}	0.53	0.086	31	33
5.00×10^{-3}	0.53	0.086	36	38
8.00×10^{-3}	0.53	0.086	23	28
1.84×10^{-3}	0.34	0.637	44	47
2.12×10^{-3}	0.34	0.637	50	46

model presented in Eq. 4 (R^2=0.99). In a similar manner, Eqs. 5 (R^2=0.96) and 6 (R^2= 0.99) describe mixing time as a function of the fluid, respectively, for another non-Newtonian fluid (n=0.53, k=0.086 Pa s^n) and the Newtonian one (n=1.00, k=0.001 Pa s^n). The exponential decreasing of mixing time by the increment in fluid velocity is notorious as the fluid increases the shear-thinning behavior. The influence of shear-thinning on t_m is possible to quantify by the values of the constant of the exponential term of the models presented in Eqs. 4 to 6. These findings have an important effect on the operation of the digester. For example, the poultry waste slurries (n=0.28, k=0.700 Pa s^n) reported by Hashimoto and Chen [6] will be expected to have higher mixing times and, at the same time, a higher influence on mixing time reduction than the beef-cattle manure (n=0.73, k=

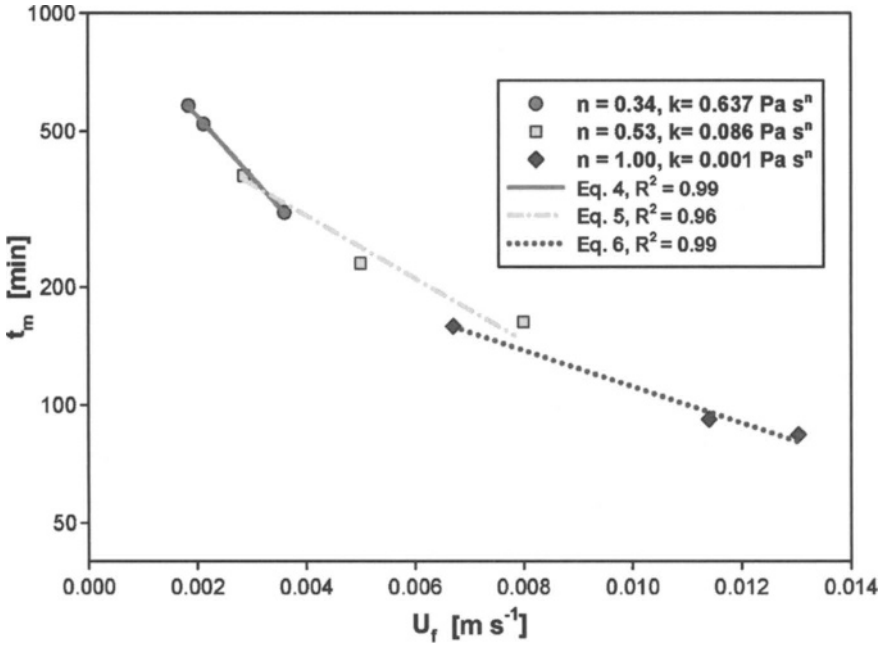


Fig. 4 Influence of velocity and flow behavior index on mixing time

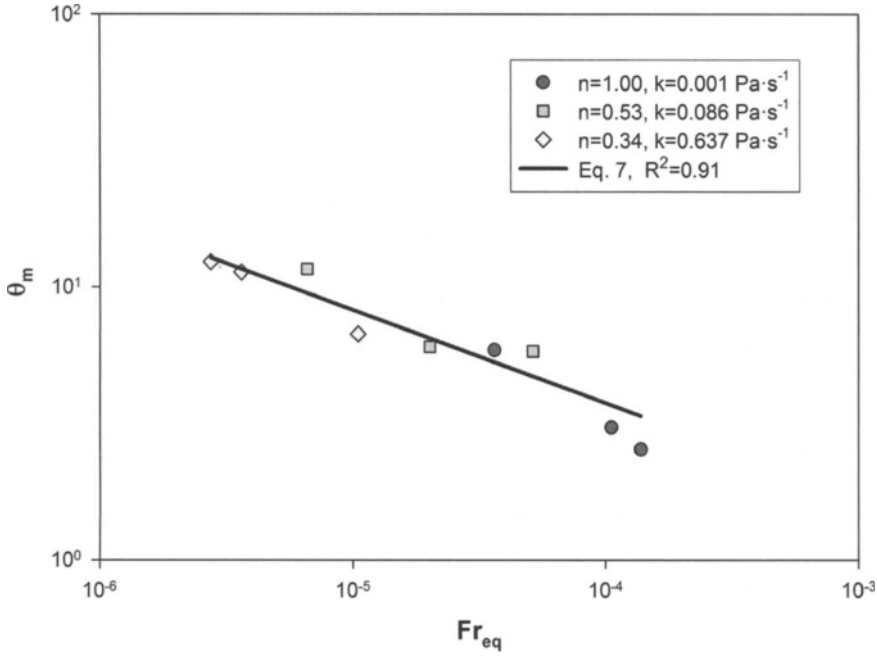


Fig. 5 Relationship between dimensionless mixing time and equivalent Froude number for the column type bioreactor

0.070 Pa s^n) referred by Chen [7]. Thus, for the latter, smaller energy requirements will be needed to achieve mixing.

$$t_m = 1119\, e^{-357\, U_f} \tag{4}$$

$$t_m = 636\, e^{-184\, U_f} \tag{5}$$

$$t_m = 324\, e^{-107\, U_f} \tag{6}$$

Dimensionless mixing time as a function of the Fr_{eq} is presented in Fig. 5 and Eq. 7. As can be observed, dimensionless mixing times for Newtonian and non-Newtonian fluids have the same trend. The model has a high coefficient of determination (R^2=0.91), suggesting that the Fr_{eq} is a parameter suitable for estimating dimensionless mixing regardless of the flow properties. The model indicates that by increasing the Fr_{eq}, a reduction in dimensionless mixing time is achieved, implying that a higher equivalent Froude number requires a fewer complete recycling circuits to achieve mixing. To illustrate this, under the operation conditions evaluated in this work, dimensionless mixing time was reduced from 12.4 to 2.5.

$$\theta_m = \frac{0.162}{Fr_{eq}^{0.34}} \tag{7}$$

Conclusions

The aim of the present work was to study the mixing performance of a novel bioreactor designed for wastewater treatment, using both Newtonian and non-Newtonian model fluids. The methodology included a blend of experimental techniques, such as flow visualization, and the evaluation of circulation and mixing times. The results showed that for the studied hydrodynamic conditions, main flow patterns are in general similar, having modifications depending on the rheological behavior of the fluids. Basically, two sections showed differences, the lower part of the draft tube and the vicinity of the top baffle. An increment in pseudoplasticity, which is related to a reduction in flow behavior index and, at the same time, to an increment in the consistence index, diminishes the mixed zones. The incorporation of a semispherical baffle at the top of the bioreactor favored agitation, while the baffle at the bottom favored particle settling. Under the operational conditions of the experiments ($Fr<1.2\times10^{-4}$), Fr_{eq} has an inversely proportional relationship with dimensionless mixing time. These findings have interesting implications for bioreactor design and operation; for high shear-thinning media, higher energy requirements will be needed to increase the fluid velocity to achieve mixing. However, imposition of hydrodynamic conditions in the bioreactor could compromise mixing needs with microbial integrity, and so further work is needed to evaluate the influence of the hydrodynamic conditions on microbial performance, which is left for future communications.

Acknowledgments The authors gratefully acknowledge the financial support from Universidad Autónoma Chapingo and Instituto Politécnico Nacional. We would also like to acknowledge to Olga Lidia Martinez-Flores and Graciela Martínez-Ramírez for their contributions during the experimental work.

References

1. Gómez, X., Cuetos, M. J., Cara, J., Morán, A., & García, A. I. (2006). *Renewable Energy, 31*, 2017–2024.
2. Shigematsu, T., Tang, Y. Q., Kawaguchi, H., Ninomiya, K., Kijima, J., Kobayashi, T., Morimura, S., & Kida, K. (2003). *Journal of Bioscience and Bioengineering, 96*, 547–558.
3. Sheng, G. P., Yu, H. Q., & Li, X. Y. (2006). *Biotechnology & Bioengineering, 93*, 1095–1102.
4. Ong, H. K., Greenfield, P. F., & Pullammanappallil, P. C. (2002). *Environmental Technology, 23*, 1081–1090.
5. Espinosa-Solares, T., Bombardiere, J., Domaschko, M., Chatfield, M., Stafford, D. A., Castillo-Angeles, S., et al. (2006). *Applied Biochemistry and Biotechnology, 129–132*, 959–968.
6. Hashimoto, A. G., & Chen, Y. R. (1976). *Transactions of the ASAE, 19*, 930–934.
7. Chen, R. Y. (1981). *Transactions of the ASAE, 24*, 187–192.
8. Achkari-Begdouri, A., & Goodrich, P. R. (1992). *Bioresource Technology, 40*, 149–156.
9. El-Mashad, H. M., van Loon, W. K. P., Zeeman, G., & Bot, G. P. A. (2005). *Bioresource Technology, 96* (5), 531–535.
10. Vesvikar, M. S., & Al-Dahhan, M. (2005). *Biotechnology and Bioengineering, 89*, 719–732.
11. Espinosa-Solares, T., Brito de la Fuente, E., Tecante, A., & Tanguy, P. A. (2001). *Chemical Engineering & Technology, 24*, 913–918.
12. Espinosa-Solares, T., Brito de la Fuente, E., Tecante, A., Medina-Torres, L., & Tanguy, P. A. (2002). *Chemical Engineering Research & Design, 80*, 817–823.
13. Ulbrecht, J. (1974). *Chemical Engineering (London)*, pp. 347–353.
14. Rzyski, E. (1993). *Chemical Engineering and Technology, 16*, 229–233.
15. Sánchez Mirón, A., Cerón García, M.-C., García Camacho, F., Molina-Grima, E., & Chisti, Y. (2004). *Chemical Engineering Research & Design, 82*, 1367–1374.
16. Ford, D. E., Mashelkar, R. A., & Ulbrecht, J. (1972). *Process Technology International, 17*, 10.
17. Wu, X., & Merchuk, J. C. (2003). *Chemical Engineering Science, 58*, 1599–1614.
18. Gouveia, E. R., Hokka, C. O., & Badino-Jr, A. C. (2003). *Brazilian Journal of Chemical Engineering, 20*, 363–374.

Appl Biochem Biotechnol (2008) 147:143–150
DOI 10.1007/s12010-008-8131-5

Thermal Effects on Hydrothermal Biomass Liquefaction

Bo Zhang · Marc von Keitz · Kenneth Valentas

Received: 15 May 2007 / Accepted: 30 November 2007 /
Published online: 6 February 2008
© Humana Press Inc. 2008

Abstract Batch pressure vessels commonly used for hydrothermal liquefaction have typical heating times in the range of 30 to 60 min. Thermodynamically, the complex set of reactions are path dependent, so that the heating rate can possibly affect yields and the composition of the resultant liquid products. It is postulated that the mode of heat transfer becomes an uncontrolled variable in kinetic studies and can seriously impact scale-up. To confirm this hypothesis and minimize these heat-transfer-related artifacts, we designed a batch pressure vessel equipped with an induction heating system, which allows the reduction of heat-up times by about two orders of magnitude to several seconds, compared to tens of minutes with standard pressure reactors. This system was used to study the direct liquefaction of corn stover and aspen wood with a pretreatment. The heating rate was found to have no significant effect on the composition of the liquid products. However, the liquid yields are dependent on the heating rate. Varying the cooling rate does not show obvious effects. The results confirm that the heating rate, as governed by the mode of heat transfer, is an important factor that needs to be considered during scale-up.

Keywords Liquefaction · Aspen · Corn stover · Heating rate · Cooling rate · Yield · Composition

Introduction

Biomass is the renewable energy source of choice for the production of liquid transportation fuels. Significant quantities of ethanol are currently being produced from corn and sugar cane via fermentation. Utilizing lignocellulosic biomass as a feedstock is seen as the next step toward significantly expanding ethanol production capacity. However, in addition to substantial technical challenges that still have to be overcome before lignocellulose-to-ethanol becomes commercially viable, any ethanol produced by fermentation has the

B. Zhang · M. von Keitz · K. Valentas (✉)
BioTechnology Institute, University of Minnesota, 240 Gortner Labs,
1479 Gortner Avenue, St. Paul, MN 55108, USA
e-mail: valentas@umn.edu

inherent drawback that it needs to be distilled from a mixture, which contains 82% to 94% water. Instead, direct thermochemical conversion of lignocellulosic biomass to a bio-crude oil or fuel gases has been proposed as an alternative. This does not require distillation, thus resulting in less energy input per unit of energy output.

There are two typical thermo-chemical conversion processes: pyrolysis and liquefaction. During pyrolysis processes, the biomass feedstock is heated in the absence of air, forming bio-oils and a gaseous product, which then condenses. Liquefaction of biomass produces a water-insoluble bio-crude oil by using treatments at high pressure (50–200 atm) and low temperature (250–450°C). The results of previous biomass liquefaction research have been reviewed by several different authors [1–5]. The advantage of liquefaction is that the bio-crude oil produced by liquefaction is not miscible with water and has a lower oxygen content and therefore higher energy content than pyrolysis-derived oils [1, 6].

Among the treatment variables, the heating rate may have a significant impact on the production of liquid bio-oil [2, 7]. For example, depending on the heating rate, the pyrolysis process can be divided into three categories: (1) conventional pyrolysis (0.1–1°C/min), (2) fast pyrolysis (10–200°C/min), (3) flash pyrolysis(>1,000°C/min). For this paper, the effects of the heating rate and the cooling rate on high-pressure liquefaction were studied. The components of the liquid products from corn stover and aspen wood with a pretreatment were identified and compared.

Material and Methods

Materials

Air-dried corn stover provided by the Agricultural Utilization Research Institute was milled and then screened, and only the fraction less than 2-mm sieve was used in this research. Aspen pulping wood chips (*Populus tremuloides*) with a pretreatment, which were the intermediates of a biorefinery process, were provided by the Department of Bioproducts and Biosystems Engineering, University of Minnesota, St. Paul, Minnesota. Aspen wood chips that passed through a 1-in. sieve but not through a 0.5-inch sieve were used. Aspen wood chips were pretreated with dilute sulfuric acid to remove partial hemicellulose.

Biomass Analytical Procedures

Moisture and ash content of biomass were determined by the methods of LAP-001 and LAP-005, respectively, which are laboratory analytical procedures (LAPs) developed by the National Renewable Energy Laboratory. Structural analyses of the samples were carried out according to the ASTM E1758-01 standard test methods. The composition of all raw materials is listed in Table 1.

Apparatus and Process

A 75-ml Parr high-pressure reactor (Parr Instrument, Moline, IL, USA) was used for liquefaction of the feedstock. The reactor consists of a reaction cylinder and a pressure gauge or valve assembly. An induction heating system, which allows the reduction of heat-up times by about two orders of magnitude, was customized by L. C. Miller, Monterey Park, CA, USA. For a typical run, 5 grams of feedstock and 45 ml distilled water were placed inside the cylinder. The cylinder was then sealed and purged through two valves on

Table 1 The composition of various lignocellulosic biomass (air dried, % by weight).

	Corn stover[a]	Aspen wood[a]	Pretreated aspen wood[b]
Glucan	36.6	41.6	51.6
Xylan	17.5	16.6	17.1
Galactan	1.1	1.2	–
Arabinan	2.5	1.2	0.3
Mannan	0.6	1.6	1.2
Klason lignin	21.0	19.7	21.4
Moisture	5.3	5.7	5.4
Ash	5.5	0.5	3.0

Endash not detectable

[a] Biomass also contains acid-soluble lignin, extractives, acetyl acid groups, and uronic acid groups.

[b] The aspen wood chips were pretreated with 1% dilute sulfuric acid at 160°C for 4 h to remove partial hemicellulose.

the reactor head with nitrogen gas at a flow rate of 80 ml/min for 5 min to remove air and prevent secondary reactions such as thermal cracking and repolymerization, and then the valves were closed. The reactor was heated to 350°C at a heating rate of about 140°C/min, and the desired temperature was held for 10 min. After completing the reaction, the cylinder was cooled down by soaking in the ice bath for 5 min. Gases were sampled into a gas bag for gas chromatography (GC) analysis later. The gas fraction was determined by measuring the weight difference of the reactor before and after gas sampling. The liquid, including both the water fraction and heavy oil fraction, was collected into a sample bottle for GC–mass spectrometry (MS) analysis later. The procedure for separating aqueous, water insoluble, and solid phases in the liquid is shown in Fig. 1. The aqueous phase was filtered to separate the water solution and the water insoluble fraction. The water insoluble fraction and the wall of the pressure reactor were washed with 10 ml acetone three times and then separated through filtration. The total amount of the acetone solution containing heavy oil and the aqueous phase were referred to as the liquid fraction. The acetone insoluble fraction was air-dried at room temperature for 48–72 h to a constant weight to yield the solid residue. Constant weight is defined as less than ± 0.01 g change in the weight upon 12 h of redrying.

The yield percentage of each fraction from liquefaction is defined as

$$\text{Gas yield (\%)} = (\text{weight of gas/weight of starting biomass}) \times 100$$

$$\text{Residue yield (\%)} = (\text{weight of residue/weight of starting biomass}) \times 100$$

$$\text{Liquid yield (\%)} = (1 - \text{weight of gas/weight of starting biomass} - \text{weight of residue/weight of starting biomass}) \times 100$$

All experiments and analysis were performed in triplicate.

Heating Rates and Cooling Rates

The heating rate was controlled by adjusting the output of the induction heater. The fast and slow heating rates were approximately 140 and 14°C/min, respectively. A 500-W band heater was used to mimic the conventional heating process. The conventional heating rate using the band heater was approximately 5°C/min.

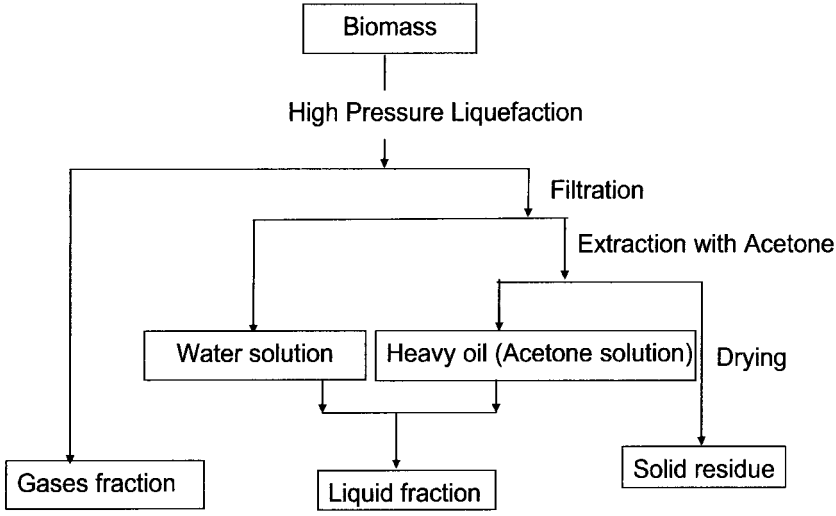


Fig. 1 Process for products separation after liquefaction

For fast cooling, the reactor was cooled to room temperature by soaking in the ice bath for 5 min. For slow cooling, the reactor was left at room temperature for 2 h until it reaches room temperature. The fast- and slow-cooling rates were approximately 66 and 5.5°C/min, respectively.

Chemical Analysis

A Perkin–Elmer Auto-system gas chromatograph (GC), which houses a 30-m, 0.53-mm (ID) fused silica capillary column (Carboxen 1010 Plot, Supelco), was used to analyze the gaseous samples from the liquefaction process. Temperature programmed step heating was performed as follows: 40°C for 1.7 min, increase by 40°C/min until 220°C, and leave at 220°C for 1.8 min. Argon was the carrier gas at a flow rate of 20 ml/min. Two detectors were used for gas analysis: a flame ionization detector (FID) for carbon-bearing species and a thermal conductivity detector (TCD) for H_2. Uncertainties in reported concentrations are estimated to be within ±5% [8].

Chemical compositions of the liquid products were identified using a Varian 3 GC/mass spectrometer with a HP-1 capillary column. The GC was programmed to hold the temperature at 40°C for 0.5 min and then increased by 10°C/min to 300°C and, finally, to hold with an isothermal for 10 min. The injector temperature was 300°C, and the injection size was 1 μl. The flow rate of the carrier gas (helium) was 0.6 ml/min. The ion source temperature was 230°C for the mass selective detector. The compounds were identified by comparison with the NIST Mass Spectral Database.

Results and Discussion

Effect of Heating Rate and Cooling Rate on Liquefaction of Corn Stover

Corn stover was used as the raw material. The reaction mixture was heated to 350°C and 20 MPa at a heating rate of about 140°C/min, 14°C/min, and 5°C/min, respectively, and the final temperature was held for 10 min. Table 2 and Fig. 2a show that the yield of liquid

Table 2 Effects of heating rate and cooling rate on liquefaction yields of corn stover.

Heating rate (°C/min)	Cooling rate (°C/min)	Liquefaction yield (% of total mass)			Gas yield (% of the total gaseous products)			
		Solid	Liquid	Gas	H_2	CO	CH_4	CO_2
140	66	8.9±2.5	70.6±2.4	20.5±4.0	3.9±0.3	15.5±0.4	1.8±0.4	78.7±1.2
140	5.5	9.3±2.1	69.6±3.3	21.1±3.7	2.7±0.9	18.9±6.2	1.1±0.5	77.2±5.8
14	66	14.9±1.8	63.6±3.0	21.5±3.8	2.6±0.6	26.9±1.6	2.6±0.4	68.0±0.6
14	5.5	15.8±2.4	61.7±4.7	22.5±4.1	2.7±0.1	24.8±1.3	2.1±0.1	70.4±1.3
5	66	18.3±3.2	53.4±2.2	28.3±4.7	3.5±0.1	23.9±0.4	2.8±0.1	69.8±0.4
5	5.5	19.8±2.6	51.5±1.8	28.7±5.2	4.8±0.8	8.2±1.5	2.2±0.5	84.7±1.2

products obtained from separation of liquefaction products increased with increasing heating rate. When the heating rate increased from 5°C/min to 140°C/min, the liquid yield increased drastically from 51–53% to 69–71% of the total biomass, but less gaseous products were generated, and the yield of solid residue also decreased from 18–20% to ~9% of the total mass.

The gaseous phase from liquefaction of corn stover primarily consisted of hydrogen (H_2), carbon monoxide (CO), methane (CH_4), and carbon dioxide (CO_2), which were 2.6–4.8%, 8–27%, 1.1–2.8%, and 68–85% of the total gaseous products, respectively.

Under the current reactor configuration, the liquid yield from the liquefaction of corn stover can be calculated from the data given in Table 2. The liquid yield as a function of the heating rate (°C/min) can be calculated from

$$\text{Liquid yield (\%)} = (0.051 \times \ln(\text{Heating rate}) + 0.4532) \times 100 \quad (1)$$

The liquid yields calculated by using Eq. 1 are also given in Fig. 2a. Equation 1 represents the correlation obtained by means of regression analysis. The correlation coefficient is 0.9181.

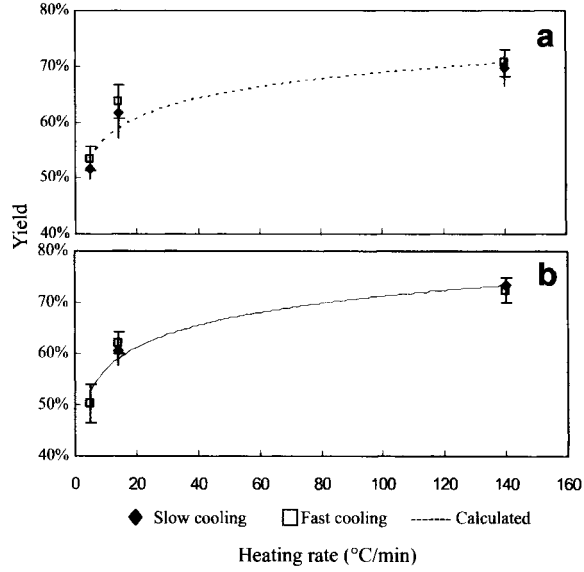


Fig. 2 Effects of heating rate and cooling rate on the liquid yields. **a** Corn stover; **b** the pretreated aspen. The fast and slow cooling rates were approximately 66°C/min and 5.5°C/min, respectively

Compared with the fast cooling process, the slow-cooling process does not show obvious effects on the profile of liquefaction products and gaseous products (Table 2). The possible reason is that the system may have reached equilibrium conditions after 10-min liquefaction.

Effect of Heating Rate and Cooling Rate on Liquefaction of Pretreated Aspen Chips

While liquefying the pretreated aspen, the reaction mixture was also heated to 350°C and 20 MPa at a heating rate of about 140°C/min, 14°C/min, and 5°C/min, respectively. The result of liquefying the pretreated aspen is similar to that of corn stover. From Table 3 and Fig. 2b, it is clear that the yield of liquid products obtained from the separation of liquefaction products increased with increasing heating rate. When the heating rate increased from 5°C/min to 140°C/min, the liquid yield increased from 50.3% to 72–74% of the total biomass, and the yield of solid residue decreased from 24.7% to 6–7% of the total mass. The cooling process did not show obvious effects on the profile of liquefaction products and gaseous products from the pretreated aspen.

Under the current reactor configuration, the liquid yield of the pretreated aspen chips as a function of the heating rate (°C/min) can be calculated from

$$\text{Liquid Yield (\%)} = (0.0627 \times \ln(\text{Heating Rate}) + 0.4239) \times 100 \quad (2)$$

The liquid yields calculated by using Eq. 2 are also given in Fig. 2b. Equation 2 represents the correlation obtained by means of regression analysis. The correlation coefficient is 0.9358. However, Eqs. 1 and 2 are only valid for the experiments within the extreme range of the heating rates between 5°C/min and 140°C/min while maintaining other variable parameters to be constant, including reactor type and dimensions, biomass conditions, etc.

Typical heating times in batch pressure vessels commonly used for thermal-chemical conversion are in the range of 30 to 60 minutes. Thus, an artifact is inadvertently introduced in kinetic studies, as the mix of reaction products is path dependant. To minimize these heat transfer artifacts, we designed a batch pressure vessel equipped with an induction heating system, which allows the reduction of heat-up times by about two orders of magnitude, from tens of minutes to several seconds, compared to standard pressure reactors. During the process of slow heating, liquefaction may involve more side reactions and result in a higher yield of solid residue but less liquid fuel. However, varying the cooling rate did not show obvious effects, as equilibrium conditions may already be reached. So, it suggests that the heating rate and mode of heat transfer are important factors, which need to be considered during scale-up.

Table 3 Effects of heating rate and cooling rate on liquefaction yields of pretreated aspen.

Heating rate (°C/min)	Cooling rate (°C/min)	Liquefaction yield (% of total mass)			Gas yield (% of the total gaseous products)			
		Solid	Liquid	Gas	H_2	CO	CH_4	CO_2
140	66	6.7±1.6	72.4±2.5	20.9±4.1	6.4±0.4	17.2±0.7	2.2±0.2	74.2±0.4
140	5.5	6.1±2.1	73.5±1.0	20.3±4.2	7.0±1.7	17.9±0.7	2.0±0.4	73.0±1.6
14	66	14.1±2.3	62.1±2.2	23.8±3.7	4.3±0.5	13.8±2.6	2.0±0.2	80.0±0.4
14	5.5	14.9±1.8	60.5±2.8	24.6±4.8	3.7±0.4	15.1±3.1	2.2±0.4	79.1±3.7
5	66	24.7±3.3	50.3±3.8	25.1±4.9	8.3±2.4	5.1±2.2	2.8±0.4	83.8±2.5

GC–MS Analysis of the Liquid Products

The components of the liquid products from various biomasses were determined by GC–MS analysis. The mass to charge ratios of the components were checked against the mass spectral library published by NIST. The peak areas shown on the GC spectra were calculated and are given in Table 4. The percentage values indicate the proportions of individual compounds in the liquid and do not represent the actual concentration of these compounds.

Within the GC–MS detectable range, the composition difference of liquid products from various origins is able to be identified. Liquid products from corn stover contain 4-ethyl-phenol, 1-(4-hydroxy-3,5-dimethoxyphenyl)-ethanone, desaspidinol, 2-hydroxy-3-methyl-2-cyclopenten-1-one, 2,5-hexanedione, and 1-hydroxy-2-propanone, and these compounds are barely detectable in the liquid products from the pretreated aspen. The liquid products from the pretreated aspen also contain unique compounds, such as 3-methyl-2-cyclopenten-1-one, 3-methyl-phenol, and 2-methoxy-4-propyl-phenol. Besides, 2,6-dimethoxy-phenol in the liquid products of the pretreated aspen is markedly higher then that of corn stover. Therefore, the composition of liquid products from liquefaction is dependent on biomass species.

With this liquefaction platform, the heating rate was found to have no effect on the individual compound of the liquid products (GC–MS data not shown), but it did affect the yield of liquefaction.

Table 4 The composition (% area) of the liquid products from corn stover and the pretreated aspen.

Retention time (min)	Possible structural formula	Chemical name	Corn stover	Pretreated aspen
3.3	$C_2H_4O_2$	Acetic acid	21.4	17.6
3.8	$C_3H_6O_2$	1-Hydroxy-2-propanone	8.4	–
6.2	C_5H_8O	Cyclopentanone	0.5	0.7
7.5	$C_5H_4O_2$	Furfural	3.5	1.7
9.3	C_6H_8O	3-Methyl-2-cyclopenten-1-one	0.9	4.5
10.1	$C_6H_{10}O_2$	2,5-Hexanedione	0.3	–
10.8	C_6H_8O	3-Methyl- 2-cyclopenten-1-one	–	2.0
11.2	C_6H_6O	Phenol	1.0	4.5
11.9	$C_6H_8O_2$	2-Hydroxy-3-methyl-2-cyclopenten-1-one	0.8	–
12.1	$C_7H_{10}O$	2,3-Dimethyl-2-cyclopenten-1-one	2.1	2.6
12.5	C_7H_8O	3-Methyl-phenol	–	1.0
12.9	$C_7H_8O_2$	Guaiacol	9.0	7.5
14.3	$C_8H_{10}O$	4-Ethyl-phenol	23.1	–
14.6	$C_8H_{10}O_2$	2-Methoxy-4-methyl-phenol	4.6	2.6
15.9	$C_9H_{12}O_2$	4-Ethylguaiacol	11.9	7.6
17.1	$C_8H_{10}O_3$	2,6-Dimethoxy-phenol	5.9	19.6
17.3	$C_{10}H_{14}O_2$	2-Methoxy-4-propyl-phenol	–	4.5
18.2	$C_9H_{12}O_3$	1,2,4-Trimethoxybenzene	1.3	7.8
19.2	$C_{10}H_{14}O_3$	5-Tert-butylpyrogallol	1.7	7.9
20.2	$C_{15}H_{16}$	1,1′-Propylidenebis-benzene	1.4	8.0
21.8	$C_{10}H_{12}O_4$	1-(4-Hydroxy-3,5-dimethoxyphenyl)-ethanone	1.5	–
22.2	$C_{11}H_{14}O_4$	Desaspidinol	0.6	–

Endash not detectable

Conclusions

In this study, we found that during thermo-chemical liquefaction of biomass, the relative proportion of the resulting solid, liquid, and gaseous fractions was dependent on the heating rate; however, variations in the heating rate did not significantly affect chemical composition of the liquid products. The composition of the liquid products is more dependent on the biomass species used for liquefaction. Varying the cooling rate did not show obvious effects on the ratio of liquid to solid to gas nor on the composition of the liquid products. These results imply that, when trying to maximize liquid yield during biomass liquefaction, it is critical to design the full-scale system for high heating rates and optimal heat transfer.

Acknowledgment The University of Minnesota Initiative for Renewable Energy and the Environment (IREE) is gratefully acknowledged for its financial support. The authors would like to thank collaborators: Dr. Shri Ramaswamy, Dr. Ulrike W Tschirner, Dr. Vernon R Eidman, Dr. Steve Polasky, Dr. Waleed Wafa Al-Dajani, and Dr. Huajiang Huang. The authors also would like to thank Dr. Qi Fu for assistance with GC and Dr. Fei Yu for comments.

References

1. Huber, G. W., Iborra, S., & Corma, A. (2006). *Chemical Reviews, 106*, 4044–4098.
2. Denirbas, A. (2004). *Energy Sources, 26*, 715–730.
3. Yu, F., Ruan, R., Lin, X., Liu, Y., Fu, R., Li, Y., et al. (2006). *Applied Biochemistry and Biotechnology, 130*, 563–573.
4. Elliott, D. C., & Schiefelbein, G. F. (1989). *Abstracts of papers of the American Chemical Society, 198*, 55–FUEL.
5. Elliott, D. C., Beckman, D., Bridgwater, A. V., Diebold, J. P., Gevert, S. B., & Solantausta, Y. (1991). *Energy & Fuels, 5*, 399–410.
6. Goudriaan, F., van de Beld, B., Boerefijn, F. R., Bos, G. M., Naber, J. E., van der Wal, S., et al. (2001). In A. V. Brigdwater (Ed.), *Progress in thermochemical biomass ConVersion 2* (pp. 1312–1325). Oxford, UK: Blackwell Science.
7. Boocock, D. G. B., & Porretta, F. (1986). *Journal of Wood Chemistry and Technology, 6*, 127–144.
8. Fu, Q., Sherwood Lollar, B., Horita, J., Lacrampe-Couloume, G., & Seyfried, Jr., W. E. (2007). *Geochimica et Cosmochimica Acta, 71*, 1982–1998.

Appl Biochem Biotechnol (2008) 148:1–13
DOI 10.1007/s12010-007-8117-8

Bundled Slash: A Potential New Biomass Resource for Fuels and Chemicals

Philip H. Steele · Brian K. Mitchell · Jerome E. Cooper · S. Arora

Received: 15 May 2007 / Accepted: 3 December 2007 /
Published online: 15 January 2008
© Humana Press Inc. 2007

Abstract Postharvest residues for southern pine species have not previously been quantified to compare volumes produced from both thinnings and clearcut volumes. A John Deere 1490 Slash Bundler bundled postharvest residues following a first thinning of a 14-year-old stand, a second thinning of a 25-year-old stand, and a clearcut of a naturally regenerated mature stand of 54 years of age. Regardless of stand type, nearly one-fifth of merchantable volume harvested was collected as postharvest residue. Initial bundle moisture contents were 127.3, 81.1, and 49.4% dry basis (db) for the first and second thinnings and mature stands, respectively. Bundle needles content was found to significantly influence the relative moisture contents of the bundles by stand type due to the high moisture content of needles compared to other bundle components. Bundles were stored outside and exposed to very hot and dry conditions and dried very rapidly to lowest moisture contents of 22.8, 14.5, and 13.5% (db) for first and second thinnings and mature stands, respectively. Response to moderating temperatures and higher precipitation resulted in rapid moisture content increase to 69.9, 46.2, and 38.1% (db) for the first and second thinnings and mature stand bundles by the end of the study. Temperature and precipitation and bundle percentage needles content all significantly influenced the rapid moisture content variations observed over the study periods.

Keywords Harvest · Residues · Bundles · Stand · Slash · Moisture content

P. H. Steele · B. K. Mitchell · J. E. Cooper (✉)
Department of Forest Products, Forest and Wildlife Research Center, Mississippi State University, Starkville, MS 39759, USA
e-mail: jcooper@cfr.msstate.edu

S. Arora
Mississippi Technology Alliance, Ridgeland, MS 39157, USA

Introduction

Postharvest Residues

Forest residues following harvesting have been shown to comprise a significant volume of total timber stand biomass. However, difficulty in recovering this biomass and low prices for this feed stock for its use in combustion have severely limited efforts to utilize this resource. In the USA, virtually 100% of this postharvest residue is unutilized. Previous research into recovery of US timber harvest residues peaked in the 1980s during the nation's last energy shortage. Relatively low fuel prices until 2005 made this resource an uneconomic feed stock as a result of the high costs of collecting and transporting the biomass. However, current high fuel costs and the current interest in conversion of lignocellulosic biomass to ethanol have increased interest in the potential recovery of post-timber-harvest residues as feed stocks for bioenergy products.

Nettles [1] performed a thorough review and summary of harvest residue volumes produced by stand type, and we are indebted to this researcher for his bibliography, from which we located most of the literature cited below. Past research on southern pine plantations was performed by Beardsell [2], which indicated that 44.7 oven-dry metric tons per hectare (ODMT/ha) was available following clear cutting. When hardwoods were present, postharvest residue volumes were significantly higher with 50 ODMT/ha for mixed species and 80.1 ODMT/ha for hardwood stands. For large-diameter bottomland hardwood stands, harvest residue volumes again increased significantly to 150.0 ODMT/ha [1, 2]. The residue volumes cited above were for clearcut timber stands.

Clearcut postharvest residue volumes were compared to thinning harvest residue volumes for UK upland spruce plantations with 44.7 ODMT/ha yield volume for clearcut and 18.0 ODMT/ha yield volume for thinned stands [1]. Watson et al. [3] quantified the energy–wood biomass available on two 22-year-old slash pine plantations and a 45-year-old natural stand of mixed slash and loblolly pine in Alabama. All stands were being clearcut for pulpwood. Two harvesting methods were applied, a one-pass system and a two-pass system. Mean residue harvest volume for the two plantation pine stands was 75.4 green metric tons per hectare (GMT/ha); for the natural mature stand the mean harvest volume was 61.5 GMT/ha.

A West Virginia study computed postharvest residue available when definition of acceptable biomass required pieces to be at least 1219.2 mm long and of rather large average small-end (122 mm) and large-end (182.9 mm) diameters. Mean length of all pieces was 3,658 mm, resulting in a mean volume collection of 32.7 m^3 per hectare [2]. A 1976 study of a maple-birch northern hardwood stand indicated that harvest residues were of relatively large diameter, with 50% having diameters exceeding 76.2 mm; 25% of the volume was greater than the minimum size for 470 mm pulpwood grade; 15% made the 2,540-mm pulpwood size class [4].

With the exception of one of the studies cited above, very little research has been performed to quantify postharvest residues for thinned stands. None provide this quantification for thinned southern pine plantations. Managers of southern pine timber stands who contemplate the total utilization of the biomass available on their forests have no information on potential postharvest residues available following thinning treatments.

A major potential between-stand difference for loblolly pines is caused by the density and moisture content differences between juvenile and mature wood. The southern pines produce juvenile wood during an approximate 10-year period beginning with germination. The juvenile wood type has larger cell lumens, resulting in increased moisture content because more water is contained in the cells. Mean southern pine juvenile wood moisture content is reported to be

139% dry weight basis (db), compared to 98% (db) for normal wood [5]. Therefore, juvenile wood is expected to have 42% higher moisture content than mature wood.

The moisture content of wood products is of interest because green wood has a moisture content ranging from 50 to 100% (db) or more depending on the species and wood type involved. For green southern pine, the weight of water is generally equal to the weight of the dry wood matter. Therefore, drying wood prior to transportation is a method to substantially reduce transportation costs. In addition, green wood must often be dried prior to processing to bioenergy products. Heat from wood combustion is considerably higher for dry compared to green wood. Pyrolysis and gasification for energy require that wood be dried to between 5 and 10% (db) moisture content. Few wood biomass feed stocks dry naturally after harvest, and large amounts of energy must be expended to dry the wood prior to processing. Development of a natural drying method for postharvest biomass to be utilized for bioenergy products would benefit the economics of the product production process.

Southern pine needles contain 154% (db) moisture content, while stems and branches average 115.5% (db) [6]. Young pine trees have a significantly higher proportion of branches with needles attached than do older pines. This is particularly true for plantation pines that generally have much wider between-tree spacing than do naturally regenerated stands. With all else equal, harvest residue from younger stands, containing large volumes of juvenile wood and needles, should have significantly higher moisture content values.

Postharvest Residue Collection Machinery

Several specialized machines have been developed to collect postharvest residues with their challenging size and distribution characteristics. Designs implemented in 2001 were reviewed by Nettles [1]. These include the Nicholson–Koch "Mobile Harvester," Georgia Pacific's "Jaws III," the Canadian Forest Engineering Research Institute's "Recufor M," and TVA's topwood harvesters.

John Deere has recently developed the 1490 Slash Bundler to collect postharvest residues following both thinnings and clearcuts. The John Deere 1490 (JD 1490) was originally developed in Scandinavia as the Timberjack 1490D (TJ 1490D). In 2003, several stand types were harvested in the western USA with the TJ 1490D to determine volume yields and efficiencies [7]. Rummer et al. quote a Swedish study that found that the TJ 1490D produced 30–40 bundles per hour with the range of costs at \$8.66 to \$11.33/m^3 harvested [7]. On the multiple sites tested by Rummer et al. in their western US studies [7], the bundles per hour produced ranged from 5 to 24, with a mean of 14.5. Site difficulty, slash arrangement, and residue density influenced the per-hour bundle production by determining the feeding time. Moisture content of the bundles on the four sites, at which this variable was measured, ranged from 11.3 to 58.1%, with a mean value of 30.8%. The TJ 1490D collected only a percentage of available material. Residues that were too scattered, short, rotten, or unproductive of retrieval were left in the field. Collection rates for available residues were highly variable, with the respective rates for the six sites being 5, 16, 20, 33, 53, and 62% [7].

Objective

The objectives of this study were (1) to compare relative bundled postharvest slash yields by stand type and (2) to monitor moisture content changes over a 4-month period during outdoor storage of the bundles.

Procedures

Slash Collection Machine

A JD 1490 Slash Bundler was used to harvest the study sites. A photograph of this machine is shown in Fig. 1, harvesting slash on one of the study stand sites. The boom grappler is utilized by the operator to collect residues for input to the in-feed deck. Multiple compression rollers forward the material into the bundler packing unit. Two pairs of compaction frames grasp and slide the compacted bundle through the wrapping unit, where bundles are wrapped with twine. The wrapped bundle is passed through the bundler until it reaches a preset length, at which time a chain saw cuts the bundle transversely, allowing it to drop to the side of the bundler.

The JD 1490 Slash Bundler is a six- or eight-wheeled device weighing about 22,000 kg; its horsepower is 182.4. The machine's length is 6,200 mm. The maximum boom reach length is 10 m. Bundle length can range from 2,400 to 3,200 mm. Bundle diameter can range from 700 to 800 mm. The manufacturer's estimate of bundler productivity is 20 to 30 bundles per hour.

Study Harvest Sites

The site of the study was on timberlands owned by Potlatch. The sites were located in Bradley County in eastern Arkansas. Company personnel identified typical first thinning, second thinning, and mature stands on which to perform the representative bundling studies. The characteristics of the three stands harvested for this study are described in Table 1. The stands were contiguous blocks, with the first-thinning site comprised of 5.11 ha, the second-thinning site comprised of 3.59 ha, and the mature stand comprised of 3.53 ha. The mature site was harvested on July 20, the second-thinning site on July 25, and the first-thinning site on July 26.

Table 2 is the Potlatch characterization of the study stands by presence of hardwood vs. pine species and by pulpwood vs. saw log size timber. The first-thinning stand was comprised of 100% pine pulpwood with no saw timber size trees. Pine timber on this young tract had not had time to grow to saw log size; likewise, ingrown hardwood had not had time to reach a merchantable size. The second-thinning stand had a small component (4.4%) of hardwood pulpwood resulting from hardwood under story invasion. The same was true of the clearcut mature stand with only 2.6% of pulpwood size hardwood under



Fig. 1 Photograph of JD 1490 Slash Bundler on a study site showing use of boom grappler to feed biomass into the compression jaw, compression of biomass into a bundle, and exit of bundle from compression system after binding with twine

Table 1 Initial and postharvest characteristics of the three study stands.

Study site	Stand size (ha)	Stand age (years)	Initial stand volume (GMT/ha)	Initial basal area (m^2)	Postharvest basal area (m^2)
1st thin	5.11	14	297.7[a]	11.4	7.9
2nd thin	3.59	25	370.9[b]	8.2	6.9
Clearcut mature stand	3.53	Approx. 54	424.0[b]	7.2	0

[a] Volume estimated from 2003 prethinning inventory.

[b] Volume estimated from 2006 prethinning modeling.

story invasion. Pine saw logs in the second thinning comprised 66.7% of total merchantable volume, while for the clearcut mature stand, this percentage was 71.1%.

Slash Bundler Production Statistics

Production and cost determination for the JD 1490 were outside the objectives of the current study. However, a team led by Dr. David W. Patterson collected time and motion and cost data, which were published in a MS Thesis in 2006. The data shown in Table 3 are from this study [8]. These results show the bundles and tons per hour production rate and costs by stand type.

Sampling Method

A subsample of five bundles was selected at random from each study site and was weighed green on the same day as they were bundled. These 15 subsamples were covered and transported by trailer from Arkansas to the Department of Forest Products, Mississippi State University, Starkville, MS. Bundles were distributed on a mowed lawn with 1,524 mm of clear space separating all sides of each bundle from its neighbor to simulate aging in a harvested setting as closely as possible. Bundles were uncovered and with no shade from any source, such that they were fully impacted by sun and rain that occurred during the study.

Each stand type's five bundles were randomly assigned to monthly destructive determination of needle and stem volume and oven-dry moisture content. The period over which the moisture content of the bundles was monitored was 4 months, with sampling occurring at 30-day intervals over this period. The sampling schedule is shown in Table 4. At the beginning of each period, three bundles, one bundle for each stand type, were sampled and their needle and stem components quantified. For this study, stem wood was defined as all solid wood components that were not needles. This included small bole wood

Table 2 Components of study stands by timber species and pulpwood vs. saw log size.

Study site	Hectares harvested (ha)	Pine logs (GMT/ha)	Pine pulpwood (GMT/ha)	Hardwood pulpwood (GMT/ha)	Total merchantable (GMT/ha)
1st thin	5.11	0	64.7	0	64.7
2nd thin	3.59	43.7	19.0	3.0	65.7
Clearcut mature stand	3.53	89.2	33.1	3.2	125.5

Table 3 JD 1490 production rate in green tons and bundles per hour with estimated production cost per bundle.

	1st thin	2nd thin	Clearcut
GMT/h	9.2	9.6	6.4
Bundles/h	21.1	23.2	16.1
Cost per bundle	$9.53	$8.72	$2.56

pieces, limbs, and small stems. Needles were separated from small needle-holding stems during sorting.

Moisture Content Analysis

Prior to destruction, to determine needle and stem component volumes, each sample bundle was weighed in total. This allowed computation of the moisture content of the bundles based on this green bundle weight and the oven dry weights of the stems, needles, and residuals. For the destructive needle and stem volume and moisture content determinations, each sample bundle was divided into five equal sections along its length, and three of these sections were randomly selected for stem and needle separation. The specimen sections were crosscut from the bundle at section demarcation boundaries by chainsaw. These specimen sections had needle and stem components segregated, and the separated components were weighed green and then placed in a biomass drier at 103 °C temperature for 24 h to obtain oven-dry weights for both stems and needles from which oven-dry moisture contents were computed. Stem and needle component percentages were computed for each of the bundles that were destructively broken down to obtain representative stem and needle moisture contents.

Bundle weights for each period, following the initial green weights obtained on the harvest site, were determined at the MSU storage site. The bundles to be broken down for component analysis were weighed prior to breakdown. Because breakdown took from 4 to 8 days to complete, the bundle section weights changed over this period as they dried. This did not influence the oven-dry section weights and estimation of section components but did not allow acquisition of a true moist bundle section weight at period beginning. To correct for this error, bundle dry section weight percentages were applied to the start-of-period moist bundle weights to estimate the start-of-period moist section weights.

During destructive separation of stem and needle components in each bundle, a small component of residue was present that was comprised of material that could not be classified as either stem or needle component. These we termed residuals, and this component consisted of dirt entrained into the bundles during harvesting, small fractured

Table 4 Dates, with number of days following stand harvest, at which bundle destructive testing to determine moisture content by component types was performed.

Period	Date and (number of days) following stand harvest		
	1st thinning	2nd thinning	Mature
Initial	8/7/2006 (12)	7/27/2006 (2)	7/24/2006 (4)
1st	8/29/2006 (34)	8/25/2006 (31)	8/23/2006 (34)
2nd	10/2/2006 (68)	9/26/2006 (62)	9/22/2006 (64)
3rd	10/24/2006 (90)	10/27/2006 (96)	10/30/2006 (102)
4th	11/30/2006 (126)	11/21/2006 (121)	11/20/2006 (123)

The 4 months over which bundles were destructively tested were divided into five periods as defined in the table.

pieces of needles and stems, dirt incorporated into the bundles from ants building nests in them during storage, and a fungally deteriorated needle and bark component resembling compost.

Results and Discussion

Bundling on the harvested stands commenced as soon as possible following harvest. Bundles from all stands averaged 635 mm in diameter and were 3,048 mm in length. On July 20, the 3.52-ha, naturally regenerated mature stand was bundled to produce a total of 238 bundles, over 14.8 h, with a mean weight per bundle of 0.4 GMT. Total bundled weight for the mature stand site was 95.3 GMT or 26.9 GMT/ha. Bundling was performed on July 25 on the 3.6-ha second-thinning site, and 100 bundles, produced over 4.3 h with a mean weight of 0.42 GMT/bundle, were harvested. Total weight of all bundles was 41.5 GMT or 11.6 GMT/ha. One-hundred and sixty nine bundles, with a mean weight of 0.43 GMT/bundle, were collected over a period of 8.0 h from the 5.1-ha first-thinning site on July 26. These bundles weighed a total of 72.8 GMT or 14.3 GMT/ha.

Per-stand merchantable volume harvested and residue bundled in GMT/ha are given in Table 2. The percentage of bundled residue per initial stand volume and per merchantable ton is also given in Table 5. For the first-thinning stand, initial stand merchantable volume harvested was 64.7 GMT/ha and bundled residue was14.3 GMT/ha. Bundled residue was 4.8% of estimated stand volume, and bundled residue was 22.0% of harvested merchantable volume. The percentage that bundled residue comprised of the first-thinning stand is probably overestimated because the computation is based on a 2003 inventory. Substantial growth since this inventory may be expected to have taken place. Second-thinning results were 65.7 GMT/ha of merchantable volume and 11.7 GMT/ha of bundled residue. Bundled residue comprised 3.1% of the estimated initial stand volume and 17.6% of the harvested merchantable volume. The naturally regenerated clearcut mature stand had 125.5 GMT/ha of merchantable volume with about double the bundled residue of the thinned stands at 26.9 GMT/ha. Bundled residue was 6.3% of the estimated initial stand volume harvested and was 21.5% of the harvested merchantable volume.

The residual component of the bundles was relatively small at 6% or less of the total green bundle volume; the exception was one bundle with 15.3% residual volume that was particularly fungally deteriorated. The needle and stem components of the destructed bundles were oven dried and weighed following their separation into these components. Figure 2 gives stem, needle, and residual component oven-dry percentage volumes for each stand type. The first-thinning needle component comprised 22% of total bundle volume. At 12.7%, the second thinning had just over one-half the percentage of the needle volume of the first thinning. Needle volume component for the naturally regenerated mature stand was

Table 5 Per-acre harvested merchantable timber and bundled residue volumes and the percentage that bundled residue comprised of the initial stand and merchantable volumes.

Study site	Harvested merchantable volume (GMT/ha)	Bundled residue per initial stand volume (%)	Bundled residue (GMT/ha)	Bundled residue per merchantable ton (%)
1st thinning	64.7	4.8	14.3	22.0
2nd thinning	65.7	3.1	11.7	17.6
Naturally regenerated stand	125.5	6.3	26.9	21.5

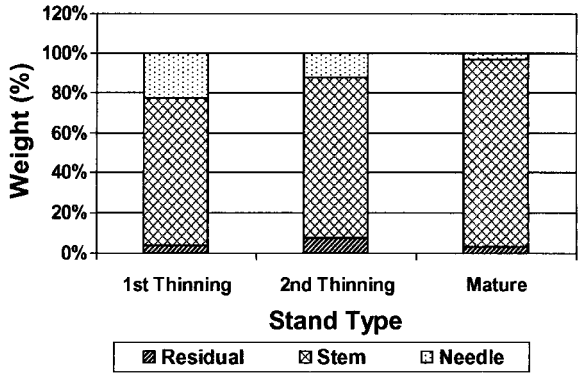


Fig. 2 Per-stand stem, needle, and residual volumes as a percentage of oven-dry bundle weight

a very low 3.4%, or about one-quarter of the needle volume of the first-thinning stand. These results correspond to the expectations discussed above that young stands would have higher needle volumes than older stands. Stem volumes are, by and large, the complement of the needle results because the residual component was a negligible amount of total bundle volume. The stem components of the bundles were 74.0, 79.6, and 93.0% of first-thinning, second-thinning, and mature-stand volumes, respectively.

Figures 3, 4, and 5 show the moisture content levels of the bundles by month over the 4-month study period. Average initial bundle moisture content value for the Fig. 3 first-thinning stand was 127.3% (db); the second-thinning stand initial moisture content value was 81.1% (db), while the mature stand value was 49.4% (db). Therefore, the first-thinning stand moisture content was 46.2% higher than that of the second thinning stand and 77.9% higher than that of the mature stand. These results appear to reflect the relative difference in magnitude of the juvenile wood prevalent and needles in the bundles by stand type. Both juvenile wood and pine needles contain higher moisture contents than stem wood and bark. The first-thinning material, at 14 years of age, was composed of a high volume of juvenile wood. Because research indicates that juvenile wood has a green moisture content of 139% (db), compared to a moisture content of 115.5% (db) for stem and branch wood, it was expected that the first-thinning and second-thinning stand bundles would have higher initial moisture contents compared to that for bundles from mature stands. In addition, as discussed above, bundles from younger timber should have considerably higher needle volumes, with a green moisture content of 154% (db), higher than any other component

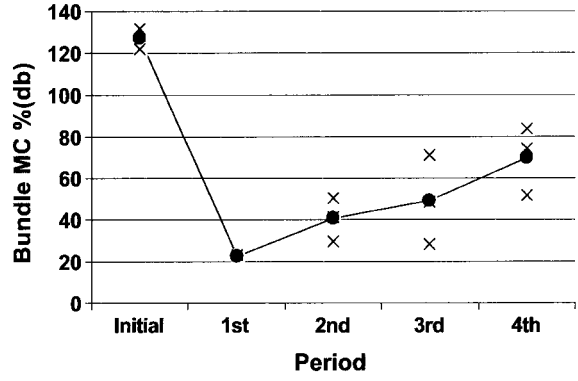


Fig. 3 Moisture content values by study period for the first-thinning stand. Means are shown as *black dots*, while observations are shown as *crosses*. For each period, three observations were made, with some observations hidden behind the mean value

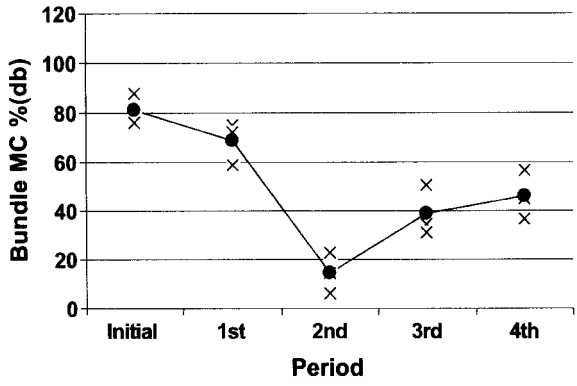


Fig. 4 Moisture content values by study period for the second-thinning stand. Means are shown as *black dots*, while observations are shown as *crosses*. For each period, three observations were made, with some observations hidden behind the mean value

shown by research to be the bundles. Therefore, bundles from first- and second-thinning material were expected to have higher moisture content from these two influences. Quantification of the actual relative needle volumes contained in the respective stand bundles confirmed our expectation that bundles from younger stands would have considerably higher needle volumes. The percentages of needles in the bundles were 22.7, 12.7, and 3.2% for first thinning, second thinning and mature wood stands, respectively.

To test our hypothesis that needle volume was an influential factor in high initial moisture content, Eq. 1 was estimated with initial moisture content (IMC) as a function of percent needle volume in each bundle (PN). Percentage needle volume (PN) was found to be highly significant at the 0.0001 level, supporting our hypothesis that magnitude of bundle needle volume influenced initial bundle moisture content.

$$\mathrm{IMC} = a + \mathrm{PN} + e \tag{1}$$

IMC	initial bundle moisture content
a	the intercept term
PN	the percentage total bundle weight comprised by needles
e	the error term

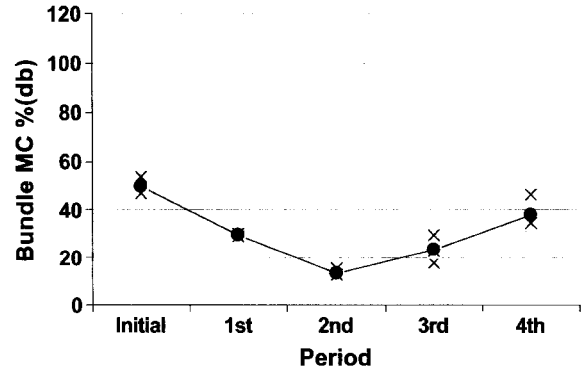


Fig. 5 Moisture content values by study period for the mature stand. Means are shown as *black dots*, while observations are shown as *crosses*. For each period, three observations were made, with some observations hidden behind the mean value

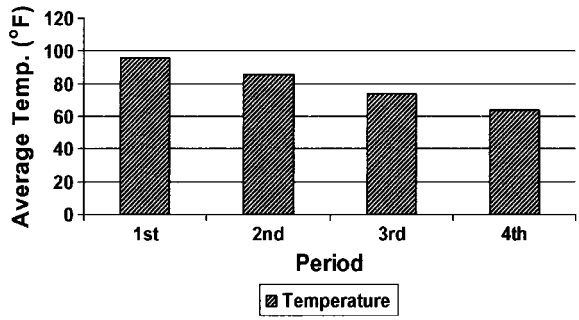


Fig. 6 Average temperature for each monthly period

Figures 3, 4, and 5 show that the study bundles dried very rapidly during what was a very hot and dry first monthly period extending from late July to late August. Bundles from each stand type lost moisture rapidly over this first period, with the first-thinning stand decreasing by 104.5 percentage points to 22.8% (db) moisture content. The second thinning and mature stand bundle moisture content values decreased to 68.7 and 29.6% (db), for respective percentage point decreases of 12.4 and 19.8%.

Over the second and subsequent periods, the first-thinning stand moisture content increased steadily to 69.9% (db) in the fourth period from its lowest moisture content [22.8% (db)] at the end of the first period. Bundles from the second thinning and mature stands, however, followed a somewhat different pattern, losing moisture over the second period to lows of 14.5 and 13.5% (db), respectively, at the end of the second period. The moisture contents of the second thinning and mature stands then steadily increased through the final period to 46.2 and 38.1% (db), respectively. These results showed that the first-thinning stand not only began with bundles containing much higher moisture content but lost moisture at a much faster rate than did the bundles of the other stand types. In addition, the first-thinning stand gained moisture at a faster rate when its moisture content began to increase. Likewise, the second-thinning stand lost moisture at a faster rate than did the mature stand; moisture content also increased at a faster rate for the second-thinning stand compared to the mature stand when their moisture contents began to increase. The difference in initial moisture content has already been identified as the difference in proportion of higher-moisture juvenile wood and needles in younger stands. Following initial drying, the juvenile wood moisture content would not be expected to increase in moisture content at a significantly faster level than the rest of the bundle components. However, the small size of the needle components of the bundles renders them very sensitive to moisture content changes. We believed it likely that the rapid bundle moisture content variations over time probably stemmed from the major difference between the

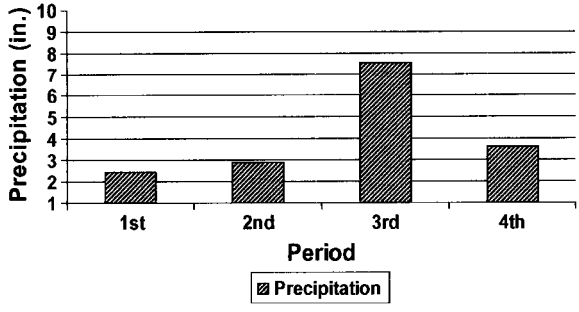


Fig. 7 Total precipitation by monthly period

bundles of each stand type: the percentage needle volume that each contained. These values differed considerably at 22.7, 12.7, and 3.2%, respectively, for the first, second, and mature stands. Below, we will test the hypothesis that the speeds of bundle moisture content change were related to the relative volume of needles in the bundles from each stand type.

Figures 6 and 7 show the average temperatures and mean precipitation amounts by period during the 4-month study. Figure 4 shows that the weather was extremely hot and dry during over the first and second periods, with a mean temperature of 35.3 °C during the first period and a mean temperature of 29.9 °C during the second period. This was accompanied by low precipitation of 63.5 and 73.7 mm during the first and second periods, respectively (Fig. 7). The very high temperatures and low rainfall during these periods explain the rapid moisture content losses from initial green to lowest moisture content of 104.5 (at the end of the first period), 66.6 (at the end of the second period), and 35.9 (at the end of the second period) percentage points for the first- and second-thinning and mature stands, respectively.

After the first period's high temperatures and low precipitation, temperatures began to moderate, and rainfall increased over subsequent periods. These weather factors appear to have combined to result in the increased moisture content values following the first period for the first-thinning stand and after the second period for the other two stand types.

The discussion above of the results in Figs. 3, 4, 5, 6, and 7 appear to indicate that weather, in the form of rainfall and temperature, expectedly influenced bundle moisture content to a high degree and that the changes varied considerably by stand type. As discussed above, we hypothesize that the volume of needles contained in each bundle, highly influenced by the weather, was the major factor responsible for the rapid fluctuation of bundle moisture content during the study. To determine the influence of the temperature, precipitation, and needle volume variables on bundle moisture content over time, a regression model (Eq. 2) containing these variables was developed.

$$\mathrm{MC} = a + \mathrm{PN} + \mathrm{PREC} + T + \mathrm{PN} * \mathrm{PREC} + \mathrm{PN} * T + \mathrm{PREC} * T + \mathrm{PN} * \mathrm{PREC} * T + e \quad (2)$$

MC	moisture content for periods 1, 2, 3, and 4
a	the intercept term
PN	the percentage total bundle weight comprised by needles
PREC	the total precipitation by period
T	the mean temperature over the period
*	interaction between the connected variables
e	the error term

Equation 2 results showed that precipitation (PREC) and needle percentage (PN) variables were highly significant at the 0.0001 level, while temperature was significant at the 0.03 level. None of the interaction terms were found to be significant variables. Percent needles (PN) contained in the bundles had the highest influence on moisture content, with a sum of squares (SS) value (44,565) more than five times as large as the 8,233 SS for precipitation. Temperature (T) had a lower SS value of 1,798.

These results indicate that the most influential factor influencing bundle moisture content was the weight of the needles present in each bundle. Precipitation and temperature significantly impacted moisture content, as would be expected, but had less impact as needle volume decreased.

This study's findings regarding the influence of bundle needle content, temperature, and precipitation are obviously only specifically relevant to slash bundling practiced during the hottest monthly weather in the south followed by storage into the fall when cooler temperatures and higher precipitation prevail. It is expected, however, that bundle needle content would have considerable influence on bundle moisture content values over time regardless of time of harvest and storage. Needles are, by far, the smallest lignocellulosic component in the bundles, and it makes sense that this small component will adsorb and desorb moisture readily as a result of precipitation and temperature variations during outdoor storage.

Summary

Postharvest loblolly pine residues were bundled with a JD 1490 Slash Bundler on Potlatch timberlands in eastern Arkansas. A first and second thinning and a clearcut of a naturally regenerated mature stand were performed on stands of 5.11, 3.59, and 3.53 ha, respectively. Bundled residue from these stands constituted 22.0, 17.6, and 21.5% of merchantable volume harvested for first and second thinning and mature stands. Bundles were stored outdoors over a 4-month period to simulate aging at the harvest site. Results showed that relative needle volume decreased as stand age increased with needle volumes of 22.7, 12.7, and 3.2% for the first- and second-thinning and mature stands, respectively. Bundles were monitored for moisture content variation over the 4-month study period. Initial green bundle moisture content values for the first- and second-thinning and mature stands were 127.3, 81.1, and 49.4% (db). The relative moisture content values were found to be significantly influenced by percentage needle content in the bundles due to the high moisture content of needles relative to other bundle components.

Temperature was very high and precipitation very low during the first period of the study. The high temperature and low precipitation were responsible for the decrease in bundle moisture contents to their lowest values of 22.8, 14.5, and 13.5% (db) for first- and second-thinning and mature stands, respectively. Temperatures moderated and rainfall increased over the remaining periods, causing a consistent rise in all bundle moisture content to 69.9, 46.2, and 38.1% (db) for the first- and second-thinning and mature stands, respectively, by the end of the study. A regression model was estimated that showed that temperature, precipitation, and percentage bundle needle volume all had significant influence on the rapid variation in moisture content over the study periods.

Acknowledgements This project would not have been possible without the cooperation of the Potlatch timberlands staff. We are particularly indebted to Matt Roberts, Potlatch Production Engineer, for coordinating the study on the Potlatch harvest sites. We are also grateful for the financial support of John Deere, who supplied the 1490 Slash Bundler at no cost to the project. This study was funded by the DOE Strategic Biomass Initiative funds administered by Mississippi Technology Alliance, Jackson, MS. This manuscript is publication # FP410-0407 of the Forest and Wildlife Research Center, Mississippi State University.

References

1. Nettles, W. R. (2001). *Improving the utilization of logging residues*. Thesis, Department of Forestry, Mississippi State University, Mississippi State, MS.
2. Beardsell, M. G. (1983). *Integrated harvesting systems to incorporate the recovery of logging residues with the harvesting of conventional forest products*. Thesis, Department of Forestry. Virginia Polytechnic Institute and State University, Blacksburg, VA.

3. Watson, W. F., Stokes, B. J., & Savelle, I. W. (1986). Comparisons of two methods of harvesting biomass for energy. *Forest Products Journal, 36*(4), 63–68.
4. Mattson, J. A., & Carpenter, E. M. (1976). Logging residue in a northern hardwood timber sale. *Northern Logger and Timber Processor, 24*(9), 16–29.
5. Zobel, B. J., & Sprague, J. R. (1998). *Juvenile wood in forest trees*. Berlin: Springer-Verlag.
6. Koch, P. (1972). *Utilization of the southern pines, vol. 1*. USDA Forest Service, So. For. Expt. Sta., US Govt. Printing Office, Wash., DC.
7. Rummer, B., Len D., & O'Brien, O. (2004). *Forest residues bundling project: New technology for residue removal*. USDA Forest Service Forest Operations Unit, Southern Research Station CD Unnumbered Report.
8. Earl, J. A. (2006). *Slash bundler performance in southeastern Arkansas*. Thesis, Department of Forest Resources, University of Arkansas, Monticello, AR.

Appl Biochem Biotechnol (2008) 148:15–22
DOI 10.1007/s12010-008-8179-2

Pretreatment Characteristics of Waste Oak Wood by Ammonia Percolation

Jun-Seok Kim · Hyunjoon Kim · Jin-Suk Lee · Joon-Pyo Lee · Soon-Chul Park

Received: 18 April 2007 / Accepted: 11 February 2008 /
Published online: 8 March 2008
© Humana Press 2008

Abstract A log of waste oak wood collected from a Korean mushroom farm has been tested for ammonia percolation pretreatment. The waste log has different physical characteristics from that of virgin oak wood. The density of the waste wood was 30% lower than that of virgin oak wood. However, there is little difference in the chemical compositions between the woods. Due to the difference in physical characteristics, the optimal pretreatment conditions were also quite different. While for waste oak the optimum temperature was determined to be 130°C, for virgin oak wood the optimum pretreatment was only achieved at 170°C. Presoaking for 12 h with ammonia solution before pretreatment was helpful to increase the delignification efficiency.

Keywords Waste oak wood · Pretreatment · Ammonia · Enzymatic hydrolysis · Lignin

Introduction

The oil crisis and global warming are the major threats to the sustainable developments of our society. Biofuels are emerging as a promising solution to overcome the barriers. However, now the biofuels are mainly produced from edible materials so that the shortage of the raw materials should be encountered in near future as the implementation of biofuels is getting more active.

Now the bioethanol is a dominant biofuel and the demand for the bioethanol continues to increase steadily for several decades [1]. To overcome the shortage of raw material, the technology developments for bioethanol production from lignocellulosic biomass have been carried out intensively. Since the collection cost of the wood biomass is too high in Korea,

Presented at the 29th Symposium on Biotechnology for Fuels and Chemicals

J.-S. Kim · H. Kim
Department of Chemical Engineering, Kyonggi University, Suwon 443-760, South Korea

J.-S. Lee (✉) · J.-P. Lee · S.-C. Park
Bioenergy Research Center, KIER 71-2 Jang-dong, Daejeon 305-343, South Korea
e-mail: bmjslee@kier.re.kr

it will not be economically feasible even though a very highly efficient technology is developed [2]. An alternative is to focus on lignocellulosic biomass which does not require too much collection cost. One of the promising candidates is the mushroom bed which can be easily collected from the mushroom farms. Currently, about 40,000 tons of oak-wood logs are used annually for growing the mushrooms, and about same amount of the waste log should be generated annually. The waste log woods are being powdered and used as soil conditioner [2].

Since the direct conversion efficiency of the lignocellulosic biomass into the fermentable sugars is not high, various pretreatment technologies have been investigated to produce sugars more economically [3]. As a pretreatment reagent, ammonia has a number of desirable characteristics: swelling of cellulosic materials, highly selective delignification reaction, low interaction with carbohydrates, and high volatility. One of the known reactions of aqueous ammonia with lignin is the cleavage of C–O–C bonding in lignin as well as ether and ester bonding in lignin carbohydrate complex. There are many advantages of removing lignin at the early phase of the conversion process before it is subjected to the biological processing. Lignin is believed to be one of the major hindering factors in the enzymatic reaction [4–6].

Previous investigations have been conducted on various pretreatment processes using a flow-through (percolation) reactor system. Among them is the ammonia recycled percolation (ARP) process that has been studied for pretreatment of various lignocellulosic biomass feedstocks including hardwood [7], corn stover [8, 9], and pulp mill sludges [10]. The recent research includes development of a novel pretreatment/delignification of biomass by soaking in aqueous ammonia for enzymatic saccharification [11]. The purpose of this investigation is to assess the effectiveness of the ARP treatment as a pretreatment process specifically for waste oak wood.

Materials and Methods

Materials

Virgin oak wood and waste oak wood were supplied from a Korean local mushroom farm. They were ground and screened. The fraction collected between 2 mm~20mesh was used in all experiments. The initial composition of virgin oak wood was determined to be: 43.3% glucan, 24.6% xylan, 2.1% arabinan, 1.0% mannan, 1.5% galactan, 19.2% Klason lignin, 2.3% acid-soluble lignin, 3.3% ash, 2.6% acetyl group, and 3.4% protein. The initial composition of waste oak wood was determined to be: 43.7% glucan, 25.5% xylan, and 17.5% Klason lignin that has similar component with virgin oak wood. The density of the waste wood was 30% lower than that of virgin oak wood. The cellulase enzyme, Celluclast 1.5L, was purchased from Novo. The average activity of the enzymes was 89.6 FPU/ml. The β-glucosidase, Novozyme 188, was also purchased from Novo.

Experimental Setup and Operation of ARP

The ARP apparatus was used in the conduction of pretreatment of virgin oak wood and waste oak wood [12]. The system consists of a stock solution reservoir, pump, temperature-programmable oven, SS-316 column reactor (9/10 in. ID×10 in. *L*, internal volume of 101.9 cm^3), and liquid holding tank. The reactor was operated in a flow-through mode, the liquid flowing through the reactor column packed with biomass. Aqueous ammonia

concentration was 15 wt%, and flow rate was 5.0 ml/min. The reactor system was pressurized by nitrogen at 325 psig to prevent vaporization. In a typical ARP experiment, 18 g of biomass sample were packed into the reactor. The reactor temperature was controlled in a forced-air convection oven. About 15 min of preheating time was necessary to reach the desired temperature. The reaction time was counted after the desired temperature was attained. The wet solids discharged from the reactor were separated into two portions. One was oven-dried at 105°C overnight for measurement of weight loss and further subjected to composition analysis. The other was used in the enzymatic digestibility test.

Digestibility Test

The enzymatic digestibility of oak wood biomass was determined according to the National Renewable Energy Laboratory (NREL) Chemical Analysis and Testing Standard Procedure no. 009 [13]. Enzymatic digestibility of pretreatment feedstocks was performed at 50°C and pH 4.8 (0.05 M sodium citrate buffer) on a shake bath agitated at 150 rpm. The digestibility is defined as percent of theoretical glucose released after 72 h of incubation with cellulase enzyme. The cellulase enzyme loading was at 10–60 FPU/g glucan. Samples were taken periodically and analyzed for glucose and cellobiose. Total glucose content after 72 h of hydrolysis was taken for calculation of the enzymatic digestibility. Untreated feedstocks and α-cellulose were subjected to the same digestibility test as a control and as a reference.

Analytical Methods

The samples of virgin oak wood and waste oak wood were analyzed for glucan, xylan, Klason lignin, and acid-soluble lignin following the procedures of NREL Chemical Analysis and Testing Standard Procedures no. 001~004 [13]. Sugars were determined by high-performance liquid chromatography using a Bio-Rad Aminex HPX-87P column for carbohydrate analysis of solids. For enzymatic digestibility, the glucose content was measured by HPX-87H column.

Results and Discussion

The density of the waste wood was 30% lower than that of virgin oak wood. The effects of ARP and pre-soaking were investigated on enzymatic digestibility for virgin oak wood and waste oak wood.

Ammonia Recycled Percolation

The feedstocks (oak wood and waste oak wood) were first put through a series of ARP processes using 15 wt% aqueous ammonia solution. Based on the previous investigations and the results of preliminary experiments of this work, 15 wt% of ammonia concentration was chosen for the ARP operation [14]. The temperature was varied over the range of 100–210°C. The weight remaining after the treatment varied from 77% to 43% for oak wood and from 76% to 38% for waste oak wood. The treated solid samples were then analyzed for sugars and Klason lignin. The results are summarized in Table 1. The glucan fraction after the ARP treatment decreased slightly as temperature was raised from 130°C to 170°C. The glucan retention at these temperatures was near 80% for oak wood and 75% for waste oak wood based on initial solid content. The xylan content and Klason lignin decreased

Table 1 Composition of oak wood (O) and waste oak wood (W) after ARP Treatment.

Reaction (°C)	% Weight remaining	Composition (%)		
		Glucan	Xylan	Klason lignin
Untreated	O 100	43.3	24.6	19.2
	W 100	43.7	25.5	17.5
ARP 100	O 77.7	42.4	20.5	15.9
	W 75.9	42.8	17.1	13.3
ARP 130	O 70.1	39.9	17.8	10.3
	W 68.3	39.4	14.5	6.6
ARP 150	O 62.5	38.1	12.2	8.9
	W 63.3	37.5	11.1	5.1
ARP 170	O 58.5	38.6	11.9	3.6
	W 55.1	29.2	4.8	2.1
ARP 190	O 50.3	32.2	6.4	2.4
	W 45.5	28.9	4.7	2.0
ARP 210	O 42.9	32.2	2.2	2.2
	W 37.7	27.7	2.0	1.5

Contents of all sugar and Klason lignin are based on untreated oven-dried biomass. Reaction condition: flow rate of ammonia (15 wt%)=5.0 ml/min

highly as temperature was raised up to 210°C. About 30–80% of the lignin and xylan were removed form feedstocks by the ARP process at various temperature conditions. Because of high retention of glucan and relatively high delignification, 170°C is deemed as the optimum operating temperature of ARP for virgin oak wood. The compositional changes in solid and liquid samples of virgin oak wood during the ARP at 170°C are summarized in Table 2. The most significant change of the composition is in the lignin. The ARP process removed 66–85% of the total lignin of virgin oak wood feedstock. The delignification reaction is rapid to the extent that 66% of lignin is removed within 10 min of treatment. About half of xylan (main component of hemicellulose) is also solubilized. The glucan content, however, remains relatively intact. The overall reduction of solid mass (expressed as solid remaining, SR) by the ARP is slightly less than half (53.3–64.4%). As indicated in Table 2 by the total of glucan and xylan (amount of carbohydrates in the solid plus that in

Table 2 Effect of reaction time on the compositions of oak wood after ARP treatment.

Time (min)	Solid (%)					Liquid (%)		Total (%)		Delignification (%)
	SR	Klason lignin	ASL	Glucan	Xylan	Glucan	Xylan	Glucan	Xylan	
Untreated	100	19.2	2.30	43.3	24.6	0.0	0.0	43.3	24.6	0.00
10	64.4	7.9	1.1	39.9	14.7	0.8	8.6	40.7	23.6	65.9
20	58.5	3.6	1.0	38.6	11.9	1.2	11.2	39.8	23.1	80.1
40	56.1	3.3	0.9	38.1	10.1	1.5	11.9	39.6	22.0	82.3
60	54.4	2.9	0.8	37.8	9.3	1.6	12.0	39.4	21.3	83.2
90	53.3	2.9	0.7	36.5	9.2	1.6	12.2	38.1	21.4	84.7

All sugar and lignin content based on the oven-dry untreated biomass. Pretreatment conditions: 15wt% of ammonia, 170°C, 5 ml/min of flow rate, 325 psig

SR Solid remaining after reaction, *ASL* acid-soluble lignin during analysis

liquid), the accountability of sugars is above 91% for glucan and 89% for xylan with up to 40 min of treatment. The carbohydrates in the biomass are thus well preserved in the ARP process, a very important benefit as a pretreatment process.

For the waste oak wood feedstock, 130°C of reaction temperature for ARP was optimum considering high retention of glucan and relatively high delignification. This optimal temperature for ARP treatment decreased for the waste oak wood feedstock presumably due to the biodegradation of this material that occurs during the mushroom cultivation. The compositional changes in solid and liquid samples of waste wood during the ARP at 130°C are summarized in Table 3. The delignification reaction is rapid to the extent that 79% of lignin is removed within 20 min of treatment.

Pre-soaking Effect

The pre-soaking effect on enzyme digestibility was investigated for waste oak wood. This work was done to achieve the higher delignification than typical ARP treatment. The waste oak wood was packed into the reactor and soaked with aqueous ammonia (15 wt%). The pre-soaking time was 0 to 48 h at room temperature. After the certain time, the pre-soaked biomass was submitted to an ARP treatment at the conditions previously optimized. The results are summarized in Table 4. The optimum pre-soaking time was selected to 24 h due to the high retention of glucan and relatively high delignification.

Enzymatic Digestibility

The data presented to this point dealt with the changes in the composition of biomass brought about by various pretreatments. The composition of biomass is an important factor in the process economics. It can also serve as an indirect index for the digestibility, the lignin content, for example. However, the true yardstick for a pretreatment must come from the direct measurement of digestibility. All of the solid samples obtained from the ARP treatment were therefore subjected to the standard enzymatic digestibility test. The digestibility data after ARP treatment for both feedstocks with pre-soaking are presented in Figs. 1 and 2. The digestibility was measured with loading of cellulose, 60 FPU/g glucan. Regardless of the treatment conditions, the digestibility of the pretreated biomass

Table 3 Effect of reaction time on the compositions of waste oak wood after ARP treatment.

Time (min)	Solid (%)					Liquid (%)		Total (%)		Delignification (%)
	SR	Klason lignin	ASL	Glucan	Xylan	Glucan	Xylan	Glucan	Xylan	
Untreated	100	17.5	2.3	43.7	25.5	0.0	0.0	43.7	25.5	0.00
10	70.2	10.1	1.1	41.8	17.5	0.5	3.6	42.3	21.1	60.4
20	68.3	6.6	1.1	39.4	14.5	0.9	9.7	40.3	23.2	78.7
40	63. 8	4.5	1.1	39.1	10.0	1.2	10.1	40.3	20.1	80.1
60	61.5	3.9	1.0	38.9	9.5	1.5	12.5	40.4	22.0	80.4
90	60.2	3.3	1.0	38.8	9.0	1.5	12.9	40.3	21.9	81.9

All sugar and lignin content based on the oven-dry untreated biomass. Pretreatment conditions: 15 wt% of ammonia, 130°C, 5 ml/min of flow rate, 300 psig

SR Solid remaining after reaction, *ASL* acid-soluble lignin during analysis

Table 4 Composition of pre-soaked waste oak wood after ARP treatment.

Pre-soaking Time (h)	% Weight remaining	Solid composition (%)		
		Glucan	Xylan	Klason lignin
0	68.3	39.4	17.5	6.6
6	68.0	38.9	16.2	5.8
12	64.8	37.6	15.4	3.1
24	63.4	38.1	15.5	3.0
48	64.6	37.7	14.9	2.9

Contents of all sugar and Klason lignin are based on untreated oven-dried biomass. Reaction temperature, 130°C; flow rate of ammonia (15 wt%), 5.0 ml/min

has significantly improved from that of the control (untreated biomass). After ARP treatment, the digestibility of virgin oak wood and waste wood is improved by about 64% (from 22.5% to 87.4% for the former feedstock and from 23.0% to 86.1% for the latter feedstock). Apparently, the lignin content is a prime factor controlling the digestibility for these feedstocks. For virgin oak wood, the enzyme digestibility was increased up to 87.4% at 170°C of ARP as shown in Fig. 1. Further increase in temperature did not have an effect on enzymatic digestibility. For waste oak wood, the enzyme digestibility was 86.1% at 130°C of ARP and had similar values of these at higher than 130°C in Fig. 2. These results provide further support that the optimum temperature of ARP for waste oak wood is lower than that for virgin oak wood.

The enzymatic digestibility data on the ARP-treated various wood feedstocks (virgin oak wood, waste oak wood, and pre-soaked waste oak wood) are shown in Fig. 3. The digestibilities were measured with three different loadings of cellulase: 60 FPU/g glucan, 30 FPU/g glucan, and 10 FPU/g glucan. With 60 FPU/g glucan enzyme loading, the digestibilities were all above 85%, the highest being near quantitative, 90.3%, which is observed with pre-soaked waste oak wood. With 10 FPU/g glucan enzyme loading, the digestibilities were about 85%. Whether this level is acceptable from a process viewpoint is debatable.

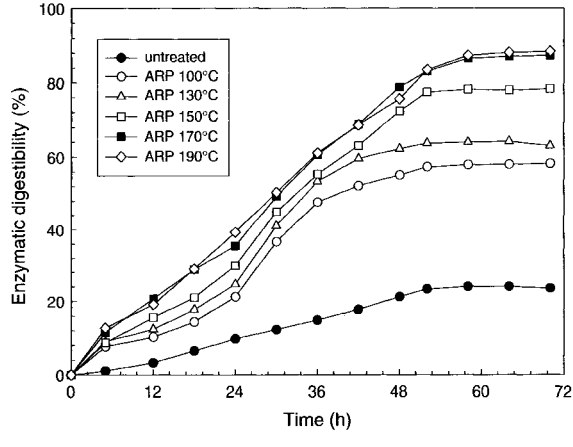


Fig. 1 Enzymatic digestibility of oak wood after ARP at various temperatures (enzyme loading, 60 FPU)

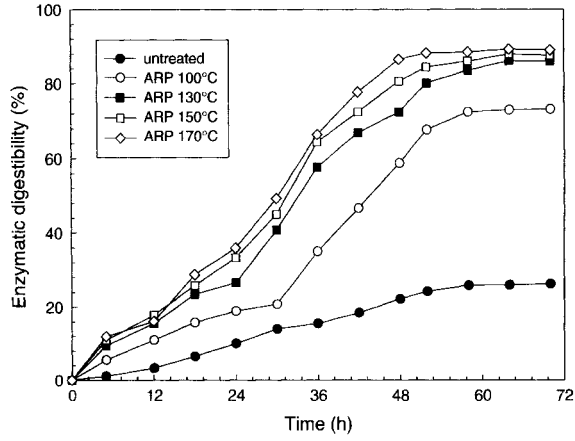


Fig. 2 Enzymatic digestibility of waste oak wood after ARP at various temperatures (enzyme loading, 60 FPU)

Conclusions

Pretreatment of oak wood and waste oak wood, especially by aqueous ammonia, is highly effective in enhancing the enzymatic digestibility and reducing lignin content. The ARP treatment removes 60–85% of the total lignin but retains more than 90% of the glucan content. Pre-soaking and ARP treatment resulted in higher extent of delignifcation as well as enzymatic digestibility. The enzymatic digestibilities of ARP-treated waste oak wood yielded 86.1% with 60 FPU/g glucan and 82.3% with 10 FPU/g glucan. The ARP process could achieve higher enzyme digestibility as well as low enzyme loading.

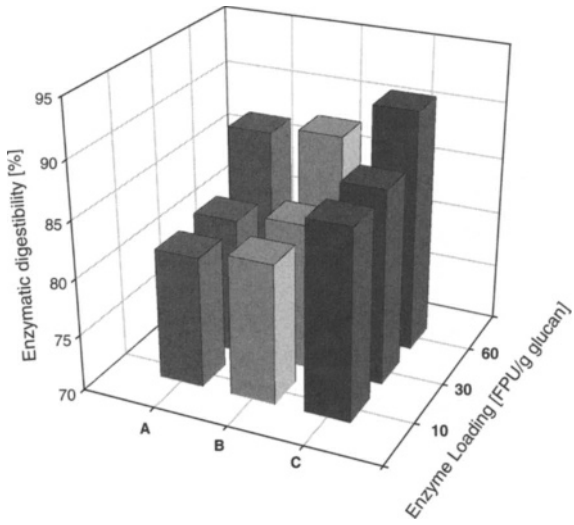


Fig. 3 Enzymatic digestibility of oak wood feedstocks (*A*, *B*, *C*) after ARP at various enzyme loadings. *A* Oak wood after ARP; *B* waste oak wood after ARP; *C* pre-soaked waste oak wood after ARP

Acknowledgment This study was supported by Korea New and Renewable Energy Center.

References

1. IEA (2004). In Biofuels for Transport. IEA Press.
2. MOCIE (2007) In A study on the energy utilization of ligneous biomass. Korea Ministry of Commerce, Industry and Energy.
3. Mosier, N., Wyman, C., Dale, B., Elander, R., Lee, Y. Y., Holtzapple, M., & Ladisch, M. (2005). *Bioresource Technology, 96*, 673–686.
4. Cowling, E. B., & Kirk, T. K. (1976). *Biotechnology and Bioengineering Symposium, 6*, 95–123.
5. Chang, V. S., & Holtzapple, M. T. (2000). *Applied Biochemistry and Biotechnology, 84/86*, 5–37.
6. Schwald, W., Brownell, H. H., & Saddler, J. (1988). *Journal of Wood Chemistry and Technology, 8*(4), 543–560.
7. Yoon, H. H., Wu, Z. W., & Lee, Y. Y. (1995). *Applied Biochemistry and Biotechnology, 51/52*, 5–19.
8. Kim, T. H., Lee, Y. Y., Sunwoo, C., & Kim, J. S. (2006). *Applied Biochemistry and Biotechnology, 133* (1), 41–58.
9. Zhu, Y., Kim, T. H., Chen, R., & Elander, R. (2006). *Applied Biochemistry and Biotechnology, 130*(1–3), 586–598.
10. Kim, J. S., Lee, Y. Y., & Park, S. C. (2000). *Applied Biochemistry and Biotechnology, 84/86*, 129–139.
11. Kim, T. H., & Lee, Y. Y. (2007). *Applied Biochemistry and Biotechnology, 136/140*, 81–92.
12. Kim, T. H., Kim, J. S., Sunwoo, C., & Lee, Y. Y. (2003). *Bioresource Technology, 90*, 39–47.
13. NREL (2004). *Chemical Analysis and Testing Laboratory Analytical Procedures (CAT)*. Golden, CO, USA: National Renewable Energy Laboratory.
14. Kim, T. H., Lee, Y. Y., Sunwoo, C., & Kim, J. S. (2006). *Applied Biochemistry and Biotechnology, 133*, 41–57.

Appl Biochem Biotechnol (2008) 148:23–33
DOI 10.1007/s12010-008-8134-2

Pretreatment of Whole-Crop Harvested, Ensiled Maize for Ethanol Production

M. H. Thomsen · J. B. Holm-Nielsen · P. Oleskowicz-Popiel · A. B. Thomsen

Received: 25 April 2007 / Accepted: 3 January 2008 /
Published online: 22 February 2008
© Humana Press 2008

Abstract To have all-year-round available feedstock, whole-crop maize is harvested premature, when it still contains enough moisture for the anaerobic ensiling process. Silage preparation is a well-known procedure for preserving plant material. At first, this method was applied to obtain high-quality animal feed. However, it was found that such ensiled crops are very suitable for bioenergy production. Maize silage, which consists of hardly degradable lignocellulosic material, hemicellulosic material, and starch, was evaluated for its potential as a feedstock in the production of bioethanol. It was pretreated at low severity (185 °C, 15 min) giving very high glucan (~100%) and hemicellulose recoveries (<80%)—as well as very high ethanol yield in simultaneous saccharification and fermentation experiments (98% of the theoretical production based on available glucan in the medium). The theoretical ethanol production of maize silage pretreated at 185 °C for 15 min without oxygen or catalyst was 392 kg ethanol per ton of dry maize silage.

Keywords Maize silage · Bioethanol · Lignocellulose · Pretreatment · Simultaneous saccharification and fermentation

Introduction

Bioethanol produced from pretreatment and microbial fermentation of biomass has great potential to become a sustainable transportation fuel in the near future [1]. Brazil and the United States are the largest producers of ethanol for transport, accounting for about 90% of world production. Both countries currently produce about 16 billion liters per year with a displacement of 40% of gasoline use in Brazil but only 3% in the United States with

M. H. Thomsen (✉) · P. Oleskowicz-Popiel · A. B. Thomsen
Bioenergy and Biomass Programme, Biosystems Department, Risø National Laboratory, Technical University of Denmark, Building BIO-301, Frederiksborgvej 399, P.O. Box 49, 4000 Roskilde, Denmark
e-mail: mette.hedegaard.thomsen@risoe.dk

J. B. Holm-Nielsen
ACABS Laboratories, Aalborg University Esbjerg, Niels Bohrs vej 8, Esbjerg, Denmark

sugarcane (*Saccharum* L.) and corn (*Zea mays* L.) as the primary feedstock, respectively [2]. In 2005, Europe produced only about 2.6% of the world's bioethanol production, but with a bioethanol sector growing with 70.5% between 2004 and 2005 primarily in Germany and Spain but with new producer countries like Hungary and Lithuania coming up [3]. The EU countries have an indicative target year 2010 at 5.75% biofuels in the transportation sector.

Recently, a 10% binding minimum target was decided to be achieved by all EU member states for the share of biofuels in overall EU transport petrol and diesel consumption by 2020 [4].

In Denmark, industrial production of bioenergy mainly exists in the form of incineration of straw, wood chips, and wood pellets in CHP plants, but extensive research is carried out to develop second-generation bioethanol production from lignocellulosic materials and successful pilot scale facilities have been developed, such as the Integrated Biomass Utilization System (IBUS) plant [5] with maximum capacity to pretreat 1 ton of straw per hour. While the production of ethanol from sugars and starch is more straightforward (first-generation bioethanol), production from lignocellulose creates additional technical challenges, such as a need for pretreatment. Lignocellulosic materials contain cellulose and hemicellulose that are bound together by lignin. Cellulose and hemicellulose are both polymers built up by long chains of sugar monomers which first after pretreatment and hydrolysis can be converted into ethanol by microbial fermentation. The aim of the pretreatment is to open up the lignocellulosic structure to enable enzymatic hydrolysis. In the enzymatic hydrolysis, the monomeric sugars bound in cellulose and hemicellulose are released and becomes available for conversion into ethanol. The mostly used microorganism for ethanol production is the ordinary baker's yeast, *Saccharomyces cerevisiae*. In the pretreatment process, some inhibitors are formed [6] and *S. cerevisiae* is one of the most inhibitor-tolerant microorganisms used for the conversion [7]. However, it can only convert the hexoses, such as glucose and mannose, and not the pentoses such as xylose and arabinose that are found in the hemicellulose part of the straw. Inhibitor formation and pentose fermentation are the main challenges in second-generation bioethanol.

Different pretreatment methods exist, such as wet oxidation [8, 9] which is also used in this study, as well as other methods such as acid treatment, steam explosion, and hydrothermal treatment [5, 10, 11]. Wet oxidation, a reaction involving oxygen and water at elevated temperature and pressure, was presented in the early 1980s to pretreat lignocellulose (wood) as an alternative to the well-studied steam explosion [9]. Compared to other pretreatment processes, wet oxidation has been proven to be more efficient for treating some lignocellulosic materials, because the crystalline structure of cellulose is opened during the process. Organic molecules, including lignin, decompose to CO_2, H_2O, and simpler and more oxidized organic compounds, mainly to low-molecular-weight carboxylic acids [12]. Wet oxidation appears to have the advantage of producing fewer byproducts, such as furfural and hydroxymethylfurfural [13, 14]. Under the conditions of wet oxidation, aliphatic aldehydes and saturated carbon bonds are very reactive; hence, the sugar degradation products, which are known inhibitors of microbial growth [15], are not expected to be produced at high concentration.

In Denmark, energy crop cultivation is taking place to a very limited extend, less than 5% of the cropland is utilized for oil seed rape to the European biodiesel sector, since the economical feasibility compared to other available feedstocks is considered poor until crude oil prices increase further. Danish growth conditions for maize for animal feeding purposes yields 12–15 tons dry matter (DM)/ha [16], but it has the potential of rising to 16–20 tons DM/ha in the context of biorefining [17]. Silage making is a method of moist forage preservation which is widely used all over the world, accounting for more than 200 million tons of dry matter stored annually in Western Europe and USA [18]. The aim of silage making is to preserve the crop with minimum loss of nutrients. Preservation can be

achieved either by encouraging the lactic acid bacteria to dominate the fermentation or alternatively by inhibiting microbial activity with chemical additives. In Denmark, maize is primarily harvested as whole crop and ensilaged to be stored as a "wet" animal fodder.

Maize silage consists of the whole harvested maize plant (stem, leaves, and grain), which is cut and ensiled anaerobically. Thus, the whole-crop maize silage consists of hardly degradable lignocellulosic material, hemicellulosic material, and starch. Preliminary trials of wet oxidation of maize silage, using optimum temperature, time, and pH found for corn stover and wheat straw [6, 13, 19] have shown that it is a promising raw material for bioethanol production [20], giving higher sugar and ethanol yields compared to wheat straw, which is the most abundant lignocellulosic resource in Denmark.

In the present study, pretreatment of whole-crop maize silage was studied with the aim of optimizing the bioethanol process. The influence of temperature, time, and pH on sugar recovery and yield after pretreatment and enzymatic hydrolysis was studied as well as the ethanol yield in simultaneous saccharification and fermentation (SSF) with *S. cerevisiae*.

Materials and Methods

Maize Silage

The maize silage was delivered from Aalborg University Esbjerg. It was collected from Niels Tobiasen, Dairy Farm, Farup Ribe and kept in the freezer at the laboratory (at −20 °C) until use in pretreatment experiments. The harvesting time for whole-crop maize in Denmark is October (2–3-week period for harvesting and chopping). The dry matter content of the maize at harvest is between 30% and 35% at harvest or 1.18–1.20 TS/Nordic Feeding Unit (which is equivalent to 1 kg of Danish spring barley grains). The harvested maize is chopped in the harvester, thoroughly compressed, and stored completely air tight. The process is fully anaerobic, and no additives were added. The silage was stored in a filed silo (approximately 1.5 m high, 15 m wide, 30–50 m long) and can be kept up to 12 months until next harvesting. Content of total solid of the silage was around 25%, and it was dried in a heating cabinet at 40 °C for 2–3 days and milled to a size of less than 2 mm prior to pretreatment and further analysis.

Pretreatment

Maize silage was pretreated using eight different set of process parameters (including wet oxidation) as shown in Table 1. The pretreatments were performed in a loop autoclave constructed at Risø National Laboratory using 6% dry matter [13]. After pretreatment, the material was separated by filtration into a solid filter cake (containing fibers and lignin) and a liquid fraction (containing soluble sugars and various degradation products). Pretreated liquids were stored at −20 °C until further analysis and use, and the filter cakes were dried and kept in a climate cabinet at 20 °C and 65% relative humidity.

Enzymatic Hydrolysis of Solid Fraction

The enzymatic convertibility of the solid fraction after pretreatment was determined for the pretreated materials as well as for the untreated maize silage. The enzymatic hydrolysis was carried out at 50 °C, pH 4.8, with 2% DM and an enzyme load of 30 FPU/g DM. The enzyme used was Cellubrix L (Novozymes, Denmark) and the amounts of hydrolyzed sugars were determined by high-performance liquid chromatography (HPLC; see "Analysis

Table 1 Experimental conditions used for screening of pretreatment of whole-crop maize silage.

Temperature (°C)	Time (min)	Catalyst Na_2CO_3 (g/l)	Oxygen (bar)
195	15	2	12
185	15	2	12
195	15	–	12
185	15	–	12
195	15	–	–
185	15	–	–
195	10	2	12
185	10	2	12

Methods" for further details). The experiments were carried out in triplicates for each solid pretreatment fraction and for the untreated maize silage.

Simultaneous Saccharification and Fermentation

After pretreatment, 8 g DM of the solid fraction (filter cakes) was mixed with 60 ml of filtrate, and the raw sample was mixed with 60 ml of water (pH 4.8) in 250-ml fermentation flasks. All experiments were done in duplicate. Liquefaction was performed at 50 °C with an enzyme (Cellubrix L) load of 15 FPU/g DM for 24 h. After cooling to room temperature, 15 FPU/g DM enzymes (Cellubrix L), 0.2 g dry commercial yeast (Malteserkors tørgær, De Danske Spritfabrikker A/S, Denmark), and 0.2 ml urea (24%) were added. The head space in the flasks was flushed with N_2, and the flasks were equipped with yeast locks filled with glycerol. The flasks were then incubated at 32 °C and the amount of produced ethanol was determined as weight loss caused by CO_2 off gassing. The final ethanol concentration was determined by HPLC (see "Analysis Methods" for further details).

Analysis Methods

Dry Matter and Ash Content

Duplicates of 0.5 g solid material or 10 ml of liquid sample were dried at 105 °C overnight to determine the dry weight. The samples were then heated to 550 °C for 3 h to determine the ash content.

Analysis of Carbohydrates in Solid Fraction

To quantify the sugar polymers in the raw material and the solid fraction after wet oxidation, a two-step acid hydrolysis was performed. The first hydrolysis step was performed at 30 °C for 60 min with 1.5 ml of H_2SO_4 (72%) for 0.16 g DM. Then, 42 ml water was added and the second step was performed at 121 °C for 60 min. The hydrolysate was filtered and the dried filter cake subtracted for ash content is reported as Klason lignin.

Analysis of Carbohydrates in Liquid Fraction

To quantify the sugar content in the liquid fraction, a weak hydrolysis was performed at 121 °C for 10 min using 4% H_2SO_4, in duplicate. The concentrations of sugar monomers were determined by HPLC as described below.

HPLC Analysis

The amounts of released sugar monomers in the hydrolysate as well as concentration of produced ethanol were determined by HPLC (Shimadzu) using a Rezex ROA column (Phenomenex) at 63 °C and 4 mM H_2SO_4 as eluent at a flow rate of 0.6 ml/min. A refractive index detector (Shimadzu Corp., Kyoto, Japan) was used.

Calculations

Recoveries were calculated according to Eq. 1. Yields were calculated as percent of theoretical (in gram per gram original cellulose or hemicellulose in raw material; Eqs. 2 and 3). Total yields were calculated as the total yield of hemicellulose/glucose in the liquid fraction and after enzymatic hydrolysis of the solid fraction (Eq. 4). The theoretical ethanol production based on the pretreatment and hydrolysis yields was calculated according to Eq. 5. The ethanol yield in SSF experiments was calculated as percentage of theoretical based on cellulose content of the fiber fraction and glucose in the filtrates (Eq. 6). The ethanol concentration was calculated from weight loss due to CO_2 of gassing by Eq. 7 .

$$\text{Recovery} = \frac{(\text{sugar in filtrate}(\text{g}/100\ \text{g}) + \text{sugar in solid}(\text{g}/100\ \text{g}))}{(\text{sugar in raw material}(\text{g}/100\ \text{g}))} \times 100\% \quad (1)$$

$$\text{Pretreatment yield}_{\text{sugar}} = \frac{(\text{mass}_{\text{sugar}}\ \text{in filtrate})}{(\text{mass}_{\text{sugar}}\ \text{in raw material})} \times 100\% \quad (2)$$

$$\text{Hydrolysis yield}_{\text{sugar}} = \frac{(\text{mass}_{\text{sugar}}\ \text{after enzymatic hydrolysis} \times 0.9)}{(\text{mass}_{\text{sugar}}\ \text{in raw material})} \times 100\% \quad (3)$$

$$\text{Total yield}_{\text{sugar}} = \frac{(\text{mass}_{\text{sugar}}\ \text{in filtrate}) + (\text{mass}_{\text{sugar}}\ \text{after enzymatic hydrolysis})}{(\text{mass}_{\text{sugar}}\ \text{in raw material})} \times 100\% \quad (4)$$

$$\text{EtOH yield} = \frac{\text{EtOH}_{\text{Gravimetric/HPLC}}}{\text{glucan in solid} \times 0.51 + \text{glucose in filtrate} \times 0.51} * 100 \quad (5)$$

$$\text{Theoretical ethanol production} = \text{TSC}^* \times \text{Yield in SSF}^{**} \times 0.51 + \text{TSH}^{***} \times \text{Recovery}^{****} \times 0.51 \quad (6)$$

*TSC=Total sugar from cellulose

**Conversion yield obtained in SSF experiments (g/100 g raw material)

***TSH=Total sugar from hemicellulose

****Total hemicellulose recovery in solid and liquid fraction (g/100 g raw material)

$$\mathrm{EtOH(g/l)} = \text{Weight loss*} \text{ of } \mathrm{CO_2}\left[\frac{\text{g total } \mathrm{CO_2} \text{ lost}}{\text{ml liquid}}\right] \cdot \frac{1}{44}\left[\frac{\text{mol } \mathrm{CO_2}}{\text{g } \mathrm{CO_2}}\right] \cdot \frac{1}{1}\left[\frac{\text{mol EtOH prod.}}{\text{mol } \mathrm{CO_2} \text{ prod.}}\right] \cdot 46\left[\frac{\text{g EtOH}}{\text{mol EtOH}}\right] \cdot 1{,}000\left[\frac{\text{ml liquid}}{\text{l}}\right] \tag{7}$$

*Off-gassed CO_2

Results and Discussions

Raw Material Composition

Maize silage has a high glucan and total sugar content compared to other lignocellulosic materials that have been examined for bioethanol production by wet oxidation [5, 19, 21, 22]. Table 2 shows the composition of the maize silage used in this study; it contained approximately 52% glucan from both starch and cellulose present in this "whole-crop" harvested material. The strong acid hydrolysis used for carbohydrate analysis makes no distinction between glucan from starch and cellulose—but the average maize silage contains approximately 20% lignocellulose and 30% starch (according to official Danish fodder quality assessment). The maize silage also contains significant amounts of hemicellulose (approximately 20%). Silage fermentation is facilitated by spontaneous conversion of water-soluble carbohydrates by lactic acid bacteria. Most strains of lactic acid bacteria are able to utilize the pentose sugars, which, to some degree, could be released from the material during shredding and compression in the silo. The DM loss during ensiling is 5–10% (see "Materials and Methods" section). The lignin content is slightly lower than in traditional lignocellulosic materials such as straw (e.g., wheat and rye), but still it is sufficient for maize silage to be a promising raw material in integrated bioethanol/power production processes such as the Danish IBUS process [5], where the lignin residue from bioethanol production is used for incineration in the power plant, thereby improving the energy balance of the ethanol process.

Sugar Recovery after Pretreatment

Maize silage was pretreated by wet oxidation and hydrothermal treatment as described in Table 1. The sugar recoveries based on analysis and overall mass balance of the pretreated fractions (solid fibers and liquid) and the raw material have been calculated according to Eq. 1, and the results are shown in Fig. 1. The total recovery of glucose was very close to a 100% in all experiments (not shown), while the recovery of hemicellulose sugars depended very much on pretreatment conditions.

In maize silage pretreated at 195 °C, 25% to 50% of the total pentoses in the raw material was degraded. The lowest recovery was observed at 195 °C in the experiment

Table 2 Composition of the maize silage raw material used in this study.

Raw material	Glucan (g/100 g DM)	Hemicellulose (g/100 g DM)	Lignin (g/100 g DM)
Maize silage	51.7	19.5	16.6

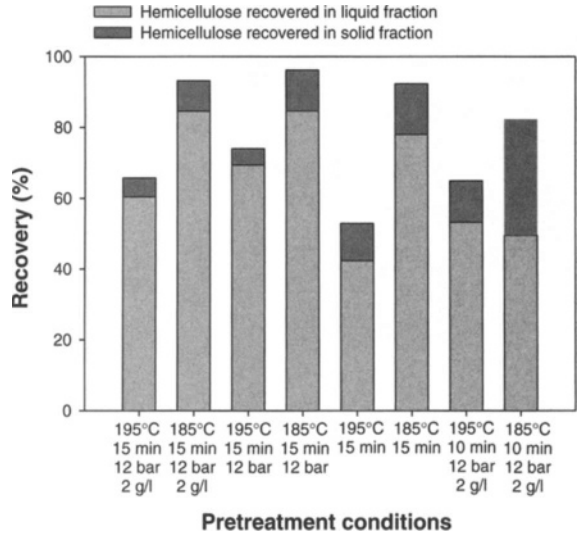


Fig. 1 Recovery of hemicellulose sugars (pentoses) in pretreatment of maize silage using different pretreatment parameters (see Table 1)

where no oxygen or alkaline catalyst was used. This is coherent with wet oxidation studies on wheat straw, which shows that oxygen and Na_2CO_3 have a positive effect on hemicellulose recovery [13]. Decreasing residence time from 15 to 10 min does not improve hemicellulose recovery in this study. However, decreasing the temperature to 185 °C has a significant effect on the recovery, and in these experiments, recoveries of 80–96% are achieved. The three experiments at 185 °C with a residence time of 15 min gave very similar results, with the wet oxidation experiment (O_2 addition) giving a slightly higher recovery.

Sugar Yield after Pretreatment and Enzymatic Hydrolysis

To evaluate the effect of the different pretreatments on the enzymatic convertibility of the materials, this was tested both on the raw maize silage and on the solid fractions of the pretreated material. Figure 2 shows the fraction of glucan (solid bars) and hemicellulose sugars (hatched bars) liberated during pretreatment (black) and enzymatic hydrolysis (gray). During pretreatment of maize silage, a significant part of both glucan and hemicellulose sugars was extracted into the liquid fraction (pretreatment yield). In "pure" lignocellulosic material such as wheat straw, which has not been ensilaged, only very small amounts of glucose are released during pretreatment (2–7%) [5]. In these experiments, 60% to 98% of the glucan and almost all the recovered hemicellulose are released during pretreatment, probably because a significant part of the glucan in this material is starch. During enzymatic hydrolysis, even more sugars were liberated (mainly glucan), giving very high total sugar yield in the best experiments (~100% of glucan). The highest glucan (~100%) and hemicellulose yields (78–89%) were obtained in the three experiments performed at 185 °C with a residence time of 15 min (enz. hydr. for exp. 185 °C, 15 min is missing—Fig. 2). The enzymatic convertibility of the raw maize silage gave a very low yield, proving that pretreatment is necessary to achieve high ethanol yields.

SSF of Pretreated Maize Silage

Simultaneous saccharification and fermentation was performed on the raw maize silage and on pretreated fibers suspended in the filtrates to a dry matter content of approximately 13%.

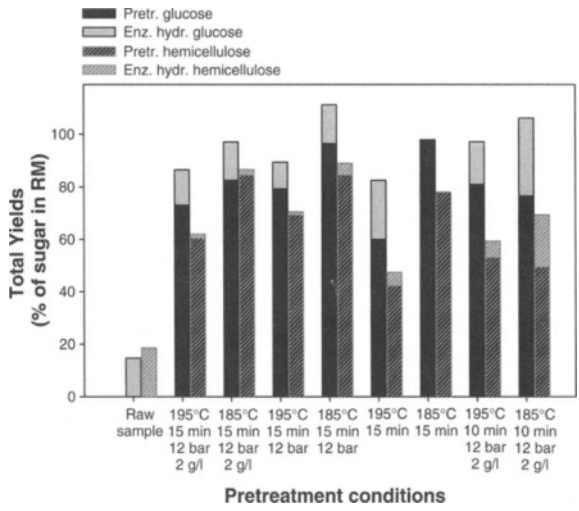


Fig. 2 Total yield of sugar after pretreatment and subsequent enzymatic hydrolysis of maize silage using different pretreatment parameters (see Table 1)

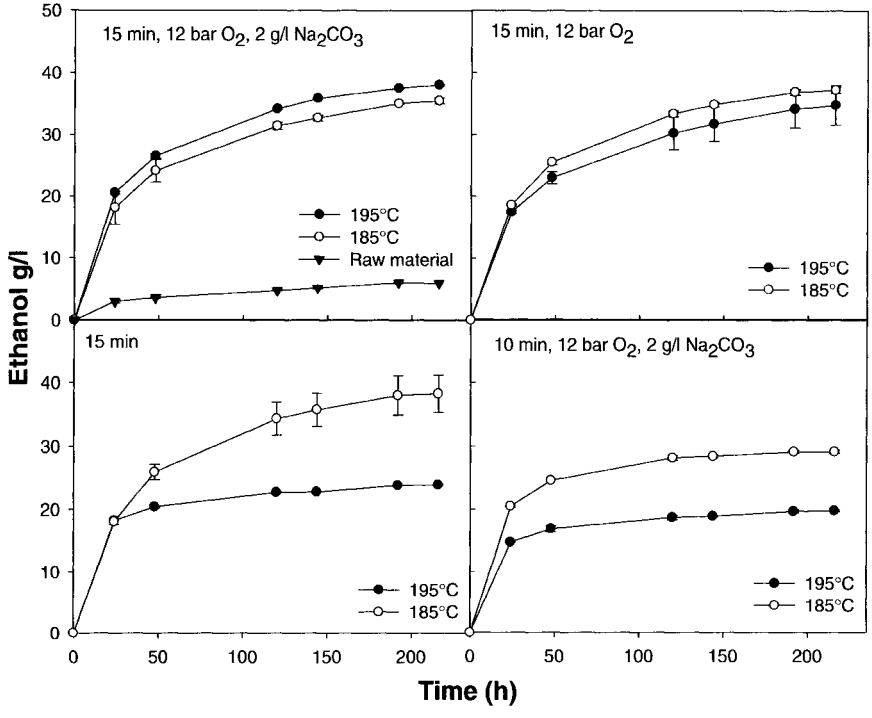


Fig. 3 Simultaneous saccharification and fermentation of raw maize silage and maize silage pretreated at different parameters settings (see Table 1). Ethanol production was followed as weight loss due to CO_2 off gassing and calculated by Eq. 7

Thirteen percent dry matter is the upper limit of what can be handled in shake flask experiments. Since *S. cerevisiae* were used in this SSF, only glucose were converted to ethanol, and yields are based only on the conversion of glucan. The ethanol production curves from SSF of the different pretreated materials are shown in Fig. 3, and the final ethanol concentrations measured by HPLC are shown in Table 3. The ethanol yield and the productivity on the raw material was low, but was improved significantly by pretreatment of the materials. This is also due to the low enzymatic convertibility of the raw material (Fig. 2). Fermentation of all pretreated materials started without a lag phase, indicating that the level of inhibitors produced in the pretreatments was low enough for the yeast to start producing ethanol. In the fermentation of toxic materials, the yeast will detoxify the medium by converting the toxic aldehydes to less toxic alcohols, giving a lag phase where no ethanol is produced [23, 24]. The best results were obtained when using maize silage pretreated with a residence time of 15 min. SSF of material pretreated for 15 min gave very similar ethanol yields of 91–98% of the theoretical production (based on available glucan in the medium determined by HPLC—Table 3), except for the experiment at 195 °C using no oxygen and no catalyst; in this experiment the yield was only approximately 61%, probably due to the low hemicellulose recovery (Fig. 1). This shows that the protective effect of hemicellulose sugars under alkaline wet oxidation conditions becomes more pronounced at higher temperatures, which is an advantage when pretreating materials such as wheat straw [13] and corn stover [19] where high temperatures are needed for high cellulose convertibility. However, these results show that in pretreatment of maize silage, 185 °C is sufficient to achieve high ethanol yields, and the addition of oxygen and catalyst can be avoided, meaning that energy can be saved and the cost of oxygen and catalyst eliminated. The ethanol yield in SSF of material pretreated at 185 °C for 15 min without oxygen or catalyst was 98% of the theoretical production (based on available glucan in the medium) when measured by HPLC (Table 3).

Theoretical Ethanol Production from Pretreated Maize Silage

A theoretical ethanol production based on the achieved yields was calculated for each wet oxidation experiment. For glucan sugars, the yield obtained in SSF was used, and for the hemicellulose sugars (which were not converted by baker's yeast in the SSF) it was assumed that all recovered sugars could be converted to ethanol at a yield of 0.51 g ethanol/g sugar (Eq. 6). These results are shown in Fig. 4 and compared to the maximum ethanol

Table 3 Final ethanol production in SSF experiments measured by HPLC.

Temperature (°C)	Time (min)	Catalyst Na_2CO_3 (g/l)	O_2 (bar)	Ethanol (g/l) HPLC	Ethanol (% of theoretical) HPLC
Raw	–	–	–	5.9	15
195	15	2	12	38.1	97
185	15	2	12	35.6	90
195	15	–	12	34.9	89
185	15	–	12	37.3	95
195	15	–	–	24.0	61
185	15	–	–	38.3	98
195	10	2	12	19.8	51
185	10	2	12	29.1	74

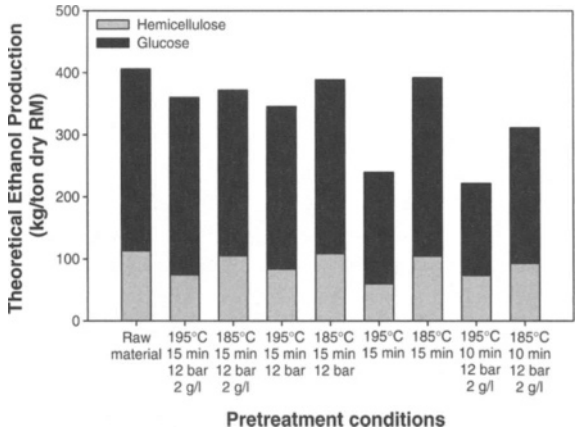


Fig. 4 Theoretical ethanol production based on sugar yield after pretreatment and enzymatic hydrolysis of maize silage pretreated at different parameters settings (see Table 1). The results are compared to the maximum production based on total sugar in the raw maize silage (*bar 1*)

production from the available sugars in the raw maize silage. Four hundred kilograms of ethanol can be produced from 1 ton of dry maize silage (corresponding to 100 kg/ton wet silage—25% DM) based on the sugar content of the material (bar 1—Fig. 4). Two experiments gave similar theoretical ethanol production of 388 kg/ton dry maize silage and 392 kg/ton dry maize silage, namely the two experiments performed at 185 °C for 15 min with and without oxygen, respectively. The experiment performed without oxygen is the best choice, because oxygen increases the cost of the bioethanol process and makes scale-up of the process more complex.

Conclusions

From the results found in this study on bioenergy potential of maize silage, it can be concluded that maize silage is a very promising raw material for bioethanol production.

Maize silage has a high glucan and total sugar content compared to other lignocellulosic materials that have been examined for bioethanol production by wet oxidation, and the result presented in this paper shows that it can be pretreated at low severity (185 °C, 15 min) giving very high glucan (~100%) and hemicellulose recoveries (89%)—as well as very high ethanol yield in SSF experiments (98% of the theoretical production based on available glucan in the medium). In contrast to other lignocellulosic materials, most of the sugars (both glucan and hemicellulose) are extracted during pretreatment, probably meaning that enzyme loadings can be reduced significantly. Furthermore, addition of oxygen and catalyst can be eliminated, which further reduces the price of ethanol production. The theoretical ethanol production of maize silage pretreated at 185 °C for 15 min without oxygen or catalyst was 392 kg ethanol per ton of dry maize silage.

The results presented in this paper were only a very preliminary study of pretreatment of maize silage. Trials should be made at lower temperatures to examine if more energy could be saved in the process. It would also be interesting to determine the content of starch and cellulose separately by enzymatic hydrolysis, instead of total glucan as is the case in this study. Also, enzymatic hydrolysis and SSF using low enzyme loadings (of both cellulases and amylases) should be made to fully see the potential of this promising raw material for bioethanol production.

Acknowledgments We thank Tomas Fernqvist from Risø National Laboratory. Dairy Farm, Farup Ribe is thanked for supplying good quality maize silage. Risø National Laboratory, Technical University of Denmark and Højteknologifonden, Denmark are thanked for financial support given to this study.

References

1. Thomsen, A. B., Medina, C., & Ahring, B. K. (2003). In H. Larsen, J. Kossmann, & L. S. Petersen (Eds.), *Risø energy report 2* (pp. 40–44).
2. Hazell, P., & Pachauri, R. K. (2006). 2020 Focus No. 14, November. http://www.ifpri.org/2020/focus/focus14.asp#dl.
3. Eurobserver (2006). Biofuels barometer May, pp. 57–66.
4. EU (2007). Brussels European Council 8–9 March—Presidency Conclusions (http://mediacontent.ig.publicus.com/PDF/IG35268339.PDF)
5. Thomsen, M. H., Thygesen, A., Christensen, B. H., Larsen, J., Jørgensen, H., & Thomsen, A. B. (2006). *Applied Biochemistry and Biotechnology, 129–132*, 448–460.
6. Klinke, H. B., Olsson, L., Thomsen, A. B., & Ahring, B. K. (2003). *Biotechnology and Bioengineering, 3*(81), 738–747.
7. Olsson, L., & Hahn-Hagerdal, B. (1993). *Process Biochemistry, 28*, 249–257.
8. Schmidt, A. S., & Thomsen, A. B. (1989). *Bioresource Technology, 64*, 139–151.
9. McGinnis, G. D. (1983a). WWWMCE. *Industrial & Engineering Chemistry Product Research and Development, 22*, 352–357.
10. Lee, Y. V., Iyer, P., & Torget, R. W. (1999). *Advances in Biochemical Engineering, Biotechnology, 65*, 93–115.
11. Galbe, M., & Zacchi, G. (2002). *Applied Microbiology and Biotechnology, 59*, 618–628.
12. McGinnis, G. D., Wilson, W. W., Prince, S. E., & Chen, C. C. (1983b). *Industrial & Engineering Chemistry Product Research and Development, 22*, 633–636.
13. Bjerre, A. B., Olesen, A. B., Fernqvist, T., Plöger, A., & Schmidt, A. S. (1996). *Biotechnology and Bioengineering, 49*, 568–577.
14. Ahring, B. K., Licht, D., Schmidt, A. S., Sommer, P., & Thomsen, A. B. (1999). *Bioresource Technology, 68*, 3–9.
15. Palmqvist, E., Hahn-Hägerdal, B., Szengyel, Z., Zacchi, G., & Reczey, K. (1997). *Enzyme and Microbial Technology, 20*, 286–293.
16. Pedersen, C. Aa. (2006). Oversigt over Landsforsøgene 2006, Dansk Landbrugsrådgivning, Landscenteret-Planteavl (Danish).
17. Holm-Nielsen, J. B., Madsen, M., & Popiel, P. O. (2006). Proceedings: World Bioenergy 2006, Conference for Biomass for Energy, 05/2006, Jönköbing Sweden.
18. Weinberg, Z. G., & Munc, R. E. (1996). *FEMS Microbiology Reviews, 19*, 53–68.
19. Varga, E., Schmidt, A. S., Reczey, K., & Thomsen, A. B. (2003). *Applied Biochemistry and Biotechnology, 104*, 37–50.
20. Thomsen, M. H., Popiel, P. O., Lisiecki, P., Varga, E., Thomsen, A. B., Esbensen, K. H., et al (2005). Proceedings: 14th European Biomass Conference and Exhibitons, 17–21 October 2005, Paris, France.
21. Petersson, A., Thomsen, M. H., Haugaard-Nielsen, H., & Thomsen, A. B. (2007). *Biomass & Bioenergy, 31*, 812–819.
22. Martín, C., Klinke, H., & Thomsen, A. B. (2007). *Enzyme and Microbial Technology, 40*(3), 426–432.
23. Taherzadeh, M. J., Gustafsson, L., Niklasson, C., & Lidén, G. (1999). *Journal of Bioscience and Bioengineering, 87*, 169–174.
24. Taherzadeh, M. J., Gustafsson, L., Niklasson, C., & Lidén, G. (2000). *Applied Microbiology and Biotechnology, 53*, 701–708.

Appl Biochem Biotechnol (2008) 148:35–44
DOI 10.1007/s12010-007-8085-z

Enzymatic Hydrolysis and Ethanol Fermentation of High Dry Matter Wet-Exploded Wheat Straw at Low Enzyme Loading

Tania I. Georgieva · Xiaoru Hou · Troels Hilstrøm · Birgitte K. Ahring

Received: 8 May 2007 / Accepted: 16 October 2007 /
Published online: 27 November 2007
© Humana Press Inc. 2007

Abstract Wheat straw was pretreated by wet explosion using three different oxidizing agents (H_2O_2, O_2, and air). The effect of the pretreatment was evaluated based on glucose and xylose liberated during enzymatic hydrolysis. The results showed that pretreatment with the use of O_2 as oxidizing agent was the most efficient in enhancing overall convertibility of the raw material to sugars and minimizing generation of furfural as a by-product. For scale-up of the process, high dry matter (DM) concentrations of 15–20% will be necessary. However, high DM hydrolysis and fermentation are limited by high viscosity of the material, higher inhibition of the enzymes, and fermenting microorganism. The wet-explosion pretreatment method enabled relatively high yields from both enzymatic hydrolysis and simultaneous saccharification and fermentation (SSF) to be obtained when performed on unwashed slurry with 14% DM and a low enzyme loading of 10 FPU/g cellulose in an industrial acceptable time frame of 96 h. Cellulose and hemicellulose conversion from enzymatic hydrolysis were 70 and 68%, respectively, and an overall ethanol yield from SSF was 68%.

Keywords Saccharomyces cerevisiae · Simultaneous saccharification and fermentation · Wet explosion · Pretreatment · Wheat straw · High dry matter · Ethanol

T. I. Georgieva · X. Hou · T. Hilstrøm · B. K. Ahring (✉)
BioScience and Technology Group, BioCentrum–DTU, Technical University of Denmark, Building 227, 2800 Lyngby, Denmark
e-mail: bka@biocentrum.dtu.dk

Present address:
T. I. Georgieva
Fluxome Science, Diplomvej 378, 2800 Lyngby, Denmark
e-mail: tig@fluxome.com

Present address:
T. Hilstrøm
BioGasol ApS, DTU, Building 205, 2800 Lyngby, Denmark

Introduction

The demand for fuel ethanol has increased tremendously because of environmental, economic, and national energy security concerns. This has increased the necessity of using lignocellulosic wastes from agriculture and forestry as alternative raw materials in addition to corn, grain, and sugarcane, which are nowadays the primary feedstocks used for production of fuel ethanol. Wheat straw is the most abundant agricultural waste in Europe and the second largest agricultural residue in the world [1]. The global annual production of bioethanol from wheat straw has been estimated to 104 million m^3 [1].

The nature of lignocellulose, such as straw, makes it rather resistant to enzymatic hydrolysis, and pretreatment is, therefore, required to open the lignocellulose structure to facilitate further hydrolysis of the carbohydrates to monomeric sugars. To obtain high overall ethanol yields, the pretreatment should maximize enzymatic convertibility, minimize sugar decomposition or loss, not require addition of chemicals toxic to the enzymes or the fermenting microorganisms, be effective for treatment of materials at high DM content, and be scalable to industrial scale [2]. Several pretreatment technologies such as wet oxidation [3], steam explosion [4], dilute acid [5], and hydrothermal [6] have been used for pretreatment of wheat straw. Recently, a new pretreatment technology, wet explosion, has been developed at The Technical University of Denmark (DTU) [7]. The method is a combination of thermal hydrolysis, wet explosion, and wet oxidation, enabling (1) operating with high biomass concentrations up to 50%, (2) handling of big particle sizes, thereby, avoiding initial energy intensive mechanical milling, (3) an easy controllable process, (4) low total energy consumption, and (5) minor generation of inhibiting compounds [7]. Since 2006, the MaxiFuels pilot plant for production of ethanol from lignocelluloses has been operating in Denmark. The pilot plant tests wheat straw as the primary feedstock.

Most studies dealing with enzymatic hydrolysis or simultaneous saccharification and fermentation (SSF) at laboratory scale are performed at low substrate concentrations, usually concentrations below 10% dry matter (DM). However, to improve process economics, operating at higher substrate concentrations would be advantageous. This is because of increased final ethanol concentration, reduced reactor volume, lower operating cost, lower downstream processing cost, and reduced wastewater [8]. It has also been stated that ethanol concentration should be above 5% (*v*/*v*) in the fermentation broth for an economically viable lignocellulose-based ethanol process. For most types of lignocellulosic materials, this requires operating enzymatic hydrolysis or SSF processes at solid concentrations above 15% DM [9]. However, operating at initial substrate concentrations above 10% DM is limited by (1) inefficient mixing because of high initial viscosity of the material, (2) higher inhibitor concentrations that could reduce the performance of cellulases and hemicellulases, (3) higher concentrations of compounds inhibitory to fermenting organism, and (4) higher enzyme loadings needed for efficient hydrolysis within an industrial acceptable time frame [9]. Many studies have shown that washing the pretreated material results in improved enzymatic hydrolysis of the cellulose fraction and more efficient fermentation of glucose to ethanol because of removal of some of the inhibitors, both for enzymes and the microorganisms [8, 10, 11]. However, in large scale, including a washing step will not be advantageous because of the generation of a large waste stream. Thus, the whole slurry after pretreatment should be further hydrolyzed and fermented.

In lab-scale hydrolysis and fermentation tests, between 10 and 35 FPU/g cellulose is commonly used as the optimum enzyme loading, depending on both substrate concentration and digestibility of the material used. However, considering both the overall cost of the

ethanol process and enzyme cost that could be up to 50% of SSF process [12], more realistic in the industrial process is enzyme concentrations in the range of 10–15 FPU/g cellulose.

The overall objective of the work presented in this paper was to investigate the efficiency of high solid enzymatic hydrolysis and SSF of wet-exploded wheat straw combined with the use of low-enzyme loading. The hydrolysis and fermentation tests were carried out with pretreated wheat straw at 14% DM, and an enzyme loading of 10 FPU/g cellulose. The effect of the use of different oxidizing agents (H_2O_2, O_2, and air) in the pretreatment is also presented as a way to improve further the effectiveness of the pretreatment.

Material and Methods

Wet-Explosion Pretreatment

Wet explosion pretreatment [7] was performed batch-wise by suspending 350 g wheat straw pellets in 1.8 l of deionized water in a 3.5-l high-pressure reactor with a paddle stirrer with a maximum stirring speed of 2,000 rpm. The reactor was equipped with an injection device for injection of H_2O_2 solution, pure oxygen, or air. The reactor was heated by water jacket, which was connected to a heat exchanger controlled by an oil heater. The highest temperature in the reactor was 190 °C. The temperature and pressure inside the reactor were monitored by two temperature sensors (one in the bottom and one in the head space) and one pressure sensor. After the pretreatment, the material was flashed into a 5-l container connected to the reactor.

In this study, the temperature for pretreatment was 180–185 °C based on the previous optimization trials. After reaching the desired temperature, the required amount of oxidant [i.e., O_2 (12–18 bars), H_2O_2 solution (35%, *v/v*), or normal air (12–18 bar)] was injected by over-pressure air supply, and the timing of the reaction was initiated. H_2O_2 solution was only injected once, whereas three or five times of injection were conducted, respectively, when O_2 or air were used as an oxidizing agent. The reaction time was in total 15 min, and the stirrer speed was 1,000 rpm for all pretreatments presented in the paper.

Straw pellets obtained from DONG Energy pellet plant in Køge, Denmark, were pretreated by wet explosion using different oxidizing agents, i.e., H_2O_2, O_2, or air. Composition of straw pellets expressed as percent of DM is given in Table 1, and it was determined by two-step acid hydrolysis according to the procedure published by the National Renewable Energy Laboratory (NREL) [13]. The pretreated wheat straw out of the reactor was with a DM of 14% and consisted of hemicellulose, cellulose, and lignin.

Enzymatic Hydrolysis

For evaluation of the effect of the different oxidants (H_2O_2, O_2, or air) used in the wet-explosion pretreatment on convertibility of the material, enzymatic hydrolysis was carried out for 72 h using the different pretreated wheat straw materials (i.e., pretreated with H_2O_2, O_2, or air). The experiment was performed in 57-ml vials with unwashed slurry (20 g) with

Table 1 Composition of straw pellets expressed as percent of DM.

Cellulose	Xylan	Klason lignin	Ash
41.8	25.3	23.4	5.6

5% DM and an enzyme loading of 20 FPU/g cellulose. The DM content was adjusted to 5% by addition of a corresponding volume of 50 mM sodium acetate buffer (pH=4.8) to undiluted pretreated wheat straw (14% DM). The experiment was done in triplicate.

Enzymatic hydrolysis with the undiluted pretreated wheat straw slurry (14% DM, pretreated with O_2) was performed in duplicate in 1-l bottles containing 400 g material with pH 4.8 and an enzyme loading of 10 FPU/g cellulose. The pH of the material was increased to 4.8 using 10 M NaOH. The pH was measured at each sampling and, if necessary, adjusted to 4.8 by addition of 2 M NaOH.

The hydrolysis tests were performed at 50 °C in a rotary shaker at 200 rpm, and samples were taken regularly for sugar analysis. In all hydrolysis experiments including the SSF, enzymes consisted of a mixture of Celluclast 1.5 l and Novozym188 (both provided by Novozymes A/S, Bagsvaerd, Denmark) in a volume ratio of 3:1.

Simultaneous Saccharification and Fermentation

The SSF experiment was performed with unwashed and undiluted slurry of pretreated wheat straw (14% DM, pretreated with O_2) in a 2-l reactor [14] with a total working volume of 1.2 l and stirring at 250 rpm under no-aseptic conditions for 4 days. Before the material was added to the reactor, pH was adjusted to 5 using 10 M NaOH. Liquification of the material was performed at 50 °C for 24 h at an enzyme loading of 10 FPU/g cellulose. After liquification, the temperature was decreased to 35 °C, trace metals and vitamins were added, and the reactor was inoculated with 2 g/l dry yeast *Saccharomyces cerevisiae* (Ethanol Red^{2122}, Fermentis). The SSF continued for another 3 days. The pH was maintained at 5 by addition of 2 M NaOH. Samples were taken for sugar and ethanol analysis. The experiment was repeated once. The composition of the specific yeast addition was in milligrams per liter as follows: *Vitamins* Biotion, 0.050; Ca–pantothenate, 1.0; myo-inositol, 25.0; thiamin HCl, 1.0; pyridoxine HCl 1.0; para-aminobenzoic acid 2.0; trace elements ethylenediaminetetraacetic acid (EDTA) 15.0; $ZnSO_4.7H_2O$, 4.5; $MnCl_2.2H_2O$, 1.0; $CoCl_2.6H_2O$, 0.3; $CuSO_4.5H_2O$, 0.3; $Na_2MoO_4.2H_2O$, 0.4; $CaCl_2.2H_2O$, 4.5; $FeSO_4.7H_2O$, 3.0; H_3BO_3, 1.0; KI, 0.1.

Analysis

Glucose, xylose, cellobiose, ethanol furfural, and hydroxymethylfurfural (HMF) were analyzed using a high-performance liquid chromatography (HPLC) refractive index (RI) equipped with an Aminex HPX-87H column (Bio-Rad Laboratories, CA, USA) at 60 °C with 4 mM H_2SO_4 as eluent with a flow rate of 0.6 ml/min. Before HPLC analysis, samples were centrifuged at 10,000 rpm for 10 min, followed by filtration through a 0.45-μm membrane filter. DM content was determined according to standard methods [15]. The composition of pretreated wheat straw, e.g, cellulose, xylan, Klason lignin, and ashes was determined by a two-step acid hydrolysis according to the procedure published by the NREL [13].

Results and Discussion

Comparison of Pretreated Materials

The effect of different oxidizing agents (H_2O_2, O_2, or air) on the pretreatment of wheat straw pellets by wet explosion was evaluated. For comparison reasons, the pretreatment

conditions used were the same for all oxidizing agents. These conditions were the optimum pretreatment conditions determined in a previous wet-explosion study employing H_2O_2 as oxidizing agent (unpublished data), which is the strongest of the tested oxidants. The evaluation was based on glucose and xylose liberated per 100 g raw material during enzymatic hydrolysis (Fig. 1). This approach takes into account solid recovery values in the pretreatment step and, thus, allows simple evaluation of the overall process efficiency (i.e., amount of potential sugar from the raw material) [4].

The use of H_2O_2 and O_2 as oxidizing agents resulted in rather similar glucose yields of 31–32 g per 100 g raw material after hydrolysis (Fig. 1), which corresponds to a glucose yield of 69% based on the glucose content in the raw material. These yields were on average 25% higher than that obtained from the material pretreated with air. However, material pretreated with H_2O_2 gave the lowest xylose yield of 16 g/100 g raw material (corresponding to a yield of 55% based on xylose content in the raw material), which was 22% lower than in the case of using oxygen as oxidant. On the other hand, material pretreated with H_2O_2 gave the highest amount of xylose and furfural present in the liquid fraction after pretreatment (Fig. 2). This combined with the fact that overall xylose yield was lowest after pretreatment with H_2O_2 indicated that more xylan was solubilized and hydrolyzed but that an increased fraction was further degraded to furfural or other degradation products. The low glucose and xylose yields obtained in the material pretreated with air were probably caused by low accessibility of the slurry to the enzymes. HMF was not detected during the HPLC analysis even for undiluted pretreated materials (data not shown).

Comparison of the total yields of the different pretreated materials combined with the generation of furfural in the liquid fraction shows that the pretreatment with O_2 was the most efficient in enhancing overall convertibility of the raw material to sugars. The total

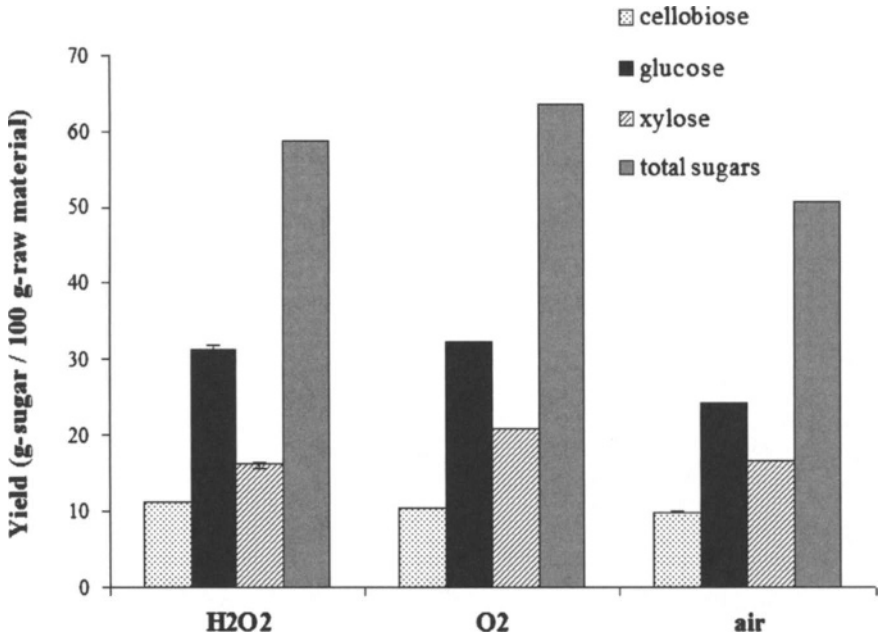


Fig. 1 Glucose, xylose, and cellobiose yields after 72 h enzymatic hydrolysis of pretreated wheat straw by wet explosion using different oxidizing agents (H_2O_2, O_2, and air). The yields are given as sugar liberated during the hydrolysis per 100 g raw wheat straw. Results are average of triplicates

overall yield of glucose, xylose, and cellobiose of this pretreatment was 63 g/g raw material, corresponding to 93% cellulose and 72% hemicellulose conversion based on the glucose and xylose content in the raw material. High recovery yield of the sugars, no production of HMF, and rather low production of furfural (Figs. 1 and 2) show that wet-explosion pretreatment using O_2 as oxidizing agent is an efficient method for fractionation of wheat straw. Moreover, replacement of H_2O_2 with oxygen could also be beneficial by reducing the cost of the pretreatment step. Based on the results, material pretreated with O_2 was used for further hydrolysis and SSF tests.

Enzymatic Hydrolysis

In this study, both enzymatic hydrolysis and SSF were investigated, because we have previously shown that the thermophilic anaerobic bacterium *Thermoanaerobacter* BG1L1 could effectively co-ferment glucose and xylose present in undetoxified wet-exploded wheat straw hydrolysate [16]. However, this organism can only be used as an ethanol producer if the process is carried out as separate hydrolysis and fermentation (SHF) because of differences in both temperature and pH optimum between this microorganism and the enzymes. Another possibility is to perform, first, SSF using *S. cerevisiae* followed by xylose fermentation by *Thermoanaerobacter* BG1L1. It is, therefore, important to know which of the two scenarios (SHF or SSF) would be the most efficient in converting the pretreated material into fermentable sugars.

To evaluate the material after wet explosion with O_2 under realistic conditions, both enzymatic hydrolysis and SSF were performed on unwashed material at high DM (14% DM) and with low enzyme loading of 10 FPU/g cellulose. Cellulose and hemicellulose conversion of 60 and 68%, respectively, were obtained in 96 h (Fig. 3). The initial

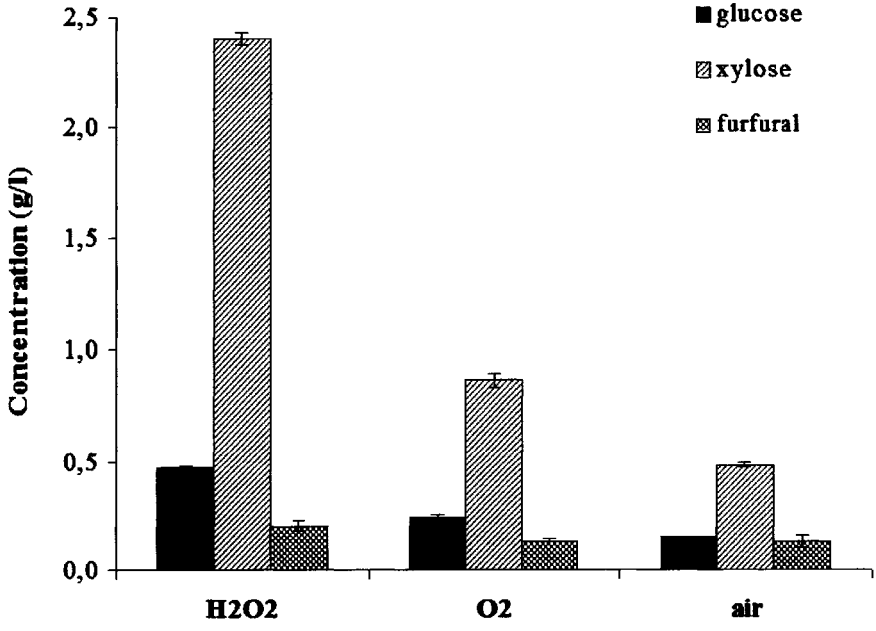


Fig. 2 Glucose, xylose, and furfural present in the liquid fraction in wet-exploded wheat straw (5% DM) pretreated with the use of H_2O_2, O_2, or air as oxidizing agents. Results are average of triplicates

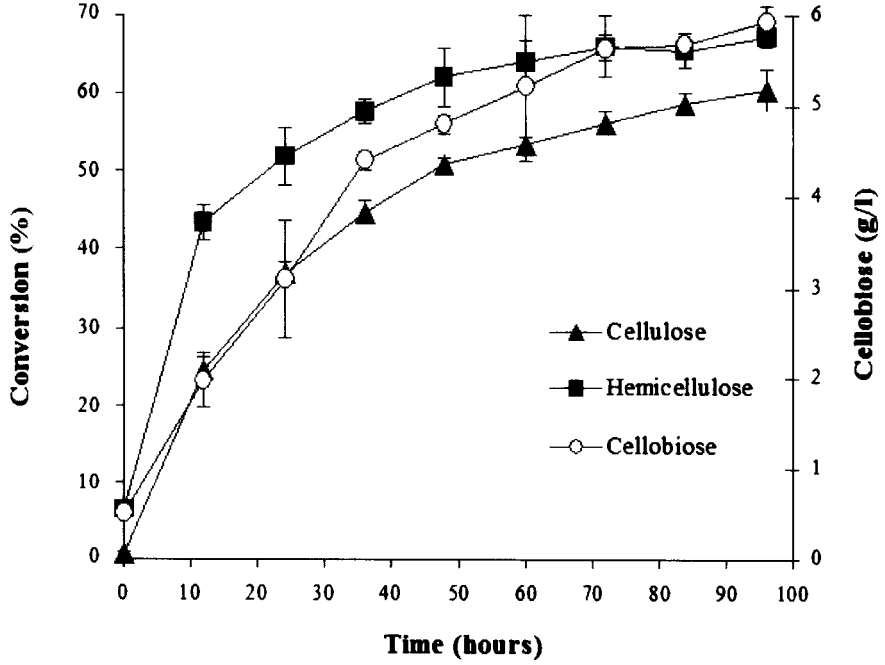


Fig. 3 Time course of cellulose and hemicellulose conversion and cellobiose production during enzymatic hydrolysis of wet-exploded wheat straw at 14% DM and an enzyme loading of 10 FPU/g cellulose. Degree of cellulose and hemicellulose conversion was calculated as amount of glucose and xylose, respectively, released during the hydrolysis relative to the maximum theoretical. Results are average of duplicates

hemicellulose hydrolysis rate appeared to be faster than the cellulose hydrolysis rate, which was probably caused by the partial solubilization of hemicelluloses during the pretreatment. These oligomers were fast hydrolyzed to xylose by the enzymes. Cellulose was hydrolyzed more slowly and a significant accumulation of cellobiose was also observed (Fig. 3). This relative large amount of cellobiose could result in pronounced inhibition of the cellulases. If the production cellobiose was taken into account, the cellulose conversion would increase by 17%, thereby, resulting in a final cellulose conversion of 70% in 96 h.

Reduced cellulose conversion in the range of 10–20% with an increase in substrate concentration from 2 to 10% DM has been reported for various substrates such as pretreated wheat straw [9] and softwood [17, 18], as well as for pure cellulose [19]. To our knowledge, only one other study has investigated enzymatic hydrolysis of pretreated wheat straw at solid concentrations higher than 10% DM [9]. In that study, cellulose conversion of approximately 65% was obtained with 12 FPU/g cellulose, which is comparable to the cellulose conversion reported herein. However, the hemicellulose conversion was 10% lower compared to that obtained in our study. This difference is most likely because of the removal of some of the easy degradable hemicelluloses in the washing step in the pretreatment in that study, whereas all hemicelluloses remain in the pretreated material used in this study. The reduced efficiency of enzymatic hydrolysis of cellulose with increased substrate concentration is primary caused by increased product inhibition (glucose) of cellulases. In this study, a significant accumulation of cellobiose was observed. Furthermore, some inhibition of the cellulases by hemicellulose-derived sugars [20] and degradation compounds formed during the pretreatment [21] have been also reported.

Simultaneous Saccharification and Fermentation

SSF is considered the most promising process for converting cellulose into ethanol. This technology enables immediate conversion of released glucose into ethanol, thus, preventing glucose accumulation in the fermentation broth and, therefore, no product (glucose) inhibition. The potential of performing the process as an SSF process was studied using *S. cerevisiae*. This fermenting organism was chosen, as it is the most efficient organism for fermentation of glucose and proven to be rather robust to the toxicity of various pretreated materials or hydrolysates [9, 22–24]. The pretreated wheat straw was liquefied for 24 h to decrease the viscosity of the material and, thus, to avoid mass transfer limitations. Glucose was consumed rapidly, and already after 10 h of SSF, the glucose liberated during the liquification step was utilized (Fig. 4). The ethanol concentration reached 12.3 g/l, corresponding to an ethanol productivity of 1.23 g/l per h (Fig. 4). These results indicate that unwashed wet-exploded wheat straw with high DM content of 14% is not toxic to the yeast and, thus, could be effectively fermented. High fermentability of the slurry at high DM is important, as detoxification or washing of the material is not needed.

After the initial fast fermentation in the first 10 h, a phase with minor increase in ethanol concentration was seen, indicating that glucose was still being released from the cellulose fraction, although at a very slow rate. The ethanol concentration reached 22.2 g/l after 72 h of SSF. Assuming a theoretical ethanol yield of 0.51 g ethanol/g consumed glucose, the cellulose conversion could be estimated to at least 68%. This result shows that, under the condition tested, the amount of cellulose hydrolyzed in the SSF was increased by at least 14% compared to that obtained in enzymatic hydrolysis (60%). It is also notable that, in the SSF, the cellobiose concentration was constantly low, thereby, avoiding the inhibition of cellulases by cellobiose. Although, that unwashed and high solids pretreated material was used for SSF process, operating the SSF in fed-batch [24], using a shorter liquification step [25] or minor increase in enzyme loading could enhance cellulose and hemicellulose conversion, thus, resulting in shorter process time and/or higher ethanol yield.

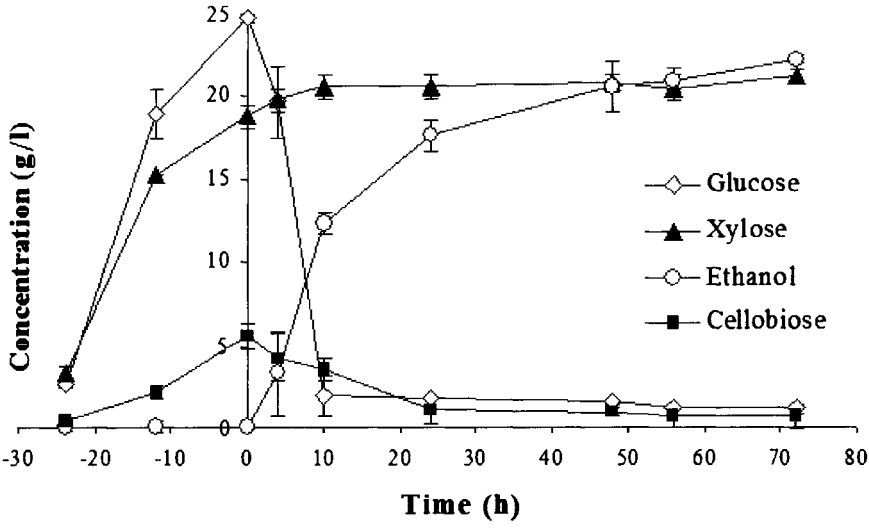


Fig. 4 Time course of ethanol, glucose, xylose and cellobiose concentrations during SSF of wet-exploded wheat straw at 14% DM and enzyme loading of 10 FPU/g-cellulose. Results are average of duplicates

Previous studies investigating the SSF of pretreated wheat straw have mostly been conducted with washed material, substrate concentrations less than 10% DM, and higher enzyme loading [6, 11, 26, 27]. Nevertheless, the overall ethanol yields obtained in those studies (60–70%) are in the same range as the results reported herein. In an SSF study with wheat straw with rather similar substrate concentration (16% DM), a cellulose conversion of 70% was obtained [8]. However, this yield was obtained with washed pretreated material, which could be due to the potential removal of inhibitors for both enzymes and the yeast.

Xylose fermentation was not tested, but with our thermophilic anaerobic bacterium *Thermoanaerobacter* BG1L1 (16), ethanol production could theoretically be increased by more than 39% by including the xylose. Based on the results from the current study, 285 l ethanol per ton DM could be possible from unwashed or undetoxified wet-exploded wheat straw. Pilot scale studies are now carried out at the Maxifuels pilot plant (DTU, Denmark) to optimize the pretreatment method at higher DM up to 30%.

Conclusions

The pretreatment of wheat straw pellets by wet explosion using three different oxidizing agents (H_2O_2, O_2, and air) under the same conditions showed that the pretreatment with O_2 was the most efficient in enhancing overall convertibility of the raw material to sugars and minimizing generation of furfural as a by-product. The wet-explosion pretreatment with O_2 as oxidizing agent enabled relatively high yields from both enzymatic hydrolysis and SSF to be obtained even on unwashed slurry with 14% DM and a low enzyme loading of 10 FPU/g cellulose in an industrial acceptable time frame of 96 h. From the enzymatic hydrolysis experiment, cellulose and hemicellulose conversion of 70 and 68%, respectively, was achieved, and the overall ethanol yield from SSF was 68%. Overall, the experimental data from the enzymatic hydrolysis and SSF reported in this paper seem rather encouraging in view of the feasibility of the wet-exploded pretreatment method as an efficient method for pretreatment of wheat straw.

Acknowledgment We thank Novozymes A/S, Bagsvaerd, Denmark, for supplying the enzymes Celluclast and Novozyme 188, and Thomas Andersen from BioCentrum for the technical help.

References

1. Kim, S., & Dale, B. E. (2004). *Biomass Bioenergy, 26*, 361–375.
2. Jørgensen, H., Kristensen, J., & Felby, C. (2007). *Biofuels Bioproducts and Biorefinery, 1*, 119–134.
3. Schmidt, A. S., & Thomsen, A. B. (1998). *Bioresource Technology, 64*, 139–151.
4. Ballesteros, I., Negro, M. J., Oliva, J. M., Cabanas, A., & Ballesteros, M. (2006). *Applied Biochemistry and Biotechnology, 129–132*, 496–508.
5. Saha, B. C., Iten, L. B., Cotta, M. A., & Wu, Y. V. (2005). *Process Biochemistry, 40*, 3693–3700.
6. Thomsen, M. H., Thygesen, A., Jørgensen, H., Larsen, J., Christensen, B. H., & Thomsen, A. B. (2006). *Applied Biochemistry and Biotechnology, 129–132*, 448–460.
7. Ahring, B. K. & Munck, J. (2006) Patent no. WO 2006-032282 A1.
8. Mohagheghi, A., Tucker, M., Grohmann, K., & Wyman, C. (1992). *Applied Biochemistry and Biotechnology, 33*, 67–81.
9. Jørgensen, H., Vibe-Pedersen, J., Larsen, J., & Felby, C. (2007). *Biotechnology and Bioengineering, 96*, 862–870.
10. Tengborg, C., Galbe, M., & Zacchi, G. (2001). *Enzyme and Microbial Technology, 28*, 835–844.

11. Felby, C., Klinke, H. B., Olsen, H. S., & Thomsen, A. B. (2003). *Applications of Enzymes to Lignocellulosics, 855*, 157–174.
12. Galbe, M., & Zacchi, G. (2002). *Applied Microbiology Biotechnology, 59*, 618–628.
13. Sluiter, A., Hames, B., Ruiz, R., Scarlata, C., Sluite, J., Templeton, D., & Crocker, D. (2006). http://devafdc.nrel.gov/pdfs/9572.pdf.
14. Hartmann, H., & Ahring, B. K. (2005). *Water Research, 39*, 1543–1552.
15. American Public Health Association/American Water Works Association/Water Environmental Federation (1995) Standard methods for the examination of water and wastewater, 19th ed. American Public Health Association/American Water Works Association/Water Environmental Federation, Washington DC, USA.
16. Georgieva, T. I., Mikkelsen, M. J., & Ahring, B. K. (2007). *Applied Biochemistry and Biotechnology* DOI 10.1007/s12010-007-8014-1.
17. Lu, Y. P., Yang, B., Gregg, D., Saddler, J. N., & Mansfield, S. D. (2002). *Applied Biochemistry and Biotechnology, 98*, 641–654.
18. Tengborg, C., Galbe, M., & Zacchi, G. (2001). *Biotechnology Progress, 17*, 110–117.
19. Ingesson, H., Zacchi, G., Yang, B., Esteghlalian, A. R., & Saddler, J. N. (2001). *Journal of Biotechnology, 88*, 177–182.
20. Xiao, Z. Z., Zhang, X., Gregg, D. J., & Saddler, J. N. (2004). *Applied Biochemistry and Biotechnology, 113–16*, 1115–1126.
21. Panagiotou, G., & Olsson, L. (2007). *Biotechnology and Bioengineering, 96*, 250–258.
22. Varga, E., Klinke, H. B., Reczey, K., & Thomsen, A. B. (2004). *Biotechnology and Bioengineering, 88*, 567–574.
23. Stenberg, K., Bollok, M., Reczey, K., Galbe, M., & Zacchi, G. (2000). *Biotechnology and Bioengineering, 68*, 204–210.
24. Sassner, P., Galbe, M., & Zacchi, G. (2006). *Enzyme and Microbial Technology, 39*, 756–762.
25. Öhgren, K., Vehmaanpera, J., Siika-Aho, M., Galbe, M., Viikari, L., & Zacchi, G. (2006). *Enzyme and Microbial Technology* EMT-7322.
26. Alfani, F., Gallifuoco, A., Saporosi, A., Spera, A., & Cantarella, M. (2000). *Journal of Industrial Microbiology and Biotechnology, 25*, 184–192.
27. Zhu, S. D., Wu, Y. X., Yu, Z. N., Zhang, X., Wang, C. W., Yu, F. Q., & Jin, S. W. (2006). *Process Biochemistry, 41*, 869–873.

Appl Biochem Biotechnol (2008) 148:45–58
DOI 10.1007/s12010-008-8200-9

A Comparison between Lime and Alkaline Hydrogen Peroxide Pretreatments of Sugarcane Bagasse for Ethanol Production

Sarita C. Rabelo · Rubens Maciel Filho · Aline C. Costa

Received: 8 May 2007 / Accepted: 16 October 2007 /
Published online: 11 April 2008
© Humana Press 2008

Abstract Pretreatment procedures of sugarcane bagasse with lime (calcium hydroxide) or alkaline hydrogen peroxide were evaluated and compared. Analyses were performed using 2 × 2 × 2 factorial designs, with pretreatment time, temperature, and lime loading and hydrogen peroxide concentration as factors. The responses evaluated were the yield of total reducing sugars (TRS) and glucose released from pretreated bagasse after enzymatic hydrolysis. Experiments were performed using the bagasse as it comes from an alcohol/sugar factory and bagasse in the size range of 0.248 to 1.397 mm (12–60 mesh). The results show that when hexoses and pentoses are of interest, lime should be the pretreatment agent chosen, as high TRS yields are obtained for nonscreened bagasse using 0.40 g lime/g dry biomass at 70 °C for 36 h. When the product of interest is glucose, the best results were obtained with lime pretreatment of screened bagasse. However, the results for alkaline peroxide and lime pretreatments of nonscreened bagasse are not very different.

Keywords Lignocellulosic materials · Sugarcane bagasse · Pretreatment · Lime · Hydrogen peroxide · Enzymatic hydrolysis · Statistical analysis

Introduction

In recent years, the worldwide trends toward scientific and technological advances in the field of new fuels point to the importance of more efficient utilization of agro-industrial residues as raw material in the ethanol production process. In Brazil, sugarcane bagasse, the major byproduct of the sugar cane industry, seems to be economically viable for the production of environmentally friendly fuels.

In general, lignocellulosic materials are resistant to bioconversion and require pretreatment to increase their biodigestibility and make cellulose more accessible to the

S. C. Rabelo · R. M. Filho · A. C. Costa (✉)
Department of Chemical Process, School of Chemical Engineering,
State University of Campinas (UNICAMP), Campinas, SP, Brazil
e-mail: accosta@feq.unicamp.br

cellulolytic enzymes. Pretreatment methods can be classified into four categories: physical, chemical, biological, and a combination of these. Chemical pretreatments have received more attention because the physical pretreatments are relatively inefficient [1] and the combined pretreatments rarely have improved digestibility when compared with simple treatments [2]; thus, chemical pretreatments have been chosen as the subject in this work.

Lynd et al. [3] has summarized the desireable properties for an ideal lignocellulosic material after chemical pretreatment; that is, it should (a) produce reactive fibers, (b) yield pentoses in nondegraded form, (c) not release the compounds that significantly inhibit fermentation, (d) work in reactors of reasonable size with moderate cost, (f) produce no solid residues, (g) have a high degree of simplicity, and (h) be effective at low moisture contents.

Pretreatment is one of the most expensive and least technologically mature steps in the process for converting biomass to fermentable sugars [4]. Costs are due to the use of steam and chemical products and the need for expensive corrosion resistant reactors; however, pretreatment also has great potential for efficiency improvement and lowering of costs through research and development [5–8].

Enzymatic hydrolysis of cellulosic material by cellulase enzymes is the most promising approach for getting high product yields vital to economic success [3, 9]. The cellulases break down cellulose to cellobiose, which is subsequently cleaved to glucose by β-glucosidase. Enzymatic hydrolysis leads to higher yields of monosaccharides than dilute-acid hydrolysis because cellulase enzymes catalyze only cellulose or hemicellulose hydrolysis reactions and not sugar degradation reactions [10]. Enzymes are naturally occurring compounds that are biodegradable and therefore environmentally friendly.

In this work, two promising pretreatment technologies are compared. They were chosen for occurring under mild conditions (temperature, pressure, and absence of acids). Both are alkaline processes, which are expected to cause less sugar degradation than acid processes [11]. The first is the pretreatment with alkaline hydrogen peroxide [12–17], which is a well-known reagent in the paper and cellulose industry, being used as a bleach agent. It has also the great advantage of not leaving residues in the biomass, as it degrades into oxygen and water. Furthermore, the formation of secondary products is practically inexistent.

The other pretreatment agent considered is lime (calcium hydroxide) [18–27], which is an inexpensive reagent and can be easily recovered as calcium carbonate by neutralization with carbon dioxide. The calcium hydroxide can be subsequently regenerated using established lime kiln technology [26].

Analyses were performed using 2 × 2 × 2 factorial designs. The factors considered were pretreatment time, temperature, and lime loading or hydrogen peroxide concentration. The responses evaluated were the total reducing sugar (TRS) and glucose yield from the pretreated bagasse after enzymatic hydrolysis. Experiments were performed using the bagasse as it comes from an alcohol/sugar factory and bagasse with a screened size of 0.248 to 1.397 mm (12–60 mesh) to evaluate the possibility of using the bagasse as it comes from the mills.

Materials and Methods

Substrate

Fresh sugarcane bagasse was obtained from the sugar plant Usina São Luiz—Dedini S/A, (Pirassununga/SP, Brazil). It was dried at 45 °C for 48 h, left for 48 h at room temperature,

put into plastic bags, and kept in a freezer until used. The dry matter content of the bagasse after being dried was 95%. The bagasse used in the tests was divided into two parts. One part was used as it came from the mill, without prior screening, and presented highly heterogeneous particle sizes. This part will be called nonscreened bagasse throughout this article. The other part was screened in the size range of 0.248 to 1.397 mm (12–60 mesh). Smaller particles were discarded because they corresponded mainly to sand. Figure 1 shows samples of the screened and nonscreened bagasse.

Chemical Analysis of Bagasse Samples

Samples of the screened and nonscreened bagasse were milled to pass through a 0.75-mm screen. Approximately 3 g of milled sample was extracted with 95% ethanol for 6 h in a Soxhlet apparatus. Ash content was determined after burning of the samples in a muffle 600 °C for 4 h [28]. Extracted bagasse samples were hydrolyzed with 72% sulfuric acid at 30 °C for 1 h (300 mg of sample and 3 ml of sulfuric acid). The acid was diluted to a final concentration of 3% (addition of 79 ml of water), and the mixture was heated at 125 °C/ 1atm for 1 h. The residual material was cooled and filtered through porous glass filter number 3. The solids were dried to constant weight at 105 °C and determined as insoluble lignin. The soluble lignin concentration in the filtrate was determined by measuring absorbance at 205 nm and using the value of 105 l g^{-1} cm^{-1} as the absorptivity of soluble lignin [29]. The concentrations of monomeric sugars in the soluble fraction were determined by high-performance liquid chromatography (HPLC) using a BIORAD HPX87H column at 45 °C, eluted at the 0.6 ml/min with 0.005 mol/l sulfuric acid. Sugars were detected in a 30 °C temperature-controlled refractive index detector (Knauer HPLC pump and detector). Under these conditions, xylose, mannose, and galactose eluted at the same retention time were integrated as a single peak. Glucose, xylose, arabinose, and acetic acid were used as external calibration standards. No corrections were performed due to sugar degradation reactions during acid hydrolysis. The factors used to convert sugar monomers to anhydromonomers were 0.90 for glucose and 0.88 for xylose and arabinose. Acetyl content was calculated as the acetic acid content multiplied by 0.7. These factors were calculated based on water addition to polysaccharides during acid hydrolysis [30–33]. Table 1 shows the composition of the screened and nonscreened bagasse.

Pretreatment

The pretreatment agents evaluated were alkaline hydrogen peroxide and lime (calcium hydroxide). Pretreatment time, temperature, and lime loading or hydrogen peroxide

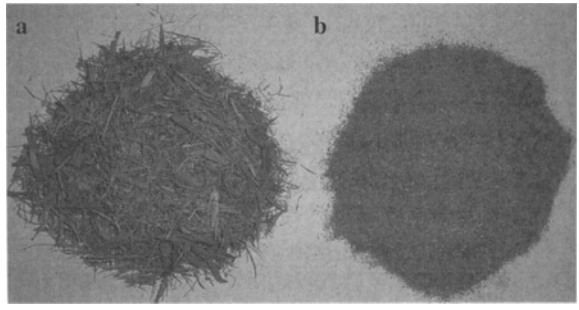


Fig. 1 **a** Nonscreened bagasse, **b** screened bagasse (12–60 mesh)

Table 1 Composition of the nonscreened and screened sugarcane bagasse.

	Nonscreened bagasse, %	Screened bagasse. %
Glucan	39.6±0.9	34.1±0.9
Xylan	19.7±0.5	17.7±0.5
Arabinan groups	1.7±0.1	2.0±0.1
Acetyl groups	2.5±0.1	2.4±0.1
Lignin	25.8±1.6	29.3±1.6
Extractives	2.3±0.1	2.3±0.1
Ash	3.8±0.1	5.3±0.1

concentration were evaluated during the experiments. The pretreatment solution of alkaline peroxide was prepared by dissolving H_2O_2 in distilled water and adjusting the pH to 11.5 with sodium hydroxide, and the lime pretreatment solution was prepared by dissolving $Ca(OH)_2$ in distilled water. In the lime pretreatment, in all the assays, a certain amount of lime remained insoluble, although this continued dissolving during pretreatment. Nonscreened bagasse (4 g) and screened bagasse (4 g) were treated with 100 ml of the pretreatment solution in 500-ml flasks in an orbital shaker (Marconi MA-832) agitated at 150 rpm.

Enzymatic Hydrolysis

After pretreatment, the substrate was washed to remove insoluble matter, dried, and weighted to measure mass loss. The present market offers many cellulase preparations (including those obtained from *Trichoderma reesei*) containing low levels of β-glucosidase, which leads to an increased accumulation of cellobiose in the enzymatic hydrolyzates of the cellulose. The inability of industrial glucose-fermenting yeasts to ferment cellobiose results in incomplete conversion of cellulose hydrolyzate to ethanol, significantly diminishing its final yield. These drawbacks may be overcome by supplementation of the cellulase complex with a β-glucosidase from other sources [34]. One gram of the pretreated bagasse was hydrolyzed with 300 ml of solution containing cellulase and β-glucosidase with the pH adjusted to 4.8. Cellulases from *T. reesei* (Sigma) loading was 3.42 filter paper units (FPU)/g dry pretreated biomass. β-glucosidase from *Aspergillus niger* (Sigma) was added to completely convert cellobiose to glucose, with loading of 1.00 IU/g dry pretreated biomass. Cellulase activity was determined as FPU per milliliter, as recommended by the International Union of Pure and Applied Chemistry [35, 36]. β-Glucosidase activity was determined through a solution of cellobiose 15 mmol/l and express in units per milliliter [37]. Enzyme activity was 47.44 FPU/ml for cellulases and 343.63 IU/ml for β-glucosidase.

Hydrolysis experiments were carried out in 500-ml flasks in an orbital shaker (Marconi MA-832) agitated at 100 rpm at 50 °C. Aliquots were taken periodically, boiled to deactivate the enzymes, and analyzed for glucose and reducing sugars. The values of glucose and reducing sugars yields used for the statistical analysis were picked at the reaction time after which no significant changes in these variables were detected.

Analytical Methods

Glucose yield was measured using a kit based on the glucose oxidase reaction (GOD-PAP, Laborlab), and TRS yield was determined by the dinitrosalycilic acid (DNS) method [38].

For glucose quantification, 10 μl of the sample and 1.0 ml of the mono-reagent glucose oxidase were added in assays pipes and put in a thermostatic bath (Marconi MA-184) at 37 °C per 10 min. At the end of the reaction, the absorbance was read in spectrophotometer (Femto 600S) at 540 nm.

For the TRS quantification, 0.5 ml of the samples and 1.5 ml of DNS were added in assay pipes and put in a thermostatic bath (Marconi MA-184) at 95 °C per 5 min. After, the samples were cooled immediately by the immersion in an ice bath. The absorbance was read in a spectrophotometer (Femto 600S) at 540 nm. In both methods, the standard glucose (Merck) was used for the preparation of the standard curve.

Results and Discussion

A 2 × 2 × 2 full factorial design with three replicates in the central point was performed for each pretreatment considered. The objective was to evaluate the influence of pretreatment time, temperature, and pretreatment agent concentration on the subsequent enzymatic hydrolysis performance.

Table 2 shows the design matrix and glucose and TRS yields after hydrolysis of pretreated bagasse for the screened and nonscreened samples for the pretreatment with alkaline hydrogen peroxide. Table 3 shows the design matrix for the pretreatment with lime. In both tables, the glucose and TRS yields were expressed as milligrams per gram of dry raw bagasse (not pretreated). The maximum TRS and glucose yield obtained are marked in italics, and the mean TRS and glucose yield obtained for the screened and nonscreened bagasse samples in all the assays are also shown. The ranges of the factors for the two pretreatments were chosen based on literature [12–27].

It can be seen from Tables 2 and 3 that under the operational conditions used in this work, maximum TRS yield was obtained with lime pretreatment of nonscreened bagasse (554.2 mg/g dry nonscreened bagasse). Lime pretreatment of screened bagasse also resulted in high TRS yield (550.6 mg/g dry screened bagasse); thus, when all the reducing sugars

Table 2 Design matrix presenting TRS and glucose yields after hydrolysis of pretreated bagasse: alkaline hydrogen peroxide (screened—S and nonscreened—NS).

Assay	Time (h)	Temperature (°C)	$[H_2O_2]$ (%)	TRS (NS), (mg/g)	Glucose (NS), (mg/g)	Glucose (NS), yield %	TRS (S) (mg/g)	Glucose (S) (mg/g)	Glucose (S), yield %
1	6	20	1	206.2	64.6	14.5	259.0	103.3	26.9
2	24	20	1	211.5	79.7	17.9	253.5	98.1	25.6
3	6	60	1	433.0	215.3	48.3	342.4	166.7	43.5
4	24	60	1	280.7	121.4	27.3	340.3	181.9	47.4
5	6	20	5	347.0	241.9	54.3	368.0	*239.3*	*62.4*
6	24	20	5	*494.7*	*309.3*	*69.4*	*452.1*	228.1	59.5
7	6	60	5	364.9	252.5	56.7	288.9	188.8	49.2
8	24	60	5	407.0	287.7	64.6	285.5	163.4	42.6
9	15	40	3	359.0	229.6	51.5	309.4	167.6	43.7
10	15	40	3	323.5	209.2	47.0	346.5	195.2	50.9
11	15	40	3	323.9	204.6	45.9	307.1	164.9	43.0
			Mean	341.0	201.4	45.2	323.0	172.5	45.0

Table 3 Design matrix presenting TRS and glucose yields after hydrolysis of pretreated bagasse: lime (screened—S and nonscreened—NS).

Assay	Time (h)	Temp (°C)	lime loading. (g/g)	TRS (NS), (mg/g)	Glucose (NS), (mg/g)	Glucose (NS), yield %	TRS (S), (mg/g)	Glucose (S), (mg/g)	Glucose (S), yield %
1	12	60	0.10	306.3	128.2	28.8	422.7	208.4	54.3
2	36	60	0.10	433.9	232.2	52.1	481.8	235.6	61.4
3	12	70	0.10	351.5	161.0	36.1	474.8	329.0	85.8
4	36	70	0.10	427.7	228.1	51.2	549.3	*335.5*	*87.5*
5	12	60	0.40	379.6	108.2	24.3	516.3	212.3	55.4
6	36	60	0.40	307.1	106.1	23.8	*550.6*	331.5	86.4
7	12	70	0.40	268.6	110.0	24.7	456.3	177.6	46.3
8	36	70	0.40	*554.2*	*296.9*	*66.7*	528.4	171.9	44.8
9	24	65	0.25	535.0	224.9	50.5	484.0	265.9	69.3
10	24	65	0.25	530.0	213.4	47.9	490.1	265.6	69.2
11	24	65	0.25	531.2	223.2	50.1	502.4	260.9	68.0
			Mean	420.5	184.7	41.5	496.1	254.0	66.2

(hexoses and pentoses) are of interest, lime pretreatment is a better choice of pretreatment agent than alkaline peroxide pretreatment. In addition, bagasse screening is not necessary, which reduces substantially the costs of the process.

Table 4 shows the effects of pretreatment time, temperature, and lime loading on TRS yield after hydrolysis for lime pretreatment of nonscreened bagasse. The statistical analysis was performed using the software Statistica (Statsoft, v. 7.0) and the confidence level considered was 90%. Significant effects are marked in italics. A statistical model is not presented because a linear model is not able to represent experimental behavior in this case.

It can be seen from Table 4 that the major effect is that of pretreatment time, followed by the three-way interaction. The interaction between pretreatment time and temperature (1 × 2) and the main effect of temperature are also significant. The main effect of lime loading has no influence on TRS yield, but its two-way interaction with temperature (2 × 3) is significant. It can be observed that all the significant effects are positive, which means that maximum TRS yield for the nonscreened bagasse is for high pretreatment time, temperature, and lime loading (see assay 8 in Table 3).

Table 4 Effects on TRS yield after hydrolysis of nonscreened bagasse pretreated with lime.

Factor	TRS (NS)	
	Effect	*p* value
Mean	*420.46*	3.4377×10^{-6}
Pretreatment time (1)	*104.23*	0.0003
Temperature (2)	*43.78*	0.0017
$Ca(OH)_2$ loading (3)	−2.48	0.3119
1×2	*76.68*	0.0006
1×3	2.33	0.3349
2×3	*24.28*	0.0057
1×2×3	*102.38*	0.0003

Significant effects marked in italics.

As the industrial fermenting microorganisms used nowadays for industrial ethanol production do not ferment pentoses, in many practical applications, the product of interest may be glucose. From Tables 2 and 3, it can be noticed that the maximum glucose yield in the range of operational conditions used in this work is for lime pretreatment of screened bagasse (335.5 mg/g dry screened bagasse). For nonscreened bagasse, alkaline hydrogen peroxide seems to be the pretreatment agent of choice, although lime pretreatment leads to just a little lower glucose yield (309.3 mg/g dry nonscreened bagasse with alkaline peroxide versus 296.9 mg/g dry nonscreened bagasse when the pretreatment agent is lime). This is not a statistically significant difference; however, the process based on alkaline hydrogen peroxide requires lower temperature and process time. Overall, it seems to be the more suitable one.

As screening is an expensive unit operation, we investigated not only the best result (lime pretreatment of screened bagasse) but also the two options for pretreatment with nonscreened bagasse: alkaline peroxide and lime pretreatments.

Table 5 shows the scaled regression coefficients of the regression model of glucose yield after hydrolysis for alkaline hydrogen peroxide pretreatment of nonscreened bagasse. It can be seen that at the 90% confidence level, pretreatment time is not significant for glucose yield. However, the interactions between pretreatment time and temperature (1 × 2) and between pretreatment time and H_2O_2 concentration (1 × 3) are significant. The concentration of H_2O_2 is the most important factor affecting this response; temperature is significant, and the interaction between temperature and peroxide concentration (2 × 3) also significantly influences glucose yield.

Table 6 depicts the scaled regression coefficients of the regression models of glucose yield after hydrolysis for lime pretreatment of nonscreened and screened bagasse. For screened bagasse, only the interaction between pretreatment time and lime loading (1 × 3) is not significant. All the other main effects and interactions are significant, and the main effect of pretreatment time is the most important. For screened bagasse, all the factors considered and all their interactions are significant. The major effect is the interaction between temperature and lime loading (2 × 3), followed by the main effect of lime loading.

Table 7 depicts the analysis of variance (ANOVA) for the model of glucose yield after hydrolysis for alkaline peroxide pretreatment of nonscreened bagasse when only the significant coefficients are taken into account. It can be seen that the model presents a high correlation coefficient and can be considered statistically significant with 90% of confidence according to the *F* test, as it presented a calculated value greater than the listed

Table 5 Scaled regression coefficients of the regression model of glucose yield for nonscreened bagasse pretreated with alkaline hydrogen peroxide.

Factor	Glu(NS)	
	Coefficient	*p* value
Mean	*201.42*	3.964×10^{-4}
Pretreatment time (1)	5.96	0.5918
Temperature (2)	*45.36*	0.0405
H_2O_2 concentration (3)	*152.58*	0.0038
1×2	*−35.29*	0.0643
1×3	*45.30*	0.0405
2×3	*−50.86*	0.0326
1×2×3	19.18	0.1781

Significant effects marked in italics.

Table 6 Scaled regression coefficients of the regression models of glucose yield.

Factor	Glu (NS)		Factor	Glu (S)	
	Coefficient	*p* value		Coefficient	*p* value
Mean	*184.75*	0.0001	Mean	*254.02*	1.100×10^{-5}
Pretreatment time (1)	*88.98*	0.0024	Pretreatment time (1)	*36.80*	0.0029
Temperature (2)	*55.33*	0.0062	Temperature (2)	*6.55*	0.0799
Lime loading (3)	*−32.08*	0.0182	Lime loading (3)	*−53.80*	0.0013
1×2	*38.03*	0.0131	1×2	*−36.40*	0.0029
1×3	3.43	0.5169	1×3	*19.95*	0.0097
2×3	*40.98*	0.0113	2×3	*−103.70*	0.0004
1×2×3	*56.48*	0.0060	1×2×3	*−26.05*	0.0057

Nonscreened and screened bagasse pretreated with lime

one [39]. Furthermore, it does not present evidence of lack of fit, as the calculated value for the F test for lack of fit is much smaller than the listed value.

Table 8 shows the ANOVA for the models of glucose yield after hydrolysis for lime pretreatment of nonscreened and screened bagasse when only the significant coefficients are taken into account. Both models present high correlation coefficients, and the F value for statistical significance of the regression are higher than the listed ones. Nevertheless, both models presented evidence of lack of fit, as they presented high lack of fit calculated F values. A model with evidence of lack of fit cannot be used for prediction or optimization purposes. However, it can be used to plot qualitative response surfaces that can aid in determining the best experimental region.

The response surface for glucose yield from nonscreened bagasse pretreated with alkaline hydrogen peroxide is depicted in Fig. 2. Figure 2a shows glucose yield versus peroxide concentration and temperature when pretreatment time is 6 h, and Fig. 2b shows the same response surface when pretreatment time is 24 h. From this figure, it can be seen

Table 7 ANOVA for the model describing glucose yield for nonscreened bagasse (NS) pretreated with alkaline peroxide.

Source of variation	Sum of squares (SQ) Glu	Degrees of freedom (*df*) Glu	Mean square (MS) Glu	*F* value Glu
Regression (R)	62,444.2	5	12,488.8	33.5[a]
Residual (r)	1,861.7	5	372.3	
Lack of fit (Lf)	1,508.2	3	502.7	2.8[b]
Pure error (Pe)	353.5	2	176.8	
Total (T)	64,305.9	10		
R^2	0.971			
F listed values (90% of confidence)				$F_{5,5}=3.45$[a] $F_{3,2}=9.16$[b]

[a] F test for statistical significance of the regression $=MS_R/MS_r$

[b] F test for lack of fit $=MS_{Lf}/MS_{Pe}$

Table 8 ANOVA for the models describing glucose yield for lime pretreatment of nonscreened (NS) and screened (S) bagasse.

Source of variation	Sum of squares (SQ)		Degrees of freedom (*df*)		Mean square (MS)		*F* value	
	Glu (NS)	Glu (S)	Glu (NS)	Glu (S)	Glu (NS)	Glu (S)	Glu (NS)	Glu (S)
Regression (*R*)	36,647.8	34,907.4	6	7	6,108.0	4,986.8	4.55[a]	34.32[a]
Residual (*r*)	5,371.0	435.9	4	3	1,342.8	145.3		
Lack of fit (Lf)	5,293.2	420.3	2	1	2,646.6	420.3	67.93[b]	53.85[b]
Pure error (Pe)	77.9	15.6	2	2	39.0	7.8		
Total (*T*)	42,018.9	35,343.3	10	10				
R^2	0.872	0.988						
F listed values (90% of confidence)							$F_{6,4}=4.01$[a] $F_{2,2}=9.00$[b]	$F_{7,3}=5.27$[a] $F_{1,2}=8.53$[b]

[a] *F* test for statistical significance of the regression=MS_R/MS_r

[b] *F* test for lack of fit=MS_{Lf}/MS_{Pe}

that high glucose yields can be obtained with both high and low pretreatment time. When pretreatment time is low, the highest glucose yields are in the region of high peroxide concentration and high temperature. For high pretreatment time, temperature has low influence, and the highest glucose yields are in the region of high peroxide concentration and low temperature. As the influence of temperature is low, pretreatment with alkaline peroxide can be performed at ambient temperature for high pretreatment time.

Figure 3 shows the response surface for glucose yield from nonscreened bagasse pretreated with lime. Figure 3a shows glucose yield versus lime loading and temperature when pretreatment time is 12 h, and Fig. 3b shows the same response surface when pretreatment time is 36 h. It can be seen that for nonscreened bagasse pretreated with lime, pretreatment time has a strong influence on glucose yield after hydrolysis, with high pretreatment time resulting in higher glucose yields. For high pretreatment time, lime loading had a weak influence and temperature a strong influence, with high temperature leading to high glucose yield. The maximum glucose yield was for high lime loadings and high temperature, but high yields are obtained even for low/moderate loadings if temperature is high.

The response surface for glucose yield from screened bagasse pretreated with lime is shown in Fig. 4. Figure 4a shows glucose yield versus lime loading and temperature when pretreatment time is 12 h, and Fig. 4b shows the same response surface when pretreatment time is 36 h. For low pretreatment time, maximum glucose yield was obtained for high temperature and low lime loading. For long pretreatment time, there was high glucose yield in two regions: low temperature and high lime loading or high temperature and low lime loading.

Conclusions

The effectiveness of alkaline hydrogen peroxide and lime pretreatment in improving sugar cane bagasse susceptibility to enzymatic hydrolysis was evaluated. Two complete 2 × 2 × 2

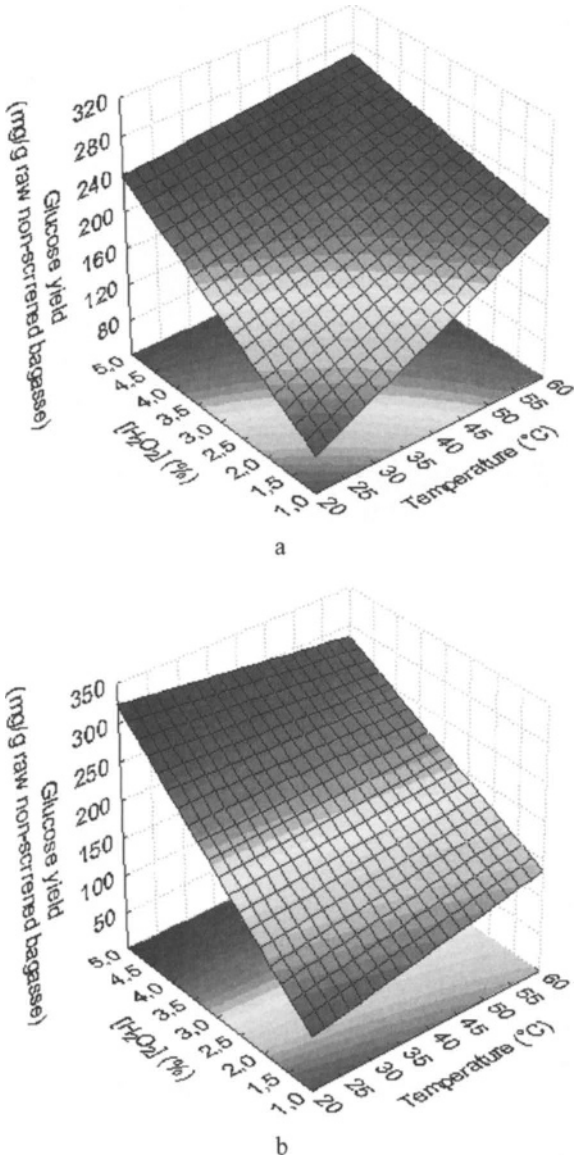


Fig. 2 Glucose yield from non-screened bagasse pretreated with alkaline hydrogen peroxide. **a** Pretreatment time of 6 h. **b** Pretreatment time of 24 h

factorial designs were carried out to determine the influence of pretreatment time, temperature, and H_2O_2 concentration or lime loading on the performance of enzymatic hydrolysis. The performance was evaluated by glucose and TRS yield after hydrolysis of the pretreated bagasse.

The influence of screening the bagasse before pretreatment in hydrolysis performance was assessed. All the tests were performed using bagasse as it comes from a sugar/alcohol factory and bagasse with screened size of 0.248 to 1.397 mm (12–60 mesh).

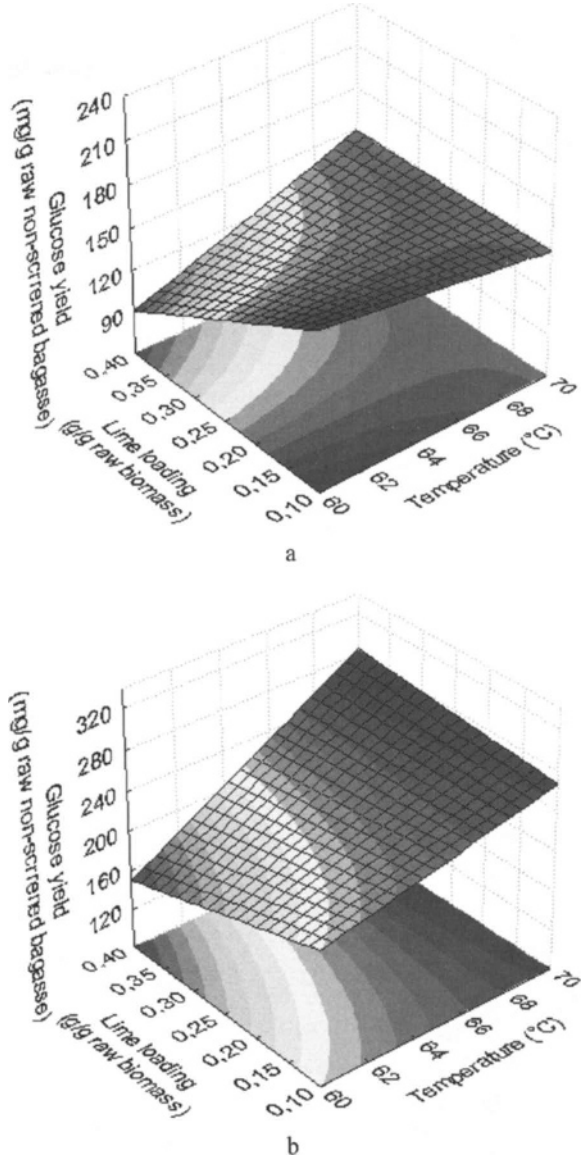


Fig. 3 Glucose yield from non-screened bagasse pretreated with lime. **a** Pretreatment time of 12 h. **b** Pretreatment time of 36 h

The results show that when hexoses and pentoses are of interest, lime should be the pretreatment agent chosen, as high TRS yields are obtained for nonscreened bagasse using 0.40 g lime/g dry biomass at 70 °C for 36 h.

When the product of interest is glucose, the best results were obtained with lime pretreatment of screened bagasse. However, the results for alkaline peroxide and lime pretreatments of nonscreened bagasse are not very different. As screening is an expensive unit operation, the use of nonscreened bagasse is preferred.

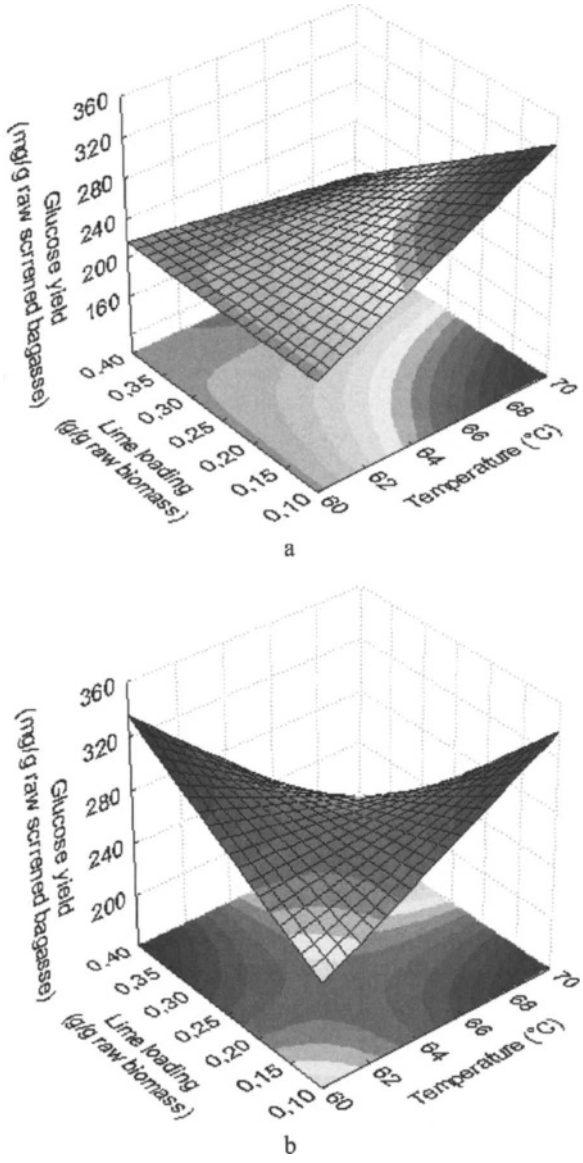


Fig. 4 Glucose yield from screened bagasse pretreated with lime. **a** Pretreatment time of 12 h. **b** Pretreatment time of 36 h

For screened bagasse, lime pretreatment can be performed under three conditions for high glucose yields: 0.10 g lime/g dry biomass at 70 °C for 12 h, 0.10 g lime/g dry biomass at 70 °C for 36 h, or 0.40 g lime/g dry biomass at 60 °C for 36 h.

For nonscreened bagasse, the best results are for alkaline peroxide pretreatment performed with 5% H_2O_2 at ambient temperature for 24 h. Lime pretreatment with 0.40 g lime/g dry biomass at 70 °C for 36 h also leads to high glucose yield. The choice between alkaline peroxide and lime pretreatment in this case is not straightforward, and fermentation of the hydrolysis product to evaluate ethanol yields should help in the

decision. There is no statistically significant difference in the processes; however, the pretreatment with peroxide can be performed at ambient temperatures and it takes less time.

As the maximum TRS and glucose yields were always found at the extremes of the studied intervals, in future work, we will investigate if it is possible to improve glucose and/or TRS yield by redefining the factor levels to cover a bigger area around the optimal conditions determined in this work.

Acknowledgments The authors acknowledge Capes for financial support.

References

1. Fan, L. T., Lee, Y. H., & Gharpuray, M. M. (1982). *Advances in Biochemical Engineering, 23*, 157–187.
2. Gharpuray, M. M., Lee, Y. H., & Fan, L. T. (1983). *Biotechnology and Bioengineering, 26*, 426–433.
3. Lynd, L. R., Elander, R. T., & Wyman, C. E. (1996). *Applied Biochemistry and Biotechnology, 57–58*, 741–761.
4. Laser, M., Schulman, D., Allen, S. G., Lichwa, J., Antal, M. J., Jr., & Lynd, L. R. (2002). *Bioresource Technology, 81*, 33–44.
5. Mosier, N., Wyman, C., Dale, B., Elander, R., Lee, Y. Y., Holtzapple, M., & Ladisch, M. (2005). *Bioresource Technology, 96*, 673–686.
6. Lee, J. (1997). *Journal of Biotechnology, 56*, 1–24.
7. Wyman, C. E., Dale, B. E., Elander, R. T., Holtzapple, M., Ladisch, M. R., & Lee, Y. Y. (2005a). *Bioresource Technology, 96*, 1959–1966.
8. Wyman, C. E., Dale, B. E., Elander, R. T., Holtzapple, M., Ladisch, M. R., & Lee, Y. Y. (2005b). *Bioresource Technology, 96*, 2026–2032.
9. Hinman, N. D., Schell, D. J., Riley, C. J., Bergeron, P. W., & Walter, P. J. (1992). *Applied Biochemistry and Biotechnology, 34/35*, 639–649.
10. Parisi, F. (1982). *Advances in Biochemical Engineering, 38*, 53–87.
11. Kaar, W. E., & Holtzapple, M. T. (2000). *Biomass Bioengineering, 18*, 189–199.
12. Gould, J. M. (1984). *Biotechnology and Bioengineering, 26*, 46–52.
13. Gould, J. M. (1985). *Biotechnology and Bioengineering, 27*, 225–231.
14. Gould, J. M. (1987). Int. Cl. C 13K1/02. US, PI 4,649,113.
15. Azzam, A. M. (1989). *Journal of Environmental Science and Health Part B, 24*(4), 421–433.
16. Amjed, M., Jung, H. G., & Donker, J. D. (1992). *Journal of Animal Science, 70*, 2877–2884.
17. Krishna, S. H., Prasanthi, K., Chowdary, G. V., et al. (1998). *Process Biochemistry, 33*, 825–830.
18. Lesoing, G., Klopfenstein, T., Rush, I., & Ward, J. (1981). *Journal of Animal Science, 51*, 263.
19. Verma, M. L. (1983). In G.R. Pearce (Ed.) (pp. 85–99). Canberra, ACT: Australian Government Publishing Service.
20. Playne, M. J. (1984). *Biotechnology and Bioengineering, 26*, 426–433.
21. Nagwani, M. (1992). M.S. thesis, Texas A&M University.
22. NREL (National Renewable Energy Laboratory—EUA). (1996)
23. Chang, V. S., Burr, B., & Holtzapple, M. T. (1997). *Applied Biochemistry and Biotechnology, 63–65*, 3–19.
24. Chang, V. S., Nagwani, M., & Holtzapple, M. T. (1998). *Applied Biochemistry and Biotechnology, 74*, 135–159.
25. Holtzapple, M. T., & Davison, R. R. (1999). Int. Cl. C 13K1/02. US, PI 5,865,898.
26. Kaar, W. E., & Holtzapple, M. T. (2000). *Biomass Bioengineering, 18*, 189–199.
27. Kim, S., & Holtzapple, M. T. (2005). *Bioresource Technology, 96*, 1994–2006.
28. Ferraz, A., Baeza, J., Rodriguez, J., & Freer, J. (2002). *Bioresource Technology, 74*(3), 201–212.
29. Lin, Y. L., & Dence, C. W. (1992). *Methods in lignin chemistry* (pp. 33–62). Berlin: Springer.
30. Irick, T. J., West, K., Brownell, H. H., Schiwald, W., & Saddler, J. N. (1988). *Applied Biochemistry and Biotechnology, 17*, 137–149.
31. Kaar, W. E., & Brink, D. L. (1991). *Journal of Wood Chemistry and Technology, 11*, 479–494.
32. Kaar, W. E., Gool, L. G., Merriman, M. M., & Brink, D. L. (1991). *Journal of Wood Chemistry and Technology, 11*, 447–463.
33. Laver, M. L., & Wilson, K. P. (1993). *Tappi Journal, 76*(6), 155–159.
34. Szczodrak, J., & Fiedurek, J. (1996). *Biomass & Bioenergy, 10*(5/6), 367–375.

35. Ghose, T. K. (1987). *Pure and Applied Chemistry, 59*(2), 257–268.
36. Adney, B., & Baker, J. (1996). Chemical analysis and testing task—Laboratory analytical procedure. LAP-006.
37. Wood, T. M., & Bhat, K. M. (1988). *Methods in enzymology.* San Diego: Academic, 160, 87–116.
38. Miller, G. L. (1959). *Analytical Chemistry, 31*(3), 426–428.
39. Barros Neto, B., Scarmin, I. S., & Bruns, R. E. (2003). 2nd ed. Campinas, SP: Editora da UNICAMP.

Appl Biochem Biotechnol (2008) 148:59–70
DOI 10.1007/s12010-007-8071-5

Substrate Dependency and Effect of Xylanase Supplementation on Enzymatic Hydrolysis of Ammonia-Treated Biomass

Rajesh Gupta · Tae Hyun Kim · Yoon Y. Lee

Received: 9 May 2007 / Accepted: 27 September 2007 /
Published online: 17 October 2007
© Humana Press Inc. 2007

Abstract Pretreatment based on aqueous ammonia was investigated under two different modes of operation: soaking in aqueous ammonia and ammonia recycle percolation. These processes were applied to three different feedstocks with varied composition: corn stover, high lignin (HL), and low lignin (LL) hybrid poplars. One of the important features of ammonia-based pretreatment is that most of the hemicellulose is retained after treatment, which simplifies the overall bioconversion process and enhances the conversion efficiency. The pretreatment processes were optimized for these feedstocks, taking carbohydrate retention as well as sugar yield in consideration. The data indicate that hybrid poplar is more difficult to treat than corn stover, thus, requires more severe conditions. On the other hand, hybrid poplar has a beneficial property that it retains most of the hemicellulose after pretreatment. To enhance the digestibility of ammonia-treated poplars, xylanase was supplemented during enzymatic hydrolysis. Because of high retention of hemicellulose in treated hybrid poplar, xylanase supplementation significantly improved xylan as well as glucan digestibility. Of the three feedstocks, best results and highest improvement by xylanase addition was observed with LL hybrid poplar, showing 90% of overall sugar yield.

Keywords Hybrid poplar · Corn stover · Xylanase · Aqueous ammonia · Pretreatment

Introduction

Various pretreatment technologies are being used to improve the digestibility of carbohydrates in biomass by making the cellulosic part more accessible by enzymes [1]. Among the major findings of recent pretreatment research is that a given pretreatment

R. Gupta · Y. Y. Lee (✉)
Department of Chemical Engineering, Auburn University, 207 Ross Hall, Auburn, AL 36830, USA
e-mail: yylee@eng.auburn.edu

T. H. Kim
Eastern Regional Research Center NAA, ARS, USDA, 600 East Mermaid Lane, Wyndmoor, PA 19038, USA

reagent exhibits selectivity toward a certain type of reaction attacking specific chemical bonds in lignin–hemicellulose–cellulose matrix. Pretreatment methods operated at low pH including steam explosion [2, 3], hot water treatment [4–6], controlled pH treatment, and dilute acid treatment [7, 8] remove substantial amount of hemicellulose. On the other hand, pretreatment methods applying high pH such as ammonia fiber explosion [9–11], lime pretreatment [12, 13], and ammonia recycle percolation (ARP) [14, 15] show little effect on hemicellulose but high interaction with lignin. In low pH pretreatments, the liquid contains hemicellulose sugars and other degradation byproducts. These byproducts are known to be inhibitory in subsequent bioconversion process. The examples of the inhibitory compounds are phenolics derived from lignin degradation, furan derivatives (hydroxymethylfurfural and furfural) from sugar decomposition, and aliphatic acids [16, 17]. Sugar–lignin condensation reactions in pretreatment liquid further reduces the sugar yield [18–22]. Glucose/xylose co-fermenting microorganisms were found to be very sensitive to these inhibitory chemicals [23, 24]. Various methods have been used to detoxify these toxins [17], but it bears substantial additional cost. From this viewpoint, hemicellulose retention is a positive feature in pretreatment because it eliminates the need of converting sugars in pretreatment liquid [25].

In most of the pretreatment studies, process conditions of pretreatment are optimized in terms of glucan digestibility. One of the factors that limit the digestibility of pretreated biomass is insufficient xylanase activity in the "cellulase" used in the hydrolysis [45]. This is particularly true for substrates with high xylan content. According to Berlin et al., the hydrolysis rate of different organosolv-treated hardwood did not show any correlation with the filter paper activity of different enzyme preparations, yet showed significant correlation with the endogenous xylanase activity [26]. Covalent and non-covalent association of xylan with cellulose and lignin is an essential factor for holding the structural integrity of cell wall [27]. Removal of xylan either by pretreatment or by xylanase would enhance enzymatic hydrolysis of cellulose. Xylanase not only degrade xylan but also assists in delignification as observed in bio-bleaching of pulp [28].

In Fig.1, lignin vs xylan content of various biomass feedstocks is shown. This data has been taken from the DOE website (http://www.eere.energy.gov/biomass/progs/search1.cgi). The data indicate that there is an inverse relationship between the lignin and xylan content of biomass. These feedstocks were divided into three different categories: Regions 1, 2, and 3 represent the feedstocks with high xylan and low lignin, low xylan and high lignin, and moderate xylan and moderate lignin, respectively. In this study, feedstocks representing the three regions were selected: corn stover, high-lignin (HL) hybrid poplar, and LL hybrid

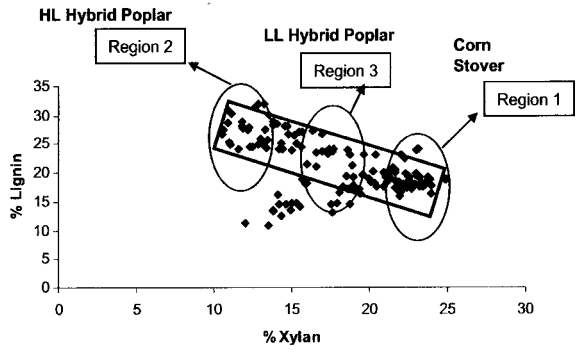


Fig. 1 Relation between lignin and xylan content in different biomass

poplar. Recent work in our laboratory has proven that SAA and ARP are very efficient for delignification of corn stover yet retaining high amount of hemicellulose [29–31].

The objective of this study is to apply pretreatments based on aqueous ammonia on feedstocks of varying physical and structural properties and seek insights on how the pretreatment effects are influenced by definable parameters. The optimum conditions were defined for different feedstocks, and the investigation was focused on the pretreatment region near optimum condition. Special attention was paid to the role of xylan and its removal by external xylanase in the enzymatic hydrolysis of biomass.

Materials and Methods

Substrates and Reagents

Corn stover was supplied by NREL. It was ground and screened, and the fraction collected between 9 and 35mesh was used in all experiments. Two different batches of hybrid poplar chips (1/4 in.) were supplied by NREL. The moisture content of both the hybrid poplar batches was approximately 50%. Avicel PH-101 was purchased from Sigma (cat. no. 11365 and lot no. 1094627). Ammonium hydroxide of 30 wt% was purchased from Fisher-Scientific.

Enzymes

Cellulase enzyme (Spezyme-CP) and xylanase (multifect xylanase) were kind gifts of Genencor International Inc. (Paulo Alto, CA, USA). Two different batches of Spezyme-CP were used in this study: Spezyme CP-A (lot no. 301-00348-257) and Spezyme CP-B (lot no. 301-04075-054). The nominal filter paper activities for Spezyme CP-A and Spezyme CP-B were 31.2 FPU/ml (determined by NREL) and 59 FPU/ml (determined by Genencor), respectively. Spezyme CP-B was used in ARP-treated samples, and Spezyme CP-A was used in SAA-treated samples. The protein content of multifect xylanase was 42 mg of protein/ml. β-Glucosidase was purchased from Sigma (Novozyme 188 from Novo Inc., Sigma no. C-6150 and lot no. 11K1088). The specified activity as determined by the authors was 750 CBU/ml.

Experimental Setup and Operation of ARP

The ARP experimental system employs a packed-bed column reactor through which the pretreatment liquid flows. Details of the reactor setup are described elsewhere [30]. ARP experiments were conducted under the following optimum set of conditions chosen for different feedstocks:

Corn Stover The temperature of 170 °C was used with 20 min of reaction time (10 min with ammonia solution followed by 10 min with deionized, DI, water) and 5ml/min of liquid flow rate. The overall solid to liquid (15% ammonia) ratio was 1:3.33 (*w/w*). The conditions for corn stover were chosen on the basis of our previous study [30].

LL and HL Hybrid Poplar Substrate was first soaked overnight in 15% ammonia solution with solid to liquid ratio of 1:3.67 (*w/w*) before ARP experiment. The temperature of the reactor containing the soaked biomass was raised to 185 °C, and DI water was passed for 27.5 min with 2 ml/min flow rate. The temperature of the reactor during the reaction

remained constant. Unless stated otherwise, all the ARP pretreatment experiments were conducted under these conditions.

It was found that overnight soaking of HL hybrid poplar before ARP treatment does not affect the hydrolysis of treated biomass much. Therefore, in other experiments where effect of different process variable in ARP process was studied (Tables 2, 3, and 4), HL hybrid poplar was soaked for only 10 min before starting the pretreatment. For HL hybrid poplar, the upper limit of temperature was set at 195 °C, above which, severe decomposition of carbohydrates were observed, and the system pressure rose to 450 psig.

Experimental Setup and Operation of SAA

Batch reactors were used for the SAA pretreatment. For low temperature operation up to 80 °C, biomass was soaked with 15% ammonia in screw-capped laboratory glass bottle and kept in an oven. For runs above 80 °C, stainless steel reactors (1.375 in. ID×6 in. l) were used. For corn stover, 60 °C temperature was used with 12 h soaking time and 1:8 solid to liquid ratio. For HL and LL hybrid poplar, the temperature of 150 °C was employed with 24 h soaking time and 1:10 solid to liquid ratio.

Enzymatic Digestibility

Enzymatic digestibility tests were done with 1.0% *w/w* glucan loading. Thus, total amount of solids in the reactor varied according to the glucan content in biomass. The reaction of enzymatic digestibility was carried out in 250 ml Erlenmeyer flask with total liquid volume of 100 ml. This test was carried out according to the NREL Chemical Analysis and Test procedures [32].

Cellulase loading of 15 FPU/g glucan and β-glucosidase loading of 30 CBU/g glucan were used in all of the enzymatic digestibility experiments. Unless noted otherwise, xylanase loading was 31.5 mg protein/g glucan in the hydrolysis experiments with xylanase supplementation. The glucan or xylan digestibility was defined as the percentage of theoretical glucan or xylan released after 72 h of incubation with enzyme.

Analytical Procedures

Composition analysis of the treated/untreated biomass was done according to the NREL Laboratory Analytical Procedures: "Preparation of samples for compositional analysis" and "determination of structural carbohydrates and lignin in biomass" (draft version) [32]. The moisture content in biomass was measured by an infrared moisture balance (Denver Instrument, IR-30). Sugar content in compositional analysis and enzymatic digestibility was determined by HPLC using a Bio-Rad Aminex HPX-87P.

Crystallinity Index

Crystallinity of treated and untreated hybrid poplar feedstock was measured by X-ray diffractometer (Rigaku DMAX). Cu–Kα radiation was generated at 40 kV and 40 mA. Samples were scanned from 2θ=10–40 with 0.01 increment. The following formula has been used for the calculation of crystallinity index of samples [33]:

$$\mathrm{CrI} = (I_{002} - I_{\mathrm{am}}/I_{002}) \times 100,$$

where I_{002} is the peak intensity corresponding to 002 lattice plane of cellulose molecule observed at 2θ equal to 22.5°, and I_{am} (at 2θ=19°) is the peak intensity corresponding to amorphous cellulose.

Results and Discussion

Observation of Feedstocks

The composition of corn stover, LL hybrid poplar, and HL hybrid poplar is shown in Table 1. Moving from corn stover to HL hybrid poplar, lignin content is increasing, and xylan content is decreasing. Among these three feedstocks, LL hybrid poplar is highest in carbohydrates.

The surface of HL hybrid poplar and LL hybrid poplar look very much similar, but the surface of corn stover shows more open structure, which would allow more adsorption capacity for pretreatment reagent into the solid, hence, higher reactivity. Diffusivity of the pretreatment reagent in agriculture residues was found to be much higher than the hardwood [34]. The surface characteristics of biomass are one of the important factors affecting the global reactivity of pretreatment reagent with biomass.

Effect of ARP Pretreatment

Table 1 shows the effect of ARP treatment on the composition and the digestibility of different feedstocks. The optimum conditions described earlier in "Materials and Method" were applied in these tests. The extent of delignification and xylan removal in corn stover is much higher than hybrid poplar. With corn stover, more than 50% xylan is lost to liquid. The glucan digestibility of ARP-treated corn stover reached 90%. Xylan removal in LL and HL hybrid poplar were 22 and 33%, respectively. The glucan digestibilities of ARP-treated LL and HL hybrid poplar were 66 and 49%, respectively.

Effects of ARP Process Variables on Hybrid Poplar

Effects of ARP temperature on pretreatment of HL hybrid poplar are shown in Table 2. Delignification or xylan removal was not significantly affected by the ARP temperature, staying relatively constant over the range of 170–195 °C. However, there was a significant effect on glucan digestibility, increasing from 27 to 52% as the temperature was raised from 170 to 195 °C. This indicates that the accessibility of enzymes to cellulose can be increased

Table 1 Effect of ARP treatment on different feedstocks.

	Composition (%)						Digestibility of treated biomass (%)	
	Glucan		Xylan		Lignin			
	Untreated	Treated	Untreated	Treated	Untreated	Treated	Glucan	Xylan
Corn stover	36.1	35.6	21.4	10.3	17.2	5.1	88.1	77.9
LL hybrid poplar	44.9	44.5	17.9	13.5	21.4	14.6	66.1	66.6
HL hybrid poplar	43.8	40.8	14.9	9.6	29.1	17.6	48.9	51.1

Table 2 Effect of temperature on the HL hybrid poplar in ARP treatment.

Temperature (°C)	Composition of treated biomass (%)			Digestibility (%)	
	Glucan	Xylan	Lignin	Glucan	Xylan
170	42.06	11.56	17.33	27.24	30.24
175	42.15	12.41	17.62	38.47	41.53
180	41.14	10.18	16.31	38.32	44.85
185	40.84	9.88	16.66	47.86	50.00
195	41.09	9.82	15.90	50.67	43.14

Liquid (DI water) flow rate, 2 ml/min; reaction time, 27.5 min

without significant change in composition. It is most likely caused by breakage of certain bonds and reconfiguration of components in lignin–hemicellulose matrix. A possibility exists that the ARP can be operated in such a way that digestibility is enhanced without further loss of carbohydrates. This claim may be limited to highly recalcitrant substrates such as hybrid poplar. Retention of carbohydrate in the solid is a desirable trait in pretreatment technology, and hybrid poplar appears to be a substrate well suited for this purpose within the context of ARP.

The effect of reaction time on the performance of ARP pretreatment with the HL hybrid poplar is shown in Table 3. Lignin removal of hybrid poplar increases with reaction time. Xylan removal, however, was only slightly affected by ARP reaction time. After a certain point, the xylan content remained constant, indicating that there is a portion of xylan that is resilient and difficult to remove. The 72-h glucan and xylan digestibilities correlate more closely with xylan removal than lignin removal.

These results are in line with the findings of Kim et al. [30] that aqueous ammonia is highly effective in delignifying lignocellulosic biomass. Reactivity of ammonia with hemicellulose appears to decline after the removal of certain fraction of hemicellulose from biomass. The reasons for this are found in previous work concerning mechanistic studies. Alkaline degradation of carbohydrate during the Kraft pulping occurs from the reducing end and the reaction of alkali with the carbohydrate chain stops when the reducing end (–OH) is replaced by the alkali stable end (–COONa) [35]. The same mechanism may apply to ammonia treatment. It has also been reported that the reducing ends of xylans consist of a combination of xylose and galacturonic acid with the sequence of β-D-Xylp-1–4–β-D-Xylp-1–3–α-L-Rhap-1–2–α-D-GalpU-1–4–β-D-Xyl. When xylose is removed from the reducing end, galacturonic acid makes the xylan molecule more stable toward alkali degradation. [36, 37]. Vian et al. [38] and Reis et al. [39] have provided evidences for tight

Table 3 Effect of reaction time on the HL hybrid poplar in ARP treatment.

Reaction time (min)	Composition of treated biomass (%)			Digestibility (%)	
	Glucan	Xylan	Lignin	Glucan	Xylan
27.5	41.13	10.68	14.51	42.34	42.23
55.0	40.33	9.88	12.41	50.75	44.77
82.5	40.01	9.83	11.05	52.38	44.43

Liquid (15% ammonia solution) flow rate, 2 ml/min; temperature, 185 °C

association of glucuronoxylans with cellulose microfibril. Mora et al. [40] have proven that there is a strong interaction and retention of heteroxylans with cellulose microfibril even after a strong alkaline treatment such as Kraft pulping. These findings suggest that the hemicellulose bound with the cellulose microfibril is difficult to remove. Among the three feedstocks, xylan loss during the ARP pretreatment is found to be inversely proportional to the cellulose content in the biomass. One plausible explanation for this is that the hemicellulose–cellulose linkage makes the hemicellulose stable, thus, making it less amenable for ammonia-induced degradation. Corn stover, having less cellulose content, possesses fewer cellulose–hemicellulose linkages than poplar. This may explain why corn stover loses more xylan than hybrid poplar during ARP pretreatment.

Sugars in ARP liquid exist only in oligomer form, i.e., xylo-oligosaccharides (XOS). After acid hydrolysis of the ARP liquor, large amount of xylose monomer appears. It proves that hemicellulose sugars in the ARP liquor is either in the form of XOS or lignin carbohydrate complex. Hemicellulose removal in ARP is proportional to the extent of lignin removal. The reason for this is unclear at this time.

Table 4 shows the effect of ammonia flow rate on the composition and digestibility. It is reaffirmed here that the digestibility correlates better with xylan removal than lignin removal, especially for hybrid poplar. This also indicates that delignification alone is not sufficient to attain high digestibility and that xylan removal is also required.

Effect of Process Variable on Crystallinity

As indicated in Fig. 2a and b, crystallinity of HL hybrid poplar increases after the ARP pretreatment. These results are in accordance with the findings of Kim et al. [30] that the total content of crystalline cellulose increases because of the removal of the amorphous part (lignin and hemicellulose) and that contributes to the increase of crystallinity. Cao and Huimin [33] also observed that the crystallinity of the treated pulp increases because of the removal of the amorphous part by enzymatic action. Figure 2a shows that the crystallinity increases with the reaction time, as removal of lignin and hemicellulose also increases. Further increase of ARP temperature from 175 to 195°C caused a slight decrease in crystallinity (Fig. 2b). In this case, the decrease of crystallinity is caused by the structural change in cellulose rather than in composition. With ARP operated below 185 °C, the basic structure of cellulose is not altered regardless of reaction time; only the removal of hemicellulose and lignin occurs.

SAA Pretreatment

Our previous work on the SAA using corn stover provided satisfactory digestibility [29]. Corn stover treated by SAA under moderate process conditions (60 °C, 1:8 S/L ratio, and

Table 4 Effect of reaction time on the HL hybrid poplar in ARP treatment.

Liquid (15% ammonia solution) flow rate (ml/min)	Composition of treated biomass (%)			Digestibility (%)	
	Glucan	Xylan	Lignin	Glucan	Xylan
2.0	41.13	10.68	14.93	42.34	42.23
5.0	40.88	11.00	12.78	44.84	39.79
7.5	40.94	9.76	11.38	48.94	45.49

Reaction time, 27.5min; temperature, 185 °C

12 h) gave approximately 90% glucan digestibility. In the case of hybrid poplar, higher severity conditions (150 °C, 24 h) were required to attain the acceptable level of digestibility. Even at the temperature as high as 150 °C, glucan digestibility of SAA-treated LL hybrid poplar and HL hybrid poplar was only 73 and 60%, respectively, with 15 FPU cellulase loading.

Composition and digestibility of the SAA-treated feedstocks are summarized in Table 5. SAA of corn stover removes 65% of lignin, yet retains 85% of xylan in solid. In case of hybrid poplar, negligible amount of xylan is lost to liquid, and delignification is much less than corn stover. The effectiveness of pretreatment is assessed with the two criteria; first, the retention of carbohydrates in solid and, second, the enzymatic digestibility of pretreated biomass. According to the first criterion, SAA is quite effective, retaining above 90% of xylan in hybrid poplar. The enzymatic digestibility of SAA-treated hybrid poplar, however, is not in acceptable range. With xylanase supplementation, the digestibility rose to 94 and 86% for LL and HL hybrid poplar, respectively (Table 6), meeting the second criterion as well.

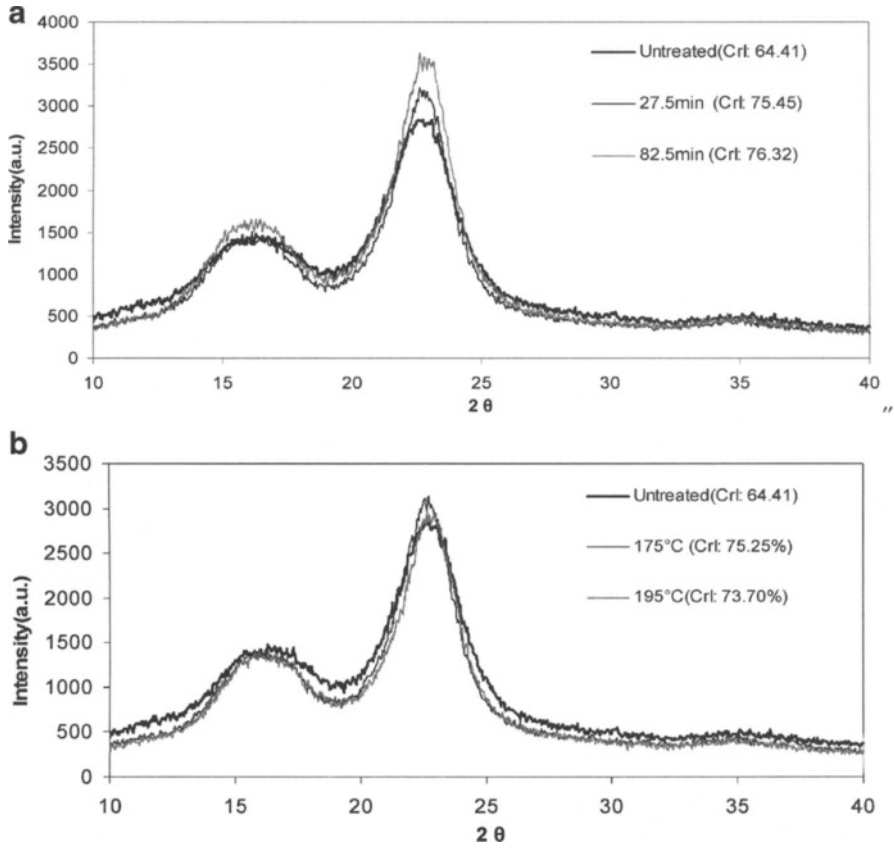


Fig. 2 **a** XRD plots of ARP-treated HL hybrid poplar samples treated with various reaction time; **b** XRD plots of ARP-treated HL hybrid poplar samples treated at different temperature

Table 5 Effect of SAA treatment on different feedstocks.

	Composition (%)						Digestibility of treated biomass (%)	
	Glucan		Xylan		Lignin			
	Untreated	Treated	Untreated	Treated	Untreated	Treated	Glucan	Xylan
Corn stover	36.1	35.3	21.4	18.4	17.2	6.1	91.2	80.6
LL hybrid poplar	44.9	44.9	17.9	16.7	21.4	19.3	72.7	67.2
HL hybrid poplar	43.8	40.5	14.9	13.6	29.1	20.0	60.0	54.7

Effect of Xylanase Supplementation on the ARP- and SAA-Treated Biomass

The effects of xylanase supplementation on glucan/xylan digestibility of ARP- and SAA-treated feedstocks are summarized in Table 6. In all cases, digestibility increased significantly after xylanase supplementation. The increase was highest with LL hybrid poplar and lowest with corn stover. Glucan and xylan digestibility of ARP-treated LL hybrid poplar increased to more than 95% after xylanase supplementation. In Fig. 3, the digestibilities of pure cellulose (Avicel) with and without xylanase addition are shown. The fact that there is no difference between them proves that the xylanase enzyme does not have any cellulase activity. This further proves that xylanase addition increases the accessibility of cellulase enzymes to cellulose chains by removing the hemicellulose barrier.

ARP of corn stover removes 70% of lignin and 50% of hemicellulose. Therefore, a large part of the hindrance for cellulase action has been removed, and high digestibility is attained without xylanase addition. On the other hand, ARP of LL hybrid poplar removes only 32% of lignin and 25% of xylan; consequently, glucan digestibility of only 65% is obtained (Table 1). When supplemented with xylanase, a drastic improvement of the digestibility was seen with LL hybrid poplar reaching 97% (Table 6). It has been reported that cellulase availability to cellulose is reduced because of unproductive binding of cellulase to lignin [41, 42]. Hydrophobic interaction of surfactants with lignin reduces the unproductive binding of cellulase with lignin. It decreases the effect of hydrophobic environment caused by lignin, thus, increasing the access of water and cellulase molecule to

Table 6 Effect of xylanase addition on the digestibility of ARP and SAA treated biomass.

	ARP treatment				SAA treatment			
	Glucan		Xylan		Glucan		Xylan	
	Digestibility (%)	Increase (%)	Digestibility (%)	Increase (%)	Digestibility (%)	Increase (%)	Digestibility (%)	Increase (%)
Corn stover	92.37	4.79	86.27	10.74	–	–	–	–
LL hybrid poplar	97.14	46.91	95.54	43.41	93.80	29.11	88.52	31.80
HL hybrid poplar	69.65	42.49	73.35	43.60	86.46	44.20	76.94	40.61

Enzymes used: cellulase + β-glucosidase + xylanase; percent increase shows the increase in digestibility because of xylanase addition

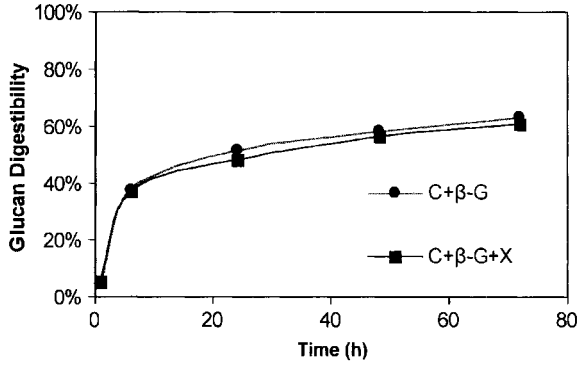


Fig. 3 Effect of xylanase addition on digestibility of Avicel (C + β-G: cellulose + β-glucosidase, C + β-G + X: cellulose + β-glucosidase + xylanase)

cellulose [43]. Despite these evidences, lignin may not be the overriding factor in cellulase action. Increase of digestibility to near quantitative level under the presence of high amount of lignin, as seen here, with LL hybrid poplar indicates that high level of lignin removal is not a necessary condition to achieve high digestibility. In the case of LL poplar, the main barrier to hydrolysis appears to be hemicellulose rather than lignin. This is not to say that lignin is not a major factor controlling digestibility. Lignin needs to be removed but only to a certain extent to achieve accessibility to carbohydrates. Kanda et al. reported that xylan molecule also binds with endo-glucanase-active site, and the Km value of endo-glucanase with xylan is greater than with cellulose by a factor of 1.6, but the *V*max value for xylan is only 18% than for the cellulose substrate [44, 45]. This suggests that the xylan acts as a competitive inhibitor to endo-glucanase.

ARP of HL hybrid poplar removes 40% lignin and 32% of xylan, which is higher than LL hybrid poplar. Yet, the lignin content in the ARP-treated HL hybrid poplar is higher than treated LL hybrid poplar (Table 1). With similar amount of xylanase supplementation, high level of digestibility was not achieved with treated HL hybrid poplar. In the case of HL hybrid poplar, lignin is still a deciding factor for enzyme accessibility to carbohydrate. Glucan digestibility increases in proportion with the amount of xylanase addition for both corn stover and LL hybrid poplar as shown in Fig. 4. For HL hybrid poplar, the effect of xylanase addition is significant only with higher xylanase loading. Unproductive binding with lignin may be the reason because HL hybrid poplar contains higher amount of residual lignin.

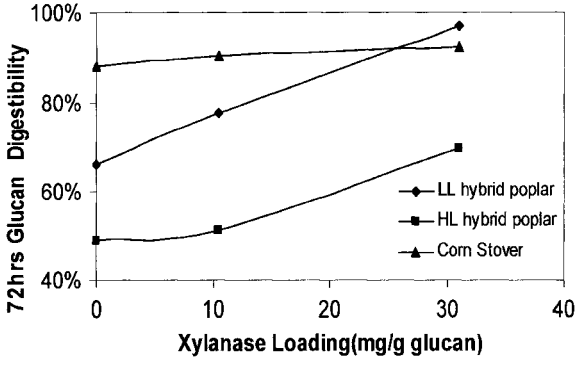


Fig. 4 Glucan digestibility of ARP-treated feedstocks with different xylanase loading

Table 7 Overall sugar yield for different feedstocks with ARP and SAA treatment.

	ARP treatment		SAA treatment	
	Without xylanase %	With xylanase %	Without xylanase %	With xylanase %
Corn stover	67.63	72.64	81.78	-
LL hybrid poplar	61.21	89.43	69.85	90.66
HL hybrid poplar	42.37	60.47	54.04	77.47

As is the case with the ARP, the glucan/xylan digestibilities with xylanase addition are higher for LL hybrid poplar than HL hybrid poplar after the SAA treatment too.

Conclusion

In ARP pretreatment of hybrid poplar, delignification is increased with the treatment severity, but xylan removal occurs only to a certain extent. Increase of temperature from 175 to 195 °C in ARP does not affect xylan/lignin removal in hybrid poplar, yet the glucan digestibility of treated solid is increased. This is caused by an increase of cellulase accessibility to cellulose created by breakage of certain bonds and reconfiguration of the components in hemicellulose–lignin matrix. Crystallinity index of hybrid poplar increases after the ARP treatment. It is primarily caused by the removal of amorphous components, i.e., hemicellulose and lignin.

Xylanase supplementation in enzymatic hydrolysis is effective for the substrates with high xylan content. Xylanase supplementation not only increases the xylan digestibility of treated biomass but also the glucan digestibility. Xylanase reduces the hindrance caused by resilient hemicellulose layer on the cellulose microfibril, thus, improving cellulase accessibility to the cellulosic part.

Addition of external xylanase improves the digestibility of ARP-treated hybrid poplar. The digestibility is higher with LL hybrid poplar than with HL hybrid poplar. Higher amount of residual lignin in HL hybrid poplar is a plausible cause of it. Lignin is the primary barrier in enzymatic hydrolysis of biomass. A certain degree of lignin removal is, therefore, necessary to facilitate enzyme access to carbohydrates in treated biomass.

In SAA treatment, higher amount of hemicellulose is retained than in ARP because of lower severity of SAA. The SAA is more effective for LL hybrid poplar than HL hybrid poplar.

Performance of ARP and SAA treatments are summarized in Table 7. In both ARP and SAA, LL hybrid poplar showed the best results. The overall sugar yield from LL hybrid poplar reached 90% (56 g of fermentable sugar/100 g of feedstock). It was achieved with xylanase supplementation. High retention of carbohydrate in the solid after pretreatment and added xylanase activity in enzymatic hydrolysis are two contributing factors for high overall sugar yield. High reactivity of aqueous ammonia with lignin over carbohydrate is the primary reason for retention of hemicellulose in ARP and SAA.

Acknowledgment The authors acknowledge the financial support for this research from the US Department of Energy (financial assistance no. DE-PS36–00GO10482, channeled through Dartmouth College). They also would like to thank Genencor International (Paulo Alto, CA, USA) for providing enzymes used in this research and NREL for providing the feedstocks.

References

1. Zhang, Y. P., & Lynd, L. R. (2004). *Biotechnology and Bioengineering, 88*(7), 797–824.
2. Fernandez-Bolanos, J., Felizon, B., Heredia, A., & Jimenez, A. (1999). *Bioresource Technology, 68*, 121–132.
3. Schwald, W., Brownell, H. H., & Saddler, J. N. (1988). *Journal of Wood Chemistry and Technology, 8*(4), 543–560.
4. Allen, S. G., Schulman, D., Lichwa, J., Antal Jr., M. J., & Lynd, L. R. (2001). *Industrial & Engineering Chemistry Research, 40*(13), 2934–2941.
5. Garrote, G., Dominguez, H., & Parajó, J. C. (2002). *Journal of Food Engineering, 52*, 211–218.
6. Váquez, M. J., Alonso, J. L., Dominguesz, H., & Parajó, J. C. (2001). *W. J. Microb. Biotechnol, 17*, 817–822.
7. Burns, D. S., Ooshima, H., & Converse, A. O. (1989). *Applied Biochemistry and Biotechnology, 20–21*, 79–94.
8. Jacobsen, S., & Wyman, C. E. (2000). *Applied Biochemistry and Biotechnology, 84–86*, 81–96.
9. Dale, B. E. (1986). US Patent 4,600,590.
10. Dale, B. E., Leong, C. K., Pham, T. K., Esquivel, V. M., Rios, I., & Latimer, V. M. (1996). *Bioresource Technology, 56*(1), 111–116.
11. Foster, B. L., Dale, B. E., & Doran-Peterson, J. B. (2001). *Applied Biochemistry and Biotechnology, 91*(3), 269–282.
12. Chang, V. S., Burr, B., & Holtzapple, M. T. (1997). *Applied Biochemistry and Biotechnology, 63–65*, 3–19.
13. Chang, V. S., & Holtzapple, M. T. (2000). *Applied Biochemistry and Biotechnology, 84*, 5–37.
14. Iyer, P. V., Wu, Z. W., Kim, S. B., & Lee, Y. Y. (1996). *Applied Biochemistry and Biotechnology, 57/58*, 121–132.
15. Kim, S. B., & Lee, Y. Y. (1996). *Applied Biochemistry and Biotechnology, 57/58*, 147–156.
16. Palmqvist, E., & Hahn-Hagerdal, B. (2000). *Bioresource Technology, 74*, 17–24.
17. Palmqvist, E., & Hahn-Hagerdal, B. (2000). *Bioresource Technology, 74*, 25–33.
18. Yang, B., & Charles, E. W. (2004). *Biotechnology and Bioengineering, 86*(1), 88–95.
19. Kim, J. S., Lee, Y. Y., & Torget, R. W. (2001). *Applied Biochemistry and Biotechnology, 91–93*, 331–340.
20. Xiang, Q., Lee, Y. Y., & Torget, R. W. (2004). *Applied Biochemistry and Biotechnology, 13–116*, 1127–1138.
21. Negro, M. J., Manzanares, P., Oliva, J. M., Ballesteros, I., & Ballesteros, M. (2003). *Biomass and Bioenergy, 25–3*, 301–308.
22. Chua, M. G. S., & Wayman, M. (1979). *Canadian Journal Chemistry, 57*, 1141–1149.
23. Du Preez, J. C. (1994). *Enzyme and Microbial Technology, 55*, 1–33.
24. Hahn-Hagerdal, B., Jeppson, H., Skoog, K., & Prior, B. A. (1994). *Enzyme and Microbial Technology, 16*, 933–943.
25. Nathan, M., Wyman, C., Dale, B., Elander, R., Lee, Y. Y., & Holtzapple, M., et al. (2005). *Bioresource Technology, 96–6*, 673–686.
26. Berlin, A., Gikes, N., Kilburn, D., Maximenko, V., Bura, R., & Markov, A., et al. (2006). *Applied Biochemistry and Biotechnology, 129–132*, 528–545.
27. Thomson, J. A. (1993). *FEMS Microbiology Reviews, 104*, 65–92.
28. Saha, B. C. (2003). *Journal of Industrial Microbiology & Biotechnology, 30*, 279–291.
29. Kim, T. H., & Lee, Y. Y. (2005). *Applied Biochemistry and Biotechnology, 121–124*, 1119–1132.
30. Kim, T. H., Kim, J. S., Sunwoo, C., & Lee, Y. Y. (2003). *Bioresource Technology, 90*, 39–47.
31. Kim, S. B., Um, B. H., & Park, S. C. (2001). *Appl. Biochem. Biotechnol, 91-93*, 81–94.
32. NREL (2004) Laboratory analytical procedures (draft version). http://www1.eere.energy.gov/biomass/analytical_procedures.html.
33. Cao, Y., & Huimin, T. (2005). *Enzyme and Microbial Technology, 36*, 314–317.
34. Kim, S. B., & Lee, Y. Y. (2002). *Bioresource Technology, 83*, 165–171.
35. Alen, R. (2000). In Paper making science and technology. Published in cooperation with the Finnish Paper Engineers Association and TAPPI, pp. 58–104.
36. Ericson, T., Peterson, G., & Samuelson, O. (1977). *Wood Science and Technology, 11*, 219–223.
37. Andersson, S. I., & Samuelson, O. (1978). *Svensk Papperstil, 81*, 79–84.
38. Vian, B., Reis, D., Mosiniak, M., & Ronald, J. C. (1986). *Protoplasm, 131*, 185–199.
39. Reis, D., Vian, B., Chanzy, H., & Ronald, J. C. (1991). *Biology of the Cell, 73*, 173–178.
40. Mora, F., Ruel, K., Comtat, J., & Joscleau, J. P. (1986). *Holzforschung, 40*, 85–91.
41. Yang, B., & Wyman, C. E. (2004). US Patent application 200401185542.
42. Lu, Y., Yang, B., Gregg, D., Saddler, J. N., & Mansfield, S. D. (2002). *Applied biochemistry and biotechnology, 98–100*, 641–654.
43. Eriksson, T., Börjesson, J., & Tjerneld, F. (2002). *Enzyme and Microbial Technology, 31*, 353–364.
44. Kanda, T., Wakabayashi, K., & Nisizawa, K. (1976). *Journal of Biochemistry (Tokyo), 79*, 989–995.
45. Wood, T. M., & McCrae, S. I. (1986). *Phytochemistry, 25*, 1053–1055.

Appl Biochem Biotechnol (2008) 148:71–81
DOI 10.1007/s12010-007-8083-1

Alkali (NaOH) Pretreatment of Switchgrass by Radio Frequency-based Dielectric Heating

Zhenhu Hu · Yifen Wang · Zhiyou Wen

Received: 9 May 2007 / Accepted: 16 October 2007 /
Published online: 13 November 2007
© Humana Press Inc. 2007

Abstract Radio-frequency (RF)-based dielectric heating was used in the alkali (NaOH) pretreatment of switchgrass to enhance its enzymatic digestibility. Due to the unique features of RF heating (i.e., volumetric heat transfer, deep heat penetration of the samples, etc.), switchgrass could be treated on a large scale, high solid content, and uniform temperature profile. At 20% solid content, RF-assisted alkali pretreatment (at 0.1 g NaOH/g biomass loading and 90°C) resulted in a higher xylose yield than the conventional heating pretreatment. The enzymatic hydrolysis of RF-treated solids led to a higher glucose yield than the corresponding value obtained from conventional heating treatment. When the solid content exceeded 25%, conventional heating could not handle this high-solid sample due to the loss of fluidity, poor mixing, and heating transfer of the samples. As a result, there was a significantly lower sugar yield, but the sugar yield of the RF-based pretreatment process was still maintained at high levels. Furthermore, the optimal particle size and alkali loading in the RF pretreatment was determined as 0.25–0.50 mm and 0.25 g NaOH/g biomass, respectively. At alkali loading of 0.20–0.25 g NaOH/g biomass, heating temperature of 90°C, and solid content of 20%, the glucose, xylose, and total sugar yield from the combined RF pretreatment and the enzymatic hydrolysis were 25.3, 21.2, and 46.5 g/g biomass, respectively.

Keywords Biomass · Enzymatic hydrolysis · Radio frequency · NaOH pretreatment · Switchgrass

Introduction

The production of fuel ethanol from corn grain is facing challenges such as limited supply and high cost of feedstock [1]. Lignocelluloses represent the most abundant and lowest-cost biomass in the world, and thus, it can be used as alternative raw material for production of fuel ethanol [1].

Z. Hu · Z. Wen (✉)
Department of Biological Systems Engineering, Virginia Polytechnic Institute and State University,
204 Seitz Hall, Virginia Tech, Blacksburg, VA 24061, USA
e-mail: wenz@vt.edu

Y. Wang
Department of Biosystems Engineering, Auburn University, Auburn, AL 36849, USA

In cellulosic ethanol production processes, a pretreatment procedure is needed to disrupt the recalcitrant structure of the lignocellulosic materials so that the cellulose can be more efficiently hydrolyzed by cellulase enzymes [2]. These pretreatments include physical, biological, and chemical ways, such as uncatalyzed steam explosion, liquid hot water, dilute acid, flow-through acid pretreatment, lime, ammonium fiber/freeze explosion, and ammonium recycle percolation [3, 4]. Most of these methods involve a high temperature requirement, which is usually achieved through convection- or conduction-based heating.

Dielectric heating is an alternative method for conventional heating [5, 6]. Compared with conduction/convection heating, which is based on superficial heat transfer, dielectric heating uses the ability of some compounds to transform electromagnetic energy into heat; thus, heating is volumetric and rapid [7]. When lignocellulose is treated by dielectric heating, the more polar (lossy) part will absorb more energy, and thus, a "hot spot" within nonhomogeneous materials will be created. It is hypothesized that this unique heating feature results in an "explosion" effect among the particles and improves the disruption of the recalcitrant structures of lignocellulose. In addition, the electromagnetic field generated in the dielectric field might create nonthermal effects that also accelerate the destruction of the crystal structures [7].

Depending on the wavelength used in the heating devices, dielectric heating can be categorized as microwave or radio frequency [8]. Microwave-based heating has been investigated in the treatment of various lignocellulosic materials [9, 10]. This technology, however, is challenging to scale up. Compared with microwave, radio-frequency (RF) heating can penetrate dielectric materials more deeply because the wavelength of RF is up to 360 times greater than that of microwave [11]. This unique feature is advantageous when treating a large amount of sample, and thus, the process is easier to scale up. When RF heating is combined with chemical (e.g., alkali) treatment, the solid content in the chemical solution can be set at a very high level. Even under nonfluid conditions, the samples can still reach a uniform temperature profile by RF heating. This will greatly reduce the reactor volume required and, thus, the capital cost.

RF as a heating method has been widely applied in the food-processing industries over the past several decades [6, 12, 13]. However, there have been no reports on using RF heating for lignocellulose pretreatment. The objective of this research was to investigate the feasibility of combining RF heating with chemical pretreatment of switchgrass, a potential energy crop for ethanol production as defined by the US Department of Energy [14]. Alkali (NaOH) will be used in this case; however, it should be noted that the technology developed here can be applied to other chemicals.

Materials and Methods

Raw Materials

Switchgrass was obtained from Southern Virginia, USA. The material was air-dried and milled. The particles passing through US standard 10# sieve (with maximum sizes of 2 mm) were used as raw material.

NaOH Pretreatment with Radio-Frequency-Assisted Heating

The RF pretreatment was carried out using a pilot-scale Strayfield 6kW RF heater system (Strayfield, Berkshire, England) with an operating frequency of 27.12 MHz and maximum

power output of 6 kW (Fig. 1). As shown in Fig. 1, treatment was performed inside the chamber which has electrically insulated walls. The radio-frequency energy was generated via a pair of parallel rectangular plate electrodes; the lower plate applicator was mounted at a fixed position, while an upper electrode was adjustable. The desired coupling of RF energy was achieved by adjusting the distance between the two plate electrodes. In this work, the distance between the two plate applicators was 272 mm. When scaling up the RF-based pretreatment process, the area of the plate electrodes can be increased to "cover" more switchgrass materials, or the distance of the two plate electrodes can be adjusted to "accommodate" larger amount of materials [15]. The average power dissipation per unit volume of switchgrass (P, unit: W m^{-3}) can be estimated by simply multiplying the current (I_p) and voltage (V) through the heated materials, both of which can be recorded from the reading of the RF-heater system. The detailed calculation of power consumption and its mechanism was described by Tang et al. [15].

Before treatment, the switchgrass particles were soaked in different concentrations of NaOH solutions at room temperature (ca. 20°C) for 2 h. The presoaked slurry was then transferred to a 5-l plastic container and treated by the RF system. Four fiber-optic sensors (UMI, FISO Technologies, Quebec, Canada) were inserted into different locations of the containers to monitor the sample temperature during the treatment. During the treatment, the temperature was controlled at 90°C with ±3°C fluctuation. Heating was maintained for 60 min.

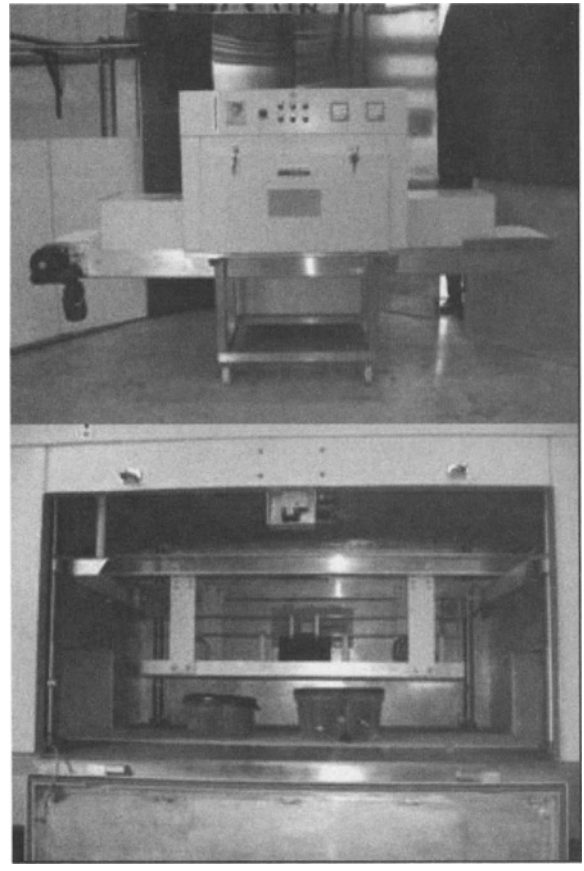


Fig. 1 Diagram of radio-frequency heating system

When the experiment was completed, the container was removed from the RF chamber and cooled at room temperature. The treated slurry was filtered through a Whatman no. 4 filter paper in a Buchner funnel. The filtered cakes were washed by deionized water to neutralize the pH to 7.0 and stored for enzymatic hydrolysis. The liquid fraction after pretreatment contained oligosaccharides, which could not be easily quantified; thus, an extra step was performed to convert those oligosaccharides into monosaccharides before monosaccharide measurement. National Renewable Energy Laboratory (NREL) procedure (LAP 002) was used for this conversion [16].

NaOH Pretreatment with Conventional Heating

NaOH pretreatment of switchgrass with conventional heating was performed to evaluate the efficiency of RF heating. Similar to the RF pretreatment, the switchgrass particles were soaked in either pure water or different concentrations of NaOH solutions at room temperature (ca. 20°C) for 2 h. The presoaked slurry was then transferred to a sealed flask, which was heated at 90°C in a water-bath shaker. Heating was maintained for 60 min. After treatment, the flask was removed from the water bath and cooled at room temperature. The procedures for handling the solid and liquid fractions were the same as those used in RF heating.

Enzymatic Hydrolysis of Pretreated Switchgrass

Two commercials enzymes, Celluclast 1.5-L and Novozyme 188 (Sigma, St Louis, MO, USA), were used for enzymatic hydrolysis. Celluclast 1.5-L contained 98.2 FPU/ml of total cellulase; β-glucosidase activity of Novozyme-188 was 540 unit/ml. One FPU is defined as the enzyme amount that releases 1 μmol of glucose equivalents from Whatman no. 1 filter paper in 1 min. One unit of β-glucosidase activity is defined as the enzyme amount that converts 1 μmol of cellubiose to 2 μmol of glucose in 1 min [17].

Hydrolysis experiments were conducted in 125-ml Erlenmeyer flasks containing a 50-ml mixture of buffer solution (pH 4.8) and pretreated switchgrass. The buffer was 50 mM acetate buffer containing 40 mg/l tetracycline and 30 mg/l cycloheximide antibiotics. The cellulase enzyme loading was 12 FPU/g (dry basis) of substrate; equivalent to 15–20 FPU/g glucan. The β-glucosidase loading was 21 units/g substrate. Flasks were incubated at 50°C in an orbital shaker (160 rpm). During hydrolysis, 1.5 ml samples were taken from the hydrolysis system, chilled on ice, and centrifuged at 10,000×*g* for 10 min. The supernatants were stored for sugar analysis.

Analysis

The sugar compositions of the raw material and the liquid and solid fractions after pretreatment were analyzed according to NREL Laboratory Analytical Procedures 002 and 003 [16, 18]. Filter paper activity and β-glucosidase activity were determined according to standard International Union of Pure and Applied Chemistry procedures [17]. Glucose and xylose were measured using a Shimadzu Prominence High Performance Liquid Chromatography System (Shimadzu Scientific Instruments, Columbia, MD, USA) with a refractive index detector. An Aminex HPX-87H (Bio-Rad, Hercules, CA, USA) column was used with 0.1% (*v*/*v*) H_2SO_4 solution as the mobile phase. The flow rate was controlled at 0.6 ml/min; the column temperature was 65°C.

Results and Discussion

Switchgrass used in this study contained 33.6% glucan, 19.3% xylan, 21.4% lignin, and 3.9% ash. Because glucose and xylose are the major sugars (>90%) in switchgrass [19–22], the yields of the two types of sugars were used to evaluate the overall pretreatment efficiency. Here, the sugar yield was expressed as grams of sugar released per 100 g (dry weight) of original, untreated biomass (switchgrass). Based on the glucan and xylan contents, the maximum yield for glucose and xylose would be $33.6 \times 1.111 = 37.3$ and $19.3 \times 1.136 = 21.9$ g/100 g biomass, respectively.

RF-Assisted NaOH Treatment of Switchgrass at Different Solid Contents

One unique feature of RF is that it has a much greater wavelength and penetrates dielectric materials more deeply compared with other types of dielectric heating such as microwave [11]; thus, RF can treat a large amount of sample at high solid content. Particularly, when the solid content reaches a level where the solid–liquid mixture is not in the fluid state, conventional heating is not able to treat the sample due to poor heating transfer. RF heating can still be used to achieve a homogenous temperature profile for the sample. In the pretreatment of lignocellulosic materials, high solid content means more solid being treated for the same reactor volume, thus reducing the reactor volume required and the capital cost.

In this work, RF-assisted NaOH treatment was performed at solid contents of 16.6, 20, 25, 33.3, and 50%. As shown in Table 1, during the pretreatment, more xylose was produced than glucose. The compositions of glucan, xylan, and lignin in the pretreated solid were similar. Throughout the experiment, the sugar yields were not significantly different among different solid contents.

The pretreated solid materials were hydrolyzed by commercial enzymes, with 20 g/l substrate concentration at pH 4.8 and 50°C. It was found that the sugar content in the hydrolysate increased sharply in the first 12 h and reached stable levels after 72 h (data not shown). Therefore, the sugar released after 72 h of incubation was used for yield calculation. As shown in Fig. 2, the yields of glucose and xylose at both the hydrolysis stage and combined pretreatment/hydrolysis stages were maintained at stable levels due to the fact that the composition of the solid after pretreatment was almost constant (Table 1).

Table 1 Sugar distributions of switchgrass (100 g) after RF pretreatment at different solid contents.

Solid content (%)	Liquid fraction (g)[a]		Solid fraction (g)			
	Glucose	Xylose	Total	Lignin	Glucan	Xylan
Untreated	–	–	100.0±0.0	26.6±0.7	31.9±1.3	19.0±0.7
16.6	1.0±0.04	5.6±0.4	67.6±2.3	10.6±0.5	32.2±0.8	14.2±0.6
20.0	1.2±0.03	5.8±0.5	68.5±2.9	11.2±0.7	31.0±0.9	14.1±0.8
25.0	1.0±0.05	5.0±0.5	70.9±3.2	12.3±0.7	30.4±1.2	14.1±0.9
33.3	1.1±0.04	5.3±0.4	68.2±2.2	10.2±0.9	30.1±0.9	13.3±0.7
50.0	1.2±0.05	5.9±0.6	68.1±3.1	10.4±0.6	29.8±1.4	13.2±1.0

[a] The liquid fraction was treated according to NREL procedure (LAP 002) [18] to convert oligosaccharides into monosaccharides.

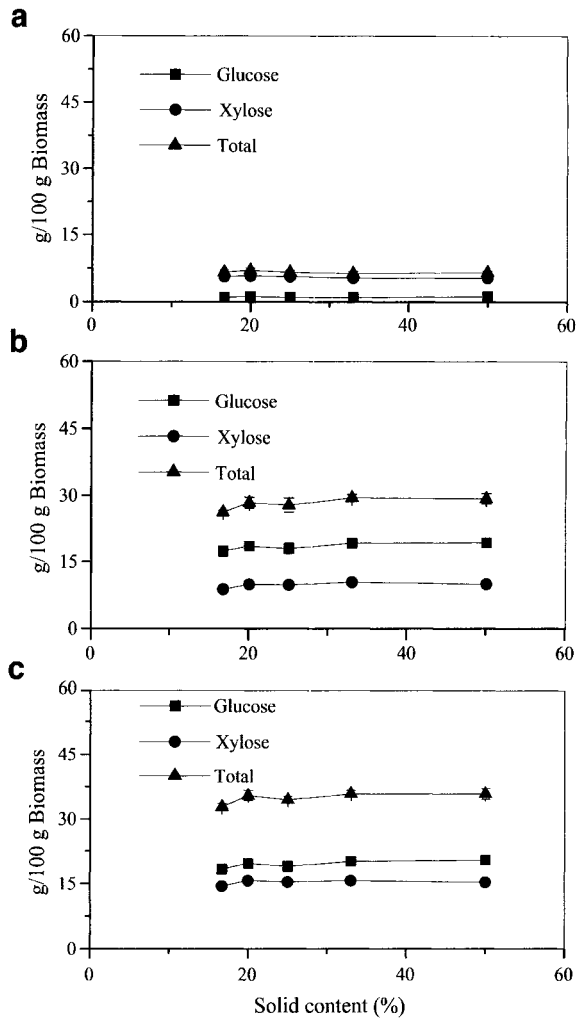


Fig. 2 Effects of switchgrass solid content of RF pretreatment on the yield of glucose (*filled squares*), xylose (*filled circles*), and the total sugars. **a** Pretreatment stage; **b** hydrolysis stage; and **c** combined two stages. Pretreatment was performed at 90°C, 0.1 g NaOH/g biomass, for 60 min

Comparison of RF and Conventional Heating Pretreatment

The RF treatment and conventional heating were compared at 20% of solid content. It should be noted that when solid loading exceeded 20%, the sample was no longer in fluid state. In this situation, the conventional heating cannot treat the samples to a homogeneous temperature profile.

The two pretreatment methods were evaluated based on the yields of the sugars (glucose and xylose) obtained from both the pretreatment and enzymatic hydrolysis. As shown in Table 2, in the pretreatment stage, RF pretreatment led to a higher xylose yield than the conventional heating pretreatment. The glucose yield was very low for both pretreatment methods. In the hydrolysis stages, RF-treated switchgrass released 19.7 g glucose/100 g biomass, ~28% higher than that released from conventionally heated switchgrass. Collectively, a total sugar yield of 36.5 g/100 g biomass was obtained from combined

Table 2 Sugar yields (g/100 g biomass) in the pretreatment and the following enzymatic hydrolysis stages from NaOH pretreatment with RF heating, conventional heating, and without heating.

	RF heating			Conventional heating			Alkali-soaked only (without heating)		
	Pretreatment	Hydrolysis	Combined	Pretreatment	Hydrolysis	Combined	Pretreatment	Hydrolysis	Combined
Xylose	5.3±0.2	10.2±0.1	15.5±0.1	4.1±0.2	8.3±0.1	12.4±0.1	1.4±0.2	6.2±0.2	7.6±0.3
Glucose	1.3±0.2	19.7±0.2	21.0±0.2	0.9±0.05	15.4±0.1	16.3±0.1	0.8±0.04	11.8±0.3	12.6±0.3
Total sugar	6.6±0.3	29.9±0.3	36.5±0.2	4.9±0.2	23.7±0.1	28.6±0.1	2.2±0.1	18.1±0.4	20.3±0.5

RF pretreatment and hydrolysis, while the corresponding yield from the conventional heating pretreatment and hydrolysis was 28.6 g/100 g biomass. It should be noted that alkali soaking itself has a significant effect on pretreatment performance, even without any heating. To account for the "alkali" effect on the pretreatment, additional experiment was conducted by soaking switchgrass with NaOH solution only (at room temperature, without any heating), and monitoring the sugar yield from this alkali-presoaked switchgrass. As shown in Table 2, the alkali treated switchgrass produced a 7.6 g xylose/100 g biomass, 12.6 g glucose/100 g biomass, and 20.3 g total sugars/100 g biomass. These sugar yields were lower than those obtained from the two heating-based pretreatments (Table 2), suggesting that the heating has a significant effect in comparison to no heating with NaOH pretreatment only. Overall, Table 2 shows that RF heating enhanced the solubilization of hemicellulose (xylan) in the pretreatment stage and enzymatic digestibility of cellulose (glucan) in the enzymatic hydrolysis stage. Such a trend (high hemicellulose removal followed by a high cellulose digestibility) has also been reported in pretreatment and hydrolysis of corn stover [23].

Effects of Particle Size on the Sugar Yield of RF-Pretreated Switchgrass

Particle size is an important substrate characteristic associated with available surface area. The reduction of particle size can increase the effective surface area to volume ratio and improve enzyme accessibility to active substrate sites [2, 24]. However, the milling of biomass is rather energy intensive, increases the pretreatment cost, and makes the process uneconomic. To investigate the effects of particle sizes of switchgrass on RF pretreatment efficiency, the milled switchgrass was further passed through US 10#, 18#, 35#, and 60# sieves and fractionated into four levels (2.0–1.0, 1.0–0.5, 0.5–0.25, and <0.25 mm). The alkali loading used was 0.1 g NaOH/g biomass. The lignin removal was similar with different particle sizes (Fig. 3a). During the pretreatment stage, the particle size reduction from 2.00 mm to <0.50 mm did not result in significant increase of xylose yield (Fig. 3b). At the particle size <0.25 mm, however, it was found that summation of xylose/glucose obtained in the liquid phase and the potential xylose/glucose released form the pretreated solid, i.e., 44.5 g/100 g biomass, was less than the maximum potential xylose/glucose contained in the original switchgrass (e.g., 52.9 g/100 g biomass; Table 3), suggesting that some sugars might degrade. In the hydrolysis stage, the glucose yield remained at a constant level, while xylose yield decreased at <0.25 mm of particles (Fig. 3c). This is probably due to the lower amount of xylan contained in the solid after RF pretreatment. Figure 3d shows that glucose, xylose, and total sugar yields from the combined the pretreatment and hydrolysis stages reached the highest level at 0.25–0.50 mm of particle size.

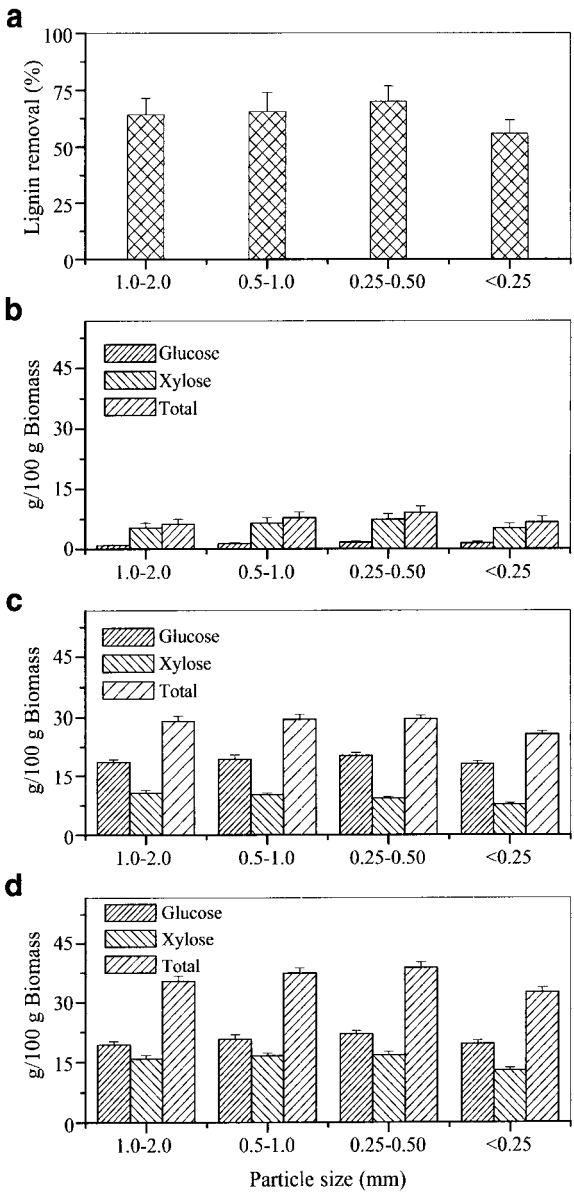


Fig. 3 Effects of switchgrass particle size of RF pretreatment on lignin removal of original switchgrass (**a**); and the yield of glucose, xylose, and the total sugars in the pretreatment stage (**b**), hydrolysis stage (**c**), and combined two stages (**d**). Pretreatment was performed at 90°C, 20% solid content for 60 min

Effects of NaOH loading on RF-Pretreated Switchgrass

The effects of NaOH loading on the pretreatment of switchgrass were investigated by varying the NaOH loading from 0 to 0.30 g NaOH per gram of raw material. Raw material was partly solubilized during the pretreatment, and solubilization increased with NaOH loading. The lignin removal increased with alkali loading from 0 to 0.2 g NaOH/g biomass, while leveled off in the range of 0.2 to 0.3 g NaOH/g biomass (Fig. 4a). As shown in Fig. 4b, in the pretreatment stage, xylose yield increased when NaOH loading increased

Table 3 Comparison of potential sugars recovered in the liquid and solid phases after the pretreatment and the original switchgrass[a].

	Glucose	Xylose	Total sugars
Liquid phase (g/100 g biomass)	1.5±0.3	5.2±1.2	6.7±1.4
Solid (g/100 g biomass)	26.9±1.3	10.9±0.9	37.8±2.0
Summation of liquid and solid phases (g/100 g biomass)	28.4±1.4	16.1±0.8	44.5±1.8
Original switchgrass(g/100 g biomass)	33.6±1.4	19.3±1.2	52.9±2.1

[a] Particle size was <0.25 mm.

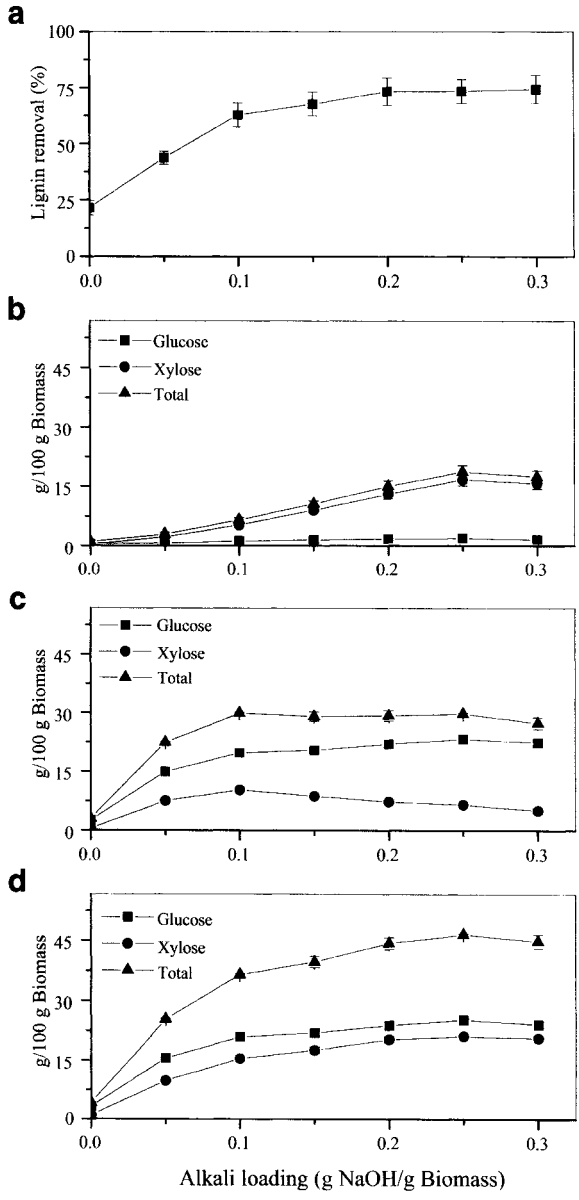


Fig. 4 Effects of NaOH loading of RF pretreatment on lignin removal of original switchgrass (**a**); and the yield of glucose, xylose, and the total sugars in the pretreatment state (**b**), hydrolysis stage (**c**), and combined two stages (**d**). Pretreatment was performed at 90°C, 20% solid content for 60 min

from 0 to 0.25 g/g biomass, with the highest xylose yield being 15.7 g/100 g biomass. The lignin removal reached the highest level (~75%) at NaOH loading of 0.20 g/g biomass (data not shown). In the subsequent hydrolysis stage, both glucose and xylose yields increased when NaOH loading increased from 0 to 0.1 g NaOH/g biomass. When alkali loading exceeded 0.1 g NaOH/g biomass, the glucose yield leveled off while xylose yield decreased (Fig. 4c). Combining the pretreatment and hydrolysis stages, it was found that both glucose and xylose yields reached the highest levels at 0.25 g NaOH/g biomass (Fig. 4d). The highest glucose and xylose yields were 25.3 and 21.2 g/100 g biomass, respectively. The total sugar yield was 46.5 g/100 g biomass, corresponding to ~80% of total maximum theoretical sugar yield contained in switchgrass. However, it should be noted that there is still room to further increase the pretreatment efficiency (i.e., sugar yield) if the RF heating could reach a temperature above 100°C.

Conclusion

In summary, the above results show the potential of using radio-frequency-based dielectric heating as an efficient method in the pretreatment of switchgrass to increase its enzymatic digestibility. When combined with chemical treatment, RF heating can treat samples at very high levels of solid contents (20–50%), at which the conventional heating was difficult to employ due to the loss of fluidity and poor mixing of the materials. Compared with conventional heating pretreatment, RF heating of switchgrass increased the sugar yield in both pretreatment and enzymatic hydrolysis stages. Our current work is under way to develop an enclosed reactor for RF heating which can reach a higher temperature so that the sugar yield could be further improved. The effects of heating time and temperature on the RF-based pretreatment need to be investigated in the future study. An appropriate combination of these two parameters, such as a lower temperature with longer time, might be an effective way to improve the pretreatment performance. Future work is needed to develop a large-scale RF-based pretreatment process. Indeed, RF-based heating has been used in a wide range of industrial applications including welding thin sheets of plastic materials to form fabricated articles, curing glue in plywood, heating rubber, and drying various products such as textile, paper, glass fiber, and foodstuffs [15]; however, there have been no reports on applying RF for biomass pretreatment. Other types of chemicals (e.g., acids or solvents) may also need to be tested with the combination of RF heating due to the relative difficulty of NaOH recovery.

Acknowledgment This work is supported by USDA CSREES (2006-38909-03484).

References

1. Dalgaard, T., Jorgensen, U., Olesen, J. E., Jensen, E. S., & Kristensen, E. S. (1998). Looking at biofuels and bioenergy. *Science, 312*, 1743–1743.
2. Chundawat, S. P. S., Venkatesh, B., & Dale, B. E. (2007). Effect of particle size based separation of milled corn stover on AFEX pretreatment and enzymatic digestibility. *Biotechnology and Bioengineering, 96*, 219–231.
3. Wyman, C. E., Dale, B. E., Elander, R. T., Holtzapple, M., Ladisch, M. R., & Lee, Y. Y. (2005). Coordinated development of leading biomass pretreatment technologies. *Bioresource Technology, 96*, 1959–1966.

4. Wyman, C. E., Dale, B. E., Elander, R. T., Holtzapple, M., Ladisch, M. R., & Lee, Y. Y. (2005). Comparative sugar recovery data from laboratory scale application of leading pretreatment technologies to corn stover. *Bioresource Technology, 96*, 2026–2032.
5. Zhao, Y. Y., Flugstad, B., Kolbe, E., Park, J. W., & Wells, J. H. (2000). Using capacitive (radio frequency) dielectric heating in food processing and preservation - A review. *Journal of Food Process Engineering, 23*, 25–55.
6. Piyasena, P., Dussault, C., Koutchma, T., Ramaswamy, H. S., & Awuah, G. B. (2003). Radio frequency heating of foods: Principles, applications and related properties - A review. *Critical Reviews in Food Science, 43*, 587–606.
7. de la Hoz, A., Diaz-Ortiz, A., & Moreno, A. (2005). Microwaves in organic synthesis: Thermal and non-thermal microwave effects. *Chemical Society Reviews, 34*, 164–178.
8. Oberndorfer, C., Pawelzik, E., & Lucke, W. (2000). Prospects for the application of dielectric heating processes in the pre-treatment of oilseeds. *European Journal Lipid Science Technology, 102*, 487–493.
9. Azuma, J., Asai, T., Isaka, M., & Koshijima, T. (1985). Enhancement of enzymatic susceptibility of lignocellulosic wastes by microwave irradiation. *Journal Fermentation Technology, 63*, 529–536.
10. Zhu, S. D., Wu, Y. X., Yu, Z. N., Chen, Q. M., Wu, G. Y., Yu, F. Q., et al. (2006). Microwave-assisted alkali pre-treatment of wheat straw and its enzymatic hydrolysis. *Biosystem Engineering, 94*, 437–442.
11. Marra, F., Lyng, J., Romano, V., & McKenna, B. (2007). Radio-frequency heating of foodstuff: Solution and validation of a mathematical model. *Journal of Food Engineering, 79*, 998–1006.
12. McKenna, B. M., Lyng, J., Brunton, N., & Shirsat, N. (2006). Advances in radio frequency and ohmic heating of meats. *Journal of Food Engineering, 77*, 215–229.
13. Marshall, M. G., & Metaxas, A. C. (1999). Radio frequency assisted heat pump drying of crushed brick. *Applied Thermal Engineering, 19*, 375–388.
14. Kaylen, M. S. (2005). An economic analysis of using alternative fuels in a mass burn boiler. *Bioresource Technology, 96*, 1943–1949.
15. Tang, J., Wang, Y., & Chan, T. V. (2004). Radio frequency heating in food processing. In: Gustavo Barbosa-Cánovas (Ed.), Novel food processing technologies, chapter 24. (pp. 501–524). Boca Raton, FL: CRC Press.
16. Ruiz, R., & Ehrman, T. (1996). Determination of carbohydrates in biomass by high performance liquid chromatography. In: Laboratory Analytic Procedure LAP-002. National Renewable Energy Laboratory (NREL), Golden, CO.
17. Ghose, T. K. (1987). Measurement of cellulase activities. *Pure and Applied Chemistry, 59*, 257–268.
18. Ruiz, R., & Ehrman, T. (1996). Determination of acid-insoluble lignin in biomass. In: Laboratory Analytic Procedure LAP-003. National Renewable Energy Laboratory (NREL), Golden, CO.
19. Adler, P. R., Sanderson, M. A., Boateng, A. A., Weimer, P. I., & Jung, H. J. G. (2006). Biomass yield and biofuel quality of switchgrass harvested in fall or spring. *Agronomy Journal, 98*, 1518–1525.
20. Dien, B. S., Jung, H. J. G., Vogel, K. P., Casler, M. D., Lamb, J. F. S., Iten, L., et al. (2006). Chemical composition and response to dilute-acid pretreatment and enzymatic saccharification of alfalfa, reed canarygrass, and switchgrass. *Biomass Bioenergy, 30*, 880–891.
21. Fike, J. H., Parrish, D. J., Wolf, D. D., Balasko, J. A., Green, J. T., Rasnake, M., et al. (2006). Long-term yield potential of switchgrass-for-biofuel systems. *Biomass Bioenergy, 30*, 198–206.
22. Fike, J. H., Parrish, D. J., Wolf, D. D., Balasko, J. A., Green, J. T., Rasnake, M., et al. (2006). Switchgrass production for the upper southeastern USA: Influence of cultivar and cutting frequency on biomass yields. *Biomass Bioenergy, 30*, 207–213.
23. Yang, B., & Wyman, C. E. (2004). Effect of xylan and lignin removal by batch and flowthrough pretreatment on the enzymatic digestibility of corn stover cellulose. *Biotechnology and Bioengineering, 86*, 88–95.
24. Mansfield, S. D., Mooney, C., & Saddler, J. N. (1999). Substrate and enzyme characteristics that limit cellulose hydrolysis. *Biotechnology Progress, 15*, 804–816.

Appl Biochem Biotechnol (2008) 148:83–95
DOI 10.1007/s12010-007-8048-4

Biological Hydrogen Production Using Chloroform-treated Methanogenic Granules

Bo Hu · Shulin Chen

Received: 28 May 2007 / Accepted: 4 September 2007 /
Published online: 26 September 2007
© Humana Press Inc. 2007

Abstract In fermentative hydrogen production, the low-hydrogen-producing bacteria retention rate limits the suspended growth reactor productivity because of the long hydraulic retention time (HRT) required to maintain adequate bacteria population. Traditional bacteria immobilization methods such as calcium alginate entrapment have many application limitations in hydrogen fermentation, including limited duration time, bacteria leakage, cost, and so on. The use of chloroform-treated anaerobic granular sludge as immobilized hydrogen-producing bacteria in an immobilized hydrogen culture may be able to overcome the limitations of traditional immobilization methods. This paper reports the findings on the performance of fed-batch cultures and continuous cultures inoculated with chloroform-treated granules. The chloroform-treated granules were able to be reused over four fed-batch cultures, with pH adjustment. The upflow reactor packed with chloroform-treated granules was studied, and the HRT of the upflow reactor was found to be as low as 4 h without any decrease in hydrogen production yield. Initial pH and glucose concentration of the culture medium significantly influenced the performance of the reactor. The optimum initial pH of the culture medium was neutral, and the optimum glucose concentration of the culture medium was below 20 g chemical oxygen demand/L at HRT 4 h. This study also investigated the possibility of integrating immobilized hydrogen fermentation using chloroform-treated granules with immobilized methane production using untreated granular sludge. The results showed that the integrated batch cultures produced 1.01 mol hydrogen and 2 mol methane per mol glucose. Treating the methanogenic granules with chloroform and then using the treated granules as immobilized hydrogen-producing sludge demonstrated advantages over other immobilization methods

B. Hu · S. Chen
Center for Multiphase Environmental Research, Washington State University, Pullman, WA 99164-6120, USA

B. Hu · S. Chen (✉)
Department of Biological Systems Engineering, Washington State University, L.J. Smith 213, Pullman, WA 99164, USA
e-mail: chens@wsu.edu

Present address:
B. Hu
Chemical Engineering Department, University of Puerto Rico at Mayaguez, Mayaguez, PR 00681-9046, USA

because the treated granules provide hydrogen-producing bacteria with a protective niche, a long duration of an active culture, and excellent settling velocity. This integrated two-stage design for immobilized hydrogen fermentation and methane production offers a promising approach for modifying current anaerobic wastewater treatment processes to harvest hydrogen from the existing systems.

Keywords Biological hydrogen production · Chloroform treatment · Granular · Immobilization · Integration with methane production

Introduction

Hydrogen gas is a clean energy; when it burns, it only produces water as the byproduct. Hydrogen also has the highest energy content per unit weight among any of the commonly known fuels. Although there are several ways to produce hydrogen—including electrolysis of water, thermo-catalytic reformation of organic compounds, and biological processes [1]—biological hydrogen production has attracted greater attention in recent years because of its capabilities as well as the growing environmental concerns regarding fossil fuel dependence. This process is particularly environmentally friendly because negative-valued waste materials such as cheese whey can be used as the raw material [2].

Biological hydrogen production using suspended-cell systems is normally inefficient and/or difficult to control in continuous operation. The low hydraulic retention rate of hydrogen-producing bacteria in a freely suspended-cell system limits the productivity of a reactor because of the long hydraulic retention time (HRT) required to maintain adequate bacteria population. Recycling biomass back to the reactor is one option for maintaining sufficient cell density, which is needed for high hydrogen production [3]. Recent studies show that immobilization of hydrogen-producing bacteria can also effectively enhance the bacteria population and increase hydrogen productivity [4, 5]. There are various challenges, however, for the polymer matrices to entrap and immobilize hydrogen-producing bacteria during the continuous operation. First, for the immobilized gel beads, as long as hydrogen gas is produced, the density of the gel beads decreases, which causes undesirable washout of the immobilized bacteria. Second, in most cases, the gel structure collapses after several batches because of damage resulting from several possible causes, including gel swelling, pH changes (many polymer matrices are pH sensitive), calcium loss, and so on. Third, bacteria leakage always decreases the biological stability of the immobilized gel beads. And finally, there are economic concerns, as entrapment of the bacteria into polymer matrices adds expense to the overall process [2, 5].

Anaerobic sludge granulation is a widely used self-immobilization method in anaerobic digestion. In an upflow anaerobic sludge bed (UASB) reactor, sludge agglutinates into granules, which results in an increase in biomass concentration and a reduction in sludge washout. The granules allow the organic loading rate of the UASB reactor to far exceed the typical loading rates applied in conventional activated sludge processes. Granules also have many advantages over other systems, which contribute to the success of the UASB design. First, the granules have faster settling velocity, which explains the reduction in sludge washout. Second, the granules provide a protective structure for microorganisms in a harsh environment, which ensures stable operation even if environmental shock occurs [6]. Third, in an anaerobic digestion system, granules are formed naturally and also have a porous structure, which is ideal for mass transfer of the nutrients required by the microorganisms and for the biogas being produced. And finally, it has been found that hydrogen-producing

biomass can develop into granules with high bioactivity [7]. Hydrogen-producing sludge has been shown to agglutinate into granules after 60 days of operation in continuous-flow tank reactors. Furthermore, granular sludge has been reported to be visible in the UASB systems after 120 days of reactor operation [8]. Rapid and efficient granular sludge formation has also been found in carrier-induced granular sludge bed (CIGSB) bioreactors with the addition of support carriers, especially activated carbon [9]. Overall, without the carrier inducement, direct granulation of hydrogen-producing bacteria is a time-consuming process, and there are many unknown factors that need to be investigated during the process.

One possible source for hydrogen producing granules is a conventional UASB reactor treating wastewaters. There are thousands of UASBs running worldwide, and once every 2 to 3 months, part of the methanogenic granules inside each of these reactors must be disposed of to maintain the reactor's efficiency. In previous research, chloroform treatment of granules was found to effectively eliminate methane production and to convert the culture into hydrogen production [6]. In this study, the use of chloroform-treated anaerobic granular sludge as immobilized hydrogen-producing bacteria in a hydrogen culture was investigated. In addition, the possibility of combining the immobilized hydrogen production with current anaerobic digestion was also examined.

Materials and Methods

Methanogenic Granules

The methanogenic granules were taken from a UASB that was treating starch wastewater. The average settling velocity of the granule was 29.5 m/h measure from 100 samples.

Glucose Culture Medium

The medium used for hydrogen (H_2) fermentation contained 20 g glucose chemical oxygen demand (COD)/L (i.e., 18.75 g glucose/L) as the carbon source and sufficient amounts of inorganic supplements [10] including: NH_4HCO_3 (5.24 g/L), $NaHCO_3$ (6.72 g/L), K_2HPO_4 (0.125 g/L), $MgCl_2$ $6H_2O$ (0.1 g/L), $MnSO_4$ $6H_2O$ (0.015 g/L), $FeSO_4$ $7H_2O$ (0.025 g/L), CuSO4 $5H_2O$ (0.005 g/L), and $CoCl_2$ $5H_2O$ (1.25×10^{-4} g/L).

Chloroform Pretreatment

To study the treatment level of the chloroform inhibition, 20 mL of culture medium was placed in a serum bottle. Chloroform was added to the culture medium for the pretreatment. Six levels of chloroform pretreatment were conducted, at 5, 2.5, 1, 0.5, 0.25, and 0.1%. Three milliliters (or another amount, if mentioned specifically) of sewage sludge granules were inoculated into the serum bottle for cultivation. The chloroform treatment level was chosen at 0.25% based on our previous studies [6]. In this case, the granules were cultured with 20 mL culture medium and 0.25% chloroform for more than 24 h. Then, the granules were filtered and washed to be used for inoculation.

Batch Culture

Twenty milliliters of culture medium was placed in a serum bottle. Three milliliters of pretreated granules from the pretreatment process was added to the serum bottle. Nitrogen

gas was then pumped into the serum bottle for 2 min before the fermentation to eliminate the oxygen inside the bottle. The culture temperature was maintained at 35 °C in an incubator (IC 600, Yamato), and the shaking speed was 100–150 rpm.

Fed-batch Culture

After the batch culture using chloroform-treated granules, 5 mL of fermentation broth was withdrawn for analysis. In addition, 5 mL of 80 g COD/L fresh culture medium with the same concentration of nutrients as the culture medium described above was added to the fermentation broth to start another batch. For the fed-batch culture without pH control, the pH was not adjusted at the beginning of each culture. For the fed-batch culture with pH adjustment, the pH was adjusted to about 7, after 5 mL of fresh culture medium was added into the serum bottles, and then a new batch was started.

Continuous Culture

An upflow reactor was set up with a volume of 450 mL and height of 18 cm. Fifty milliliters of methanogenic granules were treated with 0.1% chloroform following the method described previously. The chloroform-treated granules were packed in the upflow reactor as an expanded bed. Twenty grams of COD/L glucose culture medium was fed into the reactor from the bottom with the pump. Biogas and fermentation broth flowed out the top of the reactor then were separated in the separation bottles. Water replacement bottles were connected to the separation bottles to collect the biogas and measure the biogas volume. The reactor was maintained at a batch mode for 3 days, then at a continuous operation mode first with a HRT of 13 h. The HRT was then adjusted quickly to 5.3 h and kept in operation for 3 days until it ran constantly (here, "constantly" means that the pH of the effluent, the biogas and hydrogen production, the glucose conversion, and the volatile fatty acid [VFA] production were constant for more than 12 h). The HRT was gradually adjusted to 4 h and then held constant. The initial pH and the glucose concentration of the culture medium were then adjusted to measure their influence on the upflow reactor performance.

Scanning Electron Microscopy

The surface morphology of the granules was examined using a scanning electron microscope (Hitachi S-570). The freeze-dried granules were mounted on metal stubs, and the membranes were coated with gold for 6 min. The surfaces were then observed and photographed.

Transmission Electron Microscopy

The inside structure of the granules was examined using a transmission electron microscope (JEOL 1200 EX, equipped with digital camera and X-ray microanalysis system). The granules were fixed with 2.5% glutaraldehyde/2% paraformaldehyde in a Cacodylate buffer. They were then rinsed three times using a Cacodylate buffer, dehydrated with gradient ethanol and acetone, infiltrated and left overnight with acetone and SPURRs (1:1), infiltrated again with 100% SPURRs overnight, and embedded in the SPURRs and polymerized in the oven overnight. The resin was sectioned with Reichert-Jung ultra-microtomes at 70 nm thickness. Grids were stained with uranyl acetate for 10 min, rinsed

with water, then stained with lead citrate for 15 min and rinsed. Finally, the grids were observed and photographed.

Analysis

Total biogas production was measured at the end of the batch fermentation (Owen's method) [11]. The biogas was released into a U-tube with water. The biogas volume produced during the fermentation was measured through the water pressure out of the U-tube. The composition of biogas (H_2, CO_2, CH_4, and H_2S) in the headspace of the reactor was measured using a gas chromatograph (GC, CP-3800, Varian, Walnut Creek, CA) equipped with detectors, including a thermal conductivity detector for H_2 and CO_2, a flame ionization detector for CH_4, a Valco Instrument Pulsed Discharge Detector run in Helium Ionization Mode D2 for H_2S, an 18′×1/8″ HayeSep Q 80/100 Mesh Silcosteel column for CO_2, H_2, and CH_4 with nitrogen as the carrier gas, and a 50 m×0.53 mm×4 μm SilicaPLOT column for H_2S with helium as the carrier gas. VFAs were analyzed using a Dionex DX-500 system (Sunnyvale, CA) containing an AS11-HC (4 mm 10–32) column, a quaternary gradient pump (GP40), a CD20 conductivity detector, and an AS3500 auto-sampler [6].

Results and Discussions

Methanogenic Granules

The methanogenic granules were dark in color (probably because of the presence of sulfide produced by the sulfate-reducing bacteria in the digester) and were about 1 to 2 mm in size (Fig. 1a). The scanning electron microscopy (SEM) picture of the granules (Fig. 1b) shows the microorganisms packed together with extracellular polymers and with a porous structure, which facilitates the mass transfer, especially for the biogas to exit. There are several theories that explain the granulation process; however, the mechanism of the granules formation is not fully understood. Most researchers have concluded that filamentous *Methanosaeta concilii* is a key organism in granulation [12]. Filamentous species are clearly shown in the SEM picture (Fig. 1b), and the transmission electron microscopy (TEM) picture of the granules (Fig. 1c) also clearly shows the high activity of the *Methanosaeta* species. There is considerable consensus that the initial stage of granulation involves bacterial adhesion (a physical–chemical process), parallel to the early stages of biofilm formation. *Methanosaeta* aggregates to form nucleation centers, which in turn initiate granular development; then, acetogens adhere to the nuclei and form the second layer; finally, fermentative bacteria adhere to form the exterior layer of the granule in contact with the substrate. Methanogens can also be found in the exterior layer, which consume the free hydrogen produced by fermentative bacteria [13]. The SEM picture (Fig. 1b) confirmed that filamentous methanogens were distributed on the surface of the granules.

Chloroform Pretreatment

Chloroform pretreatment has been found to be an effective method for eliminating methanogenic activity and for switching a methane-producing system to a hydrogen-producing system [6]. It selectively inhibits methanogenic activity while allowing normal hydrogen production, so long as chloroform concentrations are low (Fig. 2). Chloroform,

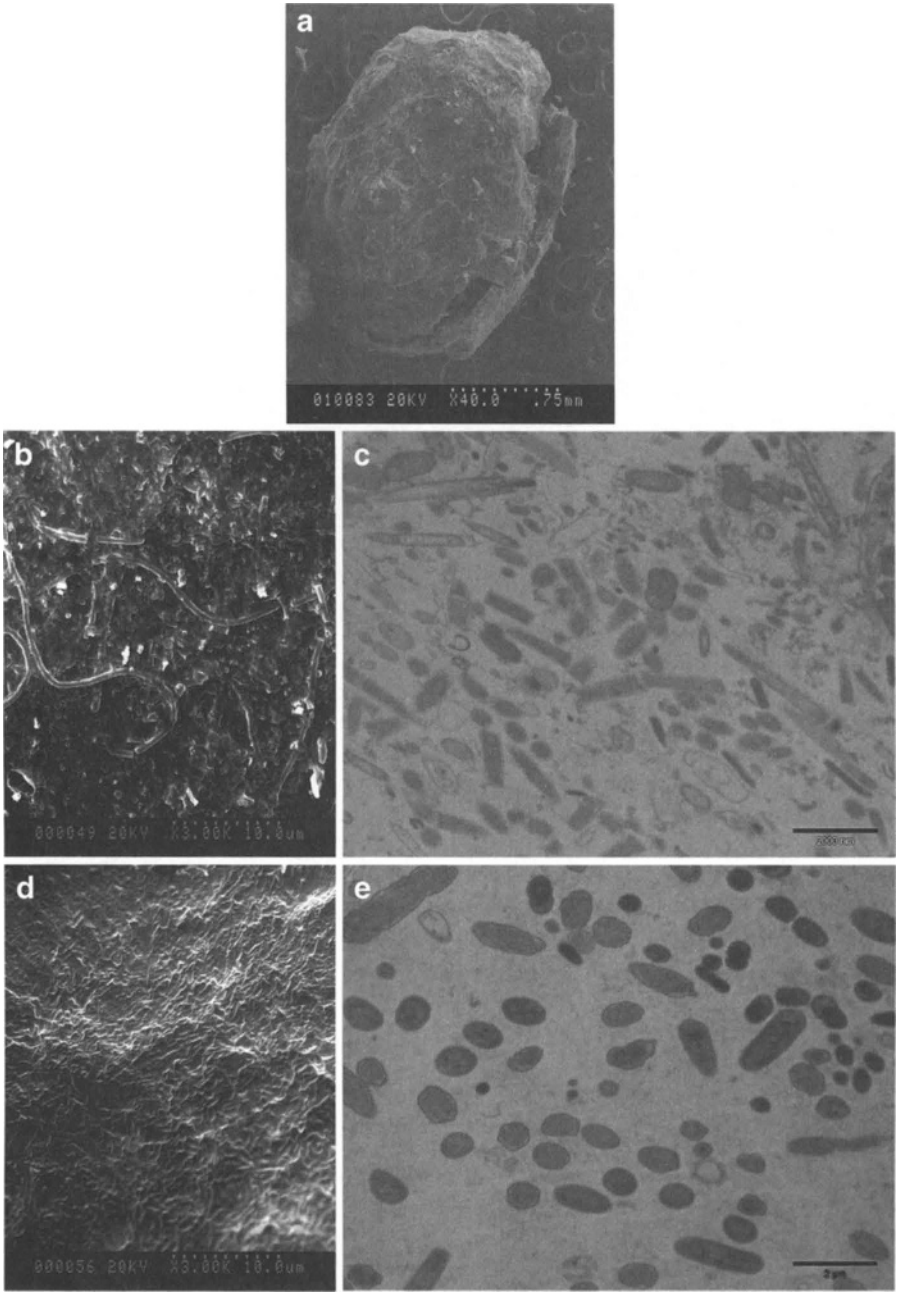


Fig. 1 **a** SEM picture of methanogenic granules. **b** SEM picture of methanogenic granules. **c** TEM picture of methanogenic granules. **d** SEM of chloroform treated granules (after 5 days culture). **e** TEM of chloroform treated granules (after 5 days culture)

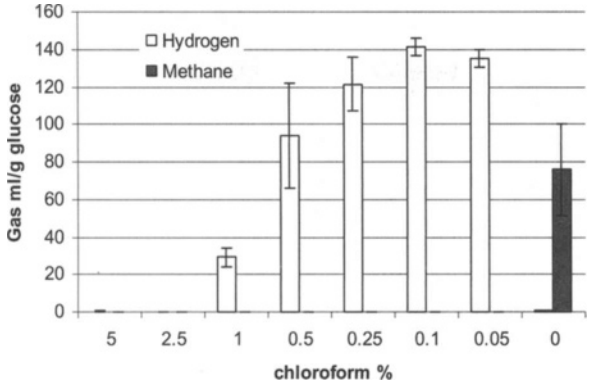


Fig. 2 Cumulative gas production for chloroform addition to granules sludge culture (Batch culture, 20 mL glucose culture medium, 3 days, inoculums 3 mL). Data are averages with *error bars* showing standard deviations (n=3)

however, causes damage to methanogens, and methanogenic activity is not easily recovered even after removal of the chloroform in subsequent cultures. In this study, the low amount of chloroform added to the culture medium in the pretreatment did not cause any damage to the structure of the granules. However, the chloroform pretreatment dramatically changed the microorganism distribution after several days of culture. Filamentous methanogens are clearly visible on the surface of the untreated granules (Fig. 1b), but there are no visible filamentous microorganisms on the chloroform-treated granules in the SEM picture (Fig. 1d). Similarly, in the TEM picture, the methanogens distributed in sections of the control methanogenic granules (Fig. 1c), while the TEM picture of the chloroform treated granules (Fig. 1e) is much clearer without the methanogens. The chloroform pretreatment showed good selectivity in inhibition of hydrogen-producing bacteria and methanogens, that is, permanently eliminating the methane production while allowing normal hydrogen production.

Fed-batch Culture

Figure 3a illustrates that for fed-batch cultures, the chloroform-treated granules can be stably reused four times with pH adjustment at the beginning of each fed-batch culture. After four fed-batches with pH adjustment, hydrogen production quickly decreased to zero, which showed strong final product inhibition. Without pH adjustment, hydrogen production was strongly inhibited after the second fed-batch, and it quickly decreased to zero. For the fed-batch cultures with pH adjustment (Fig. 3c), the metabolic pathway did not dramatically change after the first several batches because the pH of the initial culture medium was adjusted to neutral, and the VFA concentration increased with each batch. For the fed-batch cultures without pH adjustment (Fig. 3b), the metabolic pathway dramatically switched to lactic acid production, which does not produce hydrogen. VFAs can inhibit (or even be toxic to) the fermentative bacteria at high concentrations. The inhibition effect was studied by adding butyrate into the batch culture [14], and the addition of 8.36 to 12.54 g/L butyrate showed a moderate inhibitory effect. The butyrate concentration in this study reached 7.15±1.47 g/L at the third fed-batch with stable hydrogen production from cultures with pH adjustment. Then, the strong inhibition of VFA caused a drastic decrease in hydrogen production in subsequent fed-batch cultures. For the fed-batch cultures without

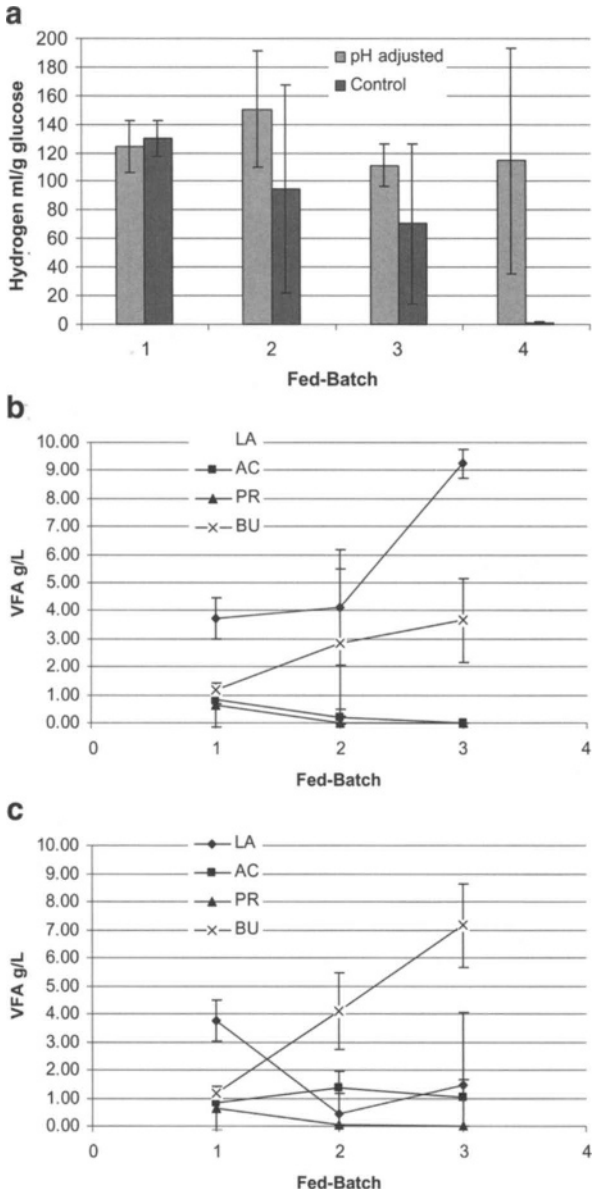


Fig. 3 **a** H_2 production from fed-batch culture of chloroform treated granules (granules were treated with 0.25% chloroform, 20 mL glucose culture medium, 3 days each batch, initial pH=8.0, inoculums 3 mL). Data are averages with *error bars* showing standard deviations (n=3). **b** VFA production from fed-batch culture of chloroform treated granules without pH adjustment (granules were treated with 0.25% chloroform, 20 mL glucose culture medium, 3 days each batch, initial pH=8.0, inoculums 3 mL). Data are averages with *error bars* showing standard deviations (n=3). *LA* Lactic acid, *AC* acetic acid, *PR* propionic acid, *BU* butyric acid. **c** VFA production from fed-batch culture of chloroform-treated granules with pH adjustment (granules were treated with 0.25% chloroform, 20 mL glucose culture medium, 3 days each batch, initial pH=8.0, inoculums 3 mL). Data are averages with *error bars* showing standard deviations (n=3). *LA* Lactic acid, *AC* acetic acid, *PR* propionic acid, *BU* butyric acid

pH adjustment, the pH value decreased batch by batch until the initial pH was too harsh for the growth of fermentative bacteria. After the second fed-batch culture, the pH of the culture medium had already been lowered to 3.8 and then increased to 4.5 with the addition of a new culture medium before the third fed-batch. The effects of VFAs on the fermentative hydrogen were associated with the pH of the solutions. At lower pH, the inhibition effects of VFAs were more likely to decrease the hydrogen fermentation activity [14]; our results clearly confirmed this finding.

VFAs, which are byproducts of the hydrogen fermentation process, can be feedstock for many other processes such as photo fermentation of hydrogen, microbial fuel cells, and methane production [15]. Higher levels of VFAs are always preferred because the separation and efficient utilization is difficult at lower concentrations. However, with the accumulation of VFAs, especially butyrate, in the fermentation broth, the switch from hydrogenesis to solventogenesis occurs. Before this "switch" to nonhydrogen production (solventogenesis), fed-batch cultures with pH adjustment seem to be an effective way to accumulate VFAs at higher concentrations.

Influence of HRT on the Continuous Fermentation with Granules

Our previous study has shown that the hydrogen productivity reached 11.6 L/L day at HRT 5.4 h [6], and remained stable even as the hydraulic resident time (HRT) decreased. In the present study, long-term continuous operation was continued to investigate the factors influencing the upflow reactor. As the HRT decreased, the hydrogen productivity gradually increased. However, the yield of hydrogen fermentation decreased dramatically when the HTR was shorter than 3 h because of the overloading of the upflow reactor (Fig. 4). For the UASB reactor, hydrogen productivity was stable at an HRT of 8 to 20 h and decreased dramatically at an HRT of 4 h [8]. A shorter HRT was reported for the CIGSB bioreactor with the addition of support carriers, where the hydrogen-producing biomass itself developed into granules [9, 10].

Influence of Culture Medium Initial pH on the Continuous Fermentation with Granules

For the continuous fermentation in the upflow reactor, the hydrogen productivity decreased when the initial pH of the culture medium was below 6.0 (Fig. 5). Our previous batch study

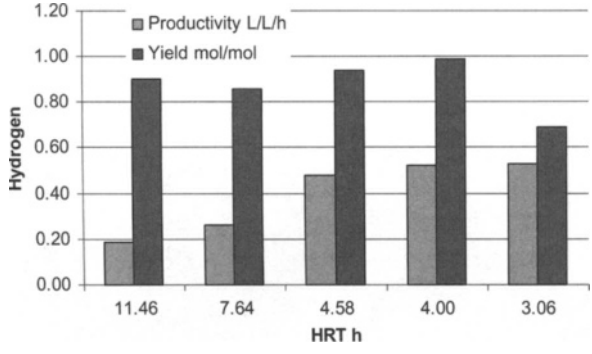


Fig. 4 Influence of HRT on the performance of the upflow hydrogen fermentation reactor (glucose culture medium 20 g COD/L, initial pH 8.0). Data were collected when they were stable for more than 12 h

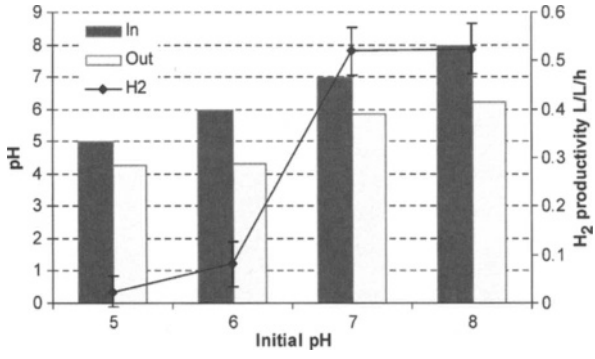


Fig. 5 Influence of initial pH of culture medium on the performance of the upflow hydrogen fermentation reactor (glucose culture medium 20 g COD/L, HRT 4 h). Data are averages with *error bars* showing standard deviations (n=3)

indicated that the culture conditions appeared to be too harsh for the hydrogen-producing bacteria to grow and nearly no hydrogen or VFA was produced when the initial pH was below 4.0 or above 9.0. The previous batch study also showed that the initial working pH for the batch culture medium ranged from 5.0 to 8.0 and that hydrogen production did not show a significant change within this initial pH range [2]. It seems that continuous culture in the upflow reactor required a narrower initial culture medium pH range. There was no significant difference for the hydrogen productivity between initial culture medium at pH 7.0 and 8.0, and the pH of the fermentation broth at these two conditions was around 6.0. When the initial pH was 5.0 or 6.0, the pH of the fermentation broth out of the reactor was about 4.2 (Fig. 5). In this case, the granules inside the reactor drifted up with the upflow and gradually washed out from the reactor, which drastically decreased the overall hydrogen productivity of the system. It is possible that this occurred because the fermentation broth was too acidic, and therefore, it might have been erosive to the extracellular polymer, which maintains the granular structure. Furthermore, because hydrogen-producing bacteria grow very slowly under acidic conditions, there might have been more bacteria detaching from the granules than bacteria reproducing and attaching to

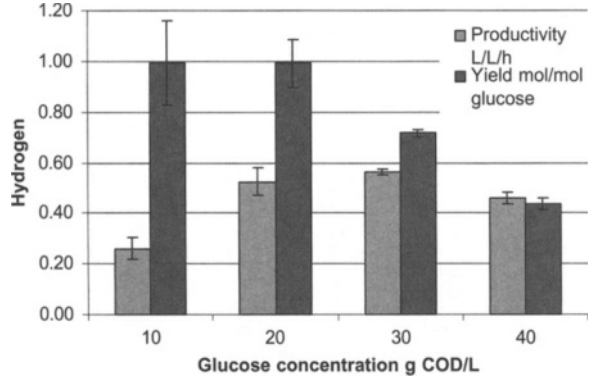


Fig. 6 Influence of glucose concentration of the culture medium on the performance of the upflow hydrogen fermentation reactor (glucose culture medium, Initial pH 8.0, HRT 4 h). Data are averages with *error bars* showing standard deviations (n=3)

the granules. The granules washing out of the reactor seems more like the floc without a granular structure, which confirms that the continuous granulized hydrogen production should remain at around neutral pH conditions because the granular structure collapsed under very acidic conditions. For many bioadsorption processes, the capacity of the adsorbent is pH sensitive, and consequently, the adsorption behavior becomes worse at very acidic conditions [16]. Most granulation theories suggest that granulation starts with bacteria adhesion to the inert nuclei [12], and our result confirms that bacterial adhesion inside the granule may be weakened when the conditions are too acidic.

Influence of Glucose Concentration of the Culture Medium on the Continuous Fermentation with Granules

Figure 6 clearly illustrates that substrate concentration influenced the continuous fermentation with granules. With an increase in glucose concentration and the associated COD loading of the upflow reactor, the hydrogen productivity reached a maximum and then decreased. There is no significant difference in hydrogen productivity between glucose concentration at 20 and at 30 g COD/L. However, when the glucose concentration was more than 20 g COD/L, the overall hydrogen yield decreased gradually because of overloading. Fermentation using high substrate concentrations is preferred because many raw materials (such as whey or manure) have a high COD content, and high concentrations of substrate are easy to heat and handle. Inhibition, however, has been found at higher feedstock concentrations [17].

Comparison of Different Immobilization Methods with Granular Treatment Method

Table 1 shows the maximum hydrogen (H_2) yield obtained in various types of H_2-producing reactors and processes. The hydrogen production yield is often influenced by several factors, such as initial glucose concentration, fermentation time, reactor type, and hydrogen partial pressure. Compared to other hydrogen-producing processes, the one investigated in this study achieved an average yield. Treating methanogenic granules and then using the treated granules as immobilized hydrogen-producing sludge, however,

Table 1 Comparison of the maximum H_2 yield obtained in various types of H_2-producing reactors.

Process	Organisms	Substrate	Maximum H_2 yield (mol H_2/mol glucose)	Reference
Batch (Blocking metabolites formation)	*Enterobacter aerogenes* HU-101 (mutant AY-2)	Glucose	1.17	[18]
Membrane reactor	Mixed culture	Glucose	1.0	[19]
N_2 sparging, continuous	Mixed culture (predominantly *Clostridium* sp.)	Glucose	1.43	[20]
UASB	Mixed culture with granular sludge	Sucrose	1.44±0.10	[21]
UASB	Mixed culture with granular sludge	Sucrose	0.92	[8]
Fluidized bed	Sewage sludge immobilized in silicone matrix	Sucrose	1.34	[22]
Batch	Chloroform treated methanogenic granules	Glucose	1.34±0.11	This study

demonstrated advantages over other immobilization methods because the granules provide the hydrogen-producing bacteria with a protective niche, a long duration, and excellent settling velocity. Different immobilization methods have been reported to enhance the biomass concentration for pure culture and mixed culture, such as calcium alginate entrapment [2]. When using a polymer matrix to trap hydrogen-producing bacteria, it is always difficult to maintain the polymer matrix because of erosion, degradation, destruction by the gas produced inside, and cell growth. In addition, the density of the matrix gel decreases as long as hydrogen and other biogases are produced, which cause the matrix gel to float and makes it more difficult to maintain the packing of the reactor. Granulation, which immobilizes the bacteria by self-flocculation, is easy to form and manipulate on an industrial scale. Fermentation using chloroform-treated granules provides a straightforward method for obtaining the hydrogen-producing granules, as methanogenic granules are available at wastewater treatment systems using a UASB.

VFA Production and Integration with Immobilized Methane Production

Table 2 shows that biohydrogen production, coupled with the subsequent step of methane production, can be an efficient process. After 3 days of biohydrogen fermentation using chloroform-treated granules, the fermentation broth was inoculated with methanogenic (untreated) granules for methane production. The initial pH of the culture medium was 8.0 for the hydrogen production, and the pH of the broth decreased to 6.5 because of VFA production before switching to the methane production reaction. Overall, the integration of the immobilized hydrogen production with immobilized methane production produced 1.01 mol hydrogen and 2 mol methane per mol glucose. It is well known that the formation of VFA during acidogenesis of organic matter precedes methanogenesis. The fermentation broth used in biohydrogen production can also be utilized with acetogensis and methanogensis to produce methane, which can alleviate the costs and environmental concerns associated with the biological hydrogen production process. The conversion of biohydrogen production follows the reaction as:

$$C_6H_{12}O_6+2H_2O \rightarrow 4H_2+2CH_3COOH+2CO_2$$

$$C_6H_{12}O_6 \rightarrow 2H_2+CH_3CH_2CH_2COOH+2CO_2$$

If acetate was considered as the final product of biohydrogen production, the biochemical reaction of the integration of biohydrogen production and methane production can be illustrated as:

$$C_6H_{12}O_6+2H_2O \rightarrow 4H_2+2CH_4+4CO_2$$

It is evident that hydrogen production can still be improved. In stage 1, only 25% of hydrogen was produced (nearly 75% was missing). There might be multiple reasons for it:

Table 2 Integration of immobilized hydrogen production and immobilized methane production (20 g COD glucose culture medium, two sequential bioreactors, 35 °C).

	Time	H_2	CO_2	CH_4	Inoculums
Stag 1. H_2 production	3 days	47.1 mL	129.6 mL	0.0 mL	Chloroform treated granules
Stag 2. CH_4 production	6 days	0.0 mL	44.7 mL	135.2 mL	Methanogenic granules
Overall	9 days	47.2 mL	174.4 mL	93.3 mL	
Integration of H_2 and CH_4 production (mol/mol glucose)	1.01	3.74	1.99		

For the batch culture, with an increase in partial hydrogen pressure of the head space, the pathway switches to butyrate production instead of acetate, which gave theoretically only 2 mol hydrogen per mol glucose. If the pathway switched to another end product, such as solvent or propionate, no hydrogen would be generated at all. Ways to further increase hydrogen production is still a topic of investigation for many researchers, including the authors of this study.

Methane production reached 1.99 mol per mol glucose, nearly the same as the theoretical value in the integrated process. Because there are many other end products in stage 1, such as butyrate and lactate, the missing hydrogen production capability might be attributable to methane production with acetogensis, which might have produced hydrogen and acetate from butyrate, propionate, and solvent, providing the necessary raw material for methanogensis.

UASB reactors are widely used for anaerobically degrading various organic wastes for methane production. This study suggested a modification process to the current anaerobic digestion system using granules by adding a separate upflow reactor packed with chloroform-treated granules to harvest hydrogen before the waste stream feeds into the UASB. The integrated two-stage design for immobilized hydrogen fermentation and methane production offers a promising approach for modifying current anaerobic wastewater treatment processes to harvest hydrogen from these systems.

Acknowledgments Funding for this project was from the Washington State University Agricultural Research Center.

References

1. Levin, D. B., Pitt, L., & Love, M. (2004). *International Journal of Hydrogen Energy, 29*, 173–185.
2. Hu, B., Liu, Y.,Chi, Z., Chen, S. (2007). *Biological Engineering* (Accepted).
3. Kraemer, J. T., & Bagley, D. M. (2005). *Environmental Science & Technology, 39*, 3819–3825.
4. Kumar, N., & Das, D. (2001). *International Journal of Hydrogen Energy, 26*, 1155–1163.
5. Wu, S. Y., Lin, C. N., Chang, J. S., & Chang, J. S. (2005). *International Journal of Hydrogen Energy, 30*, 1375–1381.
6. Hu, B., & Chen, S. (2007). *International Journal of Hydrogen Energy* (in press).
7. Fang, H. H. P., Liu, H., & Zhang, T. (2002). *Biotechnology and Bioengineering, 78*, 44–52.
8. Chang, F. Y., & Lin, C. Y. (2004). *International Journal of Hydrogen Energy, 29*, 33–39.
9. Lee, K. S., Wu, J. F., Lo, Y. S., Lo, Y. C., Lin, P. J., & Chang, J. S. (2004). *Biotechnology and Bioengineering, 87*, 648–657.
10. Fang, H. H. P., Li, Y. Y., & Chui, H. K. (1995). *Journal of Environmental Engineering-Asce, 121*, 153–160.
11. Logan, B. E., Oh, S. E., Kim, I. S., & Van Ginkel, S. (2002). *Environmental Science & Technology, 36*, 2530–2535.
12. Pol, L. W. H., Lopes, S. I. D., Lettinga, G., & Lens, P. N. L. (2004). *Water Research, 38*, 1376–1389.
13. Macleod, F. A., Guiot, S. R., & Costerton, J. W. (1990). *Applied and Environmental Microbiology, 56*, 1598–1607.
14. Zheng, X. J., & Yu, H. Q. (2005). *Journal of Environmental Management*, 74, 65–70.
15. Nath, K., & Das, D. (2004). *Applied Microbiology and Biotechnology, 65*, 520–529.
16. Tan, T. W., Hu, B., & Su, H. J. (2004). *Enzyme and Microbial Technology, 35*, 508–513.
17. Van Ginkel, S. W., & Logan, B. (2005). *Water Research, 39*, 3819–3826.
18. Rachman, M. A., Furutani, Y., Nakashimada, Y., Kakizono, T., & Nishio, N. (1997). *Journal of Fermentation and Bioengineering, 83*, 358–363.
19. Oh, S. E., Lyer, P., Bruns, M. A., & Logan, B. E. (2004). *Biotechnology and Bioengineering, 87*, 119–127.
20. Mizuno, O., Dinsdale, R., Hawkes, F. R., Hawkes, D. L., & Noike, T. (2000). *Bioresource Technology, 73*, 59–65.
21. Yu, H. Q., & Mu, Y. (2006). *Biotechnology and Bioengineering, 94*, 988–995.
22. Wu, S. Y., Lin, C. N., & Chang, J. S. (2003). *Biotechnology Progress, 19*, 828–832.

Appl Biochem Biotechnol (2008) 148:97–108
DOI 10.1007/s12010-007-8103-1

Effect of Furfural, Vanillin and Syringaldehyde on *Candida guilliermondii* Growth and Xylitol Biosynthesis

Christine Kelly · Opal Jones · Christopher Barnhart · Curtis Lajoie

Received: 16 May 2007 / Accepted: 26 November 2007 /
Published online: 23 January 2008
© Humana Press Inc. 2008

Abstract Xylitol is a five-carbon sugar alcohol with established commercial use as an alternative sweetener and can be produced from hemicellulose hydrolysate. However, there are difficulties with microbiological growth and xylitol biosynthesis on hydrolysate because of the inhibitors formed from hydrolysis of hemicellulose. This research focused on the effect of furfural, vanillin, and syringaldehyde on growth of *Candida guilliermondii* and xylitol accumulation from xylose in a semi-synthetic medium in microwell plate and bioreactor cultivations. All three compounds reduced specific growth rate, increased lag time, and reduced xylitol production rate. In general, increasing concentration of inhibitor increased the severity of inhibition, except in the case of 0.5 g vanillin per liter, which resulted in a faster late batch phase growth rate and increased biomass yield. At concentrations of 1 g/l or higher, furfural was the least inhibitory to growth, followed by syringaldehyde. Vanillin most severely reduced specific growth rate. All three inhibitors reduced xylitol production rate approximately to the same degree.

Keywords Xylitol · Inhibitor · Furfural · Vanillin · Syringaldehyde · Toxicity · Hemicellulose hydrolysate

Introduction

Lignocellulose, consisting of lignin, hemicellulose, and cellulose, is the major structural component of woody and non-woody plants and represents a major source of renewable

C. Kelly (✉) · C. Barnhart · C. Lajoie
School of Chemical, Biological, and Environmental Engineering, Oregon State University, Corvallis, OR, USA
e-mail: ckelly@engr.orst.edu

O. Jones
Department of Chemical Engineering, Syracuse University, Syracuse, NY, USA

O. Jones
MedImmune, Inc., Gaithersburg, MD, USA

organic matter. Large amounts of lignocellulosic by-products are generated through forestry and agricultural practices, paper-pulp industries, timber industries, and many agroindustries that can potentially be converted into various different value added products including biofuels, chemicals, and inexpensive energy sources for fermentation and improved animal feeds. Lignocellulosic raw materials are inexpensive and abundant, and hydrolysis of hemicellulose, a component of lignocellulose, for microbiological feedstock is currently an important and active area of research. However, there are many difficulties with microbiological growth on hydrolysate because of the inhibitors formed from hydrolysis of hemicellulose.

D-Xylose is one of the primary sugars derived from the hydrolysis of hemicellulose. One of the organisms that most efficiently produces the sweetener xylitol is *Candida guilliermondii* [1], which is used in this study. Xylitol is a five-carbon sugar alcohol with established commercial use as an alternative sweetener and has possible uses in adhesives. The unique properties of xylitol include its being an insulin-independent sweetener and its being not utilized by acid producing oral cavity bacteria, thereby reducing dental caries. Xylitol is currently produced on an industrial scale by the chemical reduction of xylose. The xylose is obtained by hydrolysis of wood [2]. However, the cost of purification of xylose from the hydrolysate makes xylitol one of the more expensive sweeteners. Xylitol is used as a sweetener in food products such as chewing gum, candy, soft drinks, and personal health products such as mouth wash and toothpaste. A process to more economically produce xylitol would result in increased xylitol use in the confectionary industry.

C. guilliermondii produces the enzyme D-xylose reductase which catalyses a reaction where the proton carrier NADPH donates a hydrogen atom to D-xylose, and D-xylose is converted to xylitol as seen in Fig. 1. The xylitol can then be converted to D-xylulose, catalyzed by xylitol dehydrogenase, which is utilized in central metabolism [3]. Under semi-aerobic conditions, xylitol accumulation is favored compared to anaerobic or aerobic conditions. Under anaerobic conditions, the ratio of NAD(P)H to $NAD(P)^+$ is low, and NAD(P)H is required for xylitol production. Under aerobic conditions, excess oxygen allows oxidation of NADH to NAD^+, and a resulting high NAD^+/NADH ratio results in a faster xylitol conversion rate to D-xylulose, eliminating the accumulation of xylitol [4, 5].

Many factors impact the xylose to xylitol fermentation process, including oxygen delivery rate and concentration, pH, temperature, and the presence of other sugars (in addition to xylose), nutrients, and inhibitors [4, 6]. The least studied of these factors is the effect of specific inhibitors derived from biomass pretreatment on the growth of xylitol-

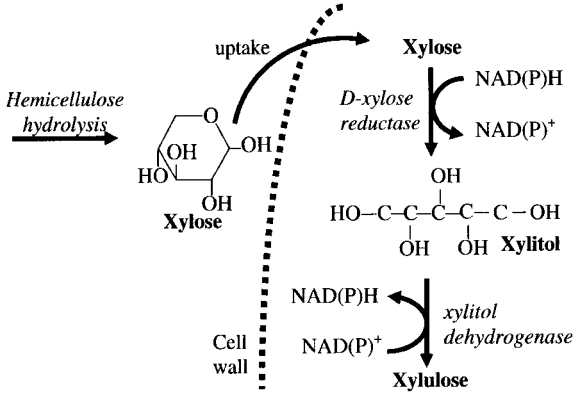


Fig. 1 Xylitol biosynthesis [3–5]

producing yeast and the effect on xylitol production. Xylose can be obtained from hydrolysis of hemicellulose after pretreatment of the lignocellulosic biomass via dilute acid hydrolysis or steam explosion. Under the high temperature and pressure conditions employed, a range of compounds are produced that are inhibitory to yeasts. Hydrolysate inhibitors include weak acids, furan derivatives, and phenolic compounds. In this study, the effects of furfural, vanillin, and syringaldehyde were investigated. Furfural is a degradation product of xylose. Vanillin and syringaldehyde are derived from the lignin fraction of lignocellulose. The chemical structures of these compounds are indicated in Fig. 2. Furfural, vanillin, and syringaldehyde can be assimilated or metabolized by the yeast *Saccharomyces cerevisiae* [7].

The xylitol production rate is highest at very high xylose concentrations (80 g/l) [8, 10]. However, concentrating the hemicellulose hydrolysates using vacuum evaporation to achieve high xylose concentrations also concentrates the non-volatile inhibitors [11]. At these inhibitor concentrations, volumetric productivity actually declines [12–14]. Many studies have demonstrated the inhibitory effect of these hydrolysis-derived compounds on growth and production of products, such as ethanol and xylitol [15–16]. Concentrated hydrolysate requires detoxification for optimum xylitol production.

Efforts to decrease the effects of inhibitors on yeast fermentations include decreasing the temperature, pressure, and residence time during dilute acid hydrolysis to minimize inhibitor formation, although decreases in xylose yield also result [17]. A number of methods have also been developed for concentrating and pretreating the hydrolysate to increase the xylose concentration and reduce the concentration of inhibitors, including precipitation by overliming, adsorption on activated carbon, removal with ion-exchange resins, and vacuum evaporation. A third approach is to adapt the yeast to the inhibitors by sequential culture and selection with increasingly concentrated hydrolysate and inhibitors [18–21].

The identity and effects of hemicellulose hydrolysis-derived inhibitors on potential ethanol and xylitol production processes have been investigated using both hemicellulose hydrolysates, followed by different detoxification processes and semi-synthetic media spiked with known concentrations of toxicants. The use of complex hemicellulose hydrolysates provides practical information on technological aspects of potential industrial designs, and when coupled with chemical analyses, also assists in identification of the major inhibitors. Semi-synthetic media can provide exposure of strains to known inhibitor concentrations and can be used to provide less ambiguous information on the microbial physiology and toxicology of specific inhibitors or combinations of inhibitors. These experiments are typically performed in shake flasks or bench-scale fermentors. In cases where it is desirable to investigate many different inhibitor concentrations and combinations microwell scale (200 µl), experiments may be useful. This approach has been employed for investigating the enzymatic hydrolysis of lignocellulosic feedstocks [22]. Although the

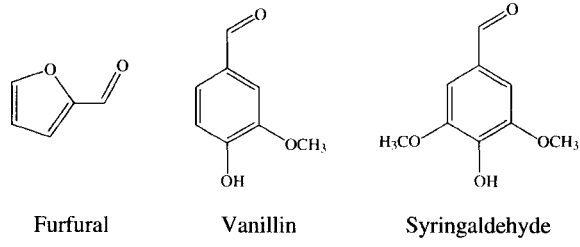


Fig. 2 Furfural, syringaldehyde, and vanillin chemical structures

scalability of the information obtained must ultimately be verified when making extrapolations to industrial processes, these approaches may prove useful in providing rapid comparison of the effects of different types and combinations of inhibitors, growth substrates, and production strains.

The yeast *C. guilliermondii* efficiently converts xylose in sugarcane bagasse to xylitol and is commonly considered for potential commercial production processes [1]. Lignin and xylose-derived degradation products are commonly found at inhibitory levels in concentrated hemicellulose hydrolysates from sugarcane bagasse [23, 16–17], although the concentrations of specific chemical species may vary widely depending on the feedstock and pretreatment conditions. The objectives of this research were to experimentally examine the effects of the inhibitors furfural, syringaldehyde, and vanillin on *C. guilliermondii* growth (low cell density) and xylitol production (high cell density) using semi-synthetic medium in microtiter plates and bench-scale fermentors, respectively. Quantitative analysis of the effects of hydrolysate inhibitors on growth and xylitol production in a semi-synthetic medium with known toxicant concentrations may contribute to further studies on the optimization of biomass pretreatment methods, thereby minimizing costs and ancillary environmental impacts.

Materials and Methods

Strain and Medium

The xylitol producing yeast *C. guilliermondii* (ATTC No. 201935) was cultivated in a semi-synthetic basal salt medium (BSM) for experiments investigating cell growth and xylitol production. This medium consisted of 40 g/l xylose (EMD Chemicals, Darmstadt, Germany) as the carbon source, 5 g/l ammonium sulfate as the nitrogen source, 0.5 g/l magnesium sulfate, 0.1 g/l calcium chloride, 1 g/l potassium sulfate, and 1 g/l yeast extract (Fisher Scientific, Rochester, NY). The medium was prepared separately for each experiment and autoclaved for 20 min at 121 °C to assure sterility.

Cultivation

Multiwell plates, shake flasks, and bioreactors were used to cultivate the *C. guilliermondii* yeast. The multiwell plates contained 96 wells each with 200-μl liquid working volume. For toxicity experiments in the multiwell plates, 0.022 g of the inhibitors vanillin, syringaldehyde (Alfa Aesar, Karlsruhe, Germany), and furfural (TCI America, Portland, OR) were each added separately to 10 ml BSM medium. The syringaldehyde solution was heated in a hot tap water bath to increase the rate of dissolution. All toxicant solutions were then filter-sterilized (0.22 μm) before preparing a series of dilutions in BSM medium. *C. guilliermondii* inoculum cultures were grown in BSM in shake flasks at 30 °C, centrifuged, and resuspended in BSM medium to an OD_{600nm} of 0.7. Multiwell plate cultivation experiments were performed by combining 180 μl BSM medium containing the appropriate concentration of inhibitor with 20 μl of the appropriate density of exponential phase *C. guilliermondii* cells in each well. Triplicates microwells were prepared and analyzed for each experimental condition. The plates were covered with plastic lids and incubated at 30 °C.

Bioreactor experiments were conducted in 3-l New Brunswick Bioflow 110 bioreactors (New Brunswick Scientific, Edison, NJ) equipped with pH, temperature,

and dissolved oxygen control. The bioreactors were autoclaved with 1 l of medium, allowed to cool, and then inoculated with 50 ml of overnight cultures of *C. guilliermondii*. The experiments consisted of two phases: batch growth and resuspension xylitol biosynthesis. During both phases, the reactor temperature was maintained at 30 °C and the pH at 6.0. The batch phase was aerated at 1.5 vvm (volume of air per volume of reactor per minute) air introduced through a sparger beneath the axial impellor, and the stirrer speed was constant at 500 rpm. At the completion of batch phase (about 30 h), the reactor contents were centrifuged and the cell pellet resuspended in new BSM medium, with or without inhibitor, and returned to the bioreactor vessel. The inhibitor was added as a dry powder (or liquid) to the BSM medium after autoclaving but before resuspending the yeast cells. The aeration rate was reduced to 0.28 vvm and introduced to the headspace (not the sparger). The agitation rate was reduced to 200 rpm. These conditions resulted in a oxygen mass transfer coefficient ($k_L a$) of ~9 h^{-1}, as measured by the gassing out method, to facilitate xylitol accumulation. Samples were taken for cell density and xylitol measurements from the bioreactor contents for about 24 h during this resuspension phase. Samples for xylitol were centrifuged and the supernatant frozen for later analysis. Individual batch fermentations were conducted for each inhibitor concentration. The inhibitor concentrations and fermentor operating conditions were chosen based on previous results using the same strain and medium [24]. Analyses were performed on triplicate samples from each bioreactor

Cell Density

Cell density was assessed using absorbance at a 600 nm wavelength ($Abs_{600\ nm}$). For the bioreactor experiments, samples were diluted to the linear range of the assay, transferred to a 1-ml cuvette, and the absorbance was measured using a Spectronic 20 Genesys spectrophotometer. In the multiwell plate experiments, the plate cover was removed, and absorbance was measured using a Perkin Elmer Victor^3 V 1420 multilabel counter. A second-order polynomial was fit (R^2=0.97) to describe the relationship between absorbance and dry mass of cells per liter (Eq. 1), and all data are reported as cell density (g/l).

$$\text{Cell Density}\left[\frac{\text{g}}{\text{L}}\right] = 3.44(\text{abs})^2 + 0.374(\text{abs}) \quad (1)$$

Xylitol

To quantify the amount of xylitol produced during each bioreactor run, the Megazyme D-sorbitol/xylitol assay kit (Wicklow, Ireland) was used. Xylitol (Calbiochem, Darmstadt, Germany) was used as a standard. In the assay, xylitol reacts with NAD^+ in the presence of sorbitol dehydrogenase to form D-xylulose and NADH. This NADH is then reacted with iodonitrotetrazolium chloride (INT) in the presence of diaphorase to form INT-formazan. The amount of INT-formazan is quantified by measuring absorbance at 492 nm. The amount of INT-formazan formed is in stoichiometric proportion to the amount of xylitol. The original assay protocol was adapted so that the assay could be performed using a microplate reader. The volumes of sample and reagents were reduced 20-fold so that the reaction mixes would fit into 96-well assay plate. In addition, sorbitol dehydrogenase was added 4 min after diaphorase because no reducing substances are present in the samples.

Results and Discussion

The effects of furfural, vanillin, and syringaldehyde as individual inhibitors and in combination on cell growth were investigated in microwell plate cultivations. At inhibitor concentrations of 1 g/l, vanillin most severely inhibited *C. guilliermondii* growth, followed by syringaldehyde. Furfural was the least inhibitory of the three compounds (Fig. 3). Each inhibitor caused a concentration-dependant decrease in growth rate, with the exception of vanillin at low concentration (Fig. 4). The initial growth rate of cells exposed to vanillin at 0.5 g/l was suppressed, but then increased dramatically after about 20 h of cultivation (Fig. 4). The biomass yield on xylose was unaffected by furfural or syringaldehyde at concentrations up to 2 g/l, whereas no growth was observed in the presence of 2 g/l vanillin. However, at 0.5 g/l vanillin, biomass yield was higher than the no inhibitor control, perhaps indicating metabolism of vanillin.

Duarte et al. [25] found that 0.5 g/l furfural decreased the specific growth rate of *Debaryomyces hansenii* CCMI 941, and at concentrations above 3.5 g/l furfural or 1.5 g/l syringaldehyde, no growth was observed. Olsson and Hahn-Hagerdal [26] reported that 1 g/l furfural resulted in a 47% inhibition of growth of *P. stipitis*, and 2 g/l furfural resulted in 99 and 90% inhibition in *P. stipitis* and *S. cerevisiae*, respectively. Syringaldehyde (0.75 g/l) and vanillin (0.5 g/l) resulted in approximately 50–88% inhibition of growth in the same strains. Generally, it is observed that log $P_{o/w}$ is a good indicator of toxicity. However, in the microtiter assays, syringaldehyde was less inhibitory to the yeast than vanillin, although it is more hydrophobic. Fitzgerald et al. [27] have shown that the toxicities of six structural analogues of vanillin are not correlated with log $P_{o/w}$, and the solubilities and availabilities of these compounds can vary between actual hemicellulose hydrolysates and defined media [7]. *S. cerevisiae* has been shown to assimilate vanillin and syringaldehyde during fermentation [28]. It is unknown whether *C. guilliermondii* has similar metabolic capabilities that may affect inhibitor toxicity.

The inhibitor compounds can affect cell growth by increasing the adaptation lag time and decreasing or altering the growth rate. The cells not exposed to inhibitor and the cells exposed to syringaldehyde exhibited a ~2-h lag time after introduction to the wells, whereas the vanillin caused a 5-h lag at all concentrations, and the furfural resulted in a concentration-dependant lag time from 0 to 15 h. Duarte et al. [25] also found a concentration-dependant lag time in response to furfural with the xylitol-producing yeast *D. hansenii*. At a furfural concentration of 2 g/l, a 13-h lag time was observed.

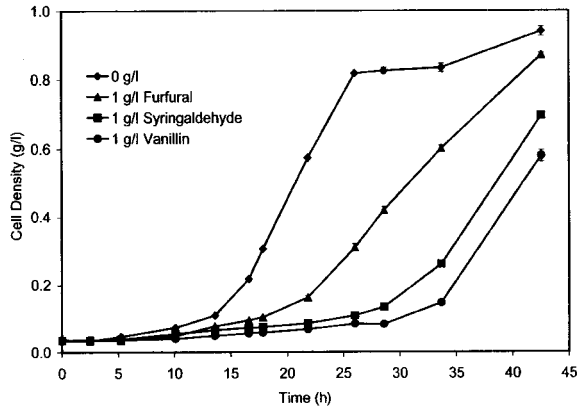


Fig. 3 Effect of inhibitor type on *C. guilliermondii* cell growth in microwell plates with a 200-µl cultivation volume and inhibitor concentrations of 1 g/l. *Filled diamond*, 0 g/l inhibitor; *filled triangle*, 1 g/l furfural; *filled square*, 1 g/l syringaldehyde; *filled circle* , 1 g/l vanillin. *Error bars* (sometimes obscured by the datum symbol) are ±standard error of the mean

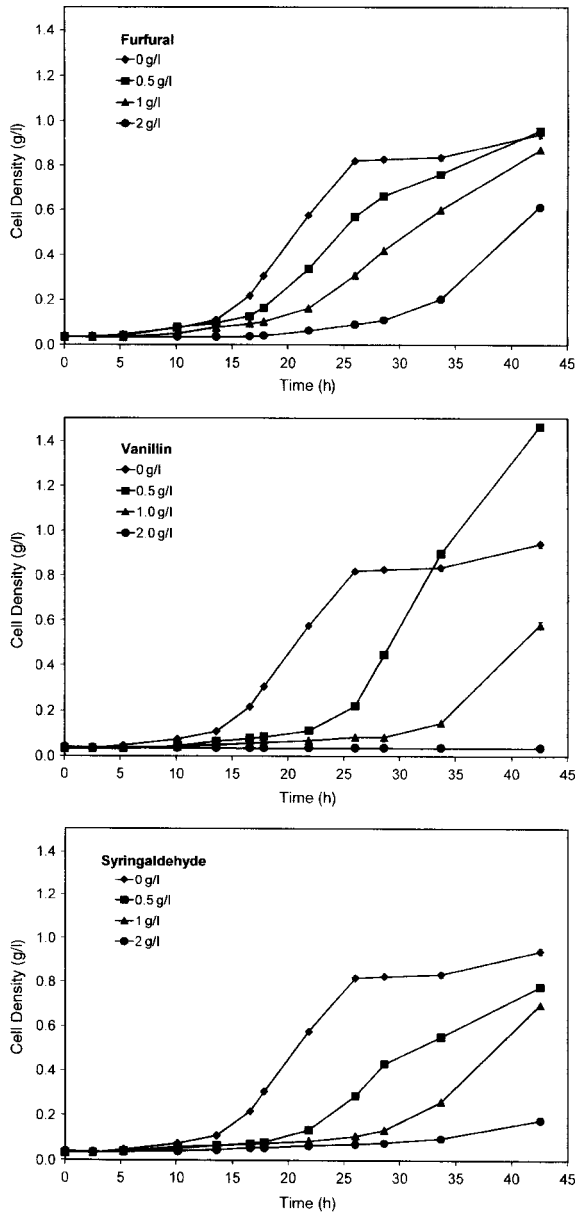


Fig. 4 Effect of inhibitor concentration on *C. guilliermondii* cell growth in microwell plates with a 200-µl cultivation volume. *Filled diamond*, 0 g/l; *filled triangle*, 0.5 g/l; *filled square*, 1.0 g/l; *filled circle*, 2.0 g/l. *Error bars* (sometimes obscured by the datum symbol) are ±standard error of the mean

The average specific growth rate of the *C. guilliermondii* cultures was determined by calculating the slope of time versus $\ln(X/X_o)$ line for each treatment, where X is cell density and X_o is initial cell density (Fig. 5). The plots for specific growth rate calculation for the 1-g/l treatments are shown in Fig. 5, and the same method was used to determine specific growth rates for inhibitor concentrations of 0.5 and 2 g/l. For the case of cultures with no inhibitor and with furfural present, *C. guilliermondii* grew with a constant growth rate. All three concentrations of furfural examined (0.5, 1 and 2 g/l) resulted in a moderately decreased specific growth rate compared to the cells not exposed to an inhibitor (Fig. 6).

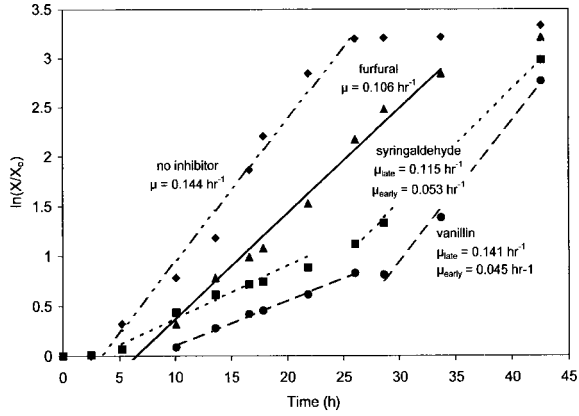


Fig. 5 Determination of specific growth rates in the presence of 1 g/l of individual inhibitors. *Lines* are linear regression, *symbols* are experimental data. Slope of the line is the specific growth rate. *Filled diamond*, no inhibitor; *filled triangle*, furfural; *filled square*, syringaldehyde; *filled circle*, vanillin

Syringaldehyde and vanillin both caused significant reductions in specific growth rate in the first 20 to 30 h of cultivation, followed by increased growth rates for late cultivation times. However, at 2 g/l vanillin, the cells did not grow in the 42 h of cultivation. Similarly, Duarte et al. [25] found no correlation between furfural concentration and specific growth rate in *D. hansenii* at concentrations above 0.5 g/l, and syringaldehyde resulted in a concentration-dependant decrease in specific growth rate in the range of 0.25 to 1.5 g/l.

In a separate multiwell plate investigation, the effects of combinations of inhibitors on *C. guilliermondii* growth were investigated. Treatments consisted of single inhibitors at 1 and 2 g/l, double inhibitor combinations of 0.5 and 1 g/l of each inhibitor, and triple inhibitor combinations of 0.33 and 0.66 g/l of each inhibitor. Figures 7 and 8 present the growth curves for the cultivations with a total of 1 and 2 g inhibitor/l, respectively. The results from this study support the single inhibitor experimental findings in that (1) the inhibition of growth was more severe with higher inhibitor concentrations, (2) vanillin at a low concentration increases biomass yield, and (3) at a high concentration, vanillin causes the most severe inhibition to *C. guilliermondii* growth rate. In addition, single inhibitors seem to be more inhibitory than multiple inhibitors at the same total concentration.

To investigate the effect of furfural, syringaldehyde, and vanillin on xylitol biosynthesis, as opposed to *C. guilliermondii* growth rate, the cells were grown to about 10 O.D in batch

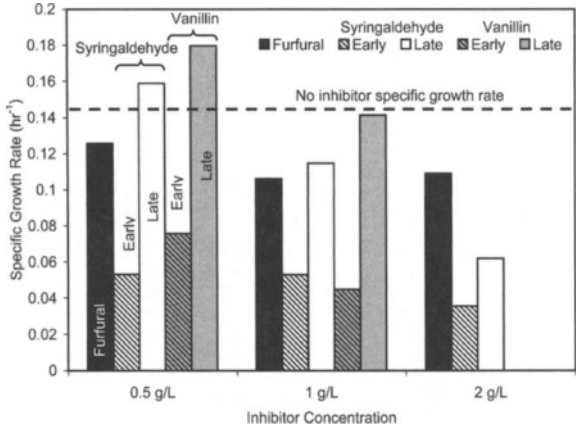


Fig. 6 Specific growth rates in the presence of individual inhibitors. Overall specific growth rate presented for furfural and two specific growth rates presented for syringaldehyde and vanillin: and early phase and late phase. The specific growth rate of *C. guilliermondii* with no inhibitor is represented by the *horizontal dashed line*

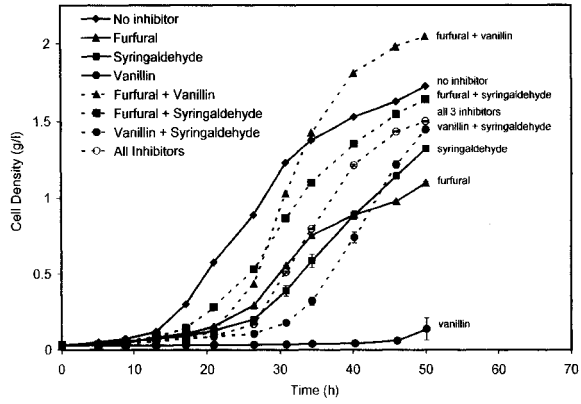


Fig. 7 Effect of 1 g/l multiple inhibitors on *C. guilliermondii* cell growth in microwell plates with a 200-µl cultivation volume. In each well the total inhibitor concentration was 1 g/l. Single inhibitor concentrations are 1 g/l, double inhibitor concentrations are 0.5 g/l each, and the triple inhibitor concentration is 0.33 g/l each. *Error bars* (sometimes obscured by the datum symbol) are ±standard error of the mean

culture in 1-l bioreactors to establish cell mass. The broth was centrifuged and the cell pellet resuspended in fresh xylose-containing medium in the bioreactor. Aeration was reduced to promote xylitol accumulation. Six bioreactor experiments were performed, including no inhibitor, 1 g/l of each inhibitor (separately), and 2 and 3 g/l of furfural. During the resuspension (xylitol accumulation) phase, the cell density remained about constant, and the dissolved oxygen concentration was stable at less than 1% of saturation in air. Figure 9 presents the xylitol concentration in the broth during the resuspension phase for each experiment. Although the cell density was the same in all experiments, the cells in the presence of 1 g/l inhibitor produced xylitol at about 85% of the no inhibitor control (0.29 versus 0.25 g xylitol per liter per hour). Furfural at 2 and 3 g/l reduced the xylitol production rate even further to about 43% of the no inhibitor control (Fig. 9).

The results of toxicity experiments performed using *C. guilliermondii* in batch fermentations are generally similar to that observed in other studies using semi-synthetic or actual hemicellulose hydrolysates for xylitol or ethanol production. Dominguez et al. [29] treated sugarcane bagasse hemicellulose hydrolysate with activated carbon before fermentation with *Candida* sp. 11-2. Starting with an initial xylose concentration of 43 g/l, this yeast produced 10.5 g/l xylitol, corresponding to a xylitol productivity of 0.2 g xylitol per liter per hour. Higher productivities may be achieved by increasing the xylose concentration to approximately 80 g/l. However, the consequent increase in the concentration of inhibitors can cause a decrease in productivity. Other important factors

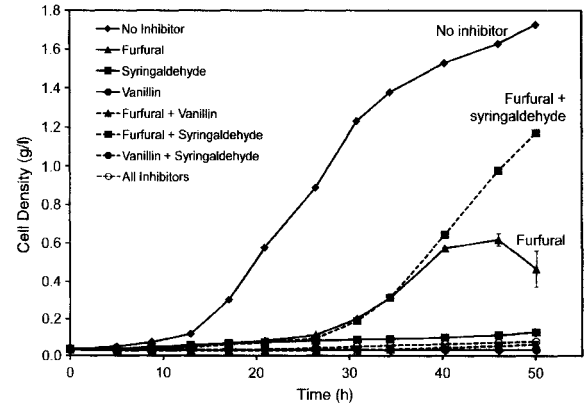


Fig. 8 Effect of 2 g/l multiple inhibitors on *C. guilliermondii* cell growth in microwell plates with a 200-µl cultivation volume. In each well, the total inhibitor concentration was 2 g/l. Single inhibitor concentrations are 2 g/l, double inhibitor concentrations are 1.0 g/l each, and the triple inhibitor concentration is 0.66 g/l each. *Error bars* (sometimes obscured by the datum symbol) are ±standard error of the mean

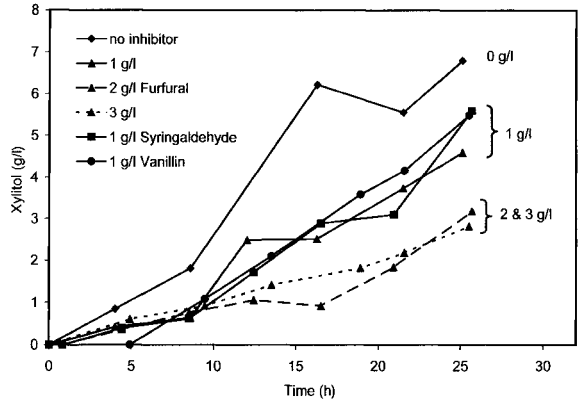


Fig. 9 Effect of inhibitors on xylitol biosynthesis in high cell density bioreactor cultivation during the resuspension phase. Time 0 is the start of resuspension. Cell density in the bioreactors was constant during the entire resuspension phase in all experiments at ~8 $OD_{600\ nm}$. *Filled diamond*, no inhibitor; *filled triangle*, furfural; *filled square*, syringaldehyde; *filled circle*, vanillin

affecting xylitol productivity include the concentrations of other growth substrates, previous adaptation of the strain, inoculum concentration, the oxygen transfer rate, the severity of the hydrolysis conditions, and the detoxification processes employed. Ding and Xia [30] found that a k_La of about 6 h^{-1} resulted in maximum xylitol accumulation during the production phase of a batch cultivation with *Candida* sp. ZU04, whereas in these experiments, the k_La was about 9 h^{-1}. Xylitol productivities of 0.66 g xylitol per liter per hour have been achieved under optimum conditions.

In fermentation experiments employing semi-synthetic sugarcane bagasse hemicellulose hydrolysate containing 60–92 g/l xylose, vanillin inhibited the metabolism of the yeast *D. hansenii* at concentrations above 0.5 g/l, and the inhibitory effects on fermentation increased with vanillin concentration up to 3 g/l. Furfural was less inhibitory to batch fermentations, with concentrations between 1 and 5 g/l exhibiting similar effects [23]. From experiments with brewers spent grain hydrolysate (85 g/l xylose) pretreated in various manners (raw, treated with activated carbon, concentrated, or amended with xylose), it appears that total phenolics (3.93 g/l), including vanillin and syringaldehyde, are the most inhibitory compounds to *C. guilliermondii* fermentations. The presence of furfural (0.61 g/l) did not effect the fermentation. Sanchez and Bautista [31] found that 2 g/l furfural inhibits oxidative metabolism and fermentation by *C. guilliermondii*, and it has been previously observed that furfural concentrations below 1 g/l are not inhibitory [32–33]. Keating et al. [34] observed that furfural had a dose-proportional effect in the range of 0.8–1.6 g/l on sugar consumption rate and ethanol productivity. Although these studies have employed a wide array of experimental approaches and extrapolation is complicated by wide differences in concentrations of specific phenolic and furaldehyde compounds in different hydrolysates, inhibitory effects of furfural, vanillin, and syringaldehyde on fermentations appear to occur in the general range of 0.5–2 g/l for individual inhibitors.

In the microwell experiments, no mixing is provided. The yeast cells grow as a layer on the bottom of the well. The inhibitory effects on cell growth are clearly visible and easily measured. This format was chosen to investigate inhibitor effects at low cell densities. Although *C. guilliermondii* appears to grow well, and reproducibly, in this environment, growth rates may be lower than that achievable in well-aerated shake flasks because of oxygen limitation. However, effects such as increased lag time and decrease in specific growth rate occur during the period of lowest cell density and oxygen consumption. Also, the concentrations of inhibitors studied (0.5–2 g/l) are within the range of those typically found in untreated hemicellulose hydrolysates, and the inhibitor concentrations observed to

effect *C. guilliermondii* growth are consistent with those reported in other toxicity studies. The primary advantages of using microtiter plates for inhibitor studies is the large number of experimental variables and synergistic effects that can be investigated, and growth can be monitored in the clear 96-well microtiter plates without any sampling by using a standard microtiter plate reader.

The batch xylitol fermentations conducted in the bench-scale fermentors were more typical of studies on inhibitor toxicities at high cell densities. It is possible that the xylitol production phase could also be considered at the microscale (100- to 200-μl volume), as this is a microaerophilic process in which low oxygen transfer rates are desirable. While this may not provide an accurate measure of the maximum volumetric productivity for a particular hydrolysate, it may be useful for investigating fundamental toxicological effects and inhibitor synergies on xylitol production.

Conclusion

Furfural, syringaldehyde, and vanillin inhibited *C. guilliermondii* growth rate, increased lag time, and reduced xylitol production rate in microwell and bioreactor cultivations. In general, increasing concentration of inhibitor increased the severity of inhibition, except in the case of 0.5 g vanillin per liter which resulted in a faster late batch phase growth rate and increased biomass yield. At concentrations of 1 g/l or higher, furfural was the least inhibitory to growth, followed by syringaldehyde, and vanillin most severely reduced growth rate. There was no synergistic effect observed by combining inhibitors, and in contrast, combinations were slightly less inhibitory to growth than single inhibitors at the same mass concentration. All three inhibitors reduced xylitol production rate approximately to the same degree. These results indicate that concentrations of these inhibitors that are easily obtained in concentrated hydrolysates can have a significant effect on both *C. guilliermondii* growth and xylitol production. For an efficient process, measures should be taken to adapt the organism to the inhibitors or remove the compounds to non-inhibitory levels.

References

1. Morita, T. A., & Silva, S. S. (2000). *Applied Biochemistry and Biotechnology, 84–86*, 801–808.
2. Saha, B. C. (2003). *Journal of Industrial Microbiology & Biotechnology, 30*(5), 279–291.
3. Preziozi-Belloy, L., Nolleau, V., & Navarro, J. M. (2000). *Biotechnology Letters, 22*, 239–243.
4. Winkelhausen, E., & Kuzmanova, S. (1998). *Journal of Fermentation and Bioengineering, 86*(1), 1–14.
5. Martinez, E. A., Silva, S. S., & Felipe, M. G. A. (2000). *Applied Biochemistry and Biotechnology, 84–86*, 633–641.
6. Felipe, M. G. A. (2004). In B. C. Saha, & K. Hayashi (Eds.) *Lignocellulose biodegradation* pp. 300–315. Washington, DC: American Chemical Society.
7. Palmquist, E., & Hahn-Hagerdal, B. (2000). *Bioresource Technology, 74*, 25–33.
8. Walthers, T., Hensirisak, P., & Agblevor, A. F. (2001). *Applied Biochemistry and Biotechnology, 91–93*, 423–435.
9. Rosa, S. M. A., Felipe, M. G. A., Silva, S. S., & Vitolo, M. (1998). *Applied Biochemistry and Biotechnology, 70–72*, 127–135.
10. Silva, C. J. S. M., & Roberto, I. C. (2001). *Processes in Biotechnology, 36*, 119–124.
11. Rodrigues, R. C. L. B., Felipe, M. G. A., Silva, J. B. A., Vitolo, M., & Gomez, P. V. (2001). *Brazilian Journal of Chemical Engineering, 18*(3), 299 311.
12. Felipe, M., Vitolo, M., Mancilha, I. M., & Silva, S. S. (1997). *Journal of Industrial Microbiology & Biotechnology, 18*, 251–254.

13. Mayerhoff, Z. D. V. L., Roberto, I. C., & Franco, T. T. (2001). *Applied Biochemistry and Biotechnology, 91–93*, 729–737.
14. Canettieri, E. V., Almeida e Silva, J. B., & Felipe, M. G. A. (2001). *Applied Biochemistry and Biotechnology, 91–93*, 423–435.
15. Cantarella, M., Cantarella, L., Gallifuoco, A., Spera, A., & Alfani, F. (2004). *Biotechnology Progress, 20* (1), 200–206.
16. Mussatto, S., Dragone, G., & Roberto, I. (2005). *Process Biochemistry, 40*, 3801–3806.
17. Silva, S. S., Matos, Z. R., & Carvalho, W. (2005). *Biotechnology Progress, 21*, 1449–1452.
18. Rao, R. S., Jyothi, C. P., Prakasham, R. S., Sarma, P. N., & Rao, L. V. (2006). *Bioresource Technology, 97*, 1974–1978.
19. Sene, L., Felipe, M. G. A., Vitolo, M., Silva, S. S., & Mancilla, I. M. (1998). *Journal of Basic Microbiology, 38*, 61–69.
20. Martin, C., Marcet, M., Almazan, O., & Jonsson, L. F. (2007). *Bioresource Technology, 98*, 1767–1773.
21. Rodrigues, R. C. L. B., Sene, L., Matos, G. S., Roberto, I. C., Pessoa Jr, A., & Felipe, M. G. A. (2006). *Current Microbiology, 53*, 53–59.
22. Berlin, A., Maximenko, V., Bura, R., Kang, K.-Y., Gilkes, N., & Saddler, J. (2005). *Biotechnology and Bioengineering, 93*(5), 880–886.
23. Sampaio, F. C., Torre, P., Lopes Passos, F. M., Alencar de Moraes, C., Perego, P., & Converti, A. (2007). *Applied Biochemistry and Biotechnology, 136*, 165–181.
24. Jones, O. T. (2004). The effect of pH and hemicellulose derived inhibitors on xylitol biosynthesis. Masters thesis, Syracuse University, Syracuse, NY.
25. Duarte, L. C., Carvalheiro, F., Neves, I., & Gírio, F. M. (2005). *Applied Biochemistry and Biotechnology, 121*, 413–426.
26. Olsson, L., & Hahn-Hagerdal, B. (1996). *Enzyme and Microbial Technology, 18*, 312–331.
27. Fitzgerald, J. D., Stratford, M., Gasson, M. J., & Narbad, A. (2005). *Journal of Agricultural and Food Chemistry, 53*, 1769–1775.
28. Delgenes, J. P., Moletta, R., & Navarro, J. M. (1996). *Enzyme Microbial Technology, 19*, 220–225.
29. Dominguez, J. M., Gong, C. S., & Tsao, G. T. (1996). *Journal of Industrial Microbiology & Biotechnology, 30*, 279–291.
30. Ding, X., & Xia, L. (2006). *Applied Biochemistry and Biotechnology, 133*, 263–270.
31. Sanchez, B., & Bautista, J. (1988). *Enzyme Microbial Technology, 10*, 315–318.
32. Roberto, I. C., Lacis, L. C., Barbosa, M. F. S., & Mancilha, I. M. (1991). *Process Biochemistry, 26*, 15–21.
33. Martinez, A., Rodriguez, M. E., York, S. W., Preston, J. F., & Ingram, L. O. (2000). *Biotechnology and Bioengineering, 69*, 526–536.
34. Keating, J. D., Panganiban, C., & Mansfield, S. D. (2006). *Biotechnology and Bioengineering, 93*(6), 1196–1206.

Appl Biochem Biotechnol (2008) 148:109–117
DOI 10.1007/s12010-007-8082-2

Production and Characterization of Biodiesel from Tung Oil

Ji-Yeon Park · Deog-Keun Kim · Zhong-Ming Wang · Pengmei Lu · Soon-Chul Park · Jin-Suk Lee

Received: 18 April 2007 / Accepted: 11 October 2007 /
Published online: 6 November 2007
© Humana Press Inc. 2007

Abstract The feasibility of biodiesel production from tung oil was investigated. The esterification reaction of the free fatty acids of tung oil was performed using Amberlyst-15. Optimal molar ratio of methanol to oil was determined to be 7.5:1, and Amberlyst-15 was 20.8wt% of oil by response surface methodology. Under these reaction conditions, the acid value of tung oil was reduced to 0.72mg KOH/g. In the range of the molar equivalents of methanol to oil under 5, the esterification was strongly affected by the amount of methanol but not the catalyst. When the molar ratio of methanol to oil was 4.1:1 and Amberlyst-15 was 29.8wt% of the oil, the acid value decreased to 0.85mg KOH/g. After the transesterification reaction of pretreated tung oil, the purity of tung biodiesel was 90.2wt%. The high viscosity of crude tung oil decreased to 9.8mm^2/s at 40 °C. Because of the presence of eleostearic acid, which is a main component of tung oil, the oxidation stability as determined by the Rancimat method was very low, 0.5h, but the cold filter plugging point, −11 °C, was good. The distillation process did not improve the fatty acid methyl ester content and the viscosity.

Keywords Biodiesel · Eleostearic acid · Esterification by Amberlyst-15 · Fuel properties · Response surface methodology · Tung oil

Introduction

An interest in biodiesel produced from triacylglycerols as an alternative fuel for diesel engines has increased because of the increase in the price of petroleum and the environmental concerns about air pollution from vehicles [1–3]. Countries produce

J.-Y. Park · D.-K. Kim · S.-C. Park · J.-S. Lee (✉)
Korea Institute of Energy Research, 71-2, Jang-dong, Yuseong-gu, Daejeon 305-343, Republic of Korea
e-mail: bmjslee@kier.re.kr

Z.-M. Wang · P. Lu
Guangzhou Institute of Energy Conversion, no.2 Nengyuan Rd, Wushan, Tianhe,
Guangzhou 510-640, China

biodiesel from various vegetable oils depending upon their agricultural policies, local crop availability, and/or feedstock price [4–6]. The focus of biodiesel production is typically on edible oils like soybean, rapeseed, and palm. Recently, waste oils and fats like used frying oil, greases, and tallow were proposed and used as biodiesel resources [3]. The basic constituent of vegetable oils is a triglyceride, which is an ester composed of three fatty acids and one glycerol. Because the fatty acids of vegetable oils vary in carbon chain length and the number of double bonds, biodiesel has different properties depending on the fatty acid composition of the feedstock [7]. Generally, saturated fatty acid methyl esters have good oxidation stability and poor low temperature properties. On the contrary, unsaturated fatty acid methyl esters have good low temperature properties and poor oxidation stability. Therefore, the standard specification concerning the minimum requirements such as EN 14214 was established to guarantee the quality of biodiesel [8–9].

The alkali process for biodiesel production can achieve high purity and yield of biodiesel in a short time. However, vegetable oils high in free fatty acids result in the production of soap and the loss of catalyst in the alkali process. To overcome this, the free fatty acids should be removed before the transesterification reaction. Because a homogeneous acid catalyst like sulfuric acid can not be recovered and is toxic, a heterogeneous acid catalyst can be used for the esterification of free fatty acids. Solid catalysts can be easily recovered after the reaction and reused [10–12].

As the supply of biodiesel increases, the interest in nonedible oils like jatropha, castor, jojoba, and tung oil has grown. Among these oils, tung oil is pressed from the nuts of the tung tree (*Vernicia fordii*), and the nut has an oil content of 30 to 40%. Tung oil has been used as a protective coating or drying agent [13–14].

As tung oil has a high acid value (AV), the esterification using solid acid catalyst, Amberlyst-15, was employed to produce biodiesel more efficiently. Optimal condition of methanol and catalyst for the esterification was established by response surface methodology. The fuel properties of tung biodiesel produced from pretreated tung oil by alkali catalyst were analyzed.

Experimental Methods

Materials

Tung oil was kindly supplied from Guangzhou Institute of Energy Conversion in China. For the pretreatment of tung oil, methanol (Duksan Pure Chemical, Ansan, Kyungki, Republic of Korea; >99.5%) and Amberlyst-15 (Aldrich Chemical, Milwaukee, WI) were used. Potassium hydroxide (Junsei Chemical, Chuo, Tokyo, Japan; >85%) and methanol was used for the transesterification reaction. For gas chromatography analyses, *n*-heptane (J.T. Baker, Phillipsburg, NJ; >99.0%), methyl heptadecanoate (Fluka, Buchs SG, Switzerland; >99.5%), 1,2,4-butanetriol (Supelco, Bellefoute, PA; >98.5%), 1,2,3-tricaproylglycerol (Supelco; >99.9%), and *N*-methyl-*N*-trimethylsilyl-trifluoroacetamide (Aldrich Chemical) were used.

Pretreatment and Transesterification of Tung Oil

For the pretreatment of tung oil, the mixture of oil, methanol, and Amberlyst-15 was mixed by a magnetic stirrer at 80 °C for 2h. After the reaction, the AV of the samples was determined. Pretreated tung oil was used for the transesterification. Tung oil was mixed

with methanol and potassium hydroxide at 80 °C for 20min. After washing with distilled water and centrifuging at 15,000rpm for 15min, biodiesel properties were analyzed.

Analyses

The AV of tung oil was measured by titration method, following American Oil Chemists' Society (AOCS) official method Cd 3d-63. The water content was measured by Karl Fischer Titrator (Mettler Toledo model DL31 Volumetric KF Titrator, Columbus, OH) in accordance with AOCS official method Ca 2e-84. The oxidation stability measurements were carried out with the model 743 Rancimat (Metrohm, Herisau, Switzerland). Samples were analyzed under constant air flow of 10L/h at 110 °C heating block temperature. The temperature correction factor ΔT was set to 1.5 °C. The cold filter plugging point (CFPP) measurements were carried out with the model FPP5Gs (ISL, Carpiquet, France). The sample was cooled following the EN 116 method. At intervals of 1 °C, a 200-mm H_2O vacuum was applied to draw up the sample into a pipette through a filter. The temperature at which either the sample ceased to flow through the filter within 60s or failed to return into the test jar was recorded as the CFPP.

The fatty acid methyl ester (FAME) content was analyzed by gas chromatography equipped with an auto-injector (Agilent 6890A, Santa Clara, CA). The INNOWax (Agilent) column (30mm × 0.32mm × 0.5μm) was used for the analysis of FAME. The oven temperature was started at 50 °C for 1min, increased to 200 °C at a rate of 15 °C/min, held at the temperature for 9min, and again increased to 250 °C at a rate of 2 °C/min, and then held at the temperature for 2min. Methyl heptadecanoate was used as the internal standard. Total glycerin was determined by gas chromatography equipped with on-column injector (Agilent 6890N). The DB-5HT (Agilent) column (15m × 0.32mm × 0.1μm) was used for the analytical work. The oven temperature was held at 50 °C for 1min, increased to 180 °C at a rate of 15 °C/min, and increased to 230 °C at a rate of 7 °C/min, and again increased to 370 °C at a rate of 10 °C/min, and then held at the temperature for 10min. 1,2,4-Butanetriol and 1,2,3-tricaproylglycerol were used as the internal standards.

Results and Discussion

Properties of Tung Oil

The AV of crude tung oil was 9.55mg KOH/g, and its viscosity was 109.4mm^2/s at 40 °C. Because the free fatty acid of oil forms soap with the alkali catalyst and prevents the separation of biodiesel from glycerin, the pretreatment process to convert the free fatty acid to biodiesel is required [3]. Therefore, it is desired that the AV of tung oil decreases to less than 1mg KOH/g before the transesterification reaction using the alkali catalyst.

Pretreatment of Tung Oil

The solid acid catalyst, Amberlyst-15, was used for the esterification reaction of the free fatty acids of the tung oil because Amberlyst-15 showed good efficiency for the esterification of oleic acid with methanol [10].

The central composite design was used to determine the optimal conditions for the esterification of tung oil using Amberlyst-15. The independent variables were the molar equivalents of methanol to oil and the weight percent of Amberlyst-15 to oil. Experiment 1

was performed to determine the condition for the lowest AV of tung oil (Table 1). Experiment 2 was performed to examine the effects of AV on methanol and catalyst when the molar equivalents of methanol to oil were less than 5 (Table 2). All experiments were performed at 80 °C for 2h, as determined from our previous works [10].

The regression analysis and the analysis of variance were performed using SAS package (SAS 9.1, SAS Institute, Cary, NC). The contour plots were developed using the fitted quadratic polynomial equation obtained from regression analysis [15–16].

From the statistical analysis of experiment 1, the relation of conversion (F) and the amount of methanol (X) and catalyst (Y) was obtained as follows:

$$F(\%) = 89.76 + 1.09X + 5.64Y - 1.39X^2 + 2.20XY - 5.50Y^2 \left(R^2 = 0.9767\right)$$

Maximum conversion was 92.5% at $X = 1.006$ and $Y = 0.777$ (Fig. 1). When the molar ratio of methanol to oil was 7.5:1 and Amberlyst-15 was 20.8wt% of oil, the final AV was 0.72mg KOH/g. At constant catalyst amount with varying methanol amount, the conversion slightly increased with the amount of methanol. At constant methanol amount with varying catalyst amount, the conversion rapidly increased with the catalyst amount but decreased again when the catalyst amount was more than 20% of oil. Therefore, the catalyst loading was an important factor to obtain the high conversion.

From the statistical analysis of experiment 2, the relation of conversion (F) and the amount of methanol (X) and catalyst (Y) was obtained as follows:

$$F(\%) = 86.39 + 9.10X + 1.55Y - 5.86X^2 + 0.51XY - 0.76Y^2 \left(R^2 = 0.9849\right)$$

Maximum conversion was 91.2% at $X = 0.833$ and $Y = 1.303$ (Fig. 2). When the molar ratio of methanol to oil was 4.1:1 and Amberlyst-15 was 29.8wt% of oil, the final AV was

Table 1 Experimental matrix for the central composite design (experiment 1).

Run	MeOH to oil (molar equivalents)	Amberlyst-15 to oil (wt%)	Final acid value (mg KOH/g)	X	Y	F (%)
1	3.41	7.5	2.03	−1	−1	78.7
2	3.41	15	1.14	−1	0	88.0
3	3.41	22.5	1.43	−1	1	85.1
4	5.45	7.5	1.38	0	−1	85.6
5	5.45	22.5	1.00	0	1	89.5
6	7.49	7.5	2.27	1	−1	76.3
7	7.49	15	0.93	1	0	90.2
8	7.49	22.5	0.82	1	1	91.4
9	2.56	15	1.40	−1.414	0	85.4
10	8.34	15	1.07	1.414	0	88.8
11	5.45	4.395	3.32	0	−1.414	65.3
12	5.45	25.605	1.05	0	1.414	89.0
13	5.45	15	0.92	0	0	90.4
14	5.45	15	1.05	0	0	89.0
15	5.45	15	0.99	0	0	89.6

MeOH to oil (molar equivalents)=2.04X+5.45, Amberlyst-15 to oil (wt%)=7.5Y+15

F (%) The conversion of free fatty acid

Table 2 Experimental matrix for the central composite design (experiment 2).

Run	MeOH to oil (molar equivalents)	Amberlyst-15 to oil (wt%)	Final acid value (mg KOH/g)	X	Y	F (%)
1	1.64	12.5	3.70	−1	−1	61.3
2	1.64	20	2.65	−1	0	72.2
3	1.64	27.5	2.75	−1	1	71.2
4	3	12.5	1.52	0	−1	84.1
5	3	27.5	1.40	0	1	85.4
6	4.36	12.5	1.32	1	−1	86.2
7	4.36	20	1.07	1	0	88.8
8	4.36	27.5	0.97	1	1	89.9
9	1.07	20	3.69	−1.414	0	61.4
10	4.92	20	1.04	1.414	0	89.1
11	3	9.395	1.27	0	−1.414	86.8
12	3	30.605	1.05	0	1.414	89.0
13	3	20	1.35	0	0	85.9
14	3	20	1.21	0	0	87.4
15	3	20	1.26	0	0	86.8

MeOH to oil (molar equivalents)=1.36X+3, Amberlyst-15 to oil (wt%)=7.5Y+20

F (%) The conversion of free fatty acid

0.85mg KOH/g. At constant catalyst amount with varying methanol amount, the conversion rapidly increased with the amount of methanol but decreased again when the ratio of methanol to oil was more than 4:1. At constant methanol amount with varying catalyst amount, the conversion nearly was not changed. Therefore, with the small loading of methanol, the effects of the catalyst loading was not significant and the methanol loading was an important factor to get the high conversion.

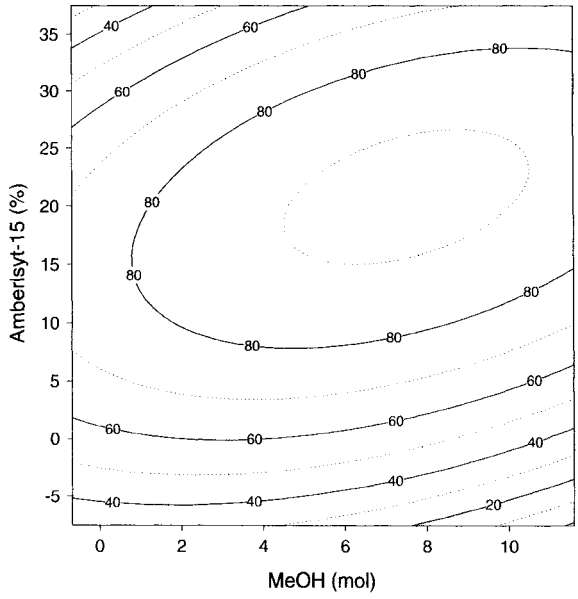


Fig. 1 Contour plot of conversion of free fatty acid of tung oil during pretreatment (experiment 1)

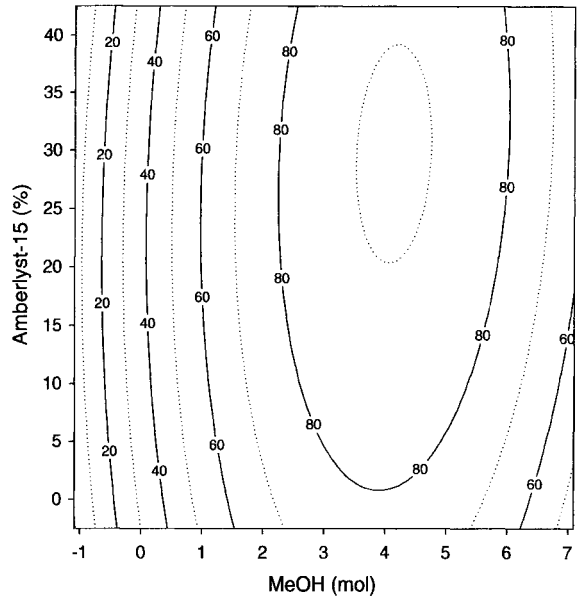


Fig. 2 Contour plot of conversion of free fatty acid of tung oil during pretreatment (experiment 2)

Transesterification of Tung Oil

Biodiesel was produced from pretreated tung oil. Reaction was performed using KOH as a catalyst at 80 °C for 20min. The final purity of tung biodiesel was 90.2wt% when the molar ratio of methanol to oil was 6:1 and KOH was 0.9% of oil and did not increase with increasing ratio of methanol to oil (Fig. 3).

Figure 4 shows the peaks of the components in the gas chromatogram. The highest peak was the peak of α-eleostearic acid. Although both eleostearic and linolenic acids have three double bonds, the structure and the properties of eleostearic acid are different from linolenic acid which was contained in soybean or rapeseed biodiesel (Fig. 5) [13, 17]. Table 3 shows the fatty acid composition of tung biodiesel. The saturated fatty acid content of tung biodiesel was 14.1% and the unsaturated fatty acid content was 84.6%. The content of

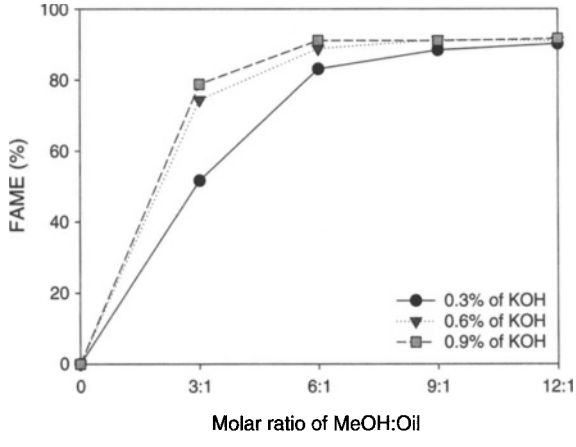


Fig. 3 Profile of FAME with amount of methanol and KOH

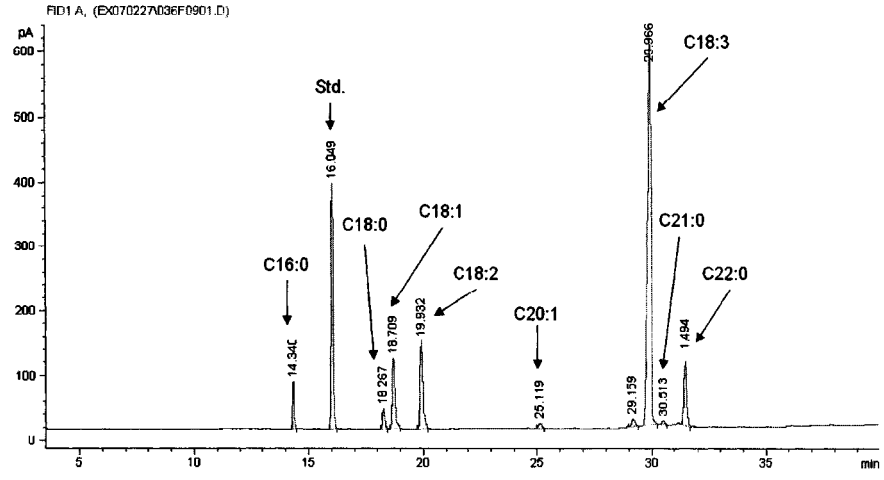


Fig. 4 Gas chromatogram of tung biodiesel

major component, α-eleostearic acid, was 63.8%. After the distillation, the amount of α-eleostearic acid decreased about 12.2%, and the unsaturated fatty acid decreased by about 8.3%. It was thought that some of α-eleostearic acid was polymerized during the distillation more than 300 °C because the eleostearic acid is more susceptible to polymerization than linolenic or linoleic acids [17–18].

Table 4 shows the properties of tung biodiesel before and after the distillation. When biodiesel was produced from rice bran oil, the purity increased more than 99% after the distillation [19]. However, the purity of tung biodiesel after the distillation was not enhanced much. The distillation of tung biodiesel was started more than 300 °C, which was a very high temperature compared with 160–220 °C of rice bran biodiesel [19]. The total glycerin of tung biodiesel was very low. The oxidation stability of tung biodiesel was very low, 0.5 h, as determined by the Rancimat method, because of the high content of eleostearic acid [8–9]. The initial AV was 9.55 mg KOH/g, but the AV of tung biodiesel was 0.59 mg KOH/g. The high viscosity of crude tung oil decreased to 9.8 mm^2/s at 40 °C after the transesterification. However, the viscosity of tung biodiesel was still much higher than the specification of biodiesel in most countries. The decrease in the viscosity by the distillation was trivial. The CFPP of tung biodiesel was −11 °C before the distillation. After

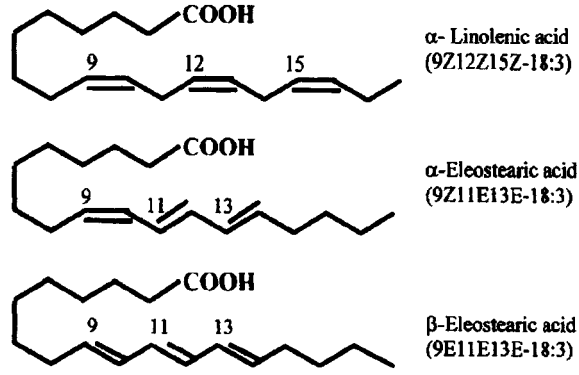


Fig. 5 Chemical structures of linolenic and eleostearic acid

Table 3 Fatty acid distribution of tung biodiesel.

Fatty acid (%)	Before distillation	After distillation
Palmitic acid (C16:0)	3.03	3.64
Stearic acid (C18:0)	2.20	2.55
Oleic acid (C18:1)	8.56	10.10
Linoleic acid (C18:2)	11.51	13.75
Eleostearic acid (C18:3)	63.80	51.64
Eicosenoic acid (20:1)	0.75	0.81
Heneicosanoic acid (C21:0)	0.46	1.02
Behenic acid (C22:0)	8.39	12.12
Not identified	1.30	4.37
Saturated fatty acid	14.08	19.33
Unsaturated fatty acid	84.62	76.30

the distillation, the CFPP increased a little because of the decrease in the unsaturated fatty acid content.

Conclusions

Tung biodiesel was produced by the esterification/transesterification reactions using Amberlyst-15 and KOH from tung oil. Amberlyst-15 showed a good esterification efficiency for the pretreatment of tung oil. The AV of tung oil decreased from 9.55 to 0.72 mg KOH/g. For the esterification of oils having a high content of free fatty acids, Amberlyst-15 will be a promising solid catalyst.

After the transesterification, the content of FAME was 90.2 wt%. The viscosity of tung oil decreased from 109.4 to 9.8 mm^2/s at 40 °C. Although the high viscosity of crude oil decreased much after transesterification, it was out of the biodiesel specification (EN 14214). Tung biodiesel contained 63.8% of α-eleostearic acid, which was an unsaturated fatty acid having three double bonds. Because of the high content of unsaturated fatty acid, tung biodiesel showed very low oxidation stability and very good cold temperature behavior. The distillation property of tung biodiesel was not good and needed a very high temperature more than 300 °C.

Tung biodiesel showed excellent cold temperature behavior, but its viscosity, FAME content, and oxidation stability did not satisfy EN 14214. If tung biodiesel is blended with palm biodiesel having a poor cold temperature performance, the blended biodiesel will have better cold temperature performance than neat palm biodiesel. The properties of tung

Table 4 Properties of tung biodiesel.

	Before distillation	After distillation
FAME (wt%)	90.2	90.4
Total glycerin (wt%)	0.046	0.016
Oxidation stability (h) at 110 °C	0.50	0.17
Water content (vol%)	0.23	0.01
Acid value (mg KOH/g)	0.59	0.46
Viscosity (mm^2/s) at 40 °C	9.8	8.7
CFPP (°C)	−11	−9

biodiesel such as viscosity, FAME content, and oxidation stability can be improved by the blending with other biodiesels. Therefore, tung biodiesel produced from nonedible tung oil can be used as a blend component of an alternative engine fuel, although tung biodiesel is not enough as a fuel for diesel engines by itself.

Acknowledgements This study was supported by the Resource Recycling R&D Center, 21C Frontier R&D Program.

References

1. Marchetti, J. M., Miguel, V. U., & Errazu, A. F. (2007). *Renewable & Sustainable Energy Reviews, 11* (6), 1300–1311.
2. Hass, M. J., Bloomer, S., & Scott, K. (2000). *Journal of the American Oil Chemists' Society, 77*(4), 373–379.
3. Ghadge, S. V., & Raheman, H. (2006). *Bioresource Technology, 97*, 379–384.
4. Foidl, N., Foidl, G., Sanchez, M., Mittebach, M., & Hackel, S. (1996). *Bioresource Technology, 58*, 77–82.
5. Canoira, L., Alcantara, R., Martinez, M. J. G., & Carrasco, J. (2006). *Biomass & Bioenergy, 30*, 76–81.
6. Conceicao, M. M., Candeia, R. A., Silva, F. C., Bezerra, A. F., Fernandes, V. J., & Souza, A. G. (2007). *Renewable & Sustainable Energy Reviews, 11*, 964–975.
7. Srivastava, A., & Prasad, R. (2000). *Renewable & Sustainable Energy Reviews, 4*, 111–133.
8. Knothe, G. (2005). *Fuel Processing Technology, 86*, 1059–1070.
9. Schober, S., & Mittelbach, M. (2004). *European Journal of Lipid Science and Technology, 106*, 382–389.
10. Kim, Y. J., Kim, D. K., Rhee, Y. W., Park, S. C., & Lee, J. S. (2005). *Korean Chemical Engineering Research, 43*(5), 621–626.
11. Marchetti, J. M., Miquel, V. U., & Errazu, A. F. (2007). *Fuel, 86*, 906–910.
12. Wang, Y., Ou, S., Liu, P., Xue, F., & Tang, S. (2006). *Journal of Molecular Catalysis A, Chemical, 252*, 107–112.
13. Sharma, V., & Kundu, P. P. (2006). *Progress Polymer Science, 31*, 983–1008.
14. Gryglewicz, S., Grabas, K., & Gryglewicz, G. (2000). *Bioresource Technology, 75*, 213–218.
15. Corino, C., Fiego, D. P. L., Macchioni, P., Pastorelli, G., Giancamillo, A. D., & Rossi, R. (2007). *Meat Science, 76*, 19–28.
16. Abdullh, A. G. L., Sulaiman, N. M., Aroua, M. K., & Noor, M. J. M. (2007). *Journal of Food Engineering, 81*, 65–71.
17. Tsuzuki, T., Tokuyama, Y., Igarashi, M., & Miyazawa, T. (2004). *Carcinogenesis, 25*(8), 1417–1425.
18. Tsuzuki, T., Igarashi, M., Iwata, T., Yamamoto, T., Ogita, K., & Miyazawa, T. (2004). *Lipids, 39*(5), 475–480.
19. Zullakah, S., Lai, C. C., Vali, S. R., & Ju, Y. H. (2005). *Bioresource Technology, 96*, 1889–1896.

Appl Biochem Biotechnol (2008) 148:119–129
DOI 10.1007/s12010-007-8046-6

Yeast Biomass Production in Brewery's Spent Grains Hemicellulosic Hydrolyzate

Luís C. Duarte · Florbela Carvalheiro · Sónia Lopes · Inês Neves · Francisco M. Gírio

Received: 17 May 2007 / Accepted: 4 September 2007 /
Published online: 26 September 2007
© Humana Press Inc. 2007

Abstract Yeast single-cell protein and yeast extract, in particular, are two products which have many feed, food, pharmaceutical, and biotechnological applications. However, many of these applications are limited by their market price. Specifically, the yeast extract requirements for culture media are one of the major technical hurdles to be overcome for the development of low-cost fermentation routes for several top value chemicals in a biorefinery framework. A potential biotechnical solution is the production of yeast biomass from the hemicellulosic fraction stream. The growth of three pentose-assimilating yeast cell factories, *Debaryomyces hansenii*, *Kluyveromyces marxianus*, and *Pichia stipitis* was compared using non-detoxified brewery's spent grains hemicellulosic hydrolyzate supplemented with mineral nutrients. The yeasts exhibited different specific growth rates, biomass productivities, and yields being *D. hansenii* as the yeast species that presented the best performance, assimilating all sugars and noteworthy consuming most of the hydrolyzate inhibitors. Under optimized conditions, *D. hansenii* displayed a maximum specific growth rate, biomass yield, and productivity of 0.34 h^{-1}, 0.61 g g^{-1}, and 0.56 g l^{-1} h^{-1}, respectively. The nutritional profile of *D. hansenii* was thoroughly evaluated, and it compares favorably to others reported in literature. It contains considerable amounts of some essential amino acids and a high ratio of unsaturated over saturated fatty acids.

Keywords *Debaryomyces hansenii* · Biomass · Single-cell protein · Hemicellulosic hydrolyzate · Brewery's spent grains · Agro-industrial residues upgrading · Yeast extract

Introduction

Yeast single-cell protein (SCP) and yeast extract (YE), in particular, are two products that have many food, feed, pharmaceutical, and biotechnological applications. However, many of these applications, e.g., yeast extract as nutrient source for industrial growth of

L. C. Duarte · F. Carvalheiro · S. Lopes · I. Neves · F. M. Gírio (✉)
INETI, Departamento de Biotecnologia, Estrada do Paço do Lumiar 22, 1649-038 Lisboa, Portugal
e-mail: francisco.girio@ineti.pt

microorganisms, are limited by the market price. Actually, yeast extract is one of the most relevant media supplements, and its replacement is one of the major technical hurdles to solve for developing low-cost fermentation routes to obtain several top value chemicals from biomass in a biorefinery framework, e.g., 3-hydroxypropionic acid, glutamic acid, and itaconic acid [1], polyols [2], and lactic acid production [3]. For the latter, an economic analysis showed that YE was the largest contributor accounting for 38% of the total production cost.

A possible cheap production approach for SCP and YE is the management of yeast biomass derived or produced within the biorefinery framework, namely, from the upgrading of the hemicellulosic fraction stream.

For this biotechnological process, there are several required traits for a yeast-cell factory, namely, the yeast should fully consume the different carbon sources present in the hydrolyzates, especially pentoses, exhibiting high yield and productivity. Other required traits include minimal byproduct formation, high tolerance to inhibitors, and to process hardiness. Simultaneous sugar utilization, minimal nutrient supplementation, and tolerance to both low pH and high temperature are also desirable traits [4]. Due to the potential food and feed applications of these products, the GRAS or QPS [5] status are additional requirements for any yeast strain.

The yeasts currently used and/or studied for SCP production, e.g., *Candida utilis*, are not able to utilize all sugars present, namely, arabinose, and as they belong to the *Candida* genus [6–8], they are not suitable for QPS status. It is thus important to develop new YE/SCP producing processes based on different yeasts.

Among other possibilities, three naturally pentose-assimilating yeasts, *Debaryomyces hansenii*, *Kluyveromyces marxianus*, and *Pichia stipitis* can be considered as strong potential candidates for cell factory. These yeasts have been used as model microorganisms mainly for the production of ethanol (*P. stipitis* and *K. marxianus*) [9, 10], SCP, and heterologous enzymes (*K. marxianus*) [11, 12] and polyols (*D. hansenii*) [2, 13]. Furthermore, they are prone, although at different levels, to genetic manipulation to achieve higher productivities from pentose metabolism [9, 14]. Moreover, *D. hansenii* and *K. marxianus* have already a QPS status [5].

In this work, we comparatively assessed the potential of brewery's spent grains (BSG) hemicellulosic hydrolyzate for YE and SCP production using *D. hansenii*, *K. marxianus*, and *P. stipitis*.

Materials and Methods

Feedstock and Hydrolysis

BSG was obtained from a local brewery (SCC-Sociedade Central de Cervejas e Bebidas, Vialonga, Portugal). The feedstock material was pretreated in an autoclave (Uniclave 88, AJC, Lisbon, Portugal) for residual starch removal, as described before [15]. The pretreated BSG was subjected to a two-step process hydrolysis consisting of an autohydrolysis followed by a sulfuric acid catalyzed posthydrolysis, as optimized before [16]. Autohydrolysis was carried out for 2.5 min at 190 °C in a 2-l stainless steel Parr reactor model 4532 (Moline, Illinois, USA), with a liquid to solid ratio of 8:1. The oligosaccharide-containing liquor was separated from the residual solid by filtration (Whatman no. 1 filter paper). Posthydrolysis were carried out in autoclave at 121 °C for 15 min after H_2SO_4 was added to the liquor to reach a final concentration of 2% (*w*/*w*).

The pH of the acid hydrolyzates was increased to 5.5 (cultivation pH) by the addition of $Ca(OH)_2$. After 1 h at pH 5.5, the precipitate was removed by centrifugation at 7,500×*g* for 25 min (Beckman Coulter, Fullerton, USA).

Microorganisms and Maintenance

The yeast strains used were *D. hansenii* CCMI 941, *P. stipitis* CBS 5773, and *K. marxianus* CBS 6556, obtained from the National Collection of Yeasts Cultures (UK), as NCYC 2597. The strains were maintained on YM agar slants containing 20 g l^{-1} glucose, 3 g l^{-1} yeast extract, 3 g l^{-1} malt extract, 5 g l^{-1} peptone, and 20 g l^{-1} agar.

Medium Preparation

To compare the performance of the three yeast species and to prevent growth limitations due to any nutritional deficiency, the BSG hydrolyzate was supplemented with several mineral nutrients and vitamins to reach the concentrations described in Duarte et al. [17]. *D. hansenii* biomass production for subsequent studies was carried out using a previously optimized medium containing 0.5 g l^{-1} KH_2PO_4 as the only supplement to BSG hydrolyzate [2]. To prevent nutrient thermal decomposition, all media were filter sterilized using a 0.22-μm Gelman membrane filters (Pall Corporation, Ann Arbor, MI, USA).

Cultivation Conditions

A 24-h-grown YM slant was used to seed 100 ml of hydrolyzate medium in a 1,000 ml baffled Erlenmeyer flask capped with cotton wool stopper. After 17 h, 2.5 ml of this culture was used to seed a similar flask and medium. Initial cell dry weight concentration was about 0.4 g l^{-1}. All cultures were carried out aerobically, in an Infors® Unitron (Bottmingen, Switzerland) orbital incubator set at 30 °C and 150 rpm. All cultivation assays were done at least in duplicate, and the mean values are reported.

At preset fermentation times, samples were withdrawn for high performance liquid chromatography (HPLC) analysis, pH, and cell growth measurements. To have enough biomass for macromolecular, amino acids and fatty acid analysis, several shake flask cultivations in media containing only 0.5 g l^{-1} KH_2PO_4 were performed. At the end of fermentation period (24 h), cells were harvested by centrifugation (Sigma, Osterode am Harz, Germany) at 9,000×*g*, 4 °C and 15 min, washed twice with 0.9% (*w*/*v*) NaCl, and freezed until further use.

Analytical Methods

D-glucose, D-xylose, L-arabinose, formic, acetic and levulinic acids, ethanol, HMF, and furfural were analyzed by HPLC using an Aminex HPX-87H column from Bio-Rad (Hercules, CA, USA). The HPLC system was a Waters LC1 module 1 plus (Millfort, MA, USA) equipped with both a refractive index and an ultraviolet detector set at 280 nm (used to detect HMF and furfural). The mobile phase was 5 mM H_2SO_4, the column temperature 50 °C, and the flow rate 0.4 ml/min. The system was equipped with a Micro-Guard Cation-H Refill Cartridge from Bio-Rad (Hercules, CA, USA) before the HPX-87H column. Due to the partial overlap of arabinose, xylitol and arabitol, samples were also analyzed by HPLC using a Waters Sugar Pak 1 column (Millfort, MA, USA). Also used was a Merck Hitachi HPLC

system (Tokyo, Japan) equipped with a refractive index detector (L-7490). The mobile phase was 50 mg l^{-1} calcium ethylenediaminetetraacetic acid (EDTA), the column temperature 90 °C, and the flow rate 0.5 ml/min. As this method does not allow to distinguish between D- and L-arabitol, the latter was used as arabitol standard. All samples were filtered by 0.45 μm Gelman membrane filters before analysis.

Phenolic compounds were quantified spectrophotometrically by a modification of the Prussian blue method as described by Graham [18]. Tannic acid was used as calibration standard.

Cell mass was followed spectrophotometrically (OD_{600nm}), diluting when necessary. At the beginning and at the end of fermentations, biomass dry weight was determined gravimetrically, by filtration of 5 ml of culture broth through 0.45 μm Gelman membrane filters, washing with a double volume of water and drying overnight at 100 °C to constant weight.

All assays were done at least in duplicate.

Macromolecular Composition

Quantitative acid hydrolysis with 72% (*w*/*w*) H_2SO_4 [19] was used to characterize the BSG feedstock. The monosaccharides and acetic acid were determined by HPLC to estimate (after corrections for stoichiometry and sugar decomposition) the contents of glucan (cellulose) and hemicelluloses (xylan, arabinan, and acetyl groups) in the sample. The acid-insoluble residue after hydrolysis was recovered by filtration and considered as Klason lignin after correction for the acid-insoluble ash. Protein was determined by the Kjeldahl method [20] using the $N \times 6.25$ conversion factor.

Protein content in the yeast biomass was also determined by the Kjeldahl method using the conversion factor of 6.25. Total carbohydrates in yeast biomass were determined by the anthrone method [21]. RNA content was determined by the Schmidt-Thannhauser method as described in Benthin et al. [22]. Fat content was determined in dried cells by a Soxhlet extraction procedure using petroleum ether (60–80 °C) as solvent [23]. Ash content was determined by igniting the samples at 575 °C for 5 h, both for the feedstock and yeast biomass. All results are reported on the dry basis.

Amino Acid Analysis

Amino acid content of the hydrolyzate and cell mass were determined in dried biomass according to Commission Directive [24] using a Biochrom 20 (Pharmacia Biotech) amino acid analyzer equipped with a photometric detector (440 nm for proline and 570 nm for all others). An external standard method was used.

Fatty Acid Analysis

Yeast biomass was freeze–dried and grounded. Fatty acid extraction and preparation of methyl esters were carried out according to Lepage and Roy [25]. Samples (100 mg) were transmethylated with 5 ml of methanol/acetyl chloride (95:5 *v*/*v*). The mixture was sealed in a light-protected Teflon-lined vial under nitrogen atmosphere and heated at 80 °C for 1 h. The vial contents were then cooled, diluted with 1 ml water, and extracted with 2 ml of *n*-heptane. The heptane layer was dried over Na_2SO_4, evaporated to dryness under nitrogen atmosphere and redissolved in heptane, which contained the methyl esters.

The methyl esters were then analyzed by gas–liquid chromatography as described before [26], on a VARIAN (Palo Alto, USA) 3800 gas-liquid chromatograph equipped with a flame ionization detector. Separation was carried out on a 0.32 mm×30 m fused silica capillary column (30 m, 0.32 mm ID, film 0.32 μm) Supelcowax 10 (SUPELCO, Bellafonte PA, USA) with helium as carrier gas at a flow rate of 1.3 ml min^{-1}. The column temperature was programmed at an initial temperature of 200 °C for 10 min, then increased at 4 °C min^{-1} to 240 °C and held there for 16 min. Injector and detector temperatures were 250 and 280 °C, respectively, and split ratio was 1:100. Peak identification and response factor calculation were carried out using known standards (Nu-Chek-Prep, Elysian, USA). For each sample, two independent derivations were prepared and injected twice.

Calculations

The specific growth rate (μ, h^{-1}) was calculated by linear regression of the $\ln(OD/OD_i)$ vs time for the exponential growth phase. The biomass volumetric production rate (productivity), Q_x (g l^{-1} h^{-1}), was calculated, at 24 h, based on cell dry weight produced per liter of culture medium per hour. The cell yield, Y_x (g/g), was calculated at 24 h, as the amount of cell dry weight formed per gram of all consumed sugars. The relative sugar consumption was calculated at 24 h, as the ratio of the amount of monosaccharide consumed to the individual initial monosaccharide amount.

Results and Discussion

Feedstock and Hydrolyzate Composition

Brewery's spent grains macromolecular composition varies much, as it is not a defined product from a single raw material; rather, it is a by-product from a mixture of several raw materials that can be processed in the brewery under quite variable conditions. The average composition of the used BSG is presented in Table 1.

Minerals and vitamins are usually found in BSG [27]. The mineral elements include aluminum, barium, calcium, chromium, cobalt, copper, iron, magnesium, manganese, phosphorus, potassium, selenium, silicon, sodium, strontium, sulfur, and zinc, typically all in concentrations lower than 0.5%, except for silicon that is the major mineral present. The vitamins include: biotin, choline, folic acid, niacin, pantothenic acid, riboflavin, thiamine, and pyridoxine. Although, many of the vitamins can be destroyed during the hydrolysis

Table 1 Average macromolecular composition of brewery's spent grains on a dry weight basis (%).

Component	BSG
Glucan	21.2
Hemicellulose	30.4
Xylan	19.8
Arabinan	9.8
Acetyl groups	0.8
Klason lignin	22.2
Protein	24.6
Ash	1.1

Table 2 Composition of brewery's spent grains hydrolyzate.

Compound	Concentration (g l^{-1})
Glucose	5.2
Xylose	14.9
Arabinose	6.2
Acetic acid	1.3
Formic acid	0.8
Levulinic acid	0.16
Furfural	0.64
HMF	0.05
Total phenolic compounds	1.3
Protein	1.2

processes, a part may become available for microbial growth, together with some nitrogen compounds.

The used BSG hydrolyzate composition is shown in Table 2. It has approximately 26 g l^{-1} of monosaccharides and a low level of microbial inhibitors, specially aliphatic acids, and furan derivatives compared to similar hemicellulosic hydrolyzates used for SCP production, e.g., eucalyptus wood [28] and sugar cane bagasse [7,8]. Also, it has a low content of phenolic compounds. Crude protein has a concentration of about 1.2 g l^{-1}. Much of this nitrogen (about half) is in ammonia form, the rest as amino acids (data not shown).

The impact of pH correction to 5.5 on the chemical composition of the hydrolyzate has been studied before [29] and leads to a decrease of about 6% in monosaccharide content and a more considerable removal of furan derivatives and phenolic compounds (10–15%). Aliphatic acid contents are not significantly affected.

Yeast Growth in Hemicellulosic BSG Hydrolyzate

All three yeast species, *D. hansenii*, *K. marxianus*, and *P. stipitis* were able to grow in fully supplemented BSG hydrolyzate medium without any detoxification step. Biomass production starts after a short lag phase, and specific growth rates are higher during glucose assimilation. It could be observed that there is a decrease in growth rate after glucose depletion, but markedly diauxic type growth was not observed for any yeast. Stationary phase was completely set in at 24 h.

Overall biomass productivity and yield differ much among the yeasts (Table 3) and reflect the ability to metabolize the different sugars and other compounds present. The high

Table 3 Kinetic and stoichiometric parameters, of *P. stipitis*, *K. marxianus*, and *D. hansenii* growth in supplemented brewery's spent grains hydrolyzate.

Parameter	*D. hansenii*	*K. marxianus*	*P. stipitis*
μ (h^{-1})	0.35	0.30	0.19
Q_x (g l^{-1} h^{-1})	0.47	0.20	0.32
Y_x (g g^{-1})	0.60	0.41	0.46
Consumed Glc (%)	100	100	100
Consumed Xyl (%)	100	70	100
Consumed Ara (%)	100	45	31

μ Specific growth rate, Q_x biomass productivity, Y_x biomass yield

D. hansenii biomass productivity reflects the ability of this yeast to fully make use of all monosaccharides present in the medium.

The yeasts exhibited a similar sugar utilization pattern (data not shown). Glucose and xylose were assimilated simultaneously, the former at a higher rate, enabling higher growth rates. Xylose was completely assimilated by *P. stipitis* and *D. hansenii*, but not by *K. marxianus*, which only consumed 70%. Arabinose was also assimilated by all yeasts simultaneously with late xylose assimilation, being only completely exhausted by *D. hansenii*. The other two yeasts, *Pichia stipitis* and *K. marxianus*, only consumed 31 and 45% of available arabinose, respectively. Furfural, acetic, and formic acid were also consumed (data not shown).

As expected for aerobic conditions, no metabolic products were found in significant amounts in the cultures supernatants, except for ethanol that was slightly produced by *P. stipitis* (maximum, 1 g l^{-1}).

Among these three yeasts, *D. hansenii* presented the best overall performance, and this comparison can be extended for other microorganisms grown in hemicellulosic hydrolyzates, e.g., *Candida tropicalis* [7] and *Paecilomyces variotii* [28]. *Candida langeronii* grown in sugar cane bagasse presented a higher biomass productivity of 0.97 g l^{-1} h^{-1} [8], but under fully controlled oxygen and pH conditions and using a higher sugar content. Nevertheless, the biomass yield for *C. langeronii* was 0.40 g g^{-1}, which is lower than that obtained for *D. hansenii*. Furthermore, *D. hansenii* has been reported to achieve, in chemostat cultures, a higher cell productivity of 2.5 g l^{-1} h^{-1} in chemically defined media using xylose as sole carbon and energy source [30].

D. hansenii has some other advantages over other yeasts, as it also tolerates high concentrations of inhibitors and is able to grow with a high biomass yield and productivity, with minimum supplement requirements. For BSG hemicellulosic two-step hydrolyzate, 0.5 g l^{-1} KH_2PO_4 was identified as the sole required supplement [2]. This has significant advantages at industrial level. Furthermore, besides its use as a polyol producer, it has many other biotechnological applications [31], namely, in food processing, e.g., cheese making, yoghurt, and meat products. Recently, it has also been reported that *D. hansenii* spent yeast was used to successfully replace yeast extract in growth media supplementation [32]. Hence, there is a need for developing efficient and economically viable procedures for its large-scale biomass production. Considering these advantages altogether with *D. hansenii* performance in BSG hydrolyzate makes this yeast species the proper choice for the subsequent analysis.

For optimized BSG supplemented media, *D. hansenii* displayed a maximum specific growth rate, biomass yield, and productivity of 0.34 h^{-1}, 0.61 g g^{-1}, and 0.56 g l^{-1} h^{-1}, respectively (data not shown).

D. hansenii Macromolecular Composition

The macromolecular composition of *D. hansenii* biomass after 24 h growth in optimized BSG medium is presented in Table 4. The total protein content of 31.8% is compared to 31.3 % reported for *C. tropicalis* [7], 37% for *Kluyveromyces fragilis* [23], and 48.1% for *C. langueronii* [8]. The protein yield per sugars consumed obtained, of 0.20 g g^{-1}, was similar to the reported value for shake flask cultures of *C. blankii* grown on xylose (0.22 g g^{-1}) [6]. Carbohydrate content was higher than the values reported for *C. langeronii* [8], and *K. fragilis* [23], but in the range of *C. blankii* [6]. These values are typical of carbon excess growth conditions for this yeast [33], and hence they can be further improved, namely, the protein content.

Table 4 Macromolecular composition of *D. hansenii* biomass grown on brewery's spent grains hydrolyzate.

Component	Relative composition (%, *w/w*)
Protein	31.8
Carbohydrates	41.6
Ash	10.8
Fat	2.3
RNA	9.0
Rest	4.5

The values obtained for the RNA content (that only include stable RNA, i.e., rRNA and tRNA) compares well to the values reported for *C. langeronii* [8], *C. kruseii* SO1, and *Saccharomyces* sp. LK3G [34] and are close to the upper end of the range (6–11%) previously reported [23]. Although this can be somewhat disadvantageous for human nutrition due to the negative health effects of a high nucleic acid intake that induces overproduction of uric acid crystals [23, 35], it may be interesting for biotechnological purposes, as in some cases, YE is used as a source of nucleic acids [36, 37]. DNA was not measured, as it usually has a fairly constant and low level regardless of the growth conditions. Typical reported values for DNA levels are 0.57 [23] and 1.4% [8]. Ash content of *D. hansenii* dried cells was found to be 10.8 %, which is within the range usually described in the literature (7–18%) [23, 38–40]. The rest value accounts for the DNA content and for pools of different building blocks and metabolites.

Amino Acid Composition

D. hansenii amino acid profile is presented in Table 5. *D. hansenii* protein contains considerable amounts of the essential amino acids. The profile compares favorably with the

Table 5 Amino acid composition (% of total protein) of *D. hansenii* biomass grown on brewery's spent grains hydrolyzate as compared to the FAO standard[a].

Amino acid	*D. hansenii*	FAO
Alanine	5.70	
Arginine	3.74	
Aspartic acid	8.51	
Cysteine	1.06	2.00
Glutamic acid	11.32	
Glycine	4.70	
Histidine	1.95	
Isoleucine	3.93	4.20
Leucine	6.00	4.80
Lysine	6.48	4.20
Methionine	0.99	2.20
Phenylalanine	3.71	2.80
Proline	3.42	
Serine	4.82	
Threonine	4.55	2.80
Tryptophan	N.d.	1.40
Tyrosine	4.88	2.80
Valine	5.21	4.20

N.d. Not determined

[a] [8, 28, 35, 45]

FAO food protein standard. All essential amino acids are present in amounts above or close to the required levels, with the exception of the sulfur-containing amino acids (methionine and cystein), which was expected, as yeast protein are described to have a low content of these amino acids [8, 23, 38]. Nevertheless, methionine and/or cysteine levels are above that described in literature for other yeast [7, 8, 23, 34, 40]. Among the nonessential amino acids, glutamic and aspartic acid are present in higher amounts as previously found for other yeasts [7, 23, 38]. Considering the overall amino acid composition, there seems to be interesting prospects for *D. hansenii* biomass use as a food/feed supplement.

Fatty Acid Composition

The distribution of fatty acids is presented in Table 6. Vaccenic acid (18:1ω7) was the major fatty acid found, which is consistent to the reported fatty acid for other *D. hansenii* strains where C18:1 was the major type of fatty acid identified [41]. The second most abundant fatty acid was linoleic acid (18:2ω6), which has been reported as the major fatty acid present in *K. fragilis* PC8002 [38]. Altogether, *D. hansenii*, compared to other yeasts, exhibited a much higher content of C18 fatty acids (more than 73%) and low levels of C16 fatty acids, which are usually the second most common fatty acids [23, 38, 41].

Concerning the degree of unsaturation, *D. hansenii* unsaturated fatty acid content is five times higher than the saturated fatty acids. This ratio is higher than the reported fatty acid content for other yeasts [23, 38], which can be advantageous as unsaturated fatty acids, namely, ω-3 and ω-6, are considered essential fatty acids that must be obtained from the diet because humans lack the anabolic processes for their synthesis [42]. Relatively to the polyunsaturated acid linolenic (C18:3ω3), *D. hansenii* has a higher content than *K. fragilis* PC8002 [38] but considerably lower than *K. fragilis* MTCC 188 [23], although the latter yeast has been reported to have a very low content of other unsaturated fatty acids. This high content of unsaturated fatty acids, specifically C18 unsaturated fatty acids, can also be an advantageous trait for a SCP/YE product. Actually, in *Saccharomyces cerevisiae*, unsaturated fatty acid composition is a significant determinant of ethanol tolerance [43]. Growing *S. cerevisiae* cells with a higher content of C18:1 fatty acids, either produced endogenously by the yeast or added as supplement to the growth media exhibit better efficacy in overcoming the toxic effects of ethanol. These results are consistent with the

Table 6 Fatty acid composition of *D. hansenii* biomass grown on brewery's spent grains hydrolyzate.

Fatty acid	Composition (% of total)
C10:0 Capric	0.36
C16:0 Palmitic	6.35
Iso C17:0 5-methyl hexadecanoic	1.66
C17:0 Margaric	2.30
C17:1 Heptadecenoic	7.86
C18:0 Stearic	3.19
C18:1ω7 Vaccenic	46.5
C18:1ω9 Oleic	0.49
C18:2ω6 Linoleic	19.5
C18:3ω3 α-Linolenic	0.70
C18:3ω6 γ-Linolenic	3.61
C20:0 Arachidic	0.35
Unidentified	7.10

current knowledge that yeast ethanol tolerance is resulting from the specific incorporation of C18:1 fatty acids in the lipidic membranes leading to a compensatory decrease in membrane fluidity. A similar trend was found in *Mucor fragilis*, where γ-linolenic acid production has increased when ethanol was added to the medium [44].

Conclusions

In non-detoxified fully supplemented BSG hemicellulosic hydrolyzate, *D. hansenii* assimilates all sugars and consumes most of the inhibitors, presenting both superior kinetic and stoichiometric performance compared to the other tested yeast species. This performance is maintained for minimal (optimized) supplemented BSG medium, and it is expected that this performance can be further improved for more controlled oxygen and pH growth conditions.

The nutritional profile of *D. hansenii* was thoroughly evaluated, and it compares favorably to others reported in literature. It contains considerable amounts of the essential amino acids and a high ratio of unsaturated over saturated fatty acids. These, together with the potential QPS and GRAS status of this yeast species, strongly support the use of *D. hansenii* as a suitable cell factory for using hemicellulosic hydrolyzates toward YE/SCP production in a biorefinery framework leading to valuable co-upgrade solutions from lignocellulosic byproducts.

Acknowledgements The authors thank Amélia Marques, Carlos Barata, and Céu Penedo for their technical support and also acknowledge Ana Partidário/Maria João Borges and Teresa Lopes da Silva for making possible the amino acid and fatty acid analysis, respectively.

References

1. Werpy, T., Petersen, G., Aden, A., Bozell, J., Holladay, J., White, J., et al. (2004). *Top value added chemicals from biomass. Volume I—Results of screening for potential candidates from sugars and synthesis gas*. Oak Ridge, TN: U.S. Department of Energy (DOE).
2. Carvalheiro, F., Duarte, L. C., Lopes, S., Parajó, J. C., Pereira, H., & Gírio, F. M. (2006). *Journal of Industrial Microbiology & Biotechnology, 33*, 646–654.
3. Tejayadi, S., & Cheryan, M. (1995). *Applied Microbiology and Biotechnology, 43*, 242–248.
4. Zaldivar, J., Nielsen, J., & Olsson, L. (2001) *Applied Microbiology and Biotechnology, 56*, 17–34.
5. European Food Safety Authority (2005). *QPS: Qualified Presumption of Safety of micro-organisms in food and feed*. EFSA, Parma, Italy.
6. Meyer, P. S., du Preez, J. C., & Kilian, S. G. (1992). *Biotechnology & Bioengineering, 40*, 353–358.
7. Pessoa, A., Jr., Mancilha, I. M., & Sato, S. (1996). *Journal of Biotechnology, 51*, 83–88.
8. Nigam, J. N. (2000). *World Journal of Microbiology & Biotechnology, 16*, 367–372.
9. Jeffries, T. W. (2006). *Current Opinion in Biotechnology, 17*, 320–326.
10. Ballesteros, M., Oliva, J. M., Negro, M. J., Manzanares, P., & Ballesteros, I. (2004). *Process Biochemistry, 39*, 1843–1848.
11. Revillion, J. P. D., Brandelli, A., & Ayub, M. A. Z. (2003). *Brazilian Archives of Biology and Technology, 46*, 121–127.
12. Bergkamp, R. J., Bootsman, T. C., Toschka, H. Y., Mooren, A. T., Kox, L., Verbakel, J. M., et al. (1993) *Applied Microbiology and Biotechnology, 40*, 309–317.
13. Rivas, B., Torre, P., Domínguez, J. M., Converti, A., & Parajó, J. C. (2006). *Journal of Agricultural and Food Chemistry, 54*, 4430–4435.
14. Terentiev, Y., Pico, A. H., Boer, E., Wartmann, T., Klabunde, J., Breuer, U., et al. (2004). *Journal of Industrial Microbiology & Biotechnology, 31*, 223–228.

15. Carvalheiro, F., Esteves, M. P., Parajó, J. C., Pereira, H., Gírio, F. M. (2004). *Bioresource Technology, 91*, 93–100.
16. Duarte, L. C., Carvalheiro, F., Lopes, S., Marques, S., Parajó, J. C., & Gírio, F. M. (2004). *Applied Biochemistry and Biotechnology, 113–116*, 1041–1058.
17. Duarte, L. C., Carvalheiro, F., Neves, I., & Gírio, F. M. (2005) *Applied Biochemistry and Biotechnology, 121*, 413–425.
18. Graham, H. D. (1992). *Journal of Agricultural and Food Chemistry, 40*, 801–805.
19. Browning, B. L. (1967). *Methods of wood chemistry.* In K. V. Sarkeanen, & C. H. Ludwig (Eds.), pp. 795–798. New York: John Wiley & Sons.
20. AOAC (1975). *AOAC official methods of analysis*. Washington, DC: AOAC International.
21. Herbert, D., Phipps, P. J., & Strange, R. E. (1971). *Methods in microbiology.* In J. R. Norris & D. W. Ribbons (Eds.), pp. 209–344. London: Academic Press.
22. Benthin, S., Nielsen, J., & Villadsen, J. (1991). *Biotechnology Techniques, 5*, 39–42.
23. Paul, D., Mukhopadhyay, R., Chatterjee, B. P., & Guha, A. K. (2002). *Applied Biochemistry and Biotechnology, 97*, 209–218.
24. 1998. Commission Directive 98/64/EC. *Establishing Community methods of analysis for the determination of aminoacids, crude oils and fats, and olaquindox in feedingstuffs and amending* Directive 71/393/EEC.
25. Lepage, G., & Roy, C. C. (1986). *Journal of Lipid Research, 27*, 114–120.
26. Silva, T. L., Santo, F. E., Pereira, P. T., & Roseiro, J. C. P. (2006). *Journal of Basic Microbiology, 46*, 34–46.
27. Mussatto, S. I., Dragone, G., & Roberto, I. C. (2006). *Journal of Cereal Science, 43*, 1–14.
28. Almeida e Silva, J. B., Mancilha, I. M., Vannetti, M. C. D., & Teixeira, M. A. (1995). *Bioresource technology, 52*, 197–200.
29. Carvalheiro, F., Duarte, L. C., Lopes, S., Parajó, J. C., Pereira, H., & Gírio, F. M. (2005).*Process Biochemistry, 40*, 1215–1223.
30. Nobre, A., Duarte, L. C., Roseiro, J. C., & Gírio, F. M. (2002). *Applied Microbiology and Biotechnology, 59*, 509–516.
31. Breuer, U., & Harms, H. (2006). *Yeast, 23*, 415–437.
32. Rivas, B., Moldes, A. B., Domínguez, J. M., & Parajó, J. C. (2004). *International Journal of Food Microbiology, 97*, 93–98.
33. Tavares, J. M., Duarte, L. C., Amaral-Collaço, M. T., & Gírio, F. M. (1999). *FEMS Microbiology Letters, 171*, 115–120.
34. Konlani, S., Delgenes, J. P., Moletta, R., Traore, A., & Doh, A. (1996). *Bioresource technology, 57*, 275–281.
35. Anupama & Ravindra, P. (2000). *Biotechnology Advances, 18*, 459–479.
36. Zhang, J. Y., Reddy, J., Buckland, B., & Greasham, R. (2003) *Biotechnology & Bioengineering, 82*, 640–652.
37. Baracat-Pereira, M. C., Coelho, J. L. C., Minussi, R. C., Chaves-Alves, V. M., Brandão, R. L., & Silva, D. O. (1999). *Applied Biochemistry and Biotechnology, 76*, 129–141.
38. Shay, L. K., & Wegner, G. H. (1986). *Journal of Dairy Science, 69*, 676–683.
39. El-Samragy, Y. A., Chen, J. H., & Zall, R. R. (1988). *Process Biochemistry, 23*, 28–30.
40. Rajoka, M. I., Kiani, M. A. T., Khan, S., Awan, M. S., & Hashmi, A. S. (2004) *World Journal of Microbiology & Biotechnology, 20*, 297–301.
41. Saldanha-da-Gama, A., Malfeito-Ferreira, M., & Loureiro, V. (1997). *International Journal of Food Microbiology, 37*, 201–207.
42. Shahidi, F., & Wanasundara, U. N. (1998). *Trends in Food Science & Technology, 9*, 230–240.
43. You, K. M., Rosenfield, C. L., & Knipple, D. C. (2003). *Applied and Environmental Microbiology, 69*, 1499–1503.
44. Silva, T. L., Pinheiro, H. M., & Roseiro, J. C. (2003). *Enzyme and Microbial Technology, 32*, 880–888.
45. Olsen, J., & Allermann, K. (1987). *Basic Biotechnology.* In J., Bu'Lock, & B., Kristiansen (Eds.), pp 285–308. London: Academic Press.

Appl Biochem Biotechnol (2008) 148:131–139
DOI 10.1007/s12010-007-8050-x

Lipase-Catalyzed Transesterification of Rapeseed Oil for Biodiesel Production with *tert*-Butanol

Gwi-Taek Jeong · Don-Hee Park

Received: 25 April 2007 / Accepted: 5 September 2007 /
Published online: 2 October 2007
© Humana Press Inc. 2007

Abstract Biodiesel is a fatty acid alkyl ester that can be derived from any vegetable oil or animal fat via the process of transesterification. It is a renewable, biodegradable, and nontoxic fuel. In this paper, we have evaluated the efficacy of a transesterification process for rapeseed oil with methanol in the presence of an enzyme and *tert*-butanol, which is added to ameliorate the negative effects associated with excess methanol. The application of Novozym 435 was determined to catalyze the transesterification process, and a conversion of 76.1% was achieved under selected conditions (reaction temperature 40 °C, methanol/oil molar ratio 3:1, 5% (w/w) Novozym 435 based on the oil weight, water content 1% (w/w), and reaction time of 24h). It has also been determined that rapeseed oil can be converted to fatty acid methyl ester using this system, and the results of this study contribute to the body of basic data relevant to the development of continuous enzymatic processes.

Keywords Biodiesel · Novozym 435 · *tert*-Butanol · Methanolysis

Introduction

Biodiesel (fatty acid methyl esters) is an alternative and renewable energy source, the development of which is hoped to reduce global dependence on petroleum, as well as air pollution. Biodiesel generated from a variety of vegetable oils and animal fats has characteristics similar to those associated with petro-diesel, including viscosity, volumetric heating value, cetane number, and flash point [1–3]. Several processes have thus far been developed for the production of biodiesel via acid-, alkali-, and enzyme-catalyzed

G.-T. Jeong
Engineering Research Institute, School of Biological Sciences and Technology,
Chonnam National University, Gwangju 500-757, Korea

D.-H. Park (✉)
School of Biological Sciences and Technology, Functional Food Research Center,
Biotechnology Research Institute, Institute of Bioindustrial Technology, Research Institute for Catalysis,
Chonnam National University, Gwangju 500-757, Korea
e-mail: dhpark@chonnam.ac.kr

transesterification reactions [3–5]. In the enzymatic process employed for the production of fatty acid methyl ester from oils, several parameters have been shown to influence both yield and rate. These parameters include the reaction solvent utilized, the reaction temperature, the type and concentration of the alcohol, the quantity of enzyme in the reaction, the water content, and the mixing rate [6].

As compared to other catalyst types used in the production of biodiesel, enzymes have several advantages. They enable conversion under reaction conditions milder than those required for chemical catalysts. Moreover, in the enzymatic process, both the transesterification of triglycerides and the esterification of free fatty acids occur in one process step. However, lipase-catalyzed transesterifications induce a series of drawbacks. As compared to conventional alkaline catalysis protocols, reaction efficiency tends to be rather poor, and thus enzymatic catalysis generally necessitates significantly longer reaction times and higher enzyme amounts. The primary obstacle to the application of enzymes in industrial processes is their relatively high cost [7].

In our study, we conducted the enzyme-catalyzed methanolysis of rapeseed oil using Novozym 435, a well-known nonspecific lipase. Novozym 435 facilitates reactions between a wide variety of alcohols and is also a remarkably heat-tolerant enzyme [6, 8]. Watanabe et al. [9] previously reported that immobilized *Candida antarctica* lipase was inactivated in the presence of more than half the stoichiometric amount of methanol against total fatty acids in the oil. This disadvantage was surmounted by the utilization of three-step methanolysis, in which only one third of the total amount of methanol was added in each stage [7, 9].

Generally, alcoholysis using long-chain or branched alcohols proceeds efficiently even in solvent-free systems, whereas methanolysis tends to result in fairly low ester conversions. This has been generally attributed to the poor solubility of methanol in oils than that of long-chain or branched alcohols and the tendency of methanol to inactive enzymes [7]. In particular, the difficulty inherent to the dissolution of both hydrophobic and hydrophilic substrates in a common low-toxicity reaction solvent has been the principal limitation of biological synthesis protocols [6, 10, 11]. Depending on the type of lipase employed, a variety of solvents for oils and alcohols have been suggested, including petroleum ether, hexane, iso-octane, 1,4-dioxane, *tert*-butanol, ionic liquids, supercritical carbon dioxide, and several others [7]. In all of our experiments, *t*-butanol was employed as the reaction solvent, primarily because of its high substrate solubility, as well as the ease inherent to the separation of the product from the by-products, a consequence of its low boiling point [6]. In addition, *tert*-butanol has been shown to ameliorate the negative effects associated with excessive methanol [12].

In the enzymatic process utilized for the production of fatty acid methyl ester (biodiesel) from rapeseed oil, several factors can influence both the yield and rate. These factors include the reaction solvent, reaction temperature, reaction time, methanol/oil molar ratio, enzyme amount, and water content [7, 9, 12–14]. The initial step of this study involved the identification of factors likely to influence the conversion.

In this study, we have attempted to determine the optimal conditions for enzyme-catalyzed methanolysis of biodiesel production, using rapeseed oil with methanol and Novozym 435.

Materials and Methods

Materials

The Novozym 435 (Lipase B from *C. antarctica*, EC 3.1.1.3, a nonspecific lipase immobilized on macroporous acrylic resin, 1–2% water content, 10,000 propyl laurate

units/g) was purchased from Novo Nordisk A/S (Bagsvaerd, Denmark). The *t*-butanol was purchased from Sigma-Aldrich (St. Louis, MO). The refined rapeseed oil originating from Jeju Island (South Korea) was supplied by Onbio (Bucheon, South Korea), and its characteristics are summarized in Table 1. Palmitic acid methyl ester, stearic acid methyl ester, oleic acid methyl ester, linoleic acid methyl ester, linolenic acid methyl ester, erucic acid methyl ester, and heptadecanoic acid methyl ester were obtained from Sigma-Aldrich and were chromatographically pure. Anhydrous methanol was acquired from Fisher Scientific. All other chemicals were of analytical grade, and the solvents were dried with molecular sieves (4Å, Yakuri Pure Chem., Japan) for 1day before use.

Lipase-catalyzed transesterification

Methanolysis was conducted in a 20mL reaction bottle, maintained at 40 °C in a rotary shaker at 260rpm. The initial weight of the rapeseed oil was 5g. To prevent direct contact between the lipases and the methanol drops, the methanol was mixed with 4mL *tert*-butanol and oil followed by the addition of lipases to the mixture. In all experiments without initial water content experiment, there was no set initial amount of water in reactant, with the exception of the water contained within the enzymes themselves.

To assess the effects of reaction temperature on enzymatic methanolysis, the reactions were conducted at 25–55°C, under the following conditions: the reactant was coupled with 5 of prepared rapeseed oil at a molar ratio of 3:1 with methanol and 5% (w/w) Novozym 435 based on the oil weight, for a reaction time of 2h. Mixing was conducted with a magnetic stirrer, which spun at approximately 200rpm. To determine the effects of enzyme amount on enzymatic methanolysis, 1–10% (w/w) Novozym 435 was added to the reactant, coupled with 5g of prepared rapeseed oil at a molar ratio of 3:1 with methanol and a reaction time of 24h at 40 °C in a rotary shaker at 260rpm. To determine the effects of the methanol/oil molar ratio on enzymatic methanolysis, a 1:1–6:1 molar ratio of methanol was added to the reactant, coupled with 5g of prepared rapeseed oil, with 5% (w/w) Novozym 435 and a reaction time of 24h at 40 °C in a rotary shaker at 260rpm. To determine the optimal initial water content and molecular sieve quantities for enzymatic methanolysis, 0–10% (w/w) water or 0–5% (w/w) molecular sieves were added to the reactant, coupled with 5g of prepared rapeseed oil at a molar ratio of 3:1 with methanol, with 5% (w/v) Novozym 435, for a reaction time of 24h at 40 °C in a rotary shaker at 260rpm. During the methanolysis, samples (100μL) were obtained from the reaction mixture at specified times. One hundred microliters of the sample, 400μL pyridine (served as solvent), and 500μL of the heptadecanoic acid methyl ester dissolved in pyridine (served as the internal standard) were measured precisely and

Table 1 Composition of fatty acids in rapeseed oils.

Properties	Value
Density	0.915
Acid value	0.01
Iodine value	112.1
Major fatty acid compositions[a] (% w/w)	Palmitic acid 4.14
	Stearic acid 1.57
	Oleic acid 35.86
	Linoleic acid 19.75
	Linolenic acid 7.77
	Erucic aicd 12.90

[a] The compositions of fatty acid in refined and crude rapeseed oils were identified by gas chromatography.

mixed for gas chromatographic analysis. The results of the experiments were expressed as the mean values from at least two independent measurements.

Analytical Methods

Gas Chromatography for Fatty Acid Methyl Ester Analysis

The fatty acid methyl ester contents in the reaction mixture were determined using a Donam 6100 GC gas chromatograph (Donam, South Korea) equipped with an HP-INNOWAX capillary column (30m × 0.32mm × 0.5μm) and an flame ionization detector. The column oven temperature was maintained at 210 °C for analysis. The injector and detector temperatures were set to 250 and 250 °C, respectively. Helium was utilized as a carrier gas. The gas chromatography calibration was conducted via the analysis of standard solutions of palmitic acid methyl ester, stearic acid methyl ester, oleic acid methyl ester, linoleic acid methyl ester, linolenic acid methyl ester, and erucic acid methyl ester. The internal standard was diluted in pyridine, as were the reaction mixture samples. The conversion was expressed as the percentage of fatty acid methyl esters generated relative to the theoretical maximum quantity, based on the amount of original oils. In this paper, the conversion was expressed as the fatty acid methyl ester content or in accordance with conversion.

Results and Discussion

In the enzymatic process utilized herein for the production of fatty acid methyl ester from rapeseed oil, several factors are known to influence conversion. The initial step of this study involved the identification of factors likely to influence conversion. In this study, *tert*-butanol was applied in lipase-catalyzed methanolysis. *tert*-Butanol has been utilized previously in several enzymatic process, including sorbitan ester synthesis [6, 15]. It has also been confirmed that *tert*-butanol is inert in the Novozym 435-catalyzed methanolysis of rapeseed oil for the production of biodiesel [12].

In the solvent-free system utilized herein, involving the following reaction conditions: 5% (w/w) Novozym, 3:1 methanol/oil molar ratio, 260rpm rotary shaker speed, and 40 °C, the conversion was found to be extremely low (only 1.8% at 24h), owing principally to the toxicity of excessive methanol on lipase activity and the difficulty of mixing, whereas the conversion (70.9% at 24h) was increased as the result of the addition of *tert*-butanol as a reaction solvent into the reaction mixture (data not shown). This has been explained as reported previously by Li et al. [12] that the presence of *tert*-butanol could improve the solubility of methanol in the reaction mixture, and thus lipase retained a high level of activity with all methanol added for lipase-catalyzed methanolysis.

Effect of Reaction Temperature on the Methanolysis

Generally, alkali-catalyzed transesterification is conducted at near the boiling point of the alcohol, but enzyme-catalyzed transesterification is performed at a low temperature to prevent the loss of lipase activity [9]. The low reaction temperature was also found to be desirable, as the reaction temperature was closely related to the energy cost inherent to the process of biodiesel production [3].

The effect of temperature on rapeseed oil methanolysis was assessed in a temperature range of 25 to 55 °C under the following conditions: 5% (w/w) Novozym 435 as a catalyst,

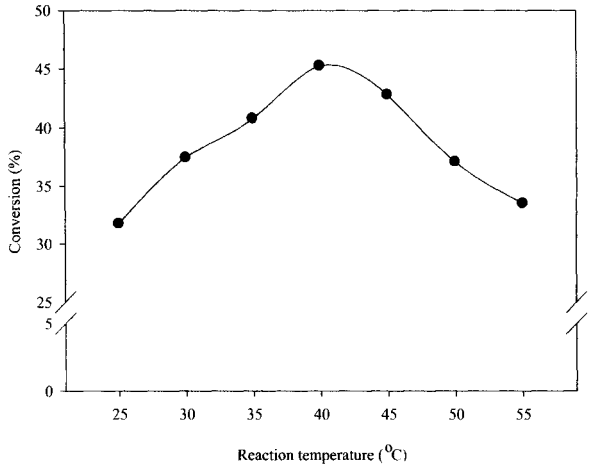


Fig. 1 Effect of reaction temperature on rapeseed oil methanolysis. Reaction conditions: 5% (w/w) Novozym 435 based on oil weight, methanol/oil molar ratio 3:1, agitation speed 300 rpm with magnetic stirrer, reaction time 2 h

a methanol/oil molar ratio of 3:1, and a 2-h reaction time. As is shown in Fig. 1, conversions decline at reaction temperatures in excess of 40 °C. The conversions at 2h increase with increasing reaction temperatures until 40 °C and after that begin to decline. At a reaction temperature of 40 °C, the conversion was approximately 45.3%. This result is similar to the results reported by Chen et al. [14], which were obtained via the methanolysis of waste cooking oil using *Rhizopus orzyae* lipase; however, they reported that reaction temperatures in excess of 40 °C induced a reduction in the methyl ester yield caused by the loss of enzyme activity, which was induced by high temperatures. Furthermore, Jeong et al. [11] previously reported that the optimal reaction temperature of Novozym 435 in sorbitan ester synthesis is 40–43 °C. However, in this study, an optimal reaction temperature of 40 °C may have allowed for the maintenance of high lipase activity and low reactant viscosity during mixing. However, this remains unclear, and the subject will require further investigation.

Effect of Enzyme Amount on Methanolysis

Novozym 435 has been reported to significantly augment the methanolysis of vegetable oils [6, 9, 12]. In this study, the effects of enzyme quantity on the enzymatic methanolysis of rapeseed oil for biodiesel production with *tert*-butanol used as a solvent has been evaluated. Figure 2 shows the effects of enzyme concentration on rapeseed oil methanolysis at 40 °C at a methanol/oil molar ratio of 3:1 for 24h. The conversion was enhanced by increases in enzyme concentration. The highest conversion attained was approximately 88.5% at 24h with 10% (w/w) Novozym 435. However, Li et al. [12] previously reported that the methyl ester yield was increased with increasing amounts of lipase and that when the lipase amount reached 2% (w/w), a methyl ester yield of 90% could be achieved at 12h. In enzyme-catalyzed methanolysis, the optimal enzyme and its usage amounts were selected in terms of optimal concentration rather than high conversion conditions, as a consequence of the significant cost associated with higher enzyme amounts. Considering the enzyme cost inherent to the enzyme-catalyzed methanolysis of rapeseed oil, an enzyme amount of 5% (w/w) was utilized in the rest of the study.

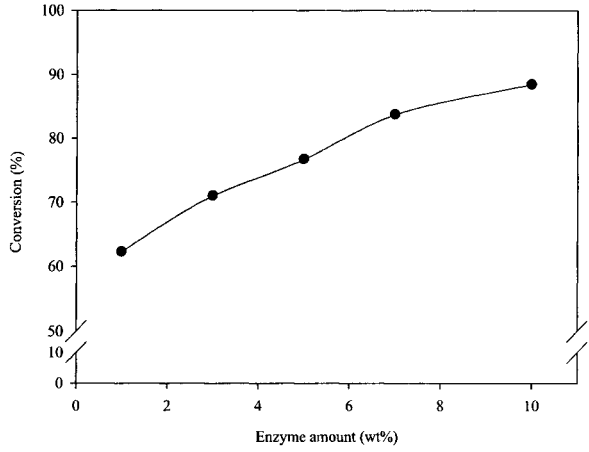


Fig. 2 Effect of enzyme amount on rapeseed oil methanolysis. Reaction conditions: Novozym 435 based on oil weight; methanol/oil molar ratio 3:1; reaction temperature 40 °C

Effect of Methanol/Oil Molar Ratio on Methanolysis

The stoichiometry of the methanolysis of oils requires 3mol of alcohol per 1mol of triglyceride to convert to 3mol of fatty acid methyl esters and 1mol of glycerol. The most significant factor in alkali/acid-catalyzed transesterification was the molar ratio of the alcohol and oil. As transesterification involves reversible and consecutive reactions, increases in the molar ratio of methanol will result in high conversions [3, 7]. However, in enzyme-catalyzed methanolysis, enzyme activity was shown to decrease in the methanolysis of oil as methanol concentration increased [13–14].

In this experiment, the effects of the methanol/oil molar ratio on rapeseed oil methanolysis oil were evaluated in a ratio range of 1:1 to 6:1, with a reaction temperature of 40 °C and 5% (w/w) Novozym 435 on the basis of oil weight as a catalyst for 24h, the results of which are indicated in Fig. 3. The conversion was enhanced in a linear fashion with increases in the methanol/oil molar ratio within a ratio range below 2:1. From the results of the methanol/oil molar ratio study, it was determined that when the molar ratio of methanol to oil was in a range of 2:1–5:1, high conversions were achieved, and no

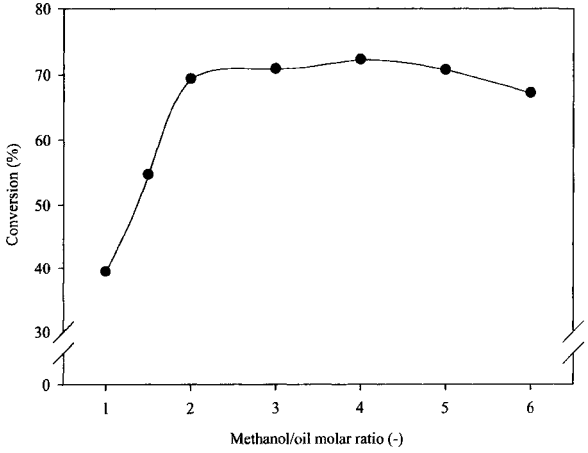


Fig. 3 Effect of methanol/oil molar ratio on rapeseed oil methanolysis. Reaction conditions: 5% (w/w) Novozym 435 based on oil weight; reaction temperature 40 °C

significant differences were detected with different methanol/oil molar ratios within this range. At methanol/oil ratios in excess of 6:1, the conversion was reduced. Considering the substantial operational stability of lipase, a methanol-to-oil molar ratio of 3 to 1 was utilized in the rest of the study.

Effect of Water Content and Molecular Sieve Amount on the Methanolysis

The activity of an enzyme in a nonaqueous reactant is known to be affected by the water content in the reactants. Additionally, the activity of the immobilized enzyme is reduced in aqueous systems, regardless of the immobilization method utilized [13].

In this study, the effects of the water content on the enzyme-catalyzed methanolysis of rapeseed oil was investigated via the addition of a small quantity of water to the reaction solution of methanol and rapeseed oil as substrates, *tert*-butanol as a solvent, and Novozym 435 as the enzyme. The reaction was conducted with the addition of water in a range from 0 to 10% (w/w) based on the weight of rapeseed oil, with a constant temperature of 40 °C and a reaction time of 24h. As is shown in Fig. 4, the highest conversion was approximately 76.1% at a water content of 1% (w/w). The conversion increased in a linear fashion with increases in the water content within a range of below 1% (w/w). At water content values in excess of 1% (w/w), the conversion was reduced in a linear fashion.

Figure 5 shows the effects of the application of molecular sieves as water absorbers on enzyme-catalyzed rapeseed oil methanolysis, using methanol as the substrate. The reaction was conducted via the addition of molecular sieves at a concentration of 0 to 10% (w/w) based on the weight of the rapeseed oil with a methanol/oil molar ratio of 3:1, a constant temperature of 40 °C, and reaction time of 24h. As can be observed in Fig. 5, the conversion evidenced no significant differences with the addition of molecular sieves within a range of 0–5% (w/w). With regard to our study, Jeong and Park [6] previously reported that the addition of molecular sieves was determined to generally inhibit sorbitan ester synthesis; however, neither the addition of water nor the dehydration of water with molecular sieves was found to be required for the enzymatic synthesis of sorbitan acrylate using Novozym 435, with the exception of the inherent water content of the enzymes.

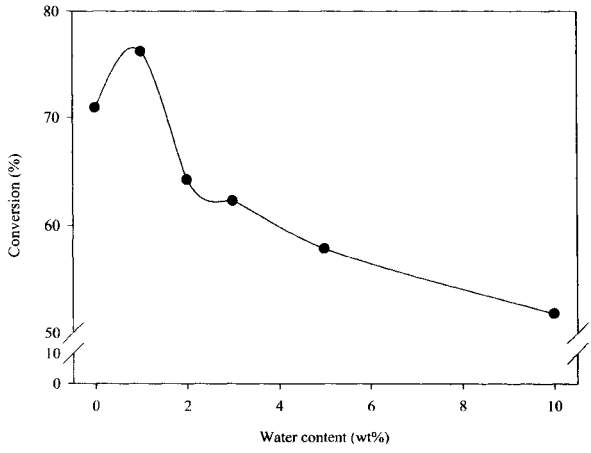


Fig. 4 Effect of water content on rapeseed oil methanolysis. Reaction conditions: 5% (w/w) Novozym 435 based on oil weight, methanol/oil molar ratio 3:1, reaction temperature 40 °C

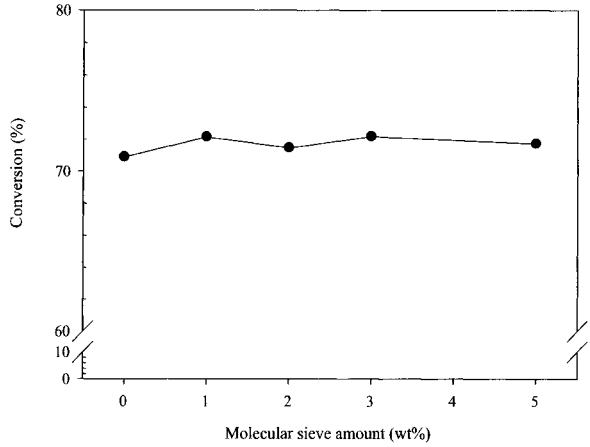


Fig. 5 Effect of molecular sieve amount on rapeseed oil methanolysis. Reaction conditions: 5% (w/w) Novozym 435 based on oil weight, methanol/oil molar ratio 3:1, reaction temperature 40 °C

Effect of Reaction Time on Methanolysis

In the process of biodiesel production, reaction temperature, methanol quantity, and reaction time were found to be significant operating parameters, which are closely associated with energy costs from an economic perspective [3]. Figure 6 shows the effects of reaction time on enzyme-catalyzed rapeseed oil methanolysis at the following conditions: 5% (w/w) Novozym, 3:1 methanol/oil molar ratio, and 40 °C. Within 10h, the reaction proceeded very fast and in a linear fashion. Rapeseed oil was converted at a rate greater than 67.7% within 12h and achieved an equilibrium state after approximately 24h.

However, Salis et al. [15] reported that solvent-free synthesis of oleic acid short-chain alcohols reached 100% of triolein conversion after only 6h at 40 °C by immobilized lipase of *Pseudomonas cepacia*. Furthermore, Kim [16] reported that the high conversion of 98.5% was possible at 45 °C of reaction temperature with 4:1 of methanol to oil molar ratio and 1% (v/v) methyl glucoside oleic polyester as an emulsifier using Novozym 435 in the presence of cosolvent. However, several researchers have reported that the conversion of

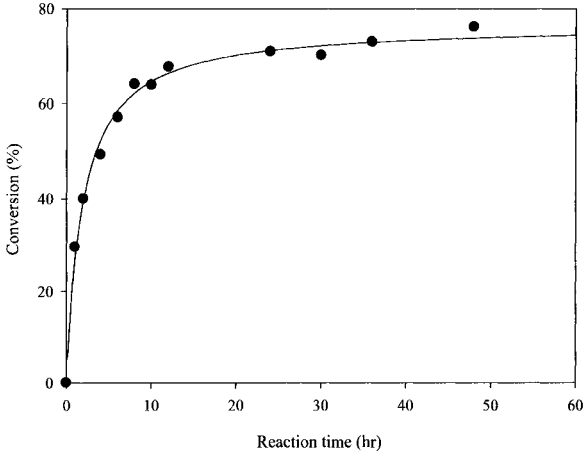


Fig. 6 Rapeseed oil methanolysis. Reaction conditions: 5% (w/w) Novozym 435 based on oil weight, methanol/oil molar ratio 3:1, reaction temperature 40 °C

vegetable oils to fatty acid methyl ester via alkali-catalyzed transesterification was achieved at a rate of above 90% within 5min with a sufficient molar ratio [2, 3, 17].

Conclusions

In this study, we have attempted to evaluate the efficacy of a technique for the production of the methyl ester of rapeseed oil via enzyme-catalyzed transesterifications using *tert*-butanol, a moderately polar organic solvent. We conducted experiments involving the alteration of several reaction conditions, including reaction temperature, methanol/oil molar ratio, enzyme amount, water content, and reaction time. The selected conditions for biodiesel production were as follows: reaction temperature 40 °C, Novozym 435 5% (w/w), methanol/oil molar ratio 3:1, water content 1% (w/w), and 24h of reaction time. Under these reaction conditions, a conversion of approximately 76.1% was achieved. Further studies are currently underway to determine a method by which the cost of fatty acid methyl ester production might be lowered, via the development of enzyme-catalyzed methanolysis protocols involving a continuous bioprocess.

Acknowledgements This work is outcome of the Specialized Graduate School supported financially by the Ministry of Commerce, Industry and Energy (MOCIE).

References

1. Lang, X., Dalai, A. K., Bakhshi, N. N., Reaney, M. J., & Hertz, P. B. (2001). *Bioresource Technology, 80*, 53–62.
2. Jeong, G. T., Oh, Y. T., & Park, D. H. (2006). *Applied Biochemistry and Biotechnology, 129–132*, 165–178.
3. Jeong, G. T., & Park, D. H., et al. (2004). *Applied Biochemistry and Biotechnology, 114*, 747–758.
4. Freedman, B., Pryde, E. H., & Mounts, T. L. (1984). *JAOCS, 61*(10), 1638–1643.
5. Nelson, L. A., Foglia, T. A., & Marmer, W. N. (1996). *JAOCS, 73*(8), 1191–1195.
6. Jeong, G. T., & Park, D. H. (2007). *Applied Biochemistry and Biotechnology, 136–140*, 595–610.
7. Mittelbach, M., & Remschmidt, C. (2004). *Biodiesel-the comprehensive handbook* pp. 69–80. Vienna, Austria: Boersedruck Ges.m.b.H.
8. Virto, C., & Adlercreutz, P. (2000). *Enzyme and Microbial Technology, 26*, 630–635.
9. Watanabe, Y., Shimada, Y., Sugihara, A., & Tominaga, Y. (2001). *Journal of the American Oil Chemists' Society, 78*, 703–707.
10. Castillo, E., Pezzotti, F., Navarro, A., & Lopez-Munguia, A. (2003). *Journal of Biotechnology, 102*, 251–259.
11. Jeong, G. T., & Park, D. H. (2006). *Enzyme and Microbial Technology, 39*, 381–386.
12. Li, L., Du, W., Liu, D., Wang, L., & Li, Z. (2006). *Journal of Molecular Catalysis B: Enzymatic, 43*, 58–62.
13. Iso, M., Chen, B., Eguchi, M., Kudo, T., & Shrestha, S. (2001). *Journal of Molecular Catalysis B: Enzymatic, 16*, 53–58.
14. Chen, G., Ying, M., & Li, W. (2006). *Applied Biochemistry and Biotechnology, 129–132*, 911–921.
15. Salis, A., Pinna, M., Monduzzi, M., & Solinas, V. (2005). *Journal of Biotechnology, 119*, 291–299.
16. Kim, H. S. (2003). *Journal of the Korean Oil Chemists' Society, 20*, 251–258.
17. Jeong, G. T., & Park, D. H. (2006). *Applied Biochemistry and Biotechnology, 129–132*, 668–679.

Appl Biochem Biotechnol (2008) 148:141–149
DOI 10.1007/s12010-008-8132-4

Bioethanol Production Optimization: A Thermodynamic Analysis

Víctor H. Álvarez · Elmer Ccopa Rivera · Aline C. Costa · Rubens Maciel Filho · Maria Regina Wolf Maciel · Martín Aznar

Received: 7 May 2007 / Accepted: 20 December 2007 /
Published online: 29 January 2008
© Humana Press Inc. 2008

Abstract In this work, the phase equilibrium of binary mixtures for bioethanol production by continuous extractive process was studied. The process is composed of four interlinked units: fermentor, centrifuge, cell treatment unit, and flash vessel (ethanol-congener separation unit). A proposal for modeling the vapor–liquid equilibrium in binary mixtures found in the flash vessel has been considered. This approach uses the Predictive Soave–Redlich–Kwong equation of state, with original and modified molecular parameters. The congeners considered were acetic acid, acetaldehyde, furfural, methanol, and 1-pentanol. The results show that the introduction of new molecular parameters r and q in the UNIFAC model gives more accurate predictions for the concentration of the congener in the gas phase for binary and ternary systems.

Keywords Bioreactors · Fermentation · Phase equilibria · Predictive Soave–Redlich–Kwong

Nomenclature

φ_i Fugacity coefficients of component i
q Area molecular parameters in the UNIFAC model
r Volume molecular parameters in the UNIFAC model
x_i Mole fraction in the liquid phase
y_i Mole fraction in the vapor phase
P Pressure of the system
T Temperature of the system

Introduction

The global demand for ethanol is increasing very quickly. In Brazil, the growth of the internal market is due to the new technology used in flex fuel vehicles (vehicles with the

V. H. Álvarez · E. C. Rivera (✉) · A. C. Costa · R. M. Filho · M. R. Wolf Maciel · M. Aznar
School of Chemical Engineering, State University of Campinas, P.O. Box 6066, 13083-970 Campinas, SP, Brazil
e-mail: elmer@feq.unicamp.br

A. C. Costa
e-mail: accosta@feq.unicamp.br

ability to operate with pure either ethanol or gasoline or even with any alcohol/gasoline blend) and the increase in oil prices. The growth of the foreign market is expected because of the enactment of the Kyoto Protocol and the implementation of environmental protection laws in many countries. Thus, there is an intensified interest in the study of all the steps involved in ethanol production and especially in the more intensive process as the extractive fermentation.

High concentrations of ethanol inhibit the fermentation process, particularly when a fermentative medium with high substrate concentration is used, as is the case in the majority of the industrial processes. Considering this, Silva et al. [1] studied a process of fermentation combined with a flash vessel, which selectively extracts ethanol from the medium as soon as it is produced. These authors have shown that this scheme presents many positive features and better performance than conventional industrial processes [2]. Cardona and Sanchez [3] point out that the reaction–separation integration is a particularly attractive alternative for the intensification of bioethanol production. When bioethanol is removed from the culture broth, its inhibition effect on the growth rate is diminished or neutralized. However, the performance of the whole process is significantly influenced by separation unit, and that means that thermodynamic knowledge of the mixture is required.

Most of the substances found in the culture broth to be separated are polar components. Besides, the very low concentration of many other components (apart from ethanol and water), called congeners, lead to difficulties to correlate and predict the concentration of the distilled product in the continuous extractive fermentation. Some of these substances (acetic acid, furfural, and methanol) are considered as a source of valuable co products [3], so that further downstream separation is justifiable.

Knowledge of the vapor–liquid equilibrium (VLE) behavior in these mixtures is necessary to design and to optimize the separation in the flash vessel, which is part of the extractive process considered in this work, described in the next section. The problem of phase equilibrium consists on the calculation of some variables of the set (T, P, x, and y) when some of them are known.

The flash vessel in the continuous extractive process operates under vacuum, but, in this study, the atmospheric pressure is considered, as no significant changes are expected to occur because of values of the used operating conditions. The classic thermodynamic models require knowledge of binary interaction parameters, which are usually determined from experimental data for binary systems.

In this study, the phase equilibrium in the binary mixtures that are expected to be found in the flash distillation was modeled with the Predictive Soave–Redlich–Kwong (PSRK) equation of state [4], using modified molecular parameters r and q. Five binary ethanol + congener mixtures were considered for new yield values for parameters r and q. The congeners considered were acetic acid, acetaldehyde, furfural, methanol, and 1-pentanol. Subsequently, the model was validated with the water + ethanol binary system, and the 1-pentanol + ethanol + water, 1-propanol + ethanol + water, and furfural + ethanol + water ternary systems.

Process Description and Modeling

Extractive Continuous Alcoholic Fermentation Process

The extractive fermentation process for bioethanol production proposed by Silva et al. [1] is shown in Fig. 1. The process is composed of four interlinked units: fermentor (ethanol

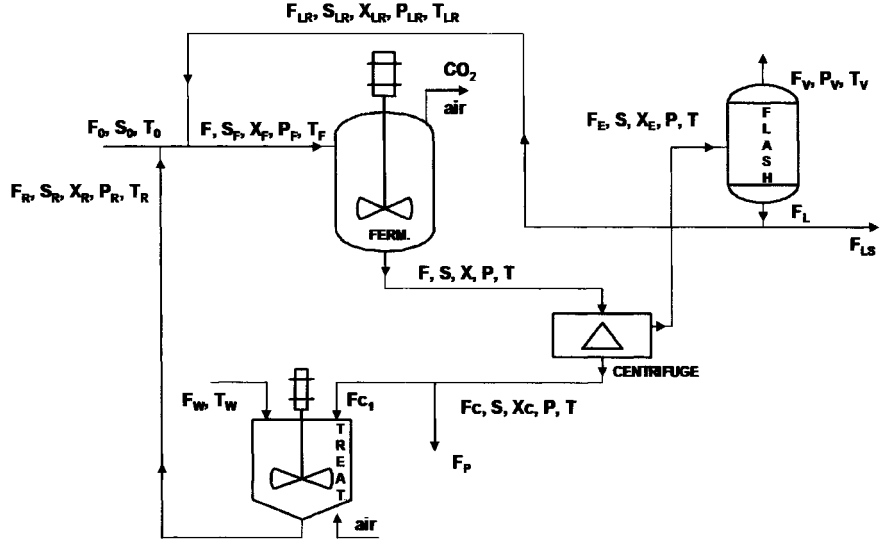


Fig. 1 Extractive alcoholic fermentation scheme

production unit), centrifuge (cell separation unit), cell treatment unit, and flash vessel (ethanol–water separation unit). This scheme attempts to simulate industrial conditions [2], with the difference that only one fermentor is used instead of a cascade system, and a flash vessel is used to extract part of the ethanol.

The flash vessel is an equipment where a close contact between a liquid and a vapor phase takes place to separate components based on the volatility difference among them. Thus, the liquid becomes rich with the less volatile components and the vapor with the most volatile components. The flash vessel is a single-stage distillation column.

The fermentation broth, without yeast, is led to the distillation flash, where the separation of the ethanol–water mixture occurs. The flash vessel must work in a temperature and pressure range to meet two main goals: cooling the broth in the fermentor to eliminate the necessity of heat exchangers in the industrial process and consequently diminishing the operational cost; and maintaining the ethanol concentration in the fermentor in levels such as it can act as antiseptic, around of 40 g/L, to prevent propagation of contaminants, typically bacteria [1]. The vapor phase pass through a condenser at 5°C to condense the rich ethanol vapor, and the liquid phase, poor in ethanol, returns to the fermentor.

The mathematical modeling of the process consists of mass and energy balance equations. All equipment, except the fermentor, are modeled assuming the hypothesis of "pseudo" steady state.

Assuming constant volume, the mass and energy balance equations for the fermentor can be written by using the intrinsic model [5, 6], with parameters adjusted as functions of the temperature from experimental data; the equations are given in Atala et al. [7]. A detailed description of the process and the mathematical model can be found in Costa et al. [8].

The Predictive Soave-Redlich-Kwong (PSRK) Equation of State: A Proposal for Modeling the Flash Vessel

The idea of combining simple cubic equations of state with excess Gibbs free energy (g^E) models, to describe the intermolecular interactions derived from the behavior of the liquid

and vapor phases, is well-known. Since Huron and Vidal [9] published their mixing rule for the attractive parameter "a" of a cubic equation of state (EoS), numerous publications have appeared, with more or less similar approaches [10].

The PSRK model was first proposed by Holderbaum and Gmehling [4] and considers the Soave–Redlich–Kwong equation of state [11] and the UNIFAC model for the excess free energy and the activity coefficient in the mixing rules, as shown below:

$$P = \frac{RT}{v-b} - \frac{a}{v(v+b)} \tag{1}$$

$$a_i = 0.42748 \frac{R^2 Tc_i^2}{Pc_i} \alpha(T) \tag{2}$$

$$b_i = 0.08664 \frac{RTc_i}{Pc_i} \tag{3}$$

For polar components, the expression proposed by Mathias and Copeman [12] is used to evaluate $\alpha(T)$ in the PSRK equation:

$$\alpha(T) = \left[1 + c_1\left(1 - T_r^{0.5}\right) + c_2\left(1 - T_r^{0.5}\right)^2 + c_3\left(1 - T_r^{0.5}\right)^3\right]^2 \quad for \quad T_r < 1 \tag{4a}$$

$$\alpha(T) = \left[1 + c_1\left(1 - T_r^{0.5}\right)\right]^2 \quad for \quad T_r > 1 \tag{4b}$$

In these equations, T_r is the reduced temperature and T_c is the critical temperature, whereas c_1, c_2, and c_3 are empirical parameters.

Table 1 UNIFAC functional groups and molecular parameters r and q.

Components	Subgroup	Contribution	R	q
Acetic acid	CH3	1	2.2024	2.0720
	COOH	1		
Acetaldehyde	CH3	1	1.8991	1.7960
	CHO	1		
Furfural	Furfural	1	3.1680	2.4810
Methanol	CH3OH	1	1.4311	1.4320
1-pentanol	CH3	1	4.5987	4.2080
	CH2	4		
	OH	1		
Ethanol	CH3	1	2.5755	2.5880
	CH2	1		
	OH	1		
Water	H2O	1	0.9200	1.4000
1-propanol	CH3	1	3.2499	3.1280
	CH2	2		
	OH	1		

Table 2 Properties for all substances involved in this study.

Components	M	T_b/K	T_c/K	P_c/MPa	V_c/m^3 kmol^{-1}	ω	Z_c
Acetic acid	60.1	391.05	591.95	5.786	0.180	0.46652	0.211
Ethanol	46.1	351.44	514.0	6.137	0.168	0.64356	0.241
Methanol	32.0	337.85	512.5	8.084	0.117	0.56583	0.222
1-pentanol	88.2	410.95	588.1	3.897	0.326	0.57314	0.260
Acetaldehyde	44.1	294.00	466.0	5.55	0.154	0.29073	0.221
Furfural	96.1	434.85	670.15	5.66	0.252	0.36778	0.256
Water	18.0	373.15	647.13	22.055	0.056	0.34486	0.229
1-pentanol	88.15	410.95	588.10	3.897	0.326	0.57314	0.260
1-propanol	60.10	370.35	536.8	5.169	0.218	0.62043	0.252

The mixing rules, which arise from combining the equation of state and a model for the excess Gibbs free energy [9, 13] are:

$$a = b\left[\frac{g^E}{A_1} + \sum x_1 \frac{a_i}{b_i} + \frac{RT}{A_1}\sum x_i \ln\frac{b}{b_i}\right] \tag{5}$$

where A_1 is a constant equal to −0.64663. Equation 5 is used together with the UNIFAC model for g^E [14] and the classical mixing and combination rule for the volume parameter b is assumed:

$$b = \sum_{i=1}^{N}\sum_{j=1}^{N} x_i x_j b_{ij} \quad b_{ij} = \frac{b_i + b_j}{2} \tag{6}$$

In these equations, a_i and b_i are the pure component constants in the equation of state as defined by Eqs. 2 and 3. A survey about the current status and potential of the PSRK equation of state has been recently presented by Horstmann et al. [15]. Different fields of

Table 3 Ranges of temperature, liquid-phase mole fraction, and vapor-phase mole fraction.

Systems	Temperature Range ΔT (K)	Liquid-Phase Fraction Δx_1	Vapor-Phase Fraction Δy_1
Ethanol (2)+			
Acetic acid	351–386	0.076–0.945	0.010–0.893
Acetaldehyde	315–339	0.100–0.450	0.495–0.959
Furfural	352–407	0.0201–0.9800	0.0048–0.35
Methanol	339–351	0.012–0.91	0.026–0.95
1-pentanol	353–406	0.083–0.985	0.012–0.875
Water	351–363	0.05–0.95	0.0526–0.6628
Ethanol (2) + water (3)			
1-pentanol	354–360	0.07–0.092	0.009–0.043
1-propanol	359–360	0.005–0.500	0.0263–0.350
Furfural	360–361	0.005–0.509	0.008–0.054

application are discussed by the authors, but applications to mixtures such as those discussed in this paper were not included. Details on how to calculate the different contributions and molecular parameters in the UNIFAC model are given in Table 1.

Modified PSRK Model

The PSRK model includes two molecular parameters, a volume parameter, r, and a surface area parameter, q. In this work, these molecular parameters are modified for ethanol, assuming them to be adjustable parameters. The VLE data for the binary systems acetic acid + ethanol, acetaldehyde + ethanol, furfural + ethanol, methanol + ethanol, and 1-pentanol + ethanol were used to obtain optimum values of r and q. This empirical approach tries to explain the modification of the molecular physical structure of ethanol mixed with some congener. An analogous empirical approach was applied for temperature-dependent variables in UNIFAC-Dortmund [16]. Then the method was validated with the binary system ethanol + water and three ternary systems, 1-pentanol + ethanol + water, 1-propanol + ethanol + water, and furfural + ethanol + water.

Table 2 shows the pure component properties of all the substances involved in this study. Here, M is the molecular weight, T_c is the critical temperature, T_b is the normal boiling temperature, P_c is the critical pressure, V_c is the critical volume, and ω is the acentric factor. Data were obtained from Diadem Public [17].

Table 3 gives some details on the experimental data used in the study. The simpler mixtures of VLE data were taken from Gmehling et al. [18].

Results and Discussion

Table 4 shows the average absolute deviations for the temperature, $\%|\Delta T|$, and for the vapor-phase concentration, $\%|\Delta y_i|$, comparing predicted and experimental values for all studied systems. These deviations are defined as follows:

$$\%|\Delta y_i| = \frac{100}{N}\sum \frac{|y_{cal} - y_{exp}|}{y_{exp}} \quad \%|\Delta T| = \frac{100}{N}\sum \left[\frac{T_{cal} - T_{exp}}{T_{exp}}\right] \tag{7}$$

The VLE data were analyzed using the PSRK model considering the molecular parameters r and q as adjustable parameters. To evaluate these parameters, a Genetic Algorithm optimization procedure, implemented and fully explained in Alvarez et al. [19]

Table 4 Percent deviations for the temperature and congener vapor-phase mole fraction used for the correlation developed in Equations 9 and 10.

Ethanol (2)+	Original. r = 2.5755, q = 2.5880		Optimized				Correlation	
	$\%\|\Delta T\|$	$\%\|\Delta y_1\|$	r	q	$\%\|\Delta T\|$	$\%\|\Delta y_1\|$	$\%\|\Delta T\|$	$\%\|\Delta y_1\|$
Acetic acid	0.3	24.4	2.8591	2.6304	0.2	22.8	0.2	22.7
Acetaldehyde	0.7	4.4	2.7217	2.4872	0.4	4.8	0.4	4.7
Furfural	0.4	22.8	2.4014	2.5911	0.5	14.6	0.5	13.3
Methanol	0.2	6.7	2.7675	2.6299	0.2	5.9	0.2	6.1
1-pentanol	0.4	7.9	2.3088	2.5764	0.3	9.3	0.3	9.2

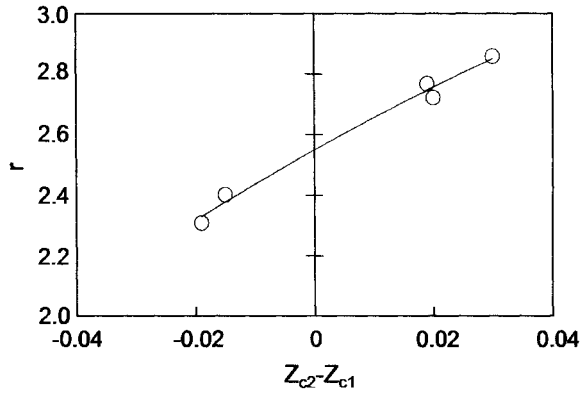


Fig. 2 Optimum molecular parameter r for the congener component in the PSRK model

was used. Thus, the optimization programs developed for this study used the objective function O_f:

$$O_f = \sum_{1}^{N} \left(y_1^{\exp} - y_1^{cal}\right)^2 \tag{8}$$

In this equation, N is the number of data points in the experimental data set and y_1 is the congener mole fraction in the vapor phase.

Results with the PSRK equation using original values for the molecular parameters r and q for ethanol in all mixtures congener (1) + ethanol (2) are shown in Table 4. As observed in this table, the PSRK model give good values for the boiling temperature, but reproduces the congener concentration in vapor phase with mean absolute deviations ranging from 4.4% to 24.4%.

The binary systems with acetic acid, acetaldehyde, furfural, methanol, and 1-pentanol congeners were used to obtain optimized molecular parameters for ethanol. The molecular parameters for ethanol, r and q, were optimized for each binary system resulting in different values for r and q, as shown in Table 4.

In the same way, the molecular r and q parameters for ethanol were optimized for each binary system, and so results in different values for these parameters.

The optimum parameters found for each of the five mixtures have been correlated with the critical compressibility factor (Z_c) for r and the acentric factor (ω) for q, as shown in

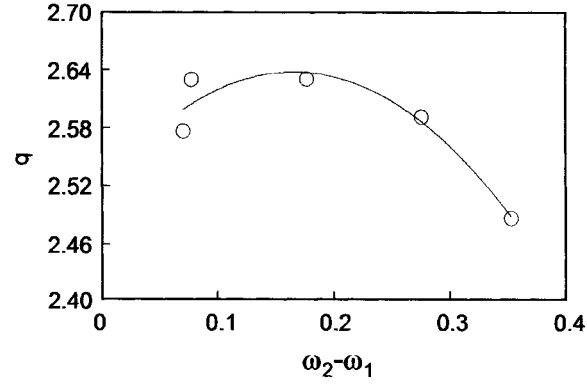


Fig. 3 Optimum molecular parameter q for the congener component in the PSRK model

Table 5 Percent deviations for the temperature and congener vapor phase mole fraction for a new binary system using original and modified PSRK model.

Ethanol (2)+	Original r=2.5755, q=2.5880			Correlation		
	%|ΔT|	%|Δy_1|	%|Δy_2|	%|ΔT|	%|Δy_1|	%|Δy_2|
Water	0.2	3.9	2.2	0.1	2.4	1.4

Figs. 2 and 3, respectively. These parameters have been fitted to quadratic functions as follows:

$$r = -30.325166(Z_{c2} - Z_{c1})^2 + 10.975229(Z_{c2} - Z_{c1}) + 2.548474 \quad (9)$$

$$q = -4.2758(\omega_2 - \omega_1)^2 + 1.4213(\omega_2 - \omega_1) + 2.5196 \quad (10)$$

In these equations, ω_2 and Zc_2 are the properties for the ethanol, and ω_1 and Zc_1 are the properties for each one of the congeners.

It can be noted that with the proposed modifications, the PSRK model becomes more empirical, but keeps the predictive capabilities of the model and, at the same time, improves its accuracy, which is demonstrated in Table 4. In addition, the model could be used for VLE in mixtures of interest for ethanol fuel.

In ternary systems, the structural parameters r and q of ethanol were calculated with the functions:

$$r = \omega_1 r_1 + \omega_2 r_2 \quad (11)$$

$$q = \omega_1 q_1 + \omega_2 q_2 \quad (12)$$

where r_i is the structural parameter r for ethanol with the congener i, and q_i is the structural parameter q for ethanol with the congener i. The experimental data for ternary systems were taken from Gmehling et al. [18].

Tables 5 and 6 showed the results of the percent deviations for the temperature and congener vapor phase mole fraction for binary and ternary systems. It can be seen that the results for the modified PSRK model are better than for the original model. In addition, different components were used as water and 1-propanol.

Table 6 Percent deviations for the temperature and congeners vapor-phase mole fraction for ternary system using original and modified PSRK model.

Ethanol (2) + water (3)	Original r=2.5755, q=2.5880				Equations 11 and 12			
	%|ΔT|	%|Δy_1|	%|Δy_2|	%|Δy_3|	%|ΔT|	%|Δy_1|	%|Δy_2|	%|Δy_3|
1-pentanol	0.3	34.7	4.9	10.2	0.9	28.7	4.4	8.2
1-propanol	0.1	19.2	4.0	3.0	0.4	19.9	3.5	2.6
1-furfural	0.5	42.1	7.4	13.8	1.8	43.4	4.3	7.3

Concluding Remarks

This work proposed the use of the Predictive Soave–Redlich–Kwong (PSRK) model to describe the phase equilibria in the flash distillation, using modified molecular parameters r and q for ethanol. In this way, the PSRK equation of state becomes more empirical, but keeps the predictive capabilities of the model. Furthermore, the introduction of new molecular parameters r and q in the UNIFAC model gives more accurate predictions for the concentration of the congener in the gas phase for binary and ternary systems.

The development presented in this work is important to be able to better understand the behavior of the flash distillation, which is a component of the extractive fermentation process. This allows the investigation of suitable operating strategies to achieve high operational performance.

Acknowledgments The authors acknowledge Fundação de Amparo à Pesquisa de Estado de São Paulo (FAPESP) and Conselho Nacional de Desenvolvimento Científico e Tecnológico (CNPq) for financial support.

References

1. Silva, F. L. H., Rodrigues, M. I., & Maugeri, F. (1999). *Journal of Chemical Technology and Biotechnology, 74*, 176–182.
2. Andrietta, S. R., & Maugeri, F. (1994). *Advances in Bioprocess Engineering, 1*, 47–52.
3. Cardona, A. C., & Sánchez, O. J. (2007). *Bioresource Technology, 98*, 2415–2457.
4. Holderbaum, T., & Gmehling, J. (1991). *Fluid Phase Equilibria, 70*, 251–265.
5. Monbouquette, H. G. (1987). *Biotechnology and Bioengineering, 29*, 1075–1080.
6. Monbouquette, H. G. (1992). *Biotechnology and Bioengineering, 39*, 498–503.
7. Atala, D. I. P., Costa, A. C., Maciel Filho, R., & Maugeri, F. (2001). *Applied Biochemistry and Biotechnology, 91–93*, 353–366.
8. Costa, A. C., Atala, D. I. P., Maugeri, F., & Maciel Filho, R. (2001). *Process Biochemistry, 37*, 125–137.
9. Huron, M. I., & Vidal, J. (1979). *Fluid Phase Equilibria, 3*, 255–271.
10. Prausnitz, J. M., Lichtenthaler, R. N., & Azevedo, E. G. (1999). *Molecular Thermodynamics of Fluid-Phase Equilibria*. New Jersey: Prentice Hall International Series.
11. Soave, G. (1972). *Chemical Engineering Science, 27*, 1197–1203.
12. Mathias, P. M., & Copeman, T. W. (1983). *Fluid Phase Equilibria, 13*, 91–108.
13. Mollerup, J. (1981). *Fluid Phase Equilibria, 7*, 121–138.
14. Fredenslund, Aa., Gmehling, J., & Rasmussen, P. (1977). *Vapor–Liquid Equilibria Using UNIFAC*. Amsterdam: Elsevier.
15. Horstmann, S., Fischer, K., & Gmehling, J. (2005). *Chemical Engineering Communications, 192*, 336–350.
16. Gmehling, J., Li, J., & Schiller, M. (1993). *Industrial & Engineering Chemistry Research, 32*, 178–193.
17. Diadem Public 1.2. (2000). The DIPPR Information and Data Evaluation Manager.
18. Gmehling, J., Onken, U., & Grenzheuser, P. (1982). *Vapor liquid equilibrium data collection*. Frankfurt: DECHEMA Chemistry Data Series.
19. Álvarez, V. H., Larico, R., Yanos, Y., & Aznar, M. (2007). *Brazilian Journal of Chemical Engineering*, in press.

Appl Biochem Biotechnol (2008) 148:151–161
DOI 10.1007/s12010-007-8120-0

Oxidation in Acidic Medium of Lignins from Agricultural Residues

Gisele Aparecida Amaral Labat · Adilson Roberto Gonçalves

Received: 9 May 2007 / Accepted: 3 December 2007 /
Published online: 3 January 2008
© Humana Press Inc. 2007

Abstract Agricultural residues as sugarcane straw and bagasse are burned in boilers for generation of energy in sugar and alcohol industries. However, excess of those by-products could be used to obtain products with higher value. Pulping process generates cellulosic pulps and lignin. The lignin could be oxidized and applied in effluent treatments for heavy metal removal. Oxidized lignin presents very strong chelating properties. Lignins from sugarcane straw and bagasse were obtained by ethanol–water pulping. Oxidation of lignins was carried out using acetic acid and Co/Mn/Br catalytical system at 50, 80, and 115 °C for 5 h. Kinetics of the reaction was accomplished by measuring the UV-visible region. Activation energy was calculated for lignins from sugarcane straw and bagasse (34.2 and 23.4 kJ mol^{-1}, respectively). The first value indicates higher cross-linked formation. Fourier-transformed infrared spectroscopy data of samples collected during oxidation are very similar. Principal component analysis applied to spectra shows only slight structure modifications in lignins after oxidation reaction.

Keywords Sugarcane bagasse · Sugarcane straw · Oxidation in acidic medium · Chelating agents · FTIR · PCA

Introduction

Agricultural residues are produced in large quantities throughout the world. Approximately 280 kg residue is produced for each ton of sugarcane in the alcohol industries. In average, 140 kg bagasse and 140 kg straw are generated. Both by-products have high potential of

G. A. A. Labat · A. R. Gonçalves (✉)
Departamento de Biotecnologia (Debiq), Escola de Engenharia de Lorena—EEL/USP, Caixa Postal 116, 12.602-810 Lorena, SP, Brazil
e-mail: adilson@debiq.eel.usp.br
URL: http://www.debiq.faenquil.br/adilson

G. A. A. Labat
e-mail: amaral@alunos.eel.usp.br

energy to be used. For example, the bagasse energy has been already extracted in thermal industries [1].

In energy terms, industries of sugar and alcohol are sustainable, in which about 90% bagasse (calorific power 18.322 kJ kg^{-1}) is used; however, the consumption can be reduced for 70% if the system of steam generation was optimized. Straw can also be mixed to the bagasse to be burned because of high calorific power (18.870 kJ kg^{-1}) [2] but with the drawback of producing more ashes.

Residues proceeding from sugarcane (bagasse and straw) are lignocellulosic materials. These materials are important sources for cellulose, hemicellulose, and lignin. Lignin is a high-complex and cross-linked macromolecule generated by dehydrogenative polymerization promoted by enzymes from hydroxycinnamylic alcohols (*p*-coumarylic, conniferylic, and synapylic). Figure 1 shows three precursors of lignin. The copolymerization from these alcohols furnishes a high-molar mass heterogenic macromolecule, optically inactive and polydisperse [3]. Figure 2 shows a schematic structure of lignin [4].

Currently, methods that use agricultural residues for chemical products obtainment have been studied, as cellulosic pulps production with applications in cardboard packing [5] and the oxidized lignin obtainment, which owns very strong chelating properties [6–8], because of its oxygenated functional groups. This becomes the oxidized lignin with great utility in the industrial effluent treatment. The use of pulps and lignins allows the integral use of the vegetable biomass and makes it possible to obtain products with higher value.

Heavy metals represent one of the major industrial contaminants of the soil and the plant ecosystem [9]. The environment pollution with toxic heavy metals is spreading throughout the world along with industrial progress [10]. The main sources of contamination with heavy metals are fertilizer impurities (Cd) [11]; the use of refuge-derived compost and sewage sludge (Cd and Ni) in irrigation, mining, and mine wastes; discharges from smelters and refineries [12]; tanneries that use chromium for a quality improvement of the leather [13]; and mainly, the use of Cd and Ni on the rise in

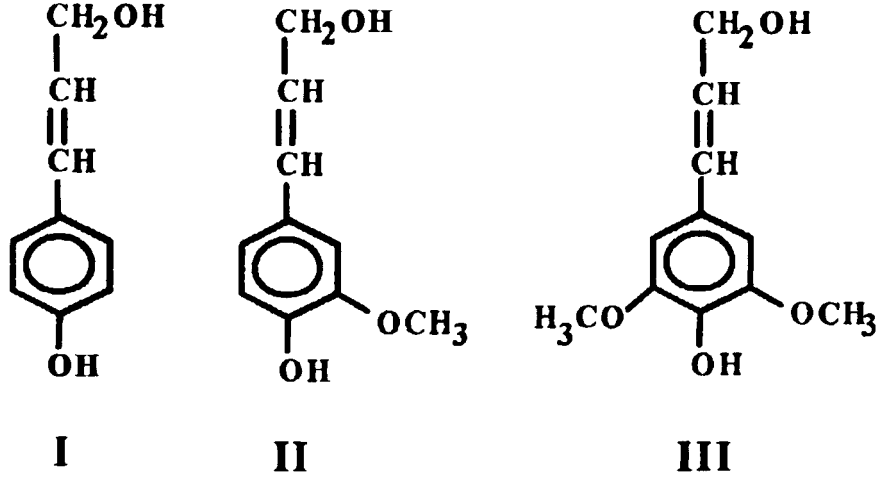


Fig. 1 Structural monomers of lignin: *p*-coumaryl alcohol (*I*), coniferyl alcohol (*II*), and sinapyl alcohol

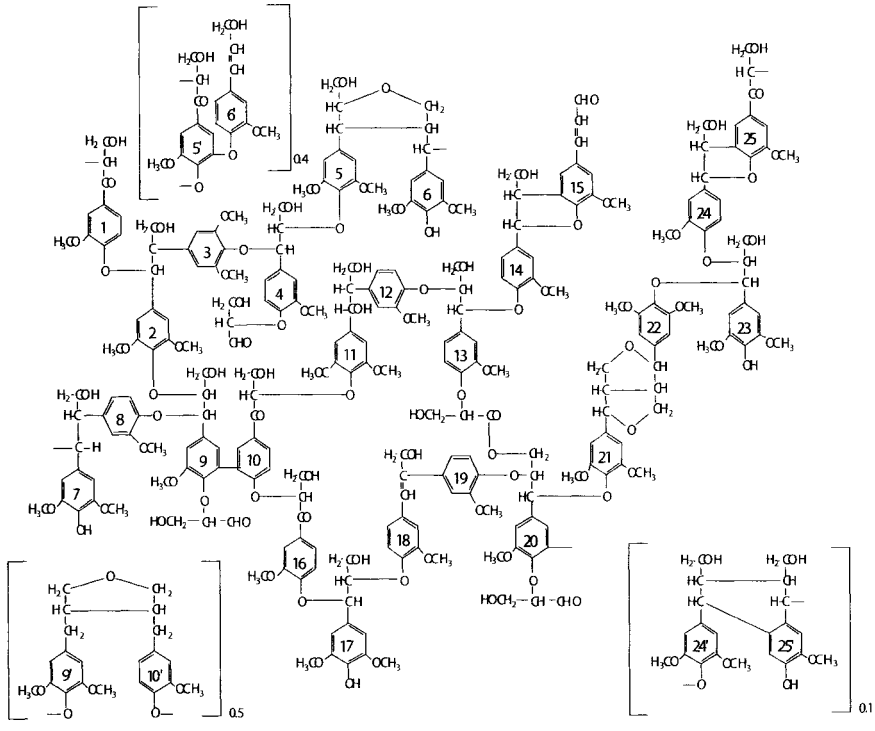


Fig. 2 Schematic structure for lignin (*Fagus sylvatica*)

electroplating, batteries, alloys, pigments, stabilizers for catalysts, and in semiconductors and TV tube phosphors [14].

An important factor is the kinetic study of the lignin oxidation in acidic medium, which is determined by the activation energy and its kinetic reaction.

In this work, lignin oxidation in acetic acid medium with the catalytic system $Co(OAc)_2$/$Mn(OAc)_2$/HBr was carried out. The catalytic system is based on oxidation of alkyl aromatic compounds by O_2. Reaction of cobalt(II) with O_2 forms cobalt(III) bromoacetate, which is catalytically decomposed through homolityc cleavage forming cobalt(II) and radical bromine. In the sequence, radical bromine removes an electron of the aromatic ring of the lignin starting the oxidation of the macromolecule. Manganese(II) ion acts on the system, decomposing the cobalt(III) [15].

$$M^{n+} + ArCH_3 \Rightarrow M^{(n-1)+} + [ArCH_3]^{\bullet +} \tag{1}$$

$$[ArCH_3]^{\bullet +} \Rightarrow ArCH_2^{\bullet} + H^+ \tag{2}$$

Methods of lignin oxidation in acidic media use mainly the Amoco system, used in the auto-oxidation of alkylbenzens into aldehydes and carboxylic acids, catalyzed by cobalt and manganese [16].

The easiness of one-electron transfer is directly related to the ionization potential of aromatic hydrocarbons and to electron donor substitutes, such as methoxyl, which decreases the oxidation potential of lignins dissolved in acetic acid [1].

To express the equation of a reaction rate, any kind of measurement proportioned to the concentration can be used. In the systems using constant volume, the action velocity (V) is simply given by

$$V = \frac{dC}{dt}, \text{where } C \text{ is the concentration and } t \text{ is the time}$$

The reaction rate of every component is given by the rate variation of its concentration, which is proportional to the time at first-order kinetics. A concentration graphic versus time shows a straight line with inclination k (reaction rate constant) [17].

The lignin oxidation from sugarcane straw and bagasse using Fourier-transformed Infrared spectroscopy (FTIR) followed by principal component analysis (PCA) was also studied.

The aim of this work was to oxidize lignins from agricultural residues, as sugarcane straw and bagasse, aiming heavy metals removal from industrial effluents, determining the activation energy, its reaction kinetics, and analysis of the infrared region.

Materials and Methods

Biomass Origin

Sugarcane bagasse and straw were obtained from Ester Industry of the São Paulo State.

Liquors and Lignins Obtainment

Ethanol–water pulping of sugarcane bagasse [18] and straw [19] were carried out as described by Curvelo and Pereira [20] using optimized temperature and times [18–19].

Lignins were precipitated from liquors by sulfuric acid and ice addition until reaching pH 2. Liquors were filtered, and the lignin was washed with distilled water and oven dried at 60 °C for 24 h for the humidity complete removal.

Oxidations Reactions

A 500-ml round-bottom flask equipped with condenser and magnetic stir was charged with 200 ml glacial acetic acid, 2 g lignin, 1.68 g cobalt acetate (II), 0.2 g manganese acetate (II), and 9.1 ml HBr 33% *w/v* under water bath at 50 and 80 °C or silicon oil bath at 115 °C. Oxygen was set at 60 ml min^{-1} flow rate.

Experiments were made in triplicates. The reaction was kept for 5 h. After the reaction temperature reached the desired value, a 2-ml sample was collected at each 30 min until the end of the reaction. One milliliter of this sample was diluted to 10 ml with acetic acid, and 1 ml aliquot of this new sample was diluted to 10 ml with distilled water. Diluted samples were filtered to remove the eventual precipitate (oxidized lignin). The absorbances of the prepared samples were measured in a CINTRA 20 spectrometer at 280 nm.

From the obtained data, graphics were done from the Neperian logarithm of the absorbance versus the reaction time that furnishes, by the straight line equation, the reaction rate constant (k) as angular coefficient. Using the best k values, the Neperian logarithm graphic, as a function of $1/RT$, was done for the determination of the activation energy.

The samples were also submitted to the analysis of the infrared region (400–4,000 cm^{-1}) in a Nicolet Avatar 320 FTIR spectrometer. A 0.15-ml aliquot was dripped on

200 mg KBr. The mixture was homogenized and evaporates in oven (60 °C) for 12 h. Pellets were obtained from the mixture after grinding and spectra recorded with 12 scans with 4 cm^{-1} resolution. The absorbances in the range of 400–4,000 cm^{-1} (935 data points per oxidized lignin spectrum) were normalized by the absorption at 1,510 cm^{-1}, corresponding to the vibrations of aromatic rings, and baseline corrected [21] using OMNIC software. Spectra were converted to text files using OMNIC software (Nicolet). Data were submitted to a statistical analysis from the variance of the intensities through the PCA using the softwares Biotec and FAEN4 compiled in Fortran, which were written based on the work of Scarminio and Bruns [22]. Graphic presentations were easily made with Microsoft Excel 2002.

Results and Discussion

Kinetics and Activation Energy

Experiments of lignin oxidation were performed in acetic acid medium in the presence of oxygen and catalysts $Co(OAc)_2/Mn(OAc)_2/HBr$.

For the kinetic study, an approach of the lignin oxidation reaction was made for a reaction of pseudo-first order, as shown in Eq. 3.

$$\text{Lignin} + [O_2] \xrightarrow{\text{cat}} \text{oxidized lignin} \tag{3}$$

The kinetic equation that represents this process independently of the oxygen concentration is given by Eq. 4.

$$V = \frac{-d[\text{lignin}]}{dt} = \frac{d[\text{oxidized lignin}]}{dt} = -k.[\text{lignin}] = k.[\text{oxidized lignin}] \tag{4}$$

The integrate shows

$$\text{Ln}[\text{oxidized lignin}] = kt + C_0 \tag{5}$$

$$\text{LNA}_{280} = Kt + C \tag{6}$$

where C_0 is the concentration of the original lignin that is constant, k is the rate constant, and t is the time. Using the Beer–Lambert's Law, the concentration of the oxidized lignin can be substituted by the absorbance at 280 nm (Eq. 6).

By this way, the logarithm of the absorbance in relation to the reaction time has as angular coefficient the reaction rate constant and the value of the linear coefficient C related to the lignin initial concentration.

The points with possible experimental errors were removed from the graphics for a better result analysis and calculated the reaction rate constant with its respective R^2 values (Table 1 and 2) based on pseudo-first order kinetics.

Values of k varied from 1.10×10^{-2} h^{-1} to 15.3×10^{-2} h^{-1} for the oxidation reaction of lignin from sugarcane straw, whereas, for oxidation reactions of lignin from sugarcane bagasse, it varied from 10.07×10^{-2} to 56.61×10^{-2} h^{-1}.

For the calculation of the activation energy, the average of the rate constants was used for each temperature, and the average of the temperature during the experiment that oscillated at ±2 °C.

Table 1 Values of rate constants and R^2 for the oxidation reaction of lignins from sugarcane straw.

Temperature (°C)	Experiment 1, k (h^{-1}) 10^{-2} (R^2)	Experiment 2, k (h^{-1}) 10^{-2} (R^2)	Experiment 3, k (h^{-1}) 10^{-2} (R^2)
115	9.90 (0.8777)	15.3 (0.9358)	12.7 (0.9522)
80	6.20 (0.9732)	1.20 (0.8893)	1.70 (0.7922)
50	1.10 (0.9711)	1.90 (0.9970)	8.00 (0.9312)

The graphic made with Neperian logarithm of k as a function of $1/RT$, where R is the universal gas constant (8.314 J mol^{-1} K^{-1}) and T is the average experimental temperature (in Kelvin), has as an angular coefficient the activation energy (Ea), as observed in the equation below:

$$\mathrm{Ln\ k} = \mathrm{LnA} - \frac{\mathrm{Ea}}{\mathrm{RT}}$$

A certain discrepancy between the values of k at the same temperature can be observed. This may be caused by the fact that the oxidation medium is not totally homogeneous, turning difficult the occurrence of an identical replication or by the difference in the oxygen amount dissolved in the medium. A difference in the linearity coefficient values was found: 8.6556 for the first (straw) and 6.5263 for the second (bagasse), a 24.6% lower value (Figs. 3 and 4). These values are related to the concentration of the original lignin; however, they are different probably by the same fact of the discrepancy between the k values.

Activation energy calculated for the oxidation reaction of lignin from sugarcane straw was 34,239 J/mol (R^2=0.9676; Fig. 3), a value higher than that found in the oxidation reaction of lignin from sugarcane bagasse, which is 2,3378 J/mol (R^2=0.9721; Fig. 4).

The differences between the activation energy and linearity coefficient values can be related to the fact that the lignin from straw presents higher cross-linked formation. This fact can be also corroborated by the colors of the original lignins. Lignin from sugarcane straw presents a darker color indicating to possess more C–C linkages.

FTIR Analysis

The spectra had the baseline corrected by the polygonal method [21]. The used region was from 400 to 4,000 cm^{-1}, and the spectra were normalized for the 1,510 cm^{-1} (characteristic vibration of aromatics), originating 390 variables for both used lignins. Spectra were recorded in a Nicolet Avatar 320 FTIR spectrometer. Spectra were converted to text file files using OMNIC software (Nicolet).

Spectra in Fig. 5 were obtained by FTIR relative to the experiment performed at 80 °C for lignin from sugarcane bagasse. The peaks at 1,600 and 1,506 cm^{-1} correspond to the

Table 2 Values of rate constants and R^2 for the oxidation reaction of lignins from sugarcane bagasse.

Temperature (°C)	Experiment 1, k (h^{-1}) 10^{-2} (R^2)	Experiment 2, k (h^{-1}) 10^{-2} (R^2)	Experiment 3, k (h^{-1}) 10^{-2} (R^2)
115	56.61 (0.9106)	28.13 (0.9995)	34.14 (0.9725)
80	14.83 (0.8588)	29.77 (0.8083)	25.11 (0.8947)
50	10.61 (0.9171)	11.09 (0.9396)	10.07 (0.9165)

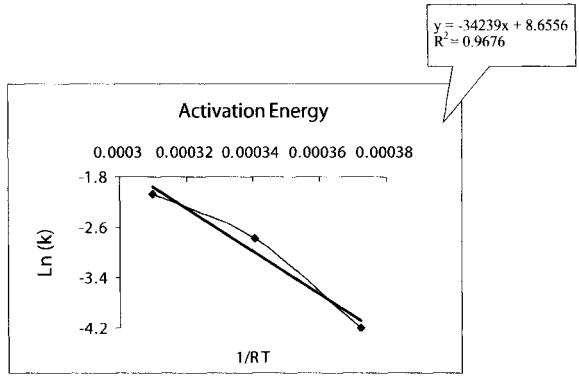


Fig. 3 Activation energy calculated for the oxidation reaction of lignins from sugarcane straw

C = C and aromatic nucleus; the region between 1,200 and 1,110 cm^{-1} is relative to the C–O bands, and the region between 800 and 400 cm^{-1} is relative to the bands of aromatic substitutes.

These spectra and those of other temperatures are very similar because they present the same picks with similar intensities. For a better evaluation of the results, spectra were submitted to analysis by PCA.

The Biotec program originated these variables for each treated spectrum, which were stored in a data file in the insert sequence of the spectra.

The program FAEN2 was used to calculate and, after treatment of the spectra, ten principal components (PCs) were originated, which contain the information of the analyzed spectra. The FAEN2 program provides each principal components with its percentage of total explained variance.

The principal component 1 PC1 explains (64.96 and 75.13%) the variance of the original data, PCs 2 and 3 explain (16.95 and 12.54%) and (11.23 and 3.43%) for straw and bagasse, respectively. The other PCs provide little explanation of the original data (6.45 and 7.96%). Figure 6 shows a graph of the variance explained in each PC; the arrow indicates the ideal number of principal components to represent the original data. These figures show that the PC3 does not have a very high variation of the explained variance. Applying the PCA was possible to reduce the original dimension of the data for three PCs.

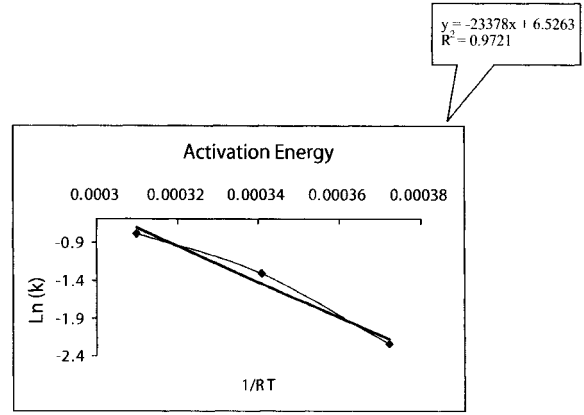


Fig. 4 Activation energy calculated for the oxidation reaction of lignins from sugarcane bagasse

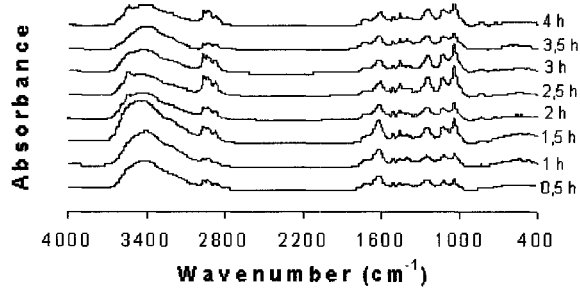


Fig. 5 FTIR spectra of the samples of the experiment performed at 80 °C for lignin from sugarcane bagasse

The first three principal components explain more than (93.14 and 91.1%) of the total variance of the system, utilizing lignin from sugarcane straw and bagasse, respectively. This means that the 390 variables for each temperature can be reduced to only three with more than 90% confidence level. Each spectrum can be reduced to a single point, as shown by PC1 × PC2 and PC1 × PC3 graphics (Figs. 7 and 8), where differences can be evaluated.

In graphs of PC1 × PC2 and PC1 × PC3, it is important to analyze the similarities and differences between the experiments carried out at different temperatures. Close points mean that the samples are similar, and spaced points mean that they are different. These graphs show that different temperatures for the oxidation reaction led to different behaviors. With the temperature increase, the score values acquired higher dispersion in the data, with exception of some points. This behavior can be better observed in the graphs of the lignin from straw. For example, in the graph of PC1 × PC2 for lignin from sugarcane bagasse, the temperature of 50 °C presented the very close scores values with exception of only three points, and the temperature of 115 °C presented distant scores values, indicating that the temperature possesses influence on the reaction of lignin oxidation in acidic medium. The ellipses show the highest concentration of the score values for the different temperatures.

The behavior of the scores values is influenced by the loadings graphics (Fig. 9). The more distant the loading value is from zero, the larger the contribution of this variable for the principal component in study.

Loadings graphs present bands more distinct from 1,170 cm^{-1}; therefore, in the region from 400 to 1,170 cm^{-1}, the sampling presented peaks with many noises, mainly for principal component 1.

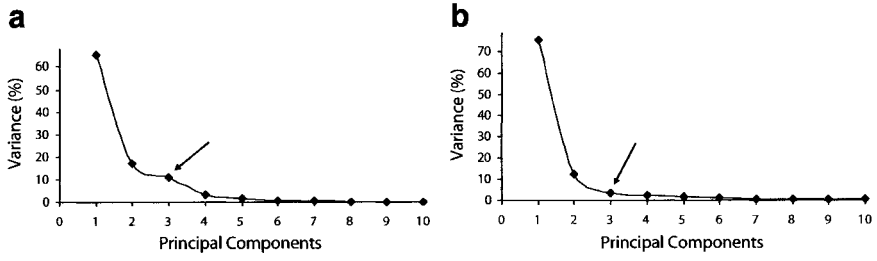


Fig. 6 Variance explained for each principal component for the oxidation reaction with lignins from **a** sugarcane straw and **b** sugarcane bagasse

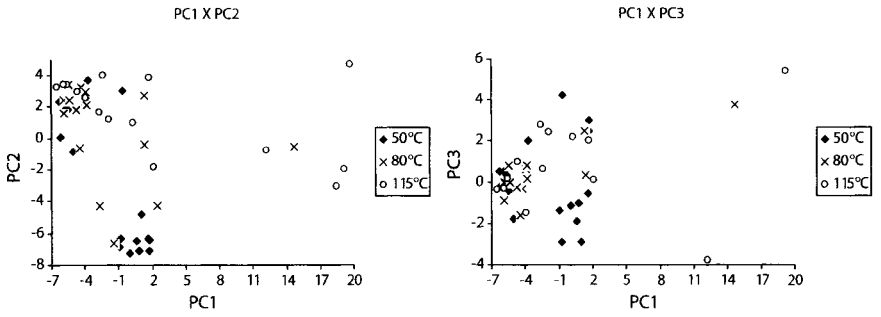


Fig. 7 Scores values of PC1 × PC2 and PC1 × PC3 from FTIR spectra of samples of lignin from sugarcane straw

The principal component 1 has a large percentage of variance (65 and 75%) for straw and bagasse, respectively, indicating to possess higher information of system.

In Fig. 9a and b, the principal component 1 presents strong contribution in the bands at 1,610, 1,630, and 1,650 cm^{-1}, characteristic of C = C aromatics and nonconjugated C = O. Figure 9a presents bands at 1,730 cm^{-1}, characteristics of C = O.

In Fig. 9b, PC3 seems to have a larger contribution on the system because of the present bands between 1,610 and 1,630 cm^{-1}. This behavior can be explained because of the variance of the sampling, by the fact that oxidation medium is not totally homogeneous and by the accumulated mistakes from the retreat of the aliquots to making pellets for reading in FTIR [23].

The existence of the C = C bands can be related to the fact that the oxygen is a soft oxidant and does not cleavage aromatic rings from lignin, and the C = O bands can be related to the lignin oxidation.

The studies carried out in this work have indicated that the original lignins obtain approximately 20% removal of heavy metal [24]. Using the oxidized lignin is intended to reach a higher value for the heavy metals removal.

Conclusions

The use of agricultural residues allows the integral use of biomass for production of materials with higher value. Pulping reactions generate cellulose that is destined for

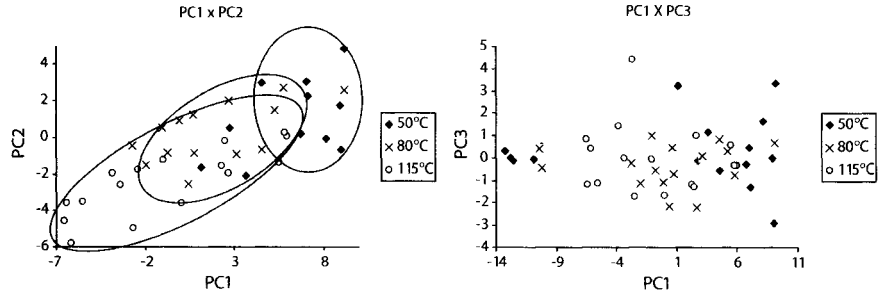


Fig. 8 Scores values of PC1 × PC2 and PC1 × PC3 from FTIR spectra of samples of lignin from sugarcane bagasse

manufacture of paper and lignins, which when being oxidized, becomes efficient in the treatment of effluent with heavy metals.

The technique of UV/visible was sufficiently viable in this work; therefore, it can supply kinetic information of the oxidation process.

The infrared spectroscopy is very important to understand what occurs with the spectrum of lignin after oxidation; therefore, it is an almost direct measure of carbonyls and hydroxyls groups responsible for the chemical modifications.

PCA is widely used in complex biotechnological processes as the lignin oxidation. This tool makes possible the differentiation between samples of oxidized lignins.

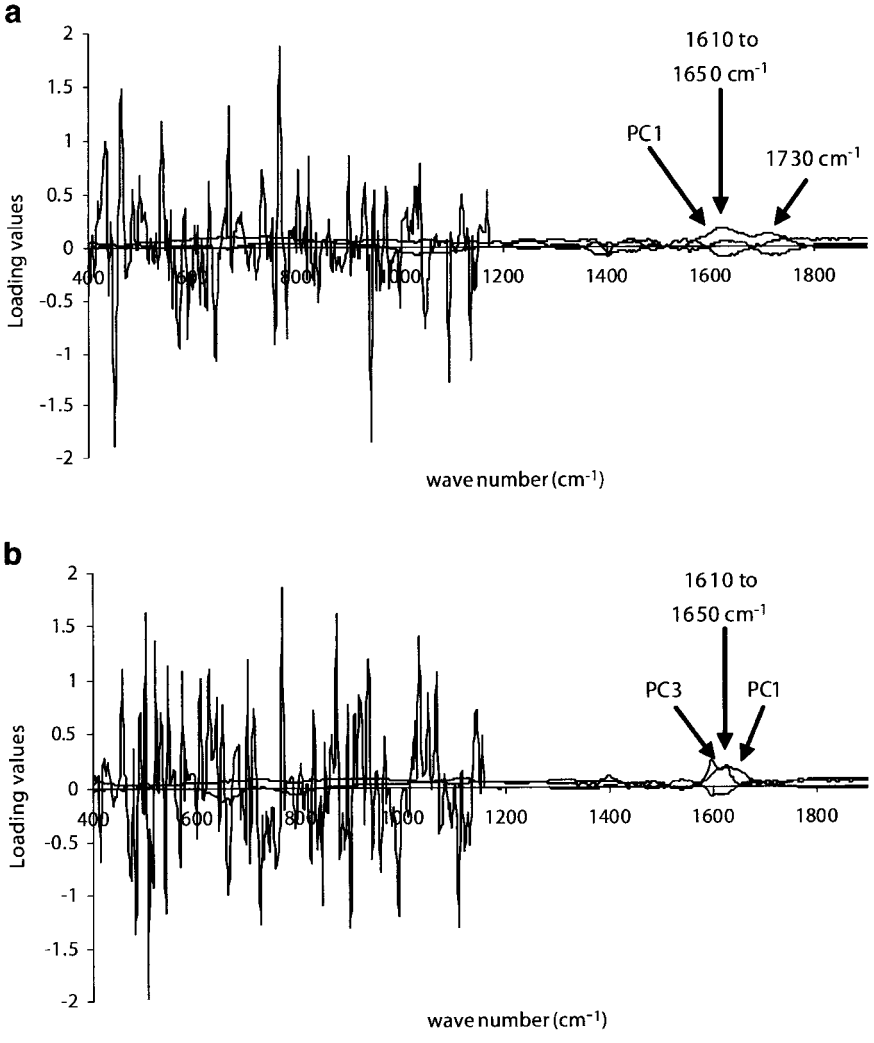


Fig. 9 Loadings values of PC1, PC2, and PC3 of FTIR spectra for the oxidation reaction of lignin from **a** sugarcane straw **b** sugarcane bagasse

The studies indicated that lignin possess strong chelating properties; however, with the oxidation, the chelating properties of the lignin become more evident and could be an alternative in the treatment of industrial effluents containing heavy metals.

Acknowledgment The authors acknowledge financial support from FAPESP, CNPq, and Lignocarb–ALFA Program.

Reference

1. Lobo, P. C., Jaguaribe, E. F., Rodrigues, J., & da Rocha, F. A. A. (2007). *Applied Thermal Engineering, 27*, 1405–1413.
2. Ripoli, T. C. C., Molina Jr, W. F., & Ripoli, M. L. C. (2000). *Science in Agriculture, 4*(57), 677–681.
3. Fengel, D., & e Wegener, G. (1989). In *Wood: Chemistry, ultra structure, reactions* (pp. 132–181). Berlin: Walter de Gruyter.
4. Nimz, H. H. (1974). *Angewandte Chemie International edition in English, 13*, 313.
5. Costa, S. M. (2005). DR thesis, Departamento de Biotecnologia/FAENQUIL, Lorena, Brazil.
6. Gonçalves, A. R., & Luz, S. M. (2000). In *Catalizadores y Adsorventes Iberoamericanos para la Remoción de Metales Pesados de Efluentes Industriales*. P. Á. Garcia (Ed.), Ediciones Cyted (pp. 159-168). Madrid
7. Gonçalves, A. R., Luz, S. M. (2001a). Poster presentations, proceedings, Guaratinguetá, pp. 345–342, Brazil.
8. Gonçalves, A. R., Luz, S. M. (2001b). Poster presentations, proceedings, Guaratinguetá, pp. 266–269, Brazil.
9. Ghoshroy, S., Freedman, K., Lartey, R., & Citovsky, V. (1998). *Plant Journal, 13*, 591–602.
10. Dönmez, G., & Aksu, Z. (1999). *Proceedings in Biochemistry, 3*, 135–142.
11. Schickler, H., & Caspi, H. (1999). *Physiologia Plantarum, 105*(1), 39–44.
12. Chaoui, A., Mazhoud, S., Ghorgbal, M. H., & El Ferjani, E. (1997). *Plant Science, 121*(2), 139–147.
13. Jordão, C. P., Da Silva, A. C., Pereira, J. L., & Brune, W. (1999). *Química Nova, 22*, 47–52.
14. Kefala, M. I., Zouboulis, A. I., & Matis, K. A. (1999). *Environmental Pollution, 94*, 283–293.
15. Partenheimer, W. (1991). *Journal of Molecular Catalysis, 67*, 35–46.
16. Sheldon, R. A., & Kochi, J. K. (1981). pp. 121–133, 315–328. New York: Academic.
17. Levenspiel, O. (2000). In *Engenharia das Reações Químicas*. São Paulo: Edgard Blücher, pp. 21–22.
18. Ruzene, D. S. (2005). DR thesis, EEL/USP, Lorena, Brazil.
19. Moriya, R. Y., Gonçalves, A. R., & Duarte, M. C. T. (2006). 28th Symposium on Biotechnology for Fuels and Chemicals, EUA.
20. Curvelo, A. A. S., & Pereira, R. (1995). 8, Helsinki 1995. Proceedings. V.2, pp. 473–478.
21. Faix, O. (1992). S. Y. Lin and C. W. Dence (eds.), Springer, Berlin, pp. 83–109.
22. Scarminio, I. S., & Bruns, R. E. (1989). *Trends in Analytical Chemistry, 8*, 326–327.
23. Benar, P., Mandelli, D., Ferreira, M. M. C., Schuchardt, U., & Gonçalves, A. R. (1999). *Journal of Wood Chemistry and Technology, 19*, 155–165.
24. Gonçalves, A. R., & Ventura, T. R. (2003). Proceedings. VII Encontro de Iniciação Científica, São José dos Campos, SP, Brazil.

Appl Biochem Biotechnol (2008) 148:163–173
DOI 10.1007/s12010-007-8062-6

Kinetic Modeling and Parameter Estimation in a Tower Bioreactor for Bioethanol Production

Elmer Ccopa Rivera · Aline Carvalho da Costa · Betânia Hoss Lunelli · Maria Regina Wolf Maciel · Rubens Maciel Filho

Received: 9 May 2007 / Accepted: 19 September 2007 /
Published online: 10 October 2007
© Humana Press Inc. 2007

Abstract In this work, a systematic method to support the building of bioprocess models through the use of different optimization techniques is presented. The method was applied to a tower bioreactor for bioethanol production with immobilized cells of *Saccharomyces cerevisiae*. Specifically, a step-by-step procedure to the estimation problem is proposed. As the first step, the potential of global searching of real-coded genetic algorithm (RGA) was applied for simultaneous estimation of the parameters. Subsequently, the most significant parameters were identified using the Placket–Burman (PB) design. Finally, the quasi-Newton algorithm (QN) was used for optimization of the most significant parameters, near the global optimum region, as the initial values were already determined by the RGA global-searching algorithm. The results have shown that the performance of the estimation procedure applied in a deterministic detailed model to describe the experimental data is improved using the proposed method (RGA–PB–QN) in comparison with a model whose parameters were only optimized by RGA.

Keywords Ethanol fermentation · Parameter estimation · Modeling · Optimization techniques · Artificial intelligence

Introduction

Bioethanol (ethanol from biomass) is nowadays the largest fermentation product obtained from sugar cane. In fact, bioethanol seems to be the most promising alternative energy source to be used as a fuel, either alone or as mixture in gasoline. Besides, from bioethanol, many chemicals products may be produced, making the sugar cane-based feedstock process

E. Ccopa Rivera (✉) · A. C. da Costa · B. H. Lunelli · M. R. W. Maciel · R. M. Filho
Laboratory of Optimization, Design and Advanced Control, School of Chemical Engineering, State University of Campinas, P.O. Box 6066, 13081-970 Campinas, SP, Brazil
e-mail: elmer@feq.unicamp.br

R. M. Filho
e-mail: maciel@feq.unicamp.br

to be very interesting from the environmental point of view and an economic attractive raw material to chemicals production. For instance, it is possible to achieve high-quality acetaldehyde, acetic acid, ethyl acetate, and ethylene and from them a huge amount of chemicals, including polymers. Although the bioethanol production is running for several years, improvements are required to increase process performance. A suitable route is to improve the fermentation process, including the investigation of an alternative process as a tower with immobilized microorganisms, to obtain bioethanol and use ethanol chemistry to obtain others chemicals.

There are many minor industrial problems associated with the ethanol fermentation processes to be solved nowadays, when optimal operation is a target. Among them, there is the lack of process robustness in the presence of fluctuations in operational conditions, which leads to changes in the kinetic behavior, with impact on yield, productivity, and conversion. These changes are very common in ethanol plants, where they occur not only because of the variations in the quality of the raw material but also because of variations of dominant microorganisms in the process.

The lack of robustness can be corrected by adjustments in the operational and control parameters of the process when fluctuations occur. To accomplish this, it is important that a mathematical model be available to aid in the decision making, mainly when the difficulties of monitoring the key process variables are taken into account. Care has to be taken with the values of the model parameters, especially the kinetic ones so that reliable predictions can be made.

Compared with growing studies of microorganism populations, few improvements on the development and application of structured deterministic models for product formation have appeared. They are essential to develop more advanced operation strategies as well as to develop control and optimization algorithms.

Estimation of kinetic parameters of deterministic models is usually complex, mainly because of nonlinearities, great number of parameters, and interactions among them. In biochemical engineering, the most classical method involves the mathematical estimation of model parameters based on the minimization of some cost function built up with the parameters to be estimated. Several kinetic models have been proposed for the alcoholic fermentation process [1–3]. Many techniques are available for minimizing the error of estimation, generally methods based on gradient search, such as the quasi-Newton algorithm (QN). At this point, it is important to bear in mind that when detailed structured models are considered, the number of the parameters to be identified and also the interactions among them increase significantly.

Artificial intelligence, such as Genetic Algorithms (GAs), covers a wide range of techniques and tools that facilitate decision making. It is often as powerful and effective as gradient search methods in many engineering applications but with some advantages related to independence of the initial guess to achieve the solution. These methods have already been successfully applied in the optimization and control of bioprocesses for more than 20 years [4]. GAs have been successfully utilized for kinetic parameter estimation in biotechnological processes [5–7].

In this work, the proposed optimization procedure is based on the combination of different optimization techniques, to know: real-coded GA (RGA), Placket–Burman (PB) design, and QN. The approach is applicable when the structure of a kinetic model has been set up and the kinetic parameters should be estimated.

The parameter estimation methodology was demonstrated on an alternative dynamic structured model [8], adapted from Rotboll and Jorgensen [9] to simulate a tower bioreactor for ethanol production by immobilized *Saccharomyces cerevisiae*. The model contains 34

kinetic parameters and nine parameters (K_E, K_{E2}, F_1, F_2, F_3, F_5, F_6, k_d, C), related to the glycolitic and respiratory (tricarboxylic acid [TCA]) paths, which were re-estimated.

Methodology

This section describes a parameter estimation methodology in three steps, which was developed to estimate kinetic parameters in structured models. First, a RGA was applied for simultaneous estimation of the parameters, and secondly, the most significant parameters were identified using the PB design. Finally, the QN was used for optimization of the most significant parameters, near to the global optimum region, as the initial values were already determined by the RGA global searching algorithm.

Case Study: Kinetic Model for a Structured Detailed Mechanistic Model

Process Description

The case study is based on a tower-type bioreactor that uses *S. cerevisiae* immobilized in pellets with 4% of citric pectin, for production of bioethanol. The bioreactor is divided in four stages with gas separators between them to prevent the CO_2 accumulation during the fermentation process because the CO_2 release may eventually result in a drop in the fermentation yield. The experiments were performed at 30 °C, pH 4.0, initial substrate concentration of 161.4 g/L, feed flow rate of 40 mL/h, and residence time of 6.12 h. After 40 h of operation, the system has reached a steady state. A diagram of the system is shown in Fig. 1.

The developed deterministic detailed model based on the work of Stremel [8] for the dynamic simulation of this system, shown in the Appendix, also includes terms for the inhibition by ethanol, substrate, and saturation by the cells inside the pellets. Stremel [8] also investigated all the parameters and their effects to identify the most significant but did not use a methodology to optimize simultaneously the parameters of the model.

Optimization by Real-coded Genetic Algorithm

The GAs used was, basically, the FORTRAN RGA developed by Yedder [10], with some modifications. In the proposed strategy, the chromosome or individual are vectors where each real value (gene) stands for each one of the unknown parameters in the kinetic model. The stopping criterion is selected when the maximum number of fixed generations is reached. The RGA parameters were adjusted to minimize the number of generations (iterations) required to reach a satisfactory fitness (objective function) value by minimizing Eq. 1, which reflects a good agreement between the measured concentration and the concentration computed by the model.

$$E(\theta) = \sum_{n=1}^{np} \left[\frac{(S_n - \mathrm{Se}_n)^2}{\mathrm{Se}_{\max}^2} + \frac{(P_n - \mathrm{Pe}_n)^2}{\mathrm{Pe}_{\max}^2} \right] = \sum_{n=1}^{np} \varepsilon_n(\theta) \tag{1}$$

In this equation, Se_n and Pe_n are the measured concentrations of substrate and ethanol at the sampling time n. S_n and P_n are the concentrations computed by the model at the sampling time n. $\mathrm{Se}_{\max}$ and $\mathrm{Pe}_{\max}$ are the maximum measured concentrations and the term np is number of sampling points. In this equation, $\varepsilon_n(\theta)$ is the error in the output because of the nth sample.

Some basic information on the GA is reported in Table 1.

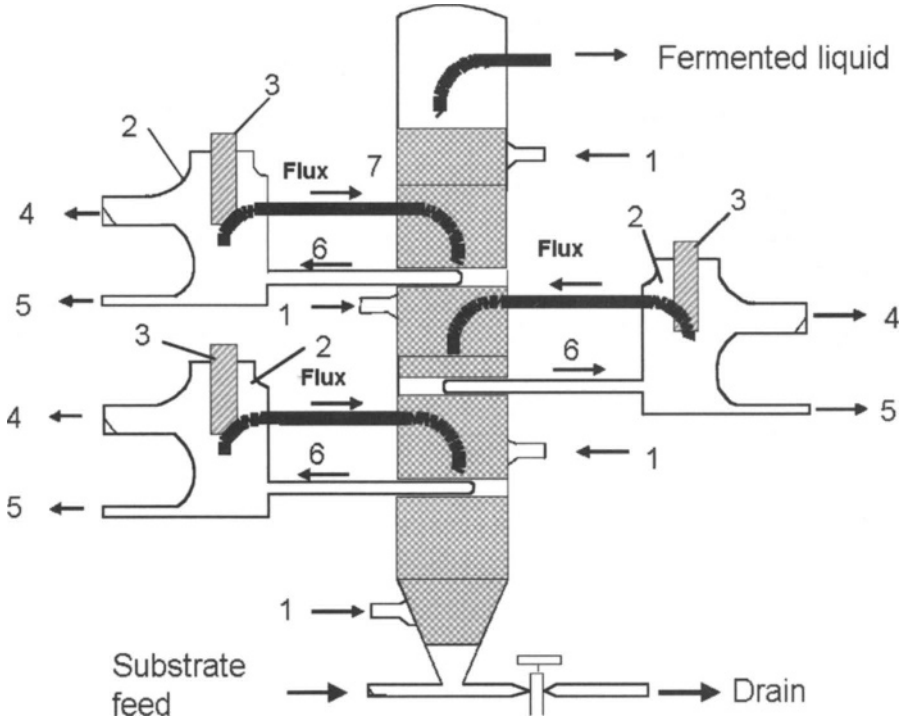


Fig. 1 Tower bioreactor. *1*, Inlet and outlet of the pellets; *2*, gas–liquid separator; *3*, inductive sensor; *4*, CO_2 outlet; *5*, evacuation of sample; *6*, fermented liquid with CO_2 flow; *7*, fermented liquid without CO_2 flow

Identification of Significant Parameters

This step consists of applying the PB design to identify the kinetic parameters that are significant on the optimization problem. The PB design is a partial factorial method that allows the testing of multiple independent process variables within a single experiment. The influence of 43 parameters on Eq. 1 was investigated using the methodology of Plackett and Burman [11]. Four variables were designated as "dummy" variables because no change is made to them, but they are used to give an estimate of the standard error for each factor. Each parameter (factor) is tested at two levels, a high (+) and a low (−) level, which will be determined after the optimization by RGA. The PB design contains a total of 47 trials.

Table 1 Main technical features used by the real-coded genetic algorithm.

Option chosen—RGA	Parameters	Parameter values
Niching, elitism, barycentric crossover, nonuniform mutation	Individual length (number of parameters in the model)	43
	Population size	10
	Crossover probability	0.9
	Mutation probability	0.03

Final Optimization by Quasi-Newton Algorithm

A simultaneous estimation of the kinetic parameters selected in the previous step is performed using the QN, whereas all other parameters remained fixed in the global optimum region, calculated by the RGA. The FORTRAN IMSL routine DBCONF was

Table 2 Optimized parameters by real-coded genetic algorithm.

Parameter	Parameter values optimized by RGA
k_1	0.469
k_2	0.262
k_3	8.112
k_4	2.467E−03
k_5	1418.132
k_6	1.150
k_8	0.377
k_9	2.883E−02
k_{10}	2.275E−03
s_1	1.213E−02
s_2	4.920E−04
s_3	8.072E−02
s_4	1.00E−06
s_5	0.358
s_6	1.801E−02
s_8	2.016E−02
s_9	1.0E−06
s_{1e}	0.147
s_{5e}	5.770E−02
s_{8e}	1.978E−03
s_{9e}	9.558
s_{10e}	168.26
k_{1e}	29.262
k_{4e}	1.264
k_{8e}	3.615E−03
k_{10e}	0.892
K_E	5.092E−02
K_{E2}	6.038E−02
k_{1i}	6.435
m_2	3.477
m_{2e}	3.476
k_{4i}	9919.791
k_{5i}	1981.616
k_{5r}	0.303
k_{9i}	2716.006
k_{10i}	504.813
k_d	7.910E−04
F_1	2.249
F_2	1.276
F_3	0.420
F_5	2.362
F_6	1.212
C	1.098

used for this purpose. The straightforward idea is to implement the optimization problem as a nonlinear programming problem that can be written as:

$$\text{Minimize Eq. 1}$$
$$\text{Subject to } l_p \leq x_p \leq u_p, p = 1, \ldots, 5$$

where x_p is the parameters. The l_p and u_p are specified lower and upper bounds on the parameters, with $l_p \leq u_p$.

Table 3 Effect estimate on Eq. 1 from results of Plackett–Burman design.

Factor	Effect	SE	t (4) value	P value	−95%	95%
Mean	0.081860*	0.000503*	162.6241*	0.000000*	0.080462*	0.083258*
k_1	0.000571	0.001007	0.5673	0.600833	−0.002224	0.003366
k_2	0.000514	0.001007	0.5107	0.636455	−0.002281	0.003309
k_3	0.000470	0.001007	0.4669	0.664869	−0.002325	0.003265
k_4	−0.000473	0.001007	−0.4696	0.663097	−0.003268	0.002322
k_5	0.000766	0.001007	0.7604	0.489370	−0.002030	0.003561
k_6	−0.012757*	0.001007*	−12.6718*	0.000223*	−0.015552*	−0.009962*
k_8	0.006145*	0.001007*	6.1039*	0.003645*	0.003350*	0.008940*
k_9	−0.001227	0.001007	−1.2185	0.289984	−0.004022	0.001568
k_{10}	0.001798	0.001007	1.7855	0.148728	−0.000998	0.004593
s_1	0.000386	0.001007	0.3830	0.721203	−0.002410	0.003181
s_2	0.000459	0.001007	0.4557	0.672248	−0.002336	0.003254
s_3	−0.000939	0.001007	−0.9324	0.403912	−0.003734	0.001856
s_4	0.000494	0.001007	0.4910	0.649146	−0.002301	0.003289
s_5	−0.000230	0.001007	−0.2285	0.830464	−0.003025	0.002565
s_6	−0.000306	0.001007	−0.3036	0.776569	−0.003101	0.002489
s_8	−0.000521	0.001007	−0.5174	0.632173	−0.003316	0.002274
s_9	0.000187	0.001007	0.1855	0.861863	−0.002608	0.002982
s_{1e}	−0.000262	0.001007	−0.2601	0.807626	−0.003057	0.002533
s_{5e}	−0.001247	0.001007	−1.2391	0.283046	−0.004043	0.001548
s_{8e}	0.000423	0.001007	0.4202	0.695930	−0.002372	0.003218
s_{9e}	−0.000205	0.001007	−0.2038	0.848458	−0.003000	0.002590
s_{10e}	−0.001174	0.001007	−1.1664	0.308253	−0.003969	0.001621
k_{1e}	−0.002425	0.001007	−2.4092	0.073619	−0.005221	0.000370
k_{4e}	−0.000807	0.001007	−0.8013	0.467855	−0.003602	0.001988
k_{8e}	0.001162	0.001007	1.1543	0.312646	−0.001633	0.003957
k_{10e}	0.000644	0.001007	0.6396	0.557227	−0.002151	0.003439
K_E	0.016200*	0.001007*	16.0913*	0.000087*	0.013405*	0.018995*
K_{E2}	0.007588*	0.001007*	7.5369*	0.001660*	0.004793*	0.010383*
k_{1i}	0.001114	0.001007	1.1065	0.330574	−0.001681	0.003909
m_2	0.000628	0.001007	0.6235	0.566748	−0.002167	0.003423
m_{2e}	0.000541	0.001007	0.5371	0.619683	−0.002254	0.003336
k_{4i}	−0.000171	0.001007	−0.1696	0.873557	−0.002966	0.002624
k_{5i}	0.000715	0.001007	0.7101	0.516848	−0.002080	0.003510
k_{5r}	0.000108	0.001007	0.1071	0.919866	−0.002687	0.002903
k_{9i}	−0.000721	0.001007	−0.7166	0.513234	−0.003517	0.002074
k_{10i}	−0.000685	0.001007	−0.6808	0.533368	−0.003481	0.002110
k_d	0.000506	0.001007	0.5027	0.641591	−0.002289	0.003301
F_1	−0.024644*	0.001007*	−24.4788*	0.000017*	−0.027439*	−0.021849*
F_2	0.022353*	0.001007*	22.2032*	0.000024*	0.019558*	0.025148*
F_3	0.023282*	0.001007*	23.1265*	0.000021*	0.020487*	0.026077*
F_5	0.021074*	0.001007*	20.9330*	0.000031*	0.018279*	0.023869*
F_6	−0.002826*	0.001007*	−2.8074*	0.048445*	−0.005621*	−0.000031*
C	−0.000778	0.001007	−0.7726	0.482874	−0.003573	0.002017

* Significant for a 95% confidence level.

Table 4 Re-estimated parameters by quasi-Newton.

Parameter	Parameter values optimized by QN
K_E	5.099E−02
F_1	2.244
F_2	1.276
F_3	0.435
F_5	2.353

Results

The optimized parameters by RGA are shown in Table 2.

By considering the values optimized by RGA as central point in a PB design, the effects for all parameters on Eq. 1 (response), for a 95% confidence level, were calculated. The effects of the parameters are given in Table 3.

A total of five most significant parameters (shown in Table 4), i.e., greater effects on error, Eq. 1, were re-estimated by QN, whereas all other parameters remained fixed in the global optimum region, in the values set by the RGA. Under such optimal model, the computed profiles for ethanol, P, and substrate, S, are shown by the dashed lines in Figs. 2 and 3, respectively.

The residual standard deviation (RSD) [12], Eq. 2, written as a percentage of the average of the experimental values, was the measurement used for characterizing the quality of the prediction of the model.

$$RSD(\%) = \frac{\left(\frac{1}{np}\left(\sum_{p=1}^{np}\left(d_p - x_p\right)^2\right)^{0.5}\right)}{\overline{d}_p} \times 100 \tag{2}$$

where x_p and d_p are, respectively, the value predicted by the mathematical model and experimental value, $\overline{d}_p$ is the average of the experimental values, and np is the number of experimental points.

The RSD (%) for the model optimized by only RGA and the methodology proposed in this work (RGA–PB–QN) are shown in Table 5. The results obtained using the methodology RGA–PB–QN were better than the results using only RGA. It can be seen that the deviations are 8.6 and 2.3% for concentrations of substrate and ethanol, respectively. In bioprocess

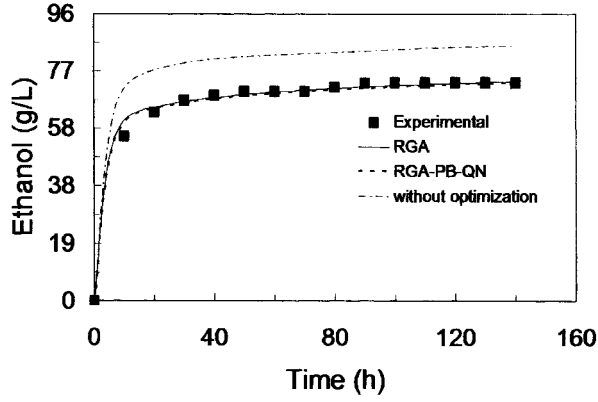


Fig. 2 Experimental (ethanol, *squares*) and modeling (model optimized by using only RGA [*solid line*]; model optimized by using RGA-PB-QN [*dashed line*]; model without optimization [*point-dash line*]) results

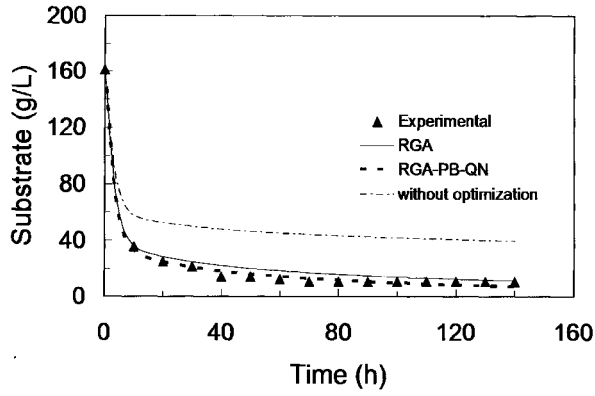


Fig. 3 Experimental (substrate, *triangles*) and modeling (model optimized by using only RGA (*solid line*); model optimized by using RGA-PB-QN [*dashed line*]; model without optimization [*point-dash line*]) results

engineering, values of RSD (%) below 10% can be considered acceptable [12]. Thus, the estimated model was able to fit experimental observations satisfactorily.

Concluding Remarks

A structured detailed mechanistic model to simulate a tower bioreactor for bioethanol production with immobilized *S. cerevisiae* was studied and coupled with an optimization procedure. This computer-aided process engineering tool allows to identify kinetic parameters as well as to explore different operational strategies.

The major problem with structured models is their large number of parameters, which makes the estimation procedure a difficult task. The use of deterministic optimization methods, such as QN, to estimate a large number of parameters (in the studied case 43) usually leads to lack of convergence. On the other hand, GAs are well suited to large-scale problems but have the drawback of slow convergence. In this work, it is proposed an estimation methodology in four steps that can be used always that a re-estimation of parameters is necessary.

The first step is to calculate the parameters in the model using a RGA. The second step is to identify the most significant of the 43 parameters using the PB design, and finally, the most significant (in the studied case five parameters) are optimized using a QN, which converges much more quickly than RGA to the optimal.

The results have shown that the performance of the model to describe the experimental data (measured as RSD (%)) is improved using the proposed methodology in comparison with a model whose parameters were only optimized by RGA.

Finally, it should be noted that the proposed methodology can be applied in many other parameter estimation problems and can be used as a reliable tool for optimizing other types of biotechnological processes.

Table 5 Residual standard deviation, RSD (%), used to characterize the prediction quality of the model.

Output variable	RSD (%)	
	RGA	RGA–PB–QN
Ethanol (g/L)	2.4	2.3
Substrate (g/L)	25.7	8.6

Acknowledgments The authors acknowledge Fundação de Amparo à Pesquisa do Estado de São Paulo (FAPESP) and Conselho Nacional de Desenvolvimento Científico e Tecnológico (CNPq) for financial support.

Appendix

A.1

The generic dynamic model for the bioparticle, where the kinetic expressions are adapted of Rotboll and Jorgensen [9] is given by Eq. 3. In the model, [ ] represents a generic concentration. Substrate conversion in the pellet through the reactions of the Embden–Meyerhof–Parnas pathway forms intermediates such as acetaldehyde [*A*] and pyruvate [*P*] that are reduced to ethanol [*E*] or oxidized in the steps of the TCA pathway.

$$\frac{\partial[\,]}{\partial t} = \alpha_{[\,]}\Delta^2_{r[\,]} \pm \left[\sum_{i,j} F_i R_j X_s\right] \exp\left(-K_E E_f\right) X_{[T]} \tag{3}$$

where

$$R_j = f(v_k,\ [S],\ [A],\ [P],\ [E],\ [X_s],\ [X_r],\ [X_{\mathrm{fe}}]) \tag{4}$$

where i=1...6 (related to Eq. 3); j=1...7 (related to Eqs. 3 and 4); k=1...34 (related to Eq. 4).

The first and second terms of Eq. 3 represent the diffusion through the particle and fluid reaction rate, respectively. The signal (±) shows if the substance is being consumed (−) or formed (+). The subscripts of the reaction rates R_j (h^{-1}) are related to the different subscripts of the factors (F_i). F_1, F_2, F_3, F_5, and F_6 are parameters to be adjusted for the glycolytic and respiratory pathways (see Table 6). The synthetic composition $X_{[S]}$ (g/g dry mass basis) is responsible for the metabolic synthesis, fermentation, and respiration.

The generic Eq. 5 is valid for the variables that do not spread outside of the pellets, where $X_{[s]}$, $X_{[p]}$, and $X_{[r]}$ (g/g dry-mass basis) are synthetic, structural, and enzymatic components of the respiratory pathway, respectively, and $X_{[\mathrm{fe}]}$ is the fermentative component.

$$\frac{\partial X_{[\,]}}{\partial t} = \left[\sum_i R_i\right] X_{[S]} - \left[\sum_k R_k X_{[S]}\right] X_{[\,]} \tag{5}$$

Table 6 Reaction rates and factors for Eq. 3.

Substance [ ]	F_i	R_j	Signal (±)	F_iR_j
Glucose [*S*]	F_1, F_6	R_1, R_6	−	F_1R_1, F_6R_6
Ethanol [*E*]	F_5, $-F_4$	R_5, R_7	+	F_5R_5, $-F_4R_7$
Acetaldehyde [*A*]	F_3, F_4	R_3, R_4, R_5, R_7	+	F_3R_3, $-F_4R_4$, $-F_4R_5$, $-F_4R_7$
Pyruvate [*P*]	F_2, $-F_4$	R_1, R_2, R_3	+	F_2R_1, $-F_4R_2$, $-F_4R_3$

Table 7 Reaction rates and factors for equation 5 and 7.

Components	R_i	R_k
$X_{[s]}$	R_6, R_7	R_6, R_7
$X_{[p]}$	R_8	R_6, R_7
$X_{[r]}$	R_9	R_6, R_7
$X_{[fe]}$	R_{10}	R_6, R_7
$X_{[T]}$	–	R_6, R_7

The reaction rates of the components (g/g h), as function of the parameters v_l and variables [ ] are:

$$R_i = f(v_l,\ [S],\ [A],\ [P],\ [E],\ [X_r]) \tag{6}$$

Equation 7 represents the concentration of total cell mass

$$\frac{\partial X_{[T]}}{\partial t} = \left[\sum_k R_k X_{[S]}\right] X_{[T]} FI_X - k_d X_{[T]} \tag{7}$$

The reaction rates R_k (see Table 7) as function of the parameters v_m and variables [ ] are:

$$R_k = f(v_m,\ [S],\ [A],\ [P],\ [E],\ [X_r]) \tag{8}$$

where i=6...10 (related to Eq. 5); k=6, 7 (related to Eq. 5 and 7), l=12...14; 21...34 (related to Eq. 6); m=12...14; 21...22 (related to Eq. 8).The number of parameters v is 34. The other constants considered are: K_E, K_{E2}, F_1, F_2, F_3, F_5, F_6, k_d, and C.

A simplification of the glycolytic and respiratory routes considered in the deterministic model to represent bioethanol synthesis is shown below by stoichiometric expressions. More details of the kinetics can be found in Stremel [8].

$$\begin{aligned}
&F_1[S] \xrightarrow{R_1} F_2[P]\\
&F_6[S] \xrightarrow{R_6} 0.732X_{[S]} \xrightarrow{0.732R_6X_{[S]}} X_{[T]}\\
&F_4[P] + O_2 \xrightarrow{R_2} TCA + CO_2\\
&F_4[P] \xrightarrow{R_3} F_3[A]\\
&F_4[A] + O_2 + X_{[r]} \xrightarrow{R_4} TCA + X_{[r]} + CO_2\\
&F_4[A] + X_{[fe]} \xrightarrow{R_5} F_5[E] + X_{[fe]} + CO_2\\
&F_4[A] \xrightarrow{R_7} 0.850X_{[S]} \xrightarrow{0.850R_7X_{[S]}} X_{[T]}\\
&X_{[S]} \xrightarrow{R_8} X_{[P]} \xrightarrow{(0.732R_6 + 0.850R_7)X_{[P]}} X_{[T]}\\
&X_{[S]} \xrightarrow{R_9} X_{[r]} \xrightarrow{(0.732R_6 + 0.850R_7)X_{[r]}} X_{[T]}\\
&X_{[S]} \xrightarrow{R_{10}} X_{[fe]} \xrightarrow{(0.732R_6 + 0.850R_7)X_{[fe]}} X_{[T]}\\
&X_{[T]} \xrightarrow{k_d} X_{[nv]}
\end{aligned} \tag{9}$$

References

1. Dourado, A., Goma, G., Albuquerque, U., & Sevely, Y. (1987). *Biotechnology and Bioengineering, 29*, 187–194.
2. Andrietta, S. R., & Maugeri, F. (1994). *Advances in Bioprocess Engineering, 1*, 47–52.
3. Blanco, M., Peinado, A. C., & Mas, J. (2006). *Analytica Chimica Acta, 556*, 364–373.
4. Schügerl, K. (2001). *Journal of Biotechnology, 85*, 149–173.
5. Park, L. J., Park, C. H., Park, C., & Lee, T. (1997). *Medical & Biological Engineering & Computing, 35*, 47–49.
6. Sáiz, J. M. G., Pizarro, C., & Vidal, D. G. (2003). *Biotechnology Progress, 19*, 599–611.
7. Rivera, E. C., Costa, A. C., Wolf, M. R., & Maciel Filho, R. (2006). *Applied Biochemistry and Biotechnology, 129–132*, 969–984.
8. Stremel, D. P. (2001). Ph.D. thesis, UNICAMP, SP, Brazil.
9. Rotboll, M., & Jorgensen, S. B. (1993). Validation of a metabolic and biomass structured model for yeast fermentation. In *European Conference on Biotechnology*, Florence, Italy.
10. Yedder, R. B. (2002). Ph.D. thesis, ENPC, Paris, France.
11. Plackett, R. L., & Burman, J. P. (1946). *Biometrika, 33*, 305–325.
12. Atala, D. I. P., Costa, A. C., Maciel Filho, R., & Maugeri, F. (2001). *Applied Biochemistry and Biotechnology, 91–93*, 353–366.

Appl Biochem Biotechnol (2008) 148:175–187
DOI 10.1007/s12010-007-8060-8

Analysis of Kinetic and Operational Parameters in a Structured Model for Acrylic Acid Production through Experimental Design

B. H. Lunelli · E. C. Rivera · E. C. Vasco de Toledo · M. R. Wolf Maciel · R. Maciel Filho

Received: 9 May 2007 / Accepted: 19 September 2007 /
Published online: 24 October 2007
© Humana Press Inc. 2007

Abstract In biotechnological processes, a great number of factors can influence the income productivity and conversion. Normally, it is not evident which of these factors are the most important and how they interact. In this work, multivariate analysis techniques are used as experimental design coupled to a detailed deterministic model to identify the parameters with the most significant impact on the model to represent well the acrylic acid production process. It is proposed as an alternative process, having sugarcane as feedstock, to the petrochemical-based ones that have significant environmental impacts for their production. To increase the competitiveness of renewable acrylic-acid-based process, it is necessary to find out working conditions near the optimal region, which is not an easy task, as the process is multivariable and non-linear. The mapping of the dynamics of the developed process is made using techniques of factorial design together with the methodology of Plackett–Burman. It is shown that it is possible to increase the process performance by choosing optimized conditions for the reactor operation.

Keywords Experimental design · Plackett–Burman design · Factorial design · Biotechnological process · Acrylic acid · Structured model

Nomenclature

AA	acrylic acid concentration
D_{Ai}	diffusivity
D_{az}	axial dispersion coefficient
D_p	particle diameter
D_r	reactor diameter
F_{in}	feed rate
k	factors number
K_A, $K_{A''}$	inhibition constant related with the product
k_i	rate constant for reaction

B. H. Lunelli (✉) · E. C. Rivera · E. C. Vasco de Toledo · M. R. Wolf Maciel · R. Maciel Filho
Laboratory of Optimization, Design and Advanced Control (LOPCA), Department of Chemical Process, School of Chemical Engineering, State University of Campinas (UNICAMP), PO Box 6066, Campinas, São Paulo 13081-970, Brazil
e-mail: betania@feq.unicamp.br

K_i	affinity constant
K_{ji}	inhibition constant
L	reactor length
p	level of fractionation
R_i	reaction rate
S_i	extracellular concentration
S_{in}	feed glucose concentration
u	superficial velocity
X_{in}	feed biomass concentration
X_i	active cell material
X_{LADH}	lactate dehydrogenase
ε	porosity
η	effectiveness factor

Introduction

In biotechnological process, a great number of factors can influence income, productivity, and conversion. Normally, it is not evident which of these factors are the most important and how they interact. This knowledge are important in an early design stage so that better process can be developed especially in terms of high production and lower environmental impact and also to define suitable operating strategies. A way to do this is to use multivariate analysis techniques as experimental design coupled to a detailed model so that several operation scenarios may be investigated. A central point in this exercise is to have a good process model, and in this sense, the knowledge of the kinetic parameters is essential.

Design of experiments is a powerful technique used for discovering a set of process factors that are most important to the process and then determine at what levels these factors must be kept to optimize the process performance [1].

This work presents an analysis of kinetic parameters, used in a dynamic structured model for the acrylic acid production process. Through this procedure, it was possible to identify the parameters with the most significant impact on the model to represent well the process of acrylic acid production.

First, an experimental design was performed to identify the key kinetics parameters that affect the response of interest (acrylic acid concentration in the steady state). For identification of these parameters, the methodology Plackett–Burman was used.

Plackett–Burman [2] is a tool for this initial screening, as it makes it possible to determine the influence of various factors with only a small number of trials, instead of using more extensive factorial design, which would furnish more complete information but which involves unfeasible complexity.

After identifying the key kinetics parameters, a full factorial was applied to identify and quantify the interactions among the key parameters and to understanding how these interactions take place. To identify the effects of the operational parameters on the acrylic acid production, a fractional factorial was applied.

Mathematical Modeling

A deterministic mathematical model for simulating the biotechnological synthesis of acrylic acid was developed in a previous study [3] to explore an alternative process. The proposed

process makes it possible to obtain acrylic acid continuously from the sugarcane fermentation. The reactor is continuously operated, and the challenge is to define operating strategy and conditions to achieve the product within the desired specifications. The kinetic model is based on the concepts of structured representation and adapted from a structured growth model developed by Lei et al. [4] and a structured model for ethanol production developed by Stremel [5].

A continuous bioreactor type plug flow reactor (PFR) with immobilized cell of *Saccharomyces cerevisiae* in spherical particle was used in the work to take into account the variations of concentrations at the reactor length and inside spherical particle.

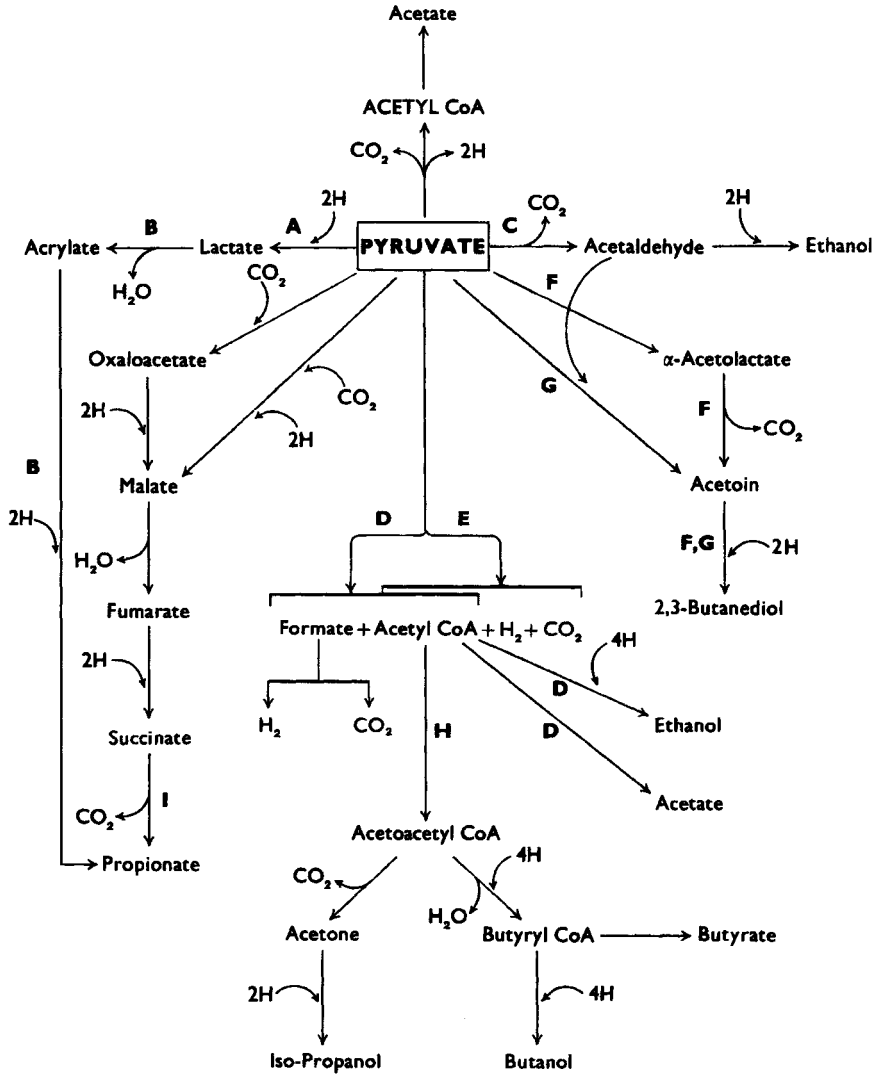


Fig. 1 Glycolytic route. Pyruvate formed by catabolism of glucose is further metabolized by pathways, which are characteristic of particular organism (see [7])

In *S. cerevisiae*, the major flux of pyruvate metabolism is to ethanol, by way of pyruvate decarboxylase and alcohol dehydrogenase. Providing an alternative route for regenerating NAD^+ through lactate dehydrogenase, which catalyzes the reduction of pyruvate to lactate, can theoretically replace ethanolic fermentation [6].

The bioreactor behavior is based on mass balances for the key chemical species of the fermentative process. The reaction stoichiometric considered was

$$\underset{\text{glucose}}{C_6H_{12}O_6} \rightarrow \underset{\text{lactate}}{2C_3H_6O_3}$$

$$\underset{\text{lactate}}{C_3H_6O_3} \rightarrow \underset{\text{acrylic acid}}{C_3H_4O_2} + H_2O$$

Figure 1 shows the scheme of the metabolic pathway for obtaining the acrylic acid. Several parallel and consecutive reactions take place and are necessary to find out operating conditions, which allow the desired product to be obtained.

Figure 2 shows a representative metabolic route involved in the process of acrylic acid production and also the reaction rates (see Table 1).

Table 1 shows the reaction rates used in the mathematical model and the kinetic parameters that are analyzed in this work.

The reaction rate (R_1) describes the glucose uptake and glycolytic pathway, and it is represented by two Michaelis–Menten equations [4].

R_2 represents the cell growth (biomass formation) from glucose with inhibition by lactate. The biomass formed is converted into active cellular material. The reaction rates (R_3) and (R_4) describe the lactate and acrylic acid formation, respectively.

Equation (R_5) corresponds to the biomass formation from lactate, where a glucose inhibition term is included in the equation. Equation (R_6) describes the formation of lactate dehydrogenase from active component in the cell material (X_a). An acrylic acid inhibition term was added in this equation. Equation (R_7) shows the degradation rate of the active compartment and depends of the glucose and acrylic acid present in the medium. These reaction rates and the kinetic parameters values were obtained from Lei et al. [4] and modified to describe the acrylic acid production process.

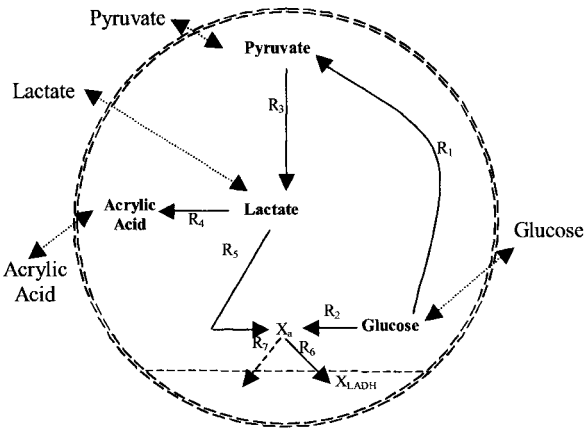


Fig. 2 Representative metabolic route

Table 1 Reaction rates.

Reactions
$R_1 = k_1 \frac{S_{glucose}}{S_{glucose}+K_1} X_a + k_{1a} \frac{S_{glucose}}{S_{glucose}+K_{1a}} X_a$
$R_2 = k_2 \frac{S_{glucose}}{S_{glucose}+K_2} \frac{1}{1+\left(\frac{S_{lactate}}{K_{2i}}\right)} X_a$
$R_3 = k_3 \frac{S_{pyruvate}}{S_{pyruvate}+K_3} X_a$
$R_4 = k_4 \frac{S_{lactate}}{S_{lactate}+K_4} X_a$
$R_5 = k_5 \frac{S_{lactate}}{S_{lactate}+K_5} \left(\frac{1}{1+K_{5i}S_{glucose}}\right) X_a$
$R_6 = k_6 \left(\frac{S_{glucose}}{S_{glucose}+K_6} + \frac{S_{lactate}}{S_{lactate}+K_{6a}}\right) \left(\frac{1}{K_{6i}S_{acrylic\ acid}+1}\right) X_a$
$R_7 = \left(k_7 \frac{S_{glucose}}{S_{glucose}+K_7} + k_{7a} \frac{S_{acrylic\ acid}}{S_{acrylic\ acid}+K_{7a}}\right) X_a$

Table 2 Mass balance for fluid and solid phase.

Reactions
Fluid phase
$\frac{\partial S_{glucose}}{dt} = D_{az}\left(\frac{\partial^2 S_{glucose}}{\partial z^2}\right) - u\left(\frac{\partial S_{glucose}}{\partial z}\right) + \frac{1-\varepsilon}{\varepsilon}\eta\left[(R_1 - R_2)_e^{-K_A S_{acrylic\ acid}} X\right]$
$\frac{\partial S_{pyruvate}}{dt} = D_{az}\left(\frac{\partial^2 S_{pyruvate}}{\partial z^2}\right) - u\left(\frac{\partial S_{pyruvate}}{\partial z}\right) + \frac{1-\varepsilon}{\varepsilon}\eta\left[(0.978R_1 - R_3)_e^{-K_A S_{acrylic\ acid}} X\right]$
$\frac{\partial S_{lactate}}{dt} = D_{az}\left(\frac{\partial^2 S_{lactate}}{\partial z^2}\right) - u\left(\frac{\partial S_{lactate}}{\partial z}\right) + \frac{1-\varepsilon}{\varepsilon}\eta\left[(1.023R_3 - R_4 - R_5)e^{-K_A S_{acrylic\ acid}} X\right]$
$\frac{\partial S_{acrylic\ acid}}{dt} = D_{az}\left(\frac{\partial^2 S_{acrylic\ acid}}{\partial z^2}\right) - u\left(\frac{\partial S_{acrylic\ acid}}{\partial z}\right) + \frac{1-\varepsilon}{\varepsilon}\eta\left[(0.8R_4 - R_7)e^{-K_A S_{acrylic\ acid}} X\right]$
Solid phase
$\frac{\partial S_{glucose}}{\partial t} = \frac{D_{Ag}}{R^2}\frac{1}{r^2}\frac{\partial}{\partial r}\left(r^2 \frac{\partial S_{glucose}}{\partial r}\right) + (R_1 + R_2)_e^{-K_A S_{acrylic\ acid}} X$
$\frac{\partial S_{pyruvate}}{\partial t} = \frac{D_{Ap}}{R^2}\frac{1}{r^2}\frac{\partial}{\partial r}\left(r^2 \frac{\partial S_{pyruvate}}{\partial r}\right) + (0.978R_1 - R_3)_e^{-K_A S_{acrylic\ acid}} X$
$\frac{\partial S_{lactate}}{\partial t} = \frac{D_{Al}}{R^2}\frac{1}{r^2}\frac{\partial}{\partial r}\left(r^2 \frac{\partial S_{lactate}}{\partial r}\right) + (1.023R_3 - R_4 - R_5)_e^{-K_A S_{acrylic\ acid}} X$
$\frac{\partial S_{acrylic\ acid}}{\partial t} = \frac{D_{Aaa}}{R^2}\frac{1}{r^2}\frac{\partial}{\partial r}\left(r^2 \frac{\partial S_{acrylic\ acid}}{\partial r}\right) + (0.8R_4 - R_7)_e^{-K_A S_{acrylic\ acid}} X$
$\frac{\partial X}{\partial t} = (0.732R_2 - 0.821R_5)X\left(1 - \frac{X}{X_{sat}}\right)e^{-K_A{}^n S_{acrylic\ acid}} - k_d X$
$\frac{\partial X_a}{\partial t} = (0.732R_2 - 0.821R_5 - R_6 - R_7) - (0.732R_2 + 0.821R_5)X_a$
$\frac{\partial X_{LADH}}{\partial t} = R_6 - (0.732R_2 + 0.821R_5)X_{LADH}$

The model consists of a set of partial differential equations describing the acrylic acid, lactate and pyruvate production, cellular growth, and glucose consumption (see Table 2).

Table 2 shows the mass balance of the main components of the process in the fluid and solid phase. The whole set of equations is solved coupling the Orthogonal Collocation Method to discretize the radial ordinates with the Method of Lines to integrated the system of equations by a stiff integrator. This work is only a theoretical study, as a predictive tool, and all presented data were simulated.

Experimental Design and Results

In the development of new process and product, the number of potential factor or variables is often excessively large. Experimental design are useful to reduce the number of variable to a manageable size so that further experiments can be performed using these key variables for a better understanding of the process/product [1].

A large number of kinetics parameters are involved in the definition of the best operating conditions to achieve the acrylic acid, taking into account all others possible products. Bearing this in mind, 24 parameters are chosen as necessary to be investigated to produce acrylic acid.

For studying such 24 kinetic parameters, Plackett–Burman design with 32 runs and 31 degrees of freedom was selected. The different parameters (variables) were prepared in two

Table 3 Kinetic parameters used in the experimental design and their levels.

Parameters	Values	
	Low level (−1)	High level (+1)
k_1	1.92	2.88
k_{1a}	0.4672	0.7008
k_2	2.64	3.96
k_3	4.16	6.24
k_4	3.40	5.10
k_5	0.96	1.44
k_6	0.024	0.036
k_7	0.032	0.048
k_{7a}	0.0032	0.0048
K_1	0.0008	0.0012
K_{1a}	0.00928	0.01392
K_2	2.32	3.48
K_3	2.56	3.84
K_4	1.68	2.52
K_5	1.88	2.82
K_6	1.56	2.34
K_{6a}	10.40	15.60
K_7	0.016	0.024
K_{7a}	0.00072	0.00108
K_{2i}	0.072	0.108
K_{5i}	1.584	2.376
K_{6i}	2.0	3.0
K_A[a]	0.072	0.108
$K_{A''}$[a]	0.152	0.228

[a] The parameters K_A and $K_{A''}$ do not appear in Table 1, but they are included in the mass balance realized inside of the particle (see Table 2).

levels, (−1) for low level and (+1) for high level. Seven dummy variables are used to estimate the standard error during analysis of data. The kinetic parameters analyzed in this study and their levels (low and high) are shown in Table 3. The values shown in Table 3 were obtained through simulation realized in the process model of acrylic acid production.

Statistica software was used to generate the matrix of the parameters values and simulation program based on a detailed model described in "Mathematical Modeling", written in Fortran language, was used to generate the desired process response. The simulations were conducted according to the 32-run Plackett–Burman design for the 24 kinetic variables, specified in Table 3. Each simulation (test) generates a result of acrylic acid concentration in the steady state (desired response).

The Pareto chart (Fig. 3) was used for identifying which estimated effects are the most important in the rote to obtain acrylic acid and to identify possible interaction effects showed later on.

Figure 3 depicts that of the 24 parameters analyzed, 10 parameters, K_A (inhibition constant by product), $K_{A'}$ (inhibition constant by product related with cell), k_1, k_{1a}, k_2, k_4 (specifics reaction rates), K_3, K_4, K_5 (affinity constants), and K_{5i} (inhibition constant) were statistically significant for acrylic acid concentration at 99% of confidence level (the dot line is the reference). These results also can be visualized in Table 4, where the results of the analysis of variance (ANOVA) for the 32-run Plackett–Burman design are shown.

As the number of significant parameters identified in the first experimental design is high, a new Plackett–Burman design was chosen to screen the most significant parameters between the ten parameters identified before.

For this study, a Plackett–Burman design with 16 runs and 15 degrees of freedom was selected. Pareto chart (Fig. 4) was used for show the obtained results.

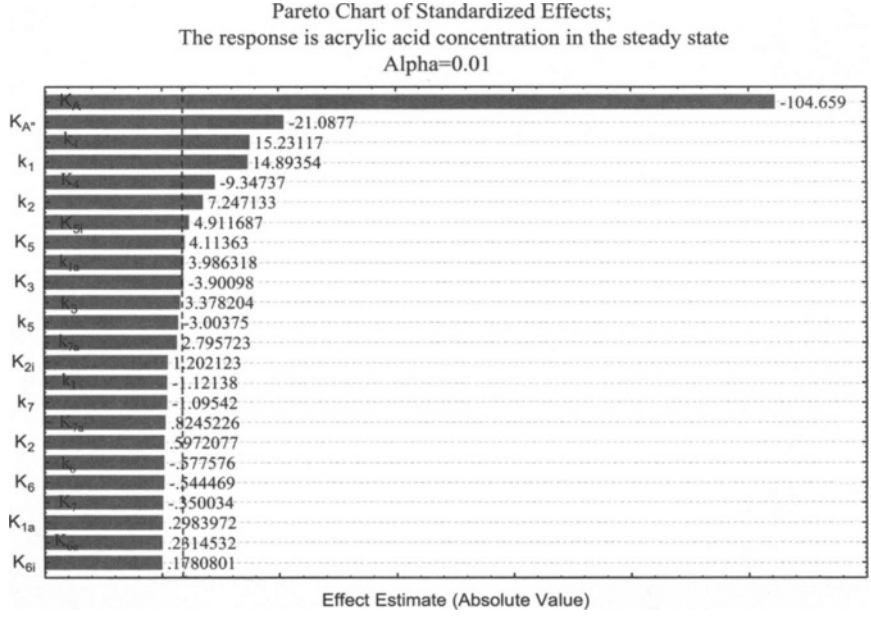


Fig. 3 Pareto chart of effects for acrylic acid concentration from 32-run Plackett–Burman design

Table 4 The results of the ANOVA for 32-run Plackett–Burman design.

Factor	Sum of squares	*df*	Mean square	*F* value	*p* value
k_1[a]	19.6748	1	19.6748	221.82	0.000001
k_{1a}[a]	1.385	1	1.3845	15.89	0.005281
k_2[a]	4.576	1	4.576	52.52	0.000170
K_3	0.994	1	0.994	11.41	0.01179
k_4[a]	20.213	1	20.213	231.99	0.000001
K_5	0.786	1	0.786	9.02	0.019837
K_6	0.0291	1	0.0291	0.33	0.58164
K_7	0.105	1	0.105	1.20	0.309583
K_{7a}	0.6810	1	0.6810	7.82	0.02669
K_1	0.110	1	0.1096	1.26	0.29912
K_{1a}	0.008	1	0.008	0.09	0.774063
K_2	0.031	1	0.0311	0.36	0.569174
K_3[a]	1.326	1	1.326	15.22	0.005891
K_4[a]	7.613	1	7.613	87.37	0.000033
K_5[a]	1.474	1	1.474	16.92	0.004495
K_6	0.026	1	0.026	0.30	0.60302
K_{6a}	0.005	1	0.005	0.05	0.82358
K_7	0.011	1	0.011	0.12	0.736609
K_{7a}	0.059	1	0.059	0.68	0.43683
K_A[a]	954.344	1	954.344	10953.43	0.00000
$K_{A''}$[a]	38.745	1	38.745	444.69	0.00000
K_{2i}	0.126	1	0.126	1.45	0.2684
K_{5i}[a]	2.102	1	2.102	24.12	0.001730
K_{6i}	0.003	1	0.003	0.03	0.863704
Error	0.610	7	0.0871		

[a] Significant parameters

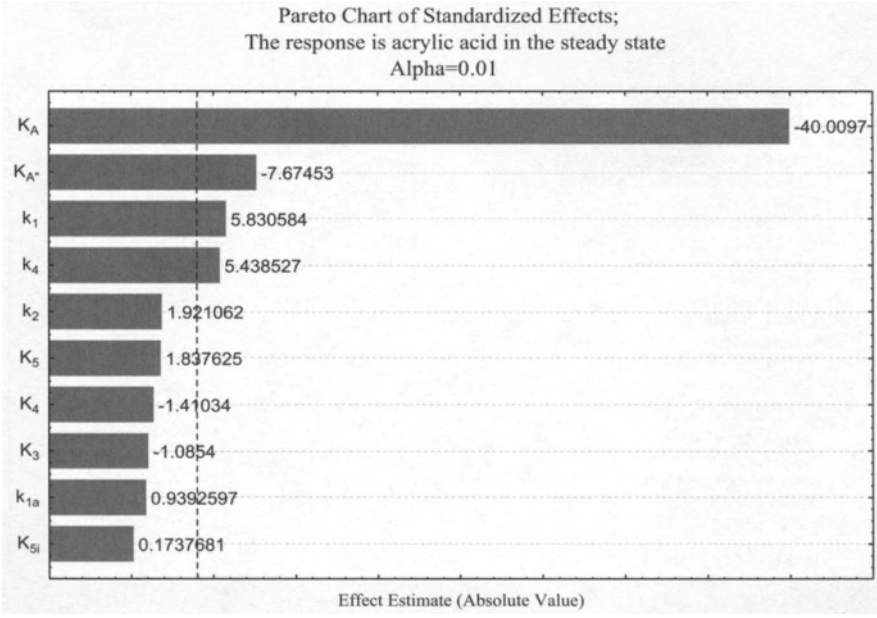


Fig. 4 Pareto chart of effects for acrylic acid concentration from 16-run Plackett–Burman design

Table 5 Coded units of parameters and response obtained from 2^4 full factorial design.

Test	Parameters				Response AA
	k_1	k_4	K_A	$K_{A''}$	
1	−1	−1	−1	−1	45.7547
2	1	−1	−1	−1	47.1526
3	−1	1	−1	−1	47.1336
4	1	1	−1	−1	49.4629
5	−1	−1	1	−1	35.5647
6	1	−1	1	−1	36.1339
7	−1	1	1	−1	36.9125
8	1	1	1	−1	37.9857
9	−1	−1	−1	1	43.7080
10	1	−1	−1	1	45.3416
11	−1	1	−1	1	44.8187
12	1	1	−1	1	47.4619
13	−1	−1	1	1	33.0871
14	1	−1	1	1	34.0245
15	−1	1	1	1	34.1258
16	1	1	1	1	35.6197

Figure 4 depicts that of the ten parameters analyzed, four parameters, K_A (inhibition constant by product), $K_{A'}$ (inhibition constant by product related with cell), k_1, and k_4 (specifics reaction rates) were statistically significant for acrylic acid concentration at 99% of confidence level. After identifying the key parameters, a full factorial design (2^k) was

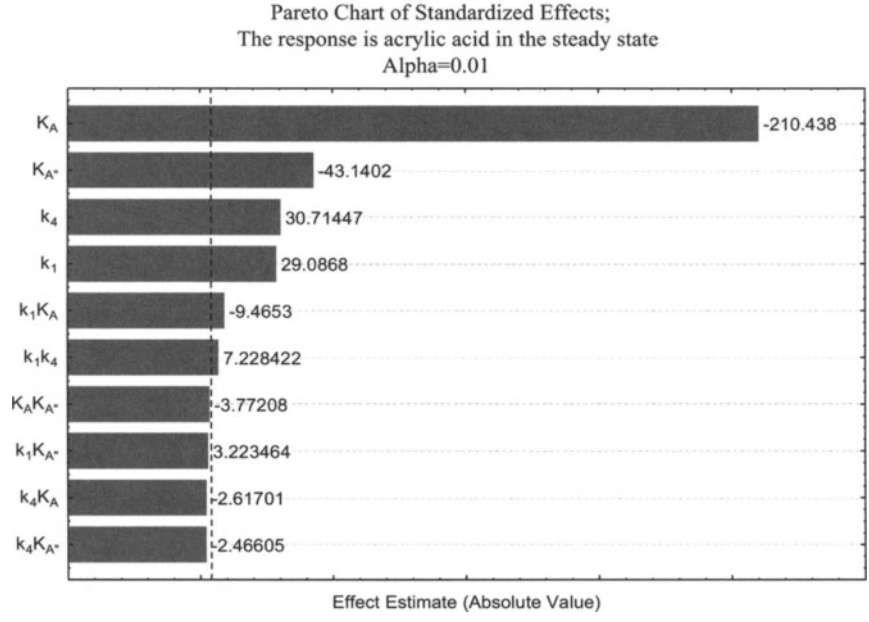
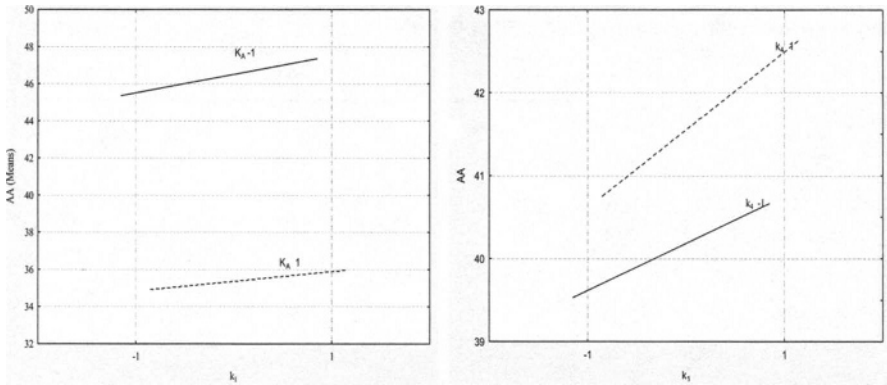


Fig. 5 Pareto chart of effects for acrylic acid concentration, from full factorial design (2^4)



a Interaction between k_1 and k_4 **b** Interaction between k_1K_A

Fig. 6 **a** Influence of the interactions between k_1 and k_4 in the acrylic acid concentration (mean value). **b** Influence of the interactions between k_1 and K_A in the acrylic acid concentration (mean value)

used to identify and to quantify the possible interactions among the key parameters. The understanding of such interactions is very important to achieve high conversion in the desired product and can be used for instance to design an optimum substrate besides the definitions of suitable operating conditions to met the objective (acrylic acid production). To do this, a full factorial design of two-level (2^4) coupled to the detailed process model was used. Four variables (k_1, k_4, K_A, and $K_{A''}$) in 16 runs were investigated in this design stage. Table 5 shows the coded units of parameters and the obtained response in each simulation (column 6). The obtained results from the 2^4 full factorial design was shown in the Pareto chart (Fig. 5).

Figure 5 also depicts that all the key parameters (k_1, k_4, K_A, and $K_{A''}$) and two interactions (k_1k_4 and k_1K_A) are statistically significant at 99% confidence level.

Figure 6a shows interaction plot between (k_1) and (K_A). Through the chart, it is possible to realize that the effect of (k_1) in the response (acrylic acid concentration in the steady state) is different at different levels of (K_A). The maximum acrylic acid concentration is

Table 6 The results of the ANOVA for 2^4 full factorial design.

Factor	Sum of squares	*df*	Mean square	Coeff. estimate	*F* value	*p* value
k_1[a]	9.1170	1	9.1170	0.75486	846.04	0.000001
k_4[a]	10.1659	1	10.1659	0.79720	943.38	0.000001
K_A[a]	477.2062	1	477.2062	−5.46126	44384.11	0.000000
$K_{A''}$[a]	20.0555	1	20.0555	−1.11957	1861.08	0.000000
k_1k_4[a]	0.5630	1	0.5630	0.18759	52.25	0.000791
k_1k_A[a]	0.9654	1	0.9654	−0.24564	89.59	0.000222
$K_1k_{A''}$	0.1120	1	0.1120	0.08366	10.39	0.023375
K_4k_A	0.0738	1	0.0738	−0.06792	6.85	0.047268
$K_4K_{A''}$	0.0655	1	0.0655	−0.06406	6.08	0.056805
$K_AK_{A''}$	0.1533	1	0.1533	−0.09789	14.23	0.012995
Error	0.0539	5	0.0108	Mean=40.8930		

[a] Significant parameters

Table 7 Operational and design parameters used in the experimental design and their levels.

Parameters	Values	
	Low level (−)	High level (+)
S_{in}	80	120
F_{in}	0.032	0.048
X_{in}	16	24
D_p	0.024	0.036
D_r	0.4	0.6
L	1.6	2.4

achieved when the (k_1) is high and (K_A) value is low. Figure 6b shows an interaction plot between (k_1) and (k_4). Through this figure, it is possible to visualize that the maximum acrylic acid concentration is achieved when (k_1) and (k_4) value is high. This can be used to guide the operator in the search for operating conditions and to design the substrate. Furthermore, this information can be used to have insights on how possible changes in the microorganism genetics should be made to potentialize the acrylic acid production. In Table 6, the results of the ANOVA for the 2^4 full factorial designs are shown.

To analyze the operational parameters used in the acrylic acid production process, a fractional factorial design of two-level (2^{k-p}) with two level of fractionation was used. In this experimental design, six variables (S_{in}, F_{in}, X_{in}, D_p, D_r, and L) were investigated in 16 runs. The values of such parameters are shown in Table 7, whereas Table 8 depicts the coded units of parameters and the obtained response in each simulation (column 8). The obtained results are shown in Pareto chart (Fig. 7).

As can be seen through the analyses of Fig. 7, it is possible to observe that the parameters, F_{in} (feed rate), X_{in} (feed biomass concentration), D_r (reactor diameter), and L (reactor length) are statistically significant at 99% confidence level. Two first variables are possible to be used as operating variables, but the last two (reactor diameter and length) are design variables that have to be chosen in a early design stage. If this investigation is not

Table 8 Coded units of parameters and response obtained from 2^{6-2} fractional factorial design.

Test	Parameters						Response
	S_{in}	F_{in}	X_{in}	D_p	D_r	L	AA
1	−1	−1	−1	−1	−1	−1	34.2994
2	1	−1	−1	−1	1	−1	41.2667
3	−1	1	−1	−1	1	1	42.1471
4	1	1	−1	−1	−1	1	34.9833
5	−1	−1	1	−1	1	1	47.6661
6	1	−1	1	−1	−1	1	40.4901
7	−1	1	1	−1	−1	−1	32.4330
8	1	1	1	−1	1	−1	39.6531
9	−1	−1	−1	1	−1	1	37.8220
10	1	−1	−1	1	1	1	45.2582
11	−1	1	−1	1	1	−1	36.9228
12	1	1	−1	1	−1	−1	30.8105
13	−1	−1	1	1	1	−1	42.6191
14	1	−1	1	1	−1	−1	35.2548
15	−1	1	1	1	−1	1	36.0530
16	1	1	1	1	1	1	43.7811

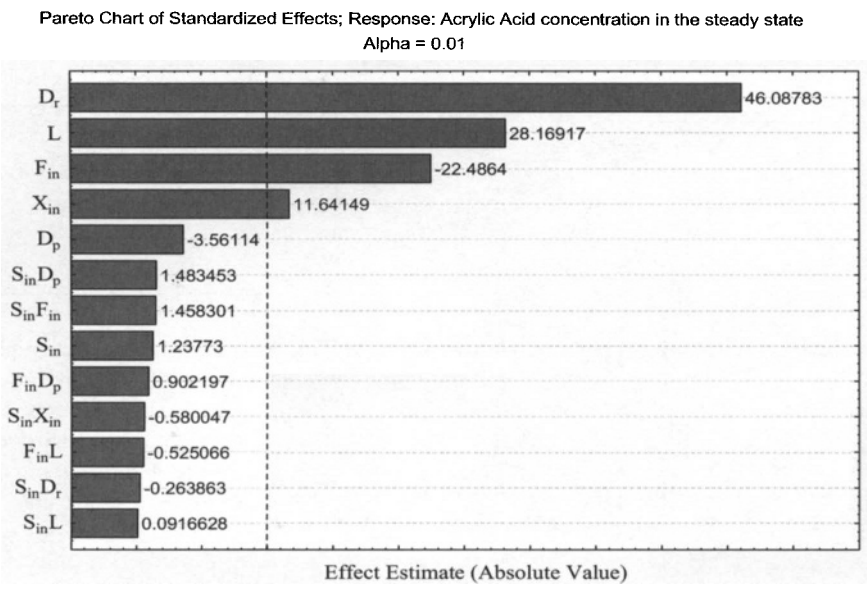


Fig. 7 Pareto chart of effects of initial and operation conditions from fractional factorial design (2^{6-2})

carried out, it is possible to have a process with lower operational performance, as changes in the operational may not be enough to drive the process to high operational performance. At this point, it is worthwhile to mention that the economical success of this alternative acrylic acid production process depends upon the achievement of high concentrations, as the downstream operations are complex and expensive, and the conventional process, even environmentally aggressive, are well established nowadays.

Through these experimental designs, it is possible to identify the optimal values of the parameters to increase the acrylic acid concentration from biotechnological process (inside of value range established for this process). Table 9 shows the optimal condition settings of factors.

Conclusions

In this work, the kinetics and operational parameters used in the acrylic acid production from biotechnological process were analyzed, bearing in mind that high operational

Table 9 Optimal values for analyzed parameters.

Factors	Optimal level
K_1	2.88
K_4	5.10
K_A	0.072
$K_{A''}$	0.152
F_{in}	0.032
X_{in}	24
D_r	0.6
L	2.4

performance are required to become this alternative process competitive with the well-established conventional ones. The appeal of the environmental less aggressive and renewable feedstock-based process is, nowadays, a target to be met; however, economical considerations have to be made. This is an issue that can be suitably dealt with through simulation tools as has been extensively made in other industry (as car makers using computational fluid dynamics to find out the best vehicle design). In this work, a procedure was proposed and used based on the experimental design that allows designing and operating the alternative process to obtain acrylic acid. This was made in two stages. First, using the methodology of Plackett–Burman design, it was possible to evaluate the kinetic parameters and identify the parameters that have significant impact in the acrylic acid production process.

Later on, through fractional factorial design, the operational parameters with a significant impact in the process were identified. In addition, it was possible to identify the optimal values for kinetic and operational parameters. The optimal values of such parameters identified in these experimental designs are able to drive the process to maximize the acrylic acid concentration.

The acrylic acid synthesis from fermentative process is a recent subject with very few works published in the literature without conclusive kinetic data of the process. Therefore, it is valuable to identify the effect of the kinetic parameters values to trace guidelines to process design and operation and to gain some insights on how genetic modifications should be made in the microorganism to met specific objectives, in this case, to enhance the acrylic acid conversion. Besides that, extensive simulation can be made allowing an understanding of the process features, which is useful to take decisions at an early design stage.

Acknowledgements The authors are grateful to the Fundação de Amparo à Pesquisa do Estado de São Paulo–FAPESP process number 05/53186–8 for the financial support.

References

1. Antony, J., & Kaye, M. (1999). In Antony, J. (2002). Training for design of experiments using a catapult. *Quality and reliability engineering international, 18*, 29–35.
2. Plackett, R. L., & Burman, J. P. (1946). The design of optimum multifactorial experiments. *Biometrika, 33*, 305–325.
3. Lunelli, B. H., Duarte, E. R., Vasco de Toledo, E. C., Wolf Maciel, M. R., & Maciel Filho, R. (2007). A new process for acrylic acid synthesis by fermentative process. *Applied Biochemistry and Biotechnology, 136-140*, 487–500.
4. Lei, F., Rotboll, M., & Jorgensen, S. B. (2001). A biochemically structured model for *Saccharomyces cerevisiae*. *Journal of Biotechnology, 88*, 205–221.
5. Stremel, D. P. (2001). Desenvolvimento de modelos estruturados alternativos para o processo de produção de etanol. PhD thesis. State University of Campinas. Campinas, Brazil.
6. Skory, C. D. (2003). Lactic acid production by *Saccharomyces cerevisiae* expressing a *Rhizopus* orizae lactate dehydrogenase gene. *Journal of Industrial Microbiology & Biotechnology., 30*, 22–27.
7. Dawes, I., & Large, P. J. (1982). Supply of carbon skeletons. In J. Mandelstam, K. McQuillen, & I. Dawes (Eds.), *Biochemistry of bacterial growth*. pp. 125–158. Oxford: Blackwell.

Appl Biochem Biotechnol (2008) 148:189–198
DOI 10.1007/s12010-007-8042-x

Optimization of Oligosaccharide Synthesis from Cellobiose by Dextransucrase

Misook Kim · Donal F. Day

Received: 10 May 2007 / Accepted: 4 September 2007 /
Published online: 2 October 2007
© Humana Press Inc. 2007

Abstract There is a growing market for oligosaccharides as sweeteners, prebiotics, anticariogenic compounds, and immunostimulating agents in both food and pharmaceutical industries. Interest in novel carbohydrate-based products has grown because of their reduced toxicity and low immune response. Cellobiose is potentially valuable as a nondigestible sugar. The reaction of cellobiose, as an acceptor with a sucrose as a donor, catalyzed by a dextransucrase from *Leuconostoc mesenteroides* B-512FMCM, produced a series of cellobio-oligosaccharides. This production system was optimized using a Box–Behnken experimental design for 289 mM of sucrose and 250 mM of cellobiose and 54 U of the enzyme at pH 5.2 and 30 °C, to produce maximum yields of oligosaccharide.

Keywords Oligosaccharide · Cellobiose · Dextransucrase · *Leuconostoc mesenteroides* B-512FMCM · Box-Behnken experimental design

Introduction

Oligosaccharides are carbohydrate polymers, generally of two to ten monomeric residues linked by *O*-glycosidic bonds [1]. Most commercial oligosaccharides were originally developed as sweeteners, but they are currently valued as soluble fiber, which decreases gastrointestinal transit time and moderates constipation and diarrhea. Oligosaccharides are considered to be low-calorie food because they are resistant to attack by digestive enzymes in human and animals and are not absorbed by the host [2]. Oligosaccharides may be produced through microbial fermentation, enzymatic synthesis, or extraction from naturally occurring sources. Currently, commercial oligosaccharides include cyclomaltodextrins, maltodextrins, fructooligosaccharides, galactooligosaccharides, and soy oligosaccharides [3].

Cellobiose is a disaccharide of two glucose molecules linked in a β-1,4 bond produced from enzymatic hydrolysis of cellulose. Enzymes capable of breaking down cellobiose are

M. Kim
Department of Food Science, Louisiana State University, Baton Rouge, LA 70803, USA

D. F. Day (✉)
Audubon Sugar Institute, St. Gabriel, LA 70776, USA
e-mail: dday@agcenter.lsu.edu

absent in the human small intestine. Nakamura et al. [4] confirmed that cellobiose may be hydrolyzed slowly by intestinal lactase in an in vitro study with rat small intestinal brush border membrane vesicles. There are some reports of new classes of sugars, containing cellobiose as a component, produced by transglycosylation reactions [5, 6]. Acarbose analogues containing cellobiose were prepared by the reaction of acarbose and *Bacillus stearothermophilus* α-maltogenic amylase (EC 3.2.1.133; [5]). Cellobiose–acarbose analogues show a potential for use as an inhibitor of β-glucosidase, whereas acarbose does not. Morales et al. [6] produced oligosaccharides with branched chains, using cellobiose as acceptor in the reaction catalyzed by alternansucrase from *Leuconostoc mesenteroides* NRRL B-23192. *L. mesenteroides* B512 FMCM mainly produces extracellularly dextransucrase (EC 2.4.1.5). This dextransucrase synthesizes a dextran that has 95% α-(1→6) linear and 5% α-(1→3) branched linkages and can transfer glucosyl units from sucrose onto the acceptor to produce oligosaccharides [7].

This work reports on optimization of some variables that play an important role in the production of cellobio-oligosaccharides; they are temperature, pH, enzymatic concentration, and the concentrations of sucrose and cellobiose.

Materials and Methods

Dextransucrase Production

L. mesenteroides B-512 FMCM was grown for 16 h at 30 °C in liquid mineral (LM) medium [0.5% (w/v) yeast extract, 0.5% (w/v) peptone, 2% (w/v) K_2HPO_4, 0.02% (w/v) $MgSO_4 \cdot 7H_2O$, 0.001% (w/v) NaCl, 0.001% (w/v) $FeSO_4 \cdot 7H_2O$, 0.001% (w/v) $MnSO_4 \cdot H_2O$, 0.013% (w/v) $CaCl_2 \cdot 2H_2O$] containing 2% glucose. The inoculum development stage required three successive transfers to build sufficient volume for inoculation for the final fermentation. A four-hundred-milliliter culture was inoculated to 14 l of LM medium and incubated for 48 h at 30 °C. The pH and agitation were not controlled during fermentation. After harvesting, cells were removed by centrifugation at 6,000 rpm×*g* for 30 min. The cell-free culture was concentrated tenfold using membrane filtration (100 K cutoff) and washed with 2 vol of sodium citrate buffer, pH 5.2. Tween 80 and NaN_3 were added at concentrations of 1 and 0.2 mg/ml to crude enzyme. The size and specific activity of dextransucrase were 180 kDa and 22.15 (U/mg).

Dextransucrase Assay

Crude dextransucrase was reacted with 100 mM sucrose for 1 h at 30 °C and then boiled for 5 min to terminate the enzyme reaction. One unit of dextransucrase activity was defined as that amount of enzyme releasing 1 μM fructose per min from 100 mM sucrose. The fructose was determined by high-performance liquid chromatography (HPLC) using an Aminex HPX 87K column (300×7.8 mm) and an HPLC analyzer coupled to a refractive index detector. The column was maintained at 85 °C and 0.01 M K_2SO_4 was used as a mobile phase at a flow rate 0.6 ml/min.

Transglycosylation Reaction

To determine optimal reaction conditions, reaction digests were prepared with various sucrose (100–800 mM), cellobiose (50–300 mM), and crude dextransucrase (13–67 U)

concentrations in 20 mM sodium citrate buffer (pH 3.2–6.0) at 20–50 °C for 24 h. The enzyme reaction products were analyzed by high-performance anion exchange chromatography using a Dionex Carbo-Pac PA 100 column (250×4 mm) by gradient elution using 1 M NaOH, water, and 480 mM sodium acetate at a constant flow rate of 0.5 ml/min. Oligosaccharide detection was carried out with an electrochemical detector (ED 40). Relative concentrations of oligosaccharide were analyzed by thin-layer chromatography (TLC). The TLC samples were loaded onto a Whatman K5 silica gel plate. The plate was irrigated three times with 2:5:1.5 volume parts of nitromethane–1-propanol–water. The carbohydrates on the TLC plate were visualized by dipping the plate into a methanol solution containing 0.3% (w/v) *N*-(1-naphthyl) ethylenediamine and 5% (v/v) sulfuric acid, followed by heating at 110 °C for 15 min. The relative percent of carbohydrates were determined using a Scion program from National Institutes of Health (NIH).

Box–Behnken Experimental Design

A three-factor and three-level Box–Behnken design was applied for the optimization procedure using Design Expert 6 software (Stat-Ease). Several factors—the amounts of sucrose, cellobiose, and dextransucrase—used to prepare each of the 17 formulations are given in Tables 1 and 2. These high, medium, and low levels were selected from the preliminary experimentation. Optimization was performed using a desirability function to obtain the levels of X_1, X_2, and X_3.

The behavior of the system has been explained by the following quadratic model equation [8]:

$$Y = \beta_0 + \beta_1 X_1 + \beta_2 X_2 + \beta_3 X_3 + \beta_{11} X_1^2 + \beta_{22} X_2^2 + \beta_{33} X_3^2 + \beta_{12} X_1 X_2 + \beta_{13} X_1 X_3 + \beta_{23} X_2 X_3 \quad (1)$$

where Y is predicted response, β_0 intercept, β_1, β_2, and β_3 linear coefficient, β_{11}, β_{22}, and β_{33} squared coefficients, and β_{12}, β_{13}, and β_{23} interaction coefficients. A total of 17 experiments were necessary to study the ten coefficients of model.

Results and Discussion

A pH of 5.2 was optimum for production of cellobio-oligosaccharides (Fig. 1). The optimum pH for oligosaccharide production was same as that for dextransucrase activity [9]. The production of cellobio-oligosaccharides was more sensitive to the changes in pH than was dextransucrase activity. Cellobio-oligosaccharide concentrations produced at pH 6.2 were 39% of that produced at pH 5.2.

Table 1 Variables in Box–Behnken design: independent variables.

Independent variables	Levels		
	Low	Middle	High
X_1: sucrose (mM)	100	250	400
X_2: cellobiose (mM)	50	150	250
X_3: dextransucrase (U)	27	40	54

Table 2 Variables in Box–Behnken design: dependent variable (Y: relative amount of cellobio-oligosaccharides produced [%])—concentrations (mM) of each independent variable used to prepare the 17 formulations.

Run	X_1	X_2	X_3
1	100	50	40
2	100	150	27
3	100	150	54
4	100	250	40
5	250	50	27
6	250	50	54
7	250	150	40
8	250	150	40
9	250	150	40
10	250	150	40
11	250	150	40
12	250	250	27
13	250	250	54
14	400	50	40
15	400	150	27
16	400	150	54
17	400	250	40

The rate of cellobio-oligosaccharide production sharply decreased above 30 °C and at 40 °C was only 46% of the maximum production (Fig. 2). The effect of temperature on the oligosaccharide production showed the same pattern as the effect of temperature on dextransucrase activity [9].

Optimization of transglycosylation was achieved by employing a Box–Behnken design for the experiments. The response surface methodology was used to study the effect of interaction among independent variables—sucrose, cellobiose, and dextransucrase on the production of cellobio-oligosaccharides. Table 3 depicts the actual and predicted values of cellobio-oligosaccharides on the basis of the experimental design. The predicted values and the observed values agreed reasonably well, as seen from Table 3. The results were

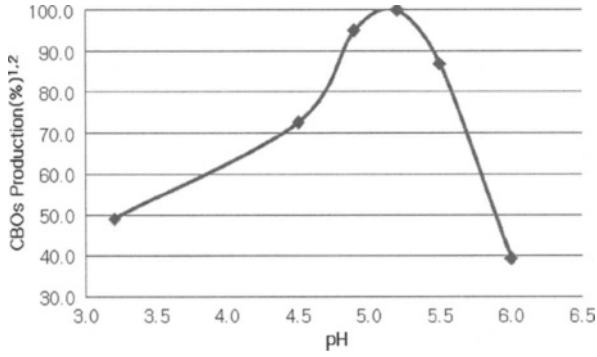


Fig. 1 Production of cellobio-oligosaccharides synthesized by *L. mesenteroides* B-512 FMCM dextransucrase at various pH values. [1]Cellobio-oligosaccharide production was calculated as the percentage concentration of cellobio-oligosaccharides at the selective pH, divided by the highest concentration of cellobio-oligosaccharide over all pH ranges. [2]Reactions conducted at 100 mM sucrose, 100 mM cellobiose, dextransucrase 27 U, and 30 °C for 24 h

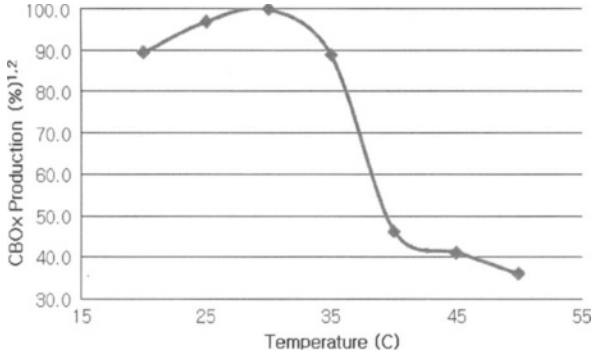


Fig. 2 Oligosaccharides produced as a function of temperature changes. [1]Cellobio-oligosaccharide production was calculated as the percentage concentration of cellobio-oligosaccharides at the selective temperature, divided by the highest concentration of cellobio-oligosaccharides over all temperature ranges. [2]Reactions conducted with 100 mM sucrose, 100 mM cellobiose, dextransucrase 27 U, and 30 °C for 24 h

analyzed using multiple regression. The coefficients of the full model were evaluated and tested for their significance through regression analysis. Concerning the p value of the coefficients, X_1, X_2, X_3, and X_1^2 were found to have significant effects on the performance of the model for the prediction of the cellobio-oligosaccharide production (Tables 4 and 5).

The final estimative response model equation was as follows:

$$Y = 71.91 + 7.64X_1 + 12.36X_2 + 17.82X_3 - 12.98X_1^2 - 3.29X_2^2 - 0.41X_3^2 - 4.25X_1X_2 + 3.31X_1X_3 - 0.52X_2X_3 \quad (2)$$

where Y is the response factor (cellobio-oligosaccharide production, percent) and X_1, X_2, and X_3 represent real values of the independent factors—sucrose (mM), cellobiose (mM), and dextransucrase (U). Table 5 shows the model coefficients and probability values. The

Table 3 Observed and predicted values and variance parameters of cellobio-oligosaccharide yield (%) recorded in experimental setup of response surface methodology.

Run number	Observed Y	Predicted Y	Residuals
1	33.60	30.83	2.77
2	35.72	36.37	−0.65
3	63.25	65.39	−2.15
4	64.12	64.09	0.02
5	35.29	37.51	−2.23
6	73.67	74.19	−0.52
7	66.78	71.25	−4.47
8	66.88	71.25	−4.36
9	74.76	71.25	3.51
10	76.06	71.25	4.81
11	71.77	71.25	0.52
12	63.90	63.27	0.62
13	100.00	97.88	2.12
14	54.34	54.37	−0.02
15	47.29	45.04	2.25
16	87.84	87.29	0.55
17	67.86	70.63	−2.77

Table 4 Regression coefficients and significance of regression model.

Factor	Coefficient estimate	*df*	Standard error	95% CI low	95% CI high
Intercept	71.91	1	1.78	67.70	76.12
X_1	7.64	1	1.41	4.32	10.97
X_2	12.36	1	1.41	9.04	15.69
X_3	17.82	1	1.41	14.50	21.14
X_1^2	−12.98	1	1.94	−17.56	−8.40
X_2^2	−3.29	1	1.94	−7.87	1.29
X_3^2	−0.41	1	1.94	−5.00	4.18
X_1X_2	−4.25	1	1.99	−8.95	0.45
X_1X_3	3.31	1	1.99	−1.39	8.01
X_2X_3	−0.52	1	1.99	−5.22	4.18

CI Confidence interval

analysis of variance of this model demonstrated that the model is highly significant, as is evident from the *F* value (F_{model}=35.99) and a very low probability value (<0.0001). A *P* value lower than 0.1 indicates that a model is considered to be statistical significant [10]. Furthermore, the lack of fit *F* value of 0.64 implies that the lack of fit is not significant relative to the pure error according to our results of analysis of factors. Nonsignificant lack of fit is a good indication that the model fits the actual relationships of the reaction parameters within the selected ranges.

The relationship between the independent and dependent variables was elucidated using contour and response surface plots (Fig. 3). Each plot represents the effect of two variables at their studied range with the other one maintained at fixed level. The shapes of contour plots display the nature and extent of the interactions [11]. As shown in Fig. 3a, an increase in sucrose concentration up to 300 mM results in increased cellobio-oligosaccharide production with increases in cellobiose concentration, at 40.5 U dextransucrase. An increase in the amount of cellobiose causes a linear increase in cellobio-oligosaccharide

Table 5 ANOVA for response surface.

Source	Sum of squares	*df*	Mean square	*F* value	Probability>*F*[a,b]
Model	5119.29	9	568.81	35.99	<0.0001
X_1	466.80	1	466.80	29.53	0.0010
X_2	1221.61	1	1221.61	77.29	<0.0001
X_3	2540.51	1	2540.51	160.73	<0.0001
X_1^2	709.29	1	709.29	44.87	0.0003
X_2^2	45.53	1	45.53	2.88	0.1335
X_3^2	0.69	1	0.69	0.04	0.8400
X_1X_2	72.19	1	72.19	4.57	0.0699
X_1X_3	43.83	1	43.83	2.77	0.1398
X_2X_3	1.08	1	1.08	0.07	0.8014
Residual	110.64	7	15.81		
Lack of fit	35.87	3	11.96	0.64	0.6282
Pure error	74.77	4	18.69		
Correlation total	5,229.93	16			

[a] Probability>*F*, level of significance

[b] Values of "probability>*F*" less than 0.05 indicate model terms are significant. Values greater than 0.1 indicate the model terms are not significant.

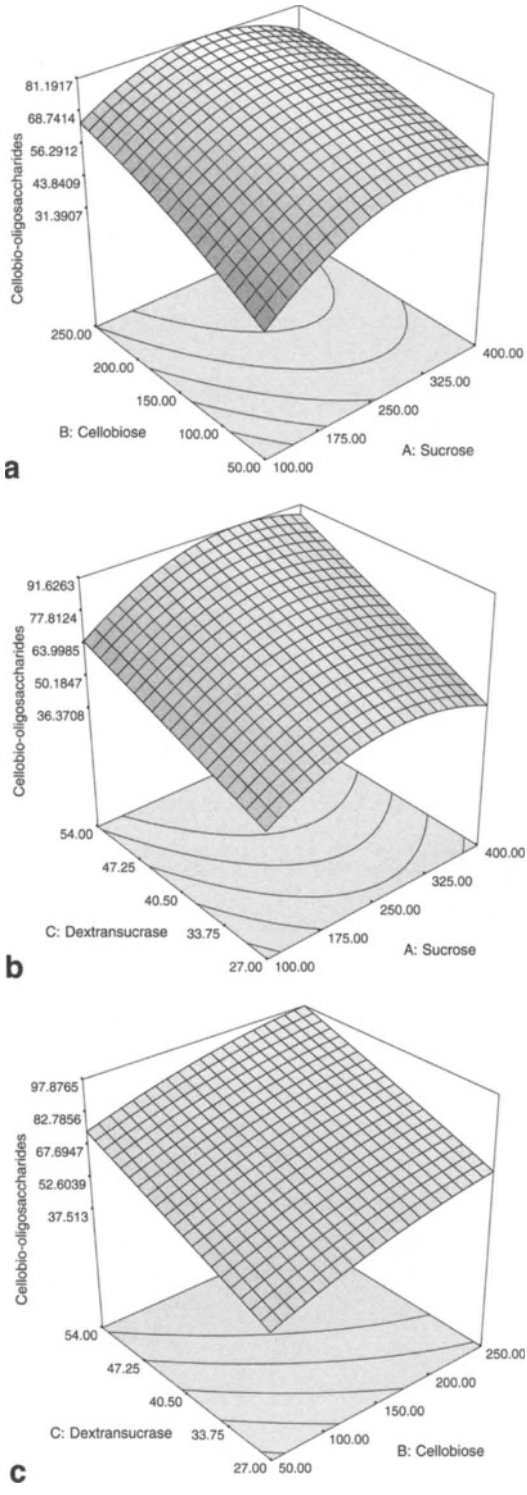


Fig. 3 Response surface plots illustrating the effect of varying concentrations of sucrose, cellobiose, and dextransucrase on their reciprocal interactions with cellobio-oligosaccharide production. Other factors are held constant at 40.5 U of dextransucrase (**a**), 150 mM of cellobiose (**b**), and 250 mM of sucrose (**c**)

produced. However, sucrose concentrations greater than 300 mM interfere with cellobio-oligosaccharide production despite increases in the concentrations of cellobiose. The reaction solutions became increasingly viscous with increases in sucrose concentration due to the concomitant formation of dextran. This finding is similar for the action of sucrose on the dextransucrase production by *L. mesenteroides* B-512 F [12].

The effects of differing dextransucrase and sucrose concentrations on the cellobio-oligosaccharide production with 150 mM cellobiose are shown in Fig. 3b. High production of cellobio-oligosaccharides was achieved at the middle level of sucrose across the entire range of dextransucrase concentrations. A linear increase in dextransucrase in selected ranges does not lead to a continuous increase of cellobio-oligosaccharide production with increased in sucrose concentration. Furthermore, product inhibition was observed because of dextran formation above 54 U of dextransucrase (data were not shown). Dextransucrase catalyzes dextran synthesis as well as oligosaccharide synthesis. Kim and Robyt [13] reported that dextran production showed a slightly sigmoidal increase suggesting an allosteric effect for the dextran.

Figure 3c illustrates the effects of different dextransucrase concentrations and cellobiose concentrations on the cellobio-oligosaccharides production in the presence of 250 mM sucrose. Increases in the amount of both dextransucrase and cellobiose resulted in linear increases in the production of cellobio-oligosaccharides when sucrose concentration was fixed. The highest concentrations were reached using high dextransucrase and cellobiose. However, the addition of cellobiose was limited by the solubility of cellobiose. Figure 3 suggests that high cellobiose and dextransucrase as well as sucrose concentration between 250 and 300 mM achieve the optimal transglycosylation of sucrose to cellobiose.

The optimum values for the selected factors were calculated from the regression equation (Eq. 2). The optimal conditions for the cellobio-oligosaccharides were as follows: X_1=288.96 mM, X_2=250 mM, X_3=54 U (Fig. 4). The theoretical cellobio-oligosaccharide yield predicted under these conditions was Y=98.74%. The prediction value by the model was confirmed using the above conditions. The actual value was 49.9 mM of cellobio-oligosaccharide (relative value to prediction value, 101.5%).

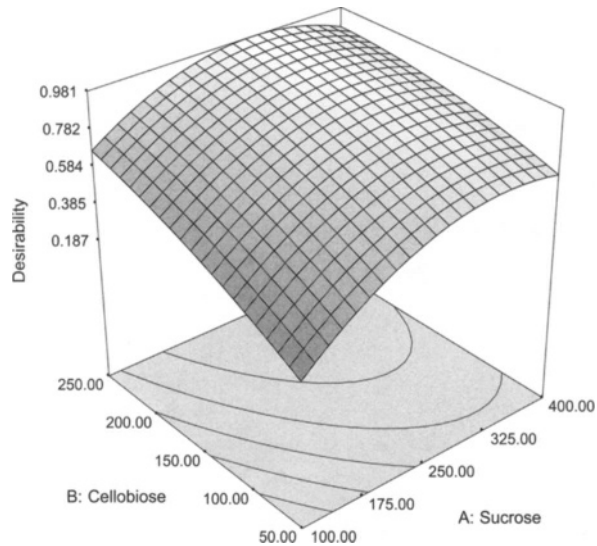


Fig. 4 Response surface plot representing the effect of varying concentrations of sucrose, cellobiose, and dextransucrase on their reciprocal interactions with cellobio-oligosaccharide (dextransucrase 54 U)

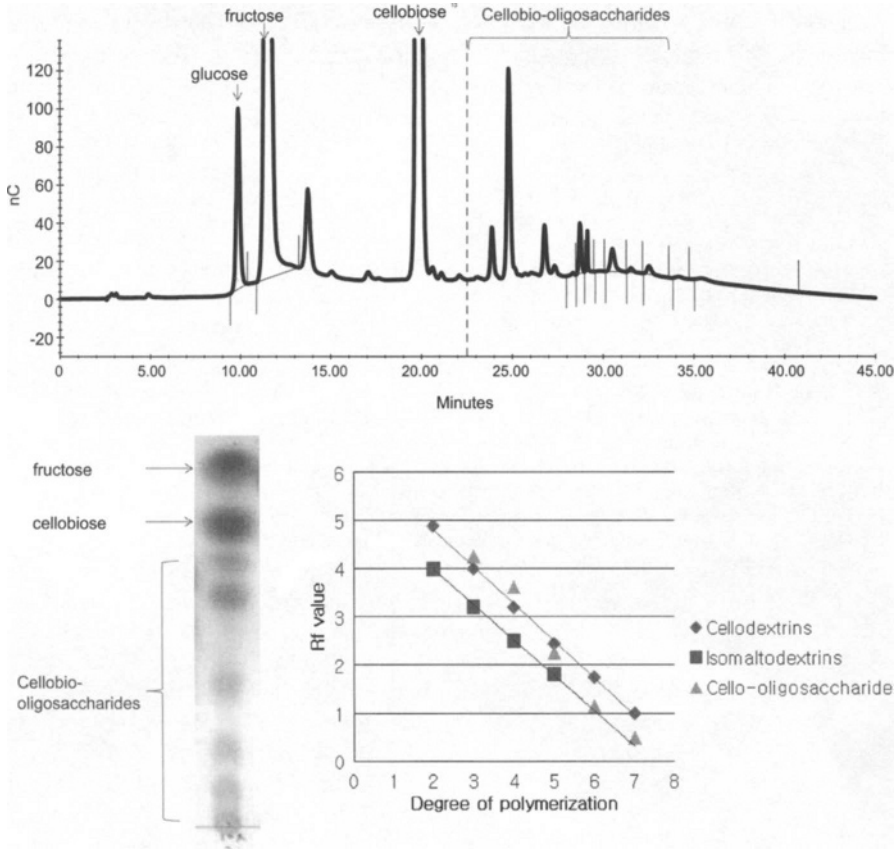


Fig. 5 Chromatogram profiles and R_f values for oligosaccharides

The cellobio-oligosaccharides showed different R_f values on TLC (Fig. 5). The sizes of five cellobio-oligosaccharides detected were compared with commercial oligosaccharide products of cellodextrins linked β-1,4 and with isomaltodextrins linked α-1,6. The degrees of polymerization (DP) of cellobio-oligosaccharides ranged from 3 to 7. Robyt and Mukerjea [14] indicated that the linkage type causes differences in migration. The migration of our cellobio-oligosaccharides with DP 3 and 4 was faster than cellodextrins containing β-1,4 linkages. However, the R_f values of the cellobio-oligosaccharides with DP 5, 6, and 7 were between cellodextrins and isomaltodextrins (α-1,6 linkages).

Conclusions

The optimal conditions for transglycosylation of sucrose onto cellobiose were a pH of 5.2 and a temperature of 30 °C. The concentration of dextransucrase was 54 U, the concentration of sucrose was 289 mM, and the concentration of cellobiose was 250 mM. The cellobio-oligosaccharide yield reached 20% based on initial cellobiose concentration under the above conditions.

Acknowledgments This research was supported by a DOE award (DE-FG36-04GO14236). This support does not constitute an endorsement by DOE of the views expressed in this article.

References

1. Staněk, J., Černý, M., & Pacák, J. (1965). *The oligosaccharides*. New York: Academic.
2. Farnworth, E. R. (2001). In R. E. C. Wildman (Ed.) *Handbook of nutraceuticals and functional foods* pp. 409–426. Florida: CRC.
3. Eggleston, G., & Côte, G. L. (2003). In G. Eggleston, & G. L. Côte (Eds.), *Oligosaccharides in food and agriculture* (pp. 2–30). MA: American Cheemical Society.
4. Nakamura, S., Oku, T., & Ichinose, M. (2004). *Nutrition, 20*, 979–983.
5. Lee, S. B., Park, K. H., & Robyt, J. F. (2001). *Carbohydrate Research, 331*, 13–18.
6. Morales, M. A. A., Remaud-Simeon, M., Willemot, R., Vignon, M. R., & Monsan, P. (2001). *Carbohydrate Research, 331*, 403–411.
7. Lindberg, B., & Svensson, S. (1968). *Acta Chemica Scandinavica, 22*, 1907–1912.
8. Box, G. E. P., & Behnken, D. W. (1960). *Technometrics, 2*, 455–475.
9. Kim, D., & Robyt, J. (1994). *Enzyme and Microbial Technology, 16*, 659–663.
10. Kim, H. M., Kim, J. G., & Hong, J. W. (2003). *Polymer, 22*, 899–906.
11. Fu, J., Zhao, Y., & Wu, Q. (2007). *Journal of Hazardous Materials, 144*, 499–505.
12. Goyal, A., & Katiyar, S. (1997). *Journal of Basic Microbiology, 37*, 197–204.
13. Kim, D., & Robyt, J. (1994). *Enzyme and Microbial Technology, 16*, 1010–1015.
14. Robyt, J. F., & Mukerjea, R. (1994). *Carbohydrate Research, 251*, 187–202.

Appl Biochem Biotechnol (2008) 148:199–209
DOI 10.1007/s12010-007-8080-4

Fermentation Kinetics for Xylitol Production by a *Pichia stipitis* D-Xylulokinase Mutant Previously Grown in Spent Sulfite Liquor

Rita C. L. B. Rodrigues · Chenfeng Lu · Bernice Lin · Thomas W. Jeffries

Received: 11 May 2007 / Accepted: 10 October 2007 /
Published online: 15 November 2007
© Humana Press Inc. 2007

Abstract Spent sulfite pulping liquor (SSL) contains lignin, which is present as lignosulfonate, and hemicelluloses that are present as hydrolyzed carbohydrates. To reduce the biological oxygen demand of SSL associated with dissolved sugars, we studied the capacity of *Pichia stipitis* FPL-YS30 (*xyl3*Δ) to convert these sugars into useful products. FPL-YS30 produces a negligible amount of ethanol while converting xylose into xylitol. This work describes the xylose fermentation kinetics of yeast strain *P.stipitis* FPL-YS30. Yeast was grown in rich medium supplemented with different carbon sources: glucose, xylose, or ammonia-base SSL. The SSL and glucose-acclimatized cells showed similar maximum specific growth rates (0.146 h^{-1}). The highest xylose consumption at the beginning of the fermentation process occurred using cells precultivated in xylose, which showed relatively high specific activity of glucose-6-phosphate dehydrogenase (EC 1.1.1.49). However, the maximum specific rates of xylose consumption (0.19 g_{xylose}/g_{cel} h) and xylitol production (0.059 $g_{xylitol}/g_{cel}$ h) were obtained with cells acclimatized in

Prepared for 29th Symposium on Biotechnology for Fuels and Chemicals.

R. C. L. B. Rodrigues · T. W. Jeffries
Departamento de Biotecnologia, DEBIQ, Escola de Engenharia de Lorena, EEL, USP, Universidade de São Paulo, P.O Box 116, 12600-970 Lorena, Sao Paulo, Brazil

T. W. Jeffries
e-mail: twjeffries@fs.fed.us

C. Lu
Department of Food Science, University of Wisconsin, Madison, WI 53706, USA

B. Lin · T. W. Jeffries
Forest Products Laboratory, USDA Forest Service, One Gifford Pinchot Dr, Madison, WI 53726-2398, USA

Present address:
R. C. L. B. Rodrigues (✉)
Forest Products Laboratory, USDA Forest Service, One Gifford Pinchot Dr, Madison, WI 53726-2398, USA
e-mail: rita@debiq.eel.usp.br

glucose, in which the ratio between xylose reductase (EC 1.1.1.21) and xylitol dehydrogenase (EC 1.1.1.9) was kept at higher level (0.82). In this case, xylitol production (31.6 g/l) was 19 and 8% higher than in SSL and xylose-acclimatized cells, respectively. Maximum glycerol (6.26 g/l) and arabitol (0.206 g/l) production were obtained using SSL and xylose-acclimatized cells, respectively. The medium composition used for the yeast precultivation directly reflected their xylose fermentation performance. The SSL could be used as a carbon source for cell production. However, the inoculum condition to obtain a high cell concentration in SSL needs to be optimized.

Keywords Xylitol · Yeast · Xylose · Ammonia spent sulfite liquor-SSL · Inoculum adaptation · Enzymes

Abbreviations

XR	xylose reductase
XDH	xylitol dehydrogenase
G6PDH	glucose-6-phosphate dehydrogenase
XK	xylulokinase
μ_x	maximum specific cell growth rate (h^{-1})
μ_s	maximum specific xylose consumption rate (g_{xylose}/g_{cell} h)
μ_p	maximum specific xylitol production rate ($g_{xylitol}/g_{cell}$ h)
$Y_{p/s}$	xylitol yield coefficient ($g_{xylitol}/g_{xylose}$)
$Y_{x/s}$	cell yield coefficient (g_{cell}/g_{xylose})
Q_p	xylitol volumetric productivity ($g_{xylitol}$/l h)

Introduction

In the sulfite-pulping process, about 50% of the wood (hemicellulose and lignin) is dissolved to produce cellulose for paper along with the effluent ("spent sulfite liquor," SSL). SSL is the only lignocellulosic hydrolysate available today in large quantities (about 90 billion liters annually worldwide) [1], and it is produced at a rate of 1 ton (dry basis) per ton of pulp [2]. Many investigators have studied the possibility of using microbes to convert SSL into usable products. Its sugar content ranges from 3 to 4%, depending on the source of wood being pulped [3]. Softwoods have been the traditional feedstock, and their hexose sugars constitute 74% of these hydrolysates. However, hardwood sulfite pulping is becoming more popular, and the pentose sugars, principally xylose, in hardwood SSL can be up to 50% [2].

Recently, the conversion of xylose into value-added chemicals, such as xylitol, ethanol, and lactic acid have made this process attractive to the fermentation industry [4]. In particular, bioconversion for xylitol production has been intensively studied during the last decade because xylitol can be used as a functional sweetener [5].

The xylose reductase (XR) catalyzes the first step of a fungal pathway that allows certain organisms to metabolize xylose, such as *Candida boidinii* [6], *Candida guilliermondii* [7], *Candida tropicalis* [8], *Candida parapsilosis* [9], and *Debaryomyces hansenii* [10]. After the reduction of xylose to xylitol by XR in a manner that can utilize nicotinamide adenine dinucleotide (reduced form; NADH) or nicotinamide adenine dinucleotide phosphate (reduced form; NADPH), xylitol is re-oxidized to xylulose by xylitol dehydrogenase, which is often specific for nicotinamide adenine dinucleotide $(NAD)^+$ [11]. Xylulose is then phosphorylated. An efficient, pathway should recycle the cosubstrate such that there is no

net conversion of NADPH into NADH resulting from xylose metabolism. Perturbations in this ratio have been linked to cell stress and xylitol excretion [12]. *Pichia stipitis* alcohol dehydrogenase-disrupted [13], xylitol dehydrogenase-defective [14], and D-xylulokinase-disrupted [15] mutants also produce xylitol from xylose. In the D-xylulokinase mutant, a metabolic pathway via arabinitol and ribulose-5-phosphate that bypasses the xylulokinase step was proposed as an alternative pathway mediating xylose assimilation. This mutant was named *P. stipitis* FPL-YS30 (*xyl3*-Δ) [15]. This pathway is also involved in L-arabinose assimilation [15].

The xylose present in SSL is difficult to ferment using native xylose-fermenting yeast strains due to the presence of sugar degradation products, acetic acid, lignosulfonates, sulfate, and occasionally, ammonia [3]. These compounds can inhibit sugar fermentation. Keating et al. [16] studied the tolerance and adaptation of ethanologenic yeasts to lignocellulosic inhibitory compounds and observed that the strains were severely affected by hardwood SSL (HSSL). This was attributed to specific syringyl lignin-derived degradation products and synergistic interactions between inhibitors [16]. Helle et al. [3] observed that xylose fermentation by genetically modified *Saccharomyces cerevisiae* 259ST in spent sulfite liquor produced up to 130% more ethanol as compared to fermentations using nonxylose-fermenting yeast. Conditions optimized for fermentation of pretreated HSSL to ethanol using an adapted strain of *P. stipitis* increased from 6.7 to 20.2 g/l [17].

The composition of the medium used for cultivation of microorganisms is directly reflected in their physiological phenotype and their fermentation performance, which in turn affect the results of strain analyses and strain performance in industrial applications [18]. In the present work, we grew cells on SSL to determine the influence of ammonium sulfite spent liquor SSL on *P. stipitis* FPL-YS30 (*xyl3*-Δ) xylitol production. The present research used SSL derived from an ammonia sulfite pulping of southern pine.

Materials and Methods

Preparation of Ammonia SSL

Ammonia SSL from pine (evaporated to 50% solids), which was obtained from Rayonier Performance Fibers, LLC (Fernandia Beach, FL, USA), was diluted to 15% *w/w* with water and adjusted to pH 6.0 with sodium hydroxide. Suspended solids were removed by centrifugation at 5,000 rpm for 5 min, and the remaining liquid was autoclaved at 111°C for 15 min.

Yeast Strain and Inoculum Media

P. stipitis FPL-YS30 (*xyl3*-Δ) was maintained on yeast peptone dextrose (YPD) agar medium (10 g/l yeast extract, 20 g/l peptone, 20 g/l glucose, and 18 g/l agar) and stored at 4°C then transferred to fresh plate to be used within 24 h of incubation at 30°C. Cells were grown in hydrophobic cotton-plugged 1,000-ml Erlenmeyer flasks containing 400 ml of either YPD (10 g/l yeast extract, 20 g/l peptone, and 30 g/l glucose), yeast peptone xylose (YPX; 10 g/l yeast extract, 20 g/l peptone, and 30 g/l xylose) or YPSSL (10 g/l yeast extract, 20 g/l peptone, and 30 g/l total sugar) in an orbital shaker at 30°C and 200 rpm. Following 24 h growth, cell cultures were harvested, centrifuged (3,000 rpm per 15 min at 21°C), and decanted to yield cell pellets. Pellets were then washed once with sterile deionized water and

subsequently adjusted to a calculated concentration of 30 g dry cell weight (DCW) per liter via standard curves relating 600 nm absorbance to DCW per liter concentration. An aliquot was transferred to fresh fermentation medium for an initial cell concentration of 0.2 g DCW/l.

Batch Fermentations

Fermentations were performed in hydrophobic cotton-plugged 125-ml Erlenmeyer flasks containing 50 ml YPX liquid medium (10 g/l yeast extract, 20 g/l peptone, 80 g/l autoclaved xylose) in an orbital shaker at 30°C and 200 rpm. Initially, the YPX media was inoculated with pure cultures from inocula grown in different media (YPD, YPX, and YPSSL) to achieve an initial cell concentration of 0.2 g DCW/l. Samples were aseptically withdrawn during fermentation in 12 h interval. All fermentation experiments were performed in duplicate.

Preparation of Cell Extract and Enzyme Assay

Cells were harvested by centrifugation (16,000×*g*) for 5 min at 4°C, immediately frozen in liquid nitrogen and stored at −80°C. For the enzymatic assays, the samples were thawed rapidly under running water and held on ice. These samples were washed once and suspended in buffer 0.1 M 3-(*N*-morpholino)propanesulfonic acid, pH 7.0 with the addition of 1 mM β-mercaptoethanol and 1 mM of a protease inhibitor cocktail (phenylmethylsulfonyl fluoride), and disrupted by vortexing with glass beads (Sigma G8772; 15 min; 0°C). Cell debris and glass beads from the cell extract were separated by centrifugation (16,000×*g*, 10 min 4°C. Enzymatic activity was measured with two different sample concentrations using a spectrophotometer (Molecular Devices spectra max plus) operating at 340 nm and 30°C. The XR (EC 1.1.1.21) activity was measured in a reaction mixture by standard assay [19] modified by using 100 mM Tris–HCl buffer, pH 7.2; 100 mM xylose; and 0.2 mM NADPH. The xylitol dehydrogenase (XDH; EC 1.1.1.9) activity was measured by standard assay [19] modified by using a reaction mixture containing 100 mM Tris–HCl buffer, pH 8.6; 0.4 mM NAD^+ ; 5 mM $MgCl_2$, and 100 mM xylitol. Glucose-6-phosphate dehydrogenase was assayed as previously described by [20]. The xylulokinase (EC 2.7.1.17) activity was measured by standard assay [19] modified by using a reaction mixture containing 50 mM Tris–HCl buffer, pH 8.6 plus 5 mM $MgCl_2$; 0.2 mM NADH; 1.5 phosphoenolpyruvate; 1.0 mM adenosine triphosphate; 4 U pyruvate kinase and 4 U lactate dehydrogenase. Specific activities are expressed as units per milligram of protein. Units are defined as micromoles of NADH or NADPH reduced or oxidized per minute.

Determination of Sugars and Extracellular Metabolites

Xylose, xylitol glycerol, arabitol, ethanol, and acetic acid were determined by high performance liquid chromatography using a refractive index detector (Hitachi High-Technologies model L-2490, Japan) and Bio Rad (Hercules, CA, USA) Aminex HPX-87H column (300×7.8 mm) at 55°C; 0.005 M H_2SO_4 as eluent, at a flow rate of 0.3 ml min^{-1} and injection volume of 20 μl. Samples of 50% SSL diluted to 15% *w/w* was analyzed using the same detector and a Bio-Rad Aminex HPX-87P column (300×7.8 mm) at 80°C; deionized water as eluent, at a flow rate of 0.6 ml min^{-1} and injection volume of 20 μl. Samples were appropriately diluted in deionized water, and then filtered through 0.45 μm polyvinylidene fluoride filters before injection (20 μl).

Determination of Biomass and Protein Concentration

Time-dependent offline sampling of 1 ml aliquots was performed aseptically during fermentations. Samples were mixed immediately before dilution in deionized water, and then subjected to duplicate absorbance determination in a spectrophotometer at 600 nm. Diluted cell-free medium was used to establish background readings and set zero absorbance levels. Values were averaged and corrected for dilution. Protein concentration in cell-free extracts was determined by Bradford method [21], using bovine serum albumin as a standard.

Determination of Total Phenolic Content

The phenolic content of 50% SSL diluted to 15% *w/w* samples was determined by Folin–Ciocalteu reagent [22]. Each sample (0.1 ml at proper dilution) was added to 4.2 ml of deionized water and 0.5 ml of Folin–Ciocalteu reagent (Sigma). After 1 min of mixing, 1 ml of an 80% solution of sodium carbonate and 4.2 ml of deionized water was added. The mixture was left for 2 h at room temperature in dark, and the absorbance at 760 nm was measured. The concentration of total phenolic content was determined by a comparison with the values obtained with a standard solution of vanillin (Sigma).

Results and Discussion

Xylose Fermentation and By-Products

The waste spent sulfite pulping liquor (SSL) had a high solid content, so dilution was necessary before fermentation. The 50% SSL after dilution to 15% *w/w* contained 2.04 g/l glucose; 4.69 g/l mannose; 0.94 g/l arabinose; 2.83 g/l xylose; 1.25 g/l galactose, and 11.2 g/l total phenolic compounds.

Cell growth in yeast peptone (YP) medium with SSL as the carbon source (YPSSL) was only 80 or 94%, respectively, of cell growth in YPX and YPD medium (data not shown); however, precultivation in YPSSL resulted in the highest cell concentration (12.0 g/l; Fig. 1a) and cellular yield ($Y_{x/s}$; 0.198 g/g; Table 1) during fermentation of 80 g/l xylose. In this case, the maximum specific growth rate (μ_x; 0.143 h^{-1}) was similar to cells precultivated in YPD (0.148 h^{-1}). Jin et al. [23] previously reported the specific growth rates of *P. stipitis* FPL YS-30 and its parental strains (*P. stipitis* FPL-UC7) cultivated in YPX (40 g/l of xylose) as 0.06 and 0.28 h^{-1}, respectively (Table 1). The increase in xylose concentration to 80 g/l did not decrease the specific growth rate of the FPL-YS30. However, xylose consumption decreased 23% compared to Jin et al. [23].

Total xylose consumption was almost the same in all fermentations (Table 1), however, the specific xylose consumption rate (μ_s) varied. The highest (0.19 g_{xylose}/g_{cell} h) was obtained using cells precultivated in YPD. The next highest was with cells cultivated in YPSSL (0.141 g_{xylose}/g_{cel} h). The specific xylose assimilation rate by *P. stipitis* FPL YS-30 in YPX with 40 g/l of xylose was previously reported as 0.98 g_{xylose}/g_{cell} h [23], which was considerably higher than what we observed here in YPX with 80 g/l xylose.

The highest xylitol production that we observed (31.6 g/l; Fig. 2a) was obtained using cells precultivated in YPD. This inoculum condition also showed the highest specific xylitol production rate (μ_p; 0.059 $g_{xylitol}/g_{cell}$ h) and xylitol volumetric productivity (Q_p; 0.267 $g_{xylitol}/l$ h; Table 1). However, the cells precultivated in YPX showed the highest

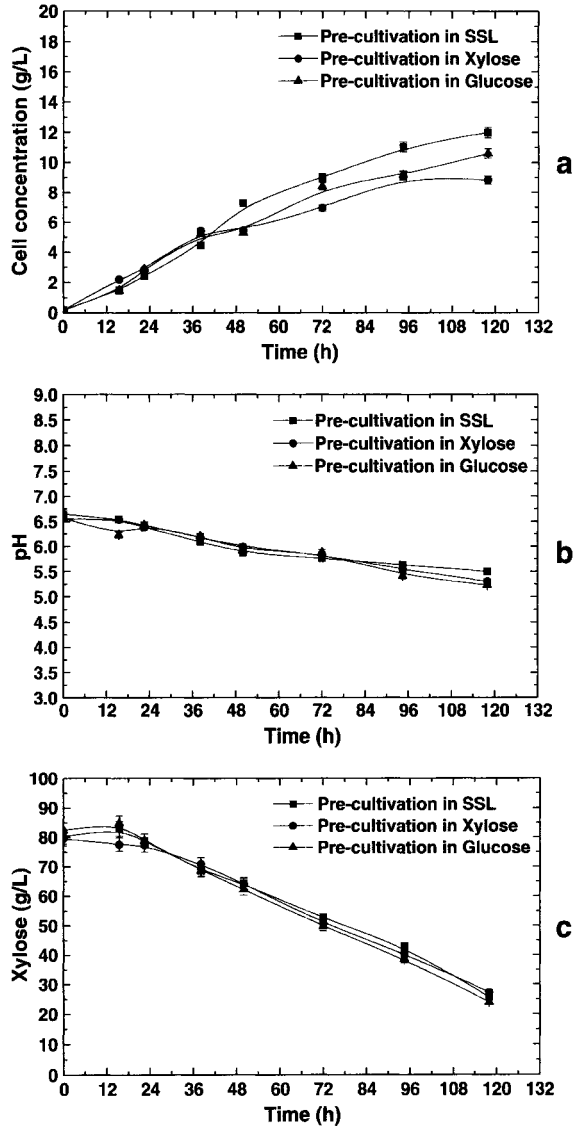


Fig. 1 Cell production (g/l; **a**), pH (**b**), and xylose consumption (g/l; **c**) during xylose bioconversion to xylitol by *P. stipitis* D-xylulokinase mutant in medium YPX

xylose conversion to xylitol ($Y_{p/s}$; 0.555 $g_{xylitol}/g_{xylose}$; Table 1) and a more stable specific xylitol production rate than cells precultivated in YPD. The highest xylitol concentration previously reported with YS30 was 13.2 g/l [23].

In general, cells precultivated in YPSSL and YPX showed similar and more stable values for specific xylose consumption and xylitol production rates than cells from YPD medium (data not shown). However, fermentation using cells precultivated in YPSSL showed lower values for specific xylose and xylitol production rates than cells precultivated in YPX.

Table 1 Parameter kinetics for xylitol production by a *P. stipitis* D-xylulokinase mutant previously grown in YP-SSL, YPX, and YPD media.

Parameters	Inoculum media		
	YP-SSL	YP-X	YP-D
Xylose consumption (%)	68.0±1.41	65.8±1.13	71.0±1.41
μ_x (h^{-1})	0.143±0.004	0.093±0.006	0.148±0.011
μ_s (g_{xylose}/g_{cell} h)	0.141±0.001	0.107±0.011	0.190±0.014
μ_p ($g_{xylitol}/g_{cell}$ h)	0.046±0.006	0.047±0.009	0.059±0.006
$Y_{p/s}$ (g/g)	0.469±0.004	0.555±0.078	0.539±0.013
$Y_{x/s}$ (g/g)	0.198±0.003	0.165±0.009	0.178±0.004
Q_p ($g_{xylitol}$/l h)	0.217±0.003	0.246±0.01	0.267±0.01

We did not observe any ethanol or acetic acid production. However, glycerol and a negligible amount of arabitol were formed (Fig. 2b, c). Cells precultivated in YPSSL showed the highest glycerol production (6.26 g/l; Fig. 2c) and the highest cellular growth (12.0 g/l; Fig. 1a). The inverse was observed using cells precultivated in YPX, which showed the lowest value for glycerol production (3.79 g/l; Fig. 2c) and cellular growth (8.8 g/l; Fig. 1a). Cells cultivated on YPSSL showed a strong tendency to produce more glycerol than cells precultivated in YPX and YPD (Fig. 2b, c).

Glycerol production could be related to cellular growth. Glycerol offsets redox imbalances that occur during yeast growth, and glycerol yields decrease as yeast growth decreases [24]. Differences in glycerol yields from cells cultivated on different media (Fig. 2b, c) indicates that the cell redox metabolism may differ. A lower glycerol yield on cells precultivated in YPX could be attributed to higher respiratory activity during growth in xylose, leading to a reduced need for glycerol production for maintenance of redox balance. The YP medium had an inherent buffering capacity (Fig. 1b) that maintained the pH around 6.0 (Fig. 1b). Glycerol yields are increased in fermentations near pH 7 [25]. However, the increased glycerol production (29%) in cell precultivated in YPSSL reduced the xylitol production (19%) compared with cells precultivated in YPD.

Cells precultivated in YPX showed the highest arabitol production (0.21 g/l; Fig. 2b). Jin et al. [15] previously proposed an alternative pathway for xylose assimilation in the D-xylulokinase mutant, *P. stipitis* FPL-YS30 (*xyl3-Δ*). This pathway (via arabinitol and ribulose-5-phosphate) is also involved in L-arabinose assimilation. Many yeast and fungi can aerobically assimilate L-arabinose, but most are enable to ferment it to ethanol or they exhibit only very low ethanol production rates and yields [29]. The rarity of ethanolic arabinose fermentation may be due to a redox imbalance in the fungal arabinose pathway as a result of the use of NADPH for the reductive reactions and the production of NADH in the oxidation reactions [29]. *P. stipitis* FPL-YS30 (*xyl3-Δ*) produces xylitol mainly because of insufficient glycolytic capacity of the alternative pathway rather than because of a redox imbalance, indicating that the oxidative phase of the pentose phosphate pathway, which produces NADPH for xylitol accumulation, is sufficient even without activity coded for by *XYL3* [15].

According to Shi et al. [26], there is a fundamental difference between the respiratory machinery supporting xylose and glucose metabolism using *P. stipitis* wild-type CBS 6054. However, addition of electron acceptors such as ketones and aldehydes in the medium [27] reduces xylitol formation. Such compounds are present also in lignocellulose hydrolysates [28] and most likely also in YP medium [29].

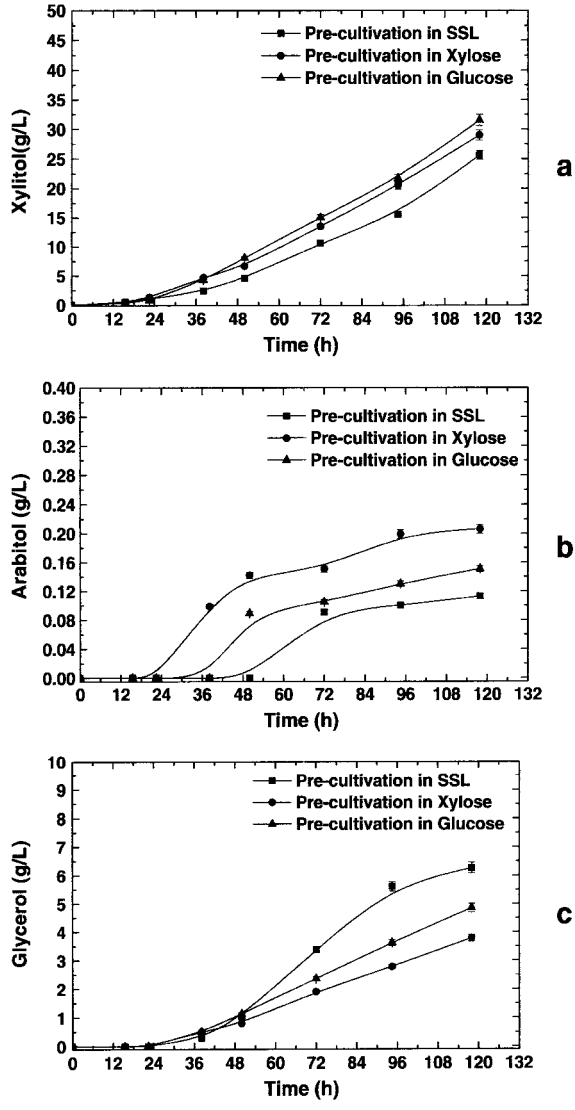


Fig. 2 Xylitol (**a**), arabitol (**b**), and glycerol (**c**) production during xylose bioconversion to xylitol by *P. stipitis* D-xylulokinase mutant in medium YPX

Enzyme Activities

Precultivation in YPX provided the highest maximum specific xylose reductase activity (0.349 U/mg_{prot}) after 38 h of fermentation (Fig. 3a). However, cells precultivated in YPSSL and YPD showed similar values for maximum specific XR activity (approximately 0.25 U/mg_{prot}) at 38 and 95 h, respectively. Initially, the XR activity in cells precultivated in YPD was not detectable, but after 23 h it was ≈0.22 U/mg_{prot}. This was also observed for cells precultivated in YPX. However, for cells precultivated in YPSSL XR, specific activity decreased approximately 44% after 38 h. Xylose consumption (Fig. 1c) and xylitol

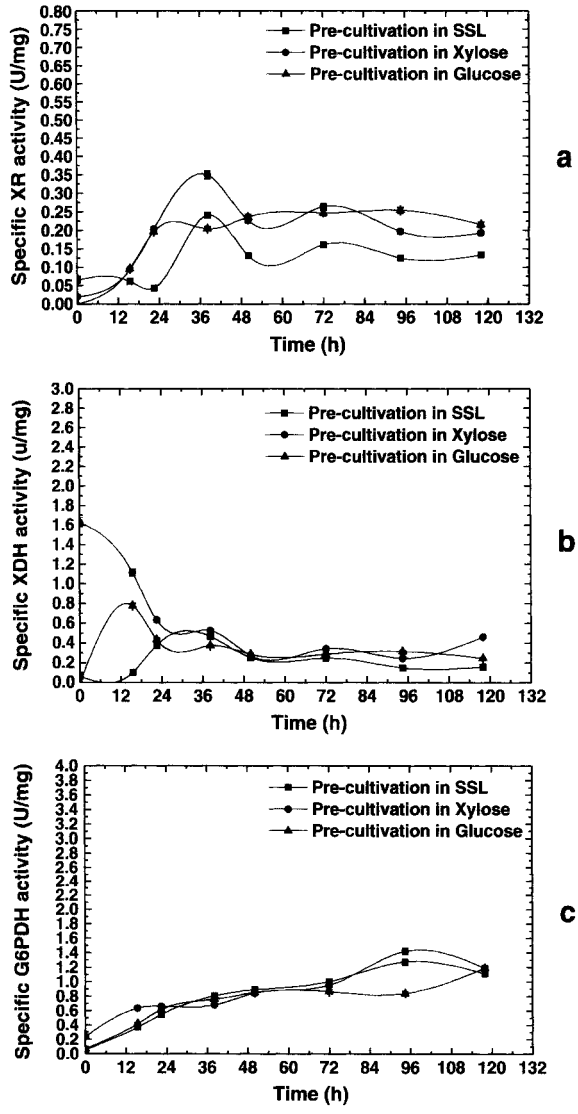


Fig. 3 Specific enzyme activities of XR (**a**), XDH (**b**), and G6PDH (**c**) during xylose bioconversion to xylitol by *P. stipitis* D-xylulokinase mutant in medium YPX

production decreased concomitantly (Fig. 2a) with enzymatic activity. The cells precultivated in YPD showed stability in XDH values around 0.3 U/mg_{prot} after 23 h of fermentation (Fig. 3b). In the other cases, there was an observed decrease in XDH maximum specific activity (Fig. 3b). The maximum specific xylitol dehydrogenase activity (1.11 U/mg_{prot}) was found using cells precultivated in YPX, followed by cells precultivated in YPD (0.778 U/mg_{prot}), in both cases after 16 h of fermentation. However, xylitol production has been partially ascribed to the difference in cofactor usage in the NAD(P)H-dependent XR and the NAD^+-dependent XDH reactions [7]. The highest xylitol production was obtained using cells precultivated in YPD, where this ratio XR/XDH was kept at higher

level (0.82). This behavior may have favored the specific xylitol production rate for cells precultivated in YPD.

A higher ratio of XR activity to XDH activity is essential for xylitol accumulation [12]. After the reduction of xylose to xylitol by XR in a manner that can utilize NADH or NADPH, xylitol is re-oxidized to xylulose by xylitol dehydrogenase, which is often specific for NAD^+ [11]. Xylulose can then be phosphorylated and enter general metabolic pathways. An efficient, high-flux pathway should recycle the cosubstrate such that there is no net conversion of NADPH into NADH resulting from xylose metabolism. In the D-xylulokinase mutant, *P. stipitis* FPL-YS30 (*xyl3-1*) [15], a metabolic pathway via arabinitol and ribulose-5-phosphate that bypasses the xylulokinase step, was proposed as an alternative pathway mediating xylose assimilation. This pathway is also involved in L-arabinose assimilation [15]. During the fermentations, the glucose 6-phosphate dehydrogenase (G6PDH) activity increased and practically reached a plateau of approximately 1.2 U/mg_{prot} (Fig. 3c). However, cells precultivated in YPX presented the highest G6PDH specific activity, 0.24 and 1.4 U/mg_{prot} at initial and 95 h of fermentation, respectively. The G6PDH enzyme regenerates NADPH, which is necessary for the consumption of xylose. The highest xylose consumption at the beginning of the fermentation process occurred using cells precultivated in YPX, which showed relatively high specific activity of G6PDH.

Conclusions

The medium composition used for *P. stipitis* FPL-YS30 inoculum development directly affected subsequent xylose fermentations. SSL could be used for cell production, but the growth conditions are not ideal. The capacities of cells cultivated in different media (YPSSL, YPX, and YPD) to procduce xylitol were equal, and thus the yields of xylitol were similar. However, differences in glycerol and arabitol yields showed that these may differ in subtle ways. We did not observe ethanol or acetic acid production. Cells exposed to a stressful environmental (YPSSL) showed high tendency to produce more glycerol than cells precultivated in YPX and YPD. The inverse was observed using cells precultivated in YPX, which showed the lowest value for glycerol production and cellular growth. However, cells precultivated in YPX showed the highest arabitol production. A portion of the reducing power is consumed in glycerol and arabitol formation that could improve xylitol production. Glycerol production in particular lowers the yield of xylitol. The highest xylitol production was obtained using cells precultivated in YPD, where the ratio XR/XDH was kept at higher level (0.82).The highest xylose consumption at the beginning of the fermentation process occurred using cells precultivated in YPX, which showed relatively high specific activity of G6PDH.

Acknowledgement Rita de C.L.B. Rodrigues gratefully acknowledges financial support by CNPq, Brazil, grant number 200702/2006-8. We thank Rayonier Performance Fibers for the SSL Xethanol for partial financial support, and Greg Hohensee for SSL sugar analysis.

References

1. Lawford, H. G., & Rousseau, J. D. (1993). *Applied Biochemistry and Biotechnology, 39–40*, 667–685.
2. Gold, D., Mohagheghi, A., Cooney, C. L., & Wang, D. I. C. (2004). *Biotechnology and Bioengineering, 23*, 2105–2116.

3. Helle, S. S., Murray, A., Lam, J., Cameron, D. R., & Duff, S. J. (2004). *Bioresource Technology, 92*, 163–71.
4. Lynd, L. R., Wyman, C. E., & Gerngross, T. U. (1999). *Biotechnology Progress, 15*, 777–793.
5. Mäkinen, K. K. (1978). Birkhäuser Verlag, Basel.
6. Vandeska, E. A. S., Kuzmanova, S., & Jeffries, T. W. (1995). *World Journal of Microbiology and Biotechnology, 11*, 213–218.
7. Rodrigues, R. C., Sene, L., Matos, G. S., Roberto, I. C., Pessoa Jr., A., & Felipe, M. G. (2006). *Current Microbiology, 53*, 53–59.
8. Kim, T. B., & Oh, D. K. (2003). *Biotechnology Letters, 25*, 2085–2088.
9. Oh, D. K., Kim, S. Y., & Kim, J. H. (1998). *Biotechnology and Bioengineering, 58*, 440–444.
10. Dominguez, J. M., Cruz, J. M., Roca, E., Dominguez, H., & Parajo, J. C. (1999). *Applied Biochemistry and Biotechnology, 81*, 119–130.
11. Lunzer, R., Mamnun, Y., Haltrich, D., Kulbe, K. D., & Nidetzky, B. (1998). *Biochemical Journal, 336*(Pt 1), 91–99.
12. Ostergaard, S., Olsson, L., & Nielsen, J. (2000). *Microbiology and Molecular Biology Reviews, 64*, 34–50.
13. Cho, J. Y., & Jeffries, T. W. (1998). *Applied Environmental Microbiology, 64*, 1350–1358.
14. Kim, M. S. C. Y., Seo, J. H., Jo, D. H., Park, Y. H., & Ryu, Y. W. D. (2001). *Journal of Microbiology and Biotechnology, 11*, 564–569.
15. Jin, Y. S., Cruz, J., & Jeffries, T. W. (2005). *Applied Microbiology and Biotechnology, 68*, 42–45.
16. Keating, J. D., Panganiban, C., & Mansfield, S. D. (2006). *Biotechnology and Bioengineering, 93*, 1196–1206.
17. Nigam, J. N. (2001). *Journal of Industrial Microbiology & Biotechnology, 26*, 145–150.
18. Hahn-Hagerdal, B., Karhumaa, K., Larsson, C. U., Gorwa-Grauslund, M., Gorgens, J., & van Zyl, W. H. (2005). *Microbial Cell Factories, 4*, 31.
19. Jin, Y. S., & Jeffries, T. W. (2003). *Applied Biochemistry and Biotechnology, 105–108*, 277–286.
20. Gurpilhares, D. B., Hasman, F. A., Pessoa Jr., A., & Roberto, I. C. (2006). *Enzyme and Microbial Technology, 39*, 591–595.
21. Bradford, M. M. (1976). *Analytical Biochemistry, 72*, 248–254.
22. Singleton, V. L., & Rossi Jr., J. A. (1965). *American Journal of Enology and Viticulture, 16*, 144158.
23. Jin, Y. S., Jones, S., Shi, N. Q., & Jeffries, T. W. (2002). *Applied Environmental Microbiology, 68*, 1232–1239.
24. Taherzadeh, M. J., Adler, L., & Liden, G. (2002). *Enzyme and Microbial Technology, 31*, 53–66.
25. Rodrigues, R. C., Felipe, M. G., Roberto, I. C., & Vitolo, M. (2003). *Bioprocess and Biosystems Engineering, 26*, 103–107.
26. Shi, N. Q., Cruz, J., Sherman, F., & Jeffries, T. W. (2002). *Yeast, 19*, 1203–1220.
27. Alexander, N. (1986). *Applied Microbiology and Biotechnology, 25*, 203–207.
28. Larsson, S., Palmqvist, E., Hägerdal, B. H., Tengborg, C., Stenberg, K., Zacchi, G., et al. (1999). *Enzyme and Microbial Technology, 24*, 151–159.
29. Dien, B. S., Kurtzman, C. P., Saha, B. C., & Bothast, R. J. (1996). *Applied Biochemistry and Biotechnology, 57*, 233–242.

Appl Biochem Biotechnol (2008) 148:211–226
DOI 10.1007/s12010-007-8028-8

Selective Enrichment of a Methanol-Utilizing Consortium Using Pulp and Paper Mill Waste Streams

Gregory R. Mockos · William A. Smith · Frank J. Loge · David N. Thompson

Received: 15 May 2007 / Accepted: 21 August 2007 /
Published online: 25 September 2007
© Humana Press Inc. 2007

Abstract Efficient utilization of carbon inputs is critical to the economic viability of the current forest products sector. Input carbon losses occur in various locations within a pulp mill, including losses as volatile organics and wastewater. Opportunities exist to capture this carbon in the form of value-added products such as biodegradable polymers. Waste-activated sludge from a pulp mill wastewater facility was enriched for 80 days for a methanol-utilizing consortium with the goal of using this consortium to produce biopolymers from methanol-rich pulp mill waste streams. Five enrichment conditions were utilized: three high-methanol streams from the kraft mill foul condensate system, one methanol-amended stream from the mill wastewater plant, and one methanol-only enrichment. Enrichment reactors were operated aerobically in sequencing batch mode at neutral pH and 25°C with a hydraulic residence time and a solids retention time of 4 days. Non-enriched waste activated sludge did not consume methanol or reduce chemical oxygen demand. With enrichment, however, the chemical oxygen demand reduction over 24-h feed/decant cycles ranged from 79 to 89%, and methanol concentrations dropped below method detection limits. Neither the non-enriched waste-activated sludge nor any of the enrichment cultures accumulated polyhydroxyalkanoates (PHAs) under conditions of nitrogen sufficiency. Similarly, the non-enriched waste activated sludge did not accumulate PHAs under nitrogen-limited conditions. By contrast, enriched cultures accumulated PHAs to nearly 14% on a dry weight basis under nitrogen-limited conditions. This indicates that selectively enriched pulp mill waste activated sludge can serve as an inoculum for PHA production from methanol-rich pulp mill effluents.

Keywords Foul condensate · Waste-activated sludge · Polyhydroxyalkanoates · Pulp mill · Natural fiber reinforced thermoplastic composite

G. R. Mockos · F. J. Loge
Department of Civil and Environmental Engineering, University of California at Davis,
1 Shields Avenue, Davis, CA 95616, USA

W. A. Smith · D. N. Thompson (✉)
Biological Sciences Department, Idaho National Laboratory, P.O. Box 1625, Idaho Falls,
ID 83415-2203, USA
e-mail: David.Thompson@inl.gov

Introduction

The ability to efficiently use waste streams and renewable resources is essential for the development of a sustainable and profitable forest products industry. The pulp and paper industry is continuously evolving to meet the demand for products that are manufactured efficiently, cost-effectively, and in an environmentally friendly manner. In striving to meet increasingly stringent environmental regulations and the socio-political pressure for sustainability, the pulp and paper industry has made process improvements resulting in an increase in the quality and diversity of its products and a decrease in its energy use and environmental impact [1]. However, opportunities exist to further reduce the environmental footprint of pulp and paper mills. Currently, several input carbon losses occur in various locations within pulp mills, including losses as volatile organic carbon (VOC) compounds such as methanol in kraft mill condensate collection systems. The kraft pulping process uses a hot sodium sulfide–hydroxide solution to digest wood chips and liberate the cellulose fibers, which are subsequently used to manufacture a wide range of paper products [2]. Condensed gases from the digesters are collected to reduce the discharge of volatile organic and reduced sulfur compounds from the mill. These contaminated condensates or "foul condensates" contain such compounds as hydrogen sulfide, methyl mercaptan, ethanol, methanol, acetone, and terpenes. Methanol is the primary hazardous air pollutant of concern and constitutes up to 80% of the organic matter and most of the chemical oxygen demand (COD) from foul condensates [3]. Condensates can either be reused (typically for pulp or chip washing) or can be treated before discharge to the wastewater treatment system. Conventional treatment methods rely on energy-intensive technologies such as incinerators and scrubbers, which ultimately produce VOC, SO_x, NO_x, and particulate emissions [4].

A sustainable alternative treatment of COD from foul condensates can be achieved through a biological conversion of the methanol into commercially useful biopolymers, such as polyhydroxyalkanoates (PHAs). Polyhydroxyalkanoates are polyesters composed of 3-hydroxy fatty acid monomers in which the carboxyl group of one monomer forms an ester bond with the hydroxyl group of the neighboring monomer [5]. Numerous bacteria are able to synthesize and store PHAs as intracellular carbon and energy reserves [6]. Bacteria accumulate PHAs under one or a combination of the following environmental conditions: macronutrient (nitrogen or phosphorus) or micronutrient (potassium, magnesium, or sulfate) limitation in the presence of excess carbon; electron donor/acceptor variability (aerobic/anaerobic cycling); or a feast–famine regime [7].

Polyhydroxyalkanoates exhibit material properties similar, in part, to conventional petroleum-based thermoplastics with the added benefit of being entirely biodegradable [8]. PHAs can serve as an alternative to petroleum-based thermoplastics in selected applications such as natural fiber reinforced thermoplastic composites. These composites are produced by co-extruding mixtures of natural fibers such as wood together with plastics such as high-density polyethylene to produce strong materials for durable applications [9]. By replacing the petroleum-derived plastics with thermoplastic bacterial polyesters such as PHAs, the composite products sector could serve as a future market for unpurified PHAs [10]. However, the integration of PHAs with natural fiber reinforced thermoplastic composites faces both technical and economic challenges that need to be met for the end product to be commercially viable. Currently, PHAs are not economically competitive with petroleum-based thermoplastics [11]. The most influential factors driving PHA production costs are extraction, purification, and carbon substrate cost. By minimizing or eliminating extraction and purification steps and by using an inexpensive substrate, the cost of PHAs can

potentially be reduced to a competitive level. In applications such as natural fiber composites, PHA extraction from the cell mass may not be required [10]. In addition, the use of pulp mill effluents such as foul condensates as an inexpensive carbon source can provide a cost-effective means by which PHA is produced using pulp mill effluents. An illustration of this approach can be seen in Fig. 1. This approach would also allow for reduced waste production and potentially create an additional profit stream within pulp and paper mills.

Extensive work has been performed using activated sludge from domestic wastewater to produce PHAs from readily degradable carbon sources such as mixed fatty acids and undefined fermentation products from anaerobic sludge digestion [12–14]. In the case of pulp mills, the raw wastewater is less conducive to PHA production because of the recalcitrant nature of the carbon and its low concentration [2]. Therefore, it is necessary to amend the wastewater with an additional carbon source to facilitate PHA production. In this instance, methanol from the foul condensates provides both an available and inexpensive biologically degradable carbon source for PHA production. As the bacteria in the pulp mill waste activated sludge are not accustomed to methanol as a primary carbon and energy source in the wastewater treatment system, the activated sludge consortium must undergo enrichment to acclimate to the foul condensates. A selective enrichment of the waste-activated sludge is required to select for a microbial consortium capable of simultaneously utilizing the methanol in foul condensates while synthesizing PHAs.

The goal of this study was to enrich a culture from pulp and paper secondary waste activated sludge that can grow aerobically using methanol-rich pulp and paper mill foul condensate streams originating from a kraft chemical recovery process. The enrichments will be used in future experiments to explore the range of environmental conditions necessary to

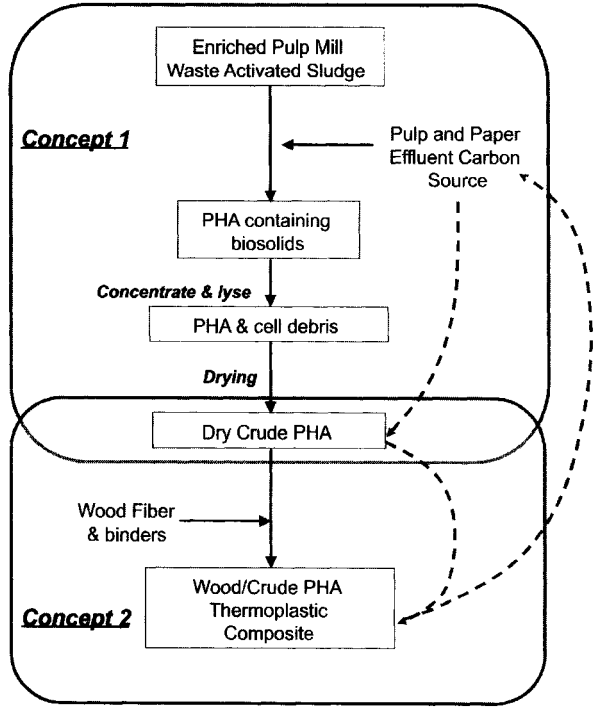


Fig. 1 Approach for minimizing costs associated with the manufacture of natural fiber reinforced thermoplastic composites using unpurified PHAs

produce and accumulate PHAs using pulp and paper effluents, with the ultimate goal of incorporating the PHA-rich biomass into natural fiber reinforced thermoplastic composite materials.

Materials and Methods

Source of Microorganisms: A mixed microbial consortium was obtained from the return waste-activated sludge line within the wastewater treatment facility at the P.H. Glatfelter pulp and paper mill in Chillicothe, OH. Activated sludge was shipped overnight at 4°C and used within 48 h of receipt. The activated sludge had a mixed liquor volatile suspended solids (MLVSS) concentration of 3,200 mg l^{-1}, a pH of 7.43, and a COD of 180 mg l^{-1}. The activated sludge was used to inoculate sequencing batch reactors used in enrichment experiments at one-fourth of the total volume of the reactors.

Pulp and Paper Mill Waste Streams: Five conditions were chosen for the enrichment of the original waste-activated sludge. Three foul condensate effluents from the pulp mill kraft chemical recovery process were selected based on their high COD: (1) the combined evaporator condensates (3200 tank foul condensate or FC 3200), (2) blow heat accumulator overflow foul condensate (FC BHAO), and (3) evaporator foul condensate (FC EVAP). The remaining two media used for enrichment consisted of primary clarifier effluent (primary out abbreviated as "1°OUT") supplemented with methanol, and waste-activated sludge supplemented with methanol (WAS-only).

The COD of the foul condensates were highly variable (see Table 1). In the FC BHAO, the COD ranged from 4,600 to 46,300 mg l^{-1}. In the FC 3200, the COD ranged from 810 to 47,400 mg l^{-1}. In the FC EVAP, the COD ranged from 4,800 to 17,400 mg l^{-1}. On the other hand, the 1°OUT received had a reasonably consistent COD between 300 and 400 mg l^{-1}. The primary carbon source in the foul condensates was methanol, which accounted for 51–72% of the COD, depending on the date sampled. This large variability demonstrates the changing compositions of the materials received, and is assumed to be a result of the variability of the wood species used as feedstocks for the pulp mill. The primary carbon source in the 1°OUT was not identified.

The foul condensates were not a significant source of total suspended solids (TSS). The average values for TSS were consistently an order of magnitude less than the TSS of the waste-activated sludge that was used as the source of inoculum. The average values for foul condensate COD, pH, and TSS are in Table 1. When samples were received from the pulp mill, pH, COD, and TSS were immediately measured. Foul condensates were adjusted to

Table 1 Average COD, TSS, and pH for the foul condensates and 1°OUT as received.

Waste stream ID	COD[a] (mg/l)	TSS[b] (mg/l)	pH
FC 3200	30,200±13,545	47±23	9.66±0.84
FC BHAO	13,314±16,433	976±1537	9.39±0.99
FC EVAP	5,487±4,247	116±29	9.48±1.11
1°OUT	480±286	600±303	7.48±0.45

[a] Chemical oxygen demand ± one standard deviation

[b] Total suspended solids ± one standard deviation

neutral pH using 1 N HCl (Fisher Scientific, Fair Lawn, NJ) and the materials were stored at 4°C to minimize biological activity and COD degradation. In some cases, the foul condensates contained a non-aqueous phase liquid that was removed by decanting and disposed before using the foul condensates.

Nutrient Media: To ensure the presence of the necessary macronutrients and micronutrients to select for a community capable of consuming methanol as the main carbon source, Methanol-Utilizing Bacteria Medium B [15] was utilized as a nutrient addition. The nutrient media was supplied to all enrichment reactors to ensure balanced growth conditions. The nutrient medium was used without methanol addition for the FC 3200, FC BHAO, and FC EVAP enrichments, as the foul condensates contained sufficient concentrations of methanol. Methanol (99.9%; Fisher Scientific, Fair Lawn, NJ) was added to the nutrient media supplied to the 1°OUT and WAS-only enrichment reactors.

System Design and Operation: Fifteen sequencing batch reactors, each with a working volume of 160 ml, were run at a hydraulic retention time (HRT) equal to the solids retention time (SRT) of 4 days. Air was supplied (200 ml min^{-1} or 1.24 vvm) to provide oxygen and mixing. Each enrichment condition was prepared in triplicate. The reactors were operated on a 24-h feed/decant cycle with one quarter of the reactor volume (40 ml) being replaced with fresh feed. In the FC 3200, FC BHAO, and FC EVAP reactors the feed consisted of a mixture of the nutrient media and the respective foul condensate. The 1°OUT reactors were fed a mixture of the nutrient medium supplemented with methanol and the 1°OUT from the pulp mill. Finally, the WAS-only reactors were simply fed the nutrient media supplemented with methanol. The ratio of nutrient media to the waste being fed was determined by reaching a final total COD in the feed of 2,500 mg l^{-1}. This value was chosen as the ceiling for COD/methanol concentration as it is within the range of methanol concentrations demonstrated to be optimal for PHA production in pure culture [16–18], yet it minimized any potential toxic effects on the microbial community [19]. The reactors were supplied continuously with oil-free instrument air, which was humidified to reduce evaporation from the reactors. Thereafter, the airflow was separated using a gang valve and then regulated using a flow meter (Cole-Parmer, Vernon Hills, IL).

The reactors were constructed using 2″×6″ ($d \times h$) glass process pipe, closed at both ends with Teflon® end caps, and sealed with rubber gaskets and stainless steel clamps (Ace Glass, Vineland, NJ). Reactors were sealed to contain the hydrogen sulfide, methyl mercaptan, and other malodorous and hazardous compounds present in the foul condensates. Reactors were vented through a series of two granular activated carbon beds (CC601 and Midas OCM; USFilter, Los Angeles, CA) that effectively removed hydrogen sulfide and methyl mercaptan from the effluent gases. The experimental process flow diagram is shown in Fig. 2.

Before initiating the enrichments, a nonsteady-state mass balance was performed to account for methanol stripping caused by aeration. The amount of methanol stripped over a 24-h period was calculated according to Eqs. 1 and 2:

$$\%\ \text{Methanol stripped} = \frac{C_i - C_f}{C_i} \times 100\% \tag{1}$$

$$C_f = C_i \exp\left[-\left(\frac{Q_{\text{air}} \Delta t H_{\text{methanol}}}{V_{\text{reactor}}}\right)\right], \tag{2}$$

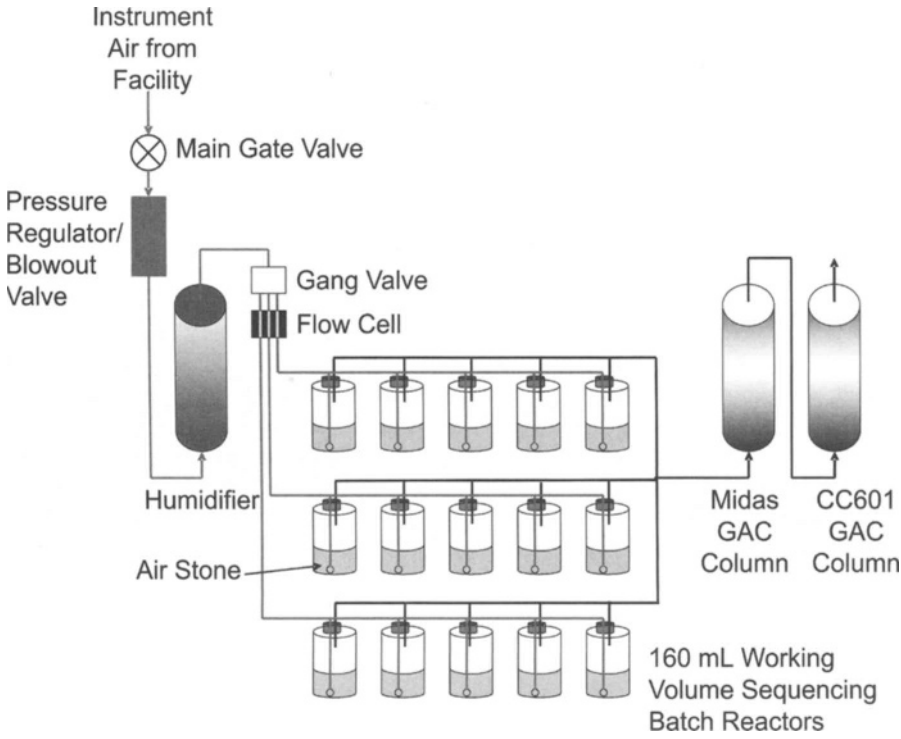


Fig. 2 Enrichment experiment process flow diagram

where C_i is the methanol concentration at time zero, C_f is the methanol concentration in reactor after 24 h, Q_{air} is the air flow rate, Δt is the time interval, $V_{reactor}$ is the reactor volume, and $H_{methanol}$ is the dimensionless Henry's constant for methanol ($1.858*10^{-4}$ for methanol at 25°C [20]).

The mass balance model predicted that 28% of the methanol would be stripped over a 24-h period (one feed/decant cycle). This was verified by an average methanol decrease of 26% over a 24-h period in five replicate stripping columns constructed and operated identically to the enrichment reactors (data not shown). Based on these results, an additional 36 μl of 99.99% methanol was added daily to the reactors along with the feed to compensate for methanol loss caused by stripping.

Sampling and Analysis: Samples were collected from the daily decants immediately before feeding and analyzed for MLVSS, COD, methanol, and ammonium (NH_4^+) concentration. A 40-ml sample was recovered from each reactor every third and fourth day of an HRT period. The unfiltered samples from the third day were stored at −80°C for future microbial community analysis. The unfiltered samples conserved on the fourth day were initially used to measure MLVSS according to ASTM Standard Method 2540 E [21] using Millipore TCLP AP40 glass fiber filters. The samples were then filtered through a Millex GP 0.22-μm Express PES Membrane filter unit (Millipore Corporation, Billerica, MA) and analyzed for soluble COD, methanol, and NH_4^+.

COD

COD was measured according to ASTM Standard Method 5220 D [21] using Hach high-range ampoules with a Hach DRB 200 digestion block and Hach DR 2010 portable data logging spectrophotometer (Hach Company, Loveland, CO) set at a 620-nm wavelength.

Methanol

Methanol was analyzed by high-performance liquid chromatography (HPLC) using a Hitachi HPLC D-6000 Series HPLC system (Tokyo, Japan) consisting of a Hewlett Packard 1047A RI Detector (Agilent Technologies, Palo Alto, CA), a Hitachi L6200A Gradient Pump (Tokyo, Japan), and a Hitachi AS-4000 autosampler (Tokyo, Japan). The mobile phase consisted of 0.01% H_2SO_4 at 0.6 ml min^{-1}. Twenty microliter samples were prepared at 1:1 dilution and injected into a BioRad Aminex HPX-87H (300×7.8 mm ID) column (Hercules, CA) with a BioRad Micro-Guard cartridge (Cat. No. 125-0131). Methanol standards were prepared at 0.01–0.1% by volume using 99.99% methanol. Samples were run at 60°C, with the detector set at 50°C. The method detection limit (MDL) for the methanol analysis was 100 mg l^{-1}.

Ammonium

Soluble ammonium ion concentrations were measured by ion chromatography using a system consisting of a Dionex ED40 conductivity detector with a GP50 gradient pump, an AS50 autosampler, an AD20 absorbance detector, and an EG40 eluent generator (Dionex Corporation, Sunnyvale, CA). Samples were analyzed using 5 μl injections at a flow rate of 1 ml min^{-1}. Samples were injected into a Dionex IonPac CS12A (250 × 4 mm ID) for cations with the Dionex ECG-MSA cartridge in the eluent generator system. Data were collected using Peaknet v. 5.21 (Dionex Corporation, Sunnyvale, CA). Cation standards were prepared using the Dionex 6 Cation Standard II #46070. A seven-level cation standardization was performed (DI water, five standards, and the non-dilute Cation Standard II solution). The MDL for the NH_4^+ analysis was 0.5 mg l^{-1}.

Polyhydroxyalkanoates

PHA analysis was conducted as described by Braunegg [22], with the following modifications. Upon completion of the 20th HRT, the reactors were fed their respective substrate media and four 40-ml samples were taken for PHA analysis per reactor over a 24-h period. The unfiltered 40-ml biomass samples were bleached by adding 2 ml of commercial grade bleach (5% NaClO) (Clorox, Oakland, CA) and centrifuged at 4,300×*g* for 15 min. The pellet was then dried at 60°C for 24 h. Between 20 and 40 mg of the dried biomass was weighed and suspended in a mixture of 2 ml acidified methanol (3% H_2SO_4, *v/v*) and 2 ml chloroform. The chloroform contained 0.5 mg ml^{-1} benzoic acid as an internal standard. The mixture was then digested at 100°C for 4 h in a Hach DRB 200 digestion block (Hach Company, Loveland, CO).

Once the digestion was completed, 1 ml of deionized water was added and the mixture was vortexed for 30 s. After allowing the organic phase to separate from the aqueous phase, Pasteur pipettes were used to remove the organic phase. The organic phase was then filtered through another Pasteur pipette packed with a cotton plug and 1 g of sodium sulfate (Fisher Scientific, Fair Lawn, NJ) to remove any remaining water. The organic phase, which

contained the methyl ester monomers of the PHA molecules, was analyzed by gas chromatography using an Agilent Technologies 6850 Network GC System with a Thermal Couple Detector system (Agilent Technologies, Palo Alto, CA). The samples were run at 60°C and at 1 ml min^{-1} with 1-μl injections using a Zebron ZB-624 column (250×1.4 mm ID) (Phenomenex Inc., Torrance, CA). The GC Chemstation 2001 software (Agilent Technologies, Palo Alto, CA) was utilized for data analysis. The concentration of PHA was quantified against standards of PHB and PHV (Poly(3-hydroxybutyric acid-co-3-hydroxyvaleric acid) standard) (Sigma-Aldrich, St. Louis, MO) as derivatized methyl esters and extraction efficiency was calculated based on the benzoic acid internal standard.

Results

The enrichments were run for a total of 20 HRTs, or 80 days, to allow the selective enrichment of a consortium capable of utilizing methanol in the various media as their main carbon source. The data shown in Figs. 3, 4, 5, and 6 are the averages of the three replicate reactors run for each medium, and represent the end point values for each HRT (40 ml fourth day samples; see above). Error bars shown indicate one standard deviation.

MLVSS: MLVSS in all reactors declined as a result of washout during enrichment of the culture for methanol-utilizing bacteria. The MLVSS, which is representative of the total microbial biomass in the cultures, stabilized in all reactors between approximately HRT 8 and 12. Because stabilization of MLVSS is not necessarily indicative of stability of the microbial community, it was decided the enrichment feedings be continued until either rebound of the MLVSS was observed (indicating growth of the selected community), or until the MLVSS was stable for an extended period (indicating steady-state cell concentration for the carbon loads supplied). The FC 3200 and FC BHAO reactors required the longest amount of time to stabilize the MLVSS (Fig. 3a,b), whereas, the WAS-only enrichments required the least amount of time (Fig. 3e). In the FC EVAP and 1°OUT reactors, the MLVSS rebounded before stabilizing (Fig. 3c,d).

Soluble COD: Soluble COD present in the reactors at the end of the 24-h feeding cycle initially varied widely for both the FC 3200 and FC BHAO reactors (Fig. 4a,b). This variability mirrored the larger-than-expected variability in the COD of these foul condensates. The large increase in COD between HRT 2 and 6 for the FC BHAO reactors was likely caused by the unexpected increase in the FC BHAO foul condensate COD from 4,600 to 46,300 mg l^{-1} (Fig. 4b). The other enrichments began COD degradation immediately (Fig. 4c–e). In all reactors the COD was degraded an average of 79–89% after enrichment for 20 HRTs. In the enrichments that were fed foul condensates, 11–21% of the input COD was found to be non-biodegradable.

Methanol: Methanol was the main contributor to COD in the enrichment reactors. Methanol comprised 51–72% of the COD in the foul condensate wastes. This wide range was caused by the varying nature of the foul condensates, and ultimately, to the composition of the wood feedstocks entering the mill. The enriched consortia in all of the reactors consumed methanol to levels below the 100 mg l^{-1} methanol (HPLC) detection limit by HRT 8 (Fig. 5a–e). This indicates functional stability in the system by HRT 8 with respect to methanol consumption. To ensure community stability in the reactors, as well as to assess the long-term functional stability of the consortia, the reactors were further run to

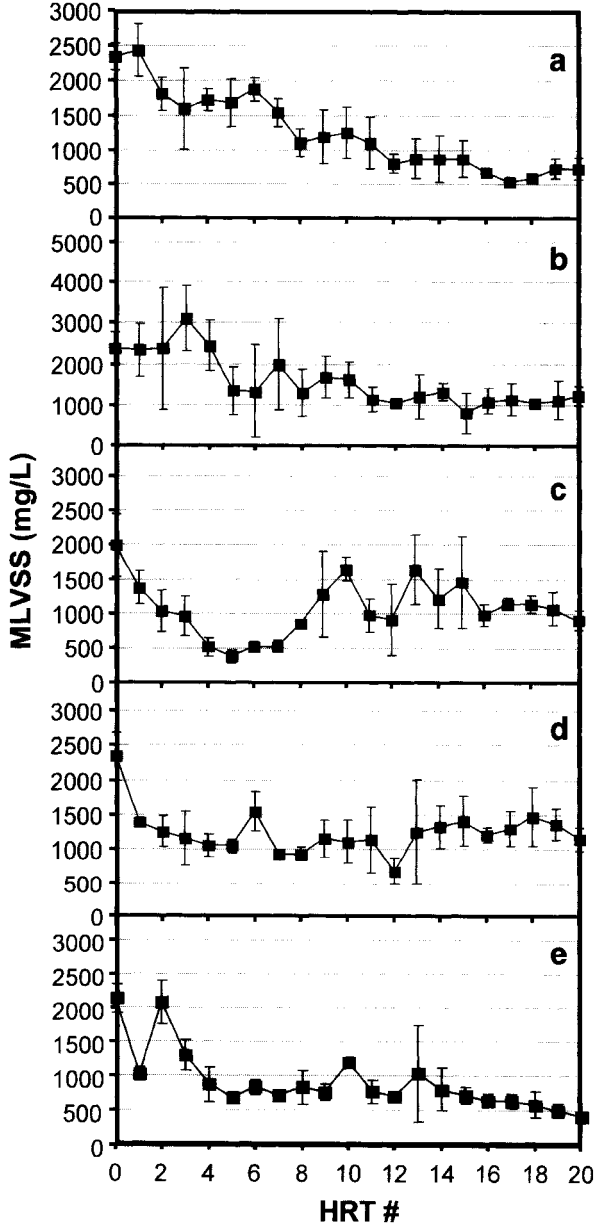


Fig. 3 (**a**–**e**) Variation of MLVSS with HRT. Data shown are from samples taken at the end of the 24-h feed period, and are the average of three replicate reactors. (**a**) FC 3200. (**b**) FC BHAO. (**c**) FC EVAP. (**d**) 1°OUT. (**e**) WAS only

HRT 20. The resulting communities were capable of degrading added methanol and methanol present in the pulp mill effluents.

Ammonium (NH_4^+): All reactors were fed a balanced growth medium containing 300 mg l^{-1} NH_4^+ as the primary source of nitrogen. Nutrient conditions were chosen to foster balanced microbial growth—no nutrient limitations were anticipated or observed. Figure 6a–e clearly demonstrates that the organisms in each enrichment scenario were not lacking in nitrogen.

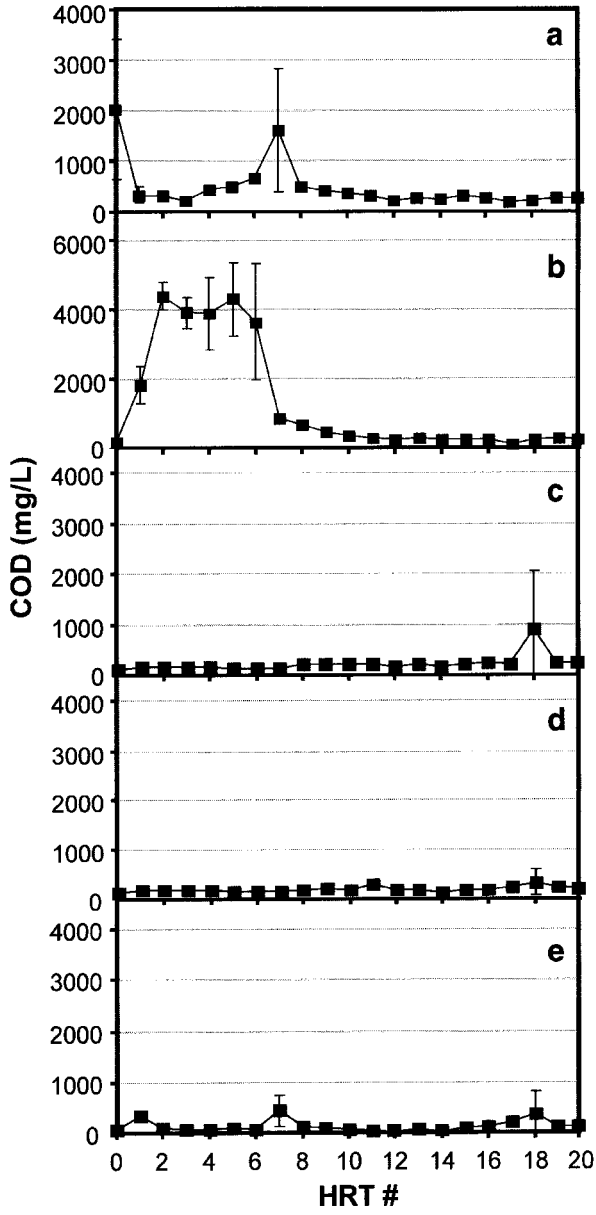


Fig. 4 (**a**–**e**) Variation of COD with HRT. Data shown are from samples taken at the end of the 24-h feed period, and are the average of three replicate reactors. (**a**) FC 3200. (**b**) FC BHAO. (**c**) FC EVAP. (**d**) 1°OUT. (**e**) WAS only

The concentration in the balanced growth medium was asymptotically reached after the community had stabilized in both the 1°OUT and WAS-only enrichments. Notably, the foul condensates from the Chillicothe mill proved to be a source of additional NH_4^+ (Fig. 6a–c), which resulted in nitrogen sufficiency reflected as C/N ratios as low as 3 in the FC 3200 enrichments. Peak COD and NH_4^+ concentrations occurred simultaneously in the FC 3200 and FC BHAO reactors (Figs. 6a–b and 4a–b).

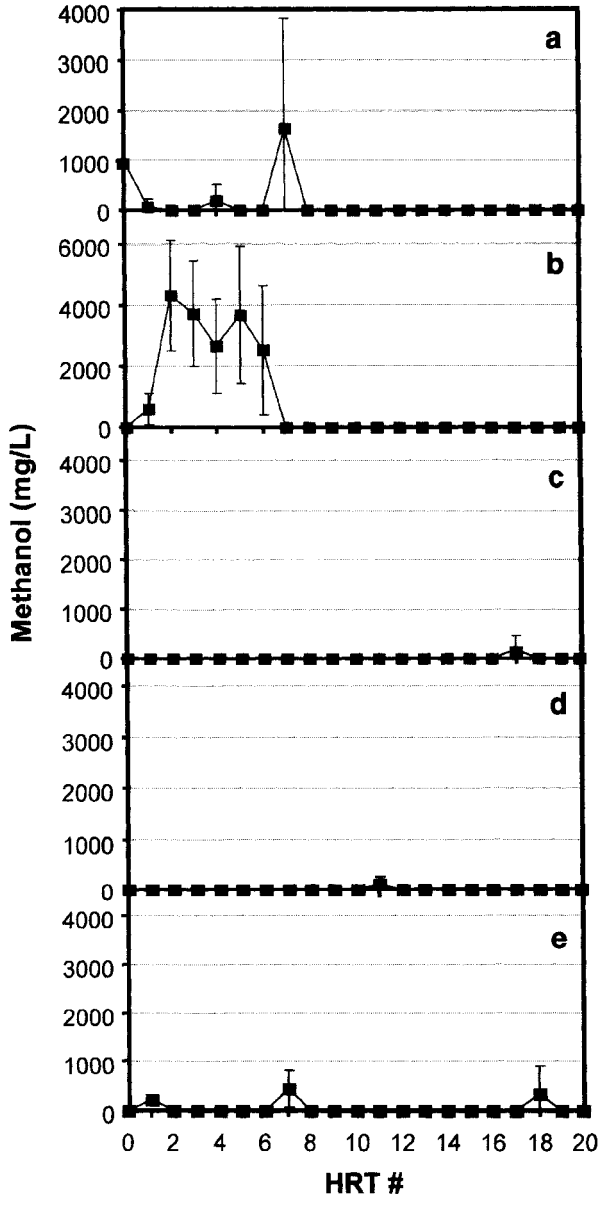


Fig. 5 (**a**–**e**) Variation of methanol with HRT. Data shown are from samples taken at the end of the 24-h feed period, and are the average of three replicate reactors. (**a**) FC 3200. (**b**) FC BHAO. (**c**) FC EVAP. (**d**) 1°OUT. (**e**) WAS only

Discussion

The objective of this work was to selectively enrich methanol-utilizing organisms from the original pulp mill waste activated sludge. Secondary waste-activated sludge from the P. H. Glatfelter wastewater treatment plant was tested for its ability to degrade methanol and produce PHA. It was found that without enrichment, the bacteria within the waste-activated sludge from the pulp mill wastewater facility did not degrade methanol or accumulate PHA over a 24-h period (data not shown). Thus, the selective enrichment of the activated sludge

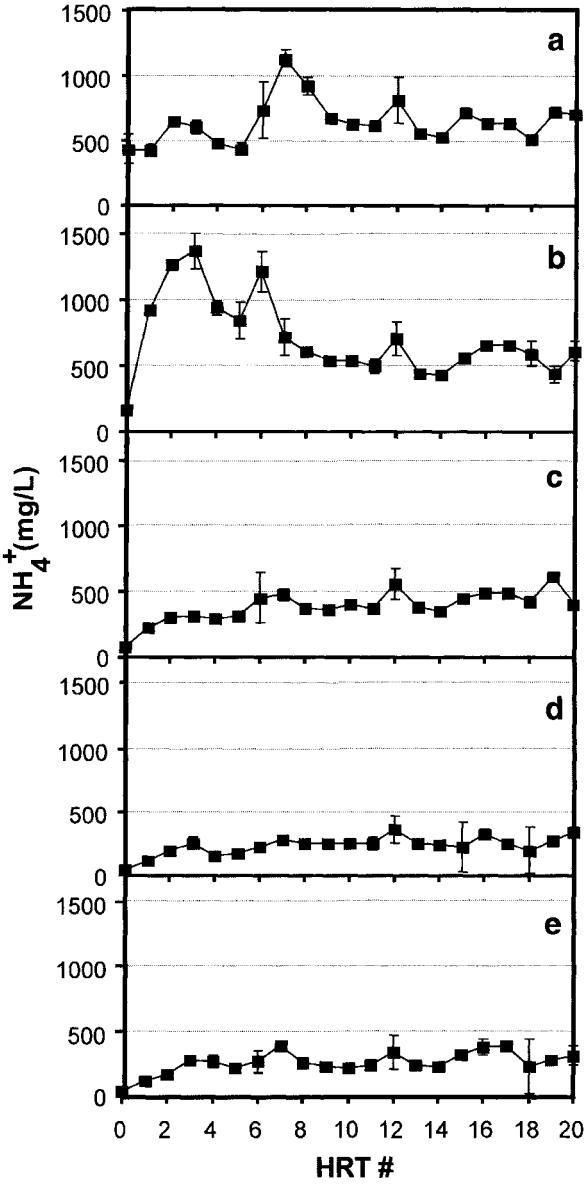


Fig. 6 (**a**–**e**) Variation of NH_4^+ with HRT. Data shown are from samples taken at the end of the 24-h feed period, and are the average of three replicate reactors. (**a**) FC 3200. (**b**) FC BHAO. (**c**) FC EVAP. (**d**) 1°OUT. (**e**) WAS only

microbial community on methanol was necessary to obtain a culture that could aerobically degrade methanol and accumulate PHA derived from methanol carbon. After a period of 20 HRTs, the pulp mill waste activated sludge was enriched for consortia capable of using the methanol from foul condensates and the methanol added to the WAS-only and 1°OUT enrichments.

As a consequence of the selection process, the MLVSS of the activated sludge initially decreased in all of the enrichment reactors as a result of washout of members of the microbial community. This was expected because the organisms present in the pulp mill activated sludge were not accustomed to methanol as a primary carbon source as significant

methanol does not reach the wastewater treatment facility but is accumulated in the foul condensates, which are combusted during disposal. After initially decreasing, the MLVSS in all reactors stabilized—FC EVAP and 1°OUT eventually showed a rebound in MLVSS, indicative of the selection for an altered microbial community. The decrease in MLVSS was evidence of the washout of non-methanol-utilizing bacteria during the enrichments, as well as washout of methanol-utilizing bacteria having doubling times longer than the SRT (4 days). Nonetheless, the underlying microbial community structure, dynamics, and functional stability and how they are related in mixed consortia are poorly understood [23]. Despite the potential structural and functional changes during the enrichment process, the mixed microbial communities were continuously capable of degrading methanol, which was their intended function. It is believed that functional stability observed in engineered systems such as sequencing batch reactors is a result of the functional redundancy within the system [24], especially with respect to microbial carbon assimilation pathways. Therefore, despite process upsets or influent changes, the dynamic changes within a biological reactor utilizing a diverse microbial community are overshadowed by functional stability when the microbial community is faced with a consistent set of operating conditions over a long period of time [25]. Based on this knowledge, the enrichment reactors were run for 20 HRTs to attempt to assess long-term functional stability and attain microbial community stability. Future work will characterize the microbial population throughout the enrichment process using t-RFLP.

The COD, pH, and TSS of the foul condensates used in the enrichments were highly variable resulting at least in part from the transient nature of the wood species utilized at the pulp mill. However, whereas COD variability was expected in the foul condensates because of varying throughput at the facility, seasonal variations, and quality of wood being processed, the magnitude of COD variation observed was not expected. The pulp mill effluents used were taken directly from preexisting sample points within the facility. It is believed that the sampling lines may not have been allowed to fully purge before sample collection because of the extensive presence of toxic and/or odorous compounds including hydrogen sulfide, methyl mercaptan, ethanol, methanol, acetone, terpenes, and various other VOCs in the foul condensates. This may have contributed to added variability in the foul condensates. This is supported by the case of the 1°OUT, as it was sampled from a well-purged sampling line and had consistent COD, pH, and TSS throughout the enrichment process. Unless improved foul condensate collection procedures are employed, the variability of the foul condensates will present a challenge in the design of a biological treatment system to synthesize PHA from pulp mill waste effluents. Such fluctuations in waste quality can negatively impact biological treatment systems if the fluctuations are not attenuated before treatment. A potential improvement to the collection procedure would be the use of feedstock mixing and dilution tank in which the condensates would be diluted to a predetermined COD using another lower carbon concentration effluent before biological treatment. Monitoring and controlling effluent carbon and nitrogen concentrations will be vital for the successful operation of a biological process that degrades methanol and produces biopolymers from pulp mill effluents.

Foul condensates were a significant source of ammonium nitrogen. Ammonia is produced in the pulping process as a result of the caustic digestion of proteins in the wood fed to the mill. The feedstock wood species has a significant impact on the concentration of ammonia present in the pulping process streams as it dictates the amount of wood nitrogen present [26]. Once the wood and pulp are digested, the primary exit point for ammonia in a pulp mill within a kraft chemical recovery process is in the foul condensates [27]. Foul condensates are a condensed caustic waste stream in which the ammonia either remains in

the gas phase or is dissolved in the foul condensate as aqueous ammonia. In the present work, once the foul condensates were received for the enrichment experiment, they were neutralized and ammonia was converted into the soluble ammonium ion. The combination of the nitrogen in the foul condensates and ammonium present in the nutrient media provided conditions of nitrogen sufficiency for all of the enrichments (C/N of 3).

The three main environmental conditions that stimulate PHA storage in a mixed consortium are: nutrient limitation, variation in electron donor/acceptor availability, or the presence of a feast–famine environment [28]. In this study, the enrichment reactors were operated with the intent of enriching the original pulp mill activated sludge for consortia capable of utilizing methanol in pulp mill effluents while synthesizing PHA in a nutrient-sufficient feast–famine environment. Therefore, it was expected that PHA production could be stimulated solely by a feast–famine regime in the presence of excess nutrients [29]. However, the enrichment reactors did not produce PHA under the nutrient-sufficient enrichment conditions, although feast–famine conditions were maintained. Although a low C/N ratio condition was more advantageous for cell growth, it did not favor PHA accumulation. Based on these observations, it was hypothesized that it would be necessary to combine a feast–famine regime with nutrient limitation (by increasing the C/N) to stimulate PHA storage using the enriched cultures. With a lower nitrogen concentration with respect to available carbon, it has been shown that a higher proportion of the carbon can be directed toward PHA synthesis [30–32]. Cultures from the WAS-only enrichments were subsequently tested for PHA production under a combined feast–famine and N-limited environment, resulting in the production of up to 13.9% PHA on a dry cell weight basis. By contrast, the original non-enriched waste-activated sludge did not yield any PHA under N-limited conditions.

The results of this study indicate that the enrichment process altered the original activated sludge community—which was originally unable to degrade methanol or produce PHA—and produced a consortium capable of degrading methanol under both N-sufficient and N-limited conditions. Alterations to the community will be studied in future experiments using molecular methods. Whereas we expected the enriched community to produce PHA from methanol under feast–famine conditions, both N-limitation and feast–famine conditions were ultimately required to stimulate PHA production. This indicates that nutrient limitation, variation in electron donor/acceptor availability, and feast–famine may not each be singly sufficient in all cases for stimulating PHA accumulation by bacteria.

Conclusions and Future Work

Activated sludge obtained from the pulp mill's wastewater treatment plant was successfully enriched for consortia capable of aerobically degrading methanol from high-strength carbon pulp mill waste streams. The COD in all of the enrichments was reduced by 79 to 89%. Foul condensates were found to be a suitable feedstock, although their variability must be mitigated to avoid process design challenges. Besides being a source of high strength COD, the foul condensates were also a significant source of ammonium nitrogen. This makes it unnecessary to add nitrogen during either growth (N-sufficient) or PHA production (N-limited) phases when using the foul condensates as the carbon source.

The enrichments were intentionally run under N-sufficient conditions to assure balanced growth, but this condition did not stimulate PHA production. The enriched cultures were later tested for PHA production under N-limited conditions and produced PHA. The non-enriched waste activated sludge did not produce PHA under N-limited conditions.

Therefore, to stimulate PHA production from pulp mill effluents it is necessary to not only provide a feast–famine regime, but also a nutrient-limited condition.

Future work will focus on optimizing the PHA yield from pulp mill effluents because successful integration of PHAs with natural fiber composites requires higher biomass PHA concentrations [10]. As part of the effort to optimize PHA production using pulp mill effluents, future work will involve characterization of the microbial community throughout the enrichment process, investigation of the influence of C/N, F/M (food to microorganism ratio), HRT, and SRT on PHA production, and a pilot test of PHA production from FC 3200 at the mill using activated sludge enriched onsite.

Acknowledgements This work is supported by the U.S. Department of Energy, Industrial Technologies Program, Forest Products Industries of the Future, under DOE-NE Idaho Operations Office Contract DE-AC07-05ID14517. The authors are grateful to Katherine Wiedeman and James Flanders of P. H. Glatfelter for providing access to their facility, the activated sludge, and the foul condensates. The authors also thank Cathy Rae of the INL for performing the PHA analyses.

References

1. Miller, M., Justiniano, M., & McQueen, S. (2005). *Energy and environmental profile of the U.S. pulp and paper industry.* Washington, DC: U.S. Department of Energy, Office of Energy Efficiency and Renewable Energy, Industrial Technologies Program.
2. Dufresne, R., Liard, A., & Blum, M. S. (2001). Anaerobic treatment of condensates: Trial at a kraft pulp and paper mill. *Water Environment Research, 73*(1), 103–109.
3. Springer, A. M. (2000). *Industrial environmental control pulp and paper industry,* (3rd ed., pp. 238–239). Atlanta, GA: Tappi Press.
4. Smook, G. A. (1992). *Handbook for pulp & paper technologists,* (2nd ed., p. 382). Bellingham, WA: Angus Wilde Publications.
5. Madison, L. L., & Huisman, G. W. (1999). Metabolic engineering of poly(3-hydroxyalkanoates): From DNA to plastic. *Microbiology and Molecular Biology Reviews, 63*(1), 21–53.
6. Anderson, A. J., & Dawes, E. A. (1990). Occurrence, metabolism, metabolic role, and industrial uses of bacterial polyhydroxyalkanoates. *Microbiological Reviews, 54*(4), 450–472.
7. Dionisi, D., Majone, M., Papa, V., & Beccari, M. (2004). Biodegradable polymers from organic acids by using activated sludge enriched by aerobic periodic feeding. *Biotechnology and Bioengineering, 85*(6), 569–579.
8. Braunegg, G., Lefebvre, G., & Genser, K. F. (1998). Polyhydroxyalkanoates, biopolyesters from renewable resources: Physiological and engineering aspects. *Journal of Biotechnology, 65*(2–3), 127–161.
9. Smith, P. M., & Wolcott, M. P. (2006). Opportunities for wood/natural fiber–plastic composites in residential and industrial applications. *Forest Products Journal, 56*(3), 4–11.
10. Coats, E. R., Loge, F. J., Englund, K., & Wolcott, M. P. (2007). Production of natural fiber reinforced thermoplastic composites through the use of PHB-rich biomass. Bioresource Technology, DOI 10.1016/j.biortech.2007.03.065, in press.
11. Philip, S., Keshavarz, T., & Roy, I. (2007). Polyhydroxyalkanoates: Biodegradable polymers with a range of applications. *Journal of Chemical Technology and Biotechnology, 82*(3), 233–247.
12. Reis, M. A. M., Serafim, L. S., Lemos, P. C., Ramos, A. M., Aguiar, F. R., & Van Loosdrecht, M. C. M. (2003). Production of polyhydroxyalkanoates by mixed microbial cultures. *Bioprocess and Biosystems Engineering, 25*(6), 377–385.
13. Satoh, H., Iwamoto, Y., Mino, T., & Matsuo, T. (1998). Activated sludge as a possible source of biodegradable plastic. *Water Science & Technology, 38*(2), 103–109.
14. Satoh, H., Mino, T., & Matsuo, T. (1999). PHA production by activated sludge. *International Journal of Biological Macromolecules, 25*, 105–199.
15. Atlas, R. M. (1997). *Handbook of microbiological media,* (2nd ed., p. 891). Boca Raton, FL: CRC Press.
16. Bourque, D., Ouellette, B., Andre, G., & Groleau, D. (1992). Production of poly-β-hydroxybutyrate from methanol: Characterization of a new isolate of Methylobacterium extorquens. *Applied Microbiology and Biotechnology, 37*(1), 7–12.

17. Kim, S. W., Kim, P., Lee, H. S., & Kim, J. H. (1996). High production of poly-β-hydroxybutyrate (PHB) from Methylobacterium organophilum under potassium limitation. *Biotechnology Letters, 18*(1), 25–30.
18. Suzuki, T., Yamane, T., & Shimizu, S. (1986). Mass production of poly-β-hydroxybutyric acid by fully automatic fed-batch culture of methylotroph. *Applied Microbiology and Biotechnology, 23*(5), 322–329.
19. Bormann, E. J., Leissner, M., & Beer, B. (1997). Growth and formation of poly(hydroxybutyric acid) by Methylobacterium rhodesianum at methanol concentrations of above 25 g/l. *Acta Biotechnologica, 17*(4), 279–289.
20. Weast, R. C. (1984). *Handbook of chemistry and physics* (64th ed.). Boca Raton, FL: CRC Press.
21. APHA (1992). *Standard methods for the examination of water and wastewater* (20th ed.). Washington D.C.: American Public Health Association.
22. Braunegg, G., Sonnleitner, B., & Lafferty, R. M. (1978). A rapid gas chromatographic method for the determination of poly-β-hydroxybutyric acid in microbial biomass. *European Journal of Applied Microbiology and Biotechnology, 6*(1), 29–37.
23. Gentile, M. E., Jessup, C. M., Nyman, J. L., & Criddle, C. S. (2007). Correlation of functional instability and community dynamics in denitrifying dispersed-growth reactors. *Applied and Environmental Microbiology, 73*(3), 680–690.
24. Briones, A., & Raskin, L. (2003). Diversity and dynamics of microbial communities in engineered environments and their implications for process stability. *Current Opinions in Biotechnology, 14*, 270–276.
25. Kaewpipat, K., & Grady, J. C. P. L. (2002). Microbial population dynamics in laboratory-scale activated sludge reactors. *Water Science & Technology, 46*(1–2), 19–27.
26. Kymäläinen, M., Holmström, M., Forssén, M., & Hupa, M. (2001). The fate of nitrogen in the chemical recovery process in a kraft pulp mill. Part III: The effect of some process variables. *Journal of Pulp and Paper Science, 27*(9), 317–324.
27. Kymäläinen, M., Forssén, M., & Hupa, M. (1999). The fate of nitrogen in the chemical recovery process in a kraft pulp mill. Part I. A general view. *Journal of Pulp and Paper Science, 25*(12), 410–417.
28. Dionisi, D., Beccari, M., Di Gregorio, S., Majone, M., Papini, M. P., & Vallini, G. (2005). Storage of biodegradable polymers by an enriched microbial community in a sequencing batch reactor operated at high organic load rate. *Journal of Chemical Technology and Biotechnology, 80*, 1306–1318.
29. Salehizadeh, H., & Loosdrecht M. C. M. V. (2004). Production of polyhydroxyalkanoates by mixed culture: Recent trends and biotechnological importance. *Biotechnology Advances, 22*(3), 261–279.
30. Serafim, L. S., Lemos, P. C., Oliveira, R., & Reis, M. A. M. (2004). Optimization of polyhydroxybutyrate production by mixed cultures submitted to acrobic dynamic feeding conditions. *Biotechnology and Bioengineering, 87*(2), 145–160.
31. Chua, H., Yu, P. H. F., & Ma, C. K. (1999). Accumulation of biopolymers in activated sludge biomass. *Applied Biochemistry and Biotechnology, 77–79*(1–3), 389–399.
32. Ma, C. K., Chua, H., Yu, P. H. F., & Hong, K. (2000). Optimal production of polyhydroxyalkanoates in activated sludge biomass. *Applied Biochemistry and Biotechnology, 84*(1–9), 981–990.

Appl Biochem Biotechnol (2008) 148:227–234
DOI 10.1007/s12010-007-8118-7

Evaluation of Cashew Apple Juice for the Production of Fuel Ethanol

Álvaro Daniel Teles Pinheiro · Maria Valderez Ponte Rocha · Gorete R. Macedo · Luciana R. B. Gonçalves

Received: 14 May 2007 / Accepted: 3 December 2007 /
Published online: 26 February 2008
© Humana Press 2007

Abstract A commercial strain of *Saccharomyces cerevisiae* was used for the production of ethanol by fermentation of cashew apple juice. Growth kinetics and ethanol productivity were calculated for batch fermentation with different initial sugar (glucose + fructose) concentrations. Maximal ethanol, cell, and glycerol concentrations were obtained when 103.1 g L^{-1} of initial sugar concentration was used. Cell yield ($Y_{X/S}$) was calculated as 0.24 (g microorganism)/(g glucose + fructose) using cashew apple juice medium with 41.3 g L^{-1} of initial sugar concentration. Glucose was exhausted first, followed by fructose. Furthermore, the initial concentration of sugars did not influence ethanol selectivity. These results indicate that cashew apple juice is a suitable substrate for yeast growth and ethanol production.

Keywords Ethanol · Cashew apple juice · *Saccharomyces cerevisiae* · Batch cultivation · Kinetic parameters

Introduction

One of the greatest challenges for society in the twenty-first century is to meet the growing demand for energy for transportation, heating, and industrial processes and to provide raw material for the industry in a sustainable way. An increasing concern for the security of oil supply has been evidenced by increasing oil prices, which, during 2006, approached US$80 per barrel [1]. More importantly, the future energy supply must be fulfilled with a simultaneous substantial reduction of green house gas emissions [2]. Ethanol satisfies that

Á. D. T. Pinheiro · M. V. P. Rocha · L. R. B. Gonçalves (✉)
Departamento de Engenharia Química, Universidade Federal do Ceará, Campus do Pici, Bloco 709, 60455-760 Fortaleza, Ceará, Brazil
e-mail: lrg@ufc.br

G. R. Macedo
Laboratório de Engenharia Bioquímica (LEB), Departamento de Engenharia Química, Universidade Federal do Rio Grande do Norte, Natal, Rio Grande do Norte, Brazil

requirement because its production and combustion do not contribute significantly to the total amount of carbon dioxide in the atmosphere [3].

Ethanol has already been introduced on a large scale in Brazil, USA, and some European countries, and it is expected to be one of the dominating renewable biofuels in the transport sector within the coming 20 years. Ethanol can be blended with petrol or used as neat alcohol in dedicated engines, taking advantage of the higher octane number and higher heat of vaporization; furthermore, it is an excellent fuel for future advanced flexfuel hybrid vehicles [1]. Nearly all fuel ethanol is produced by fermentation of sucrose in Brazil or corn glucose in the USA; however, these raw material bases will not be sufficient to satisfy the international demand [4].

A very common argument against ethanol is its economic competitiveness against fossil fuels. Nevertheless, Goldemberg et al. [5] demonstrated, through the Brazilian experience with ethanol, that economy of scale and technological advances can lead to increased competitiveness of this renewable alternative, reducing the gap with conventional fossil fuels. Consequently, there is an intensified interest in the study of all the steps involved in ethanol production to reduce costs [6].

Impelled by the creation of the "Proálcool" project in the 1970s and 1980s, Brazil has become, in 2005–2006, the world's largest ethanol producer via fermentation, developing and improving many fermentative processes [5] using sugar cane as a source of sucrose. In the northeast of Brazil, however, the volume of ethanol produced does not represent an important amount compared to the national production. So, the optimization of alternative low-cost processes is imperative. In the state of Ceará, the cashew agroindustry has an outstanding role in the local economy. However, only 12% of the total peduncle, the part of the tree that connects it to the cashew nut, is processed and it does not play an important role in the economy of the state. Furthermore, the majority of the cashew apple production spoils in the soil. Those facts, together with its rich composition (reducing sugar, fibers, vitamins, and minerals salts), turns cashew apple juice (CAJ) into an interesting and inexpensive (R$1.00/kg) culture medium [7].

Cashew is produced in around 32 countries of the world, and the major cashew apple-producing countries and their production figures in the year of 2004, based on the Food and Agriculture Organization [8], are, approximately, Vietnam, 8.4 million tons; Nigeria, 5 million tons; India, 4 million tons; Brazil, 1.6 million tons; and Indonesia, 1 million tons. The official estimate for the Brazilian cashew crop for 2006/2007 is around 266 million tons [9], which accounts for 11% of the world production and corresponds to more than 2 billion tons of cashew apple. Considering that the use of agroindustrial residues can contribute for the reduction of production costs, cashew apple appears as an alternative raw material for ethanol production, due to its vast availability and high concentration of reducing sugars. Therefore, the aim of this work was to investigate the potential use of this alternative substrate (CAJ) as a carbon source for ethanol production by *Saccharomyces cerevisiae* (commercial strain). Experiments were conducted in a batch bioreactor and the process was monitored by measuring biomass, glucose, fructose, and ethanol concentrations.

Materials and Methods

Microorganism

The microorganism used was a commercial yeast *S. cerevisiae* Saf-Instant (SAF Argentina, Buenos Aires, Argentina).

CAJ Preparation

CAJ was extracted by compressing the cashew apple (*Anarcardium occidentale* L.). After compressing, the juice was centrifuged at 3,500 rpm for 20 min (BIO ENG, BE-6000, Piracicaba, São Paulo, Brazil).

Media and Fermentation Assays

The medium for fermentation consisted of CAJ supplemented with the following components: $MgSO_4$ 0.65 g L^{-1}, KH_2PO_4 0.50 g L^{-1}, $(NH_4)_2SO_4$ 2.50 g L^{-1}, and $ZnSO_4$ (0.65 g L^{-1}). It was sterilized in autoclave (Phoenix, Araraquara, São Paulo, Brazil) at 110 °C for 10 min, and the initial pH was adjusted to 4.50 by using 1 N HCl. Batch fermentation was carried out in 500-ml Erlenmeyer flasks with 250 ml of medium in a rotary shaker TE240 (Tecnal, Piracicaba, São Paulo, Brazil) at 30 °C and 150 rpm. The initial yeast concentration inoculated into the fermentation medium was 10 g L^{-1} using dry baker yeast. Samples were collected at time-defined intervals and submitted to analysis.

Influence of CAJ (glucose + fructose) Concentration on Ethanol Production by *S. cerevisiae*

The effects of initial concentrations of glucose + fructose, present in CAJ, were examined. Different initial sugar concentrations (glucose + fructose) were evaluated, from 24.4 to 103.1 g L^{-1}. The initial sugar concentration was achieved by diluting or concentrating the CAJ, which has a natural concentration around 80 g L^{-1}. For each initial sugar concentration, specific microbial growth rates (μ_x), specific ethanol production rates (μ_p), maximum ethanol (P_{em}) or glycerol concentration (P_{gm}), maximum dry weight (X_m), ethanol ($Y_{P/So}$), and cell yields ($Y_{X/So}$) were calculated (variables are listed in the Appendix).

Analytical Methods

Biomass Content

Cell concentration was determined by dry weight [10]. Samples were taken from the fermentation media at certain time intervals and centrifuged at 3,000 rpm for 30 min in a BE-6000 centrifuge (BIO ENG). The pellet was dried at 80 °C on a Tecnal TE-397/4 stove (Tecnal) until constant weight was achieved. Supernatant was used for glucose, fructose, ethanol, and glycerol analysis.

pH Measurement

The pH of the fermentation medium was measured using a Tec-3MP model pH meter (Tecnal, Campinas, São Paulo, Brazil).

Glucose, Fructose, Ethanol, and Glycerol Concentrations

Substrate concentration (glucose and fructose) and product concentration (ethanol and glycerol) were measured by high-performance liquid chromatography (HPLC) using a Waters HPLC system (Waters, Milford, MA, USA) equipped with a refractive index Waters 2414 detector and a Shodex Sugar SC1011 column 8.0×300 mm (Shodex, Kawasaki,

Kanagawa, Japan). Water MiliQ (simplicity 185, Millipore, Billerica, MA, USA) was used as solvent with a flow rate of 0.6 mL min^{-1} at 80 °C. Samples were identified by comparing the retention times with those of carbohydrate, ethanol, and glycerol standards.

Yield Coefficients and Selectivity

The experimental data of products, substrates, and cells concentrations in a given period of time were used to calculate the yields in product ($Y_{P/S}$) and cells ($Y_{X/S}$) related to substrate and the specific rates for growth (μ_x), substrate consumption (μ_S), and product formation (μ_p).

Equations 1 and 2 represented a productivity (Pm) and ethanol selectivity (Se), respectively.

$$\mathrm{Pm} = \frac{C_{im} - C_{i0}}{t} \tag{1}$$

Where i stands for ethanol or glycerol, C_{i0} is the initial concentration, C_{im} is the highest i concentration, and t is the fermentation time when the highest i concentration is achieved.

$$\mathrm{Se} = \frac{C_{\mathrm{ETHANOL}}}{C_{\mathrm{GLICEROL}}} \tag{2}$$

Results and Discussion

In a previous work [11], CAJ was characterized in terms of physical–chemical parameters, and results showed it was rich in glucose, fructose, and several amino acids. However, some macro- and micronutrients were not present at the desired level for ethanol production and had to be supplemented. In this work, the effect of initial sugar concentrations (glucose + fructose − S_0) on ethanol production was investigated in the range of 24.4–103.1 g L^{-1}. Figure 1 shows the experimental results obtained for substrate consumption and ethanol and glycerol production and dry weights of the strain during fermentation time for each substrate concentration studied. It can be observed that, for all initial sugar concentrations evaluated, the biomass concentration with time is a typical curve of microbial growth. Furthermore, log phase growth occurred between 4 and 6 h for CAJ medium.

The yeast consumed both glucose and fructose, sugars that are present in CAJ, to produce ethanol and glycerol (Fig. 1), but glucose was exhausted first, followed by fructose. Maximum ethanol concentration, 44.4±4 g L^{-1}, was obtained when 103.1 g L^{-1} of the initial sugar concentration was used; however, higher productivity, 9.71±0.3 g L^{-1}, was achieved with 87.7 g L^{-1} (Fig. 1, Tables 1 and 2) of the initial concentration of substrate. Highest ethanol concentration was obtained after 4 h of fermentation in the medium with an initial sugar concentration of 87.7 g L^{-1} and after 6 h in the medium with an initial sugar concentration of 103.1 g L^{-1}. This result is probably due to yeast metabolism, which may be inhibited by the substrate or suffer from glucose repression. It can be observed that the rate of sugar consumption is very low when S_0=103.1 g $L^{-1}$was used; fructose and glucose concentrations remained almost constant for 2 h at the beginning of fermentation. Other authors [12] found that the growth of *S. cerevisiae* is inhibited equally by glucose and fructose. Another possibility is the presence of other chemicals that are partially inhibitory to the yeast fermentation, which had its concentration enhanced when concentrating the juice.

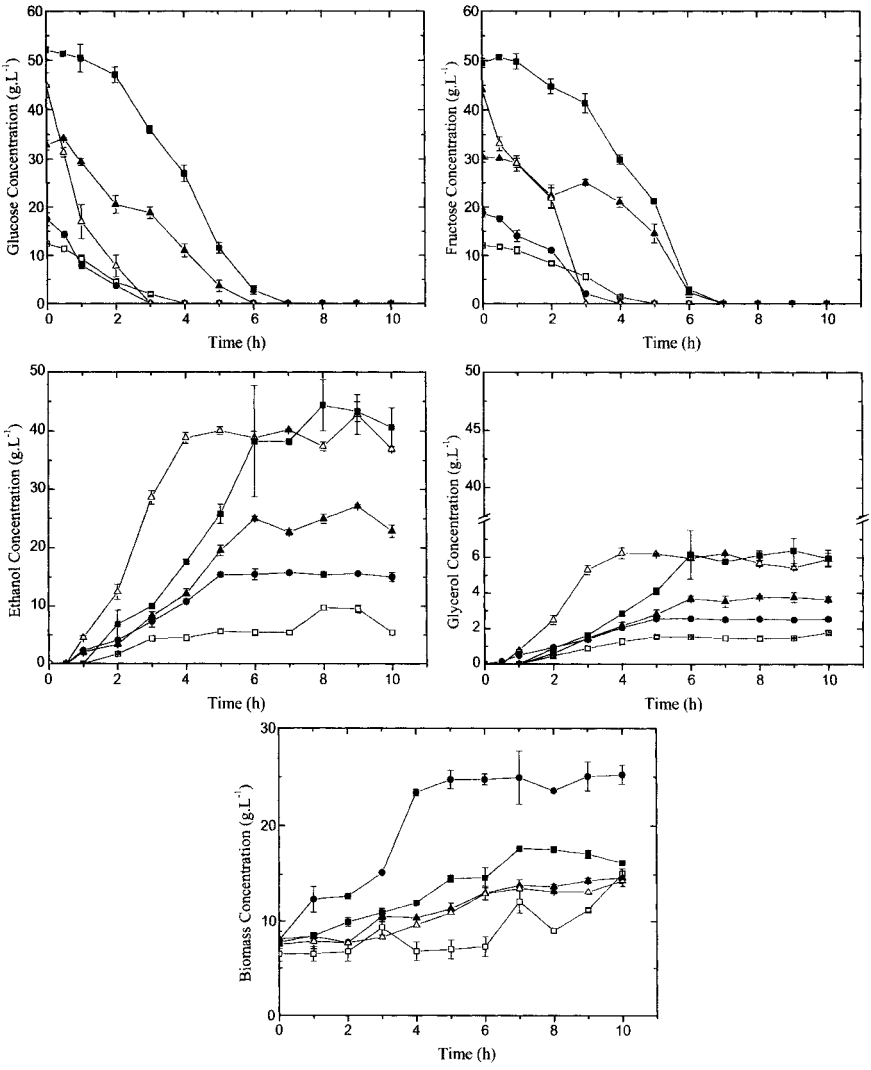


Fig. 1 Effect of sugar (glucose + fructose) on ethanol production by *S. cerevisiae* at 30 °C and 150 rpm. Initial sugar (glucose + fructose) concentration: *open squares*, 24.4; *closed circles*, 41.3; *closed triangles*, 62.9; *open triangles*, 87.7; and *closed squares*, 103.1 g L^{-1}. Data points represent the mean and standard deviation from at least three separate experiments

It can be observed that glycerol was produced in all assays (Fig. 1 and Table 2), and maximum glycerol concentration was obtained (5.8±0.1 g L^{-1}) when 103.1 g L^{-1} of initial sugar concentration was used. Glycerol is produced and accumulated in the yeast cell as a response to osmotic stress. In addition to osmotic regulation, glycerol also has a role in the redox balance of the yeast cell. Under anaerobic conditions, glycerol is formed to reoxidize the NADH formed in anabolism and in the synthesis of organic acids [13, 14]. Yalçin and Özbas [15] evaluated grape juice as a medium for glycerol production; their obtained maximum glycerol concentration and dry weight were 14.1 and 8.0 g L^{-1}, respectively. Although the objective of this work is to produce ethanol, glycerol has been an important

Table 1 Effect of initial sugar (glucose + fructose) concentration (S_0) on ethanol and glycerol productivity (Pm) and ethanol selectivity (Se) during fermentation of CAJ by *S. cerevisiae* at 30 °C and 150 rpm.

S_0 (g L^{-1})	Productivity (g L^{-1} h^{-1})[a]		Selectivity (Se)
	Ethanol	Glycerol	
24.4	1.455±0.06	0.255±0.01	5.86±0.3
41.3	3.082±0.02	0.429±0.01	6.18±0.1
62.9	4.168±0.22	0.418±0.03	6.70±0.5
87.7	9.708±0.25	0.889±0.00	6.64±0.2
103.1	6.370±0.38	0.747±0.02	6.64±0.6

[a] Values were calculated at maximum ethanol and glycerol concentrations.

industrial material with different uses in many industries, such as food, pharmaceutical, cosmetics, drug, toothpaste, leather, textile, tobacco, and other industries [15]. Many growth factors affect glycerol metabolism of yeast cells, such as the type of substrate and the initial substrate concentration, temperature, pH, inoculation rate, aeration rate, nitrogen source, etc. [15]. It is reported that an increase in the initial sugar concentration enhances glycerol production because of osmotic stress. In this study, however, initial sugar concentration had no important effect on ethanol selectivity (Table 1).

Specific growth rates (μ_x), specific substrate rates (μ_S), and ethanol production rates (μ_p) were calculated, and results are shown in Fig. 2 for S_0=103.1 g L^{-1}. Similar profiles were obtained for the other initial substrate concentration studied (data not shown). As can be observed, specific growth rates, substrate consumption, and product formation followed a typical pattern for ethanol fermentation [16]. The specific rate of substrate consumption (μ_S) and ethanol production (μ_p) present similar profiles, thus correlating it very well. The specific growth rate (μ_x) presents, approximately, the same course of the others two curves. Then, ethanol formation is associated with growth, consumption of substrate, and catabolism reaction, typical of a primary metabolite (Fig. 2).

Table 2 shows the effect of initial sugar (glucose + fructose) concentration on maximum ethanol concentration (C_{em}), together with dry weight (X_m) and glycerol concentration (C_g) when C_{em} was achieved. Table 3 shows the results on cell ($Y_{X/S}$), ethanol ($Y_{Pe/S}$), and glycerol ($Y_{Pg/S}$) yield coefficients, as well as those on ethanol yield that were calculated considering theoretical yield ($Y_{Pe/S}$=0.511) as reference [17]. The specific growth rate (Table 3) increased almost twofold when sugar concentration was increased from 24.4 to 87.7 or 103.1 g L^{-1}. However, specific growth rate remained almost constant when sugar concentration was increased from 87.7 to 103.1 g L^{-1}. The biomass yield ($Y_{X/S}$) in the media decreased from 0.228 to 0.091 g per gram of sugar concentration. Other authors [17]

Table 2 CAJ fermentation by *S. cerevisiae* at 30 °C and 150 rpm: maximum ethanol (C_{em}), glycerol (C_{gm}), and biomass concentrations (dry weight) for media with different initial concentrations of sugar (glucose + fructose).

S_0 (g L^{-1})	X_0 (g L^{-1})	X_m (g L^{-1})	C_{em} (g L^{-1})	C_g (g L^{-1})	ΔX (g L^{-1})	ΔS (g L^{-1})
24.4	6.50±0.8	12.07±1.2	9.7±1	1.4±0.1	5.57	24.4
41.3	8.00±0.9	16.85±4.9	15.6±0	2.5±0.1	8.85	41.3
62.9	8.13±0.1	14.67±1.0	27.1±0	3.8±0.1	6.54	62.9
87.7	7.55±0.1	14.33±0.1	42.8±3	5.4±0.1	6.78	87.7
103.1	7.75±0.1	17.17±0.4	44.4±4	5.8±0.1	9.42	103.1

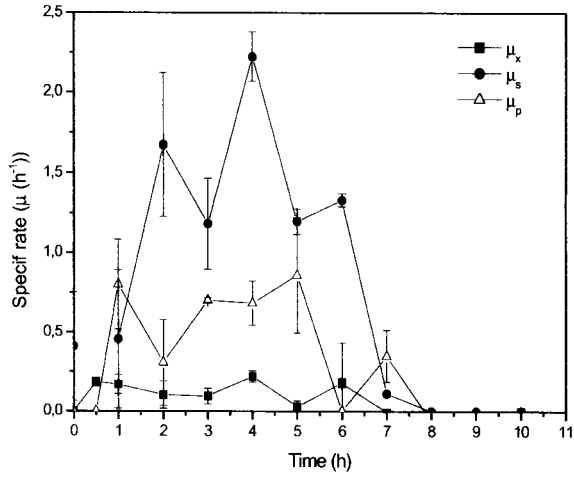


Fig. 2 Specific rates of growth (μ_X), substrate consumption (μ_S), and ethanol production (μ_P) for the fermentation of CAJ medium by *S. cerevisiae* at 30 °C, 150 rpm, and initial sugar (glucose + fructose) concentration of 101.05 g L^{-1}

observed the same behavior for biomass yield, which decreased from 0.217 to 0.075 g per gram of sugar concentration when sucrose concentration was increased from 34.6 to 257.4 g L^{-1}, and they attributed the decrease on $Y_{X/S}$ to growth inhibition due to high substrate concentrations. Ethanol yield varied from 74 to 95.5% of the theoretical values, the highest value being achieved when 87.7 g L^{-1} of initial sugar concentration was used.

Conclusion

Maximum ethanol concentration was obtained (≅44 g L^{-1}) when 87.7 and 103.1 g L^{-1} of initial sugar concentration was used in the fermentation medium. Specific rates of growth, substrate consumption, and product formation followed a typical pattern for ethanol fermentation. Maximum ethanol yield (0.488 g g^{-1}) and productivity (9.71 g L^{-1} h^{-1}) were obtained when 87.7 g L^{-1} of initial sugar concentration was used. Finally, initial sugar concentration had no important effect on selectivity. The results obtained indicate that CAJ is a suitable substrate for ethanol production. Moreover, the use of the CAJ as a medium will not only reduce the cost of the resulting ethanol production, but it will also make use of an agricultural waste that is otherwise discarded in the field.

Table 3 Effect of initial sugar (glucose + fructose) concentration on specific growth rates, yield coefficients and ethanol yield during CAJ fermentation by *S. cerevisiae* at 30 °C and 150 rpm.

S_0 (g L^{-1})	X_0 (g L^{-1})	$Y_{X/S}$ (g g^{-1})	$Y_{X/Pe}$ (g g^{-1})	$Y_{Pe/S}$ (g g^{-1})	$Y_{Pg/S}$ (g g^{-1})	Specific growth rate, μ_X (h^{-1})	Ethanol yield[a] (%)
24.4	6.50±0.8	0.228	0.574	0.398	0.059	0.061±0.02	77.8
41.3	8.00±0.9	0.214	0.567	0.378	0.061	0.071±0.01	73.9
62.9	8.13±0.1	0.104	0.241	0.431	0.060	0.078±0.01	84.3
87.7	7.55±0.1	0.077	0.158	0.488	0.062	0.115±0.01	95.5
103.1	7.75±0.1	0.091	0.212	0.431	0.056	0.120±0.01	84.3

[a] Values were calculated as a comparison between experimental and theoretical values of ethanol yield coefficients ($Y_{Pe/S}$).

Acknowledgments The authors acknowledge *Financiadora de Estudos e Projetos*, *Conselho Nacional de Desenvolvimento Cientifico e Tecnologico*, and *Agência Nacional do Petróleo* (from Brazil) for the financial support that made this work possible.

Appendix

Ks	substrate saturation parameter (g L^{-1})
P_{max}	product concentration when cell growth ceases (g L^{-1})
S	substrate concentration (g L^{-1})
X	biomass concentration (g L^{-1})
X_{max}	biomass concentration when cell growth ceases (g L^{-1})
$Y_{P/X}$	yield of product based on cell growth (g/g)
$Y_{X/S}$	yield of cell growth based on substrate consumptions (g/g)
$Y_{P/S}$	yield of product based on substrate consumptions (g/g)
C_{em}	maximum ethanol concentration (g L^{-1})

Greek letter

μ_{max}	maximum specific growth rate (h^{-1})
μ_p	specific rate of product formation (g/[L.h])
μ_S	specific rate of substrate consumption (g/[L.h])
μ_x	specific rate of growth (g/[L.h])

References

1. Hahn-Hägerdal, B., Galbe, M., Gorwa-Grauslund, M. F., Lidén, G., & Zacchi, G. (2006). *Trends in Biotechnology, 24*(12), 549–556.
2. Martin, C., Galbe, M., Wahlbom, C. F., Hahn-Hagerdal, B., & Jonsson, L. F. (2002). *Enzyme and Microbial Technology, 31*, 274–282.
3. Nigam, J. N. (2001). *Journal of Applied Microbiology, 90*, 208–215.
4. Rosillo-Calle, F., & Cortez, L. A. B. (1998). *Biomass and Bioenergy, 14*(2), 115–124.
5. Goldemberg, J., Coelho, S. T., Nastari, P. M., & Lucon, O. (2004). *Biomass and Bioenergy, 26*, 301–304.
6. Rivera, E. C., Costa, A. C., Atala, D. I. P., Maugeri, F., Maciel, M. R. W., & Maciel, F. R. (2006). *Process Biochemistry, 41*, 1682–1687.
7. Rocha, M. V. P., Oliveira, A. H. S., Souza, M. C. M., & Gonçalves, L. R. B. (2006). *World Journal of Microbiology and Biotechnology, 22*, 1295–1299.
8. Food and Agriculture Organization of the United Nations in http://faostat.fao.org/site/408/DesktopDefault.aspx?PageID=408 accessed in August 24th, 2007.
9. Instituto Brasileiro de Pesquisa e Estatística in www.ibge.gov.br accessed in August 24th, 2007.
10. Atala, D. I. P., Costa, A. C., Maciel, R., et al. (2001). *Applied Biochemistry and Biotechnology, 91–3*, 353–365.
11. Rocha, M. V. P., Souza, M. C. M., Benedicto, S. C. L., Bezerra, M. S., Macedo, G. R., Pinto, G. A. S., et al. (2007). *Applied Biochemistry and Biotechnology, 136–140*, 185–194.
12. Koren, D. W., & Duvnjak, Z. (1993). *Acta Biotechnologica, 13*, 311–322.
13. Albers, E., Larsson, C., Lidén, G., Niklasson, C., & Gustafsson, L. (1996). *Applied and Environmental Microbiology, 62*(9), 3187–3195.
14. Costenoble, R., Valadi, H., Gustafsson, L., Franzén, C. J., & Niklasson, C. (2000). *Yeast, 16*(16), 1483–1495.
15. Yalçin, K. S., & Özbas, Z. Y. (2004). *Process Biochemistry, 39*, 1285–1291.
16. Schmidell, W., Lima, U. A., Aquarone, E., & Borzani, W. (2001). *Biotecnologia Industrial* (vol. 2). São Paulo: Edgard Blucher.
17. Atiyeh, H., & Duvnjak, Z. (2001). *Applied Microbiology and Biotechnology, 57*, 407–411.

Appl Biochem Biotechnol (2008) 148:235–243
DOI 10.1007/s12010-007-8040-z

Atmospheric Pressure Liquefaction of Dried Distillers Grains (DDG) and Making Polyurethane Foams from Liquefied DDG

Fei Yu · Zhiping Le · Paul Chen · Yuhuan Liu · Xiangyang Lin · Roger Ruan

Received: 15 May 2007 / Accepted: 4 September 2007 /
Published online: 2 October 2007
© Humana Press Inc. 2007

Abstract In this study, dried distillers grains (DDG) was liquefied in acidic conditions at atmospheric pressure, and polyurethane foams were subsequently prepared from the liquefied DDG. Liquefaction was examined over a range of conditions including liquefaction time of 1–3 h, temperature of 150–170 °C, sulfuric acid (as catalyst) concentration of 1.0–3.0 wt%, and liquefaction solvent (ethylene carbonate) to DDG ratio of 3:1–5:1. The bio-polyols in the liquefied DDG were rich in hydroxyl groups, which can react with methylene diphenyl diisocyanate (MDI) to form cross-linked polyurethane networks. The biodegradability of the prepared polyurethane foams was also evaluated. This study strives to broaden the application of DDG as a feedstock for bio-polyurethane preparation.

Keywords Dried distillers grains · Liquefaction · Bio-polyols · Polyurethane · Biodegradable

Introduction

Dried distillers grains (DDG), a co-product of the distillery industry is abundant in Minnesota. About 98% of the DDG in North America comes from corn plants that produce ethanol for oxygenated fuels. The remaining 1–2% of DDG is produced by the alcohol beverage industry. Approximately 3.2 million metric tons of DDG are produced in North America annually. In recent years, some regions of the USA, especially the Midwest, have required more use of oxygenated fuels (e.g., ethanol–gasoline blends) to reduce air pollution

F. Yu
Department of Forest Products, Mississippi State University, Box 9820,
Mississippi State, MS 39762, USA

F. Yu · P. Chen · R. Ruan (✉)
Center for Biorefining and Department of Bioproducts and Biosystems Engineering,
University of Minnesota, 1390 Eckles Ave., St. Paul, MN 55108, USA
e-mail: ruanx001@umn.edu

Z. Le · Y. Liu · X. Lin · R. Ruan
Jiangxi Biomass Engineering Center, Nanchang University, Nanchang, China, 330047

and dependency on foreign petroleum. Because of the increased demand on ethanol, the production of DDG is expected to double within the next decade. However, in North America, over 80% of DDG is used as animal feed at a price just a little more than the cost of the corn that goes into it. The economics of ethanol production facilities depends very much on the price of ethanol as well as processing and marketing of byproducts such as DDG and carbon dioxide. Thus, decreasing prices for the dry-grind ethanol process coproducts, especially DDG, suggest that there is significant potential for value-added process by using ethanol coproducts. However, to determine the overall techno-economical feasibility of using DDG as raw material, the general process route, the chemical and physical characteristics of the final products, and the associated capital and operation costs must be determined [1–4]. This research focuses on an innovative method for the preparation of polyurethane from liquefied DDG.

Polyurethane is an important polymer, and its annual market in North America is about 2.8 million tons. Currently, polyurethane is synthesized mainly from isocyanate and hydroxyl groups containing polyols from petroleum resources, such as polyesters and polyethers. The present work was to develop and evaluate a three-step process for making polyurethane foams from renewable biomass, which may be used as packaging material, insulating material in construction, and so on. First, bio-polyols were obtained from liquefaction of DDG in acidic conditions. DDG was pretreated over a range of conditions including liquefaction solvent, residence time, temperature, sulfuric acid concentration, and liquefaction solvent to DDG ratio. Secondly, dilution, pH adjustment, filtration, and evaporation process were developed to separate and purify the bio-polyols in the liquefied DDG. Last, flexible and rigid polyurethane foams were prepared from the liquefied bio-polyols by reacting with diisocyanate.

Materials and Methods

Materials

DDG, provided by Agricultural Utilization Research Institute (Waseca, MN, USA), was milled to 2.0-mm meals before liquefaction [1]. Ethylene carbonate and ethylene glycol (Sigma, Minneapolis, MN, USA) was used as liquefying solvent. Stannous 2-ethyl hexanoate (Sigma), polyether modified polysiloxane (Sigma), and methylene diphenyl diisocyanate (MDI such as Isonate 181 and Papi 27, Dow Chemical, Midland, MI, USA) were used for the preparation of polyurethane foams. All chemicals were reagent grade.

Atmospheric Pressure Liquefaction Procedure

The lab apparatus used for atmospheric pressure liquefaction consisted of a stirring system, a temperature controller, and a 500-ml three-neck flask. One hundred grams liquefying solvent (ethylene carbonate or ethylene glycol) and catalyst (1–5 wt% concentrated sulfuric acid) were first placed in the flask and preheated to 100 °C. Weighed DDG was then added to the flask and well mixed with the liquefying chemicals. The ratio of liquefaction solvent to DDG ranged from 3 to 5. Liquefaction was carried out by continuously stirring at atmospheric pressure. After a preset reaction time, the heater was turned off and the stirrer kept running until the mixture cooled down. The liquefied mixture (bio-polyol) was collected for later use and analysis. All experiments and analysis were performed in three replicates.

When liquefaction reached a predetermined time, the resulting liquefied mixture was washed into a beaker with 200 ml dioxane–water solution (4/1, *v*/*v*) and then filtrated

through filter paper under vacuum. The residue was dried to a constant weight at 105 °C. The percent of liquefaction yield was calculated by the following equation:

$$\text{Liquefaction yield (\%)} = (1 - \text{weight of dried residue/dry weight of starting DDG}) \times 100$$

Separation and Purification of Bio-Polyols

A series of chemical unit operations were undertaken to obtain pure bio-polyols. The purified bio-polyols can be used for making higher quality polymers or they can be broken down into hydrocarbon and hydrogen by means of catalytic reforming. Figure 1 shows the procedure used for separating and purifying bio-polyols from liquefied DDG. Raw material (DDG), catalyst (sulfuric acid), and liquefying solvent (ethylene carbonate) were first added to the liquefaction apparatus, holding for 2 h at 160 °C. After that, the liquefied material was diluted tenfold with dioxane–water solution (1/1, *v/v*). As only liquefied polyols can be dissolved in this solution, it was then separated from the unliquefied residues. To obtain the pH neutralized polyols, the pH of the solvent was adjusted to 6.5–7 with 1 mol/l NaOH followed by filtration to separate the unliquefied residues from the solution. These residues can be recycled to the liquefaction apparatus for secondary liquefaction, resulting in less harm to the environment. This unliquefied mixture included some ash and also some unliquefied substrate. Subsequently, the filtrate was evaporated under reduced pressure to 1% water content. Using evaporation process to get rid of dioxane and water, eventually, pure polyols are obtained. The dioxane–water solution can also be recycled to the dilution process. The purified polyols can be recycled to the liquefaction process, using as a substitute solvent, which will decrease the costs of production [3].

Determination of Hydroxyl Value of Bio-Polyols

One gram liquefied DDG was placed in a 150-ml beaker, and 10 ml of phthalic anhydride solution (dissolving 150 g phthalic anhydride in 900 ml of dioxane and 100 ml pyridine) was added. The beaker was covered with aluminum foil and the beaker put into a boiling

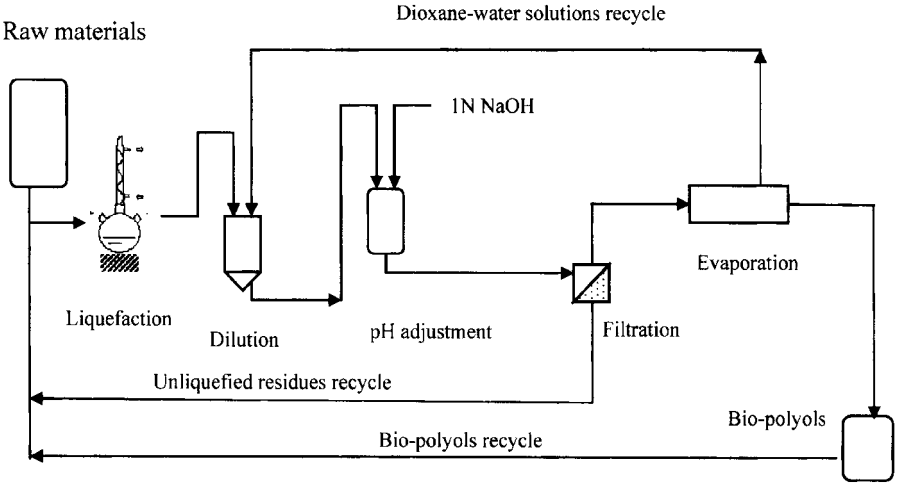


Fig. 1 Procedure used for separating and purifying of bio-polyols

water bath for 20 min. After cooling down, 20 ml of dioxane–water solution (4/1, *v*/*v*) and 5 ml of water were added to the beaker and then titrated with 1 mol/l NaOH to pH 8.3 using a pH-meter to indicate the end-point. Blank titration was conducted using the same procedure. Hydroxyl value was calculated by the formula below.

$$\text{Hydroxyl value (mg KOH/g)} = (B - S) \cdot N \times 56.1/W$$

where

B volume of NaOH standard solution consumed in blank titration (ml)
S volume of NaOH standard solution consumed in sample titration (ml)
W sample weight (g)
N equivalent concentration of NaOH standard solution (mol/l)

Preparation of Polyurethane Foams from Bio-Polyols

Weighed amounts of bio-polyols, catalyst (Stannous 2-ethyl hexanoate), surfactant (polyether-modified polysiloxane), and blowing reagent (distilled water) were mixed well in a paper cup. A prescribed amount of MDI was added to the mixture, which was then stirred with a high-speed stirrer (5,000 rpm) for 15 s. After stirring, the mixture was poured immediately into another paper cup, and the foam was allowed to rise and set at ambient conditions (22 °C). Finally, the foam samples were cured at room temperature for 24 h before any analysis can be conducted. The formulations of the prepared foams are shown in Table 2.

Biodegradability of Polyurethane Foams from Bio-Polyols

To evaluate the biodegradability of polyurethane foams, a natural degradation of polymers in soil was simulated in the laboratory [2]. The soil used in this research is merchandised potting soil (Menards, St. Paul, MN, USA). The test samples (about 2×2×2 cm) were buried in flowerpots filled with potting soil. The flowerpots were kept in a cultivating room at 25 °C. The samples were watered once a day to keep the moisture constant. Every month, five samples were taken out, washed with 200 ml water, and dried to a constant weight at 105 °C to determine weight loss of the samples. The rate of biodegradation was indicated by the average weight loss.

Results and Discussion

Bio-Polyols from DDG by Atmospheric Pressure Liquefaction

The effect of liquefaction solvent and processing time on the liquefaction of DDG is shown in Fig. 2. It was found that the liquefaction with ethylene carbonate was very rapid and almost completed within 1 h. On the other hand, the liquefaction with ethylene glycol was much slower, and about 18% residue still remained after 3 h of liquefaction [3, 4]. This result agrees with that obtained by Yamada and Ono [4] who found ethylene carbonate promoted the acid-catalyzed solvolysis of cellulose. Ethylene carbonate is an effective liquefaction solvent because of its high permittivity and high boiling point. Atmospheric pressure liquefaction is regarded as a non-aqueous reaction, which can be assisted by sulfuric acid as a catalyst. The acid potential depends on the permittivity of the solvent. The higher the permittivity of the solvent, the larger the acid potential. Therefore, sulfuric acid could

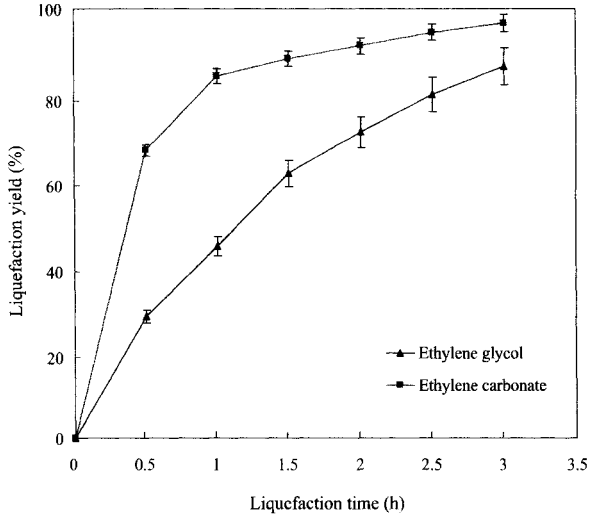


Fig. 2 Effect of solvent and time on the liquefaction of DDG. [Liquefaction solvent/DDG ratio (g/g): 4; catalyst content: 3%; liquefaction temperature 160 °C]. *Error bars* represent standard deviations calculated from the data obtained from three replicated experiments

promote rigorous reactions when ethylene carbonate is chosen as liquefying solvent, resulting in a complete liquefaction in a short period of time. In subsequent experiments, ethylene carbonate was used as liquefaction solvent to achieve a reasonable liquefaction yield in an acceptable time range.

DDG contains little starch, but is a good source of fiber and protein. Distillers grains typically contain 42% highly digestible neutral detergent fiber [1], and thus, are alternative biomass feedstock. Figure 3 shows that the reaction mechanism occurs during the DDG liquefaction process. Under the catalysis of sulfuric acid, DDG fibers experience a partial chemical degradation; meanwhile, it reacts with ethylene carbonate to form a series of glucosides. Figure 4 shows that decomposition of ethylene carbonate generates carbon dioxide which caused the bubbles observed during the liquefaction. The reactions illustrated in Figs. 3 and 4 suggest that the liquefied DDG may consist of degraded DDG fragments (oligosaccharides), glucosides, and residual and decomposed liquefying solvent, all of which contain one or more hydroxyl groups. Therefore, it is feasible to cross-link the bio-polyol into a network of polyurethane through the esterification reaction between the

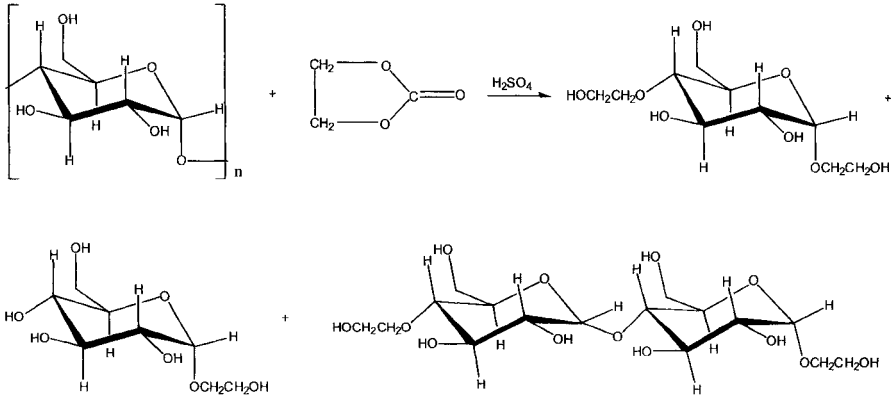


Fig. 3 Reaction mechanism between DDG fiber and ethylene carbonate

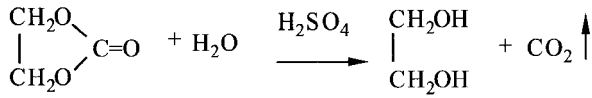


Fig. 4 Decomposition of ethylene carbonate in the atmospheric pressure liquefaction

hydroxyl groups of the bio-polyol and isocyanate in cross-linking chemicals having two or more functionalities, such as diisocyanate [5].

Liquefaction yield achieved by the liquefaction process were 80–98%, indicating that the selected liquefaction conditions, such as temperature, time, sulfuric acid content, and liquefaction solvent to DDG ratio, promoted the atmospheric pressure liquefaction process. These results are summarized in Table 1. Clearly, an increase in liquefaction time and temperature results in increased liquefaction yield. For instance, when the temperature was 160 °C, the liquefaction yield reaches 94.6% at 2 h, whereas further increase in temperature and time resulted in a depressed increase in liquefaction yield. A similar trend has also been observed in the case of liquefaction of corn stover [3]. Typically, the increase of catalyst content should increase in the liquefaction yield. As can be seen in Table 1, 94.6% liquefaction yield was obtained at 3% sulfuric acid in 160 °C 2 h. However, the use of sulfuric acid will cause condensation of degraded residues and increase the viscosity of the liquefied materials. The amount of insoluble residue increased with decreasing liquefaction solvent/DDG ratio. When the liquefaction solvent/DDG ratio reaches 5, the liquefaction yield is 97.8% after 2 h. A higher yield could be expected at even higher liquefaction solvent/DDG ratio, but at the cost of more solvents or lower productivity.

Another key characteristic of bio-polyols from atmospheric pressure liquefaction was their hydroxyl functionality and the structure of the hydroxyl group [6]. The hydroxyl value in liquefied DDG is one of the important factors in the preparation of polyurethane having the desired mechanical properties. The total hydroxyl value was, therefore, evaluated in relation to the liquefaction conditions (Table 1).

An inverse decreasing relationship was found between the hydroxyl value and the reaction time for the liquefaction system. Figure 5 shows the hydroxyl value decreased steadily from h 0 to h 1.5 and then increased slightly until the end of the liquefaction (h 3). Such decrease in hydroxyl number resulted from dehydration and thermal oxidative degradation of the liquefaction solvent (ethylene carbonate). Yao et al. [7] also reported that alcohol-D-glycosides were produced by the liquefaction between polysaccharides and ethylene glycol under a temperature of 150 °C and catalyst (sulfuric acid) concentration of 3% as used in their

Table 1 Effect of processing conditions on the liquefaction of DDG[a].

Temperature (°C)	Time (h)	Sulfuric acid (%)	Liquefaction solvent/DDG ratio (g/g)	Hydroxyl value (mgKOH/g)	Liquefaction yield (%)
150	2	3	4	226	92.1
160	2	3	4	158	94.6
170	2	3	4	144	94.9
160	1	3	4	176	87.6
160	3	3	4	165	95.1
160	2	1	4	178	80.9
160	2	5	4	151	96.4
160	2	3	3	137	88.3
160	2	3	5	221	97.8

[a] Mean values for three replicates are indicated.

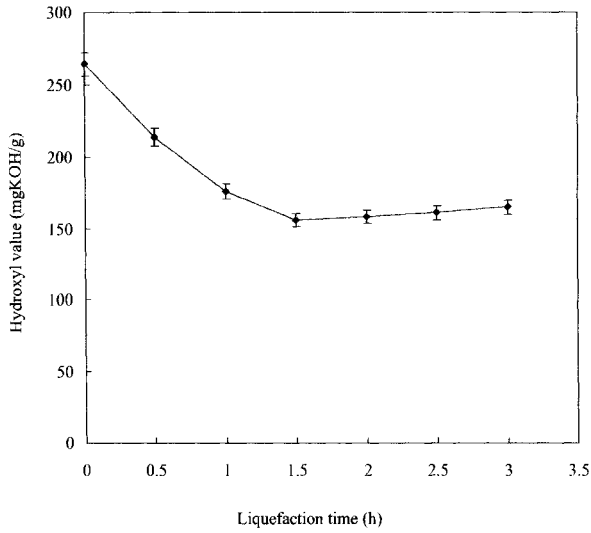


Fig. 5 Changes in hydroxyl value in the atmospheric pressure liquefaction of DDG. [Liquefaction solvent (ethylene carbonate)/DDG ratio (g/g): 4; catalyst content: 3%; liquefaction temperature 160 °C]. *Error bars* represent standard deviations calculated from the data obtained from three replicated experiments

experiment [7]. A reduced hydroxyl value of wood and starch samples with the increase of reaction time was reported.

Preparation of Polyurethane Foams

DDG-based bio-polyols were applied to produce flexible and/or rigid polyurethane foams with a preliminary investigation. Properties of the bio-polyols, diisocyanates, formulate, and other factors showed significant effects on formation, color, and physical properties of bio-polyurethane foams [8]. Table 2 gives example formulas for the preparation of polyurethane foams from the bio-polyols. In general, the formulas consist of two mutually separated phases. One phase includes bio-polyol, blowing agent (to form bubbles), catalyst, and surfactant, and the other is MDI (Isonate 181 or Papi 27). During the polyurethane foaming reaction, carbon dioxide is generated by the reaction between water and isocyanate. Increasing the water content expanded the foam volume, resulting in thinner foam cell walls and larger foam. It was also found that without the catalyst, the bio-polyols phase did not dissolve in the isocyanate phase. Just after addition of the catalyst, the mixture became brown. Up to 2 min after the catalyst addition, the phase separation could be observed in

Table 2 Formulas of polyurethane foams from DDG-based bio-polyols.

Foams	Ingredients	Parts (wt%)
Rigid	DDG-based bio-polyol	100
	Blowing agent (water)	2–5
	Catalyst (stannous 2-ethyl hexanoate)	2–3
	Surfactant (polyether modified polysiloxane)	3–4
	MDI (Isonate 181)	150–200
Flexible	DDG-based bio-polyol	100
	Blowing agent (water)	2–5
	Catalyst (stannous 2-ethyl hexanoate)	2–3
	Surfactant (polyether-modified polysiloxane)	2–3
	MDI (Papi 27)	100–150

portions of mixture, and a considerable increase in viscosity was noted in the mixture. Further continuation of the reaction with vigorous stirring (5,000 rpm) at room temperature resulted in disappearance of the phase separation, enhanced coloration, and the production of an appreciable quantity of water as byproduct. Thus, it was suggested that 2 min was enough for the formation of polyurethane foams.

The foam prepared from the rigid foam formula smelled strongly of MDI even 3 days after preparation, and contracted considerably, which indicates incomplete polyurethane formation. In the preparation of polyurethane using the flexible foam formula, the resulting foam was whitened and never imparted any odor or shrinking behavior. As has been stated above, when DDG-based bio-polyols were used as the starting material for polyurethane synthesis, a strong color change occurred in the ring-opening polymerization at room temperature within a relatively short time.

Biodegradability of Polyurethane Foams

Figure 6 shows the biodegradability result of polyurethane foams from DDG-based bio-polyols. The result showed that polyurethane foam lost about 12.6% of its initial weight in 10 months, which may be attributed to the fact that DDG contains many natural extracts, especially proteins and fats. In addition, there is a small amount of uncross-linked or partially cross-linked materials in the polyurethane foams, which might be less resistant to polymer degradation than fully cross-linked materials, and thus, more susceptible to biodegradation. No microorganisms were observed on the surface of the foams or in the surrounding soil, suggesting that less degraded chemicals were carried from the bio-polyurethane foams in 10 months [9]. Further investigation is required to elucidate the pathway and final products of polyurethane foams' degradation.

Conclusions

Bio-polyols were prepared from DDG liquefied using our unique atmospheric pressure liquefaction process. These DDG-based bio-polyols possess suitable characteristics for

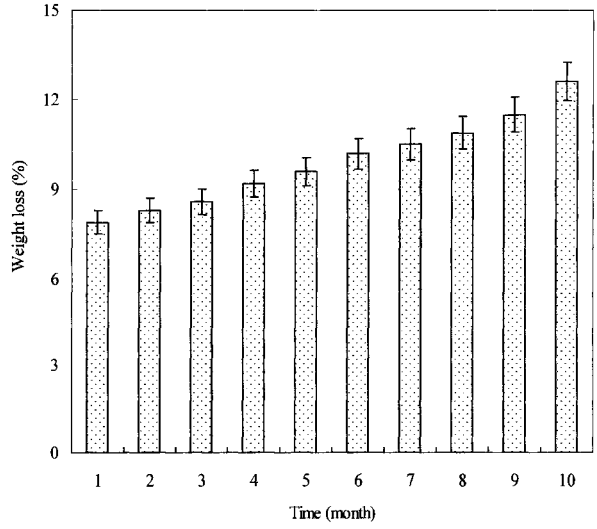


Fig. 6 Biodegradability of polyurethane foams from DDG-based bio-polyols. *Error bars* represent standard deviations calculated from the data obtained from five replicated experiments

making polyurethane foams. The properties of the bio-polyols can be adjusted by changing the liquefaction process conditions. Ethylene carbonate was proven to be an effective liquefying solvent for DDG. The optimum conditions for liquefaction of DDG are liquefaction solvent/DDG ratio of 4, liquefaction temperature 160 °C, liquefaction time 2 h, and catalyst content 3 wt%. Flexible and rigid polyurethane foams can be synthesized from the DDG-based bio-polyols. Polyurethane foams degraded about 12.6% in 10 months.

Acknowledgment This work was supported by University of Minnesota Initiative for Renewable Energy and the Environment (IREE) and the China Ministry of Education PCSIRT Program (IRT0540).

References

1. AURI. (2005). Distillers' dried grains flowability report. Agricultural Utilization Research Institute Fuels Initiative. Online: http://www.auri.org/research/Flowability _summary_10_17_05.pdf.
2. Karunanandaa, K., & Varga, G. A. (1996). Colonization of rice straw by white-rot fungi (Cyathus stercoreus): Effect on ruminal fermentation pattern, nitrogen metabolism, and fiber utilization during continuous culture. *Animal Feed Science and Technology, 61*, 1–16.
3. Yu, F., Ruan, R., Lin, X., Liu, Y., Fu, R., Li, Y., et al. (2006). Reaction kinetics of stover liquefaction in recycled stover polyol. *Applied Biochemistry and Biotechnology, 129–132*, 563–573.
4. Yamada, T, & Ono, H. (1999). Rapid liquefaction of lignocellulosic waste by using ethylene carbonate. *Bioresource Technology, 70*, 61–67.
5. Ravve, A. (2000). Principles of polymer chemistry (2nd ed., pp. 338). New York: Kluwer Academic/ Plenum Publishers.
6. Alma, M. H., Basturk, M. A., & Digrak, M. (2003). New polyurethane-type rigid foams from liquified wood powders. Journal of Materials Science Letters. *Journal of Materials Science Letters, 22*, 1225–1228.
7. Yao, Y. G., Yoshioka, M., & Shiraishi, N. (1995). Rigid polyurethane foams from combined liquefaction mixtures of wood and starch. *Mokuzai Gakkaishi, 41*, 659–668.
8. Yao, Y. G., Yoshioka, M., & Shiraishi, N. (1996). Water-absorbing polyurethane foams from liquefied starch. *Journal of Applied Polymer Science, 60*, 1939–1949.
9. Gomes, M. E., Ribeiro, A. S., Malafaya, P. B., Reis, R. L., & Cunha, A. M. (2001). A new approach based on injection moulding to produce biodegradable starchbased polymeric scaffolds: morphology, mechanical and degradation behavior. *Biomaterials, 22*, 883–889.

Appl Biochem Biotechnol (2008) 148:245–256
DOI 10.1007/s12010-007-8119-6

Bacterial Cellulose Production by *Acetobacter xylinum* Strains from Agricultural Waste Products

Sasithorn Kongruang

Received: 15 May 2007 / Accepted: 3 December 2007 /
Published online: 3 January 2008
© Humana Press Inc. 2007

Abstract Bacterial cellulose is a biopolysaccharide produced from the bacteria, *Acetobacter xylinum*. Static batch fermentations for bacterial cellulose production were studied in coconut and pineapple juices under 30 °C in 5-l fermenters by using three *Acetobacter* strains: *A. xylinum* TISTR 998, *A. xylinum* TISTR 975, and *A. xylinum* TISTR 893. Experiments were carried out to compare bacterial cellulose yields along with growth kinetic analysis. Results showed that *A. xylinum* TISTR 998 produced a bacterial cellulose yield of 553.33 g/l, while *A. xylinum* TISTR 893 produced 453.33 g/l and *A. xylinum* TISTR 975 produced 243.33 g/l. In pineapple juice, the yields for *A. xylinum* TISTR 893, 975, and 998 were 576.66, 546.66, and 520 g/l, respectively. The strain TISTR 998 showed the highest productivity when using coconut juice. Morphological properties of cellulose pellicles, in terms of texture and color, were also measured, and the textures were not significantly different among treatments.

Keywords Bacterial cellulose · *Acetobacter xylinum* · Texture · Coconut juice · Pineapple

Introduction

Cellulose is composed of the homopolymer of β-1, 4-linked D-glucose. The degree of polymerization of cellulose varies from 100–15,000 glucose units with the crystallization of the long linear chains to form microfibrils of a single crystalline entity [1, 2]. Relatively pure cellulose is produced by the bacteria *Acetobacter xylinum*. This microorganism has been studied for more than 100 years. Unlike the cellulose from wood pulp, bacterial cellulose is devoid of other contaminating polysaccharides such as lignin and hemicellulose, and its isolation and purification are relatively simple, not requiring energy- or chemical-intensive processes [3]. This bacterium has been used as the model system of choice in the exploration of the processes of biogenesis [4–6]. Although the process of formation of cellulose by *A. xylinum* had been investigated quite extensively in earlier studies, most investigations have dealt with the elucidation of cellulose biosynthesis [7–10],

S. Kongruang (✉)
Department of Biotechnology, Faculty of Applied Science, King Mongkut's Institute of Technology North Bangkok, Piboonsongkram Road, Bangsue, Bangkok 10800, Thailand
e-mail: stk@kmitnb.ac.th

and most strains studied so far produce only a smaller amount of pellicle under nonagitated conditions. Moreover, a standard medium used for the cultivation of bacterial producing organisms, the Hestrin–Schramm medium [11], is expensive and requires many additional resources for cultivation.

Polysaccharide-producing microorganisms are simple and capable of constructing a polymer from available raw materials and secondary raw material sources. Products from beets (molasses, sugar syrup, and saccharose), corn (starch, hydrolyzed starch, glucose syrup, and glucose), and potatoes (starch and starch hydrolyzates) can be used for producing such polymers. Inedible substrates such as peat hydrolyzates, wood, dextran production wastes, petrochemical wastes and products, ethanol, methanol, glycerin, and ethylene glycol are often suitable [12]. Coconut and pineapple are popular fruits grown in many tropical countries, and they are available over a large part of the year. Coconut juice is mostly discarded as waste from various agro-industries. Since the juices are rich in carbohydrates, proteins, and trace elements, they can be used as a substrate for the production of food grade bacterial cellulose, and also as a raw material for a pure quality paper. Although these two substrates have been used for the traditional cultivation of bacterial cellulose in Southeast Asia, an efficient medium composition has never been reported. Therefore, the main objective of this study was to develop a simple and relatively inexpensive fermentation process for the production of bacterial cellulose employing static batch fermentation with nonconventional agro-residues. Comparison of bacterial strains, growth kinetics, and parameters related to cellulose production were also investigated.

Materials and Methods

Culture Media and Conditions

Three different strains of *A. xylinum*: *A. xylinum* TISTR 998, *A. xylinum* TISTR 975, and *A. xylinum* TISTR 893 were obtained from the Thailand Institute of Scientific and Technological Research, Bangkok, Thailand. Inoculum preparations were transferred from the stock solution to Yeast Malt extract agar slants and incubated for 2 days at 30 °C before being transferred to 5 ml of immature coconut juice to accelerate the growth for a week and then scaled up to 50 ml with the same substrate. The filtrated juices from commercially available coconut and pineapple juices were sterilized before cultivation. A 10% portion of the total volume of each inoculum media was then inoculated into the mature sterilized coconut and pineapple juices with 1% yeast extract supplementation and 14 ml of 95% ethanol in 500 ml for 6 days at 30 °C at a pH of 4.75. Scaling up to 5,000-ml cultivation, at the same pH of sterilized coconut and pineapple juices, was accomplished by static culturing for 2 weeks in a 5-l container to allow for pellicle formation. Cultures were grown in triplicate and repeated twice. Bacterial cellulose pellicles grown on the liquid surface were collected and washed overnight with running water and then immersed in 1 N NaOH for 2 days at 30 °C to dissolve the cells in the pellicle. The pellicles were then immersed under distilled water with 0.02% NaN_2 to reduce microbial contamination and then kept under 4 °C.

Analytical Methods

Samples were collected at regular intervals for 2 weeks of fermentation to quantify cell mass, substrate consumption, and bacterial cellulose production. The cells were collected after centrifugation at 9,200×*g* force for 30 min at 4 °C. The cell mass was estimated by

measuring the optical density at 600 nm after treating the culture broth with 5% cellulase (Celluclast 1.5 l, Novozyme A/S, Bagsvaerd, Denmark) at 50 °C for 30 min. Dry weight determinations for the dry cell mass were also measured. The supernatant was collected to determine residual sugar content by using the Anthrone method [13]. To measure the total cellulose produced, cellulose in the culture broth was washed twice with distilled water and then treated with 1% NaOH at 90 °C for 30 min to dissolve the cell mass. Purified cellulose was washed twice with distilled water and weighed. Total acidity and pH of the medium were also measured over the course of the fermentation. The growth kinetics were reported in terms of growth rate (r_x, g/l/h), specific growth rate (μ, h^{-1}), rate of substrate utilization (r_s, g/l/h), rate of product formation (r_p, g/l/h), specific rate of substrate utilization (Q_s, g/g/h), and specific rate of product formation (Q_p, g/g/h).

Total Viable Count

The number of viable cells in the inocula was determined at timed intervals by the pour plate technique with HS medium. Colonies were counted after 5 days of incubation at 30 °C.

Texture Evaluation

Bacterial celluloses, sized 7.5×7.5×1 cm, were used after incubation in a hot oven at 100 °C for 3 h. Texture was analyzed with a texture analyzer (TA-XT21, Memmert, Germany) with Crip Sracture Rig (HDP/CFS). The instrument was set as follows: 4 cm distance between probe and samples, 1.0 mm/s pretest speed, 1.0 mm/s test speed, and 10.0 mm/s post-test speed. The compression test was run at a rate of 20 times per sample. The compression force was reported.

Color Analysis

A section of 10 g of bacterial cellulose was cut into 1 cm^3 sections to measure color appearance. The values of L^*, a^*, and b^* were measured by a Hunter Lab Color Quest (Memmert, Germany) colorimeter with the CIELAB color system. These values were then used to calculate chroma (C^*) and hue angle (h_{ab}) values. L^* indicates lightness, with a scale ranging from 0 (black) to 100 (white). Positives and negatives in a^* represent red and green, whereas positives and negatives in b^* represent yellow and blue, respectively.

Statistical Analysis

Each treatment was conducted in triplicate and all experiments were repeated at least twice. The statistical significance of the evaluated data was analyzed by one-way analysis of variance. Differences among the mean values were tested using the least significant difference multiple range test. Values were considered significant when $p<0.05$, except when otherwise indicated.

Results and Discussion

Cell Growth and Substrate Utilization in Different Strains

This study aimed to select the best strain for bacterial cellulose (BC) production along with the investigation of the cell growth and substrate utilization. The kinetics of growth and

substrate conversion during BC production by all three strains are shown in Table 1. It was found that TISTR 998 produced BC at approximately a twofold higher rate than the rates of both TISTR 893 and 975. Although the specific growth rate of biomass revealed the same values for all strains, with no significant difference among TISTR 998 with 975 and 893 (p=0.139 and 0.165), TISTR 998 showed a higher efficiency of metabolization for sucrose, glucose, and fructose in coconut juice, and conversion into BC with a value of specific rate of substrate utilization that was 2.75-fold higher than that for TISTR 975. There was a significant difference between the substrate utilization rates of TISTR 998 and 975 (p= 0.0066). This resulted in highest specific rate of product formation (6548.33 g/g/h) that was obtained. Figure 1, which includes values from which the values of Table 1 were calculated, illustrates the bacterial growth curve as the consumption of substrate occurred. All three strains grown in coconut and pineapple juice had a similar pattern of increase in biomass concentrations with decreasing substrate concentrations (Figs. 1 and 2), which is supported by the similarity of growth rates that were seen in Table 1. A rapid increase in cell growth during the 8-day period of fermentation was found for all strains cultured in coconut juice.

Table 1 summarizes the fermentation kinetics of the strains grown on pineapple juice. The final yield of BC from all strains resulted in approximately the same concentration. Both TISTR 893 and 975 showed higher values of specific rate of substrate utilization than TISTR 998, while the growth rates of all strains showed the same profile (Fig. 2). There was, however, a significant difference in substrate utilization when TISTR 998 is compared with both 893 and 975 (p=0.091, p=0.210 respectively). For pineapple, TISTR 893 showed the highest level of BC production, which was different from coconut juice, as TISTR 998 yielded the highest BC production. The changes over the time course of fermentation (Fig. 3) also showed an obvious slower rate of increasing BC after the 6 days of TISTR 975 cultivation, as can be seen in the lower cellulose yield. This result provides strong support for the notion that the static culture method for BC production is more suitable for commercial-scale production, as higher production rates can be achieved. Our strategy for using strains capable of producing cellulose with a high yield have been accomplished, as shown in the high specific rates of product formation (Q_p values, Table 1). This approach is the easiest way to culture BC, with a low production cost, and without extreme attempts to perform chemical mutations and gene modifications to obtain potent strains.

Bacterial Cellulose Production in Different Strains

In a static culture condition, the amount of BC produced gradually increased when produced on coconut juice, these values were 21.85, 18.24, 13.52 cm^3/l per day of TISTR

Table 1 The growth kinetic parameters during the static fermentation of *Acetobacter xylinum* strains in coconut and pineapple juice at 30 °C for 2 weeks.

Substrate	Strains	Bacterial cellulose (g/l)	r_x (g/l/h)	μ (h^{-1})	r_s (g/l/h)	Q_s (g/g/h)	r_p (g/l/h)	Q_p (g/g/h)
Coconut juice	998	553.33	0.041	0.50	3.48	42.96	530.42	6,548.33
	893	453.33	0.045	0.50	1.52	17.12	191.20	2,148.32
	975	243.33	0.050	0.50	1.56	15.57	155.74	1,557.39
Pineapple juice	998	520.00	0.002	0.021	2.871	25.78	213.60	2,080.24
	893	576.66	0.002	0.022	2.922	34.24	401.24	4,702.08
	975	546.66	0.002	0.021	2.734	34.46	434.38	5,475.32

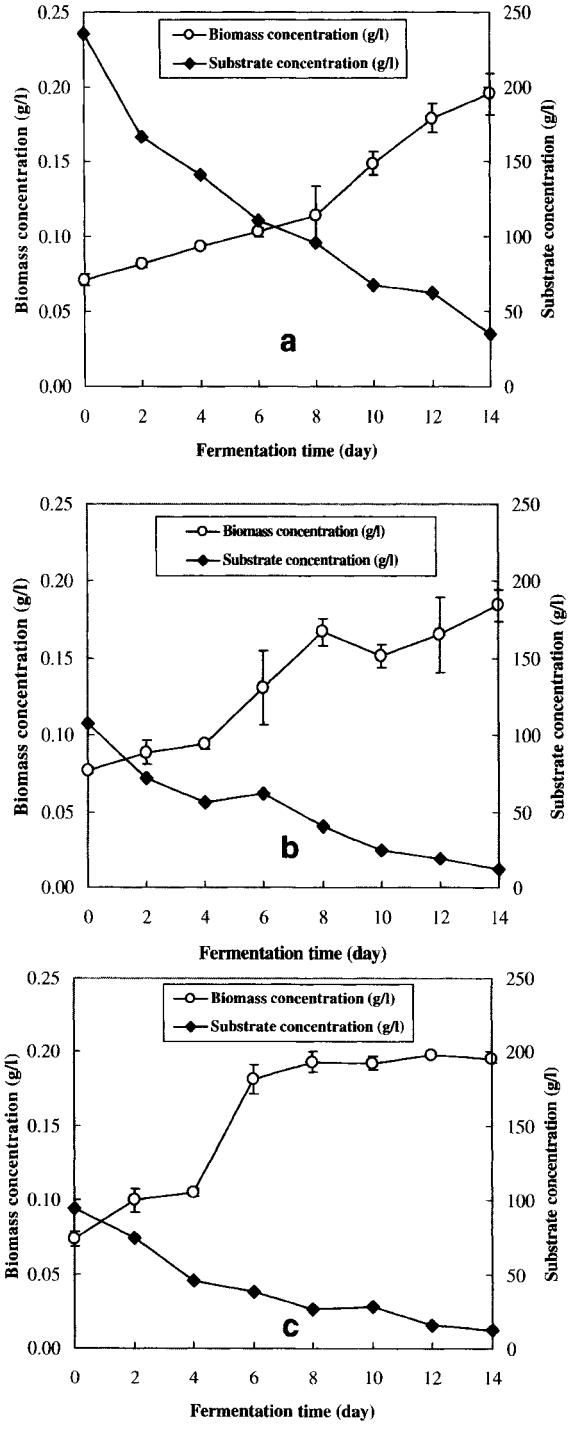


Fig. 1 Time course of cell growth and substrate utilization using *Acetobacter xylinum* grown in coconut juice, **a** TISTR 998, **b** TISTR 893, and **c** TISTR 975. *Values* represent the mean of triplicate determination; *error bars* represent ±standard deviation. When not shown, the error bars fall within the symbols

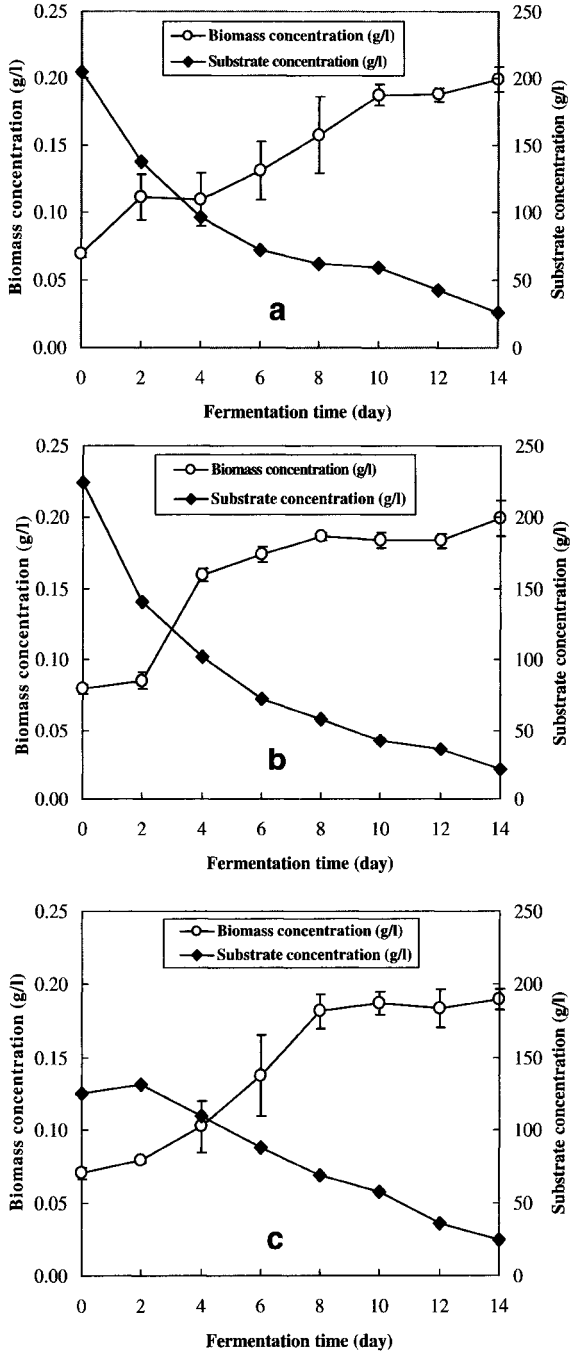


Fig. 2 Time course of cell growth and substrate utilization using *Acetobacter xylinum* grown in pineapple juice, **a** TISTR 998, **b** TISTR 893, and **c** TISTR 975

998, 893, and 975, respectively (Fig. 3a). Cellulose produced in this static condition occurred as a big oval pellicle with a diameter of 26 cm and with a thickness between 2.7 and 3.6 cm. Rates of BC formation on pineapple juice are illustrated in Fig. 3b. Bacterial strains TISTR 998, 893, and 975 produced cellulose at rates of 8.96, 19.02, and 15.25 cm^3/

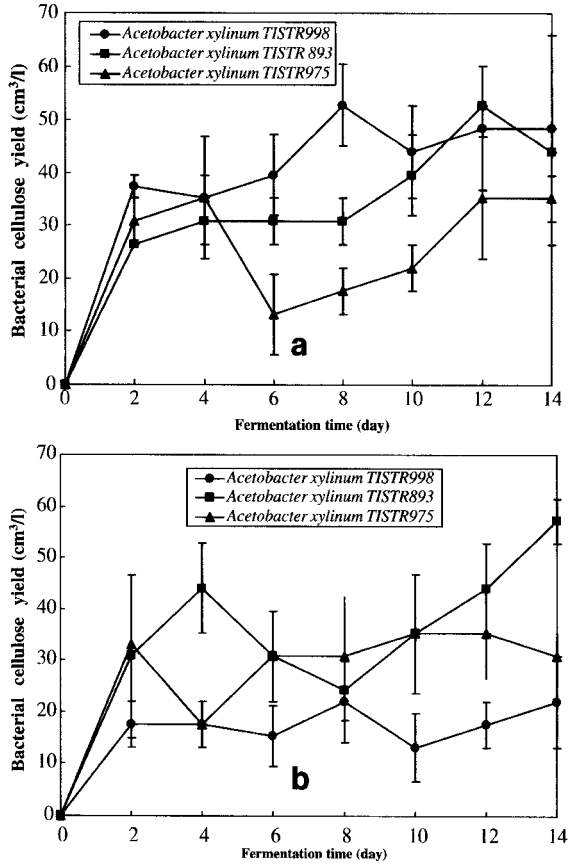


Fig. 3 Rates of bacterial cellulose production during the course of fermentation on **a** coconut juice and **b** pineapple juice

l per day, respectively. In contrast to an agitated culture, *A.xylinium*, a gram-negative, obligate aerobic, rod-shaped organism, produces cellulose at the air–water interface as an assembly of highly crystalline interwoven ribbons that are chemically pure, free of lignin and hemicellulose, and have a high degree of polymerization. The cells and fibrils of cellulose attach to the surfaces of the disks to form tough gelatinous mats that become limited in thickness only by the distance to the adjacent disk. The majority *A. xylinum* cells are found at the top of the growing pellicle, where cellulose production takes place. Since new cellulose is produced at the surface, the pellicle is formed in a downward direction. The steady increase in bacterial cellulose yield in both substrates reveals a spontaneous appearance of cellulose non-producing mutants, and a serious clump-forming problem, which is normally found in an agitated culture. As a consequence of this disturbed condition, a decline in cellulose yield as well as a non-uniform structure may occur.

Viable Cell Growth in Different Strains

The changes in total viable cell count during the course of the fermentations are given for both juices in Fig. 4a,b. Bacterial growth exponentially increased, reaching 10^{11} times the value of the initial day after 8 days of cultivation (Fig. 4a,b). Both substrates showed similar curves of cell growth and the curves approached stationary growth after 8 days of fermentation time. Both substrates clearly showed two phases of cell generation that had

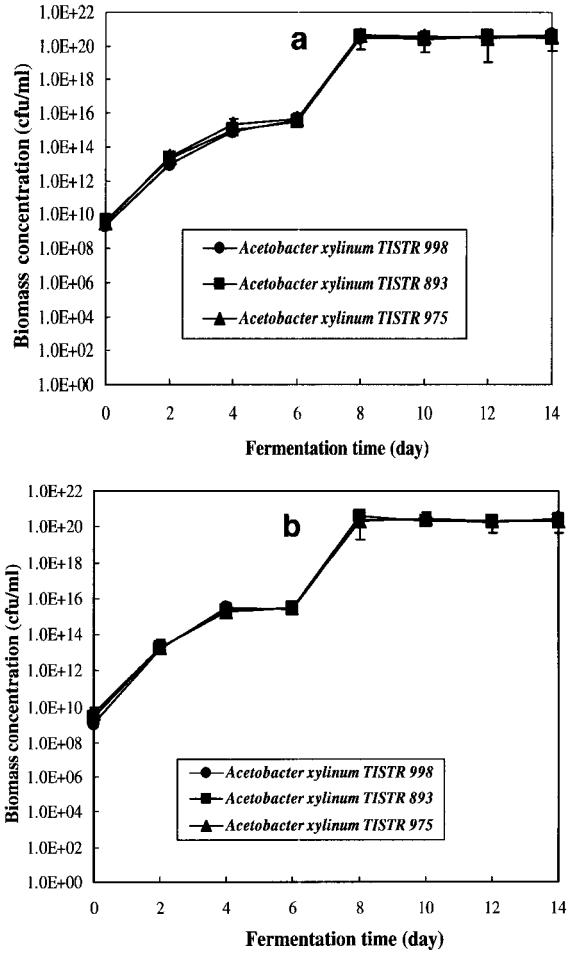


Fig. 4 Viable cell count during the fermentation of bacterial cellulose on **a** coconut juice and **b** pineapple juice

both exponential and stationary growth phases during the fermentation time. There was no cell death phase during this period because of the substantial amount of substrate still remaining in the fermentation broth. Cellulose levels increased the whole time due to continuous cell growth. The doubling time of this type of bacteria is known to be within the range 1.5 to 8 h [14], and our data showed a doubling time of 2 h. The growth rate of fibrils is not well-known, but a rate of ~2 μm min^{-1} has been reported as the rate observed for isolated cells during the initial stage of cultivation [15].

Total Acid and pH Changes During Fermentation

As fermentation time increased, there was an increase in the total acid observed (as measured by the presence of acetic acid secreted during bacterial growth and cellulose production, Fig. 5a,b). This is because *A. xylinum* is unique in its family for being able to convert carbohydrates to acetic acid by synthesizing and extruding fibrils of cellulose. Its metabolism is respiratory, which involves oxidizing ethanol to acetic acid and converting glucose to gluconic acid. Acetic acid is a by-product of cellulose, which influences the

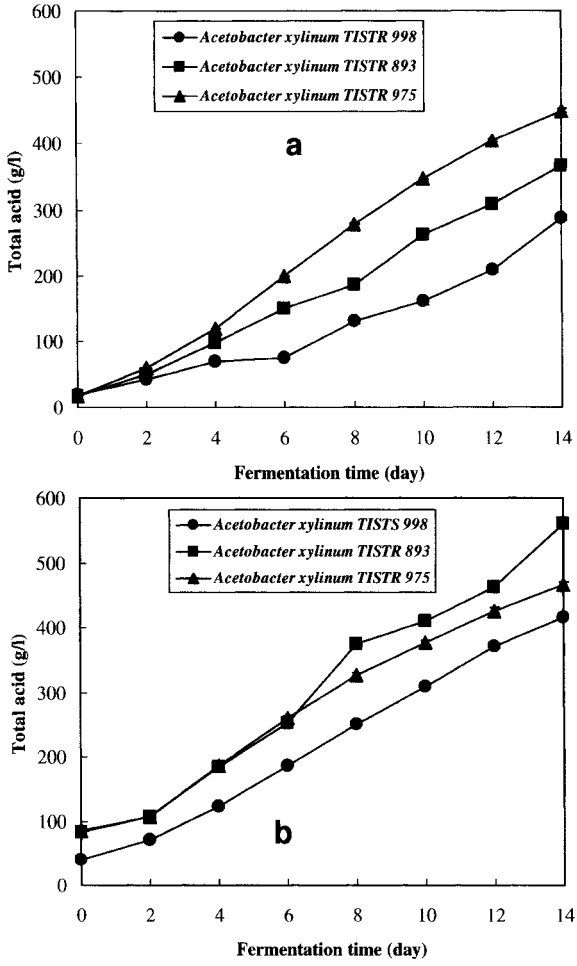


Fig. 5 Total acid production from the fermentation by three strains of *Acetobacter xylinum* of **a** coconut juice and **b** pineapple juice

decreased pH in the culture medium. As proposed by Seto et al. [16], a decrease in pH of the culture medium has an effect on both cellulose production and cell growth for *A. xylinum*. The pH of both substrates had changed to lower the acidity (Fig. 6a,b). While bacterial cellulose is being produced, this change in acidity can be difficult to control by the pH buffer system, as has been observed by some investigators [17, 18]. This pH reduction was also observed in the Hestrin–Schramm medium when cultured with the same strains (TISTR 893,975) in molasses, as reported by Premjet et al. [19]. When coconut juice was the substrate, the highest acetic acid concentration was found in TISTR 975, with a 24.96-fold increase (Fig. 5a). Acetic acid content at levels of about 20.37-fold and 14.58-fold were detected in TISTR 893 and 998, respectively. For pineapple juice (Fig. 5b), TISTR 998, 893, and 975 produced acetic acid at levels of increase of 10-, 6.68-, and 5.47-fold, respectively. The only significant difference in total acid production between substrates for a given strain was seen in the higher rate of production by TISTR 975 over that of 998 on pineapple substrate (Fig. 5b). This value was also significantly greater than the values seen for the other strains (Fig. 5a).

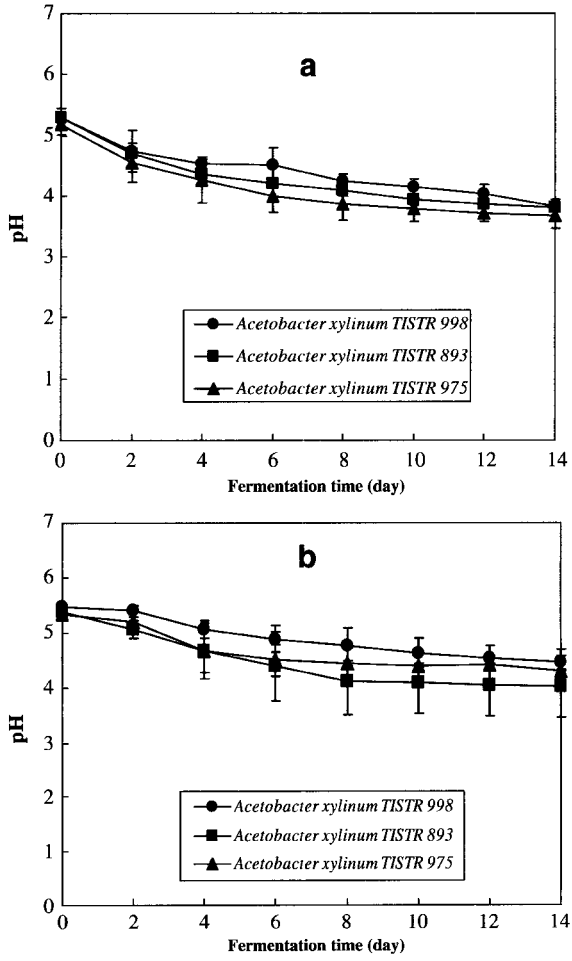


Fig. 6 Time course of pH change during fermentation using **a** coconut juice and **b** pineapple juice

Effect of Texture on Bacterial Cellulose in Different Strains

The strengths of the resulting dried sheets were tested by applying mechanical compression forces to determine the relative effects of the bacterial strains. As shown (Table 2), there were no significant differences between the textures of all bacterial cellulose strength levels derived from the three strains. Both coconut and pineapple juices yielded the same strength rating. The mechanical properties of bacterial cellulose, both air-dried and hot-pressed

Table 2 Comparison of the compression forces on bacterial celluloses.

Bacterial strains	Force (kg)	
	Coconut juice	Pineapple juice
TISTR 893	0.086±0.043	0.076±0.016
TISTR 975	0.072±0.013	0.090±0.038
TISTR 998	0.070±0.022	0.073±0.037

Table 3 Color comparison of bacterial cellulose.

Substrate	Bacterial strain	CIELab values (standard error)				
		L^*	a^*	b^*	C^*	h_{ab}
Coconut juice	893	52.46 (1.67)	−2.45 (0.10)	−0.47 (0.60)	2.78 (0.08)	194.02 (13.70)
	975	53.62 (2.78)	−3.33 (0.03)	0.13 (0.64)	3.58 (0.29)	195.69 (19.85)
	998	53.02 (1.37)	−3.05 (0.18)	1.18 (0.72)	3.59 (0.17)	158.41 (13.32)
Pineapple juice	893	47.17 (0.99)	0.01 (0.31)	13.30 (0.49)	13.00 (0.63)	88.40 (0.75)
	975	54.00 (1.41)	2.12 (0.33)	19.41 (0.11)	19.22 (0.79)	83.62 (0.57)
	998	52.46 (1.54)	−2.45 (0.20)	−0.47 (0.70)	2.78 (0.36)	194.02 (0.25)

preparations [20], also showed that there were no differences detected on BC among different bacterial strains. Comparison of two bacterial strains (ATCC 10821 from the American Type Culture Collection, Maryland, USA and AJ 12368 from Central Research Laboratories, Ajinomoto, Tokyo, Japan) did not show any substantial difference (data not shown). The lack of significant differences in mechanical effects among strains was also observed among varying cultivation times and cellulose contents. The experiment depicted in Table 3 also emphasized that the sheets obtained from the pellicles of different strains have the same mechanical properties. All of these strains are useful for producing BC for paper making.

Effect of Color on Bacterial Cellulose in Different Strains

As shown in Table 3, all strains yielded an opaque, white, thick pellicle, as the L^* value shifted slightly toward the lightness side. However, the values obtained from strains 893 and 975 detected higher values of positive b^*, indicating yellowness. Values from the calculated chroma and hue angle for strains 893 and 975 are also shown in Table 3. The samples cultivated on pineapple juice yielded an opaque yellow color, which contained a carotene color, (h_{ab} values approach to 90°, Table 3), while those bacterial celluloses derived from the coconut juice showed a white color.

Conclusions

This study showed that the bacterial cellulose derived from coconut and pineapple juices can be converted efficiently to bacterial cellulose by the supplementation of yeast extract and ethanol under static fermentation conditions at 30 °C. Bacterial celluloses produced from all strains are growth associated products. Coconut juice seems to be a better substrate than pineapple juice. In view of energy consumption, the productivity of BC on this medium is high, which makes the production costs lower than expected. It is also clear that different *A. xylinum* strains produce different BC content levels under the same inoculation volumes and under static cultivation conditions. These results suggest that bacterial cellulose pellicles of all strains appear to be easily applied to use in many applications such as food, paper, and textile industries, without requiring additional steps of decolorization and purification. Furthermore, the properties of cellulose, in terms of crystallinity, high water-absorption capacity, and mechanical strength of the reported strains, have additional applications in cosmetics and medicine.

Acknowledgements This work has been supported by the Faculty of Applied Science, King Mongkut's Institute of Technology North Bangkok, Bangkok, Thailand. The author is very much grateful to Dr. Mario Ambrosino, Oregon State University, for his kind critical reading of the manuscript.

References

1. Hon, D. (1994). *Cellulose*, *1*, 1–25.
2. Koyama, M., Helbert, W., Imai, T., Sugiyama, J., & Henrissat, B. (1997). *Proceedings of the National Academy of Sciences of the United States of America*, *94*, 9091–9095.
3. Embuscado, M. E., Marks, J. S., & BeMiller, J. N. (1994). *Food Hydrocolloids*, *8*, 407–418.
4. Delmer, D. P., & Amor, Y. (1995). *The Plant Cell*, *7*, 987–1000.
5. Delmer, D. P. (1999). *Annual Review of Plant Physiology and Plant Molecular Biology*, *50*, 245–276.
6. Einfeldt, L., & Klemm, D. (1997). *Journal of Carbohydrate Chemistry*, *16*, 635–646.
7. Koyama, M., Helbert, W., Imai, T., Sugiyama, J., & Henrissat, B. (1997). *Proceedings of the National Academy of Sciences of the United States of America*, *94*, 9091–9095.
8. Ross, P., Mayer, R., & Benziman, M. (1991). *Microbiology and Molecular Biology Reviews*, *55*(1), 35–58.
9. Hirai, A., Tsuji, M., Yamamoto, H., & Horii, F. (1998). *Cellulose*, *5*, 201–213.
10. Lynd, L. R., Weimer, P. J., Vanzyl, W. H., & Pretorius, I. S. (2002). *Microbiology and Molecular Biology Reviews*, *66*, 506–577.
11. Schramm, M., & Hestrin, S. (1954). *Biochemical Journal*, *56*, 163–166.
12. Shamolina, I. (1997). *Fibre Chemistry*, *29*(1), 3–10.
13. Herbert, P. J., Phipps, P. J., & Strange, R. E. (1971). London: Academic, *5*, 266–272.
14. Marx-Figini, M., & Pion, B. G. (1974). *Biochimica Biophysica Acta*, *338*, 232.
15. Brown, R. M., Willison, J. H. M., & Richardson, C. L. (1976). *Proceedings of the National Academy of Sciences of the United States of America*, *72*, 4565.
16. Seto, A., Kojima, Y., Tonouchi, N., Tsuchida, T., & Yoshinaga, F. (1997). *Bioscience, Biotechnology, and Biochemistry*, *61*, 735–736.
17. Dudman, W. F. (1995). *Journal of General Microbiology*, *21*, 327–337.
18. Ishikawa, A., Matsuoka, M., Tsuchida, T., & Yoshinaga, F. (1995). *Bioscience, Biotechnology, and Biochemistry*, *59*, 2259–2262.
19. Premjet, S., Vorasingha, A., Somsiri, A., Ohtani, Y., & Sameshima, K. (2003). *Thai Journal of Biotechnology*, *4*(1), 30–36.
20. Yamanaka, S., Watanabe, K., Kitamura, N., Iguchi, M., Mitsuhashi, S., Nishi, Y., & Uryu, M. (1989). *Journal of Materials Science*, *24*, 3141–3145.

Appl Biochem Biotechnol (2008) 148:257–260
DOI 10.1007/s12010-007-8029-7

Overview of Special Session B—Compositional and Structural Analysis of Biomass

Bonnie Hames

Received: 29 May 2007 / Accepted: 21 August 2007 /
Published online: 12 February 2008
© Humana Press Inc. 2007

Abstract Special Session B at the 29th Symposium on Biotechnology for Fuels and Chemicals was the first invited session at this symposium devoted to analytical methods. The special topic was added in response to numerous requests for information on new and innovative methods that could be applied in the growing renewable fuels industry. Presentation topics include analytical methods for the characterization and analysis of maize traits, tools for investigating cell wall limitations to enzymatic degradation, methods for customizing enzyme cocktails for biomass, new techniques for the analysis of carbohydrates, analytical methods that enhance our understanding of pretreatment, improved methods for monitoring process intermediates, and published standard analytical methods for biomass conversion processes.

Keywords Analytical chemistry · Enzymes · Chromatography · Standard methods · Feedstock · Biomass · Forage · Carbohydrates · Imaging · Pretreatment · Saccharification · Process monitoring

Special Session B at the 29th Symposium on Biotechnology for Fuels and Chemicals Invited was the first session at this symposium devoted entirely to analytical methods. The special topic was added in response to numerous requests for information on new and innovative methods that could be applied in the growing renewable fuels industry. Quality analytical methods are needed in all areas of biomass conversion. Feedstock methods support breeding and agronomic programs that improve yields and quality. Process methods improve our understanding of pretreatment, saccharification, fermentation, combustion, and recycle steps. Imaging tools provide new insight into recalcitrance and inhibition. Methods that retain precision and accuracy but enhance sample throughput are being developed in many forms. This session captured a diverse cross section of the innovative analytical methods supporting biotechnology approaches to fuels and chemicals production. The

B. Hames (✉)
Ceres, Inc., 1535 Rancho Conejo Blvd.,
Thousand Oaks, CA 91320, USA
e-mail: bhames@ceres-inc.com

following excerpts from presentation abstracts help summarize the diverse topics presented in this inaugural session on analytical methods

The session opened with a presentation by Dr. Brigette Chabbert, research scientist at *Institut National de la Recherche Agronomique, Unite Mixte de Recherche*, in Reims, France, who discussed "Cell Wall Limitations to Efficient Lignocellulosic Bioconversion."

> Improvement and development of efficient enzymatic tools for biomass conversion require in depth knowledge of the main limitations brought by lignified cell-walls. Non-invasive methods such (immuno)cytochemistry provide specific information on the cell wall heterogeneity at both cellular and subcellular levels. Notably, complexity of the cell wall networks can be clearly evidenced following enzymatic destructuration. Enzyme engineering aimed at modulating enzyme size and activity can provide a variety of molecular tools that will allow significant knowledge of the organizational heterogeneity of plant cell walls. Strategy based on in muro probing of the wall network in plant tissues would take advantage from comparative studies on various botanical plant materials. The use of in vitro systems of the lignin-polysaccharide matrix provides information on the way supramolecular organization of the wall polymers may affect the enzymatic breakdown of lignocellulosics.

Dr. Justin Stege, Associate Director of Alternative Fuels at Diversa in San Diego, CA, presented "Analytical Techniques for Enzyme Cocktails."

> Effective saccharification of pretreated biomass requires the synergistic activities of multiple enzymes, particularly when significant hemicellulose structures remain. With over 1000 plant cell wall-degrading enzymes in our collection, Diversa develops cocktails of enzymes that are customized for each particular feedstock, pretreatment and for different process conditions. Diversa has developed a 96-well capillary electrophoresis system for profiling oligosaccharide and monosaccharide reaction products. This high throughput CE technology enables us to rapidly screen hundreds of enzymes or enzyme combinations under different conditions with different substrates to select for desirable product profiles. These customized cocktails can be further improved by analyzing the undigested carbohydrates remaining after enzyme digestion. Using this compositional information, enzymes have been identified that saccharify the resistant material, greatly improving the yield of fermentable sugars.

Dr. Neil Price, from the USDA National Center for Agricultural Utilization Research in Peoria, IL, presented, "New Techniques for the Analysis of Carbohydrates."

> Carbohydrates are complex. In addition to the size/mass differences increasing from monosaccharides to oligosaccharides to polysaccharides, the carbohydrate analyst must also contend with which sugars are present (composition), how they are joined together (linkage), and their stereochemistry (configuration and anomericity). New techniques developed for glycomics and glycoproteomics are highly applicable for the analysis of most complex carbohydrate products. This talk reviewed methods for composition and linkage analysis of sugars, and introduced new methods of end-labeling, chiral isotopic labeling, and deuterium exchange (HX) that are compatible with MALDI-TOF MS, electrospray mass spectrometry, and NMR for the analysis of carbohydrates.

Dr. David Johnson, from the National Renewable Energy Lab, in Golden, CO, gave an overview of "Methods that Enhance our Understanding of Pretreatment Processes."

Conversion of lignocellulosic biomass to sugars and ethanol requires an effective pretreatment before the cellulose can be efficiently hydrolyzed by enzymes. Pretreatment conditions cover the entire range from low to high pH, from moderate to high temperatures, and from minutes to weeks. As with all chemical processes, pretreatments are only successful if they generate the desired products in high yield and undesirable products are minimized. Development of tools to understand the effect of pretreatment processes on lignocellulosic feedstocks is an active area of research at NREL. Characteristics typically tracked are cellulose crystallinity (by solid-state 13C NMR or X-ray diffraction), cellulose accessibility (measured using fluorescence labeled enzymes) and porosity (measured by thermoporometry or solute exclusion). Various microscopic imaging techniques can be used to follow changes in lignin and xylan distribution in the plant cell wall. By labeling with carbohydrate specific probes changes in the cell wall structure can be revealed. Immunoelectron microscopy has been used to monitor how major enzyme components of biomass degrading enzyme cocktails penetrate the cell wall matrix following pretreatment. Using these tools, we are attempting to gain a better understanding of how pretreatment processes can generate highly digestible.

The session's student speaker, Aaron Lorenz, a doctoral candidate in the Department of Agronomy at the University of Wisconsin in Madison, discussed "Silage Breeding Programs and their Connection to Energy Feedstock Production."

The University of Wisconsin has conducted a silage breeding program for the past 15 years using NIRS-based predictions of forage quality. A review of the development and operation of this breeding program provides some perspective on the future of lignocellulosic biofeedstock development programs. Evaluation of biomass yield and composition, followed by recombination of selected genotypes require logistical efficiency if significant gains are to be realized in the near future. Prior experience with measures of forage quality (e.g., fiber concentration and forage digestibility) may help if these relate well to requirements for lignocellulosic ethanol production, particularly with respect to the characteristics of the germplasm used to initiate genetic improvement programs.

Dr. Kevin Chamblis, Assistant Professor in the Department of Chemistry and Biochemistry, at Baylor University in Waco, TX, described "Improved Analytical Methods for Monitoring Process Intermediates in Biomass-to-Ethanol Conversion."

Qualitative and quantitative analysis of lignocellulosic degradation products is critical to any technical or economic valuation of biomass conversion. The majority of degradation products are introduced into process streams during biomass pretreatment. Pretreatment liquids contain not only cellulose and fermentable sugars, but also a wide variety of aliphatic and aromatic acids, phenols, and aromatic aldehydes that may exert an inhibitory effect on downstream bioconversion processes. Accordingly, there is broad interest in the development of reliable methods for assessment of an increasing number of target analytes in biomass process streams.

This presentation highlighted recent advances in the development of a high performance liquid chromatography-photodiode array-tandem mass spectrometry (HPLC-PDA-MS/MS) method, targeting 40 potentially-inhibitory degradation products, and an improved high performance anion exchange-pulsed amperometry (HPAE-PAD) technique for rapid monitoring of biomass sugars in pretreatment liquids.

Closing the session, Dr Foster Agblevor, Associate Professor in the Department of Biological Systems Engineering at Virginia Tech in Blacksburg, described "ASTM E48 Activities in the Area of Standard Analytical Methods Supporting Biomass Conversion Processes."

> Realizing the goals of the US DOE 30x'30 initiative will require the development, standardization and validation of hundreds of new analytical methods specifically for biomass. The data generated from these analytical methods will be used to evaluate feedstocks, optimize reactors and determine process economics for bench-scale to commercial-scale processes that convert biomass feedstocks to liquid transportation fuels. Efficient utilization of the slate of biomass feedstocks proposed in the DOE Billion Ton Study will require a multitude of individual analytical methods capable of tracking as many as 20 constituents from feedstock to products.
>
> Deployment of biomass analysis into the private sector will more likely be in the form of high-throughput methods that will be calibrated using, and validated relative to, the best chemical and structural tools available, providing a research environment rich in high quality data.
>
> Since engineering concepts and economic projections will be dependent on process analytical data, a clear QA/QC trail should be established linking high-throughput analysis methods to rigorous scientific and statistical standards. This can most easily be accomplished by establishing industry-wide consensus methods and publishing them through existing standards organization such as American Society for Testing and Materials (ASTM).

The response to this new special session topic was overwhelmingly positive, clearly indicating a need for increased research focus on analytical methods and forums for presenting innovative analytical methods used in fuels and chemical production.

Appl Biochem Biotechnol (2008) 148:261–270
DOI 10.1007/s12010-007-8116-9

What can be Learned from Silage Breeding Programs?

Aaron J. Lorenz · James G. Coors

Received: 18 May 2007 / Accepted: 3 December 2007 /
Published online: 9 January 2008
© Humana Press Inc. 2007

Abstract Improving the quality of cellulosic ethanol feedstocks through breeding and genetic manipulation could significantly impact the economics of this industry. Attaining this will require comprehensive and rapid characterization of large numbers of samples. There are many similarities between improving corn silage quality for dairy production and improving feedstock quality for cellulosic ethanol. It was our objective to provide insight into what is needed for genetic improvement of cellulosic feedstocks by reviewing the development and operation of a corn silage breeding program. We discuss the evolving definition of silage quality and relate what we have learned about silage quality to what is needed for measuring and improving feedstock quality. In addition, repeatability estimates of corn stover traits are reported for a set of hybrids. Repeatability of theoretical ethanol potential measured by near-infrared spectroscopy is high, suggesting that this trait may be easily improved through breeding. Just as cell wall digestibility has been factored into the latest measurements of silage quality, conversion efficiency should be standardized and included in indices of feedstock quality to maximize overall, economical energy availability.

Keywords Silage breeding · Corn stover · Repeatability · Quality

Introduction

Large amounts of funding and significant advances in research are making the production of fuels from cellulosic sources a reality. At least six "biorefineries" received funding from the Department of Energy and are expected to be completed within the next 5years [1]. Corn stover is widely recognized as a low-cost feedstock for initial use on a large scale because of its current abundance and proximity to existing corn grain ethanol plants. Examples of other potential feedstocks include perennials such as switchgrass, miscanthus,

A. J. Lorenz (✉) · J. G. Coors
Department of Agronomy, University of Wisconsin—Madison, 1575 Linden Drive,
Madison, WI 53706, USA
e-mail: alorenz@wisc.edu

J. G. Coors
e-mail: jgcoors@wisc.edu

popular, and native prairie grass mixtures. Energy for fuel production from any cellulosic source will be derived from the plant cell wall, which is primarily composed of cellulose (polysaccharide of glucose) and hemicellulose (complex polymer of both five- and six-carbon sugars). These sugars will be made available for fermentation through chemical pretreatment of the feedstock followed by enzymatic hydrolysis of the remaining cellulose [2].

Carbohydrates bound in cellulosic biomasses are also the primary energy source for ruminant animals. One example is corn silage, which is a high-yielding and high-quality feed commonly fed to dairy cows. Corn silage is produced by harvesting whole corn plants a few weeks before physiological maturity and ensiling. The most significant carbohydrate sources in corn silage are from the starch and cell wall fractions, which are made available to the animal by a complex community of anaerobic microbes that reside in the gastrointestinal tract [3]. Both highly degradable (starch and simple sugars) and less degradable (cell wall bound) carbohydrates are converted to volatile fatty acids and absorbed through the rumen wall [4]. Metabolizable energy that exceeds maintenance requirements in a healthy, lactating dairy cow is used for milk production.

Crop varieties with greater biomass yield, carbohydrate concentration, and carbohydrate availability would be better adapted for use as cellulosic feedstocks and could significantly improve the economics of this industry by increasing the amount of energy produced from an area of land as well as reducing costs associated with pretreatment and enzyme hydrolysis [2]. When a plant breeder wants to improve a species for novel uses, three simple but fundamental questions must be answered: (1) "What are we selecting for?" (2) "How are we going to measure it?" (3) "Can we do it efficiently?" Evaluation of biomass yield and composition for selection and recombination requires logistical efficiency if significant gains are to be realized in the near future. Characterizing biomass properties that influence ethanol production, developing tools for efficient measurement of these properties, and synthesizing relevant properties into a single, accurate, and intuitive index would facilitate variety selection and breeding. Novel variation for cell wall properties has been generated through genetic engineering, and its potential for increasing biomass yield is being investigated by manipulating genes involved in photosynthesis and nitrogen metabolism [5]. However, the need for these tools still remains as such engineered variation must be entered into breeding programs for recombination with agronomically elite genetic backgrounds. The effect different genetic backgrounds have on transgene expression and phenotype should be studied in a field setting.

The University of Wisconsin (UW) has conducted a silage breeding program for the past 15years using near-infrared spectroscopy (NIRS) based predictions of forage quality. Collaboration with nutritionists and agronomists has been instrumental in defining agronomic and quality characteristics for their improvement. The relationship between developing corn varieties for silage use and developing varieties for use as a cellulosic feedstock is obvious: In both cases, we want to maximize total available energy from plant biomass that is converted into a product through the action of microorganisms. The objective of this paper is to provide insight into what is needed for the measurement and thus genetic improvement of cellulosic feedstocks. We will accomplish this by reviewing the development and operation of a corn silage breeding program and discuss the evolving analysis of silage quality. Although yield is tremendously important, this paper will focus on quality because it is harder to measure, and the session topic under which this paper was originally presented centered on feedstock composition. We will also highlight the concept of repeatability, discuss why it is important for breeding, and report repeatability estimates of corn stover composition measurements related to ethanol production.

Measuring Energy Value of Corn Silage

Because grain makes up 40–45% of the total silage dry matter and starch, the largest constituent of grain, is a highly available energy source, it was previously believed that the best grain-producing varieties were also the best silage varieties [6]. However, we now know that this is not necessarily true because of variability in neutral detergent fiber (NDF, total cell wall concentration determined by Van Soest detergent analysis) digestibility and thus amount of energy that can be utilized from this substantial fraction [7]. Public and private breeding projects as well as university extension programs have developed and identified corn varieties for dedicated silage use. High quality is desired in a silage variety and is important for maximizing the amount of milk that can be produced from 1ton of silage; it is influenced by both total available energy content and dry matter intake potential of the silage [6]. Dry matter intake is defined as the amount of silage an animal can consume in a given amount of time. Feeding trials for determining the quality of individual varieties are practically impossible, so ranking varieties based on milk potential must rely on measuring chemical constituents and in vitro assays that are functionally and statistically associated with milk production in vivo. Constituent concentrations and their availability are entered into a model for prediction of total available energy for lactation.

The calculation of net energy of lactation (NEL) has been continually refashioned to better reflect both the amount, as well as the ruminal availability, of nutrients contributing to dietary energy used for milk production. Up until the early 1990s, the energy value of forages, including corn silage, was commonly assessed by measuring acid detergent fiber (ADF) [8]. The negative correlation of ADF, which is mostly composed of cellulose, lignin, and mineral constituents, with fiber digestibility is largely due to the fact that lignin restricts ruminal microbial degradation of plant fiber. When evaluating corn silage, nutritionists usually assumed complete digestion of starch and calculated dietary energy accordingly. This approach was used in spreadsheets for prediction of milk potential developed at the UW named MILK91 and MILK95.

It has long been recognized that the simplistic calculation of NEL based solely on amount of starch, lignin, or ADF ignores variation in the digestibility of fiber, starch, and other dietary components. Digestibility and NEL predictions based on ADF concentration alone can have high errors and empirical equations used depend upon the set of samples evaluated [6, 9]. However, initially, there were few analytical tools that accurately measured rate or extent of degradation of individual dietary constituents in the rumen. Furthermore, dry matter intake was assumed to be solely a function of NDF concentration in the diet because fiber increases bulk density in the rumen and decreases the amount of feed an animal can process over time. Results from feeding trials in which NDF was held constant and NDF digestibility (NDFD) was varied showed that digestibility of the NDF fraction also affects dry matter intake [10, 11]. These deficiencies have been addressed in the several refinements of early dietary models (MILK1991, MILK1995, MILK2000) that eventually resulted in the current system of ration evaluation, MILK2006.

The major refinement during these revisions was the development a multicomponent summative energy equation [12, 13]. The digestibility of protein, fatty acids, fiber (as measured by NDF), nonfiber carbohydrates, and starch are all used in the calculation of NEL. Because dry matter intake is not only a function of NDF concentration but also of NDFD, both factors were taken into consideration. MILK2006, therefore, now combines a robust summative energy calculation of NEL along with an estimate of intake potential to predict potential milk production per unit weight of forage.

Table 1 depicts the relative effects of NDF and starch on potential milk production as the dietary models changed over the last 15+years. It is apparent that the early nutritional models (MILK1991 and MILK 1995) did not consider effects of the ruminal availability of these constituents, and this is reflected in the lack of correlation between milk production potential and digestibility of either NDF or starch. MILK91 and MILK95 applied no weight to starch digestibility and NDFD. The small, negative correlations are due to the lack of independence between constituent concentrations and their digestibilities. This was corrected with the advent of MILK2000 and the further modifications for MILK2006. Nutritional studies have shown that varieties with higher fiber concentrations (low starch percentage) can outperform varieties with lower fiber concentrations (high starch percentage) with respect to actual milk production measured in vivo [6]. This is thought to be due to differences in fiber digestibility and the earlier models (MILK91 and MILK95) would have incorrectly ranked these varieties. Moreover, MILK2006 more accurately predicts actual production values taken from the literature than MILK2000 [13].

It is important to recognize why these nutritional models were first established and what use they currently serve. In well-managed dairies, rations are balanced to provide a nutritionally complete feed with maximum energy value. Feedstocks vary on a daily and seasonal basis, so a flexible and rapid nutritional assay is necessary. MILK2006 provides means for predicting energy content and intake potential of harvested forages so that these forages can be appropriately combined with other fiber and nonfiber dietary components when fed as part of a complete ration. Plant breeders also quickly realized the utility of these simple and rapid predictive assays to provide selection indices when choosing among new forage strains or cultivars for breeding purposes. In addition, MILK2006 is now commonly used in extension trials of new silage corn hybrids throughout the USA and Europe, and these evaluations are used by individual farmers to purchase hybrid seeds for planting [14].

Fortunately, NIRS can be employed to estimate most components of nutritive value important for forages, and these estimates can be used directly with MILK2006. For example, NDF, starch, protein, and NDFD of corn silage can easily be measured with NIRS, and these constituents along with MILK2006 have been routinely used by the UW corn breeding program to develop superior silage varieties [4, 15]. In a typical year, the UW silage breeding program collects forage samples from 4,000 to 6,000 field plots. Based on forage yield, approximately one half of the samples from the most productive hybrids are then analyzed for quality. This must be completed within a 4–6-week period between early

Table 1 Correlation coefficients (r) for neutral detergent fiber (NDF) and starch, as well as NDF and starch digestibilities (NDFD and StarchD) with milk per ton estimates from MILK1991 to 2006 dietary models.

r values	MILK2006[a]	MILK2000[b]	MILK1995[c]	MILK1991[d]
NDF	−0.46	−0.40	−0.94	−0.99
Starch	0.48	0.44	0.75	0.74
NDFD, % of NDF	0.49	0.70	0.16	−0.10
StarchD, % of starch	0.30	0.21	−0.25	−0.27

Data provided by J. G. Lauer (UW—Madison Agronomy Department, n=3727 treatment means for corn silage hybrids evaluated in Wisconsin). Adapted from Shaver [13].

[a] Calculated as per Shaver [13]

[b] Calculated as per Schwab et al. [12]

[c] Calculated as per Undersander et al. [8] except for in vitro dry matter digestibility adjustment

[d] Calculated as per Undersander et al. [8] using ADF and NDF.

September and mid-October so seeds of selected families can be sent to a winter nursery for generation advancement. Finally, after each season of silage evaluation, the ability to predict the nutritive value of the germplasm under development is upgraded by including new NIRS spectral samples and corresponding laboratory evaluations in the calibration database.

Although NIRS prediction equations have proven to be reliable and accurate, knowledge of nutritional requirements has increased from the time the equations were initially developed. This will always be the case because of the need to assemble a large nutritional database encompassing a large array of different forages grown in different environments for NIRS prediction to work adequately. Assembling such a database takes several years to accomplish. While data are being accumulated, the nutritional concepts validating the initial effort of NIRS prediction change somewhat requiring that altered or new nutritional characteristics be considered. The UW NIRS calibration data for NDF, NDFD, and protein were developed through compositional evaluations of a large number of corn hybrids by the UW corn breeding project beginning in 1992 and continuing to the present time (Table 2). Starch concentration was added in 1995.

Without doubt, important new nutritional characteristics will emerge as our knowledge increases and our analytical abilities improve. One potential improvement relates to the fact that current NDF digestion analyses may not provide the best representation of how fiber is utilized. The energy from the fiber component of a diet is a function of amount of total fiber and both rate and extent of fiber digestion. A single time point (e.g., 48-h) determination of NDFD represents a combination of both potential rate of digestion and total extent of fiber digestion, but it may be more efficient to deal with these factors independently. Increasing the rate of digestion would permit a greater extent of digestion before particles pass from the rumen, and many researchers have recommended that NDF digestion rate should be included, if possible, in the nutritional assessment of corn silage [16]. There is considerable variation in the rate of NDF digestion, especially apparent in hybrids carrying the *brown midrib3* (*bm3*) mutation such as F657 (Fig. 1), and perhaps this characteristic will eventually be included in the suite of traits used to evaluate silage hybrids.

Issues Related to Measuring Energy Value of Corn Stover as an Ethanol Feedstock

Similar to the silage quality situation, carrying out complete fermentations for determining the relative energy value of different crop varieties for breeding is impractical considering the large number of samples requiring analysis. High-throughput methods for determining

Table 2 NIRS calibration statistics for corn silage used at the University of Wisconsin for broad-based prediction equations used to estimate neutral detergent fiber (NDF), in vitro true digestibility (IVTD), protein, and starch of corn silage.

Trait	Number	Mean	R^2	SEC	SEV(C)	# PLS terms	Math trt.
NDF (%)	838	47.0	0.93	1.53	1.60	13	1,4,4,1
IVTD (%)	642	80.0	0.82	1.47	1.56	11	1,4,4,1
Protein (%)	844	7.5	0.92	0.32	0.34	13	1,4,4,1
Starch (%)	293	28.4	0.94	1.83	2.02	9	1,4,4,1

NDF digestibility is calculated from NDF and IVTD.

SE Standard error, *R* coefficient of determination, *SEC* standard error of calibration, *SEV(C)* standard error of cross-validation, *#PLS terms* number of terms used for modified partial least squares regression.

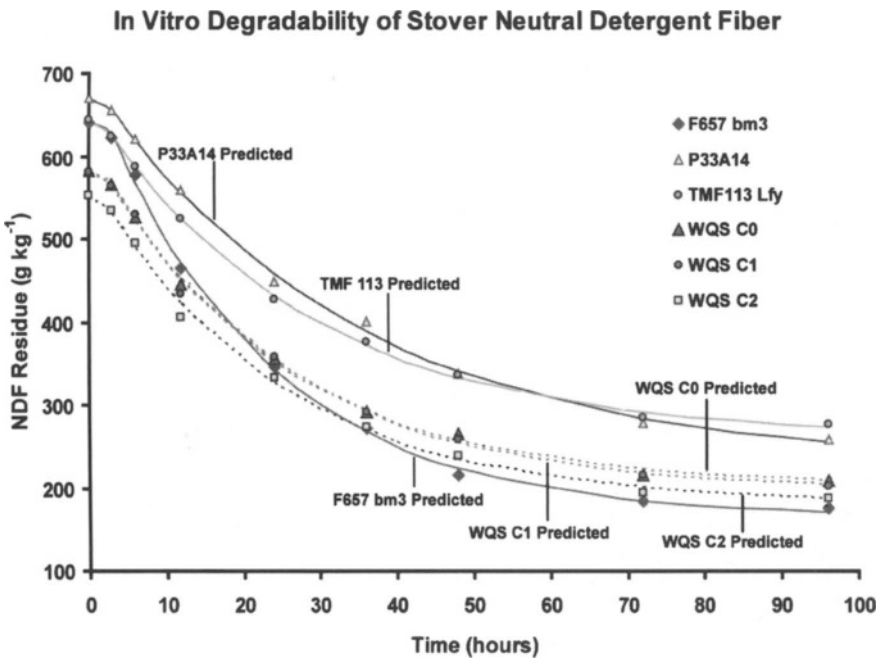


Fig. 1 In vitro neutral detergent fiber digestion for stover collected from six corn varieties over six time periods of incubation with rumen microbes. The hybrid designated P33A14 is a conventional high-yielding grain hybrid. Hybrid TMF113 carries the leafy gene that increases the number of leaves above the ear. The brown-midrib hybrid F657 carries the *bm3* gene that reduces lignin concentration of the stover. The germplasm designated *WQS C0*, *C1*, *C2* are breeding populations produced by two cycles of selection for silage yield and quality [14]. Data from Justen [20]

feedstock constituents, their energy value, and conversion efficiency will be required and must be combined into an index that accurately ranks varieties for cellulosic ethanol quality at the industrial scale. The National Renewable Energy Laboratory (NREL) has developed an NIRS equation for predicting the concentration of individual cell wall carbohydrates and theoretical ethanol potential of corn stover [17]. However, the theoretical ethanol potential assumes the cell wall carbohydrates to be completely available for fermentation and does not reflect variability in stover digestibility among varieties. Moreover, hydrolysis of cellulose carried out by costly cellulases and chemical pretreatment—to make the cellulose more accessible to enzymatic hydrolysis—are currently among the most expensive steps in the process [2]. Identifying and breeding varieties with stover that is more conducive to chemical and enzymatic digestion could be of more value than those varieties that contain higher carbohydrate concentrations but are more recalcitrant. Because cellulosic ethanol production practices are under development and will likely not be uniform anyway, determining a standard method for assessing the economically available energy through combining composition and degradability will allow for breeders to make progress in improving the overall ethanol quality of corn stover, just as silage breeding and quality analysis has added additional variables for a more comprehensive model of quality.

As discussed above, the rate of digestion impacts the energy value of corn silage, and hopefully, future tools allow ruminant nutritionists and breeders to include this characteristic in quality evaluations. Likewise, genetic variability for rate of chemical degradation or conversion into ethanol may impact the economics of cellulosic ethanol plants by influencing

the rate of biofeedstock throughput that can be achieved. Determining the relative importance of conversion rate, how to measure this trait, and how to incorporate it into a comprehensive model would be essential to developing a variety that is completely converted in substantially less time. While more immediate hurdles have priority (total carbohydrate content and conversion efficiency), genetic improvement of these characteristics will reach limits, making conversion rate one of the next feedstock properties that could contribute to overall process efficiency in the future.

Accurate prediction of NEL, dry matter intake, and thus milk production potential provides correct ranking of varieties for silage use, and the use of NIRS for prediction of silage constituents has made large-scale breeding and variety evaluation possible. The current status of cellulosic biofeedstock development for corn is directly analogous to that of silage breeding before the development of a dedicated breeding effort. For biofeedstock development, what now remains is to determine the logistical requirements for large-scale field evaluations. To this end, we need information on the appropriate number of unique field environments (locations and years of evaluation) as well as the amount of replication within each environment that are necessary to correctly rank potential germplasm sources. Plant breeders use the concept of "repeatability" to address these requirements for accurate assessment at the field level.

Repeatability of Corn Stover Traits Related to Cellulosic Ethanol Production

Measurement precision combined with genetic variation of a characteristic is vital to its improvement. Genetic gain for a trait made each cycle of selection by plant breeders directly relates to the heritability (h^2) of a trait and its selection differential (S: difference between mean of selected individuals and population mean).

$$\text{Genetic gain per cycle} = h^2 S$$

The selection differential is directly related to the selection intensity. The selection intensity can be increased by either selecting a smaller number of individuals for recombination or increasing the total number of individuals evaluated. The latter approach is preferred because a reduction in genetic diversity through selecting too few individuals may compromise future gains. Therefore, rapid methods of measurement are necessary to evaluate large numbers of families with adequate replication over different environments. The h^2 of a trait represents the proportion of S expected to be inherited by the next generation and is determined by the ratio of heritable genetic variance to total phenotypic variance. Repeatability sets an upper limit to h^2 and is a statistical measure used to quantify the importance of variation among individuals or families under evaluation (usually referred to as genotypes) relative to variation within genotypes [18]. Repeatabilities are dependent upon the genotypes evaluated as well as the environments in which they were evaluated. When genotypes are randomly sampled from a defined reference population, repeatability is termed broad-sense heritability or coefficient of genetic determination. Plant breeders typically calculate repeatability (R) on a family mean basis with:

$$R = \frac{\sigma^2_{\mathrm{G}}}{\sigma^2_{\mathrm{G}} + \left(\sigma^2_{\mathrm{GE}}/e\right) + \left(\sigma^2_e/re\right)}$$

where σ^2_G is the variation among genotypes, σ^2_{GE} is the variation because of genotype by environment interaction, σ^2_e is the variation because of error, e is the number of environments

individuals were evaluated in, and r is the number of replications within environments. Essentially, the presence of genotype by environment interaction and random environmental noise (measurement error, within environment variation) reduces repeatability and thus reduces efficiency of selection. Increasing replication and/or the number of environments used for evaluation increases repeatability at the expense of additional resources.

We calculated repeatability values for a set of silage traits and a set of stover traits measured in a nearly identical set of corn hybrids. Forty hybrids were evaluated for silage traits at 30–40% dry matter, and 44 hybrids were evaluated for stover traits at physiological maturity (approximately 50% dry matter) during 2005 and 2006. Hybrids were evaluated in a randomized complete block design with three replications within each of four environments (480 silage plots, 528 stover plots). Plots consisted of two rows (0.76m apart and 6.08m long) planted to a density of 79,000 plants per hectare. A single sample was obtained from each plot and ground to pass a 1-mm screen for compositional analysis. The global NIRS equations discussed above were used to predict NDF, NDFD, and starch concentrations of each sample. These constituents were then entered into MILK2006 for prediction of milk per ton. The stover constituents glucan, xylan, galactan, mannan, arabinan, and lignin were predicted by Stover9, a NIRS equation developed at the NREL in Golden, CO [17]. Polysaccharide concentrations were used to calculate theoretical ethanol potential according to NREL's website (http://www1.eere.energy.gov/biomass/ethanol_yield_calculator.html). Silage and stover yield values were on a dry-matter basis.

Repeatability estimates of the silage traits were in the expected range and indicate that the majority of total variation observed was due to variation among hybrids (Table 3). The repeatability estimates for the stover characteristics predicted by Stover9 were excellent and mostly exceeded those of the silage traits. Stover9 predictions of individual hybrids were reliable across environments and replications within environments and suggest that ethanol potential and its components may be highly heritable. Both silage and stover yield repeatabilities were lower than those of the composition type traits, which is not surprising given the complex nature of yield and difficulty in obtaining reliable measurements in a field setting. Nevertheless, significant gains have been made for grain yield of corn through persistent breeding and selection [19].

Table 3 Repeatability estimates for silage and stover traits. Silage traits were predicted with the global NIRS equations discussed in text and MILK2000 was used to calculate milk per ton.

	R
Silage trait	
Milk per ton	0.72
NDF	0.65
NDFD	0.84
Starch	0.74
Silage yield	0.58
Stover trait	
Ethanol potential[a]	0.82
Glucan	0.81
Xylan	0.83
Galactan	0.87
Arabinan	0.95
Mannan	0.74
Lignin	0.85
Stover yield	0.75

Stover composition was predicted with Stover9 [17].

[a] Theoretical ethanol potential calculated with NREL's ethanol calculator (http://www1.eere.energy.gov/biomass/ethanol_yield_calculator.html).

Conclusions

Lessons from measuring and ranking silage varieties for potential milk production can be applied to the analogous situation of determining how to rank varieties for use as cellulosic feedstocks. Rapid methods of measurement capable of analyzing the large number of samples generated by breeding and variety evaluation programs will be required. In addition, a simple method of assigning an intuitive quality value to different varieties would be advantageous, and such an index should include total carbohydrate concentration and conversion efficiency. Commercial procedures such as pretreatment type and severity as well as specifics on hydrolysis reactions are not yet established. However, inclusion of conversion efficiency standardized by pretreatment severity, enzyme loading, and cost would better rank varieties based on economically available energy given the variation for cell wall digestibility among varieties. As more is learned about energy sources and inhibitors in cellulosic biomasses and how they relate to ethanol production, models for energy prediction will change. However, selection and improvement of feedstocks should still proceed, even when knowledge of the energy value is known to be incomplete. The rate of digestion is a silage property known to vary and impact NEL. Because increased rate of digestion could affect the economics of ethanol plants by increasing feedstock throughput in the future, this property may deserve attention, and simple measurement techniques will need to be developed that are statistically and functionally associated.

Repeatability of ethanol potential and corn stover composition as determined by NIRS prediction is high and suggests that these traits may be highly heritable. Improvements in feedstock composition through breeding could be realized with sufficient funding and effort. A comprehensive model for predicting economically available energy for ethanol production should be developed so the net amount of energy per ton of feedstock and per dollar can be maximized.

References

1. Service, R. F. (2007). *Science, 315*, 1488–1491.
2. Wyman, C. E. (2007). *Trends in Biotechnology, 25*, 153–157.
3. Van Soest, P. J. (1994). *Nutritional ecology of the ruminant* (2nd ed.). Ithaca, NY: Cornell University Press.
4. Coors, J. G., & Lauer, J. G. (2001). In A. R. Hallauer (Ed.) *Specialty corns* pp. 347–392. Boca Raton, FL: CRC.
5. Ragauskas, A. J., Williams, C. K., Davison, B. H., Britovsek, G., Cairney, J., Eckert, C. A., et al. (2006). *Science, 311*, 484–489.
6. Allen, M. S., Coors, J. G., & Roth, G. W. (2003). In D. R. Buxton, R. E. Muck, & J. H. Harrison (Eds.) *Silage science and technology* pp. 547–608. Madison, WI: ASA–CSSA–SSSA.
7. Lauer, J. G., Coors, J. G., & Flannery, P. J. (2001). *Crop Science, 41*, 1449–1455.
8. Undersander, D. J., Howard, W. T., & Shaver, R. D. (1993). *Journal of Production Agriculture, 6*, 231–235.
9. Weiss, W. P. (1994). In G. C. Fahey (Ed.) *Forage quality, evaluation, and utilization* pp. 644–681. Madison, WI: ASA–CSSA–SSSA.
10. Mertens, D. R. (1987). *Journal of Animal Science, 64*, 1548–1558.
11. Oba, M., & Allen, M. S. (1999). *Journal of Dairy Science, 82*, 589–596.
12. Schwab, E. C., Shaver, R. D., Lauer, J. G., & Coors, J. G. (2003). *Journal of Animal Feed Science and Technology, 109*, 1–18.
13. Shaver, R. D. (2006). *Corn silage evaluation: MILK2000 challenges and opportunities with MILK2006.* Available at: http://www.wisc.edu/dysci/uwex/nutritn/pubs/milk2006weblinktext.pdf.
14. Lauer, J., Kohn, K., & Flannery, P. J. (2005). Wisconsin corn hybrid performance trials grain and silage. University of Wisconsin Ext. Publ. A3653. Available at: http://corn.agronomy.wisc.edu/HT/2005/Text.htm.

15. Coors, J. G. (2007). UW corn silage breeding program. Available: http://www.silagebreeding.agronomy.wisc.edu/Corn/corn_home.htm.
16. Jung, H. G., Mertens, D. R., & Buxton, D. R. (1998). *Crop Science, 38*, 205–210.
17. Hames, B. R., Thomas, S. R., Sluiter, A. D., Roth, C. J., & Templeton, D. W. (2003). *Applied Biochemistry and Biotechnology, 105*, 5–16.
18. Lessells, C. M., & Boag, P. T. (1987). *Auk, 104*, 116–121.
19. Duvick, D. N., Smith, J. S. C., & Cooper, M. (2004). *Plant Breeding Reviews, 24*, 109–151.
20. Justen, B. (2004). M.S. thesis, University of Wisconsin, Madison, WI.

Appl Biochem Biotechnol (2008) 148:271–276
DOI 10.1007/s12010-007-8044-8

Permethylation Linkage Analysis Techniques for Residual Carbohydrates

Neil P. J. Price

Received: 23 May 2007 / Accepted: 4 September 2007 /
Published online: 2 October 2007
© Humana Press Inc. 2007

Abstract Permethylation analysis is the classic approach to establishing the position of glycosidic linkages between sugar residues. Typically, the carbohydrate is derivatized to form acid-stable methyl ethers, hydrolyzed, peracetylated, and analyzed by gas chromatography-mass spectrometry. The position of glycosidic linkages in the starting carbohydrate are apparent from the mass spectra as determined by the location of acetyl residues. The completeness of permethylation is dependent upon the choice of base catalyst and is readily confirmed by matrix-assisted laser desorption/ionization time-of-flight mass spectrometry mass spectrometry. For the permethylation of β-cyclodextrin, Hakomori dimsyl base is shown to be superior to the NaOH–dimethyl sulfoxide system, and the use of the latter resulted in selective under-methylation of the 3-hydroxy groups. These techniques are highly applicable to residual carbohydrates from biofuel processes.

Keywords Carbohydrate · Linkage analysis · Permethylation · Mass spectrometry

Introduction

Permethylation analysis of sugars is a useful technique for establishing the position of glycosidic linkages (Fig. 1) [1–3]. Free hydroxyl groups on the carbohydrate under study are initially converted to methyl ethers by application of a strongly based-catalyzed Williamson ether synthesis. Because this reaction is sensitive to the presence of water, the permethylation reaction is generally undertaken in a dry solvent such as dimethyl sulfoxide (DMSO) or dimethylformamide. The methylating reagent itself is usually methyl iodide or dimethyl sulfate, although the use of the latter is generally discouraged because of the high toxicity.

Mention of trade names or commercial products in this article is solely for the purpose of providing specific information and does not imply recommendation or endorsement by the US Department of Agriculture.

N. P. J. Price (✉)
USDA-ARS-NCAUR, Bioproducts & Biocatalysis Research Unit, 1815 North University Street, Peoria, IL 61604, USA
e-mail: neil.price@ars.usda.gov

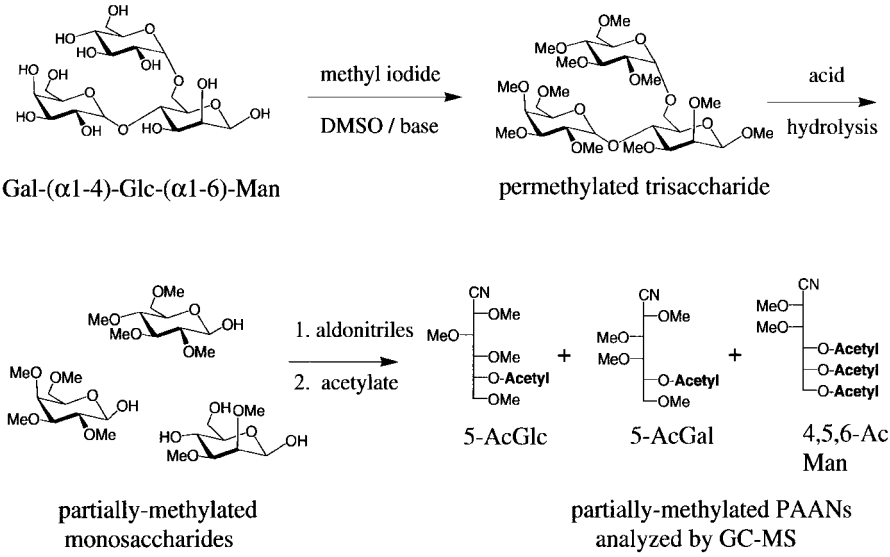


Fig. 1 Schematic for the permethylation linkage analysis, exemplified by a hypothetical trisaccharide, Gal-(α-1,4)-Glc-(α-1,6)-Man. The acid-hydrolyzed partially methylated monosaccharides generated are analyzed by GC-MS, typically as alditol or aldononitrile derivatives

Complete methylation (termed, "per"methylation) is essential to achieving good linkage analysis results because under-methylation of the hydroxyl groups can lead to linkage artifacts. Two factors are important here; firstly, the choice of base catalyst, and secondly, to ensure good solubility and miscibility of the carbohydrate and methylation reagent [4–9]. DMSO is generally the solvent of choice because it may be commercially acquired and stored water-free and has a high solvation for most oligosaccharides and polysaccharides. In addition, those polysaccharides that are insoluble can sometimes be analyzed as a fine suspension in DMSO. The use of DMSO as solvent has also specified the choice of either sodium hydride of dry sodium hydroxide as the base catalyst [4, 5]. Sodium hydride has the advantage that it actually reacts with the DMSO solvent to form its anion, methyl sulfinyl carbanion, also called the dimsyl ion, first reported by Corey and Chaykovsky [10]. Dimsyl base is highly suited to ether preparation, but is difficult to handle and must be stored under oil. This led to the introduction of suspended sodium hydroxide as base catalyst [4]. However, sodium hydroxide is hygroscopic, and because it is not soluble in DMSO, it must be ground up to form a suspension. This can result in non-miscible methylation conditions, especially with DMSO-insoluble polysaccharides, and may therefore result in under-methylation.

In this paper, we have compared two commonly used permethylation methods [4, 5] and have applied them to a model carbohydrate compound. The completeness of the methylation steps was established by matrix-assisted laser desorption/ionization time-of-flight mass spectrometry (MALDI-TOF MS). The methylated carbohydrate products were acid-hydrolyzed and converted to methylated partially acetylated aldononitrile derivatives (Me PAANs) for linkage analysis by gas chromatography-mass spectrometry (GC-MS) [11].

Methods

All reagents were obtained commercially from Sigma-Aldrich, St. Louis. Permethylations were undertaken as described, using either NaOH–DMSO suspension [4] or dimsyl base [5] as the catalyst. The acid hydrolysis (2.0 M trifluoroacetic acid) was undertaken at 121 °C, and aldononitrile acetates were prepared as described [11]. GC-MS analyses of the derivatized samples employed an Agilent 6890N gas chromatograph (Agilent Technologies, Palo Alto, CA, USA) equipped with an HP 7683 autoinjector interfaced with an HP 5973 series mass spectrometer configured in electron impact mode. Chromatography was accomplished with a capillary HP-1 column (25 m long; 0.2-mm diameter) using helium as the carrier gas at a flow rate of 0.8 ml/min. The oven temperature was ramped over a linear gradient from 150 to 250 °C at 4 °C/min. Mass spectra were recorded in positive-ion mode over the range 50 to 500 m/z. MALDI-TOF MS spectra were obtained on a Bruker–Daltonic Omniflex instrument (Bruker, Billerica, MA, USA) operating in reflectron mode. Samples were dried under a lamp on a conventional 49-place stainless steel target. The matrix used was 2,5-dihydroxybenzoic acid. A 200-ns pulsed ion extraction was used, with matrix suppression up to 200 Da. Excitation was at 337.1 nm, typically at 60% of a 150-μJ maximum output, and 80 shots were accumulated. Ion sources 1 and 2 were 19.0 and 14.0 kV, with lens and reflector voltages of 9.20 and 20.00 kV, respectively.

Results

A comparison study was undertaken of two bases commonly used for the permethylation analysis of sugars [4, 5]. A model carbohydrate, β-cyclodextrin (β-CD) was chosen because it contains a single type of sugar residue, β-1,4-linked glucose and because of its comparatively poor solubility in DMSO [12, 13]. β-CD was dissolved in DMSO and methylated using methyl iodide, essentially as described by Hakomori (using dimsyl base [5]) or Kerek and Ciucanu (using NaOH base [4]). At the end of the reactions, the methylated β-CDs were extracted into hexane and split into three aliquots. Two of these aliquots were analyzed by either MALDI-TOF mass spectrometry or thin layer chromatography (TLC) to determine the completeness of methylation (Fig. 2). The third aliquots were acid-hydrolyzed to their component sugar residues, converted to the corresponding partially methylated aldononitriles (PMANs), and analyzed by GC-MS (Fig. 3). This was undertaken to confirm that the linkages present for the β-CD were correctly identified and also to ascertain the positions of under-methylated hydroxyl groups.

The dimsyl base was seen to be highly effective for the permethylation of β-CD. A molecular $[M+Na]^+$ adduct ion was observed at m/z 1451, which corresponds to the molecular mass of β-CD with all of the 21 free hydroxyls replaced by methyl groups (Fig. 2). Except for a single $[M-14+Na]^+$ at m/z 1437, there was little evidence for partially methylated β-CDs. Moreover, the fully methylated β-CD was also observed as a single band by the TLC analysis (Fig. 2). By contrast, MALDI-MS analysis of the NaOH-catalyzed reaction showed a series of ions incrementally 14 mass units less than the fully methylated m/z 1451 molecular ion. This ion series is evidence of a mixture of under-methylated β-CDs. Hence, under-methylated ions are observed at m/z 1437, 1423, 1409, etc. (Fig. 2) where the observed 14 mass unit differentials are due to the mass difference between –H and a $–CH_3$. Furthermore, under-methylated β-CDs formed under the NaOH-catalyzed conditions are also apparent as a less motile "ladder" when analyzed by TLC (Fig. 2).

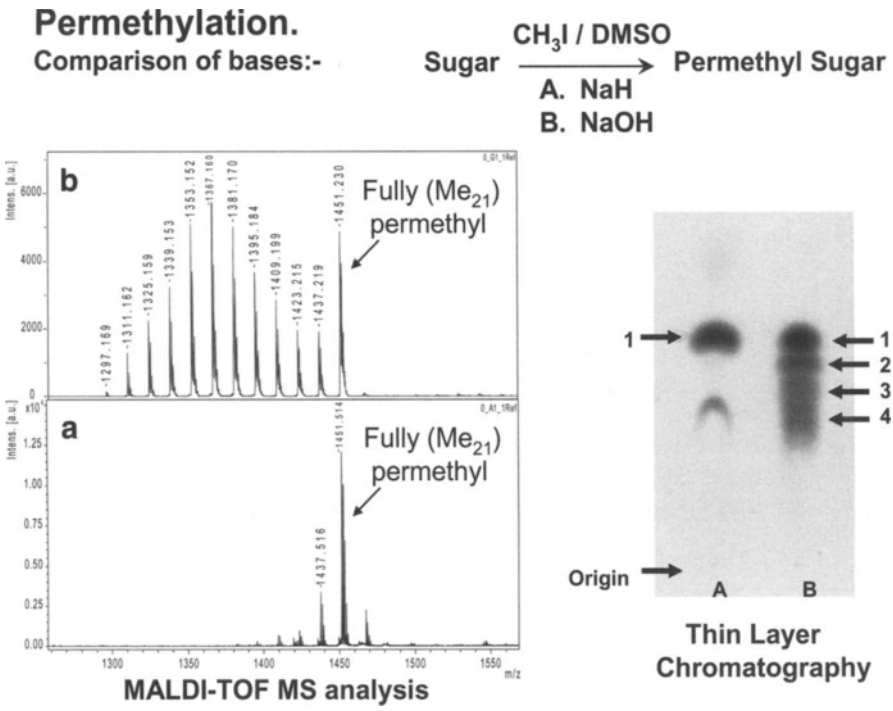


Fig. 2 Comparison of the effectiveness of the base catalysts used in permethylation of β-cyclodextrin. The catalyst used was Hakomori dimsyl base (**a**) or NaOH–DMSO suspension (**b**). The analysis was by MALDI-TOF MS (*left*) and thin layer chromatography (*right*)

To ascertain the positions of the under-methylated hydroxyl groups and also to confirm the 1,4-linkages of β-CD, the methylation products from the above reactions were acid-hydrolyzed, converted to aldononitrile acetates, and analyzed by GC-MS (Fig. 3). The dimsyl-catalyzed reaction gave rise to a single chromatographic peak, which, in the mass spectrometer, was identified as due to 2,3,6-trimethyl-4-*O*-acetyl-glucose. Because the position of *O*-acetyl groups corresponds to the original linkage position, the 2,3,6-trimethyl-4-*O*-acetyl-glucose peak (peak 1, Fig. 3) confirmed that the only linkage present in the original β-CD is the expected 1,4. Other glycosidic linkages are absent, as evident from the lack of other GC peaks. Moreover, the lack of other GC peaks also shows that the original β-CD sample was fully methylated under dimsyl-catalyzed conditions. By contrast, two peaks were observed for the NaOH-catalyzed reaction corresponding to 2,3,6-trimethyl-4-*O*-acetyl-glucose peak (peak 1) plus 2,6-dimethyl-3,4-di-*O*-acetyl-glucose (peak 2, Fig. 3). Integration results indicates peak 1/peak 2 ratio of ~3:1. The more intense peak 1 confirmed the expected 1,4-linkage, and also indicates ~66% of the β-CD was in fact fully methylated. However, the 3,4-di-*O*-acetylated derivative (peak 2) shows that 33% under-methylation of β-CD occurs with NaOH–DMSO. Furthermore, the under-methylated hydroxy groups all occur selectively at the 3-position, with no evidence of under-methylation at the 6-hydroxyl or 2-hydroxyl groups. Importantly, when taken together, the MALDI-TOF MS data (Fig. 2) and GC-MS data (Fig. 3) indicate that the under-methylated β-CDs occur as a complex mixture in which

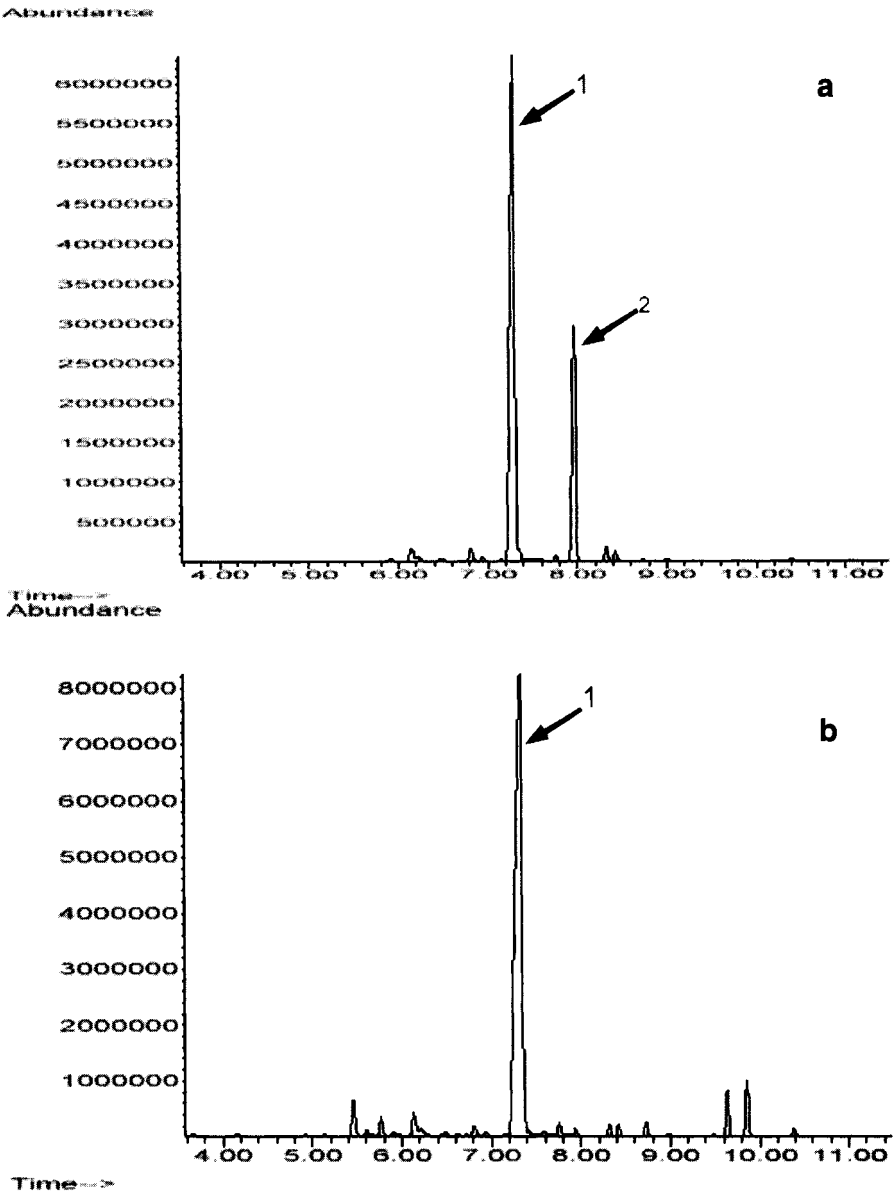


Fig. 3 GC-MS traces of PMANs derived from permethylation of β-cyclodextrin. **a** Using NaOH–DMSO base; **b** using dimsyl base. Peak 1 is due to 2,3,6-trimethyl-4-*O*-acetyl-glucose, and peak 2 to 2,6-dimethyl-3,4-di-*O*-acetyl-glucose. The latter peak is evidence of under-methylation of the β-cyclodextrin at position 3 of each glucose residue

the 3-*O*-methyl groups may be absent from one, two, three, or more of the seven glucose residues of the starting β-CD. Hence, after GC-MS, the under-3-*O*-methylated glucose residues of the mixture of partially methylated β-CD give rise to peak 2, whereas the remaining fully methylated Glc residues are identified by GC peak 1.

Discussion

This paper discussed some issues involved in permethylation linkage analysis of carbohydrates and highlights the importance of solvation of the sample and reactant and the choice of base catalyst. Complete permethylation is shown to be essential to obtaining confident results. For the example carbohydrate, β-CD, it was shown that the Hakomori dimsyl reagent is a superior base catalyst than NaOH–DMSO suspension. Under the latter condition, under-methylation of β-CD occurs selectively at 3-hydroxy groups, which might be interpreted as artifactual 3-*O*-linkages. This may occur because the 3-hydroxy groups are buried within the relatively hydrophobic torus of β-CD where they are excluded from deprotonation by the NaOH base [14]. Consistent with this, maltoheptoase, a linear form of β-CD, is permethylated equally well using either dimsyl or NaOH, and several mannose oligosaccharides are more completely permethylated using NaOH–DMSO (data not shown). The conclusion is that permethylation conditions are not universally applicable to all carbohydrate types, and it is therefore recommended that the completeness of permethylation of carbohydrate samples be checked by MALDI-TOF MS analysis before the acid hydrolysis step. Under-methylation can then be corrected either by changing the base-catalyst or by exhaustive re-methylation of the sample.

Acknowledgment Jim Nicholson and Trina Hartman (NCAUR-ARS-USDA) are both thanked for their technical assistance.

References

1. Fernández, L. E. M., Sørensen, H. R., Jørgensen, C., Pedersen, S., Meyer, A. S., & Roepstorff, P. (2007). Characterization of oligosaccharides from industrial fermentation residues by matrix-assisted laser desorption/ionization, electrospray mass spectrometry, and gas chromatography mass spectrometry. *Molecular Biotechnology, 35*, 149–160.
2. Jay, A. (1996). The methylation reaction in carbohydrate analysis. *Journal of Carbohydrate Chemistry, 15*, 897–923.
3. Ciucanu, I. (2006). Per-*O*-methylation reaction for structural analysis of carbohydrates by mass spectrometry. *Analytica Chimica Acta, 576*, 147–155.
4. Ciucanu, I., & Kerek, F. (1984). A simple and rapid method for the permethylation of carbohydrates. *Carbohydrate Research, 131*, 209–217.
5. Hakomori, S. (1964). A rapid permethylation of glycolipid and polysaccharide catalyzed by methylsulfinyl carbanion in dimethyl sulfoxide. *Journal of Biochemistry, 55*, 205–208.
6. Parente, J. P., Cardon, P., Leroy, Y., Montreuil, J., Fournet, B., & Ricart, G. (1985). A convenient method for methylation of glycoprotein glycans in small amounts by using lithium methylsulfinyl carbanion. *Carbohydrate Research, 141*, 41–47.
7. Needs, P. W., & Selvendran, R. R. (1993). Avoiding oxidative degradation during sodium hydroxide/methyl iodide-mediated carbohydrate methylation in dimethyl sulfoxide. *Carbohydrate Research, 245*, 1–10.
8. Funakoshi, I., & Yamashina, I. (1980). Quantitative determination of partially methylated alditol acetate of amino sugar by gas chromatography-mass spectrometry. *Analytical Biochemistry, 107*, 265–270.
9. Harris, P. J., Henry, R. J., Blakeney, A. B., & Stone, B. A. (1984). An improved procedure for the methylation analysis of oligosaccharides and polysaccharides. *Carbohydrate Research, 127*, 59–73.
10. Corey, E. J., & Chaykovsky, M. (1962). Methylsulfinylcarbanion. *Journal of American Chemical Society, 84*, 866–867.
11. Price, N. P. (2006). Acylic sugar derivatives for GC/MS analysis of 13C-enrichment during carbohydrate metabolism. *Analytical Chemistry, 76*, 6566–6574.
12. Bender, M. L., & Komiyama, M. (1978). *Cyclodextrin chemistry*. NY: Springer
13. Szejtli, J. (1998). Introduction and general overview of cyclodextrin chemistry. *Chemical Review, 98*, 1743–1753.
14. Rao, C. T., & Pitha, J. (1991). Reactivities at the *O*-2, *O*-3, and *O*-6 positions of cycloamyloses in Hakomori methylation. *Carbohydrate Research, 220*, 209–213.